VOLUME 27 / NUMBER 16
AUGUST 23, 1989
ACC. NOS. N89-22568 TO N89-23405

STAR
AN ABSTRACT JOURNAL

Scientific and Technical Aerospace Reports

PRODUCED BY THE
SCIENTIFIC AND TECHNICAL
INFORMATION
DIVISION

NASA

NATIONAL AERONAUTICS AND SPACE ADMINISTRATION

WHAT YOU CAN DO FOR *STAR*

All users of this abstract service are urged to forward reports to be considered for announcement in *STAR*. This will aid NASA in its efforts to provide the fullest possible coverage of all scientific and technical publications that might support aeronautics and space research and development. If you have prepared relevant reports (other than those that you will transmit to NASA, DoD, or DOE through the usual contract- or grant-reporting channels), please send them for consideration to the NASA Scientific and Technical Information Facility, P.O. Box 8757, BWI Airport, Maryland 21240.

Reprints of journal articles, book chapters, and conference papers are also welcome. These will be considered for announcement in *STAR's* companion journal, *International Aerospace Abstracts*.

You may specify a particular source to be included in a report announcement if you wish; otherwise the report will be placed on public sale at the National Technical Information Service. Copyrighted publications will be announced but not distributed or sold.

PURCHASE OF *STAR*

The semimonthly issues are available to registered users on annual subscription for $99.00 from the NASA Scientific and Technical Information Facility, ATTN: Registration Services, P.O. Box 8757, BWI Airport, MD 21240. *STAR* is publically available on annual subscription for $99.00 from the Superintendent of Documents, U.S. Government Printing Office, Washington, DC 20402.

PUBLISHED BY:

UNITED STATES GOVERNMENT
NATIONAL AERONAUTICS AND SPACE ADMINISTRATION
SCIENTIFIC AND TECHNICAL INFORMATION DIVISION
Scientific and Technical Aerospace Reports, Volume 27, is prepared by the NASA Scientific and Technical Information Facility operated for the National Aeronautics and Space Administration by RMS Associates.

The Administrator of the National Aeronautics and Space Administration has determined that the publication of this periodical is necessary in the transaction of the public business required by law of this Agency. Use of funds for printing this periodical has been approved by the Director of the Office of Management and Budget through March 22, 1989.

US ISSN 0036-8741

INTRODUCTION

Scientific and Technical Aerospace Reports (STAR) is a major component of a comprehensive National Aeronautics and Space Administration information system covering aeronautics, space, and supporting disciplines. *STAR* is issued on the 8th and 23rd of each month and announces current publications of the following types:

- NASA, NASA contractor, and NASA grantee reports
- Reports issued by other U.S. Government Agencies, domestic and foreign institutions, universities, and private firms
- Translations in report form
- NASA-owned patents and patent applications
- Other U.S. Government Agency and foreign patents and patent applications
- Domestic and foreign dissertations and theses

Journal, book, and conference literature, cover-to-cover journal translations, and certain foreign dissertations are announced in a companion journal, *International Aerospace Abstracts (IAA),* available on subscription from the American Institute of Aeronautics and Astronautics, Technical Information Service, 555 West 57th Street, 12th Floor, New York, New York 10019.

SUBJECT SCOPE

Subject scope of *STAR,* and *IAA* includes all aspects of aeronautics and space research and development, supporting basic and applied research, and applications. Aerospace aspects of earth resources, energy development, conservation, oceanography, environmental protection, urban transportation, and other topics of high national priority are also covered.

OTHER NASA PUBLICATIONS

Other NASA publications and information services are described in the publication, *The NASA Scientific and Technical Information System ... and How to Use It,* available without charge from the NASA Scientific and Technical Information Facility, P.O. Box 8757, BWI Airport, Maryland 21240.

HOW TO USE *STAR* SUBJECT CATEGORIES

STAR is categorized by 10 major subject divisions divided into 76 specific subject categories and one general category/division. The major subject divisions are listed in the Table of Contents, together with a note for each that defines its scope and provides any cross-references. For example:

AERONAUTICS

Includes aeronautics (general); aerodynamics; air transportation and safety; aircraft communications and navigation; aircraft design, testing and performance; aircraft instrumentation; aircraft propulsion and power; aircraft stability and control; and research and support facilities (air).

For related information see also *Astronautics.*

Each major division is further divided into as many as nine specific categories, which are identified by category numbers.

Abstracts in *STAR* are grouped by specific category, the categories appearing in sequential order. Category breaks in the abstract section are identified by the category number and title, and a scope note. Cross-references to other categories are provided as appropriate. For example:

02 AERODYNAMICS

Includes aerodynamics of bodies, combinations, wings, rotors, and control surfaces; and internal flow in ducts and turbomachinery.

For related information see also *34 Fluid Mechanics and Heat Transfer.*

CROSS-REFERENCES

Individual *STAR* abstracts are not ordinarily cross-referenced, except for certain conference reports or book translations that have had separate abstracts written for their component papers or chapters. Citations and abstracts of the components follow immediately after those of the parent document. When the subject content of a component differs sufficiently from the general content of the parent, a cross-reference citation also is printed at the end of the category to which it normally would have been assigned if it were independent.

DOCUMENTS ON MICROFICHE

Documents on microfiche[1] are designated by a pound sign (#) following the accession number. The pound sign is used without regard to the source or quality of the microfiche.

AVAILABILITIES

One or more sources from which a document announced in *STAR* is available to the public is given in each citation. The most commonly indicated sources and their acronyms or abbreviations are listed below. If the publication is available from a source other than those listed, the publisher and his address will be displayed on the availability line or in combination with the corporate source line.

Avail: NTIS. Sold by the National Technical Information Service. Prices for hard copy (HC) and microfiche (MF) are indicated by a price code following the letters HC or MF in the *STAR* citation. Current values for the price codes are given in the tables on page vii.

Initially distributed microfiche under the NTIS SRIM (Selected Research in Microfiche) is available at greatly reduced unit prices. For this service and for information concerning subscription to NASA printed reports, consult the NTIS Subscription Section, Springfield, Va. 22161.

NOTE ON ORDERING DOCUMENTS: When ordering NASA publications (those followed by the * symbol), use the N accession number. NASA patent applications (only the specifications are offered) should be ordered by the US-Patent-Appl-SN number. Non-NASA publications (no asterisk) should be ordered by the AD, PB, or other *report number* shown on the last line of the citation, not by the N accession number. It is also advisable to cite the title and other bibliographic identification.

Avail: SOD (or GPO). Sold by the Superintendent of Documents, U.S. Government Printing Office, in hard copy. The current price and order number are given following the availability line. (NTIS will fill microfiche requests, as indicated above, for those documents identified by a # symbol.)

(1) A microfiche is a transparent sheet of film, 105 by 148 mm in size, containing as many as 60 to 98 pages of information reduced to micro images (not to exceed 26:1 reduction).

Avail: BLL (formerly NLL): British Library Lending Division, Boston Spa, Wetherby, Yorkshire, England. Photocopies available from this organization at the price shown. (If none is given, inquiry should be addressed to the BLL.)

Avail: DOE Depository Libraries. Organizations in U.S. cities and abroad that maintain collections of Department of Energy reports, usually in microfiche form, are listed in *Energy Research Abstracts*. Services available from the DOE and its depositories are described in a booklet, *DOE Technical Information Center - Its Functions and Services* (TID-4660), which may be obtained without charge from the DOE Technical Information Center.

Avail: ESDU. Pricing information on specific data, computer programs, and details on ESDU topic categories can be obtained from ESDU International Ltd. Requesters in North America should use the Virginia address while all other requesters should use the London address, both of which are on page vi.

Avail: Fachinformationszentrum, Karlsruhe. Sold by the Fachinformationszentrum Energie, Physik, Mathematik GMBH, Eggenstein Leopoldshafen, Federal Republic of Germany, at the price shown in deutschmarks (DM).

Avail: HMSO. Publications of Her Majesty's Stationery Office are sold in the U.S. by Pendragon House, Inc. (PHI), Redwood City, California. The U.S. price (including a service and mailing charge) is given, or a conversion table may be obtained from PHI.

Avail: NASA Public Document Rooms. Documents so indicated may be examined at or purchased from the National Aeronautics and Space Administration, Public Documents Room (Room 126), 600 Independence Ave., S.W., Washington, D.C. 20546, or public document rooms located at each of the NASA research centers, the NASA Space Technology Laboratories, and the NASA Pasadena Office at the Jet Propulsion Laboratory.

Avail: Univ. Microfilms. Documents so indicated are dissertations selected from *Dissertation Abstracts* and are sold by University Microfilms as xerographic copy (HC) and microfilm. All requests should cite the author and the Order Number as they appear in the citation.

Avail: US Patent and Trademark Office. Sold by Commissioner of Patents and Trademarks, U.S. Patent and Trademark Office, at the standard price of $1.50 each, postage free. (See discussion of NASA patents and patent applications below.)

Avail: (US Sales Only). These foreign documents are available to users within the United States from the National Technical Information Service (NTIS). They are available to users outside the United States through the International Nuclear Information Service (INIS) representative in their country, or by applying directly to the issuing organization.

Avail: USGS. Originals of many reports from the U.S. Geological Survey, which may contain color illustrations, or otherwise may not have the quality of illustrations preserved in the microfiche or facsimile reproduction, may be examined by the public at the libraries of the USGS field offices whose addresses are listed in this Introduction. The libraries may be queried concerning the availability of specific documents and the possible utilization of local copying services, such as color reproduction.

Avail: Issuing Activity, or Corporate Author, or no indication of availability. Inquiries as to the availability of these documents should be addressed to the organization shown in the citation as the corporate author of the document.

NASA PATENTS AND PATENT APPLICATIONS

Patents and patent applications owned by NASA are announced in *STAR* under appropriate subject categories and are referenced in the *STAR* indexes. In the Report/Accession Number Index, patents are indexed by the NASA Case Number (which appears in lieu of the report number in other indexes), the U.S. Patent Number, the U.S. Patent Application Serial Number, and the U.S. Patent Class. Patent applications for which patents have not yet been issued are indexed by the NASA Case Number and the U.S. Patent Application Serial Number.

NASA *patent application specifications* are sold in paper copy by the National Technical Information Service at price code A02. Microfiche are sold at price code A01. The US-Patent-Appl-SN- number should be used in ordering either paper copy or microfiche from NTIS. Printed copies of *patents* (which are not microfiched) are available for purchase at $1.50 per copy from:

Commissioner of Patents and Trademarks
U.S. Patent and Trademark Office
Washington, D.C. 20231

When ordering patents, the U.S. Patent Number should be used, and payment must be remitted in advance, preferably by money order or check payable to the Commissioner of Patents and Trademarks. Prepaid purchase coupons for ordering are also available from the Patent and Trademark Office. The patents and patent applications announced in *STAR* are owned by NASA and are available for royalty-free licensing. Requests for licensing terms and further information should be addressed to:

Associate General Counsel for Intellectual Property/Code GP
National Aeronautics and Space Administration
Washington, D.C. 20546

ELIGIBILITY AND REGISTRATION FOR NASA INFORMATION PRODUCTS AND SERVICES

A variety of services is available to organizations of the following types that have registered with NASA to receive specific services or products:

1. NASA offices, research centers, contractors, subcontractors, grantees, and consultants;
2. Other U.S. Government agencies and their contractors;
3. Libraries in the United States that have arrangements with NASA to maintain collections of NASA documents for public reference;
4. Other organizations in the United States having a need for NASA documents in work related to aeronautics and space research;
5. Organizations abroad that have established reciprocal document exchange arrangements with NASA.

Only the central service points or central points of document acquisition and control within qualified organizations are eligible to register for NASA products and services. Domestic organizations that may be eligible to receive various classes of NASA publications and services should address their requests for registration or for further information to:

NASA Scientific and Technical Information Facility
ATTN: Registration Services
Post Office Box 8757
BWI Airport, Maryland 21240

Organizations abroad should direct requests to Manager, International STI Activities, NTT, NASA Headquarters, Washington, D.C. 20546.

AVAILABILITY OF *STAR* ABSTRACTS ON MICROFICHE

Microfiche of the abstract sections of this issue and other issues of *STAR* are available on annual subscription from NTIS as PB89-911300, Attn: Subscriptions, 5285 Port Royal Road, Springfield, Virginia 22161. Annual subscription rates are $70.00 North America; $140.00 foreign. Abstract sections for previous years retroactive to 1964 are available at the current rates. Microfiche for individual *STAR* issue abstract sections are not available.

PUBLIC COLLECTIONS OF NASA DOCUMENTS

DOMESTIC: NASA and NASA-sponsored documents and a large number of aerospace publications are available to the public for reference purposes at the library maintained by the American Institute of Aeronautics and Astronautics, Technical Information Service, 555 West 57th Street, 12th Floor, New York, New York 10019

EUROPEAN: An extensive collection of NASA and NASA-sponsored publications is maintained by the British Library Lending Division, Boston Spa, Wetherby, Yorkshire, England for public access. The British Library Lending Division also has available many of the non-NASA publications cited in *STAR*. European requesters may purchase facsimile copy or microfiche of NASA and NASA-sponsored documents, those identified by both the symbols # and * from ESA - Information Retrieval Service European Space Agency, 8-10 rue Mario-Nikis, 75738 Paris CEDEX 15, France.

FEDERAL DEPOSITORY LIBRARY PROGRAM

In order to provide the general public with greater access to U.S. Government publications, Congress established the Federal Depository Library Program under the Government Printing Office (GPO), with 50 regional depositories responsible for permanent retention of material, inter-library loan, and reference services. At least one copy of nearly every NASA and NASA-sponsored publication, either in printed or microfiche format, is received and retained by the 50 regional depositories. A list of the regional GPO libraries, arranged alphabetically by state, appears on the inside back cover. These libraries are *not* sales outlets. A local library can contact a Regional Depository to help locate specific reports, or direct contact may be made by an individual.

ADDRESSES OF ORGANIZATIONS

American Institute of Aeronautics and Astronautics
Technical Information Service
555 West 57th Street, 12th Floor
New York, New York 10019

British Library Lending Division,
Boston Spa, Wetherby, Yorkshire,
England

Commissioner of Patents and Trademarks
U.S. Patent and Trademark Office
Washington, D.C. 20231

Department of Energy
Technical Information Center
P.O. Box 62
Oak Ridge, Tennessee 37830

ESA-Information Retrieval Service
ESRIN
Via Galileo Galilei
00044 Frascati (Rome) Italy

ESDU International
P.O. Box 1633
Manassas, Virginia 22110

ESDU International, Ltd.
251-259 Regent Street
London, W1R 7AD, England

Fachinformationszentrum Energie, Physik, Mathematik GMBH
7514 Eggenstein Leopoldshafen
Federal Republic of Germany

Her Majesty's Stationery Office
P.O. Box 569, S.E. 1
London, England

NASA Scientific and Technical Information Facility
P.O. Box 8757
B.W.I. Airport, Maryland 21240

National Aeronautics and Space Administration
Scientific and Technical Information Division (NTT)
Washington, D.C. 20546

National Technical Information Service
5285 Port Royal Road
Springfield, Virginia 22161

Pendragon House, Inc.
899 Broadway Avenue
Redwood City, California 94063

Superintendent of Documents
U.S. Government Printing Office
Washington, D.C. 20402

University Microfilms
A Xerox Company
300 North Zeeb Road
Ann Arbor, Michigan 48106

University Microfilms, Ltd.
Tylers Green
London, England

U.S. Geological Survey Library
National Center - MS 950
12201 Sunrise Valley Drive
Reston, Virginia 22092

U.S. Geological Survey Library
2255 North Gemini Drive
Flagstaff, Arizona 86001

U.S. Geological Survey
345 Middlefield Road
Menlo Park, California 94025

U.S. Geological Survey Library
Box 25046
Denver Federal Center, MS914
Denver, Colorado 80225

NTIS PRICE SCHEDULES

(Effective January 1, 1989)

Schedule A
STANDARD PRICE DOCUMENTS AND MICROFICHE

PRICE CODE	NORTH AMERICAN PRICE	FOREIGN PRICE
A01	$ 6.95	$13.90
A02	10.95	21.90
A03	13.95	27.90
A04-A05	15.95	31.90
A06-A09	21.95	43.90
A10-A13	28.95	57.90
A14-A17	36.95	73.90
A18-A21	42.95	85.90
A22-A25	49.95	99.90
A99	*	*
NO1	55.00	70.00
NO2	55.00	80.00

Schedule E
EXCEPTION PRICE DOCUMENTS AND MICROFICHE

PRICE CODE	NORTH AMERICAN PRICE	FOREIGN PRICE
E01	$ 9.00	18.00
E02	11.50	23.00
E03	13.00	26.00
E04	15.50	31.00
E05	17.50	35.00
E06	20.50	41.00
E07	23.00	46.00
E08	25.50	51.00
E09	28.00	56.00
E10	31.00	62.00
E11	33.50	67.00
E12	36.50	73.00
E13	39.00	78.00
E14	42.50	85.00
E15	46.00	92.00
E16	50.50	101.00
E17	54.50	109.00
E18	59.00	118.00
E19	65.50	131.00
E20	76.00	152.00
E99	*	*

*Contact NTIS for price quote.

IMPORTANT NOTICE

NTIS Shipping and Handling Charges

U.S., Canada, Mexico — ADD $3.00 per TOTAL ORDER

All Other Countries — ADD $4.00 per TOTAL ORDER

Exceptions — Does NOT apply to:

ORDERS REQUESTING NTIS RUSH HANDLING

ORDERS FOR SUBSCRIPTION OR STANDING ORDER PRODUCTS *ONLY*

NOTE: Each additional delivery address on an order requires a separate shipping and handling charge.

VOLUME 27 NUMBER 16 / AUGUST 23, 1989

TABLE OF CONTENTS

AERONAUTICS

Includes aeronautics (general); aerodynamics; air transportation and safety; aircraft communications and navigation; aircraft design, testing and performance; aircraft instrumentation; aircraft propulsion and power; aircraft stability and control; and research and support facilities (air).

For related information see also *Astronautics.*

01 AERONAUTICS (GENERAL) 2217

02 AERODYNAMICS 2217

Includes aerodynamics of bodies, combinations, wings, rotors, and control surfaces; and internal flow in ducts and turbomachinery.

For related information see also *34 Fluid Mechanics and Heat Transfer*

03 AIR TRANSPORTATION AND SAFETY 2221

Includes passenger and cargo air transport operations; and aircraft accidents.

For related information see also *16 Space Transportation* and *85 Urban Technology and Transportation.*

04 AIRCRAFT COMMUNICATIONS AND NAVIGATION 2221

Includes digital and voice communication with aircraft; air navigation systems (satellite and ground based); and air traffic control.

For related information see also *17 Space Communications, Spacecraft Communications, Command and Tracking* and *32 Communications and Radar.*

05 AIRCRAFT DESIGN, TESTING AND PERFORMANCE 2222

Includes aircraft simulation technology.

For related information see also *18 Spacecraft Design, Testing and Performance* and *39 Structural Mechanics.* For land transportation vehicles see *85 Urban Technology and Transportation.*

06 AIRCRAFT INSTRUMENTATION 2223

Includes cockpit and cabin display devices; and flight instruments.

For related information see also *19 Spacecraft Instrumentation* and *35 Instrumentation and Photography.*

07 AIRCRAFT PROPULSION AND POWER 2223

Includes prime propulsion systems and systems components, e.g., gas turbine engines and compressors; and onboard auxiliary power plants for aircraft.

For related information see also *20 Spacecraft Propulsion and Power, 28 Propellants and Fuels,* and *44 Energy Production and Conversion.*

08 AIRCRAFT STABILITY AND CONTROL 2224

Includes aircraft handling qualities; piloting; flight controls; and autopilots.

For related information see also *05 Aircraft Design, Testing and Performance.*

09 RESEARCH AND SUPPORT FACILITIES (AIR) 2225

Includes airports, hangars and runways; aircraft repair and overhaul facilities; wind tunnels; shock tubes; and aircraft engine test stands.

For related information see also *14 Ground Support Systems and Facilities (Space).*

ASTRONAUTICS

Includes astronautics (general); astrodynamics; ground support systems and facilities (space); launch vehicles and space vehicles; space transportation; space communications, spacecraft communications, command and tracking; spacecraft design, testing and performance; spacecraft instrumentation; and spacecraft propulsion and power.

For related information see also *Aeronautics*

12 ASTRONAUTICS (GENERAL) 2227

For extraterrestrial exploration see *91 Lunar and Planetary Exploration.*

13 ASTRODYNAMICS 2228

Includes powered and free-flight trajectories; and orbital and launching dynamics.

14 GROUND SUPPORT SYSTEMS AND FACILITIES (SPACE) 2228

Includes launch complexes, research and production facilities; ground support equipment, e.g., mobile transporters; and simulators.

For related information see also *09 Research and Support Facilities (Air).*

15 LAUNCH VEHICLES AND SPACE VEHICLES 2229

Includes boosters; operating problems of launch/space vehicle systems; and reusable vehicles.

For related information see also *20 Spacecraft Propulsion and Power.*

16 SPACE TRANSPORTATION N.A.

Includes passenger and cargo space transportation, e.g., shuttle operations; and space rescue techniques.

For related information see also *03 Air Transportation and Safety* and *18 Spacecraft Design, Testing and Performance.* For space suits see *54 Man/System Technology and Life Support.*

17 SPACE COMMUNICATIONS, SPACECRAFT COMMUNICATIONS, COMMAND AND TRACKING N.A.

Includes telemetry; space communications networks; astronavigation and guidance; and radio blackout.

For related information see also *04 Aircraft Communications and Navigation* and *32 Communications and Radar.*

18 SPACECRAFT DESIGN, TESTING AND PERFORMANCE 2229

Includes satellites; space platforms; space stations; spacecraft systems and components such as thermal and environmental controls; and attitude controls.

For life support systems see *54 Man/System Technology and Life Support.* For related information see also *05 Aircraft Design, Testing and Performance, 39 Structural Mechanics,* and *16 Space Transportation.*

19 SPACECRAFT INSTRUMENTATION N.A.

For related information see also *06 Aircraft Instrumentation* and *35 Instrumentation and Photography.*

20 SPACECRAFT PROPULSION AND POWER 2231

Includes main propulsion systems and components, e.g. rocket engines; and spacecraft auxiliary power sources.

For related information see also *07 Aircraft Propulsion and Power, 28 Propellants and Fuels, 44 Energy Production and Conversion,* and *15 Launch Vehicles and Space Vehicles.*

CHEMISTRY AND MATERIALS

Includes chemistry and materials (general); composite materials; inorganic and physical chemistry; metallic materials; nonmetallic materials; propellants and fuels; and materials processing.

23 CHEMISTRY AND MATERIALS (GENERAL) 2232

24 COMPOSITE MATERIALS 2237

Includes physical, chemical, and mechanical properties of laminates and other composite materials.

For ceramic materials see *27 Nonmetallic Materials.*

25 INORGANIC AND PHYSICAL CHEMISTRY 2241

Includes chemical analysis, e.g., chromatography; combustion theory; electrochemistry; and photochemistry.

For related information see also *77 Thermodynamics and Statistical Physics.*

26 METALLIC MATERIALS 2243

Includes physical, chemical, and mechanical properties of metals, e.g., corrosion; and metallurgy.

27 NONMETALLIC MATERIALS 2248

Includes physical, chemical, and mechanical properties of plastics, elastomers, lubricants, polymers, textiles, adhesives, and ceramic materials.

For composite materials see *24 Composite Materials.*

28 PROPELLANTS AND FUELS 2252

Includes rocket propellants, igniters and oxidizers; their storage and handling procedures; and aircraft fuels.

For related information see also *07 Aircraft Propulsion and Power, 20 Spacecraft Propulsion and Power,* and *44 Energy Production and Conversion.*

29 MATERIALS PROCESSING 2252

Includes space-based development of products and processes for commercial application.

For biological materials see *55 Space Biology.*

ENGINEERING

Includes engineering (general); communications and radar; electronics and electrical engineering; fluid mechanics and heat transfer; instrumentation and photography; lasers and masers; mechanical engineering; quality assurance and reliability; and structural mechanics.

For related information see also *Physics.*

31 ENGINEERING (GENERAL) 2253

Includes vacuum technology; control engineering; display engineering; cryogenics; and fire prevention.

32 COMMUNICATIONS AND RADAR 2253

Includes radar; land and global communications; communications theory; and optical communications.

For related information see also *04 Aircraft Communications and Navigation* and *17 Space Communications, Spacecraft Communications, Command and Tracking.* For search and rescue see *03 Air Transportation and Safety,* and *16 Space Transportation.*

33 ELECTRONICS AND ELECTRICAL ENGINEERING 2258

Includes test equipment and maintainability; components, e.g., tunnel diodes and transistors; microminiaturization; and integrated circuitry.

For related information see also *60 Computer Operations and Hardware* and *76 Solid-State Physics.*

34 FLUID MECHANICS AND HEAT TRANSFER 2260

Includes boundary layers; hydrodynamics; fluidics; mass transfer and ablation cooling.

For related information see also *02 Aerodynamics* and *77 Thermodynamics and Statistical Physics.*

35 INSTRUMENTATION AND PHOTOGRAPHY 2268

Includes remote sensors; measuring instruments and gages; detectors; cameras and photographic supplies; and holography.

For aerial photography see *43 Earth Resources and Remote Sensing.* For related information see also *06 Aircraft Instrumentation* and *19 Spacecraft Instrumentation.*

36 LASERS AND MASERS 2270

Includes parametric amplifiers.

For related information see also *76 Solid-State Physics.*

37 MECHANICAL ENGINEERING 2272

Includes auxiliary systems (nonpower); machine elements and processes; and mechanical equipment.

38 QUALITY ASSURANCE AND RELIABILITY 2279

Includes product sampling procedures and techniques; and quality control.

39 STRUCTURAL MECHANICS 2280

Includes structural element design and weight analysis; fatigue; and thermal stress.

For applications see *05 Aircraft Design, Testing and Performance* and *18 Spacecraft Design, Testing and Performance.*

GEOSCIENCES

Includes geosciences (general); earth resources and remote sensing; energy production and conversion; environment pollution; geophysics; meteorology and climatology; and oceanography.

For related information see also *Space Sciences.*

42 GEOSCIENCES (GENERAL) **2285**

43 EARTH RESOURCES AND REMOTE SENSING **2285**

Includes remote sensing of earth resources by aircraft and spacecraft; photogrammetry; and aerial photography.

For instrumentation see *35 Instrumentation and Photography.*

44 ENERGY PRODUCTION AND CONVERSION **2287**

Includes specific energy conversion systems, e.g., fuel cells; global sources of energy; geophysical conversion; and windpower.

For related information see also *07 Aircraft Propulsion and Power, 20 Spacecraft Propulsion and Power,* and *28 Propellants and Fuels.*

45 ENVIRONMENT POLLUTION **2297**

Includes atmospheric, noise, thermal, and water pollution.

46 GEOPHYSICS **2298**

Includes aeronomy; upper and lower atmosphere studies; ionospheric and magnetospheric physics; and geomagnetism.

For space radiation see *93 Space Radiation.*

47 METEOROLOGY AND CLIMATOLOGY **2301**

Includes weather forecasting and modification.

48 OCEANOGRAPHY **2303**

Includes biological, dynamic, and physical oceanography; and marine resources.

For related information see also *43 Earth Resources and Remote Sensing.*

LIFE SCIENCES

Includes life sciences (general); aerospace medicine; behavioral sciences; man/system technology and life support; and space biology.

51 LIFE SCIENCES (GENERAL) **2303**

52 AEROSPACE MEDICINE **2304**

Includes physiological factors; biological effects of radiation; and effects of weightlessness on man and animals.

53 BEHAVIORAL SCIENCES **N.A.**

Includes psychological factors; individual and group behavior; crew training and evaluation; and psychiatric research.

54 MAN/SYSTEM TECHNOLOGY AND LIFE SUPPORT **2305**

Includes human engineering; biotechnology; and space suits and protective clothing.

For related information see also *16 Space Transportation.*

55 SPACE BIOLOGY **N.A.**

Includes exobiology; planetary biology; and extraterrestrial life.

MATHEMATICAL AND COMPUTER SCIENCES

Includes mathematical and computer sciences (general); computer operations and hardware; computer programming and software; computer systems; cybernetics; numerical analysis; statistics and probability; systems analysis; and theoretical mathematics.

59 MATHEMATICAL AND COMPUTER SCIENCES (GENERAL) **N.A.**

60 COMPUTER OPERATIONS AND HARDWARE **2306**

Includes hardware for computer graphics, firmware, and data processing.

For components see *33 Electronics and Electrical Engineering.*

61 COMPUTER PROGRAMMING AND SOFTWARE **2306**

Includes computer programs, routines, algorithms, and specific applications, e.g., CAD/CAM.

62 COMPUTER SYSTEMS **2329**

Includes computer networks and special application computer systems.

63 CYBERNETICS **2330**

Includes feedback and control theory, artificial intelligence, robotics and expert systems.

For related information see also *54 Man/System Technology and Life Support.*

64 NUMERICAL ANALYSIS **2333**

Includes iteration, difference equations, and numerical approximation.

65 STATISTICS AND PROBABILITY **2338**

Includes data sampling and smoothing; Monte Carlo method; and stochastic processes.

66 SYSTEMS ANALYSIS **2339**

Includes mathematical modeling; network analysis; and operations research.

67 THEORETICAL MATHEMATICS **2339**

Includes topology and number theory.

PHYSICS

Includes physics (general); acoustics; atomic and molecular physics; nuclear and high-energy physics; optics; plasma physics; solid-state physics; and thermodynamics and statistical physics.

For related information see also *Engineering.*

70 PHYSICS (GENERAL) **2339**

For precision time and time interval (PTTI) see *35 Instrumentation and Photography;* for geophysics, astrophysics or solar physics see *46 Geophysics, 90 Astrophysics,* or *92 Solar Physics.*

71 ACOUSTICS 2340
Includes sound generation, transmission, and attenuation.
For noise pollution see *45 Environment Pollution.*

72 ATOMIC AND MOLECULAR PHYSICS 2340
Includes atomic structure, electron properties, and molecular spectra.

73 NUCLEAR AND HIGH-ENERGY PHYSICS 2341
Includes elementary and nuclear particles; and reactor theory.
For space radiation see *93 Space Radiation.*

74 OPTICS 2342
Includes light phenomena and optical devices.
For lasers see *36 Lasers and Masers.*

75 PLASMA PHYSICS 2343
Includes magnetohydrodynamics and plasma fusion.
For ionospheric plasmas see *46 Geophysics.* For space plasmas see *90 Astrophysics.*

76 SOLID-STATE PHYSICS 2345
Includes superconductivity.
For related information see also *33 Electronics and Electrical Engineering* and *36 Lasers and Masers.*

77 THERMODYNAMICS AND STATISTICAL PHYSICS 2352
Includes quantum mechanics; theoretical physics; and Bose and Fermi statistics.
For related information see also *25 Inorganic and Physical Chemistry* and *34 Fluid Mechanics and Heat Transfer.*

SOCIAL SCIENCES

Includes social sciences (general); administration and management; documentation and information science; economics and cost analysis; law, political science, and space policy; and urban technology and transportation.

80 SOCIAL SCIENCES (GENERAL) N.A.
Includes educational matters.

81 ADMINISTRATION AND MANAGEMENT 2354
Includes management planning and research.

82 DOCUMENTATION AND INFORMATION SCIENCE 2354
Includes information management; information storage and retrieval technology; technical writing; graphic arts; and micrography.
For computer documentation see *61 Computer Programming and Software.*

83 ECONOMICS AND COST ANALYSIS N.A.
Includes cost effectiveness studies.

84 LAW, POLITICAL SCIENCE AND SPACE POLICY 2357
Includes NASA appropriation hearings; aviation law; space law and policy; international law; international cooperation; and patent policy.

85 URBAN TECHNOLOGY AND TRANSPORTATION 2357
Includes applications of space technology to urban problems; technology transfer; technology assessment; and surface and mass transportation.
For related information see *03 Air Transportation and Safety, 16 Space Transportation,* and *44 Energy Production and Conversion.*

SPACE SCIENCES

Includes space sciences (general); astronomy; astrophysics; lunar and planetary exploration; solar physics; and space radiation.
For related information see also *Geosciences.*

88 SPACE SCIENCES (GENERAL) N.A.

89 ASTRONOMY 2358
Includes radio, gamma-ray, and infrared astronomy; and astrometry.

90 ASTROPHYSICS 2359
Includes cosmology; celestial mechanics; space plasmas; and interstellar and interplanetary gases and dust.
For related information see also *75 Plasma Physics.*

91 LUNAR AND PLANETARY EXPLORATION 2361
Includes planetology; and manned and unmanned flights.
For spacecraft design or space stations see *18 Spacecraft Design, Testing and Performance.*

92 SOLAR PHYSICS 2361
Includes solar activity, solar flares, solar radiation and sunspots.
For related information see *93 Space Radiation.*

93 SPACE RADIATION 2361
Includes cosmic radiation; and inner and outer earth's radiation belts.
For biological effects of radiation see *52 Aerospace Medicine.* For theory see *73 Nuclear and High-Energy Physics.*

GENERAL

Includes aeronautical, astronautical, and space science related histories, biographies, and pertinent reports too broad for categorization; histories or broad overviews of NASA programs.

99 GENERAL 2362

Note: N.A. means that no abstracts were assigned to this category for this issue.

SUBJECT INDEX I-1
PERSONAL AUTHOR INDEX I-51
CORPORATE SOURCE INDEX I-59
CONTRACT NUMBER INDEX I-71
REPORT/ACCESSION NUMBER INDEX I-75

TYPICAL CITATION AND ABSTRACT

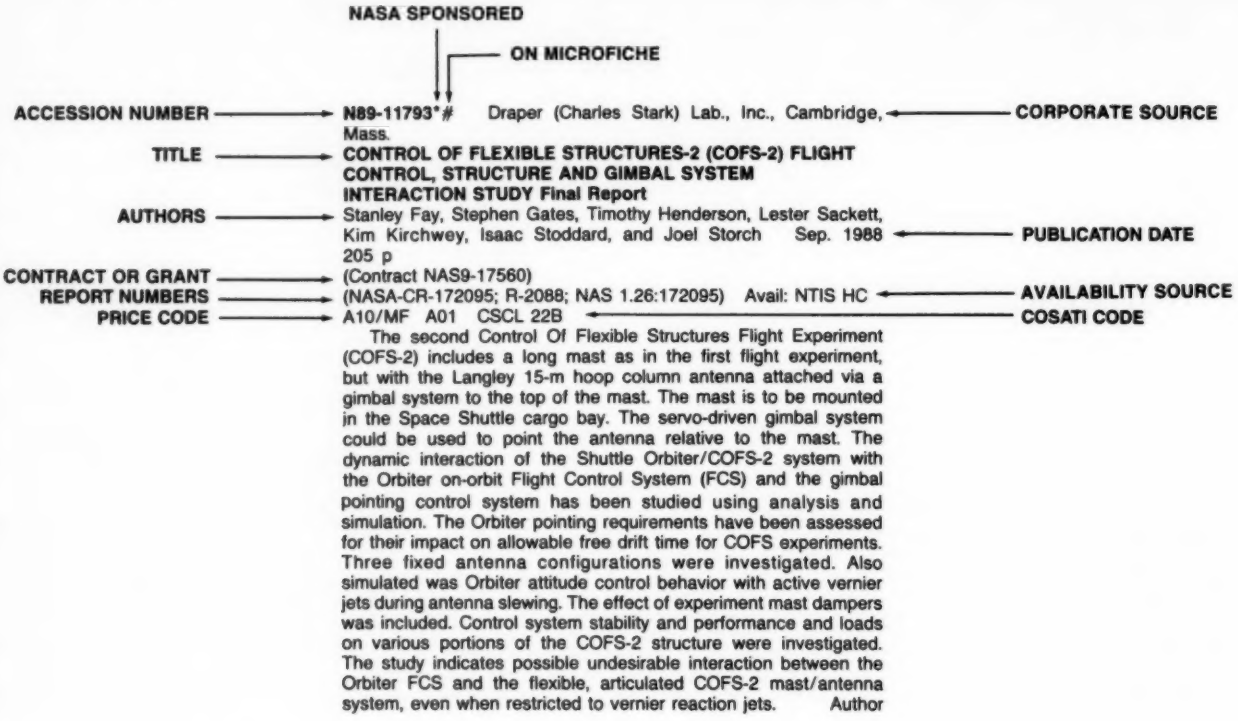
NASA SPONSORED
ON MICROFICHE
ACCESSION NUMBER
N89-11793*# Draper (Charles Stark) Lab., Inc., Cambridge, Mass.
CORPORATE SOURCE
TITLE
CONTROL OF FLEXIBLE STRUCTURES-2 (COFS-2) FLIGHT CONTROL, STRUCTURE AND GIMBAL SYSTEM INTERACTION STUDY Final Report
AUTHORS
Stanley Fay, Stephen Gates, Timothy Henderson, Lester Sackett, Kim Kirchwey, Isaac Stoddard, and Joel Storch Sep. 1988
PUBLICATION DATE
205 p
CONTRACT OR GRANT
(Contract NAS9-17560)
REPORT NUMBERS
(NASA-CR-172095; R-2088; NAS 1.26:172095) Avail: NTIS HC
AVAILABILITY SOURCE
PRICE CODE
A10/MF A01 CSCL 22B
COSATI CODE
The second Control Of Flexible Structures Flight Experiment (COFS-2) includes a long mast as in the first flight experiment, but with the Langley 15-m hoop column antenna attached via a gimbal system to the top of the mast. The mast is to be mounted in the Space Shuttle cargo bay. The servo-driven gimbal system could be used to point the antenna relative to the mast. The dynamic interaction of the Shuttle Orbiter/COFS-2 system with the Orbiter on-orbit Flight Control System (FCS) and the gimbal pointing control system has been studied using analysis and simulation. The Orbiter pointing requirements have been assessed for their impact on allowable free drift time for COFS experiments. Three fixed antenna configurations were investigated. Also simulated was Orbiter attitude control behavior with active vernier jets during antenna slewing. The effect of experiment mast dampers was included. Control system stability and performance and loads on various portions of the COFS-2 structure were investigated. The study indicates possible undesirable interaction between the Orbiter FCS and the flexible, articulated COFS-2 mast/antenna system, even when restricted to vernier reaction jets. Author

VOLUME 27 NUMBER 16 / AUGUST 23, 1989

Scientific and Technical Aerospace Reports

A Semimonthly Publication of the National Aeronautics and Space Administration

01 AERONAUTICS (GENERAL)

N89-22568*# National Aeronautics and Space Administration. Langley Research Center, Hampton, VA.
EVALUATION OF THE RIDE QUALITY OF A LIGHT TWIN ENGINE AIRPLANE USING A RIDE QUALITY METER
Eric C. Stewart Jun. 1989 27 p
(NASA-TP-2913; L-16524; NAS 1.60:2913) Avail: NTIS HC A03/MF A01 CSCL 01B

A ride quality meter was used to establish the baseline ride quality of a light twin-engine airplane planned for use as a test bed for an experimental gust alleviation system. The ride quality meter provides estimates of passenger ride discomfort as a function of cabin noise and vibration (acceleration) in five axes (yaw axis omitted). According to the ride quality meter, in smooth air the cabin noise was the dominant source of passenger discomfort, but the total discomfort was approximately the same as that for the smooth-air condition. The researcher's subjective opinion, however, is that the total ride discomfort was much worse in the moderate turbulence than it was in the smooth air. The discrepancy is explained by the lack of measurement of the low-frequency accelerations by the ride quality meter. Author

N89-22569*# National Aeronautics and Space Administration. Lewis Research Center, Cleveland, OH.
NASA's PROGRAM ON ICING RESEARCH AND TECHNOLOGY
John J. Reinmann, Robert J. Shaw, and Richard J. Ranaudo 1989 55 p Presented at the Symposium on Flight in Adverse Environmental Conditions, Gol, Norway, 8-12 May 1989; sponsored by AGARD
(NASA-TM-101989; E-4692; NAS 1.15:101989) Avail: NTIS HC A04/MF A01 CSCL 01B

NASA's program in aircraft icing research and technology is reviewed. The program relies heavily on computer codes and modern applied physics technology in seeking icing solutions on a finer scale than those offered in earlier programs. Three major goals of this program are to offer new approaches to ice protection, to improve our ability to model the response of an aircraft to an icing encounter, and to provide improved techniques and facilities for ground and flight testing. This paper reviews the following program elements: (1) new approaches to ice protection; (2) numerical codes for deicer analysis; (3) measurement and prediction of ice accretion and its effect on aircraft and aircraft components; (4) special wind tunnel test techniques for rotorcraft icing; (5) improvements of icing wind tunnels and research aircraft; (6) ground de-icing fluids used in winter operation; (7) fundamental studies in icing; and (8) droplet sizing instruments for icing clouds. Author

N89-22570# Air Force Systems Command, Wright-Patterson AFB, OH. Foreign Technology Div.
ACTA AERONAUTICA ET ASTRONAUTICA SINICA (SELECTED ARTICLES)
7 Feb. 1989 41 p Transl. into ENGLISH from Hong Kong Xueboa (Peoples Republic of China), v. 8, no. 12, Dec. 1987 p B578-B584, B594-B600
(AD-A205128; FTD-ID(RS)T-0912-88) Avail: NTIS HC A03/MF A01 CSCL 01B

The formula of requisite linear damping for overcoming landing-gear shimmy according to the point-contact theory is derived. However, the damping property of the hydraulis shimmy damper is mostly nonlinear. Two methods are presented to treat this case; the tangent method and the minimum equivalent linear damping method. Their correlation is also found. It is demonstrated by computation that both methods are effective and reliable. The requirements for measuring ground load on an aircraft is discussed. A practical data treatment method has been developed for the case that the measurement satisfy the minimum requirement. Although the method is illustrated with taxiing data, however, it is also applicable to the treatment of turning and braking load data. Author

02 AERODYNAMICS

Includes aerodynamics of bodies, combinations, wings, rotors, and control surfaces; and internal flow in ducts and turbomachinery.

For related information see also *34 Fluid Mechanics and Heat Transfer.*

N89-22571# Jiaotong Univ., Shanghai (China).
UNSTEADY AERODYNAMIC COMPUTATIONAL METHOD OF NON-COPLANAR WING-TAIL COMBINATIONS IN SUBSONIC FLOW
Jiguang An, Wenbo Zhou, Ming Yan, Kangyan Chen, Xianchai Sun, Zhen Yan, and Chuanren Qiu (Shanghai Aircraft Co., China) 1987 12 p Sponsored by Institute of Scientific and Technical Information of China, Beijing
(PB89-111470; ISTIC-TR-C-000196) Avail: NTIS HC A03/MF A01 CSCL 01A

An unsteady aerodynamic computational method is presented for 3-D non-coplanar wing-tail combination (namely, an airplane with horizontal tail plane located higher or lower than wing) at subsonic speed. The velocity potential function of unsteady vortex ring is chosen as an elementary solution of governing equation of flow field. The whole computational method follows strictly the physical mechanism of unsteady aerodynamic phenomenon, so it can be widely used in predicting those unsteady aerodynamic data needed in aircraft design and performance evaluation. Author

N89-22572 Stanford Univ., CA.
A NUMERICAL STUDY OF VISCOUS VORTEX RINGS USING A SPECTRAL METHOD Ph.D. Thesis
Sharon Kay Stanaway 1988 199 p
Avail: Univ. Microfilms Order No. DA8826238

Viscous, axisymmetric vortex rings are investigated numerically by solving the incompressible Navier-Stokes equations using a spectral method designed for this type of flow. The results presented are axisymmetric, but the method is developed to be naturally extended to three dimensions. The spectral method relies on divergence-free basis functions. The basis functions are formed in spherical coordinates using Vector Spherical Harmonics in the angular directions, and Jacobi polynomials together with a mapping in the radial direction. Simulations are performed of a single ring over a wide range of Reynolds numbers (Re is identical with gamma nu), 0.001 is less than or equal to Re is less than or equal to 1000, and of two interacting rings. At large times, regardless of

the early history of the vortex ring, it is observed that the flow approaches a Stokes solution that depends only on the total hydrodynamic impulse, which is conserved for all time. At small times, from an infinitely thin ring, the propagation speeds of vortex rings of varying Re are computed and comparisons are made with the asymptotic theory by Saffman. The results are in agreement with the theory; furthermore, the error is found to be smaller than Saffman's own estimate by a factor of the square root of (nu t/r squared) (at least for Re=0). The error also decreases with increasing Re at fixed core-to-ring radius ratio, and appears to be independent of Re as Re approaches infinity. Following a single ring, with Re = 500, the vorticity contours indicate shedding of vorticity into the wake and a settling of an initially circular core to a more elliptical shape, similar to Norbury's steady inviscid vortices. Finally, the case of leapfrogging vortex rings with Re = 1000 is considered. The results show severe straining of the inner vortex core in the first pass and merging of the two cores during the second pass. Dissert. Abstr.

N89-22573*# National Aeronautics and Space Administration. Lewis Research Center, Cleveland, OH.

SECOND-ORDER ACCURATE NONOSCILLATORY SCHEMES FOR SCALAR CONSERVATION LAWS

Hung T. Huynh 1989 16 p Proposed for presentation at the 6th International Conference on Numerical Methods in Laminar and Turbulent Flow, Swansea, England, 11-15 Jul. 1989; cosponsored by the Univ. Coll. of Swansea, ONR Branch Office London, Journal for Numerical Methods in

(NASA-TM-102010; E-4721; NAS 1.15:102010) Avail: NTIS HC A03/MF A01 CSCL 01A

Explicit finite difference schemes for the computation of weak solutions of nonlinear scalar conservation laws is presented and analyzed. These schemes are uniformly second-order accurate and nonoscillatory in the sense that the number of extrema of the discrete solution is not increasing in time. Author

N89-22574*# Institute for Computer Applications in Science and Engineering, Hampton, VA.

THE INVISCID AXISYMMETRIC STABILITY OF THE SUPERSONIC FLOW ALONG A CIRCULAR CYLINDER Final Report

Peter W. Duck (Manchester Univ., England) Feb. 1989 74 p

(Contracts NAS1-18605; NAS1-18107)

(NASA-CR-181816; NAS 1.26:181816; ICASE-89-19) Avail: NTIS HC A04/MF A01 CSCL 01A

The supersonic flow past a thin straight circular cylinder is investigated. The associated boundary layer flow (i.e., the velocity and temperature field) is computed; the asymptotic, far downstream solution is obtained, and compared with the full numerical results. The inviscid, linear, axisymmetric (temporal) stability of this boundary layer is also studied. A so called doubly generalized inflexion condition is derived, which is a condition for the existence of so called subsonic neutral modes. The eigenvalue problem (for the complex wavespeed) is computed for two freestream Mach numbers (2.8 and 3.8), and this reveals that curvature has a profound effect on the stability of the flow. The first unstable inviscid mode is seen to rapidly disappear as curvature is introduced, while the second (and generally the most important) mode suffers a substantially reduced amplification rate. Author

N89-22575# National Aeronautical Establishment, Ottawa (Ontario).

COMPARISON OF BOUNDARY LAYER TRIPS OF DISK AND GRIT TYPES ON AIRFOIL PERFORMANCE AT TRANSONIC SPEEDS

Y. Y. Chan Dec. 1988 40 p

(AD-A205206; NAE-AN-56; NRC-29908) Avail: NTIS HC A03/MF A01 CSCL 21A

The effects on aerodynamic performance of a supercritical airfoil applying disk or grit tripping for boundary layer transition has been investigated for a typical supercritical airfoil at transonic speeds. It is observed that by allowing the laminar flow passing through the space between the disks, transition takes place a short distance downstream from the disk trip line. The boundary layer developed downstream from disk trip is therefore slightly thinner than that from a grit trip. The vortex generating mechanism of the disks may also enhance this development. This small difference has negligible effect on aerodynamics of the airfoil at low lift. However, at high lift, the difference in boundary layer developments is amplified by the strong shock wave and the severe adverse pressure gradient. The thinner and more energetic boundary layer induced by the disk trip will yield higher lift, lower drag and higher trailing edge pressure. GRA

N89-22576# Sandia National Labs., Albuquerque, NM. Parachute Systems Div.

A PRELIMINARY CHARACTERIZATION OF PARACHUTE WAKE RECONTACT

James H. Strickland and J. Michael Macha 1989 8 p Presented at the 10th AIAA Aerodynamic Decelerator Systems Technical Conference, Cocoa Beach, FL, 18 Apr. 1989

(Contract DE-AC04-76DP-00789)

(DE89-006442; SAND-88-3058C; CONF-8904118-3) Avail: NTIS HC A02

A series of tests was conducted on a 10 ft diameter ringslot parachute with a geometric porosity of 20 percent to establish the conditions under which wake recontact occurs. The vertical helicopter drop tests covered a range of mass ratios from 0.5 to 3.0 and a range of Froude numbers from 70 to 400. Data consisted of velocity time histories obtained using a laser tracker and diameter time histories obtained from photometric data. A collapse parameter based on the ratio of the maximum parachute diameter to the subsequent minimum diameter was correlated with the mass ratio M sub R and the Froude number Fr or equivalently with the initial to final velocity ratio V sub o/V sub t. For large values of V sub o/V sub t the collapse parameter R sub c appears to be a function of M sub R alone. Non-dimensional opening time and collapse time data were also correlated with M sub R and V sub o/V sub t. DOE

N89-22577*# National Aeronautics and Space Administration. Lewis Research Center, Cleveland, OH.

RECTANGULAR NOZZLE PLUME VELOCITY MODELING FOR USE IN JET NOISE PREDICTION

U. H. vonGlahn 1989 36 p Presented at the 25th Joint Propulsion Conference, Monterey, CA, 10-12 Jul. 1989; sponsored by AIAA, ASME, SAE and ASEE

(NASA-TM-102047; E-4739; NAS 1.15:102047; AIAA-89-2357)

Avail: NTIS HC A03/MF A01 CSCL 01A

A modeling technique for predicting the axial and transverse velocity characteristics of rectangular nozzle plumes is developed. In this technique, modeling of the plume cross section is initiated at the nozzle exit plane. The technique is demonstrated for the plume issuing from a rectangular nozzle having an aspect ratio of 6.0 and discharging into quiescent air. Application of the present procedures to a nozzle discharging into a moving airstream (flight effect) are then demonstrated. The effects of plume shear layer structure modification on the velocity flowfield are discussed and modeling procedures are illustrated by example. Author

N89-22578# Aeronautical Research Inst. of Sweden, Stockholm. Aerodynamics Dept.

COMPRESSIBLE EULER SOLUTION AROUND A WING CANARD STING CONFIGURATION

Torsten Berglind 12 Feb. 1988 33 p

(Contract FMV-FlygFl-82260-88-061-73-001)

(FFA-TN-1988-62; ETN-89-94316) Avail: NTIS HC A03/MF A01

A patched multiblock grid around a 65 deg canard attached to a sting is constructed by transfinite interpolation. The wing-sting is enveloped by a C-O type grid with a polar singularity at the apex. The grid emanates from the wing-sting surface via axisymmetric surfaces, the first contiguous to the trailing edge of the canard, the second contiguous to the leading edge of the canard, and finally the farfield boundary. The grid contains 310,000 grid points. A multiblock Euler solver with a high degree of

vectorization (MESCI) was used for the flow computations. The canard is treated as a slit, whereby the grid has to be divided into two blocks, since MESCI does not allow slits in the interior domain. Each time step requires 7.6 CPU seconds on a CYBER-205. The flow field is computed at 10 and 20 deg angle of attack at a free stream Mach number of 0.85. The transonic flow cases are both of high complexity, containing local shock waves and the interaction of the canard tip vortex and the delta wing vortex. The flow solver in conjunction with the grid system is able to capture the dominant flow phenomena such as the canard and delta wing vortices. The C sub p-distributions on the upper side of the wing agree reasonably well with measurements. ESA

N89-22579# Centre d'Etudes Aerodynamiques et Thermiques, Poitiers (France).

INTERACTION BETWEEN AN ISOLATED VORTEX AND A WING PROFILE Final Report [INTERACTION ENTRE UN TOURBILLON ISOLE ET UN PROFIL D'AILE]

Mar. 1988 67 p In FRENCH

(Contract DRET-85-092)

(ETN-89-94364) Avail: NTIS HC A04/MF A01

Wind tunnel measurements were carried out in a two-dimensional configuration. A reproducible vortex with an axis parallel to the profile is created by mechanical means in the subsonic wind tunnel. The measurements include the velocity fields with and without profile, the wall pressures, and the lift. Smoke flow visualization was also used. The viscous vortex structure is disintegrated when passing over the profile, and three-dimensional effects appear. The modification of the wall pressure field is most important near the leading edge. ESA

N89-22580# Deutsche Forschungs- und Versuchsanstalt fuer Luft- und Raumfahrt, Goettingen (Germany, F.R.). Abteiling Hochgeschwindigkeitsstroemungen.

TRANSONIC AND SUPERSONIC FLOW PAST A 65 DEG DELTA WING WITH ROUNDED LEADING EDGES: ANALYSIS OF EXPERIMENTAL DATA

Krishnaswami Yegna Narayan and Klaus Hartmann Sep. 1988 67 p

(DFVLR-FB-88-44; ISSN-0171-1342; ETN-89-94378) Avail: NTIS HC A04/MF A01; DFVLR, VB-PL-DO, Postfach 90 60 58, 5000 Cologne, Fed. Republic of Germany, DM 20.50

Data on a sweptback cropped delta wing with rounded leading edges over a Mach number range of 0.4 to 4, and from tests at Mach 0.85 over a Reynolds number range of 2.4 to 13 million (based on root chord) are discussed. It is shown that the first occurrence of leading edge separation can be determined from one of three (related) criteria: a sudden drop in the peak suction pressure on the leeside, a rapid inboard movement of the location of the suction peak, and a rapid inboard movement of the foot of the pressure rise following the suction peak. Fully attached flow, mixed flow and leading edge separated flow types are identified. Flow attachment at the rounded leading edge occurs at a lower Mach number compared to a wing with sharp leading edge. Leading edge separation on a wing with a drooped leading edge occurs at an angle of attack higher than in the undrooped case by an angle equal to the droop. An increase in Reynolds number causes leading edge separation to occur at higher angles of attack. ESA

N89-22581# Deutsche Forschungs- und Versuchsanstalt fuer Luft- und Raumfahrt, Goettingen (Germany, F.R.). Abteilung Instabilitaeten und Abloesung.

FLOW OVER A LEADING EDGE WITH DISTRIBUTED ROUGHNESS

Jerzy M. Floryan and Uwe Dallmann Sep. 1988 52 p

(DFVLR-FB-88-45; ISSN-0171-1342; ETN-89-94379) Avail: NTIS HC A04/MF A01; DFVLR, VB-PL-DO, Postfach 90 60 58, 5000 Cologne, Fed. Republic of Germany, DM 19

Flow over a leading edge with distributed roughness (assumed to have small amplitude, which permits linearization of the governing equations) was analyzed. Explicit solutions are obtained in the limits of large and small wave numbers. Results show that roughness can produce modifications of the flow far away from the solid surface, while modifications of the temperature field are confined to within the thermal boundary layer. Surface stresses tend to eliminate roughness if erosion or wall flexibility are admitted. It is noted that heat flow tends to concentrate at the tips of the roughness. ESA

N89-22582# Aeronautical Research Inst. of Sweden, Stockholm. Aerodynamics Dept.

WIND TUNNEL TESTS OF 16 PERCENT THICK AIRFOIL SECTION WITH SPOILERS AT DIFFERENT CHORDWISE POSITIONS

Anders Bjorck Dec. 1988 44 p Sponsored by the Swedish National Energy Administration

(FFA-TN-1987-39; ETN-89-94544) Avail: NTIS HC A03/MF A01

Wind tunnel tests were carried out at low speeds on a 16 percent thick, moderately cambered airfoil section equipped with spoilers at 7 different chordwise positions on the forward half part of the airfoil. Two spoiler positions were on the pressure side, two at the leading edge, and three on the suction side of the airfoil. The effect of spoiler height was examined. The spoiler height varied between 2.5 to 12.5 percent of the airfoil chord. The results indicate that a spoiler on the airfoil suction side positioned 5 percent of the chord from the leading edge is capable of eliminating the strong driving tangential force of the basic airfoil for the entire range of positive angles of attack tested. ESA

N89-22583# Aeronautical Research Inst. of Sweden, Stockholm. Aerodynamics Dept.

THE INFLUENCE OF THE LEADING EDGE GEOMETRY ON THE WAVE DRAG FOR A 65 DEGREE DELTA WING AT LOW SUPERSONIC SPEED AND SMALL ANGLES OF ATTACK

Torsten Berglind, Georg Drougge, and Peter Eliasson 25 Oct. 1988 15 p Sponsored by the Defence Material Administration of Sweden, Stockholm

(FFA-141; ISSN-0081-5640; ETN-89-94550) Avail: NTIS HC A03/MF A01; Almgvist and Wiksell Booksellers, Printers, Publishers, Stockholm, Sweden, 100 Finnish marks

High speed wind tunnel tests were performed to validate the Euler code WINGA2 at supersonic speeds. As test cases, three 65 deg wings (so-called Euler wings) were used at M=1.2. The influence of the body on the flow over the wing was computed with the Euler code MESCI. The agreement between computations and experiments is good. Wing design problems were considered. The results show that rather blunt leading edges, drooped or not, can result in good drag performance at low lift and moderate supersonic speeds. Such geometry could be beneficial for the subsonic maneuvering case. ESA

N89-22584# Centre d'Etudes et de Recherches, Toulouse (France). Dept. d'Etudes et de Recherches en Aerothermodynamique.

SIDEWALL BOUNDARY LAYER STUDY, WITH AND WITHOUT SUCTION, FOR THE 150 mm CHORD CAST 7 AIRFOIL AT THE T2 WIND TUNNEL

J. B. Dor, J. P. Archambaud, and J. F. Breil Dec. 1987 105 p In FRENCH

(Contract Phase-3075-AN-225-D)

Avail: NTIS HC A06/MF A01

Tests to investigate sidewall effects realized at the T2 transonic wind tunnel equipped with top and bottom adaptive walls are described. The model was the 150 mm chord CAST 7 airfoil tested with fixed transition at 0.5 deg angle of attack. The flow field was studied near the solid sidewall, above the downstream part of the model upper side and in the wake, at Mach number 0.705 and 0.755, utilizing directional boundary layer probing, static pressure measurements, and wall visualizations. Suction rate (q suction / q test section) of about 4/1000 was achieved on sidewalls, on the downstream part of the model upperside and around the trailing edge. The velocity distribution on the airfoil, the lift coefficient and the modifications of the sidewall boundary layers (measurements, visualizations) allowed the suction effect to be analyzed. Author

N89-22585 Georgia Inst. of Tech., Atlanta.
CONVERGENCE OF DISCRETE-VORTEX INDUCED-FLOW CALCULATIONS BY OPTIMUM CHOICE OF MESH Ph.D. Thesis
Yihwan Danny Chiu 1988 239 p
Avail: Univ. Microfilms Order No. DA8904804

A brief review of numerical solutions for the lifting thin-airfoil theories for both fixed-wing and rotary-wing problems is presented. Errors are noted in numerical calculations by conventional VORTEX LATTICE METHODS (VLM) for two-dimensional thin-airfoil, Lifting-Line, and Lifting-Surface theories. Emphasis is made on the optimum choice of mesh and collocation points for VLM to ensure that numerical results will converge and that this convergence will be as rapid as possible. The Fourier Series Method of Lifting-Line theory for fixed-wing problems is extended for rotary-wings problems. An efficient and accurate numerical technique is offered to calculate the induced velocities due to trailing vortices. Applications of these new findings are made in order to develop a simple tip-loss formula for lightly-loaded rotors with rectangular planforms. Dissert. Abstr.

N89-22586 Georgia Inst. of Tech., Atlanta.
AERODYNAMICS OF NONRIGID BODIES UNDERGOING LARGE AMPLITUDE TIME-DEPENDENT MOTIONS Ph.D. Thesis
Jatinder Singh 1988 191 p
Avail: Univ. Microfilms Order No. DA8904829

A simplified zonal approach is described to evaluate unsteady aerodynamic forces on nonrigid bodies undergoing large amplitude time-dependent motions or deformations. It analyzes unsteady flow in the limit of high Reynolds numbers. The kinematic aspect of the incompressible viscous flows in the form of an integral representation for the velocity vector is utilized to determine the surface vortex sheet strength representing the vorticity content of the boundary layers. Wake is modeled by the vortex filaments and knowing the surface vortex sheet strength and the strengths and locations of the wake vortices, a viscous theory of aerodynamics is then used to evaluate the resulting unsteady aerodynamic forces. The simplified zonal approach is cast into two alternate formulations, namely, the conformal transformation approach and the boundary element approach. The conformal transformation approach allows for the explicit evaluation of the unsteady aerodynamic forces, while the boundary element approach can solve flows about arbitrary bodies. Using the simplified zonal approach, a number of problems were solved for flows around rigid and nonrigid bodies undergoing a variety of prescribed motions. For the bodies undergoing high frequency oscillations or deformations, even for small amplitude motions, well formed vortex clusters dominate the near wake. The movement of these vortex clusters and the time-dependent changes in the strength of the vortex sheets gives rise to the unsteady aerodynamic forces. Results obtained for some problems are compared with the theoretical and experimental results of other researchers and good quantitative agreement is observed.
Dissert. Abstr.

N89-22587 Georgia Inst. of Tech., Atlanta.
A STUDY OF UNSTEADY TURBULENT FLOW PAST AIRFOILS Ph.D. Thesis
Jiunn-Chi Wu 1988 213 p
Avail: Univ. Microfilms Order No. DA8904832

When a helicopter is in forward flight, the aerodynamics of the rotor blade is very complex. The rotor blade may have transonic flow on the advancing side and may experience dynamic stall on the retreating side. In order to predict the characteristics of above complex flow, a solution procedure must be able to predict the large separated flow, unsteadiness, compressibility effects, and turbulence characteristics. For this purpose, an efficient solution procedure solving the two-dimensional and quasi three-dimensional, unsteady, compressible Navier-Stokes equations were developed and applied to rotor blade sections. Specifically, this work addresses the following areas: (1) reliable prediction of static airloads and dynamic stall hystersis loops for arbitrary airfoils; (2) investigation of yaw effects on the airload characteristics; (3) transonic and/or stall flutter characteristics; (4) evaluation of algebraic, one-equation and two-equation turbulence models for strongly separated flows. Numerical results show that good prediction of static loads and dynamic stall hystersis loops of rotor blade sections was feasible. Yaw effects on airloads were predicted to be less profound than observed in experiments. The present solution procedure was found to be capable of predicting transonic and stall flutter. In attached flows the three turbulence models considered gave good correlation with experimental data. For steady or unsteady separated flows, the three turbulence models only exhibit fair correlation with experimental data. No clear trend could be found favoring the use of higher order turbulence models in separated flows. Dissert. Abstr.

N89-22588 Purdue Univ., West Lafayette, IN.
AERODYNAMIC DETUNING OF A LOADED AIRFOIL CASCADE IN AN INCOMPRESSIBLE FLOW BY A LOCALLY ANALYTICAL METHOD Ph.D. Thesis
Hsiao-Wei David Chiang 1988 268 p
Avail: Univ. Microfilms Order No. DA8900647

A mathematical model is developed and utilized to demonstrate the enhanced aeroelastic stability and forced response behavior associated with aerodynamic detuning of a rotor operating in an incompressible flow field. The validity of the tuned cascade model and solution technique are demonstrated by considering the steady and unsteady aerodynamics of both theoretical and experimental cascade configurations. To verify the detuned cascade model and influence coefficient technique, predictions from this model are compared to the steady theoretical results and also the tuned cascade unsteady aerodynamic model predictions. The capabilities of this detuned cascade model are then demonstrated by predicting the flutter stability and forced response behavior of detuned rotor configurations. Nonuniform circumferential airfoil spacing and alternate blade structural detuning are both shown to enhance stability. The greatest stability enhancement resulted from a combination of aerodynamic and structural detuning. Also, the unstable baseline configuration can be stabilized by the introduction of splitter blades. For the forced response behavior, both the alternate circumferential spaced detuning and the alternate blade structural detuning can be beneficial on the response amplitude of the airfoils. By including aspect ratio effects, the alternate splitter blade detuning results in significantly reduced amplitudes of response for most cases considered. In conclusion, this detuning analysis has demonstrated that both the aeroelastic stability and forced responsive behavior can be greatly enhanced by aerodynamic detuning. Therefore, aerodynamic detuning appears to be a viable passive control mechanism for aeroelastic problems of an incompressible cascade. Dissert. Abstr.

N89-22589# Georgia Tech Research Inst., Atlanta.
SUPERSONIC PARTICLE PROBES: MEASUREMENT OF INTERNAL WALL LOSSES Final Report, 10 Jun. 1986 - 10 Jun. 1988
J. J. Ivie, L. J. Forney, and R. L. Roach Mar. 1989 106 p
(Contract F40600-86-K-0004)
(AD-A205863; AEDC-TR-88-37) Avail: NTIS HC A06/MF A01
CSCL 20D

The operating characteristics of supersonic particle probes were investigated. The characteristics such as internal wall deposition, pressure recovery, and ease of operation and construction were examined. Three basic probe designs were tested in a cold flow experiment designed to simulate the hot, hostile environment of rocket and jet engine plumes. The probe designs consisted of two internal shock probes (Dehne and Colket probes) and one external shock probe (McGregor probe). In the internal shock probes, the compression from supersonic to subsonic flow occurred either in a constant area throat (Dehne) or at a sudden expansion (Colket). In the external shock, or McGregor probe the shock was positioned slightly outside the entrance of the probe. From deposition studies performed on the probes, three factors were found to enhance deposition. These factors were: (1) shock-boundary layer interaction, (2)

particle-boundary layer interaction, and (3) stagnation zones at sudden expansions. The probe with the lowest deposition was a McGregor probe with a 2.0-deg divergence angle. Using test particles with diameters of 1.0, 1.5, 2.0, and 2.5 micron, the average losses in the McGregor probe were 14 percent, whereas in the Colket and Dehne probes, the losses were 18 and 22 percent, respectively. A correlation was developed to predict the deposition (E) in the McGregor probe using Willeke's dimensionless parameter (Omega): E = 1011 Omega + 1.55. GRA

N89-22590# Naval Postgraduate School, Monterey, CA.
COMPUTATIONAL INVESTIGATION OF INCOMPRESSIBLE AIRFOIL FLOWS AT HIGH ANGLES OF ATTACK M.S. Thesis
John M. Mathre Dec. 1988 158 p
(AD-A205885) Avail: NTIS HC A08/MF A01 CSCL 01A

Cebeci's viscous/inviscid interaction program was applied to the analysis of steady, two dimensional, incompressible flow past four airfoils, the NACA 66 sub 3-018, 0010 (Modified), 4412 and the Wortmann FX 63-137. Detailed comparisons with the available experimental results show that the essential features are correctly modelled, but that significant discrepancies are found in regions of flow separations. GRA

N89-22830*# Stanford Univ., CA.
TRANSITION TO TURBULENCE IN LAMINAR HYPERSONIC FLOW
Jaap VanDerVegt *In its* Annual Research Briefs, 1988 Feb. 1989 p 115-119 (For primary document see N89-22817 16-34)
Avail: NTIS HC A08/MF A01 CSCL 01A

03 AIR TRANSPORTATION AND SAFETY

Includes passenger and cargo air transport operations; and aircraft accidents.

For related information see also *16 Space Transportation* and *85 Urban Technology and Transportation.*

N89-22591# Office of Technology Assessment, Washington, DC.
SAFE SKIES FOR TOMORROW: AVIATION SAFETY IN A COMPETITIVE ENVIRONMENT
Jul. 1988 194 p
(PB89-114318; OTA-SET-381; LC-88-600550) Avail: NTIS HC A09/MF A01; also available SOD HC $8.50 as 052-003-01126-3 CSCL 01C

How well existing safety policies, regulations and technologies meet the government's responsibility for ensuring safety in commercial aviation are assessed and the role and capability of FAA to carry out its function are reviewed. Author

N89-22592# Sandia National Labs., Albuquerque, NM. Parachute Systems Div.
TESTING OF A NEW RECOVERY PARACHUTE SYSTEM FOR THE F111 AIRCRAFT CREW ESCAPE MODULE: AN UPDATE
Donald W. Johnson 1989 7 p Presented at the 10th AIAA Aerodynamic Decelerator Systems Technical Conference, Cocoa Beach, FL, 18 Apr. 1989
(Contract DE-AC04-76DP-00789; AF Proj. SM-MMK-87-10-324) (DE89-007139; SAND-89-0410C; CONF-8904118-4) Avail: NTIS HC A02/MF A01

A new recovery parachute system has been designed for the F111 crew escape module (CEM). The system includes a cluster of three 49 ft diameter ringslot-solid parachutes, a Kevlar deployment bag, and an explosively fired drogue gun to deploy the pilot parachute. Tests have been conducted that indicate the parachute system will meet the rate of descent requirement of 25 ft/sec at 5000 ft pressure altitude. To control the drag load developed by the parachutes, a new central reefing/disreefing system has been developed. Since the recovery parachute system is normally deployed crosswind from the CEM, line sail of the suspension lines during early tests was a problem but has been minimized by a dual pilot parachute system. DOE

N89-22593# National Transportation Safety Board, Washington, DC.
AIRCRAFT ACCIDENT REPORT: TRANS-COLORADO AIRLINES, INC., FLIGHT 2286, FAIRCHILD METRO 3, SA227 AC, N68TC BAYFIELD, COLORADO, JANUARY 19, 1988
4 Feb. 1989 91 p
(PB89-910401; NTSB/AAR-89/01) Avail: NTIS HC A05/MF A01 CSCL 01C

About 1920 mountain standard time on January 19, 1988, N68TC, a Trans-Colorado Airlines Inc., Fairchild Metro 3, operating as a Continental Express flight 2286 from Stapleton International Airport, Denver, Colorado, with 2 flightcrew members and 15 passengers on board, crashed on approach to Durango, Colorado. The two flightcrew members and seven passengers were killed as a result of the accident. The National Transportation Safety Board determines that the probable cause of this accident was the first officer's flying and the captain's ineffective monitoring of an unstabilized approach which resulted in a descent below the published descent profile. Contributing to the accident was the degradation of the captain's performance resulting from his use of cocaine before the accident. The safety issues examined include the execution of a special approach by flightcrews and the effects of cocaine on human performance. Author

N89-22594# Wichita State Univ., KS. Inst. for Aviation Research.
ELECTRO-IMPULSE DE-ICING RESEARCH: FATIGUE AND ELECTROMAGNETIC INTERFERENCE TESTS Final Report
G. W. Zumwalt, R. A. Friedberg, and J. A. Schwartz Mar. 1989 64 p
(DOT/FAA/CT-88/27) Avail: NTIS HC A04/MF A01

Electro-Impulse Deicing (EIDI) was recently developed and tested with very encouraging results. Questions remain, however, regarding the fatigue life and electromagnetic compatibility of the system. Fatigue tests were conducted on two production aluminum wing leading edges and one composite material leading edge. These were done at realistic temperatures and impulse energies for an estimated aircraft lifetime of ice protection. Coil mounting brackets were the main casualties. Wing components did not fail. Tests were also conducted for metal and composite wings of electromagnetic radiation of EIDI over a wide frequency range. The aluminum wing was found to be an excellent shield. All wires external to the aluminum wing were shown to require careful shielding. The composite wing required all wiring and the metal doublers to be shielded and grounded. Author

04 AIRCRAFT COMMUNICATIONS AND NAVIGATION

Includes digital and voice communication with aircraft; air navigation systems (satellite and ground based); and air traffic control.

For related information see also *17 Space Communications, Spacecraft Communications, Command and Tracking* and *Communications and Radar.*

N89-22595# Civil Aeromedical Inst., Oklahoma City, OK.
STUDIES OF POSTSTRIKE AIR TRAFFIC CONTROL SPECIALIST TRAINEES. PART 2: SELECTION AND SCREENING PROGRAMS
Carol A. Manning, Pamela S. Kegg, and William E. Collins Jul. 1988 25 p
(AD-A199177; DOT/FAA/AM-88/3) Avail: NTIS HC A03/MF A01

Specific contributions of aviation psychologists to the selection and Academy training of FAA air traffic control specialists are presented in a historical context. Research results which formed the basis for the written aptitude selection tests, The Occupational

Knowledge Test (for assessing prior experience), and the pass/fail screens for the Academy's nonradar and radar programs are noted. Results of continuing validation research on all aspects of these selection/screening programs are presented in detail as well as the means by which the results are used to: (1) predict training and performance outcomes; (2) model the impact of program changes; (3) allow the introduction of changes (improvements) without compromising the validity of the programs; and (4) assure compliance with the Uniform Guidelines on Employee Selection Procedures. The application of this line of research has produced considerable cost benefits to the agency. Author

N89-22596# Federal Aviation Administration, Washington, DC.
NATIONAL AIRSPACE SYSTEM PLAN: FACILITIES, EQUIPMENT, ASSOCIATED DEVELOPMENT AND OTHER CAPITAL NEEDS
Jun. 1988 364 p
(AD-A202615; AD-E900870) Avail: NTIS HC A16/MF A01 CSCL 01D

This is the sixth annual update of the NAS Plan. The Plan addresses the compelling problems of how best to improve safety and efficiency, accommodate spiraling demands for aviation services, deal with the problems of aging or obsolete facilities, recognize and users desires for minimal restrictions on the use of the airspace, allow for a reduced Federal role, and create a foundation for continued evolution which exploits newer technologies and developments obtained through continuing research. The recurring theme throughout the Plan is that the solution lies in greater use of automation, consolidations of major facilities, and application of cost effective technological solutions. Topics of interest included in this update follow: Demand on the System; Air Traffic Control System - En Route, Terminal, and Flight Service and Weather; Ground-to-Air Systems; Interfacility Communications Systems; Maintenance and Operations Support Systems; Other Capital Needs; and Transition. GRA

N89-22597# Massachusetts Univ., Amherst. Dept. of Computer and Information Science.
DYNAMIC IMAGE INTERPRETATION FOR AUTONOMOUS VEHICLE NAVIGATION Annual Report, 26 Feb. 1987 - 25 Feb. 1988
Edward M. Riseman and Allen R. Hanson Sep. 1988 33 p
(Contract DACA76-85-C-0008)
(AD-A204167; ETL-0516) Avail: NTIS HC A03/MF A01 CSCL 12I

The results of the project on Dynamic Image Interpretation for Autonomous Land Vehicle (ALV) Navigation is presented for the time period 2/26/87 to 2/25/88. The purpose of the ALV project is to develop algorithms and tools to enable a vehicle to navigate autonomously through realistic landscapes. Contents: Visual Motion Analysis- Computation of the Optical Flow Field; The Recovery of Environmental Motion and Structure from a Mobile Vehicle; Alternatives to General Motion Analysis; Stereoscopic Motion Analysis; Analysis of Constant General Motion; Token-Based Approaches to Motion and Perceptual Organization; Mobile Vehicle Navigation; Perceptual Organization (Grouping)- The Perceptual Organization of Image Curves; Extracting Geometric Structure; Database Support for Symbolic Vision Processing- ISR1, ISR2, Generic Views and Indexing. GRA

N89-22598# Service Hydrographique et Oceanographique de la Marine, Paris (France). Section Geodesie-Geophysique.
GEODETIC POSITIONING SYSTEM FOR FLYING AIRCRAFT (MAY 1987) [POSITIONNEMENT GPS D'UN AVION EN VOL (MAI 1987)]
Gildas Cozian Nov. 1988 49 p In FRENCH
(Rept-013/88; ETN-89-94358) Avail: NTIS HC A03/MF A01

Flight tests were performed in on a Caravelle aircraft to evaluate a geodetic positioning system. A Strada laser trajectographic system furnished a precision submetric reference used to evaluate the real time geodetic position values and the same after differential data treatment. The tests show that the receiver allows in real time to determine the position of a flying aircraft with a three-dimensional precision better than 50 m. After differential treatment the precision is 5 m. ESA

N89-22599# European Space Agency, Paris (France).
NAVIGATION EXPERIMENT NAVEX: THE READING DIFFERENCES BETWEEN ALL GROUND STATION MEASURING CLOCKS DURING SPACELAB PASS OF THE D1 MISSION
Herbert Schild (Deutsche Forschungs- und Versuchsanstalt fuer Luft- und Raumfahrt, Oberpfaffenhofen, West Germany) Jan. 1989 38 p Transl. into ENGLISH of Navigationsexperiment NAVEX die Uhrenstaende Zwischen allen Messuhren der Bodenstationen fuer Jeden Spaceshuttle-Ueberflug Waehrend der D1-Mission (Oberpfaffenhofen, Fed. Republic of Germany, DFVLR), Oct. 1987 37 p Original language document was announced as N88-22880
(ESA-TT-1113; DFVLR-Mitt-87-23; ETN-89-94445) Avail: NTIS HC A03/MF A01; original German version available from DFVLR, VB-PL-DO, Postfach 90 60 58, 5000 Cologne, Fed. Republic of Germany, DM 14.50

The reading differences between the measuring clock of the NAVEX master ground station and the measuring clocks of the receiving stations are calculated for each pass of the space shuttle. The reading rates between all clocks participating in the NAVEX experiment are given. It is possible to connect the readings of all clocks with each other in each second, i.e., the sequence of measurement. ESA

05 AIRCRAFT DESIGN, TESTING AND PERFORMANCE

Includes aircraft simulation technology.

For related information see also *18 Spacecraft Design, Testing and Performance* and *39 Structural Mechanics*. For land transportation vehicles see *85 Urban Technology and Transportation*.

N89-22600# Messerschmitt-Boelkow-Blohm G.m.b.H., Bremen (Germany, F.R.). Unternehmensberetch Transport- und Verkehrsflugzeuge.
DEVELOPMENT AND TESTING OF CRITICAL COMPONENTS FOR TECHNOLOGICAL PREPARATION OF AN AIRBUS-CFRP-FUSELAGE, PHASE 2 Final Report, 1 May 1986 - 30 Jun. 1987
M. Koblax Nov. 1987 75 p In GERMAN; ENGLISH summary
(Contract BMFT-LKF-8652/7)
(MBB-UT-129/87; ETN-89-93769) Avail: NTIS HC A04/MF A01

Essential technological premises for the introduction of composite materials into the fuselage structure of future commercial aircraft were prepared. Selected critical as well as production-development components were manufactured, tested and evaluated. Tests were developed and prepared in order to continue post crash fire research. The possibilities to improve materials and processes were analyzed. The structural efficiency of the selected critical components was proved. The development risks are therefore sufficiently minimized. ESA

N89-22601# Aeronautical Research Inst. of Sweden, Stockholm. Aerodynamics Dept.
TRANSONIC AND SUPERSONIC WIND TUNNEL TESTS ON CONTROL EFFECTIVENESS ON SCHEMATIC MISSILE CONFIGURATIONS WITH CANARD CONTROLS
Sven Erik Gudmundson and Lars Torngren Dec. 1987 76 p
(Contract FMV-FlygFl-82223-78-170-21-001)
(FFA-TN-1988-11; ETN-89-94314) Avail: NTIS HC A05/MF A01

A wind tunnel investigation of pitch, yaw, and roll control effectiveness was performed at transonic and supersonic speeds for two body-canard-wing cruciform missile configurations. At zero roll angle position the setting angles were varied from 0 to 20

deg in steps of 5 or 10 deg for the two horizontal canard controls for pitch control tests, and for the two vertical canard controls for yaw control tests. At 45 deg roll angle position the setting angles were varied for all controls in both pitch and yaw control tests. At the roll control tests the setting angles were varied from 0 to 5 and 10 deg for all controls at both 0 and 45 deg roll angle position. Pitch control tests were done with the canard controls interdigitated 45 deg in relation to the wing planes. ESA

N89-22602# Aeronautical Research Inst. of Sweden, Stockholm. Aerodynamics Dept.
PREDICTION OF LOADS ON WING/BODY/EXTERNAL STORE/FINS PYLON-CONFIGURATIONS AT TRANSONIC SPEEDS
Dieqian Wang and Sven G. Hedman 29 Aug. 1988 78 p
(Contract FMV-FlygFl-82260-88-061-73-001)
(FFA-TN-1988-44; ETN-89-94547) Avail: NTIS HC A05/MF A01

A computational method for prediction of loads on configurations consisting of wing, body, external store, and pylon at transonic speeds is described. The geometric flexibility required for treatment of underwing pylon-mounted stores is achieved by the embedded grid technique. The store modeling capability permits a body of revolution with multiple aft fins in cruciform positions. The chosen formulation of the small perturbation equation and the selected mass flux boundary condition enhance the numerical stability and the accuracy of the computed store body flow field. Computed pressure distributions at zero angle of attack for two parabolic arc bodies of different thickness ratios were compared with experimental data, and an excellent agreement between calculation and experiment is obtained in a wide range of transonic speed, including Mach number 1 and a Mach number larger than 1. For a complete configuration it is observed that the method predicted the features of the flow. ESA

N89-22603 Georgia Inst. of Tech., Atlanta.
AN EFFICIENT INVERSE METHOD FOR THE DESIGN OF BLENDED WING-BODY CONFIGURATIONS Ph.D. Thesis
Neep Hazarika 1988 180 p
Avail: Univ. Microfilms Order No. DA8904811

A numerical inverse design technique was developed for designing body-alone and wing-body configurations directly in the physical plane. Although numerous inverse design techniques exist, they are closely tied to the basic analyses, and can not be upgraded as improved analysis techniques become available. Moreover, many of these tools are configuration-specific, i.e., they are restricted to the design of specific configurations such as airfoils or wings. A general purpose analysis-and configuration-independent design scheme is developed. The present design technique is capable of incorporating a variety of analysis tools and is capable of designing body-alone and wing-body configurations with a minimum of modifications. The present method of designing directly in the physical plane derives its roots from panel methods and was applied to isolated aircraft components such as airfoils and nacelles in transonic flow. The present work avoids chordwise distortions when applied to blended wing-body configuration design, and trailing edge closure is ensured naturally within the solution scheme. The flow solver used to compute pressures over the initial, final and intermediate configurations is a full potential solver. The present work can be used to modify existing configurations to meet certain target requirements. The presence of shock waves and lifting surfaces does not seem to complicate or restrict the design process. Since the analysis is separate from the design, one can substitute Euler or Navier-Stokes solvers as they become more efficient and available. This technique thus provides a methodology for the inverse design of realistic configurations that are typical of high performance transonic aircraft. Dissert. Abstr.

06 AIRCRAFT INSTRUMENTATION

Includes cockpit and cabin display devices; and flight instruments.

For related information see also *19 Spacecraft Instrumentation* and *35 Instrumentation and Photography.*

N89-22604# SLI Avionic Systems Corp., Grand Rapids, MI.
PRE AND POST MODIFICATION ELECTROMAGNETIC COMPATIBILITY TEST REPORT FOR THE C-130H SELF CONTAINED NAVIGATION SYSTEM WITH MLS A-KIT, REVISION
C. Snider 20 Jan. 1989 100 p
(Contract F09603-85-C-1224)
(AD-A205167; Rept-6216-055-Rev) Avail: NTIS HC A05/MF A01 CSCL 20N

The specific tests performed on the Self Contained Navigation System (SCNS) with MLS A-Kit, were a Pre-Modification Electromagnetic Interference (EMI) Signature of the aircraft equipment bays, flight deck and connecting wiring, followed by a Post-Modification EMI Signature and a functional compatibility test of the avionic systems with the SCNS system operating. The tests performed were an engineering evaluation of post-installation EMI and Electromagnetic Compatibility (EMC) with existing electronic and avionic systems in the C-130H Aircraft. The test objectives were to verify the proper EMI/EMC design, installation, and operation of the associated C-130H Aircraft subsystems prior to beginning flight test. This determines if the new installation, or the new or modified equipment would emit radiated or conducted EMI, and if emitted, whether the levels would create interference or degradation in existing equipment. GRA

07 AIRCRAFT PROPULSION AND POWER

Includes prime propulsion systems and systems components, e.g., gas turbine engines and compressors; and onboard auxilliary power plants for aircraft.

For related information see also *20 Spacecraft Propulsion and Power, 28 Propellants and Fuels,* and *44 Energy Production and Conversion.*

N89-22605*# National Aeronautics and Space Administration. Lewis Research Center, Cleveland, OH.
ACTIVE VIBRATION CONTROL FOR FLEXIBLE ROTOR BY OPTIMAL DIRECT-OUTPUT FEEDBACK CONTROL
Kenzou Nonami, Eliseo DiRusso, and David P. Fleming 1989 9 p Proposed for presentation at the 12th Biennial Conference on Mechanical Vibration and Noise, Montreal, Quebec, 17-20 Sep. 1989; sponsored by ASME
(NASA-TM-101972; E-4672; NAS 1.15:101972) Avail: NTIS HC A02/MF A01 CSCL 21E

Experimental research tests were performed to actively control the rotor vibrations of a flexible rotor mounted on flexible bearing supports. The active control method used in the tests is called optimal direct-output feedback control. This method uses four electrodynamic actuators to apply control forces directly to the bearing housings in order to achieve effective vibration control of the rotor. The force actuators are controlled by an analog controller that accepts rotor displacement as input. The controller is programmed with experimentally determined feedback coefficients; the output is a control signal to the force actuators. The tests showed that this active control method reduced the rotor resonance peaks due to unbalance from approximately 250 micrometers down to approximately 25 micrometers (essentially runout level). The tests were conducted over a speed range from 0 to 10,000 rpm; the rotor system had nine critical speeds within this speed range. The method was effective in significantly reducing the rotor vibration for all of the vibration modes and critical speeds. Author

N89-22606*# National Aeronautics and Space Administration. Lewis Research Center, Cleveland, OH.
INVESTIGATION OF LOW NOx STAGED COMBUSTOR CONCEPT IN HIGH-SPEED CIVIL TRANSPORT ENGINES
Hung Lee Nguyen, David A. Bittker, and Richard W. Niedzwiecki 1989 23 p Presented at the 25th Joint Propulsion Conference, Monterey, CA, 10-12 Jul. 1989; cosponsored by the AIAA, ASME, SAE, and ASEE
(NASA-TM-101977; E-4071; NAS 1.15:101977; AIAA-89-2942)
Avail: NTIS HC A03/MF A01 CSCL 21E

Levels of exhaust emissions due to high temperatures in the main combustor of high-speed civil transport (HSCT) engines during supersonic cruise are predicted. These predictions are based on a new combustor design approach: a rich burn/quick quench/lean burn combustor. A two-stage stirred reactor model is used to calculate the combustion efficiency and exhaust emissions of this novel combustor. A propane-air chemical kinetics model is used to simulate the fuel-rich combustion of jet fuel. Predicted engine exhaust emissions are compared with available experimental test data. The effect of HSCT engine operating conditions on the levels of exhaust emissions is also presented. The work described in this paper is a part of the NASA Lewis Research Center High-Speed Civil Transport Low NO(x) Combustor program. Author

N89-22607*# National Aeronautics and Space Administration. Lewis Research Center, Cleveland, OH.
TRANSONIC VISCOUS FLOW CALCULATIONS FOR A TURBINE CASCADE WITH A TWO EQUATION TURBULENCE MODEL
A. A. Boretti (Florence Univ., Italy) Apr. 1989 16 p
(NASA-TM-101944; E-4634; NAS 1.15:101944) Avail: NTIS HC A03/MF A01 CSCL 21E

A numerical method for the study of steady, transonic, turbulent viscous flow through plane turbine cascades is presented. The governing equations are written in Favre-averaged form and closed with a first order model. The turbulent quantities are expressed according to a two-equation kappa-epsilon model where low Reynolds number and compressibility effects are included. The solution is obtained by using a pseudo-unsteady method with improved perturbation propagation properties. The equations are discretized in space by using a finite volume formulation. An explicit multistage dissipative Runge-Kutta algorithm is then used to advance the flow equations in the pseudo-time. First results of calculations compare fairly well with experimental data. Author

N89-22608 Motoren- und Turbinen-Union Muenchen G.m.b.H. (Germany, F.R.).
PROPULSION SYSTEMS WITH IMPROVED EFFICIENCY FOR FUTURE PASSENGER AIRCRAFT. MAIN TASK A: CONCEPTUAL INVESTIGATIONS OF FUTURE PROPULSION SYSTEMS WITH ENHANCED PROPULSIVE EFFICIENCY [ANTRIEBE MIT VERBESSERTER WIRTSCHAFTLICHKEIT FUER ZUKUENFTIGE VERKEHRSFLUGZEUGE. HAUPTAUFGABE A: KONZEPTIONELLE UNTERSUCHUNGEN VON ZUKUENFTIGEN ANTRIEBEN MIT ERHOEHTEM VORTRIEBSWIRKUNGSGRAD]
Schill, Gumucio, Wildner, Geidel, and Tracksdorf 30 Jun. 1987 186 p In GERMAN
(Contract BMFT-LFT-8510/4)
(MTU-TB-87/010; ETN-89-93765) Avail: Fachinformationszentrum Karlsruhe, 7514 Eggenstein-Leopoldshafen 2, Fed. Republic of Germany

Open counter-rotating propfan propulsion systems as pusher with and without transmission were investigated. The variant with transmission is shown to be the most advantageous concept with respect to specific fuel consumption, weight and noise. The main advantages of the pusher without transmission are (besides the omission of the transmission) the smaller length and the smaller propeller diameter. The concept CRISP (Counter-Rotating Integrated Shrouded Propfan) was selected for further studies. Questions concerning CRISP, such as electrical auxiliary apparatus in samarium-cobalt technology and alternative transmission variants, are discussed. A nuclear propulsion system with single-rotor gas generator and innovative component technology was designed. ESA

N89-22609 Cincinnati Univ., OH.
LDV MEASUREMENTS AND INVESTIGATION OF FLOW FIELD THROUGH RADIAL TURBINE GUIDE VANES Ph.D. Thesis
Hasan Eroglu 1988 216 p
Avail: Univ. Microfilms Order No. DA8903591

The results of laser Doppler velocimeter (LDV) measurements and investigation of detailed flow field through radial inflow turbine guide vanes are presented. A three-component LDV system was used for the velocity measurements. The results are presented as contour plots of mean velocities, flow angles and turbulent stresses. Significant end wall cross flows were observed inside the blade passages close to the trailing edges. However, these cross flows are different from the ones in axial turbines because of the counter effects of the radial pressure gradient, the blade shape, and the high negative incidence angle. The flow field through the blade passages was found to be strongly influenced by the scroll geometry. The lack of periodicity between flow channels and asymmetry with respect to the two end walls were attributed to this upstream influence. The rapid mixing of the free stream flow with the wakes occurred downstream of the trailing edges. The average flow angle at downstream measuring station was found to be lower than the exit blade angle showing flow overturning at this radial location. The turbulence intensity increased in the downstream direction. The turbulent stresses also generally increased in the flow direction, but at different rates. The cross plane contour plots of turbulent stress components indicated that the turbulence is anisotropic. The mass flow rate increase did not change the inlet flow angle, but it decreased the passage averaged exit flow angle. The turbulence intensity and stresses decreased with the increase of the mass flow rate. In addition to the experimental investigation, an analytical study of the flow field through the guide vanes of the experimental radial turbine was performed. The flow field was computed using an inviscid, panel method computer code on the blade-to-blade surface of revolution at midspan position. Dissert. Abstr.

N89-22659# Ministry of Defence, London (England).
FUTURE ADVANCED AERO-ENGINES: THE MATERIALS CHALLENGE
D. R. Highton and W. J. Chrispin *In* AGARD, Application of Advanced Material for Turbomachinery and Rocket Propulsion Mar. 1989 10 p (For primary document see N89-22654 16-23)
Avail: NTIS HC A13/MF A01

08 AIRCRAFT STABILITY AND CONTROL

Includes aircraft handling qualities; piloting; flight controls; and autopilots.

For related information see also *05 Aircraft Design, Testing and Performance.*

N89-22610 Purdue Univ., West Lafayette, IN.
MODEL-BASED ANALYSIS AND COOPERATIVE SYNTHESIS OF CONTROL AND DISPLAY AUGMENTATION FOR PILOTED FLIGHT VEHICLES Ph.D. Thesis
Sanjay Garg 1988 281 p
Avail: Univ. Microfilms Order No. DA8825537

The thrust of this research is to develop and validate a systematic technique for pilot-optimal control/display synthesis in complex, closed-loop manual control tasks. The suggested methodology makes extensive use of an Optimal Control Model of human behavior, both for synthesis as well as analysis. The use of the Optimal Control Modeling approach to adequately predict the effects of control/display interaction on human performance and workload, is first validated by performing a detailed model-based study of a set of configurations previously evaluated

in an in-flight experimental study. The mathematical formulation of the Cooperative Control Synthesis technique is then extended to allow for simultaneously augmenting the display dynamics as well as plant or controlled element dynamics. The first order necessary conditions for the optimality of the control/display augmentation control laws are derived and a numerical solution algorithm is developed to solve for these control laws. The methodology is exercised to synthesize control and display augmentation in a compensatory tracking task with a generic controlled element. Analytical evaluations of the designs indicate the applicability of the methodology to meet pilot-centered requirements and to provide a task specific, systematic trade-off between control and display augmentation. An extensive real-time man-in-the-loop simulation study is performed to validate the results from the methodology. Finally, the utility of the methodology is demonstrated by synthesizing control-display designs in the longitudinal approach and landing task for a modern, statically unstable fighter-type aircraft. Dissert. Abstr.

N89-22611# Aeronautical Research Labs., Melbourne (Australia).
SINGLE CHANNEL TEST CONTROLLERS Aircraft Structures Technical Memo.
I. Powlesland and E. S. Moody Jun. 1988 55 p
(AD-A204088; ARL-STRUC-TM-488; DODA-AR-005-525) Avail: NTIS HC A04/MF A01 CSCL 14B

The stand-alone controllers in single and coupled-channel forms are described. Details of hardware and software are given, and notes on the associated data acquisition system and test boxes are included. A number of appendices provide data for preparation and reading of floppy disks, for cycling and communication rate adjustments and detailed information on other aspects of these units. GRA

N89-22612*# Systems Technology, Inc., Hawthorne, CA.
ORBITER FLYING QUALITIES (OFQ) WORKSTATION USER'S GUIDE Final Report, Oct. 1988
Thomas T. Myers, Zareh Parseghian, and Jeffrey R. Hogue Jun. 1988 202 p
(Contract NAS2-12454)
(NASA-CR-179440; H-1537; NAS 1.26:179440) Avail: NTIS HC A10/MF A01 CSCL 22B

This project was devoted to the development of a software package, called the Orbiter Flying Qualities (OFQ) Workstation, for working with the OFQ Archives which are specially selected sets of space shuttle entry flight data relevant to flight control and flying qualities. The basic approach to creation of the workstation software was to federate and extend commercial software products to create a low cost package that operates on personal computers. Provision was made to link the workstation to large computers, but the OFQ Archive files were also converted to personal computer diskettes and can be stored on workstation hard disk drives. The primary element of the workstation developed in the project is the Interactive Data Handler (IDH) which allows the user to select data subsets from the archives and pass them to specialized analysis programs. The IDH was developed as an application in a relational database management system product. The specialized analysis programs linked to the workstation include a spreadsheet program, FREDA for spectral analysis, MFP for frequency domain system identification, and NIPIP for pilot-vehicle system parameter identification. The workstation also includes capability for ensemble analysis over groups of missions. Author

N89-22613# Aeronautical Research Inst. of Sweden, Stockholm. Aerodynamics Dept.
TRANSONIC AND SUPERSONIC WIND TUNNEL TESTS ON CONTROL EFFECTIVENESS ON SCHEMATIC MISSILE CONFIGURATION WITH CANARD CONTROL
Sven Erik Gudmundson and Lars Torngren Dec. 1987 133 p
(Contract FMV-FlygFl-82223-78-170-21-001)
(FFA-TN-1988-11-Suppl; ETN-89-94315) Avail: NTIS HC A07/MF A01

A wind tunnel investigation of pitch, yaw, and roll control effectiveness was performed at transonic and supersonic speeds for two body-canard-wing cruciform missile configurations. At zero roll angle position the setting angles were varied from 0 to 20 deg in steps of 5 or 10 deg for the two horizontal canard controls for pitch control tests and for the two vertical canard controls for yaw control tests. At 45 deg roll angle position the setting angles were varied for all controls in both pitch and yaw control tests. At the roll control tests the setting angles were varied from 0 to 5 and 10 deg for all controls at both zero and 45 deg roll angle position. Pitch control tests were done with the canard controls interdigitated 45 deg in relation to the wing planes. Tables of results are presented. ESA

09 RESEARCH AND SUPPORT FACILITIES (AIR)

Includes airports, hangars and runways; aircraft repair and overhaul facilities; wind tunnels; shock tubes; and aircraft engine test stands.

For related information see also *14 Ground Support Systems and Facilities (Space).*

N89-22614*# National Aeronautics and Space Administration. Langley Research Center, Hampton, VA.
HARDWARE AND OPERATING FEATURES OF THE ADAPTIVE WALL TEST SECTION FOR THE 0.3-METER TRANSONIC CRYOGENIC TUNNEL
Raymond E. Mineck Jun. 1989 41 p
(NASA-TM-4114; L-16548; NAS 1.15:4114) Avail: NTIS HC A03/MF A01 CSCL 14B

A 13- by 13-inch adaptive wall test section was installed in the Langley 0.3-Meter Transonic Cryogenic Tunnel circuit. This test section has four solid walls and is configured for two-dimensional airfoil testing. The top and bottom walls are flexible and movable, whereas the sidwalls are rigid and fixed. The test section has a turntable to support airfoil models, a survey mechanism to probe the model wake, and provisions for a sidewall boundary-layer-control system. Details of the adaptive wall test section, the tunnel circuit modifications, the supporting instrumentation, the monitoring and control hardware, and the wall adaptation strategy are discussed. Sample results of shakedown tests with the test section empty and with an airfoil installed are also included. Author

N89-22615# Air Force Systems Command, Wright-Patterson AFB, OH. Foreign Technology Div.
VISTING CHINA'S AERODYNAMICS RESEARCH AND DEVELOPMENT CENTER
Yongdai Hu and Yaping Li 5 Jan. 1989 12 p Transl. into ENGLISH from Sichuan Huabao (People's Republic of China), no. 5, Iss. 53, Sep. 1987 p 7-9
(AD-A203980; FTD-ID(RS)T-0639-88) Avail: NTIS HC A03/MF A01 CSCL 14B

A visit ot the reseach and development facility is detailed. The facility was developed to meet the needs of China's aviation and space industry and it's peoples' economic development. One highlight of the visit was the wind tunnel. Photographs are presented. E.R.

N89-22616*# Vigyan Research Associates, Inc., Hampton, VA.
MICROCOMPUTER BASED CONTROLLER FOR THE LANGLEY 0.3-METER TRANSONIC CRYOGENIC TUNNEL
S. Balakrishna and W. Allen Kilgore Mar. 1989 149 p
(Contract NAS1-17919)
(NASA-CR-181808; NAS 1.26:181808) Avail: NTIS HC A07/MF A01 CSCL 14B

Flow control of the Langley 0.3-meter Transonic Cryogenic Tunnel (TCT) is a multivariable nonlinear control problem. Globally stable control laws were generated to hold tunnel conditions in the presence of geometrical disturbances in the test section and precisely control the tunnel states for small and large set point changes. The control laws are mechanized as four inner control

loops for tunnel pressure, temperature, fan speed, and liquid nitrogen supply pressure, and two outer loops for Mach number and Reynolds number. These integrated control laws have been mechanized on a 16-bit microcomputer working on DOS. This document details the model of the 0.3-m TCT, control laws, microcomputer realization, and its performance. The tunnel closed loop responses to small and large set point changes were presented. The controller incorporates safe thermal management of the tunnel cooldown based on thermal restrictions. The controller was shown to provide control of temperature to + or - 0.2K, pressure to + or - 0.07 psia, and Mach number to + or - 0.002 of a given set point during aerodynamic data acquisition in the presence of intrusive geometrical changes like flexwall movement, angle-of-attack changes, and drag rake traverse. The controller also provides a new feature of Reynolds number control. The controller provides a safe, reliable, and economical control of the 0.3-m TCT. Author

N89-22617*# National Aeronautics and Space Administration. Lewis Research Center, Cleveland, OH.
NEW HYPERSONIC FACILITY CAPABILITY AT NASA LEWIS RESEARCH CENTER
Jeffrey E. Haas, Roger Chamberlin, and John H. Dicus 1989 16 p Presented at the 25th Joint Propulsion Conference, Monterey, CA, 10-12 Jul. 1989; sponsored by AIAA, ASME, SAE and ASEE
(NASA-TM-102028; E-4760; NAS 1.15:102028; AIAA-89-2534) Avail: NTIS HC A03/MF A01 CSCL 14B

Four facility activities are underway at NASA Lewis Research Center to develop new hypersonic propulsion test capability. Two of these efforts consist of upgrades to existing operational facilities. The other two activities will reactivate facilities that have been in a standby condition for over 15 years. These four activities are discussed and the new test facilities NASA Lewis will have in place to support evolving high speed research programs are described. Author

N89-22618# Aeronautical Research Inst. of Sweden, Stockholm. Structures Dept.
FATIGUE EVALUATION OF WTS-3 WIND TURBINE BLADE AND RETENTION
Anders I. Gustavsson and Anders F. Blom Dec. 1987 38 p Sponsored by the Swedish National Energy Administration
(FFA-TN-1987-81; ETN-89-94313) Avail: NTIS HC A03/MF A01

The WTS-3 wind turbine blade and retention computed stress levels are compared to material properties, and potentially fatigue critical areas are identified. For the blade, these are flatwise spar stresses, and blade shell flatwise stresses. It is not possible to judge the fatigue criticallity of the inner 30 percent of the blade due to limited information. For the retention, which consists of two steel rings bolted to the fiber glass spar shank and a redundant bonded joint, the bolted joint appears to be strong enough to fulfil the design life. It is, however, not possible to assess the load transfer pin joint stress with the available information. Computed stress levels in the bonded joints are low enough for the joint to sustain the design life when the mean stress distribution along the bond line is considered. However, the steep stress gradient at the tapered end of the steel ring may promote debonding during fatigue cycling. This area should be thoroughly studied by NDT techniques during service operation. ESA

N89-22619# Deutsche Forschungs- und Versuchsanstalt fuer Luft- und Raumfahrt, Brunswick (Germany, F.R.). Hauptabteilung Windkanaele.
THE LOW-SPEED WIND TUNNEL AT DVFLR IN BRUNSWICK (FED. REPUBLIC OF GERMANY) Status Report, 1988
Gerhard Kausche, Horst Otto, Dietmar Christ, and Ruediger Siebert Sep. 1988 96 p In GERMAN; ENGLISH summary Original contains color illustrations
(DFVLR-Mitt-88-25; ISSN-0176-7739; ETN-89-94371) Avail: NTIS HC A05/MF A01; DFVLR, VB-PL-DO, Postfach 90 60 58, 5000 Cologne, Fed. Republic of Germany, DM 43

Information for users of the low-speed wind tunnel Braunschweig (NWB) of DFVLR is presented. The wind tunnel has a closed return circuit comprising an open and a closed test section, the cross-section being 3.25 m x 2.80 m. A maximum velocity of 90 m/sec in the closed test section and of 75 m/sec in the open one can be achieved. The information required for the preliminary planning of test programs and for the preliminary layout of models for intended tests is given. ESA

N89-22620 Council for National Academic Awards (England).
INVESTIGATION OF THE EFFECTS OF INCREASED SOPHISTICATION OF SIMULATION OF THE ATMOSPHERIC WIND IN WIND TUNNELS Ph.D. Thesis
Allan Hodgson Cusick 1988 413 p
Avail: Univ. Microfilms Order No. BRD-84076

The influence of the sophistication of the simulation of the natural wind in wind tunnels was investigated upon the correlation of model and full scale ground wind speeds and directions. A model of a section of the Manchester University campus, centered about the Mathematics Tower, was made at a scale of 1:250. It extended, at this scale, for a distance of one meter in all directions. This model was tested in three wind tunnels. Two are of high, one of low, sophistication of simulation of the natural wind. It was found that results in all three wind tunnels were significantly affected by model limitations such as the artificial ending of wind dominant building formations at the edge of the model, and potentially, by mis-positioning of ground wind probes at measuring stations in areas of high horizontal velocity gradient. The least sophisticated simulation produced local defects which were markedly worse than corresponding defects in the other two simulations in one particular wind direction. However, the measurements at points in the least sophisticated simulation, which were free of effects directly related to the limited size of the wind tunnel relative to the model, exhibited a similar level of correlation with full scale results to that in the sophisticated simulations. Following the normal custom in pre-construction environmental wind tunnel testing of large buildings in an urban area, only the buildings and major features were included in the model. In these circumstances the effect of the ground-cover on the completed site is expected to give an extra safety factor over the model ground wind predictions made using the smooth base board. The results in all three wind tunnels indicated conformity with these expectations. Dissert. Abstr.

N89-22621 Colorado Univ., Boulder.
NUMERICAL STUDY OF A MULTIPURPOSE TRANSONIC WIND TUNNEL WITH AN ADAPTABLE INJECTION-SUCTION SYSTEM Ph.D. Thesis
Shing-Chung Onn 1988 117 p
Avail: Univ. Microfilms Order No. DA8902928

For the simplicity in installation and operation, an adaptable injection-suction (AIS) system was implemented to see if it can be used to replace the conventional convergent-divergent nozzle in a multipurpose transonic wind tunnel. Results for three different AIS systems indicate that such an idea is feasible. Without viscous effects, an isentropic small-disturbance velocity potential formulation is used to solve this transonic flow problem. Based on the examined cases, it can be found that: (1) before choking, with increasing M sub infinity, the normal shock can be gradually moved down the channel and the supersonic bubble grows like the flow in a conventional convergent-divergent nozzle, (2) after choking, both the location and shape of the sonic line are invariant with respect to decreased exit pressure, (3) in a subcritical flow, the pressure distribution at the AIS system is approximately symmetric with respect to the center of the AIS system, and the pressure distribution is no longer symmetric in a supercritical flow, (4) the supersonic bubble in a supercritical flow may disappear by reducing the strength of the AIS system, (5) after choking, by lowering the choked exit pressure, the shock can be moved further downstream to become a lambda shock near the exit of the channel, (6) for the case by using an AIS system with injection only, a sonic flow at the exit section can be obtained by locating the trailing edge of this injection system at the wall exit and specifying the exit Mach number to be unity, and (7) an originally

choked flow may not be choked if the AIS system is shifted to a different location. From the first three findings, it can be concluded that the present numerical calculations of this transonic flow problem are fairly reliable. Dissert. Abstr.

12 ASTRONAUTICS (GENERAL)

For extraterrestrial exploration see *91 Lunar and Planetary Exploration.*

N89-22622# Joint Publications Research Service, Arlington, VA.
JPRS REPORT: SCIENCE AND TECHNOLOGY. USSR: SPACE
17 Aug. 1988 78 p Transl. into ENGLISH from various Russian articles
(JPRS-USP-88-003) Copyright Avail: NTIS HC A05/MF A01

Topics addressed include: aerospace engineering, administration of space policy, life sciences, interplanetary sciences, aerospace sciences, and manned mission highlights. For individual titles, see N89-22623 through N89-22630.

N89-22623# Joint Publications Research Service, Arlington, VA.
PROJECT RADIOASTRON **c89**
B. Konovalov *In its* JPRS Report: Science and Technology. USSR: Space 17 Aug. 1988 p 15-16 Transl. into ENGLISH from Izvestiya (Moscow, USSR), 10 Apr. 1988 p 2 (For primary document see N89-22622 16-12)
Copyright Avail: NTIS HC A05/MF A01

A consortium of European radio observatories, the Technological University of Finland, the Australian Scientific Research Society, the Australian Radio Observatory, and the United States National Radio Astronomical Observatory, in addition to the Soviet Union, will develop on-board equipment necessary for the Project Radioastron space radio telescope and the means required for information processing. Four special centers, outfitted with the most powerful and high-speed computers, are being organized in Western Europe, Australia, the United States, and the Soviet Union for the processing of the enormous flow of anticipated information. The design of the space telescope is briefly discussed. B.G.

N89-22624# Joint Publications Research Service, Arlington, VA.
METHODS AND ALGORITHMS FOR PROCESSING TELEVISION IMAGES OF NUCLEUS OF HALLEY'S COMET. SOME RESULTS Abstract Only **c90**
R. Z. Sagdeyev, G. A. Avanesov, Ya. L. Ziman, V. A. Shamis, and V. A. Krasikov *In its* JPRS Report: Science and Technology. USSR: Space 17 Aug. 1988 p 26 Transl. into ENGLISH from Kosmicheskiye Issledovaniya (Moscow, USSR), v. 25, no. 6, Nov.-Dec. 1987 p 820-830 (For primary document see N89-22622 16-12)
Copyright Avail: NTIS HC A05/MF A01

About 50 television images of Halley's Comet obtained from the Vega spacecraft at distances of 500 to 8000 km are now processed. The main processing stages were: retrieval of images and noise elimination; defining boundaries of the nuclear regions; discrimination objets; discrimination of structural elements on the nucleus surface; determination of nucleus configuration and size. In a generalized way, the specialized methods and algorithms developed for the solution of these problems and the results of their applications are examined. Author

N89-22625# Joint Publications Research Service, Arlington, VA.
HISTORICAL SURVEY OF BIOSATELLITES **c18**
V. B. Pishchik *In its* JPRS Report: Science and Technology. USSR: Space 17 Aug. 1988 p 35-38 Transl. into ENGLISH from Zemlya i Vselennaya (Moscow, USSR), no. 2, Mar.-Apr. 1988 p 33-38 (For primary document see N89-22622 16-12)
Copyright Avail: NTIS HC A05/MF A01

The history of animal experimentation on Soviet spacecraft is briefly reviewed. The biosatellite research made huge contributions to the understanding of many fundamental problems of space science. The development of modern space technology opens further possibilities to continue conducting medical and biological research. B.G.

N89-22626# Joint Publications Research Service, Arlington, VA.
CONSTRUCTION IN WEIGHTLESSNESS **c18**
Sergey Dmitriyevich Grishin and Sergey Vasilyevich Chekalin *In its* JPRS Report: Science and Technology. USSR: Space 17 Aug. 1988 p 40-43 Transl. into ENGLISH from Problemy Osvoyeniya Kosmosa (Novoye v Zhizni, Nauke, Tekhnike: Seriya Kosmonavtika, Astronomiya) (Moscow, USSR), no. 1, Jan. 1988 p 36-44 (For primary document see N89-22622 16-12)
Copyright Avail: NTIS HC A05/MF A01

Large-scale structures (LSSs), the conditions for their operation, the demands made on them, and the problems of deployment and assembly in orbit are discussed. B.G.

N89-22627# Joint Publications Research Service, Arlington, VA.
POWER SUPPLY IN SPACE **c44**
Sergey Dmitriyevich Grishin and Sergey Vasilyevich Chekalin *In its* JPRS Report: Science and Technology. USSR: Space 17 Aug. 1988 p 43-46 Transl. into ENGLISH from Problemy Osvoyeniya Kosmosa (Novoye v Zhizni, Nauke, Tekhnike: Seriya Kosmonavtika, Astronomiya) (Moscow, USSR), no. 1, Jan. 1988 p 27-36 (For primary document see N89-22622 16-12)
Copyright Avail: NTIS HC A05/MF A01

With the increased complexity of the problems that must be solved and with the longer active service life of spacecraft, the power needs of on-board equipment are growing rapidly. This necessitates the improvement of the present spacecraft power supplies and development of space power engineering. Storage batteries, use of solar energy, and radioisotope and nuclear power units are examined. B.G.

N89-22628# Joint Publications Research Service, Arlington, VA.
DEVELOPMENT OF ORBITAL WELDING TECHNOLOGY **c37**
A. Tarasov *In its* JPRS Report: Science and Technology. USSR: Space 17 Aug. 1988 p 46-49 Transl. into ENGLISH from Pravda (Moscow, USSR), 29 Mar. 1988 p 2 (For primary document see N89-22622 16-12)
Copyright Avail: NTIS HC A05/MF A01

The history of Soviet orbital welding is briefly outlined, starting with the ground design up to and including the actual performance in space. B.G.

N89-22629# Joint Publications Research Service, Arlington, VA.
GLAVKOSMOS OFFICIAL YU. P. SEMENOV INTERVIEWED ON DEVELOPMENT OF USSR SPACE PROGRAM
In its JPRS Report: Science and Technology. USSR: Space 17 Aug. 1988 p 61-65 Transl. into ENGLISH from Pod Znamenem Leninizma (Kiev, USSR), no. 4, Feb. 1988 p 74-78 (For primary document see N89-22622 16-12)
Copyright Avail: NTIS HC A05/MF A01

Humanity has begun counting down the fourth decade since that memorable day of 4 October 1957, when the Earth's gravity was overcome for the first time and an artificial satellite was placed in a near-Earth orbit. Since then, an intensive exploitation of space has begun. The first steps into space and the prospects for the exploitation of interstellar space are discussed. Author

N89-22630# Joint Publications Research Service, Arlington, VA.
FUTURE SPACE PROJECTS DISCUSSED AT MOSCOW SPACE FORUM
Tamara Breus *In its* JPRS Report: Science and Technology. USSR: Space 17 Aug. 1988 p 65-67 Transl. into ENGLISH from Nauka i Tekhnika (Riga, USSR), no. 2, Feb. 1988 p 26-28 (For primary document see N89-22622 16-12)
Copyright Avail: NTIS HC A05/MF A01

Goals in mission planning for circumterrestrial space data acquisition, extra-atmospheric astronomy; planetary investigations, and the flight to Mars are discussed. B.G.

N89-22631# Air War Coll., Maxwell AFB, AL.
SPACE CONTROL: A NATIONAL IMPERATIVE

Raymond H. Barker, Jr. Apr. 1988 72 p
(AD-A202612; AD-E900870) Avail: NTIS HC A04/MF A01
CSCL 22A

This report provides a discussion on various aspects of the new mission of space control--a mission which seeks to maintain access to and assure an ability to operate in space and, when so directed, deny such freedom to an enemy. In doing so, it first reviews some relevant history applicable to the space control mission. Then, it reviews the utility of space systems in supporting various elements of national security. After a brief review of the threat, the report discusses some dimensions of the policy debate between the executive and legislative branches of government over the proper investment path for the mission. Finally, the report seeks to provide a framework for developing a space control strategy as a foundation for defining future mission capability. Building upon existing national strategy elements of strategic deterrence, The Maritime Strategy, and the AirLand Battle Doctrine: the report discusses a potential approach to building a strategy for the space control mission. GRA

N89-22985*# National Aeronautics and Space Administration. Lewis Research Center, Cleveland, OH.
HUMAN EXPLORATION MISSION STUDIES Abstract Only
Robert L. Cataldo *In its* Space Electrochemical Research and Technology Conference: Abstracts 1989 p 4 (For primary document see N89-22982 16-44)
Avail: NTIS HC A03/MF A01 CSCL 22A

13 ASTRODYNAMICS

Includes powered and free-flight trajectories; and orbital and launching dynamics.

N89-22632# Air Force Inst. of Tech., Wright-Patterson AFB, OH. School of Engineering.
OPTIMAL LOW THRUST TRAJECTORIES FOR PLANETARY CAPTURE M.S. Thesis
David E. Gaylor Dec. 1988 58 p
(AD-A202604; AD-E900870; AFIT/EN/AA/88D-04) Avail: NTIS HC A04/MF A01 CSCL 22C

The purpose of this study is to find optimal low thrust capture trajectories in the restricted three body problem. The region of phase space which corresponds to capture by a body is bounded by the curve of zero velocity passing through the equilibrium point (Lagrange point) L2. If the spacecraft is driven to rest at L2, capture has been achieved by adding the least amount of energy. An optimal control law is developed to achieve this based on maximizing the Jacobi integral. The dynamics are then linearized around L2 for the Earth Moon system and the shooting method is used to solve the two point boundary value problem. This problem was found to be singular so the shooting method was modified to avoid making corrections along the null eigenvector. Four trajectories were found which demonstrate the optimal control law which successfully caused the spacecraft to be captured by the Moon. GRA

N89-22633 Colorado Univ., Boulder.
TEN YEAR LIFETIME ORBITS ABOUT THE PLANET MARS PH.D. Thesis
Rodney Donald Bain 1988 117 p
Avail: Univ. Microfilms Order No. DA8902876

A spacecraft designed for a mapping or photographic planetary mission will need to penetrate the atmosphere of Mars at its upper levels to gather the required data. The problem investigated is the determination of an envelope (called the Critical Envelope) about the planet Mars with the criteria of non-impact with the Martian surface for at least ten earth-years. The major constituent of the envelope involves the determination of the minimum value of the Periapsis Altitude of such an envelope. The purpose of this non-impact (quarantine) condition is to insure non-introduction of foreign materials into the Martian environment. This quarantine condition requires the determination of long-term perturbative effects upon the envelope. The problem was modeled as an astrodynamic perturbation problem affected by atmospheric drag (modeled as an exponential atmosphere) and aspherical gravitational effects, along with the geometric oblateness of the planet. In order to determine the gravity effects three different models were employed (2 x 0, 4 x 4, and 8 x 8). To reduce the configuration space, the Mean Anomaly and the Argument of Periapsis are set to zero. The number of orbits (2,263) investigated indicated that the Periapsis Altitude should be set at 441 km or above. Orbital data included the ranges of eccentricities from .01 to .1, variations of the inclination from 0.5 degrees to 85.5 degrees, and the Longitude of the Ascending Node varying from 0 to 360 degrees. Dissert. Abstr.

14 GROUND SUPPORT SYSTEMS AND FACILITIES (SPACE)

Includes launch complexes, research and production facilities; ground support equipment, e.g., mobile transporters; and simulators.

For related information see also *09 Research and Support Facilities (Air).*

N89-22634# Illinois Univ., Urbana.
VARIATIONAL ANALYSIS OF RAILGUN PLASMA-ARC-ARMATURE FOR ACCELERATION OF SOLID HYDROGEN PELLETS FOR FUSION REACTOR REFUELING
W. H. Choe and Kevin Kim Dec. 1988 24 p
(Contract DE-FG02-84ER-52111)
(DE89-009556; DOE/ER-52111/T4) Avail: NTIS HC A03/MF A01

This paper discusses fueling magnetically confined plasmas using a railgun plasma-arc-armature. The topics covered are: the plasma model; variational analysis; current density in the plasma arc and arc voltage; and magnetic field and the net railgun force. DOE

N89-22635# Illinois Univ., Urbana. Fusion Technology Lab.
DEVELOPMENT AND STUDY OF A 3.2-mm-DIAMETER, 1.2-m-LONG TWO-STAGE PLASMA-ARC-DRIVEN RAILGUN FOR HYPERVELOCITY HYDROGEN PELLET INJECTION
David Zhang and Kevin Kim Dec. 1988 68 p
(Contract DE-FG02-84ER-52111)
(DE89-009557; DOE/ER-52111/T5) Avail: NTIS HC A04/MF A01

A detailed description of a prototype, fuseless, plasma-arc-driven, two-stage railgun system with a 1.2-m-long railgun barrel and a 3.2-mm-diameter circular bore is presented, along with the preliminary results indicating its capabilities and limitations. A hydrogen pellet generator, which has a straight-tube configuration and which is also operated as a gas gun, is employed as the first stage of the two-stage acceleration system. The design details of this preacceleration system and the results illustrating its performance are first presented. The second-stage accelerator which acts as a booster accelerator, is a fuseless plasma-arc-driven railgun, and constitutes the core of the entire two-stage acceleration scheme. Details of its design, ancillary systems, operation, and performance are described next in this report. The experimental data included herein represent only the preliminary data, and the system modifications that led to the improvements are described in the accompanying two other progress reports that precede this. DOE

N89-22636# Societe Europeenne de Propulsion, Vernon (France). Div. Propulsion a Liquides et Espace.
ADVANCED CARTRIDGE TECHNOLOGY: EXECUTIVE SUMMARY
R. Petit Paris, France ESA 25 Aug. 1988 34 p
(Contract ESTEC-7502/87)
(SEP-TS/F-6972/88-RP; ESA-CR(P)-2716; ETN-89-94452)
Copyright Avail: NTIS HC A03/MF A01

Materials and technologies for the cartridges of furnaces such

as the Advanced Gradient Heating Facility, where temperatures on the diffusers can reach 1500 C, were reviewed. Nickel superalloy, refractory metal, ceramic and thermostructural composite mechanical, thermal, and chemical properties were investigated, as well as commercial data. The informations on 50 materials was entered in a data base to provide users with an information source which can be constantly updated. It is possible to select all the materials in the data base satisfying several criteria as for instance a service temperature higher than 900 C and a good chemical compatibility with aluminum. Cartridge configurations using these materials are proposed and development priorities are defined. ESA

15 LAUNCH VEHICLES AND SPACE VEHICLES

Includes boosters; operating problems of launch/space vehicle systems; and reusable vehicles.

For related information see also *20 Spacecraft Propulsion and Power.*

N89-22637# Office of Technology Assessment, Washington, DC.
LAUNCH OPTIONS FOR THE FUTURE: SPECIAL REPORT
Jul. 1988 110 p
(PB89-114268; OTA-ISC-383; LC-88-600540) Avail: NTIS HC A06/MF A01; also available SOD HC $5.00 as 052-003-01117-4 CSCL 22B

The range of launch systems that exist now or could be available before 2010 are described and the costs of meeting different demand levels are explored for launching humans and spacecraft to orbit. Also discussed is the importance of developing advanced technologies for space transportation. Author

16 SPACE TRANSPORTATION

Includes passenger and cargo space transportation, e.g., shuttle operations; and space rescue techniques.

For related information see also *03 Air Transportation and Safety* and *18 Spacecraft Design, Testing and Performance.* For space suits see *54 Man/System Technology and Life Support.*

No abstracts in this category.

17 SPACE COMM., SPACECRAFT COMM., COMMAND & TRACKING

Includes telemetry; space communications networks; astronavigation and guidance; and radio blackout.

For related information see also *04 Aircraft Communications and Navigation* and *32 Communications and Radar.*

No abstracts in this category.

18 SPACECRAFT DESIGN, TESTING AND PERFORMANCE

Includes satellites; space platforms; space stations; spacecraft systems and components such as thermal and environmental controls; and attitude controls.

For life support systems see *54 Man/System Technology and Life Support.* For related information see also *05 Aircraft Design, Testing and Performance, 39 Structural Mechanics,* and *16 Space Transportation.*

N89-22638*# National Aeronautics and Space Administration. Lyndon B. Johnson Space Center, Houston, TX.
ORBITAL DEBRIS ENVIRONMENT FOR SPACECRAFT DESIGNED TO OPERATE IN LOW EARTH ORBIT
Donald J. Kessler, Robert C. Reynolds, and Phillip D. Anz-Meador 1 Sep. 1988 19 p Prepared in cooperation with Lockheed Engineering and Sciences Co., Houston, TX
(NASA-TM-100471; NAS 1.15:100471) Avail: NTIS HC A03/MF A01 CSCL 22B

The orbital debris environment model is intended to be used by the spacecraft community for the design and operation of spacecraft in low Earth orbit. This environment, when combined with material-dependent impact tests and spacecraft failure analysis, is intended to be used to evaluate spacecraft vulnerability, reliability, and shielding requirements. The environment represents a compromise between existing data to measure the environment, modeling of this data to predict the future environment, the uncertainty in both measurements and modeling, and the need to describe the environment so that various options concerning spacecraft design and operations can be easily evaluated. Author

N89-22639# Naval Postgraduate School, Monterey, CA.
DESIGN OF AN ELF/VLF SATELLITE FOR UNDER THE ICE SUBMARINE COMMUNICATIONS M.S. Thesis
Gary C. Thompson Sep. 1988 131 p
(AD-A202607; AD-E900870) Avail: NTIS HC A07/MF A01 CSCL 25E

The design of a space based tethered antenna satellite system for ELF/VLF communications with submarines in the far northern latitudes, and under the polar ice is proposed. By using the dynamo effect of a moving wire in a (geo) magnetic field, the tether cable can produce tens of kilowatts of its own radiation power. The transmitted signal of IKHz-3KHz will be whistler mode propagation to couple to the Earth's field lines and follow them down to the surface. The signal can penetrate 100m of seawater, and ice of unlimited thickness. A constellation of 12 satellites will provide 75 percent duty cycle coverage for each submarine operating area of over four million square kilometers. Author

N89-22640# British Aerospace Public Ltd. Co., Bristol (England). Space and Communications Div.
SECOND GENERATION METEOSAT PRE-PHASE A SYSTEM STUDY Final Report
R. Flower and P. G. Hardtke (Dornier-Werke G.m.b.H., Friedrichshafen, Germany, F.R.) Paris, France ESA Jul. 1988 637 p Sponsored in part by Laben Space Instrumentation and and Systems, Milan, Italy; Matra-Espace, Paris, France; MBB GmbH, Ottobrunn, Fed. Republic of Germany; ANT Nachrichtentechnik, Backnang, Fed. Republic of Germany and Meteorological Office
(Contract ESA-7197/87/NL/JS)
(BA-SGM-FR-01; ESA-CR(P)-2706; ETN-89-94238) Copyright Avail: NTIS HC A99/MF A01

Technical and cost options for the 2nd generation Meteosat satellite were compared. Instruments, systems, configuration, payload accommodation, control, and program aspects were studied. The recommended configuration is three axis stabilized with separate bus and payload modules. The payload includes an imaging radiometer, an IR sounder with 16 km resolution, a microwave sounder, 20 kg scientific package, and a mission performance telecommunication package. No preference between

onboard and ground processing is decided. Two rigid foldout solar arrays are suggested, but no eclipse power to scientific instruments. The attitude and orbit control system is zero momentum biased, with four star trackers. A combined bipropellant system is used for apogee boost and stationkeeping lattitude control. Mass and volume are compatible with Ariane 4 launch in upper or lower passenger position, depending on instrument assumptions. Four spacecrafts are needed for a 10 to 15 yr program life. ESA

N89-22641# Alcatel Espace, Toulouse (France).
STUDY OF A WIDEBAND TELECOMMUNICATIONS SATELLITE FOR EUROPE Final Report
F. Arzpayma, C. Combes, X. Henrion, B. Jarrousse, R. Lenormand, J. P. Marre, and D. Rene Paris, France ESA 31 Jan. 1987 215 p
(Contract ESTEC-5847/84/NL/GM(SC))
(ATES/DMA/TRM/162-86; ESA-CR(P)-2707; ETN-89-94239)
Copyright Avail: NTIS HC A10/MF A01

The system requirements and constraints, and configuration for a 20 to GHz satellite telecommunication network for Europe were assessed. A mixed TDMA/single channel per carrier access technique and waveguide beam forming network antennas was compared with hybrid TDMA/FDMA access technique and electronically phased array antenna. The hybrid technique is preferred. ESA

N89-22642# Universidad Politecnica de Madrid (Spain). Lab. de Aerodinamica.
SPACECRAFT THERMAL CONTROL DESIGN DATA HANDBOOK Final Report
I. DaRiva, D. Rivas, and J. Meseguer Paris, France ESA Dec. 1987 5 p
(Contract ESTEC-6115/84/NL/MA(SC))
(LAMF-8712; ESA-CR(P)-2712; ETN-89-94242) Avail: NTIS HC A02/MF A01

Updates to certain pages of the ESA spacecraft thermal control design data handbook are indicated. ESA

N89-22643# Standard Elektrik Lorenz A.G., Stuttgart (Germany, F.R.). Avionics and Aerospace System Group.
GPS TERMINAL: STUDY OF A GPS RECEIVER FOR COLUMBUS PLATFORM ELEMENTS, EXECUTIVE SUMMARY
Paris, France ESA Jun. 1988 30 p Prepared in cooperation with Bell Telephone Mfg. Co., Antwerp, Belgium and Sener SA, Madrid, Spain
(Contract ESTEC-6818/86/NL/PB(SC))
(GPS-REP-SEL-002; ESA-CR(P)-2719; ETN-89-94453) Avail: NTIS HC A03/MF A01

The specification, analysis, design, simulation, and measurements show that the requirements as derived from applications for Columbus Space Station elements and as stated in the Global Positioning System (GPS) terminal performance specification can be met. Modifications in the GPS Core Module and in the GPS Simulator designs existing for ground based applications are necessary to adapt them to the specific space environment. The main modifications with respect to Core Module are: (1) implementation of space qualifiable parts and materials; (2) replacement of the EPROM by a RAM; (3) development of the GPS Time Generator, the power supply, and the GNC interfaces; (4) design of the housing; (5) adaptation of the signal processor software to the loop parameters required for Columbus applications and to the multi-antenna control requirement; and (6) adaptation of the data processor software to the new initialization procedure, the modified signal acquisition strategy used in the loops, the new ionospheric delay compensation model; the Kalman filtering algorithms required for orbiting receivers, the new calculations necessary for performing range measurement corrections and antenna selections according to the actual station element attitude, and the control from the GNC to perform measurements for differential mode. ESA

N89-22644# Centre National d'Etudes Spatiales, Toulouse (France). Dept. Structures.
ELECTRODYNAMIC TRANSIENT TESTS Final Report
R. Dardel and F. Mercier Paris, France ESA 19 Jan. 1988 81 p
(Contract ESTEC-6328/85/NL/BP)
(CNES-CT/DRT/TVE/SM-024; ESA-CR(P)-2727; ETN-89-94456)
Avail: NTIS HC A05/MF A01

The Arabsat satellite structural and thermal model (STM) underwent tests representing longitudinal excitations occurring during the first stage and second ends of flight of Ariane. Sine tests were performed on a 170 kN shaker. Results show the validity of the tests, and reveal differences between sine and transient excitations. The transient signal energy is mainly located in frequency spectrum bands which do not contain the resonance frequencies of the important modes of the damped satellite. The sine signal energy is mainly located, in spite of notchings, at satellite resonance frequencies. The transient excitation can generate levels higher than those produced by sine excitation. If the low frequency range is not taken into account, the acceleration levels reached on local modes are usually lower in the transient case than in the sine one. Calculations show that the stresses due to sine excitation are higher for appendices than those obtained by a transient excitation. The damping coefficient has a low influence on responses in transient excitation. Transient excitation, although less severe on almost all satellite appendices than the sine excitation, can induce, by its rigid motion component, high accelerations and stresses on satellite parts. ESA

N89-22645# Erno Raumfahrttechnik G.m.b.H., Bremen (Germany, F.R.). Main Dept. for Advanced Launcher Systems.
ARIANE 5 TRANSFER VEHICLE (ATV) Final Report
N. Deutscher and C. Cougnet (MATRA Espace, Toulouse, France) Paris, France ESA Jul. 1988 97 p Prepared in cooperation with SAAB-Space AB, Goteborg, Sweden
(Contract ESTEC-7357/87/NL/MA(SC))
(Rept-OX-1-005; ESA-CR(P)-2735; ETN-89-94461) Avail: NTIS HC A05/MF A01

An Ariane Transfer Vehicle (ATV), an unmanned liquid propulsion Ariane 5 upper stage (L5) plus an enhanced Vehicle Equipment Bay (VEB), equipped with all needed subsystems, namely with Rendezvous and Docking (RVD) capability, to perform logistics supply missions to the International Space Station (ISS) is described. The ATV is an L5/VEB derivate and fits into the family of Ariane 5 upper stages. The ATV is a flexible intelligent basis on which to build a logistic vehicle by adaption of payload modules. It is a low-cost vehicle because it reuses to a maximum extent existing hardware and software from other ESA programs like AR5, Hermes and Columbus. Analysis shows the feasibility of the ATV, establishes the requirements, defines the hardware and dynamical configuration and the needed L5/VEB upgrades. A development plan which shows the coherence with the other space programs is given. ESA

N89-22646# Aerospatiale, Les Mureaux (France). Direction Technique Systems Futurs.
ATV: ARIANE 5 TRANSFER VEHICLE STUDY Final Report
C. Bonnal Paris, France ESA 11 Jul. 1988 81 p
(Contract ESTEC-7356/87/NL/MA)
(STF/E-39-005/CB; ESA-CR(P)-2738; ETN-89-94463) Avail: NTIS HC A05/MF A01

Mission and system requirements of the Ariane Transfer Vehicle (ATV) were defined, and an overall ATV concept was derived. The ATV subsystems (structure, propulsion, thermal control, electrical power, communications, guidance, navigation, control, data handling, and mechanisms) are discussed. Payload accommodation and mission configurations are described. The design relies heavily on Ariane 5 upper composite hardware to achieve a logistics vehicle compatible with Hermes and STS servicing needs. It allows transfer and rendezvous functions, with destructive reentry at the end of the mission. It fully exploits the Ariane low Earth orbit capability (20 tons). ESA

N89-22647# Erno Raumfahrttechnik G.m.b.H., Bremen (Germany, F.R.).
COLUMBUS MTFF UTILIEATION, PHASE B2X: EXECUTIVE SUMMARY FOR MAIN STUDY
G. Zelck Paris, France ESA 25 Nov. 1988 85 p Prepared in cooperation with Fokker BV, Amsterdam, Netherlands and Dornier System GmbH, Friedrichshafen, Fed. Republic of Germany
(Contract ESA-7451/87/F/SC)
(CUT-MBER-800-RP-220; ESA-CR(P)-2744; ETN-89-94466)
Avail: NTIS HC A05/MF A01

Columbus Man-Tended Free Flyer (MTFF) payload operation planning/timelining and the corresponding logistics requirements; and telecommunication during the MTFF operational phase were studied. Critical areas for system development and operation are summarized. ESA

N89-22648# Alcatel Espace, Toulouse (France).
STUDY OF A DRS EXPERIMENTAL PAYLOAD FOR SINGLE AND MULTIPLE ACCESS AT S BAND: EXECUTIVE SUMMARY
J. Neron Paris, France ESA 10 May 1988 46 p
(Contract ESTEC-7140/87/NL/DG)
(PSD88/00017; ESA-CR(P)-2751; ETN-89-94472) Copyright
Avail: NTIS HC A03/MF A01

Antenna concepts for ESA's DRS sateilite were studied, and the possibility of reusing the reflector for an experimental land mobile telecommunications mission was investigated. Concerning the large reflector, there is no significant advantage for any technology and the choice depends on the antenna and even spacecraft configuration. When a central attachment of the reflector is requested, the MBB UMA technology is the most suitable. For offset configurations, the light weight of the ISRS is interesting but, for unsymmetrical configurations, it induces a solar torque which leads to tens of kilograms of propellant consumption to compensate it. Thus, for unsymmetrical configurations, the Aerospatiale technology is more adequate. The antenna concept depends on the final mission priorities. To provide one S band single access beam, the center fed fully steerable antenna concept offers the best performances. But as this mission will be requested only for a small percentage of the time, the interest of this configuration for a flight on SAT-2 is limited. For implementation of several missions such as S band plus land mobile plus, as an option, LOCSTAR, offset fed concepts are more suitable. ESA

N89-22625# Joint Publications Research Service, Arlington, VA.
HISTORICAL SURVEY OF BIOSATELLITES
V. B. Pishchik *In its* JPRS Report: Science and Technology. USSR: Space 17 Aug. 1988 p 35-38 Transl. into ENGLISH from Zemlya i Vselennaya (Moscow, USSR), no. 2, Mar.-Apr. 1988 p 33-38 (For primary document see N89-22622 16-12)
Copyright Avail: NTIS HC A05/MF A01

N89-22626# Joint Publications Research Service, Arlington, VA.
CONSTRUCTION IN WEIGHTLESSNESS
Sergey Dmitriyevich Grishin and Sergey Vasilyevich Chekalin *In its* JPRS Report: Science and Technology. USSR: Space 17 Aug. 1988 p 40-43 Transl. into ENGLISH from Problemy Osvoyeniya Kosmosa (Novoye v Zhizni, Nauke, Tekhnike: Seriya Kosmonavtika, Astronomiya) (Moscow, USSR), no. 1, Jan. 1988 p 36-44 (For primary document see N89-22622 16-12)
Copyright Avail: NTIS HC A05/MF A01

19 SPACECRAFT INSTRUMENTATION

For related information see also *06 Aircraft Instrumentation* and *35 Instrumentation and Photography.*

No abstracts in this category.

20 SPACECRAFT PROPULSION AND POWER

Includes main propulsion systems and components, e.g., rocket engines; and spacecraft auxilliary power sources.

For related information see also *07 Aircraft Propulsion and Power, 28 Propellants and Fuels, 44 Energy Production and Conversion,* and *15 Launch Vehicles and Space Vehicles.*

N89-22649# Air Force Inst. of Tech., Wright-Patterson AFB, OH. School of Engineering.
SPACECRAFT CHARGE AS A SOURCE OF ELECTRICAL POWER FOR SPACECRAFT M.S. Thesis
Wayne Gale Nov. 1988 107 p
(AD-A202621; AD-E900870; AFIT/GSO/ENP/88D-2) Avail: NTIS HC A06/MF A01 CSCL 22B

This thesis examines the suitability of spacecraft charge, collected at geosynchronous altitude, as a source of electrical power for spacecraft. An analytical plasma probe model is used to describe the flux of charged particle currents on two isolated (conductive) hemispheres of a spacecraft. Surface potentials are evaluated for both a body-stabilized and spin-stabilized spacecraft under average and worst case plasma conditions. A discharge current is simulated, between differentially charged surfaces, to examine the current flow required to balance the surface potentials. This current approximates the maximum current flow available from the spacecraft charge. The results show that surface potential differences can be large in in worst case plasma conditions, but the current available is too small to be useful as a power source. The discharge current does scale up in proportion to spacecraft surface area exposed to the plasma; however, the design of large conductive spacecraft surfaces is a problem in itself. GRA

N89-22650# Martin Marietta Corp., Denver, CO. Astronautics Group.
SPACE PROPULSION HAZARDS ANALYSIS MANUAL (SPHAM). VOLUME 2: APPENDICES Final Report, Dec. 1983 - Jun. 1986
David C. Erdahl, Douglas W. Banning, and Elvis D. Simon Oct. 1988 1178 p
(Contract F04611-84-C-0003)
(AD-A204601; MCR-88-590-Vol-2; AFAL-TR-88-096-Vol-2) Avail: NTIS HC A09/MF A04 CSCL 22A

The Space Propulsion Hazards Analysis manual (SPHAM) is a compilation of methods and data directed at hazards analysis and safety for space propulsion and associated vehicles, but broadly applicable to other environments and systems. It includes methods for compiling imposed requirements and deriving design requirements. It describes in detail the steps to constructing accident scenarios for formal risk assessment. It discusses the approaches to developing probabilities for events in scenarios, and probabilities for scenarios. It illustrates data analysis from experience data for the purpose of probability modeling. The SPHAM provides methods for predicting blast, fragmentation, thermal, acoustic and toxicity post accident environments. The SPHAM describes in overview fashion a large number of qualitative and quantitative analytical methods available to perform hazards analysis complete with guidelines for application. Examples are FMEA, Fault-tree and Energy Analysis. It describes methods to organize analysis by type, phase, or subsystem. Examples are interface hazards analysis, preliminary hazards analysis, and ordnance hazards analysis. Qualitative and quantitative risk assessments are described. The appendices to SPHAM contain voluminous data on available references in the form of an annotated bibliography, summary of the hazardous nature of 27 commodities common to space propulsion, and system description for a variety of space launch vehicles, upper stage vehicles, and spacecraft. GRA

N89-22651*# National Aeronautics and Space Administration. Lewis Research Center, Cleveland, OH.
THE NASA SPACE SOLAR CELL ADVANCED RESEARCH PROGRAM
Dennis J. Flood 1989 9 p Presented at International PVSEC-4, Sydney, Australia, 14-17 Feb. 1989; sponsored by The Institution of Radio and Electronics Engineers of Australia and the Univ. of New South Wales
(NASA-TM-102020; E-4747; NAS 1.15:102020) Avail: NTIS HC A02/MF A01 CSCL 10A

Two major requirements for space solar cells are high efficiency and survivability in the naturally occurring charged particle space radiation environment. Performance limits for silicon space cells are well understood. Advanced cells using GaAs and InP are under development to provide significantly improved capability for the future. Author

N89-22652*# National Aeronautics and Space Administration. Lewis Research Center, Cleveland, OH.
ANALYSIS OF THE NONVENTED FILL OF A 4.96-CUBIC-METER LIGHTWEIGHT LIQUID HYDROGEN TANK
David J. Chato 1989 12 p Proposed for presentation at the 27th National Heat Transfer Conference, Philadelphia, PA, 5-8 Aug. 1989; sponsored by ASME
(NASA-TM-102039; E-4750; NAS 1.15:102039) Avail: NTIS HC A03/MF A01 CSCL 21H

As part of its development of cryogenic fluid management techniques for spacecraft, the NASA Lewis Research Center Cryogenic Fluid Technology Office (CFTO) is planning to perform ground tests of nonvented fill techniques on a 4.96-cubic-meter lightweight liquid hydrogen tank. This tank is similar in size and shape to the tankage planned for CFTO's COLD-SAT liquid hydrogen flight experiment. The analyses used to select two injection systems are presented for nonvented fills of this tank at design flow rates between 220 and 450 kg/hr. The first system uses multiple nozzles spraying from the top of the tank through the ullage space. This system should be capable of liquid fill levels in excess of 95 percent. The second system injects the liquid through a submerged nozzle and should produce fill levels on the order of 80 percent liquid. Author

N89-22653*# National Aeronautics and Space Administration. Lewis Research Center, Cleveland, OH.
NUMERICAL MODEL OF SOLAR DYNAMIC RADIATOR FOR PARAMETRIC ANALYSIS
Jennifer L. Rhatigan 1989 10 p Prepared for presentation at the 24th Intersociety Energy Conversion Engineering Conference, Washington, DC, 6-11 Aug. 1989; sponsored in part by IEEE, AIAA, ANS, ASME, SAE, and AIChE
(NASA-TM-102054; E-4807; NAS 1.15:102054) Avail: NTIS HC A02/MF A01 CSCL 21H

Growth power requirements for Space Station Freedom will be met through addition of 25 kW solar dynamic (SD) power modules. The SD module rejects waste heat from the power conversion cycle to space through a pumped-loop, multi-panel, deployable radiator. The baseline radiator configuration was defined during the Space Station conceptual design phase and is a function of the state point and heat rejection requirements of the power conversion unit. Requirements determined by the overall station design such as mass, system redundancy, micrometeoroid and space debris impact survivability, launch packaging, costs, and thermal and structural interaction with other station components have also been design drivers for the radiator configuration. Extensive thermal and power cycle modeling capabilities have been developed which are powerful tools in Station design and analysis, but which prove cumbersome and costly for simple component preliminary design studies. In order to aid in refining the SD radiator to the mature design stage, a simple and flexible numerical model was developed. The model simulates heat transfer and fluid flow performance of the radiator and calculates area mass and impact survivability for many combinations of flow tube and panel configurations, fluid and material properties, and environmental and cycle variations. A brief description and discussion of the numerical model, it's capabilities and limitations, and results of the parametric studies performed is presented. Author

23 CHEMISTRY AND MATERIALS (GENERAL)

N89-22654# Advisory Group for Aerospace Research and Development, Neuilly-Sur-Seine (France). Propulsion and Energetics Panel.
APPLICATION OF ADVANCED MATERIAL FOR TURBOMACHINERY AND ROCKET PROPULSION
Mar. 1989 282 p In ENGLISH and FRENCH Meeting held in Bath, England, 3-5 Oct. 1988
(AGARD-CP-449; ISBN-92-835-0498-4) Avail: NTIS HC A13/MF A01

The proceedings of the conference are presented. The specialists' meetings were arranged in the following sessions: Overview and Combined Applications; Gas Turbine Applications; Rocket Applications; and Special Applications. A Technical Evaluation report is included at the beginning of the proceedings. The aim of the specialists' meetings was to review the advances made in the field of materials applicable in the hot parts of aerospace propulsion system during the last few years. The meetings offered a forum for the users of new materials in the fields of turbomachines and rockets to report on recent achievements and to discuss the various applications. For individual titles, see N89-22655 through N89-22680.

N89-22655# Air Force Materials Lab., Wright-Patterson AFB, OH. Metals and Ceramics Div.
TECHNICAL EVALUATION REPORT
Norman M. Tallan *In* AGARD, Application of Advanced Material for Turbomachinery and Rocket Propulsion Mar. 1989 11 p
(For primary document see N89-22654 16-23)
Avail: NTIS HC A13/MF A01

A technical evaluation is presented of the materials presented at the 72nd Propulsion and Energetics Panel Specialists' Meeting. The objective of the meeting was to bring together the designers, developers and users of aerospace propulsion systems and the developers and producers of aerospace materials to provide a forum in which the material requirements of both current and future propulsion systems and the ability of emerging new materials to meet those requirements could be reviewed. The scope included the properties and potential applications of superalloys, refractory metals, advanced intermetallic alloys, and metal matrix composites based on them; carbon-carbon and ceramic matrix composites; coatings and the processes used to prepare them; bearing and insulation materials; braze and weld repair methods; innovative design approaches to the use of these new materials; and the damage tolerance and life prediction of these materials and their implications with regard to damage tolerant design and applications to real propulsion systems. E.R.

N89-22656# Pratt and Whitney Aircraft, West Palm Beach, FL. Materials Engineering.
APPLICATION OF ADVANCED MATERIALS FOR TURBOMACHINERY AND ROCKET PROPULSION
Joseph B. Moore *In* AGARD, Application of Advanced Material for Turbomachinery and Rocket Propulsion Mar. 1989 5 p
(For primary document see N89-22654 16-23)
Avail: NTIS HC A13/MF A01

Gas turbine engines of the 1980's and 1990's will require improved nickel and titanium alloys as well as certain intermetallic compounds and low temperature composites. Engines of the 2000's with significantly higher thrust to weight ratios will require lighter weight, higher temperature non-conventional materials including aluminum alloys, titanium metal matrix composites, intermetallic compounds, and ceramic matrix composites. Major concerns once these materials are developed will be the design, manufacture,

inspection, and repair of required components at affordable cost. Current or near-term liquid rocket engines having technology levels equivalent to those being studied for the space transportation and advanced launch systems can benefit from improved materials for turbomachinery, high heat flux throat regions of the thrust chamber, high strength, hydrogen resistant materials for cases and ducts, and refractory materials for uncooled or partially cooled nozzle extensions. To meet the far term goals for advanced rocket engines required for single-stage-to-orbit (SSTO) vehicles materials requirements are not unlike those described above for 21st century gas turbine engines. Author

N89-22657# Deutsche Forschungs- und Versuchsanstalt fuer Luft- und Raumfahrt, Stuttgart (Germany, F.R.). Inst. for Structures and Design.

MONOLITHIC AND FIBER CERAMIC COMPONENTS FOR TURBOENGINES AND ROCKETS **c27**

R. Kochendoerfer *In* AGARD, Application of Advanced Material for Turbomachinery and Rocket Propulsion Mar. 1989 10 p (For primary document see N89-22654 16-23)
Avail: NTIS HC A13/MF A01

From the design point of view, whether or not the existing experience gained during the automotive ceramic turbine development can be transferred to aero jet engines is reviewed. It is well known that design considerations strongly influence the failure tolerance of ceramic structures. Following material adequate design concepts will increase component reliability. Focussing these topics, the future application of ceramics for thermally and/or mechanically high-loaded structures within the propulsion system are discussed. Actual available data of emerging materials as C/C, C/SiC, SiC/Sic are presented. The material's behavior, their potential for structural applications as well as design consequences are evaluated. Author

N89-22658# Royal Aircraft Establishment, Farnborough (England). Space Dept.

CVD AND DIFFUSION COATINGS FOR HIGH TEMPERATURE APPLICATIONS IN TURBOMACHINERY AND ROCKET MOTORS **c27**

S. P. Field, J. E. Restall, C. D. Chalk, and C. Hayman (Fulmer Research Inst. Ltd., Stoke Poges, England) *In* AGARD, Application of Advanced Material for Turbomachinery and Rocket Propulsion Mar. 1989 12 p (For primary document see N89-22654 16-23)
Avail: NTIS HC A13/MF A01

A brief but critical review is presented of recent developments in Chemical Vapor Deposition (CVD) metal and ceramic coatings for aerospace applications, covering in addition to standard CVD, activated CVD, diffusion CVD, pressure pulsed CVD and the more recently explored chemical vapor infiltration (CVI) processing. Fused slurry diffusion coatings are also covered. Important applications of such coatings and free-standing shapes are outlined and illustrated, particularly CVD diffusion aluminizing, chromizing and siliconizing of turbine blades, refractory metal coatings and free-standing components of rocket motors. Future trends in materials technology are also discussed with particular reference to the CVD coating of fibers, including modified carbon-carbon and other ceramic composites for high temperature operation in oxidizing environments. Author

N89-22659# Ministry of Defence, London (England).

FUTURE ADVANCED AERO-ENGINES: THE MATERIALS CHALLENGE **c07**

D. R. Highton and W. J. Chrispin *In* AGARD, Application of Advanced Material for Turbomachinery and Rocket Propulsion Mar. 1989 10 p (For primary document see N89-22654 16-23)
Avail: NTIS HC A13/MF A01

A balanced program of aero-engine advanced engineering is pursued in the UK, and an important and growing element of this program is that devoted to materials and processing technology. The quest for more capable materials is an essential element of that program. The powerplant continues to be a critical factor in improving vehicle capability in all military and civil applications. A position has been reached where further improvements in propulsion depend not only on maintaining current effort in aerothermodynamic technology, but also making substantial investments in new high risk materials technology. E.R.

N89-22660# Rolls-Royce Ltd., Derby (England). Materials Research.

NEW METALLIC MATERIALS FOR GAS TURBINES **c26**

M. A. Hicks *In* AGARD, Application of Advanced Material for Turbomachinery and Rocket Propulsion Mar. 1989 13 p (For primary document see N89-22654 16-23)
Avail: NTIS HC A13/MF A01

The mix of properties required for high performance components in the gas turbine will continue to necessitate the use of metallic materials for the forseeable future. Examples are shown which indicate how a detailed understanding of material/component behavior and a better understanding and control of the manufacturing process are becoming increasingly important in meeting the anticipated design targets. Author

N89-22661# Pratt and Whitney Aircraft, West Palm Beach, FL.

DAMAGE TOLERANCE CONCEPTS FOR ADVANCED MATERIALS AND ENGINES

T. E. Farmer and M. C. VanWanderham *In* AGARD, Application of Advanced Material for Turbomachinery and Rocket Propulsion Mar. 1989 7 p (For primary document see N89-22654 16-23)
Avail: NTIS HC A13/MF A01

Planned increases in thrust to weight for future gas turbine engines require dramatically higher operating temperatures and rotor speeds. This necessitates simpler design, improved materials and sophisticated fabrication techniques. Damage Tolerance Design (DTD) has been established as the basis for gas turbine engine design and maintenance in the U.S. Consideration of damage tolerance has significant influence on configurations and materials. The advanced configurations, bonded structures, composites, anisotropic alloys and less ductile materials required to meet the advanced engine goals challenge the current DTD philosophy. Fortunately, interim plans for incremental increases in performance and engine configuration to meet long-term goals afford the opportunities for developing transition technologies to meet these objectives. Author

N89-22662# Rolls-Royce Ltd., Derby (England).

MATERIAL/MANUFACTURING PROCESS INTERACTION IN ADVANCED MATERIAL TECHNOLOGIES

G. W. Meetham *In* AGARD, Application of Advanced Material for Turbomachinery and Rocket Propulsion Mar. 1989 7 p (For primary document see N89-22654 16-23)
Avail: NTIS HC A13/MF A01

Since the first flight of a gas turbine powered aircraft some forty years ago, tremendous advances in engine performance have been made in terms of thrust, thrust-weight ratio and specific fuel consumption. The performance and efficiency of gas turbine engines is a direct function of the maximum cycle temperature and, throughout the forty years in which the aero gas turbine has existed, this has provided the motivation for the continuous development of materials which are capable of operating at higher temperatures in the turbine section of the engine. Turbine entry temperatures have risen from around 700 C in the Whittle W1 engine in 1941 to around 1350 C in current advanced engines. Author

N89-22663# Fiat Aviazione S.p.A., Turin (Italy). Stress Dept.

DEVELOPMENT OF STRESS AND LIFING CRITERIA FOR SINGLE CRYSTAL TURBINE BLADES **c26**

S. Salvano, M. Stanisci, and E. Campo *In* AGARD, Application of Advanced Material for Turbomachinery and Rocket Propulsion Mar. 1989 9 p (For primary document see N89-22654 16-23)
Avail: NTIS HC A13/MF A01

The stress and lifing criteria applied to turbine blades are discussed, by focusing the relevant features which make single crystal materials different from conventional alloys. The discussion

basis is provided by the material data and blade finite element analyses, collected for the application of single crystal alloys to advanced aircraft engines. Author

N89-22664# Cranfield Inst. of Tech., Bedford (England). School of Industrial Science.

ADVANCED MATERIALS TO COMBAT THE HIGH TEMPERATURE DEGRADATION PROCESSES IN TURBOMACHINERY **c27**

P. Hancock and J. F. Restall (Royal Aircraft Establishment, Farnborough, England) *In* AGARD, Application of Advanced Material for Turbomachinery and Rocket Propulsion Mar. 1989 11 p (For primary document see N89-22654 16-23)

Avail: NTIS HC A13/MF A01

The reasons for the necessity of protective surface coatings on conventional superalloy components are examined. Diffusion coatings, together with newer overlay coatings based on MCrALY compositions produced by electron beam plasma vapor, are examined and their mechanisms of surface breakdown identified. It is suggested that further developments could be made with compositions that are outside the current commercially available coatings. The limitations of the upper operating temperature of conventional coating systems suggest the need for thermal barrier coatings and the conflict between dense coatings for surface protection and porous coatings for essential mechanical stability is examined. Finally, the advantages of fiber reinforced ceramic components are considered, together with potential mechanisms of surface breakdown. Author

N89-22665# Garrett Turbine Engine Co., Phoenix, AZ.

THE DEMONSTRATION OF MONOLITHIC AND COMPOSITE CERAMICS IN AIRCRAFT GAS TURBINE COMBUSTORS **c27**

Frank G. Davis and Dale A. Hudson *In* AGARD, Application of Advanced Material for Turbomachinery and Rocket Propulsion Mar. 1989 10 p (For primary document see N89-22654 16-23)

Avail: NTIS HC A13/MF A01

Since the mid seventies, the Air Force Wright Aeronautical Laboratories Aero Propulsion Laboratory has been on a course to evaluate and demonstrate the application of advanced non-metallic materials in experimental gas turbine engines. Potential increases of several hundred degrees or more in operating temperature represents a quantum leap in engine capability. Since the seventies, combustion rig tests have been successfully performed at near-stoichiometric conditions on two ceramic combustor configurations. These combustors were annular, through-flow designs similar to the metallic burners used in present-day military propulsion gas turbines. The first configuration used monolithic ceramic segments as a portion of the inner and outer combustor liners. The segments were supported by an external metal structure. These segments were fabricated from silicon carbide material. In the most recent program ceramic composite rings were used to form the inner and outer liners. The rings were composed of silicon carbide fibers and a silicon carbide matrix. The ceramic composite rings required no external support structure. Testing consisted of both steady-state and transient operations. During transient testing, the combustors were subjected to rapid thermal cycling. Testing of silicon carbide and silicon nitride ceramic materials has just begun. Author

N89-22666# United Technologies Research Center, East Hartford, CT. Materials Technology.

COMPOSITE MATERIAL SYSTEMS FOR HIGH TEMPERATURE APPLICATIONS **c24**

Earl R. Thompson *In* AGARD, Application of Advanced Material for Turbomachinery and Rocket Propulsion Mar. 1989 13 p (For primary document see N89-22654 16-23)

Avail: NTIS HC A13/MF A01

One approach to the demands of high temperature, structural applications, being actively pursued, is through the development of composite materials. For applications up to approximately 1200 C, the materials research is primarily centered upon the fiber reinforcement of glass and glass-ceramic matrices. For applications above 1200 C, the development of coating systems for the protection of high-strength carbon-carbon composites is the prime focus. In terms of fabrication, the glass and glass-ceramic matrix composites reinforced by carbon and silicon carbide fiber yearns can be understood by considering the thermoplastic nature of the matrix constituent. Continuous, as well as chopped, fibers were successfully used to reinforce these brittle matrices. When optimally fabricated, the resultant composites have displayed a combination of high apparent toughness and high strength at room and elevated temperature. Carbon-carbon composites have extremely high temperature (greater than 2000 C) capability and excellent strength retention in inert environments. The major application limiting property of these composites is the lack of coatings which will provide the required long life, high-temperature oxidation resistance. Multilayer coating approaches which depend upon silicon nitride as the primary oxidation resistant barrier were developed. The background leading to this choice and a consideration of the experience with this coating are considered. Author

N89-22667# Centre de Villaroche, Moissy (France).

UTILIZATION OF HIGH TEMPERATURE COMPOSITES IN TURBOJET ENGINES [UTILISATION DES COMPOSITES HAUTES TEMPERATURES DANS LES TURBOREACTEURS] **c24**

R. Mestre *In* AGARD, Application of Advanced Material for Turbomachinery and Rocket Propulsion Mar. 1989 11 p In FRENCH (For primary document see N89-22654 16-23)

Avail: NTIS HC A13/MF A01

The design of modern military turbojet engines yields a high performance thrust/weight nozzle of composite materials in the hot section of the engine. Within that context, SNECMA, developed ceramic composites for use as afterburning nozzles in the turbines, areas of the engine where the temperature of the gas goes above 2000 K, especially after prolonged use. The materials, CERASEP (SiC-SiC) and SEPCARB (C-SiC) provided by the European Societe of Propulsion is used for nozzle flaps and other pieces of the structure. Some tests were made on the prototype, in order to validate the fabrication procedures and the design concept. The engine parts were made and tested for endurance, while the engine was in operational use. Author

N89-22668# Motoren- und Turbinen-Union Muenchen G.m.b.H. (Germany, F.R.).

INITIAL RESULTS OF TESTS ON METAL-CERAMIC GUIDE VANES **c24**

W. Huether and W. Krueger *In* AGARD, Application of Advanced Material for Turbomachinery and Rocket Propulsion Mar. 1989 5 p (For primary document see N89-22654 16-23)

Avail: NTIS HC A13/MF A01

Metal-ceramic guide vanes consist of an outer ceramic shell and an inner metallic core, which is cooled. The hot gas contacts only the uncooled ceramic shell, so that the total amount of cooling air is reduced to a low value compared with conventional guide vanes. A linear arrangement of four guide vanes in a size which would be suitable for the RB 199 was built and tested with hot gas at atmospheric pressure. It could be shown that material temperature of the ceramic shell higher than 1870 K (2900 F) are possible, under static as well as cyclic loading. Author

N89-22669# Brown, Boveri und Cie A.G., Mannheim (Germany, F.R.). Materials Technology Lab.

INTERACTION OF COATINGS WITH BASE METALS AT HIGH TEMPERATURE **c27**

Hermann W. Gruenling, K. Schneider, and L. Singheiser *In* AGARD, Application of Advanced Materials for Turbomachinery and Rocket Propulsion Mar. 1989 23 p (For primary document see N89-22654 16-23)

Avail: NTIS HC A13/MF A01

The interaction of aluminide, CoCrAlY- and NiCrAlY-based coatings on the nickel-based alloy IN 738 LC was investigated in the temperature range 850 to 1000 C. Due to intensive interdiffusion behavior of CoCrAlY-coatings with Ni-based alloys the coating composition changes to CoNiCrAlY at high temperature. The

degradation of the coating occurs primarily by Al-diffusion into the alloy. NiCrAlY-coatings show less interdiffusion with Ni-based alloys. Coating degradation occurs by oxidation. A similar behavior was observed for aluminide coatings. Interdiffusion effects between coatings and alloys increase N sub v - numbers in the interdiffusion zone resulting in the precipitation of brittle phases. Author

N89-22670*# National Aeronautics and Space Administration. Marshall Space Flight Center, Huntsville, AL.
VACUUM PLASMA SPRAY COATING **c27**
Richard R. Holmes and Timothy N. McKechnie (Rockwell International Corp., Huntsville, AL.) *In* AGARD, Application of Advanced Material for Turbomachinery and Rocket Propulsion Mar. 1989 5 p (For primary document see N89-22654 16-23)
Avail: NTIS HC A13/MF A01 CSCL 11C

Currently, protective plasma spray coatings are applied to space shuttle main engine turbine blades of high-performance nickel alloys by an air plasma spray process. Originally, a ceramic coating of yttria-stabilized zirconia (ZrO2.12Y2O3) was applied for thermal protection, but was removed because of severe spalling. In vacuum plasma spray coating, plasma coatings of nickel-chromium-aluminum-yttrium (NiCrAlY) are applied in a reduced atmosphere of argon/helium. These enhanced coatings showed no spalling after 40 MSFC burner rig thermal shock cycles between 927 C (1700 F) and -253 C (-423 F), while current coatings spalled during 5 to 25 test cycles. Subsequently, a process was developed for applying a durable thermal barrier coating of ZrO2.8Y2O3 to the turbine blades of first-stage high-pressure fuel turbopumps utilizing the enhanced NiCrAlY bond-coating process. NiCrAlY bond coating is applied first, with ZrO2.8Y2O3 added sequentially in increasing amounts until a thermal barrier coating is obtained. The enchanced thermal barrier coating has successfully passed 40 burner rig thermal shock cycles. Author

N89-22671*# National Aeronautics and Space Administration. Lewis Research Center, Cleveland, OH.
THRUST CHAMBER THERMAL BARRIER COATING TECHNIQUES **c27**
Richard J. Quentmeyer *In* AGARD, Application of Advanced Material for Turbomachinery and Rocket Propulsion Mar. 1989 10 p Previously announced as N88-24690 (For primary document see N89-22654 16-23)
Avail: NTIS HC A13/MF A01 CSCL 11C

Methods for applying thermal barrier coatings to the hot-gas side wall of rocket thrust chambers in order to significantly reduce the heat transfer in high heat flux regions has been the focus of technology efforts for many years. A successful technique developed by NASA-Lewis that starts with the coating on a mandrel and then builds the thrust chamber around it by electroforming appropriate materials is described. This results in a smooth coating with exceptional adherence, as was demonstrated in hot fire rig tests. The low cycle fatigue life of chambers with coatings applied in this manner was increased dramatically compared to uncoated chambers. Author

N89-22672# SIGRI Electrogradhit G.m.b.H., Meitingen (Germany, F.R.).
SILICON-CARBIDE COATED CARBON-CARBON: AN ADVANCED MATERIAL FOR ROCKET SYSTEMS **c24**
E. v. Gellhorn, U. Gruber, and H. Leis (Messerschmitt-Boelkow-Blohm G.m.b.H., Munich, Germany, F.R.) *In* AGARD, Application of Advanced Material for Turbomachinery and Rocket Propulsion Mar. 1989 10 p (For primary document see N89-22654 16-23)
Avail: NTIS HC A13/MF A01

To increase the resistance of rocket systems, materials have to be used which can withstand temperatures above 2000 C, as well as erosion and corrosion attack. Carbon fiber-reinforced carbon coated with silicon carbide seems to be the outstanding material suited to resist temperature as well as mechanical requirements. The manufacture of the nozzles is described. Carbon fibers are impregnated with resins, the resins are carbonized to form a closed carbon matrix and the shaped body is coated with silicon carbide. The nozzles were tested for up to 300 seconds in a semi-free jet and a connected pipe test rig for the ramrocket under regular operating conditions. The tests proved the excellent thermal shock resistance of the material, as well as its oxidation resistance. A better understanding of the material properties demanded was obtained. Author

N89-22673*# National Aeronautics and Space Administration. Lewis Research Center, Cleveland, OH.
FIBER REINFORCED SUPERALLOYS FOR ROCKET ENGINES **c26**
Donald W. Petrasek and Joseph R. Stephens *In* AGARD, Application of Advanced Material for Turbomachinery and Rocket Propulsion Mar. 1989 13 p Previously announced as N89-15990 (For primary document see N89-22654 16-23)
Avail: NTIS HC A13/MF A01 CSCL 11F

High pressure turbopumps for advanced reusable liquid propellant rocket engines such as that for the Space Shuttle Main Engine (SSME) require turbine blade materials that operate under extreme conditions of temperature, hydrogen environment, high-cycle fatigue loading, thermal fatigue and thermal shock. Such requirements tax the capabilities of current blade materials. Based on projections of properties for tungsten fiber reinforced superalloy (FRS) composites, it was concluded that FRS turbine blades offer the potential of a several fold increase in life and over a 200 C increase in temperature capability over the current SSME blade material. FRS composites were evaluated with respect to mechanical property requirements for SSME blade applications. Compared to the current blade material, the thermal shock resistance of FRS materials is excellent, two to nine times better, and their thermal fatigue resistance is equal to or higher than the current blade material. FRS materials had excellent low and high-cycle fatigue strengths, and thermal shock-induced surface microcracks had no influence on their fatigue strength. The material also exhibited negligible embrittlement when exposed to a hydrogen environment. Author

N89-22674# Metallwerk Plansee, A.G., Reutte (Austria).
BEHAVIOR OF TUNGSTEN, MOLYBDENUM AND ALLOYS UNDER UNUSUAL HEATING CONDITIONS **c26**
R. Eck, H. Bildstein, F. Simader, R. Stickler (Technische Univ., Vienna, Austria), and J. Tinzl *In* AGARD, Application of Advanced Material for Turbomachinery and Rocket Propulsion Mar. 1989 11 p (For primary document see N89-22654 16-23)
Avail: NTIS HC A13/MF A01

State of the art of fabricability of tungsten by powder metallurgy methods for relevant configurations in relation to final properties desired are summarized. Effects of unisotropy through metal forming and its relevance to design are discussed. For tungsten-thoria alloys, as an example of a refractory ODS alloy, mechanical properties such as DBTT for low temperature stresses and strength, ductility and microstructural data at temperatures up to 3000 K are presented and discussed in context with application considerations. As an alternative tungsten-rhenium alloys containing up to 26 percent Re are discussed in comparison with tungsten-thoria emphasizing advantages of ductility at low temperatures. A simple model of interference of heat dissipation and buildup of thermal stresses in a plate configuration of tungsten is shortly discussed. Relevant properties of the molybdenum alloys Mo5Re to Mo41Re, a selection of Ti, Zr, Hf carbide-oxide dispersion strengthened alloys and molybdenum tungsten alloys are discussed. Limitations of erosion and oxidation inhibiting coatings for refractory metals are explained for advanced chemical and physical methods. Author

N89-22675# Aerospatiale, Saint Medard-en-Jalles (France). Etablissement d'Aquitaine.
HIGH-PERFORMANCE REFRACTORY COMPOSITE MATERIALS [LES MATERIAUX COMPOSITES REFRACTAIRES A HAUTE PERFORMANCE] **c24**
A. Hordonneau *In* AGARD, Application of Advanced Materials for Turomachinery and Rocket Propulsion Mar. 1989 9 p In

FRENCH (For primary document see N89-22654 16-23)
Avail: NTIS HC A13/MF A01

Applications of carbon and ceramic composites to throats and inlet/outlet sections of solid rocket nozzles, combustion chamber elements, and rocket engine mechanical parts are discussed. Application of these materials for hot structures of the Hermes hypersonic vehicle and the STS 2000 space transport vehicle is also discussed. In addition, various procedures associated with the fabrication of carbon and ceramic composites are discussed including the automatic weaving of fiber preforms, automatic densification, and surface treatment. E.R.

N89-22676# Societe Europeene de Propulsion, Saint-Medard-en-Jalles (France).
HIGH TEMPERATURE COMPOSITE MATERIALS FOR ROCKET PROPULSION **c24**
Paul Donguy and Jacques Broca *In* AGARD, Application of Advanced Material for Turbomachinery and Rocket Propulsion Mar. 1989 11 p (For primary document see N89-22654 16-23)
Avail: NTIS HC A13/MF A01

The promises of the composite materials with non degradable matrix like carbon or ceramics in rocket propulsion is shown by examples. From an historial point of view, carbon-carbon materials were first used in solid rocket motor nozzles. More recently, successful all composite hot gas valving systems have incorporated not only carbon-carbon materials, but also thermostable insulators and oxidation resistant materials with silicon carbide matrix. These oxidation resistant materials open the way now for liquid propellant rocket applications such as small thrusters and large nozzle exit-cone. The design philosopy to be followed to reach the best compromise between propulsion requirements and material properties is discussed. Author

N89-22677# Office National d'Etudes et de Recherches Aerospatiales, Palaiseau (France).
CERAMIC HEAT EXCHANGERS AND TURBINE BLADES: THEORY AND EXPERIMENTAL RESULTS [ECHANGEURS DE CHALEUR ET AUBES DE TURBINE EN CERAMIQUE THEORIE ET RESULTATS EXPERIMENTAUX] **c27**
P. Avran and S. Boudigues *In* AGARD, Application of Advanced Material for Turbomachinery and Rocket Propulsion Mar. 1989 11 p In FRENCH; ENGLISH summary (For primary document see N89-22654 16-23)
Avail: NTIS HC A13/MF A01

Theoretical and experimental research on the use of ceramics in gas turbines developed at O.N.E.R.A (the French Aerospace Research Institute) during the last five years is reviewed and discussed. The two main lines of this research are ceramic heat exchangers for high efficiency, low specific fuel consumption gas turbine cycles, and use of ceramics for fixed or moving turbine blades. Author

N89-22678*# National Aeronautics and Space Administration. Marshall Space Flight Center, Huntsville, AL.
CRYOGENIC TURBOPUMP BEARING MATERIALS
Biliyar N. Bhat *In* AGARD, Application of Advanced Material for Turbomachinery and Rocket Propulsion Mar. 1989 10 p (For primary document see N89-22654 16-23)
Avail: NTIS HC A13/MF A01 CSCL 07A

Materials used for modern cryogenic turbopump bearings must withstand extreme conditions of loads and speeds under marginal lubrication. Naturally, these extreme conditions tend to limit the bearing life. It is possible to significantly improve the life of these bearings, however, by improving the fatigue and wear resistance of bearing alloys, and improving the strength, liquid oxygen compatibility and lubricating ability of the bearing cage materials. Improved cooling will also help to keep the bearing temperatures low and hence prolong the bearing life. Author

N89-22679# Defence Research Establishment Valcartier (Quebec).
DEVELOPMENT OF AN ASBESTOS-FREE INSULANT FOR ROCKET MOTORS **c27**
D. Sanschagrin and G. Couture *In* AGARD, Application of Advanced Material for Turbomachinery and Rocket Propulsion Mar. 1989 10 p (For primary document see N89-22654 16-23)
Avail: NTIS HC A13/MF A01

As a result of concerns about restrictions on the industrial use of asbestos, DREV initiated a research project aimed at replacing asbestos in the rocket motor insulant designated RF/B. RF/B is a polymer composite consisting of a carboxyl terminated polybutadiene filled with asbestos. While retaining the same polymeric resin, a combination of fibers (Kevlar, Refrasil and Pyron) and fillers (kaolin and Mg(OH)2) was used to obtain formulations compatible with the processing of RF/B, which is based on the use of a sigma-blade mixer and two roll mills. The mechanical properties of the new material and its suitability in CRV7 rocket motors were assessed. Author

N89-22680# Centre de Recherches Metallurgiques, Liege (Belgium).
METALLURGICAL STUDY OF SUPERALLOY BRAZING ALLOYS **c26**
Ch. Lecomte-Mertens and W. Bex (FN Moteurs, Mimort, Belgium) *In* AGARD, Application of Advanced Material for Turbomachinery and Rocket Propulsion Mar. 1989 12 p (For primary document see N89-22654 16-23)
Avail: NTIS HC A13/MF A01

For a better understanding of the new superalloy repair or joining process, it is important to know the metallurgical behavior of more conventional brazing alloys more or less doped with melting point depressants such as aluminum boron and/or silicon especially during the diffusion-brazing treatment. Therefore, the brazing results on calibrated slots of different widths were metallographically compared after variable brazing and diffusion time-temperature cycles. The composition of the different phases present in the tested brazing alloys were also determined with the scanning electron microscope. Moreover, evaluation testings as fatigue and thermal shocks were performed to compare new and repaired parts. Finally, it was possible to evaluate the best time-temperature cycles bringing a satisfactory homogenization, while keeping them compatible with the eventual subsequent heat treatments and with the requirements of an economical industrial production. Author

N89-22681# Midwest Research Inst., Golden, CO. Solar Energy Research Inst.
MEASUREMENT UNCERTAINTY OF ADSORPTION TESTING OF DESICCANT MATERIALS
Carl E. Bingham and Ahmad A. Pesaran Dec. 1988 8 p Presented at the American Society of Mechanical Engineers Solar Energy Conference, San Diego, CA, 2-4 Apr. 1989
(Contract DE-AC02-83CH-10093)
(DE89-000841; SERI/TP-254-3454; CONF-890436-8) Avail: NTIS HC A02/MF A01

The technique of measurement uncertainty analysis as described in the current ANSI/ASME standard is applied to the testing of desiccant materials in SERI's Sorption Test Facility. This paper estimates the elemental precision and systematic errors in these tests and propagates them separately to obtain the resulting uncertainty of the test parameters, including relative humidity (+ or - .03) and sorption capacity (+ or - .002 g/g). Errors generated by instrument calibration, data acquisition, and data reduction are considered. Measurement parameters that would improve the uncertainty of the results are identified. Using the uncertainty in the moisture capacity of a desiccant, the design engineer can estimate the uncertainty in performance of a dehumidifier for desiccant cooling systems with confidence. DOE

N89-22682*# National Aeronautics and Space Administration. Lyndon B. Johnson Space Center, Houston, TX.
IN-SPACE TECHNOLOGY DEVELOPMENT: ATOMIC OXYGEN AND ORBITAL DEBRIS EFFECTS
James T. Visentine and Andrew E. Potter, Jr. May 1989 42 p
(NASA-TM-102154; S-593; NAS 1.15:102154) Avail: NTIS HC A03/MF A01 CSCL 07A

Earlier Shuttle flight experiments have shown atomic oxygen within the orbital environment can interact with many materials to produce surface recession and mass loss and combine catalytically with other constituents to generate visible and infrared glows. In addition to these effects, examinations of returned satellite hardware have shown many spacecraft materials are also susceptible to damage from high velocity impacts with orbital space debris. These effects are of particular concern for large, multi-mission spacecraft, such as Space Station and SDI operational satellites, that will operate in low-Earth orbit (LEO) during the late 1990's. Not only must these spacecraft include materials and exterior coatings that are resistant to atomic oxygen surface interactions, but these materials must also provide adequate protection against erosion and pitting that could result from numerous impacts with small particles (less than 100 microns) of orbital space debris. An overview of these concerns is presented, and activities now underway to develop materials and coatings are outlined that will provide adequate atomic protection for future spacecraft. The report also discusses atomic oxygen and orbital debris flight experiments now under development to expand our limited data base, correlate ground-based measurments with flight results, and develop an orbital debris collision warning system for use by future spacecraft. Author

24 COMPOSITE MATERIALS

Includes physical, chemical, and mechanical properties of laminates and other composite materials.
For ceramic materials see *27 Nonmetallic Materials.*

N89-22683# Air Force Inst. of Tech., Wright-Patterson AFB, OH. School of Engineering.
DAMAGE INITIATION IN TWO-DIMENSIONAL, WOVEN, CARBON-CARBON COMPOSITES M.S. Thesis
James C. Dendis Dec. 1988 134 p
(AD-A202617; AD-E900870; AFIT/GAE/AA/88D-7) Avail: NTIS HC A07/MF A01 CSCL 11D

This thesis examines the failure initiation characteristics of uncoated, 2-D, warp-aligned, ACC-4 Carbon Carbon Composites in standard three-point bend experiments. ASTM-2344 short beam shear tests were run on specimens with a span-to-depth ratio of four, five, and fifteen. Failure load and indications of failure initiation were recorded on a load-displacement curve. Actual specimen mid-span displacement was recorded instead of the usual cross-head displacement. Specimens were micro photographed for pre- and post-test comparisons. Halftone repreductions of the photographs are included to show similarities and differences in failures of the various length specimens. A linear elastic NASTRAN finite element model was used to predict the global stress field. Displacements predicted by this model are within 5 percent of mean experimental values. Failure initiation sites and loads were predicted with contour plots of the Tsai-Wu and Tsai-Hill failure criteria. This model predicts failure initiation at loads near 50 percent of maximum loan in the short specimens. A series of increasing step load test were run to collect photos of specimen damage at loads less than maximum. The results are consistent with model predictions with initial damage occurring at 45 percent of max load in the short beam. Author

N89-22684*# National Aeronautics and Space Administration. Lewis Research Center, Cleveland, OH.
THE ISOTHERMAL FATIGUE BEHAVIOR OF A UNIDIRECTIONAL SIC/TI COMPOSITE AND THE TI ALLOY MATRIX
John Gayda, Jr., Timothy P. Gabb, and Alan D. Freed Apr. 1989 36 p
(NASA-TM-101984; E-4683; NAS 1.15:101984) Avail: NTIS HC A03/MF A01 CSCL 11D

The high temperature fatigue behavior of a metal matrix composite (MMC) consisting of Ti-15V-3Cr-3Al-3Sn (Ti-15-3) matrix reinforced by 33 vol percent of continuous unidirectional SiC fibers was experimentally and analytically evaluated. Isothermal MMC fatigue tests with constant amplitude loading parallel to the fiber direction were performed at 300 and 550 C. Comparative fatigue tests of the Ti-15-3 matrix alloy were also conducted. Composite fatigue behavior and the in-situ stress state of the fiber and matrix were analyzed with a micromechanical model, the Concentric Cylinder Model (CCM). The cyclic stress-strain response of the composite was stable at 300 C. However, an increase in cyclic mean strain foreshortened MMC fatigue life at high strain ranges at 550 C. Fatigue tests of the matrix alloy and CCM analyses indicated this response was associated with stress relaxation of the matrix in the composite. Author

N89-22685# Aeronautical Research Labs., Melbourne (Australia).
ENVIRONMENTAL PROGRAM ON DURABILITY OF GRAPHITE/EPOXY HONEYCOMB SPECIMENS WITH REPRESENTATIVE DAMAGE AND REPAIRS Interim Report
P. D. Chalkley and R. J. Chester Jul. 1988 39 p
(AR-005-504; ARL-MAT-TM-397) Avail: NTIS HC A03/MF A01

An experimental trial is underway to determine the effect of tropical exposure, cyclic loading, and thermal cycling on the long term durability of damaged graphite-epoxy laminates. No damage growth was observed after 300,000 cycles at a strain level of 2500 microstrain. Author

N89-22686# Rockwell International Science Center, Thousand Oaks, CA.
FIBER MATRIX INTERFACE EFFECTS IN FAILURE OF CERAMIC MATRIX FIBER COMPOSITES Annual Report No. 3, 15 Jul. 1987 - 14 Jul. 1988
D. Marshall Jan. 1989 176 p
(Contract N00014-85-C-0416)
(AD-A204618; SC5432.AR) Avail: NTIS HC A09/MF A01 CSCL 11B

Macroscopic and microscopic mechanical properties of ceramic composites have been investigated. A general analytical expression was obtained for the steady-state matrix cracking stress in composites that fail noncatastrophically. The solution is expressed in terms of the stress-displacement relation that characterizes stretching of the fibers between the crack surfaces, and is applicable to any reinforcement that forms crack bridging ligaments, including ductile reinforcements. The influence of statistical distributions of fiber strengths on nonsteady state and steady state matrix cracking, as well as on transitions in failure mechanism between catastrophic and noncatastrophic modes, has been evaluated. The indentation fiber-pushing technique that was developed previously under this contract for measuring fiber-matrix interfacial properties has been further extended to allow measurement of residual stresses in individual fibers. GRA

N89-22687# Adtech Systems Research, Inc., Dayton, OH.
THREE-DIMENSIONAL RESPONSE OF COMPOSITES Final Report, 1 Jun. 1985 - 31 May 1988
S. R. Soni, S. Chandrashekara, G. P. Tandon, U. Santosh, and Ten-Lu Hsiao Jan. 1989 146 p
(Contract F33615-85-C-5034)
(AD-A204623; AFWAL-TR-88-4242) Avail: NTIS HC A07/MF A01 CSCL 11D

This report contains analytical models developed for the prediction of three-dimensional response of composites. Two aspects of the problem of stress and failure analysis are considered. One pertains to a macromechanical model which the development of a global-local finite element method for stress analysis of composite laminates is given. The other aspect incorporates a micromechanics approach leading to a model, termed NDSANDS, for the stress and failure analysis of carbon-carbon composites.

Again, the global-local formulation for the laminate stress analysis is numerically solved by two different finite element techniques. The NDSANDS model incorporates the effects of processing by evaluating the residual stresses due to hygrothermal effects. A number of problems has been solved for illustrating the effectiveness of all the above mentioned models, It is believed that these models are of extreme importance in studying the optimum design parameters in structural composites. GRA

N89-22688# Naval Air Development Center, Warminster, PA. Aircraft and Crew Systems Technology Directorate.
THE EFFECTS OF PLASTIC MEDIA BLASTING PAINT REMOVAL ON THE MICROSTRUCTURE OF GRAPHITE/EPOXY COMPOSITE MATERIALS Final Report, Oct. 1986 - Oct. 1987
Joseph Kozol, Steven Thoman, and Kenneth Clark 7 Oct. 1988 45 p
(AD-A204801; NADC-88109-60) Avail: NTIS HC A03/MF A01 CSCL 11D

Plastic media blasting (PMB) was assessed as a paint removal method for AS4/3501-6 and IM6/3501-6 graphite epoxy (Gr/Ep) composite materials. Microstructural effects on these composite materials were evaluated after repeated paint/blast cycles. Polyester (type 1) and urea formaldehyde (type 2) plastic media materials were used in a variety of blast conditions. Ultrasonic inspection, optical microscopy and scanning electron microscopy were used to assess the damage induced during paint removal. After one paint/blast cycle, most of the blast conditions caused little or no visual damage to the composite substrates. After four paint/blast cycles, several of the conditions caused minimal visual damage. Paint removal by sanding caused more visual damage after one paint removal cycle than any of the repeat blast conditions that were evaluated. GRA

N89-22689# Pittsburgh Univ., PA. Dept. of Physics and Astronomy.
FAR- AND MID-INFRARED PROPERTIES OF METAL-INSULATOR COMPOSITE MATERIALS Annual Letter Report, 1 Jan. - 31 Dec. 1988
Robert P. Devaty 1988 40 p
(Contract N00014-85-K-0808)
(AD-A204914) Avail: NTIS HC A03/MF A01 CSCL 11D

The infrared properties of thin Pt/Al2O3 granular metal-insulator composite films (cermets) were investigated using Fourier transform spectroscopy. The films were grown by dual electron beam evaporation onto polished single crystal sapphire substrates. They were borrowed from Dr. J. V. Mantese of General Motors Research Labs. The metallic volume fraction, which was controlled by the deposition conditions, ranged from 23 percent to 100 percent in the set of samples. The percolation threshold estimate from the temperature dependence of the dc resistance is greater than 50 percent, which implies that the Pt particles are highly correlated. The percolation threshold for a random metal-insulator mixture is less than 20 percent. The transmission and relative reflection of the films were measured at room temperature using a Nicolet 740 Fourier transform infrared spectrometer (FTIR), which arrived at the beginning of the year. The mid and near infrared regions (400 to 15250 cm-1) were covered using three combinations of sources, beamsplitters, and detectors. The reflection standard was a 100 percent Pt film from the sample set. GRA

N89-22690# Utah Univ., Salt Lake City. Dept. of Materials Science and Engineering.
ALUMINA REINFORCED TETRAGONAL ZIRCONIA (TZP) COMPOSITES Progress Report
D. K. Shetty 1988 10 p
(Contract DE-FG02-87ER-45312)
(DE89-008880; DOE/ER-45312/1) Avail: NTIS HC A02/MF A01

During the past year, research progressed in three areas. These are: (1) Studies of Interfacial Bonding and Sliding Friction in Ceramic-Matrix Composites, (2) Fabrication and Characterization of Al2O3 - Reinforced Zirconia Composites, and (3) Application of Electrical-Mechanical Analog to Composites. During this period, one technical paper appeared in the Journal of the American Ceramic Society and three other technical papers are in different stages of publication. A list of publications and their current status are given separately in this report. DOE

N89-22691 National Physical Lab., Teddington (England). Div. of Materials Applications.
NEW THEORETICAL MODEL OF STRESS TRANSFER BETWEEN FIBRE AND MATRIX IN A UNIAXIALLY FIBRE REINFORCED COMPOSITE
L. N. McCartney Nov. 1988 46 p Presented at the World Materials Congress, Chicago, IL, 26-30 Sep. 1988
(NPL-DMA(A)168; ISSN-0143-7313; ETN-89-94205) Copyright Avail: National Physical Lab., Teddington, Middlesex, TW11 0LW, England

An analytical method was developed to predict the stress transfer between fiber and matrix in a uniaxially fiber reinforced composite, associated with either a single matrix crack or a fiber break. Thermal residual stresses arising from a mismatch in thermal expansion coefficients between the fiber and matrix, and Poisson ratio mismatches are accounted for. The theoretical approach retains all relevant stress and displacement components and satisfies exactly the equilibrium equations and the boundary conditions involving stresses. Two of the four stress-strain-temperature relations are satisfied exactly while the remaining two are satisfied only in an average sense, as are the displacement boundary conditions. The general representation is used to solve three types of stress transfer problem. A matrix crack and a broken fiber are analyzed for the case when there is perfect bonding between fiber and matrix. The third type of problem takes account of frictional slip at the interface governed by the Coulomb friction law. Predictions are presented of the stress distributions along the fiber matrix interface and in particular the length of the frictional slip zone is related to applied strain, friction coefficient, fiber volume fraction, and the difference between the test and manufacturing temperatures. ESA

N89-22692*# National Aeronautics and Space Administration. Langley Research Center, Hampton, VA.
SOLUTION OF MULTI-CENTER MOLECULAR INTEGRALS OF SLATER-TYPE ORBITALS
H. Tai Jan. 1989 35 p
(NASA-TM-101545; NAS 1.15:101545) Avail: NTIS HC A03/MF A01 CSCL 11D

The troublesome multi-center molecular integrals of Slater-type orbitals (STO) in molecular physics calculations can be evaluated by using the Fourier transform and proper coupling of the two center exchange integrals. A numerical integration procedure is then readily rendered to the final expression in which the integrand consists of well known special functions of arguments containing the geometrical arrangement of the nuclear centers and the exponents of the atomic orbitals. A practical procedure was devised for the calculation of a general multi-center molecular integrals coupling arbitrary Slater-type orbitals. Symmetry relations and asymptotic conditions are discussed. Explicit expressions of three-center one-electron nuclear-attraction integrals and four-center two-electron repulsion integrals for STO of principal quantum number n=2 are listed. A few numerical results are given for the purpose of comparison. Author

N89-22693# Oak Ridge National Lab., TN.
BEHAVIOR OF IRON ALUMINIDES IN OXIDIZING AND SULFIDIZING ENVIRONMENTS
P. F. Tortorelli, J. H. DeVan, and J. R. DiStefano 1989 15 p Presented at WESTEC '89: High Temperature Intermetallics Symposium, Los Angeles, CA, 21 Mar. 1989
(Contract DE-AC05-84OR-21400)
(DE89-008919; CONF-890394-1) Avail: NTIS HC A03/MF A01

To date, use of iron aluminides based on Fe3Al (less than or equal to 30 at. percent Al) or FeAl (30 to 50 at. percent Al) for structural applications has been limited by their low ductility and poor fracture toughness at room temperature and inadequate

strength above 600 C. However, in recent years, a renewed effort has been devoted to the development of ductile iron aluminides with increased strength, particularly in view of their good potential for use in hostile environments. While it is expected that such aluminides will be able to form oxide scales for corrosion protection in oxidizing high temperature environments, resistance to degradation in oxidizing salt or oxidizing/sulfidizing gas environments has not been adequately addressed as a function of compositional and microstructural changes. This paper reviews and extends results for iron aluminides exposed to an oxidizing/sulfidizing gas and presents the first data for corrosion of this class of materials by an aggressive oxidizing molten nitrate salt of 48.5NaNO3-50.5KNO3-1Na2O2. DOE

N89-22694# Brookhaven National Lab., Upton, NY. Medical Dept.

EXAFS STUDIES OF MULTILAYER INTERFACES

S. M. Heald and G. M. Lamble 1988 13 p Presented at the Fall Meeting of the Materials Research Society, Boston, MA, 28 Nov. 1988

(Contract DE-AC02-76CH-00016)

(DE89-009527; BNL-41404; CONF-881155-55) Avail: NTIS HC A03/MF A01

Important for the understanding of multilayer materials is a determination of their interface structure. The extended X-ray absorption fine structure (EXAFS) technique can be useful, particularly for interfaces with a high degree of structural disorder. This paper reviews the application of EXAFS to multilayers, and describes the standing wave enhancement of the EXAFS from multilayer interfaces. Examples are given for W-C and Ni-Ti multilayers. DOE

N89-22695# Argonne National Lab., IL. Materials and Components Technology Div.

OBSERVATIONS ON THE TOUGHENING OF Al2O3-SiC COMPOSITES

J. P. Singh, S. Smith, and R. O. Scattergood (North Carolina State Univ., Raleigh.) Dec. 1988 10 p Presented at the 7th International Symposium on Ceramics, Bologna, Italy, 14-16 Dec. 1988

(Contract W-31-109-eng-38)

(DE89-009843; CONF-881207-2) Avail: NTIS HC A02/MF A01

Findings are presented regarding the effects of the volume fraction of SiC whiskers and the oxygen content of the whiskers on the mechanical properties of SiC-whisker-reinforced Al2O3 matrix composites. The fracture toughness (K sub IC) of the composites increased with increasing whisker content and a value of 10.7 MPa sq root of m was obtained at 25 vol. pct whisker content. This approximately threefold increase in K sub IC of Al2O3 with whisker addition is believed to be due to energy absorption as a result of interaction between whiskers and crack front, causing crack deflection, whisker pullout, and crack bridging. The strength of the composites, on the other hand, remained generally unchanged up to approximately 25 vol. pct whisker content, above which it decreased slightly. The slight decrease in strength is attributed to the presence of residual tensile stresses in the matrix and the large critical flaws introduced during processing. The presence of a large silica layer on the whisker surface degraded the whiskers during hot pressing in vacuum (6.7 x 10(-2)Pa) environment, which resulted in reduced fracture toughness. DOE

N89-22696# Argonne National Lab., IL. Materials and Components Technology Div.

FRACTURE TOUGHNESS OF MgCr2O4-BASED REFRACTORY COMPOSITES

J. P. Singh and R. B. Poeppel Nov. 1988 18 p Presented at the 7th International Symposium on Ceramics, Bologna, Italy, 14-16 Dec. 1988

(Contract W-31-109-eng-38)

(DE89-009847; CONF-881207-3) Avail: NTIS HC A03/MF A01

The effects of unstabilized ZrO2 and W inclusions on the fracture surface energy and thermal-shock resistance of MgCr2O4 have been characterized. The fracture surface energy increased with increasing ZrO2 content and decreased as the ZrO2 content increased further. The increase in fracture surface energy for MgCr2O4-W with increasing W content was monotonic for the range of composition studied (less than or equal to 10.3 vol pct W). It is proposed that these fourfold increases in fracture surface energy result from the absorption of energy due to microcrack formation in the MgCr2O4 matrix, which results from the tensile stresses due to the mismatch in thermal expansion coefficient and/or elastic modulus between the matrix and inclusions. In addition, for MgCr2O4-ZrO2 composites, a major cause of microcracking is the tetragonal yields monoclinic phase transformation of ZrO2 and the associated volume expansion. Thermal quench experiments indicated substantial improvements in the thermal-shock resistance of MgCr2O4 with appropriate ZrO2 and W additions. DOE

N89-22697# Argonne National Lab., IL. Materials and Components Technology Div.

INTERNAL STRESSES IN CERAMIC COMPOSITE CONSTITUENTS DETERMINED BY NEUTRON DIFFRACTION TECHNIQUE

J. P. Singh, D. S. Kupperman, and S. Majumdar Jun. 1988 18 p Presented at the 3rd International Symposium on Ceramic Materials and Components for Engines, Las Vegas, NV, 28-30 Nov. 1988

(Contract W-31-109-eng-38)

(DE89-009883; CONF-881125-5) Avail: NTIS HC A03/MF A01

The volumetric internal strains in the constituents of two ceramic composites, SiC whisker-reinforced Al2O3 matrix and monoclinic ZrO2 dispersed in cubic ZrO2 matrix have been measured with the Argonne Intense Pulsed Neutron Source and Powder Diffractometer. The corresponding stresses were determined from strain measurements. The internal strains in Al2O3/SiC have been observed to relax with increasing temperature, extrapolating to zero strain at approximately 1400 C. For ZrO2 composites, 0.29 pct compressive strain was measured in monoclinic ZrO2 particles for composites with 4 wt pct monoclinic ZrO2 content. This strain was observed to relax to 0.12 pct at 10 wt pct monoclinic ZrO2 contents. It is believed that this strain relaxation is probably due to the microcracking of cubic ZrO2 matrix as a result of large hydrostatic tensile stresses developed in the matrix at higher monoclinic ZrO2 content. DOE

N89-22698# Lawrence Livermore National Lab., CA. Chemistry and Materials Science.

ATOMIC IMAGING OF Au/Ni MULTILAYERS

M. A. Wall and A. F. Jankowski Mar. 1989 19 p Presented at the 16th International Conference on Metallurgical Coatings and Equipment Exhibit, San Diego, CA, 17-21 Apr. 1989 Submitted for publication

(Contract W-7405-eng-48)

(DE89-009903; UCRL-99853; CONF-890468-4) Avail: NTIS HC A03

The role of interfaces in materials often plays a decisive part in determining physical properties. The order/disorder state of the interfacial structure, induced during the composition modulated synthesis, becomes increasingly property significant as the multilayer period decreases, i.e., the proportional number of interfaces increases. The presence or lack of interlayer coherency is dependent on the atomic misfit between host lattices compounded with short-long range interactions, as well as the deposition dependent growth morphology. The use of high resolution electron microscopy (HREM) to atomically image the structure of Au/Ni multilayers will provide unique insight into the interfacial role in the supermodulus effect (a several fold increase in the biaxial modulus above homogeneous solution values which takes place over a narrow layer thickness range). This critical range of multilayer periods, between 1 and 3 nm, corresponds to a high interface volume fraction. A strain-wave description of atomic displacements coincident with the multilayer period appears appropriate to explain the highly distorted, single phase structure observed on an atomic scale. DOE

N89-22699# Etablissement Technique Central de l'Armement, Arcueil (France). Service Technologie des Materiaux.
FILAMENT WINDING MANUFACTURING OF LONG FIBER COMPOSITE MATERIALS IN THERMOPLASTIC MATRIX Final Report [ETUDE DE LA MISE EN OEUVRE PAR ENROULEMENT FILAMENTAIRE DE MATERIAUX COMPOSITES A FIBRES LONGUES ET MATRICES THERMOPLASTIQUES]
Didier Lucas and Delamare 25 May 1987 53 p In FRENCH
(Contract DRET/SDCE-85-1487)
(ETCA-87-R-047; ETN-89-94349) Avail: NTIS HC A04/MF A01

The manufacturing procedure includes the preheating of preimpregnated ribbons to the resin melt point, keeping it hot once deposited on the rotating spindle, and a precise temperature regulation system to avoid resin degradation. A classical winding machine was used, adding heating and temperature regulating systems. The microscope examination of specimens show an excellent fiber wetting and compactation. ESA

N89-22700# Etablissement Technique Central de l'Armement, Arcueil (France). Service Technologie des Materiaux.
INFLUENCE OF CONDITIONING ON THE TRAPEZOIDAL FATIGUE BEHAVIOR OF A CARBON EPOXY COMPOSITE [INFLUENCE DE DIFFERENTS CONDITIONNEMENTS SUR LE COMPORTEMENT EN FATIGUE TRAPEZOIDALE D'UN COMPOSITE CARBONE/EPOXY]
C. Cazeneuve and P. Herrou 9 Jun. 1987 71 p In FRENCH
(Contract DRET/SDR/G8-83-1028)
(ETCA-87-R-052; ETN-89-94351) Avail: NTIS HC A04/MF A01

The effects of heat and moisture conditioning on the viscoelastic and fatigue behavior of a T300/914 composite were studied. The evolution of composite behavior is characterized by an increase of deformation capacity which allows the reorientation of fibers and an increase of rigidity and the possibility of creating damage associated to this fiber reorientation. This behavior is in good agreement with the viscoelastic properties shown at the torsion pendulum test. ESA

N89-22701# Etablissement Technique Central de l'Armement, Arcueil (France). Service Technologie des Materiaux.
DYNAMIC BEHAVIOR OF A CARBON EPOXY COMPOSITE Final Report [COMPORTEMENT DYNAMIQUE D'UN COMPOSITE CARBONE/EPOXY]
C. Cazeneuve 5 Jan. 1987 54 p In FRENCH
(Contract DRET/SDR-84-1022)
(ETCA-87-R-001; ETN-89-94352) Avail: NTIS HC A04/MF A01

Starting from microfracturographic analysis of unidirectional composites exposed to dynamic compression loading, the degradation and mechanical behavior of a carbon epoxy composite are studied. The fracture surfaces obtained in quasi-static regime are examined. It is shown that the 5208 epoxy matrix is involved in the degradation mechanism. There is shear of the matrix itself when loading is oriented in the fiber direction. These observations allow us to assess the viscoelastic character of the mechanical behavior. ESA

N89-22702# Aerospatiale, Suresnes (France). Direction Centrale de la Qualite.
TESTS OF NEW MATERIALS WITH SECOND GENERATION CARBON FIBERS, TEST REPORT [ESSAIS CSPC 319-20 SONDAGE SUR NOUVEAUX MATERIAUX AVEC FIBRES DE CARBONE DE DEUXIEME GENERATION. PROCES-VERBAL 47-188F]
J. Odorico, G. Pellan, and R. Perrier 23 Jan. 1987 51 p In FRENCH
(Contract STPA-83-96-003)
(Rept-47-188/F; ETN-89-94355) Avail: NTIS HC A04/MF A01

Material to implement the mainframe structure of future aircraft were tested. The results presented refer to five carbon-epoxy systems. The tests include tensile tests, interlayer shearing, flexion on unidirectional specimens, tensile on crossed ply specimens, delamination sensitivity, and influence of holes on the mechanical behavior. Improvements of up to 50 pct of the mechanical characteristics are found. ESA

N89-22703# Aerospatiale, Suresnes (France). Direction Centrale de la Qualite.
CSPC TEST 319.30: STUDY ON IMPACT TOLERANCE OF PREIMPREGNATED CARBON-EPOXY SYSTEMS [ESSAI CSPC 319.30: ETUDE DE LA TOLERANCE AUX CHOCS DES PREIMPREGNES CARBONE-EPOXY. PROCES-VERBAL 47-323/F]
B. Soulezelle and J. Odorico 21 Dec. 1988 57 p In FRENCH
(Rept-47-323/F; ETN-89-94356) Avail: NTIS HC A04/MF A01

Standard tests aiming to evaluate the impact behavior of carbon epoxy structural aircraft components are described. After impact testing, the specimens are tested in compression or static traction. The method allows to determine the loss of mechanical characteristics due to impact. The designer must then use a maximum admissible stress corresponding to maximum invisible impact damage. ESA

N89-22704# Aerospatiale, Suresnes (France). Direction Centrale de la Qualite.
IMPROVING HOLE BORING YIELD IN CARBON EPOXY COMPOSITES WITH TENSILE LOADING [AMELIORATION DU RENDEMENT DE PERCAGE DES COMPOSITES CARBONE EPOXY TRAVAILLANT EN TRACTION. PROCES-VERBAL 47-324/F]
J. Odorico and G. Pellan 3 Mar. 1987 70 p In FRENCH
(Contract STPA-84-96-023)
(Rept-47-324/F; ETN-89-94357) Avail: NTIS HC A04/MF A01

Experimental tests were performed using three types of composite materials and specimens with varying ply orientations with and without holes. The results show that the orientation of plys within a 10 deg range does not affect the mechanical characteristics of holed specimens. A local fiber reinforcement at the edge of the hole improves the yield up to 50 percent. ESA

N89-22705# Office National d'Etudes et de Recherches Aerospatiales, Paris (France). Direction Scientifique de la Resistance des Structures.
ULTRASONIC DETECTION OF DAMAGE IN CARBON EPOXY COMPOSITE MATERIALS Final Report [DETECTION PAR ULTRASONS DE L'ENDOMMAGEMENT DES MATERIAUX COMPOSITES CARBONE EPOXY]
H. Kaczmarek and J. Renard May 1988 71 p In FRENCH
(Contract STPA-85-95-004)
(ONERA-RT-3/7256-RY-071-R; ETN-89-94361) Avail: NTIS HC A04/MF A01

Theoretical and experimental flaw detection are presented. The measurements were carried on with a 15 MHz transducer. A data processing and defect visualization computer program is detailed. The visualization of transversal cracking is only partially solved. Possible corrective measures and improvements are discussed. ESA

N89-22706# Deutsche Forschungs- und Versuchsanstalt fuer Luft- und Raumfahrt, Brunswick (Germany, F.R.). Inst. fuer Strukturmechanik.
MECHANICAL PROPERTIES AND DAMAGE MECHANISMS OF CARBON FIBER REINFORCED COMPOSITES: COMPRESSION LOADING
Heinrich W. Bergmann Aug. 1988 423 p
(DFVLR-FB-88-41; ISSN-0171-1342; ETN-89-94376) Avail: NTIS HC A18/MF A01; DFVLR, VB-PL-DO, Postfach 90 60 58, 5000 Cologne, Fed. Republic of Germany, DM 150

The fracture properties and the damage mechanisms of unnotched and notched graphite/epoxy laminates were investigated. The response of unidirectional and multidirectional stacking sequences under static compression loading, under

constant amplitude cycling in the compression-compression and tension-compression regime, and under thermal cycling simulating the temperatures in a low Earth orbit was studied. The relationships between damage state and residual stiffness and strength under different environmental conditions were examined. Multidirectional laminates containing delaminations were emphasized. The X-ray radiography, ultrasonic C-scanning, and acoustic emission techniques, and a reflection method were used to characterize and monitor the damage states. The laminates were sectioned to compare the global laminate properties with macro and microscopic modes of failure. The understanding of the damage mechanisms and fatigue behavior of carbon fiber reinforced composites was enhanced. ESA

N89-22707# Aeronautical Research Inst. of Sweden, Stockholm. Structures Dept.
A SURVEY OF POLY-ETHER-ETHER-KETONE AND ITS ADVANCED COMPOSITES
Soren Nilsson Dec. 1988 55 p
(Contract FMV-FFL-82250-86-169-25-001)
(FFA-TN-1988-37; ETN-89-94545) Avail: NTIS HC A04/MF A01

The suitability of PEEK for aircraft structures was reviewed. Its major advantages compared to present epoxy matrix systems are: increased toughness; better impact resistance; greater ease of repair; less hygroscopic; infinite shelf-life; some metal forming operations are transferable to thermoplastic forming; and quality of material may be better in terms of less batch-to-batch variation. However, in processing thermoplastics one can encounter; higher pressures and temperatures; and difficulties with fiber-wet-out at the higher molecular weights and consequently higher void contents. ESA

N89-22708 Northwestern Univ., Evanston, IL.
DAMAGE DEVELOPMENT, PROPERTY DEGRADATION AND LIFE PREDICTION IN COMPOSITE LAMINATES Ph.D. Thesis
Jae-Won Lee 1988 326 p
Avail: Univ. Microfilms Order No. DA8902656

Damage mechanisms and accumulation and associated stiffness reduction in cross-ply graphite/epoxy laminates subjected to quasi-static and tension-tension fatigue loadings were investigated. The initiation of longitudinal matrix cracking was observed at approximately 65 percent of the normalized logarithmic lifetime (log n/log N). The reduction in axial modulus, even in normalized form, is a function of the cyclic stress level. The characteristic features of the typical axial modulus curve are: (1) initial drop due to first cycle damage, (2) gradual reduction or plateau due to transverse crack multiplication or saturation up to the characteristic damage state (CDS), (3) accelerated reduction corresponding primarily to fiber fractures. The in-plane shear modulus was more sensitive to longitudinal matrix cracking than the axial modulus of the laminate. An attempt was made to express the in-plane shear modulus degratation mathematically based on the Nair-Reissner cantilever beam solution for a simple shear test. A model, based on static and fatigue properties of the single lamina, was developed for predicting the fatigue life of cross-ply laminates. Fatigue life consists of two parts, the first portion necessary to reach the CDS and the residual life after attainment of the CDS. A procedure for estimating the CDS life is described based on the relationship between residual stiffness and crack density and the in-situ S-N curve of the 90 deg lamina. The residual life after the CDS was obtained by calculating the stress carried by the 0 deg plies and assuming that these plies within the damaged laminate behave like a 0 deg lamina under cycle loading.
Dissert. Abstr.

N89-22666# United Technologies Research Center, East Hartford, CT. Materials Technology.
COMPOSITE MATERIAL SYSTEMS FOR HIGH TEMPERATURE APPLICATIONS
Earl R. Thompson *In* AGARD, Application of Advanced Material for Turbomachinery and Rocket Propulsion Mar. 1989 13 p
(For primary document see N89-22654 16-23)
Avail: NTIS HC A13/MF A01

N89-22667# Centre de Villaroche, Moissy (France).
UTILIZATION OF HIGH TEMPERATURE COMPOSITES IN TURBOJET ENGINES [UTILISATION DES COMPOSITES HAUTES TEMPERATURES DANS LES TURBOREACTEURS]
R. Mestre *In* AGARD, Application of Advanced Material for Turbomachinery and Rocket Propulsion Mar. 1989 11 p In FRENCH (For primary document see N89-22654 16-23)
Avail: NTIS HC A13/MF A01

N89-22668# Motoren- und Turbinen-Union Muenchen G.m.b.H. (Germany, F.R.).
INITIAL RESULTS OF TESTS ON METAL-CERAMIC GUIDE VANES
W. Huether and W. Krueger *In* AGARD, Application of Advanced Material for Turbomachinery and Rocket Propulsion Mar. 1989 5 p (For primary document see N89-22654 16-23)
Avail: NTIS HC A13/MF A01

N89-22672# SIGRI Electrogradhit G.m.b.H., Meitingen (Germany, F.R.).
SILICON-CARBIDE COATED CARBON-CARBON: AN ADVANCED MATERIAL FOR ROCKET SYSTEMS
E. v. Gellhorn, U. Gruber, and H. Leis (Messerschmitt-Boelkow-Blohm G.m.b.H., Munich, Germany, F.R.) *In* AGARD, Application of Advanced Material for Turbomachinery and Rocket Propulsion Mar. 1989 10 p (For primary document see N89-22654 16-23)
Avail: NTIS HC A13/MF A01

N89-22675# Aerospatiale, Saint Medard-en-Jalles (France). Etablissement d'Aquitaine.
HIGH-PERFORMANCE REFRACTORY COMPOSITE MATERIALS [LES MATERIAUX COMPOSITES REFRACTAIRES A HAUTE PERFORMANCE]
A. Hordonneau *In* AGARD, Application of Advanced Materials for Turomachinery and Rocket Propulsion Mar. 1989 9 p In FRENCH (For primary document see N89-22654 16-23)
Avail: NTIS HC A13/MF A01

N89-22676# Societe Europeene de Propulsion, Saint-Medard-en-Jalles (France).
HIGH TEMPERATURE COMPOSITE MATERIALS FOR ROCKET PROPULSION
Paul Donguy and Jacques Broca *In* AGARD, Application of Advanced Material for Turbomachinery and Rocket Propulsion Mar. 1989 11 p (For primary document see N89-22654 16-23)
Avail: NTIS HC A13/MF A01

25 INORGANIC AND PHYSICAL CHEMISTRY

Includes chemical analysis, e.g., chromatography; combustion theory; electrochemistry; and photochemistry.

For related information see also *77 Thermodynamics and Statistical Physics.*.

N89-22709*# Stanford Univ., CA. Dept. of Physics.
HIGH ACCURACY THERMAL CONDUCTIVITY MEASUREMENTS NEAR THE LAMBDA TRANSITION OF HELIUM WITH VERY HIGH TEMPERATURE RESOLUTION Final Report
William M. Fairbank and John A. Lipa Mar. 1989 26 p
(Grant NAG2-276)
(NASA-CR-184836; NAS 1.26:184836) Avail: NTIS HC A03/MF A01 CSCL 07D

Over the past few years extensive thermal conductivity measurements near the lambda point of helium were made. The original goal of measuring the thermal conductivity with a resolution

of t = T/T sub lambda -1 of 3 x 10(-8) was reached, but with somewhat less accuracy than was hoped. Subtle effects in the apparatus near the transition were observed which reduced the ability to interpret the results. Nevertheless, for resolution of t is greater than or equal to 10(-7) reliable data was obtained, extending previous measurements by more than an order of magnitude. Deviations from theoretical predictions were observed for t is less than or equal to 3 x 10(-6) leading to the question of the validity of the present renormalization group analysis of transport properties, at least for the case of helium. This anomaly led to closer examination of the boundary effects in the measurements. During the experiments a totally unexpected effect in the very dilute He-3 - He-4 mixtures was observed which led to the explanation of the anomalous results. The concentration dependence of the thermal conductivity near T sub lambda in the superfluid phase was found to deviate strongly from the predictions. The results gave an independent verification of this behavior and caused reanalysis of the Khalatnikov theory of hydrodynamics of the mixtures. An alternative solution was found which is in better agreement with the experiment. Author

N89-22710*# National Aeronautics and Space Administration. Lewis Research Center, Cleveland, OH.
LIGHTWEIGHT FIBROUS NICKEL ELECTRODES FOR NICKEL-HYDROGEN BATTERIES
Doris L. Britton 1989 10 p Presented at the 4th Annual Battery Conference on Applications and Advances, Long Beach, CA, 17-19 Jan. 1989; sponsored by California State Univ., Long Beach
(NASA-TM-101997; E-4701; NAS 1.15:101997) Avail: NTIS HC A02/MF A01 CSCL 10C

The NASA Lewis Research Center is currently developing nickel electrodes for nickel-hydrogen batteries. These electrodes are lighter in weight and have higher energy densities than the heavier state-of-the-art sintered nickel electrodes. Lightweight fibrous materials or plaques are used as conductive supports for the nickel hydroxide active material. These materials are commercial products that are fabricated into nickel electrodes by electrochemically impregnating them with active material. Evaluation is performed in half cells structured in the bipolar configuration. Initial performance tests include capacity measurements at five discharge levels, C/2, 1.0C, 1.37C, 2.0C, and 2.74C. The electrodes that pass the initial tests are life cycle-tested in a low Earth orbit regime at 80 percent depth of discharge. Author

N89-22711# Oxford Univ. (England). Dept. of Engineering Science.
MEASUREMENT OF THE TOTAL GAS CONTENT OF A LIQUID
R. E. Franklin and J. Rozewicz 1986 13 p
(Contract ER1/9/4/2057/093)
(OUEL-1643/86; ETN-89-94208) Avail: NTIS HC A03/MF A01

An apparatus for the measurement of the total gas content of a liquid is described and its use illustrated. The operation of the apparatus is based on the same basic principle as that of the constant volume van Slyke apparatus. The use of mercury which was a cause of substantial operating problems in the old apparatus, is eliminated. The weight and dimensions are both several times smaller and permit its use as a portable instrument. The estimated value is correct to 0.5 percent. ESA

N89-22712# Iowa Univ., Iowa City. Dept. of Chemistry.
MODELS FOR SURFACE INTERMEDIATES IN CO HYDROGENATION Final Report
Louis Messerle 1988 15 p
(Contract DE-FG22-85PC-80513)
(DE89-004348; DOE/PC-80513/T5) Avail: NTIS HC A03/MF A01

We have discovered the first example of intermolecular C-H bond activation by a metal-metal multiply-bonded complex. Reductive dimerization of the Ta(V) organometallic (eta-C5Me4R)TaX4 (R = Me, Et; X = Cl, Br) yields a novel class of highly-reactive dinuclear complexes (C5Me4R)2Ta2(mu-X)4, which possess quadrupole bridged Ta(III)-Ta(III) double bonds of sigma(sup2)delta(sup 2) electronic configuration. The nonbonded ditantalum(IV) intermediate in the reduction, (C5Me4R) 2Ta2(mu-X)2X4, has been characterized. The Ta = Ta complexes insert into the vinylic C-H bond of 1-alkenes under mild conditions to yield the ditantalum vinyl hydride (C5Me4R)2Ta2X4(mu-H)(mu, eta (sup 2)-CHCHR prime). The Ta = Ta complex inserts into other sigma-bonds, adding H2 to yield (C5Me4R)2Ta2(mu-H)2X4. It inserts into B-H bonds, resulting in dehydrodimerization of BH4(-) groups to (C5Me4R)2Ta2 (mu-X)2(mu-B2H6) with a mu-diborane group. These reactions with olefins and BH4(-) are unprecedented in dinuclear M-M multiple bond and early metal chemistry. We have also found an example of direct enolate generation from CO insertion into a metal alkyl, and have made a major breakthrough for developing lower-valent organovanadium and divanadium chemistry. DOE

N89-22713# Argonne National Lab., IL. Materials Science Div.
PRECIPITATION OF Ar, Kr AND Xe IN Ni AT ROOM TEMPERATURE
A. S. Liu and R. C. Birtcher Nov. 1988 6 p Presented at the Fall Meeting of the Materials Research Society, Boston, MA, 28 Nov. - 2 Dec. 1988
(Contract W-31-109-eng-38)
(DE89-009879; CONF-881155-58) Avail: NTIS HC A02/MF A01

Transmission electron microscopy has been used to study the precipitation of inert gases (Ar, Kr and Xe) injected into Ni at room temperature. The nucleation and size distribution of the precipitates were found to be insensitive to the type of gas atom but dependent upon gas concentration (ion fluence). The precipitate density decreases and the sizes increases with increasing gas concentration. In all cases, the gases precipitate as solid fcc crystals with their axes aligned with host Ni lattice, For the same gas concentration, the lattice parameter is larger for higher atomic mass in accord with bulk thermodynamics. The lattice parameter of each gas type increases with increasing gas concentration owing to the pressure relaxation that accompanies precipitate growth. This results in melting of large precipitates in accord with the behavior of bulk quantities of the gases at low temperatures. DOE

N89-22714 National Physical Lab., Teddington (England). Div. of Materials Applications.
CRITERIA FOR SELECTION OF PHASE NAMES FOR OXIDES
T. I. Barry and F. P. Glasser (Aberdeen Univ., Scotland) Dec. 1988 10 p
(NPL-DMA(A)169; ISSN-0143-7313; ETN-89-94339) Copyright Avail: National Physical Lab., Teddington, Middlesex, TW11 0LW, United Kingdom

Guidelines for the selection of generic unambiguous phase names for oxides needed for the thermodynamic modeling of phase equilibria in multicomponent systems (CaO-MgO-FeO sub x-Al sub 2O sub 3-SiO sub 2 are presented. These are required for immediate use and are not intended for formal recognition. Examples of phase names which fulfil the requirements and of others which are acceptable but pose certain difficulties are given. ESA

N89-22715# European Space Agency, Paris (France).
MATERIAL DEGRADATION IN A BARIUM HYDROXIDE LATENT HEAT STORAGE PILOT UNIT
Siegfried Krause and Michael vonBradke (Deutsche Forschungs- und Versuchsanstalt fuer Luft- und Raumfahrt, Stuttgart, Germany, F.R.) Jan. 1989 65 p Transl. into ENGLISH of Degradationsuntersuchungen bei einer Bariumhydroxid-Latent-waermespeicher-Pilotanlage (Stuttgart, Fed. Republic of Germany, DFVLR), Aug. 1987 74 p Original language document was announced as N88-22961
(ESA-TT-1107; DFVLR-FB-87-49; ETN-89-94443) Avail: NTIS HC A04/MF A01; original German version available from DFVLR, VB-PL-DO, Postfach 90 60 58, 5000 Cologne, Fed. Republic of Germany, DM 29.50

Barium hydroxide's chemical interaction with the heat transfer

oil, the stainless steel container, and the ambient air was investigated in a pilot storage unit. Chemical analysis, and electron microscope, and EDX were applied. Degradations observed after 40 test months are remarkably small. Long useful lives may therefore be expected for practical latent heat storage plants. The results also concern latent heat storage at high temperatures in solar dynamic energy systems in space, where the latent heat storage medium and its container also interact. ESA

N89-22716 Southampton Univ. (England).
THEORETICAL PREDICTIONS OF TURBULENT BURNING VELOCITIES OF STEADY AND ACCELERATING UNCONFINED TURBULENT FLAMES WITH PREMIXED REACTANTS Ph.D. Thesis
Howard Lester Gray 1988 196 p
Avail: Univ. Microfilms Order No. BRDX84434

The equations governing premixed turbulent combustion which result from the modelling methods are used to predict turbulent burning speeds for both steady and accelerating flames. The method exploits the characteristics arising at the flame edges because of the hyperbolic nature of the governing partial differential equations there. The analysis predicts an enhancement of burning speed with flame acceleration. This will only be apparent for large scale flames such as those which would occur in unconfined vapor cloud explosions, or if a large external acceleration field is imposed. This burning speed enhancement is used to describe how an accelerating flame can undergo a transition to a self-accelerating regime, which is then used to estimate possible flame speeds and accelerations in an unconfined vapor cloud explosion. The model does not give any limit to this self-acceleration, although it is expected that the burning speed will be limited by the modelling assumptions described below being violated at high burning speeds. The stability of the profiles of the various dependent variables (e.g., turbulence intensity, reaction progress variable) is examined for the cases of no heat release and moderate heat release using numerical solutions of the governing equations. These solutions predict that the flame will not propagate in a manner in which the profiles are preserved, and various causes for this are discussed. This analysis is limited to intense, large length scale turbulence, where the mean reaction rate is mixing rather than chemistry limited. The flow Mach number must be small to avoid compressibility effects. Dissert. Abstr.

N89-22717# City Univ. of New York, Brooklyn.
PREPARATION, CHARACTERIZATION AND PERFORMANCE OF MoS3 AS AN ACTIVE CATHODE MATERIAL Final Report, 15 Jun. 1985 - 14 Dec. 1988
Fred H. Pollak 14 Feb. 1989 61 p
(Contract DAAG29-85-K-0118)
(AD-A205866; ARO-22450.1-CH) Avail: NTIS HC A04/MF A01 CSCL 07B

We report on a program of the preparation, characterization and performance of amorphous MoS3 (a-MoS3) as an active cathode material. We have, for the first time, prepared thin films (approx. 1 micro of a-MoS3). This was accomplished by electrodeposition from both aqueous and non-aqueous solutions of (NH4)2MoS4 (ATTM) at room temperature. These thin films were studied by several experimental methods including X-rays, Raman scattering, optical transmission and electrolyte electro-reflectance. GRA

N89-22718# Universal Energy Systems, Inc., Dayton, OH.
COMBUSTOR FLOW VISUALIZATION USING INNOVATIVE INFRARED THERMOGRAPHICS TECHNIQUES Final Report, 1 Jul. 1986 - 2 Jan. 1987
Gary D. Streby Mar. 1989 227 p
(Contract F33615-86-C-2670)
(AD-A205905; WRDC-TR-89-2015) Avail: NTIS HC A11/MF A01 CSCL 21B

Innovative computational analysis methods and image processing techniques were combined with a commercially available infrared (IR) thermal imaging video system to produce complete surface thermographic data of a ramjet combustor configuration. The components of the data analysis system, the data-reduction procedures, and typical test data are presented. Data precision and the limitations of the infrared system are discussed. Unique capabilities of the system included continuous infrared color or gray-scale video monitoring of a heated test article, full-frame video digitizing and image enhancement of infrared thermal images, and computer processing to produce complete surface 3-dimensional thermal topographic data plots of a heated combustor under actual operating conditions. GRA

N89-23003*# SRI International Corp., Menlo Park, CA.
THE APPLICATION OF ELECTROCHEMICAL IMPEDANCE SPECTROSCOPY FOR CHARACTERIZING THE DEGRADATION OF NI(OH)2/NIOOH ELECTRODES Abstract Only
Digby D. Macdonald *In* NASA, Lewis Research Center, Space Electrochemical Research and Technology Conference: Abstracts 1989 p 30 (For primary document see N89-22982 16-44)
Avail: NTIS HC A03/MF A01 CSCL 07D

26 METALLIC MATERIALS

Includes physical, chemical, and mechanical properties of metals, e.g., corrosion; and metallurgy.

N89-22719# Yunnan Tin Corp., Gejiu (China).
INNOVATION IN SEPARATION TECHNOLOGY FOR FINE GRAVITY SEMI-PRODUCTS
Juan-zhi He and Meng-xing Liu 1987 13 p Sponsored by Institute of Scientific and Technical Information of China, Beijing
(PB89-112478; ISTIC-TR-C-000157) Avail: NTIS HC A03/MF A01 CSCL 11F

New methods were developed to recover a number of valuable by-products from the rougher tin concentrates obtained by gravity concentration. Separation of cassiterite from zircon was achieved by flotation in a weak alkaline medium with sodium carbonate as modifier and mixed tolyl arsenic acid as collector. A tin concentrate of 56.55 percent Sn with 4.51 percent ZrO2 and a zircon concentrate of 56.80 percent ZrO2 with 2.44 percent Sn are produced at recoveries 94.83 percent Sn and 94.09 percent ZrO2, respectively. The rougher tin concentrate, containing large amounts of oxide minerals of lead and iron, was recovered more successfully and economically by the above scheme, with addition of sodium carboxymethyl cellulose (CMC), as compared with the old tin-lead separation scheme. A tin concentrate of 47.62 percent Sn with lead content of 5.14 percent and a lead concentrate of 41.0 percent Pb with tin content of 0.85 percent are obtained at recoveries of 92.66 percent Sn and 97.14 percent Pb, respectively. A new process combined with chemical treatment was developed to clean rougher tin concentrates containing sulphur, bismuth and wolfram. Author

N89-22720 Utah Univ., Salt Lake City.
HYDROGEN EMBRITTLEMENT STUDY AND POSITRON ANNIHILATION RESPONSE OF HYDROGEN IN AISI 4340 STEEL Ph.D. Thesis
In-Ok Shim 1988 138 p
Avail: Univ. Microfilms Order No. DA8825797

Hydrogen degradation of mechanical properties and the positron annihilation response of hydrogen in ultra-high strength 4340 steel were studied. Hydrogen dissolved in the steel up to about 8 wt. ppm with very high diffusivity of the order of 10 to the -7 sq cm/sec at room temperature during cathodic charging. The strength was greatly lowered by implanted hydrogen, and as the hydrogen was removed by aging at room and elevated temperature, the strength was recovered fully or partially depending on the hydrogen-induced damage. Intergranular fracture along prior austenite grain boundaries was produced by initial hydrogen and with further implantation of high fugacity hydrogen the fracture mode changed to transgranular fracture. Severe charging increased dislocation density and formed dislocation substructures. Hydrogen-induced damage could be nondestructively detected by

the Dopper broadening technique by virtue of a higher value of the parameter, P/W. On the other hand, immediately after charging, the P/W parameter has a lower value, since hydrogen as an electron screened proton gets trapped in defects and prevents positrons from being trapped at those. Positron annihilation spectroscopy was also shown to be sensitive to the microstructural changes during heat-treatment and plastic deformation in this steel. Dissert. Abstr.

N89-22721# Harvard Univ., Cambridge, MA.
DEVELOPMENT OF METASTABLE PROCESSING PATHS FOR HIGH TEMPERATURE ALLOYS Semiannual Technical Report, 1 Apr. - 30 Sep. 1988
William J. Boettinger 30 Sep. 1988 59 p
(Contract N00014-86-K-0753)
(AD-A202614; AD-E900870) Avail: NTIS HC A04/MF A01 CSCL 11F

The possibility of developing new processing strategies for high temperature intermetallic compounds is being investigated. In particular rapid solidification followed by controlled heat treatment may provide new and unusual microstructures of multiphase materials. This report describes research performed at NIST to develop predictive models for solubility extension and metastable phase formation of intermetallic compounds and research to improve the phase diagram modeling of systems involving ordered phases. GRA

N89-22722*# National Inst. of Standards and Technology, Boulder, CO. Chemical Engineering Science Div.
IGNITION CHARACTERISTICS OF THE IRON-BASED ALLOY UNS S66286 IN PRESSURIZED OXYGEN
James W. Bransford, Phillip A. Billard, James A. Hurley, Kathleen M. McDermott, and Isaura Vazquez Nov. 1988 49 p
(NASA Order H-43201-B)
(NASA-CR-183612; NAS 1.26:183612; NISTIR-88/3904) Avail: NTIS HC A03/MF A01 CSCL 11F

The development of ignition and combustion in pressurized oxygen atmospheres was studied for the iron based alloy UNS S66286. Ignition of the alloy was achieved by heating the top surface of a cylindrical specimen with a continuous-wave CO2 laser. Two heating procedures were used. In the first, laser power was adjusted to maintain an approximately linear increase in surface temperature. In the second, laser power was periodically increased until autoheating (self-heating) was established. It was found that the alloy would autoheat to destruction from temperatures below the solidus temperature. In addition endothermic events occurred as the alloy was heated, many at reproducible temperatures. Many endothermic events occurred prior to abrupt increases in surface temperature and appeared to accelerate the rate of increase in specimen temperature to rates greater than what would be expected from increased temperature alone. It is suggested that the source of these endotherms may increase the oxidation rate of the alloy. Ignition parameters are defined and the temperatures at which these parameters occur are given for the oxygen pressure range of 1.72 to 13.8 MPa (25 to 2000 psia). Author

N89-22723# Northwestern Univ., Evanston, IL. Dept. of Materials Science and Engineering.
INVESTIGATION AND SYNTHESIS OF HIGH TEMPERATURE AND INCREASED STIFFNESS RSP ALUMINUM ALLOYS Final Report, 1 Oct. 1985 - 30 Sep. 1988
Morris E. Fine and Julia R. Weertman 30 Nov. 1988 92 p
(Grant AF-AFOSR-0337-85; AF Proj. 2306)
(AD-A204162; AFOSR-89-0081TR) Avail: NTIS HC A05/MF A01 CSCL 11F

Two promising systems as the basis for high temperature aluminum alloys useful to 425 C (800 F) were investigated. The first is a metal matrix composite consisting of an aluminum-magnesium alloy matrix reinforced by spinel (magnesium aluminate) particulate. The second system is Al3(ZrX), where X is vanadium or titanium dispersed in aluminum matrix. Here the lattice parameter of the Al3(ZrX) intermetallic particles nearly matches that of the matrix. Research on dilute alloys has shown a low coarsening rate for these intermetallics at 425 C. A study of aluminum alloys with a higher concentration of zirconium and vanadium was completed. The creep resistance at 410 C of the spinel composite was much better than that of the alumina composite. Extrusions containing 5 vol. percent Al3(V.75Zr.25) were prepared. The measured creep rate at 425 C is much lower than that of the current aluminum-iron-cerium alloys. An aluminum-vanadium intermetallic compound, however, forms at grain boundaries leading to a precipitate free zone which grows slowly at 425 C. Dilute alloys containing 1 vol. percent Al3(ZrTi) were then prepared and these show more promise than the aluminum-zirconium-vanadium alloys. GRA

N89-22724# Johns Hopkins Univ., Baltimore, MD. Dept. of Materials Science and Engineering.
MECHANISMS OF CREVICE CORROSION IN CHLORINATED ENVIRONMENTS Final Report
Patrick J. Moran and Barbara A. Shaw Jan. 1989 64 p
(Contract N00014-87-K-0294)
(AD-A204621) Avail: NTIS HC A04/MF A01 CSCL 11F

Crevice corrosion is considered by many to be the most deleterious form of corrosion because it occurs on shielded areas of a metal surface where visual examination of the underlying metal is difficult, if not possible, and unpredicted catastrophic failures can result. Crevice corrosion has been observed on a variety of passive film forming metals exposed in a number of different environments ranging from high purity water to the human body. This type of corrosion is inherent in metals and alloys that are easily passivated (e.g., stainless steels, aluminum and aluminum alloys, titanium and titanium alloys, and nickel base alloys), but also occurs on iron and mild steel exposed to highly oxidizing or passivating environments. Metal surfaces shielded by gaskets, washers, bolt heads, o-rings, barnacles or other surface deposits are typical sites for this type of corrosion. GRA

N89-22725# Virginia Univ., Charlottesville. Dept. of Materials Science.
PROCESSING AND PROPERTIES OF ADVANCED ALUMINUM ALLOYS Annual Report, 1 Jan. - 31 Dec. 1988
John A. Wert and Edgar A. Starke, Jr. Feb. 1989 85 p
(Grant AF-AFOSR-0082-87)
(AD-A205187; UVA/525671/MS89/101; AFOSR-89-0230TR)
Avail: NTIS HC A05/MF A01 CSCL 11F

This project has as its focus microstructure control for improving fracture resistance of advanced aluminum alloys. Our progress report is divided into two major parts: Part 1 which is concernec with the quench sensitivity of the Al-Li-Cu-Mg alloy 2090 and the effect of quench rate on fracture behavior, and Part 2 which is concerned with the recovery and recrystallization mechanisms that occur in an alloy having a high density of dispersoid particles. The grain size of aluminum alloys can affect both strength and deformation behavior and often controls the degree of superplasticity during elevated temperature deformation. Author

N89-22726# Du Pont de Nemours (E. I.) and Co., Aiken, SC.
AQUEOUS IMPURITY EFFECTS ON STAINLESS STEEL IGSCC (INTERGRANULAR STRESS CORROSION CRACKING): A CENTRAL COMPOSITE MATRIX ANALYSIS
R. S. Ondrejcin, G. R. Caskey, P. Aldred, W. L. Clarke, and S. A. Wilson (General Electric Co., San Jose, CA.) 1988 20 p
Presented at Corrosion '89, New Orleans, LA, 17 Apr. 1989
(Contract DE-AC09-76SR-00001)
(DE88-017382; DP-MS-88-177; CONF-890437-1) Avail: NTIS HC A03/MF A01

Sixty sensitized Type 304 stainless steel CERT samples were tested in a central composite statistical matrix to determine the effects of temperature, hydrogen peroxide, oxygen, carbon dioxide, sulfate and chloride concentrations and to rank them with respect to aggressiveness. Measurement and control of the variables was in real time. The ranges of these variables were based on the moderator conditions in Savannah River Plant reactors and are similar to conditions during some light-water reactor start-ups. DOE

N89-22727# International Centre for Theoretical Physics, Trieste (Italy).
ROLE OF ALUMINIUM CONCENTRATION ON THE STRUCTURE BEHAVIOUR OF Cu-Al ALLOYS
A. M. Nassar, A. S. Taha, K. A. Ragab, and S. El-Mossalamy (Al-Azhar Univ., Cairo, Egypt) Jun. 1988 11 p Submitted for publication
(DE88-705647; IC-88/115) Avail: NTIS (US Sales Only) HC A03/MF A01

Effect of Al(5, 10, 15 and 20) percent on the structure behaviour of Cu-Al alloys was investigated by both microhardness measurements and optical microscopic investigations. Pure Cu was used for comparison. The analysis of the hardness-temperature curve shows a type of dependence which obeys an empirical exponential law, but consists of several distinguishable regions. For Cu 20 percent Al, one region is observed, and two regions for pure Cu, while for alloys of 5 and 10 percent Al concentration three regions were observed. The activation energy varies between 0.03 and 0.9 ev. for these regions, depending on the Al-concentration as well as the annealing temperature. The recrystallization temperature was found to increase with increasing Al-concentration. It was also observed that Cu-20 percent Al alloy is very hard and brittle owing to the formation of gamma-2 phase, and also to phase separation as being detected from optical microscopic investigations. DOE

N89-22728# Sandia National Labs., Albuquerque, NM.
CORROSION MONITORING WITH ACOUSTIC WAVE DEVICES
N. R. Sorenson, A. J. Ricco, and S. J. Martin 1989 13 p Presented at Corrosion '89, New Orleans, LA, 17 Apr. 1989
(Contract DE-AC04-76DP-00789)
(DE89-005235; SAND-88-2891C; CONF-890437-9) Avail: NTIS HC A03/MF A01

Acoustic wave devices have been used to study atmospheric and aqueous corrosion of thin metal films. By monitoring the change in propagation velocity of a surface acoustic wave (SAW), atmospheric corrosion by gases can be recorded. Sulfidation of copper and inhibition of the sulfidation process by organic inhibitors has been studied to demonstrate the extreme mass sensitivity of the SAW devices. By exciting the same substrate at a different frequency, a shear horizontal acoustic plate mode (SH-APM) was used to monitor corrosion of aluminum in an aqueous sodium hydroxide environment. DOE

N89-22729# Oak Ridge National Lab., TN. Materials and Ceramics Div.
TEMPERATURE EFFECTS ON THE BREAK-IN OF NICKEL ALUMINIDE ALLOYS
Peter J. Blau and C. E. DeVore 1989 26 p Presented at the International Conference on Wear of Materials, Denver, CO, 9 Apr. 1989
(Contract DE-AC05-84OR-21400)
(DE89-005341; CONF-8904103-1) Avail: NTIS HC A03/MF A01

Nickel aluminide alloys are ordered intermetallic compounds which show promise for elevated temperature applications, some of which involve sliding contact. The present investigation was conducted to develop an understanding of the unlubricated sliding break-in behavior of three nickel aluminide alloys at room and elevated temperatures. In a particular, the variations in both the friction coefficient and the wear track morphology were studied. Pin-on-disk sliding experiments were conducted at room temperature and 923 K (650 C) in air using fixed 9.5-mm-diam polycrystalline alumina balls as the pin material. Friction break-in behavior changed as the test temperature was increased. Friction coefficient changes corresponded to changes in the wear track morphology. At elevated temperatures, the oxidation of the disk surfaces affected the friction coefficient. Repeat runs on unworn parts of disks exposed to elevated temperatures had little effect on break-in behavior. DOE

N89-22730# Brookhaven National Lab., Upton, NY. Dept. of Applied Science.
LOCATING PITTING SITES FROM PROPAGATING SURFACE POTENTIAL TRANSIENTS
Hugh S. Isaacs, Alison J. Davenport, and Philip J. Rulon (University of Southeastern Massachusetts, North Dartmouth.) 1989 11 p Presented at the Corrosion '89, New Orleans, LA, 17 Apr. 1989
(Contract DE-AC02-76CH-00016)
(DE89-006171; BNL-42094; CONF-890437-7) Avail: NTIS HC A03/MF A01

The propagation of potential transients along passive metal surfaces has been measured and modeled in order to analyze those transients detected following pit initiation. From the positioning of three or more detecting reference electrodes over the exposed surface the location of the pit site can be determined. DOE

N89-22731# Lawrence Livermore National Lab., CA.
EFFECTS OF GRAIN SIZE AND STRAIN RATE ON THE MECHANICAL RESPONSE OF COPPER
David H. Lassila 1989 7 p Presented at the 4th International Conference on Mechanical Properties of Materials at High Rates of Strain, Oxford, United Kingdom, 20 Mar. 1989
(Contract W-7405-eng-48)
(DE89-008811; UCRL-100134; CONF-890324-5) Avail: NTIS HC A02/MF A01

The effects of grain size and strain rate on the flow stress of copper were studied at room temperature. The Hall-Petch relationship was used to analyze the test results. Results of the study suggest that the strengthening effects of grain boundaries in copper are independent of strain rate over the range of strain rates .001/s to 500/s DOE

N89-22732# Kernforschungsanlage, Juelich (Germany, F.R.). Inst. fuer Grenzflaechenforschung und Vakuumphysik.
ION-INDUCED KINETIC ELECTRON EMISSION ON CLEAN AND GAS COATED METAL SURFACES Thesis - Tecnische Univ., Vienna [IONENINDUZIERTE KINETISCHE ELEKTRONENEMISSION AN REINEN UND GASBEDECKTEN METALLOBERFLAECHEN]
Mona M. Ferguson May 1988 133 p In GERMAN; ENGLISH summary
(JUEL-2201; ISSN-0366-0885; ETN-89-93958) Avail: NTIS HC A07/MF A01

The ion-induced electron emission from clean and gas-covered gold, silver, palladium, copper, and titanium, as well as from stainless steel, brass, titanium nitride, and technical aluminum was investigated. Each surface was bombarded with up to 23 different ion types from Li(+) to Sn(+) with a kinetic energy of 20 keV. The results for clean metals show that the electron yield depends on the electronic structures of both projectile ion and target atom. The yield from gold, silver, and palladium exhibits in every case the same dependence on the atomic number of the projectile, Z1. A different dependence is observed for each of copper and titanium. The adsorption of oxygen, hydrogen, or nitrogen causes a small decrease in the electron yield from silver, palladium, and copper in accord with the expected increase in work function. In contrast, an increase in the yield from titanium following adsorption of oxygen is observed and is explained by the formation of an oxide layer with a greater escape depth for electrons. The investigation of the Z1-dependence of the electron yield from the clean metals after exposure to air and from stainless steel, brass, titanium nitride, and technical aluminum reveals a universal Z1-dependence. It is explained by the superposition of the yields from the various components of the surface layers to these targets. ESA

N89-22733# Kernforschungsanlage, Juelich (Germany, F.R.). Inst. fuer Grenzflaechenforschung und Vakuumphysik.
RECONSTRUCTION AND RELAXATION OF METAL SURFACES Thesis - Technische Univ., Aachen [REKONSTRUKTION UND RELAXATION METALLISCHER OBERFLAECHEN]

Matthias Wuttig Jul. 1988 135 p In GERMAN; ENGLISH summary
(JUEL-2213; ISSN-0366-0885; ETN-89-93961) Avail: NTIS HC A07/MF A01

High resolution electron energy loss spectroscopy was used to study the relationship between surface structure and surface dynamics for different metal surfaces. The measurement of the Rayleigh wave dispersion for the clean Cu(100) surface shows a change of the force field in the vicinity of the surface. The introduction of an attractive surface stress indicates a tendancy of the surface layer to contract as a consequence of an increased charge density within the first layer. With the concept of surface stress the frequency reduction of the Rayleigh wave for the oxygen overlayer can be explained phenomenologically. The surface stress is repulsive since the oxygen adsorption leads to a reduction of bonding charge between the first layer nickel atoms and hence a more effective repulsion of the ion cores. For carbon adsorption the charge transfer is even stronger and leads to a surface reconstruction in the lattice dynamical calculations as is observed by the experiment. ESA

N89-22734# Technische Univ., Clausthal-Zellerfeld (Germany, F.R.). Inst. fuer Nichmetallische Werkstoffe.
MELTING BEHAVIOR OF HEAVY METAL BATCH COMPONENTS [EINSCHMELZVERHALTEN VON SCHWERMETALLOXIDTRAEGERN]
G. H. Frischat, E. Gehrmann, and P. Frolow Jul. 1988 59 p In GERMAN
(Contracts BMFT-01-YQ-113-6; BMFT-01-ZH-85062)
(ETN-89-93986) Avail: NTIS HC A04/MF A01

The melting and vaporization behavior of heavy metal batch components (CdO, CdS, CdSe, CdCO3, CdO + Se, CdS + CdSe, Se, As2O3, Sb2O3, PbO, Pb3O4) is investigated in connection with a base glass. The heavy metal compounds were either added to the batch or substituted for CaO.MgO (PbO). A gradient furnace was used to study the batch reactions between 550 and 1050 C. The batch moisture and the atmosphere was varied. It is found that the batch moisture is of strongest importance, and different phases appear at lower temperatures and also the decarbonization temperature is lowered. The formation of K2SeO4 is strongly influenced too. The second strongest influence on the batch reactions is given by changing the atmosphere (air, nitrogen, H2O loaded air). The transpiration method was used to study the evaporation behavior at high temperatures. The volatilized products were quantitatively gathered in borosilicate and silica glass wool thimbles, and analyzed by flame photometry. The vapor pressure data are reported, and the influence of inert and reactive atmospheres is discussed. ESA

N89-22735# University of Southern Illinois, Carbondale. Dept. of Mechanical Engineering and Energy Processes.
THERMAL HEALING OF DEFECTS IN OXIDE FILMS ON METALS AND ALLOYS Final Report, 1 Jan. - 31 Dec. 1988
J. H. Swisher, W. D. Cho, and S. C. Chang (National Tsing Hua Univ., Hsinchu, Taiwan) Mar. 1989 30 p
(Contract DE-FC22-88PC-88861)
(DE89-009580; DOE/PC-88861/T13) Avail: NTIS HC A03/MF A01

In the initial part of a continuing program on the thermal healing of defects in oxide films on metals and alloys, a study was undertaken on the healing of defects in wustite (FeO) layers on unalloyed iron. Experiments were performed isothermally at 900 and 720 C, and with an imposed temperature gradient in the specimens. Defects which simulated damage caused by abrasive particles in a gas stream were made by scribing through preformed oxide layers and by diffusion-bonding gold bands in grooves on the iron surfaces. It was found that lateral mass transport of FeO into or over the defects occurs readily, capillarity being the driving force. In the presence of a temperature gradient, as would be present in heat exchangers, turbine blades, etc., the extent of mass transport was somewhat larger and the FeO grain size in the flaw areas was larger also. The mechanism of mass transport is believed to be either surface or bulk diffusion of Fe2(+) ions. DOE

N89-22736# Oak Ridge National Lab., TN.
IMPROVED HIGH TEMPERATURE CREEP RESISTANT AUSTENITIC ALLOY Patent Application
Philip J. Maziasz, inventor (to DOE), Robert W. Swindeman, inventor (to DOE), and Gene M. Goodwin, inventor (to DOE) 13 May 1988 12 p
(Contract DE-AC05-84OR-21400)
(DE89-009664; PATENTS-US-A7193705;
US-Patent-Appl-SN-193705) Avail: NTIS HC A03/MF A01

An improved austenitic alloy having in wt percent 19-21 Cr, 30-35 Ni, 1.5-2.5 Mn, 2-3 Mo, 0.1-0.4 Si, 0.3-0.5 Ti, 0.1-0.3 Nb, 0.1-0.5 V, 0.001-0.005 P, 0.08-0.12 C, 0.01-0.03 N, 0.005-0.01 B and the balance iron that is further improved by annealing for up to 1 hour at 1150 to 1200 C and then cold deforming 5 to 15 percent. The alloy exhibits dramatically improved creep rupture resistance and ductility at 700 C. GRA

N89-22737# Argonne National Lab., IL. Materials and Components Technology Div.
SPINODAL DECOMPOSITION OF AUSTENITE IN LONG-TERM-AGED DUPLEX STAINLESS STEEL
H. M. Chung Feb. 1989 25 p Presented at the Metallurgical Society Annual Meeting, Las Vegas, NV, 27 Feb. - 3 Mar. 1989
(Contract W-31-109-eng-38)
(DE89-009827; CONF-890215-5) Avail: NTIS HC A03

Spinodal decomposition of austenite phase in the cast duplex stainless steels CF-8 and -8M grades has been observed after long-term thermal aging at 400 and 350 C for 30,000 h (3.4 yr). At 320 C, the reaction was observed only at the limited region near the austenite grain boundaries. Ni segregation and worm-holes corresponding to the spatial microchemical fluctuations have been confirmed. The decomposition was observed only for heats containing relatively high overall Ni content (9.6 to 12.0 wt pct) but not in low-Ni (8.0 to 9.4 wt pct) heats. In some specimens showing a relatively advanced stage of decomposition, localized regions of austenite with a Vickers hardness of 340 to 430 were observed. However, the effect of austenite decomposition on the overall material toughness appears secondary for aging up to 3 to 5 yr in comparison with the effect of the faster spinodal decomposition in ferrite phase. The observation of the thermally driven spinodal decomposition of the austenite phase in cast duplex stainless steels validates the proposition that a miscibility gap occurs in Fe-Ni and ancillary systems. DOE

N89-22738# Illinois Univ., Chicago.
CORROSION OF IRON, NICKEL AND COBALT BASED ALLOYS IN HIGH TEMPERATURE ENVIRONMENTS CONTAMINATED WITH CHLORINE Final Report
Michael McNallan Jan. 1989 6 p
(Contract DE-FG02-85ER-45178)
(DE89-009829; DOE/ER-45178/3) Avail: NTIS HC A02/MF A01

This report contains a summary of research, and lists the graduate theses completed under this program. The results in print, press and those presented at public meetings are also listed. DOE

N89-22739# Argonne National Lab., IL. Materials and Component Technology Div.
MICROSTRUCTURAL STUDIES OF IAD AND PVD Cr COATINGS BY CROSS SECTION TRANSMISSION ELECTRON MICROSCOPY
C. C. Cheng, R. A. Erck, and G. R. Fenske 1988 8 p Presented at the Fall Meeting of the Materials Research Society, Boston, MA, 28 Nov. - 3 Dec. 1988
(Contract W-31-109-eng-38)
(DE89-009877; CONF-881155-57) Avail: NTIS HC A02/MF A01

Cross section transmission electron microscopy was used to study the microstructure and interface structure of Cr films

deposited by ion-assisted deposition as a function of the incident ion energy. High-energy ion bombardment (1 keV) was found to enhance the adhesion of the deposited film owing to the formation of an intermixed layer, whereas deposition with low-energy ions (100 eV) was found to reduce or eliminate gain boundary porosity. A tailored Cr film with excellent adhesion and no grain boundary porosity was deposited by combining high- and low-energy ion bombardment. DOE

N89-22740# Illinois Univ., Urbana. Dept. of Materials Science and Engineering.
MECHANISMS OF CASCADE COLLAPSE
T. DiazdelaRubia, K. Smalinskas, R. S. Averback, I. M. Robertson, H. Hseih, and R. Benedek (Argonne National Lab., IL.) Dec. 1988 8 p Presented at the Fall Meeting of the Materials Research Society, Boston, MA, 28 Nov. - 3 Dec. 1988
(Contract W-31-109-eng-38)
(DE89-009882; CONF-881155-59) Avail: NTIS HC A02/MF A01

The spontaneous collapse of energetic displacement cascades in metals into vacancy dislocation loops has been investigated by molecular dynamics (MD) computer simulation and transmission electron microscopy (TEM). Simulations of 5 keV recoil events in Cu and Ni provide the following scenario of cascade collapse: atoms are ejected from the central region of the cascade by replacement collision sequences; the central region subsequently melts; vacancies are driven to the center of the cascade during resolidification where they may collapse into loops. Whether or not collapse occurs depends critically on the melting temperature of the metal and the energy density and total energy in the cascade. Results of TEM are presented in support of this mechanism. DOE

N89-22741# California Univ., Berkeley. Lawrence Berkeley Lab. Materials and Chemical Sciences Div.
AB INITIO CALCULATIONS OF ORDERED INTERMETALLIC PHASE EQUILIBRIA
M. Sluiter, D. DeFontaine, X. Q. Guo, R. Podloucky, and A. J. Freeman Dec. 1988 15 p Presented at the Fall Meeting of the Materials Research Society, Boston, MA, 28 Nov. 1988
(Contract DE-AC03-76SF-00098)
(DE89-009974; LBL-26727; CONF-881155-69) Avail: NTIS HC A03/MF A01

General procedures for computing alloy phase equilibria from ab initio electronic structure calculations are reviewed and applied to the Al-Li phase diagram. Free energies were calculated by the cluster variation method (CVM) in the tetrahedron approximation for the fcc and bcc lattices and ordered superstructures. Input was provided by first principles FLAPW calculations. The computed phase diagram for both stable and metastable structures agrees remarkably well with the experimental one. GRA

N89-22742# Etablissement Technique Central de l'Armement, Arcueil (France). Service Structure des Materiaux.
WEAR PROTECTION COATINGS AND TREATMENTS FOR THE TA6V ALLOY [DEPOTS ET TRAITEMENTS DE SURFACE ANTIEROSION DU TA6V]
J. P. Massoud and G. Coquerelle 7 Jan. 1988 45 p In FRENCH
(Contract DCA/STPA-86-96-901)
(ETCA-88-R-003; ETN-89-94348) Avail: NTIS HC A03/MF A01

The treatments studied include oven heat treatment, nitriding, carbiding, and borum surface treatments. The particle impact wear test procedure is described. On average 30,000 impacts per sec and 0.33 g/s of SiC particles at 100 m/s over 3 sq cm were used. Best results are obtained with titanium nitride coatings. ESA

N89-22743# Etablissement Technique Central de l'Armement, Arcueil (France). Service Technologie des Materiaux.
FRACTURE TOUGHNESS AND MECHANICAL BEHAVIOR OF STEEL AND ALUMINUM ALLOYS [TENACITE ET LOIS DE COMPORTEMENT D'ACIER ET D'ALLIAGES D'ALUMINIUM]
J. Clisson 22 Sep. 1987 103 p In FRENCH
(Contract DRET/SDR-84-1022)
(ETCA-87-R-090; ETN-89-94353) Avail: NTIS HC A06/MF A01

The influence of loading rate on the yield limit and toughness was studied for three aluminum alloys and one austenitic steel with high elasticity limit. The results show a small influence of deformation rate on the characteristics. A large influence of chemical composition and heat treatment is shown. ESA

N89-22744# Etablissement Technique Central de l'Armement, Arcueil (France). Service Chimie-Physique.
APPLICATION OF ELECTROCHEMICAL NOISE SPECTRAL ANALYSIS TO THE STUDY OF THE PITTING CORROSION OF ALUMINUM ALLOYS [APPLICATION DE L'ANALYSE SPECTRALE DU BRUIT ELECTROCHIMIQUE A L'ETUDE DE LA CORROSION PAR PIQURES DES ALLIAGES D'ALUMINIUM]
C. Bataillon 8 Oct. 1987 149 p In FRENCH Sponsored by Direction des Recherches, Etudes et Techniques, Paris, France
(ETCA-87-R-102; ETN-89-94354) Avail: NTIS HC A07/MF A01

The electrochemical noise measuring technique applied to aluminum alloys in a corrosive media containing chloride ions, is described. The study characterizes quantitatively the pitting corrosion resistance. The parameters used include the kinetics of pitting development and structural aspects of pitting corrosion. A propagation mechanism is suggested, based on the experimental data, to explain the intermittent behavior of pitting propagation. ESA

N89-22745# Deutsche Forschungs- und Versuchsanstalt fuer Luft- und Raumfahrt, Cologne (Germany, F.R.). Inst. for Raumsimulation.
DIAGNOSTICS OF PHASE FORMATION IN METASTABLE SOLIDIFICATION OF METALS
Berndt Feuerbacher Oct. 1988 57 p Submitted for publication
(DFVLR-FB-88-43; ISSN-0171-1342; ETN-89-94377) Avail: NTIS HC A04/MF A01; DFVLR, VB-PL-DO, Postfach 90 60 58, 5000 Cologne, Fed. Republic of Germany, DM 23.50

The solidification of metals in metastable phases is treated. The usual processing method of rapid quenching does not allow investigations on the detailed solidification and phase selection phenomena. Solidification techniques including slow but deep undercooling, which allow for diagnostic measurements during the early steps of nucleation and phase selection, are considered. Theoretical and experimental methods in nucleation and free dendritic growth are reviewed. Deviations from local equilibrium at the solidification front are discussed. The results lead to a better understanding of the metastable solidification process and to a controlled production of materials with advanced properties. ESA

N89-22746# Army Lab. Command, Watertown, MA. Material Technology Lab.
ASSESSING HYDROGEN ASSISTED CRACKING MODES IN HIGH STRENGTH STEEL WELDS Final Report
Steven A. Gedeon and Thomas W. Eagar Dec. 1988 21 p
(AD-A205431; MTL-TR-88-44) Avail: NTIS HC A03/MF A01 CSCL 11F

The stress intensity which causes crack propagation in high strength steel weldments was quantified as a function of the hydrogen content at the crack location. This relationship was used to assess previously proposed theoretical hydrogen assisted cracking mechanisms. It was found that the microplasticity theory of Beachem can best describe how the stress intensity factor and hydrogen content affect the modes of intergranular, quasi-cleavage,

and microvoid coalescence fracture. Implant test results were analyzed with the aid of fracture mechanics to determine the stress intensity associated with various modes of fracture. Diffusible weld hydrogen results were analyzed with the aid of hydrogen distribution model developed by Coe and Chano to determine the amount of hydrogen present at the crack location at the time of fracture.
GRA

N89-22660# Rolls-Royce Ltd., Derby (England). Materials Research.
NEW METALLIC MATERIALS FOR GAS TURBINES
M. A. Hicks *In* AGARD, Application of Advanced Material for Turbomachinery and Rocket Propulsion Mar. 1989 13 p (For primary document see N89-22654 16-23)
Avail: NTIS HC A13/MF A01

N89-22663# Fiat Aviazione S.p.A., Turin (Italy). Stress Dept.
DEVELOPMENT OF STRESS AND LIFING CRITERIA FOR SINGLE CRYSTAL TURBINE BLADES
S. Salvano, M. Stanisci, and E. Campo *In* AGARD, Application of Advanced Material for Turbomachinery and Rocket Propulsion Mar. 1989 9 p (For primary document see N89-22654 16-23)
Avail: NTIS HC A13/MF A01

N89-22673*# National Aeronautics and Space Administration. Lewis Research Center, Cleveland, OH.
FIBER REINFORCED SUPERALLOYS FOR ROCKET ENGINES
Donald W. Petrasek and Joseph R. Stephens *In* AGARD, Application of Advanced Material for Turbomachinery and Rocket Propulsion Mar. 1989 13 p Previously announced as N89-15990 (For primary document see N89-22654 16-23)
Avail: NTIS HC A13/MF A01 CSCL 11F

N89-22674# Metallwerk Plansee, A.G., Reutte (Austria).
BEHAVIOR OF TUNGSTEN, MOLYBDENUM AND ALLOYS UNDER UNUSUAL HEATING CONDITIONS
R. Eck, H. Bildstein, F. Simader, R. Stickler (Technische Univ., Vienna, Austria), and J. Tinzl *In* AGARD, Application of Advanced Material for Turbomachinery and Rocket Propulsion Mar. 1989 11 p (For primary document see N89-22654 16-23)
Avail: NTIS HC A13/MF A01

N89-22680# Centre de Recherches Metallurgiques, Liege (Belgium).
METALLURGICAL STUDY OF SUPERALLOY BRAZING ALLOYS
Ch. Lecomte-Mertens and W. Bex (FN Moteurs, Mimort, Belgium) *In* AGARD, Application of Advanced Material for Turbomachinery and Rocket Propulsion Mar. 1989 12 p (For primary document see N89-22654 16-23)
Avail: NTIS HC A13/MF A01

27 NONMETALLIC MATERIALS

Includes physical, chemical, and mechanical properties of plastics, elastomers, lubricants, polymers, textiles, adhesives, and ceramic materials.

For composite materials see *24 Composite Materials.*

N89-22747# National Inst. of Standards and Technology, Gaithersburg, MD.
FORMATION OF LUBRICATING FILMS AT ELEVATED TEMPERATURES FROM THE GAS PHASE
E. E. Klaus, J. L. Duda, S. K. Naidu (Pennsylvania State Univ., University Park.), R. G. Munro, ed., and S. Hsu, ed. Sep. 1988 103 p Sponsored by DOE, Washington, DC
(PB89-129530; NIST/SP-744; LC-88-600554) Avail: NTIS HC A06/MF A01; also available SOD HC $4.75 as 003-003-02897-5 CSCL 11H

Conventional liquid lubricants, when subjected to temperatures of 250 C and above for extended time in an air atmosphere, degrade rapidly to make large amounts of solid sludge and deposits. Based on boundary lubrication of bearings, these same lubricants, when subjected to 250 C to the melting point of the bearing metal, produce in the micro-to-milli-second residence time in the bearing contact enough friction polymer to result in good lubrication. The use of these conventional liquid lubricants delivered in a homogeneous vapor phase where the carrier gas is nitrogen, air or mixtures of these two gases is described. The lubricants studied include alkyl and aryl phosphate esters, organic acid esters, polyphenyl ethers, and mineral oil.
Author

N89-22748# National Inst. of Standards and Technology, Gaithersburg, MD. Building Materials Div.
ELECTROCHEMICAL TECHNIQUE FOR RAPIDLY EVALUATING PROTECTIVE COATINGS ON METALS Final Technical Note
Changjian Lin (Xiamen Univ., China) and Tinh Nguyen Oct. 1988 25 p
(PB89-134209; NIST/TN-1253) Avail: NTIS HC A03/MF A01 CSCL 11B

A new electrochemical technique based on multicyclic scanning potentials applied to a specimen in an electrolyte was developed and evaluated as a method for rapidly evaluating the corrosion protection performance of organic coatings on metal. Opaque alkyd and clear acylic coated steel samples prepared at different thicknesses, curing conditions, defect inclusions, and contamination concentrations were used for the evaluation. The applied potentials were between -1.8 and + 1.8 V, and the electrolyte was a 3 percent NaCl solution. Preliminary results indicate that the technique is useful for evaluating the corrosion protection properties of organic coatings on steel. The technique appears to offer a number of advantages; fast and in situ measurements, good reproducibility, high sensitivity, and minimal damage to the coating.
Author

N89-22749# Sandia National Labs., Albuquerque, NM.
PROGRESS IN CRYSTALLINE SILICON RESEARCH
Dan E. Arvizu and David L. King 1989 10 p Presented at the 4th International Photovoltaic Science and Engineering Conference, Sydney, Australia, 14 Feb. 1989 Submitted for publication
(Contract DE-AC04-76DP-00789)
(DE89-007423; SAND-89-0381C; CONF-890211-3) Avail: NTIS HC A02/MF A01

This paper discusses progress in US sponsored crystalline silicon photovoltaic cell technology for one-sun and concentrating applications, from the research laboratory to the production line. A summary of field experience, present economics, projected utility requirements, cell efficiency status, and the US DOE research direction will be presented.
DOE

N89-22750# Pennsylvania State Univ., University Park. Dept. of Chemistry.
REACTIONS OF INORGANIC HIGH POLYMERS AS A ROUTE TO TAILORED SOLIDS
Harry R. Allcock 9 Feb. 1989 16 p
(Contract N00014-84-K-0477)
(AD-A204602; TR-48) Avail: NTIS HC A03/MF A01 CSCL 07F

A new class of reactive inorganic polymers—the polyphosphazenes—can be used as macromolecular intermediates for the synthesis of a wide range of inorganic-organic solids. By reactions that change the polymer side groups, it is possible to bias the properties toward elastomers or microcrystalline polymers, liquid crystalline materials, bioerodable solids, solids with bioactive surfaces, solid electrolytes, semiconductors, or ultrastructures.
GRA

N89-22751# Sao Paulo Univ. (Brazil). Inst. de Quimica.
EFFECTS OF X-RAYS ON ISOTACTIC POLYPROPYLENE. VOLUME 2: POLYMERS AND CERAMICS
Yoshio Kawano and Sandra Soares 1988 6 p Presented at the 6th Japan-Brazil Symposium on Sciience and Technology, Sao Paulo, Brazil, 10 Aug. 1988
(DE88-705606; ACIESP-60-Vol-2; CONF-8808156) Avail: NTIS (US Sales Only) HC A02/MF A01

In order to understand the structural change caused by radiation, isotactic PP films were irradiated with X-radiation, and their structures by X-ray diffraction and infrared and ultraviolet spectroscopies were studied. DOE

N89-22752# International Centre for Theoretical Physics, Trieste (Italy).
DYNAMIC SCATTERING FROM MULTICOMPONENT POLYMER SYSTEMS
Mustapha Benmouna (INES Sciences Exactes, Tiemcen, Algeria) Sep. 1988 12 p Submitted for publication
(DE88-705677; IC-88/285) Avail: NTIS (US Sales Only) HC A03/MF A01

The application of Random Phase Approximation to dynamic scattering from multicomponent polymer systems is considered. The effect of excluded volume interaction between polymer species is investigated. A simple method of introducing solvent dynamics is proposed. This method allows for obtaining dynamics of pure polymer mixtures from dynamics of corresponding solutions. The scattering functions of mixtures of three polymers is shown to be characterized by two exponential decay modes. DOE

N89-22753# International Centre for Theoretical Physics, Trieste (Italy).
APPLICATION OF THE ORNSTEIN-ZERNIKE FORMALISM TO POLYMER AND COPOLYMER BLENDS
Mustapha Benmouna (INES Sciences Exactes, Tiemcen, Algeria) Sep. 1988 11 p Submitted for publication
(DE88-705686; IC-88/302) Avail: NTIS (US Sales Only) HC A03/MF A01

The Ornstein Zernike formalism is shown to be applicable to polymer and copolymer blends. Direct correlation functions are obtained from the solution problem by using a simple procedure which was suggested before (M. Benmouna, H. Benoit and W. Wu, to be published in Macromolecules). This procedure consists essentially of replacing the volume fraction of solvent by the quantity phi sub c N sub c P sub c (q) where phi sub c, N sub c and P sub c (q) are the volume fraction, the degree of polymerization and the form factor as a function of momentum transfer q, respectively. DOE

N89-22754# International Centre for Theoretical Physics, Trieste (Italy).
SPINODAL DECOMPOSITION IN POLYMER BLENDS
Mustapha Benmouna Sep. 1988 12 p Submitted for publication
(DE88-705687; IC-88/303) Avail: NTIS (US Sales Only) HC A03/MF A01

The kinetic of spinodal decomposition in polymer blends is investigated. The time evolution of the polymer composition fluctuations is determined using the multiple time-scales method. It is shown that for short times, the initial growth rate is consistent with the prediction of the linear theory based on the Random Phase Approximation. As the time increases, the composition fluctuations tend to a constant value due to nonlinear effects. DOE

N89-22755# New Energy Development Organization, Tokyo (Japan).
TECHNICAL FEASIBILITY STUDY ON THE DEVELOPMENT OF CERAMIC THERMOELECTRIC CONVERSION, PART 2
May 1988 78 p In ENGLISH and JAPANESE
(DE88-756481; NEDOJ-P-8708-Pt-2) Avail: NTIS (US Sales Only) HC A05/MF A01

A survey was conducted on the current trends and problems with ceramic thermoelectric conversion, which converts thermal energy directly to the electric energy. The conversion efficiency of 19 percent and the output density of more than 0.5W/sq cm have been accomplished in the laboratory. A possible application is the space power source. The Jet Propulsion Laboratory has been conducting the conceptual design. Present tasks include the development of electrodes with high output density and durability and construction of modular structures. The Ford has developed a 100 W class module with 6 single cells, which is under testing. The application of ceramic thermoelectric conversion will be widely advanced and the R and D will be accelerated when its advantages are demonstrated with modular structures in aspects of meeting the diversified energy needs and developing clean energy source. DOE

N89-22756# Lawrence Livermore National Lab., CA.
LOW-DENSITY FOAMS FROM MACROPOROUS EPOXY GELS
James D. LeMay Nov. 1988 11 p Presented at the American Chemical Society Polymeric Materials Division Meeting, Dallas, TX, 9 Apr. 1989
(Contract W-7405-eng-48)
(DE89-004042; UCRL-99995; CONF-890483-1) Avail: NTIS HC A03/MF A01

A technology for making low-density, microcellular epoxy foams was described. The foam precursor was a heterogeneous (two-phase), macroporous gel made by homopolymerizing an epoxy novolac oligomer in an inert diluent. Dry foam was recovered from the gel with little shrinkage by exchanging the diluent with liquefied carbon dioxide then processing at supercritical conditions. Foams were made with densities ranging from 0.034 to 0.150 g/cc. SEM micrographs of the dry foams reveal a highly porous, ramified morphology that is self-similar over at least 1 to 2 orders of magnification. The structure contains open cells with diameters ranging from 0.1 to several microns. The foams are characterized by high BET surface areas (100 to 300 sq m/g). GRA

N89-22757 Motoren- und Turbinen-Union Muenchen G.m.b.H. (Germany, F.R.).
BASIC PROGRAM FOR THE DEVELOPMENT OF A RELIABLE HIGH STRENGTH CONSTRUCTION CERAMIC MODE OF SIC Final Report [GRUNDLAGENPROGRAMM ZUR ENTWICKLUNG EINER ZUVERLAESSIGEN H.T.-KONSTRUKTIONSKERAMIK AUS SIC]
W. Huether, Andrees, and Rossmann 30 Apr. 1987 85 p In GERMAN; ENGLISH summary
(MTU-TB-87/927; ETN-89-93764) Avail: Fachinformationszentrum Karlsruhe, 7514 Eggenstein-Leopoldshafen 2, Fed. Republic of Germany

Methods were developed for the reproducable production of high strength ceramic parts with large volume for engines. By improvements of the powder preparation it was possible to reach an average strength of 250 Mla in turbine disks with a volume of 300 cu cm. The disks were manufactured by cold isostatic pressing and sintering of alpha-Sic. Strength measurements were performed at four-point bend specimens and using cold spinning tests of the turbine disks. ESA

N89-22758# Construcciones Aeronauticas S.A., Madrid (Spain). Div. de Proyectos.
PAINT COMPATIBILITY TEST
A. Buendia 24 Jun. 1988 13 p
(I-266/88; ETN-89-94128) Avail: NTIS HC A03/MF A01

The compatibility of different polyurethane finishes applied on epoxy primer, with different primer drying intervals, was checked. The F-580-280 epoxy primer from ICI does not show any adhesion problem when covered by the finishes: PU-66 from International Celomer, N-53624 from Wiederhold, and Aerodur Finish C-21/100 from Sikkens, neither when the primer was aged for 4 hr nor for 72 hr. ESA

N89-22759# Technische Univ., Delft (Netherlands).
INTERFACIAL ADHESION AND MECHANICAL PROPERTIES OF POLYAMIDE-6/GLASS BEAD COMPOSITES Ph.D. Thesis
Edwin Adriaan Andre vanHartingsveldt 1987 129 p Original contains color illustrations
(ETN-89-94136) Avail: NTIS HC A07/MF A01

The relationship between the interfacial adhesion and the mechanical properties of polyamide-6 filled with small glass beads was studied. The measurement of interfacial debonding in described. The influence of interfacial debonding on the elastic properties and tensile strength of the composite is shown. The

way the interfacial adhsion is influenced by a chemical modification of the glass surface, by the absorption of water from the environment, or by the rate of testing is summarized. A photoelastic technique was used to study the stresses and strains around a glass disk embedded in an epoxy matrix, which can be considered as a two-dimensional model. The effect of interfacial debonding on the local stress field was examined. Debonding of the glass disk occurs during a creep test at constant load. This observation is in agreement with a critical strain criterion for debonding observed in the polyamide-6/glass bead composites. ESA

N89-22760# National Inst. of Standards and Technology, Boulder, CO.
DIAGNOSTICS OF GLOW DISCHARGES USED TO PRODUCE HYDROGENATED AMORPHOUS SILICON FILMS Annual Report, 15 Jun. 1987 - 30 Nov. 1988
A. Gallagher, D. A. Doughty, J. Doyle, M. He, and G. H. Lin (Colorado Univ., Boulder.) Mar. 1989 21 p
(Contract DE-AC02-83CH-10093)
(DE89-000887; SERI/STR-211-3473) Avail: NTIS HC A03/MF A01

A simple, inexpensive, accurate method of measuring surface reaction probabilities (beta) of depositing species has been developed. This method has been applied to low-power silane discharges, obtaining beta = 0.4 for typical, high-film-quality deposition conditions. Explaining this result will require further developments, such as introducing more than one type of surface bond, in current deposition models. A method has also been developed to measure the spatial distribution of depositing species between the electrodes of a deposition discharge. This method has been applied to low-power, RF silane discharges under conditions in which excellent a-Si:H film quality is obtained. This has unmistakably verified rapid H reactions with SiH4, and the dominance of SiH3 deposition, and several other conclusions of the standard model reported here. In particular, it supports the predictions of the model regarding the cause of film-quality deterioration at high powers, partly the result of a loss in SiH3 deposition by SiH3 + SiH3 reactions. DOE

N89-22761# Polytechnic Univ., Brooklyn, NY.
POLYMER ELECTROLYTES WITH EXCLUSIVELY CATIONIC CONDUCTIVITY
H. Liu, Y. Okamoto, T. Skotheim, Y. S. Pak, S. G. Greenbaum, and K. J. Adamic (Hunter Coll., New York.) 1988 5 p Presented at the Fall Meeting of the Materials Research Society, Boston, MA, 28 Nov. 1988
(Contract DE-AC02-76CH-00016)
(DE89-009521; BNL-42371; CONF-881155-54) Avail: NTIS HC A02/MF A01

The synthesis of exclusively cation conducting polymer electrolytes based on a nylon-1 backbone, ethylene-oxide side chains, and attached dibutyl phenolate anions is described. The tendency for ion pair formation appears to be reduced as the conductivity of the sodium-containing compound reaches approximately 2 times 10 sup minus 6 S-cm sup minus 1 at 50 C. Na(23) nuclear magnetic resonance measurements demonstrate: (1) motional narrowing of the mobile Na resonance above the glass transition temperature; (2) mobile Na concentrations of approximately 75 percent at 40 C; and (3) insensitivity of the linewidth to applied hydrostatic pressure up to 2 kbar. Similarities between these findings, and those in conventional polymer-salt electrolytes are discussed. DOE

N89-22762# Oak Ridge National Lab., TN.
CARBONACEOUS FILM COATING Patent Application
Leon Maya, inventor (to DOE) 27 Apr. 1988 14 p
(Contract DE-AC05-84OR-21400)
(DE89-009592; PATENTS-US-A7186427;
US-Patent-Appl-SN-186427) Avail: NTIS HC A03/MF A01

A method of making a carbonaceous film comprising heating tris(1,3,2-benzodiazaborolo)borazine or dodecahydro tris borazine in an inert atmosphere in the presence of a substrate to a temperature at which the borazine compound decomposes, and the decomposition products deposit onto the substrate to form a thin, tenacious, highly reflective conductive coating having a narrow band gap which is susceptible of modification and a relatively low coefficient of friction. DOE

N89-22763# Los Alamos National Lab., NM.
MICROWAVE SINTERING OF BORON CARBIDE Patent Application
Rodger D. Blake, inventor (to DOE), Joel D. Katz, inventor (to DOE), John J. Petrovic, inventor (to DOE), and Haskell Sheinberg, inventor (to DOE) 10 Jun. 1988 8 p
(Contract W-7405-eng-36)
(DE89-009652; PATENTS-US-A7206153;
US-Patent-Appl-SN-206153) Avail: NTIS HC A02/MF A01

A method for forming boron carbide into a particular shape and densifying the green boron carbide shape was considered. Boron carbide in powder form was pressed into a green shape and then sintered, using a microwave oven, to obtain a dense boron carbide body. Densities of greater than 95 percent of theoretical density were obtained. GRA

N89-22764# Sandia National Labs., Albuquerque, NM.
CHEMICAL STATE DEPTH PROFILING BY AUGER SIGNAL DECOMPOSITION: SILICON OXYNITRIDE
G. C. Nelson 1989 17 p Presented at the 16th International Conference on Metallurgical Coatings and Equipment Exhibit, San Diego, CA, 17 Apr. 1989
(Contract DE-AC04-76DP-00789)
(DE89-009830; SAND-89-0706C; CONF-890468-5) Avail: NTIS HC A03/MF A01

Thin silicon nitride (Si3N4) films are widely used as a dielectric in metal-nitride-oxide-silicon (MNOS) structures for radiation hard non-volatile memories. The retention of charge in these devices depends, among other things, on the chemistry of the films. It has been reported that charge transport in MNOS structures can be reduced by replacing the Si3N4 film by a silicon oxynitride (SiO sub x N sub y) film. In order to understand the relationship between chemistry and retention of charge, it is necessary to have a technique that can determine the chemistry of the films as a function of depth. This can be accomplished with Auger electron spectroscopy by using fingerprint spectra for each of the elements and compounds present in the sample. By using classical least-squares techniques, a unique combination of the standard spectra can be found that best fits the unknown spectrum. When this method is repeated for each spectrum in a depth profile, a chemical state depth profile is obtained. The use of this technique to profile oxynitride films where the SiO2 content varies between 0 and 12 atomic percent is presented. DOE

N89-22765# Etablissement Technique Central de l'Armement, Arcueil (France). Service Structure des Materiaux.
APPLICATION OF INDENTATION TO THE STUDY OF THE TOUGHNESS OF YTTRIUM-ZIRCON PLASMA COATINGS Final Report [APPLICATION DE L'INDENTATION A L'ETUDE DE LA TENACITE DE REVETEMENTS DE ZIRCONES YTTRIEES OBTENUS PAR PLASMA]
R. Mouginot and M. C. Foujanet 3 Apr. 1987 44 p In FRENCH
(Contract DRET/SDCE/MA-841471)
(ETCA-87-R-040; ETN-89-94343) Avail: NTIS HC A03/MF A01

Ceramic thermal barrier fragility is studied by determination of the toughness in Vicker tests. The observation of indentation fracture permitted to classify the specimens according to toughness and brittelness. It is suggested that the fracture energy absorption capacity is due, at least for some of the specimens, to the transformation of tetragonal to monoclinic structures. ESA

N89-22766# Etablissement Technique Central de l'Armement, Arcueil (France). Service Technologie des Materiaux.
GLASS TRANSITION TEMPERATURE OF THE M10 RESIN ASSOCIATED TO CARBON, KEVLAR OR GLASS FIBERS Final Report [TEMPERATURE DE TRANSITION VITREUSE DE LA RESINE M10 ASSOCIEE A DES FIBRES DE CARBONE, VERRE OU KEVLAR]
Daniel Bouvart, C. Guibe, and B. Foucher 25 Feb. 1987 54 p In FRENCH
(Contract DRET/SDR/G8-84-1022)
(ETCA-87-R-022; ETN-89-94344) Avail: NTIS HC A04/MF A01

The influence of the fiber presence on glass transition temperature of an epoxy resin is studied. It is shown that resin without fibers has a glass transition up to 30 C above the resin with reinforcing fibers. It is suggested that a modification of the crosslinked molecular network in the vicinity of the fibers is responsible for the observed phenomena. ESA

N89-22767# Centre d'Etudes et de Recherches, Toulouse (France). Dept. d'Etudes et de Recherches en Technologie Spatiale.
COATING OF SILICON CARBIDE FIBERS Final Report [REVETEMENTS DE FIBRES DE CARBURE DE SILICIUM]
J. Bernard and J. Siffre Sep. 1987 51 p In FRENCH
(Contract DRET-86-002-15)
(CERT-423900/RF; ETN-89-94362) Avail: NTIS HC A04/MF A01

A thin niobium oxide coating was applied by reactive cathodic spraying. The method allows a homogeneous deposit without affecting the fiber mechanical properties. A complementary study about the high temperature behavior of the coated fibers helps to define the coating material and width. It is shown that the crystallization of the coating could seriously affect the fiber mechanical properties. ESA

N89-22768# Army Materials Technology Lab., Watertown, MA. Polymer Research Branch.
ENVIRONMENTALLY INDUCED DISCONTINUITIES IN TRANSPARENT POLYMERS Final Report
Janice J. Vanselow, Alex J. Hsieh, and Jennie H. Brown Feb. 1989 13 p Presented at the US Army CRDEC Conference, Chemical Defense Research, Nov. 1988
(AD-A205483; MTL-TR-89-11) Avail: NTIS HC A03/MF A01 CSCL 07F

Several grades of poly(methyl methacrylate) (PMMA) used in the aircraft industry have been selected for evaluation of their resistance to chemically-induced stress crazing and cracking. Solvents include simulants for CW agents, the decontaminant, DS2, and another surface active agent, o-xylene. Craze initiation due to solvents applied to the surface of these materials is determined, and the improved stress crazing resistance due to biaxial stretching of PMMA is demonstrated. Fracture toughness is determined for all formulations. Crack propagation is measured in the isotropic samples via a static dead-weight loading apparatus while the solvent, o-xylene, is applied. Results demonstrate varying comparative resistances based on the different test methods. GRA

N89-22769# Princeton Univ., NJ. Dept. of Chemical Engineering.
ANNEALING STUDIES ON A FULLY CURED EPOXY RESIN: EFFECT OF THERMAL PREHISTORY, AND TIME AND TEMPERATURE OF ANNEALING Technical Report, No. 18, 7 Jan. 1988 - 15 Mar. 1989
K. P. Pang and John K. Gillham Mar. 1989 35 p
(Contract N00014-84-K-0021)
(AD-A205875) Avail: NTIS HC A03/MF A01 CSCL 11I

The dynamic mechanical behavior at about 1 Hz of a fully cured epoxy resin (maximum glass transition temperature, T ca. 170 C) has been studied during and after isothermal annealing in terms of the influence of thermal prehistory, time of annealing, and temperature of annealing (Ta). Annealing temperatures ranged from Tg-15 Tg-130 C. The rate of isothermal annealing was observed to decrease by a decade for each decade increase of annealing time when the material was far from equilibrium. Annealing at high temperatures did not measurably affect the material properties during cooling; similarly the effect of annealing at lwo temperatures was not measurable during heating. GRA

N89-22770# Carnegie-Mellon Univ., Pittsburgh, PA. Dept. of Chemistry.
PHYSICAL-CHEMICAL STUDIES OF SOLUTIONS PROCESSING OF NEMATIC POLYMERS Final Report, 1 Sep. 1985 - 31 Aug. 1988
Guy C. Berry 8 Feb. 1989 32 p
(Contracts F49620-85-C-0140; F49620-85-C-1040)
(AD-A205921; AFOSR-89-0288TR) Avail: NTIS HC A03/MF A01 CSCL 07C

Investigations have involved solutions of the rodlike chain poly(1,4-phenylene-2,6-benzobisthiazole), PBT, and related copolymers containing a small fraction of the phenylene replaced by bipyridyl ether. Studies include: (1) The kinetics of polymerization of PBT in the nematic phase; (2) The supramolecular structure of PBT in solution; (3) The phase equilibria of blends of PBT and nylon in solution; (4) The rheological properties of blends of PBT and nylon in solution; and (5) The properties of fully aligned monodomains of nematic solutions of PBT. The polymerization kinetics of PBT did not show any change in rate at the isotropic to an anisotropic phase transition for the solutions studied. At higher conversions (above 90 percent), the polymerization rate constant decreased markedly. This is attributed to effects on the diffusion of the chains along their axes, and comparisons are made to available theoretical models. GRA

N89-22657# Deutsche Forschungs- und Versuchsanstalt fuer Luft- und Raumfahrt, Stuttgart (Germany, F.R.). Inst. for Structures and Design.
MONOLITHIC AND FIBER CERAMIC COMPONENTS FOR TURBOENGINES AND ROCKETS
R. Kochendoerfer *In* AGARD, Application of Advanced Material for Turbomachinery and Rocket Propulsion Mar. 1989 10 p (For primary document see N89-22654 16-23)
Avail: NTIS HC A13/MF A01

N89-22658# Royal Aircraft Establishment, Farnborough (England). Space Dept.
CVD AND DIFFUSION COATINGS FOR HIGH TEMPERATURE APPLICATIONS IN TURBOMACHINERY AND ROCKET MOTORS
S. P. Field, J. E. Restall, C. D. Chalk, and C. Hayman (Fulmer Research Inst. Ltd., Stoke Poges, England) *In* AGARD, Application of Advanced Material for Turbomachinery and Rocket Propulsion Mar. 1989 12 p (For primary document see N89-22654 16-23)
Avail: NTIS HC A13/MF A01

N89-22664# Cranfield Inst. of Tech., Bedford (England). School of Industrial Science.
ADVANCED MATERIALS TO COMBAT THE HIGH TEMPERATURE DEGRADATION PROCESSES IN TURBOMACHINERY
P. Hancock and J. F. Restall (Royal Aircraft Establishment, Farnborough, England) *In* AGARD, Application of Advanced Material for Turbomachinery and Rocket Propulsion Mar. 1989 11 p (For primary document see N89-22654 16-23)
Avail: NTIS HC A13/MF A01

N89-22665# Garrett Turbine Engine Co., Phoenix, AZ.
THE DEMONSTRATION OF MONOLITHIC AND COMPOSITE CERAMICS IN AIRCRAFT GAS TURBINE COMBUSTORS
Frank G. Davis and Dale A. Hudson *In* AGARD, Application of Advanced Material for Turbomachinery and Rocket Propulsion Mar. 1989 10 p (For primary document see N89-22654 16-23)
Avail: NTIS HC A13/MF A01

N89-22669# Brown, Boveri und Cie A.G., Mannheim (Germany, F.R.). Materials Technology Lab.
INTERACTION OF COATINGS WITH BASE METALS AT HIGH TEMPERATURE
Hermann W. Gruenling, K. Schneider, and L. Singheiser *In* AGARD, Application of Advanced Materials for Turbomachinery and Rocket Propulsion Mar. 1989 23 p (For primary document see N89-22654 16-23)
Avail: NTIS HC A13/MF A01

N89-22670*# National Aeronautics and Space Administration. Marshall Space Flight Center, Huntsville, AL.
VACUUM PLASMA SPRAY COATING
Richard R. Holmes and Timothy N. McKechnie (Rockwell International Corp., Huntsville, AL.) *In* AGARD, Application of Advanced Material for Turbomachinery and Rocket Propulsion Mar. 1989 5 p (For primary document see N89-22654 16-23)
Avail: NTIS HC A13/MF A01 CSCL 11C

N89-22671*# National Aeronautics and Space Administration. Lewis Research Center, Cleveland, OH.
THRUST CHAMBER THERMAL BARRIER COATING TECHNIQUES
Richard J. Quentmeyer *In* AGARD, Application of Advanced Material for Turbomachinery and Rocket Propulsion Mar. 1989 10 p Previously announced as N88-24690 (For primary document see N89-22654 16-23)
Avail: NTIS HC A13/MF A01 CSCL 11C

N89-22677# Office National d'Etudes et de Recherches Aerospatiales, Palaiseau (France).
CERAMIC HEAT EXCHANGERS AND TURBINE BLADES: THEORY AND EXPERIMENTAL RESULTS [ECHANGEURS DE CHALEUR ET AUBES DE TURBINE EN CERAMIQUE THEORIE ET RESULTATS EXPERIMENTAUX]
P. Avran and S. Boudigues *In* AGARD, Application of Advanced Material for Turbomachinery and Rocket Propulsion Mar. 1989 11 p In FRENCH; ENGLISH summary (For primary document see N89-22654 16-23)
Avail: NTIS HC A13/MF A01

N89-22679# Defence Research Establishment Valcartier (Quebec).
DEVELOPMENT OF AN ASBESTOS-FREE INSULANT FOR ROCKET MOTORS
D. Sanschagrin and G. Couture *In* AGARD, Application of Advanced Material for Turbomachinery and Rocket Propulsion Mar. 1989 10 p (For primary document see N89-22654 16-23)
Avail: NTIS HC A13/MF A01

28 PROPELLANTS AND FUELS

Includes rocket propellants, igniters, and oxidizers; their storage and handling procedures; and aircraft fuels.

For related information see also *07 Aircraft Propulsion and Power, 20 Spacecraft Propulsion and Power,* and *44 Energy Production and Conversion.*

N89-22771# New Energy Development Organization, Tokyo (Japan).
SURVEY OF DEVELOPMENT TRENDS OF METHANOL AUTOMOBILES AND METHANOL FUEL IN CHINA
Tsuyoshi Hashimoto, Takehiko Sato, Ryo Suzuki, Tsutomu Toichi, and Tomoya Kikuchi May 1988 158 p In JAPANESE
(DE88-756492; NEDOJ-P-8743) Avail: NTIS (US Sales Only) HC A08/MF A01

This report was prepared basing upon the results of the field survey in China during the period from January through May 1988. In China, the Seventh Five-Year Program is now being carried out and the established target is to quadruple her national income in a 20 year period from 1981 through 2000. It is planned to secure the supply of energy in the future mainly with coal and from the viewpoints that the demand of fuel for transportation in the future is expected to increase greatly and that she has such feedstock for methanol as coal abundantly, she is very active in the development concerning the introduction of methanol as automobile fuel. In this survey, the basic survey concerning the policy of oil alternate energy includes: (1) the countermeasure concerning fuel for transportation, (2) the current situation of the research and development of methanol automobiles as one of the oil alternate policies and its appropriate assessment, and (3) the current situation and the future prospect of methanol as fuel was conducted and the consolidation of information for the examination of the feasibility of the cooperation between Japan and China in the future was made. DOE

N89-22772# Air Force Inst. of Tech., Wright-Patterson AFB, OH. School of Engineering.
INTERNAL DEBONDING OF SOLID ROCKET FUEL: AN EXPERIMENTAL INVESTIGATION M.S. Thesis
James N. Hanley Dec. 1988 111 p
(AD-A205903; AFIT/GAE/AA/88D-19) Avail: NTIS HC A06/MF A01 CSCL 21I

The objective of this study was the development of a method to compute the fracture energy required to debond crystal particles in a solid rocket fuel. A blister test was defined that pressurizes an initially debonded region to generate an adhesive fracture. An LVDT measures the displacement of the blister. The fracture energy is expressed in terms of the critical loading, displacement, specimen geometry and material properties. Consistent results required developing a proper casting and curing method for thin polymeric layers onto a crystal substrate. Various thicknesses and substrates were examined. The study found that the deflection of the blister behaved like a plate and could be analyzed as one to compute the adhesive fracture energy. The dimensionless values of fracture energy fell along predictable curves for small values of adhesive thicknesses to blister radii. The adhesive fracture energy was found to be a function of force applied, adhesive material properties and blister geometry. The value for adhesive fracture energy on a crystal substrate is compared to a Plexiglass substrate for an epoxy resin. And a polished and unpolished crystal specimen's fracture energy are compared. GRA

29 MATERIALS PROCESSING

Includes space-based development of products and processes for commercial applications.

For biological materials see *55 Space Biology.*

N89-22773*# Alabama Univ., Huntsville.
CONSORTIUM FOR MATERIALS DEVELOPMENT IN SPACE Annual Report, 1 Oct. 1987 - 30 Sep. 1988
30 Sep. 1988 48 p
(Grant NAGw-812)
(NASA-CR-181405; NAS 1.26:181405) Avail: NTIS HC A03/MF A01 CSCL 22A

The status of the Consortium for Materials Development in Space (CMDS) is reviewed. Individual projects are outlined and the status of Get Away Special (GAS) 105 is summarized. B.G.

N89-22774# Ruhr Univ., Bochum (Germany, F.R.). Arbeitsgruppe Physikalische Chemie der Grenzflaechen.
ADSORPTION STUDIES IN THE CRITICAL REGION OF A PURE FLUID. DEVELOPMENT OF AN APPARATUS FOR ADSORPTION MEASUREMENTS UNDER MICROGRAVITY CONDITIONS Final Report
Gerhard Helmut Findenegg and Hans Lewandowsij Dec. 1987 77 p In ENGLISH and GERMAN Original contains color illustrations
(Contract BMFT-01-QV-070)
(ETN-89-93767) Avail: NTIS HC A05/MF A01

A differential-volumetric measuring apparatus was developed for the determination of the adsorption of supercritical fluids as a function of temperature at constant bulk density. The

measurements of thermophysical properties of the microscopic boundary layer at fluid/solid interfaces in the near-critical region are affected by the gravitational field of the Earth that causes a density gradient in the fluid. The developed differential-volumetric technique allows measurements under microgravity conditions on a free-flying space platform like EURECA. The scientific background of these experiments is outlined. Preliminary results for the adsorption of sulfur hexafluoride on graphite and graphitized carbon are presented. ESA

N89-22775# Dornier-Werke G.m.b.H., Friedrichshafen (Germany, F.R.).
MINI PROTEIN CRYSTALLIZATION FACILITY (MPCF), PHASE A STUDY: EXECUTIVE SUMMARY
R. Bosch and Stapelmann May 1988 43 p Prepared in cooperation with Carrar, France and Cosurvey, Belgium
(Contract ESA-7403/87/F/FL(SC))
(ESA-CR(P)-2709; ETN-89-94240) Avail: NTIS HC A03/MF A01

A protein facility for a Biokosmos flight is discussed. Existing facilities designed for Spacelab, shuttle, and EURECA are unsuitable, so a system was designed. It carries 90 experiment cells mounted on 9 stacks (LPCF-type) or optionally, 70 cells where 2 cells can be observed and crystals can be detected and photographed. Mass is 40 kg; box dimensions 582 x 268 mm; power consumption is 50 W nominal; one process temperature; temperature accuracy is 1 K for all phases. The facility is integrated into Biokosmos in Moscow and thermal preconditioned prior to stack insertion. The stacks are inserted at launch site, where Biokosmos power is used for the thermal control; prelaunch power breakdowns of Biokosmos are acceptable up to 30 hr. ESA

31 ENGINEERING (GENERAL)

Includes vacuum technology; control engineering; display engineering; cryogenics; and fire prevention.

N89-22776# Technische Univ., Delft (Netherlands).
SIMULATION OF A REFRIGERANT EVAPORATOR Ph.D. Thesis
Jakob Stefanus vanderMeer 1987 164 p
(ETN-89-94133) Avail: NTIS HC A08/MF A01

A computer model for the design and optimization of the compressor refrigeration cycle especially with respect to dynamic behavior was developed. A steady state version was also developed. The model describing the refrigerant is divided into the evaporation and superheating regions. A mechanism based on empirics corrects the model for the influence of transportation times in the evaporation region. The mass balance of the refrigerant in the superheat region is regarded as quasi-static, because of the small mass of the vapor. The energy balance accounts for a distributed model and is represented by the steady state solution of the partial differential equation which describes this area for the steady conditions. A correction for the dynamical effects was added to this solution, for all influencing parameters, according to the analytical dynamic solution for the case of the evaporation temperature as input parameter. The expansion device model was worked out for the usual type of device in combination with a dry evaporator, the thermostatic expansion valve. Validation tests are described. ESA

N89-22777# Aeronautical Research Inst. of Sweden, Stockholm. Wind Energy Dept.
PRELIMINARY BLADE DESIGN USING INTEGRATED COMPUTER CODES
Arve Ryan Dec. 1988 28 p Sponsored by the Swedish National Energy Administration
(FFA-TN-1988-67; ETN-89-94317) Avail: NTIS HC A03/MF A01

Loads on the root of a horizontal axis wind turbine (HAWT) rotor blade were analyzed. A design solution for the root area is presented. The loads on the blades are given by different load cases that are specified. To get a clear picture of the influence of different parameters, the whole blade is designed from scratch. This is only a preliminary design study and the blade should not be looked upon as a construction reference. The use of computer programs for the design and optimization is extensive. After the external geometry is set and the aerodynamic loads calculated, parameters like design stresses and laminate thicknesses are run through the available programs, and a blade design optimized on basis of facts and estimates used is shown. ESA

N89-22778# Aeronautical Research Inst. of Sweden, Stockholm. Aerodynamics Dept.
BLADE ROOT DESIGN: A STATE OF ART SURVEY
Olof Sandberg Nov. 1988 21 p Sponsored by the Swedish National Energy Administration
(FFAP-201; ETN-89-94318) Avail: NTIS HC A03/MF A01

Glass fiber reinforced plastic wind turbine blades are discussed, and 10 blade root designs are presented. They are considered to represent the state of the art. Suggestions are made as to how to proceed in the development of the bonded bolt type of root retention. For this type of very high cycle fatigue designs there is a need for two redundant design principles. ESA

32 COMMUNICATIONS AND RADAR

Includes radar; land and global communications; communications theory; and optical communications.

For related information see also *04 Aircraft Communications and Navigation* and *17 Space Communications, Spacecraft Communications, Command and Tracking.* For search and rescue see *03 Air Transportation and Safety,* and *16 Space Transportation.*

N89-22779*# City Coll. of the City Univ. of New York, NY. Inst. of Marine and Atmospheric Sciences.
PROBABILITIES AND STATISTICS FOR BACKSCATTER ESTIMATES OBTAINED BY A SCATTEROMETER WITH APPLICATIONS TO NEW SCATTEROMETER DESIGN DATA
Willard J. Pierson, Jr. Washington NASA Apr. 1989 132 p
(Grant NAGw-690)
(NASA-CR-4228; NAS 1.26:4228) Avail: NTIS HC A07/MF A01 CSCL 20N

The values of the Normalized Radar Backscattering Cross Section (NRCS), sigma (o), obtained by a scatterometer are random variables whose variance is a known function of the expected value. The probability density function can be obtained from the normal distribution. Models for the expected value obtain it as a function of the properties of the waves on the ocean and the winds that generated the waves. Point estimates of the expected value were found from various statistics given the parameters that define the probability density function for each value. Random intervals were derived with a preassigned probability of containing that value. A statistical test to determine whether or not successive values of sigma (o) are truly independent was derived. The maximum likelihood estimates for wind speed and direction were found, given a model for backscatter as a function of the properties of the waves on the ocean. These estimates are biased as a result of the terms in the equation that involve natural logarithms, and calculations of the point estimates of the maximum likelihood values are used to show that the contributions of the logarithmic terms are negligible and that the terms can be omitted. Author

N89-22780*# Smithsonian Astrophysical Observatory, Cambridge, MA.
THEORETICAL INVESTIGATION OF EM WAVE GENERATION AND RADIATION IN THE ULF, ELF, AND VLF BANDS BY THE ELECTRODYNAMIC ORBITING TETHER Final Report, 1 May 1987 - 31 Jul. 1988
Robert D. Estes and Mario D. Grossi Mar. 1989 74 p
(Grant NAG8-638)
(NASA-CR-181560; NAS 1.26:181560) Avail: NTIS HC A04/MF A01 CSCL 20N

The problem of electromagnetic wave generation by an electrodynamic tethered satellite system is important both for the ordinary operation of such systems and for their possible application as orbiting transmitters. The tether's ionospheric circuit closure problem is closely linked with the propagation of charge-carrying electromagnetic wave packets away from the tethered system. Work is reported which represents a step towards a solution to the problem that takes into account the effects of boundaries and of vertical variations in plasma density, collision frequencies, and ion species. The theory of Alfen wave packet generation by an electrodynamic tethered system in an infinite plasma medium is reviewed, and brief summary of previous work on the problem is given. The consequences of the presence of the boundaries and the vertical nonuniformity are then examined. One of the most significant new features to emerge when ion-neutral collisions are taken into account is the coupling of the Alfven waves to the fast magnetosonic wave. This latter wave is important, as it may be confined by vertical variations in the Alfven speed to a sort of leaky ionospheric wave guide, the resonances of which could be of great importance to the signal received on the Earth's surface. The infinite medium solution for this case where the (uniform) geomagnetic field makes an arbitrary angle with the vertical is taken as the incident wave-packet. Even without a full solution, a number of conclusions can be drawn, the most important of which may be that the electromagnetic field associated with the operation of a steady-current tethered system will probably be too weak to detect on the Earth's surface, even for large tethered currents. This is due to the total reflection of the incident wave at the atmospheric boundary and the inability of a steady-current tethered system to excite the ionospheric wave-guide. An outline of the approach to the numerical problem is given. The use of numerical integrations and boundary conditions consistent with a conducting Earth is proposed to obtain the solution for the horizontal electromagnetic field components at the boundary of the ionosphere with the atmospheric cavity. Author

N89-22781# Air Force Inst. of Tech., Wright-Patterson AFB, OH. School of Engineering.
POSITION, SCALE, AND ROTATION INVARIANT OPTICAL PATTERN RECOGNITION FOR TARGET EXTRACTION AND IDENTIFICATION M.S. Thesis
J. T. Walrond and Timothy G. Childress Dec. 1988 148 p
(AD-A202600; AD-E900870; AFIT/GE/ENG/88D-4) Avail: NTIS HC A07/MF A01 CSCL 17K

The feasibility of optically implementing a real-time, pattern recognition system using correlation techniques in a position, scale, and rotation invariant (PSRI) feature space was investigated. Input target templates were optically Fourier transformed using an improved high-resolution, high-pass filter positioned in the focal plane of the transforming lens. A logarithmic-polar coordinate transform of the magnitude-squared of the Fourier transform (/FT/2) was performed with an improved method of focusing the magnified /FT/2 onto a computer generated hologram (CGH), which was shown to scale linearly along the horizontal axis and logarithmically along the vertical axis. Optical, matched-filter correlations on the magnitude-squared Fourier transform logarithmic-polar (FLRT) feature space were performed using thermoplastic, phase-relief holography and Vander Lugt filtering. Correlation results prove that scale and rotation changes of the input can be predicted accurately based on linear shifts of the correlation peak. Also, the FLRT feature space is shown to provide excellent discrimination for multiple-input scenes. The need for a cyclic correlation was verified, and digital simulations prove the validity of the optical results. GRA

N89-22782# Air Force Inst. of Tech., Wright-Patterson AFB, OH. School of Engineering.
VERIFICATION AND LIMITATIONS OF THE MONOSTATIC-BISTATIC RADAR CROSS SECTION DERIVED BY KELL M.S. Thesis
Jeffrey M. MacLennan Dec. 1988 127 p
(AD-A202601; AD-E900870; AFIT/GE/ENG/88D-24) Avail: NTIS HC A07/MF A01 CSCL 17I

Robert Kell developed a relationship between monostatic radar cross section (RCS) and bistatic RCS whereby bistatic RCS can be predicted from monostatic RCS measure under certain conditions. This study found Kell's relationship to be mathematically sound given certain assumptions. Kell's relationship was then tested by comparing computer generated bistatic and monostatic cross sections for simple shapes. Four parameters were varied during testing in order to discern possible limitations of Kell's method: bistatic angle, angle of incidence, electrical size of the target, and continuity. Results of the testing show Kell's method has some merit. The difference between the bistatic RCS and its related monostatic RCS for electrically large spheres is less than 1-dB up to bistatic angles of 80 deg. For electrically large flat and singly curved surfaces the monostatic and bistatic cross sections were within 3-dB for angles of incidence up to 30 deg from broadside and bistatic angles up to 15 deg. Finally, the accuracy of Kell's relationship proved to be polarization dependent when surface discontinuities in the form of 90 deg wedges were present. GRA

N89-22783# Stanford Linear Accelerator Center, CA.
COMPUTER AIDED DESIGN OF THREE-DIMENSIONAL WAVEGUIDE LOADED CAVITIES
Yehuda Goren and David U. L. Yu (DULY Consultants, Rancho Palos Verdes, CA.) Feb. 1989 20 p
(Contracts DE-AC03-76SF-00515; DE-AC03-87ER-80529)
(DE89-007733; SU-SLAC/AP-73) Avail: NTIS HC A03/MF A01

We have developed two simple methods to calculate the power transport through an external waveguide of a loaded cavity utilizing the RF parameters obtained from the frequency domain codes. In the first method the external power loss through an open waveguide is expressed in terms of equivalent circuit coupling parameters between a closed waveguide and a cavity to which it is connected. As we shall see, this equivalent circuit approach is limited in it applicability only to structures with high loaded Q values, say Q(sub L) less than 200. In the second method, the power flow through an external waveguide is calculated from an analysis of the electromagnetic field components of the standing waves in the closed waveguide-cavity structure. Our models make use of the MAFIA code to obtain values of structural parameters and fields when an external waveguide is abruptly terminated with a metal surface. A typical model consists of an output cavity attached via an iris to a short waveguide section ended with a conducting cap. Our methodologies of calculating the loaded Q(sub L) in terms of the parameters of the closed waveguide-cavity model are described in the following sections. We have obtained reasonable and encouraging results for several loaded cavities whose values of Q(sub L) have been experimentally measured. Of particular interest is the application to low-Q structures such as the relativistic klystron output cavities. The electromagnetic field method yields good agreement with experimental measurements. This method has also been successfully applied to high gradient accelerating structures with slots for damping out higher modes as recently proposed by Palmer. DOE

N89-22784# Boys Town National Inst., Omaha, NE.
DETECTION OF KNOWN SIGNALS IN ARBITRARY BACKGROUNDS Annual Report, 1 Sep. 1987 - 30 Sep. 1988
Donna L. Neff, Walt Jesteadt, and Brian P. Callaghan Oct. 1988 25 p
(Grant AF-AFOSR-0374-87; AF Proj. 2313)
(AD-A204076; AFOSR-88-1227TR) Avail: NTIS HC A03/MF A01 CSCL 06J

Psychophysical masking studies examined conditions in which the basic task was the detection of a target sound presented simultaneously with maskers whose component frequencies changed with each presentation. Experiments focused on the important determinants of performance when maskers are randomized. Specific experiments found: (1) that psychometric functions for individual maskers were extremely shallow relative to slopes under minimal uncertainty, (2) that the masking produced by combinations of broadband noise and multicomponent maskers

was greater than that predicted from a linear sum of the effects of each masker alone, (3) that the effects of masker uncertainty were greatly reduced or eliminated in forward masking, (4) that the large individual differences observed were not reflected in measures of peripheral filter shape, and (5) that masking produced by uncertainty was extremely resistant to change as masker energy was progressively removed from the frequency region around the signal. GRA

N89-22785# International Centre for Theoretical Physics, Trieste (Italy).
DISTORTIONS CAUSED BY THE SIGNAL PROCESSING IN ANALOG AM MODULATORS
Ernest C. Njau (Dar-es-Salaam Univ., Tanzania) Aug. 1988 10 p
(DE88-705657; IC-88/225) Avail: NTIS (US Sales Only) HC A02/MF A01

Complete analytical expressions for distortions caused by signal processing in analog AM modulators are developed. The salient features in these expressions are shown to be consistent with displays of actual spectra of AM signals. Finally suggestions are given on how the distortions may be practically minimized. DOE

N89-22786# Oak Ridge National Lab., TN. Instrumentation and Controls Div.
APPROXIMATION TECHNIQUE FOR DETERMINING GAIN AND RADIATION PATTERN OF THE HORN ANTENNA
Paul D. Ewing 1989 6 p Presented at the Southeastcon '89 Conference and Exhibition, Columbia, SC, 9 Apr. 1989
(Contract DE-AC05-84OR-21400)
(DE89-006136; CONF-8904111-3) Avail: NTIS HC A02/MF A01

An approximation can be used to avoid the complex mathematics and computation methods for calculating the gain and radiation pattern of the electromagnetic horn antenna. Because of the curvature of the antenna wave front, calculations using conventional techniques typically involve solving the Fresnel integrals and using computer-aided numerical integration. With this model, linear approximations give a reasonable estimate of the gain and radiation pattern using simple trigonometric functions, allowing a hand calculator to replace the computer. The case of the E-plane horn antenna was used to evaluate this technique, applying selected criteria. Results showed that the gain approximation holds for an antenna flare angle of less than 10 degrees for typical antenna dimensions, and the E field radiation pattern approximation holds until the antenna's phase error approaches 60 degrees, both within typical design parameters. This technique is a useful engineering tool. DOE

N89-22787# Oak Ridge National Lab., TN.
THE INDUCED CURRENT IN PARALLEL WIRES OVER AN IMPERFECT GROUND FROM AN INCIDENT EMP
Herbert P. Neff, Jr. and Dennis A. Reed 1989 29 p Presented at the Southeastcon 1989 Conference and Exhibition, Columbia, SC, 9 Apr. 1989
(Contract DE-AC05-84OR-21400)
(DE89-007209; CONF-8904111-4) Avail: NTIS HC A03/MF A01

The current that is induced in infinitely long, finitely conducting, and parallel wires over a finitely conducting plane earth from an incident electromagnetic pulse is investigated. Frequency-domain expressions for this current are derived. Time-domain results are obtained for the case of two wires at the same height above the earth for several wire spacings and ground parameters. It was found that the maximum current was about 8 kA for grazing incidence (theta = 6(degree)) when the wire spacing is large, corresponding to the single wire case. When the wire spacing is small, the current approaches one-half the value above (4 kA) as it should. This suggest the use of multiple wires in a cage arrangement for reducing the induced current. DOE

N89-22788# Lawrence Livermore National Lab., CA.
GENERAL GRID FINITE DIFFERENCE METHODS FOR TIME DEPENDENT ELECTROMAGNETIC PROBLEMS IN TWO DIMENSIONS
Scott L. Ray Nov. 1988 9 p Presented at the 7th International Conference on Finite Element Methods in Flow Problems, Huntsville, AL, 3 Apr. 1989 Submitted for publication
(Contract W-7405-eng-48)
(DE89-007225; UCRL-99865; CONF-890479-7) Avail: NTIS HC A02/MF A01

A new method for solving Maxwell's equations in the time domain on two-dimensional irregular grids has been developed. The method is based on finite-difference approximations to Ampere's and Faraday's laws in both their differential and integral forms. These difference approximations are derived, in part, using finite element notions of coordinate transformations and isoparametric function mapping. Key features of the general-grid method are that it is a direct generalization of the familiar, orthogonal grid finite-difference, time-domain technique and that it is more accurate than previous irregular grid methods. DOE

N89-22789# Lawrence Livermore National Lab., CA.
SPECIAL TECHNIQUES USED FOR TIME DOMAIN, THREE DIMENSIONAL FINITE ELEMENT MODELING OF ELECTROMAGNETICS
J. Brian Grant Nov. 1988 9 p Presented at the 7th International Conference on Finite Element Methods in Flow Problems, Huntsville, AL, 3 Apr. 1989
(Contract W-7405-eng-48)
(DE89-007227; UCRL-97689; CONF-890479-5) Avail: NTIS HC A02/MF A01

Accurate and reliable electromagnetic modeling codes, which may be specific or general purpose, help Lawrence Livermore National Laboratory carry out its research. However, a need for a three-dimensional coded prompted the development of a finite element code. MAXWELL3 is a general electromagnetic modeling code (solves the differential Maxwell equations in the time domain) allows arbitrary geometrical shapes for simulation regions. The finite element technique was chosen over the finite difference technique because of the boundary-conforming discretization of the former. This paper focuses on some of the techniques used to make 3D finite elements tractable in electromagnetics. Sample models are presented to illustrate some of the effects certain techniques, e.g., a free space boundary, have on the solution. DOE

N89-22790# Los Alamos National Lab., NM.
SUPERFISH ACCURACY DEPENDENCE ON MESH SIZE
J. L. Merson and G. P. Boicourt 1989 4 p Presented at the 13th Particle Accelerator Conference, Chicago, IL, 20-23 Mar. 1989
(Contract W-7405-eng-36)
(DE89-007992; LA-UR-89-599; CONF-890335-4) Avail: NTIS HC A02

The RF cavity code SUPERFISH is extensively used for the design of drift-tube linac (DTL), radio-frequency quadrupole (RFQ), and coupled-cavity linac (CCL) structures. It has been known for some time that considerably finer meshes are required near the nose of a drift tube to ensure accurate calculation of the resonant frequency and related secondary quantities. This paper discusses the results of numerical experiments designed to provide rules to set proper mesh sizes for DTL, RFQ, and CCL problems. During this work, SUPERFISH problems involving more than 100,000 mesh points were solved. DOE

N89-22791# Wisconsin Univ., Madison. Dept. of Electrical and Computer Engineering.
ICRF WAVEGUIDE LAUNCHER RESEARCH Final Progress Report, Jun. 1986 - Feb. 1989
J. E. Scharer 28 Feb. 1989 19 p
(Contract DE-FG02-86ER-52133)
(DE89-009151; DOE/ER-52133/3) Avail: NTIS HC A03/MF A01

The research we have accomplished during the past year includes the topics of ICRF fast wave coupling to L- and H-mode edge profiles, measurements of simulated plasma loads on a dielectric-filled 85 MHz waveguide launcher and an analysis of coupling of ion Bernstein waves. We have also carried out a computer simulation, fabrication and initial laboratory measurements on a 2 GHz scale model vacuum folded guide launcher. We have also begun to examine coupling between launched fast waves and ion Bernstein waves driven by density gradients near the plasma edge and the effects of known edge turbulence and ponderomotive forces on the direct launching of ion Bernstein waves. DOE

N89-22792# Forschungsinstitut der Deutschen Bundespost, Darmstadt (Germany, F.R.).
THE RADIATION PERFORMANCE OF OFFSET REFLECTOR ANTENNAS WITH HORN FEEDS EXCITED BY HIGH ORDER MODES
Herbert Thielen Jul. 1988 16 p In GERMAN; ENGLISH summary
(FI-454-TB-43; ETN-89-93771) Copyright Avail: NTIS HC A03/MF A01

The physical reasons for alignment errors in the antenna tracking of asymmetric reflector systems were investigated. The radiation behavior of offset reflector antennas, employing higher-order modes was theoretically and experimentally analyzed. In the case of TE21-mode excitation, a cross-polarization component is produced in single-reflector antennas due to feed tilt which is considerably larger than with the communication mode (TE11 or HE11 mode). In the case of circular polarization, this causes a null shift amounting to 1/10 or 1/5 of the half-power beam width of the main lobe. No null shift exists for the TM01- and TE01-modes. When the TE21-mode is used, the cross-polarization component is considerably smaller for dual-offset than for single-reflector antennas. In the case of ground station antennas where beam-waveguides consisting of two reflectors are used, a similar performance is obtained as for single-reflector antennas. ESA

N89-22793 Forschungsinstitut fuer Hochfrequenzphysik, Werthhoven (Germany, F.R.).
OBSERVATION PARAMETERS FOR A GROUND-BASED RADAR STATION TO SURVEY NEAR-EARTH SATELLITES
Dieter Mehrholz May 1988 64 p In GERMAN; ENGLISH summary
(Contract BMVg-T/RF31/D0038/D1332)
(Rept-4-88; Lfd-273; ETN-89-93774) Copyright Avail: Forschunginstitut fuer Hochfrequenzphysik, Wachtberg-Werthhoven, Fed. Republic of Germany

Parameters of observation were defined for a ground-based radar station aiming at the survey of noncooperative objects in the near-Earth space. The parameters are quantitatively illustrated by satellite orbits. The examples are chosen in such a way that upper limits for the corresponding observation parameters are deduced, leading to requirements for radar equipment. The parameters are used for the quality control of radar data. ESA

N89-22794# Technische Univ., Delft (Netherlands).
SELECTED ASPECTS OF DISCRETE-TIME FILTERING TECHNIQUES AS APPLIED TO SENSOR CONTROL AND SIGNAL PROCESSING PROBLEMS Ph.D. Thesis
Lars Bjorset 1988 237 p
(ETN-89-94134) Avail: NTIS HC A11/MF A01

The general structure of the discrete-time linear filter and basic rules for paralleling and cascading multiple filters are defined. Rules for feedback and feedforward within complexes of interconnected filters are established. Discrete-time initial and final value theorems are defined, and applications for the analysis of control systems are discussed. Basic filter synthesis techniques are defined. Implications of sampling rate conversions (decimation and interpolation) in discrete-time control systems are analyzed, and applications to sensor systems are considered. The solution of sensor signal processing problems through the application of discrete-time finite impulse response (FIR) filters is treated. Complex signal representations are defined, together with the generalized complex filter, and basic properties are discussed. The feasibility of parallel-shifting the characteristics of FIR filters along the frequency axis is analyzed. The resulting filters are shown to have close similarities to filters banks realized by windowing and subsequent discrete Fourier transform processing. ESA

N89-22795# Technische Univ., Delft (Netherlands).
HIFI: A DESIGN METHOD FOR IMPLEMENTING SIGNAL PROCESSING ALGORITHMS ON VLSI PROCESSOR ARRAYS Ph.D. Thesis
Jurgen Annevelink 1988 212 p
(ETN-89-94138) Avail: NTIS HC A10/MF A01

A design method, called HIFI, that makes it possible to systematically implement a large class of signal processing algorithms on systolic and wavefront arrays is defined. The model underlying the definition of the design method is a combination of a process oriented model and an applicative, function oriented model. The result is a model that combines a high level of abstraction with powerful decomposition mechanisms. The model is used to define the HIFI design method, which allows both top-down and bottom-up design styles. The HIFI design-method is based on two different design steps: refinement, which makes it possible to define the decomposition of a function with a dependence graph; and partitioning, used to project a dependence graph on a so-called signal flow graph, which allows a more efficient implementation, of the function defined by the dependence graph. The design method is illustrated by an algorithm for the solution of a system of linear equations, and the transitive closure algorithm. ESA

N89-22796# Los Alamos National Lab., NM.
SCALING RELATIONS FOR A BEAM-DEFLECTING TM(110) MODE IN AN ASYMMETRIC CAVITY
H. Takeda 1989 4 p Presented at the 13th Particle Accelerator Conference, Chicago, IL, 20 Mar. 1989
(Contract W-7405-eng-36)
(DE89-009277; LA-UR-89-949; CONF-890335-33) Avail: NTIS HC A02/MF A01

A deflecting mode in an rf cavity caused by an aperture of the coupling hole from a waveguide is studied. If the coupling hole was a finite size, the rf modes in the cavity can be distorted. We consider the distorted mode as a sum of the accelerating mode, and the deflecting mode. The finite-size coupling hole can be considered as radiating dipole sources in a closed cavity. Following the prescription given by H. Bethe, the relative strength of the deflecting mode TM sub 110 to the accelerating TM sub 010 mode is calculated by decomposing the dipole source field into cavity eigenmodes. Scaling relations are obtained as a function of the coupling hole radius. DOE

N89-22797# Lawrence Livermore National Lab., CA. Technology Information Systems.
PixMail: PICTURES THROUGH MAIL
Meera Blattner, Francisco Sierra, and Peter Prassinos Feb. 1989 13 p Prepared in cooperation with California Univ., Davis
(Contract W-7405-eng-48)
(DE89-009682; UCID-21652) Avail: NTIS HC A03/MF A01

PixMail is a set of procedures for sending pictures through internet mail. The pictures can be sent or received by personal computers, terminals with or without raster capability, and facsimile machines. Optical scanners may be used as input to the picture file and printers may be used as an output device once the raster file is stored in a form used by a paint editor. No additional equipment needs to be purchased by the users to send or receive PixMail (unless facsimile input/output is desired) and it is no more difficult to send or receive than ordinary UNIX mail. PixMail uses the protocols of existing electronic mail for transmission from any ARPAnet or MILnet user to any other. DOE

N89-22798# Argonne National Lab., IL.
CALCULATION OF LONGITUDINAL AND TRANSVERSE WAKE-FIELD EFFECTS IN DIELECTRIC STRUCTURES
W. Gai 1989 10 p Presented at the Advanced Accelerator Concepts Workshop, Lake Arrowhead, CA, 9 Jan. 1989
(Contract W-31-109-eng-38)
(DE89-009814; ANL-HEP-CP-89-24; CONF-890197-6) Avail: NTIS HC A02/MF A01

The electro-magnetic radiation of a charged particle passing through a dielectric structure has many applications to accelerator physics. Recently a new acceleration scheme, called the dielectric wake field accelerator, has been proposed. It also can be used as a pick up system for a storage ring because of its slow wave characteristics. In order to study these effects in detail, in this paper we will calculate the wake field effects produced in a dielectric structure by a charged particle. DOE

N89-22799# Swedish Inst. of Space Physics, Uppsala. Inst. foer Rymdfysik.
EFFECT OF PUMP-INDUCED DENSITY DEPLETIONS ON THE SPECTRUM OF STIMULATED ELECTROMAGNETIC EMISSIONS
T. B. Leyser and B. Thide Jun. 1988 21 p Sponsored in part by the Swedish Natural Science Research Council, Stockholm
(IRF-Preprint-107; ISSN-0284-1711; ETN-89-94319) Avail: NTIS HC A03/MF A01

Analytical formulas describing the standing wave pattern in the ionospheric reflection region of a vertically propagating HF electromagnetic wave in the O mode are used to estimate density depletions due to the ponderomotive force of the successive wave maxima. The frequencies of Langmuir waves enhanced through the parametric decay instability in the created density wells are determined. It is suggested that a spectral feature of the stimulated electromagnetic emissions, downshifted by 1 to 2 kHz from the pump frequency, is evidence of parametrically excited Langmuir waves mode converted to electromagnetic waves. Stimulated radiation then provides a means for remote sensing of the peak electric field strength in the reflection region. ESA

N89-22800# Deutsche Forschungs- und Versuchsanstalt fuer Luft- und Raumfahrt, Oberpfaffenhofen (West Germany). Abteilung Hochfrequenzphysik.
COHERENT POLARIMETRIC RADAR TECHNIQUES FOR MICROWAVE PROPAGATION AND CLOUD PHYSICS RESEARCH
Arno Schroth, Peter Meischner, and Madhukar Chandra Oct. 1988 104 p
(DFVLR-FB-88-47; ISSN-0171-1342; ETN-89-94380) Avail: NTIS HC A06/MF A01; DVFLR, VB-PL-DO, Postfach 90 60 58, 5000 Cologne, Fed. Republic of Germany, DM 25.50

A polarimetric C-Band radar is presented. Real-time processing of data, especially the determination of the scattering matrix and the Stokes-matrix of the targets, is discussed. The phenomenological description of targets with the aid of special parameters is reviewed. The utilization of a radar observable in deriving microphysical information about the target is explained. Examples of real-time polarimetric measurements of meteorological targets by the radar are presented. ESA

N89-22801# Telebit, Copenhagen (Denmark).
STUDY ON COMMUNICATIONS COSTS FOR COLUMBUS UTILIZATION
Svend Moller Nielsen and Nicolaj Sorensen Paris, France ESA 15 Sep. 1988 77 p
(Contract ESA-7266/87/D/IM)
(Rept-871126/1/FR; ESA-CR(P)-2731; ETN-89-94457) Copyright Avail: NTIS HC A05/MF A01

On the basis of a hypothetical communications scenario established for cost calculations, the expected communications costs for Columbus utilization in the year 1995 and onwards to the year 2025, are estimated to provide initial considerations for a charging policy in relation to potential Columbus users. A hypothetical sample of five European countries is established, and current telecommunications tariffs for the data, voice, and video communications required for the Columbus utilization in and between these five countries and the USA are identified. Technological, political, and commercial development trends are analyzed as to their likely influences on future telecommunications tariff development. Communications costs for the study period are estimated, assuming telecommunications administrations to be providers of service and considering estimated equipment and operations costs. Alternative communications solutions are indicated. ESA

N89-22802# Telespazio, S.p.A., Rome (Italy).
PSDE/SAT-2: COMMUNICATION SYSTEM ARCHITECTURE STUDY, EXECUTIVE SUMMARY
Paris, France 1988 27 p Prepared in cooperation with Italspazio, Rome, Italy
(Contract ESTEC-7570/88/NL/DG)
(ESA-CR(P)-2732; ETN-89-94458) Copyright Avail: NTIS HC A03/MF A01

The PSDE/SAT-2 multimission satellite designed to offer a flight opportunity to different experimental communication payloads and verify the feasibility of advanced space technologies is described. It was conceived for expriment in the framework of the European DRS (Data Relay Satellite) program thus providing intersatellite and interorbit communication links, but also experimental and preoperative services. Payloads include optical communication single access payload (LSA); S-Band single access payload; S-Band multiple access payload; land mobile experimental payload; navigation payload; 40/50 GHz communication payload; and millimeter wave propagation payload. The orbital slot and interference analysis identified a limited number of orbital positions for the mission interleaved between Eutelsat satellites (i.e., 14 deg 30 min E and 17 deg 30 min E). A coordination is required in Ku-Band with Eutelsat satellites and in Ka-Band with ITALSAT (Italy) and TOR-12 (USSR) systems. The link budget analysis shows that the feeder link can be correctly dimensioned assuming the ground segment as specified by ESA and the feeder link payload interface compatible with the presently available hardware technology. A feeder link interface payload was designed, matching the overall system specifications. The TT and C system architecture is shown to be adequate. ESA

N89-22803# Stockholm Univ. (Sweden). Inst. of Physics.
A SIGNAL PROCESSING SYSTEM USING MC68000 AND TMS320 MICROPROCESSORS
Eddie Alestedt 1988 23 p
(USIP-88-07; ETN-89-94551) Avail: NTIS HC A03/MF A01

A VME based signal processing system using an MC68000 supervising processor and two high speed numeric processors, TMS 32020 and TMS 32010, was designed. The TMS32020 is used for numeric calculations, while the TMS32010 handles A/D and D/A conversions for input and output of analog signals. Program and data administration are handled by the 68000 processor. All three processors operate concurrently. An application of the system to real-time calculations of power spectra is described. ESA

N89-22804# Arizona Univ., Tucson. Dept. of Speech and Hearing Sciences.
COORDINATED NONINVASIVE STUDIES (CNS) PROJECT Final Report, 15 Sep. 1985 - 31 Oct. 1988
Judith Lauter Nov. 1988 186 p Original contains color illustrations
(Grant AF-AFOSR-0379-85; AF Proj. 2313)
(AD-A205413; AFOSR-89-0264TR) Avail: NTIS HC A09/MF A01 CSCL 25D

Research activities during this period include: data collection related to the interface between complex-sound production and perception, specifically, studies on speech acoustics including two experiments on voice-onset-time variability in productions by speakers of several languages, and a series on acoustical characteristics of emotional expression; data collection regarding individual differences in the effect of stimulus characteristic on

relative ear advantages; continuing data analysis and new collections documenting individual differences in auditory evoked potentials, with details related to auditory-systems asymmetries preliminary tests regarding the match between behavioral measures of relative ear advantages and quantitative-electroencephalographic asymmetries observed during auditory stimulation; pilot testing using a combination of Nuclear Magnetic Resonance's (NMR) anatomical-imaging and chemical-spectral-analysis capabilities to study phsiological activation in the human brain. GRA

N89-22805# Illinois Univ., Urbana. Coll. of Engineering.
SIGNAL DETECTION IN FRACTIONAL GAUSSIAN NOISE AND AN RKHS (REPRODUCING KERNEL HILBERT SPACE) APPROACH TO ROBUST DETECTION AND ESTIMATION
Richard J. Barton Feb. 1989 149 p
(Contracts N00014-81-K-0014; N00014-89-J-1321)
(AD-A205441; UILU-ENG-89-2203) Avail: NTIS HC A07/MF A01 CSCL 25B

This report is divided into two parts. In the first part, the problem of signal detection in fractional Gaussian noise is considered. To facilitate the study of this problem, several results related to the reproducing kernel Hilbert space of fractional Brownian motion are presented. In particular, this reproducing kernel Hilbert space is characterized completely, and an alternative characterization for the restriction of this class of functions to a compact interval, O,T is given. Infinite-interval whitening filters for fractional Brownian motion are also developed. Application of these results to the signal detection problem yields necessary and sufficient conditions for a deterministic or stochastic signal to produce a nonsingular shift when embedded in additive fractional Gaussian noise. Also, a formula for the likelihood ratio corresponding to any deterministic nonsingular shift is developed. Finally, some results concerning detector performance in the presence of additive fractional Gaussian noise are presented. GRA

N89-22806# IIT Research Inst., Chicago, IL.
ELF COMMUNICATIONS SYSTEM TERMINAL GROUNDS SEASONAL VARIATION PILOT STUDY Technical Report, May 1987 - Nov. 1988
J. R. Gauger and R. G. Drexler Mar. 1989 45 p
(Contract N00039-88-C-0065)
(AD-A205900; IITRI-E06595-4) Avail: NTIS HC A03/MF A01 CSCL 25B

A pilot study was conducted to determine the nature and magnitude of seasonal variations in ELF Communications System ground terminal safety parameters land to identify the most appropriate methodology for ground terminal seasonal monitoring. This study was conducted at the Navy's ELF communications System's Wisconsin Transmitter Facility in northwestern Wisconsin over a seventeen month period from may 1987 to November 1988. Measurements of ground terminal step voltages and body currents at twelve test locations encompassing the principle terrain and soil types of the area were taken using several measurement methodologies. This report documents the pilot study and measurements, presents an analysis of the nature and magnitude of seasonal ground terminal variations, identifies the measurement methodology of choice for all-season monitoring, and makes recommendations for future monitoring of the ELF terminal grounds. GRA

N89-22950*# George Washington Univ., Washington, DC.
FINITE ELEMENT MODELING OF ELECTROMAGNETIC FIELDS AND WAVES USING NASTRAN
E. Thomas Moyer, Jr. and Erwin Schroeder (Naval Ship Research and Development Center, Bethesda, MD.) *In* Computer Software Management and Information Center Seventeenth NASTRAN (R) Users' Colloquium Mar. 1989 p 214-246 (For primary document see N89-22940 16-39)
Avail: NTIS HC A17/MF A01; also available from COSMIC, Athens, GA 30602 CSCL 20N

33 ELECTRONICS AND ELECTRICAL ENGINEERING

Includes test equipment and maintainability; components, e.g., tunnel diodes and transistors; microminiaturization; and integrated circuitry.

For related information see also *60 Computer Operations and Hardware* and *76 Solid-State Physics.*

N89-22807# China Aeronautical Establishment, Beijing.
ACCELERATION TEST FOR AIRCRAFT LOW-PASS FILTER
Zhufeng Zhang 1988 17 p
(PB89-116263; HJB-860367) Avail: NTIS HC A03/MF A01 CSCL 09C

A constant intensive acceleration endurance test method is introduced. Forty paper-capacitor low-pass filters were selected at random sampling for the reliability endurance test at four intensive levels on the increased temperature. According to the measured data during reliability test and using the graphic method, the normal intensive endurance distribution curve can be obtained by extension of the points on the accelerating endurance curve, preliminary judging the filter testing with the distribution tendency, and evaluating the product reliable life-time and the characteristic life-time, the accelerating factor can be calculated. It is to get the theoretical basis to conduct the accelerating endurance test at the increased temperature. Author

N89-22808# Sandia National Labs., Albuquerque, NM. Primary Standards Lab.
A COMPUTER CONTROLLED 100 KV PULSE GENERATOR
Stuart L. Kupferman, Stanley R. Booker, and Heidi J. Meissner 1989 7 p Presented at the IMTC Conference, Washington, DC, 25 Apr. 1989
(Contract DE-AC04-76DP-00789)
(DE89-005922; SAND-88-2960C; CONF-8904116-1) Avail: NTIS HC A02/MF A01

A high voltage pulse generator used primarily for calibrating precision high voltage dividers has been redesigned and rebuilt for state of the art operation. It now has the capability to run a divider calibration, compare the results with historical data for the divider, and then print a calibration certificate, all under computer control. Thirteen component instruments are controlled via three IEEE 488 buses. A voice synthesizer is used to inform the operator of the progress of the calibration. Measurement precision is in the 0.1 percent range. A heat exchanger is used to control the temperature of the oil bath to allow calibration of dividers between 13 C (55 F) and 21 C (70 F). Positive or negative pulse polarity may be selected and pulse magnitude is settable from less than 10 kV to greater than 300 kV. DOE

N89-22809# Universities Research Association, Inc., Batavia, IL.
DOUBLE SIDED CIRCUIT BOARD AND A METHOD FOR ITS MANUFACTURE Patent Application
Carl W. Lindenmeyer, inventor (to DOE) 14 Apr. 1988 11 p
(Contract DE-AC02-76CH-03000)
(DE89-009601; PATENTS-US-A7182671;
US-Patent-Appl-SN-182671) Avail: NTIS HC A03/MF A01

Conductance between the sides of a large double sided printed circuit board is provided using a method which eliminates the need for chemical immersion or photographic exposure of the entire large board. A plurality of through-holes are drilled or punched in a substratum according to the desired pattern, conductive laminae are made to adhere to both sides of the substratum covering the holes and the laminae are pressed together and permanently joined within the holes, providing conductive paths. DOE

N89-22810# Argonne National Lab., IL.
ITER EQUILIBRIUM WITH BOOTSTRAP CURRENTS, LOWER HYBRID CURRENT DRIVE AND FAST WAVE CURRENT DRIVE
David A. Ehst Mar. 1989 59 p

(Contract W-31-109-eng-38)
(DE89-009676; ANL/FPP/TM-238) Avail: NTIS HC A04/MF A01

A current drive system is proposed for the technology phase of ITER which relies on RF power and bootstrap currents. The RF/bootstrap system permits operation at high safety factor, and we consider the axial value to be q(sub a) approximate or = to 1.9, which minimizes the need for seed current near the magnetic axis. Lower hybrid power (approximately 30 MW) provides current density near the surface, ICRF (approximately 65 MHz, approximately 30 MW) fast waves generate current near the axis, and high frequency fast waves (approximately 250 MHz, approximately 74 MW) supply the remaining current density. The system is not yet optimized but appears to offer great flexibility (ion heating for ignition, current rampup, etc.) with relatively inexpensive and well developed technology. DOE

N89-22811# Edgerton, Germeshausen and Grier, Inc., Idaho Falls, ID.
ASSESSMENT OF EV BATTERIES AND APPLICATION TO R AND D PLANNING
Gary L. Henriksen, Pandit G. Patil, Elliot Z. Ratner, and Charles J. Warde (Warde Associates, Inc., Greensboro, NC.) 1989 8 p Presented at the Society of Automotive Engineers International Congress and Exposition, Detroit, MI, 27 Feb. 1989
(Contract DE-AC07-76ID-01570)
(DE89-009720; EGG-M-88460; CONF-890240-2) Avail: NTIS HC A02/MF A01

To guide future EV battery R and D programs, the U.S. Department of Energy (DOE) commissioned a comprehensive assessment of secondary battery technologies. A total of 67 battery developers---from the United States, Canada, Europe, Asia, and Africa---were solicited to submit battery design concepts for an Improved Dual-Shaft Electric Propulsion (IDSEP) van. A team of 10 consultants and 7 representatives from DOE laboratories evaluated 42 developer responses and consultant-prepared designs. Using six criteria---five technical/economic criteria and a maturity/technical barriers criterion---the assessment identified 12 most-promising batteries. Employing a generic EV-battery development-system framework, the assessment results are being used to formulate multi-year R and D plans and schedules for the most-promising developmental batteries. DOE

N89-22812# Edgerton, Germeshausen and Grier, Inc., Idaho Falls, ID.
EVALUATION OF SEVERAL STATE-OF-CHARGE ALGORITHMS
J. M. Espinosa, M. E. Martin, and A. F. Burke Sep. 1988 191 p
(Contract DE-AC07-76ID-01570)
(DE89-009752; DOE/ID-10214) Avail: NTIS HC A09

One of the important needs in marketing an electric vehicle is a device which reliably indicates battery state-of-charge for all types of driving. The purpose of the state-of-charge indicator is analogous to a gas gauge in an internal combustion engine powered vehicle. Many different approaches have been tried to accurately predict battery state-of-charge. This report evaluates several of these approaches. Four different algorithms were implemented into software on an IBM PC and tested using a battery test database for ALCO 2200 lead-acid batteries generated at the INEL. The database was obtained under controlled conditions which compare with the battery response in real EV use. Each algorithm is described in detail as to theory and operational functionality. Also discussed is the hardware and data requirements particular to implementing the individual algorithms. The algorithms were evaluated for accuracy using constant power, stepped power, and simulated vehicle (SFUDS79) discharge profiles. Attempts were made to explain the cause of differences between the predicted and actual state-of-charge and to provide possible remedies to correct them. Recommendations for future work on battery state-of-charge indicators are presented that utilize the hardware and software now in place in the INEL Battery Laboratory. DOE

N89-22813# Argonne National Lab., IL.
ADVANCED BATTERIES FOR ELECTRIC VEHICLES
Paul A. Nelson 1989 19 p Presented at the 4th International Seminar on Lithium Battery Technology and Applications, Deerfield Beach, FL, 6 Mar. 1989
(Contract W-31-109-eng-38)
(DE89-009771; CONF-890315-1) Avail: NTIS HC A03/MF A01

Over the past twenty years, some of the most difficult problems have been solved in the development of long-lived lithium/sulfide secondary batteries having molten chloride electrolytes. Recent tests of Li-Al/FeS2 cells have demonstrated 1000 cycles of operation and the practicality of achieving a specific energy of 175 Wh/kg for prismatic cells. Bipolar cells now under study may achieve even higher specific energy. Also, bipolar cells make possible the use of low-cost coated current collectors for the positive electrode instead of the expensive molybdenum current collectors that have been required for prismatic cells. Very compact batteries to power an electric van have been conceptually designed with this approach. These batteries would provide a range for the loaded vehicle of more than 100 miles for a battery weighing 280 kg, only 15 percent of the loaded vehicle weight (1930 kg). DOE

N89-22814# Argonne National Lab., IL. Chemical Technology Div.
LABORATORY EVALUATION OF ADVANCED BATTERY TECHNOLOGIES FOR ELECTRIC VEHICLE APPLICATIONS
W. H. DeLuca, J. E. Kulaga, R. L. Hogrefe, A. F. Tummilo, and C. E. Webster 1989 6 p Presented at the SAE International Congress and Exposition, Detroit, MI, 27 Feb. 1989
(Contract W-31-109-eng-38)
(DE89-009810; CONF-890240-5) Avail: NTIS HC A02/MF A01

During 1988, battery technology evaluations were performed for the Department of Energy and Electric Power Research Institute at the Argonne Analysis and Diagnostic Laboratory. Cells and multicell modules from four developers were examined to determine their performance and life characteristics for electric vehicle propulsion applications. The results provide an interim measure of the progress being made in battery R and D programs, a comparison of battery technologies, and a source of basic data for modeling and continuing R and D. This paper summarizes the performance and life characterizations of twelve single cells and six 3- to 24-cell modules that encompass four technologies (Na/S, Ni/Fe, lead-acid, and Fe/Air). DOE

N89-22815# Institut National des Sciences Appliquees, Lyon (France). Lab. de Composants de Puissance et Applications.
DEVELOPMENT OF BEHAVIORIST MODELS TO SIMULATE COMMUTED POWER SWITCHES Ph.D. Thesis
Olivier Hamel 1988 166 p In FRENCH; ENGLISH summary
(ISAL-88-0065; ETN-89-94367) Avail: NTIS HC A08/MF A01

Black box analysis is applied to MOS diodes and transistors. Even if the analysis is based on the classical semiconductor equations, the approach provides a model presenting good performances over a large variety of commuting conditions. In the case of the MOS transistor, a model taking in account the nonlinear capacities is developed. This model behaves correctly on either resistive or inductive loading. The procedure is a part of a set of power switching computer aided design tools. ESA

N89-22816# Utah Div. of Water Resources, Salt Lake City. Dept. of Physics.
CURRENT AND THERMAL NOISE IN MIXED Na/Ag BETA ALUMINA Technical Report, No. 21, Jun. 1988 - Mar. 1989
James J. Brophy Mar. 1989 11 p
(Contract N00014-82-K-0603)
(AD-A205869) Avail: NTIS HC A03/MF A01 CSCL 20A

Current noise in mixed-ion Na/Ag Beta alumina ceramics is characteristic of conductivity fluctuations due to diffusion noise of the mobile ions as previously observed in Na, Ag, and Pb Beta alumina single-ion conductors and for mixed-ion Na/Ca Beta alumina. The measured diffusion noise levels are greater for current injection of Ag ions from AgNO3 solution electrodes. Room temperature conductivities calculated from thermal noise

measurements are the same for both Na and Ag electrodes and show a strong mixed alkali effect. Correlation effects between the mobile ions are the same for both Na and Ag ion injection and are strongest near the 50/50 concentration ratio. Diffusion noise, Mobile ions, Conductivity fluctuations, Beta alumina single-ion conductors, Mixed alkali effect. GRA

N89-22993*# Giner, Inc., Waltham, MA.
ADVANCED DOUBLE LAYER CAPACITORS Abstract Only
S. Sarangapani, P. Lessner, J. Forchione, and A. B. LaConti *In* NASA, Lewis Research Center, Space Electrochemical Research and Technology Conference: Abstracts 1989 p 14-15 (For primary document see N89-22982 16-44)
(Contract N00014-88-0391)
Avail: NTIS HC A03/MF A01 CSCL 09C

N89-23001*# Michigan Technological Univ., Houghton.
STRUCTURAL COMPARISON OF NICKEL ELECTRODES AND PRECURSOR PHASES Abstract Only
Bahne C. Cornilsen, Xiaoyin Shan, and Patricia Loyselle *In* NASA, Lewis Research Center, Space Electrochemical Research and Technology Conference: Abstracts 1989 p 28 (For primary document see N89-22982 16-44)
Avail: NTIS HC A03/MF A01 CSCL 09C

N89-23002*# National Aeronautics and Space Administration. Lewis Research Center, Cleveland, OH.
IMPEDANCE STUDIES OF Ni/Cd AND Ni/H CELLS USING THE CELL CASE AS REFERENCE ELECTRODE Abstract Only
Margaret A. Reid *In its* Space Electrochemical Research and Technology Conference: Abstracts 1989 p 29 (For primary document see N89-22982 16-44)
Avail: NTIS HC A03/MF A01 CSCL 09C

N89-23005*# Eagle-Picher Industries, Inc., Joplin, MO.
ADVANCES IN LIGHTWEIGHT NICKEL ELECTRODE TECHNOLOGY Abstract Only
Dwaine Coates, Gary Paul, James R. Wheeler, and Paul Daugherty *In* NASA, Lewis Research Center, Space Electrochemical Research and Technology Conference: Abstracts 1989 p 32 (For primary document see N89-22982 16-44)
Avail: NTIS HC A03/MF A01 CSCL 09C

N89-23007*# National Aeronautics and Space Administration. Lewis Research Center, Cleveland, OH.
NICKEL-HYDROGEN CAPACITY LOSS ON STORAGE Abstract Only
Michelle A. Manzo *In its* Space Electrochemical Research and Technology Conference: Abstracts 1989 p 34 (For primary document see N89-22982 16-44)
Avail: NTIS HC A03/MF A01 CSCL 09C

34 FLUID MECHANICS AND HEAT TRANSFER

Includes boundary layers; hydrodynamics; fluidics; mass transfer; and ablation cooling.

For related information see also *02 Aerodynamics* and *77 Thermodynamics and Statistical Physics.*

N89-22817*# Stanford Univ., CA. Center for Turbulence Research.
ANNUAL RESEARCH BRIEFS, 1988
Feb. 1989 163 p
(Contract NCC2-460)
(NASA-CR-184906; NAS 1.26:184906) Avail: NTIS HC A08/MF A01 CSCL 20D

The primary objective of the Center for Turbulence Research (CTR) is to stimulate and produce advances in physical understanding of turbulence, in turbulence modeling and simulation, and in turbulence control. Topics addressed include: fundamental modeling of turbulence; turbulence structure and control; transition and turbulence in high-speed compressible flows; and turbulent reacting flows. For individual titles, see N89-22818 through N89-22834.

N89-22818*# Stanford Univ., CA.
THE LENGTH SCALE FOR SUB-GRID-SCALE PARAMETERIZATION WITH ANISOTROPIC RESOLUTION
Douglas K. Lilly (Oklahoma Univ., Norman.) *In its* Annual Research Briefs, 1988 Feb. 1989 p 3-9 (For primary document see N89-22817 16-34)
Avail: NTIS HC A08/MF A01 CSCL 20D

Use of the Smagorinsky eddy-viscosity formulation and related schemes for subgrid-scale parameterization of large eddy simulation models requires specification of a single length scale, earlier related by Lilly to the scale of filtering and/or numerical resolution. An anisotropic integration of the Kolmogoroff enstrophy spectrum allows generalization of that relationship to anisotropic resolution. It is found that the Deardorff assumption is reasonably accurate for small anisotropies and can be simply improved for larger values. Author

N89-22819*# Stanford Univ., CA.
TURBULENCE MODELING
Tsan-Hsing Shih *In its* Annual Research Briefs, 1988 Feb. 1989 p 11-17 (For primary document see N89-22817 16-34)
Avail: NTIS HC A08/MF A01 CSCL 20D

In recent years codes that use the Navier-Stokes equations to compute aerodynamic flows have evolved from computing two-dimensional flows around simple airfoils to computing flows around full scale aircraft configurations. Most flows of engineering interest are turbulent and turbulence models are needed for their prediction. Yet, it is known that present turbulence models are adequate only for simple flows and do poorly in complicated flows such as three-dimensional separation, or large-scale unsteadiness. The same progress that allowed the development of these aerodynamic codes, namely the introduction of supercomputers, has allowed us to compute directly turbulent flows, albeit only for simple flows at moderate Reynolds numbers. These direct turbulence simulations provide us with detailed data that experimentalists were not able to measure. This work is motivated by the fact that data exists for developing better turbulence models and by the need for better models to compute flows of engineering interest. The objective is to develop turbulence models for engineering applications. The model categories that show promise for immediate use are on the two-equation level and the Reynolds-stress level. Author

N89-22820*# Stanford Univ., CA.
ON CURVE AND SURFACE STRETCHING IN TURBULENT FLOW
Nassrollah Etemadi (Illinois Univ., Chicago.) *In its* Annual Research Briefs, 1988 Feb. 1989 p 19-27 (For primary document see N89-22817 16-34)
Avail: NTIS HC A08/MF A01 CSCL 20D

Cocke (1969) proved that in incompressible, isotropic turbulence the average material line (material surface) elements increase in comparison with their initial values. Good estimates of how much they increase in terms of the eigenvalues of the Green deformation tensor were rigorously obtained. Author

N89-22821*# Stanford Univ., CA.
RENORMALIZATION GROUP ANALYSIS OF TURBULENCE
Leslie M. Smith *In its* Annual Research Briefs, 1988 Feb. 1989 p 29-33 (For primary document see N89-22817 16-34)
Avail: NTIS HC A08/MF A01 CSCL 20D

The objective is to understand and extend a recent theory of turbulence based on dynamic renormalization group (RNG) techniques. The application of RNG methods to hydrodynamic turbulence was explored most extensively by Yakhot and Orszag (1986). An eddy viscosity was calculated which was consistent with the Kolmogorov inertial range by systematic elimination of the small scales in the flow. Further, assumed smallness of the

nonlinear terms in the redefined equations for the large scales results in predictions for important flow constants such as the Kolmogorov constant. It is emphasized that no adjustable parameters are needed. The parameterization of the small scales in a self-consistent manner has important implications for sub-grid modeling. Author

N89-22822*# Stanford Univ., CA.
LOW-DIMENSIONAL CHAOS IN TURBULENCE
John A. Vastano *In its* Annual Research Briefs, 1988 Feb. 1989 p 35-37 (For primary document see N89-22817 16-34)
Avail: NTIS HC A08/MF A01 CSCL 20D

Direct numerical simulations are being performed on two different fluid flows in an attempt to discover the mechanism underlying the transition to turbulence in each. The first system is Taylor-Couette flow; the second, two-dimensional flow over an airfoil. Both flows exhibit a gradual transition to high-dimensional turbulence through low-dimensional chaos. The hope is that the instabilities leading to chaos will be easier to relate to physical processes in this case, and that the understanding of these mechanisms can then be applied to a wider array of turbulent systems. Author

N89-22823*# Stanford Univ., CA.
CLOSE INTERACTIONS OF 3-D VORTEX TUBES
Mogens V. Melander (Southern Methodist Univ., Dallas, TX.) *In its* Annual Research Briefs, 1988 Feb. 1989 p 39-50 (For primary document see N89-22817 16-34)
Avail: NTIS HC A08/MF A01 CSCL 20D

The motivation for studying close vortex interactions is briefly discussed in the light of turbulence and coherent structures. Particular attention is given to the interaction known as reconnection. Two reconnection mechanisms are discussed. One is annihilation of vorticity by cross-diffusion, the other is an inviscid head-tail formation. At intermediate Reynolds numbers both mechanisms are operating. Author

N89-22824*# Stanford Univ., CA.
NUMERICAL SIMULATION OF VISCOUS VORTEX RINGS
Sharon Kay Stanaway *In its* Annual Research Briefs, 1988 Feb. 1989 p 51-54 (For primary document see N89-22817 16-34)
Avail: NTIS HC A08/MF A01 CSCL 20D

Vortex interactions and their role in turbulent flow are examined. The objectives are twofold. First, to use the existing axisymmetric code to study the annihilation process of colliding vortex rings and determine the relevance of this problem to similar 3-D phenomena. The second objective is to extend the code to three dimensions. The code under development is unique in that it can compute flows in a truly infinite domain (i.e., without periodic boundary conditions or approximations from truncating the domain). Because of this, the far field sound can be computed, and therefore, contribute to improved models of turbulence generated noise for this class of flows. Issues which can be addressed by the code include: effects of viscosity on mode selection in azimuthal breakdown of vortex rings (i.e., the Widnall instability); reconnection, the associated production of small scales, and the time scale of the process. Author

N89-22825*# Stanford Univ., CA.
THE EFFECTS OF PARTICLE LOADING ON TURBULENCE STRUCTURE AND MODELLING
Kyle D. Squires and J. K. Eaton *In its* Annual Research Briefs, 1988 Feb. 1989 p 55-61 (For primary document see N89-22817 16-34)
Avail: NTIS HC A08/MF A01 CSCL 20D

The objective of the present research was to extend the Direct Numerical Simulation (DNS) approach to particle-laden turbulent flows using a simple model of particle/flow interaction. The program addressed the simplest type of flow, homogeneous, isotropic turbulence, and examined interactions between the particles and gas phase turbulence. The specific range of problems examined include those in which the particle is much smaller than the smallest length scales of the turbulence yet heavy enough to slip relative to the flow. The particle mass loading is large enough to have a significant impact on the turbulence, while the volume loading was small enough such that particle-particle interactions could be neglected. Therefore, these simulations are relevant to practical problems involving small, dense particles conveyed by turbulent gas flows at moderate loadings. A sample of the results illustrating modifications of the particle concentration field caused by the turbulence structure is presented and attenuation of turbulence by the particle cloud is also illustrated. Author

N89-22826*# Stanford Univ., CA.
ANALYSIS OF TURBULENCE STRUCTURES IN SHEAR FLOWS
Moon J. Lee *In its* Annual Research Briefs, 1988 Feb. 1989 p 63-78 (For primary document see N89-22817 16-34)
Avail: NTIS HC A08/MF A01 CSCL 20D

Outline of the research program and a recent progress in the studies of sheared turbulence are described. The research program reported is directed at two goals: (1) understanding of fundamental physics of organized structures in turbulent shear flows; and (2) development of phenomenological models of turbulence based on physical arguments. Three projects that were carried out are: (1) structure of sheared turbulence near a plane boundary; (2) distortion of turbulence by axisymmetric strain and dilation; and (3) study of energy transfer in turbulent shear flow. Author

N89-22827*# Stanford Univ., CA.
DIRECT NUMERICAL SIMULATION OF COMPRESSIBLE FREE SHEAR FLOWS
Sanjiva K. Lele *In its* Annual Research Briefs, 1988 Feb. 1989 p 79-98 Presented at the AIAA meeting, Reno, NV, 1989 (For primary document see N89-22817 16-34)
(AIAA-89-0374) Avail: NTIS HC A08/MF A01 CSCL 20D

Direct numerical simulations of compressible free shear layers in open domains are conducted. Compact finite-difference schemes of spectral-like accuracy are used for the simulations. Both temporally-growing and spatially-growing mixing layers are studied. The effect of intrinsic compressibility on the evolution of vortices is studied. The use of convective Mach number is validated. Details of vortex roll up and pairing are studied. Acoustic radiation from vortex roll up, pairing and shape oscillations is studied and quantified. Author

N89-22828*# Stanford Univ., CA.
DIRECT SIMULATION OF COMPRESSIBLE REACTING FLOWS
Thierry J. Poinsot *In its* Annual Research Briefs, 1988 Feb. 1989 p 99-106 (For primary document see N89-22817 16-34)
Avail: NTIS HC A08/MF A01 CSCL 20D

A research program for direct numerical simulations of compressible reacting flows is described. Two main research subjects are proposed: the effect of pressure waves on turbulent combustion and the use of direct simulation methods to validate flamelet models for turbulent combustion. The interest of a compressible code to study turbulent combustion is emphasized through examples of reacting shear layer and combustion instabilities studies. The choice of experimental data to compare with direct simulation results is discussed. A tentative program is given and the computation cases to use are described as well as the code validation runs. Author

N89-22829*# Stanford Univ., CA.
TURBULENT TRANSPORT IN THE SOLAR NEBULA
Kevin W. Thompson *In its* Annual Research Briefs, 1988 Feb. 1989 p 107-114 (For primary document see N89-22817 16-34)
Avail: NTIS HC A08/MF A01 CSCL 20D

It is likely that turbulence played a major role in the evolution of the solar nebula, which is the flattened disk of dust and gas out of which our solar system formed. Relevant turbulent processes include the transport of angular momentum, mass, and heat, which were critically important to the formation of the solar system. This research will break ground in the modeling of compressible

turbulence and its effects on the evolution of the solar nebula. The computational techniques which were developed should be of interest to researchers studying other astrophysical disk systems (e.g., active galactic nuclei), as well as turbulence modelers outside the astrophysics community. Author

N89-22830*# Stanford Univ., CA.
TRANSITION TO TURBULENCE IN LAMINAR HYPERSONIC FLOW **c02**
Jaap VanDerVegt *In its* Annual Research Briefs, 1988 Feb. 1989 p 115-119 (For primary document see N89-22817 16-34)
Avail: NTIS HC A08/MF A01 CSCL 01A

Progress in a recently started project aimed at the prediction of transition to turbulence in hypersonic flow is briefly discussed. The prediction of transition to turbulence is a very important issue in the design of space vessels. Two space vehicles currently under investigation, namely the aeroassisted transfer vehicle (AOTV) and the trans-atmospheric vehicle (TAV), suffer from strong aerodynamic heating. This heating is strongly influenced by the boundary layer structure. These aerospace vehicles fly in the upper atmospheric layer at a Mach number between 10 and 30 at very low atmospheric pressures. At very high altitudes the flow is laminar, but when the space vessel returns to a lower orbit, the flow becomes turbulent and the heating is dramatically increased. The prediction of this transition process is commonly done by means of experiments. The experimental facilities available nowadays cannot model the hypersonic flow field accurately enough by limitations in Mach and Reynolds number. These facilities also have a large free stream disturbance level which makes it very difficult to investigate transition accurately. An alternative approach is to study transition by theoretical means. Up to now numerical studies of hypersonic flow only discussed steady laminar or turbulent flow. This theoretical approach is extended to the study of transition in hypersonic flow by means of direct numerical simulations and additional theoretical investigations to explain the mechanisms leading to transition. A brief outline of how this research is to be performed is given. Author

N89-22831*# Stanford Univ., CA.
DIRECT NUMERICAL SIMULATIONS OF TURBULENT CONVECTION WITH A VARIABLE GRAVITY AND KEPLERIAN ROTATION
William H. Cabot *In its* Annual Research Briefs, 1988 Feb. 1989 p 121-125 (For primary document see N89-22817 16-34)
Avail: NTIS HC A08/MF A01 CSCL 20D

Thermal convection was proposed as a possible mechanism for generation and maintenance of turbulence in the inner accretion disk regime of the primordial solar nebula. It is of fundamental interest to design experiments with the basic physical features of the solar nebula conditions cannot be produced in the laboratory, numerical simulations of hydrodynamic flows, which have been very successful in describing aerodynamic flows, can be suitable modified to provide experimental data for solar nebula modelling. The goals are to modify an extant, proven hydrodynamics code with the most important features of the solar nebula and other thin accretion disks: bouyancy terms to generate convection, internal heating representing the release of gravitational potential energy, a variable gravity linearly proportional the the distance from the vertical midplane due to centrifugal balance, rapid rotation with axis aligned with gravity, and Keplerian rotational shear; to determine the effect that these features have on the turbulent convection by introducing them individually and to determine the cumulative nature of the turbulent convection for accretion disk conditions; and to model the convection and the turbulence. In this manner, prior solar nebula models can be tested and their deficiencies rectified. Author

N89-22832*# Stanford Univ., CA.
EXPERIMENTAL INVESTIGATION OF FLOW OVER A BACKWARD FACING STEP-PROGRESS REPORT
L. W. B. Browne (Newcastle Univ., Australia) *In its* Annual Research Briefs, 1988 Feb. 1989 p 127-146 (For primary document see N89-22817 16-34)
Avail: NTIS HC A08/MF A01 CSCL 20D

The sizes and arrangement of the wind tunnel used for the experimentation are described. The specifications for the cold-wire anemometers, hot-wire anemometers, cold-wire rakes, and miniature 3-wire probe are proveded. The results of the experiment are briefly discussed. B.G.

N89-22833*# Stanford Univ., CA.
THE EFFECTS OF STABILIZING AND DESTABILIZING LONGITUDINAL CURVATURE ON THE STRUCTURE OF TURBULENT, TWO-STREAM MIXING LAYERS
Michael W. Plesniak and J. P. Johnston *In its* Annual Research Briefs, 1988 Feb. 1989 p 147-152 (For primary document see N89-22817 16-34)
Avail: NTIS HC A08/MF A01 CSCL 20D

The construction and development of the multi-component traversing system and associated control hardware and software are presented. A hydrogen bubble/laser sheet flow visualization technique was developed to visually study the characteristics of the mixing layers. With this technique large-scale rollers arising from the Taylor-Gortler instability and its interaction with the primary Kelvin-Helmholtz structures can be studied. Author

N89-22834*# Stanford Univ., CA.
AN EXPERIMENTAL INVESTIGATION OF A LOW REYNOLDS NUMBER TURBULENT BOUNDARY LAYER SUBJECT TO AN ADVERSE PRESSURE GRADIENT
Jonathan H. Watmuff *In its* Annual Research Briefs, 1988 Feb. 1989 p 153-166 (For primary document see N89-22817 16-34)
Avail: NTIS HC A08/MF A01 CSCL 20D

A very low Reynolds number turbulent boundary layer subject to an adverse pressure gradient is studied. The aim is to obtain highly accurate mean-flow and turbulence measurements under conditions that can be closely related to the numerical simulations of Philippe Spalart for the purposes of CFD validation. Much of the Boundary Layer Wind Tunnel was completely rebuilt with a new wider contraction and working section which will improve compatibility with the simulations. A unique sophisticated high-speed computer controlled 3-D probe traversing mechanism was integrated into the test section. Construction of the tunnel and traverse is discussed in some detail. The hardware is now complete, and measurements are in progress. The mean-flow data indicate that a suitably two-dimensional base flow was established. Automation of the probe positioning and data acquistion have led to a decreased running time for total pressure measurements. However, the most significant benefits are expected to occur when using hot-wire probes. Calibrations can be performed automatically and there is no need to handle fragile probes when moving between measuring stations. Techniques are being developed which require sampling of the signals from moving hot-wire probes on the basis of their position in the flow. Measurements can be made in high intensity turbulence by flying probes upstream at high speed so that the relative magnitude of the turbulent velocity fluctuations are reduced. In regions, where the turbulence intensity is not too large, the probe can also be repetitively scanned across very dense spatial grids in other directions. With this technique, a complete profile can be measured in about 1/3 the time and with a spatial density about 50 times that obtainable using a stationary probe. Author

N89-22835# Naval Postgraduate School, Monterey, CA.
CONTROL OF EMBEDDED VORTICES USING WALL JETS M.S. Thesis
Geoffrey E. Schwartz Sep. 1988 291 p
(AD-A202606; AD-E900870) Avail: NTIS HC A13/MF A01 CSCL 20K

A wall jet inclined at 30 deg to horizontal was used to alter the structural characteristics of streamwise vortices embedded in a turbulent boundary layer developing in a zero pressure gradient. The vortices were created using a half delta wing attached to the

floor of a wind tunnel. With the jet opposing the vortex downwash and blowing ratio increasing from 0 to 4.8, streamwise vorticity decreased from approx. 750 to approx. 150/s while circulation decreased from approx. 0.15 sq m/s. The average vortex core radius increased from approx. 0.9 to approx. 2.4 cm, while the vortex moved approx. 3 cm spanwise toward the jet. With the jet at the vortex upwash and blowing ratio increasing from 0 to 6.7, streamwise vorticity decreased from approx. 860 to approx. 570/s while circulation decreased from approx. 0.17 to approx. 0.15 sq m/s. GRA

N89-22836*# Institute for Computer Applications in Science and Engineering, Hampton, VA.
NON-LINEAR EVOLUTION OF A SECOND MODE WAVE IN SUPERSONIC BOUNDARY LAYERS Final Report
Gordon Erlebacher (National Aeronautics and Space Administration. Langley Research Center, Hampton, VA.) and M. Y. Hussaini Feb. 1989 41 p
(Contract NAS1-18605)
(NASA-CR-181811; NAS 1.26:181811; ICASE-89-15) Avail: NTIS HC A03/MF A01 CSCL 20D

The nonlinear time evolution of a second mode instability in a Mach 4.5 wall-bounded flow is computed by solving the full compressible, time-dependent Navier-Stokes equations. High accuracy is achieved by using a Fourier-Chebyshev collocation algorithm. Primarily inviscid in nature, second modes are characterized by high frequency and high growth rates compared to first modes. Time evolution of growth rate as a function of distance from the plate suggests this problem is amenable to the Stuart-Watson perturbation theory as generalized by Herbert. Author

N89-22837*# Institute for Computer Applications in Science and Engineering, Hampton, VA.
INVISCID SPATIAL STABILITY OF A COMPRESSIBLE MIXING LAYER. PART 2: THE FLAME SHEET MODEL Final Report
T. L. Jackson and C. E. Grosch (Old Dominion Univ., Norfolk, VA.) Mar. 1989 33 p
(Contracts NAS1-18107; NAS1-18605)
(NASA-CR-181815; NAS 1.26:181815; ICASE-89-18-Pt-2) Avail: NTIS HC A03/MF A01 CSCL 20D

The results of an inviscid spatial calculation for a compressible reacting mixing layer are reported. The limit of infinitive activation energy is taken and the diffusion flame is approximated by a flame sheet. Results are reported for the phase speeds of the neutral waves and maximum growth rates of the unstable waves as a function of the parameters of the problem: the ratio of the temperature of the stationary stream to that of the moving stream, the Mach number of the moving streams, the heat release per unit mass fraction of the reactant, the equivalence ratio of the reaction, and the frequency of the disturbance. These results are compared to the phase speeds and growth rates of the corresponding nonreacting mixing layer. We show that the addition of combustion has important, and complex effects on the flow stability. Author

N89-22838*# Virginia Polytechnic Inst. and State Univ., Blacksburg. Dept. of Aerospace and Ocean Engineering.
COMPUTATIONAL FLUID DYNAMICS RESEARCH IN THREE-DIMENSIONAL ZONAL TECHNIQUES Final Technical Report
Robert W. Walters Apr. 1989 16 p
(Grant NAG1-866)
(NASA-CR-181406; NAS 1.26:181406) Avail: NTIS HC A03/MF A01 CSCL 20D

Patched-grid algorithms for the analysis of complex configurations with an implicit, upwind-biased Navier-Stokes solver were investigated. Conservative and non-conservative approaches for performing zonal interpolations were implemented. The latter approach yields the most flexible technique in that it can handle both patched and overlaid grids. Results for a two-dimensional blunt body problem show that either approach yield accurate steady-state shock locations and jump conditions. In addition, calculations of the turbulent flow through a hypersonic inlet on a three-zone grid show that the numerical prediction is in good agreement with the experimental results. Through the use of a generalized coordinate transformation at the zonal interface between two or more blocks, the algorithm can be applied to highly stretched viscous grids and to arbitrarily-shaped zonal boundaries. Applications were made to the F-18 aircraft at subsonic, high-alpha conditions, in support of the NASA High-Alpha Research Program. The calculations were compared to ground-based and flight test experiments and were used as a guide to understanding the ground-based tests, which are laminar and transitional, and their relationship to flight. Calculations about a complete reconnaissance aircraft were also performed in order to further demonstrate the capability of the patched-grid algorithm. Author

N89-22839# Purdue Univ., West Lafayette, IN.
TWO-PHASE FLOW CHARACTERISTIC OF INVERTED BUBBLY, SLUG AND ANNULAR FLOW IN POST-CRITICAL HEAT FLUX REGION
M. Ishii and James P. Denten 1988 25 p Presented at the 16th Water Reactor Safety Information Meeting, Gaithersburg, MD, 24 Oct. 1988 Prepared in cooperation with Argonne National Lab., IL
(Contract W-31-109-eng-38)
(DE89-007384; CONF-8810155-43) Avail: NTIS HC A03/MF A01

Inverted annular flow can be visualized as a liquid jet-like core surrounded by a vapor annulus. While many analytical and experimental studies of heat transfer in this regime have been performed, there is very little understanding of the basic hydrodynamics of the post-Convective Heat Flux (CHF) flow field. However, a recent experimental study was done that was able to successfully investigate the effects of various steady-state inlet flow parameters on the post-CHF hydrodynamics of the film boiling of a single phase liquid jet. This study was carried out by means of a visual photographic analysis of an idealized single phase core inverted annular flow initial geometry (single phase liquid jet core surrounded by a coaxial annulus of gas). In order to extend this study, a subsequent flow visualization of an idealized two-phase core inverted annular flow geometry (two-phase central jet core, surrounded by a coaxial annulus of gas) was carried out. The objective of this second experimental study was to investigate the effect of steady-state inlet, pre-CHF two-phase jet core parameters on the hydrodynamics of the post-CHF flow field. In actual film boiling situations, two-phase flows with net positive qualities at the CHF point are encountered. Thus, the focus of the present experimental study was on the inverted bubbly, slug, and annular flow fields in the post dryout film boiling region. Observed post dryout hydrodynamic behavior is reported. A correlation for the axial extent of the transition flow pattern between inverted annular and dispersed droplet flow (the agitated regime) is developed. It is shown to depend strongly on inlet jet core parameters and jet void fraction at the dryout point. DOE

N89-22840# International Centre for Theoretical Physics, Trieste (Italy).
FORCED AND FREE CONVECTION FLOW WITH VISCOUS DISSIPATION EFFECTS: THE METHOD OF PARAMETRIC DIFFERENTIATION
M. A. Hossain and O. Arbad (Centre for Research in Basic Science, Misurata, Libya) Jul. 1988 18 p Submitted for publication
(DE88-705649; IC-88/141) Avail: NTIS (US Sales Only) HC A03/MF A01

Effect of buoyancy force in a laminar uniform forced convection flow past a semi-infinite vertical plate has been analyzed near the leading edge, taking into account the viscous dissipation. The coupled non-linear locally similar equations, which govern the flow, are solved by the method of parametric differentiation. Effects of the buoyancy force and the heat due to viscous dissipation on the flow and the temperature fields as well as on the wall shear-stress and the heat transfer at the surface of the plate are shown graphically for the values of the Prandtl number sigma ranging from 10 sup -1 to 1.0. DOE

N89-22841# Central Research Inst. of Electric Power Industry, Tokyo (Japan).
DEVELOPMENT OF ADVANCED HEAT PUMP. PART 2: PRELIMINARY TEST OF TWO-STAGE COMPRESSION HEAT PUMP
Tetsushiro Iwatsubo, Michinori Saikawa, and Teruhide Hamamatsu Mar. 1988 33 p In JAPANESE; ENGLISH summary
(DE88-756838; CRIE-W-87020-Pt-2) Avail: NTIS (US Sales Only) HC A03/MF A01

A heat pump driven by electricity is one of the excellent electricity utilization systems and is promoted to be widely used. An advanced heat pump has been investigated to enlarge its applications in the field of hot water supply for domestic use which will be competitive with city gas and air conditioning in large scale buildings. An experimental unit with two-stage compression system was designed, which has the multi-function of air conditioning and hot water supply, and the trial system was fabricated. In the design, followings were considered; cooperative operations of two compressors by inverter driving, the temperature conditions of both the air for the air conditioning and the heat source, additional setting of the intermediate heat exchanger. The test operation was carried out with checking the start up procedure, the control sequence and so on. The probability of five operation modes: cooling, heating, hot water supply, cooling/hot water supply, and heating/hot water supply, were confirmed. In the mode of heating/hot water supply the hot water temperature was increased to 65 C, the excellent performance in hot water supply was demonstrated. DOE

N89-22842# Central Research Inst. of Electric Power Industry, Tokyo (Japan).
DEVELOPMENT OF ADVANCED HEAT PUMPS. PART 3: FUNDAMENTAL APPROACH ON TWO-STAGE COMPRESSION SYSTEM
Michinori Saikawa, Tetsushiro Iwatsubo, and Teruhide Hamamatsu Mar. 1988 22 p In JAPANESE; ENGLISH summary
(DE88-756842; CRIE-W-87029-Pt-3) Avail: NTIS (US Sales Only) HC A03/MF A01

A heat pump using electricity has benefits in many aspects such as energy conservation, pollution abatement and so on. As one of the measures for developing power demand, the electric power industry is engaged in its usuage and improving the performance. In addition to usual air conditioning, the performance of the system with hot water supply mode was mainly studied aiming at drastic improvement. By adopting the two-stage compression method, the irreversible losses in the heat exchanges were reduced. Though the Coefficient of Performance of the conventional system adopting the single-stage method is shown the value of 1.67, it is shown the values of 2.16 to 2.8 in the two-stage method, the performance was increased by about 70 percent. The results of experiments using a miniature experimental device showed good agreement with the predicted performance. In the annual hot water supply load of 4,240 mcal, the annual running cost of this system is evaluated as 38,800 yen, this figure is lower than that of city gas of 47,100 yen. When only night time electricity is used, the cost is reduced to 10,700 yen which is less than that of kerosene. DOE

N89-22843# Midwest Research Inst., Golden, CO. Solar Energy Research Inst.
HEAT TRANSFER AND PRESSURE DROP MEASUREMENTS IN AN AIR/MOLTEN SALT DIRECT-CONTACT HEAT EXCHANGER
Mark S. Bohn Nov. 1988 10 p Presented at the American Society of Mechanical Engineers Solar Energy Conference, San Diego, CA, 2-5 Apr. 1989
(Contract DE-AC02-83CH-10093)
(DE89-000837; SERI/TP-253-3426; CONF-890436-7) Avail: NTIS HC A02/MF A01

This paper presents a comparison of experimental data with a recently published model of heat exchange in irrigated packed beds. Heat transfer and pressure drop were measured in a 150 mm (ID) column with a 610 mm bed of metal Pall rings. Molten nitrate salt and preheated air were the working fluids with a salt inlet temperature of approximately 440 C and air inlet temperatures of approximately 230 C. A comparison between the experimental data and the heat transfer model is made on the basis of heat transfer from the salt. For the range of air and salt flow rates tested, 0.3 to 1.2 kg/sq m/s air flow and 6 to 18 kg/sq m/s salt flow, the data agree with the model within 22 percent standard deviation. In addition, a model for the column pressure drop was validated, agreeing with the experimental data within 18 percent standard deviation over the range of column pressure drop from 40 to 1250 Pa/m. DOE

N89-22844# California Univ., Berkeley. Lawrence Berkeley Lab. Materials and Chemical Sciences Div.
ON THE NUMERICAL INTEGRATION OF VISCOELASTIC FLOW EQUATIONS
J. Rosenberg and R. Keunings (Universite Catholique de Louvain, Belgium) Oct. 1988 8 p Presented at the 7th International Conference on Finite Element Methods in Flow Problems, Huntsville, AL, 3-7 Apr. 1989 Submitted for publication
(Contract DE-AC03-76SF-00098)
(DE89-007135; LBL-26467; CONF-890479-4) Avail: NTIS HC A02/MF A01

Various numerical techniques are compared in the integration of the upper-convected Maxwell (UCM) constitutive model on the basis of known kinematics. They include Galerkin's method, streamline upwinding schemes and the method of characteristics. The results show the superiority of the latter in flows endowed with stress singularities. Solutions of the full set of momentum, mass and constitutive equations are computed with the method of characteristics and a Picard iterative scheme. Convergence difficulties are addressed. DOE

N89-22845# Sandia National Labs., Albuquerque, NM. Parachute Systems Div.
A VORTEX PANEL ANALYSIS OF CIRCULAR-ARC BLUFF-BODIES IN UNSTEADY FLOW
James H. Strickland 1989 28 p Presented at the 10th AIAA Aerodynamic Decelerator Systems Technical Conference, Cocoa Beach, FL, 18 Apr. 1989
(Contract DE-AC04-76DP-00789)
(DE89-007141; SAND-89-0366C; CONF-8904118-2; AIAA-89-0930) Avail: NTIS HC A03/MF A01

A method which is capable of calculating the unsteady flow field around circular-arc bluff bodies of zero thickness is presented. This method utilizes linear vortex panels to model the body surface and a portion of the wake surfaces. Discrete vortices are used to model the remainder of the wake surfaces. Separation is assumed to occur at the sharp edges of the bodies. Numerical results for circular-arc bodies with included angles of less than 180 degrees are compared with experimental data and found to be in good agreement. DOE

N89-22846 Gesellschaft fuer Mathematik und Datenverarbeitung, Saint Augustin (Germany, F.R.). Inst. fuer Methodische Grundlagen.
MULTIGRID FOR THE STEADY-STATE INCOMPRESSIBLE NAVIER-STOKES EQUATION: A SURVEY
Johannes Linden, Guy Lonsdale, Barbara Steckel, and Klaus Stueben Jul. 1988 21 p
(GMD-322; ISSN-0723-0508; ETN-89-93759) Copyright Avail: Fachinformationszentrum Karlsruhe, 7514
Eggenstein-Leopoldshafen 2, Fed. Republic of Germany

The present status of multigrid solver methods and related discretizaion aspects for the steady state Navier-Stokes equations is reviewed. Stable discretizations of the Navier-Stokes equations are discussed, with emphasis on non-staggered grid discretizations. Relaxation schemes (including pressure correction based methods, distributive and box schemes), which are used as smoothers in multigrid methods, are discussed. The analysis and algorithmic aspects of the construction of smoothing schemes are discussed.

A stable discretization for non-staggered grids is proposed, as well as a generalized form of box-relaxation which turns out to be an effective and simple smoother and which is easily extendable to general boundary fitted grids. ESA

N89-22847# Technische Univ., Delft (Netherlands).
AN EXPERIMENTAL STUDY OF TURBULENT MIXING OF VISCOELASTIC FLUIDS Ph.D. Thesis
Paul Vincent Bartels 1988 237 p
(ETN-89-94140) Avail: NTIS HC A11/MF A01

The viscoelastic behavior of fluids was related to the hydrodynamics, energy dissipation, and homogenization for turbulent pipeline flow and stirred tank reactors. For both mixing systems a significant influence of viscoelasticity on the hydrodynamics is found in locations with a high shear rate, such as occur in the boundary layer of pipeline flow and in the trailing vortices of the blade of a Rushton turbine. This results in a dramatic drop of the overall energy dissipation for very low values of elasticity number. In tube flow there is a threshold for the drag reduction phenomenon. The friction factor appears to be also a function of the elasticity number. The homogenization process of polymer solutions is also slower due to the lower energy dissipation, causing less dispersion. The energy dissipation and homogenization can be related to a characteristic fluid time and the elasticity number. The effect of inserted mixing elements on turbulent pipe flow was studied. The pressure drop of the mixers is almost independent of the concentration of polyacrylamide, but mixing will be less when the characteristic time of the solutions increases. ESA

N89-22848# Oxford Univ. (England). Dept. of Engineering Science.
CAVITATION IN A SUBMERGED JET AT CONSTANT PRESSURE
R. E. Franklin and J. Rozewicz 1986 64 p
(Grant ER1/9/4/093-ARE(T))
(OUEL-1658/86; ETN-89-94209) Avail: NTIS HC A04/MF A01

It is argued that most of the features of the noise from cavitating submerged jets, including the effect of changes in nozzle diameter, may be accounted for by inference from a knowledge of the flow structure in a single-phase jet. Evidence comes from flow visualizations and measurements, and from a statistical theory of cavitation in a turbulent flow. ESA

N89-22849# Swedish Defence Research Establishment, Stockholm.
VELOCITY MEASUREMENTS DOWNSTREAM OF A SUDDEN EXPANSION USING LDV. PART 2: EXPERIMENTAL RESULTS
Jan Eriksson Nov. 1988 64 p In SWEDISH; ENGLISH summary
(FOA-C-20736-2.1-Pt-2; ISSN-0347-3694; ETN-89-94222) Avail: NTIS HC A04/MF A01

Detailed laser Doppler velocimeter (LDV) measurements downstream of a sudden axially symmetrical expansion, together with a discussion of the experimental uncertainties are reported. Maximum radial and tangential turbulences are 70 % to 80 % of the maximum intensity of the axial turbulence. Compared with other studies of similar geometries, the experimental results are good, and may be considered as a reference for this type of flow and disturbance. ESA

N89-22850*# National Aeronautics and Space Administration. Ames Research Center, Moffett Field, CA.
PERFORMANCE OF ALL-METAL DEMOUNTABLE CRYOGENIC SEALS AT SUPERFLUID HELIUM TEMPERATURES
Louis J. Salerno, Alan L. Spivak (Trans-Bay Electronics, Richmond, CA.), and Peter Kittel Apr. 1989 7 p Presented at the AIAA 24th Thermophysics Conference, Buffalo, NY, 12-15 Jun. 1989
(NASA-TM-102190; A-89101; NAS 1.15:102190) Avail: NTIS HC A02/MF A01 CSCL 20D

Two all-metal demountable cryogenic seals with an outside diameter of 36.6 mm, inside diameter of 27.2 mm, and thickness of 0.51 mm were leak-tested at room temperature (300 K), liquid nitrogen temperature (21 cycles at 77 K), liquid helium temperature (9 cycles at 4.2 K), and susperfluid helium temperature (4 cycles at 1.6 K). Each seal was mounted and demounted for 13 cycles. Thickness measurements at 90 deg intervals along the circumference showed a maximum seal compression of 0.038 mm. Leak-rate measurements at all temperatures showed no detectable leak above the helium background level, typically 0.1 x 10(-9) std-cc/sec, during testing. Author

N89-22851# Carnegie-Mellon Univ., Pittsburgh, PA. Dept. of Mechanical Engineering.
EXPERIMENTAL AND THEORETICAL STUDIES OF VERTICAL ANNULAR LIQUID JETS
N. Chigier, J. I. Ramos, and K. Kihm 1988 8 p Presented at the Society for Industrial and Applied Mathematics (SIAM), Minneapolis, MN, 11 Jul. 1988
(Contract DE-FG02-86ER-13597)
(DE89-009153; CONF-8807159-1; CONF-8805106-3) Avail: NTIS HC A02/MF A01

The stability, dynamics and convergence of vertical annular liquid jets as a function of the initial radius, sheet thickness and velocity have been studied. The influence of the Froude, Reynolds, and Weber numbers and geometry on convergence and stability are examined. Analytical and numerical techniques were used to solve the steady state and time-dependent form of the Navier-Stokes equations for inviscid curtains. Experiments were carried out on annular liquid curtains with an initial radius of 50 mm and initial sheet thicknesses of 0.5 and 1.0 mm. Three Froude numbers have been studied: 1.27, 4.27 and 8.87 by variation of the liquid flow rate. Pressure within the curtains was varied progressively from 0 to 3 Pa. Several flow regimes were found: (1) non-pressurized, (2) pressurized, (3) oscillating, and (4) punctured. Curtain shape and convergence length were determined by photography. Velocity in the liquid curtain was measured by Laser Doppler Anemometry. The variation of liquid film thickness with axial distance was determined. Good agreement was found between predictions and experiments. DOE

N89-22852# Office National d'Etudes et de Recherches Aerospatiales, Paris (France). Direction de l'Aerodynamique.
COMPUTERIZED SIMULATION OF TURBULENT FLOW IN A CHANNEL Final Report [SIMULATION NUMERIQUE D'ECOULEMENTS TURBULENTS DANS UN CANAL]
K. Dang Aug. 1988 87 p In FRENCH
(Contract DRET-87-34-001)
(ONERA-RSF-16/3419-AY-112-A; ETN-89-94359) Avail: NTIS HC A05/MF A01

A direct numerical solution code for Navier-Stokes unsteady incompressible flow is described. It is based on high order finite difference methods. The procedure is used to model channel turbulent flows with two periodical variation directions. The optimization of the vectorial computation algorithm allows a processing time of 15 sec per million network points. ESA

N89-22853# Office National d'Etudes et de Recherches Aerospatiales, Paris (France). Direction de l'Aerodynamique.
NUMERICAL SIMULATION OF VORTEX BREAKDOWN Final Report [SIMULATION NUMERIQUE DE L'ECLATEMEMT TOURBILLONNAIRE]
T. H. Le Jul. 1988 24 p In FRENCH
(Contract DRET/RP-87-34-001)
(ONERA-RSF-3/4368-AY-502-A; ETN-89-94360) Avail: NTIS HC A03/MF A01

A finite difference method and a particulate method were developed to simulate vortex breakdown. The finite difference method is used to compute a free vortex breakdown example. The results are encouraging since the main known characteristic of the phenomena are simulated, including three-dimensional structure, unsteady flow, and a region with negative axial velocity. ESA

N89-22854# Centre d'Etudes et de Recherches, Toulouse (France). Dept. d'Etudes et de Recherches en Informatique.
A FLUX SPLITTING METHOD FOR HYPERBOLIC SYSTEMS: APPLICATION TO THE SOLUTION OF THE EULER EQUATIONS Final Report [UNE METHODE DE FLUX SPLITTING POUR LES SYSTEMES HYPERBOLIQUES. APPLICATION A LA RESOLUTION DES EQUATIONS D'EULER]
Pierre-Alain Mazet and Francoise Bourdel Feb. 1988 104 p In FRENCH
(Contract DRET-87-002-21)
(CERT-RF-1/3290/DERI; ETN-89-94363) Avail: NTIS HC A06/MF A01

A variational entropy method is changed to flux splitting to improve the central unit processing time cost. The method uses the fundamental convexity notion inherent to hyperbolic systems. The method is developed as linear and then generalized in nonlinear. A discontinuous Galerkin approximation is used. The application to the numerical solution of the Euler equation is demonstrated. ESA

N89-22855# Deutsche Forschungs- und Versuchsanstalt fuer Luft- und Raumfahrt, Goettingen (Germany, F.R.). Inst. fuer Experimentelle Stroemungsmechanik.
LECTURES IN FLUID PHYSICS HELD AT THE PHYSICS DEPARTMENT OF THE GEORG-AUGUST-UNIVERSITY. VOLUME 1: SOURCE STRENGTH OF VORTICITY
Hans G. Hornung Jun. 1987 68 p In GERMAN; ENGLISH summary Lectures held in Goettingen, Fed. Republic of Germany, 1987
(DFVLR-Mitt-88-26-Vol-1; ISSN-0176-7739; ETN-89-94372)
Avail: NTIS HC A04/MF A01; DFVLR, VB-PL-DO, Postfach 90 60 58, 5000 Cologne, Fed. Republic of Germany, DM 21

It is shown how vorticity may be generated in a fluid continuum. The source strength of vorticity at a wall is derived explicitly. It is shown that this may be expressed in a form that is independent of material properties. Among the examples of other sources of vorticity, viscoelasticity, turbulence, body forces, and numerical effects are discussed. ESA

N89-22856# Deutsche Forschungs- und Versuchsanstalt fuer Luft- und Raumfahrt, Goettingen (Germany, F.R.). Inst. fuer Experimentelle Stroemungsmechanik.
LECTURES IN FLUID PHYSICS HELD AT THE PHYSICS DEPARTMENT OF THE GEORG-AUGUST-UNIVERSITY. VOLUME 2: EXAMPLES OF THE APPLICATION OF DIMENSIONAL ANALYSIS
Hans G. Hornung Jul. 1987 70 p In GERMAN; ENGLISH summary Lectures held in Goettingen, Fed. Republic of Germany, 1987
(DFVLR-Mitt-88-27-Vol-2; ISSN-0176-7739; ETN-89-94373)
Avail: NTIS HC A04/MF A01; DFVLR, VB-PL-DO, Postfach 90 60 58, 5000 Cologne, Fed. Republic of Germanmy, DM 22

It is shown how dimensional analysis may lead relatively quickly to the formal relation between the dimensionless quantities that determine a physical situation. The efficacy of symmetry arguments is emphasized. Examples from gas dynamics, and turbulent, thermocapillary, and viscoelastic flow, as well as from surface waves and statistical mechanics are used to elucidate these principles. ESA

N89-22857# Von Karman Inst. for Fluid Dynamics, Rhode-Saint-Genese (Belgium).
THEORETICAL STUDY OF THE UNSTEADY FLOW IN A STRAIGHT CHANNEL WITH VARIABLE AND CONSTANT CROSS SECTION
M. T. Sideris and R. A. vandenBraembussche Jun. 1988 54 p
(VKI-TN-168; ETN-89-94450) Avail: NTIS HC A04/MF A01

Wave propagation in one-dimensional channels was analyzed. In incompressible flows, the disturbances propagate with infinite speed (rigid column theory). High reduced frequencies result in a large phase shift between pressure and velocity. In compressible flows, the perturbations propagate as compression and expansion waves, with a speed equal to the speed of sound relative to the flow velocity. The amplitude of the variations increases considerably at resonant frequency and higher harmonics. The amplitude of the variations decreases along the tube length due to the superposition of waves travelling in the one-dimensional space. The numerical results of the compressible flow case show good agreement when compared to the method of characteristics. The results of the two discretization schemes used (MacCormack and Runge-Kutta) are of similar accuracy. However the Runge-Kutta scheme allows much higher numerical time steps and proves to be numerically more efficient than the MacCormack scheme. ESA

N89-22858# Societe Nationale Industrielle Aerospatiale, Paris (France). Div. Engins Tactiques.
NUMERICAL SIMULATION OF BLAST WAVES [SIMULATION NUMERIQUE D'ONDES DE SOUFFLE]
Pascal Garnero 1988 11 p In FRENCH Sponsored by the Service Technique des Engins Tactiques, France
(Rept-882-320-102; ETN-89-94480) Avail: NTIS HC A03/MF A01

A two-dimensional numerical code was developed to simulate the spherical propagation of the shock wave from an explosion. The code is based on the solution of Euler equations and includes the study of interactions with obstacles in the wave path. The first results are encouraging, but further development is necessary. ESA

N89-22859# Aeronautical Research Inst. of Sweden, Stockholm. Aerodynamics Dept.
A HIGHER-ORDER SCHEME FOR THE BURGERS EQUATION
Peter Wilde 24 Aug. 1988 22 p
(FFA-TN-1988-43; ETN-89-94546) Avail: NTIS HC A03/MF A01

An implicit higher-order scheme for solving the nonlinear boundary value problem to the Burger equation is studied. The Rothe method is used to approximate the time dependent boundary value problem by a set of ordinary boundary value problems depending only in the space variable. For the time discretization a second order one-sided finite difference operator is used. For the resulting set of ordinary boundary value problems a fourth order finite difference scheme is used. The nonlinear term in the Burger equation is discretized in a way leading to a linear finite difference equation. Methods to handle the problems near the boundary, obtained by using higher-order finite difference stencils were assessed. The usefulness of the scheme is demonstrated by numerical examples. ESA

N89-22860*# National Aeronautics and Space Administration. Ames Research Center, Moffett Field, CA.
ON THE STRUCTURE OF PRESSURE FLUCTUATIONS IN SIMULATED TURBULENT CHANNEL FLOW
John Kim Apr. 1989 45 p Submitted for publication
(NASA-TM-101084; A-89073; NAS 1.15:101084) Avail: NTIS HC A03/MF A01 CSCL 20D

Pressure fluctuations in a turbulent channel flow are investigated by analyzing a database obtained from a direct numerical simulation. Detailed statistics associated with the pressure fluctuations are presented. Characteristics associated with the rapid (linear) and slow (nonlinear) pressure are discussed. It is found that the slow pressure fluctuations are larger than the rapid pressure fluctuations throughout the channel except very near the wall, where they are about the same magnitude. This is contrary to the common belief that the nonlinear source terms are negligible compared to the linear source terms. Probability density distributions, power spectra, and two-point correlations are examined to reveal the characteristics of the pressure fluctuations. The global dependence of the pressure fluctuations and pressure-strain correlations are also examined by evaluating the integral associated with Green's function representations of them. In the wall region where the pressure-strain terms are large, most contributions to the pressure-strain terms are from the wall region (i.e., local), whereas away from the wall where the pressure-strain

terms are small, contributions are global. Structures of instantaneous pressure and pressure gradients at the wall and the corresponding vorticity field are examined. Author

N89-22861*# National Aeronautics and Space Administration. Lewis Research Center, Cleveland, OH.
ON THE LAGRANGIAN DESCRIPTION OF UNSTEADY BOUNDARY LAYER SEPARATION. PART 2: THE SPINNING SPHERE
Leon L. VanDommelen May 1989 26 p
(NASA-TM-102027; E-4771; NAS 1.15:102027) Avail: NTIS HC A03/MF A01 CSCL 20D

A theory to explain the initial stages of unsteady separation was proposed by Van Dommelen and Cowley (1989). This theory is verified for the separation process that occurs at the equatorial plane of a sphere or a spheroid which is impulsively spun around an axis of symmetry. A Lagrangian numerical scheme is developed which gives results in good agreement with Eulerian computations, but which is significantly more accurate. This increased accuracy, and a simpler structure to the solution, also allows verification of the Eulerian structure, including the presence of logarithmic terms. Further, while the Eulerian computations broke down at the first occurrence of separation, it is found that the Lagrangian computation can be continued. It is argued that this separated solution does provide useful insight into the further evolution of the separated flow. A remarkable conclusion is that an unseparated vorticity layer at the wall, a familiar feature in unsteady separation processes, disappears in finite time. Author

N89-22862*# National Aeronautics and Space Administration. Lewis Research Center, Cleveland, OH.
A GENERALIZED ONE-DIMENSIONAL COMPUTER CODE FOR TURBOMACHINERY COOLING PASSAGE FLOW CALCULATIONS
Ganesh N. Kumar, Richard J. Roelke, and Peter L. Meitner (Army Aviation Systems Command, Cleveland, OH.) 1989 14 p Prepared for presentation at the 25th Joint Propulsion Conference, Monterey, CA, 10-12 Jul. 1989; sponsored in part by AIAA, ASME, SAE, and ASEE
(DA Proj. 1L1-61102-AH-45)
(NASA-TM-102079; E-4839; NAS 1.15:102079; AVSCOM-TR-89-C-013) Avail: NTIS HC A03/MF A01 CSCL 20D

A generalized one-dimensional computer code for analyzing the flow and heat transfer in the turbomachinery cooling passages was developed. This code is capable of handling rotating cooling passages with turbulators, 180 degree turns, pin fins, finned passages, by-pass flows, tip cap impingement flows, and flow branching. The code is an extension of a one-dimensional code developed by P. Meitner. In the subject code, correlations for both heat transfer coefficient and pressure loss computations were developed to model each of the above mentioned type of coolant passages. The code has the capability of independently computing the friction factor and heat transfer coefficient on each side of a rectangular passage. Either the mass flow at the inlet to the channel or the exit plane pressure can be specified. For a specified inlet total temperature, inlet total pressure, and exit static pressure, the code computers the flow rates through the main branch and the subbranches, flow through tip cap for impingement cooling, in addition to computing the coolant pressure, temperature, and heat transfer coefficient distribution in each coolant flow branch. Predictions from the subject code for both nonrotating and rotating passages agree well with experimental data. The code was used to analyze the cooling passage of a research cooled radial rotor. Author

N89-22863 Washington State Univ., Pullman.
STUDY OF UNSTEADY BOUNDARY LAYERS WITH ADVERSE PRESSURE GRADIENT Ph.D. Thesis
Boguslaw Felix Gajdeczko 1988 158 p
Avail: Univ. Microfilms Order No. DA8902784

Experimental data on oscillatory turbulent boundary layers in adverse pressure gradient are presented. The experiments were conducted in an unsteady flow water tunnel using 2-component laser Doppler anemometry (LDA). While these experimental data compliment those obtained earlier by other investigators, they are characterized by large values of amplitude (approx.=0.4) and frequency (Strouhal number up to 25). Two sets of experiments in mild and one set in strong adverse pressure gradient were conducted. The experiments indicate the existence of a multilayer structure in the oscillatory properties of the flow. This structure appears to correlate strongly with the local Strouhal number. It is also affected significantly by the pressure gradient and by the occurrence of flow reversal during the oscillation cycle. The experimental data are complimented by results of a numerical simulation of the unsteady boundary layer using the (kappa-epsilon) model of turbulence. While this model was not found to be adequate for the quantitative predictions of the flow (as was expected), it nevertheless was found to simulate (and thereby confirm) some of the interesting and important features of unsteady turbulent boundary layers in adverse pressure gradient that were observed experimentally. Dissert. Abstr.

N89-22864# Naval Research Lab., Washington, DC. Lab. for Computational Physics and Fluid Dynamics.
LOW REYNOLDS NUMBER CALCULATION OF TURBULENT CHANNEL FLOW: A GENERAL DISCUSSION Interim Report, Oct. - Nov. 1988
R. A. Handler, E. W. Hendricks, and R. I. Leighton 23 Feb. 1989 105 p
(AD-A205883; NRL-MR-6410) Avail: NTIS HC A06/MF A01 CSCL 20D

The statistical properties of turbulent flow in a channel at a wall Reynolds number of 125 using a moderate resolution direct numerical simulation is investigated. We have found that the use of a Green function method results in turbulent statistics which are significantly closer to experimental results than those produced by the Orszag-Kells (1980) splitting method. We have found some differences between our calculations and those of Kim, Moin and Moser (1987) (KMM). Our calculation gives somewhat lower turbulent intensities and longer streamwise correlation lengths. In general, however, the one and two point statistics are in good agreement with the KMM results. Conditional sampling calculations on the simulated data indicate a definite relationship between VITA and Q2 events. We have also found that aliasing errors cause strong damping effects on the final steady state turbulent velocity field. GRA

N89-22865# SRI International Corp., Menlo Park, CA.
COMPRESSION AND SHEAR WAVE PROPAGATION IN EXPLOSIVES Final Report, 1 Feb. 1984 - 30 Sep. 1988
M. Cowperthwaite and Y. M. Gupta Jan. 1989 84 p
(Contract DAAG29-84-K-0018)
(AD-A205917; ARO-21117.2-EG) Avail: NTIS HC A05/MF A01 CSCL 19I

The objective of the experimental study was to investigate the occurrence of shear-induced reaction (SIR) in an explosive subjected to the type of one-dimensional compression and shear (1DCS) loading produced by the parallel-inclined impact (PII) technique pioneered by Gupta. The objective of the theoretical study was to formulate a treatment of the reactive flow produced in an explosive subjected to 1DCS loading and thereby provide a framework for interpreting the results of the PII experiments. Our theoretical study was based on a model analysis of the PII experiment with the shock-loaded target treated as an inert elastic solid and the resulting flow treated ideally as a pure compression wave followed by a pure shear wave. A complete equation of state for a reactive elastic solid was formulated and used to derive the thermodynamic equations governing the one-dimensional adiabatic flows produced by PII. The experimental study was based on Gupta's premise that significant differences between the sets of longitudinal particle velocity histories recorded in an explosive subjected to normal impact and PII producing equivalent nonreactive compression waves can be taken as evidence for the occurrence of SIR in the PII experiment. Results of shear particle

measurements led to the conclusion that the shear deformation produced in Composition B3 by PII remains close to the impact surface. GRA

N89-22866# Princeton Univ., NJ. Dept. of Mechanical and Aerospace Engineering.
THE STRUCTURE AND CONTROL OF THREE-DIMENSIONAL SHOCK WAVE TURBULENT BOUNDARY LAYER INTERACTIONS Final Report, 15 Jul. 1986 - 30 Sep. 1988
Seymour M. Bogdonoff 14 Feb. 1989 39 p
(Contract F49620-86-C-0094)
(AD-A205923; MAE-1851; AFOSR-89-0285TR) Avail: NTIS HC A03/MF A01 CSCL 20D

The present report briefly reviews the work accomplished on the study of three-dimensional shock wave turbulent boundary layer interactions at a Mach 3. The work consisted of two major thrusts: (1) Modeling of the complex interaction and detailed experiments coordinated with extensive computations; and (2) Exploratory studies of control concepts for a 20 deg fin and crossing shock configurations. The completed works have been reported and are briefly reviewed. A brief resume is presented of incompleted results on complex interactions, new heat transfer techniques, initial spanwise boundary layer effects, and studies in a new Low Turbulence Variable Geometry facility. GRA

35 INSTRUMENTATION AND PHOTOGRAPHY

Includes remote sensors; measuring instruments and gages; detectors; cameras and photographic supplies; and holography.

For aerial photography see *43 Earth Resources and Remote Sensing.* For related information see also *06 Aircraft Instrumentation,* and *19 Spacecraft Instrumentation.*

N89-22867# Liaoning Inst. of Metrology, Shenyang (China).
NEW THERMOCOUPLE: CHARACTERISTIC INVESTIGATION OF Au+Pd+Ni/Ni+Cr THERMOCOUPLE BELOW 273K
Dehua Song, Jichun Xiao, and Yuzhu Mao (Academia Sinica, Beijing, China) 1987 11 p Sponsored by Institute of Scientific and Technical Information of China, Beijing
(PB89-112940; ISTIC-TR-C-000181) Avail: NTIS HC A03/MF A01 CSCL 14B

Experimental investigation of AuPdNi/NiCr thermocouple characteristic below 273K is described. The thermoelectric force of the thermocouple is as high as 14.5 mv at 4.2K. Its sensitivity is 15 to 79 microvolts/k in the temperature range from 20 to 273K, and these are the highest of all thermocouples now. The inhomogeneity, E-T relation and the Seebeck coefficients are given, and it is compared with AuFe/NiCr thermocouple. Finally, the T-E-S reference table is given also. Author

N89-22868*# National Aeronautics and Space Administration. Langley Research Center, Hampton, VA.
SURFACE TEMPERATURE MEASUREMENTS USING A THIN FILM THERMAL ARRAY
L. A. Dillon-Townes, P. B. Johnson, R. L. Ash (Old Dominion Univ., Norfolk, VA.), K. Daryabeigi, and J. C. Whipple Mar. 1989 22 p
(Contract NAS1-17993)
(NASA-TM-101549; NAS 1.15:101549) Avail: NTIS HC A03/MF A01 CSCL 14B

A thin film device was designed and fabricated to measure surface temperatures. An array of eight integrated thermal sensors are mounted on a 0.002 inch (0.05 mm) Kapton film and multiplexed to obtain an area thermal measurement. The device was tested on a flat plate airfoil and demonstrated a temperature variation of 0.55 C maximum and 0.05 C minimum compared to embedded thermocouples. Future improvements are also discussed. Author

N89-22869# EG and G Energy Measurements, Inc., Los Alamos, NM.
THE PROPAGATION OF NOISE THROUGH STREAK SYSTEMS
Adam Whiteson 1988 8 p Presented at the 32nd International Technical Symposium on Optical and Opto-Electronic Applied Science and Engineering, San Diego, CA, 14 Aug. 1988
(Contract DE-AC08-88NV-10617)
(DE89-006600; CONF-880887-31) Avail: NTIS HC A02/MF A01

The influence of a streak tube system on the noise properties of the signal is analyzed. The streak system is modeled as a cascade of stochastic amplifiers and a system transfer function for the signal statistics developed in terms of the Z transform of each stage. The output signal variance is calculated from the model and compared with experimental data. DOE

N89-22870# California Univ., Berkeley. Lawrence Berkeley Lab. National Center for Electron Microscopy.
TRANSMISSION ELECTRON MICROSCOPY: IMAGING OF MATERIALS
Gareth Thomas Oct. 1988 33 p Presented at the Metallurgical Society Fall Meeting and American Society for Metals Materials Week, Chicago, IL, 24 Sep. 1988
(Contract DE-AC03-76SF-00098)
(DE89-007418; LBL-26144; CONF-880901-18) Avail: NTIS HC A03/MF A01

This report was an invited paper for a symposium and only covers general aspects of transmission electron microscopy. A history, and examples of work done on ceramics and alloys are covered. DOE

N89-22871# International Centre for Theoretical Physics, Trieste (Italy).
DISTORTIONS IN THE OUTPUT SIGNALS OF CONVENTIONAL SPECTRUM ANALYZERS
Ernest C. Njau (Dar-es-Salaam Univ., Tanzania) Aug. 1988 9 p
(DE88-705656; IC-88/224) Avail: NTIS (US Sales Only) HC A02/MF A01

We show that the output signals of conventional spectrum analyzers contain distortions which basically originate from the signal processing performed inside the analyzers' frequency convertors. Total elimination of these distortions through normal filtering techniques is difficult owing to the closeness of some of their frequencies to the corresponding frequencies of the required signals. Simple design adjustments that can minimize these distortions are suggested. DOE

N89-22872# Los Alamos National Lab., NM. Materials Science and Technology Div.
ULTRA-SENSITIVE X-RAY SENSORS GIVE IMPROVED CONTRAST SENSITIVITY
David M. Stupin 1989 10 p Presented at the 12th World Conference on Non-Destructive Testing, Amsterdam, Netherlands, 23 Apr. 1989
(Contract W-7405-eng-36)
(DE89-003581; LA-UR-88-3865; CONF-890478-1) Avail: NTIS HC A02/MF A01

Low-light-level cameras used with phosphors detect very small contrast differences and very small features in X-ray images. I used (1) a Silicon-Intensifier-Tube (SIT) television camera coupled by a fiber optic to a phosphor screen and (2) an integrating CCD camera focused on a phosphor to detect a 0.1 percent contrast difference and 2-micrometer-diameter wires in a digital image. Flannery, et al., and Kinney, et al., reported spatial resolution as small as 1 micrometer in computer X-ray tomography (CAT scans) using synchrotron X-ray sources and CCD cameras. I thought that these cameras could be used with industrial X-ray sources with microfocal spot sizes to produce X-ray images with spatial resolution as small as 1 micrometer and contrast sensitivity as small as 0.01 percent. Hence, near-real time X-ray inspection system could be made that have the resolution of X-ray film and 20 times better contrast sensitivity. As a proof of principle

experiment, I used an X-ray camera composed of an X-ray phosphor deposited on a fiber optic that is coupled to a night vision camera (SIT). Using a digital subtraction technique and an 8-bit frame grabber, this camera detected wires as small as 2 micrometers in diameter and X-ray attenuations as small as 0.27 percent. Verhoeven reported 0.14 percent for a free-standing foil without a substrate. However, some CCD cameras have 64 times more levels of digitization than the frame grabber and can integrate images for as long as 30 minutes before the images are digitized. Hence, I predicted that the CCD camera would also detect wires 2 micrometers in diameter and contrast differences as small as 0.02 percent, ten times better than the SIT and 20 better than film. Unfortunately, my preliminary experiments with CCD camera duplicate, but do not improve upon, the performance of the SIT. DOE

N89-22873# Los Alamos National Lab., NM.
ALEXIS: A NARROW-BAND SURVEY/MONITOR OF THE ULTRASOFT X-RAY SKY
W. C. Priedhorsky, J. J. Bloch, F. Cordova, B. W. Smith, M. Ulibarri, J. Chavez, E. Evans, O. H. W. Seigmund, H. Marshall, and J. Vallerga (Sandia National Labs., Albuquerque, NM.) et al 1989 29 p Presented at the Berkeley Colloquium on Extreme Ultraviolet Astronomy, Berkeley, CA, 19 Jan. 1989
(Contract W-7405-eng-36)
(DE89-007980; LA-UR-89-479; CONF-890189-3) Avail: NTIS HC A03/MF A01

Los Alamos and Sandia National Laboratories are building an ultrasoft X-ray monitor experiment. This experiment, called ALEXIS (Array of Low-Energy X-Ray Imaging Sensors), consists of six compact normal-incidence telescopes. ALEXIS will operate in the range 70 to 110 eV. The ultrasoft X-ray/EUV band is nearly uncharted territory for astrophysics. ALEXIS, with its wide fields-of-view and well-defined wavelength bands, will complement the upcoming NASA Extreme Ultraviolet Explorer and ROSAT EUV Wide Field Camera, which are sensitive broad-band survey experiments. The program objectives of ALEXIS are to: (1) demonstrate the feasibility of a wide field-of-view, normal incidence ultrasoft X-ray telescope system, and (2) to determine ultrasoft X-ray backgrounds in the space environment. As a dividend, ALEXIS will pursue the following scientific objectives: (1) to map the diffuse background, with unprecedented angular resolution, in several emission-line bands, (2) to perform a narrow-band survey of point sources, (3) to search for transient phenomena in the ultrasoft X-ray band, and (4) to provide synoptic monitoring of variable ultrasoft X-ray sources such as cataclysmic variables and flare stars. ALEXIS is designed to be flown on a small autonomous payload carrier (a minisat) that could be launched from any expendable launch vehicle. The experiment weighs 100 pounds, draws 40 watts, and produces 10 kbps of data. It can be flown in any low earth orbit. Onboard data storage allows operation and tracking from a single ground station at Los Alamos. DOE

N89-22874# Lawrence Livermore National Lab., CA.
WAVELENGTH STREAK CAMERA
C. McConaghy and J. Koo 1988 5 p Presented at SPIE O-E Laser: International Symposium and Exhibition on Fiber Optics, Optoelectronics and Laser Applications, Boston, MA, 6 Sep. 1988
(Contract W-7405-eng-48)
(DE89-008612; UCRL-98426; CONF-8809105-13) Avail: NTIS HC A02/MF A01

We have demonstrated the recording of 8 GHz electrical signals by optically encoding time into wavelength and deflecting, by means of a diffraction grating, the optical signal across a readout array. The experiments were performed at 820 nm and show promise for circumventing the material dispersion in fibers at this wavelength to allow propagation of high bandwidth microwave signals (up to 10 GHz) over 1 km distances. DOE

N89-22875# Westinghouse Electric Corp., West Mifflin, PA.
MEASURING ELECTRODE ASSEMBLY Patent Application
John E. Bordenick, inventor (to DOE) 26 Apr. 1988 16 p
(Contract DE-AC11-76PN-00014)
(DE89-009591; PATENTS-US-A7186419;
US-Patent-Appl-SN-186419) Avail: NTIS HC A03/MF A01

A pH measuring electrode assembly for immersion in a solution includes an enclosed cylindrical member having an aperture at a lower end thereof. An electrolyte is located in the cylindrical member above the level of the aperture and an electrode is disposed in this electrolyte. A ring formed of an ion porous material is mounted relative to the cylindrical member so that a portion of this ring is rotatable relative to and is covering the aperture in the cylindrical member. A suitable mechanism is also provided for indicating which one of a plurality of portions of the ring is covering the aperture and to keep track of which portions of the ring have already been used and become clogged. Preferably, the electrode assembly also includes a glass electrode member in the center thereof including a second electrolyte and electrode disposed therein. The cylindrical member is resiliently mounted relative to the glass electrode member to provide for easy rotation of the cylindrical member relative to the glass electrode member for changing of the portion of the ring covering the aperture. DOE

N89-22876# Fermi National Accelerator Lab., Batavia, IL.
THE NEW EXPERIMENTAL AREAS OXYGEN MONITOR
D. Schoo Aug. 1988 7 p
(Contract DE-AC02-76CH-03000)
(DE89-009700; FNAL-TM-1567) Avail: NTIS HC A02/MF A01

Because of the nature of the beamline requirements for oxygen monitoring equipment to operate ancillary equipment, such as exhaust fans, doors and cryogenic valves, and because of the well known problems of the oxygen sensors installed in high radiation areas, a new design for sensing the oxygen content of ambient air was needed. A new monitor system was designed to solve these problems and some others that compromised the reliability and the maintenance of the monitoring system. From the operating experience gained with the Accelerator Standard Oxygen Monitor System currently installed in many locations in the experimental area, from suggestions solicited from the Safety Group and from the Cryogenics Group, I designed a new Experimental Areas Standard Oxygen Monitor. Many suggestions were carefully considered and a design that incorporates most of them was constructed. I will summarize a list of the important improvements that will be of interest to the users of the system, and explain how these functions will make the oxygen system easier to live with. DOE

N89-22877# European Space Agency, Paris (France).
APPLICATION OF THE SINGLE-AXIS-RATE-TABLE (SAT) OF THE DFVLR FOR THE EVALUATION OF STATIONARY AND DYNAMIC GYRO PROPERTIES
Egmar Luebeck (Deutsche Forschungs- und Versuchsanstalt fuer Luft- und Raumfahrt, Brunswick, Germany, F.R.) Nov. 1988 47 p Transl. into ENGLISH of Zum Einsatz des Einachs-Drehtisches (SAT) der DFVLR fuer die Erprobung Stationaerer und Dynamischer Kreiseleigenschafter (Brunswick, Fed. Republic of Germany, DFVLR), 1988 46 p Original language document was announced as N88-27533
(ESA-TT-1122; DFVLR-Mitt-88-09; ETN-89-94235) Avail: NTIS HC A03/MF A01; original German version available from DFVLR, VB-PL-DO, Postfach 90 60 58, 5000 Cologne, Fed. Republic of Germany, DM 22

The wake behind a flat plate, held parallel to the free-stream, is simulated numerically using a finite difference Galerkin method for the solution of the time-dependent, incompressible Navier-Stokes equations. The temporal amplification process of perturbations at supercritical Reynolds numbers, leading finally to the saturation state, is studied. The Orr-Sommer-feld stability analysis of the quasi-steady state, occurring during the wake development, reveals that the flow can be divided into a locally absolutely unstable and a locally convectively unstable region. The influence of these stability properties on the wake, as well as their changes with Reynolds number and based bleed, is discussed based on the numerical simulation and the linear, local stability analysis. ESA

N89-22878# Nationaal Inst. voor Kernfysica en Hoge Energiefysica, Amsterdam (Netherlands).
EXPERIMENTAL STUDY OF URANIUM PLASTIC SCINTILLATOR CALORIMETERS
G. dAgostini, A. Bamberger, F. Barreiro, E. Bernardi, K. Dierks, G. Drews, Jos J. Engelen, M. Garcia, R. Klanner, and U. Koetz (Deutsches Elektronen-Synchrotron, Hamburg, Germany, F.R.) et al Apr. 1988 27 p Prepared in cooperation with Toronto Univ., Ontar io
(NIKHEF-H/88-4; ETN-89-94250) Avail: NTIS HC A03/MF A01

As preparation for the ZEUS high resolution calorimeter, sampling calorimeters made from 3.2 mm plates of depleted uranium read out by plastic scintillator of 3 mm and 5 mm thickness were built. The response of hadrons, electrons, and muons was measured in the energy range between 3 and 100 GeV. In agreement with predictions, the relative response of electrons and hadrons as well as the hadronic energy resolution depend strongly on the thickness of the plastic scintillator. For 3.2 mm depleted uranium and 3 mm thick scintillator equal response for electrons and hadrons is seen over the full energy range. A hadronic energy resolution of 34.5 percent/rt e(GeV) is obtained. Results for the spatial resolution for electrons and hadrons are given. Results from a lead scintillator calorimeter built as a prestudy before uranium plates were available are reported. ESA

N89-22879# Centre d'Etudes et de Recherches, Toulouse (France). Dept. d'Etudes et de Recherches en Aerothermodynamique.
IMPLEMENTATION OF A TWO-COMPONENT LASER ANEMOMETER AT THE T2 WIND TUNNEL
J. L. Bonnet, A. Seraudie, J. P. Archambaud, and A. Mignosi Jul. 1987 123 p In FRENCH Original contains color illustrations
(A-501-H; T-114-A) Avail: NTIS HC A06/MF A01

A series of tests for perfecting the velocity measurement with a two-component laser anemometer was carried out on a 180 mm chord RA16SC1 airfoil at the T2 wind tunnel, in September 1986. Measurements were performed on boundary layers, wake, and shock probing on the upper side of the model, mainly for two Mach number values (M = 0.6 and 0.725) at 2 deg angle of attack, corresponding respectively to a steady shock and to a buffeting configuration. The anemometer system was tested to determine its limitations and practical problems of its use: theoretical limitations due to the filter, to the wall approach, to the density gradients etc. In conclusion, good velocity measurements are reliable with this laser anemometer at the T2 wind tunnel, with respect to the use limitations. Author

N89-23136# Columbia Univ., New York, NY. Dept. of Computer Science.
MODELING SENSORS AND APPLYING SENSOR MODEL TO AUTOMATIC GENERATION OF OBJECT RECOGNITION PROGRAM
Katsushi Ikeuchi and Takeo Kanade *In* Science Applications International Corp., Proceedings: Image Understanding Workshop, Volume 2 Apr. 1988 p 697-710 (For primary document see N89-23115 16-61)
(Contract F33615-84-K-1520; ARPA Order 4976)
Avail: NTIS HC A99/MF E03 CSCL 14B

36 LASERS AND MASERS

Includes parametric amplifiers.
For related information see also *76 Solid-State Physics*.

N89-22880# Lawrence Livermore National Lab., CA.
MAGNETIC AXIS ALIGNMENT AND THE POISSON ALIGNMENT REFERENCE SYSTEM
Lee V. Griffith, Richard F. Schenz, and Gary E. Sommargren (Zygo Corp., Santa Cruz, CA.) 31 Jan. 1989 37 p
(Contract W-7405-eng-48)
(DE89-007687; UCID-21591) Avail: NTIS HC A03/MF A01

Three distinct metrological operations are necessary to align a free-electron laser (FEL): the magnetic axis must be located, a straight line reference (SLR) must be generated, and the magnetic axis must be related to the SLR. This paper begins with a review of the motivation for developing an alignment system that will assure better than 100 micrometer accuracy in the alignment of the magnetic axis throughout an FEL. The paper describes techniques for identifying the magnetic axis of solenoids, quadrupoles, and wiggler poles. Propagation of a laser beam is described to the extent of revealing sources of nonlinearity in the beam. Development and use of the Poisson line, a diffraction effect, is described in detail. Spheres in a large-diameter laser beam create Poisson lines and thus provide a necessary mechanism for gauging between the magnetic axis and the SLR. Procedures for installing FEL components and calibrating alignment fiducials to the magnetic axes of the components are also described. An error budget shows that the Poisson alignment reference system will make it possible to meet the alignment tolerances for an FEL. DOE

N89-22881# MCR Technology Corp., Chicago, IL.
DEVELOPMENT OF AN EFFICIENT HIGH BRIGHTNESS TI:AL2O3 LASER AMPLIFIER Final Report, 15 Aug. 1987 - 14 Feb. 1988
D. Cullen, W. Haddad, K. Boyer, and C. K. Rhodes Apr. 1988 15 p
(Contract F49620-87-C-0086)
(AD-A204187; AFOSR-88-1311TR) Avail: NTIS HC A03/MF A01 CSCL 09C

Ti:Al(2)O(3) represents an exciting new material with application to many areas including atmospheric research, laser radar, and spectroscopy. It is particulary suitable for short pulse generation, since it has a very large bandwidth. In the context of short wavelength high brightness sources, MCR Technology Corporation has pursued the development of Ti:Al(2)O(3) as a system which can be frequency doubled or tripled to produce high energy picosecond and femtosecond duration pulses at short wavelengths. To data we have demonstrated a flashlamp excited device capable of 450 mJ output at 750 nm in a 300 nsec pulse. The overall electrical to optical energy conversion was 0.18 percent. On the basis of this result, it is projected that overall efficiencies greater than 1 to 2 percent should be achievable in relatively simple and practical configurations. GRA

N89-22882# Science Research Lab., Inc., Somerville, MA.
COMPACT, LIGHTWEIGHT CO2 LASERS FOR SDIO APPLICATIONS Technical Progress Report, 30 Sep. 1988 - 31 Jan. 1989
Jonah Jacob 31 Jan. 1989 10 p
(Contract N00014-88-C-0727)
(AD-A204300; AD-E801786; SRL-P-01-1989) Avail: NTIS HC A02/MF A01 CSCL 09C

Two rate equations are important in determining the stability of the discharge. The first is the electron production and loss. The ionization rate constant v in the first equation is assumed to be the result of metastable ionization. Since the metastable levels have a much smaller ionization energy than the ground state the ionization rate of the discharge is dominated by electron impact ionization of the metastables. The stability of both equations will be analyzed assuming that the applied discharge is sinusoidally varying. Hence the various rates are determined by the local RF electric field of frequency which is generated externally by the system shown. From the analysis performed in Phase 1 Science Research Laboratory (SRL) has shown that a current source is volumetrically stable and so the initial analysis will assume an RF current source. GRA

N89-22883# General Coherent Technology, Inc., Richardson, TX.
GAMMA RAY LASER PUMP DIAGNOSTIC Final Report
C. B. Collins 18 Jan. 1989 80 p
(Contract N00014-88-C-2257)
(AD-A205221) Avail: NTIS HC A05/MF A01 CSCL 09C

The nuclear analog of the ruby laser would embody the most straightforward of the several concepts for a gamma ray laser. The greatest progress toward an ultrashort wavelength laser has been achieved along that direction. For ruby the identification and exploitation of a bandwidth funnel were the critical keys in the development of the first laser. There was a broad absorption band linked through efficient cascading to the narrow laser level. The search for the analogous situation on the nuclear scale is proceeding quite fruitfully. Significant amounts of nuclear fluorescence have been pumped by pulsed bremsstrahlung sources; thus proving that the concept of bandwidth funneling works as well at the nuclear level as it does for the ruby. This critical process was found to produce eleven orders of magnitude increase in the amount of X-ray pump energy absorbed into demonstration nuclei of Se-77. Most recently, the first of the 29 candidate materials for a gamma ray laser was successfully pumped with intense pulses of bremsstrahlung. The yield of nuclear fluorescence was about 10,000 times greater than what was predicted by even the theories including the large factor for funneling. Selected over 28 alternatives solely on the basis of availability, this first material narrowly missed the threshold of feasibility for gamma ray laser. These results with a relatively unattractive candidate indicate that the probabilities should be raised for full success of one of the other 28 materials. GRA

N89-22884# Mission Research Corp., Albuquerque, NM.
KINETIC STUDIES OF THE ELECTRON-BEAM-PUMPED ARF LASER
Thomas C. Genoni, Lawrence A. Wright, and Thomas A. Bida 1989 4 p Presented at CLEO '89: Conference on Lasers and Electro Optics, Baltimore, MD, 24 Apr. 1989
(Contract DE-AC04-76DP-00789)
(DE89-004041; SAND-88-7162C; CONF-890423-4) Avail: NTIS HC A02/MF A01

Results from ArF kinetics calculations -- including vibrational relaxation, B/C state mixing and amplified spontaneous emission -- are compared to experiments measuring extracted intensity and fluorescence yield. An efficient two-stage amplifier is then designed. DOE

N89-22885# Los Alamos National Lab., NM.
PROGRESS TOWARD THE DELIVERY OF HIGH ENERGY PULSES WITH THE AURORA KrF/ICF LASER SYSTEM
L. A. Rosocha, R. G. Anderson, S. J. Czuchlewski, J. A. Hanlon, R. G. Jones, M. Kang, C. R. Mansfield, S. J. Thomas, R. G. Watt, and J. F. Figueira 1988 7 p Presented at the LASERS '88, Lake Tahoe, NV, 5-9 Dec. 1988
(Contract W-7405-eng-36)
(DE89-007750; LA-UR-89-366; CONF-881244-9) Avail: NTIS HC A02/MF A01

Because of the attractiveness of short wavelength lasers for inertial confinement fusion (ICF), the Los Alamos National Laboratory is engaged in a program to investigate the feasibility of high power KrF lasers as future ICF drivers. The main hardware element in this program is the Aurora KrF laser system, which is a prototype for demonstrating the applicability of optical angular multiplexing and serial amplification by large electron-beam-driven KrF laser amplifiers to potential large-scale fusion drivers. Multiplexing is a straightforward scheme for matching the energetic component (approx. 5 ns) of the required target pulse to the longer pulse time (approx. 500 ns) required for practical, efficient large-scale KrF laser amplifier operation. Aurora uses a multiplexed 96-element train of 5-ns pulses, which is amplified and passed through a demultiplexer, where all pulses in the train are stacked in time by using suitable time-of-flight delays. Presently, the laser system is configured to deliver 48 stacked 5-ns pulses to the target at multikilojoule energy levels. In principal, it is possible to extract energy levels exceeding 10 kJ from the final Aurora amplifier. In this paper, we will report on the performance of the front end, amplifiers, and the optical train. Amplifier improvements, energy extraction experiments, and subsequent progress in the delivery of demultiplexed pulses to the target plane will also be discussed. As of this conference, we have tested the amplifier upgrade hardware, measured the gain on two modified amplifiers, installed optics on the main power amplifier, sized the beams to the target chamber, and begun firing the amplifier chain in a step-by-step process of integration from the front end lasers to the target plane. At the time of presentation, the second amplifier in the chain of four has exceeded the original design output of 50 J by more than 20 percent. DOE

N89-22886# Lawrence Livermore National Lab., CA.
TUNABLE CHROMIUM LASERS
Lloyd L. Chase and Stephen A. Payne Jan. 1989 9 p Presented at the SPIE Conference on Optics, Electro-optics and Laser Applications in Science and Engineering: OE/LASE '89, Los Angeles, CA, 15 Jan. 1989
(Contract W-7405-eng-48)
(DE89-008814; UCRL-99077; CONF-890145-23) Avail: NTIS HC A02/MF A01

During the decade that has passed since the discovery of the alexandrite laser, many other tunable vibronic sideband lasers based on Cr(3+) have been developed. These lasers span the wavelength range from 700 nm to at least 1235 nm. Experimental and theoretical research has provided an understanding of the important factors that influence the performance of these Cr(3+) lasers and other solid state vibronic lasers. The intrinsic performance levels of some of the most promising Cr(3+) lasers are evaluated from extrapolated slope efficiency measurements. DOE

N89-22887# Los Alamos National Lab., NM.
FIBER OPTIC LASER ROD Patent Application
George F. Erickson, inventor (to DOE) 13 Apr. 1988 10 p
(Contract W-7405-eng-36)
(DE89-009598; PATENTS-US-A7180939;
US-Patent-Appl-SN-180939) Avail: NTIS HC A02/MF A01

A laser rod is formed from a plurality of optical fibers, each forming an individual laser. Synchronization of the individual fiber lasers is obtained by evanescent wave coupling between adjacent optical fiber cores. The fiber cores are dye-doped and spaced at a distance appropriate for evanescent wave coupling at the wavelength of the selected dye. An interstitial material having an index of refraction lower than that of the fiber core provides the optical isolation for effective lasing action while maintaining the cores at the appropriate coupling distance. DOE

N89-22888# Lawrence Livermore National Lab., CA.
Cr3(+)-DOPED COLQUIRIITE SOLID STATE LASER MATERIAL Patent Application
Stephen A. Payne, inventor (to DOE), Lloyd L. Chase, inventor (to DOE), Herbert W. Newkirk, inventor (to DOE), and William F. Krupke, inventor (to DOE) 31 Mar. 1988 16 p
(Contract W-7405-eng-48)
(DE89-010106; PATENTS-US-A7176014;
US-Patent-Appl-SN-176014) Avail: NTIS HC A03/MF A01

Chromium doped colquiriite, LiCaAlF6:Cr(3+), is useful as a tunable laser crystal that has a high intrinsic slope efficiency, comparable to or exceeding that of alexandrite, the current leading performer of vibronic sideband Cr(3+) lasers. The laser output is tunable from at least 720 nm to 840 nm with a measured slope efficiency of about 60 percent in a Kr laser pumped laser configuration. The intrinsic slope efficiency (in the limit of large output coupling) may approach the quantum defect limited value of 83 percent. The high slope efficiency implies that excited state absorption (ESA) is negligible. The potential for efficiency and the tuning range of this material satisfy the requirements for a pump laser for a high density storage medium incorporating Nd(3+) or Tm(3+) for use in a multimegajoule single shot fusion research facility. DOE

N89-22889# European Space Agency, Paris (France).
ON THE SMALL-SIGNAL GAIN OF FREE-ELECTRON LASERS IN THE LOW-CURRENT REGION
Gerhard Spindler (Deutsche Forschungs- und Versuchsanstalt fuer Luft- und Raumfahrt, Stuttgart, Germany, F.R.) Nov. 1988

48 p Transl. into ENGLISH of Zur Kleinsignalverstaerkung von Free-Electron-Lasern im Bereich Schwacher Elektronenstroeme (Stuttgart, Fed. Republic of Germany, DFVLR) Feb. 1987 58 p Original language document was announced as N88-27552
(ESA-TT-1120; DFVLR-FB-87-10; ETN-89-94234) Avail: NTIS HC A03/MF A01; original German version available from DFVLR, VB-PL-DO, Postfach 90 60 58, 5000 Cologne, Fed. Republic of Germany, DM 15

A physically transparent method for calculating the small-signal gain of a free-electron laser (FEL) in the low-current regime is presented. The approach, performed within the framework of the single-particle model, makes explicit use of the modulation of the electron distribution function (bunching). In comparison with the usual method (expansion of the energy perturbation to second order by the amplitude of the signal wave; averaging over a homogeneous initial distribution) a gain formula with a factor twice as high in case of the FEL with a helical periodic wiggler is obtained. This is in best agreement with the Stanford-Experiment (1975). For the wiggler-free FEL (gyration in a homogeneous longitudinal magnetic field in combination with relatistic longitudinal motion) there are significant deviations of the gain formula with respect to published results. ESA

N89-22890*# David Sarnoff Research Center, Princeton, NJ.
PARALLEL OPTICAL RANDOM ACCESS MEMORY (PORAM) Final Report, 24 Aug. 1987 - 23 Mar. 1988
G. A. Alphonse Washington NASA Jun. 1989 35 p (Contract NAS1-18226)
(NASA-CR-4241; NAS 1.26:4241) Avail: NTIS HC A03/MF A01 CSCL 20E

It is shown that the need to minimize component count, power and size, and to maximize packing density require a parallel optical random access memory to be designed in a two-level hierarchy: a modular level and an interconnect level. Three module designs are proposed, in the order of research and development requirements. The first uses state-of-the-art components, including individually addressed laser diode arrays, acousto-optic (AO) deflectors and magneto-optic (MO) storage medium, aimed at moderate size, moderate power, and high packing density. The next design level uses an electron-trapping (ET) medium to reduce optical power requirements. The third design uses a beam-steering grating surface emitter (GSE) array to reduce size further and minimize the number of components. Author

37 MECHANICAL ENGINEERING

Includes auxiliary systems (nonpower); machine elements and processes; and mechanical equipment.

N89-22891*# National Aeronautics and Space Administration. Lewis Research Center, Cleveland, OH.
ROTORDYNAMIC INSTABILITY PROBLEMS IN HIGH-PERFORMANCE TURBOMACHINERY, 1988
Washington, DC Feb. 1989 454 p Workshop held in College Station, TX, 16-18 May 1988; sponsored by NASA, Lewis Research Center, Cleveland, OH, Texas A and M Univ., College Station, ARO, Durham, NC, and Aeropropulsion Lab., Wright-Patterson AFB, OH
(NASA-CP-3026; E-4227; NAS 1.55:3026) Avail: NTIS HC A20/MF A01 CSCL 13I

The continuing trend toward a unified view is supported with several developments in the design and manufacture of turbomachines with enhanced stability characteristics along with data and associated numerical/theoretical results. The intent is to provide a continuing impetus for an understanding and resolution of these problems. Topics addressed include: field experience, dampers, seals, impeller forces, bearings, and compressor and rotor modeling. For individual titles, see N89-22892 through N89-22917.

N89-22892*# Zhejiang Univ. (China).
SOME FIELD EXPERIENCE WITH SUBSYNCHRONOUS VIBRATION OF CENTRIFUGAL COMPRESSORS
Xi-xuan Wang, Jin-chu Gu, Qin-gen Shen, Yong-li Hua, Lan-sheng Zhu, and Yun-tian Du (Zhengzhou Polytechnic Inst., Henan, China) NASA, Lewis Research Center, Rotordynamic Instability Problems in High-Performance Turbomachinery, 1988 Feb. 1989 p 1-18 (For primary document see N89-22891 16-37)
Avail: NTIS HC A20/MF A01 CSCL 13I

A lot of large chemical fertilizer plants producing 1000 ton NH3/day and 1700 ton urea/day were constructed in the 1970's in China. During operation, subsynchronous vibration takes place occasionally in some of the large turbine-compressor sets and has resulted in heavy economic losses. Two cases of subsynchronous vibration are described: Self-excited vibration of the low-pressure (LP) cylinder of one kind of N2-H2 multistage compressor; and Forced subsynchronous vibration of the high-pressure (HP) cylinder of the CO2 compressor. Author

N89-22893*# Sulzer Bros. Ltd., Winterthur (Switzerland). Lab. for Vibrations and Acoustics.
ROTOR INSTABILITY DUE TO A GEAR COUPLING CONNECTED TO A BEARINGLESS SUN WHEEL OF A PLANETARY GEAR
E. T. Buehlmann and A. Luzi (Swiss Locomotive and Machine Works Ltd., Winterthrup.) *In* NASA, Lewis Research Center, Rotordynamic Instability Problems in High-Performance Turbomachinery, 1988 Feb. 1989 p 19-39 (For primary document see N89-22891 16-37)
Avail: NTIS HC A20/MF A01 CSCL 13I

A 21 MW electric power generating unit comprises a gas turbine, a planetary gear, and a generator connected together by gear couplings. For simplicity of the design and high performance the pinion of the gear has no bearing. It is centered by the planet wheels only. The original design showed a strong instability and a natural frequency increasing with the load between 2 and 6.5 MW. In this operating range the natural frequency was below the operating speed of the gas turbine, n sub PT = 7729 RPM. By shortening the pinion shaft and reduction of its moment of inertia the unstable natural frequency was shifted well above the operating speed. With that measure the unit now operates with stability in the entire load range. Author

N89-22894*# CESI, Milan (Italy).
SOME IN-FIELD EXPERIENCES OF NON-SYNCHRONOUS VIBRATIONS IN LARGE ROTATING MACHINERY
Giuseppe Colnago, Claudio Frigeri, Andrea Vallini, and Gian Antonio Zanetta (Ente Nazionale per l'Energia Elettrica, Rome, Italy) *In* NASA, Lewis Research Center, Rotordynamic Instability Problems in High-Performance Turbomachinery, 1988 Feb. 1989 p 41-59 (For primary document see N89-22891 16-37)
Avail: NTIS HC A20/MF A01 CSCL 13I

Some problems associated with non-synchronous vibrations are analyzed by describing three cases experienced with fairly large rotating machines in operating conditions. In each case, a brief description is first given of the machine and of the instrumentation used. The experimental results are then presented, with reference to time or frequency domain recordings. The lines followed in diagnosis are then discussed and, lastly, the corrective action undertaken is presented. Author

N89-22895*# Southampton Univ. (England). Dept. of Mechanical Engineering.
THE SPECTRAL ANALYSIS OF AN AERO-ENGINE ASSEMBLY INCORPORATING A SQUEEZE-FILM DAMPER
R. Holmes and M. M. Dede *In* NASA, Lewis Research Center, Rotordynamic Instability Problems in High-Performance Turbomachinery, 1988 Feb. 1989 p 61-86 (For primary document see N89-22891 16-37)
Avail: NTIS HC A20/MF A01 CSCL 13I

Aero-engine structures have very low inherent damping and so artificial damping is often introduced by pumping oil into annular gaps between the casings and the outer races of some or all of

the rolling-element bearings supporting the rotors. The thin oil films so formed are called squeeze film dampers and they can be beneficial in reducing rotor vibration due to unbalance and keeping to reasonable limits the forces transmitted to the engine casing. However, squeeze-film dampers are notoriously non-linear and as a result can introduce into the assembly such phenomena as subharmonic oscillations, jumps and combination frequencies. The purpose of the research is to investigate such phenomena both theoretically and experimentally on a test facility reproducing the essential features of a medium-size aero engine. The forerunner of this work was published. It was concerned with the examination of a squeeze-film damper in series with housing flexibility when supporting a rotor. The structure represented to a limited extent the essentials of the projected Rolls Royce RB401 engine. That research demonstrated the ability to calculate the oil-film forces arising from the squeeze film from known motions of the bearing components and showed that the dynamics of a shaft fitted with a squeeze film bearing can be predicted reasonably accurately. An aero-engine will normally have at least two shafts and so in addition to the excitation forces which are synchronous with the rotation of one shaft, there will also be forces at other frequencies from other shafts operating on the squeeze-film damper. Theoretical and experimental work to consider severe loading of squeeze-film dampers and to include these additional effects are examined.

Author

N89-22896*# Texas A&M Univ., College Station. Dept. of Mechanical Engineering.

PIEZOELECTRIC PUSHERS FOR ACTIVE VIBRATION CONTROL OF ROTATING MACHINERY

A. B. Palazzolo, A. F. Kascak, R. R. Lin, J. Montague (Sverdrup Technology, Inc., Cleveland, OH.), and R. M. Alexander *In* NASA, Lewis Research Center, Rotordynamic Instability Problems in High-Performance Turbomachinery, 1988 Feb. 1989 p 87-110 (For primary document see N89-22891 16-37)

Avail: NTIS HC A20/MF A01 CSCL 13I

The active control of rotordynamic vibrations and stability by magnetic bearings and electromagnetic shakers was discussed extensively in the literature. These devices, though effective, are usually large in volume and add significant weight to the stator. The use of piezoelectric pushers may provide similar degrees of effectiveness in light, compact packages. Analyses are contained which extend quadratic regulator, pole placement and derivative feedback control methods to the prescribed displacement character of piezoelectric pushers. The structural stiffness of the pusher is also included in the theory. Tests are currently being conducted at NASA Lewis Research Center with piezoelectric pusher-based active vibration control. Results performed on the NASA test rig as preliminary verification of the related theory are presented.

Author

N89-22897*# Texas A&M Univ., College Station. Dept. of Mechanical Engineering.

CAVITATION EFFECTS ON THE PRESSURE DISTRIBUTION OF A SQUEEZE FILM DAMPER BEARING

Fouad Y. Zeidan and John M. Vance *In* NASA, Lewis Research Center, Rotordynamic Instability Problems in High-Performance Turbomachinery, 1988 Feb. 1989 p 111-132 Sponsored in part by General Electric Co., Aircraft Engine Business Group (For primary document see N89-22891 16-37)

Avail: NTIS HC A20/MF A01 CSCL 13I

High speed motion pictures have revealed several operating regimes in a squeeze film damper. Pressure measurements corresponding to these distinct regimes were made to examine their effect on the performance of such dampers. Visual observation also revealed the means by which the pressure in the feed groove showed higher amplitudes than the theory predicts. Comparison between vapor and gaseous cavitation are made based on their characteristic pressure wave, and the effect this has on the total force and its phase.

Author

N89-22898*# Texas A&M Univ., College Station. Dept. of Mechanical Engineering.

AN ELECTROVISCOUS DAMPER

Jorgen L. Nikolajsen and M. S. Hoque *In* NASA, Lewis Research Center, Rotordynamic Instability Problems in High-Performance Turbomachinery, 1988 Feb. 1989 p 133-141 Sponsored in part by TAMU Turbomachinery Research Consortium (For primary document see N89-22891 16-37)

Avail: NTIS HC A20/MF A01 CSCL 13I

A new type of vibration damper for rotor systems was developed and tested. The damper contains electroviscous fluid which solidifies and provides Coulomb damping when an electric voltage is imposed across the fluid. The damping capacity is controlled by the voltage. The damper was incorporated in a flexible rotor system and found to be able to damp out high levels of unbalanced excitation. Other proven advantages include controllability, simplicity, and no requirement for oil supply. Still unconfirmed are the capabilities to eliminate critical speeds and to suppress rotor instabilities.

Author

N89-22899*# Texas A&M Univ., College Station.

ANNULAR HONEYCOMB SEALS: TEST RESULTS FOR LEAKAGE AND ROTORDYNAMIC COEFFICIENTS; COMPARISONS TO LABYRINTH AND SMOOTH CONFIGURATIONS

Dara W. Childs, David Elrod, and Keith Hale *In* NASA, Lewis Research Center, Rotordynamic Instability Problems in High-Performance Turbomachinery, 1988 Feb. 1989 p 143-159 Previously announced in X89-10207 (For primary document see N89-22891 16-37)

(Contract NAG3-181; F49620-82-K-0033)

Avail: NTIS HC A20/MF A01 CSCL 11A

Test results are presented for leakage and rotordynamic coefficients for seven honeycomb seals. All seals have the same radius, length, and clearance; however, the cell depths and diameters are varied. Rotordynamic data, which are presented, consist of the direct and cross-coupled stiffness coefficients and the direct damping coefficients. The rotordynamic-coefficient data show a considerable sensitivity to changes in cell dimensions; however, no clear trends are identifiable. Comparisons of test data for the honeycomb seals with labyrinth and smooth annular seals show the honeycomb seal had the best sealing (minimum leakage) performance, followed in order by the labyrinth and smooth seals. For prerotated fluid entering the seal, in the direction of shaft rotation, the honeycomb seal has the best rotordynamic stability followed in order by the labyrinth and smooth. For no prerotation, or fluid prerotation against shaft rotation, the labyrinth seal has the best rotordynamic stability followed in order by the smooth and honeycomb seals.

Author

N89-22900*# Kaiserslautern Univ. (Germany, F.R.). Dept. of Mechanical Engineering.

ROTORDYNAMIC COEFFICIENTS FOR LABYRINTH SEALS CALCULATED BY MEANS OF A FINITE DIFFERENCE TECHNIQUE

R. Nordmann and P. Weiser *In* NASA, Lewis Research Center, Rotordynamic Instability Problems in High-Performance Turbomachinery, 1988 Feb. 1989 p 161-175 (For primary document see N89-22891 16-37)

Avail: NTIS HC A20/MF A01 CSCL 11A

The compressible, turbulent, time dependent and three dimensional flow in a labyrinth seal can be described by the Navier-Stokes equations in conjunction with a turbulence model. Additionally, equations for mass and energy conservation and an equation of state are required. To solve these equations, a perturbation analysis is performed yielding zeroth order equations for centric shaft position and first order equations describing the flow field for small motions around the seal center. For numerical solution a finite difference method is applied to the zeroth and first order equations resulting in leakage and dynamic seal coefficients respectively.

Author

N89-22901*# Rockwell International Corp., Canoga Park, CA. Rocketdyne Div.
ROTORDYNAMIC COEFFICIENTS FOR STEPPED LABYRINTH GAS SEALS
Joseph K. Scharrer *In* NASA, Lewis Research Center, Rotordynamic Instability Problems in High-Performance Turbomachinery, 1988 Feb. 1989 p 177-195 (For primary document see N89-22891 16-37)
Avail: NTIS HC A20/MF A01 CSCL 11A

The basic equations are derived for compressible flow in a stepped labyrinth gas seal. The flow is assumed to be completely turbulent in the circumferential direction where the friction factor is determined by the Blasius relation. Linearized zeroth and first-order perturbation equations are developed for small motion about a centered position by an expansion in the eccentricity ratio. The zeroth-order pressure distribution is found by satisfying the leakage equation while the circumferential velocity distribution is determined by satisfying the momentum equations. The first order equations are solved by a separation of variables solution. Integration of the resultant pressure distribution along and around the seal defines the reaction force developed by the seal and the corresponding dynamic coefficients. The results of this analysis are presented in the form of a parametric study, since there are no known experimental data for the rotordynamic coefficients of stepped labyrinth gas seals. The parametric study investigates the relative rotordynamic stability of convergent, straight and divergent stepped labyrinth gas seals. The results show that, generally, the divergent seal is more stable, rotordynamically, than the straight or convergent seals. The results also show that the teeth-on-stator seals are not always more stable, rotordynamically, then the teeth-on-rotor seals as was shown by experiment by Childs and Scharrer (1986b) for a 15 tooth seal. Author

N89-22902*# Kaiserslautern Univ. (Germany, F.R.). Dept. of Mechanical Engineering.
INFLUENCE OF DIFFERENT TYPES OF SEALS ON THE STABILITY BEHAVIOR OF TURBOPUMPS
W. Diewald and R. Nordmann *In* NASA, Lewis Research Center, Rotordynamic Instability Problems in High-Performance Turbomachinery, 1988 Feb. 1989 p 197-210 (For primary document see N89-22891 16-37)
Avail: NTIS HC A20/MF A01 CSCL 11A

One of the main problems in designing a centrifugal pump is to achieve a good efficiency while not neglecting the dynamic performance of the machine. The first aspect leads to the design of grooved seals in order to minimize the leakage flow. But the influence of these grooves to the dynamic behavior is not well known. Experimental and theoretical results of the rotordynamic coefficients for different groove shapes and depths in seals is presented. In addition, the coefficients are applied to a simple pump model. Author

N89-22903*# Kaiserslautern Univ. (Germany, F.R.). Dept. of Mechanical Engineering.
A 3-DIMENSIONAL FINITE-DIFFERENCE METHOD FOR CALCULATING THE DYNAMIC COEFFICIENTS OF SEALS
F. J. Dietzen and R. Nordmann *In* NASA, Lewis Research Center, Rotordynamic Instability Problems in High-Performance Turbomachinery, 1988 Feb. 1989 p 211-227 (For primary document see N89-22891 16-37)
Avail: NTIS HC A20/MF A01 CSCL 11A

A method to calculate the dynamic coefficients of seals with arbitrary geometry is presented. The Navier-Stokes equations are used in conjunction with the k-e turbulence model to describe the turbulent flow. These equations are solved by a full 3-dimensional finite-difference procedure instead of the normally used perturbation analysis. The time dependence of the equations is introduced by working with a coordinate system rotating with the precession frequency of the shaft. The results of this theory are compared with coefficients calculated by a perturbation analysis and with experimental results. Author

N89-22904*# Kobe Univ. (Japan). Faculty of Engineering.
AN EXPERIMENTAL STUDY ON THE STATIC AND DYNAMIC CHARACTERISTICS OF PUMP ANNULAR SEALS
T. Iwatsubo, B. C. Sheng, and T. Matsumoto *In* NASA, Lewis Research Center, Rotordynamic Instability Problems in High-Performance Turbomachinery, 1988 Feb. 1989 p 229-251 (For primary document see N89-22891 16-37)
Avail: NTIS HC A20/MF A01 CSCL 11A

A test apparatus was constructed and was applied to investigate static and dynamic characteristics of annular seals for turbopumps. The fluid forces acting on the seals were measured for various parameters such as the preswirl velocity, the pressure difference between the inlet and outlet of the seal, the whirling amplitude, and the ratio of whirling speed to spinning speed of the rotor. Influence of these parameters on the static and dynamic characteristics was investigated from the experimental results. As a result, preswirl affects the dynamic characteristics strongly. Especially, the preswirl opposing the rotating direction has a stabilizing role on the rotor system. Author

N89-22905*# Case Western Reserve Univ., Cleveland, OH.
A SEAL TEST FACILITY FOR THE MEASUREMENT OF ISOTROPIC AND ANISOTROPIC LINEAR ROTORDYNAMIC CHARACTERISTICS
M. L. Adams, T. Yang, and S. E. Pace (Electric Power Research Inst., Palo Alto, CA.) *In* NASA, Lewis Research Center, Rotordynamic Instability Problems in High-Performance Turbomachinery, 1988 Feb. 1989 p 253-267 (For primary document see N89-22891 16-37)
Avail: NTIS HC A20/MF A01 CSCL 11A

A new seal test facility for measuring high-pressure seal rotor-dynamic characteristics has recently been made operational at Case Western Reserve University (CWRU). This work is being sponsored by the Electric Power Research Institute (EPRI). The fundamental concept embodied in this test apparatus is a double-spool-shaft spindle which permits independent control over the spin speed and the frequency of an adjustable circular vibration orbit for both forward and backward whirl. Also, the static eccentricity between the rotating and non-rotating test seal parts is easily adjustable to desired values. By accurately measuring both dynamic radial displacement and dynamic radial force signals, over a wide range of circular orbit frequency, one is able to solve for the full linear-anisotropic model's 12 coefficients rather than the 6 coefficients of the more restrictive isotropic linear model. Of course, one may also impose the isotropic assumption in reducing test data, thereby providing a valid qualification of which seal configurations are well represented by the isotropic model and which are not. In fact, as argued in reference (1), the requirement for maintaining a symmetric total system mass matrix means that the resulting isotropic model needs 5 coefficients and the anisotropic model needs 11 coefficients. Author

N89-22906*# Kaiserslautern Univ. (Germany, F.R.). Dept. of Mechanical Engineering.
FINITE DIFFERENCE ANALYSIS OF ROTORDYNAMIC SEAL COEFFICIENTS FOR AN ECCENTRIC SHAFT POSITION
R. Nordmann and F. J. Dietzen *In* NASA, Lewis Research Center, Rotordynamic Instability Problems in High-Performance Turbomachinery, 1988 Feb. 1989 p 269-284 (For primary document see N89-22891 16-37)
Avail: NTIS HC A20/MF A01 CSCL 11A

The dynamic coefficients of seals are calculated for shaft movements around an eccentric position. The turbulent flow is described by the Navier-Stokes equations in connection with a turbulence model. The equations are solved by a finite-difference procedure. Author

N89-22907*# Tokyo Univ. (Japan).
INFLUENCE OF IMPELLER AND DIFFUSER GEOMETRIES ON THE LATERAL FLUID FORCES OF WHIRLING CENTRIFUGAL IMPELLER
Hideo Ohashi, Akira Sakurai, and Jiro Nishihama (Asahi Glass Co. Ltd., Yokohama, Japan) *In* NASA, Lewis Research Center,

Rotordynamic Instability Problems in High-Perforance Turbomachinery, 1988 Feb. 1989 p 285-306 (For primary document see N89-22891 16-37)
Avail: NTIS HC A20/MF A01 CSCL 13I

Lateral fluid forces on two-dimensional centrifugal impellers, which whirl on a circular orbit in a vaneless diffuser, were reported. Experiments were further conducted for the cases in which a three-dimensional centrifugal impeller, a model of the boiler feed pump, whirls in vaneless and vaned diffusers. The influence of the clearance configuration between the casing and front shroud of the impeller was also investigated. The result indicated that the fluid dynamic interaction between the impeller and the guide vanes induces quite strong fluctuating fluid forces to the impeller, but nevertheless its influence on radial and tangential force components averaged over a whirling orbit is relatively small.
Author

N89-22908*# Osaka Univ., Toyonaka (Japan).
A THEORETICAL STUDY OF FLUID FORCES ON A CENTRIFUGAL IMPELLER ROTATING AND WHIRLING IN A VANED DIFFUSER
Yoshinobu Tsujimoto, Allan J. Acosta, and Yoshiki Yoshida (Mitsubishi Heavy-Industries Ltd., Takasago, Japan) *In* NASA, Lewis Research Center, Rotordynamic Instability Problems in High-Performance Turbomachinery, 1988 Feb. 1989 p 307-322 (For primary document see N89-22891 16-37)
Avail: NTIS HC A20/MF A01 CSCL 13I

The fluid forces on a centrifugal impeller rotating and whirling in a vaned diffuser are analyzed on the assumption that the number of impeller and diffuser vanes is so large that the flows are perfectly guided by the vanes. The flow is taken to be two dimensional, inviscid, and incompressible, but the effects of impeller and diffuser losses are taken into account. It is shown that the interaction with the vaned diffuser may cause destabilizing fluid forces. From these discussions, it is found that the whirling forces are closely related to the steady head-capacity characteristics of the impeller. This physical understanding of the whirling forces can be applied also to the cases with volute casings. At partial capacities, it is shown that the impeller forces change greatly when the flow rate and whirl velocity are near to the impeller or vaned diffuser attributed rotating stall onset capacity, and the stall propagation velocity, respectively. In such cases the impeller forces may become destabilizing for impeller whirl.
Author

N89-22909*# Textron Bell Helicopter, Fort Worth, TX.
INFLUENCE OF IMPELLER SHROUD FORCES ON TURBOPUMP ROTOR DYNAMICS
Jim P. Williams and Dara W. Childs (Texas A&M Univ., College Station.) *In* NASA, Lewis Research Center, Rotordynamic Instability Problems in High-Performance Turbomachinery, 1988 Feb. 1989 p 323-339 Previously announced as X89-10213 (For primary document see N89-22891 16-37)
Avail: NTIS HC A20/MF A01 CSCL 13I

The shrouded-impeller leakage path forces calculated by Childs (1987) have been analyzed to answer two questions. First, because of certain characteristics of the results of Childs, the forces could not be modeled with traditional approaches. Therefore, an approach has been devised to include the forces in conventional rotordynamic analyses. The forces were approximated by traditional stiffness, damping and inertia coefficients with the addition of whirl-frequency-dependent direct and cross-coupled stiffness terms. The forces were found to be well-modeled with this approach. Finally, the effect these forces had on a simple rotor-bearing system was analyzed, and, therefore, they, in addition to seal forces, were applied to a Jeffcott rotor. The traditional methods of dynamic system analysis were modified to incorporate the impeller forces and yielded results for the eigenproblem, frequency response, critical speed, transient response and an iterative technique for finding the frequency of free vibration as well as system stability. All results lead to the conclusion that the forces have little influence on natural frequency but can have appreciable effects on system stability. Specifically, at higher values of fluid swirl at the leakage path entrance, relative stability is reduced. The only unexpected response characteristics that occurred are attributed to the nonlinearity of the model.
Author

N89-22910*# Mechanical Technology, Inc., Latham, NY.
MAGNETIC BEARING STIFFNESS CONTROL USING FREQUENCY BAND FILTERING
H. Ming Chen *In* NASA, Lewis Research Center, Rotordynamic Instability Problems in High-Performance Turbomachinery, 1988 Feb. 1989 p 341-352 (For primary document see N89-22891 16-37)
Avail: NTIS HC A20/MF A01 CSCL 13I

Active magnetic bearings can be implemented with frequency band-reject filtering that decreases the bearing stiffness and damping at a small bandwidth around a chosen frequency. The control scheme was used for reducing a rotor dynamic force, such as an imbalance force, transmitted to the bearing stator. The scheme creates additional system vibration modes at the same frequency. It also shows that the amount of force reduction is limited by the stability requirement of these modes.
Author

N89-22911*# Rotor Bearing Dynamics, Inc., Wellsville, NY.
A MAGNETIC DAMPER FOR FIRST MODE VIBRATION REDUCTION IN MULTIMASS FLEXIBLE ROTORS
M. E. F. Kasarda, P. E. Allaire, R. R. Humphris, and L. E. Barrett (Virginia Univ., Charlottesville.) *In* NASA, Lewis Research Center, Rotordynamic Instability Problems in High-Performance Turbomachinery, 1988 Feb. 1989 p 353-372 (For primary document see N89-22891 16-37)
Avail: NTIS HC A20/MF A01 CSCL 13I

Many rotating machines such as compressors, turbines and pumps have long thin shafts with resulting vibration problems, and would benefit from additional damping near the center of the shaft. Magnetic dampers have the potential to be employed in these machines because they can operate in the working fluid environment unlike conventional bearings. An experimental test rig is described which was set up with a long thin shaft and several masses to represent a flexible shaft machine. An active magnetic damper was placed in three locations: near the midspan, near one end disk, and close to the bearing. With typical control parameter settings, the midspan location reduced the first mode vibration 82 percent, the disk location reduced it 75 percent and the bearing location attained a 74 percent reduction. Magnetic damper stiffness and damping values used to obtain these reductions were only a few percent of the bearing stiffness and damping values. A theoretical model of both the rotor and the damper was developed and compared to the measured results. The agreement was good.
Author

N89-22912*# Aerojet TechSystems Co., Sacramento, CA.
INCORPORATING GENERAL RACE AND HOUSING FLEXIBILITY AND DEADBAND IN ROLLING ELEMENT BEARING ANALYSIS
R. R. Davis and C. S. Vallance *In* NASA, Lewis Research Center, Rotordynamic Instability Problems in High-Performance Turbomachinery, 1988 Feb. 1989 p 373-387 (For primary document see N89-22891 16-37)
Avail: NTIS HC A20/MF A01 CSCL 13I

Methods for including the effects of general race and housing compliance and outer race-to-housing deadband (clearance) in rolling element bearing mechanics analysis is presented. It is shown that these effects can cause significant changes in bearing stiffness characteristics, which are of major importance in rotordynamic response of turbomachinery and other rotating systems. Preloading analysis is demonstrated with the finite element/contact mechanics hybrid method applied to a 45 mm angular contact ball bearing.
Author

N89-22913*# Texas A&M Univ., College Station. Dept. of Mechanical Engineering.
EXPERIMENTAL VERIFICATION OF AN EDDY-CURRENT BEARING
Jorgen L. Nikolajsen *In* NASA, Lewis Research Center,

Rotordynamic Instability Problems in High-Performance Turbomachinery, 1988 Feb. 1989 p 389-394 Sponsored in part by TAMU Turbomachinery Research Consortium (For primary document see N89-22891 16-37)
Avail: NTIS HC A20/MF A01 CSCL 13I

A new type of electromagnetic bearing was built and tested. It consists of fixed AC-electromagnets in a star formation surrounding a conducting rotor. The bearing works by repulsion due to eddy-currents induced in the rotor. A single bearing is able to fully support a short rotor. The rotor support is inherently stable in all five degrees of freedom. No feedback control is needed. The bearing is also able to accelerate the rotor up to speed and decelerate the rotor back to standstill. The bearing design and the experimentation to verify its capabilities are described.
Author

N89-22914*# Sulzer-Escher Wyss Ltd., Zurich (Switzerland).
ROTORDYNAMIC STABILITY PROBLEMS AND SOLUTIONS IN HIGH PRESSURE TURBOCOMPRESSORS
J. Schmied *In* NASA, Lewis Research Center, Rotordynamic Instability Problems in High-Performance Turbomachinery, 1988 Feb. 1989 p 395-413 (For primary document see N89-22891 16-37)
Avail: NTIS HC A20/MF A01 CSCL 13I

The stability of a high pressure compressor is investigated with special regard to the self-exciting effects in oil seals and labyrinths. It is shown how to stabilize a rotor in spite of these effects and even increase its stability with increasing pressure. Author

N89-22915*# Bently Rotor Dynamics Research Corp., Minden, NV.
ROLE OF CIRCUMFERENTIAL FLOW IN THE STABILITY OF FLUID-HANDLING MACHINE ROTORS
D. E. Bently and A. Muszynska *In* NASA, Lewis Research Center, Rotordynamic Instability Problems in High-Performance Turbomachinery, 1988 Feb. 1989 p 415-430 (For primary document see N89-22891 16-37)
Avail: NTIS HC A20/MF A01 CSCL 13I

The recent studies of the dynamic stiffness properties of fluid lubricated bearing and seals by the authors have yielded most of the generalized characteristics discussed and used in this paper. They include bearing and seal nonlinear fluid film properties associated with stiffness, damping, and fluid average circumferential velocity ratio. Analytical relationships yield the rotor system's dynamic stiffness characteristics. This paper shows the combination of these data to provide the fluid-induced rotor stability equations.
Author

N89-22916*# Aerojet TechSystems Co., Sacramento, CA.
ENHANCED ROTOR MODELING TAILORED FOR RUB DYNAMIC STABILITY ANALYSIS AND SIMULATION
R. R. Davis *In* NASA, Lewis Research Center, Rotordynamic Instability Problems in High-Performance Turbomachinery, 1988 Feb. 1989 p 431-444 (For primary document see N89-22891 16-37)
Avail: NTIS HC A20/MF A01 CSCL 13I

New methods are presented that allow straightforward application of complex nonlinearities to finite element based rotor dynamic analyses. The key features are: (1) the methods can be implemented with existing finite element or dynamic simulation programs, (2) formulation is general for simple application to a wide range of problems, and (3) implementation is simplified because nonlinear aspects are separated from the linear part of the model. The new techniques are illustrated with examples of inertial nonlinearity and torquewhirl which can be important in rubbing turbomachinery. The sample analyses provide new understanding of these nonlinearities which are discussed.
Author

N89-22917*# Mitsubishi Heavy-Industries Ltd., Takasago (Japan).
HIGH STABILITY DESIGN FOR NEW CENTRIFUGAL COMPRESSOR
H. Kanki, K. Katayama, S. Morii, Y. Mouri, S. Umemura, U. Ozawa, and T. Oda *In* NASA, Lewis Research Center, Rotordynamic Instability Problems in High-Performance Turbomachinery, 1988 Feb. 1989 p 445-459 (For primary document see N89-22891 16-37)
Avail: NTIS HC A20/MF A01 CSCL 13I

It is essential that high-performance centrifugal compressors be free of subsynchronous vibrations. A new high-performance centrifugal compressor has been developed by applying the latest rotordynamics knowledge and design techniques: (1) To improve the system damping, a specially designed oil film seal was developed. This seal attained a damping ratio three times that of the conventional design. The oil film seal contains a special damper ring in the seal cartridge. (2) To reduce the destabilizing effect of the labyrinth seal, a special swirl canceler (anti-swirl nozzle) was applied to the balance piston seal. (3) To confirm the system damping margin, the dynamic simulation rotor model test and the full load test applied the vibration exciting test in actual load conditions.
Author

N89-22918*# Stanford Univ., CA. Aerospace Robotics Lab.
CONTROL OF FREE-FLYING SPACE ROBOT MANIPULATOR SYSTEMS Semiannual Report No. 7
Robert H. Cannon, Jr. 20 Mar. 1989 116 p
(Contract NCC2-333)
(NASA-CR-184837; NAS 1.26:184837) Avail: NTIS HC A06/MF A01 CSCL 13I

Control techniques for self-contained, autonomous free-flying space robots are being tested and developed. Free-flying space robots are envisioned as a key element of any successful long term presence in space. These robots must be capable of performing the assembly, maintenance, and inspection, and repair tasks that currently require astronaut extra-vehicular activity (EVA). Use of robots will provide economic savings as well as improved astronaut safety by reducing and in many cases, eliminating the need for human EVA. The focus of the work is to develop and carry out a set of research projects using laboratory models of satellite robots. These devices use air-cushion-vehicle (ACV) technology to simulate in two dimensions the drag-free, zero-g conditions of space. Current work is divided into six major projects or research areas. Fixed-base cooperative manipulation work represents our initial entry into multiple arm cooperation and high-level control with a sophisticated user interface. The floating-base cooperative manipulation project strives to transfer some of the technologies developed in the fixed-base work onto a floating base. The global control and navigation experiment seeks to demonstrate simultaneous control of the robot manipulators and the robot base position so that tasks can be accomplished while the base is undergoing a controlled motion. The multiple-vehicle cooperation project's goal is to demonstrate multiple free-floating robots working in teams to carry out tasks too difficult or complex for a single robot to perform. The Location Enhancement Arm Push-off (LEAP) activity's goal is to provide a viable alternative to expendable gas thrusters for vehicle propulsion wherein the robot uses its manipulators to throw itself from place to place. Because the successful execution of the LEAP technique requires an accurate model of the robot and payload mass properties, it was deemed an attractive testbed for adaptive control technology.
Author

N89-22919*# National Aeronautics and Space Administration. Lewis Research Center, Cleveland, OH.
EFFECTS OF LUBRICATION ON THE PERFORMANCE OF HIGH SPEED SPUR GEARS
Hachiro Mizutani, Yuuichi Isikawa (Mechanical Engineering Lab., Tsukuba, Japan), and Dennis P. Townsend Apr. 1989 10 p
Presented at the 5th International Power Transmission and Gearing Conference, Chicago, IL, 24-27 Apr. 1989; sponsored in part by ASME
(NASA-TM-101969; E-4666; NAS 1.15:101969) Avail: NTIS HC A02/MF A01 CSCL 13I

An experimental analysis was conducted to determine power loss and gear noise of high speed spur gears with long addendum

under various conditions of load, speed, and oil jet pressure for into mesh lubrication. Power losses were calculated from temperature measurements of lubricating oil, gears, gear box, and oil flow rate. Furthermore, power loss was divided into windage loss, friction loss and churning loss. The results show that windage loss and churning loss were the main components of gear power loss of high gear speed. In addition, lubricating conditions had some influences on gear noise especially under low oil temperature or high viscosity. Author

N89-22920*# Illinois Univ., Chicago. Dept. of Mechanical Engineering.
TOPOLOGY OF MODIFIED HELICAL GEARS AND TOOTH CONTACT ANALYSIS (TCA) PROGRAM Final Report
Faydor L. Litvin and Jiao Zhang Washington NASA Apr. 1989 159 p
(Grant NAG3-655; DA Proj. 1L1-62209-A-47-A)
(NASA-CR-4224; E-4626; NAS 1.26:4224; AVSCOM-TR-89-C-002) Avail: NTIS HC A08/MF A01 CSCL 13I

The contents of this report covers: (1) development of optimal geometries for crowned helical gears; (2) a method for their generation; (3) tooth contact analysis (TCA) computer programs for the analysis of meshing and bearing contact of the crowned helical gears; and (4) modelling and simulation of gear shaft deflection. The developed method for synthesis was used to determine the optimal geometry for a crowned helical pinion surface and was directed to localize the bearing contact and guarantee favorable shape and a low level of transmission errors. Two new methods for generation of the crowned helical pinion surface are proposed. One is based on the application of a tool with a surface of revolution that slightly deviates from a regular cone surface. The tool can be used as a grinding wheel or as a shaver. The other is based on a crowning pinion tooth surface with predesigned transmission errors. The pinion tooth surface can be generated by a computer-controlled automatic grinding machine. The TCA program simulates the meshing and bearing contact of the misaligned gears. The transmission errors are also determined. The gear shaft deformation was modelled and investigated. It was found that the deflection of gear shafts has the same effect as gear misalignment. Author

N89-22921# Air Force Inst. of Tech., Wright-Patterson AFB, OH. School of Engineering.
CONFIGURATION COMPARISON ANALYSIS FOR THE AFIT/AAMRL ANTHROPOMORPHIC ROBOTIC MANIPULATOR M.S. Thesis
Steven L. Parker Dec. 1988 92 p
(AD-A202618; AD-E900870; AFIT/GA/AA/88D-08) Avail: NTIS HC A05/MF A01 CSCL 12I

A method of calculating mechanical efficiency was developed as a means of comparing the performance of different types of manipulators. As an initial approach to this problem takes into account inertial and gravitational terms of the robot configurations in addition to a variable payload. The method included developing a numerical integration algorithm to calculate the work done by each manipulator at any point in that manipulator's workspace. The efficiencies of two robotic manipulator configurations that are candidates for the design of the AFIT, AAMRL, Anthropomorphic Robotic Manipulator, were analyzed. The two designs were a serial open link direct drive manipulator, and the closed parallel kinematic chain direct drive manipulator design by Dr. Asada at MIT. The difference between the manipulator was actual mass and kinematic design. The efficiency measure used to analyze both manipulators was based on the magnitude of the total work done by the manipulator to move a payload a prescribed distance. The effects of a variable mass payload on efficiency have now been individually examined for the cases when the arm has been tuned for some nominal payload by means of compensating for gravity, making the robotic configuration invariant, and decoupling the manipulator's dynamic equations of motion. GRA

N89-22922*# Oak Ridge National Lab., TN.
TRACTION-DRIVE FORCE TRANSMISSION FOR TELEROBOTIC JOINTS
D. M. Williams and D. P. Kuban 1989 15 p Presented at the NASA Conference on Space Telerobotics, Pasadena, CA, 31 Jan. 1989 Sponsored by NASA, Langley Research Center, Hampton, VA
(Contract DE-AC05-84OR-21400)
(NASA-CR-183331; NAS 1.26:183331; DE89-006687; CONF-890153-3) Avail: NTIS HC A03/MF A01 CSCL 13I

The U.S. Space Station Program is providing many technological developments to meet the increasing demands of designing such a facility. One of the key areas of research is that of telerobotics for space station assembly and maintenance. Initial implementation will be teleoperated, but long-term plans call for autonomous robotics. One of the essential components for making this transition successful is the manipulator joint mechanism. Historically, teleoperated manipulators and industrial robotics have had very different mechanisms for force transmission. This is because the design objectives are almost mutually exclusive. A teleoperator must have very low friction and inertia to minimize operator fatigue; backlash and stiffness are of secondary concern. A robot, however, must have minimum backlash, and high stiffness for accurate and rapid positioning. A joint mechanism has yet to be developed that can optimize these divergent performance objectives. A joint mechanism that approaches this optimal performance was developed for NASA Langley, Automation Technology Branch. It is a traction-drive differential that uses variable preload mechanisms. The differential provides compact, dexterous motion range with a torque density similar to geared systems. The traction drive offers high stiffness and zero backlash---for good robotic performance, and the variable-loading mechanism (VLM) minimizes the drive-train friction---for improved teleoperation. As a result, this combination provides a mechanism to allow advanced manipulation with either teleoperated control or autonomous robotic operation. This paper will address the design principles of both of these major components of the joint mechanism. DOE

N89-22923# Applied Research Associates, Inc., Albuquerque, NM.
NUMERICAL METHOD TO PREDICT PROJECTILE PENETRATION
Larry A. Schoof, Frank A. Maestas, and C. Wayne Young (Sandia National Labs., Albuquerque, NM.) 1989 6 p Presented at the 4th Annual Symposium on Interaction of Non-nuclear Munitions With Structures, Panama City, FL, 17 Apr. 1989
(Contract DE-AC04-76DP-00789)
(DE89-007140; SAND-89-0266C; CONF-8904119-1) Avail: NTIS HC A02/MF A01

The Simplified Analytical Model of Penetration with Lateral Loading (SAMPLL) computer code developed at Sandia National Laboratories has been modified to allow additional penetration capabilities. The new capabilities include the ability to model penetration by other than cylindrical penetrators (flares, tapers, and boattails) and the ability to calculate penetration/perforation of multiple layers of different materials. Additionally, updated soil and rock empirical equations have been added to the model. A broader range of problems can now be modeled more accurately with the modified SAMPLL. DOE

N89-22924# Sandia National Labs., Albuquerque, NM.
A CALORIMETRIC-BASED COMPARISON OF GAS TUNGSTEN AND PLASMA ARC WELDING PROCESSES
Gerald A. Knorovsky and Phillip W. Fuerschbach 1988 18 p Presented at the JOWOG 22D Joining Subgroup, Aldermasten, United Kingdom, 4 Oct. 1988
(Contract DE-AC04-76DP-00789)
(DE89-008712; SAND-89-0809C; CONF-8810176-4) Avail: NTIS HC A03/MF A01

Measurements of arc and melting efficiencies have been made for pulsed and continuous mode Gas Tungsten Arc Welding (GTAW) and Plasma Arc Welding (PAW) processes. Welds were

made on 2.5 mm total thickness pure Ni and 304 Stainless Steel in a standing edge weld geometry at constant nominal machine output settings which varied average current with travel speed. Under continuous current conditions, the measured heat input remained approximately constant for the conditions examined (250 to 1250 mm/min), while melting efficiency increased dramatically (0 to approx. 0.4). Arc efficiencies were relatively constant, remaining in the range of approx. 0.75 to 0.85 for GTAW and somewhat less for PAW. Values of melting efficiency for Ni were slightly less than those for 304 when compared at similar travel speeds, though both tended toward the same limit (approx. 0.4). The PAW results were not appreciably higher than the GTAW. In addition to melting efficiency the centerline depth of penetration was also measured. In contrast to the GTAW results, which increased with speed at lower travel speeds and then plateaued at 0.8 mm, the PAW results increased monotonically with speed to a maximum of 1.0 mm. In conclusion, calorimetric measurements of nonconsumable arc welding processes have been found helpful in understanding conditions under which efficient arc welds with minimal heat inputs for a desired weld penetration can be made. DOE

N89-22925*# National Aeronautics and Space Administration. Lewis Research Center, Cleveland, OH.
TRANSMISSION OVERHAUL AND REPLACEMENT PREDICTIONS USING WEIBULL AND RENEWEL THEORY
M. Savage and D. G. Lewicki (Army Aviation Systems Command, Cleveland, OH.) 1989 12 p Presented at the 25th Joint Propulsion Conference, Monterey, CA, 10-12 Jul. 1989; cosponsored by the AIAA, ASME, SAE and ASEE
(DA Proj. 1L1-62209-A-47-A)
(NASA-TM-102022; E-4756; NAS 1.15:102022; AVSCOM-TR-89-C-007; AIAA-89-2919) Avail: NTIS HC A03/MF A01 CSCL 13I

A method to estimate the frequency of transmission overhauls is presented. This method is based on the two-parameter Weibull statistical distribution for component life. A second method is presented to estimate the number of replacement components needed to support the transmission overhaul pattern. The second method is based on renewal theory. Confidence statistics are applied with both methods to improve the statistical estimate of sample behavior. A transmission example is also presented to illustrate the use of the methods. Transmission overhaul frequency and component replacement calculations are included in the example. Author

N89-22926# Pacific Northwest Labs., Richland, WA. Applied Physics Center.
DESIGN OF A LIGHTWEIGHT, LOW-COST GEOPHYSICAL SURVEY VEHICLE
K. R. Ames Mar. 1989 6 p Presented at the 3rd ANS Topical Meeting on Robotics and Remote Systems, Charleston, SC, 13-16 Mar. 1989
(Contract DE-AC06-76RL-01830)
(DE89-009383; PNL-SA-16548; CONF-890304-35) Avail: NTIS HC A02/MF A01

A remote-controlled vehicle has been designed at Pacific Northwest Laboratory for surveying sites that are dangerous for manned vehicles. The vehicle is required to be small, maneuverable, inexpensive, and as free of metallic parts as practicable. The prototype being fabricated will have a mostly aluminum engine, dual bicycle tire wheel assemblies, a two-clutch steering system for selective engagement of pairs of wheels on either side of the vehicle, and radio control with fiber-optic umbilical video link. Wireless control and telemetry are planned for the future. Other future possibilities include a mostly plastic engine and a global positioning system that uses satellite signals. DOE

N89-22927 National Physical Lab., Teddington (England). Div. of Materials Applications.
THE EFFECT OF THERMOCAPILLARY FLOW ON WELD-POOL PROFILE
B. J. Keene Nov. 1988 83 p
(NPL-DMA(A)167; ISSN-0143-7313; ETN-89-94338) Copyright Avail: National Physical Lab., Teddington, Middlesex, TW11 0LW, United Kingdom

Literature on the Heiple-Roper (1982) theory, which predicts that thermocapillary flow in a weld pool can often be the dominant factor controlling weld penetration and thus, differences in surface properties of melts could account for the phenomenon of variable weld penetration, was reviewed. All the mathematical models based on convective flow in a Tungsten Inert Gas weld pool come to the same conclusion, in that, depending on the magnitudes of d gamma (dT and dT/dx, (where gamma is surface tension, T temperature) the thermocapillary flow in the fluid could be the major factor controlling weld pool velocities and shapes, and it follows that provided the models are correct, surface tension forces must always be taken into account when assessing weldability of materials. The buoyancy forces in the pool are shown to be relatively unimportant. Experimental evidence supports the view that thermocapillary flow in a weld pool can be an important or dominant factor in controlling the final profile of the weld. Differences in weldability can often be directly related to the concentration of surfactants which are present in the melt. It is established that, in the absence of gettering elements, the relative levels of surfactants in iron and steel dictate both the magnitude and direction of the thermocapillary flow induced by the temperature gradient across the surface and thus control the direction of thermal transfer from the heat source. ESA

N89-22928# Etablissement Technique Central de l'Armement, Arcueil (France). Service Structure des Materiaux.
TRIBOLOGICAL CHARACTERIZATION OF 15 SURFACE TREATMENTS FOR ALUMINUM ALLOYS [CARACTERISATION TRIBOLOGIQUE DE 15 TRAITEMENTS DE SURFACE POUR LES ALLIAGES D'ALUMINIUM]
J. P. Bosch 2 Dec. 1987 58 p In FRENCH
(Contract DRET/SDR/G8-83-1028)
(ETCA-87-R-132; ETN-89-94350) Avail: NTIS HC A04/MF A01

Metallographic and tribological tests were carried out on treated Al alloy specimens. The treatments include anodizing with graphite added, anodizing with MoS2 added, same with sanding before treatment, anodizing with teflon added, diffusion treatments, MoS2 vanish coating, and Ni or Cr coatings. It is shown that while anodizing improves wear resistance, the friction coefficient is increased. The use of graphite, MoS2, or teflon improves friction without affecting wear. Sanding improves further the wear resistance. ESA

N89-22929# Societe Europeenne de Propulsion, Vernon (France). Div. Propulsion a Liquides en Espace.
IMPLEMENTATION OF ACTIVE MAGNETIC BEARINGS ON ADVANCED ROCKET ENGINE TURBOPUMPS
J. P. Girault 1988 13 p
(ETN-89-94365) Avail: NTIS HC A03/MF A01

Advantages and drawbacks of using S2M active magnetic bearings (AMB) to suspend rotors of rocket engine turbopumps were assessed. Technological keys for development are presented: AMB materials properties (mechanical and chemical); miniaturization of the electronic controller; rotordynamic prediction; and fluid and electrical interfaces. ESA

N89-22930 Wayne State Univ., Detroit, MI.
A GENERAL NON-LINEAR DYNAMICAL THEORY OF ELASTIC CURVED BEAMS Ph.D. Thesis
Kun-Ik Lee 1988 70 p
Avail: Univ. Microfilms Order No. DA8903237

The direct form of elastic curved beam theory (C-W-D theory) in Lagrangian coordinates was investigated and expressions in the inertia terms were included which gives a coupling of the neutral axis motion and cross section motion. Next the three-dimensional theory of classical continuum mechanics (descent or reduction method) was considered and the field equations boundary conditions, stress measures, and constitutive equations were derived for the motion terms in terms of the three

Piola-Kirchhoff vectors. These reproduce completely all of the equations of C-W-D theory. The stress measures may be regarded as constitutive equations if they are Piola-Kirchhoff constitutive functions. The classical strain tensor was derived in terms of the C-W-D position vector. Applying the constitutive equations obtained by descent method, the constitutive equations were obtained for the stress measures in terms of this modified classical strain tensor. The inertia constitutive equations were also obtained. The derivation of the strain measures in the direct C-W-D theory was reconsidered and their special form valid at any point in the curved beam obtained. The exact nonlinear expressions for these strains, valid for a general deformation (including stretching and shearing of the cross section) were given. Linearizing these expressions, the results obtained by descent or reduction from three-dimensional theory were recovered. Finally, a complete linear dynamical theory of elastic curved beams was recorded. Dissert. Abstr.

N89-22628# Joint Publications Research Service, Arlington, VA.
DEVELOPMENT OF ORBITAL WELDING TECHNOLOGY
A. Tarasov *In its* JPRS Report: Science and Technology. USSR: Space 17 Aug. 1988 p 46-49 Transl. into ENGLISH from Pravda (Moscow, USSR), 29 Mar. 1988 p 2 (For primary document see N89-22622 16-12)
Copyright Avail: NTIS HC A05/MF A01

38 QUALITY ASSURANCE AND RELIABILITY

Includes product sampling procedures and techniques; and quality control.

N89-22931# Information Research Lab., Inc., Dartmouth, MA.
INTERACTIVE ULTRASONIC NONDESTRUCTIVE EVALUATION Final Report, 1 Sep. 1987 - 30 Sep. 1988
C. H. Chen and S. K. Sin Oct. 1988 48 p
(Contract DAAL04-88-C-0003)
(AD-A204166; MTL-TR-88-34) Avail: NTIS HC A03/MF A01 CSCL 12E

It has been shown that modern DSP (Digital Signal Processing) and Pattern Recognition techniques are very effective tools for Ultrasonic NDE (Non-Destructive Evaluations) of materials. In our recent researches 1, such techniques as High Resolution Spectral Analysis, Deconvolution, K-mean Clustering, Non-linear Mapping and Multipe Fisher's Discriminant, have been applied to the classification of hidden defect geometries with high accuracy. In view of this uprising needs for DSP and Pattern Recognition in Ultrasonic NDE, and software package that effectively combines the two is in order. Interactive Ultrasonic NDE (IUNDE) TM developed by Information Research Laboratory, Inc. is such a package created especially to meet the needs of researches and practicing engineers in this field. It also includes a variety of feature extraction functions that allow the user to choose features extracted from the time series of his or her interest for classification. GRA

N89-22932# Houston Univ., TX. Dept. of Electrical Engineering.
NONDESTRUCTIVE EVALUATION OF STRESS USING ULTRASOUND AND PULSED HEAT Final Report, 1 Dec. 1986 - 30 Nov. 1988
Wallace L. Anderson Jan. 1989 4 p
(Contract DAAL03-87-K-0009)
(AD-A205176; ARO-24513.8-EG) Avail: NTIS HC A02/MF A01 CSCL 20A

Unique instrumentation was developed for high-precision time-resolved ultrasonic velocity measurement. Such instrumentation is not available commercially nor, as far as is known, has such a capability ever been developed previously. It has a significant potential for materials studies and possibly other areas as well, as for instance noninvasive biomedical applications. It was demonstrated that with such instrumentation, applied stress even of modest values can be detected at depths of at least 1 cm in aluminum. Furthermore, such detection was shown to be quantitative, i.e., the amplitude of the effect is proportional to stress magnitude, and its shape is responsive in the predicted manner to locality of the stress. In view of item 3, below, it is evident that this concept is a viable basis for nondestructive characterization of subsurface residual stress in metals. Methods for data inversion to obtain stress profiles from measured velocity were explored and it was found that two techniques give good results with simulated data and relatively large amounts of additive noise, namely: (1) generalized matrix inversion with constraints, and (2) least mean squares parameter fitting. Author

N89-22933# Fraunhofer-Inst. fuer Zerstoerungsfreie Pruefverfahren, Saarbruecken (Germany, F.R.).
MULTIFREQUENCY EDDY CURRENT TESTING, OPTIMIZATION OF THE METHOD FOR STEAM GENERATOR TESTING. PHASE 2: NONLINEAR DESCRIPTION OF SIGNAL LOCATION CURVES DYNAMICS OF THE SIGNAL LOCATION CURVES Final Report [MEHRFREQUENZ-WIRBELSTOMPRUEFUNG VERFAHRENSOPTIMIERUNG FUER DIE DAMPFERZEUGERHEIZROHRPRUEFUNG. PHASE 2: NICHTLINEARE BESCHREIBUNG DER SIGNALORTSKURVEN, DYNAMIK DER SIGNALORTSKURVEN]
R. Becker and K. Betzold 29 Aug. 1986 100 p In GERMAN
(Contract BMFT-GRS-150610)
(Rept-860142-TW; ETN-89-93772) Avail: NTIS HC A05/MF A01

The defect detection capability and the signal analysis for defect size and type were improved for the testing of steam generator heating pipes at the pipe base and the roll connection. The nonlinear curve path of the disturb signal is described by linear terms in the impedance planes; the signal pattern of the disturber is directly described by second order polynomials and the measuring values are quadratically coupled. These two measures improve the suppression quality. Interior defects can be distinguished from exterior ones. These are special calibration curves for all angular defect positions in order to convert signal amplitude into defect depth. The time and space dependence of the dynamic signal location curves provide an additional decision criterion to distinguish hole-like defects from crack-like defects. A multifrequency testing equipment with frequency optimization realizes the signal processing. ESA

N89-22934# Fraunhofer-Inst. fuer Zerstoerungsfreie Pruefverfahren, Saarbruecken (Germany, F.R.).
RECONSTRUCTION OF DEFECTS FROM AMPLITUDE LOCATION CURVES Final Report [FEHLERREKONSTRUKTION AUS AMPLITUDENORTSKURVEN]
R. Werneyer, F. Walte, and W. Mueller 1988 122 p In GERMAN
(Contract BMFT-RS-102-17)
(Rept-780852-TW; ETN-89-93773) Avail: NTIS HC A06/MF A01

Ultrasonic testing methods for thick-walled components are described. Besides maximum amplitude and time of flight, these methods also use the dynamic behavior of the echo for the description of the reflector. The reflection behavior of circles, stripes, cones, and cylinder were investigated using refraction theory and geometric reflection, and the amplitude location curves were determined. It is possible to distinguish voluminous reflectors from plane reflectors (including sloping positions). The inversion of the amplitude location curves makes it possible to reconstruct using single model reflectors. Comparative measurements on artificial reflectors in water and in solids are discussed. ESA

N89-22935# Construcciones Aeronauticas S.A., Madrid (Spain). Div. de Proyectos.
NDT RESULTS FOR COMPARABILITY PROGRAM SPF/DB
V. Cortes and J. M. Martin 7 Jun. 1988 20 p
(I-264/88; ETN-89-94127) Avail: NTIS HC A03/MF A01

Ultrasonic flaw detection results from techniques using

immersion reflector plates (for the whole test piece) and pulse echoes (for areas with artificial defects) are given. ESA

N89-22936# Institut National des Sciences Appliquees, Lyon (France). Lab. de Traitement du Signal et Ultrasons.
SIGNAL TREATMENT AND DATA ANALYSIS METHODS APPLIED TO NONDESTRUCTIVE CONTROL OF ADHESIVE BONDED JOINTS Ph.D. Thesis [METHODES DE TRAITEMENT DU SIGNAL ET D'ANALYSE DES DONNEES APPLIQUEES AU CONTROLE NON DESTRUCTIF DES COLLAGES]
Marc Lethiecq 1989 175 p In FRENCH
(ISAL-IDI-8809; ETN-89-94368) Avail: NTIS HC A08/MF A01

Adhesive bonding of a piezoelectric ceramic to an aluminium substrate was assessed. The methods tested include longitudinal and transversal pulsed ultrasonics and electric impedance measurement. The correlation between the nondestructive measurements and the destructive tests was performed by the principal components method. The error rate in detecting defective elements is 10 percent. The transversal ultrasonics method is shown to be the best for quality control. ESA

39 STRUCTURAL MECHANICS

Includes structural element design and weight analysis; fatigue; and thermal stress.

For applications see *05 Aircraft Design, Testing and Performance* and *18 Spacecraft Design, Testing and Performance*.

N89-22937# Southwest Inst. of Fluid Physics, Chengdu (China).
DYNAMIC FRACTURE IN SOLIDS
Desheng Wang, Shonghe Ma, Gongxun Shi, Yannian Li, and Danian Chen (Beijing Inst. of Tech., China) 1987 13 p Sponsored by Institute of Scientific and Technical Information of China, Beijing
(PB89-112650; ISTIC-TR-C-000139) Avail: NTIS HC A03/MF A01 CSCL 20K

Dynamic fracture in expanding shells and spallation are two main problems of dynamic fracture in solids. Even in the absence of possible adiabatic shear banding and classical necking instability, models of spall fracture are found to be inapplicable to fracture of expanding shells. The NAG model developed by Seaman et al is more suitable to different situations of dynamic fracture, however it requires numerous material constants that are difficult to obtain. Hence, some simple models and criteria are still developed and discussed. For fracture in expanding shells, there are two rupture criteria, namely, the Taylor's criterion and Ivanov's criterion. The simple model is developed by Johnson. One- and two-dimensional deformation and rupture of expanding shells of the work are presented. For spallation, simple criteria seem to be abandoned but the Tuler-Butcher criterion is still used. Some simple models of spall fracture are developed by Cochran et al and Johnson, respectively. The work on spallation is also presented. Finally, some problems are discussed. Author

N89-22938# Texas A&M Univ., College Station. Mechanics and Materials Center.
ANALYSIS OF THE MECHANICAL BEHAVIOR OF ADHESIVELY BONDED COMPOSITE JOINTS Final Report, Aug. 1986 - Aug. 1988
L. A. Mignery and R. A. Schapery 4 Nov. 1988 10 p
(Contract N00014-86-K-0590)
(AD-A202616; AD-E900870; MM-5558-88-20) Avail: NTIS HC A02/MF A01 CSCL 11D

This report summarizes research on characterizing a composite polymeric adherend material and studying, experimentally and theoretically, its reaction in one adhesive joint configuration. The particular material investigated is a continuous fiber graphite/epoxy composite material with a rubber toughened matrix. The composite is nonlinear and viscoelastic at room temperature. A constitutive equation is developed to account for this behavior, and it is then used in a finite element analysis of an adhesive joint. Experimental verifications of the constitutive model and adhesive joint are made. GRA

N89-22939*# National Aeronautics and Space Administration. Lewis Research Center, Cleveland, OH.
STRUCTURAL DYNAMICS BRANCH RESEARCH AND ACCOMPLISHMENTS FOR FY 1988
Apr. 1989 48 p
(NASA-TM-101406; E-4498; NAS 1.15:101406) Avail: NTIS HC A03/MF A01 CSCL 20K

Fiscal year 1988 research highlights from the Structural Dynamics Branch at NASA Lewis Research Center are described. Highlights from the branch's major work areas -- aeroelasticity, vibration control, dynamic systems, and computational structural methods -- are included as well as a complete listing of the FY 88 branch publications. Author

N89-22940*# Computer Software Management and Information Center, Athens, GA.
SEVENTEENTH NASTRAN (R) USERS' COLLOQUIUM
Mar. 1989 400 p Colloquium held in San Antonio, TX, 24-28 Apr. 1989
(NASA-CP-3029; NAS 1.55:3029) Avail: NTIS HC A17/MF A01; also available from COSMIC, Athens, GA 30602 CSCL 20K

General application of finite element methodology and the specific application of the NASA Structural Analysis System, NASTRAN, to a variety of static and dynamic structural problems were reviewed. For individual titles, see N89-22941 through N89-22956.

N89-22941*# Unisys Corp., Huntsville, AL.
IMPROVED PERFORMANCE IN NASTRAN (R)
Gordon C. Chan *In* Computer Software Management and Information Center Seventeenth NASTRAN (R) Users' Colloquium Mar. 1989 p 1-90 (For primary document see N89-22940 16-39)
Avail: NTIS HC A17/MF A01; also available from COSMIC, Athens, GA 30602 CSCL 20K

Three areas of improvement in COSMIC/NASTRAN, 1989 release, were incorporated recently that make the analysis program run faster on large problems. Actual log files and actual timings on a few test samples that were run on IBM, CDC, VAX, and CRAY computers were compiled. The speed improvement is proportional to the problem size and number of continuation cards. Vectorizing certain operations in BANDIT, makes BANDIT run twice as fast in some large problems using structural elements with many node points. BANDIT is a built-in NASTRAN processor that optimizes the structural matrix bandwidth. The VAX matrix packing routine BLDPK was modified so that it is now packing a column of a matrix 3 to 9 times faster. The denser and bigger the matrix, the greater is the speed improvement. This improvement makes a host of routines and modules that involve matrix operation run significantly faster, and saves disc space for dense matrices. A UNIX version, converted from 1988 COSMIC/NASTRAN, was tested successfully on a Silicon Graphics computer using the UNIX V Operating System, with Berkeley 4.3 Extensions. The Utility Modules INPUTT5 and OUTPUT5 were expanded to handle table data, as well as matrices. Both INPUTT5 and OUTPUT5 are general input/output modules that read and write FORTRAN files with or without format. More user informative messages are echoed from PARAMR, PARAMD, and SCALAR modules to ensure proper data values and data types being handled. Two new Utility Modules, GINOFILE and DATABASE, were written for the 1989 release. Seven rigid elements are added to COSMIC/NASTRAN. They are: CRROD, CRBAR, CRTRPLT, CRBE1, CRBE2, CRBE3, and CRSPLINE. Author

N89-22942*# Naval Ship Research and Development Center, Bethesda, MD. Numerical Structural Mechanics Branch.
USING PATRAN AND SUPERTAB AS PRE- AND POSTPROCESSORS TO COSMIC/NASTRAN

Robert R. Lipman *In* Computer Software Management and Information Center Seventeenth NASTRAN (R) Users' Colloquium Mar. 1989 p 91-101 (For primary document see N89-22940 16-39)
Avail: NTIS HC A17/MF A01; also available from COSMIC, Athens, GA 30602 CSCL 20K

Patran and Supertab are interactive computer graphics pre- and postprocessors that can be used to generate NASTRAN bulk data decks and to visualize results from a NASTRAN analysis. Both of the programs are in use at the Numerical Structural Mechanics Branch of the David Taylor Research Center (DTRC). Various aspects of Patran and Supertab are discussed including: geometry modeling, finite element mesh generation, bulk data deck creation, results translation and visualization, and the user interface. Some advantages and disadvantages of both programs will be pointed out. Author

N89-22943*# Deutsch Metal Components, Gardena, CA.
INCREASING MARKETABILITY AND PROFITABILITY OF PRODUCT LINE THRU PATRAN AND NASTRAN
Art Hyatt *In* Computer Software Management and Information Center Seventeenth NASTRAN (R) Users' Colloquium Mar. 1989 p 102-129 (For primary document see N89-22940 16-39)
Avail: NTIS HC A17/MF A01; also available from COSMIC, Athens, GA 30602 CSCL 20K

Starting with the design objective the operational cycle life of the Swaging Tool was increased. To accomplish this increase in cycle life without increasing the size or weight of the tool would be engineering achievement. However, not only was the operational cycle life increased between 2 to 10 times but simultaneously the size and weight of the Swage Tool was decreased by about 50 percent. This accomplishment now becomes an outstanding engineering achievement. This achievement was only possible because of the computerized Patran, Nastran and Medusa programs. Author

N89-22944*# Intergraph Corp., Huntsville, AL.
THE USE OF COSMIC NASTRAN IN AN INTEGRATED CONCEPTUAL DESIGN ENVIRONMENT
Gil White *In* Computer Software Management and Information Center Seventeenth NASTRAN (R) Users' Colloquium Mar. 1989 p 130-132 (For primary document see N89-22940 16-39)
Avail: NTIS HC A17/MF A01; also available from COSMIC, Athens, GA 30602 CSCL 20K

Changes in both software and hardware are rapidly bringing conceptual engineering tools like finite element analysis into mainstream mechanical design. Systems that integrate all phases of the manufacturing process provide the most cost benefits. The application of programming concepts like object oriented programming allow for the encapsulation of intelligent data within the design geometry. This combined with declining cost in per seat hardware bring new alternatives to the user. Author

N89-22945*# DYNACS Engineering Co., Inc., Clearwater, FL.
A NASTRAN/TREETOPS SOLUTION TO A FLEXIBLE, MULTI-BODY DYNAMICS AND CONTROLS PROBLEM ON A UNIX WORKSTATION
Javier E. Benavente and Norris R. Luce *In* Computer Software Management and Information Center Seventeenth NASTRAN (R) Users' Colloquium Mar. 1989 p 133-158 (For primary document see N89-22940 16-39)
Avail: NTIS HC A17/MF A01; also available from COSMIC, Athens, GA 30602 CSCL 20K

Demands for nonlinear time history simulations of large, flexible multibody dynamic systems has created a need for efficient interfaces between finite-element modeling programs and time-history simulations. One such interface, TREEFLX, an interface between NASTRAN and TREETOPS, a nonlinear dynamics and controls time history simulation for multibody structures, is presented and demonstrated via example using the proposed Space Station Mobile Remote Manipulator System (MRMS). The ability to run all three programs (NASTRAN, TREEFLX and TREETOPS), in addition to other programs used for controller design and model reduction (such as DMATLAB and TREESEL, both described), under a UNIX Workstation environment demonstrates the flexibility engineers now have in designing, developing and testing control systems for dynamically complex systems. Author

N89-22946*# RPK Corp., Hayes, VA.
ENHANCEMENTS TO THE IBM VERSION OF COSMIC/NASTRAN
W. Keith Brown *In* Computer Software Management and Information Center Seventeenth NASTRAN (R) Users' Colloquium Mar. 1989 p 159-168 (For primary document see N89-22940 16-39)
Avail: NTIS HC A17/MF A01; also available from COSMIC, Athens, GA 30602 CSCL 20K

Major improvements were made to the IBM version of COSMIC/NASTRAN by RPK Corporation under contract to IBM Corporation. These improvements will become part of COSMIC's IBM version and will be available in the second quarter of 1989. The first improvement is the inclusion of code to take advantage of IBM's new Vector Facility (VF) on its 3090 machines. The remaining improvements are modifications that will benefit all users as a result of the extended addressing capability provided by the MVS/XA operating system. These improvements include the availability of an in-memory data base that potentially eliminates the need for I/O to the PRIxx disk files. Another improvement is the elimination of multiple load modules that have to be loaded for every link switch within NASTRAN. The last improvement allows for NASTRAN to execute above the 16 mega-byte line. This improvement allows for NASTRAN to have access to 2 giga-bytes of memory for open core and the in-memory data base. Author

N89-22947*# RPK Corp., Columbia, MD.
A POWERFUL ENHANCEMENT TO THE DMAP ALTER CAPABILITY
P. R. Pamidi *In* Computer Software Management and Information Center Seventeenth NASTRAN (R) Users' Colloquium Mar. 1989 p 169-186 (For primary document see N89-22940 16-39)
Avail: NTIS HC A17/MF A01; also available from COSMIC, Athens, GA 30602 CSCL 20K

A powerful enhancement to the DMAP alter capability was developed and is available on all RPK-supported versions of COSMIC/NASTRAN. This enhancement involves the addition of two alter control cards, called INSERT and DELETE, to the Executive Control Deck. These cards allow for DMAP alters to be made by referencing DMAP statements by their module names rather than by their statement numbers in the rigid format DMAP sequence. This allows for increased user convenience and flexibility and makes alters more meaningful to the user. In addition, DMAP alter packages employing the alter control cards will be much less susceptible to future changes in rigid format DMAPs than alter packages employing the standard ALTER control cards. The usage of the cards is illustrated by examples. Author

N89-22948*# National Aeronautics and Space Administration. Lewis Research Center, Cleveland, OH.
A NASTRAN DMAP ALTER FOR LINEAR BUCKLING ANALYSIS UNDER DYNAMIC LOADING
Robert A. Aiello and Joseph E. Grady *In* Computer Software Management and Information Center Seventeenth NASTRAN (R) Users' Colloquium Mar. 1989 p 187-200 Previously announced as N89-13522 (For primary document see N89-22940 16-39)
Avail: NTIS HC A17/MF A01; also available from COSMIC, Athens, GA 30602 CSCL 20K

A modification to the NASTRAN solution sequence for transient analysis with direct time integration (COSMIC NASTRAN rigid format 9) was developed and incorporated into a DMAP alter. This DMAP alter calculates the buckling stability of a dynamically loaded structure, and is used to predict the onset of structural buckling under stress-wave loading conditions. The modified

solution sequence incorporates the linear buckling analysis capability (rigid format 5) of NASTRAN into the existing Transient solution rigid format in such a way as to provide a time dependent eigensolution which is used to assess the buckling stability of the structure as it responds to the impulsive load. As a demonstration of the validity of this modified solution procedure, the dynamic buckling of a prismatic bar subjected to an impulsive longitudinal compression is analyzed and compared to the known theoretical solution. In addition, a dynamic buckling analysis is performed for the analytically less tractable problem of the localized dynamic buckling of an initially flawed composite laminate under transverse impact loading. The addition of this DMAP alter to the transient solution sequence in NASTRAN facilitates the computational prediction of both the time at which the onset of dynamic buckling occurs in an impulsively loaded structure, and the dynamic buckling mode shapes of that structure. Author

N89-22949*# RPK Corp., Columbia, MD.
IMPROVEMENTS TO THE CONTINUE FEATURE IN TRANSIENT ANALYSIS
P. R. Pamidi *In* Computer Software Management and Information Center Seventeenth NASTRAN (R) Users' Colloquium Mar. 1989 p 201-213 (For primary document see N89-22940 16-39)
Avail: NTIS HC A17/MF A01; also available from COSMIC, Athens, GA 30602 CSCL 20K

The CONTINUE feature in transient analysis as implemented in the standard release of COSMIC/NASTRAN has inherent errors associated with it. As a consequence, the results obtained by a CONTINUEd restart run do not, in general, match the results that would be obtained in a single run without the CONTINUE feature. These inherent errors were eliminated by improvements to the restart logic that were developed by RPK Corporation and that are available on all RPK-supported versions of COSMIC/NASTRAN. These improvements ensure that the results of a CONTINUEd transient analysis run are the same as those of a non-CONTINUEd run. In addition, the CONTINUE feature was extended to transient analysis involving uncoupled modal equations. The improvements and enhancement were illustrated by examples. Author

N89-22950*# George Washington Univ., Washington, DC.
FINITE ELEMENT MODELING OF ELECTROMAGNETIC FIELDS AND WAVES USING NASTRAN **c32**
E. Thomas Moyer, Jr. and Erwin Schroeder (Naval Ship Research and Development Center, Bethesda, MD.) *In* Computer Software Management and Information Center Seventeenth NASTRAN (R) Users' Colloquium Mar. 1989 p 214-246 (For primary document see N89-22940 16-39)
Avail: NTIS HC A17/MF A01; also available from COSMIC, Athens, GA 30602 CSCL 20N

The various formulations of Maxwell's equations are reviewed with emphasis on those formulations which most readily form analogies with Navier's equations. Analogies involving scalar and vector potentials and electric and magnetic field components are presented. Formulations allowing for media with dielectric and conducting properties are emphasized. It is demonstrated that many problems in electromagnetism can be solved using the NASTRAN finite element code. Several fundamental problems involving time harmonic solutions of Maxwell's equations with known analytic solutions are solved using NASTRAN to demonstrate convergence and mesh requirements. Mesh requirements are studied as a function of frequency, conductivity, and dielectric properties. Applications in both low frequency and high frequency are highlighted. The low frequency problems demonstrate the ability to solve problems involving media inhomogeneity and unbounded domains. The high frequency applications demonstrate the ability to handle problems with large boundary to wavelength ratios. Author

N89-22951*# Naval Ship Research and Development Center, Bethesda, MD. Applied Mathematics Div.
CALCULATION OF LOW FREQUENCY VIBRATIONAL RESONANCES OF SUBMERGED STRUCTURES
Gordon C. Everstine *In* Computer Software Management and Information Center Seventeenth NASTRAN (R) Users' Colloquium Mar. 1989 p 247-261 (For primary document see N89-22940 16-39)
Avail: NTIS HC A17/MF A01; also available from COSMIC, Athens, GA 30602 CSCL 20K

Numerical techniques for calculating the low frequency vibrational resonances of submerged structures are reviewed. Both finite element and boundary element approaches for calculating fully-coupled added mass matrices for use in NASTRAN analysis are described and illustrated. The finite element approach is implemented using existing capability in NASTRAN. The boundary element approach uses the NASHUA structural-acoustics program to compute the added mass matrix. The two procedures are compared to each other for the case of a submerged cylindrical shell with flat end closures. It is concluded that both procedures are capable of computing accurate submerged resonances and that the more elegant boundary element procedure is easier to use but may be more expensive computationally. Author

N89-22952*# Naval Ship Research and Development Center, Bethesda, MD. Applied Mathematics Div.
POWER FLOWS AND MECHANICAL INTENSITIES IN STRUCTURAL FINITE ELEMENT ANALYSIS
Stephen A. Hambric *In* Computer Software Management and Information Center Seventeenth NASTRAN (R) Users' Colloquium Mar. 1989 p 262-289 (For primary document see N89-22940 16-39)
Avail: NTIS HC A17/MF A01; also available from COSMIC, Athens, GA 30602 CSCL 20K

The identification of power flow paths in dynamically loaded structures is an important, but currently unavailable, capability for the finite element analyst. For this reason, methods for calculating power flows and mechanical intensities in finite element models are developed here. Formulations for calculating input and output powers, power flows, mechanical intensities, and power dissipations for beam, plate, and solid element types are derived. NASTRAN is used to calculate the required velocity, force, and stress results of an analysis, which a post-processor then uses to calculate power flow quantities. The SDRC I-deas Supertab module is used to view the final results. Test models include a simple truss and a beam-stiffened cantilever plate. Both test cases showed reasonable power flow fields over low to medium frequencies, with accurate power balances. Future work will include testing with more complex models, developing an interactive graphics program to view easily and efficiently the analysis results, applying shape optimization methods to the problem with power flow variables as design constraints, and adding the power flow capability to NASTRAN. Author

N89-22953*# Texas Instruments, Inc., Dallas.
FINITE ELEMENT ANALYSIS OF A MICROMECHANICAL DEFORMABLE MIRROR DEVICE
T. J. Sheerer, W. E. Nelson, and L. J. Hornbeck *In* Computer Software Management and Information Center Seventeenth NASTRAN (R) Users' Colloquium Mar. 1989 p 290-310 (For primary document see N89-22940 16-39)
Avail: NTIS HC A17/MF A01; also available from COSMIC, Athens, GA 30602 CSCL 20K

A monolithic spatial light modulator chip was developed consisting of a large number of micrometer-scale mirror cells which can be rotated through an angle by application of an electrostatic field. The field is generated by electronics integral to the chip. The chip has application in photoreceptor based non-impact printing technologies. Chips containing over 16000 cells were fabricated, and were tested to several billions of cycles. Finite Element Analysis (FEA) of the device was used to model both the electrical and mechanical characteristics. Author

N89-22954*# Butler Analyses, Towson, MD.
RITZ METHOD FOR TRANSIENT RESPONSE IN SYSTEMS HAVING UNSYMMETRIC STIFFNESS
Thomas G. Butler *In* Computer Software Management and Information Center Seventeenth NASTRAN (R) Users' Colloquium Mar. 1989 p 311-362 (For primary document see N89-22940 16-39)
Avail: NTIS HC A17/MF A01; also available from COSMIC, Athens, GA 30602 CSCL 20K

The DMAP coding was automated to such an extent by using the device of bubble vectors, that it is useable for analyses in its present form. This feasibility study demonstrates that the Ritz Method is so compelling as to warrant coding its modules in FORTRAN and organizing the resulting coding into a new Rigid Format. Even though this Ritz technique was developed for unsymmetric stiffness matrices, it offers advantages to problems with symmetric stiffnesses. If used for the symmetric case the solution would be simplified to one set of modes, because the adjoint would be the same as the primary. Its advantage in either type of symmetry over a classical eigenvalue modal expansion is that information density per Ritz mode is far richer than per eigenvalue mode; thus far fewer modes would be needed for the same accuracy and every mode would actively participate in the response. Considerable economy can be realized in adapting Ritz vectors for modal solutions. This new Ritz capability now makes NASTRAN even more powerful than before. Author

N89-22955*# Air Force Flight Dynamics Lab., Wright-Patterson AFB, OH.
MODAL STRAIN ENERGIES IN COSMIC NASTRAN
B. D. Snyder and V. B. Venkayya *In* Computer Software Management and Information Center Seventeenth NASTRAN (R) Users' Colloquium Mar. 1989 p 363-381 (For primary document see N89-22940 16-39)
Avail: NTIS HC A17/MF A01; also available from COSMIC, Athens, GA 30602 CSCL 20K

A computer program was developed to take a NASTRAN output file from a normal modes analysis and calculate the modal strain energies of selected elements. The FORTRAN program can determine the modal strain energies for CROD, CBAR, CELAS, CTRMEM, CQDMEM2, and CSHEAR elements. Modal strain energies are useful in estimating damping in structures. Author

N89-22956*# Southern Methodist Univ., Dallas, TX. Dept. of Civil and Mechanical Engineering.
DEFINITION OF NASTRAN SETS BY USE OF PARAMETRIC GEOMETRY
Terry V. Baughn and Mehran Tiv *In* Computer Software Management and Information Center Seventeenth NASTRAN (R) Users' Colloquium Mar. 1989 p 382-394 (For primary document see N89-22940 16-39)
Avail: NTIS HC A17/MF A01; also available from COSMIC, Athens, GA 30602 CSCL 20K

Many finite element preprocessors describe finite element model geometry with points, lines, surfaces and volumes. One method for describing these basic geometric entities is by use of parametric cubics which are useful for representing complex shapes. The lines, surfaces and volumes may be discretized for follow on finite element analysis. The ability to limit or selectively recover results from the finite element model is extremely important to the analyst. Equally important is the ability to easily apply boundary conditions. Although graphical preprocessors have made these tasks easier, model complexity may not lend itself to easily identify a group of grid points desired for data recovery or application of constraints. A methodology is presented which makes use of the assignment of grid point locations in parametric coordinates. The parametric coordinates provide a convenient ordering of the grid point locations and a method for retrieving the grid point ID's from the parent geometry. The selected grid points may then be used for the generation of the appropriate set and constraint cards. Author

N89-22957# Sandia National Labs., Albuquerque, NM. Applied Mechanics Div.
AN EXPERIMENTAL AND ANALYTICAL SYNTHESIS OF CONTROLLED STRUCTURE DESIGN
Lee D. Peterson, James J. Allen, James P. Lauffer, and A. Keith Miller 1989 32 p Presented at the 30th Structures, Structural Dynamics and Materials Conference, Mobile, AL, 3 Apr. 1989 Previously announced in IAA as A89-30651
(Contract DE-AC04-76DP-00789)
(DE89-006506; SAND-88-2377C; CONF-8904112-1) Avail: NTIS HC A03/MF A01

An overview of the experimental and analytical results from a controlled structure technology development project are reported and discussed. A controller was designed to reject disturbances from a lightly damped truss structure, in which twenty structural modes lie within the controller bandwidth. The signals from four strain sensors are fed back through an eighteenth order dynamic controller into four stress actuators (not collocated with the sensors) to reduce the vibration of the structure. Five independent performance measures are simultaneously minimized to synthesize the controller. An optimal projection controller, designed from a 58th order state space model, experimentally reduces the structural vibration by up to 65 percent without saturating the actuators and without destabilizing high frequency modes. By comparing analytical and experimental performance predictions, the robustness of the controller to model imperfections is demonstrated. The overall procedure reported here demonstrates a complete analysis, control synthesis, and test of a realistic controlled structure. DOE

N89-22958# Argonne National Lab., IL. Reactor Analysis and Safety Div.
ADAPTIVE CONTACT ELEMENTS FOR THREE-DIMENSIONAL EXPLICIT TRANSIENT ANALYSIS
R. F. Kulak 1989 73 p
(Contract W-31-109-eng-38)
(DE89-008436; ANL/PPRNT-89-111) Avail: NTIS HC A04/MF A01

A finite element method was developed for treating the mechanics of contact between deformable bodies. The method uses a family of adaptive interface elements, which were based on the penalty method, to handle the changing contact configurations that can occur between discretized contacting bodies. The nodal connectivity of these interface elements was allowed to change during the computations in order to accommodate finite sliding. The infusion of these elements in the interface satisfies the stress equilibrium condition during contact. Explicit forms for the nodal internal forces are presented. The methodology has been coded and several sample problems are presented. DOE

N89-22959# IKO Software Service G.m.b.H., Stuttgart (Germany, F.R.).
THE PROJECT ASKA-SPACE, PHASE 1 Final Report
Gerhard Baumann 1988 54 p In GERMAN; ENGLISH summary Presented at a DFVLR Conference, Cologne, Fed. Republic of Germany, 3 Dec. 1987
(Contract BMFT-01-TB-8503)
(ETN-89-93768) Avail: NTIS HC A04/MF A01

The finite element program ASKA was further developed to fulfil the special requirements of spacecraft structures. The following items received special consideration: data compatibility on the problem definition level; new elements (shell elements and beams); composite elements; thermal and thermo-elastic analysis; sensitivity analysis and optimization; interface programs for the pre and postprocessors and for data base managment systems. Studies showed how state of the art analysis methods can be integrated, especially for dynamic analysis. ESA

N89-22960# GKSS-Forschungszentrum Geesthacht (Germany, F.R.). Inst. fuer Anlagentechnik.
FINITE ELEMENT ANALYSIS FOR CALIBRATION CURVE COMPUTATION FOR MEASUREMENT OF CRACK PROPAGATION OF ELLIPSE SHAPED SURFACE CRACKS [FINITE-ELEMENT-ANALYSE ZUR BERECHNUNG VON EICHKURVEN FUER DIE MESSUNG DES RISSFORTSCHRITTES VON ELLIPSENFOERMIGEN OBERFLAECHENRISSEN]
R. A. Dietrich and W. Schoenfeld 4 Jul. 1988 28 p In GERMAN; ENGLISH summary
(GKSS-88/E/34; ISSN-0344-9629; ETN-89-93953) Copyright Avail: NTIS HC A03/MF A01

The finite element method is utilized to calculate the calibration curves for measurement of crack propagation for elliptical surface cracks in fracture mechanics specimens. The calibration curves are required for measurement of the crack propagation using the electrical direct-current method. The calibration curves are calculated for fracture mechanics specimens with the thickness from 5 to 20 mm. The starting crack specimens thickness is of 2 mm. ESA

N89-22961# Oxford Univ. (England). Dept. of Engineering Science.
THE HERTZIAN CONE CRACK: THEORETICAL NUMERICAL AND EXPERIMENTAL STUDIES
Li Yingzhi and D. A. Hills 1988 56 p
(OUEL-1743/88; ETN-89-94216) Avail: NTIS HC A04/MF A01

The fracture analysis of problems for a half space containing an axisymmetric crack is studied. A general solution of stress strain fields at the crack tip is proposed. Based on the stress strain fields obtained, a high order special finite element is established to calculate the stress intensity factors for Hertzian cone cracks. Experimental work, permitting the fracture toughness of glass to be found is compared with data obtained by other methods. In experiments, the difficulty is mainly is measuring the crack accurately. A greater spread of dimensions (especially the cone angle) is found, and no account is taken of interfacial shear traction. In the case of opaque materials it is impossible to acquire sufficient data from surface measurements alone. There is a large number of independent variables in the calibration. Also, although small, there is a finite mode 2 component of crack tip loading present, whose magnitude (and possibly sign) changes as the crack extends. ESA

N89-22962# Los Alamos National Lab., NM.
GENERALIZED FINITE STRAINS, GENERALIZED STRESSES, AND A HYBRID VARIATIONAL PRINCIPLE FOR FINITE-ELEMENT COMPUTER PROGRAMS USING CURVILINEAR COORDINATES
W. A. Cook Apr. 1989 20 p
(Contract W-7405-eng-36)
(DE89-009923; LA-11546-MS) Avail: NTIS HC A03/MF A01

A Generalized hybrid variational principle is presented that includes, as special cases, hybrid variational principles for the Lagrangian and Eulerian formulations. This generalized hybrid principle approximates force equilibrium and constitutive equations. This report is an extension of a similar report entitled Generalized Finite Strains, Generalized Stresses, and a Hybrid Variational Principle for Finite-Element Computer Programs. The difference between these reports is in the use of curvilinear coordinates. Presented in these reports are two approaches for solving nonlinear stress analysis problems with this generalized hybrid variational principle. Both approaches use the finite-element method: one iterates the nodal displacements, and the other iterates the incremental displacements. DOE

N89-22963 National Physical Lab., Teddington (England). Div. of Materials Applications.
APPROXIMATE LARGE DEFLECTION ANALYSIS OF SIMPLY SUPPORTED ORTHOTROPIC PLATES
D. H. Ferriss Dec. 1988 27 p
(NPL-DMA(A)171; ISSN-0143-7313; ETN-89-94340) Copyright Avail: National Physical Lab., Teddington, Middlesex, TW11 0LW, United Kingdom

Equations describing the large deflection of simply supported rectangular orthotropic plates subjected to transverse uniform and centre point loading are presented. An approximate solution to these equations is determined using a Galerkin technique involving polynomial and trigonometric functions. The resulting cubic equations are solved numerically for deflections up to 10 times the plate thickness and results are presented in tables. It is shown that the behavior can be approximated by design formulae involving one or more cubic expressions of the plate displacement. ESA

N89-22964# Fraunhofer Inst. fuer Werkstoffmechanik, Freiburg (Germany, F.R.).
RECENT ADVANCES IN MODELING CREEP CRACK GROWTH
H. Riedel Aug. 1988 31 p Presented at the 7th International Conference on Fracture, Houston, TX, Mar. 1989
(W-2/88; ETN-89-94402) Avail: NTIS HC A03/MF A01

Progress in describing transient crack growth including the effect of primary creep is reviewed. The effect of crack tip geometry changes by blunting and by crack growth on the crack tip fields and on the validity of the C asterisk integral is analyzed by idealizing the growing-crack geometry by a sharp notch and using solutions for the notch-tip fields. Three-dimensional calculations of the C asterisk integral are cited and theoretical points are emphasized regarding the three-dimensional fields at crack tips. Creep growth is described by continuum-damage models for which similarity solutions can be obtained. Crack growth under small-scale creep conditions turns out to be difficult to understand. Slightly different models yield very different crack growth rates. ESA

N89-22965# Aeronautical Research Inst. of Sweden, Stockholm. Structures Dept.
ON THE SEMI-ELLIPTICAL SURFACE CRACK PROBLEM: DETAILED NUMERICAL SOLUTIONS FOR COMPLETE ELASTIC STRESS FIELDS
Anders F. Blom and Borje Andersson Dec. 1988 42 p Presented at the ASTM International Symposium on Surface Crack Growth: Models, Experiments and Structures, Reno, NV, Apr. 1988 Submitted for publication Sponsored by the Swedish Board for Technical Development
(FFA-TN-1988-74; ETN-89-94549) Avail: NTIS HC A03/MF A01

The p-version of the finite element method together with carefully designed meshes are used to obtain accurate numerical solutions for complete elastic stress fields in a linearly elastic plate containing a semi-elliptical surface crack for two materials having a Poisson ratio of 0.3 and 0.499, respectively. A priori known convergence properties are used to estimate bounds for the error in the numerical solutions. The calculated displacements are accurate at all points located not closer than 0.001a, a being the crack size, from the crack front. It is demonstrated that pointwise values for the traditional edge stress intensity factors are readily obtained with very high accuracy even when using a very simple mesh and a modest computational effort. Socalled vertex and vertex-edge intensity factors are derived which together with numerically determined eigenfunctions fully characterize the complete solution in the vicinity of the vertex where the crack front intersects with the stress free surface. For the nearly incompressible material the second order vertex intensity factor strongly influences the solution close to the vertex. The first order vertex intensity factor may, under different boundary conditions, be of negligible importance (except for extremely small distances from the vertex). The size of the domain where the vertex singularity strongly influences the solution is of the order 0.02a. ESA

N89-22966 Lehigh Univ., Bethlehem, PA.
CORROSION FATIGUE CRACK GROWTH: THE ROLE OF CRACK-TIP DEFORMATION AND FILM FORMATION KINETICS Ph.D. Thesis
Stephen John Hudak, Jr. 1988 234 p
Avail: Univ. Microfilms Order No. DA8901871

The mechanical and electrochemical conditions were examined at the crack-tip, then this information was used to critically assess anodic dissolution versus hydrogen embrittlement mechanisms of crack growth. The system studied as sensitized 304 stainless steel in an aqueous 0.1M Na2SO4 environment at temperatures of 343 to 363K. The measurements of crack-tip strains at growing corrosion fatigue cracks were obtained using the stereoimaging technique. Results showed that the crack-tip strains, and thus strain rates, were significantly less than those attending crack growth in an inert environment. The local environment was determined using a crack simulation experiment involving cyclic straining of a creviced electrode. Cyclic straining was found to decrease the electrode potential and promote acidification of the occluded environment. The evolution of the local environment was explained in terms of the formation of both oxide and sulfide films. Using the above information, it is shown that film rupture/anodic dissolution concepts are incapable of predicting the measured dependence of corrosion fatigue crack growth rates on stress intensity factor range, cyclic frequency, and degree of cold work. However, these growth rate trends are shown to be consistent with a hydrogen enbrittlement mechanism. Based on these results, as well as the reduction in the critical crack-tip strain attending crack growth, hydrogen embrittlement is the predominant mechanism of corrosion fatigue crack growth in the 304 stainless steel-aqueous environment system. Dissert. Abstr.

N89-22967 Alabama Univ., University.
A STUDY OF HIGH STRAIN RATE GENERATION OF ADIABATIC SHEAR BANDS IN A TITANIUM ALLOY Ph.D. Thesis
Abdelhay Mohamed Abdelhay 1988 167 p
Avail: Univ. Microfilms Order No. DA8826939

The Split Hopkinson Pressure Bar (SHPB) apparatus capable of subjecting specimens to dynamic shear at rates of strain between 3.6 E04 and 1.2 E05 /s is described. Results are given for two heat treatments (Type A as received alloy, and Type B was heat treated alloy) of the titanium alloy Ti6Al4V. Both types of the Ti6Ala4V alloy showed a strain rate sensitivity, but the degree was less for type B alloy. Yield strengths for some of the specimens tested were observed up to 8.46 E04 /s. No evidence was obtained of adiabatic shear band formation or thermal softening up to a strain rate of 7.87 E04 /s for type A treatment, and up to 8.83 E04 /s for the other type. Above these values of strain rate failure of specimens by adiabatic shear banding was evident, and at higher values of strain rates voids and micro cracks were observed along these shear bands. An experimental finding was found to be useful to mark the onset of such plastic instability at high strain rate deformation. This criterion was based on the global amount of specific energy absorbed by the plastically deformed zone. The function relating specific energy and strain rate has a discontinuity which divide the behavior under dynamic loading into two zones. Before the discontinuity there is a steady increase in the specific energy with the strain rate, and there was no evidence of formation of adiabatic shear bands. At the discontinuity there is a large increase in specific strain energy. After the discontinuity there was always the formation of shear bands. Such a criterion was found to be suitable to mark the point of plastic instability by adiabatic shear banding. Dissert. Abstr.

N89-22968 Iowa Univ., Iowa City.
A RECURSIVE FORMULATION FOR FLEXIBLE MULTIBODY DYNAMICS Ph.D. Thesis
Sung-Soo Kim 1988 207 p
Avail: Univ. Microfilms Order No. DA8903945

A recursive formulation is developed for dynamic simulation of multi-body mechanical systems that consist of rigid and flexible bodies, using a variational-vector calculus approach for both open and closed loop systems. Kinematics between pairs of contiguous flexible bodies is defined using relative joint coordinates and deformation modal coordinates, for a library of standard joints. Closed loops in the flexible mechanical system are cut to form a spanning tree structure. Reaction forces due to cut joints are treated as external forces in the spanning tree structure. Linear relationships between absolute, deformation, and joint relative coordinate variational quantities and velocities are recursively applied to derive variational equations of motion. Numerical performance of the recursive formulation is evaluated by comparing solutions with those obtained with absolute coordinate formulations. A method for selecting boundary conditions and deformation modes for redundantly constrained flexible components in mechanical systems is presented. Gaussian elimination is used to partition the coefficient matrix in equilibrium equations for each flexible component, leading to definition of a retained statically determinate set and a redundant set of boundary conditions. Constraint and attachment modes are employed, to account for deformation due to constraint reaction forces. Numerical experiments are carried out to demonstrate validity of the method. Dissert. Abstr.

42 GEOSCIENCES (GENERAL)

N89-22969*# National Aeronautics and Space Administration, Washington, DC.
EARTH SYSTEM SCIENCE: A PROGRAM FOR GLOBAL CHANGE
1989 305 p Original document contains color illustrations
(NASA-TM-101186; NAS 1.15:101186) Avail: NTIS HC A14/MF A01 CSCL 08E

The Earth System Sciences Committee (ESSC) was appointed to consider directions for the NASA Earth-sciences program, with the following charge: review the science of the Earth as a system of interacting components; recommend an implementation strategy for Earth studies; and define the role of NASA in such a program. The challenge to the Earth system science is to develop the capability to predict those changes that will occur in the next decade to century, both naturally and in response to human activity. Sustained, long-term measurements of global variables; fundamental descriptions of the Earth and its history; research foci and process studies; development of Earth system models; an information system for Earth system science; coordination of Federal agencies; and international cooperation are examined.
B.G.

43 EARTH RESOURCES AND REMOTE SENSING

Includes remote sensing of earth resources by aircraft and spacecraft; photogrammetry; and aerial photography.

For instrumentation see *35 Instrumentation and Photography.*

N89-22970*# Stanford Univ., CA. Remote Sensing Lab.
EVALUATION OF THE PORTABLE INSTANTANEOUS DISPLAY ANALYSIS SPECTROMETER (PIDAS) Final Report, 1 Oct. 1987 - 30 Nov. 1988
R. J. P. Lyon, Tod Rubin, and Makoto Ohashi 3 Jun. 1988
90 p Prepared in cooperation with Pasco Corp. (Japan)
(Grant NAGw-1252)
(NASA-CR-184878; NAS 1.26:184878) Avail: NTIS HC A05/MF A01 CSCL 14B

The Portable Instantaneous Display Analysis System (PIDAS) was evaluated by measuring 125 spectra of mineral specimens and rock samples under the following conditions: in the laboratory under artificial illumination and outdoors, on the building patio, while still using the line voltage electric power supplies. The PIDAS was compared and contrasted with the GEOSCAN PFS, Daedalus-Spectrafax 440, and the Geophysical Environmental Research (GER) IRIS Mark 4. B.G.

N89-22971*# Massachusetts Inst. of Tech., Cambridge. Lab. of Electronics.
REMOTE SENSING OF EARTH TERRAIN Final Report, 1 Sep. 1982 - 31 Mar. 1989

J. A. Kong 31 Mar. 1989 26 p
(Grant NAG5-270)
(NASA-CR-184937; NAS 1.26:184937; OSP-92790) Avail: NTIS HC A03/MF A01 CSCL 08B

A mathematically rigorous and fully polarimetric radar clutter model used to evaluate the radar backscatter from various types of terrain clutter such as forested areas, vegetation canopies, snow covered terrains, or ice fields is presented. With this model, the radar backscattering coefficients for the multichannel polarimetric radar returns can be calculated, in addition to the complex cross correlation coefficients between elements of the polarimetric measurement vector. The complete polarization covariance matrix can be computed and the scattering properties of the clutter environment characterized over a broad range of incident angle and frequencies. Author

N89-22972# Freiburg Univ. (Germany, F.R.). Inst. fuer Physische Geographie.
DERIVATION OF A LARGE-SCALE MAP OF HEAT LOAD IN THE REGION FREIBURG-BASEL (GERMANY, F.R.) USING SATELLITE DATA. A CONTRIBUTION TO THE PRODUCTION OF BIOCLIMATE DATA BASED ON A GEOGRAPHIC INFORMATION SYSTEM Ph.D. Thesis [ABLEITUNG EINER GROSSMASSSTAEBIGEN KARTE DER WAERMEBELASTUNG IM RAUM FREIBURG-BASEL MIT HILFE VON SATELLITENDATEN. EIN BEITRAG ZUR ERZEUGUNG VON BIOKLIMAKARTEN AUF DER BASIS EINES GEOGRAPHISCHEN INFORMATIONSSYSTEMS]
Gunter Menz 1987 222 p In GERMAN Color map as supplement
(Rept-27; ETN-89-93781) Avail: NTIS HC A10/MF A01

The computer-aided production of a map of the heat load on man in the southern Black Forest (West Germany) on the Upper Rhine plane between Freiburg and Basel was investigated. A geographic information system was established using data from a climate model, a digital height model, LANDSAT data, and data from the Heat Capacity Mapping Mission. Using a stochastic model the heat load values were estimated. The form and significance of the estimation equation depends on the data collection. The effect of the local land use on the bioclimate of neighboring locations can only be determined with sufficient environment data. The highest variance information is obtained if the land use is differentiated in 6 classes, allowing a heat load mapping. Heat load mapping on scales 1:200,000, 1:100,000 and 1:50,000 prove to be possible, enabling the transition from a mesoscale to a microscale cartographic determination of climatic effects on human beings. ESA

N89-22973# Technische Univ., Delft (Netherlands). Faculty of Geodesy.
INTEGRATION OF TIE-POINTS IN DIGITAL MOSAICING Thesis
Herman Ryks Jun. 1988 79 p
(ETN-89-94147) Avail: NTIS HC A05/MF A01

A mosaicing method which includes the use of tie-points, which are points in the overlap of two or more images that have known image-coordinates in these images, but of which no ground coordinates are necessary, is presented. This enables one to make mosaics, using very few ground control points, or none at all. The FORTRAN program that calculates the transformation parameters of the images to be mosaiced is given. The tests performed are described. Recommendations to achieve an operational mosaicing system are made. ESA

N89-22974# Swedish Defence Research Establishment, Stockholm.
A MULTINATIONAL VERIFICATION SATELLITE: A PRELIMINARY INVESTIGATION
Lars B. Wallin, Ulf Ekblad, Sven Grahn, Troliev Orhaug, and Ulf Sveding Sep. 1988 66 p In SWEDISH; ENGLISH summary Sponsored by the Ministry of Foreign Affairs, Sweden
(FOA-C-10312-9.3; ISSN-0281-0247; ETN-89-94221) Avail: NTIS HC A04/MF A01 Swedish Defense Research Establishment, P.O. Box 27322, S-102 54 Stockholm, Sweden, 50 Swedish crowns

The possibilities of using observation satellites for arms control verification is reported. The problems of using existing military and civilian satellites are noted, and organization alternatives, differing in their degree of multinationality are given. ESA

N89-22975*# Max-Planck-Inst. fuer Meteorologie, Hamburg (Germany, F.R.).
DEVELOPMENT OF A SATELLITE SAR IMAGE SPECTRA AND ALTIMETER WAVE HEIGHT DATA ASSIMILATION SYSTEM FOR ERS-1
Klaus Hasselmann, Susanne Hasselmann, Eva Bauer, Claus Bruening, Susanne Lehner, Hans Graber, and Piero Lionello (Consiglio Nazionale delle Ricerche, Venice, Italy) Paris, France ESA Jul. 1988 165 p
(Contracts NAS7-918; JPL-957652; ESA-6875/87/HGE/I(SC); N00014-83-G-0126; ST2J-0044-8-D; BMFT-07-KR-2121)
(NASA-CR-182685; NAS 1.26:182685; ESA-CR(P)-2710; ETN-89-94241; Rept-19) Avail: NTIS HC A08/MF A01 CSCL 05B

The applicability of ERS-1 wind and wave data for wave models was studied using the WAM third generation wave model and SEASAT altimeter, scatterometer and SAR data. A series of global wave hindcasts is made for the surface stress and surface wind fields by assimilation of scatterometer data for the full 96-day SEASAT and also for two wind field analyses for shorter periods by assimilation with the higher resolution ECMWF T63 model and by subjective analysis methods. It is found that wave models respond very sensitively to inconsistencies in wind field analyses and therefore provide a valuable data validation tool. Comparisons between SEASAT SAR image spectra and theoretical SAR spectra derived from the hindcast wave spectra by Monte Carlo simulations yield good overall agreement for 32 cases representing a wide variety of wave conditions. It is concluded that SAR wave imaging is sufficiently well understood to apply SAR image spectra with confidence for wave studies if supported by realistic wave models and theoretical computations of the strongly nonlinear mapping of the wave spectrum into the SAR image spectrum. A closed nonlinear integral expression for this spectral mapping relation is derived which avoids the inherent statistical errors of Monte Carlo computations and may prove to be more efficient numerically. ESA

N89-22976# Swedish Defence Research Establishment, Linkoeping. Dept. of Information Technology.
MINIMUM NUMBER OF SATELLITES FOR PERIODIC COVERAGE
Ulf Ekblad Dec. 1988 22 p
(FOA-C-30511-9.4; ISSN-0347-3708; ETN-89-94308) Avail: NTIS HC A03/MF A01; Swedish Defence Research Establishment, P.O. Box 1165, S-581 Linkoeping, Sweden, 50 Swedish crowns

The problem of obtaining a periodic coverage of a site by satellites is considered. Periodic coverage is defined as a certain number of observations of a specified site per time interval. This reduces the number of satellites required substantially. One can e.g., obtain periodic coverage of a site from low Earth orbit with as few as one or two satellites if the revisit time is three days or longer. ESA

N89-22977# GEC-Marconi Electronics Ltd., Chelmsford (England).
THEORETICAL STUDIES FOR ERS-1 WAVE MODE, VOLUME 1 Final Report
J. T. Macklin, R. A. Cordey, and J. M. Pielou Paris, France ESA Aug. 1988 130 p
(Contract ESA-6878/87/HGE/I(SC))
(GEC-MTR-87/110-Vol-1; ESA-CR(P)-2750; ETN-89-94471)
Copyright Avail: NTIS HC A07/MF A01

The theory of how the sea surface is imaged by synthetic aperture radar (SAR), as well as inverse methods for recovering quantitative information about ocean waves from SAR data are

discussed. Short-wave spectra, wave-wave interactions (hydrodynamic modulation) and wave nonlinearities (including breaking waves) are reviewed. Backscattering from breaking waves and the imaging effects due to their motions are considered. An inverse method using complex imagery is developed and is shown to offer improved prediction of the speckle component in the power spectra of SAR intensity images. The possibility of an iterative inverse method for nonlinear imaging conditions is discussed. The available optimum inverse methods are reviewed, and the potential of the maximum entropy method is considered. The requirements for validating the imaging theory are examined, and recommendations are made for future work, highlighting aspects relevant to the operation of the wave mode of ERS-1. ESA

N89-22978# European Space Agency, Paris (France).
IMAGING RADAR APPLICATIONS IN EUROPE. ILLUSTRATED EXPERIMENTAL RESULTS (1978-1987)
M. G. Wooding, A. J. Sieber, P. N. Churchill (Joint Research Centre of the European Communities, Ispra, Italy), J. Lichtenegger, M. Fea, T.-D. Guyenne, ed., and N. Longdon, ed. Oct. 1988 85 p Original contains color illustrations
(ESA-TM-01; ETN-89-94474) Copyright Avail: NTIS HC A05/MF A01

The potential of imaging radar for agriculture, forestry, geology, snow and ice, and oceanography applications is illustrated. Image processing techniques and data availability are mentioned. ESA

N89-22979*# California Univ., Santa Barbara.
REMOTE SENSING INFORMATION SCIENCES RESEARCH GROUP: BROWSE IN THE EOS ERA Final Report
John E. Estes and Jeffrey L. Star 1 May 1989 155 p
(Grant NAGw-987)
(NASA-CR-184637; NAS 1.26:184637) Avail: NTIS HC A06/MF A01 CSCL 08B

The problem of science data browse was examined. Given the tremendous data volumes that are planned for future space missions, particularly the Earth Observing System in the late 1990's, the need for access to large spatial databases must be understood. Work was continued to refine the concept of data browse. Further, software was developed to provide a testbed of the concepts, both to locate possibly interesting data, as well as view a small portion of the data. Build II was placed on a minicomputer and a PC in the laboratory, and provided accounts for use in the testbed. Consideration of the testbed software as an element of in-house data management plans was begun. Author

N89-23101# Carnegie-Mellon Univ., Pittsburgh, PA. Digital Mapping Lab.
COOPERATIVE METHODS FOR ROAD TRACKING IN AERIAL IMAGERY
David M. McKeown, Jr. and Jerry L. Denlinger *In* Science Applications International Corp., Proceedings: Image Understanding Workshop, Volume 1 Apr. 1988 p 327-341 (For primary document see N89-23074 16-61)
(Contracts DACA72-84-C-0002; F33615-84-K-1520; DARPA Order 4976)
Avail: NTIS HC A22/MF A01 CSCL 08B

N89-23102# General Electric Co., Schenectady, NY. Corporate Research and Development Center.
PACE: AN ENVIRONMENT FOR INTELLIGENCE ANALYSIS
N. R. Corby, Joseph L. Mundy, P. A. Vrobel, A. J. Hanson, Lynn H. Quam, G. B. Smith, and Thomas M. Strat (SRI International Corp., Menlo Park, CA.) *In* Science Applications International Corp., Proceedings: Image Understanding Workshop, Volume 1 Apr. 1988 p 342-350 (For primary document see N89-23074 16-61)
(Contract DACA76-86-C-0007)
Avail: NTIS HC A22/MF A01 CSCL 08B

N89-23122# SRI International Corp., Menlo Park, CA. Artificial Intelligence Center.
OVERVIEW OF THE SRI CARTOGRAPHIC MODELING ENVIRONMENT
Andrew J. Hanson and Lynn H. Quam *In* Science Applications International Corp., Proceedings: Image Understanding Workshop, Volume 2 Apr. 1988 p 576-582 (For primary document see N89-23115 16-61)
(Contract MDA903-86-C-0084; NSF IST-85-11751)
Avail: NTIS HC A99/MF E03 CSCL 08B

44 ENERGY PRODUCTION AND CONVERSION

Includes specific energy conversion systems, e.g., fuel cells; global sources of energy; geophysical conversion; and windpower.

For related information see also *07 Aircraft Propulsion and Power, 20 Spacecraft Propulsion and Power,* and *28 Propellants and Fuels.*

N89-22980*# Space Power, Inc., San Jose, CA.
MEGAWATT CLASS NUCLEAR SPACE POWER SYSTEMS (MCNSPS) CONCEPTUAL DESIGN AND EVALUATION REPORT. VOLUME 3, TECHNOLOGIES 2: POWER CONVERSION Final Report
J. R. Wetch et al Sep. 1988 136 p
(Contract NAS3-23867)
(NASA-CR-179614-Vol-3; NAS 1.26:179614-Vol-3; SPI-25-1-Vol-3)
Avail: NTIS HC A07/MF A01 CSCL 10B

The major power conversion concepts considered for the Megawatt Class Nuclear Space Power System (MCNSPS) are discussed. These concepts include: (1) Rankine alkali-metal-vapor turbine alternators; (2) in-core thermionic conversion; (3) Brayton gas turbine alternators; and (4) free piston Stirling engine linear alternators. Considerations important to the coupling of these four conversion alternatives to an appropriate nuclear reactor heat source are examined along with the comparative performance characteristics of the combined systems meeting MCNSPS requirements. M.G.

N89-22981*# Space Power, Inc., San Jose, CA.
MEGAWATT CLASS NUCLEAR SPACE POWER SYSTEMS (MCNSPS) CONCEPTUAL DESIGN AND EVALUATION REPORT. VOLUME 2, TECHNOLOGIES 1: REACTORS, HEAT TRANSPORT, INTEGRATION ISSUES Final Report
J. R. Wetch et al Sep. 1988 143 p
(Contract NAS3-23867)
(NASA-CR-179614-Vol-2; NAS 1.26:179614-Vol-2; SPI-25-1-Vol-2)
Avail: NTIS HC A07/MF A01 CSCL 10B

The objectives of the Megawatt Class Nuclear Space Power System (MCNSPS) study are summarized and candidate systems and subsystems are described. Particular emphasis is given to the heat rejection system and the space reactor subsystem. Author

N89-22982*# National Aeronautics and Space Administration. Lewis Research Center, Cleveland, OH.
SPACE ELECTROCHEMICAL RESEARCH AND TECHNOLOGY CONFERENCE: ABSTRACTS Abstracts Only
Washington 1989 49 p Conference held in Cleveland, OH, 11-13 Apr. 1989
(NASA-CP-10029; E-4708; NAS 1.55:10029) Avail: NTIS HC A03/MF A01 CSCL 10A

The objectives of the conference were to examine current technologies, research efforts, and advanced ideas, and to identify technical barriers which affect the advancement of electrochemical energy storage systems for space applications. Papers were presented and workshops were conducted in four technical areas: advanced concepts, hydrogen-oxygen fuel cells and electrolyzers, the nickel electrode, and advanced rechargeable batteries. For individual titles, see N89-22983 through N89-23011.

N89-22983*# National Aeronautics and Space Administration. Goddard Space Flight Center, Greenbelt, MD.

OVERVIEW OF BATTERY USAGE IN NASA/GSFC LEO AND GEO MISSIONS Abstract Only

Thomas Yi *In* NASA, Lewis Research Center, Space Electrochemical Research and Technology Conference: Abstracts 1989 p 1-2 (For primary document see N89-22982 16-44)
Avail: NTIS HC A03/MF A01 CSCL 10A

In July, 1989, Cosmic Background Explorer (COBE) will be launched from a Delta rocket to study the big bang theory. The COBE, which is in a LEO/Polar orbit, will have two 20 Ah NiCd batteries, and 18 cells per battery, made by McDonnell Douglas Company. In December, 1989, National Oceanic and Atmospheric Administration (NOAA-D) will be launched from an Atlas rocket for weather observation purposes. NOAA-D, which is in a LEO/Polar morning orbit, will have two 26.5 Ah NiCd batteries, and 17 cells per battery, made by Ge-Astro East Windor. NOAA-I, which is scheduled for May, 1991 launch in a LEO/Polar afternoon orbit, will have three 26.5 Ah NiCd batteries, 17 cells per battery, made by GE-Astro East Windor. In April, 1990, Gamma Ray Observatory (GRO) will be launched from STS37 to study the gamma ray radiation phenomenon. GRO, which is in a LEO orbit, will have two modular power systems (MPS) made by McDonnell Douglas, each MPS consisting of three 50 Ah NiCd batteries, 22 cells per battery. In July, 1990, Geostationary Operational Environmental Satellite (GOES-I) will be launched from an Atlas I rocket for weather observation purposes. GOES-I, which is in a GEO orbit, will have two 12 Ah NiCd batteries, 28 cells per battery, made by Ford Aerospace and Communications Company. In December, 1990, Tracking and Data Relay Satellite (TDRS-E) will be launched from STS43 for communication purposes. TDRS-E, which is in a GEO orbit, will have three 40 Ah NiCd batteries, 24 cells per battery, made by TRW. In August, 1991, Extreme Ultraviolet Explorer (EUVE) will be launched from a Delta rocket. EUVE, which is in a LEO orbit, will have one modular power system (MPS) made by McDonnell Douglas. In December, 1991, Upper Atmosphere Research Satellite (UARS) will be launched from STS50 to study the Earth's ozone layer and other environmental concerns. UARS, which is in a 56 deg inclination LEO orbit, will have one modular power systems (MPS) made by McDonnell Douglas. Author

N89-22984*# Jet Propulsion Lab., California Inst. of Tech., Pasadena.

THE IMPORTANCE OF BATTERIES IN UNMANNED MISSIONS Abstract Only

John W. Klein *In* NASA, Lewis Research Center, Space Electrochemical Research and Technology Conference 1989 p 3 (For primary document see N89-22982 16-44)
Avail: NTIS HC A03/MF A01 CSCL 10A

A brief overview of the current set of unmanned missions that are currently in operation and those planned for the next 5 to 10 years was presented. The important role of batteries in the development of successful missions was discussed. The workhorse battery, the NiCd, and its use throughout historical missions was explored. Its role on Observers and Landers was discussed, and the success those batteries had. The recent events in the issues of quality and life for NiCd batteries were discussed. These discussions focused on the current design activities for Mars Observer (MO), TOPEX, and Mariner Mark II. Separator selection and the need for uniform testing procedures to develop a quality battery product that can perform to mission requirements were discussed. The recent experiences with the GRO battery failure and the other events have led JPL to the decision to develop a testing program in conjunction with other NASA centers to determine the best separator material for these two missions. The decision for separator material and battery design must be made a year from now. Thus there will not be time to perform a total 2-year accelerated test. The JPL plan for coping with this compromise was discussed. A discussion of where NiH2 batteries are beginning to have an impact and the difficulties with their implementation were addressed. Such missions at Earth Observing System (EOS) and the NOAA series of satellites rely upon NiH2 for success but were not chosen for TOPEX or MO due to their large volume requirements. Author

N89-22985*# National Aeronautics and Space Administration. Lewis Research Center, Cleveland, OH.

HUMAN EXPLORATION MISSION STUDIES Abstract Only

c12

Robert L. Cataldo *In its* Space Electrochemical Research and Technology Conference: Abstracts 1989 p 4 (For primary document see N89-22982 16-44)
Avail: NTIS HC A03/MF A01 CSCL 22A

The Office of Exploration has established a process whereby all NASA field centers and other NASA Headquarters offices participate in the formulation and analysis of a wide range of mission strategies. These strategies were manifested into specific scenarios or candidate case studies. The case studies provided a systematic approach into analyzing each mission element. First, each case study must address several major themes and rationale including: national pride and international prestige, advancement of scientific knowledge, a catalyst for technology, economic benefits, space enterprise, international cooperation, and education and excellence. Second, the set of candidate case studies are formulated to encompass the technology requirement limits in the life sciences, launch capabilities, space transfer, automation, and robotics in space operations, power, and propulsion. The first set of reference case studies identify three major strategies: human expeditions, science outposts, and evolutionary expansion. During the past year, four case studies were examined to explore these strategies. The expeditionary missions include the Human Expedition to Phobos and Human Expedition to Mars case studies. The Lunar Observatory and Lunar Outpost to Early Mars Evolution case studies examined the later two strategies. This set of case studies established the framework to perform detailed mission analysis and system engineering to define a host of concepts and requirements for various space systems and advanced technologies. The details of each mission are described and, specifically, the results affecting the advanced technologies required to accomplish each mission scenario are presented.
Author

N89-22986*# Jet Propulsion Lab., California Inst. of Tech., Pasadena.

A SURVEY OF ADVANCED BATTERY SYSTEMS FOR SPACE APPLICATIONS Abstract Only

Alan I. Attia *In* NASA, Lewis Research Center, Space Electrochemical Research and Technology Conference: Abstracts 1989 p 6 (For primary document see N89-22982 16-44)
Avail: NTIS HC A03/MF A01 CSCL 10A

The results of a survey on advanced secondary battery systems for space applications are presented. The objectives were: to identify advanced battery systems capable of meeting the requirements of various types of space missions, with significant advantages over currently available batteries, to obtain an accurate estimate of the anticipated improvements of these advanced systems, and to obtain a consensus for the selection of systems most likely to yield the desired improvements. Few advanced systems are likely to exceed a specific energy of 150 Wh/kg and meet the additional requirements of safety and reliability within the next 15 years. The few that have this potential are: (1) regenerative fuel cells, both alkaline and solid polymer electrolyte (SPE) types for large power systems; (2) lithium-intercalatable cathodes, particularly the metal ozides intercalatable cathodes (MnO2 or CoO2), with applications limited to small spacecrafts requiring limited cycle life and low power levels; (3) lithium molten salt systems (e.g., LiAl-FeS2); and (4) Na/beta Alumina/Sulfur or metal chlorides cells. Likely technological advances that would enhance the performance of all the above systems are also identified, in particular: improved bifunctional oxygen electrodes; improved manufacturing technology for thin film lithium electrodes in combination with polymeric electrolytes; improved seals for the lithium molten salt cells; and improved ceramics for sodium/solid electrolyte cells. Author

N89-22987*# California Univ., Berkeley. Lawrence Berkeley Lab.
NOVEL NITROGEN-BASED ORGANOSULFUR ELECTRODES FOR ADVANCED INTERMEDIATE TEMPERATURE BATTERIES Abstract Only
S. J. Visco and L. C. DeJonghe *In* NASA, Lewis Research Center, Space Electrochemical Research and Technology Conference: Abstracts 1989 p 7 (For primary document see N89-22982 16-44)
Avail: NTIS HC A03/MF A01 CSCL 10A

Advanced secondary batteries operating at intermediate temperatures (100 to 200 C) have attracted considerable interest due to their inherent advantages (reduced corrosion and safety risks) over higher temperature systems. Current work in this laboratory has involved research on a class of intermediate temperature Na/beta double prime- alumina/RSSR batteries conceptually similar to Na/S cells, but operating within a temperature range of 100 to 150 C, and having an organosulfur rather than inorganic sulfur positive electrode. The organosulfur electrodes are based on the reversible, two electron eduction of organodisulfides to the corresponding thiolate anions, RSSR + 2 electrons yield 2RS(-), where R is an organic moiety. Among the advantages of such a generic redox couple for battery research is the ability to tailor the physical, chemical, and electrochemical properties of the RSSR molecule through choice of the organic moiety. The viscosity, liquidus range, dielectric constant, equivalent weight, and redox potential can in fact be verified in a largely predictable manner. The current work concerns the use of multiple nitrogen organosulfur molecules, chosen for application in Na/RSSR cells for their expected oxidizing character. In fact, a Na/RSSR cell containing one of these materials, the sodium salt of 5-mercapto 1-methyltetrazole, yielded the highest open circuit voltage obtained yet in the laboratory; 3.0 volts in the charged state and 2.6 volts at 100 percent discharge. Accordingly, the cycling behavior of a series of multiple nitrogen organodisulfides as well as polymeric organodisulfides are presented in this manuscript. Author

N89-22988*# Jet Propulsion Lab., California Inst. of Tech., Pasadena.
ADVANCED RECHARGEABLE SODIUM BATTERIES WITH NOVEL CATHODES Abstract Only
S. DiStefano, B. V. Ratnakumar, and C. P. Bankston *In* NASA, Lewis Research Center, Space Electrochemical Research and Technology Conference: Abstracts 1989 p 8 (For primary document see N89-22982 16-44)
Avail: NTIS HC A03/MF A01 CSCL 10A

Various high energy density rechargeable batteries are being considered for future space applications. Of these, the sodium-sulfur battery is one of the leading candidates. The primary advantage is the high energy density (760 Wh/kg theoretical). Energy densities in excess of 180 Wh/kg were realized in practical batteries. Other technological advantages include its chemical simplicity, absence of self-discharge, and long cycle life possibility. More recently, other high temperature sodium batteries have come into the spotlight. These systems can be described as follow: Na/Beta Double Prime-Al2O3/NaAlCl4/Metal Dichloride Sodium/metal dichloride systems are colloquially known as the zebra system and are currently being developed for traction and load leveling applications. The sodium-metal dichloride systems appear to offer many of the same advantages of the Na/S system, especially in terms of energy density and chemical simplicity. The metal dichloride systems offer increased safety and good resistance to overcharge and operate over a wide range of temperatures from 150 to 400 C with less corrosion problems. Author

N89-22989*# Argonne National Lab., IL.
MONOLITHIC SOLID OXIDE FUEL CELL DEVELOPMENT Abstract Only
K. M. Myles and C. C. McPheeters *In* NASA, Lewis Research Center, Space Electrochemical Research and Technology Conference: Abstracts 1989 p 9 (For primary document see N89-22982 16-44)
Avail: NTIS HC A03/MF A01 CSCL 10A

The Monolithic Solid Oxide Fuel Cell (MSOFC) is an oxide-ceramic structure in which appropriate electronic and ionic conductors are fabricated in a honeycomb shape similar to a block of corrugated paperboard. These electronic and ionic conductors are arranged to provide short conduction paths to minimize resistive losses. The power density achievable with the MSOFC is expected to be about 8 kW/kg or 4 kW/L, at fuel efficienceis over 50 percent, because of small cell size and low resistive losses in the materials. The MSOFC operates in the range of 700 to 1000 C, at which temperatures rapid reform of hydrocarbon fuels is expected within the nickel-YSZ fuel channels. Tape casting and hot roll calendering are used to fabricate the MSOFC structure. The performance of the MSOFC has improved significantly during the course of development. The limitation of this system, based on materials resistance alone without interfacial resistances, is 0.093 ohm-sq cm area-specific resistance (ASR). The current typical performance of MSOFC single cells is characterized by ASRs of about 0.4 to 0.5 ohm-sq cm. With further development the ASR is expected to be reduced below 0.2 ohm-sq cm, which will result in power levels greater than 1.4 W/sq cm. The feasibility of the MSOFC concept was proven, and the performance was dramatically improved. The differences in thermal expansion coefficients and firing shrinkages among the fuel cell materials were minimized. As a result of good matching of these properties, the MSOFC structure was successfully fabricated with few defects, and the system shows excellent promise for development into a practical power source. Author

N89-22990*# Eltron Research, Inc., Aurora, IL.
THE ELECTROCHEMICAL GENERATION OF USEFUL CHEMICAL SPECIES FROM LUNAR MATERIALS Abstract Only
Kan J. Tsai, Daniel J. Kuchynka, and Anthony F. Sammells *In* NASA, Lewis Research Center, Space Electrochemical Research and Technology Confernece: Abstracts 1989 p 10 (For primary document see N89-22982 16-44)
(Contract NAS9-17991)
Avail: NTIS HC A03/MF A01 CSCL 10A

The current status of work on an electrochemical technology for the simultaneous generation of oxygen and lithium from a Li2O containing molten salt (Li2O-LiCl-LiF) is discussed. The electrochemical cell utilizes an oxygen vacancy conducting solid electrolyte, yttria-stabilized zirconia, to effect separation between the oxygen evolving and lithium reduction half-cell reactions. The cell, which operates at 700 to 800 C, possesses rapid electrode kinetics at the lithium-alloy electrode with exchange current density values being greater than 60 mA/sq cm, showing high reversibility for this reaction. When used in the electrolytic mode, lithium produced at the negative electrode would be continuously removed from the cell for later use (under lunar conditions) as an easily storable reducting agent (compared to H2) for the chemical refining of lunar ores via the general reaction: 2Li + MO yields Li2O + M where MO represents a lunar ore. Emphasis to this time has been on the simulated lunar ore ilmenite (FeTiO3), which we have found becomes chemically reduced by Li at 432 C. Furthermore, both Fe2O3 and TiO2 have been reduced by Li to give the corresponding metal. This electrochemical approach provides a convenient route for producing metals under lunar conditions and oxygen for the continuous maintenance of human habitats on the Moon's surface. Because of the high reversibility of this electrochemical system, it has also formed the basis for the lithium-oxygen secondary battery. This secondary lithium-oxygen battery system posses the highest theoretical energy density yet investigated. Author

N89-22991*# Texas A&M Univ., College Station.
A NEW CONCEPT FOR HIGH-CYCLE-LIFE LEO: RECHARGEABLE MnO2-HYDROGEN Abstract Only
A. John Appleby, Y. J. Dhar, O. J. Murphy, and Supramaniam Srinivasan *In* NASA, Lewis Research Center, Space

Electrochemical Research and Technology Conference: Abstracts 1989 p 11 (For primary document see N89-22982 16-44)
Avail: NTIS HC A03/MF A01 CSCL 10A

The nickel-hydrogen secondary battery system is now the one of choice for use in GEO satellites. It offers superior energy density to that of nickel-cadmium, with a lifetime that is at least comparable in terms of both cycle life and overall operating life. While the number of deep cycles required for GEO use is small, LEO satellites with long lifetimes (5 to 10 years) will require secondary battery systems allowing 30,000 to 60,000 useful cycles which are characterized by an approximately 2C charge rate and C average discharge rate. Recent work has shown that birnessite MnO2 doped with bismuth oxide can be cycled at very high rates (6C) over a very large number of cycles (thousands) at depths-of-discharge in the 85 to 90 percent range, based on two electrons, which discharge at the same potential in a flat plateau. The potential is about 0.7 V vs. hydrogen, with a cut-off at 0.6 V. At first sight, this low voltage would seem to be a disadvantage, since the theoretical energy density will be low. However, it permits the use of lightweight materials that are immune from corrosion at the positive. The high utilization and low equivalent weight of the active material, together with the use of teflon-bonded graphite for current collection, result in very light positives, especially when these are compared with those in a derated nickel-hydrogen system. In addition, the weight of the pressure vessel falls somewhat, since the dead volume is lower. Calculations show that a total system will have 2.5 times the Ah capacity of a derated nickel-hydrogen LEO battery, so that the energy density, based on 1.2 V for nickel-hydrogen and 0.7 V for MnO2-hydrogen, will be 45 percent higher for comparable cycling performance.

Author

N89-22992*# National Aeronautics and Space Administration. Marshall Space Flight Center, Huntsville, AL.
CHARACTERIZATION TESTING OF A 40 AHR BIPOLAR NICKEL HYDROGEN BATTERY Abstract Only
Jeffrey C. Brewer, Michelle A. Manzo, and Randall F. Gahn (National Aeronautics and Space Administration. Lewis Research Center, Cleveland, OH.) *In* NASA, Lewis Research Center, Space Electrochemical Research and Technology Conference: Abstracts 1989 p 12-13 (For primary document see N89-22982 16-44)
Avail: NTIS HC A03/MF A01 CSCL 10A

In a continuing effort to develop NiH2 bipolar technology to a point where it can be used efficiently in space flight, testing of a second 40 Ahr, 10-cell bipolar battery has begun. This battery has undergone extensive characterization testing to determine the effects of such operating parameters as charge and discharge rates, temperature, and pressure. The fundamental design of this actively cooled bipolar battery is the same as the first battery. Most of the individual components, however, are from different manufacturers. Different testing procedures as well as certain unique battery characteristics make it difficult to directly compare the two sets of results. In general, the performance of this battery throughout characterization produced expected results. The main differences seen between the first and second batteries occurred during the high-rate discharge portion of the test matrix. The first battery also had poor high-rate discharge results, although better than those of the second battery. Minor changes were made to the battery frame design used for the first battery in an attempt to allow better gas access to the reaction sites for the second build and hopefully improve performance. The changes, however, did not improve the performance of the second battery and could have possibly contributed to the poorer performance that was observed. There are other component differences that could have contributed to the poorer performance of the second battery. The H2 electrode in the second battery was constructed with a Goretex backing which could have limited the high-rate current flow. The gas screen in the second battery had a larger mesh which again could have limited the high-rate current flow. Small scale 2 x 2 batteries are being tested to evaluate the effects of the component variations.

Author

N89-22993*# Giner, Inc., Waltham, MA.
ADVANCED DOUBLE LAYER CAPACITORS Abstract Only
c33
S. Sarangapani, P. Lessner, J. Forchione, and A. B. LaConti *In* NASA, Lewis Research Center, Space Electrochemical Research and Technology Conference: Abstracts 1989 p 14-15 (For primary document see N89-22982 16-44)
(Contract N00014-88-0391)
Avail: NTIS HC A03/MF A01 CSCL 09C

There is a need for large amounts of power to be delivered rapidly in a number of airborne and space systems. Conventional, portable power sources, such as batteries, are not suited to delivering high peak power pulses. The charge stored at the electrode-electrolyte double layer is, however, much more assessible on a short time scale. Devices exploiting this concept were fabricated using carbon and metal oxides (Pinnacle Research) as the electrodes and sulfuric acid as the electrolyte. The approach reported, replaces the liquid sulfuric acid electrolyte with a solid ionomer electrolyte. The challenge is to form a solid electrode-solid ionomer electrolyte composite which has a high capacitance per geometric area. The approach to maximize contact between the electrode particles and the ionomer was to impregnate the electrode particles using a liquid ionomer solution and to bond the solvent-free structure to a solid ionomer membrane. Ruthenium dioxide is the electrode material used. Three strategies are being pursued to provide for a high area electrode-ionomer contact: mixing of the RuOx with a small volume of ionomer solution followed by filtration to remove the solvent, and impregnation of the ionomer into an already formed RuOx electrode. RuOx powder and electrodes were examined by non-electrochemical techniques. X-ray diffraction has shown that the material is almost pure RuO2. The electrode structure depends on the processing technique used to introduce the Nafion. Impregnated electrodes have Nafion concentrated near the surface. Electrodes prepared by the evaporation method show large aggregates of crystals surrounded by Nafion.

Author

N89-22994*# Texas A&M Univ., College Station.
RECENT ADVANCES IN SOLID POLYMER ELECTROLYTE FUEL CELL TECHNOLOGY WITH LOW PLATINUM LOADING ELECTRODES Abstract Only
Supramaniam Srinivasan, David J. Manko, Mohammad Enayatullah, and A. John Appleby *In* NASA, Lewis Research Center, Space Electrochemical Research and Technology Conference: Abstracts 1989 p 16-17 (For primary document see N89-22982 16-44)
Avail: NTIS HC A03/MF A01 CSCL 10A

High power density fuel cell systems for defense and civilian applications are being developed. Taking into consideration the main causes for efficiency losses (activation, mass transport and ohmic overpotentials) the only fuel cell systems capable of achieving high power densities are the ones with alkaline and solid polymer electrolyte. High power densities (0.8 W/sq cm at 0.8 V and 1 A/sq cm with H2 and O2 as reactants), were already used in NASA's Apollo and Space Shuttle flights as auxiliary power sources. Even higher power densities (4 W/sq cm - i.e., 8 A sq cm at 0.5 V) were reported by the USAF/International Fuel Cells in advanced versions of the alkaline system. High power densities (approximately 1 watt/sq cm) in solid polymer electrolyte fuel cells with ten times lower platinum loading in the electrodes (i.e., 0.4 mg/sq cm) were attained. It is now possible to reach a cell potential of 0.620 V at a current density of 2 A/sq cm and at a temperature of 95 C and pressure of 4/5 atm with H2/O2 as reactants. The slope of the linear region of the potential-current density plot for this case is 0.15 ohm-sq cm. With H2/air as reactants and under the same operating conditions, mass transport limitations are encountered at current densities above 1.4 A/sq cm. Thus, the cell potential at 1 A/sq cm with H2/air as reactants is less than that with H2/O2 as reactants by 40 mV, which is the expected value based on electrode kinetics of the oxygen reduction reaction, and at 2 A/sq cm with H2/air as reactant is less than the corresponding value with H2/O2 as reactants by 250 mV, which is due to the considerably greater mass transport limitations in the former case.

Author

N89-22995*# Dow Chemical Co., Freeport, TX.
THE APPLICATION OF DOW CHEMICAL'S PERFLUORINATED MEMBRANES IN PROTON-EXCHANGE MEMBRANE FUEL CELLS Abstract Only
G. A. Eisman *In* NASA, Lewis Research Center, Space Electrochemical Research and Technology Conference: Abstracts 1989 p 18 (For primary document see N89-22982 16-44)
Avail: NTIS HC A03/MF A01 CSCL 10A

Dow Chemical's research activities in fuel cell devices revolves around the development and subsequent investigation of the perfluorinated inomeric membrane separator useful in proton-exchange membrane systems. Work is currently focusing on studying the effects of equivalent weight, thickness, water of hydration, pretreatment procedures, as well as the degree of water management required for a given membrane separator in the cell. The presentation will include details of certain aspects of the above as well as some of the requirements for high and low power generation. Author

N89-22996*# National Aeronautics and Space Administration. Lewis Research Center, Cleveland, OH.
HYDROGEN-OXYGEN PROTON-EXCHANGE MEMBRANE FUEL CELLS AND ELECTROLYZERS Abstract Only
R. Baldwin, M. Pham, A. Leonida, J. McElroy, and T. Nalette (Hamilton Standard, Windsor Locks, CT.) *In its* Space Electrochemical Research and Technology Conference: Abstracts 1989 p 19-20 (For primary document see N89-22982 16-44)
Avail: NTIS HC A03/MF A01 CSCL 10A

Hydrogen-oxygen SPE fuel cells and SPE electrolyzers (products of Hamilton Standard) both use a Proton-Exchange Membrane (PEM) as the sole electrolyte. The SPE cells have demonstrated a ten year life capability under load conditions. Ultimate life of PEM fuel cells and electrolyzers is primarily related to the chemical stability of the membrane. For perfluorocarbon proton-exchange membranes an accurate measure of the membrane stability is the fluoride loss rate. Millions of cell hours have contributed to establishing a relationship between fluroride loss rates and average expected ultimate cell life. Several features were introduced into SPE fuel cells and SPE electrolyzers such that applications requiring greater than or equal to 100,000 hours of life can be considered. Equally important as the ultimate life is the voltage stability of hydrogen-oxygen fuel cells and electrolyzers. Here again the features of SPE fuel cells and SPE electrolyzers have shown a cell voltage stability in the order of 1 microvolt per hour. That level of stability were demonstrated for tens of thousands of hours in SPE fuel cells at up to 500 amps per square foot (ASF) current density. The SPE electrolyzers have demonstrated the same at 1000 ASF. Many future extraterrestrial applications for fuel cells require that they be self recharged. To translate the proven SPE cell life and stability into a highly reliable extraterrestrial electrical energy storage system, a simplification of supporting equipment is required. Static phase separation, static fluid transport and static thermal control will be most useful in producting required system reliability. Although some 200,000 SPE fuel cell hours were recorded in earth orbit with static fluid phase separation, no SPE electrolyzer has, as yet, operated in space. Author

N89-22997*# Case Western Reserve Univ., Cleveland, OH.
ELECTROCATALYSTS FOR OXYGEN ELECTRODES IN FUEL CELLS AND WATER ELECTROLYZERS FOR SPACE APPLICATIONS Abstract Only
Jai Prakash, Donald Tryk, and Ernest Yeager *In* NASA, Lewis Research Center, Space Electrochemical Research and Technology Conference: Abstracts 1989 p 21-22 (For primary document see N89-22982 16-44)
Avail: NTIS HC A03/MF A01 CSCL 10A

In most instances separate electrocatalysts are needed to promote the reduction of O2 in the fuel cell mode and to generate O2 in the energy storage-water electrolysis mode in aqueous electrochemical systems operating at low and moderate temperatures (T greater than or equal to 200 C). Interesting exceptions are the lead and bismuth ruthenate pyrochlores in alkaline electrolytes. These catalysts on high area carbon supports have high catalytic activity for both O2 reduction and generation (1,2). Rotating ring-disk electrode measurements provide evidence that the O2 reduction proceeds by a parallel four-electron pathway. The ruthenates can also be used as self-supported catalysts to avoid the problems associated with carbon oxidation, but the electrode performance so far achieved in the research at Case Western Reserve University (CWRU) is considerably less. At the potentials involved in the anodic mode the ruthenate pyrochlores have substantial equilibrium solubility in concentrated alkaline electrolyte. This results in the loss of catalyst into the bulk solution and a decline in catalytic activity. Furthermore, the hydrogen generation counter electrode may become contaminated with reduction products from the pyrochlores (lead, ruthenium). A possible approach to this problem is to immobilize the pyrochlore catalyst within an ionic-conducting solid polymer, which would replace the fluid electrolyte within the porous gas diffusion O2 electrode. For bulk alkaline electrolyte, an anion-exchange polymer is needed with a transference number close to unity for the Oh(-) ion. Preliminary short-term measurements with lead ruthenates using a commercially available partially-fluorinated anion-exchange membrane as an overlayer on the porous gas-fed electrode indicate lower anodic polarization and virtually unchanged cathodic polarization. Author

N89-22998*# Giner, Inc., Waltham, MA.
OXYGEN ELECTRODES FOR RECHARGEABLE ALKALINE FUEL CELLS Abstract Only
L. Swette and N. Kackley *In* NASA, Lewis Research Center, Space Electrochemical Research and Technology Conference: Abstracts 1989 p 23-24 (For primary document see N89-22982 16-44)
(Contract NAS3-24635)
Avail: NTIS HC A03/MF A01 CSCL 10A

Electrocatalysts and supports for the positive electrode of moderate temperature single-unit rechargeable alkaline fuel cells are being investigated and developed. Candidate support materials were drawn from transition metal carbides, borides, nitrides and oxides which have high conductivity (greater than 1 ohm/cm). Candidate catalyst materials were selected largely from metal oxides of the form ABO sub x (where A = Pb, Cd, Mn, Ti, Zr, La, Sr, Na, and B = Pt, Pd, Ir, Ru, Ni (Co) which were investigated and/or developed for one function only, O2 reduction or O2 evolution. The electrical conductivity requirement for catalysts may be lower, especially if integrated with a higher conductivity support. All candidate materials of acceptable conductivity are subjected to corrosion testing. Materials that survive chemical testing are examined for electrochemical corrosion activity. For more stringent corrosion testing, and for further evaluation of electrocatalysts (which generally show significant O2 evolution at at 1.4 V), samples are held at 1.6 V or 0.6 V for about 100 hours. The surviving materials are then physically and chemically analyzed for signs of degradation. To evaluate the bifunctional oxygen activity of candidate catalysts, Teflon-bonded electrodes are fabricated and tested in a floating electrode configuration. Many of the experimental materials being studied have required development of a customized electrode fabrication procedure. In advanced development, the goal is to reduce the polarization to about 300 to 350 mV. Approximately six support materials and five catalyst materials were identified to date for further development. The test results will be described. Author

N89-22999*# Giner, Inc., Waltham, MA.
NON-NOBLE ELECTROCATALYSTS FOR ALKALINE FUEL CELLS Abstract Only
S. Sarangapani, P. Lessner, M. Manoukian, and J. Giner *In* NASA, Lewis Research Center, Space Electrochemical Research and Technology Conference: Abstracts 1989 p 25-26 (For primary document see N89-22982 16-44)
(Contract DE-AC02-87ER-80500)
Avail: NTIS HC A03/MF A01 CSCL 10A

Carbons activated with macrocyclics have attracted increasing attention as alternative electrocatalysts for oxygen reduction. Initial activity of these catalysts is good, but performance declines rapidly.

Pyrolyzing the macrocyclic on the carbon support leads to enhanced stability and the catalysts retain good activity. The approach described is designed to develop bulk doped catalysts with similar structures to pyrolyzed macrocyclic catalysts. The transition metal and coordinated ligands are dispersed throughout the bulk of the conductive carbon skeleton. Two approaches to realizing this concept are being pursued, both involving the doping of carbon precursors. In one approach, the precursor is a solid phase carbon-containing ion-exchange resin. The precursor is doped with a transition metal and/or nitrogen, and the resulting mixture is pyrolyzed. In the other approach, the precursor is a gas-phase hydrocarbon. This is introduced with a transition metal species and nitrogen species into a reactor and pyrolyzed. Several studies have been conducted to determine if there is a synergistic effect between the transition metal and nitrogen and the effect of different methods of introducing the metal-nitrogen (M-N) coordination on performance. One approach was to introduce the metal and nitrogen separately, for example, by sequentially doping FeCl3 and NH4OH into the resin. Catalysts were prepared from an undoped ion-exchange resin, a resin doped only with N, a resin doped only with Fe, and a resin doped with both Fe and N. Introduction of nitrogen alone has no beneficial effect on the performance of the catalysts. The introduction of the Fe alone significantly improves the performance in both the high and low current density regions. When both Fe and N are introduced, the performance at lower current densities (catalytic activity) is increased beyond that of the Fe-doped carbon, but the performance at higher current densities is similar to the carbon containing only Fe. Catalysts prepared from resins-Fe(bipy)3SO4 precursors have performance that is only slightly less then CoTMPP adsorbed and pyroloyzed on Vulcan XC-72. Their performance is much better than carbons which have had the N and Fe introduced separately. Author

N89-23000*# National Aeronautics and Space Administration. Lewis Research Center, Cleveland, OH.

CORROSION TESTING OF CANDIDATES FOR THE ALKALINE FUEL CELL CATHODE Abstract Only

Joseph Singer and William L. Fielder *In its* Space Electrochemical Research and Technology Conference: Abstracts 1989 p 27 (For primary document see N89-22982 16-44)
(Contract NAS3-25119)
Avail: NTIS HC A03/MF A01 CSCL 10A

It is desirable to employ a corrosion screening test for catalyst or support candidates for the fuel cell cathode before entering upon optimization of the candidate or of the catalytic electrode. To this end, corrosion test electrodes, intended for complete immersion and maximum wetting, have been made with 30 to 40 vol. pct Teflon; with perovskites this is about 10 to 15 pct. The candidates were synthesized by methods intended for single-phase product without special emphasis on high surface area, although the substances tested were no coarser than 2 m squared/g. A typical loading was 25 mg/cm sq of the pure substance, usually on gold screen, a few mm squared of which were left bare for contacting. Contact to the gold lead wire was made by welding with a micro-torch or a spot-welder. Corrosion testing consisted of obtaining current-voltage data under flowing inert gas in the potential region for reduction of O2. The electrode was immersed in 30 pct KOH. Observations were made at 20 C and 80 C, and the results compared with data from gold standards. Results with some perovskites, pyrochlores, spinels, and interstitial compounds will be discussed. Author

N89-23001*# Michigan Technological Univ., Houghton.

STRUCTURAL COMPARISON OF NICKEL ELECTRODES AND PRECURSOR PHASES Abstract Only c33

Bahne C. Cornilsen, Xiaoyin Shan, and Patricia Loyselle *In* NASA, Lewis Research Center, Space Electrochemical Research and Technology Conference: Abstracts 1989 p 28 (For primary document see N89-22982 16-44)
Avail: NTIS HC A03/MF A01 CSCL 09C

A summary of previous Raman spectroscopic results and a discussion of important structural differences in the various phases of active mass and active mass precurors are presented. Raman spectra provide unique signatures for these phases, and allow one to distinguish each phase, even when the compound is amorphous to X-rays (i.e., does not scatter X-rays because of a lack of order and/or small particle size). The structural changes incurred during formation, charge and discharge, cobalt addition, and aging will be discussed and related to electrode properties. Important structural differences include NiO2 layer stacking, nonstoichiometry (especially cation-deficit nonstoichiometry), disorder, dopant content, and water content. The results indicate that optimal nickel active mass is non-close packed and nonstoichiometric. The formation process transforms precursor phases into this structure. Therefore, the precursor disorder, or lack thereof, influences this final active mass structure and the rate of formation. Aging processes induce structural change which is believed to be detrimental. The role of cobalt addition can be appreciated in terms of structures favored or stabilized by the dopant. In recent work, the in situ Raman technique to characterize the critical structural parameters was developed. An in situ method relates structure, electrochemistry, and preparation. In situ Raman spectra of cells during charge and discharge, either during cyclic voltammetry or under constant current conditions were collected. With the structure-preparation knowledge and the in situ Raman tool, it will be possible to define the structure-property-preparation relations in more detail. This instrumentation has application to a variety of electrode systems. Author

N89-23002*# National Aeronautics and Space Administration. Lewis Research Center, Cleveland, OH.

IMPEDANCE STUDIES OF Ni/Cd AND Ni/H CELLS USING THE CELL CASE AS REFERENCE ELECTRODE Abstract Only c33

Margaret A. Reid *In its* Space Electrochemical Research and Technology Conference: Abstracts 1989 p 29 (For primary document see N89-22982 16-44)
Avail: NTIS HC A03/MF A01 CSCL 09C

Many impedance studies were carried out on Ni electrodes and Ni/Cd and Ni/H batteries. In order for impedance to become a diagnostic tool, accurate and reproducible measurements must be made, and some way of separating the contributions of the individual electrodes must be found. Using the PAR and the Solartron impedance equipment, studies have found that consistent measurements can be made if the cells or electrodes are equilibrated at the voltage of interest. In the charged state, equilibration times required are short, on the order of a few hours or less, but the equilibration time required becomes progessively longer as the voltage is lowered. The cell case can be used as a reference electrode during impedance measurements. The voltage of the case with respect to the electrodes is unimportant provided that it does not change appreciably during the course of the measurement. Measurements were made with several uncycled Ni/Cd cells, one from a lot which was known to have faulty Cd electrodes and another from a lot which showed excellent cycle life and presumably had good Cd electrodes. The impedances of the Ni electrodes vs. the case were similar, while the impedance of the poor Cd electrodes vs. the case. A 50 AH Ni/H cell was also investigated. After subtraction of the ohmic resistances, the sums of the impedances of the individual electrodes were very close to the impedance of the total cell. This indicates that the method is valid for examining the characteristics of the individual electrodes in situ. Author

N89-23003*# SRI International Corp., Menlo Park, CA.

THE APPLICATION OF ELECTROCHEMICAL IMPEDANCE SPECTROSCOPY FOR CHARACTERIZING THE DEGRADATION OF Ni(OH)2/NiOOH ELECTRODES Abstract Only c25

Digby D. Macdonald *In* NASA, Lewis Research Center, Space Electrochemical Research and Technology Conference: Abstracts 1989 p 30 (For primary document see N89-22982 16-44)
Avail: NTIS HC A03/MF A01 CSCL 07D

The use of wide-band electrochemical impedance spectroscopy is described for characterizing the degradation of porous

Ni(OH)2/NiOOH electrodes in concentrated KOH electrolyte solutions. The impedance spectra are interpreted in terms of a finite electrical transmission line and the changes in the components of the electrical analog are followed as a function of cycle number. The degradation of the capacity of rolled and bonded Ni(OH)2/NiOOH electrodes is caused by rupture of ohmic contacts within the active mass and by restructuring which results in a decrease in the number of active pores. Author

N89-23004*# Hughes Aircraft Co., Los Angeles, CA.
KOH CONCENTRATION EFFECT ON THE CYCLE LIFE OF NICKEL-HYDROGEN CELLS. 4: RESULTS OF FAILURE ANALYSE Abstract Only
H. S. Lim and S. A. Verzwyvelt *In* NASA, Lewis Research Center, Space Electrochemical Research and Technology Conference: Abstracts 1989 p 31 (For primary document see N89-22982 16-44)
Avail: NTIS HC A03/MF A01 CSCL 10A

Effects of KOH concentrations on failure modes and mechanisms of nickel-hydrogen cells were studied using long cycled boiler plate cells containing electrolytes of various KOH concentrations ranging 21 to 36 percent. Life of these cells were up to 40,000 cycles in an accelerated low earth orbit (LEO) cycle regime at 80 percent depth of discharge. An interim life test results were reported earlier in J. Power Sources, 22, 213-220, 1988. The results of final life test, end-of-life cell performance, and teardown analyses are discussed. These teardown analyses included visual observations, measurements of nickel electrode capacity in an electrolyte-flooded cell, dimensional changes of cell components, SEM studies on cell cross section, BET surface area and pore volume distribution in cycled nickel electrodes, and chemical analyses. Cycle life of a nickel-hydrogen cell was improved tremendously as KOH concentration was decreased from 36 to 31 percent and from 31 to 26 percent while effect of further concentration decrease was complicated as described in our earlier report. Failure mode of high concentration (31 to 36 percent) cells was gradual capacity decrease, while that of low concentration (21 to 26 percent) cells was mainly formation of a soft short. Long cycled (25,000 to 40,000 cycles) nickel electrodes were expanded more than 50 percent of the initial value, but no correlation was found between this expansion and measured capacity. All electrodes cycled in low concentration (21 to 26 percent) cells had higher capacity than those cycled in high concentration (31 to 36 percent) cells. Author

N89-23005*# Eagle-Picher Industries, Inc., Joplin, MO.
ADVANCES IN LIGHTWEIGHT NICKEL ELECTRODE TECHNOLOGY Abstract Only **c33**
Dwaine Coates, Gary Paul, James R. Wheeler, and Paul Daugherty *In* NASA, Lewis Research Center, Space Electrochemical Research and Technology Conference: Abstracts 1989 p 32 (For primary document see N89-22982 16-44)
Avail: NTIS HC A03/MF A01 CSCL 09C

Studies are currently underway to further the development of lightweight nickel electrode technology. Work is focused primarily on the space nickel-hydrogen system and nickel-iron system but is also applicable to the nickel-cadmium and nickel-zinc systems. The goal is to reduce electrode weight while maintaining or improving performance thereby increasing electrode energy density. Two basic electrode structures are being investigated. The first is the traditional nickel sponge produced from sintered nickel-carbonyl powder and the second is a new material for this application which consists of a non-woven mat of nickel fiber. Electrodes are being manufactured, tested and evaluated at the electrode and cell level. Author

N89-23006*# Eagle-Picher Industries, Inc., Joplin, MO.
MULTI-MISSION NI-H2 BATTERY CELL FOR THE 1990'S Abstract Only
Lee Miller, Jack Brill, and Gary Dodson *In* NASA, Lewis Research Center, Space Electrochemical Research and Technology Conference: Abstracts 1989 p 33 (For primary document see N89-22982 16-44)
Avail: NTIS HC A03/MF A01 CSCL 10A

A sufficient production, test and operational database is now available to permit design technology optimization for the next decade. The evolved battery cell design features standardized technology intended to support multiple type missions (e.g., both GEO and LEO). Design analyses and validation test cells demonstrate improved performance plus attractive specific-energy characteristics will be achieved. Author

N89-23007*# National Aeronautics and Space Administration. Lewis Research Center, Cleveland, OH.
NICKEL-HYDROGEN CAPACITY LOSS ON STORAGE Abstract Only **c33**
Michelle A. Manzo *In its* Space Electrochemical Research and Technology Conference: Abstracts 1989 p 34 (For primary document see N89-22982 16-44)
Avail: NTIS HC A03/MF A01 CSCL 09C

Nickel-hydrogen batteries are rapidly becoming accepted for use in low-earth-orbit and geosynchronous orbit applications. With their increased use it has become evident that the storage procedures commonly used for nickel-cadmium cells are not adequate for the nickel-hydrogen system. The capacity loss exhibited by nickel electrodes from various manufacturers when exposed to different storage conditions was determined. A comprehensive test matrix was developed to evaluate capacity loss in nickel electrodes from four different manufacturers. Two types of tests were run; individual electrode tests, which involved flooded capacity and impedance measurements before and after storage under varied conditions of temperature, hydrogen pressure, and electrolyte concentration; and cell tests which primarily evaluated the effects of state-of-charge on storage. The cell tests evaluated capacity loss on cells stored open circuit, shorted and trickle charged at C/100 following a full charge. The results indicate that capacity loss varies with the specific electrode manufacturing process, storage temperature and hydrogen pressure. In general, electrodes stored at low temperatures or low hydrogen pressures exhibited a smaller loss in capacity over the twenty-eight day storage period than those stored at high pressure and high temperature. The capacity loss appears to correlate with the level of cobalt in the nickel electrode, with the most significant loss of capacity occurring in electrodes with higher cobalt levels. Impedance measurements appear to correlate well with the capacity loss observed for a given type of electrode but do not correlate well with the capacity loss between electrodes fabricated by different manufacturers. There was a definite correlation between the electrode potential measured immediately following storage and the measured capacity loss. Author

N89-23008*# Boeing Aerospace Co., Seattle, WA.
HYDROGEN EMBRITTLEMENT IN NICKEL-HYDROGEN CELLS Abstract Only
Sidney Gross *In* NASA, Lewis Research Center, Space Electrochemical Research and Technology Conference: Abstracts 1989 p 35 (For primary document see N89-22982 16-44)
Avail: NTIS HC A03/MF A01 CSCL 10A

It was long known that many strong metals can become weakened and brittle as the result of the accumulation of hydrogen within the metal. When the metal is stretched, it does not show normal ductile properties, but fractures prematurely. This problem can occur as the result of a hydrogen evolution reaction such as corrosion or electroplating, or due to hydrogen in the environment at the metal surface. High strength alloys such as steels are especially susceptible to hydrogen embrittlement. Nickel-hydrogen cells commonly use Inconel 718 alloy for the pressure container, and this also is susceptible to hydrogen embrittlement. Metals differ in their susceptibility to embrittlement. Hydrogen embrittlement in nickel-hydrogen cells is analyzed and the reasons why it may or may not occur are discussed. Although Inconel 718 can display hydrogen embrittlement, experience has not identified any problem with nickel-hydrogen cells. No hydrogen embrittlement problem is expected with the 718 alloy pressure container used in nickel-hydrogen cells. Author

N89-23009*# Ford Aerospace and Communications Corp., Palo Alto, CA.
SODIUM SULFUR BATTERY FLIGHT EXPERIMENT DEFINITION STUDY Abstract Only
Rebecca R. Chang and Robert Minck (Ford Aerospace and Communications Corp., Newport Beach, CA.) *In* NASA, Lewis Research Center, Space Electrochemical Research and Technology Conference: Abstracts 1989 p 36 (For primary document see N89-22982 16-44)
Avail: NTIS HC A03/MF A01 CSCL 10A

Sodium-sulfur batteries were identified as the most likely successor to nickel-hydrogen batteries for space applications. One advantage of the Na/S battery system is that the usable specific energy is two to three times that of nickel-hydrogen batteries. This represents a significant launch cost savings or increased payload mass capabilities. Sodium-sulfur batteries support NASA OAST's proposed Civil Space Technology Initiative goal of a factor of two improvement in spacecraft power system performance, as well as the proposed Spacecraft 2000 initiative. The sodium-sulfur battery operates at between 300 and 400 C, using liquid sodium and sulfur/polysulfide electrodes and solid ceramic electrolyte. The transport of the electrode materials to the surface of the electrolyte is through wicking/capillary forces. These critical transport functions must be demonstrated under actual microgravity conditions before sodium-sulfur batteries can be confidently utilized in space. Ford Aerospace Corporation, under contract to NASA Lewis Research Center, is currently working on the sodium-sulfur battery space flight experiment definition study. The objective is to design the experiment that will demonstrate operation of the sodium-sulfur battery/cell in the space environment with particular emphasis on evaluation of microgravity effects. Experimental payload definitions were completed and preliminary designs of the experiment were defined. Author

N89-23010*# Argonne National Lab., IL.
ADVANCED HIGH-TEMPERATURE BATTERIES Abstract Only
Paul A. Nelson *In* NASA, Lewis Research Center, Space Electrochemical Research and Technology Conference: Abstracts 1989 p 37-38 (For primary document see N89-22982 16-44)
Avail: NTIS HC A03/MF A01 CSCL 10A

The promise of very high specific energy and power was not yet achieved for practical battery systems. Some recent approaches are discussed for new approaches to achieving high performance for lithium/DeS2 cells and sodium/metal chloride cells. The main problems for the development of successful LiAl/FeS2 cells were the instability of the FeS2 electrode, which has resulted in rapidly declining capacity, the lack of an internal mechanism for accommodating overcharge of a cell, thus requiring the use of external charge control on each individual cell, and the lack of a suitable current collector for the positive electrode other than expensive molybdenum sheet material. Much progress was made in solving the first two problems. Reduction of the operating temperatures to 400 C by a change in electrolyte composition has increased the expected life to 1000 cycles. Also, a lithium shuttle mechanism was demonstrated for selected electrode compositions that permits sufficient overcharge tolerance to adjust for the normally expected cell-to-cell deviation in coulombic efficiency. Sodium/sulfur batteries and sodium/metal chloride batteries have demonstrated good reliability and long cycle life. For applications where very high power is desired, new electrolyte coinfigurations would be required. Design work was carried out for the sodium/metal chloride battery that demonstrates the feasibility of achieving high specific energy and high power for large battery cells having thin-walled high-surface area electrolytes. Author

N89-23011*# Jet Propulsion Lab., California Inst. of Tech., Pasadena.
ADVANCES IN AMBIENT TEMPERATURE SECONDARY LITHIUM CELLS Abstract Only
S. Subbarao, D. H. Shen, F. Deligiannis, C-K. Huang, and G. Halpert *In* NASA, Lewis Research Center, Space Electrochemical Research and Technology Conference: Abstracts 1989 p 39 (For primary document see N89-22982 16-44)
Avail: NTIS HC A03/MF A01 CSCL 10A

The Jet Propulsion Laboratory is involved in a Research and Development program sponsored by NASA/OAST on the development of ambient temperature secondary lithium cells for future space applications. Some of the projected applications are planetary spacecraft, planetary rovers, and astronaut equipment. The main objective is to develop secondary lithium cells with greater than 100 Wh/kg specific energy while delivering 1000 cycles at 50 percent Depth of Discharge (DOD). To realize these ambitious goals, the work was initially focused on several important basic issues related to the cell chemistry, selection of cathode materials and electrolytes, and component development. The performance potential of Li-TiS2, Li-MoS3, Li-V6O13 and Li-NbSe3 electrochemical systems was examined. Among these four, the Li-TiS2 system was found to be the most promising system in terms of realizable specific energy and cycle life. Some of the major advancements made so far in the development of Li-TiS2 cells are in the areas of cathode processing technology, mixed solvent electrolytes, and cell assembly. Methods were developed for the fabrication of large size high performance TiS2 cathodes. Among the various electrolytes examined, 1.5M LiAsF6/EC + 2-MeTHF mixed solvent electrolyte was found to be more stable towards lithium. Experimental cells activated with this electrolyte exhibited more than 300 cycles at 100 percent Depth of Discharge. Work is in progress in other areas such as selection of lithium alloys as candidate anode materials, optimization of cell design, and development of 5 Ah cells. The advances made at the Jet Propulsion Laboratory on the development of secondary lithium cells are summarized. Author

N89-23012# Sandia National Labs., Albuquerque, NM.
PHOTOVOLTAIC SYSTEMS FOR TODAY'S REMOTE POWER APPLICATIONS
H. N. Post, M. G. Thomas, and V. Vernon Risser 1989 7 p Presented at the 4th International Photovoltaic Science and Engineering Conference, Sydney, Australia, 14 Feb. 1989
(Contract DE-AC04-76DP-00789)
(DE89-007431; SAND-89-0332C; CONF-890211-2) Avail: NTIS HC A02/MF A01

The Design Assistance Center (DAC) has developed a database of design, performance, and operating experience for remote photovoltaic (PV) systems. The DAC uses this database to assist potential users in evaluating PV for their specific applications and to accelerate the acceptance of PV as a viable power option for remote applications. DOE

N89-23013# Sandia National Labs., Albuquerque, NM.
ADVANCES IN CONCENTRATOR CELL TECHNOLOGY
David L. King 1989 9 p Presented at the 4th International Photovoltaic Science and Engineering Conference, Sydney, Australia, 14 Feb. 1989
(Contract DE-AC04-76DP-00789)
(DE89-007432; SAND-89-0382C; CONF-890211-1) Avail: NTIS HC A02/MF A01

The dramatic improvement in silicon concentrator cell efficiency recently demonstrated in university laboratories has had a significant influence on concentrator technology development. This paper briefly describes concentrator field experience, economics, current technology paths, and concludes with a detailed summary of concentrator cell performance. DOE

N89-23014# Industrial Science and Technology Agency, Tokyo (Japan).
JAPAN'S SUNSHINE PROJECT 1987 ANNUAL SUMMARY OF SOLAR ENERGY R AND D PROGRAM
Apr. 1988 460 p In JAPANESE
(DE88-756452; AIST-8805) Avail: NTIS (US Sales Only) HC A20

Results on Japanese sunshine project in 1987 are summarized as to fundamental research, development for practical use and international cooperation to utilize solar photo and thermal energy

as follows: Solar photo-utilizing technology consists of the research of solar photo-voltatic power generating system (basic research, new type solar cell, amorphous silicon), and the practical utilization of solar photo-voltatic power generating system (lower cost silicon, solar panel, high efficiency crystal type solar cell, amorphous solar cell, solar cell evaluation system, peripheral technology, independent dispersive and centralized solar photo-voltatic power generating systems, photo and thermal hybrid solar photo-voltatic power generating system). Solar thermal utilizing technology consists of research of solar thermal and photo-voltatic power generating system (combined thermal-power solar system), solar air conditioning and hot water supplying system, and development of real industrial solar system. International cooperation means the solar energy technical cooperation project between Japan and Australia. DOE

N89-23015# Sandia National Labs., Albuquerque, NM.
AN ASSESSMENT OF THE OPTICAL PERFORMANCE OF STRETCHED-MEMBRANE MIRROR MODULES
D. J. Alpert and R. M. Houser 1988 16 p Presented at the American Society of Mechanical Engineers Solar Energy Conference, San Diego, CA, 2 Apr. 1989
(Contract DE-AC04-76DP-00789)
(DE88-017347; SAND-88-1651C; CONF-890436-2) Avail: NTIS HC A03/MF A01

The United States Department of Energy's solar thermal program is developing an innovative concept for the heliostats used in a solar central-receiver power plant: replacing the familiar glass mirrors with stretched-membrane reflectors. This paper presents Sandia's assessment of first- and second-generation mirror modules made of stretched membranes. The first of these prototype mirror modules were built in 1986 by two contractors to Sandia. Solar Kinetics, Inc., produced a module with optical characteristics equaling those of heliostats that use glass mirrors. The first design produced by Science Applications International Corp. proved to be unworkable. Using the experience gained with the first models, the same two contractors are currently building improved prototypes. The improved designs will be easier to fabricate and will perform better than the first-generation designs. SAIC's second design has been installed at the Central Receiver Test Facility, and Sandia's preliminary assessment shows the quality of its beam to be as good as SKI's original design. SKI is currently in the process of installing its second prototype. The final paper will include detailed results of the second-generation prototypes' beam quality, focusing systems, defocusing capabilities, and durability. DOE

N89-23016# Sandia National Labs., Albuquerque, NM.
COMPARISON OF A CAVITY SOLAR RECEIVER NUMERICAL MODEL AND EXPERIMENTAL DATA
R. E. Hogan, R. B. Diver, and W. B. Stine (California State Polytechnic Univ., Pomona.) 1988 8 p Presented at the American Society of Mechanical Engineers Solar Energy Conference, San Diego, CA, 2 Apr. 1989
(Contract DE-AC04-76DP-00789)
(DE89-003609; SAND-88-1847C; CONF-890436-3) Avail: NTIS HC A02/MF A01

A numerical model which predicts the thermal environment in axisymmetric solar cavity receivers is described. The computed energy transfer rates and temperatures are compared to experimental data for tests of a novel test bed receiver in the Sandia National Laboratories solar furnace. In general, the numerical model captures the trends observed in the experimental data. Sensitivity analyses show that the total solar energy input rate and the convective heat loss coefficient have a significant effect on the thermal performance and that the input solar flux distribution has a significant effect on the receiver temperature distribution in these experiments. DOE

N89-23017# Sandia National Labs., Albuquerque, NM.
DESIGN CONSIDERATIONS FOR HEAT-PIPE SOLAR RECEIVERS
Douglas R. Adkins 1989 24 p Presented at the American Society of Mechanical Engineers Solar Energy Conference, San Diego, CA, 2 Apr. 1989
(Contract DE-AC04-76DP-00789)
(DE89-004037; SAND-88-3072C; CONF-890436-5) Avail: NTIS HC A03/MF A01

Heat pipes are being developed to transfer solar energy from the focal point of a parabolic dish concentrator to the working fluid of Stirling engines. With these receivers, concentrated solar energy that is absorbed on the concave surface of a dome is removed by the evaporation of liquid sodium on the convex side of the dome. Vaporized sodium then condenses on an engine's heater tubes and transfers energy to the working fluid of the engine. The condensed sodium returns to the absorber surface where it is redistributed across the dome by the capillary action of a wick. Issues concerning the flow of sodium in a heat pipe solar receiver are investigated in this paper. A comparison is made between various wick options, and general issues concerning the design of heat pipe receivers are also discussed. DOE

N89-23018# Argonne National Lab., IL.
SOLAR RADIATION AT THE EARTH'S SURFACE: WHAT ARE WE DOING TO IT AND WITH IT?
David R. Cook 1989 20 p
(Contract W-31-109-eng-38)
(DE89-008446; ANL/PPRNT-89-98) Avail: NTIS HC A03/MF A01

This document is a brief overview of current and future applications of solar energy. Topics include solar radiation and climate, surface absorption and reflection, solar collectors, energy storage devices, and solar radiation protection. DOE

N89-23019# California Univ., Berkeley. Lawrence Berkeley Lab. Applied Sciences Div.
TECHNOLOGY BASE RESEARCH PROJECT FOR ELECTROCHEMICAL ENERGY STORAGE Annual Report, 1987
Kim Kinoshita, ed. Jul. 1988 63 p
(Contract DE-AC03-76SF-00098)
(DE89-008860; LBL-25507) Avail: NTIS HC A04/MF A01

The progress made by the technology base research (TBR) project for electrochemical energy storage during calendar year 1987 was summarized. The primary objective of the TBR Project, which is sponsored by the Department of Energy (DOE) and managed by Lawrence Berkeley Laboratory (LBL), is to identify electrochemical technologies that can satisfy stringent performance and economic requirements for electric vehicles and stationary energy storage applications. The ultimate goal is to transfer the most promising electrochemical technologies to the private sector or to another DOE project (e.g., Sandia National Laboratories' Exploratory Technology Development and Testing Project) for further development and scale-up. Besides LBL, which has overall responsibility for the TBR Project, Los Alamos National Laboratory (LANL), Brookhaven National Laboratory (BNL) and Argonne National Laboratory (ANL) participate in the TBR Project by providing key research support in several of the project elements. The TBR Project consists of three major project elements: exploratory research; applied science research; and air systems research. The objectives and the specific battery and electrochemical systems addressed by each project element are discussed in the following sections, which also include technical summaries that relate to the individual projects. Financial information that relates to the various projects and a description of the management activities for the TBR Project are described in the Executive Summary. GRA

N89-23020# Midwest Research Inst., Golden, CO. Solar Energy Research Inst.
SOLAR THERMAL PROGRAM SUMMARY. VOLUME 1: OVERVIEW, FISCAL YEAR 1988
Feb. 1989 22 p
(Contract DE-AC02-83CH-10093)
(DE89-000860; DOE/CH-10093/45-Vol-1) Avail: NTIS HC A03/MF A01

The goal of the solar thermal program is to improve overall

solar thermal systems performance and provide cost-effective energy options that are strategically secure and environmentally benign. Major research activities include energy collection technology, energy conversion technology, and systems and applications technology for both CR and DR systems. This research is being conducted through research laboratories in close coordination with the solar thermal industry, utilities companies, and universities. The Solar Thermal Technology Program is pursuing the development of critical components and subsystems for improved energy collection and conversion devices. This development follows two basic paths: for CR systems, critical components include stretched membrane heliostats, direct absorption receivers (DARs), and transport subsystems for molten salt heat transfer fluids. These components offer the potential for a significant reduction in system costs; and for DR systems, critical components include stretched membrane dishes, reflux receivers, and Stirling engines. These components will significantly increase system reliability and efficiency, which will reduce costs. The major thrust of the program is to provide electric power. However, there is an increasing interest in the use of concentrated solar energy for applications such as detoxifying hazardous wastes and developing high-value transportable fuels. These potential uses of highly concentrated solar energy still require additional experiments to prove concept feasibility. The program goal of economically competitive energy reduction from solar thermal systems is being cooperatively addressed by industry and government. DOE

N89-23021# Midwest Research Inst., Golden, CO. Solar Energy Research Inst.
RESEARCH ON AMORPHOUS-SILICON-BASED, THIN-FILM PHOTOVOLTAIC DEVICES, TASK B Annual Report, 1 Jan. - 31 Aug. 1988
W. Bottenberg and K. Mitchell Mar. 1989 70 p
(Contract DE-AC02-83CH-10093)
(DE89-000885; SERI/STR-211-3446) Avail: NTIS HC A04/MF A01

This report contains results of research undertaken to develop 13 percent efficient four-terminal hybrid tandem photovoltaic submodules with an aperture area of 850 sq cm. The modules would have a copper-indium-diselenide-based (CIS) bottom circuit and a semitransparent thin-film silicon-hydrogen (TFS) top circuit. The work resulted in a measured efficiency of 14.5 percent for the 4-sq cm CIS/TFS tandem device and 12.3 percent for the tandem 30 x 30 cm submodule, which exceeded project goals. Stability remained an important issue for TFS in terms of performance, however. An initial loss of 15 to 20 percent was typical. The data suggest no fundamental stability problem with CIS. DOE

N89-23022# Midwest Research Inst., Golden, CO. Solar Energy Research Inst.
RESEARCH ON AMORPHOUS-SILICON-BASED, THIN-FILM PHOTOVOLTAIC DEVICES, TASK B Annual Report, 16 Mar. 1987 - 15 Mar. 1988
A. E. Delahoy, E. Eser, and F. Kampas Mar. 1989 71 p
(Contract DE-AC02-83CH-10093)
(DE89-000886; SERI/STR-211-3487) Avail: NTIS HC A04

This report describes the results of Phase 1 of research undertaken to study area-related problems associated with the performance of amorphous silicon based photovoltaic submodules. Objectives are to determine the optimum submodule configuration; demonstrate proof-of-concept, single-junction submodules with 10 percent conversion efficiency over an area larger than 900 sq cm; and demonstrate proof-of-concept tandem submodules with 9 percent conversion efficiency over an area larger than 900 sq cm. The research was divided into three subtask areas: semiconductor materials, nonsemiconductor materials, and submodules. DOE

N89-23023# Argonne National Lab., IL.
FABRICATION OF SOLID OXIDE FUEL CELL BY ELECTROCHEMICAL VAPOR DEPOSITION Patent Application
Brian Riley, inventor (to DOE) and Bernard E. Szreders, inventor (to DOE) 26 Apr. 1988 20 p Prepared in cooperation with Combustion Engineering, Inc., Stamford, CT
(Contract W-31-109-eng-38)
(DE89-009605; PATENTS-US-A7184476;
US-Patent-Appl-SN-184476) Avail: NTIS HC A03/MF A01

In a high temperature solid oxide fuel cell (SOFC), the deposition of an impervious high density thin layer of electrically conductive interconnector material, such as magnesium doped lanthanum chromite, and of an electrolyte material, such as yttria stabilized zirconia, onto a porous support/air electrode substrate surface is carried out at high temperatures (approx. 1100 to 1300 C) by a process of electrochemical vapor deposition. In this process, the mixed chlorides of the specific metals involved react in the gaseous state with water vapor resulting in the deposit of an impervious thin oxide layer on the support tube/air electrode substrate of between 20 and 50 microns in thickness. An internal heater, such as a heat pipe, is placed within the support tube/air electrode substrate and induces a uniform temperature profile therein so as to afford precise and uniform oxide deposition kinetics in an arrangement which is particularly adapted for large scale, commercial fabrication of SOFCs. DOE

N89-23024# Argonne National Lab., IL.
SOLID OXIDE FUEL CELL MATRIX AND MODULES Patent Application
Brian Riley, inventor (to DOE) 22 Apr. 1988 33 p Prepared in cooperation with Combustion Engineering, Inc., Stamford, CT
(Contract W-31-109-eng-38)
(DE89-009607; PATENTS-US-A7184918;
US-Patent-Appl-SN-184918) Avail: NTIS HC A03/MF A01

Porous refractory ceramic blocks arranged in an abutting, stacked configuration and forming a three dimensional array provide a support structure and coupling means for a plurality of solid oxide fuel cells (SOFCs). The stack of ceramic blocks is self-supporting, with a plurality of such stacked arrays forming a matrix enclosed in an insulating refractory brick structure having an outer steel layer. The necessary connections for air, fuel, burnt gas, and anode and cathode connections are provided through the brick and steel outer shell. The ceramic blocks are so designed with respect to the strings of modules that by simple and logical design the strings could be replaced by hot reloading if one should fail. The hot reloading concept has not been included in any previous designs. DOE

N89-23025*# National Aeronautics and Space Administration. Lewis Research Center, Cleveland, OH.
InP (INDIUM PHOSPHIDE): INTO THE FUTURE
Henry W. Brandhorst, Jr. Mar. 1989 10 p Presented at the 1st International Conference on Indium Phosphide, Norman OK, 20-22 Mar. 1989; sponsored by the Society of Photo-Optical Instrumentation Engineers
(NASA-TM-102058; E-4816; NAS 1.15:102058) Avail: NTIS HC A02/MF A01 CSCL 10A

Major industry is beginning to be devoted to indium phosphide and its potential applications. Key to these applications are high speed and radiation tolerance; however the high cost of indium phosphide may be an inhibitor to progress. The broad applicability of indium phosphide to many devices will be discussed with an emphasis on photovoltaics. Major attention is devoted to radiation tolerance and means of reducing cost of devices. Some of the approaches applicable to solar cells may also be relevant to other devices. The intent is to display the impact of visionary leadership in the field and enable the directions and broad applicability of indium phosphide. Author

N89-22627# Joint Publications Research Service, Arlington, VA.
POWER SUPPLY IN SPACE
Sergey Dmitriyevich Grishin and Sergey Vasilyevich Chekalin *In its* JPRS Report: Science and Technology. USSR: Space 17 Aug. 1988 p 43-46 Transl. into ENGLISH from Problemy Osvoyeniya Kosmosa (Novoye v Zhizni, Nauke, Tekhnike: Seriya Kosmonavtika, Astronomiya) (Moscow, USSR), no. 1, Jan. 1988 p

27-36 (For primary document see N89-22622 16-12)
Copyright Avail: NTIS HC A05/MF A01

45 ENVIRONMENT POLLUTION

Includes atmospheric, noise, thermal, and water pollution.

N89-23026# Gesellschaft fuer Strahlen- und Umweltforschung m.b.H., Munich (Germany, F.R.). Projekttraegerschaften.
SEASONAL AND LATITUDINAL VARIATIONS OF THE TEMPORAL VARIANCE OF OZONE AND OF THE POTENTIAL TEMPERATURE Final Report
Ernest-Peter Roeth (Essen Univ., Germany, F.R.) 1988 80 p In GERMAN; ENGLISH summary
(Contract BMFT-0704590-4)
(BPT-3/88; ISSN-0176-0777; ETN-89-93760) Copyright Avail: NTIS HC A05/MF A01

The time variance of stratospheric gases was used to derive transport parameters of the lower stratosphere, applying the method of the equivalent displacement height (EDH). The 18-yr series of measurements of ozone and of the potential temperature observed by the Meteorological Observatory Hohenpeissenberg (West Germany) and the LIMS satellite measurements (Limb Infrared Monitor of the Stratosphere) were analyzed. From the Hohenpeissenberg data the seasonal variation of the EDH as well as of the horizontal and vertical displacements were derived. The satellite measurements gave the latitudinal variations of these parameters for the observation period from November 1978 to May 1979. It is shown that the EDH is a powerful parameter to describe the transport effects in the lower stratosphere. ESA

N89-23027# Gesellschaft fuer Strahlen- und Umweltforschung m.b.H., Munich (Germany, F.R.). Projekttraeger Umwelt- und Klimaforschung.
QUANTITATIVE ANALYSIS OF ATMOSPHERIC TRACE GASES Final Report
Gerhard Schmidtke, Wolfgang Kohn, Ulrich Klocke, Manfred Knothe, Wolfgang Julius Riedel, and Helmut Wolf (Fraunhofer Inst., Freiburg, Germany, F.R.) 28 Apr. 1988 104 p In GERMAN; ENGLISH summary
(Contract BMFT-FKZ-0704569-8)
(BPT-10/88; ISSN-0176-0777; ETN-89-93762) Copyright Avail: NTIS HC A06/MF A01

A fully automatic diode laser spectrometer was developed and tested for the measurement of the trace gases NO, NO2, HNO3, O3 and SO2, which are involved in the ozone cycle. The choice of the suitable measuring methods is outlined. The development of the different components and the testing of the apparatus concept are discussed. Up to five different gases can be monitored in the ppb and sub-ppb ranges of concentration. The diffraction-limited reflection optics and the long-path gas cell (White cell) corrected for astigmatism are of special interest. ESA

N89-23028# Kernforschungsanlage, Juelich (Germany, F.R.). Abteilung Sicherheit und Strahlenschutz.
INVESTIGATION ON LONG TIME DISPERSION AND WASHOUT FACTOR. VEGETATION CONTAMINATION COMPUTATION WITH METEOROLOGICAL WHOLE YEAR OR SUMMER STATISTICS [UNTERSUCHUNGEN ZUM LANGZEITAUSBREITUNGS- UND ZUM WASHOUT-FAKTOR. BERECHNUNG DER KONTAMINATION DER VEGETATION MIT DER METEOROLOGISCHEN GANZJAHRES- ODER SOMMERSTATISTIK]
E. Pomplun and K. Heinemann Jun. 1988 53 p In GERMAN Original contains color illustrations
(JUEL-Spez-449; ISSN-0343-7639; ETN-89-93957) Avail: NTIS HC A04/MF A01

Long time dispersion and washout factors are studied for the quantitative evaluation of vegetation pollution. Effects of meteorological statistics on both factors are considered. Direct vegetation contamination analysis is performed using whole year statistics instead of summer statistics. Meteorological statistics should give 5 yr measurement results to constitute a representative dispersion analysis method. ESA

N89-23029# Kernforschungsanlage, Juelich (Germany, F.R.). Inst. fuer Chemie 2: Chemie der Belasteten Atmosphaere.
COUPLING OF A CHEMILUMINESCENCE DETECTOR WITH A GAS CHROMATOGRAPHEN FOR THE SELECTIVE MEASUREMENT OF OXIDIZED NITROGEN BONDS IN THE ATMOSPHERE [KOPPLUNG EINES CHEMOLUMINESZENZDEKEKTORS MIT EINEM GASCHROMATOGRAPHEN ZUR SELEKTIVEN MESSUNG OXIDIERTER STICKSTOFFVERBINDUNGEN IN DER ATMOSPHAERE]
Frank Flocke, Andreas Volz, and Dieter Kley Jul. 1988 83 p In GERMAN; ENGLISH summary
(JUEL-2217; ISSN-0366-0885; ETN-89-93962) Avail: NTIS HC A05/MF A01

An analytical technique for the measurement of organic nitrates is presented. Separation of the different nitrogen species is achieved by capillary gas-chromatography. Chemiluminescence (NO/O3) in combination with catalytic conversion (Au/CO AT 300 C) is used for detection. This combination converts individual NOx species including organic nitrates to NO, which is then detected by its chemiluminescence upon reaction with O3. For atmospheric samples with low concentrations of organic nitrates, cryogenic preconcentration from 3l of air is employed. The different components of the analytical system were tested in the laboratory. The detection limit is of the order of a few ppt in a 3l sample. Separation of the nitrates by chain length is best achieved on an unpolar stationary phase. Reproducibility, including cryogenic sampling, is +/- 5%. Measurements at a test site confirm the existence of organic nitrates in ambient air. ESA

N89-23030# Westinghouse Hanford Co., Richland, WA.
THE LONG-TERM CLIMATE CHANGE ASSESSMENT TASK OF THE HANFORD SITE, WASHINGTON, PROTECTIVE BARRIER DEVELOPMENT PROGRAM
K. L. Petersen Mar. 1989 6 p Presented at the 6th Annual PACLIM Workshop, Pacific Grove, CA, 5 Mar. 1989
(Contract DE-AC06-87RL-10930)
(DE89-008704; WHC-SA-0537; CONF-890385-1) Avail: NTIS HC A02/MF A01

Development of a study plan is under way to guide a multiyear program of long-term climate change assessment of the protective barriers alternative being considered for the disposal of some radioactive defense waste stored near the surface at the Hanford Site, Washington. These barriers are being designed to limit movement of radionuclides and other contaminants to the accessible environment for as long as 10,000 yr. A stepwise approach to climatic data acquisition will be relied on in obtaining needed information for concurrent barrier tasks and in developing a local climate forecast model. These models will need to couple past climate patterns to models of regional and global climate drivers to provide bounding conditions for barrier performance assessment analyses. DOE

N89-23031 Colorado Univ., Boulder.
THE RESPONSE OF THERMOSPHERIC NITRIC OXIDE TO AN AURORAL STORM Ph.D. Thesis
David Eric Siskind 1988 189 p
Avail: Univ. Microfilms Order No. DA8902936

The response of thermospheric nitric oxide (NO) to the auroral storm of September 19, 1984 is analyzed. Measurements of nitric oxide from the Solar Mesosphere Explorer (SME) ultraviolet spectrometer are compared with the calculations of a one-dimensional photochemical model of the lower thermosphere. The NCAR thermospheric General Circulation Model (TGCM) is used to calculate the response of the background neutral atmosphere to auroral forcings such as Joule and particle heating. The output of the TGCM is used as input to the photochemical model. The time history of the auroral energy input is assessed using particle data from the NOAA 6 and 7 satellites. Calculations

of the mid-latitude NO response show that temperature increases which result from Joule heating lead to NO enhancements. A larger response is initially seen for altitudes greater than 120 km. After several days, downward diffusion leads to NO increases at lower altitudes. Equatorial NO shows little response because the combined effects of temperature enhancements and atomic oxygen enhancements largely cancel. At auroral latitudes the effects of particle precipitation are dominant with Joule heating contributing only 15 percent to the peak NO density. Calculations of the auroral NO response predict an enhancement; however, the amplitude of the response, as well as the absolute magnitude of the calculated NO, greatly exceed the observations. Vertical winds on the order of 1 to 5 m/sec in the E region are proposed as an important loss process. The NO density is sensitive to changes in the O/O2 ratio, the N(D-2) yield from N2 dissociative excitation and the quenching of N(D-2) by O. Dissert. Abstr.

46 GEOPHYSICS

Includes aeronomy; upper and lower atmosphere studies; ionospheric and magnetospheric physics; and geomagnetism.

For space radiation see *93 Space Radiation.*

N89-23032# Naval Research Lab., Washington, DC. Plasma Physics Div.

EFFECTS OF ION COLLISIONS ON QUASILINEAR HEATING BY THE CURRENT-DRIVEN ION CYCLOTRON INSTABILITY IN THE HIGH LATITUDE IONOSPHERE

P. Satyanarayana (Science Applications International Corp., McLean, VA.), M. J. Keskinen, P. K. Chaturvedi, and S. L. Ossakow 14 Oct. 1988 25 p

(AD-A202512; NRL-Memo-6335) Avail: NTIS HC A03/MF A01 CSCL 04A

Using an effective relaxation time model, the effects of ion-ion and ion-neutral collisions on quasilinear ion heating by the current-driven ion cyclotron instability in the high latitude ionosphere have been studied. For conditions typical of the high latitude lower (200 to 300 km) F-region ionosphere, it is found that the combined effects of ion-neutral and ion-ion collisions tend to isotropize (S(tet)/T(par) approx. 1) the perpendicular T(per) and parallel S(tet) ion temperatures on time scales on the order of several tens to hundreds of NO+ cyclotron periods for wave amplitudes e(phi)/T sub e = 0.2. Here, phi is the wave electrostatic potential, T(par) the electron temperature (in energy units), e is the electron charge. In addition, for the high latitude upper (600 km) F-region ionosphere it is found that stronger anisotropy (T(per)/T(par) greater than 3) can be sustained even in the presence of ion collisions with waves with amplitudes e(phi)/T sub e = 0.2. For larger amplitude waves e(phi)/T sub e = 0.4, we find that the heating is weakly anisotropic at low altitudes (200-300 km) and strongly anisotropic at higher (600 km) altitudes. In both wave amplitude regimes (0.2 and 0.4), we find perpendicular ion heating factors about 2 to 10 for altitudes in the range 300 to 600km, with the larger perpendicular heating occurring at higher altitudes and larger wave amplitudes. The results are compared with recent rocket and satellite observations in the high latitude ionosphere. GRA

N89-23033# Systems Integration Engineering, Inc., Lexington, MA.

TECHNICAL SUPPORT FOR OPTICAL TURBULENCE RESEARCH Final Report, 6 Mar. 1985 - 31 Aug. 1988

Frank C. Regan, Jr. 26 Sep. 1988 107 p

(Contract F19628-85-C-0052)

(AD-A204776; AFGL-TR-88-0269) Avail: NTIS HC A06/MF A01 CSCL 04A

This report documents technical support provided to AFGL's Atmospheric Optics Branch. Specific tasking areas in this contract include the following: system integration; testing; field support; printed circuit board fabrication; analysis and design; documentation. GRA

N89-23034# SRI International Corp., Menlo Park, CA.

IONOSPHERIC SCINTILLATION STUDIES Final Report, Oct. 1984 - Sep. 1987

Robert C. Livingston 1 May 1988 43 p

(Contract F19628-84-K-0019)

(AD-A205210; AFGL-TR-88-0148) Avail: NTIS HC A03/MF A01 CSCL 04A

Irregular structure in ionospheric plasma density can significantly affect Department of Defense (DOD) communications and radar systems which utilize transionospheric radiowave paths. Transport and dissipation of ionospheric structure is therefore of direct relevance. Such an understanding can aid the long-term goal of developing a predictive capability for global ionospheric structure. Experimental observation of the ionosphere over the past few years has concentrated on high latitudes. This is the most complex portion of the global ionospheric system; the auroral zone, the polar cap, and the boundary between them can all be regions of highly dynamic and structured plasma. In the polar cap, very large scale plasma patches and sun-aligned arcs occur, and can convect rapidly from their source regions to the entire high latitude region. Much of what has been learned about this extended regime of irregularity structure at high latitudes has been through the application of complementary diagnostics: Optics, ionosonde, incoherent scatter radar, in-situ satellite, and scintillation measurements. These various techniques allow the observation of structure over several orders of magnitude in spatial scale. The optics, ionosonde and radar provide an overall view of large-scale production and dynamics; the satellites diagnose the inputs to the large- and medium-scale irregularities; from the scintillation data, the strength, shape, and motion of the kilometer-scale structure can be identified. Author

N89-23035# Los Alamos National Lab., NM.

MONTE CARLO APPLIED TO RESONANCE SCATTERING OF HIGH ALTITUDE FLUORESCENT RADIATION

Dave Collins, Henry Horak, Redus Holland, and Dexter Sutherland 1989 15 p Presented at the Advances in Nuclear Engineering Computation and Radiation Shielding, Santa Fe, NM, 9-13 Apr. 1989

(Contract W-7405-eng-36)

(DE89-006519; LA-UR-89-265; CONF-890408-8) Avail: NTIS HC A03/MF A01

Monte Carlo sampling methods developed during a recent study of resonance scattering of high altitude fluorescent radiation are discussed. The techniques employed in this study include treating the fluorescent radiation in the form of spectral lines, taking advantage of azimuthal symmetry by converting point emission data and point collision data to emission rings and collision rings to gain statistical accuracy, and using backward Monte Carlo to increase the number of samples within the field of view of highly collimated detectors. The models developed to sample spectral lines emitted by transitions within the N2(+) first negative system are described as well the methods for propagating and scattering complete spectral lines as single entities. DOE

N89-23036# Pacific Northwest Labs., Richland, WA.

PRELIMINARY RESULTS OF THE MLAM (MULTI-LAYER AIR MASS) LAGRANGIAN TRANSPORT MODEL SIMULATION OF ANATEX (ACROSS NORTH AMERICA TRACER EXPERIMENT)

William E. Davis, Anthony R. Olsen, and Trudy A. Erb Jan. 1989 5 p Presented at the American Meteorological Society, Anaheim, CA, 29 Jan. - 2 Feb. 1989

(Contract DE-AC06-76RL-01830)

(DE89-008123; PNL-SA-16432; CONF-890135-8) Avail: NTIS HC A02

The 1987 Across North America Tracer Experiment (ANATEX), for the study of regional to continental-scale transport and diffusion, released perfluorocarbon tracers for three hours every 2.5 days in January, February and March (Draxler et. al. 1985, 1987). The experiment resulted in 33 days of releases at two sites; Glasgow, Montana and St. Cloud, Minnesota. Each release consisted of approximately 50 kg of perfluoro ortho-dimenthoyl cyclohexane (PDCH) at St. Cloud and 83 kg of perfluoro trimethyl cyclohexane

(PTCH) at Glasgow. The experiment included the release of a third tracer, 50 kg of perfluoro methyl cyclohexane (PMCH), every five days from St. Cloud; designed to serve as a means to distinguish consecutive releases from St. Cloud. A surface sampling network of 77 sampling sites, located east of 105 degree longitude in the United States and Canada, measured 24-hour average tracer concentrations out to a distance of 3000 km from Glasgow. The network, organized in eight arcs east of Glasgow, collected daily concentrations of each tracer from January 5 through March 29, 1987. The network design provides average daily surface footprint information for the three tracers. DOE

N89-23037# Gesellschaft fuer Strahlen- und Umweltforschung m.b.H., Munich (Germany, F.R.). Projekttraeger Umwelt- und Klimaforschung.

MASS-SPECTROSCOPIC MEASUREMENTS OF STRATOSPHERIC IONS, TRACE GASES AND PRECONDENSATION NUCLEI USING BALLOON-BORNE MEASURING PROBES Final Report [MASSENSPEKTROMETRISCHE MESSUNGEN STRATOSPHAERISCHER IONEN, SPURENGASE UND PRAEKONDENSATIONSKERNE MITTELS BALLONGETRAGENER MESSSONDEN]

F. Arnold and H. Schlager (Max-Planck-Inst. fuer Kernphysik, Heidelberg, Germany, F.R.) 1988 100 p In GERMAN
(Contract BMFT-FKZ-0704562)
(BPT-7/88; ISSN-0176-0777; ETN-89-93761) Copyright Avail: NTIS HC A05/MF A01

Ion mass spectroscopic measurements from balloons are presented. The experimental method and the instruments used for mass spectroscopic analysis of stratospheric ions and for trace gas analysis are described. The instrument nacelle and the tandem balloon are outlined. The telemetric method, remote control system, and the ground station are described. The balloon flights from France and from Kiruna in Sweden are depicted. The identification of stratospheric icns, the height distribution of stratospheric ions, reaction schemes of stratospheric ions, trace gas determination, the deduction of thermochemical data from stratospheric ion measurements, and the investigation of stratospheric aerosols are discussed. Laboratory investigations of ion-neutral interactions are discussed. ESA

N89-23038# Johann-Wolfgang-Goethe-Univ., Frankfurt am Main (Germany, F.R.). Inst. fuer Physikalische und Theoretische Chemie.

DETERMINATION OF THE DYNAMIC CO2 SOURCE-SINK FUNCTION OF DIFFERENT BIOMES WITH THE OBJECT OF VERIFYING SEASONALITY AND TREND OF ATMOSPHERIC CO2 MEASUREMENTS OF DIFFERENT STATIONS Final Report

Gundolf Hans Kohlmaier 1988 40 p In GERMAN; ENGLISH summary
(Contract BMFT-KF-2007/4)
(ETN-89-93763) Avail: NTIS HC A03/MF A01

The exchange of CO2 between different biota (vegetation family) and the atmosphere was modeled with respect to the seasonal course as well as the long-term trend. From the analysis of the seasonal trend of atmospheric CO2, it is concluded that the land vegetation can be considered as a sink as well as a source for atmospheric CO2. A release of 0.8 to Gt C/a can be regarded as a result of the presently cleared tropical woodland. A probable uptake of 0.4 to 2.4 Gt C/a by the vegetation is due to a CO2 fertilization effect under the assumption that the rising CO2 levels lead to a long-term rise of productivity and not only to an acceleration of growth in the young vegetation stands. The increase of the amplitude of the seasonal CO2 cycle cannot be explained exclusively by a CO2 fertilization effect; a variety of other factors must be considered as well, (especially change in land use strategies) and the variability of the climate. ESA

N89-23039# Technische Univ., Delft (Netherlands). Faculty of Geodesy.

DETAILED GRAVITY ANOMALIES DERIVED FORM SEASAT ALTIMETER DATA. A COMPARISON OF TWO ALTERNATIVE APPROACHES: LEAST SQUARES COLLOCATION AND A METHOD BASED ON FFT Thesis

Rogers H. N. Haagmans Aug. 1988 103 p
(ETN-89-94144) Avail: NTIS HC A06/MF A01

Gravity anomalies computed from Seasat data using a geodetic least squares collocation and a geophysical fast Fourier transformation (FFT) technique were compared with each other and with a set of high precision data from the NAVGRAV North Sea gravimetry study. The collocation results show good resemblance with the NAVGRAV set. An rms difference of 7 mgal is found. If the noise of the NAVGRAV set is included, the noise in the computed gravity anomalies becomes 7.4 mgal. These results are obtained from a part of the altimeter data within the North Sea area. It is excepted that optimal use of the complete altimeter data set may result in better accuracy. The obtained accuracy seems to open possibilities for using the altimeter anomalies for exploration purposes. The geophysical method has more disappointing results. The reason for this may be found in insufficient orbit error removal from the altimeter profiles. If this is improved, for instance by using the technique which was used for the collocation set, then much better results are expected from this method. ESA

N89-23040*# Texas Univ., San Antonio. Div. of Earth and Physical Sciences.

KILOMETRIC RADIATION POWER FLUX DEPENDENCE ON AREA OF DISCRETE AURORA

N. A. Saflekos, J. L. Burch, D. A. Gurnett, R. R. Anderson, and R. E. Sheehan (Boston Coll., Chestnut Hill, MA.) [1989] 65 p
(Grants NAG5-227; NAGw-1254; NSF ATM-85-21590; NSF ATM-86-46122; NSF ATM-88-05819)
(NASA-CR-184993; NAS 1.26:184993) Avail: NTIS HC A04/MF A01 CSCL 04A

Kilometer wavelength radiation, measured from distant positions over the North Pole and over the Earth's equator, was compared to the area of discrete aurora imaged by several low-altitude spacecraft. Through correlative studies of auroral kilometric radiation (AKR) with about two thousand auroral images, a stereoscopic view of the average auroral acceleration region was obtained. A major result is that the total AKR power increases as the area of the discrete auroral oval increases. The implications are that the regions of parallel potentials or the auroral plasma cavities, in which AKR is generated, must possess the following attributes: (1) they are shallow in altitude and their radial position depends on wavelength, (2) they thread flux tubes of small cross section, (3) the generation mechanism in them reaches a saturation limit rapidly, and (4) their distribution over the discrete auroral oval is nearly uniform. The above statistical results are true for large samples collected over a long period of time (about six months). In the short term, AKR frequently exhibits temporal variations with scales as short as three minutes (the resolution of the averaged data used). These fluctuations are explainable by rapid quenchings as well as fast starts of the electron cyclotron maser mechanism. There were times when AKR was present at substantial power levels while optical emissions were below instrument thresholds. A recent theoretical result may account for this set of observations by predicting that suprathermal electrons, of energies as low as several hundred eV, can generate second harmonic AKR. The indirect observations of second harmonic AKR require that these electrons have mirror points high above the atmosphere so as to minimize auroral light emissions. The results provide evidence supporting the electron cyclotron maser mechanism. Author

N89-23041# Deutsche Forschungs- und Versuchsanstalt fuer Luft- und Raumfahrt, Oberpfaffenhofen (West Germany). Abteilung Atmosphaerische Dynamik.

THE LARGE EDDY SIMULATION (LES) OF MESOSCOP FOR ATMOSPHERIC BOUNDARY LAYER FLOWS INCLUDING PASSIVE SCALARS

Helmut Schmidt Oct. 1988 125 p In GERMAN; ENGLISH summary

(Contract BMFT-KF-3012/4)

(DFVLR-Mitt-88-28; ISSN-0176-7739; ETN-89-94374) Avail: NTIS HC A06/MF A01; DFVLR, VB-PL-DO, Postfach 90 60 58, 5000 Cologne, Fed. Republic of Germany, DM 41

The MESOSCOP three-dimensional time-dependent numerical hydrodynamic model version as operated in Large-Eddy Simulation (LES) is described. It can be applied to the turbulent atmospheric boundary layer over flat terrain. The model comprises the full continuity and Navier-Stokes equation. Balance equations for one or a number of active and passive scalars can be integrated. The thermodynamic variable is the (potential) temperature. The model equations might easily be simplified by filtering the continuity equation (anelastic approximation or incompressible flow), applying the Boussinesq approximation or neglecting the Coriolis terms. A variety of boundary conditions is implemented and the subgrid scale fluxes are derived from simplified balance equations for the second-order moments. The description of the model can be read as an introduction to the theory of second-order closure. The FORTRAN code is described, to enable a newcomer to handle the model without much additional personal support. ESA

N89-23042 Harvard Univ., Cambridge, MA.

TOPICS IN GRAVITATIONAL THEORY Ph.D. Thesis

Gary Freeman Hinshaw 1988 63 p

Avail: Univ. Microfilms Order No. DA8901581

In chapter one the gravitational lensing properties were calculated for an isothermal sphere in which the singularity at the origin is replaced by a finite core, and contrasted with the singular case. It is shown that this can significantly alter the statistics of the lensing of distant quasars by both the known distribution of intervening galaxies, and also by a possible distribution of dark galaxies, as might be predicted in biased galaxy formation models. In chapter two the results of chapter one were used to investigate the effect of distortions in the temperature of the cosmic microwave background radiation due to the presence of soft cored clusters of galaxies acting as gravitational lenses. The observability of the temperature, and distortion in large separation lens systems was discussed. It was concluded that the effect should be observable in systems where the angular image separation is as little as 20 in. In chapter three a generalization of the gauge invariant gravitational perturbation theory is presented, it was first introduced by Bardeen and subsequently refined by Brandenberger, Kahn, and Press. The resulting formalism offers a simpler scheme for calculating the growth of scalar gravitational perturbations. Dissert. Abstr.

N89-23043 Edinburgh Univ. (Scotland).

DIABATIC CIRCULATIONS IN THE STRATOSPHERE Ph.D. Thesis

Steven Pawson 1988 220 p

Avail: Univ. Microfilms Order No. BRD-84141

Three-dimensional fields of radiative heating and cooling rates have been calculated from satellite observations of temperature, ozone and water vapor distributions in the stratosphere. Net radiative heating rates were obtained from these components. The data were used to show that the mean pressure of each isentropic surface in the stratosphere changes by less than 1 pct each day. Correlated monthly, zonal-mean fields qualitatively agree with the broad range of previous calculations. Three-dimensional heating fields are analyzed for the Northern Hemisphere winter and spring; comparison with the potential vorticity distribution reveals that the strongest net cooling tends to occur at the eastern edge of the displaced polar vortex. The net radiative heating rates give the vertical component of the diabatic circulation in isentropic coordinates. The horizontal component of the diabatic circulation is calculated from the vertical mass convergence, for both three-dimensional and zonal-mean cases, using the steady state continuity equation; the satellite data are used to validate the assumption that density changes can be neglected over long times, so that the diabatic circulation is the dominant part of the divergent flow; that is not the case over short periods. The zonal-mean diabatic circulation agrees well with the most convincing previous calculations; there is ascent in the tropics and descent at the winter pole, with ascent overlying weaker descent at the summer pole, with poleward flow which is strongest near the winter hemisphere stratopause. These circulations were used with the eddy vertical velocity, determined from the three-dimensional heating field, to examine various terms in the zonal-mean tracer budget. Dissert. Abstr.

N89-23044# Auroral Observatory, Tromso (Norway).

OPTICAL STUDIES OF THE MAGNETOSPHERIC CUSP FROM SVALBARD Technical Report, 30 Sep. 1987 - 29 Sep. 1988

Kjell Henriksen 2 Jan. 1989 5 p

(AD-A205432) Avail: NTIS HC A02/MF A01 CSCL 04A

The present investigation was made on spectrometric auroral data obtained on the dayside and nightside of the auroral oval in Svalbard. Synthetic spectra of O2(+) 1NG and N2(+) 1NG bands were calculated. The transition probabilities were obtained by particular solutions of the Schrodinger equation. The synthetic spectra were used to analyze the auroral spectrum from 5200 to 5800 A, deriving the intensities of all the auroral emissions of this spectral region. The same spectral technique was used to analyze solar spectra, deriving ozone column densities and spectral UV irradiances. GRA

N89-23045# Massachusetts Inst. of Tech., Cambridge. Earth Resources Lab.

ANALYSIS OF REGIONAL PHASES USING THREE COMPONENT DATA Report, 19 Aug. 1987 - 31 Aug. 1988

Michael Prange and M. N. Toksoz 28 Nov. 1988 69 p

(Contract F19628-87-K-0054)

(AD-A205480; AFGL-TR-88-0322; SR-1) Avail: NTIS HC A04/MF A01 CSCL 08K

A method is presented for computing three-dimensional seismic wave scattering from a rough interface. It is derived using a perturbation approach which requires interface height perturbations to be small relative to the wavelengths of scattered waves, and interface slope perturbations to be much less than one. These validity conditions are based on an order of error analysis of the truncation of the perturbation series. Comparison of reflection and transmission coefficients generated by the perturbation method with those generated from a second-order finite difference method for several rough interface models with Gaussian auto-correlation functions shows that the perturbation method is accurate for RMS interface height deviations of less than about a tenth of the smallest wavelength in the scattered field. This result is independent of RMS interface slope in the tested range of 0.037 to 0.99. GRA

N89-23046# Alaska Univ., Fairbanks.

GRAVITY WAVE AND TURBULENCE STUDIES USING A HIGH-RESOLUTION ST RADAR Annual Technical Report, 1 Jan. - 31 Dec. 1988

David C. Fritts 1 Feb. 1989 5 p

(Contract F49620-87-C-0024)

(AD-A205592; AFOSR-89-0284TR) Avail: NTIS HC A02/MF A01 CSCL 04A

Research during the past year included both theoretical and observational studies of gravity waves and their effects in the lower and middle atmosphere. Theoretical studies examined the stability conditions of inertio-gravity waves in order to address the most likely form of wave instability conditions of inertio-gravity waves in order to address the most likely form of wave instability and saturation as well as the atmospheric structures leading to ducting and wave energy transports. Ongoing theoretical studies are addressing nonlinear wave interactions and wave interactions and wave forcing via geostrophic adjustment. Observational work has dealt with mesospheric momentum fluxes at high latitudes

and with continuing studies of wave and turbulence effects using a variety of data sets. Future work will address increasingly the sources and variability of such motions. GRA

N89-23047# Naval Postgraduate School, Monterey, CA.
DEVELOPMENT OF A DIFFERENTIAL TEMPERATURE PROBE FOR THE MEASUREMENT OF ATMOSPHERIC TURBULENCE AT ALL LEVELS M.S. Thesis
Michael R. Olmstead Dec. 1988 91 p
(AD-A205893; NPS61-89-003) Avail: NTIS HC A05/MF A01 CSCL 20F

Fluctuating temperature structures in the atmosphere induce phase perturbations in a propagating laser beam. These turbulent conditions occur throughout the atmosphere and cause the laser beam to spread and alter its centroid. There are several methods to measure the parameters of optical turbulence in the atmosphere, but few that will determine them as a function of altitude at all levels. One method of measuring altitude profiles of turbulence is with a temperature probe launched via a balloon system. This thesis involves the development of a differential temperature probe sensor to measure the temperature fluctuations at all altitudes in the atmosphere. In addition, it investigates the effect of solar heating on the probes in the atmosphere and the subsequent effects on the measurements. A validation of the probe system was made by a comparison test with an acoustic echosounder developed earlier. In addition to validating the probe system, the absolute (C sub T)-sq analysis of the echosounder was confirmed. GRA

47 METEOROLOGY AND CLIMATOLOGY

Includes weather forecasting and modification.

N89-23048*# National Oceanic and Atmospheric Administration, Boulder, CO. Wave Propulsion Lab.
HAZARD INDEX CALCULATION FOR 31 MAY 1984 MICROBURST AT ERIE, COLORADO Final Report
R. A. Kropfli Oct. 1988 54 p Sponsored by NASA, Langley Research Center, Hampton, VA
(NASA-CR-184968; NAS 1.26:184968; PB89-127831; NOAA-TM-ERL-WPL-155) Avail: NTIS HC A04/MF A01 CSCL 04B

Two x-band Doppler radars, operated by NOAA, were used to collect high resolution data within a small, benign looking microburst during the PHOENIX II boundary layer experiment. The lowest 2.5 km of the microbursts was observed throughout its development and dissipation over a 15 minute period. These observations presented an excellent opportunity to compute a quantitative threat to a hypothetical aircraft whose flight track would carry it through the microburst. The hazard index is based on the kinetic energy loss to the aircraft that would be produced by the microburst; it is a function of the vertical air motion, horizontal spatial derivatives of the wind field, and the assumed aircraft air speed and direction. Indices were computed and plotted for all 8 volume scans and peak values were observed to be sufficiently high to present a significant hazard to an aircraft. Author

N89-23049# Central Research Inst. of Electric Power Industry, Tokyo (Japan).
CHARACTERISTICS OF WINTER LIGHTNING TO HIGH STRUCTURES. OBSERVATION FROM DECEMBER 1978 TO MARCH 1987
Kunihiko Miyake, Hiroshi Mitani, Atsuyuki Inoue, and Shigeru Yokoyama May 1988 38 p In JAPANESE; ENGLISH summary
(DE88-756454; CRIE-T-37040) Avail: NTIS (US Sales Only) HC A03/MF A01

From the observation results of winter lightning to independent high structures during nine years from the year 1978, a data base was structured and statistically analyzed. Totally 416 times of observation were made at the three points, ie, Kashiwazaki, Fukui and Nakanoto. Lightning stroke was recorded 181 times/8 years at Kashiwazaki, 184 times/7 years at Fukui and 51 times/6 years at Nakanoto. The number of annual winter lightning strokes to the structure, to which the number of lightning strokes is the largest at each point, was larger than that of summer's and propotional to the height above ground of structure. Their cumulative frequency distribution of lightning stroke current peaks does not largely differ from that of summer's. The ratio of positive polarity to negative polarity for the number of lightning strokes is 1 to 2, which indicates a larger number of positive polarity's than 1 to 19 being that of summer's. The wave front time of lightning stroke of positive polarity current is wide in distribution, while 90 percent of the negative polarity's is within 50 microseconds. The electric charge quantity of winter lightning extends in a range from less than 1 Coulomb to more than thousands of coulomb which is much larger than the summer's being tens of coulomb. The vertical lightning stroke angle is mostly approx. 35 degrees and may reach 85 degrees. DOE

N89-23050# International Centre for Theoretical Physics, Trieste (Italy).
ON THE PHYSICAL CAUSES OF ENSO EVENTS AND THE ITCZ's EXTREME LATITUDINAL DISPLACEMENTS
Ernest C. Njau (Dar-es-Salaam Univ., Tanzania) Aug. 1988 15 p
(DE88-705654; IC-88/205) Avail: NTIS (US Sales Only) HC A03/MF A01

We predict the maximum latitudinal shifts of the Inter-Tropical convergence zone (ITCZ) over land masses due to variations in the surface or near-surface temperature fields. We also predict the mean locations of the ITCZ over oceans during Northern Hemisphere (NH) and Southern Hemisphere (SH) summers. All our predictions are shown to agree well with observations. Finally, on the basis of the association between the latitudinal location of the eastern pacific portion of the ITCZ and El Nino-Southern Oscillation (ENSO) events as well as some previous related work (Njau, 1985a; 1985b; 1986; 1987; 1988), we suggest possible physical causes of the ENSO events. DOE

N89-23051 Deutscher Wetterdienst, Offenbach am Main (Germany, F.R.).
CLIMATOLOGICAL AND STATISTICAL FUNDAMENTALS FOR THE EXPLANATION OF CLIMATE DATA PROCESSING [KLIMATOLOGISCHE UND STATISTISCHE GRUNDLAGEN ALS ERLAEUTERUNGEN FUER KLIMABEARBEITUNGEN]
A. Cappel, M. Kalb, and H. Schmidt 1988 16 p In GERMAN
(ETN-89-93775) Copyright Avail: Deutscher Wetterdienst, Frankfurter Strasse 135, D-6050 Offenbach am Main, Fed. Republic of Germany

The climatological and statistical fundamentals, used by the German weather services, are explained in order to simplify the processing of climate data series and to provide better information to users of climatological data tables. The following climatological elements and concepts, their definitions, measurement and measuring units are described: observation dates, cloudiness, atmospheric pressure, humidity, atmospheric temperature, precipitation, visual range, sunshine duration, daily averages, and wind. Averages and frequency distributions are discussed. ESA

N89-23052 Deutscher Wetterdienst, Offenbach am Main (Germany, F.R.).
REPORTS FROM THE GERMAN METEOROLOGICAL SERVICE. NO. 175: GLOBAL RADIATION DURING TWILIGHT [BERICHTE DES DEUTSCHEN WETTERDIENSTES NR. 175: GLOBALBELEUCHTUNGSSTAERKE WAEHREND DER DAEMMERUNG]
Klaus Dehne, Uwe Bergholter, and Fritz Kasten 1988 69 p In GERMAN; ENGLISH summary Original contains color illustrations
(ISBN-3-88148-241-5; ISSN-0072-4130; ETN-89-93776) Copyright Avail: Deutscher Wetterdienst, Frankfurter Strasse 135, D-6050 Offenbach am Main, Fed. Republic of Germany

A continuous measuring series was performed with an automatic device at Hamburg-Fuhlsbuettel airport from October 1984 to July

1986, with a view to the study of the incoming global radiation Gv during twilight and in particular its dependence on cloudiness. The cloudiness data were derived from photographs taken with a fish-eye camera, quality controlled and supplemented using observation journals of the aeronautical meteorological office. Part of the 1200 observed twilight phases were attributed to groups of clouds marked by a predominant type of cloud and a mean interval cloudiness. The average course of Gv during twilight as a function of solar altitude, as well as standard deviations and/or variation coefficients were determined. The Gv in cloudless twilight was parameterized as a function of solar altitude. For the parameterization in clouded twilight a constant factor was determined for each group of clouds. The average values for cloudless sky deviate from previous data. ESA

N89-23053 Deutscher Wetterdienst, Offenbach am Main (Germany, F.R.).
REPORTS FROM THE GERMAN METEOROLOGICAL SERVICE. NO. 177: SMALL-SCALE VARIABILITY OF SOLAR RADIATION [BERICHTE DES DEUTSCHEN WETTERDIENSTS NR. 177: KLEINSKALIGE VARIABILITAET DER SONNENSTRAHLUNG]
Reinhard Trapp and Fritz Kasten 1988 74 p In GERMAN; ENGLISH summary
(ISBN-3-88148-224-X; ISSN-0072-4130; ETN-89-93777)
Copyright Avail: Deutscher Wetterdienst, Frankfurter Strasse 135, D-6050 Offenbach am Main, Fed. Republic of Germany

The small-scale variability of the daily relative global radiation (rg) was investigated on the basis of data obtained at the 28 radiometric stations of the German Weather Service in 1982 to 1985. The frequency distributions of rg of at least 20-year measuring series at four stations differ only slightly from the above-mentioned 4-year series. The correlation coefficient (cc) of rg of two stations each time was determined as a function of the length of the correlation time interval and the season. The dependance of cc on the distance between stations is presented according to geographic location and orientation of the stations from month to month. Two-dimensional frequency distributions of rg illustrate the simultaneous appearance of given values of rg at two stations in the different seasons. The connection between rg and wind direction was analyzed. Monthly maps of rg in the FRG are drawn and converted into maps of monthly global radiation. ESA

N89-23054 Royal Netherlands Meteorological Inst., De Bilt. Physical Meteorology Dept.
RADIATIVE COOLING IN THE NOCTURNAL BOUNDARY LAYER Ph.D. Thesis - Wageningen Agricultural Univ.
S. A. Tjemkes 1988 119 p
(KNMI-WR-88-05; ISSN-0169-1651; ETN-89-94153) Copyright Avail: Royal Netherlands Meteorological Inst., P.O. Box 201, 3730 DeBilt, Wilhelminalaan 10, Netherlands

The transfer of infrared radiation through a cloudfree nocturnal boundary layer is studied. A narrow band model which simulates the absorption and emission of longwave radiation by water vapor and carbon dioxide is tested. It is shown that the narrow band model simulates the surface downward flux within 3 W/sqm and the cooling rate within 0.2 K/day. To analyze the interaction between turbulence and infrared radiation in a horizontally homogenenous cloudless nocturnal boundary layer, the radiation scheme is combined with a turbulence model, in which a prognostic equation for the turbulent kinetic enrgy is solved together with a diagnostic length scale equation for the turbulence. The performance of this combined radiation turbulence model is compared with observations of the mean thermodynamic and turbulence structure throughout the nocturnal boundary layer. Agreement between the calculated and observed profiles of turbulence and mean thermodynamic variables and between the calculated and observed evolution of the surface fluxes is satisfactory. The inclusion of radiative cooling within the boundary layer increases the boundary layer height by 25 percent. The combined radiation-turbulence model is also used to study the influence of the geostrophic wind velocity on the surface minimum temperature. A parametrization scheme is derived which is able to reproduce the surface minimum temperature over an almost saturated vegetated clay soil within 2.5 K. ESA

N89-23055 Royal Netherlands Meteorological Inst., De Bilt.
SURFACE FLUX PARAMETERIZATION SCHEMES: DEVELOPMENTS AND EXPERIENCES AT KNMI
A. A. M. Holtslag and A. C. M. Beljaars 1988 32 p Presented at the Workshop on Parameterization of Fluxes over Land Surface, Reading, England, 24-26 Oct. 1988 Submitted for publication
(KNMI-WR-88-06; ISSN-0169-1651; ETN-89-94154) Copyright Avail: Royal Netherlands Meteorological Inst., P.O. Box 201, 3730 DeBilt, Wilhelminalaan 10, Netherlands

Observations and modeling efforts on surface fluxes are reviewed, emphasizing aspects that are important for numerical weather and climate models, e.g., surface roughness lengths for momentum and heat, surface stomatal resistance for evaporation and related quantities. Comparisons of flux estimates with observations are given. Exchange coefficients for momentum and heat in stable and very stable conditions are discussed. Formulas for the exchange coefficients are proposed. ESA

N89-23056 California Univ., Los Angeles.
RETRIEVING THE DISTRIBUTION OF LIQUID WATER CONTENT IN CLOUDS FROM OBSERVATIONS OF THERMAL MICROWAVE RADIATION Ph.D. Thesis
James Frederick Drake 1988 204 p
Avail: Univ. Microfilms Order No. DA8824656

Two methods were developed for retrieving the distribution of liquid water content in nonprecipitating clouds by using passive microwave remote sensing with a radiometer on the ground or on board an aircraft. One gives the distribution in a cross-section through a cloud from an analysis of measurements of intersecting beams of radiation; the other determines a coarse vertical profile. The physical principle of the methods is the proportionality between the liquid water content and the liquid absorption/emission coefficient. Mie theory was used to determine the scattering and absorption coefficients when the liquid distribution contained large, precipitating drops as well as 0.5 g/m(3) of small droplets. The scattering coefficient and the departure from proportionality between the absorption coefficient and the water content were not significant for precipitation rates less than 1 mm/hr. Computer simulation and mathematical analysis were used to estimate the accuracy that could be anticipated in the retrievals. It was not especially sensitive to the width of the radiometer antenna pattern. With the tomographic technique it was estimated that 2 to 3 min are sufficient to obtain data that permit reconstruction with a spatial resolution of 400 m with an expected error of about 0.1 g/m(3) in a cloud with a maximum liquid water content of 2 g/m(3). Expressions relating the expected error to cloud properties, radiometer characteristics, and retrieval resolution were derived. The profiling technique, which is only capable of partitioning the liquid in a vertical profile into an upper and a lower layer, was estimated to be capable of determining the fraction to within about 5 percent for clouds with column-integrated liquid contents of 0.1 to 0.5 g/m(3). Dissert. Abstr.

N89-23057 Texas A&M Univ., College Station.
REMOTE SENSING OF OCEANIC RAINRATES BY PASSIVE MICROWAVE SENSORS: A STATISTICAL-PHYSICAL APPROACH Ph.D. Thesis
David Allen Short 1988 98 p
Avail: Univ. Microfilms Order No. DA8903406

An analysis of microwave brightness temperatures (T) from the Nimbus-5 Electrically Scanning Microwave Radiometer (ESMR-5) and coincident, high resolution radar rainrates (R) over the GATE area during Phase I has shown them to be related in a manner consistent with radiative transfer theory and recent model calculations. The observed brightness temperatures can be simulated accurately from the rainrate field by direct application of an appropriate R, T relation. However, the inference of rainrates from the ESMR-5 temperatures, via the same R, T relation, is hampered by a fundamental remote sensing problem: The R, T relation is non-linear while the sensor field-of-view (FOV) is large

enough to encompass substantial rainrate inhomogeneity. These factors combine to produce retrieved rainrates that are, on average, too low, with large random errors. The ESMR-5 rainrate retrieval errors were found to be dominated by this rainrate retrieval problem, generally referred to as the beam filling problem. ESMR-5 inferred rainrates are half as large as, and highly correlated (0.96) with radar rainrates, when both are averaged over the 400 km diameter radar circle. A simple multiplicative correction factor of 2 brings them into close agreement. A statistical model of the beam filling problem was developed by envisioning an idealized instrument FOV that encompasses an entire gamma distribution of rainrates. This ensemble FOV model was used to calculate FOV temperatures, FOV averaged rainrates, retrieved rainrates and correction factors. The statistical model suggests that the correction factor varies from 1.6 to 2.7 for suppressed to enhanced tropical convective regimes and decreases to 1.5 as the freezing level and average rain column height decreases to 2.5 km.

Dissert. Abstr.

48 OCEANOGRAPHY

Includes biological, dynamic, and physical oceanography; and marine resources.

For related information see also *43 Earth Resources and Remote Sensing.*

N89-23058# Woods Hole Oceanographic Institution, MA.
MEASUREMENTS OF A BAROTROPIC PLANETARY VORTICITY MODE IN AN EDDY-RESOLVING QUASI-GEOSTROPHIC MODEL USING ACOUSTIC TOMOGRAPHY M.S. Thesis
Wendy B. Lawrence Aug. 1988 31 p
(Contract N00228-85-G-3262)
(AD-A205409; WHOI-88-36) Avail: NTIS HC A03/MF A01 CSCL 08C

The resonant barotropic oscillations (modes) predicted by the quasi-geostrophic (QG) theory are difficult to observe in the ocean. Large-scale measurements over lengthy durations may be required in order to observe these waves. The capability of receiving long-range sound transmissions in the ocean implies that acoustic methods may be well-suited for study of large-scale motions. In particular, basin-scale tomographic arrays may provide the coverage over sufficient time periods as well as the sensitivity needed to resolve the modes. In this study we investigate whether the analysis of the travel time fluctuations of tomographic transmissions can detect large-scale barotropic planetary oscillations in a QG model. A tomographic array is placed in a 2-layer, flat bottom, steady-wind driven QG circulation model to investigate whether analysis of acoustic travel time changes can detect large-scale barotropic oscillations. Time series of sea surface elevation and upper and lower layer meridional currents are generated for comparison against a series of acoustic travel times. The spectra of these time series exhibit a broad mesoscale peak near a period of 40 days. The spectrum of the acoustic travel time contains a significant peak due to a resonant barotropic oscillation with a period of 28.6 days which is not present in the spectra of the point measurements. GRA

N89-23059# Army Cold Regions Research and Engineering Lab., Hanover, NH.
SEAFLOOR TEMPERATURE AND CONDUCTIVITY DATA FROM COASTAL WATERS OF THE US BEAUFORT SEA
Paul V. Sellmann, Erk Reimnitz, and Edward W. Kempema Jan. 1989 26 p
(AD-A205428; CRREL-89-1) Avail: NTIS HC A03/MF A01 CSCL 08C

Important and unique seabed engineering properties and conditions observed on the shallow shelf of the Beaufort Sea may be caused by low temperatures and variable salinities of bottom waters. A year-long monitoring program was initiated during the fall of 1985 to make daily measurements of these parameters using small, self-contained, low-cost instrumentation units placed on the seabed in four locations. The four sites selected were in areas where overconsolidated sediments, seasonal seabed freezing and shallow ice-bounded permafrost are known to occur. The instruments were recovered during the fall of 1986; three units contained useful data. The longest record was 341 days at station 8 in outer Harrison Bay. Seabed temperatures above 0 C, for the period of record, occurred only 15 days at one site and 13 days at another. The mean annual temperatures for these sites were -1.55 C and -1.60 C. Estimates of the onset of seabed freezing suggest that the seabed can freeze on all but 82 days of the year. GRA

51 LIFE SCIENCES (GENERAL)

N89-23060# Office of Technology Assessment, Washington, DC.
NEW DEVELOPMENTS IN BIOTECHNOLOGY: US INVESTMENT IN BIOTECHNOLOGY, PART 4
Jul. 1988 300 p
(PB88-246939; OTA-BA-360-Pt-4; LC-88-600538) Avail: NTIS HC A13/MF A01; also available SOD HC $7.50 as 052-003-01060-7 CSCL 06C

The levels and types of investment currently are described being made by the Federal, State, and private sectors. Issues that affect investment: levels of R and D funding, research priorities, interagency coordination, information requirements, training and education needs, monitoring of university industry research, State efforts to promote biotechnology, the effects of tax law on commercial biotechnology, the adequacy of Federal assistance for biotechnology start-ups, and the effects of export control on biotechnology commerce are identified. Author

N89-23061*# National Aeronautics and Space Administration. Ames Research Center, Moffett Field, CA.
ACCLIMATIZATION TO COLD IN HUMANS
Hanna Kaciuba-Uscilko (Polish Academy of Sciences, Warsaw.) and John E. Greenleaf Apr. 1989 43 p
(NASA-TM-101012; A-88223; NAS 1.15:101012) Avail: NTIS HC A03/MF A01 CSCL 06S

This review focuses on the responses and mechanisms of both natural and artificial acclimatization to a cold environment in mammals, with specific reference to human beings. The purpose is to provide basic information for designers of thermal protection systems for astronauts during intra- and extravehicular activities. Hibernation, heat production, heat loss, vascular responses, body insulation, shivering thermogenesis, water immersion, exercise responses, and clinical symptoms and hypothermia in the elderly are discussed. Author

N89-23062# Pacific Northwest Labs., Richland, WA.
INHALATION DEVELOPMENTAL TOXICOLOGY STUDIES: TERATOLOGY STUDY OF METHYL ETHYL KETONE IN MICE Final Report
Terryl J. Mast, J. A. Dill, J. J. Evanoff, R. L. Rommereim, Richard J. Weigel, and R. Bruce Westerberg Feb. 1989 246 p
(Contract DE-AC06-76RL-01830)
(DE89-009563; PNL-6833; NTH-Y01-ES-70153) Avail: NTIS HC A11/MF A01

Methyl Ethyl Ketone (MEK) is a widely used industrial solvent which results in considerable human exposure. In order to assess the potential for MEK to cause developmental toxicity in rodents, four groups of Swiss (CD-1) mice were exposed to 0, 400, 1000 or 3000 ppM MEK vapors, 7 h/day, 7 dy/wk. Ten virgin females and approx.30 plug-positive females per group were exposed concurrently for 10 consecutive days (6--15 dg for mated mice). Body weights were obtained throughout the study period, and uterine and fetal body weights were obtained at sacrifice on 18 dg. Uterine implants were enumerated and their status recorded. Live fetuses were sexed and examined for gross, visceral, skeletal, and soft-tissue craniofacial defects. Exposure of pregnant mice to

these concentrations of MEK did not result in apparent maternal toxicity, although there was a slight, treatment-correlated increase in liver to body weight ratios which was significant for the 3000-ppM group. Mild developmental toxicity was evident at 3000-ppM as a reduction in mean fetal body weight. This reduction was statistically significant for the males only, although the relative decrease in mean fetal body weight was the same for both sexes. DOE

52 AEROSPACE MEDICINE

Includes physiological factors; biological effects of radiation; and effects of weightlessness on man and animals.

N89-23063# Severn Communications Corp., Millersville, MD.
ASTRONAUT RADIATION EXPOSURE IN LOW-EARTH ORBIT. PART 1: GALACTIC COSMIC RADIATION
John R. Letaw 31 Mar. 1988 45 p
(Contract N00014-87-C-2251)
(AD-A204598; SCC-88-01) Avail: NTIS HC A03/MF A01 CSCL 06G

In recent years, there has been increasing concern about the radiation doses which will be suffered by astronauts on present-day and future space missions. In order to characterize radiation exposure risks on space missions one requires models of space radiation environments, codes for transporting the components of ionizing radiation, and procedures for assessing radiation risks of a given exposure. To verify their accuracy, predictions based on these transport results must then be compared with existing dosimetry data. Linear energy transfer (LET) spectra, absorbed dose, and dose equivalent from galactic cosmic radiation and its fragments are presented for four, representative low-earth orbit configurations. The orbits include a high (STS-5IJ) and low (STS-61C) altitude, low-inclination (28.5 degs) flight; a high inclination (49.5 degs) flight (STS-51F); and a polar flight. Results are compared with computations for an exo-magnetospheric flight. GRA

N89-23064# Westinghouse Electric Corp., Cockeysville, MD. Product Support and Equipment Dept.
MOTOR THEORY OF AUDITORY PERCEPTION Final Report, 1 Sep. 1987 - 31 Aug. 1988
Heather Williams 2 Dec. 1988 53 p
(Grant AF-AFOSR-0336-86; AF Proj. 2313)
(AD-A204951; AFOSR-89-0213TR) Avail: NTIS HC A04/MF A01 CSCL 06D

Behavioral paradigms have been developed that yield quantifiable, reliable results for testing the discriminability of two auditory stimuli (operant go-nogo) and individuals' preferences between two stimuli (two-speaker choice test). The copulation solicitation response is not reliable. Zebra finches can learn to produce and discriminate variants in the timbre' of song syllables. Adult males learn a discrimination between two similar songs more quickly when one of those songs is their own. Auditory responses have been recorded, measured, and cataloged in all the forebrain nuclei with connections to the song motor system. The latencies may give indications of how this auditory information is processed. Deafening studies had led to the conclusion that vocal plasticity ceased at sexual maturity in closed-ended song learners. This is not so: when a hearing male's song is altered by cutting the vocal motor nerves, a limited form of plasticity in production is seen. GRA

N89-23065# Air Force Inst. of Tech., Wright-Patterson AFB, OH. School of Engineering.
A NEW PERSPECTIVE IN THE ETIOLOGY, TREATMENT, PREVENTION AND PREDICTION OF SPACE MOTION SICKNESS M.S. Thesis
Rogelio Morales, Jr. Dec. 1988 169 p
(AD-A205660; AFIT/GSO/ENG/88D-2) Avail: NTIS HC A08/MF A01 CSCL 06O

Seven male subjects were given the drug phenytoin (dilantin) in double blind, placebo-controlled crossover experiment. Subjects were rotated in a motion stimulus chair while several of their physiological parameters were measured. Subjects treated with dilantin were found to have a greater tolerance to motion sickness than when they were treated with a placebo. Also, dilantin did not affect the physical performance and cognitive skills of the subjects. The research analyzed heart rate, respiration, gastro-intestinal activity, and brain wave activity. The research found an increase in mean heart rates, mean respiration intake volume, and electrosplanchnogram root mean square voltages during motion sickness. Root mean square voltage of subdelta-delta (.05 to 1 Hz) electroencephalogram (EEG) activity increased in subjects that were least susceptible to motion sickness while subjects that were highly susceptible to motion sickness had insignificant subdelta-delta EEG activity. Motion sickness models were developed using the Barron Associates' Abductive Reasoning Mechanism (ARM) software. Motion sickness prediction models were developed using the ARM software and linear regression. GRA

N89-23066# Naval Health Research Center, San Diego, CA.
BENZODIAZEPINES AND CAFFEINE: EFFECT ON DAYTIME SLEEPINESS, PERFORMANCE, AND MOOD Interim Report
L. C. Johnson, C. L. Spinweber, and S. A. Gomez 21 Dec. 1988 31 p
(AD-A205862; NHRC-88-51) Avail: NTIS HC A03/MF A01 CSCL 06O

In a double-blind parallel group design, 80 young adult males were divided into eight treatment groups. Subjects received 15 or 30 mg of flurazepam, 0.25 or 0.50 mg of triazolam, or placebo at bedtime, and 250 mg of caffeine or placebo in the morning for two treatment days. Two objective (MSLT and lapses) and two subjective (Stanford Sleepiness Scale and Visual Analog) measures of sleepiness, five performance tests, and two mood measures (Profile of Mood Scale and Visual Analog Scale) were administered repeatedly on both days. Significant treatment effects were found for sleepiness but not for performance or mood. Early morning caffeine significantly antagonized next day hypnotic induced drowsiness and enhanced alertness in the subjects who received bed time placebo. Flurazepam, 30 mg, subjects were more sleepy than all other groups, but the flurazepam, 15 mg, group did not differ significantly from those receiving triazolam. Although not significantly different, the flurazepam, 30 mg, group had a poorer performance score and more negative mood than the other groups. Performance in this group was most improved by caffeine. In all groups, sleepiness was greatest and performance and mood poorest in early morning trials and caffeine was most effective at this time. GRA

53 BEHAVIORAL SCIENCES

Includes psychological factors; individual and group behavior; crew training and evaluation; and psychiatric research.

No abstracts in this category.

54 MAN/SYSTEM TECHNOLOGY AND LIFE SUPPORT

Includes human engineering; biotechnology; and space suits and protective clothing.

For related information see also *16 Space Transportation.*

N89-23067# Air Force Inst. of Tech., Wright-Patterson AFB, OH. School of Engineering.

A REAL-TIME SIMULATOR FOR MAN-IN-THE-LOOP TESTING OF AIRCRAFT CONTROL SYSTEMS (SIMTACS-RT) M.S. Thesis

Gary G. Dameron Dec. 1988 136 p

(AD-A202599; AD-E900870; AFIT/GE/ENG/88D-8) Avail: NTIS HC A07/MF A01 CSCL 01D

A real time, high fidelity simulator is constructed to model F-16 dynamics and control laws. Built around and Electronics Associates Incorporated (EAI) SIMSTAR hybrid computer, the simulator (SIMTACS-RT) uses nonlinear, coupled differential equations for its dynamic model. An EAI FGS 300 function generator is used to access an aerodynamic data base of 25000 values in real time. Man-in-the-loop simulation is supported with a force stick for pilot inputs and an oscilloscope display for pitch and roll information (the lateral program is still in development). Four hybrid computer programs are presented as user ready simulation/analysis tools, supporting both multi-rate digital and analog control laws. Recommendations for further improvement in simulator realism are presented. GRA

N89-23068*# National Aeronautics and Space Administration. Langley Research Center, Hampton, VA.

THE SPACE STATION FLIGHT TELEROBOTIC SERVICER AND THE HUMAN

Kelli F. Willshire, James G. Watzin (National Aeronautics and Space Administration. Goddard Space Flight Center, Greenbelt, MD.), and Phyllis K. Millen Apr. 1989 34 p Presented at the 2nd International Conference on the Human-Computer Interaction, Honolulu, HI, 10-15 Aug. 1987

(NASA-TM-100615; NAS 1.15:100615) Avail: NTIS HC A03/MF A01 CSCL 05H

The Space Station Flight Telerobotic Servicer (FTS) and its human-machine interaction issues are described. Included is a discussion of the FTS strawman concept and the FTS workstation human factor issues. Author

N89-23069# CHI Systems, Inc., Blue Bell, PA.

AN EXPERIMENTAL ENVIRONMENT AND LABORATORY FOR STUDYING HUMAN INFORMATION PROCESSING IN NAVAL AIR ASW (NAVAL AIR ANTISUBMARINE WARFARE) Technical Report, 30 Sep. 1987 - 29 Sep. 1989

Wayne Zachary and Monica C. Zubritzky 20 Oct. 1988 71 p

(Contract N00014-87-C-0814)

(AD-A204774; TR-881020-8704) Avail: NTIS HC A04/MF A01 CSCL 23B

This report documents a laboratory facility to support experimental research into human-computer interaction and decision-making in Naval Air Anti-Submarine Warfare mission management. The facility contains three components, all of which run on a SUN Workstation; 1) a simulated Air ASW workstation and mission, 2) experimental design tools, and 3) a data collection and transformation tools. The workstation/simulation simulation provides a realistic yet simplified version of ASW mission management as performed by the Tactical Coordinator (TACCO) on board a Naval ASW aircraft. Embedded in this simulation are automated data collection programs which collect keystroke-level data on TACCO actions as well as on the situational and display context within which the actions were taken. Additional tools translate these data into timelines and other forms needed to support the building of GOMS- and blackboard-based cognitive models of the human operator. The experimental design tools provide experimenter-friendly utilities for the creation of experimental problems with desired physical and cognitive demands on the subject. The laboratory is also designed to support implementation and experimentation with advanced adaptive user interfaces to the TACCO based on the cognitive models currently being developed. GRA

N89-23070# National Aerospace Lab., Amsterdam (Netherlands). Flight Div.

AN IN-FLIGHT INVESTIGATION OF WORKLOAD ASSESSMENT TECHNIQUES FOR CIVIL AIRCRAFT OPERATIONS

R. C. vandeGraaf 26 Aug. 1987 132 p

(Contract NIVR-01406N)

(NLR-TR-87119-U; ETN-89-94197) Avail: NTIS HC A07/MF A01

An in-flight study to assess short-term workload was set up to investigate the problem of drawing conclusions from a variety of experimental measures in a complex task situation. Several implications are pointed out, such as dealing with mutually different outcomes, the designation of artefacts, and the problem of formulating final conclusions without the (a priori) availability of a method for evaluating other methods. An experimental program based on normal approach conditions for transport aircraft is outlined. The considered measures include pilot and safety pilot ratings (McDonnell 10-point rating scale, SWAT 3x3 rating matrix), measures of the pilot's heart rate, and measures reflecting control activity and task performance. The usefulness of two (pilot-aircraft) model-based methods (using the HRA and PROCRU computer programs) was examined. The experimental results show the necessity of the use of a set of different measures to guarantee a reliable assessment. Pros and cons of different measures are discussed. A strategy dealing with the formulation of final conclusions based on the outcomes of a variety of measures is considered. ESA

N89-23071# State Univ. of New York, Buffalo. Pulmonary Div.

EFFICACY OF CONVENTIONAL AND HIGH-FREQUENCY VENTILATION AT ALTITUDE Final Report, Jul. 1985 - Dec. 1986

Robert A. Klocke, Alan T. Aquilina, Brydon J. Grant, Alan R. Saltzman, Patricia A. Land, and Neel B. Ackerman, Jr. (Department of the Air Force, Washington, DC.) Dec. 1988 62 p

(Contract F33615-83-D-0601)

(AD-A205922; USAFSAM-TR-88-10) Avail: NTIS HC A04/MF A01 CSCL 23E

High-frequency ventilation (HFV) is a promising mode of ventilatory support and could be useful in aeromedical evacuation. There have been no studies to date to examine the feasibility of maintaining gas exchange with HFV at reduced barometric pressure. This report investigates: (1) the role of molecular diffusion in gas transport during HFV, and (2) the ability to maintain gas exchange with HFV at simulated altitude in healthy and in diseased lungs. The role of molecular diffusion was tested by determining the rate of pulmonary uptake of six tracer gases with low aqueous solubility but different molecular weights during conventional and high-frequency ventilation. The inspired gas and the subsequent rate of appearance of these gases in arterial blood were monitored. With conventional mechanical ventilation (CMV), there was separation of the gases with appearance in arterial blood occurring in order of increasing molecular weight. With HFV, there was a slight molecular weight effect, but substantially less than that seen with CMV. These findings indicate that the role of molecular diffusion during HFV is minimal, but a significantly greater effect of diffusion is present during CMV. GRA

55 SPACE BIOLOGY

Includes exobiology; planetary biology; and extraterrestrial life.

No abstracts in this category.

59 MATHEMATICAL AND COMPUTER SCIENCES (GENERAL)

No abstracts in this category.

60 COMPUTER OPERATIONS AND HARDWARE

Includes hardware for computer graphics, firmware, and data processing.

For components see *33 Electronics and Electrical Engineering.*

N89-23072# Sandia National Labs., Albuquerque, NM.
IMPLEMENTING SECURITY MEASURES FOR COMPUTER-BASED SECURITY SYSTEMS
Debra A. Faculjak Feb. 1989 55 p
(Contract DE-AC04-76DP-00789)
(DE89-008995; SAND-88-3114) Avail: NTIS HC A04/MF A01

The purpose of this document is to ensure that system designers: (1) become familiar with security issues, policy, and directives, and (2) are able to integrate protection of the computer, its peripherals, and its data into the system at an early stage in its design. This document provides a comprehensive and uniform review of those security issues that are pertinent to the applications developed within Directorate 5200. The intention of this document is to provide guidance in the development of appropriate computer security protection for the SNLA-developed security systems. The policies and standards of computer security, set forth by the Department of Defense (DOD) and the DOE, are provided to enhance the designers' understanding of the rationale for such security. DOE

N89-23073*# Institute for Computer Applications in Science and Engineering, Hampton, VA.
IMPLEMENTING NESTED CONDITIONAL STATEMENTS IN SIMD MACHINES Final Report
David Middleton Apr. 1989 17 p Prepared in cooperation with NASA, Langley Research Center
(Contract NAS1-18605)
(NASA-CR-181832; ICASE-89-27; NAS 1.26:181832) Avail: NTIS HC A03/MF A01 CSCL 09B

Single instruction, multiple data (SIMD) computers consist of a very large number of processors executing a common sequence of instructions. Maintaining the full speedup potential of such machines is most sensitive to conditional execution in their programs, regions of code where some processing elements (PEs) perform no useful work. Techniques are presented for efficiently implementing nested conditional statements, specifically if and case statements, in SIMD machines, while adding minimal specialized hardware. Author

N89-23093# Massachusetts Inst. of Tech., Cambridge. Artificial Intelligence Lab.
THE MIT VISION MACHINE
T. Poggio, J. Little, E. Gamble, W. Gillett, D. Geiger, Daphna Weinshall, M. Villalba, N. Larson, Todd Anthony Cass, and H. Buelthoff et al *In* Science Applications International Corp., Proceedings: Image Understanding Workshop, Volume 1 Apr. 1988 p 177-198 (For primary document see N89-23074 16-61)
Avail: NTIS HC A22/MF A01 CSCL 09B

61 COMPUTER PROGRAMMING AND SOFTWARE

Includes computer programs, routines, alogorithms, and specific applications, e.g., CAD/CAM.

N89-23074# Science Applications International Corp., McLean, VA.
PROCEEDINGS: IMAGE UNDERSTANDING WORKSHOP, VOLUME 1 Annual Technical Report, Feb. 1987 - Apr. 1988
Lee S. Baumann, ed. Apr. 1988 525 p Workshop held in Cambridge, MA, 6-8 Apr. 1988; sponsored by DARPA
(Contract N00014-86-C-0700; ARPA Order 5605)
(AD-A197558) Avail: NTIS HC A22/MF A01 CSCL 09B

This document contains the annual progress reports and technical papers presented on the research activities in image understanding at a workshop conducted on 6 to 8 April 1988, in Cambridge, Massachusetts. Also included are copies of invited papers presented at the workshop and additional technical papers from the research activities which were not presented due to lack of time but are germane to this research field. Topics discussed include: intelligent systems, robotics, knowledge-based vision, algorithms, pattern matching, feedback, tracking, autonomous navigation, parallel processing, target recognition, data integration, motion recognition, and image analysis. For individual titles, see N89-23075 through N89-23114.

N89-23075# Massachusetts Inst. of Tech., Cambridge. Artificial Intelligence Lab.
MIT PROGRESS IN UNDERSTANDING IMAGES
T. Poggio et al *In* Science Applications International Corp., Proceedings: Image Understanding Workshop, Volume 1 Apr. 1988 p 1-12 (For primary document see N89-23074 16-61)
Avail: NTIS HC A22/MF A01 CSCL 09B

Work in the past year has concentrated on three main projects, each one representing a complementary aspect of a complete vision system. The first project - a parallel Vision Machine - has the goal of developing a system for integrating early vision modules and computing a robust description of the discontinuities of the surfaces and of their physical properties. Additional goals of the project are the refinement of early vision algorithms and their implementation on a massively parallel architecture such as the Connection Machine System. The second project concerns visual recognition; several schemes for model based recognition were developed and implemented. Finally, work has continued on autonomous navigation. Around these main themes, additional work, at the theoretical and implementation level, has been done in motion analysis, navigation, photogrammetry, visual routines, and learning. Author

N89-23076# University of Southern California, Los Angeles. Inst. for Robotics and Intelligent Systems.
USC IMAGE UNDERSTANDING RESEARCH: 1987-1988
Ramakant Nevatia *In* Science Applications International Corp., Proceedings: Image Understanding Workshop, Volume 1 Apr. 1988 p 13-16 (For primary document see N89-23074 16-61)
(Contracts DACA76-85-C-0009; F33615-87-C-1436)
Avail: NTIS HC A22/MF A01 CSCL 09B

University of Southern California Image Understanding research projects are summarized and references to more detailed projects and papers are provided. The work has focussed on the topics of: mapping from aerial images, robotics vision, motion analysis for autonomous land vehicles (ALV), some general techniques, and parallel processing. Author

N89-23077# Stanford Univ., CA. Robotics Lab.
IMAGE UNDERSTANDING: INTELLIGENT SYSTEMS
Thomas O. Binford *In* Science Applications International Corp., Proceedings: Image Understanding Workshop, Volume 1 Apr. 1988 p 17-28 (For primary document see N89-23074 16-61)
(Contract F33615-85-C-5106)
Avail: NTIS HC A22/MF A01 CSCL 09B

Progress in model-based vision, implemented in the SUCCESSOR system, is summarized. Results are presented in three areas. The first is representation and geometric modeling. New generic modeling of object classes was achieved, models of three classes were built, and a generic model of a hallway was used to build a model of the hallway of the Robotics Laboratory building. A general painted-surface model for metals and non-metals, specular and non-specular reflection; a new physical model for diffuse reflection; curved-axis solids of revolution (CSR); set operations with CSRs; and boundary representation by trimmed-surfaces have been added. The second area is interpretation of scenes and data. Initial results were obtained in expressing structural relations, measurement evidence, and predictive evidence in a Bayesian network model. Computational complexity was addressed by basing generation of hypotheses on quasi-invariant observables. A new generic observability model for diffuse reflection from surfaces was obtained. New results were obtained on differential geometry of generalized cylinders and ribbons. The third area is segmentation and building structured descriptions of scenes. New results are described from a hierarchical stereo correspondence system which builds descriptions of objects and surfaces. Stereo reconstruction of curved surfaces is shown. Preliminary results on texture segmentation are presented. Edge segmentation into regions, global color region segmentation, and local color segmentation of edges are described. Author

N89-23078# Maryland Univ., College Park. Computer Vision Lab.

IMAGE UNDERSTANDING RESEARCH AT THE UNIVERSITY OF MARYLAND, DECEMBER 1986 - JANUARY 1988

Azriel Rosenfeld, Larry S. Davis, and John Aloimonos *In* Science Applications International Corp., Proceedings: Image Understanding Workshop, Volume 1 Apr. 1988 p 29-39 (For primary document see N89-23074 16-61)

Avail: NTIS HC A22/MF A01 CSCL 09B

Research in image understanding is briefly summarized. The areas covered include: motion analysis, 3D vision, range sensing, navigation, interpretation of aerial images, digital and computational geometry, parallel algorithms, and pyramid techniques. Author

N89-23079# Carnegie-Mellon Univ., Pittsburgh, PA. Dept. of Computer Science.

CMU IMAGE UNDERSTANDING PROGRAM

Takeo Kanade *In* Science Applications International Corp., Proceedings: Image Understanding Workshop, Volume 1 Apr. 1988 p 40-52 (For primary document see N89-23074 16-61)

Avail: NTIS HC A22/MF A01 CSCL 09B

Image Understanding covers a wide range of topics ranging from the basic computer vision issues in color, motion, and shape to the vision system issues in parallel architectures and outdoor navigation systems. Progress in this field is reviewed. Highlights include: continuous stereo by Kahlman filtering, color image segmentation by dichromatic reflection model, sensor modeling for model-based vision, 3D FORM system for geometric modeling, Navlab demonstration systems, range data analysis for outdoor scenes, precise camera calibration process, microscopic traffic simulator, parallel vision software on Warp, and Scan Line Array Processors (SLAP). Author

N89-23080# SRI International Corp., Menlo Park, CA. Artificial Intelligence Center.

IMAGE UNDERSTANDING RESEARCH AT SRI INTERNATIONAL

Martin A. Fischler and Robert C. Bolles *In* Science Applications International Corp., Proceedings: Image Understanding Workshop, Volume 1 Apr. 1988 p 53-61 (For primary document see N89-23074 16-61)

(Contracts MDA903-86-C-0084; DACA76-85-C-0004)

Avail: NTIS HC A22/MF A01 CSCL 09B

The Image Understanding research program is a broad effort spanning the entire range of machine vision research. The progress in two programs is described: the first is concerned with modeling the earth's surface from aerial photographs; the second is concerned with visual interpretation for land navigation. In particular, the following are described: progress in the design of a core knowledge structure; representing, recognizing, and rendering complex natural and man-made objects; recognizing and modeling terrain features and man-made objects in image sequences; interactive techniques for scene modeling and scene generation; automated detection and delineation of cultural objects in aerial imagery; and automated terrain modeling from aerial imagery. Author

N89-23081# Massachusetts Univ., Amherst. Dept. of Computer and Information Science.

SUMMARY OF IMAGE UNDERSTANDING RESEARCH AT THE UNIVERSITY OF MASSACHUSETTS

Edward M. Riseman and Allen R. Hanson *In* Science Applications International Corp., Proceedings: Image Understanding Workshop, Volume 1 Apr. 1988 p 62-72 (For primary document see N89-23074 16-61)

(Contracts DACA76-85-C-0008; DACA76-86-C-0015; F30602-87-C-0140; N00014-82-K-0464; DMA800-85-C-0012; AF-AFOSR-0021-86; NSF DCR-85-00332)

Avail: NTIS HC A22/MF A01 CSCL 09B

Several areas of research in the Image Understanding Program are summarized, including: (1) knowledge-based vision; (2) database support for symbolic vision processing; (3) motion processing; (4) perceptual organization (grouping); (5) image understanding architecture; (6) integrated vision benchmark for parallel architectures; and (7) mobile vehicle navigation. A fundamental goal of the computer vision research environment is the integration of a diverse set of research efforts into a system that is ultimately intended to achieve real-time image interpretation. Two major system integration efforts are the VISIONS static interpretation system, which is a knowledge-based computer vision system utilizing parallel modular processes that communicate via a blackboard, and an autonomous mobile vehicle for navigation through a partially known environment. Author

N89-23082# Rochester Univ., NY. Dept. of Computer Science.

PROGRESS IN IMAGE UNDERSTANDING AT THE UNIVERSITY OF ROCHESTER

Christopher M. Brown *In* Science Applications International Corp., Proceedings: Image Understanding Workshop, Volume 1 Apr. 1988 p 73-77 (For primary document see N89-23074 16-61)

Avail: NTIS HC A22/MF A01 CSCL 09B

Progress in various areas of image understanding is discussed. Areas included are active vision, object recognition, multi-model segmentation with Markov random fields, high-level issues in vision, hardware and systems support for parallel vision, and vision theory. Author

N89-23083# Columbia Univ., New York, NY. Dept. of Computer Science.

IMAGE UNDERSTANDING AND ROBOTICS RESEARCH AT COLUMBIA UNIVERSITY

John R. Kender, Peter K. Allen, Terrance E. Boult, and Hussein A. H. Ibrahim *In* Science Applications International Corp., Proceedings: Image Understanding Workshop, Volume 1 Apr. 1988 p 78-87 (For primary document see N89-23074 16-61)

(Contract DACA76-86-C-0024)

Avail: NTIS HC A22/MF A01 CSCL 09B

Diverse research investigations in vision and robotics are identified and summarized. Since it is difficult to separate those aspects of robotic research that are purely visual from those that are vision-like (for example, tactile sensing) or vision-related (for example, integrated vision-robotic systems), all robotic research that is not purely manipulative is listed. Areas of research that are identified are low-level vision: theories involving stereo, data representations, and applications to graphics; middle-level vision: regularized surface reconstruction and stereo, sensory fusion, shape from dynamic shadowing, and application to range data; spatial relations: representations of objects and space, and theory

and practice of navigation; parallel algorithms: low- and middle-level vision theory, research and applications on tree machines, and research and applications on pipelined machines; and, finally, robotics and tactile sensing: system development, and multi-fingered object recognition. Author

N89-23084# Hughes Research Labs., Calabasas, CA. Artificial Intelligence Center.

KNOWLEDGE-BASED VISION TECHNOLOGY PROGRESS AT HUGHES AI CENTER

K. E. Olin, M. J. Dally, John G. Harris, and Kurt Reiser *In* Science Applications International Corp., Proceedings: Image Understanding Workshop, Volume 1 Apr. 1988 p 88-93 (For primary document see N89-23074 16-61)

(Contracts DACA76-85-C-0007; DACA76-85-C-0017)

Avail: NTIS HC A22/MF A01 CSCL 09B

The research progress reported is concerned primarily with two topic areas; first, vision and systems for navigation, and second, object recognition. The first cross-country map and sensor-based autonomous operation of a robotic vehicle in natural terrain was achieved in August 1987 and repeated with extended capabilities in December 1987. The vehicle avoided difficult obstacles such as bushes, gullies, rock outcrops, and steep slopes. In preparation for experiments onboard the autonomous land vehicle, an extensive simulation capability was developed. In Section 1 an overview is presented of the approach, the perception system development, and the planning system. Details of the perception and planning techniques are presented in other papers. A multisolution image interpretation system was developed for object detection. The objective of this system was to detect objects by reasoning with multiple feature sets represented in object models. A feature set is comprised of a rich variety of image primitives together with spatial relationships. The multiresolution interpretation used lower resolutions to focus attention and higher resolution for object details. An overview of this system is presented in Section 2. Author

N89-23085# General Electric Co., Schenectady, NY. Corporate Research and Development Center.

IMAGE UNDERSTANDING RESEARCH AT GE

Joseph L. Mundy *In* Science Applications International Corp., Proceedings: Image Understanding Workshop, Volume 1 Apr. 1988 p 94-95 (For primary document see N89-23074 16-61)

(Contract DACA76-86-C-0007)

Avail: NTIS HC A22/MF A01 CSCL 09B

Major goals and research results for the Image Understanding Project are reviewed. The primary research emphasis is on model based object recognition and geometric reasoning. Author

N89-23086# Honeywell Systems and Research Center, Minneapolis, MN.

QUALITATIVE REASONING AND MODELING FOR ROBUST TARGET TRACKING AND RECOGNITION FROM A MOBILE PLATFORM

Bir Bhanu and Durga Panda *In* Science Applications International Corp., Proceedings: Image Understanding Workshop, Volume 1 Apr. 1988 p 96-102 (For primary document see N89-23074 16-61)

Avail: NTIS HC A22/MF A01 CSCL 09B

The DARPA Strategic Computer Vison Program focuses on demonstrating robust techniques for target tracking and recognition from a moving robotic combat vehicle. The work is specifically directed towards significant enhancements in the performance of existing target tracking techniques under high clutter and low contrast situations in a ground-to-ground scenario when the robotic conbat vehicle is in motion and multiple targets may appear at varying ranges. The topics currently under investigation are: decomposition of complex vehicle motion into its constituent parts; qualitative 3-D scene modeling; target motion detection and tracking; landmark recognition; 3-D target model acquisition and refinement; and the use of recognition and map information in an integrated motion detection and tracking system. The research results are useful in vision controlled navigation/guidance of a robotic combat vehicle for practical military missions such as targeting, reconnaissance, and surveillance. Progress made during the period from March 1987 to January 1988 is summarized. Technology transfer aspects of the work are also discussed. Author

N89-23087# Advanced Decision Systems, Mountain View, CA.

KNOWLEDGE BASED VISION FOR TERRESTRIAL ROBOTS

Daryl T. Lawton, Tod S. Levitt, and Patrice Gelband *In* Science Applications International Corp., Proceedings: Image Understanding Workshop, Volume 1 Apr. 1988 p 103-110 (For primary document see N89-23074 16-61)

(Contract DACA76-85-C-0005)

Avail: NTIS HC A22/MF A01 CSCL 09B

The Knowledge Based Vision Project is concerned with developing terrain recognition and modeling capabilities for an autonomous land vehicle for functioning in outdoor environments. The vehicle will be provided with a laser range finder, controllable cameras, limited inertial sensing, and have limited, inexact, and undetailed a priori terrain information, generally in the form of labeled grid data. One of the basic functions of the vehicle is to elaborate this terrain map of the environment. Another is to successfully navigate through the environment using landmarks. The scene data base is where the interpretation of images from a single location is developed. The developed scene is referred to as a viewframe. Other data bases store views from different locations, relationships between views, and objects, such as landmarks, that viewframes have in common. In the underlying functional architecture two different types of processing flow are being studied. The first involves accessing an existing viewframe and using it to recognize predicted objects. The second involves developing a viewframe without any a priori information. The work is based upon a generic terrestrial viewframe model which includes several constraints on the formation of perceptual groups based upon the relative direction of gravity, the horizon line determined by the orientation to the immediate ground plane, and the projected egocentric directions from the observer on this plane. Author

N89-23088# Massachusetts Univ., Amherst. Dept. of Computer and Information Science.

AN INTEGRATED IMAGE UNDERSTANDING BENCHMARK: RECOGNITION OF A 2 1/2 D MOBILE

Charles C. Weems, Edward M. Riseman, Allen R. Hanson, and Azriel Rosenfeld (Maryland Univ., College Park.) *In* Science Applications International Corp., Proceedings: Image Understanding Workshop, Volume 1 Apr. 1988 p 111-126 (For primary document see N89-23074 16-61)

(Contract DACA76-86-C-0015)

Avail: NTIS HC A22/MF A01 CSCL 09B

This benchmark is the second in a series of efforts to evaluate the merits of various parallel architectures as applied to Image Understanding. The first benchmark exercise considered only execution times for a set of isolated vision-related tasks. This second benchmark exercise addresses the issue of system performance on an integrated set of tasks where the task interactions that are typical of complex vision applications are present. The goal of this exercise is to gain a better understanding of vision architecture requirements, that can be used to guide the development of the next generation of vision architectures. Author

N89-23089# Massachusetts Univ., Amherst. Dept. of Computer and Information Science.

SOME SAMPLE ALGORITHMS FOR THE IMAGE UNDERSTANDING ARCHITECTURE

Charles C. Weems *In* Science Applications International Corp., Proceedings: Image Understanding Workshop, Volume 1 Apr. 1988 p 127-138 (For primary document see N89-23074 16-61)

(Contracts F49620-86-C-0041; DACA76-86-C-0015)

Avail: NTIS HC A22/MF A01 CSCL 09B

The Image Understanding Architecture (IUA) is a heterogenous, multi-level, associative, parallel architecture that is designed to

support real-time knowledge-based computer vision research and applications. A 1/64th scale proof-of-concept prototype is currently under construction. The IUA architecture and a programmer's model of the machine are briefly summarized, and several algorithms are presented that demonstrate some of the features of the low and intermediate levels of the architecture in performing computer vision tasks. These include both local and global associative operations, horizontal and vertical communication, and Single Instruction Stream/Multiple Data (SIMD), multi-SIMD, and synchronous-Multiple Instruction/Multiple Data (MIMD) processing modes. Author

N89-23090# David Sarnoff Research Center, Princeton, NJ.
ALGORITHMS AND ARCHITECTURES FOR SMART SENSING
Peter J. Burt *In* Science Applications International Corp., Proceedings: Image Understanding Workshop, Volume 1 Apr. 1988 p 139-153 (For primary document see N89-23074 16-61)
Avail: NTIS HC A22/MF A01 CSCL 09B

Human vision is a distinctly dynamic process in which the eyes move through a sequence of fixations to selectively gather scene information for the task at hand. Similar strategies are being developed for computer vision. Included in these smart sensing techniques are mechanisms analogous to peripheral alerting and foveal attention in humans. Perhaps most importantly, smart sensing requires a close interaction between low and high level vision mechanisms, as image understanding processes guide information gathering processes even as initial image data is being interpreted. Smart sensing techniques can have a profound effect on the efficiency of a vision system, increasing its speed often by several orders of magnitude. The multiresolution, pyramid structure provides a computational framework for smart sensing. Computer architectures for hierarchical image analysis that support smart sensing, and hardware to perform multiresolution image analysis at video rates are discussed. Author

N89-23091# Maryland Univ., College Park. Computer Vision Lab.
THE MARYLAND APPROACH TO IMAGE UNDERSTANDING
John Aloimonos, Larry S. Davis, and Azriel Rosenfeld *In* Science Applications International Corp., Proceedings: Image Understanding Workshop, Volume 1 Apr. 1988 p 154-165 (For primary document see N89-23074 16-61)
(Contract DAAB07-86-K-F073)
Avail: NTIS HC A22/MF A01 CSCL 09B

In an effort to understand images, while still working on initial processes of low and middle level vision, emphasis is being placed on the integration of multiple sources of information for visual reconstruction, on navigation and on object recognition. A methodological paradigm for research in vision is introduced, namely: while research is continuing top-down in the Marr paradigm, work also progresses in a bottom-up fashion in that paradigm. It is suggested that the Marr paradigm (computational theory, algorithms, data structures, and implementation) should be augmented with one more level, that of robustness, that Marr left implicit in his writings. Author

N89-23092# Columbia Univ., New York, NY. Dept. of Computer Science.
AN INTEGRATED APPROACH TO STEREO MATCHING, SURFACE RECONSTRUCTION AND DEPTH SEGMENTATION USING CONSISTENT SMOOTHNESS ASSUMPTIONS
Liang-Hua Chen and Terrance E. Boult *In* Science Applications International Corp., Proceedings: Image Understanding Workshop, Volume 1 Apr. 1988 p 166-176 (For primary document see N89-23074 16-61)
(Contract N00039-84-C-0165)
Avail: NTIS HC A22/MF A01 CSCL 09B

A stereo matching algorithm is presented. It makes use of simultaneous matching, surface reconstruction, and segmentation of world surfaces. By integrating these three phases, which are traditionally temporally separated, the algorithm can make use of the current surface information to help diambiguate the potential matches. After discussing the required mathematical background, the integrated process of matching, reconstruction and segmentation is discussed. Unlike past attempts at integrating these processes, the presented algorithm uses a single smoothness criterion for both matching, reconstruction and segmentation. The segmentation part of the process is based on estimates of surface ending energy, and is significantly different from previous segmentation algorithms. Examples are presented showing results on both synthetic images and camera acquired images. The camera-based examples include both a traditional type scene with two objects, and a scene with transparent objects. Author

N89-23093# Massachusetts Inst. of Tech., Cambridge. Artificial Intelligence Lab.
THE MIT VISION MACHINE **c60**
T. Poggio, J. Little, E. Gamble, W. Gillett, D. Geiger, Daphna Weinshall, M. Villalba, N. Larson, Todd Anthony Cass, and H. Buelthoff et al *In* Science Applications International Corp., Proceedings: Image Understanding Workshop, Volume 1 Apr. 1988 p 177-198 (For primary document see N89-23074 16-61)
Avail: NTIS HC A22/MF A01 CSCL 09B

The vision Machine, its goals, and achievements to date are described. The Vision Machine is a computer system that attempts to integrate several vision cues to achieve high performance in unstructured environments for the tasks of recognition and navigation. It is also a test-bed for theoretical progress in early vision algorithms, their parallel implementation and their integration. The Vision Machine consists of a movable two-camera Eye-Head system (the input device) and a 16K Connection Machine (the main computational engine). Several parallel early vision algorithms which compute edge detection, stereo, motion, texture and surface color in close to real-time were developed and implemented. The integration stage is based on the technique of coupled Markov Random Field models, and leads to a cartoon-like map of the discontinuities in the scene, with a partial labeling of the brightness edges in terms of their physical origin. Available recognition algorithms will interface with the output of the integration stage and the analog and hybrid Very Large Scale Integration (VLSI) implementations of the Vision Machine main components has begun. Author

N89-23094# Carnegie-Mellon Univ., Pittsburgh, PA. Dept. of Computer Science.
KALMAN FILTER-BASED ALGORITHMS FOR ESTIMATING DEPTH FROM IMAGE SEQUENCES
Larry Matthies, Richard Szeliski, and Takeo Kanade *In* Science Applications International Corp., Proceedings: Image Understanding Workshop, Volume 1 Apr. 1988 p 199-213 (For primary document see N89-23074 16-61)
(Contract F33615-87-C-1499)
Avail: NTIS HC A22/MF A01 CSCL 09B

Using known camera motion to estimate depth from image sequences is an important problem in robot vision. Many applications of depth from motion, including navigation and manipulation, require algorithms that can estimate depth in an on-line, incremental fashion. This requires a representation that records the uncertainty in depth estimates and a mechanism that integrates new measurements with existing depth estimates to reduce the uncertainty over time. Kalman filtering provides this mechanism. Previous applications of Kalman filtering to depth from motion have been limited to estimating depth at the location of a sparse set of features. A pixel-based (iconic) algorithm is introduced which estimates depth and depth uncertainty at each pixel and incrementally refines these estimates over time. The algorithm for translations parallel to the image plane is described and its formulation and performance contrasted to that of a feature-based Kalman filtering algorithm. The performance of the two approaches is compared by analyzing their theoretical convergence rates, by conducting quantitative experiments with images of a flat poster, and by conducting qualitative experiments with images of a realistic outdoor scene model. The results show that the method is an

effective way to extract depth from lateral camera translations and suggest that it will play an important role in low-level vision. Author

N89-23095# Rochester Univ., NY. Dept. of Computer Science.
MULTIMODAL RECONSTRUCTION AND SEGMENTATION WITH MARKOV RANDOM FIELDS AND HCF OPTIMIZATION
P. B. Chou and C. M. Brown *In* Science Applications International Corp., Proceedings: Image Understanding Workshop, Volume 1 Apr. 1988 p 214-221 (For primary document see N89-23074 16-61)
(Contracts F30602-85-C-0008; DACA76-85-C-0001; N00014-82-K-0193; NSF DCR-83-20136)
Avail: NTIS HC A22/MF A01 CSCL 09B

Segmentation of a visual input into regions corresponding to three-dimensional objects is an important step in many image analysis algorithms. Reconstruction of physical properties (such as depth or surface orientation) is similarly important. Fusing multiple sources of visual data seems a practical way to improve robustness, as does guiding interpretation with prior domain knowledge. Coupled Markov random fields provide a unifying mechanism to accomplish all these goals simultaneously. The Highest Confidence First algorithm is an optimization heuristic that yields good results in finding high-probability reconstruction and discontinuity values. Its use in this context involves making precise the relation between intensity and depth discontinuities. In synthetic data, the contribution of intensity information to depth reconstruction and segmentation is significant. Author

N89-23096# Illinois Univ., Urbana. Coordinated Science Lab.
IU AT UI: AN OVERVIEW AND AN EXAMPLE ON SHAPE FROM TEXTURE
Narendra Ahuja and Thomas Huang *In* Science Applications International Corp., Proceedings: Image Understanding Workshop, Volume 1 Apr. 1988 p 222-253 Sponsored in part by NSF, Washington, DC, AFOSR, Washington, DC, NBS, Washington, DC, AT and T, Rockwell International, Eastman Kodak and Northrop (For primary document see N89-23074 16-61)
Avail: NTIS HC A22/MF A01 CSCL 09B

An overview of some recent research in image understanding (IU) is presented, including an overview of the integration approach used in a number of IU problems. Several examples of research that uses integration for image interpretation are summarized. The use of integration in solving the shape from texture problem is described in detail. Author

N89-23097# Schlumberger Palo Alto Research, CA.
PHYSICALLY BASED MODELING FOR VISION AND GRAPHICS
Andrew Witkin, Michael Kass, Demetri Terzopoulos, and Kurt Fleischer *In* Science Applications International Corp., Proceedings: Image Understanding Workshop, Volume 1 Apr. 1988 p 254-278 (For primary document see N89-23074 16-61)
Avail: NTIS HC A22/MF A01 CSCL 09B

Work on unified solutions to problems in computer vision and computer graphics including animation, motion control and planning, and design is described. The key problems in model synthesis are inverse problems in which a compact specification of the constraints that a shape or motion must fulfill is converted into an explicit description of the shape or motion itself. Viewed this way, model synthesis in graphics differs from visual shape and motion analysis primarily in the source of the constraints. In graphics, the constraints are supplied by a user, encoding desiderata, while in vision they encode evidence extracted from the image data. The approach taken to solve both sets of problems uses the machinery of physics. Models are composed of simulated materials that move and deform in response to applied forces. Constraints, whether derived from images or specified by a human model-builder, are imposed by applying carefully designed constraint forces to the models. These forces serve to mold the model into a form that satisfies the constraints they represent, vanishing only when the constraints are met. The manner in which a model responds to various forces is used to encode expected or desired properties of the object, such as a tendency toward smoothness. Additional forces, applied dynamically by the user, provide a remarkably effective mode of user interaction. Mathematically, this approach yields systems of ordinary or partial differential equations governing the evolution of the model through time. The results that this approach has yielded are described. Author

N89-23098# Pennsylvania Univ., Philadelphia. Dept. of Computer and Information Science.
PERCEPTION WITH FEEDBACK
Ruzena Bajcsy *In* Science Applications International Corp., Proceedings: Image Understanding Workshop, Volume 1 Apr. 1988 p 279-288 (For primary document see N89-23074 16-61)
(Contracts F49620-85-K-0018; DAAG29-84-K-0061; DAAG29-84-9-0027; N00014-85-K-0807; NSF DCR-82-19196; NSF MCS-82-19196; NSF DCR-84-10771)
Avail: NTIS HC A22/MF A01 CSCL 09B

Active perception is defined as a problem of an intelligent data acquisition process. For that, parameters and errors from the scene need to be defined and measured, which in turn can be fed back to control the data acquisition process. This is a difficult though important problem. The difficutly is in the fact that many of the feedback parameters are context and scene dependent. The precise definition of these parameters depends on thorough understanding of the data acquisition devices (camera parameters, illumination and reflectance parameters), algorithms (edge detectors, region growers, 3D recovery procedures) as well as the goal of the visual processing. Author

N89-23099# Honeywell Systems and Research Center, Minneapolis, MN.
QUALITATIVE MOTION DETECTION AND TRACKING OF TARGETS FROM A MOBILE PLATFORM
Bir Bhanu and Wilhelm Burger *In* Science Applications International Corp., Proceedings: Image Understanding Workshop, Volume 1 Apr. 1988 p 289-318 (For primary document see N89-23074 16-61)
Avail: NTIS HC A22/MF A01 CSCL 09B

The problem of understanding scene dynamics is to find consistent and plausible 3-D interpretations for any change observed in the 2-D image sequence. Due to the motion of the Autonomous Land Vehicle (ALV), stationary in the image, whereas moving objects are not necessarily seen in motion. The three main tasks of target motion detection and tracking approach presented here are: to estimate the vehicle's motion, to derive the 3-D structure of the stationary environment, and to detect and classify the motion of individual targets in the scene. These three tasks strongly depend on each other. The direction of heading (i.e., translation) and rotation of the vehicle are estimated with respect to stationary locations in the scene. The focus of expansion (FOE) is not determined as a particular image location, but as a region of possible FOE-locations called the Fuzzy FOE. A qualitative strategy of reasoning and modeling for the perception of 3D space from motion information is presented. Instead of refining a single quantitative description of the observed environment over time, multiple qualitative interpretations are maintained simultaneously. This offers superior robustness and flexibility over traditional numerical techniques which are often ill-conditioned and noise-sensitive. A rule-based implementation of this approach is discussed and results on real ALV imagery are presented. Author

N89-23100# Advanced Decision Systems, Mountain View, CA.
QUALITATIVE NAVIGATION 2 **c63**
Tod S. Levitt, Daryl T. Lawton, David M. Chelberg, Kerry V. Koitzsch, and John W. Dye *In* Science Applications International Corp., Proceedings: Image Understanding Workshop, Volume 1 Apr. 1988 p 319-326 (For primary document see N89-23074 16-61)
Avail: NTIS HC A22/MF A01 CSCL 09B

A multi-level theory of representation of large-scale space based

upon the observation and re-acquisition of distinctive visual events, i.e., landmarks, was developed. The theory provides a method for integrating the visual information from many images into a uniform database as a sensor-based robot moves through its environment. It incorporates the outputs of tracking of significant perceptual events, as well as providing a high-level visual description of places that can be used to robustly guide a robot with visual predictions even with a poorly stablized sensor platform. The representation provides the theoretical foundations for visual memory databases and path planning and execution algorithms that include coordinate free, topological representation of relative spatial location, yet smoothly integrate available metric knowledge of relative or absolute angles and distances. A qualitative navigation simulator, called the QUALNAV model, was built to provide a software laboratory for experimenting with spatial relationships in visual memory and their relationship to vision-based path planning and execution. Author

N89-23101# Carnegie-Mellon Univ., Pittsburgh, PA. Digital Mapping Lab.

COOPERATIVE METHODS FOR ROAD TRACKING IN AERIAL IMAGERY **c43**

David M. McKeown, Jr. and Jerry L. Denlinger *In* Science Applications International Corp., Proceedings: Image Understanding Workshop, Volume 1 Apr. 1988 p 327-341 (For primary document see N89-23074 16-61)

(Contracts DACA72-84-C-0002; F33615-84-K-1520; DARPA Order 4976)

Avail: NTIS HC A22/MF A01 CSCL 08B

Research in digital mapping and image understanding in the area of automated feature extraction from aerial imagery is described. A system for road tracking, (ARF) A Road Follower that uses multiple cooperative methods for extracting information about road location and structure from complex aerial imagery is discussed. This system is a multi-level architecture for image analysis that allows for cooperation among low-level processes and aggregation of information by high-level analysis components. Two low-level methods were implemented: road surface texture correlation and road edge following. Each low level method works independently to establish a model of the enter line of the road, its width, and other local properties. Intermediate-level processes monitor the state of the low-level feature extraction methods and make evaluations concerning the success of each method. They also extract various road properties such as width changes, surface material changes, and overpasses. As a result of these evaluations one tracking method may be suspended due to apparent failure and restarted from the model generated by other successful trackers. Finally a high-level module generates a symbolic description of the road in terms of various attributes of the road such as center line, road width, surface material, overpasses, and an indication of potential vehicles on the road. This description is available in both map and image coordinate systems, and can be used to generate a textual description of the road. Author

N89-23102# General Electric Co., Schenectady, NY. Corporate Research and Development Center.

PACE: AN ENVIRONMENT FOR INTELLIGENCE ANALYSIS **c43**

N. R. Corby, Joseph L. Mundy, P. A. Vrobel, A. J. Hanson, Lynn H. Quam, G. B. Smith, and Thomas M. Strat (SRI International Corp., Menlo Park, CA.) *In* Science Applications International Corp., Proceedings: Image Understanding Workshop, Volume 1 Apr. 1988 p 342-350 (For primary document see N89-23074 16-61)

(Contract DACA76-86-C-0007)

Avail: NTIS HC A22/MF A01 CSCL 08B

The system design for an environment to aid intelligence analysis is described. The goal of this system development is to provide an integrated set of tools for analyzing the status of a military site from a set of aerial images and collateral reports. The system, called Perceptual Analysis and Control Environment (PACE) is to be implemented by integrating various research tools that were developed and will be focussed on the application of airbase monitoring. Author

N89-23103# New York Univ., New York.

AFFINE INVARIANT MATCHING

Robert Hummel and Haim Wolfson *In* Science Applications International Corp., Proceedings: Image Understanding Workshop, Volume 1 Apr. 1988 p 351-364 (For primary document see N89-23074 16-61)

(Contracts N00014-82-K-0381; N00014-85-K-0077; NSF DCR-83-20085; NSF IRI-87-03335)

Avail: NTIS HC A22/MF A01 CSCL 09B

A selected overview of computer vision research is presented, emphasizing work on representation of images, and on model-based vision and including a technique for fast matching of shape descriptions of objects to preprocessed models. The matching process permits general affine transformations of the shape, and thus is applicable to the problem of recognizing flat, or nearly flat, objects viewed from an arbitrary angle and distance in 3-D. Different methods apply when the boundary of the objects consist primarily of line segments, or general (non-convex) curves, or (the most difficult case), convex curves. The case of recognizing 3-D objects, as opposed to flat objects is also discussed. The novelty of the approach and the computational efficiency is achieved by a hashing technique indexed over possible affine transformations. Author

N89-23104# SRI International Corp., Menlo Park, CA. Artificial Intelligence Center.

CONSTRUCTING SIMPLE STABLE DESCRIPTIONS FOR IMAGE PARTIONING

Yvan G. Leclerc *In* Science Applications International Corp., Proceedings: Image Understanding Workshop, Volume 1 Apr. 1988 p 365-382 (For primary document see N89-23074 16-61)

(Contract MDA903-86-C-0084)

Avail: NTIS HC A22/MF A01 CSCL 09B

A formulation of the image partitioning problem is presented: construct a complete and stable description of an image, in terms of a specified descriptive language, that is simplest in the sense of shortest description length. A suitable descriptive language that results in intuitively satisfying partitionings can be limited to a low-order polynomial description of the intensity variation within each region and a measure of the length of the region boundaries; other aspects of the shape and semantic properties of the regions need not be explicitly considered. Experiments performed on a variety of both natural and synthetic images demonstrate the superior performance of this approach over partitioning techniques based on clustering vectors of local image attributes and over standard edge-detection techniques. Author

N89-23105# University of Southern California, Los Angeles. Inst. for Robotics and Intelligent Systems.

THREE-DIMENSIONAL OBJECT RECOGNITION USING SURFACE DESCRIPTIONS

T. J. Fan, Gerard Medioni, and Ramakant Nevatia *In* Science Applications International Corp., Proceedings: Image Understanding Workshop, Volume 1 Apr. 1988 p 383-397 (For primary document see N89-23074 16-61)

(Contract F33615-87-C-1436)

Avail: NTIS HC A22/MF A01 CSCL 09B

A previously developed method to segment and describe range images using surface properties to establish correspondences between 3-D objects as needed in recognition is described. In a first step, labeled curves corresponding to jump boundaries, creases, and limbs of objects are grouped into boundaries of regions. Each region is therefore described by its boundaries, and by a polynomial approximation, which allows reconstruction of each patch individually, and also the complete scene. The scene is represented by a graph with the patch as the nodes and relations between them as the links. In a second step, objects (or partial objects) are inferred from surface patches, then two range images at this partial object level are matched. Graphs of objects are

matched using a best-first search under three types of constraints. The matching is data-driven in the sense that no a priori information is required. Substantial partial occlusion is also allowed. The results are presented in two instances. In matching two complex scenes, objects that appear in two images are identified without a priori information of these objects. Objects may vary in orientation and position or be occluded by other objects. Various real range images have been used in the testing with very good results. In multi-view model building and object recognition, the descriptions of objects are used to build multi-view models. Each model consists of 6 to 8 views, arranged so that most of the significant surfaces of the model object will be contained in at least one view. Given a new scene containing various objects, a model matching is applied, and a best model, if any, is selected for each scene object.

Author

N89-23106# Massachusetts Inst. of Tech., Cambridge. Artificial Intelligence Lab.

SELF CALIBRATION OF MOTION AND STEREO VISION FOR MOBILE ROBOT NAVIGATION **c63**

Rodney A. Brooks, Anita M. Flynn, and Thomas Marill *In* Science Applications International Corp., Proceedings: Image Understanding Workshop, Volume 1 Apr. 1988 p 398-410 (For primary document see N89-23074 16-61)

Avail: NTIS HC A22/MF A01 CSCL 09B

Experiments with a mobile robot are described, in which one vision process (forward motion vision) to calibrate another (stereo vision) without resorting to any external units of measurement. Both are calibrated to a velocity dependent coordinate system which is natural to the task of obstacle avoidance. The foundations of these algorithms, in a world of perfect measurement, are quite elementary. The contribution of this work is to make them noise tolerant while remaining simple computationally. Both the algorithms and the calibration procedure are easy to implement and have shallow computational depth, making them run at reasonable speed on moderate uni processors, appear practical to run continuously, maintaining an up-to-the second calibration on a mobile robot, and appear to be good candidates for massively parallel implementations.

Author

N89-23107# Hughes Research Labs., Calabasas, CA. Artificial Intelligence Center.

AUTONOMOUS NAVIGATION IN CROSS-COUNTRY TERRAIN **c63**

David M. Keirsey, David W. Payton, and J. Kenneth Rosenblatt *In* Science Applications International Corp., Proceedings: Image Understanding Workshop, Volume 1 Apr. 1988 p 411-416 (For primary document see N89-23074 16-61)

(Contract DACA76-85-C-0017)

Avail: NTIS HC A22/MF A01 CSCL 09B

Progress and experimentation with an autonomous robotic vehicle in cross-country terrain is described. Experiments were performed on the Autonomous Land Vehicle in natural terrain. An overview of the software architecture used for this achievement is discussed; descriptions of experiments and details of planning techniques are presented. Experiments describe the vehicle's avoidance of both known and unknown obstacles in its path.

Author

N89-23108# University of Southern California, Los Angeles. Inst. for Robotics and Intelligent Systems.

INTEGRATION EFFORT IN KNOWLEDGE-BASED VISION TECHNIQUES FOR THE AUTONOMOUS LAND VEHICLE PROGRAM **c63**

Keith Price and Igor Pavlin *In* Science Applications International Corp., Proceedings: Image Understanding Workshop, Volume 1 Apr. 1988 p 417-422 (For primary document see N89-23074 16-61)

(Contract DACA76-85-C-0009)

Avail: NTIS HC A22/MF A01 CSCL 09B

A methodology is presented and some early results are demonstrated in the integration of knowledge-based image analysis programs. The domain of complete three-dimensional motion analysis in the context of the Autonomous Land Vehicle is specifically addressed. The integrated system exploits the strengths and minimizes the weaknesses of the individual techniques, resulting in performance which is considerably improved over the performance of any of the independently developed programs.

Author

N89-23109# University of Southern California, Los Angeles. Inst. for Robotics and Intelligent Systems.

CONTOUR CORRESPONDENCES IN DYNAMIC IMAGERY

S. L. Gazit and Gerard Medioni *In* Science Applications International Corp., Proceedings: Image Understanding Workshop, Volume 1 Apr. 1988 p 423-432 (For primary document see N89-23074 16-61)

(Contract DACA76-85-C-0009)

Avail: NTIS HC A22/MF A01 CSCL 09B

One of the fundamental problems in Computer Vision is the problem of establishing correspondences between two (or more) images. The approach described here differs from previous approaches in the choice of matching primitives and the preference criterion. Super-segments are used, which are objects that can dually be represented either as groups of connected line segments or as chains of points, and sections of super-segments are matched. The correspondence is based on similar shape and translation of matching sections. Segment matching to limit search space are used then a chain matching algorithm is applied on sections. The method seems very robust, as demonstrated by the examples.

Author

N89-23110# University of Southern California, Los Angeles. Inst. for Robotics and Intelligent Systems.

SPATIO-TEMPORAL ANALYSIS OF AN IMAGE SEQUENCE WITH OCCLUSION

Shou-Ling Peng and Gerard Medioni *In* Science Applications International Corp., Proceedings: Image Understanding Workshop, Volume 1 Apr. 1988 p 433-442 (For primary document see N89-23074 16-61)

(Contract DACA76-85-C-0009)

Avail: NTIS HC A22/MF A01 CSCL 09B

A method is presented for analyzing a sequence of image frames taken close apart in time, forming a spatio-temporal volume. Edgels in each spatial image are detected, then an analysis is done of individual slice centered on each edgel and taken in the temporal direction. The combination of results from these multiple slices enables us to compute an estimate of the velocity in the direction normal to the tangent to the curve. This resulting normal velocity field may then be used to compute the real velocity field and to perform object segmentation. In contrast to most previous approaches, the system is quite robust, it is capable of handling occlusion as well as disocclusion as they are explicitely modelled. Results on synthetic data consisting of two objects moving with occlusion and results on real image sequences are presented.

Author

N89-23111# University of Southern California, Los Angeles. Inst. for Robotics and Intelligent Systems.

NATURAL REPRESENTATION OF MOTION IN SPACE-TIME

Wolfgang O. Franzen *In* Science Applications International Corp., Proceedings: Image Understanding Workshop, Volume 1 Apr. 1988 p 443-452 (For primary document see N89-23074 16-61)

Avail: NTIS HC A22/MF A01 CSCL 09B

An approach to the representation of rigid and nonrigid 3D motion in time-varying imagery is described. The homogeneous coordinate representation of rigid transformations is extended by adding time as an explicit component. Characterized are the classes of motion and/or structural change that have a constant matrix representation under this notation. The coefficients of this matrix representation have a natural interpretation as the constant coefficients of a certain nonhomogeneous system of linear difference equations. Among the classes of object motion having a constant representation are the following: a constantly deforming object undergoing translation; a rigid object rotating about a fixed

axis at a constant angular velocity while undergoing translation in any direction and acceleration in the direction of the axis of rotation; a nonrotating rigid object undergoing constant translation and/or acceleration in any direction. Camera motion, object motion, or simultaneous motion, may be described using this representation. A vector equation expresses the position of a point on an object, at an arbitrary juncture in time, as a function of its initial position, and the matrices describing the motion of the camera, and the motion of the object. The matrix representation presented is compact and should allow the efficient computation of the motion of computer generated objects. If a rigid object, undergoing constant motion of the form described, is accelerating solely due to a constant external force of known magnitude, the absolute distances to points on the object, and the absolute parameters of motion, may be recovered from a monocular image sequence. Author

N89-23112# Stanford Univ., CA. Robotics Lab.
GENERIC MODELS FOR ROBOT NAVIGATION **c63**
David J. Kriegman, Thomas O. Binford, and Thilaka S. Sumanaweera *In* Science Applications International Corp., Proceedings: Image Understanding Workshop, Volume 1 Apr. 1988 p 453-460 Sponsored in part by the Fannie and John Hertz Foundation (For primary document see N89-23074 16-61)
(Contract F33615-85-C-5106)
Avail: NTIS HC A22/MF A01 CSCL 09B

The concept of generic modeling is introduced. A particular application is an explicit abstract generic building model which is valid for a broad class of buildings. It is built with mechanisms that were used to create generic models for other object classes including machine screws and generalized cylinders. These methods extend the generality of object classes which can be implemented, compared to previous implementations of object classes. Ultimately, given sensor information and a generic model, the model can be instantiated. Using a combination of epipolar stereo vision along with monocular vision, a portion of the generic building model has been instantiated. This instantiation can then be used for mobile robot navigation. Generic Models will be used to represent object class in the SUCCESSOR vision system. Author

N89-23113# Washington Univ., Seattle. Intelligent Systems Lab.
MATHEMATICAL MORPHOLOGY AND THE MORPHOLOGICAL SAMPLING THEOREM
Robert M. Haralick *In* Science Applications International Corp., Proceedings: Image Understanding Workshop, Volume 1 Apr. 1988 p 461-487 (For primary document see N89-23074 16-61)
Avail: NTIS HC A22/MF A01 CSCL 09B

For the purpose of object or defect identification required in vision applications in manufacturing, the operations of mathematical morphology are perhaps more useful than the convolution operations. This is because mathematical morphology provides a natural algebraic theory for working with shape. The morphological sampling theorem described states how a digital image must be morphologically filtered before sampling in order to preserve relevant information after sampling. The sampling theorem indicates to what precision an appropriately morphologically filtered image can be reconstructed after sampling, and it specified the relationship between morphological processing before sampling and the more computationally efficient scheme of morphologically operating on the sampled image. Thus, the morphological sampling theorem provides a sound basis for recognizing and extracting shape information in a computationally efficient, multi-resolution pyramid processing approach. Author

N89-23114# Stanford Univ., CA. Robotics Lab.
USING GENERIC GEOMETRIC AND PHYSICAL MODELS FOR REPRESENTING SOLIDS
Jean Ponce and Glenn Healey *In* Science Applications International Corp., Proceedings: Image Understanding Workshop, Volume 1 Apr. 1988 p 488-503 (For primary document see N89-23074 16-61)
(Contract F33615-85-C-5106)
Avail: NTIS HC A22/MF A01 CSCL 09B

A solid modelling system based on powerful geometric and physical representations is presented. The geometric representation combines constructive solid geometry (CSG) and boundary (Brep) representations. Solids are built as CSG trees by applying set operations to a very general set of primitives: generalized cylinders with either a straight or a curved axis. Using an efficient and robust boundary evaluator, corresponding Breps are constructed in terms of trimmed surface patches and their boundaries. In addition to geometric models, the system describes the physical properties of material surfaces using very general physical models. The optical properties of both homogeneous and inhomogeneous materials are accurately modeled. The described model for the scattering of light from the body of inhomogeneous materials based on modified Kubelka-Munk theory is significantly more general than previous models used in computer graphics and vision for this process. Physical and geometric representations are unified using a method to map material surface properties onto geometric models. Representations allow for computationally efficient and physically accurate display of complex solids. Several rendering algorithms exploiting these advantages are presented, including fast ray tracing for line drawing and shaded display. The system described was implemented. Several examples demonstrate the effectiveness of the geometric and physical models. Author

N89-23115# Science Applications International Corp., McLean, VA.
PROCEEDINGS: IMAGE UNDERSTANDING WORKSHOP, VOLUME 2 Annual Technical Report, Feb. 1987 - Apr. 1988
Lee S. Baumann, ed. Apr. 1988 678 p Workshop held in Cambridge, MA, 6-8 Apr. 1988; sponsored by DARPA
(Contract N00014-86-C-0700; ARPA Order 5605)
(AD-A197559) Avail: NTIS HC A99/MF E03 CSCL 09B

Annual progress reports and technical papers presented by the participants at the Image Understanding Workshop sponsored by the Information Science and Technology Office, Defense Advanced Research Projects Agency are presented. Also included are copies of invited papers presented at the workshop and additional technical papers which were not presented (volume 2). Topics addressed included: intelligent image understanding, machine vision and robotics, knowledge-based systems, motion detection and tracking, object and target recognition, parallel computation, stereo vision, and image processing. For individual titles, see N89-23116 through N89-23180.

N89-23116# Hughes Research Labs., Calabasas, CA. Artificial Intelligence Center.
MULTIRESOLUTION AERIAL IMAGE INTERPRETATION
Teresa M. Silberberg *In* Science Applications International Corp., Proceedings: Image Understanding Workshop, Volume 2 Apr. 1988 p 505-511 (For primary document see N89-23115 16-61)
Avail: NTIS HC A99/MF E03 CSCL 09B

The interpretation system presented in this paper uses multiple image resolutions to detect objects in large, cluttered, high resolution, aerial images. Lower resolutions are processed first so attention is focused in the higher resolutions to those areas where there is evidence of the objects. The system provides a framework for modeling objects at each resolution using a variety of complementary image features. The approach (both data-driven and model-driven) utilizes hypothesis generation and verification, and employs evidential reasoning to evaluate the hypotheses. The system was exercised on two aerial images; one consisting of a single submarine and analyzed using three resolutions, and the other consisting of three airplanes and analyzed using two resolutions. Author

N89-23117# University of Southern California, Los Angeles. Inst. for Robotics and Intelligent Systems.

PERCEPTUAL GROUPING FOR THE DETECTION AND DESCRIPTION OF STRUCTURES IN AERIAL IMAGES

Rakesh Mohan and Ramakant Nevatia *In* Science Applications International Corp., Proceedings: Image Understanding Workshop, Volume 2 Apr. 1988 p 512-526 (For primary document see N89-23115 16-61)

(Contracts F33615-87-C-1436; DMA800-85-C-0008; DARPA Order 3119)

Avail: NTIS HC A99/MF E03 CSCL 09B

Vision systems which rely on low-level representations such as edges and regions have difficulty handling complex natural images for high and mid level visual tasks. Representations of structural relationships in the arrangements of primitive image features, as detected by the perceptual organization process, are essential for analyzing complex imagery. These representations are termed collated features. In the detection of collated features, structural informatiuon is utilized to overcome local problems such as noise and poor contrast of real image. The structural information encoded in collated features is essential for such processes as visual reasoning, object segmentation and shape description. Their influence is not limited to the above mentioned high-level visual processes as the collated features also actively interact with such mid-level processes as stereo and serve as attentional mechanisms for low-level feature detection. A vision system is presented that illustrates, for a particular visual domain, the concept of collated features, the process of their detection and their interaction with the diverse visual processes of stereo, monocular and 3-D reascning, shape description and object extraction. Author

N89-23118# Honeywell Systems and Research Center, Minneapolis, MN.

DYNAMIC MODEL MATCHING FOR TARGET RECOGNITION FROM A MOBILE PLATFORM

Hatem Nasr and Bir Bhanu *In* Science Applications International Corp., Proceedings: Image Understanding Workshop, Volume 2 Apr. 1988 p 527-536 (For primary document see N89-23115 16-61)

(Contract DACA76-86-C-0017)

Avail: NTIS HC A99/MF E03 CSCL 09B

A novel technique called dynamic model matching (DMM) is presented for target recognition from a moving platform such as an autonomous combat vehicle. The DMM technique overcomes major limitations in present model-based target recognition techniques that use a single, static target model, and therefore cannot account for continuous changes in the target's appearance caused by varying range and perspective, DMM addresses this problem by combining a moving camera model, 3-D object models, spatial models, and expected range and perspective to generate multiple 2-D image models for matching. DMM also generates recognition strategies that can emphasize different object features at varying ranges. DMM operates within a larger system for landmark recognition based on the perception, reasoning, action, and expectation paradigm called PREACTE. Results are presented on a number of test sites using color video data obtained from the autonomous land vehicle. Author

N89-23119# Honeywell Systems and Research Center, Minneapolis, MN.

TRIPLE: A MULTI-STRATEGY MACHINE LEARNING APPROACH TO TARGET RECOGNITION

Bir Bhanu and John C. Ming *In* Science Applications International Corp., Proceedings: Image Understanding Workshop, Volume 2 Apr. 1988 p 537-547 (For primary document see N89-23115 16-61)

Avail: NTIS HC A99/MF E03 CSCL 09B

Current target recognition systems are unable to modify their behavior based on the dynamic environmental changes which occur around them. In order to perform robustly in unconstrained, outdoor environments, a target recognition system must be able to adapt its representation of this dynamic environment while maintaining acceptable performance levels. Machine learning technology offers some promising solutions to many of these problems faced in the target recognition scenario. Learning allows a system to use situation context, to adapt its representation of the changing environment, and to improve the system's recognition performance over time. An innovative system is described which combines learning and target recognition into an integrated system which accomplishes the above tasks. This system is called TRIPLE: Target Recognition Incorporating Positive Learning Expertise. It uses two machine learning techniques known as explanation-based learning and conceptual clustering, combined with a knowledge-based reasoning system, to provide robust target recognition. A complete description of the TRIPLE system, as well as a simple example showing the system's behavior, is presented. Author

N89-23120# Maryland Univ., College Park. Computer Vision Lab.

USING FLOW FIELD DIVERGENCE FOR OBSTACLE AVOIDANCE IN VISUAL NAVIGATION **c63**

Randal C. Nelson and John Aloimonos *In* Science Applications International Corp., Proceedings: Image Understanding Workshop, Volume 2 Apr. 1988 p 548-567 Sponsored in part by DARPA, Washington, DC (For primary document see N89-23115 16-61)

Avail: NTIS HC A99/MF E03 CSCL 09B

The practical recovery of quantitative structural information about the world from visual data has proven to be a very difficult task. In particular, the recovery of motion information which is sufficiently accurate to allow practical application of theoretical shape from motion results has so far been infeasible. Yet a large body of evidence suggests that use of motion is an extremely important process in biological vision systems. It has been suggested that qualitative visual measurements can provide powerful perceptual cues, and that practical operations can be performed on the basis of such clues without the need for a quantitative reconstruction of the world. The use of such information is termed inexact vision. The investigation of one such approach to the analysis of visual motion is described. Specifically, the use of certain measures of flow field divergence was investigated as a qualitative cue for obstacle avoidance during visual navigation. It is shown that a quantity termed the directional divergence of the 2-D motion field can be used as a reliable indicator of the presence of obstacles in the visual field of an observer undergoing generalized rotational and translational motion. Moreover, the necessary measurements can be robustly obtained from real image sequences. A simple differential procedure for robustly extracting divergence information from image sequences which can be performed using a highly parallel, connectionist architecture is described. The procedure is based on the twin principles of directional separation of optical flow components and temporal accumulation of information. Experimental results are presented showing that the system responds as expected to divergence in real world image sequences, and the use of the system to navigate between obstacles is demonstrated. Author

N89-23121# Hughes Research Labs., Calabasas, CA. Artificial Intelligence Center.

AN OPERATIONAL PERCEPTION SYSTEM FOR CROSS-COUNTRY NAVIGATION **c63**

Michael J. Daily, John G. Harris, and Kurt Reiser *In* Science Applications International Corp., Proceedings: Image Understanding Workshop, Volume 2 Apr. 1988 p 568-575 (For primary document see N89-23115 16-61)

(Contract DACA87-85-C-0007)

Avail: NTIS HC A99/MF E03 CSCL 09B

An operational perception system for cross-country navigation which has been verified in both simulated and real world environments is presented. Range data from a laser range scanner is transformed into an alternate representation called the Cartesian Elevation Map (CEM). A detailed vehicle model operates on the CEM to produce traversability information along selected trajectories. This information supports a real-time reflexive planning system. The successful demonstration of obstacle detection and

avoidance algorithms on board an Autonomous Land Vehicle is discussed. Author

N89-23122# SRI International Corp., Menlo Park, CA. Artificial Intelligence Center.
OVERVIEW OF THE SRI CARTOGRAPHIC MODELING ENVIRONMENT **c43**
Andrew J. Hanson and Lynn H. Quam *In* Science Applications International Corp., Proceedings: Image Understanding Workshop, Volume 2 Apr. 1988 p 576-582 (For primary document see N89-23115 16-61)
(Contract MDA903-86-C-0084; NSF IST-85-11751)
Avail: NTIS HC A99/MF E03 CSCL 08B

Image manipulation capabilities provided to support research on interactive, semiautomated, and automated computer-based cartographic activities are described. The cartographic features and data that can be entered include multiple images, camera models, digital terrain elevation data, point, line, and area cartographic features, and a wide assortment of three-dimensional objects. Interactive capabilities include free-hand feature entry, altering features while constraining them to conform to the terrain and lighting geometry, adjustment of feature parameters, and the adjustment of the camera model to display the scene features from arbitrary viewpoints. Cartographic features are depictable either as wire-frame sketches for interactive purposes or as texture-mapped renderings for realistic scene synthesis. High-quality simulated scenes are created by texture-mapping images onto terrain data and adding renderings of cartographic features using depth-buffering and anti-aliasing techniques. Motion sequences can be created by choosing a series of camera models and rendering the simulated appearance of the scene from each viewpoint. Author

N89-23123# Columbia Univ., New York, NY. Dept. of Computer Science.
ON THE COMPUTATIONAL COMPLEXITY OF LINEAR NAVIGATION **c63**
John R. Kender and Avraham Leff *In* Science Applications International Corp., Proceedings: Image Understanding Workshop, Volume 2 Apr. 1988 p 583-592 (For primary document see N89-23115 16-61)
(Contracts DACA76-86-C-0024; N00039-84-C-0165)
Avail: NTIS HC A99/MF E03 CSCL 09B

A model of topological navigation in one-dimensional spaces, such as single roads, corridors, or transportation routes is formalized. The concepts of a direction and a custom map are defined as well as some specifications for motor and sensor models, including the idea of sensor synchronicity. The representations necessary to model and exploit differences between the world itself (here, a version of Lineland), the world as perceived by the map-maker, and the world as experienced by the navigator are discussed. The difficulties of giving precise meaning to what is meant by a good map, and what is meant by a landmark are demonstrated. Proof is offered to show that even in the simplest case where both motor and sensor control is error-free, NP-complete problems arise in Lineland, even while attempting to navigate from one single object to another. Forced to use the A* search method, heuristics that appear reasonable for map creation are provided, and examples are given of several maps that are good under varying criteria. Author

N89-23124# Carnegie-Mellon Univ., Pittsburgh, PA. Robotics Inst.
THREE-DIMENSIONAL VISION FOR OUTDOOR NAVIGATION BY AN AUTONOMOUS VEHICLE **c63**
Martial Hebert and Takeo Kanade *In* Science Applications International Corp., Proceedings: Image Understanding Workshop, Volume 2 Apr. 1988 p 593-601 (For primary document see N89-23115 16-61)
(Contracts DACA76-85-C-0003; F33615-87-C-1499; NSF DCR-86-04199)
Avail: NTIS HC A99/MF E03 CSCL 09B

Progress in range image analysis for autonomous navigation in outdoor environments is reported. The goal of the work is to use range data from an ERIM laser range finder to build a three-dimensional description of the environment. Techniques are described for building both low-level description, such as obstacle maps or terrain maps, as well as higher level description using model-based object recognition. These techniques have been integrated in the NAVLAB system. Author

N89-23125# Carnegie-Mellon Univ., Pittsburgh, PA. Dept. of Computer Science.
MACHINE-INDEPENDENT IMAGE PROCESSING: PERFORMANCE OF APPLY ON DIVERSE ARCHITECTURES
Richard S. Wallace, Jon A. Webb, and I-Chen Wu *In* Science Applications International Corp., Proceedings: Image Understanding Workshop, Volume 2 Apr. 1988 p 602-608 Prepared in cooperation with Hughes Research Labs., Calabasas, CA (For primary document see N89-23115 16-61)
(Contracts F33615-81-K-1539; N00039-95-C-0134; DACA76-85-C-0002; N00014-80-C-0236; N00014-85-K-0152; NR-048-659; NR-SDRJ-007)
Avail: NTIS HC A99/MF E03 CSCL 09B

One of the most important obstacles standing in the way of widespread use of parallel computers for low-level vision is the lack of a programming language that can be mapped efficiently onto different computer architectures which is suited for low-level vision. Such a language is presented and its capabilities by comparing the performance of the Hughes HBA, the Carnegie Mellon Warp machine, and the Sun 3 on a large set of low-level vision programs. In order to demonstrate its efficiency performance of the Sun code is compared with routines of similar function written by professional programmers. Author

N89-23126# University of Southern California, Los Angeles. Inst. for Robotics and Intelligent Systems.
PARALLEL ARCHITECTURES FOR IMAGE PROCESSING AND VISION **c62**
V. K. Prasanna-Kumar and Dionisios Reisis *In* Science Applications International Corp., Proceedings: Image Understanding Workshop, Volume 2 Apr. 1988 p 609-619 (For primary document see N89-23115 16-61)
(Contract F33615-87-C-1436; NSF IRI-87-10863; DARPA Order 3119)
Avail: NTIS HC A99/MF E03 CSCL 09B

Activities in developing parallel architectures and parallel techniques for various image and vision problems are summarized. The proposed architectures include the enchanced mesh, the reconfigurable mesh and the mesh of meshes. These architectures are illustrated by parallelizing known techniques and/or developing new parallel algorithms for image processing and vision. Efficient algorithms are developed to support data routing among the processors. By using these routing techniques, a variety of problems related to digitized images are solved, as well as problems in image understanding using linear segments as primitives. Author

N89-23127# Rochester Univ., NY. Dept. of Computer Science.
PARALLEL HARDWARE FOR CONSTRAINT SATISFACTION **c62**
Michael J. Swain and Paul R. Cooper *In* Science Applications International Corp., Proceedings: Image Understanding Workshop, Volume 2 Apr. 1988 p 620-624 Sponsored in part by NSERC, Canada (For primary document see N89-23115 16-61)
(Contract F30602-85-C-0008)
Avail: NTIS HC A99/MF E03 CSCL 09B

A parallel implementation of constraint satisfaction by arc consistency is presented. The implementation is constructed of standard digital hardware elements, used in a very fine-grained, massively parallel style. As an example of how to specialize the design, a parallel implementation for solving graph isomorphism with arc consistency is also given. Complexity analyses are given for both circuits. Running time for the algorithms turns out to be linear or O(n squared), and if the I/O must be serial, it will dominate the computation time. Fine-grained parallelism trades off time

complexity for space complexity, but the number of gates required is only O(n to the fourth). Author

N89-23128# Carnegie-Mellon Univ., Pittsburgh, PA. Dept. of Computer Science.
SCAN LINE ARRAY PROCESSORS: WORK IN PROGRESS **c62**
Allan L. Fisher, Peter T. Highnam, and Todd E. Rockoff *In* Science Applications International Corp., Proceedings: Image Understanding Workshop, Volume 2 Apr. 1988 p 625-633 (For primary document see N89-23115 16-61)
(Contract F33615-87-K-1499; ARPA Order 4976)
Avail: NTIS HC A99/MF E03 CSCL 09B

Motivation for and progress toward the implementation and use of a special-purpose very large scale integration (VLSI) processor array for computer vision are described. A Scan Line Array Processor (SLAP) includes one processing element (PE) for each pixel on a single image scan line, arranged in a linear array. Each PE has internal fixed-point functional units and a register bank. A SLAP operates with a system controller broadcasting a single instruction to all PEs in each cycle. Adjacent processing elements can exchange data in each cycle, and a dedicated video shift register performs concurrent image I/O. The simple control structure and linear topology of a SLAP promises great cost effectiveness. A key issue is the efficiency with which problems can be mapped onto the array for which a number of algorithms and algorithm mapping schemes have been designed. In order to fully assess the practical value of the SLAP approach, a prototype array with 512 processing elements is being constructed. Built around custom 2 micron CMOS chips, the array and its controller will occupy three standard-size circuit cards and deliver some 4 billion 16 bit integer operations per second. Performance estimates on some commonly used algorithms indicate that this raw throughput can be put to good use. In addition to developing hardware and algorithms, low-level programming tools and an optimizing compiler for a high-level parallel language tailored for image processing are also being built. An overview of the SLAP concept, implementation work, and some comparative performance predictions are provided. Author

N89-23129# Columbia Univ., New York, NY. Dept. of Computer Science.
PYRAMID ALGORITHMS IMPLEMENTATION ON THE CONNECTION MACHINE
Hussein A. H. Ibrahim *In* Science Applications International Corp., Proceedings: Image Understanding Workshop, Volume 2 Apr. 1988 p 634-639 (For primary document see N89-23115 16-61)
(Contract DACA76-86-C-0024)
Avail: NTIS HC A99/MF E03 CSCL 09B

Pyramid architectures have lately been proposed in the literature to implement a large number of image understanding algorithms, such as multi-resolution, pipelined, and bottom/up algorithms. In these architectures each processing element (PE) on an intermediate layer is connected to nine other PE's, four on the same level, four in layer below it, and to a single parent in the layer above it. Hardware implementation of such pyramid machines is expensive because of the extensive wiring involved. The Connection Machine (CM), a highly parallel fine-grained single instruction stream/multiple data (SIMD) machine with a hypercube and mesh interconnection networks, has been available for some time now to the vision community. Described here is the implementation of an address mapping scheme that efficiently maps the pyramid architecture onto the CM, resulting in an efficient way of implementing pyramid algorithms on the CM. In this mapping, each PE in the CM simulates a PE on the base of the pyramid, and at most one PE on the intermediate levels. Top/Bottom communication in the pyramid can be simulated in this scheme using only three hypercube communication cycles in the CM. On the other side, mesh communication occurring in all intermediate levels of the pyramid architecture can be simulated using at most a number of hypercube communication cycles that is proportional to the dimension of the cube (16 in the case of a 64 K CM). A programming environment for pyramid algorithms, using this addressing scheme, has been implemented on the CM. It allows the user to create pyramid data structures, load/unload images from various pyramid levels, move data up/down, and perform several operations such as convolution and hierarchical operators on the created data structures. Author

N89-23130# Massachusetts Inst. of Tech., Cambridge. Artificial Intelligence Lab.
ROBUST PARALLEL COMPUTATION OF 2-D MODEL-BASED RECOGNITION
Todd Anthony Cass *In* Science Applications International Corp., Proceedings: Image Understanding Workshop, Volume 2 Apr. 1988 p 640-650 (For primary document see N89-23115 16-61)
(Contracts N00014-86-K-0685; N00014-85-K-0124; DACA76-85-C-0010)
Avail: NTIS HC A99/MF E03 CSCL 09B

An approach to 2-D model-based object recognition is developed, suitable for implementation on a highly parallel single instruction stream/multiple data (SIMD) computer. Object models and image data are represented as contour features. Transformation sampling is used to determine the optimal model feature to image feature transformation by sampling the space of possible transformations. It is shown that only a small part of this space need actually be sampled due to the constraints placed on possible transformations by individual matches of image features to model features. The procedure requires O(Tmn) processors and O(lg squared (Tmn)) time, where m is the number of model features, m is the number of image features, and T depends on the size of the image. The resulting procedure works well and is extremely robust in the presence of occlusion. An implementation of the procedure on the Connection Machine is described, and some experimental results given. Author

N89-23131# General Electric Co., Schenectady, NY. Corporate Research and Development Center.
THE CONCEPT OF AN EFFECTIVE VIEWPOINT
Joseph L. Mundy, A. J. Heller, and D. W. Thompson *In* Science Applications International Corp., Proceedings: Image Understanding Workshop, Volume 2 Apr. 1988 p 651-659 (For primary document see N89-23115 16-61)
(Contract DACA76-86-C-0007)
Avail: NTIS HC A99/MF E03 CSCL 09B

The power of object recognition features as a function of viewpoint is explored. A prior system for model-based recognition is examined, using the geometries of the relevant match feature to define a viewpoint based error function. General rules for determining degenerate viewpoints of a feature are proposed. The uses of the function in selecting promising match features is discussed. Finally, results of the recognition system are presented along with an analysis of the relevant error values, demonstrating the ability of the error metric to predict the reliability of features at arbitrary viewpoints and to derive a minimal set of effective features. Author

N89-23132# SRI International Corp., Menlo Park, CA. Artificial Intelligence Center.
CORE KNOWLEDGE SYSTEM: STORAGE AND RETRIEVAL OF INCONSISTENT INFORMATION **c82**
Thomas M. Strat and Grahame B. Smith *In* Science Applications International Corp., Proceedings: Image Understanding Workshop, Volume 2 Apr. 1988 p 660-665 (For primary document see N89-23115 16-61)
Avail: NTIS HC A99/MF E03 CSCL 05B

An information storage and retrieval mechanism that avoids the requirement of consistency maintenance imposed by tradition knowledge-based systems is described. By viewing data as opinions rather than facts, the system is able to combine knowledge that is generally accepted as being true with data that may be from unreliable sources. A formal account of the semantics of the approach is also given. The information management system described has been implemented and used to store information

derived from image processing along with opinions from other sources about objects in the visible world. It appears to be well suited for the requirements of an autonomous robot, and for information storage in general. Author

N89-23133# Advanced Decision Systems, Mountain View, CA.
IU SOFTWARE ENVIRONMENTS
Christopher C. McConnell and Daryl T. Lawton *In* Science Applications International Corp., Proceedings: Image Understanding Workshop, Volume 2 Apr. 1988 p 666-677 (For primary document see N89-23115 16-61)
(Contract DACA76-85-C-0005)
Avail: NTIS HC A99/MF E03 CSCL 09B

The development of Image Understanding (IU) environments and their significant features are reviewed, beginning with a history of machine vision environments. The basic components of general IU environments with respect to representations, programming constructs, system-specific data bases and user interfaces are described with a look, finally, at examples of how these components have been realized in several different systems. Author

N89-23134# Maryland Univ., College Park. Computer Vision Lab.
USING PROBABILISTIC DOMAIN KNOWLEDGE TO REDUCE THE EXPECTED COMPUTATIONAL COST OF MATCHING
Azriel Rosenfeld, Avraham Margalit, and Rameshkumar Sitaraman *In* Science Applications International Corp., Proceedings: Image Understanding Workshop, Volume 2 Apr. 1988 p 678-689 (For primary document see N89-23115 16-61)
(Contract DAAB07-86-K-F073)
Avail: NTIS HC A99/MF E03 CSCL 09B

Matching of data structures such as digital images or labeled graphs is computationally expensive, because it requires node-by-node comparisons of the labels. Probabilistic models for the classes of data structures being matched, can reduce the expected computational cost of matching by comparing the nodes in an appropriate order. Some general results about this approach are presented, and also experimental results for digital images, when the probability densities of their gray levels, or more generally, the probability densities of arrays of local property values derived from the images are known. Author

N89-23135# Rochester Univ., NY. Dept. of Computer Science.
OBJECT RECOGNITION FROM A LARGE DATABASE USING A DECISION TREE
Michael J. Swain *In* Science Applications International Corp., Proceedings: Image Understanding Workshop, Volume 2 Apr. 1988 p 690-696 (For primary document see N89-23115 16-61)
Avail: NTIS HC A99/MF E03 CSCL 09B

The decision tree data structure can be employed as successfully outside of the pattern recognition domain as it has been within. This claim is substantiated by describing a system for recognition from a large database that recognizes polyhedra in crowded scenes and uses object topology, comparisons of length and angle, and viewpoint consistency as tests. Given the a priori probability of polyhedra to appear in the image, viewpoints from which they are seen, and the errors that occur in detecting their edges, the decision tree is automatically constructed from the database using the criterion of minimizing the expected recognition time. Since the optimal solution of this problem is intractible, a greedy method is used based on minimizing the expected entropy of the a posteriori distribution of possible matches. The motivation for the entropy measure is derived. Since object topology is a major source of information for the recognition system, the space of viewpoints is divided according to principal view regions. The large number of regions that this results in does not reduce the run-time efficiency of the system, since any number of regions can be considered at one time by the recognition system, whose state is determined by a position in the decision tree. Other measurements are also used, for example angle measurements and comparisons of length, where they will provide more information than the topological data. The viewpoint consistency constraint is used to provide an exact viewpoint determination as soon as is economical from information-theoretical point of view. By considering matches directly to the model at run-time instead of principal views the redundancy of the principal view representation is avoided and the viewpoint consistency constraint can be efficiently applied. Author

N89-23136# Columbia Univ., New York, NY. Dept. of Computer Science.
MODELING SENSORS AND APPLYING SENSOR MODEL TO AUTOMATIC GENERATION OF OBJECT RECOGNITION PROGRAM c35
Katsushi Ikeuchi and Takeo Kanade *In* Science Applications International Corp., Proceedings: Image Understanding Workshop, Volume 2 Apr. 1988 p 697-710 (For primary document see N89-23115 16-61)
(Contract F33615-84-K-1520; ARPA Order 4976)
Avail: NTIS HC A99/MF E03 CSCL 14B

A model-based vision system requires models to predict object appearances. How an object appears in the image is a result of interaction between the object properties and the sensor characteristics. Thus, in model-based vision, the sensor should be modeled as well as modeling the object. In the past, however, the sensor model was not used in model-based vision or, at least, was contained in the object model implicitly. A framework between an object model and the object's appearances is presented. Two aspects of sensor characteristics are considered: sensor detectability and sensor reliability. Sensor detectability specifies what kinds of features can be detected and in what condition the features are detected; sensor reliability is a confidence for the detected features. The configuration space is defined to represent sensor characteristics. A representation method for sensor detectability and reliability in the configuration space is proposed. Finally, an investigation is made of how to apply the sensor model to a model-based vision system, in particular, automatic generation of an object recognition program from a given model. Author

N89-23137# Massachusetts Univ., Amherst. Dept. of Computer and Information Science.
RAPID OBJECT RECOGNITION FROM A LARGE MODEL BASE USING PREDICTION HIERARCHIES
J. Brian Burns and Leslie J. Kitchen (University of Western Australia, Nedlands.) *In* Science Applications International Corp., Proceedings: Image Understanding Workshop, Volume 2 Apr. 1988 p 711-719 (For primary document see N89-23115 16-61)
(Contract F30602-87-C-0140; NSF DCR-85-00332)
Avail: NTIS HC A99/MF E03 CSCL 09B

An object recognition system is presented to handle the computational complexity posed by a large model base, an unconstrained viewpoint, and the structural complexity and detail inherent in the projection of an object. The design is based on two ideas. The first is to compute descriptions of what the objects should look like in the image, called predictions, before the recognition task begins. This reduces actual recognition to a 2-D matching process, improving the efficiency of 3-D object recognition during run-time. The second design feature is to represent all the predictions by a single, combined IS-A and PART-OF hierarchy called a prediction hierarchy that speeds up the indexing, or selection, of the correct object and viewpoint. The modes in this hierarchy are partial descriptions that are common to views and hence constitute shared processing subgoals during matching. The recognition time and storage demands of large model bases and complex models are substantially reduced by subgoal sharing: projections with similarities explicitly share the recognition and representation of their common aspects. A prototype system for the automatic compilation of a prediction hierarchy from a 3-D model base is demonstrated using a set of polyhedral objects and projections from an unconstrained range of viewpoints. In addition, a recognition system is proposed that can efficiently search for matches to the object-specific goal nodes of the hierarchy. Author

N89-23138# Maryland Univ., College Park. Computer Vision Lab.

EVALUATION OF QUANTIZATION ERROR IN COMPUTER VISION

Behrooz Kamgar-Parsi and Behzad Kamgar-Parsi *In* Science Applications International Corp., Proceedings: Image Understanding Workshop, Volume 2 Apr. 1988 p 720-730 (For primary document see N89-23115 16-61)

Avail: NTIS HC A99/MF E03 CSCL 09B

Due to the important role that digitization error plays in the field of computer vision, a careful analysis of its impact on the computational approaches used in the field is necessary. Mathematical tools for the computation of the average error due to quantization are discussed. They can be used in estimating the actual error occurring in the implementation of a method. Also derived is the analytic expression for the probability density of error distribution of a function of an arbitrarily large number of independently quantized variables. The probability of the error of the function to be within a given range can thus be obtained accurately. In analyzing the applicability of an approach one must determine whether the approach is capable of withstanding the quantization error. If not, then regardless of the accuracy with which the experiments are carried out the approach will yield unacceptable results. The tools developed here can be used in the analysis of the applicability of a given algorithm, hence revealing the intrinsic limitations of the approach. Author

N89-23139# General Electric Co., Schenectady, NY. Corporate Research and Development Center.

ALGEBRAIC REASONING IN VIEW CONSISTENCY AND PARAMETERIZED MODEL MATCHING PROBLEMS

David A. Cyriuk, Deepak Kapur, and Joseph L. Mundy *In* Science Applications International Corp., Proceedings: Image Understanding Workshop, Volume 2 Apr. 1988 p 731-739 (For primary document see N89-23115 16-61)

(Contract DACA76-86-C-0007)

Avail: NTIS HC A99/MF E03 CSCL 09B

A view consistency approach was proposed in the 1987 DARPA Image Understanding workshop as a way to extract three-dimensional information from multiple images of a polyhedral scene, without any knowledge of a model or information about the scene. Further experiments in the use of this approach are reported. Also explored is the use of this approach for matching parameterized models in the absence of complete knowledge about the orientation of the camera. Towards this end, an algebraic reasoning system was developed which combines a Grobner basis algorithm for reasoning about polynomial equational constraints and Bledsoe-Shostak-Brooks' extended least upper bound-greatest lower bound (SUP INF) method for reasoning about inequality constraints. Inequalities can be used to express the range of parameter values as well as imprecise data. It is shown how the Grobner basis algorithm extends the domain of application of the SUP-INF method as well as increases the efficiency of the SUP-INF method, especially in the presence of equational constraints. A number of improvements over Brooks' extension of the SUP-INF method are discussed. Author

N89-23140# SRI International Corp., Menlo Park, CA. Artificial Intelligence Center.

TEST RESULTS FROM SRI'S STEREO SYSTEM

Marsha Jo Hannah *In* Science Applications International Corp., Proceedings: Image Understanding Workshop, Volume 2 Apr. 1988 p 740-744 (For primary document see N89-23115 16-61)

(Contracts MDA903-83-C-0027; MDA903-86-C-0084)

Avail: NTIS HC A99/MF E03 CSCL 09B

Briefly described is the automatic system, STEREOSYS, which has been developed for stereo compilation. This system uses area-based correlation, but applies this basic technique in a variety of novel ways to develop a disparity model for a given stereo image pair. The techniques used are hierarchical in nature, and incorporate iterative refinement, as well as a best-first strategy, in the matching process. Also presented are results obtained with this system on test data recently distributed by the International Society of Photogrammetry and Remote Sensing, Working Group III/4 (Mathematical Aspects of Pattern Recognition and Image Analysis) as part of their Test A on Image Matching. Detailed analysis of these results is not completed, but preliminary indications are that STEREOSYS performed better than all other tested algorithms. Author

N89-23141# Maryland Univ., College Park. Computer Vision Lab.

PRELIMINARY DESIGN OF A PROGRAMMED PICTURE LOGIC

David Harwood, Raju Prasannappa, and Larry S. Davis *In* Science Applications International Corp., Proceedings: Image Understanding Workshop, Volume 2 Apr. 1988 p 745-755 (For primary document see N89-23115 16-61)

Avail: NTIS HC A99/MF E03 CSCL 09B

The objective of the Programmed Picture Logic (PPL) project is to design and implement a general and modular logic-programmed system for two-dimensional interpretation of image theories in image structures obtained by image analysis. Important subsystems include heuristic search for object instances with optimization of goodness-of-figure, and procedures for computing basic image components, locales for searches, and predicates. Some of these are illustrated in an application to aerial images of suburban neighborhoods. Author

N89-23142# Columbia Univ., New York, NY. Dept. of Computer Science.

AN INTRODUCTION TO GENERALIZED STEREO TECHNIQUES

Lawrence Brill Wolff *In* Science Applications International Corp., Proceedings: Image Understanding Workshop, Volume 2 Apr. 1988 p 756-768 Sponsored in part by IBM Prepared in cooperation with Bell Telephone Labs., Holmdel, NJ (For primary document see N89-23115 16-61)

(Contract N00039-84-C-0165)

Avail: NTIS HC A99/MF E03 CSCL 09B

Developed herein is a formal theory for stereo vision which unifies existing stereo methods and predicts a large variety of stereo methods not yet explored. The notion of stereo is defined axiomatically using terms which are both general and precise giving stereo vision a broader and more rigorous foundation. The variations in imaging geometry between successive images used in parallax stereo and conventional photometric stereo techniques are extended to stereo techniques which involve variations of arbitrary sets of physical imaging parameters. Physical measurement of visual object features is defined in terms of solution loci in feature space arising from constraint equations that model the physical laws that relate the object feature to specific image features. Ambiguity in physical measurements results from a solution locus which is a subset of feature space larger than a single measurement point. Stereo methods attempt to optimally reduce ambiguity of physical measurement by intersecting solution loci obtained from successive images. A number of examples of generalized stereo techniques are presented. This new conception of stereo vision offers a new perspective on many areas of computer vision including areas that have not been previously associated with stereo vision (e.g., color imagery). As the central focus of generalized stereo vision methods is on measurement ambiguity mathematical developments are presented that characterize the size of measurement ambiguity as well as the conditions under which disambiguation of a solution locus takes place. The dimension of measurement ambiguity at a solution point is defined using the structure of a differentiable manifold and an upper bound is established using the implicit function theorem. The symmetry group of bijective transformations of feature space into itself, which leave a solution locus invariant, are used to analyze the ambiguity of a solution locus. A purely group theoretic characterization of the conditions under which measurement disambiguation takes place is given. Author

N89-23143# SRI International Corp., Menlo Park, CA. Artificial Intelligence Center.

STOCHASTIC STEREO MATCHING OVER SCALE

Stephen T. Barnard *In* Science Applications International Corp., Proceedings: Image Understanding Workshop, Volume 2 Apr. 1988 p 769-778 (For primary document see N89-23115 16-61)
(Contracts DACA76-85-C-0004; MDA903-86-C-0084)
Avail: NTIS HC A99/MF E03 CSCL 09B

A stochastic optimization approach to stereo matching is presented. Unlike conventional correlation matching and feature matching, the approach provides a dense array of disparities, eliminating the need for interpolation. First, the stereo matching problem is defined in terms of finding a disparity map that satisfies two competing constraints: (1) matched points should have similar image intensity, and (2) the disparity map should vary as slowly as possible. These constraints are interpreted as specifying the potential energy of a system of oscillators. Ground states are approximated by a new variant of simulated annealing, which has two important features. First, the microcanonical assemble is simulated using a new algorithm that is more efficient and more easily implemented than the familiar Metropolis algorithm (which simulates the canonical ensemble). Secondly, it uses a hierarchical, coarse-to-fine control structure employing Laplacian pyramids of the stereo images. In this way, quickly computed results at low resolutions are used to initialize the system at higher resolutions. Author

N89-23144# Massachusetts Inst. of Tech., Cambridge.
QUALITATIVE VERSUS QUANTITATIVE DEPTH AND SHAPE FROM STEREO
Daphna Weinshall *In* Science Applications International Corp., Proceedings: Image Understanding Workshop, Volume 2 Apr. 1988 p 779-785 (For primary document see N89-23115 16-61)
Avail: NTIS HC A99/MF E03 CSCL 09B

The problem of obtaining depth information from binocular disparities is presented. It is motivated by the fact that implementing registration algorithms and using the results for depth computations is hard in practice with real images due to noise and quantization errors. It is shown that qualitative depth information can be obtained from stereo disparities with almost no computations, and with no prior knowledge (or computation) of camera parameters. The only constraint is that the epipolar plane of the fixation point includes the X-axes of both cameras. Two expressions are derived which order all matched points in the images in two distinct depth-consistent fashions from image coordinates only. One is a tilt-related order lambda, which depends only on the polar angles of the matched points, the other is a depth-related order chi. Using lambda for tilt estimation and point separation (in depth) demonstrates some anomalies and unusual characteristics which have been observed in psychophysical experiments. Furthermore, the same approach can be applied to estimate some qualitative behavior of the normal to the surface of any object in the field of view. More specifically, one can follow changes in the curvature of a contour on the surface of an object, with either chi or lambda coordinate fixed. Author

N89-23145# Columbia Univ., New York, NY. Dept. of Computer Science.
THE INTEGRATION OF INFORMATION FROM STEREO AND MULTIPLE SHAPE-FORM-TEXTURE CUES
Mark L. Moerdler and Terrance E. Boult *In* Science Applications International Corp., Proceedings: Image Understanding Workshop, Volume 2 Apr. 1988 p 786-793 (For primary document see N89-23115 16-61)
(Contract N00039-84-C-0165)
Avail: NTIS HC A99/MF E03 CSCL 09B

In numerous computer vision applications, there is both the need for and the ability to access multiple types of information about the three-dimensional aspects of objects or surfaces. When this information comes from different sources the combination becomes non-trivial. An approach is described that integrates multiple visual sensing methodologies yielding three-dimensional information. The current system integrates feature based stereo algorithms with various shape-from-texture algorithms (multi-view shape-from-texture and shape-from-motion modules expected to be incorporated in the future). Unlike most systems for multi-sensor integration, that fuse all the information at one conceptual level, e.g., the surface level, the system under development uses two levels of data fusion, intra-process integration and inter-process integration. Intra-process integration techniques for feature-based stereo and shape-from-texture algorithms are discussed. Also discussed is an inter-process integration technique based on smooth models of surfaces. Examples are presented using camera acquired images. Author

N89-23146# Stanford Univ., CA. Robotics Lab.
STRUCTURAL CORRESPONDENCE IN STEREO VISION **c63**
Hong Seh Lim and Thomas O. Binford *In* Science Applications International Corp., Proceedings: Image Understanding Workshop, Volume 2 Apr. 1988 p 794-808 (For primary document see N89-23115 16-61)
(Contract N00039-84-C-0211)
Avail: NTIS HC A99/MF E03 CSCL 09B

Additional results on the work which appeared in last Image Understanding Workshop are described. The design and implementation of a high-level stereo-vision system which achieves global correspondence between high-level structures of stereo pairs is discussed. This structural correspondence reduces matching complexity, and provides globally consistent matching results avoiding local mismatches. Recovered range data is segmented into surfaces and bodies. Author

N89-23147# Stanford Univ., CA. Robotics Lab.
CURVED SURFACE RECONSTRUCTION USING STEREO CORRESPONDENCE **c63**
Hong Seh Lim and Thomas O. Binford *In* Science Applications International Corp., Proceedings: Image Understanding Workshop, Volume 2 Apr. 1988 p 809-819 (For primary document see N89-23115 16-61)
(Contract N00039-84-C-0211)
Avail: NTIS HC A99/MF E03 CSCL 09B

An inherent problem in stereo correspondence is that apparent boundaries of a curved surface from a pair of stereo images do not correspond to the same physical points on the curved surface; therefore, they can not be matched directly. Described here is a high-level stereo vision system which replaces the inappropriate correspondence constraint with an accurate constraint that the curved surface is tangent to lines of sight along four rays on each epipolar plane. Equations were derived from apparent boundaries of a curved surface in both images in order to reconstruct an approximation to the curved surface in space. The terminator, an edge bounding the curved surface, is used as an additional constraint whenever it is available. This is particularly applicable to objects that can be described in terms of generalized cylinders. Surface maps are obtained from reconstructed curved surfaces; thus, surface interpolation is not necessary. Author

N89-23148# Martin Marietta Corp., Denver, CO.
GEOMETRIC CAMERA CALIBRATION USING SYSTEMS OF LINEAR EQUATIONS **c74**
Keith D. Gremban, Charles E. Thorpe, and Takeo Kanade (Carnegie-Mellon Univ., Pittsburgh, PA.) *In* Science Applications International Corp., Proceedings: Image Understanding Workshop, Volume 2 Apr. 1988 p 820-825 Previously announced in IAA as A89-11980 (For primary document see N89-23115 16-61)
(Contracts DACA76-85-C-0003; DACA76-84-C-0005; NSF DCR-84-19990; NSF DCR-86-04199)
Avail: NTIS HC A99/MF E03 CSCL 20F

Geometric camera calibration is the process of determining a mapping between points in world coordinates and the corresponding image locations of the points. In previous methods, calibration typically involved the iterative solution to a system of nonlinear equations. A method is presented for performing camera calibration that provides a complete, accurate solution, using only linear systems of equations. By using two calibration planes, a line-of-sight vector is defined for each pixel in the image. The effective focal point of a camera can be obtained by solving the

system that defines the intersection point of the line-of-sight vectors. Once the focal point has been determined, a complete camera model can be obtained with a straightforward least-squares procedure. This method of geometric camera calibration has the advantages of being accurate, efficient, and practical for a wide variety of applications. Author

N89-23149# Massachusetts Inst. of Tech., Cambridge. Artificial Intelligence Lab.

RELATIVE ORIENTATION

Berthold K. P. Horn *In* Science Applications International Corp., Proceedings: Image Understanding Workshop, Volume 2 Apr. 1988 p 826-837 Previously announced as N88-22449 (For primary document see N89-23115 16-61)

(Contracts DACA76-85-C-0100; N00014-85-K-0124)

Avail: NTIS HC A99/MF E03 CSCL 09B

Before corresponding points in images taken with two cameras can be used to recover distances to objects in a scene, one has to determine the position and orientation of one camera relative to the other. This is the classic photogrammetric problem of relative orientation, central to the interpretation of binocular stereo information. Iterative methods for determining relative orientation were developed long ago; without them we would not have most of the topographic maps we do today. Relative orientation is also of importance in the recovery of motion and shape from an image sequence when successive frames are widely separated in time. Described here is a particularly simple iterative scheme for recovering relative orientation that, unlike existing methods, does not require a good initial guess for the baseline and the rotation. The data required is a set of pairs of corresponding rays from the two projection centers to points in the scene. It is well known that at least five pairs of rays are needed. Less appears to be known about the existence of multiple solutions and their interpretation. These issues are discussed here in detail. The unambiguous determination of all of the parameters of relative orientation is not possible when the observed points lie on a critical surface. Author

N89-23150# Carnegie-Mellon Univ., Pittsburgh, PA. Dept. of Computer Science.

IMAGE SEGMENTATION AND REFLECTION ANALYSIS THROUGH COLOR **c63**

Gudrun J. Klinker, Steven A. Shafer, and Takeo Kanade *In* Science Applications International Corp., Proceedings: Image Understanding Workshop, Volume 2 Apr. 1988 p 838-853 (For primary document see N89-23115 16-61)

(Contract F33615-84-K-1520; NSF DCR-84-19990; ARPA Order 4976)

Avail: NTIS HC A99/MF E03 CSCL 09B

A color image understanding approach that can be used to segment and analyze surfaces with color variations due to highlights and shading is presented. Discussed first is a theory that relates the reflected light from dielectric materials, such as plastic, to fundamental physical reflection processes, and describes the color of the reflected light as a linear combination of the color of the light due to surface reflection (highlights) and body reflection (object color). This theory is used in an algorithm that separates a color image into two parts: an image of just the highlights, and the original image with the highlights removed. In the past, this method has been applied to hand-segmented images. Shown here is how to perform automatic segmentation by applying this theory in stages to identify the object and highlight colors. The result is a combination of segmentation and reflection analysis that is better than traditional heuristic segmentation methods (such as histogram thresholding), and that provides important physical information about the surface geometry and material properties at the same time. Also shown is the importance of modeling the camera properties for this kind of quantitative analysis of color. This line of research can lead to physics-based image segmentation methods that are both more reliable and more useful than traditional segmentation methods. Author

N89-23151# Stanford Univ., CA. Robotics Lab.

A COLOR METRIC FOR COMPUTER VISION **c63**

Glenn Healey and Thomas O. Binford *In* Science Applications International Corp., Proceedings: Image Understanding Workshop, Volume 2 Apr. 1988 p 854-861 (For primary document see N89-23115 16-61)

(Contract F33615-85-C-5106)

Avail: NTIS HC A99/MF E03 CSCL 09B

A color space metric which is useful for computer vision is discussed. While there is no shortage of proposed methods for quantifying how the human eye perceives color differences, these perceptual metrics are inherently inappropriate for computer vision. The metric developed is appropriate for images sensed using color filters (e.g., R, G, B) as is often done in computer vision. This approach is more general than previous approaches in that the analysis makes use of the special characteristics of the filters and camera and accounts for their noise properties. The color distance function derived is an estimate of the physical distance between normalized spectral power distributions. Components of this distance are weighted to account for sensor noise properties. A color metric has several possible uses in a computer vision system. A color metric is useful for detecting color edges, classifying intensity edges, and estimating color variation within image regions. The usefulness of the color metric is demonstrated by evaluating its performance on regions of real images. Author

N89-23152# Maryland Univ., College Park. Computer Vision Lab.

COMBINING INFORMATION IN LOW-LEVEL VISION **c63**

John Aloimonos and Anup Basu *In* Science Applications International Corp., Proceedings: Image Understanding Workshop, Volume 2 Apr. 1988 p 862-906 (For primary document see N89-23115 16-61)

(Contract DAAB07-86-K-F073)

Avail: NTIS HC A99/MF E03 CSCL 09B

Low level modern computer vision is not domain dependent, but concentrates on problems that correspond to identifiable modules in the human visual system. Several theories have been proposed in the literature for the computation of shape from shading, shape from texture, retinal motion from spatiotemporal derivatives of the image intensity function and the like. The basic problems with some of the existing approaches if several available cues are combined, disappear in most cases; the resulting algorithms compute robustly and uniquely the intrinsic parameters (shape, depth, motion, etc.). The problem of machine vision is explored here from its basics. A low level mathematical theory is presented for the unique and robust computation of intrinsic parameters. The computational aspect of the theory envisages a cooperative highly parallel implementation, bringing in information from five different sources (shading, texture, motion, contour and stereo), to resolve ambiguities and ensure uniqueness of the intrinsic parameters. Author

N89-23153# Massachusetts Univ., Amherst. Computer Vision Research Lab.

COMPUTATION OF MOTION IN DEPTH PARAMETERS: A FIRST STEP IN STEREOSCOPIC MOTION INTERPRETATION **c63**

Poornima Balasubramanyam and M. A. Snyder *In* Science Applications International Corp., Proceedings: Image Understanding Workshop, Volume 2 Apr. 1988 p 907-920 (For primary document see N89-23115 16-61)

Avail: NTIS HC A99/MF E03 CSCL 09B

The need to obtain the three parameters of absolute 3-D motion in depth of objects in a dynamic scene using visual information motivated this research. Motion in depth (MID) parameters refer to the following three components of the object or camera motion, i.e., the single component of translation in depth (parallel to the line of sight) and the two components of rotation in depth (or rotational components that are not about the line of sight. The use of stereoscopic motion enables the MID parameters to be computed in a quick and robust manner for a stereo camera system moving through an environment that may have several

independently moving rigid bodies. It has been shown elsewhere that use of temporal binocular imagery permits the formulation of the ratio of the relative optic flow between a stereo pair of images and the disparity between them as a linear function of the image coordinates. The coefficients of this linear function are the translation in depth and rotation in depth components which are precisely the MID parameters being computed in our approach. Author

N89-23154# Maryland Univ., College Park. Computer Vision Lab.

IS CORRESPONDENCE NECESSARY FOR THE PERCEPTION OF STRUCTURE FROM MOTION **c63**

Eiki Ito and John Aloimonos *In* Science Applications International Corp., Proceedings: Image Understanding Workshop, Volume 2 Apr. 1988 p 921-929 (For primary document see N89-23115 16-61)

(Contract DAAB07-86-K-F073)

Avail: NTIS HC A99/MF E03 CSCL 09B

The fundamental assumption of almost all existing computational theories for the perception of structure from motion is that moving elements on the retina correspond projectively to identifiable moving points in three-dimensional space. Furthermore, these computational theories are based on the fundamental idea of retinal motion, (i.e., they use as their input the velocity with which image points are moving optic flow or discrete displacements). In this research, the possibility is investigated for the development of computational theories for the perception of structure from motion that are not based on the concept of the velocity of individual image elements, i.e., they do not use optic flow or displacements as input. Author

N89-23155# Massachusetts Univ., Amherst. Dept. of Computer and Information Science.

MOTION FROM A SEQUENCE OF IMAGES **c63**

Igor Pavlin *In* Science Applications International Corp., Proceedings: Image Understanding Workshop, Volume 2 Apr. 1988 p 930-937 Previously announced in IAA as A89-11835 (For primary document see N89-23115 16-61)

(Contracts N00014-82-K-0464; DACA76-85-C-0008)

Avail: NTIS HC A99/MF E03 CSCL 09B

A method is proposed for the recovery of motion parameters of a rigid object moving through an environment with constant but arbitrary linear and angular velocities. The method uses temporal information from a sequence of images such as those taken by a mobile robot. Spatial information contained in the images is also used. The temporal sequence, combined with the assumption of constant velocities, provides powerful constraints for the motion trajectory of rigid objects. A closed form solution is derived for the rigid object trajectory by integrating the differential equations describing the motion of a point on the tracked object. The integrated equations are non-linear only in angular velocity and are linear in all other motion parameters. These equations allow the use of a simple least-square error minimization criterion during an iterative search for the motion parameters. Experimental results demonstrate the power of this method in fast and reliable convergence. Author

N89-23156# Rochester Univ., NY. Dept. of Computer Science.

RECOGNIZING ANIMAL MOTION **c63**

Nigel H. Goddard *In* Science Applications International Corp., Proceedings: Image Understanding Workshop, Volume 2 Apr. 1988 p 938-944 Prepared in cooperation with Hughes Research Labs., Calabasas, CA (For primary document see N89-23115 16-61)

Avail: NTIS HC A99/MF E03 CSCL 09B

A method is proposed for recognizing animal motion from pure motion cues. A graphical representation for animal gait is introduced, and its connectionist implementation given. Assuming principal views, a way of indexing into this gait representation from low level invariants is described. Preliminary results from the first implementation are presented. The approach is motivated and constrained by biological considerations. Author

N89-23157# Massachusetts Univ., Amherst. Dept. of Computer and Information Sciences.

ISSUES IN EXTRACTING MOTION PARAMETERS AND DEPTH FROM APPROXIMATE TRANSLATIONAL MOTION

R. Dutta, R. Manmatha, Edward M. Riseman, and M. A. Snyder *In* Science Applications International Corp., Proceedings: Image Understanding Workshop, Volume 2 Apr. 1988 p 945-960 (For primary document see N89-23115 16-61)

(Contracts DACA76-85-C-0008; F30602-87-C-0140; NSF DCR-85-00332)

Avail: NTIS HC A99/MF E03 CSCL 09B

In dynamic imaging situations where the sensor is undergoing primarily translational motion with a relatively small rotational component, it might seem likely that approximate translational motion algorithms can be effective in determining depth. By restricting the processing to the two dimensions of translational motion there is a great reduction in complexity from the five dimensions of general motion (excluding the scaling component of sensor velocity or displacement). In an attempt to recover depth of points over a sequence of frames in such situations a set of three algorithms was applied sequentially: elimination of the effect of small rotations, then extraction of the focus of expansion (FOE), and then determination of depth of points. The goal was the extraction of obstacles at a distance beyond the accuracy of the range sensors in the autonomous land vehicle (ALV) research program. It was found, however, that even small rotations significantly affect the performance of algorithms designed for pure translational motion. A theoretical analysis of the problems in computing the FOE is presented. The attempt to correct for small rotations in the motion system described above was ineffective. A pair of previously developed algorithms have been combined to yield a general motion algorithm and have been applied to sequences of approximate translational motion. The conclusion is that in order to determine depth of points in many real situations, general motion analysis must be applied even when sensor motion is primarily translational. Various alternatives for extracting depth from motion are briefly considered. Author

N89-23158# Columbia Univ., New York, NY. Dept. of Computer Science.

A REAL TIME HIERARCHICAL MODEL FOR OPTIC FLOW DETERMINATION VIA SPATIOTEMPORAL FREQUENCY CHANNELS **c63**

Ajit Singh and Peter K. Allen *In* Science Applications International Corp., Proceedings: Image Understanding Workshop, Volume 2 Apr. 1988 p 961-969 (For primary document see N89-23115 16-61)

Avail: NTIS HC A99/MF E03 CSCL 09B

The recent work on perception and measurement of visual motion has consistently advocated the use of hierarchical representation and analysis. In most of the practical applications of motion perception, such as robotics, object tracking in space applications, etc., it is absolutely necessary to be able to construct and process these hierarchical image representations in real time, and this calls for an inherently parallel implementation. Past work on motion perception that makes use of hierarchical models is reviewed and the need for their real time implementation is identified. A new hierarchical model is described for extraction of one form of motion information from an image sequence, namely optic-flow, based on the recently proposed spatiotemporal frequency approach. The inherent parallelism in the model is identified and how to exploit that to implement the model in real-time on the PIPE image processing architecture is shown. In the implementation, the underlying image pyramids and the optic flow is computed in real time. Finally the results of the PIPE implementation are presented. They are also available on a video-tape to display the real-time nature of the computations. Author

N89-23159# Massachusetts Univ., Amherst. Dept. of Computer and Information Science.

TRANSLATING OPTICAL FLOW INTO TOKEN MATCHES **c63**

Lance R. Williams and Allen R. Hanson *In* Science Applications

International Corp., Proceedings: Image Understanding Workshop, Volume 2 Apr. 1988 p 970-980 (For primary document see N89-23115 16-61)
(Contracts F30602-87-C-0140; DMA800-85-C-0012)
Avail: NTIS HC A99/MF E03 CSCL 09B

Motion in the environment manifests itself in changes of many kinds, not just image plane velocities, yet these are all that an optical flow field makes explicit. Optical flow is viewed as a useful low-level representation from which a symbolic description of change, in the form of token matches, can be computed. The tokens of interest are those produced by perceptual organization processes, and are more abstract than edges or interest points. A demonstration is given of a working system for matching line tokens which uses the optical flow field in a heuristic manner to limit the search for the minimal bipartite cover of the set of tokens from each frame. Author

N89-23160# Rochester Univ., NY. Dept. of Computer Science.
STRUCTURE RECOGNITION BY CONNECTIONIST RELAXATION: FORMAL ANALYSIS
Paul R. Cooper *In* Science Applications International Corp., Proceedings: Image Understanding Workshop, Volume 2 Apr. 1988 p 981-993 (For primary document see N89-23115 16-61)
(Contract F30602-85-C-0008)
Avail: NTIS HC A99/MF E03 CSCL 09B

A connectionist implementation of discrete relaxation, for labelled graph matching is described. The application is fast parallel indexing from structure descriptions. The network is limited by complexity considerations to the detection and propagation of unary and binary consistency constraints. The convergence of the algorithm is proved. The desired behavior of the algorithm is formally specified, and the fact that the network correctly computes this is proved. Explicit and exact space and time resource requirements are developed. Author

N89-23161# SRI International Corp., Menlo Park, CA. Artificial Intelligence Center.
EXTRACTING GENERIC SHAPES USING MODEL-DRIVEN OPTIMIZATION **c63**
Pascal Fua and Andrew J. Hanson *In* Science Applications International Corp., Proceedings: Image Understanding Workshop, Volume 2 Apr. 1988 p 994-1004 (For primary document see N89-23115 16-61)
(Contract MDA903-86-C-0084)
Avail: NTIS HC A99/MF E03 CSCL 09B

A model-driven approach is developed for extracting generic shapes from monoscopic and stereographic imagery. Generic geometric constraints are used to obtain model candidates and to suggest missing model components in the image data. Competing scene parses are ranked using objective functions that include the cost of encoding the scene information in terms of a set of generic primitives and a measure of the geometric quality of the parse. As examples, generic models are formulated for buildings, roads, and vegetation clumps. The model definitions include edge characteristics, two- and three-dimensional geometric properties, region characteristics, and procedures for predicting and verifying missing shape components. Results are shown for a variety of aerial imagery. Author

N89-23162# Stanford Univ., CA. Robotics Lab.
TEXTURE MODELS AND IMAGE MEASURES FOR SEGMENTATION **c63**
Richard Vistnes *In* Science Applications International Corp., Proceedings: Image Understanding Workshop, Volume 2 Apr. 1988 p 1005-1015 (For primary document see N89-23115 16-61)
Avail: NTIS HC A99/MF E03 CSCL 09B

The problem of texture segmentation is to identify image curves that separate different textures. The segmentation problem has two phases: detecting differences between textures, followed by localizing the edges thus detected. This paper focuses on texture discrimination, which is based on differences in texture measures between two image regions. Texture is treated not merely as image pattern, but as the projection of scene structure; two image textures differ when the scene textures of which they are projections differ. A model is proposed for a large class of scene textures and examines their images under projection. A set of image texture measures is proposed that allows the reliable discrimination of physically different textures. Textures are characterized by distributions of shape, position and color of image substructures; methods for estimating these distributions are discussed. A forced-choice method is proposed for evaluating the ability of texture measures to discriminate textures. The proposed texture measures have been implemented, and empirical tests show that the measures can discriminate a large set of natural textures with 90 to 100 percent accuracy, compared with about 40 percent accuracy for another popular set of texture measures. Author

N89-23163# SRI International Corp., Menlo Park, CA. Artificial Intelligence Center.
MODAL DRIVEN EDGE DETECTION
Pascal Fua and Yvan G. Leclerc *In* Science Applications International Corp., Proceedings: Image Understanding Workshop, Volume 2 Apr. 1988 p 1016-1021 (For primary document see N89-23115 16-61)
(Contracts DACA76-85-C-0004; MDA903-86-C-0084)
Avail: NTIS HC A99/MF E03 CSCL 09B

Standard edge-detectors fail to find most relevant edges, finding either too many or too few, because they lack a geometrical model to guide their search. A technique that integrates both photometric and geometric models with an initial estimate of the boundary is presented. The strength of this approach lies in the geometric model's ability to overcome various photometric anomallies, thereby finding boundaries that could not otherwise be found. Furthermore, the model can be used to score edges based on their goodness of fit, thus allowing one to use the semantic model information to accept or reject them. Author

N89-23164# SRI International Corp., Menlo Park, CA. Artificial Intelligence Center.
GENERALIZING EPIPOLAR-PLANE IMAGE ANALYSIS ON THE SPATIOTEMPORAL SURFACE
H. Harlyn Baker and Robert C. Bolles *In* Science Applications International Corp., Proceedings: Image Understanding Workshop, Volume 2 Apr. 1988 p 1022-1030 (For primary document see N89-23115 16-61)
(Contract DACA76-85-C-0004)
Avail: NTIS HC A99/MF E03 CSCL 09B

The previous implementation of an Epipolar-Plane Image Analysis mapping technique demonstrated the feasibility and benefits of the approach, but were carried out for restricted camera geometrics. The question of more general geometrics made utility for autonomous navigation uncertain. Discussed here is the development of a generalization of the analysis that: (1) enable varying view direction, including varying over time, (2) provides three-dimensional connectivity information for building coherent spatial descriptions of observed objects, and (3) operates sequentially, allowing initiation and refinement of scene feature estimates while the sensor is in motion. To implement this generalization it was necessary to develop an explicit description of the evolution of images over time. This was achieved by building a process that creates a set of two-dimensional manifolds defined at the zeroes of a three-dimensional spatiotemporal Laplacian. These manifolds represent explicitly both the spatial and temporal structure of the temporally-evolving imagery, and they are termed spatiotemporal surfaces. The surfaces are constructed incrementally, as the images are acquired. Also described is a tracking mechanism that operates locally on these evolving surfaces in carrying out three-dimensional scene reconstruction. Author

N89-23165# SRI International Corp., Menlo Park, CA. Artificial Intelligence Center.
BUILDING SURFACES OF EVOLUTION: THE WEAVING WALL
H. Harlyn Baker *In* Science Applications International Corp.,

Proceedings: Image Understanding Workshop, Volume 2 Apr. 1988 p 1031-1040 (For primary document see N89-23115 16-61)
(Contract DACA76-85-C-0004)
Avail: NTIS HC A99/MF E03 CSCL 09B

We describe a three-dimensional surface construction process designed for the analysis of image sequences. Named the Weaving Wall, the process operates over images as they arrive from the sensor, knitting together, along a parallel frontier, connected descriptions of images as they evolve over time. Developed to support a tracking mechanism for recovering the three-dimensional structure of a scene being traversed, other applications have since become apparent. These include rendering and computation on tomographic medical data, display of higher-dimensioned analytic functions, edge detection on the scale-space surface, and display and analysis of material fracture data. Displays from some of these applications are presented. The Weaving Wall may be of use in representing the evolution of any two-dimensional imagery varying in a nearly continuous manner along a third dimension, and possibly four dimensions. Author

N89-23166# Aule-Tek, Inc., Schenectady, NY.
GENERATION OF FACE-EDGE-VERTEX MODELS DIRECTLY FROM IMAGES
C. I. Connolly and J. R. Stenstrom *In* Science Applications International Corp., Proceedings: Image Understanding Workshop, Volume 2 Apr. 1988 p 1041-1046 (For primary document see N89-23115 16-61)
(Contract DACA76-86-C-0007)
Avail: NTIS HC A99/MF E03 CSCL 09B

Computer models of objects are necessary for a variety of tasks including model-based vision. Techniques are presented to construct face-edge-vertex models directly from intensity images. A corresponding technique is developed to build face-edge-vertex models from range images. The results are compared. Author

N89-23167# Massachusetts Univ., Amherst. Dept. of Computer and Information Science.
DEPTH FROM LOOMING STRUCTURE
Lance R. Williams and Allen R. Hanson *In* Science Applications International Corp., Proceedings: Image Understanding Workshop, Volume 2 Apr. 1988 p 1047-1051 (For primary document see N89-23115 16-61)
(Contracts DACA76-85-C-0008; F30602-87-C-0140)
Avail: NTIS HC A99/MF E03 CSCL 09B

A technique for computing distance to environmental surfaces suitable for obstacle recognition by a mobile robot is presented. Accurate knowledge of the camera motion parameters is not required. We demonstrate how motion in depth manifests itself in the projected lengths and areas of environmental surfaces whose extent in depth is small relative to their distance from the camera. Results on a sequence taken by a mobile robot are presented to demonstrate the accuracy of the method. Finally, examples are presented of organizational principles which would allow suitable environmental structures to be recognized automatically. Author

N89-23168# Columbia Univ., New York, NY. Dept. of Computer Science.
ON THE RECOVERY OF SUPERELLIPSOIDS
Terrance E. Boult and Ari D. Gross *In* Science Applications International Corp., Proceedings: Image Understanding Workshop, Volume 2 Apr. 1988 p 1052-1063 (For primary document see N89-23115 16-61)
(Contract N00039-84-C-0165)
Avail: NTIS HC A99/MF E03 CSCL 09B

Superellipsoids are parameterized solids which can appear like cubes or spheres or octahedrons or 8-pointed stars or anything in between. They can also be stretched, bent, tapered and combined with boolean to model a wide range of objects. Superquadrics are of interest as model primitives for computer vision applications because they are flexible enough to allow modelling of many objects, yet they can be described by a few (5 to 14) numbers. Research into the recovery of superellipsoids from 3-D information, in particular range data, is discussed. This research can be divided into two parts, a study of potential error-of-fit measures for recovering superquadrics, and implementation and experimentation with a system which attempts to recover superellipsoids by minimizing an error-of-fit measure. An overview of work in both areas is presented. Included are data from an initial comparison of 4 error-of-fit measures in terms of the inter-relationship between each measure and the parameters defining the superellipsoid. Also discussed is an experimental system which employs a nonlinear least square minimization technique to recover the parameters. Both the advantages of this technique are discussed, and some of its major drawbacks. Examples are presented, using both synthetic and range-data, where the system successfully recovers superellipsoids, including negative volumes as would occur if superellipsoids were used in a constructive solid modeling system. Author

N89-23169# Stanford Univ., CA. Robotics Lab.
STRAIGHT HOMOGENEOUS GENERALIZED CYLINDERS: DIFFERENTIAL GEOMETRY AND UNIQUENESS RESULTS
Jean Ponce *In* Science Applications International Corp., Proceedings: Image Understanding Workshop, Volume 2 Apr. 1988 p 1064-1073 (For primary document see N89-23115 16-61)
(Contract F33615-85-C-5106)
Avail: NTIS HC A99/MF E03 CSCL 09B

The differential geometry of straight homogeneous generalized cylinders (SHGC's) is discussed. A necessary and sufficient condition that a SHGC must verify to parameterize a regular surface is derived, the Gaussian curvature of a regular SHGC is computed, and proof is offered that the parabolic lines of a SHGC are either meridians or parallels. Using these results, the following problem is addressed: Under which conditions can a given surface have several descriptions by SHGC's. Several new results are reported. In particular, it was proven that two SHGC's with the same cross-section plane and axis direction are necessarily deduced from each other through inverse scalings of their cross-sections and sweeping rule curve. Shafer's pivot and slant theorems were extended. Finally, that a surface with at least two parabolic lines has at most three different SHGC descriptions, and that a surface with at least four parabolic lines has at most a unique SHGC description. Author

N89-23170# Stanford Univ., CA. Robotics Lab.
RIBBONS, SYMMETRIES AND SKEWED SYMMETRIES
Jean Ponce *In* Science Applications International Corp., Proceedings: Image Understanding Workshop, Volume 2 Apr. 1988 p 1074-1079 (For primary document see N89-23115 16-61)
(Contract F33615-85-C-5106)
Avail: NTIS HC A99/MF E03 CSCL 09B

Following Rosenfeld, comparisons were made of Blum, Brooks, and Brady ribbons. It was proven that Blum and Brady ribbons are not, in general, Brooks ribbons. Conversely, Brooks ribbons are, in general, neither Blum nor Brady ribbons. For Blum and Brooks ribbons, it is in principle trivial to decide whether two contour points may form a ribbon pair: they have to form a local symmetry, i.e., the angles between the line joining these two points and the outward normals to the contour at these points must be the same. This property is not true for Brooks ribbons. Is it then possible to characterize locally the pairs of contour points which form a Brooks ribbon pair. Using the curvature of the contour of a Brooks ribbon, the answer to this question proved to be yes for some classes of Brooks ribbons, including skewed symmetries. This result has potential practical applications for three-dimensional shape recovery from image contours. Author

N89-23171# Maryland Univ., College Park. Computer Visual Lab.
SYMBOLIC PIXEL LABELING FOR CURVILINEAR FEATURE DETECTION
John Canning, J. John Kim, Nathan Netanyahu, and Azriel Rosenfeld *In* Science Applications International Corp.,

Proceedings: Image Understanding Workshop, Volume 2 Apr. 1988 p 1080-1090 (For primary document see N89-23115 16-61)
Avail: NTIS HC A99/MF E03 CSCL 09B

A method of detecting thin curvillinear features in an image based on a detailed analysis of the local gray level patterns at each pixel is described. This method allows operations such as thinning and gap filling to be based on more accurate information. Author

N89-23172# Stanford Univ., CA. Robotics Lab.
IMAGE SEGMENTATION USING GEOMETRIC AND PHYSICAL CONSTRAINTS
Thilaka S. Sumanaweera, Glenn Healey, Byung-Uk Lee, Thomas O. Binford, and Jean Ponce *In* Science Applications International Corp., Proceedings: Image Understanding Workshop, Volume 2 Apr. 1988 p 1091-1099 (For primary document see N89-23115 16-61)
(Contract F33615-85-C-5106)
Avail: NTIS HC A99/MF E03 CSCL 09B

Segmentation is an important step in scene analysis. Segmentation algorithms based on geometry alone are easily confused by image artefacts due to physical processes, for example, specularities. On the other hand, segmentation algorithms based on purely local properties are rarely adequate for segmenting complex images. Segmentation algorithms are described which use both geometric and physical properties. The performance of these algorithms is discussed. Author

N89-23173# University of Southern California, Los Angeles. Inst. for Robotics and Intelligent Systems.
ADAPTIVE SMOOTHING FOR FEATURE EXTRACTION
Philippe Saint-Marc and Gerard Medioni *In* Science Applications International Corp., Proceedings: Image Understanding Workshop, Volume 2 Apr. 1988 p 1100-1113 (For primary document see N89-23115 16-61)
(Contracts DACA76-85-C-0009; F33615-98-C-1436)
Avail: NTIS HC A99/MF E03 CSCL 09B

A method to smooth a signal is presented whether the signal be an intensity image, a range image or a contour - which preserves discontinuities and facilitates their detection. This is achieved by repeatedly convolving the image with a very small averaging filter modulated by a measure of the continuousness at each pixel. This process is related to the Anisotropic Diffusion reported by Perona and Malik recently, but is not subject to instability or divergence. It is shown first how this basic approach can be applied when it is reasonable to model an image as piecewise constant (such as most aerial or outdoor images), discussion then turns to the case when it becomes necessary to detect discontinuities of the first derivatives, as is the case for range images, and finally the case when the input signal is a connected curve is presented. The method is extremely attractive as there is a single parameter to adjust, analogous to the variance omega in the Scale-Space paradigm, and produces a robust segmentation as no tracking is needed. The method is illustrated with results on real intensity and range images, and on actual contours. Author

N89-23174# Massachusetts Inst. of Tech., Cambridge. Artificial Intelligence Lab.
RECOGNIZING SOLID OBJECTS BY ALIGNMENT
Daniel P. Huttenlocher and Shimon Ullman *In* Science Applications International Corp., Proceedings: Image Understanding Workshop, Volume 2 Apr. 1988 p 1114-1124 (For primary document see N89-23115 16-61)
(Contracts DACA76-85-C-0010; N00014-86-K-0685; N00014-85-K-0124)
Avail: NTIS HC A99/MF E03 CSCL 09B

It is shown that a correspondence between three points on a rigid solid object and three points in a two-dimensional image is sufficient to align the object with the image. The method uses a weak perspective viewing model, where true perspective is approximated by orthographic projection plus scale. It is also demonstrated that the alignment transformation exists, and is unique up to a reflection, for any non-colinear triple of object and image points. The transformation can also be computed from edge fragments, where the endpoints are unknown. For planar objects, the transformation is equivalent to a two-dimensional affine transform from the object to the image. A recognition system that was implemented uses one or two pairs of model and image features to hypothesize potential alignments of object models with an image. Each hypothesis is verified by projecting the model features into the image. Examples using points and edges extracted from grey-level images are shown. Author

N89-23175# Maryland Univ., College Park. Center for Automation Research.
PROJECTIVE INVARIANTS OF SHAPES
Isaac Weiss *In* Science Applications International Corp., Proceedings: Image Understanding Workshop, Volume 2 Apr. 1988 p 1125-1134 (For primary document see N89-23115 16-61)
Avail: NTIS HC A99/MF E03 CSCL 09B

A major goal of computer vision is object recognition, which involves matching of images of an object, obtained from different, unknown points of view. Since there are infinitely many points of view, one is faced with the problem of a search in a multidimensional parameter space. A related problem is the stereo reconstruction of 3-D surfaces from multiple 2-D images. A method is proposed to solve these fundamental problems by using geometrical properties of the visible shape that are invariant to a change in the point of view. To obtain such invariants, classical theories for differential and algebraic invariants not previously used in image understanding were used as a starting point. As they stand, these theories are not directly applicable to vision. Extensions and adaptation of these methods to the needs of machine vision are suggested. General projective transformation, which include both perspective and orthographic projections as special cases are being studied. Author

N89-23176# Columbia Univ., New York, NY. Dept. of Computer Science.
AN OPTIMAL ALGORITHM FOR THE DERIVATION OF SHAPE FROM SHADOWS
Michael Hatzitheodorou and John R. Kender *In* Science Applications International Corp., Proceedings: Image Understanding Workshop, Volume 2 Apr. 1988 p 1135-1139 (For primary document see N89-23115 16-61)
Avail: NTIS HC A99/MF E03 CSCL 09B

The study problem is that of recovering a surface slice from the shadows it casts on itself when lighted by the sun at various times of the day. The problem is formulated and solved in a Hilbert space setting. The spline algorithm interpolating the date that result from the shadows is constructed. This algorithm is optimal in terms of the approximation error and has low cost. The optimal error algorithm is implemented and a series of test runs presented. In addition another modified version of the algorithm that improves the cost considerably is shown. This version is suited for parallel computation with further reductions in the cost of the solution. Author

N89-23177# Stanford Univ., CA. Robotics Lab.
PREDICTING MATERIAL CLASSES
Glenn Healey and Thomas O. Binford *In* Science Applications International Corp., Proceedings: Image Understanding Workshop, Volume 2 Apr. 1988 p 1140-1146 (For primary document see N89-23115 16-61)
(Contract F33615-85-C-5106)
Avail: NTIS HC A99/MF E03 CSCL 09B

Given the physical properties of a class of materials, it is possible to predict the properties of images of these materials. Examined here are the properties of metals and dielectrics which allow them to be distinguished in color images. First general physical models were adopted for the properties of materials which determine how they interact with light. From these models, an analysis was made of the geometric, spectral, and intensity properties of the light reflected from an arbitrary material. The

goal of this work is to isolate those properties of the reflected light which provide evidence for the classification of a material as either a metal or a dielectric. The ability to achieve this level of classification is a first step towards a more general material identification system. Author

N89-23178# Stanford Univ., CA. Robotics Lab.
TEXTURE EDGE LOCALIZATION
Richard Vistnes *In* Science Applications International Corp., Proceedings: Image Understanding Workshop, Volume 2 Apr. 1988 p 1147-1154 (For primary document see N89-23115 16-61)
Avail: NTIS HC A99/MF E03 CSCL 09B

Texture segmentation may be separated into two phases: edge detection, followed by edge localization; the latter topic is discussed. In the first part some simple, abstracted textures are used to illustrate the issues involved in texture edge localization. Some of the limits of localization are discussed. The second part suggests a simple approach to localization based on interpreting the responses of edge detectors spaced at fixed intervals in position and orientation space. The results of this algorithm as applied to some synthetic and natural textures are presented. Author

N89-23179# Columbia Univ., New York, NY. Dept. of Computer Science.
SURFACE ORIENTATION FROM PROJECTIVE FORESHORTENING OF ISOTROPIC TEXTURE AUTOCORRELATION
Lisa Gottesfeld Brown and Haim Shvaytser *In* Science Applications International Corp., Proceedings: Image Understanding Workshop, Volume 2 Apr. 1988 p 1155-1159 (For primary document see N89-23115 16-61)
(Contract N00039-84-C-0165)
Avail: NTIS HC A99/MF E03 CSCL 09B

A new method for determining local surface orientation from the autocorrelation function of statistically isotropic textures is introduced. It relies on the foreshortening that occurs in the image of an oriented surface, and the analogous foreshortening produced in the texture autocorrelation function. This method assumes textural isotropy, but does not require the texture to be composed of texels or assume texture regularities such as equal area texels or equal spacings between texels. This technique is applied to natural images of planar textured surfaces and found to give good results in many instances. The simplicity of the method and its use of information from all parts of the image are emphasized. Author

N89-23180# General Electric Co., Schenectady, NY. Corporate Research and Development Center.
LABELING POLYHEDRAL IMAGES
Van-Duc Nguyen *In* Science Applications International Corp., Proceedings: Image Understanding Workshop, Volume 2 Apr. 1988 p 1160-1165 (For primary document see N89-23115 16-61)
Avail: NTIS HC A99/MF E03 CSCL 09B

Recognizing that a polyhedral image is a segmentation of the plane into connected regions, called faces, joined by vertices and edges, the input image is represented as a planar network of nodes (vertices, edges, faces) linked by adjacency links. By introducing junction-pairs and junction-loops as labelings of edges and faces, globally consistent labelings of the whole image can be found through achieving node and arc consistencies at all nodes and links in the network. This proves that labeling of polyhedral images and line drawings is linear in the number of edges in the image, and exponential only in the maximum number of edges intersecting at a node. Text examples on ideal and real polyhedral images are illustrated. Author

N89-23181*# National Aeronautics and Space Administration. Langley Research Center, Hampton, VA.
A KNOWLEDGE-BASED TOOL FOR MULTILEVEL DECOMPOSITION OF A COMPLEX DESIGN PROBLEM
James L. Rogers Washington May 1989 23 p
(NASA-TP-2903; L-16557; NAS 1.60:2903) Avail: NTIS HC A03/MF A01 CSCL 09B

Although much work has been done in applying artificial intelligence (AI) tools and techniques to problems in different engineering disciplines, only recently has the application of these tools begun to spread to the decomposition of complex design problems. A new tool based on AI techniques has been developed to implement a decomposition scheme suitable for multilevel optimization and display of data in an N x N matrix format. Author

N89-23182*# National Aeronautics and Space Administration. Goddard Space Flight Center, Greenbelt, MD.
SEAPAK USER'S GUIDE, VERSION 1.0
Charles R. McClain, Daniel Endres, Judy Chen, Michael Darzi, and James Firestone (General Sciences Corp., Laurel, MD.) 1989 448 p
(Contract NAS5-29371)
(NASA-TM-100728; NAS 1.15:100728) Avail: NTIS HC A19/MF A01 CSCL 09B

The SEAPAK is a user-interactive satellite data analysis package that was developed for the processing and interpretation of Nimbus-7/Coastal Zone Color Scanner (CZCS) and the NOAA Advanced Very High Resolution Radiometer (AVHRR) data. The various hardware and software components of the Laboratory for Oceans Computer Facility (LOCF) relevant to SEAPAK, a number of data processing scenarios, the SEAPAK menu and the procs it contains, a reference section containing the SEAPAK procs, references, and a glossary are described. B.G.

N89-23183*# SRI International Corp., Menlo Park, CA.
SPECIFYING REAL-TIME SYSTEMS WITH INTERVAL LOGIC Final Report
John Rushby 30 Nov. 1988 81 p
(Contract NAS1-17067)
(NASA-CR-181804; NAS 1.26:181804) Avail: NTIS HC A05/MF A01 CSCL 09B

Pure temporal logic makes no reference to time. An interval temporal logic and an extension to that logic which includes real time constraints are described. The application of this logic by giving a specification for the well-known lift (elevator) example is demonstrated. It is shown how interval logic can be extended to include a notion of process. How the specification language and verification environment of EHDM could be enhanced to support this logic is described. A specification of the alternating bit protocol in this extended version of the specification language of EHDM is given. Author

N89-23184*# Northwestern Univ., Evanston, IL. Dept. of Civil Engineering.
PARALLEL PROCESSORS AND NONLINEAR STRUCTURAL DYNAMICS ALGORITHMS AND SOFTWARE Semiannual Progress Report, 1 Mar. - 31 Aug. 1988
Ted Belytschko 21 Apr. 1989 36 p
(Grant NAG1-650)
(NASA-CR-184938; NAS 1.26:184938) Avail: NTIS HC A03/MF A01 CSCL 09B

A nonlinear structural dynamics finite element program was developed to run on a shared memory multiprocessor with pipeline processors. The program, WHAMS, was used as a framework for this work. The program employs explicit time integration and has the capability to handle both the nonlinear material behavior and large displacement response of 3-D structures. The elasto-plastic material model uses an isotropic strain hardening law which is input as a piecewise linear function. Geometric nonlinearities are handled by a corotational formulation in which a coordinate system is embedded at the integration point of each element. Currently, the program has an element library consisting of a beam element based on Euler-Bernoulli theory and trianglar and quadrilateral plate element based on Mindlin theory. Author

N89-23185# Air Force Inst. of Tech., Wright-Patterson AFB, OH. School of Engineering.
IMPLEMENTATION OF THE NETOS (NETWORK OPERATING SYSTEM) OPERATED SYSTEM IN Ada WITH MODIFICATIONS TO ALLOW VARIABLE LENGTH MESSAGES M.S. Thesis
Robert Rodriguez Dec. 1988 109 p
(AD-A202602; AD-E900870; AFIT/GE/ENG/88D-43) Avail: NTIS HC A06/MF A01 CSCL 25E

This thesis redeveloped the Network Operating System (NETOS) software, which is patterned after the OSI 7-Layer Model and runs on a Local Area Network at the Air Force Institute of Technology, from the programming language C to the programming language Ada, with modifications to support variable length messages. The approach taken used a software development methodology which contains the following phases; requirements analysis, design, implementation, and testing. The requirement analysis phase consisted of an enumerated listing of the requirement specifications supported by SADT diagrams. The design phase transformed these diagrams to a structural chart representation of the design. Implementation of the software was written in Janus/Ada for the work stations and Whitesmith C for the central system. Testing was an integral part of the implementation phase and was accomplished at each level of the 7-Layer model. GRA

N89-23186# Air Force Inst. of Tech., Wright-Patterson AFB, OH. School of Engineering.
THE DESIGN AND IMPLEMENTATION OF A GRAPHICAL VHDL (VHSIC HARDWARE DESCRIPTION LANGUAGE) USER INTERFACE M.S. Thesis
Stephen M. Matechik Dec. 1988 141 p
(AD-A202619; AD-E900870; AFIT/GE/ENG/88D-25) Avail: NTIS HC A07/MF A01 CSCL 12E

This thesis effort outlines the design and implementation of a Graphical VHDL User Interface (GVUI). Though the GVUI is designed as an integral component of the UNIX based Air Force Institute of Technology (AFIT) VHDL Environment (AVE), it is a stand alone tool that operates under MS-DOS on an IBM PC-XT personal computer. The goal of the GVUI is to automatically generate VHDL source code from a graphic schematic diagram. To meet this goal, two phases of development were identified. Phase 1 primarily addresses the schematic generation and editing capabilities of the system. Phase 2 shall focus on the system's automatic code generation capabilities. This thesis specifically addresses and completes the first of these two phases. This research paper is organized in the following manner. A brief introduction of VHDL and current VHDL programming environments is presented as background information. The GVUI development is then tracked from its requirements analysis and system design, through detailed design, and on through functional testing. In conclusion, recommendations for future enhancements are provided. A comprehensive user's guide is included as an appendix. GRA

N89-23187# Argonne National Lab., IL. Mathematics and Computer Science Div.
USE OF LANGUAGE FEATURES IN THE IMPLEMENTATION AND VALIDATION OF A STANDARDIZED GENERIC PACKAGE OF ELEMENTARY FUNCTIONS FOR Ada
Ping Tak Peter Tang 28 Oct. 1988 7 p Presented at the Sandia Workshop on Ada in Real-Time and Scientific Environments, Albuquerque, NM, 30 Oct. 1988
(Contract W-31-109-eng-38)
(DE89-007385; CONF-8810320-1) Avail: NTIS HC A02/MF A01

The creators of Ada envisioned it to be a fine language for portable numerical programming by incorporating into Ada a formal floating-point model that is further supported by numerous environment inquiries. It is therefore somewhat ironic that there is no mention at all in the language of a library of elementary functions, one of the most basic building blocks for scientific computations. Do the language features allow such a library to be rigorously specified in the spirit of the floating-point model. If so, can a specification-conforming library be implemented portably in Ada itself. This paper is a summary of our investigations of the functions EXP and LOG pertaining to the second question. With careful use of the language features, we have shown that portable implementations are achievable, with minor qualifications. Moreover, we have also shown that the accuracy of such portable implementations can themselves be validated by programs implemented portably in Ada. The organization of this paper is as follows. We discuss the specifications and outline the implementations. We report the results of our analysis on the implementations. The idea and the implementations of the validation method are then discussed. Finally, we discuss the extension of our present work. DOE

N89-23188# Decision Science Consortium, Inc., Reston, VA.
CONSENSUS THEORY IN EXPERT SYSTEMS: AN ADAPTIVE INFERENCE FRAMEWORK AND APPLICATION TO IMAGE UNDERSTANDING Final Report, May 1986 - Dec. 1988
Kathryn B. Laskey, Marvin S. Cohen, William G. Roman, Paul K. Black, and James R. Mcintyre Dec. 1988 74 p
(Contract DACA72-86-C-0003)
(AD-A204253; DSCI-TR-88-16; ETL-0524) Avail: NTIS HC A04/MF A01 CSCL 12F

Advances in automated image understanding technology are essential to our ability to exploit today's sophisticated imagery capabilities to support battlefield intelligence requirements. This report describes the application of a unique inference framework, Non-Monotonic Probabilist, to the problem of achieving consensus among modules, each of which supports a different part of the image understanding problem. Non-Monotonic Probabilist combines symbolic default reasoning with numerical uncertainty propagation to support a flexible ability to make and revise assumptions, to examine the degree of conflict associated with the current set of assumptions, and to resolve conflicts by reaching inside arguments and adjusting the underlying assumptions. GRA

N89-23189# Techplan Corp., San Diego, CA.
OVERVIEW OF THE SOFTWARE TECHNOLOGY PROJECT RS34C71, DOCUMENTATION, MANAGEMENT/TECHNICAL ADVANCED CONCEPTS FOR SOFTWARE ENGINEERING Final Report
Jul. 1988 63 p
(Contract N66001-86-D-0020)
(AD-A204921; NOSC/TD-1301) Avail: NTIS HC A04/MF A01 CSCL 12E

An overview of the Software Technology Project is presented. This multi-laboratory exploratory development program is taking a unique approach to the identification and demonstration of new technologies capable of facilitating the entire life-cycle of the software development process. GRA

N89-23190# Carnegie-Mellon Univ., Pittsburgh, PA. Management Sciences Research Group.
AN ALGORITHM FOR THE THREE-INDEX ASSIGNMENT PROBLEM Management Science Research Report
Egon Balas and Matthew J. Saltzman (Arizona Univ., Tucson.) Sep. 1988 36 p
(Contract N00014-85-K-0198; NSF ECS-86-01660)
(AD-A205172; MSRR-550; WP-88-89-23) Avail: NTIS HC A03/MF A01 CSCL 12A

A branch and bound algorithm is described for solving the axial three-index assignment problem. The main features of the algorithm include a Lagrangian relaxation incorporating a class of facet inequalities and solved by a modified subgradient procedure to find a good lower bounds, a primal heuristic based on the principle of minimizing maximum regret plus a variable depth interchange phase for finding good upper bounds, and a novel branching strategy that exploits problem structure to fix several variables at each node and reduce the size of the total enumeration tree. Computational experience is reported on problems with up to 78 equations and 16,376 variables. The primal heuristics were tested on problems with up to 210 equations and 343,000 variables. GRA

N89-23191# Colorado Univ., Boulder. Dept. of Computer Science.
A NEW MODIFIED CHOLESKY FACTORIZATION
Robert B. Schnabel and Elizabeth Eskow 30 Dec. 1988 40 p
(Contract DAAL03-88-K-0086; NSF CCR-87-02403; NSF DCR-84-20944)
(AD-A205174; ARO-24923.3-MA) Avail: NTIS HC A03/MF A01 CSCL 12B

The modified Cholesky factorization plays an important role in optimization algorithms. Given a symmetric but not necessarily positive matrix A, it computes a Cholesky factorization of A+E, where E=O if A is safely positive definite, and E is a diagonal matrix chosen to make A+E positive definite otherwise. The factorization costs only a small multiple of n-square operations more than the standard Cholesky factorization. A algorithm that has these same properties is presented, but the theoretical bound on (E) is substantially smaller. It is based upon two techniques, the use of Gerschgorin bounds in selecting the elements of E, and a new way of monitoring positive definiteness. In extensive computational tests on indefinite matrices, the factorization virtually always produces smaller values of (E) than the existing method, without impairing the conditioning of A+E. In some cases the improvements are substantial. The factorization may prove useful in optimization algorithms. GRA

N89-23192# Dynamics Research Corp., Andover, MA.
DEVELOPING SOFTWARE TO USE PARALLEL PROCESSING EFFECTIVELY Final Report, Jun. - Dec. 1987
Julian Center Oct. 1988 199 p
(Contract F19628-86-D-0006)
(AD-A205184; RADC-TR-88-203) Avail: NTIS HC A09/MF A01 CSCL 12E

This report describes the difficulties involved in writing efficient parallel programs and describes the hardware and software support currently available for generating software that utilizes processing effectively. Historically, the processing rate of single-processor computers has increased by one order of magnitude every five years. However, this pace is slowing since electronic circuitry is coming up against physical barriers. Unfortunately, the complexity of engineering and research problems continues to require ever more processing power (far in excess of the maximum estimated 3 Gflops achievable by single-processor computers). For this reason, parallel processing architectures are receiving considerable interest, since they offer high performance more cheaply than a single-processor supercomputer, such as the Cray. GRA

N89-23193# Los Alamos National Lab., NM.
OPTIMIZATION FOR OBJECT LOCALIZATION OF THE CONSTRAINED ALGEBRAIC RECONSTRUCTION TECHNIQUE
Kenneth M. Hanson 1989 9 p Presented at the 3rd Conference on Medical Imaging, Newport Beach, CA, 29 Jan. 1989
(Contract W-7405-eng-36)
(DE89-007755; LA-UR-89-266; CONF-890115-1) Avail: NTIS HC A02/MF A01

A method for optimizing image-recovery algorithms is presented that is based on how well the specified task of object localization can be performed using the reconstructed images. The task performance is numerically assessed by a Monte Carlo simulation of the complete imaging process including the generation of scenes appropriate to the desired application, subsequent data taking, image recovery, and performance of the stated task based on the final image. This method is used to optimize the constrained Algebraic Reconstruction Technique (ART), which reconstructs images from their projections under a nonnegativity constraint by means of an iterative updating procedure. The optimization is performed by finding the relaxation factor, which is employed in the updating procedure, that yields the minimum rms error in estimating the position of discs in the reconstructed images. It is found that the optimum operating points for the best object localization are essentially the same as those obtained earlier when the performance of simple object detection is to be optimized. DOE

N89-23194# Sandia National Labs., Albuquerque, NM.
AUTOMATING THE IDENTIFICATION OF STRUCTURAL MODEL PARAMETERS
James J. Allen and David R. Martinez Jan. 1989 29 p Presented at the 30th Structures, Structural Dynamics and Materials Conference, Mobile, AL, 3 Apr. 1989
(Contract DE-AC04-76DP-00789)
(DE89-006327; SAND-88-2347C; CONF-8904112-3) Avail: NTIS HC A03/MF A01

System identification methods are analytical techniques for resolving the correct model form and parametric values. However, for system identification to become a practical tool for engineering analysis, the estimation techniques/codes must communicate with finite element software packages, without intensive analyst intervention and supervision. This paper presents a technique used to integrate commercial software packages for finite element modeling (MSC/NASTRAN), mathematical programming techniques (ADS), and general linear system analysis (PRO-MATLAB). The parameter estimation techniques and the software for controlling the overall system were programmed in PRO-MATLAB. Two examples of application of this software are presented. The examples consist of a truss structure in which the model form is well defined and an electronics package whose model form is ill-defined since it is difficult to model with finite elements. A comparison of the resulting updated models with the experimental data showed significant improvement. DOE

N89-23195# Lawrence Livermore National Lab., CA.
A NEW APPROACH TO SYSTEM TESTING
Nancy Storch 1 Jun. 1988 7 p Presented at the Structured Development Forum X, San Francisco, CA, 8 Aug. 1988
(Contract W-7405-eng-48)
(DE89-008660; UCRL-98873; CONF-880894-4) Avail: NTIS HC A02/MF A01

This paper describes actual experiences in designing system level test cases for a large on-line commercial transaction system which had just been implemented. Real world, less than perfect conditions existed. Although software engineering methods had been used during the development, up-to-date available documentation was limited as was the availability of knowledgeable persons. Even so, test cases were needed in a timely fashion. An approach was taken to identify a major section of the software as an object and then to develop a state model for it based on the implementation and availability of certain process information in the database such as: track flags, status, and time stamps. A flow graph was derived from the state transition diagram. Application of basis path testing to a simplified version of the flow graph lead to a meaningful set of test cases which when run found errors. Not only was this testing a success, but the creation of the state model provided valuable documentation for further understanding and maintenance of the software. DOE

N89-23196# Sandia National Labs., Albuquerque, NM.
TWO TIME STEPPING ALGORITHMS FOR PARALLEL COMPUTERS
David E. Womble 1989 5 p Presented at the 4th Hypercube, Concurrent Computers and Applications, Monterey, CA, 6 Mar. 1989
(Contract DE-AC04-76DP-00789)
(DE89-008679; SAND-89-0580C; CONF-890372-2) Avail: NTIS HC A02/MF A01

Time stepping algorithms are often used to solve parabolic and hyperbolic differential equations numerically. These algorithms are generally regarded as sequential in time; that is, the solution on a time level must be known before the computation of the solution at subsequent time levels can start. While this remains true in principle, we demonstrate that it is possible for processors to perform useful work on many time levels simultaneously. Specifically, it is possible for a processor assigned to a later time level to compute a very good initial guess for the solution based on approximations to the solutions on previous time levels, thus reducing the time required for solution. The reduction in the solution time can be measured as parallel speedup. We demonstrate two

parallel time stepping algorithms that can be used for both linear and nonlinear problems. We compare the two algorithms and discuss their performance in terms of parameters associated with classical time stepping algorithms. DOE

N89-23197# Oak Ridge National Lab., TN. Mathematical Sciences Section.
REDUCTION OF A GENERAL MATRIX TO TRIDIAGONAL FORM USING A HYPERCUBE MULTIPROCESSOR
G. A. Geist 1989 7 p Presented at the 4th Hybercube, Concurrent Computers and Applications, Monterey, CA, 6 Mar. 1989
(Contract DE-AC05-84OR-21400)
(DE89-006721; CONF-890372-3) Avail: NTIS HC A02/MF A01

Recently there has been a renewed interest in finding reliable methods of reducing general matrices to tridiagonal form. We have developed a serial reduction algorithm that appears to be very reliable in practice. In this paper we describe a parallel version of our algorithm, which has been implemented using a portable library developed at Oak Ridge National Laboratory (ORNL). The library allows the code to be portable across most commercial hypercubes. The algorithm was developed as one step in the process of finding eigenvalues of nonsymmetric matrices. Our original parallel eigenvalue routines reduced the matrix to Hessenberg form and then applied QR iteration, but their performance was disappointing. Our new parallel routines reduce the matrix to tridiagonal form and then apply LR iteration. Using an iPSC/2, we compare the performance of the new parallel routines with our previous parallel routines and show that the new routines are nearly an order of magnitude faster, allowing us to solve much larger problems than previously attempted. DOE

N89-23198# Los Alamos National Lab., NM. Theoretical Biology and Biophysics Theoretical Div.
SIMULATION AND ANALYSIS OF PHYSICAL MAPPING
Karl Sirotkin and John Joseph Loehr 1988 22 p Presented at the Interface Between Computational Science and Nucleic Acid Sequencing, Santa Fe, NM, 12-16 Dec. 1988
(Contract W-7405-eng-36)
(DE89-009399; LA-UR-89-817; CONF-881276-1) Avail: NTIS HC A03/MF A01

The current talk involves objects smaller than those that are macro-restriction mapped but larger than the bases that are sequenced. Specifically, we describe simulations of the alignment of recombinant lambdoid and cosmid clones by fingerprinting methods. The purpose of the simulation is to compare methods, as realistically as desired, while preparing for the analysis of actual physical mapping data. Furthermore, we will eventually begin to submit data to the Human Genome Information Resource (HGIR) to exercise its database. A simulation has advantages over a formal mathematical analysis. Not only can a simulation be as realistic as desired (for example by using actual sequences from GenBank(trademark)) but if desired properly, when finished much of the code could be used on actual data. Furthermore, a simulation can be designed to utilize any degree of parameterization, while analyses usually must make simplifying assumptions to minimize the number of parameters. For example, the way this simulation is designed one could, by simply adding a short module, mimic rearrangements that might occur during cloning in order to discover the effect that they would have on the contig generating algorithms and to learn how to recognize and deal with such rearrangements. This talk describes the structure and announces the availability of the code for the simulation modules. We tested the method for aligning clones based upon oligonucleotide hybridizing sites comparing its efficacy on actual human DNA sequences from GenBank to its efficacy on random, completely uncorrelated sequence. Surprisingly, its performance was about the same on both sequences. DOE

N89-23199# Sandia National Labs., Albuquerque, NM. Advanced Systems Development Dept.
ENGINEERING GRAPHICS SYSTEM (EGS) USER'S MANUAL
David E. Salguero 31 Jan. 1989 395 p
(Contract DE-AC04-76DP-00789)
(DE89-009668; SAND-89-0156) Avail: NTIS HC A17/MF A01

The Engineering Graphics System (EGS) is a computer program for use on Digital Equipment Corporation VAXstation color workstations. Its purpose is to manage and plot sets of engineering analysis data for use in reports and presentations. It is capable of producing nearly any type of x-y plot from a set of tabulated data. After the plot curves have been retrieved from the tabulated data, EGS can be used to interactively modify the appearance of the plot for use in a report or presentation. Modifications appear on the workstation display exactly as they appear on final hardcopy, which avoids costly iterations. Hardcopy plots can be made on two different black and white laser printers and on two different color printers, and plots can be converted for use by the Interleaf technical publishing software. GRA

N89-23200# Edgerton, Germeshausen and Grier, Inc., Idaho Falls, ID.
MIRAP, MICROCOMPUTER RELIABILITY ANALYSIS PROGRAM
J. N. T. Jehee Jan. 1989 33 p Sponsored in part by US Nuclear Regulatory Commission; and Netherlands Energy Research Foundation
(Contract DE-AC07-76ID-01570)
(DE89-009749; EGG-SSRE-8137) Avail: NTIS HC A03/MF A01

A program for a microcomputer is outlined that can determine minimal cut sets from a specified fault tree logic. The speed and memory limitations of the microcomputers on which the program is implemented (Atari ST and IBM) are addressed by reducing the fault tree's size and by storing the cut set data on disk. Extensive well proven fault tree restructuring techniques, such as the identification of sibling events and of independent gate events, reduces the fault tree's size but does not alter its logic. New methods are used for the Boolean reduction of the fault tree logic. Special criteria for combining events in the AND and OR logic avoid the creation of many subsuming cut sets which all would cancel out due to existing cut sets. DOE

N89-23201# Swedish Defence Research Establishment, Stockholm.
A STATISTICAL PACKAGE IN Ada
Nils Roman Nov. 1988 65 p In SWEDISH; ENGLISH summary
(FOA-C-20740-2.7; ISSN-0347-3694; ETN-89-94303) Avail: NTIS HC A04/MF A01

The construction and the function of an Ada statistical analysis system is described. Statistical formulas and algorithms used in the computing of distribution functions and percentiles are outlined. The most important parts of the system are three Ada packages which contain routines for the collection of data, for computing the confidence intervals and the most common distribution functions and percentiles. Its routines can be used as well in independent programs to perform statistical analysis on data stored on external files, and directly in large simulation programs with immediate need for statistical analysis. ESA

N89-23202 National Physical Lab., Teddington (England). Div. of Electrical Science.
REPORT ON ROUND ROBIN MEASUREMENTS OF 6 DIGITAL MAGNETIC TAPES
A. E. Drake Dec. 1988 9 p
(NPL-DES-91; ISSN-0143-7305; ETN-89-94341) Copyright Avail: National Physical Lab., Teddington, Middlesex, TW11 0LW, United Kingdom

Problems encountered in the calibration of 12.7 mm wide digital magnetic tape recorded at a packing density of 356 flux transitions/mm were highlighted by round robin measurements. The agreement between the measurements is between 6 and 10 percent. Reasons for this poor agreement are changes in the value of the NBS SRM 6250 tapes with usage, and the method of calibrating tape systems by setting the bias current at the value

of 1.4 l(f) for a particular NBS SRM tape. For making comparable measurements, the present method of using NBS SRM tapes to certify tertiary tapes is not sufficiently well defined in either ISO 1864 or in the application notes given on the certificate accompanying the SRM. A well defined method of test should be included in ISO 1864 and in the corresponding standard for 18 track digital tape cartridges. ESA

N89-23203# European Space Agency, Paris (France).
NEW STABLE, VECTORISABLE KALMAN FILTER ALGORITHMS BASED ON ORTHOGONAL TRANSFORMATIONS
Hans-Jurgen Hotop (Deutsche Forschungs- und Versuchsanstalt fuer Luft- und Raumfahrt, Brunswick, Germany, F.R.) Jan. 1989 215 p Transl. into ENGLISH of Neue Stabile und Vektorisierbare Kalmanfilter-Algorithms auf der Grundlage von Orthogonal-transformationen (Brunswick, Fed. Republic of Germany, DFVLR), Dec. 1987 210 p Original language document was announced as N88-23494
(ESA-TT-1108; DFVLR-FB-87-52; ETN-89-94444) Avail: NTIS HC A10/MF A01; original German version available from DFVLR, VB-PL-DO, Postfach 90 60 58, 5000 Cologne, Fed. Republic of Germany, DM 68

A stable Kalman filter algorithm based on a Givens transformation is developed theoretically together with three separate update formulations. The backward filter of Rauch-Tung-Striebel is reformulated. As an alternative orthogonal transformation the singular value decomposition is investigated. The advantage of the Kalman filter algorithm vs. conventional formulations is examined for the support of inertial navigation systems (simulation and flight data) on serial computers and a vector processor. ESA

N89-23204# Software Sciences Ltd., Farnborough (England).
HOOD TOOLSET DEVELOPMENT PROJECT: ECLIPSE/HOOD/REP, ISSUE 1.1 Final Report
A. E. Elliston and P. Flood Paris, France ESA 16 Nov. 1988 45 p Prepared in cooperation with Computer Resources International A/S, Denmark; CISI Ingenierie, Toulouse, France and MATRA Espace, Toulouse, France
(Contract ESTEC-7435/87/NL/MAC)
(ESA-CR(P)-2746; ETN-89-94467) Copyright Avail: NTIS HC A03/MF A01

A toolset was developed for the Hierarchical Object Oriented Design method (HOOD) for the architectural design phase of the ESA software engineering lifecycle, specifically for software to be developed in Ada. The main functions provided by the Toolset are: HOOD diagram editing, HOOD text editing, design checking, document production, Ada code production, management services, and Toolset maintenance facilities. The Toolset itself follows the object oriented approach. Hence, to perform an operation on an entity, the user first has to select the entity and then select the operation to be performed. The Toolset uses the multiwindow capabilities of the SUN3 workstation. Within each window user interaction with the tool is accomplished largely using the mouse. Keyboard input is also used for efficiency during text editing. ESA

N89-23205# San Diego State Univ., CA. Center for Research in Mathematics and Science Education.
STORY PROBLEM SOLVER: A SCHEMA-BASED SYSTEM OF INSTRUCTION Technical Report, 1 Sep. 1987 - 1 Jan. 1989
Sandra P. Marshall, Kathryn E. Barthuli, Margaret A. Brewer, and Frederic E. Rose 3 Feb. 1989 33 p
(Contract N00014-85-K-0661; RR04206)
(AD-A205594; CRMSE-RN-89-01) Avail: NTIS HC A03/MF A01 CSCL 05G

This report describes a computer-based instructional system, the Story Problem Solver (SPS). SPS provides students with instruction about the semantic structure of story problems. It was developed to test a specific schema theory of knowledge organization in long-term memory. For this reason SPS depends explicitly upon a theory of the relationship between the form of instruction and the memory structures that develop as a result. In this report we describe the schema theory underlying SPS, the design of SPS with respect to the theory, and the systems's operational features. The report concludes with a short description of ongoing extensions to the basic instructional program. GRA

62 COMPUTER SYSTEMS

Includes computer networks and special application computer systems.

N89-23206# Stanford Univ., CA. Knowledge Systems Lab.
EXPERT SYSTEMS ON MULTIPROCESSOR ARCHITECTURES, PHASE 1 Final Report, Mar. 1985 - Jul. 1987
Edward A. Feigenbaum and Robert S. Engelmore Aug. 1988 325 p
(Contract F30602-85-C-0012)
(AD-A204907; RADC-TR-88-187) Avail: NTIS HC A14/MF A01 CSCL 12E

The military has a demonstrated need for knowledge-based systems with significantly higher quantitative performance. The current hardware and software architectures for knowledge based systems cannot support such requirements. Based on near-term projections for integrated circuit technologies, it is clear that highly parallel multiprocessor computers consisting of 100s to 1000s of processors and realizing a variety of concurrent architectures can be built. The most promising approach for achieving orders of magnitude improvement in the quantitative performance of knowledge-based systems is by exploiting concurrency on multiprocessor systems. The major issue is whether such computer systems can be effectively used to enhance the performance of knowledge-based systems. Expert systems on Multiprocessor Architectures project is addressing the following questions: (1) Can multiprocessor computers be used to achieve significant execution speedup (two to three orders of magnitude) over serial machines for knowledge-based system applications. (2) What are the limiting factors in achieving speedup for such systems. (3) What are appropriate software models and methodologies for programming such systems. (4) What are appropriate hardware architectures for supporting such systems. Given the lack of any formal foundations for studying concurrent knowledge-based systems, the approach taken to answering these questions is empirical rather than theoretical. GRA

N89-23207# Maryland Univ., College Park. Dept. of Computer Science.
PARALLEL PROBLEM SOLVING SYSTEM, PRISM (PARALLEL INFERENCE SYSTEM) Final Report, Nov. 1986 - Feb. 1988
Jack Minker 19 Apr. 1988 12 p
(Grant AF-AFOSR-0303-82; AF Proj. 2304)
(AD-A204915; AFOSR-89-0113TR) Avail: NTIS HC A03/MF A01 CSCL 12G

A parallel problem solving problem solving system, PRISM (Parallel Inference System), that was implemented on the VAX/11-780, the PYRAMID and SUN machines, was ported successfully to McMOB and then to the BBN Butterfly parallel architecture. The McMOB architecture is essentially the ZMOB architecture with 16 Motorola 68000 processors, upgrading the Z80A microprocessors, interconnected in a ring structure. Experimental testing of PRISM on McMOB was undertaken. In addition, several enhancements were made to PRISM to permit experimental analyses to be made, and to incorporate additional features to take full advantage of parallelism in a problem solving environment. The tracing and statistical gathering packages were extended. An ability to display AND-parallelism was added to the trace program which displays the execution of a program on the parallel machines. Heuristic techniques were developed to determine which information to display to a user. The system software for ZMOB/McMOB is now robust and considered completed. This has allowed us to re-emphasize our studies on parallel software. A new formalism for slicing/splicing was developed which eliminates much of the run-time overhead of the

technique, allowing for the development of a splicing compiler. Work has also focused on the development of debugging tools for parallel software and the integration of artificial intelligence techniques into debugging software. GRA

N89-23208# Sandia National Labs., Albuquerque, NM.
FACTORING VERY LARGE NUMBERS USING A MASSIVELY PARALLEL COMPUTER
Diane B. Holdridge and James A. Davis 1989 3 p Presented at the 4th Hypercube, Concurrent Computers and Applications, Monterey, CA, 6 Mar. 1989
(Contract DE-AC04-76DP-00789)
(DE89-008198; SAND-89-0581C; CONF-890372-1) Avail: NTIS HC A02/MF A01

A good many words have been spoken and written (some by the present authors) about factoring very large numbers. Therefore, the thrust of this paper is a discussion of how the quadratic sieve algorithm has been adapted to work on a 1024-processor hypercube at Sandia National Laboratories. A brief description of the hypercube, an NCUBE/ten, its idiosyncrasies and its power, as well as some comparisons of timings between numbers factored on the CRAY and on the hypercube, are included. DOE

N89-23126# University of Southern California, Los Angeles. Inst. for Robotics and Intelligent Systems.
PARALLEL ARCHITECTURES FOR IMAGE PROCESSING AND VISION
V. K. Prasanna-Kumar and Dionisios Reisis *In* Science Applications International Corp., Proceedings: Image Understanding Workshop, Volume 2 Apr. 1988 p 609-619 (For primary document see N89-23115 16-61)
(Contract F33615-87-C-1436; NSF IRI-87-10863; DARPA Order 3119)
Avail: NTIS HC A99/MF E03 CSCL 09B

N89-23127# Rochester Univ., NY. Dept. of Computer Science.
PARALLEL HARDWARE FOR CONSTRAINT SATISFACTION
Michael J. Swain and Paul R. Cooper *In* Science Applications International Corp., Proceedings: Image Understanding Workshop, Volume 2 Apr. 1988 p 620-624 Sponsored in part by NSERC, Canada (For primary document see N89-23115 16-61)
(Contract F30602-85-C-0008)
Avail: NTIS HC A99/MF E03 CSCL 09B

N89-23128# Carnegie-Mellon Univ., Pittsburgh, PA. Dept. of Computer Science.
SCAN LINE ARRAY PROCESSORS: WORK IN PROGRESS
Allan L. Fisher, Peter T. Highnam, and Todd E. Rockoff *In* Science Applications International Corp., Proceedings: Image Understanding Workshop, Volume 2 Apr. 1988 p 625-633 (For primary document see N89-23115 16-61)
(Contract F33615-87-K-1499; ARPA Order 4976)
Avail: NTIS HC A99/MF E03 CSCL 09B

63 CYBERNETICS

Includes feedback and control theory, artificial intelligence, robotics and expert systems.

For related information see also *54 Man/System Technology and Life Support.*

N89-23209*# Charles River Analytics, Inc., Cambridge, MA.
EXPERT SYSTEMS FOR REAL-TIME MONITORING AND FAULT DIAGNOSIS Final Report
S. J. Edwards and A. K. Caglayan Apr. 1989 116 p
(Contract NAS2-12725)
(NASA-CR-179441; NAS 1.26:179441; H-1540) Avail: NTIS HC A06/MF A01 CSCL 09B

Methods for building real-time onboard expert systems were investigated, and the use of expert systems technology was demonstrated in improving the performance of current real-time onboard monitoring and fault diagnosis applications. The potential applications of the proposed research include an expert system environment allowing the integration of expert systems into conventional time-critical application solutions, a grammar for describing the discrete event behavior of monitoring and fault diagnosis systems, and their applications to new real-time hardware fault diagnosis and monitoring systems for aircraft. Author

N89-23210# Lawrence Livermore National Lab., CA.
SYSTOLIC IMPLEMENTATION OF NEURAL NETWORKS
A. J. DeGroot and S. R. Parker Jan. 1989 10 p Presented at the SPIE Conference on Optics, Electro-optics and Laser Applications in Science and Engineering: OE/LASE '89, Los Angeles, CA, 15 Jan. 1989
(Contract W-7405-eng-48)
(DE89-008031; UCRL-100353; CONF-890145-19) Avail: NTIS HC A02/MF A01

The backpropagation algorithm for error gradient calculations in multilayer, feed-forward neural networks is derived in matrix form involving inner and outer products. It is demonstrated that these calculations can be carried out efficiently using systolic processing techniques, particularly using the SPRINT, a 64-element systolic processor developed at Lawrence Livermore National Laboratory. This machine contains one million synapses, and forward-propagates 12 million connections per second, using 100 watts of power. When executing the algorithm, each SPRINT processor performs useful work 97 percent of the time. The theory and applications are confirmed by some nontrivial examples involving seismic signal recognition. DOE

N89-23211# Lawrence Livermore National Lab., CA. Dept. of Electrical Engineering.
DESIGN OF A NEW HIGH PRECISION COMPUTER NUMERICAL CONTROL
Douglas J. Sweeney and George F. Weinert 23 Jun. 1988 6 p Presented at the 32nd International Technical Symposium on Optical and Opto-electronic Applied Science and Engineering, San Diego, CA, 14-19 Aug. 1988
(Contract W-7405-eng-48)
(DE89-008032; UCRL-98957; CONF-880887-33) Avail: NTIS HC A02/MF A01

The purpose of this project is to produce a generic high precision computer numerical controller (CNC) for use on microinch- and sub-microinch-resolution machine tools at the Lawrence Livermore National Laboratory. In order to fully utilize the potential of these machine tools, the CNC must include the ability to use multiple feedback sensors on each machine axis, incorporate corrections for quasistatic geometric errors (such as straightness, and squareness), be able to function over a relatively large range of motion (in excess of 60 inches per axis), and be able to produce motion updates at a rate sufficient to take advantage of the high bandwidth of the servo systems. At present, no commercially available CNC can presently meet all of the resolution, feed rate, and length of travel requirements of these machines. In order to minimize the complexity of the system, and thereby increase its reliability and maintainability, the programming was done in a high level language. The number of processors was kept as small as possible while still maintaining the performance requirements. We also used commercially available hardware in preference to building, in order to increase both reliability and maintainability. Special emphasis was given to making the CNC's operator interface as friendly as possible. We have completed a prototype control. We plan to install and test it in 1988. DOE

N89-23212# Swedish Defence Research Establishment, Linkoeping. Dept. of Information Technology.
SOME METHODS FOR UNCERTAIN REASONING
Nils Olander May 1988 58 p In SWEDISH; ENGLISH summary
(FOA-C-30492-3.3; ISSN-0347-3708; ETN-89-94125) Avail: NTIS HC A04/MF A01; Swedish Defence Research Establishment, P.O. Box 1165, S-581 11 Linkoeping, Sweden, 50 Swedish crowns

Computer programs for the analysis and interpretation of sensory data, including methods for uncertain reasoning are

discussed. Bayes' method, the Dempster-Shafer method, certainty factor method, and fuzzy reasoning are considered. There is no generally accepted method. No suggested method can handle spatial and temporal data at the same time. ESA

N89-23213# Swedish Defence Research Establishment, Linkoeping. Dept. of Information Technology.
FUSION OF MULTISENSOR DATA: A SUMMARY OF THE JASMIN PROJECT
Nils Olander and Bengt Rosen Jun. 1988 23 p In SWEDEN; ENGLISH summary
(FOA-C-30498-3.3; ISSN-0347-3708; ETN-89-94126) Avail: NTIS HC A03/MF A01; Swedish Defence Research Establishment, P.O. Box 1165, S-581 11 Linkoeping, Sweden, 50 Swedish crowns

The Jasmin project studied how knowledge based techniques could be used to combine symbolic data from different sensors. The application in mind concerned reconnaissance data from an aircraft. The system can also deal with geographical items. To keep the effectiveness of the sensors, various types of automation shall be necessary to interpret the data. ESA

N89-23214# Oxford Univ. (England). Dept. of Engineering Science.
A PSEUDO SINGULAR VALUE DECOMPOSITION AND INNER FUNCTIONS IN SUPER OPTIMAL CONTROL
M. C. Tsai, D.-W. Gu, I. Postlethwaite, and B. D. O. Anderson 1988 23 p
(OUEL-1738/88; ETN-89-94215) Avail: NTIS HC A03/MF A01

A pseudo singular value decomposition (PSVD) and inner functions which arise in super optimal H sup inf design are studied. Uniqueness properties of the PSVD are derived, and structural inner functions are defined in order to characterize particular PSVDs. Two examples are given to illustrate the properties of a structural inner function and the different PSVDs. ESA

N89-23215# Technische Hogeschool Twente, Enschede (Netherlands). Faculty of Applied Mathematics.
ON THE STABILIZATION OF BILINEAR SYSTEMS VIA CONSTANT FEEDBACK
R. Luesink and H. Nijmeijer Apr. 1988 26 p
(MEMO-706; ISSN-0921-1969; ETN-89-94258) Avail: NTIS HC A03/MF A01

The problem of stabilization of a bilinear system via a constant feedback is studied. Using the idea of simultaneous triangularization of the matrices involved, easy checkable conditions for the solvability of this question are obtained. Algorithms for checking these conditions are given and illustrated. ESA

N89-23216# Technische Hogeschool Twente, Enschede (Netherlands). Faculty of Applied Mathematics.
ADAPTIVE LQ CONTROL: CONFLICT BETWEEN IDENTIFICATION AND CONTROL
J. W. Polderman Jun. 1988 18 p
(MEMO-718; ISSN-0921-1969; ETN-89-94264) Avail: NTIS HC A03/MF A01

One of the fundamental limitations of indirect adaptive control based on the minimization of a quadratic cost criterion and the certainty equivalence principle is considered. It is shown that the iteraction between (closed-loop) identification and optimal control is conflictual in the sense that almost all possible limits of the sequence of parameter estimates induce suboptimal behavior of the adaptively controlled system. ESA

N89-23217# Technische Hogeschool Twente, Enschede (Netherlands). Faculty of Applied Mathematics.
THE LOCAL DISTURBANCE DECOUPLING PROBLEM WITH STABILITY FOR NONLINEAR SYSTEMS
L. L. M. vanderWagen and H. Nijmeijer Jun. 1988 18 p
(MEMO-721; ISSN-0921-1969; ETN-89-94266) Avail: NTIS HC A03/MF A01

The Disturbance Decoupling Problem with Stability (DDPS) for nonlinear systems is considered. The DDPS is the problem of finding a feedback such that after applying this feedback the disturbances do not influence the output anymore and x = 0 is an asymptotically stable equilibrium point of the feedback system. Under fairly mild assumptions it is possible to define a distribution Delta s sup asterisk which is the nonlinear analog of the linear V s sup asterisk, the largest stabilizable controlled invariant subspace in the kernel of the output mapping, and to prove that the DDPS is locally solvable if and only if the disturbance vector fields are contained in Delta s sup asterisk. ESA

N89-23218# Technische Hogeschool Twente, Enschede (Netherlands). Faculty of Applied Mathematics.
OPTIMAL PROCESSES DESCRIBED BY A PARABOLIC DIFFERENTIAL EQUATION WITH CONTROL IN THE COEFFICIENTS, PART 3
E. A. vanMarle and R. Nottrot Jul. 1988 35 p
(MEMO-725-Pt-3; ISSN-0921-1969; ETN-89-94270) Avail: NTIS HC A03/MF A01

By extending a distillation column in a fictive way and continuizing the material-balances a partial differential equation of parabolic type is found. By introducing an integral criterion the dynamics of the column can be considered as an optimal process. Necessary conditions are derived. Special attention is given to the effect of a variation of the control variables to the solution of the parabolic equation. ESA

N89-23219# Technische Hogeschool Twente, Enschede (Netherlands). Faculty of Applied Mathematics.
ON THE USE OF STABLE DISTRIBUTIONS IN DESIGN PROGRAMS
L. L. M. vanderWegen Sep. 1988 18 p
(MEMO-736; ISSN-0169-2690; ETN-89-94280) Avail: NTIS HC A03/MF A01

The role of stable distributions in nonlinear design problems is pointed out. Stable distributions are controlled invariant distributions for which the dynamics restricted to the integral manifold through an equilibrium is asymptotically stable. These distributions can be calculated by prolongating a certain stable manifold through the equilibrium. The nonlinear analog Delta sub s sup asterisk of V sub s sup asterisk, the maximal stabilizable controlled invariant subspace in the kernel of the output mapping, is such a stable distribution. It is proved that (under extra conditions) the disturbance decoupling problem with Stability is (locally) solvable if and only if the disturbance vectorfields are contained in Delta sub s sup asterisk. An important role in the noninteracting control problem with stability is played by the radical. It is proved that, if this problem is solvable, then the radical is a stable distribution. ESA

N89-23220# Technische Hogeschool Twente, Enschede (Netherlands). Faculty of Applied Mathematics.
ROBUST STABILIZATION OF AN INVERTED DOUBLE PENDULUM SYSTEM VIA A POLYNOMIAL APPROACH TO H(INFINITY) OPTIMAL CONTROL
K. G. Woodgate Oct. 1988 88 p
(Grant ST2J-0101-2-NL(EDB))
(MEMO-742; ISSN-0169-2690; ETN-89-94285) Avail: NTIS HC A05/MF A01

It is shown how the polynomial approach to H inf to optimal control due to Kwakernaak may be used to design a linear discrete-time feedback controller that robustly stabilizes a linear discrete-time model of an inverted double pendulum. This is done by first transforming the discrete-time problem into continuous-time and thereafter formulating and solving a continuous-time mixed sensitivity problem. Attention is paid to the choice of weighting functions that arise in the problem formulation. Designs for a simpler, related system, the inverted single pendulum, are presented as an introduction to the final design. Results concerning the numerical problem which ultimately has to be solved are also presented. ESA

N89-23221# Loughborough Univ. of Technology (England). Dept. of Mathematics.
SOME LOCAL RESULTS FOR LINEAR SYSTEMS AND IMPLICATIONS FOR STATE VARIABLE FEEDBACK
A. C. Pugh, A. Kafai, and G. E. Hayton (Hull Univ., England) Aug. 1987 17 p Previously announced in IAA as A89-23507 (Maths-Res-202; ETN-89-94321) Avail: NTIS HC A03/MF A01

A result concerning the invariance of the infinite zero structure of a general transfer function matrix under state feedback is obtained. The approach indicates the need for a localized theory of linear systems and basic results in this area are derived. It is shown that linear state feedback should leave invariant the infinite pole structure of the open-loop system. This phenomenon can to some extent be explained by the fact that the state is determined from entirely finite frequency considerations and that the feeding back of such information can only reasonably be expected to alter that part of the system structure to which it relates. In such circumstances the infinite frequency structure could well be imagined to be immune. ESA

N89-23222# Centre National de la Recherche Scientifique, Toulouse (France). Lab. d'Automatique et d'Analyse des Systemes.
AUTOMATIC GENERATION OF NONCOLLIDING TRAJECTORIES AND MANIPULATION TASK PLANNING IN ROBOTICS Ph.D. Thesis - Toulouse Univ. [GENERATION AUTOMATIQUE DE TRAJECTOIRES SANS COLLISION ET PLANIFICATION DE TACHES DE MANIPULATION EN ROBOTIQUE]
Thierry Simeon 1989 139 p In FRENCH; ENGLISH summary (LAAS-89-002; ETN-89-94370) Avail: NTIS HC A07/MF A01

A set of tools implementing a robotics collision avoiding system is presented. The system is based on a representation of free regions of the configuration spaces of the robotic system. The obstacle avoidance algorithm is based on computation of distance between pairs of primitives and transformation in discrete configuration parameters. The approach allows an integration of geometric reasoning and artificial intelligence to solve the manipulation task planning problem. ESA

N89-23223# Aerospatiale, Paris (France). Div. Engins Tactiques.
CONTRIBUTIONS OF EXPERT SYSTEMS TO LOGISTICS [POINT DE VUE SUR LA CONTRIBUTION DES SYSTEMES EXPERTS A LA LOGISTIQUE]
Serge Dupuy 1988 5 p In FRENCH
(Rept-882-320-101; Note-E/ES4-21-387; ETN-89-94479) Avail: NTIS HC A02/MF A01

Methodological comments are presented including the need to associate user, expert, and engineer, the function of the expert in modelling incertitude, the contributions of knowledge engineering, and the validation and maintenance procedure which are necessry to any artificial intelligence development. ESA

N89-23100# Advanced Decision Systems, Mountain View, CA.
QUALITATIVE NAVIGATION 2
Tod S. Levitt, Daryl T. Lawton, David M. Chelberg, Kerry V. Koitzsch, and John W. Dye *In* Science Applications International Corp., Proceedings: Image Understanding Workshop, Volume 1 Apr. 1988 p 319-326 (For primary document see N89-23074 16-61)
Avail: NTIS HC A22/MF A01 CSCL 09B

N89-23106# Massachusetts Inst. of Tech., Cambridge. Artificial Intelligence Lab.
SELF CALIBRATION OF MOTION AND STEREO VISION FOR MOBILE ROBOT NAVIGATION
Rodney A. Brooks, Anita M. Flynn, and Thomas Marill *In* Science Applications International Corp., Proceedings: Image Understanding Workshop, Volume 1 Apr. 1988 p 398-410 (For primary document see N89-23074 16-61)
Avail: NTIS HC A22/MF A01 CSCL 09B

N89-23107# Hughes Research Labs., Calabasas, CA. Artificial Intelligence Center.
AUTONOMOUS NAVIGATION IN CROSS-COUNTRY TERRAIN
David M. Keirsey, David W. Payton, and J. Kenneth Rosenblatt *In* Science Applications International Corp., Proceedings: Image Understanding Workshop, Volume 1 Apr. 1988 p 411-416 (For primary document see N89-23074 16-61)
(Contract DACA76-85-C-0017)
Avail: NTIS HC A22/MF A01 CSCL 09B

N89-23108# University of Southern California, Los Angeles. Inst. for Robotics and Intelligent Systems.
INTEGRATION EFFORT IN KNOWLEDGE-BASED VISION TECHNIQUES FOR THE AUTONOMOUS LAND VEHICLE PROGRAM
Keith Price and Igor Pavlin *In* Science Applications International Corp., Proceedings: Image Understanding Workshop, Volume 1 Apr. 1988 p 417-422 (For primary document see N89-23074 16-61)
(Contract DACA76-85-C-0009)
Avail: NTIS HC A22/MF A01 CSCL 09B

N89-23112# Stanford Univ., CA. Robotics Lab.
GENERIC MODELS FOR ROBOT NAVIGATION
David J. Kriegman, Thomas O. Binford, and Thilaka S. Sumanaweera *In* Science Applications International Corp., Proceedings: Image Understanding Workshop, Volume 1 Apr. 1988 p 453-460 Sponsored in part by the Fannie and John Hertz Foundation (For primary document see N89-23074 16-61)
(Contract F33615-85-C-5106)
Avail: NTIS HC A22/MF A01 CSCL 09B

N89-23120# Maryland Univ., College Park. Computer Vision Lab.
USING FLOW FIELD DIVERGENCE FOR OBSTACLE AVOIDANCE IN VISUAL NAVIGATION
Randal C. Nelson and John Aloimonos *In* Science Applications International Corp., Proceedings: Image Understanding Workshop, Volume 2 Apr. 1988 p 548-567 Sponsored in part by DARPA, Washington, DC (For primary document see N89-23115 16-61)
Avail: NTIS HC A99/MF E03 CSCL 09B

N89-23121# Hughes Research Labs., Calabasas, CA. Artificial Intelligence Center.
AN OPERATIONAL PERCEPTION SYSTEM FOR CROSS-COUNTRY NAVIGATION
Michael J. Daily, John G. Harris, and Kurt Reiser *In* Science Applications International Corp., Proceedings: Image Understanding Workshop, Volume 2 Apr. 1988 p 568-575 (For primary document see N89-23115 16-61)
(Contract DACA87-85-C-0007)
Avail: NTIS HC A99/MF E03 CSCL 09B

N89-23123# Columbia Univ., New York, NY. Dept. of Computer Science.
ON THE COMPUTATIONAL COMPLEXITY OF LINEAR NAVIGATION
John R. Kender and Avraham Leff *In* Science Applications International Corp., Proceedings: Image Understanding Workshop, Volume 2 Apr. 1988 p 583-592 (For primary document see N89-23115 16-61)
(Contracts DACA76-86-C-0024; N00039-84-C-0165)
Avail: NTIS HC A99/MF E03 CSCL 09B

N89-23124# Carnegie-Mellon Univ., Pittsburgh, PA. Robotics Inst.
THREE-DIMENSIONAL VISION FOR OUTDOOR NAVIGATION BY AN AUTONOMOUS VEHICLE
Martial Hebert and Takeo Kanade *In* Science Applications International Corp., Proceedings: Image Understanding Workshop, Volume 2 Apr. 1988 p 593-601 (For primary document see N89-23115 16-61)

(Contracts DACA76-85-C-0003; F33615-87-C-1499; NSF DCR-86-04199)
Avail: NTIS HC A99/MF E03 CSCL 09B

N89-23146# Stanford Univ., CA. Robotics Lab.
STRUCTURAL CORRESPONDENCE IN STEREO VISION
Hong Seh Lim and Thomas O. Binford *In* Science Applications International Corp., Proceedings: Image Understanding Workshop, Volume 2 Apr. 1988 p 794-808 (For primary document see N89-23115 16-61)
(Contract N00039-84-C-0211)
Avail: NTIS HC A99/MF E03 CSCL 09B

N89-23147# Stanford Univ., CA. Robotics Lab.
CURVED SURFACE RECONSTRUCTION USING STEREO CORRESPONDENCE
Hong Seh Lim and Thomas O. Binford *In* Science Applications International Corp., Proceedings: Image Understanding Workshop, Volume 2 Apr. 1988 p 809-819 (For primary document see N89-23115 16-61)
(Contract N00039-84-C-0211)
Avail: NTIS HC A99/MF E03 CSCL 09B

N89-23150# Carnegie-Mellon Univ., Pittsburgh, PA. Dept. of Computer Science.
IMAGE SEGMENTATION AND REFLECTION ANALYSIS THROUGH COLOR
Gudrun J. Klinker, Steven A. Shafer, and Takeo Kanade *In* Science Applications International Corp., Proceedings: Image Understanding Workshop, Volume 2 Apr. 1988 p 838-853 (For primary document see N89-23115 16-61)
(Contract F33615-84-K-1520; NSF DCR-84-19990; ARPA Order 4976)
Avail: NTIS HC A99/MF E03 CSCL 09B

N89-23151# Stanford Univ., CA. Robotics Lab.
A COLOR METRIC FOR COMPUTER VISION
Glenn Healey and Thomas O. Binford *In* Science Applications International Corp., Proceedings: Image Understanding Workshop, Volume 2 Apr. 1988 p 854-861 (For primary document see N89-23115 16-61)
(Contract F33615-85-C-5106)
Avail: NTIS HC A99/MF E03 CSCL 09B

N89-23152# Maryland Univ., College Park. Computer Vision Lab.
COMBINING INFORMATION IN LOW-LEVEL VISION
John Aloimonos and Anup Basu *In* Science Applications International Corp., Proceedings: Image Understanding Workshop, Volume 2 Apr. 1988 p 862-906 (For primary document see N89-23115 16-61)
(Contract DAAB07-86-K-F073)
Avail: NTIS HC A99/MF E03 CSCL 09B

N89-23153# Massachusetts Univ., Amherst. Computer Vision Research Lab.
COMPUTATION OF MOTION IN DEPTH PARAMETERS: A FIRST STEP IN STEREOSCOPIC MOTION INTERPRETATION
Poornima Balasubramanyam and M. A. Snyder *In* Science Applications International Corp., Proceedings: Image Understanding Workshop, Volume 2 Apr. 1988 p 907-920 (For primary document see N89-23115 16-61)
Avail: NTIS HC A99/MF E03 CSCL 09B

N89-23154# Maryland Univ., College Park. Computer Vision Lab.
IS CORRESPONDENCE NECESSARY FOR THE PERCEPTION OF STRUCTURE FROM MOTION
Eiki Ito and John Aloimonos *In* Science Applications International Corp., Proceedings: Image Understanding Workshop, Volume 2 Apr. 1988 p 921-929 (For primary document see N89-23115 16-61)
(Contract DAAB07-86-K-F073)
Avail: NTIS HC A99/MF E03 CSCL 09B

N89-23155# Massachusetts Univ., Amherst. Dept. of Computer and Information Science.
MOTION FROM A SEQUENCE OF IMAGES
Igor Pavlin *In* Science Applications International Corp., Proceedings: Image Understanding Workshop, Volume 2 Apr. 1988 p 930-937 Previously announced in IAA as A89-11835 (For primary document see N89-23115 16-61)
(Contracts N00014-82-K-0464; DACA76-85-C-0008)
Avail: NTIS HC A99/MF E03 CSCL 09B

N89-23156# Rochester Univ., NY. Dept. of Computer Science.
RECOGNIZING ANIMAL MOTION
Nigel H. Goddard *In* Science Applications International Corp., Proceedings: Image Understanding Workshop, Volume 2 Apr. 1988 p 938-944 Prepared in cooperation with Hughes Research Labs., Calabasas, CA (For primary document see N89-23115 16-61)
Avail: NTIS HC A99/MF E03 CSCL 09B

N89-23158# Columbia Univ., New York, NY. Dept. of Computer Science.
A REAL TIME HIERARCHICAL MODEL FOR OPTIC FLOW DETERMINATION VIA SPATIOTEMPORAL FREQUENCY CHANNELS
Ajit Singh and Peter K. Allen *In* Science Applications International Corp., Proceedings: Image Understanding Workshop, Volume 2 Apr. 1988 p 961-969 (For primary document see N89-23115 16-61)
Avail: NTIS HC A99/MF E03 CSCL 09B

N89-23159# Massachusetts Univ., Amherst. Dept. of Computer and Information Science.
TRANSLATING OPTICAL FLOW INTO TOKEN MATCHES
Lance R. Williams and Allen R. Hanson *In* Science Applications International Corp., Proceedings: Image Understanding Workshop, Volume 2 Apr. 1988 p 970-980 (For primary document see N89-23115 16-61)
(Contracts F30602-87-C-0140; DMA800-85-C-0012)
Avail: NTIS HC A99/MF E03 CSCL 09B

N89-23161# SRI International Corp., Menlo Park, CA. Artificial Intelligence Center.
EXTRACTING GENERIC SHAPES USING MODEL-DRIVEN OPTIMIZATION
Pascal Fua and Andrew J. Hanson *In* Science Applications International Corp., Proceedings: Image Understanding Workshop, Volume 2 Apr. 1988 p 994-1004 (For primary document see N89-23115 16-61)
(Contract MDA903-86-C-0084)
Avail: NTIS HC A99/MF E03 CSCL 09B

N89-23162# Stanford Univ., CA. Robotics Lab.
TEXTURE MODELS AND IMAGE MEASURES FOR SEGMENTATION
Richard Vistnes *In* Science Applications International Corp., Proceedings: Image Understanding Workshop, Volume 2 Apr. 1988 p 1005-1015 (For primary document see N89-23115 16-61)
Avail: NTIS HC A99/MF E03 CSCL 09B

64 NUMERICAL ANALYSIS

Includes iteration, difference equations, and numerical approximation.

N89-23224# Air Force Inst. of Tech., Wright-Patterson AFB, OH. School of Engineering.
NONLINEAR OPTIMIZATION INVOLVING POLYNOMIAL MATRICES AND THEIR GENERALIZED INVERSES M.S. Thesis
Raymond R. Hill, Jr. Dec. 1988 120 p
(AD-A202620; AD-E900870; AFIT/GOR/MA/88D-4) Avail: NTIS HC A06/MF A01 CSCL 12A

This thesis examines the applications of the generalized inverse

of a matrix. In particular, use is made of the generalized inverse of a matrix containing variable elements. Such matrices are referred to as multiparameter, polynomial, or variable element matrices. The notion of a generalized inverse in fact generalizes the concept of a matrix inverse. A matrix inverse exists only for square, non-singular matrices. The generalized inverse extends this notion to non-square, singular matrices. The classical matrix inverse, when it exists, is a unique element of the set of generalized inverses for the matrix. Many modern problems involve multiparameter matrices. The ability to obtain inverses for such matrices, both singular and non-singular, is a necessity in solving these problems. This thesis consolidates the theory of generalized inverses, including extensions to multiparameter matrices. An in depth discussion is made of the ST method for computing all generalized inverses of a matrix as well as the strong interface between the ST method and the Fundamental Theorem of Linear Algebra. Finally selected application problems are solved demonstrating the utility of the generalized inverse in such problems. GRA

N89-23225# Wisconsin Univ., Madison. Center for Mathematical Sciences.
ON POLYNOMIAL IDEALS OF FINITE CODIMENSION WITH APPLICATIONS TO BOX SPLINE THEORY Technical Summary Report
Carl DeBoor and Amos Ron Dec. 1988 29 p
(Contract DAAL03-87-K-0030; NSF DMS-87-01275)
(AD-A204095; CMS-TSR-89-21) Avail: NTIS HC A03/MF A01 CSCL 12A

This document investigates the relations between an ideal I of finite codimension in the space pi of multivariate polynomials and various ideals which are generated by lower order perturbations of the generators of I. Special emphasis is given to the question of the codimension of I and its perturbed counterpart and to the local approximation order of their kernels. The discussion, stimulated by certain results in approximation theory, allows us to provide a simple analysis of the polynomial and exponential spaces associated with box splines. This includes their structure, dimension, local approximation order and an algorithm for their construction. The resulting theory is extended to subspaces of the above exponential/polynomial spaces. GRA

N89-23226# Wisconsin Univ., Madison. Center for Mathematical Sciences.
ON MULTIVARIATE POLYNOMIAL INTERPOLATION Technical Summary Report
Carl DeBoor and Amos Ron Nov. 1988 16 p
(Contract DAAL03-87-K-0030; NSF DMS-87-01275)
(AD-A204099; CMS-TSR-89-17) Avail: NTIS HC A03/MF A01 CSCL 12A

This document provides a map of a finite subset Theta onto a polynomial space pi sub theta from which interpolation to arbitrary data given at the points in theta is possible and uniquely so. Among all polynomial spaces Q from which interpolation at theta is uniquely possible, the documented pi sub theta is of smallest degree. It is also D and scale-invariant. This mapping is monotone, thus providing a Newton form for the resulting interpolant. This mapping is also continuous within reason, allowing interpretation of certain cases of coalescence as Hermite interpolation. In fact, this mapping can be extended to the case where, with each theta within set theta, there is associated a polynomical space P sub theta, and, for given smooth f, a polynomial q in the group of polynomial spaces is sought for which p(D)(f-q)(theta) = 0, for all p elements of P sub theta, and theta an element of set theta. We obtain pi sub theta as the scaled limit at the origin least term (exp sub theta) of the exponential space exp sub theta with frequencies theta, and base our results on a study of the map H onto the least term H defined on subspaces H of the space of functions analytic at the origin. This study also allows determining of the local approximation order from such H and provides an algorithm for the construction of the least term H from any basis for H. GRA

N89-23227# Gosudarstvennyi Komitet po Ispolzovaniyu Atomnoi Energii, Obninsk (USSR). Fiziko-Ehnergeticheskij Inst.
ON HAUSDORFF DIMENSION OF INVARIANT MANIFOLDS OF INFINITE-DIMENSIONAL DYNAMIC SYSTEMS
D. A. Kamaev 1988 4 p In RUSSIAN
(DE88-705628; FEI-1906) Avail: NTIS (US Sales Only) HC A02/MF A01

Dependence of Hausdorff dimension of limited invariant manifolds of infinite-dimensional dynamic systems on the choice of phase space is studied. DOE

N89-23228# Gosudarstvennyi Komitet po Ispolzovaniyu Atomnoi Energii, Obninsk (USSR). Fiziko-Ehnergeticheskij Inst.
ON THE AVERAGING METHOD FOR QUASILINEAR HYPERBOLIC EQUATIONS
D. A. Kamaev 1988 11 p In RUSSIAN; In RUSSIAN
(DE88-705629; FEI-1908) Avail: NTIS (US Sales Only) HC A03/MF A01

A study was made on the averaging method, applied to hyperbolic equations in the Hilbert space. The selected class of equations includes as particular case the system of one-dimensional quasilinear equations with partial derivatives of hyperbolic type with the right part being periodical with respect to time variable. The version of averaging method, not considered earlier in publications, has been substantiated. The analog of the first main N. N. Bogolyubov theorem about the approximate solution in finite, but as much as is desired long time interval, has been proved. The obtained statements are applied to investigation of induced vibrations of elastic string in nonlinear force field. DOE

N89-23229# International Centre for Theoretical Physics, Trieste (Italy).
COHOMOLOGY THEORY AND DEFORMATIONS OF Z SUB 2-GRADED LIE ALGEBRAS
K. C. Tripathy and M. K. Patra (Delhi Univ., India) Sep. 1988 19 p Submitted for publication
(DE88-705694; IC-88/314) Avail: NTIS (US Sales Only) HC A03/MF A01

The algebraic cohomology and the spectral sequences for a Z sub 2-graded Lie algebra are briefly reviewed. The reducibility property of a strongly semisimple Lie superalgebra is established. The role of second and third cohomologies in the deformation of a Lie superalgebra is discussed. Using spectral sequences, the second cohomology of full BRS algebra is shown to be F sup 1 and the third cohomology being trivial implying that osp(1,2) is the only graded Lie algebra obtained by deformation of the full BRS algebra. DOE

N89-23230# Sandia National Labs., Albuquerque, NM. Applied Mechanics Div.
NONLINEAR FINITE ELEMENT SIMULATION OF THE LARGE ANGLE MOTION OF FLEXIBLE BODIES
Lee D. Peterson 1989 32 p Presented at the 30th Structures, Structural Dynamics and Materials Conference, Mobile, AL, 3 Apr. 1989
(Contract DE-AC04-76DP-00789)
(DE89-006505; SAND-88-2366C; CONF-8904112-2; AIAA-89-1201) Avail: NTIS HC A03/MF A01

Finite element simulations of the geometrically nonlinear, large angle motion of flexible bodies are presented and discussed. The simulations use ABAQUS, a commercially available nonlinear, large strain-displacement structural finite element program. To evaluate the capabilities of ABAQUS, simulation results for three examples are presented: a large angle maneuver of a cantilevered beam, the nutation of a rotating free-free beam observed from a rotating frame, and the spin-up of a cantilevered beam from rest. The spin-up problem is a standard test case which tests for false divergence of the beam above a critical spin rate. In these simple examples, ABAQUS successfully simulates the large rotational motion, correctly capturing the geometrically nonlinear effects. The success of these simple examples indicates that ABAQUS, or similar nonlinear finite element programs, could be used to simulate

the large angle rotation of arbitrary structures when a high fidelity truth model is desired. DOE

N89-23231# California Univ., Berkeley. Lawrence Berkeley Lab. Accelerator and Fusion Research Div.
INCORPORATION OF A BOUNDARY CONDITION TO NUMERICAL SOLUTION OF POISSON's EQUATION
S. Caspi, M. Helm, and L. J. Laslett Oct. 1988 8 p Presented at the 7th International Conference on Finite Element Methods in Flow Problems, Huntsville, AL, 3-7 Apr. 1989
(Contract DE-AC03-76SF-00098)
(DE89-007132; LBL-24106; CONF-890479-6; SSC-MAG-166)
Avail: NTIS HC A02/MF A01

Two-dimensional and axially-symmetric problems in electrostatics, magnetostatics or potential fluid flow frequently are solved numerically by means of relaxation techniques -- employing, for example, the finite-difference program POISSON. In many such problems, the sources (charges or currents, vorticity, and regions of permeable material) lie exclusively within a finite closed boundary curve and the relaxation process, in principle, then can be confined to the region interior to such a boundary -- provided that a suitable boundary condition is imposed on the solution at the boundary. This paper is a review and illustration of a computational method that uses a boundary condition of such a nature as to avoid the inaccuracies and more extensive meshes present when, alternatively, a simple Dirichlet or Neumann boundary condition is specified on a somewhat more remote outer boundary. DOE

N89-23232# Technische Univ., Delft (Netherlands).
SEMILINEAR ELLIPTIC EIGENVALUE PROBLEMS Ph.D. Thesis
Guido Sweers 1988 162 p
(ETN-89-94142) Avail: NTIS HC A08/MF A01

Existence and multiplicity results for a semilinear elliptic eigenvalue problem are presented. The maximum of solutions for a semilinear elliptic problem is discussed. Results for the boundary layer of solutions for a semilinear elliptic problem are obtained. Getting a solution between sub- and supersolutions without monotone iteration is considered. Semilinear elliptic problems on domains with corners are analyzed. Existence and stability for a nonautonomous semilinear elliptic eigenvalue problem are treated. Eigenvalues and eigenfunctions of a special elliptic system are mentioned. A counterexample with convex domain to a conjecture of De Saint Venant (1856) is proposed. A strong maximum principle for a non-cooperative elliptic system is outlined. ESA

N89-23233# Lawrence Livermore National Lab., CA.
APPROXIMATE BAYESIAN METHODS FOR NONLINEAR MEASUREMENT ERROR MODELS
Kevin K. Anderson 22 Mar. 1989 23 p Presented at the Symposium on the Interface of Computing Science and Statistics, Orlando, FL, 9 Apr. 1989
(Contract W-7405-eng-48)
(DE89-009224; UCRL-100680; CONF-8904155-1) Avail: NTIS HC A03/MF A01

Approximations to posterior density functions for the unknown parameters in nonlinear measurement error models are presented. Three computationally convenient approximations are compared with exact calculations for a circular model and a location finding problem with measurement errors in the locations of the sensors. DOE

N89-23234# Technische Hogeschool Twente, Enschede (Netherlands). Faculty of Applied Mathematics.
GENERALIZED MULTICOMPONENT KP-HIERARCHIES
G. F. Helminck and G. F. Post Apr. 1988 21 p
(MEMO-708; ISSN-0921-1969; ETN-89-94260) Avail: NTIS HC A03/MF A01

To any maximal commutative subalgebra n of Mn (C) is associated a hierarchy of matrix equations, which is a generalization of the multicomponent KP-hierarchy. A wide variety of solutions of this hierarchy is constructed, using the Grassmannian approach. It is shown that the N-wave equations as described in the work of Drinfeld-Sokolov (1985) are reductions of the present hierarchy. ESA

N89-23235# Technische Hogeschool Twente, Enschede (Netherlands). Faculty of Applied Mathematics.
RESTRICTIONS ON INDUCED SUBGRAPHS ENSURING HAMILTONICITY OR PANCYCLICITY OF K SUB 1,3-FREE GRAPHS
H. J. Broersma and H. J. Veldman Apr. 1988 17 p
(MEMO-709; ISSN-0921-1969; ETN-89-94261) Avail: NTIS HC A03/MF A01

The Goodman and Hedetniemi (1974) result that every 2-connected graph containing no induced subgraph isomorphic to K sub 1, 3 or K sub 1, 3 +e is Hamiltonian is improved by showing that a graph G is pancyclic if G contains no induced K sub 1,3 while in every induced subgraph H isomorphic to K sub 1,3 +e certain pairs of vertices have a common neighbor outside H. It is shown that other sufficient conditions for Hamiltonicity or pancyclicity in terms of forbidden induced subgraphs can be relaxed in a similar way. Results of Gould and Jacobson (1982) are generalized. ESA

N89-23236# Technische Hogeschool Twente, Enschede (Netherlands). Faculty of Applied Mathematics.
THE SEPARATION NUMBER
F. Goebel May 1988 21 p
(MEMO-710; ISSN-0921-1969; ETN-89-94262) Avail: NTIS HC A03/MF A01

Bounds for the separation number of a graph are obtained in terms of simpler parameters. With the aid of these bounds, the separation number for various special graphs are determined, in particular multiples of small graphs. This leads to concepts like robustness and asymptotic separation number. ESA

N89-23237# Technische Hogeschool Twente, Enschede (Netherlands). Faculty of Applied Mathematics.
SHORT PROOFS OF SOME FAN-TYPE RESULTS
H. J. Veldman May 1988 9 p
(MEMO-711; ISSN-0921-1969; ETN-89-94263) Avail: NTIS HC A02/MF A01

For a graph G, define theta (G) = min (max(d(u), d(v))/d(u,v) = 2) if G contains two vertices at distance 2, and theta (G) = infinity otherwise. Fan (1984) proved that every 2-connected graph on n vertices with theta G greater than or = 1/2 n is Hamiltonian. Short proofs of this result and a number of analogs are presented. It is shown that if G is 2-connected, theta (G) greater than or = 1/2 (n-i) and G - (v is a member of V(G)/d(v) is greater than or = 1/2 (n-i)) has at least three components with more than i vertices, then G is Hamiltonian (i greater than or = 1). ESA

N89-23238# Technische Hogeschool Twente, Enschede (Netherlands). Faculty of Applied Mathematics.
GEOMETRICAL INTERPRETATION OF THE BILINEAR EQUATIONS FOR THE KP-HIERARCHY
G. F. Helminck and G. F. Post Jun. 1988 10 p
(MEMO-720; ISSN-0921-1969; ETN-89-94265) Avail: NTIS HC A02/MF A01

An interpretation in the context of the Grassmann manifold is given of the Hirota bilinear equations for the KP-hierarchy and its modified versions. ESA

N89-23239# Technische Hogeschool Twente, Enschede (Netherlands). Faculty of Applied Mathematics.
INPUT-OUTPUT DECOUPLING WITH STABILITY FOR HAMILTONIAN SYSTEMS
H. J. C. Huijberts and A. J. vanderSchaft 6 Jul. 1988 23 p Revised
(MEMO-722; MEMO-648; ISSN-0921-1969; ETN-89-94267)
Avail: NTIS HC A03/MF A01

The input-output decoupling problem with stability for Hamiltonian systems is treated, using decoupling feedbacks which all make the system maximally unobservable. Using the fact that

the dynamics of the maximal unobservable subsystem are again Hamiltonian, a condition for input-output decoupling with (critical) stability is deduced, which easily can be checked. ESA

N89-23240# Technische Hogeschool Twente, Enschede (Netherlands). Faculty of Applied Mathematics.
A BOREL-RITT THEOREM WITH PRESCRIBED ERROR BOUNDS
B. L. J. Braaksma (Groningen Rijksuniversiteit, Netherlands) and G. K. Immink Jul. 1988 36 p
(MEMO-723; ISSN-0921-1969; ETN-89-94268) Avail: NTIS HC A03/MF A01

Given a formal power series the coefficients of which satisfy certain growth conditions, it is shown that there exists an analytic function admitting this series as asymptotic expansion in a sector, with corresponding estimates of the remainder terms. This result can be applied in the asymptotic theory of difference and q-difference equations. ESA

N89-23241# Technische Hogeschool Twente, Enschede (Netherlands). Faculty of Applied Mathematics.
ASYMPTOTIC EXPANSIONS WITH ERROR BOUNDS FOR SOLUTIONS OF DIFFERENCE EQUATIONS OF LEVEL 1 SUP +
G. K. Immink Jul. 1988 29 p
(MEMO-724; ISSN-0921-1969; ETN-89-94269) Avail: NTIS HC A03/MF A01

A class of nonlinear analytic difference equations is considered. It is shown that there exist solutions admitting asymptotic power series expansions such that the remainder terms satisfy a growth condition. This result is applied to a block-diagonalization problem for systems of homogeneous linear difference equations. ESA

N89-23242# Technische Hogeschool Twente, Enschede (Netherlands). Faculty of Applied Mathematics.
SMOOTHING AND LIKELIHOOD RATIO FOR GAUSSIAN BOUNDARY VALUE PROCESSES
Arunabha Bagchi and Hans Westdijk Jul. 1988 28 p
(MEMO-726; ISSN-0921-1969; ETN-89-94271) Avail: NTIS HC A03/MF A01

A derivation, which does not need the invertibility assumption of the covariance matrix of the boundary data, is given for the smoothing of Gaussian two point boundary value processes (TPBVP). The likelihood ratio for TPBV processes are derived in terms of the system parameters by using the Krein factorization. The likelihood ratio involves the smoother of the process. An alternate expression for the likelihood ratio based on the filtered estimate of the state is also given. ESA

N89-23243# Technische Hogeschool Twente, Enschede (Netherlands). Faculty of Applied Mathematics.
MODEL MATCHING FOR LINEAR HAMILTONIAN SYSTEMS
H. J. C. Huijberts Aug. 1988 13 p
(MEMO-730; ISSN-0921-1969; ETN-89-94275) Avail: NTIS HC A03/MF A01

The Hamiltonian model matching problem of designing a compensating feedback for a given Hamiltonian system in such a way that the resulting input-output behavior matches that of a prespecified Hamiltonian model is solved by formulating it as a Hamiltonian disturbance decoupling problem with observation feedback and disturbance measurements. It turns out that the conditions for solvability of the Hamiltonian model matching problem are the same as those for solvability of the normal model matching problem. A procedure for reducing the compensator order is given. ESA

N89-23244# Technische Hogeschool Twente, Enschede (Netherlands). Faculty of Applied Mathematics.
NONLINEAR MODEL MATCHING WITH PRESCRIBED TRACKING ERROR WITH AN APPLICATION TO HAMILTONIAN SYSTEMS
H. J. C. Huijberts Aug. 1988 18 p
(MEMO-731; ISSN-0921-1969; ETN-89-94276) Avail: NTIS HC A03/MF A01

The model matching problem is addressed via the notion of clamped dynamics or zero dynamics and a version of the modified Hirschorn algorithm. Results on the nonlinear Model Matching Problem with prescribed tracking error for SISO-systems are extended to MIMO-systems. Results are applied to the problem of matching Hamiltonian models by means of Hamiltonian plants. Special attention is paid to the structural properties of the system after solving the Model Matching Problem with prescribed tracking error. ESA

N89-23245# Technische Hogeschool Twente, Enschede (Netherlands). Faculty of Applied Mathematics.
SMOOTH INTERPOLATION TO SCATTERED DATA BY BIVARIATE PIECEWISE POLYNOMIALS OF ODD DEGREE
R. H. J. Gmelig-Meyling and P. R. Pfluger (Amsterdam Univ., Netherlands) Aug. 1988 38 p
(MEMO-732; ISSN-0921-1969; ETN-89-94277) Avail: NTIS HC A03/MF A01

An algorithm which determines a bivariate smooth piecewise polynomial interpolant to function values given at points scattered in R squared is presented. The degree of the polynomials is as small as possible for arbitrary triangulations and a high degree of polynomial precision is achieved. Experiments and numerical tests for quintic splines of class C squared are described. ESA

N89-23246# Technische Hogeschool Twente, Enschede (Netherlands). Faculty of Applied Mathematics.
LOCALIZATION OF SOLUTIONS OF A NONLINEAR FOKKER-PLANCK EQUATION WITH DIRICHLET BOUNDARY CONDITIONS
B. H. Gilding Sep. 1988 49 p
(MEMO-733; ISSN-0169-2690; ETN-89-94278) Avail: NTIS HC A03/MF A01

The Cauchy-Dirichlet problem for a nonlinear degenerate second-order parabolic equation in one space dimension is considered. The equation possesses the property that if the initial data function for the Cauchy-Dirichlet problem is nonnegative and has compact support then at all later times the (generalized) solution of the problem also is nonnegative and has compact support as a function of the spatial variable. Such equations arise in the theory of soil moisture infiltration. A solution of the Cauchy-Dirichlet problem is said to be localized if its support with respect to the spatial variable is uniformly bounded in time. The influence of the coefficients in the equation and of the lateral boundary data on the localization of solutions is investigated. With regard to the physical background to the problem, the results relate to the role of soil characteristics, gravity, and boundary conditions in determining the finite penetration of a wetting front during soil-moisture infiltration. ESA

N89-23247# Technische Hogeschool Twente, Enschede (Netherlands). Faculty of Applied Mathematics.
NUMERICAL SOLUTION OF THE BIHARMONIC EQUATION USING DIFFERENT TYPES OF BIVARIATE SPLINE FUNCTIONS
R. H. J. Gmelig-Meyling Sep. 1988 11 p
(MEMO-734; ISSN-0169-2690; ETN-89-94279) Avail: NTIS HC A03/MF A01

The numerical solution of a boundary value problem by the finite element method is discussed. The partial differential equation is the so-called biharmonic equation, which is elliptic and of fourth order. This equation describes the deformation of a thin elastic plate subject to load. As approximate solutions, piecewise polynomial functions of minimal degree with respect to a triangular mesh are used. To obtain conforming finite elements suitable spline functions are of class C sup 1 at least. Accuracy and computational cost of three different (conforming) finite elements are compared. The elements are either polynomial or piecewise polynomial per triangle. A preconditioned conjugate gradient method is used to solve the resulting large (but sparse) systems of linear equations.

The different elements applied to model problems described in the literature are compared. ESA

N89-23248# Technische Hogeschool Twente, Enschede (Netherlands). Faculty of Applied Mathematics.
ON THE ASYMPTOTIC BEHAVIOR OF THE COEFFICIENTS OF ASYMPTOTIC POWER SERIES AND ITS RELEVANCE TO STOKES PHENOMENA
G. K. Immink Sep. 1988 29 p
(MEMO-738; ISSN-0169-2690; ETN-89-94282) Avail: NTIS HC A03/MF A01

The relevance of the asymptotic behavior of the coefficients of asymptotic power series for the study of Stokes phenomena is considered. A connection problem in the theory of linear difference equations is used as an illustration. ESA

N89-23249# Technische Hogeschool Twente, Enschede (Netherlands). Faculty of Applied Mathematics.
APPROXIMATION OF SURFACES CONSTRAINED BY A DIFFERENTIAL EQUATION USING SIMPLEX SPLINES
C. R. Traas Jan. 1908 11 p
(MEMO-739; ISSN-0169-2690; ETN-89-94283) Avail: NTIS HC A03/MF A01

The utility of bivariate quadratic simplex splines for the approximation of surfaces was investigated. The surface is constrained to satisfy a differential equation. It is shown that with a fair amount of automation these splines can be used very well. ESA

N89-23250# Technische Hogeschool Twente, Enschede (Netherlands). Faculty of Applied Mathematics.
NONLOCAL HIGHER ORDER SYMMETRIES FOR THE FEDERBUSH MODEL
W. M. Sluis and P. H. M. Kersten Oct. 1988 59 p Revised
(MEMO-740; MEMO-719; ISSN-0169-2690; ETN-89-94284)
Avail: NTIS HC A04/MF A01

By introduction of nonlocal variables, four first order nonlocal Lie-Backlung transformations are obtained for the Federbush model. The Lie algebraic structure of the nonlocal symmetries is discussed. ESA

N89-23251# Technische Hogeschool Twente, Enschede (Netherlands). Faculty of Applied Mathematics.
ON THE MAXIMUM PERIOD OF A PERMUTATION OF N ELEMENTS
H. J. Broersma and F. Goebel Oct. 1988 13 p
(MEMO-743; ISSN-0169-2690; ETN-89-94286) Avail: NTIS HC A03/MF A01

Asymptotic upper and lower bounds for the maximum period of a permutation of n elements are given. ESA

N89-23252# Technische Hogeschool Twente, Enschede (Netherlands). Faculty of Applied Mathematics.
MONOTONICITY-PRESERVING QUADRATIC C SUP 1-SPLINE INTERPOLATION TO SCATTERED DATA
R. H. J. Gmelig-Meyling Oct. 1988 30 p
(MEMO-744; ISSN-0169-2690; ETN-89-94287) Avail: NTIS HC A03/MF A01

The problem of constructing a visually pleasing, monotone and derivative-continuous interpolant to positional data is considered. The data are assumed to be drawn from a monotone, bivariate function at points which are distributed arbitrarily over the plane. An efficient interpolation algorithm is presented which ensures the monotonicity of the data. The convex hull of the data points is triangulated and every triangle is partitioned into six subtriangles. The interpolating function is a piecewise quadratic C sup 1-spline with respect to the subtriangles. The interpolant is determined uniquely by function and first derivative values at the data points. A collection of linear inequality constraints on the derivative parameters is established in order to ensure monotonicity. Quadratic programming techniques are employed to determine derivative values which define a monotone and visually pleasing interpolating surface. ESA

N89-23253 National Physical Lab., Teddington (England). Div. of Information Technology and Computing.
THE STABLE EVALUATION OF A SIMPLE RATIONAL FUNCTION AND ITS APPLICATION TO SPLINE APPROXIMATION
M. G. Cox and P. M. Harris Nov. 1988 19 p
(NPL-DITC-135/88; ISSN-0262-5369; ETN-89-94342) Copyright Avail: National Physical Lab., Teddington, Middlesex, TW11 0LW, United Kingdom

The simple formula f = (x sup p/q-1)/(x-1), where p and q are relatively prime positive integers and x is real and positive, is considered. This formula cannot be used directly when x = 1 and, for x close to one, it suffers from cancellations which may yield considerable error in the computed value of f. An alternative formula for evaluating f that is unconditionally stable, even for x arbitrarily close to unity, is given. Perturbation and floating-point error analyses of the two formulae are presented. An application to knot placement in the context of spline approximation of discrete data sets is given. ESA

N89-23254# Aeronautical Research Inst. of Sweden, Stockholm. Aerodynamics Dept.
THE INFLUENCE OF OPEN BOUNDARY CONDITIONS AND DIFFERENCE OPERATORS ON THE TIME-INTEGRATION OF THE BURGER'S EQUATION
Anders Bengtsson, Evdokia Ziakouli, and Jan Nordstrom 10 Nov. 1988 45 p Sponsored by the Swedish Board for Technical Advancement
(FFA-TN-1988-57; ETN-89-94548) Avail: NTIS HC A03/MF A01

The influence of open boundary conditions and difference operators on the time-integration of the Burger's equation are investigated. The continuous and semidiscrete problems are analyzed. The energy method is used to investigate well-posedness of the problem. The Laplace transform technique is used to compute the spectrum for different boundary conditions and difference operators. It is shown how to predict the rate of convergence to steady-state by using the spectrum of the problem. Linear and nonlinear computations are performed and the resulting convergence rates agree well with the theoretical analysis. ESA

N89-23255# Naval Postgraduate School, Monterey, CA.
A DIVIDE AND CONQUER METHOD FOR UNITARY AND ORTHOGONAL EIGENPROBLEMS Technical Report, 1 Oct. 1988 - 30 Jan. 1989
William Gragg and L. Reichel 22 Feb. 1989 41 p
(AD-A205433; NPS53-89-007) Avail: NTIS HC A03/MF A01 CSCL 12A

Let H epsilon C be a unitary upper Hessenberg matrix whose eigenvalues, and possibly also eigenvectors, are to be determined. We describe how this eigenproblem can be solved by a divide and conquer method, in which the matrix H is split into two smaller unitary right Hessenberg matrices H1 and H2 by a rank-one modification of H. The eigenproblems for H1 and H2 can be solved independently, and the solutions of these smaller eigenproblems define a rational function, whose zeros on the unit circle are the eigenvalues of H. The eigenvectors of H can be determined from the eigenvalues of H and the eigenvectors of H1 and H2. The outlined splitting of unitary upper Hessenberg matrices into smaller such matrices is carried out recursively. This gives rise to a divide and conquer method that is suitable for implementation on a parallel computer. When H epsilon R sub nxn is orthogonal, the divide and conquer scheme simplifies and is described separately. Our interest in the orthogonal eigenproblem stems from applications in signal processing. Numerical examples for the orthogonal eigenproblem conclude the paper. GRA

N89-23256# Bath Univ. (England). School of Mathematical Sciences.
STATISTICAL SMOOTHING METHODS AND IMAGE ANALYSIS Final Report, 1 Oct. 1986 - 31 Sep. 1988
C. Jennison and B. W. Silverman Dec. 1988 271 p

(Contract DAJA45-86-C-0054; DA Proj. 1L1-61103-BH-57)
(AD-A205643; R/D-5421-MA-01) Avail: NTIS HC A12/MF A01 CSCL 12C

This document covers a number of different areas. The methodology of density estimation has been considered with particular reference to the smoothed bootstrap. A new method of fitting parsimonious additive models has been devised. The topic of statistical integral equations has been investigated in detail and algorithms for two main cases of particular interest have been developed and investigated. Applications to image analysis have been considered. Contributions to the theory of estimation from indirect information have been made. There has been careful consideration of the appropriate way to penalize an edge process model in an image reconstruction. The methodology of nonparametric discriminant analysis, with particular reference to the CART approach, has been the subject of considerable attention. The ICM method of image reconstruction has been studied. A new method of image refinement has been developed. GRA

N89-23257# Stanford Univ., CA. Dept. of Computer Science.
PROJECTIONS OF VECTOR ADDITION SYSTEM REACHABILITY SETS ARE SEMILINEAR
Hans Kleine Buening, Theodor Lettmann (Karlsruhe Univ., Germany, F.R.), and Ernst W. Mayr 29 Mar. 1988 11 p
(Contract N00014-85-C-0731)
(AD-A205914; SU-STAN-CS-88-1199) Avail: NTIS HC A03/MF A01 CSCL 12B

The reachability sets of Vector Addition Systems of dimension six or more can be non-semilinear. This may be one reason why the inclusion problem (as well as the equality problem) for reachability sets of vector addition systems in general is undecidable, even though the reachability problem itself is known to be decidable. We show that any one-dimensional projection of the reachability set of an arbitrary vector addition system is semilinear, and hence simple. GRA

65 STATISTICS AND PROBABILITY

Includes data sampling and smoothing; Monte Carlo method; and stochastic processes.

N89-23258# Purdue Univ., West Lafayette, IN. Dept. of Statistics.
MONTE CARLO APPROXIMATIONS IN BAYESIAN DECISION THEORY. PART 3: LIMITING BEHAVIOR OF MONTE CARLO APPROXIMATIONS
Jun Shao Dec. 1988 18 p
(Contract N00014-88-K-1070; NSF DMS-87-17799)
(AD-A204173; TR-88-65C) Avail: NTIS HC A03/MF A01 CSCL 12C

Monte Carlo approximation is a useful method in obtaining a numerical approximation to a Bayesian action (an action which minimizes the posterior expected loss). The behavior of the Monte Carlo approximation is studied when the Monte Carlo sample size is large. Convergence and convergence rate of the Monte Carlo approximation are established under some weak conditions on the loss function. GRA

N89-23259# International Centre for Theoretical Physics, Trieste (Italy).
IMPLEMENTATION OF COMPARATIVE PROBABILITY BY GLEASON MEASURES: INFINITE DIMENSIONAL CASE
Simba A. Mutangadura (Zimbabwe Univ., Salisbury.) Sep. 1988 12 p
(DE88-705683; IC-88/299) Avail: NTIS (US Sales Only) HC A03/MF A01

In this paper we give one necessary and sufficient condition for a Classical Comparative Probability (CCP) associated with an infinite dimensional Hilbert space to be implemented by a Gleason measure. This condition automatically renders the CCP a Quantum Comparative Probability. DOE

N89-23260# Los Alamos National Lab., NM.
THE MULTIGROUP AND CYLINDRICAL GEOMETRY FORMULATION OF THE Sn MONTE CARLO HYBRID METHOD
R. S. Baker, W. L. Filippone (Arizona Univ., Tucson.), and R. E. Alcouffe 1988 10 p Presented at the American Nuclear Society Meeting, Santa Fe, NM, 10-15 Apr. 1989
(Contract W-7405-eng-36)
(DE89-000326; LA-UR-88-3281; CONF-890438-1) Avail: NTIS HC A02/MF A01

We describe a general formulation of the Sn/Monte Carlo hybrid method which couples a region where a Monte Carlo calculation has been performed to regions where Sn calculations are to be done. This coupling is completely consistent in that the solution obtained is not dependent upon any assumptions of geometric separation or decoupling. In this paper we demonstrate this consistency both theoretically and through example problems in R-Z cylindrical geometry and in the multigroup case. We have also reformulated the method to handle multigroup problems with a minimum impact upon storage requirements. As such we conclude that we have brought this method to the verge of solving practical problems in neutral particle transport. The hybrid technique consists of defining spatial regions of a problem in which either a Monte Carlo calculation or an Sn calculation is to be done. The calculations are then connected through the common boundary fluxes which are determined iteratively using the response matrix technique. The hybrid method is being developed so that the best features of the Monte Carlo and Sn techniques can be exploited in a single problem. It is advantageous to use precalculated response matrices in the Monte Carlo regions but not in the Sn regions. However, because the response matrices are stored, a brute force extension of the hybrid method to multigroup problems would increase the number of response matrix elements by a factor of G^2, where G is the number of energy groups. This quickly leads to unacceptable amounts of storage requirements. To address this, we have reformulated the method for multigroup problems which makes it possible to solve pure down scatter problems without significant increases in memory requirements. DOE

N89-23261# Sandia National Labs., Albuquerque, NM.
TECHNIQUES FOR APPLYING SETS CODE PROCEDURES TO LARGE FAULT TREES IN PRA (PROBABILISTIC RISK ASSESSMENT) ANALYSIS
Sharon L. Daniel and Arthur C. Payne, Jr. 1988 6 p Presented at the International Topical Meeting on Probability, Reliability and Safety Assessment, Pittsburgh, PA, 2 Apr. 1989
(Contract DE-AC04-76DP-00789)
(DE89-004823; SAND-88-1463C; CONF-890405-10) Avail: NTIS HC A02/MF A01

In this paper, we describe some of the new techniques developed in the Risk Methods Integration and Evaluation Program (RMIEP) for solving large fault trees and for performing external event analysis to the same level of detail as the internal event analysis by manipulating the original internal event fault trees to include component location information. Approximations or simplifications of these techniques were used in the NUREG-1150 analyses for both internal and external events. DOE

N89-23262# Technische Hogeschool Twente, Enschede (Netherlands). Faculty of Applied Mathematics.
ASYMPTOTICALLY OPTIMAL NONPARAMETRIC EXPERIMENTAL DESIGN TESTS FOR THE LOG LINEAR MODEL UNDER CENSORING
T. J. Terpstra Jul. 1988 14 p
(MEMO-727; ISSN-0921-1969; ETN-89-94272) Avail: NTIS HC A03/MF A01

Lifetime distributions with failure rates given by the Cox regression model are considered. The basic failure rate is unknown. The failure of n objects is observed during an interval where censoring is allowed. An asymptotically minimax most powerful nonparametric test is obtained for the null hypothesis. Test statistics for composite hypotheses are also obtained. ESA

N89-23263# Technische Hogeschool Twente, Enschede (Netherlands). Faculty of Applied Mathematics.
ON THE EXPECTED NUMBER OF ASSIGNMENTS IN REDUCED MATRICES FOR THE LINEAR ASSIGNMENT PROBLEM
W. M. Nawijn and B. Dorhout Jul. 1988 13 p
(MEMO-728; ISSN-0921-1969; ETN-89-94273) Avail: NTIS HC A03/MF A01

A linear nxn assignment problem for which the elements of the cost matrix are sampled from a continuous probability distribution is considered. Based on the zero entries of the reduced matrix the expectation of the maximum number of initial assignments is determined for general n, as well as an asymptotic value for large n. ESA

N89-23264# Technische Hogeschool Twente, Enschede (Netherlands). Faculty of Applied Mathematics.
LIMITING EXACT EFFICIENCY OF QUADRATIC STATISTICS
G. A. M. Jeurnink and W. C. M. Kallenberg Sep. 1988 40 p
(MEMO-737; ISSN-0169-2690; ETN-89-94281) Avail: NTIS HC A03/MF A01

Application of exact Bahadur efficiencies in testing theory or exact inaccuracy rates in estimation theory is discussed. It needs evaluation of large deviation probabilities. Because of the complexity of the expressions frequently a local limit of the nonlocal measure is considered. Local limits of large deviation probabilities of general quadratic statistics are obtained by relating them to large deviation probabilities of sums of k-dimensional random vectors. The results are applied, e.g., to generalized Cramer-von Mises statistics, including the Anderson-Darling statistic, Neyman's smooth tests, and likelihood ratio tests. ESA

66 SYSTEMS ANALYSIS

Includes mathematical modeling; network analysis; and operations research.

N89-23265# Los Alamos National Lab., NM.
TRANSITIONAL STRATEGIC DEFENSE ARCHITECTURES
Gregory H. Canavan Mar. 1989 24 p
(Contract W-7405-eng-36)
(DE89-008312; LA-11524-MS) Avail: NTIS HC A03/MF A01

Transitional deployments permit the rational evolution of increasing capability in each defensive layer. Boost-phase and midcourse transitions are discussed; a key feature is the need for balance between deployment and development. DOE

N89-23266# Technische Hogeschool Twente, Enschede (Netherlands). Faculty of Applied Mathematics.
RELATIONSHIPS BETWEEN THE PRENUCLEOLUS, ENSC-SOLUTION AND RELATED SOLUTION CONCEPTS FOR COOPERATIVE GAMES
Theo Driessen and Yukihiko Funaki (Toyo Univ., Kawagoe, Japan) July. 1988 18 p
(MEMO-729; ISSN-0921-1969; ETN-89-94274) Avail: NTIS HC A03/MF A01

The Egalitarian NonSeparable Contribution (ENSC) solution of a cooperative n-person game in characteristic function form is considered. Given that the separable contributions of the single players to the grand coalition are already allocated, the ENSC-method prescribes the egalitarian allocation of the remaining nonseparable contribution in the game. Conditions sufficient for the coincidence of the ENSC-method and the so-called prenucleolus concept are treated. The main result states that both solutions coincide whenever the maximal excesses at the ENSC-solution are determined by the (n-1)-person coalitions in the n-person game. The relationship between the ENSC-method and the so-called Shapley value for a specific type of n-person games is studied. The main result states that the Shapley value of a so-called k-person coalitional game is a linear or convex combination of the ENSC-solution and the center of the set of all nonnegative efficient payoff vectors. ESA

67 THEORETICAL MATHEMATICS

Includes topology and number theory.

N89-23267# International Centre for Theoretical Physics, Trieste (Italy).
ON A FUNCTIONAL EQUATION OVER HILBERT SPACES
A. B. Thaheem and Noor Mohammad (Quaid-i-Azam Univ., Islamabad, Pakistan) Jun. 1988 4 p
(DE88-705645; IC-88/38-Rev) Avail: NTIS (US Sales Only) HC A02/MF A01

Let (u sub t:t is an element of R) and (v sub t:t is an element of R) be commuting one-parameter groups of unitary operators on a Hilbert space H such that u sub t + u sub - t = v sub t + v sub - t for all t is an element of R. It is shown here that H can be decomposed into two parts by a projection p such that u sub t = v sub t on pH and u sub t = v sub - t on (1-p)H. DOE

70 PHYSICS (GENERAL)

For precision time and time interval (PTTI) see *35 Instrumentation and Photography;* for geophysics, astrophysics or solar physics see *46 Geophysics, 90 Astrophysics,* or *92 Solar Physics.*

N89-23268 National Physical Lab., Teddington (England). Div. of Materials Applications.
MODEL CALCULATIONS OF THE ELECTRON-OPTICAL PROPERTIES OF COMPACT FARADAY CUPS
G. D. Ingram and M. P. Seah Aug. 1988 35 p
(NPL-DMA(A)165; ISSN-0143-7313; ETN-89-94204) Copyright Avail: National Physical Lab., Teddington, Middlesex, TW11 0LW, England

Calculations are made of compact model Faraday cups comprising an earthed outer box with a small aperture surrounding an inner box, coated internally with graphite, which may be positively biased. The trajectories of incident electrons or positive ions are calculated for a range of energy to bias ratios to define the change in effective cup aperture as a function of the bias or energy value. The effect of the bias is calculated to determine the number of generated secondary electrons which escape from the cup. These calculations define the cup efficiency for four types of measurement: electron beam current, electron beam current densities, positive ion beam currents, and positive ion beam current densities. Traditional criteria, developed for measuring electron beam currents, are shown not to be valid for the other three categories. General design rules are evaluated separately for all four types of measurement in compact Faraday cups. ESA

N89-23269# Netherlands Energy Research Foundation, Petten.
THE HALF-METALLIC FERROMAGNETIC NiMnSb: A POSITRON-ANNIHILATION STUDY Ph.D. Thesis - Amsterdam Univ.
Karl Hanssen Apr. 1988 110 p
(ECN-209; ETN-89-94248) Avail: NTIS HC A06/MF A01

The electronic structure of NiMnSb is investigated by spin-polarized measurements of the angular correlation of annihilation radiation; NiMnSb is predicted to be a half-metallic ferromagnet. To interpret the experimental data, the electronic structure, the Fermi surface, and the two-photon momentum density were calculated. The calculations, based on self-consistent potentials evaluated according to the augmented spherical wave method, were performed scalar-relativistically. From the measured distribution, the sum and difference of the spin-dependent momentum densities are obtained once integrated along three different directions in p space, namely (100), (110), and (111). The distributions show a clear impression of the majority-spin Fermi-surface. A good quantitative agreement between theory and

experiment is established. A value for the three photon difference effect in NiMnSb is established: 0.0084 + or - 0.1. To test the half-metallic nature of the band structure the experimental distributions are compared with theoretical ones obtained from modelled band structures in which small numbers of electrons near the Fermi level are transferred from one spin population to the other. The best agreement is obtained for a band occupation in which no electrons are transferred, i.e., for the half-metallic state. ESA

71 ACOUSTICS

Includes sound generation, transmission and attenuation. For noise pollution see *45 Environmental Pollution.*

N89-23270*# National Aeronautics and Space Administration. Langley Research Center, Hampton, VA.
COMPARISON OF MEASURED AND CALCULATED SOUND PRESSURE LEVELS AROUND A LARGE HORIZONTAL AXIS WIND TURBINE GENERATOR
Kevin P. Shepherd, William L. Willshire, Jr., and Harvey H. Hubbard (Planning Research Corp., Hampton, VA.) Mar. 1989 46 p
(NASA-TM-100654; NAS 1.15:100654) Avail: NTIS HC A03/MF A01 CSCL 20A

Results are reported from a large number of simultaneous acoustic measurements around a large horizontal axis downwind configuration wind turbine generator. In addition, comparisons are made between measurements and calculations of both the discrete frequency rotational harmonics and the broad band noise components. Sound pressure time histories and noise radiation patterns as well as narrow band and broadband noise spectra are presented for a range of operating conditions. The data are useful for purposes of environmental impact assessment. Author

N89-23271# National Center for Physical Acoustics, University, MS.
EXPERIMENTAL OBSERVATION OF THE NONLINEAR RESPONSE OF SINGLE BUBBLES TO AN APPLIED ACOUSTIC FIELD Technical Report, 1 Jan. 1986 - 31 Dec. 1988
R. Glynn Hold and Lawrence A. Crum 31 Dec. 1988 119 p
(Contract N00014-86-K-0134)
(AD-A205191; NCPA-LC-02-1988) Avail: NTIS HC A06/MF A01 CSCL 20A

An experimental technique for measuring the time-varying response of an oscillating, acoustically levitated bubble in water is developed. The bubble is levitated in a cell consisting of two concentric, cylindrical, piezoceramic transducers mounted on either end of a short glass tube. The entire apparatus forms a closed-open cylindrical tube which is driven in the cylindrical mode of (1, 0, 1) at a frequency f= 24kHz. Linearly polarized laser light (He-Ne 632.8, Ar-I 488.) is scattered from a bubble, and the scattered intensity is measured with a suitable photodetector positioned at some known angle from the forward, subtending some solid acceptance angle. The output photodetector current, which is linearly proportional to the light intensity, is converted into a voltage, digitized, and then stored on a computer for analysis. The scattered intensity I sub exp (t) thus obtained contains, in principle, all of the dynamical information about the oscillating bubble, and various methods of analysis are employed to examine the behavior. Complex I exp (t) behavior is also measured, with subharmonics and broad-band noise apparent in the Fourier spectra. This behavior is shown to exhibit high (greater than 2) correlation dimension, indicating the presence of more than one degree of freedom in the motion. Possible explanations for this phenomenon are discussed, including shape oscillations and chaos. Author

N89-23272*# National Aeronautics and Space Administration. Langley Research Center, Hampton, VA.
ENVIRONMENTAL NOISE CHARACTERISTICS OF THE MOD5-B (3.2 MW) WIND TURBINE GENERATOR
Kevin P. Shepherd and Harvey H. Hubbard (Planning Research Corp., Hampton, VA.) Mar. 1989 29 p
(NASA-TM-101567; NAS 1.15:101567) Avail: NTIS HC A03/MF A01 CSCL 20A

Both narrow band and broad band acoustic data were obtained for the MOD5-B wind turbine for a range of wind speeds from 5.8 to 14.3 m/s; for a range of power outputs from 300 to 3100 kW; and for various azimuth angles and distances. Comparisons are made with those of other large machines and with predictions by available methods. The highest levels occur at the lower frequencies and generally decrease as the frequency increases. Low frequency rotational noise components were more intense than expected for an upwind machine and are believed to result from localized wind gradients across the rotor disk due to upwind terrain features. Predicted broad band spectra follow the general trends of the data but tend to underestimate the levels in the frequency range where the turbulent boundary layer-trailing edge interaction noise is expected to be significant. Author

N89-23273# AT and T Technologies, Inc., Greensboro, NC.
ACOUSTIC WAVE DEVICE USING PLATE MODES WITH SURFACE-PARALLEL DISPLACEMENT Patent Application
Stephen J. Martin, inventor (to DOE) and Antonio J. Ricco, inventor (to DOE) 29 Apr. 1988 20 p
(Contract DE-AC04-76DP-00789)
(DE89-009719; PATENTS-US-A7187776; US-Patent-Appl-SN-187776) Avail: NTIS HC A03

Solid-state acoustic sensors for monitoring conditions at a surface immersed in a liquid and for monitoring concentrations of species in a liquid and for monitoring electrical properties of a liquid are formed by placing interdigital input and output transducers on a piezoelectric substrate and propagating acoustic plate modes therebetween. The deposition or removal of material on or from, respectively, a thin film in contact with the surface, or changes in the mechanical properties of a thin film in contact with the surface, or changes in the electrical characteristics of the solution, create perturbations in the velocity and attenuation of the acoustic plate modes as a function of these properties or changes in them. DOE

72 ATOMIC AND MOLECULAR PHYSICS

Includes atomic structure, electron properties, and molecular spectra.

N89-23274# California Univ., Davis. Dept. of Applied Science.
MOLECULAR DYNAMICS AND IRREVERSIBILITY, FROM BOLTZMANN TO NOSE
William G. Hoover Jan. 1989 73 p Presented at The Boltzmann Seminar, Hohe Wand, Austria, 1 Jan. 1989 Prepared in cooperation with Lawrence Livermore National Lab., CA
(Contract W-7405-eng-48)
(DE89-006740; UCRL-100259; CONF-890180-1) Avail: NTIS HC A04/MF A01

Throughout Boltzmann's life-long atomistic study of irreversibility, he emphasized the one-body distribution function f sub 1, averaged over many particles, with the underlying dynamics taken to be a series of two-body collisions. His derivation of the H theorem, linking dynamics and thermodynamics, remains the major accomplishment in understanding the Second Law of Thermodynamics. Today his analytic one-body approach has largely been superceded by using fast computers to simulate many-body Molecular Dynamics. Fermi originated Molecular Dynamics at Los Alamos in 1953. His few-body one-dimensional chains launched a generation of numerical studies of Lyapunov-unstable ordinary different equations. By 1972 computers could simulate 1000-body gases, liquids, or solids, and a new nonequilibrium mechanics was developed to facilitate this work. In 1984, Nose made a major contribution. He showed how to introduce macroscopic variables, such as temperature, pressure, and heat flux, directly into time-reversible microscopic equations of motion. When Nose's mechanics is applied to nonequilibrium systems zero-volume strange attractors form in the many-body phase space. The

attractors provide a new explanation for the classical problem of irreversibility that fascinated Boltzmann. Here I trace the evolution of molecular dynamics from Fermi's work at Los Alamos to Nose recent work, and I speculate on the applicability of the new nonequilibrium ideas to quantum systems. DOE

N89-23275 National Physical Lab., Teddington (England). Div. of Radiation Science and Acoustics.
DETERMINATION OF THE He3 NUMBER DENSITY FOR THE PROPORTIONAL COUNTER USED IN THE NPL BONNER SPHERE SYSTEM
D. J. Thomas and N. Soochak Jul. 1988 50 p
(NPL-RS(EXT)104; ISSN-0143-7315; ETN-89-94206) Copyright Avail: National Physical Lab., Teddington, Middlesex, TW11 0LW, England

The He3 number density for the gas in an He3 proportional counter was evaluated from a determination of the number of (n,p) reactions detected in a known thermal fluence. Accuracy is 4 percent. The thermal fluence determination, and the analysis of reaction rates for He3 proportional counters in thermal fluences are discussed. It is stressed that the applicability of any approximate expressions relating the measured response to the amount of detecting material should be checked. If the detector is fairly opaque to neutrons, the effective temperature of the Maxwellian distribution does need to be known. This is true even for a detector with a 1/v dependence. For such a detector the reaction rate is independent of the shape of the thermal neutron distribution in the limiting case of a thin detector, but this is not true for one where the neutrons have a high probability of being absorbed. The epithermal component of the field needs to be determined since the detector response may be quite different in this energy region. The response of the detector as a function of energy needs to be known over all the relevant neutron energy range. The effects of absorption and scattering in any cladding material around the detecting element must be considered. ESA

N89-23276# Nationaal Inst. voor Kernfysica en Hoge Energiefysica, Amsterdam (Netherlands).
HARD SCATTERING OF (ALMOST) REAL PHOTONS AT HERA
Sijbrand J. deJong and Jos J. Engelen 13 Mar. 1988 28 p Presented at the DESY Theory Workshop Physics at HERA, Amsterdam, Netherlands, 1987
(NIKHEF-H/88-3; ETN-89-94249) Avail: NTIS HC A03/MF A01

Photoproduction reactions producing large transverse momenta are reviewed, as well as the possibility of using them for tests of perturbative QCD. Pointlike coupling of the photon to the proton constituents is considered in leading log approximation. Although the cross sections of these processes, photon gluon fusion and QCD Compton scattering, get their largest contribution from low Qsq (almost) real photons, they are calculated over the full Qsq range. Photoproduction as a background to the standard deep inelastic physics at HERA and to exotic phenomena is discussed. Heavy flavor production through photon gluon fusion may offer good possibilities of studying charm and bottom quarks. An attempt is made to determine a possible strategy to identify the top quark at HERA. ESA

N89-23277# Nationaal Inst. voor Kernfysica en Hoge Energiefysica, Amsterdam (Netherlands).
ELECTRON DRIFT VELOCITY CLOSE TO A SENSE WIRE
Jan Konijn and Fred Hartjes Jun. 1988 11 p
(NIKHEF-H/88-5; ETN-89-94251) Avail: NTIS HC A03/MF A01

Using a focused UV nitrogen laser beam, electrons were liberated from an argon - ethane gas mixture in a drift chamber. The drift time was measured for distances from the sense wire between 30 mm and 30 microns. From these measurements a drift velocity curve was derived for electric field strengths between 1 and 15 kV/cm. ESA

N89-23278# Nationaal Inst. voor Kernfysica en Hoge Energiefysica, Amsterdam (Netherlands).
NEUTRINO HELICITY FLIPS VIA ELECTROWEAK INTERACTIONS AND SN1987a
K. J. F. Gaemers, R. Gandhi, and J. M. Lattimer (State Univ. of New York, Stony Brook.) Oct. 1988 13 p
(Contract DE-AC02-87ER-40317)
(NIKHEF-H/88-18; ETN-89-94257) Avail: NTIS HC A03/MF A01

Electroweak mechanisms via which neutrinos may flip helicity and become sterile are examined. Exact and approximate expression for flip processes relevant in astrophysics and cosmology, mediated by W, Z, and gamma exchange, including their interference, are derived. It is shown that within the context of the Standard Model with massive neutrinos, for nu e to nu e scattering, sigma flip z/sigma flip gamma = 6000, independent of particle masses and energies to a good approximation. It is also shown that using general considerations and the fact that the observed nu bar e burst from SN1987a lasted several seconds, these weak interaction flip cross-sections can be used to derive an upper limit on mu and tau netrino masses of 40 keV. ESA

N89-23279# Swedish Defence Research Establishment, Stockholm. Dept. of Weapons Technology.
MIE SCATTERING CALCULATIONS FOR HEAT RADIATION
Per Cederstam Nov. 1988 62 p In SWEDISH; ENGLISH summary
(FOA-C-20738-2.1; ISSN-0347-3694; ETN-89-94302) Avail: NTIS HC A04/MF A01

A program package which computes scattering efficiencies, absorption efficiencies, and phase-functions with Mie scattering theory is described. An approximation to the relation between isotropic and forward scattering is evaluated, as an input to the discrete transfer method. The distribution of the heat radiated in the combustion chamber is not of an exact wavelength, its spectrum approximately follows the Planck function and depends on the temperature. ESA

73 NUCLEAR AND HIGH-ENERGY PHYSICS

Includes elementary and nuclear particles; and reactor theory.

For space radiation see *93 Space Radiation.*

N89-23280# Continuous Electron Beam Accelerator Facility, Newport New, VA.
RADIATION CONTROL AT THE CONTINUOUS ELECTRON BEAM ACCELERATOR FACILITY (CEBAF), A NEW HIGH POWER CW ELECTRON ACCELERATOR INSTALLATION
Geoffrey B. Stapleton and Ralph H. Thomas (California Univ., Berkeley. Lawrence Berkeley Lab.) 1989 6 p
(Contract DE-AC05-84ER-40150)
(CEBAF-PR-89-001) Avail: NTIS HC A02/MF A01

A description is given of the design goals and radiation control measures, for a 4 GeV, 1 MW electron accelerator under construction in the USA. The importance of cooperation between designers and regulators is illustrated. Author

N89-23281# Los Alamos National Lab., NM.
SPACE NUCLEAR SAFETY PROGRAM Progress Report, Jul. - Sep. 1987
T. G. George, comp. Feb. 1989 20 p
(Contract W-7405-eng-36)
(DE89-008308; LA-11440-PR) Avail: NTIS HC A03/MF A01

This quarterly report describes studies related to the use of Pu-238O2 in radioisotope power systems, carried out for the Office of Special Nuclear Projects of the U.S. Department of Energy by Los Alamos National Laboratory. The studies discussed are ongoing; the results and conclusions described may change as the work progresses. DOE

N89-23282# Lawrence Livermore National Lab., CA.
BEAM RESEARCH TECHNICAL ABSTRACTS, 1987
Arthur L. Henry, ed. Nov. 1988 44 p
(Contract W-7405-eng-48)
(DE89-009013; UCRL-53889) Avail: NTIS HC A03/MF A01

This document is a summary of the published, unclassified scientific work of the Beam Research Program at Lawrence Livermore National Laboratory during the calendar year 1987. It includes the complete abstract of each report as well as three indexes: author, key word, and report number. Most abstracts represent work that was completed and published in report form. DOE

74 OPTICS

Includes light phenomena; and optical devices.
For lasers see *36 Lasers and Masers.*

N89-23283# Edo Corp., Shelton, CT. Engineering Div.
UNITY VISION BLOCK WITH FOCAL PLANE Final Report, Jul. 1987 - Oct. 1988
Robert W. Astheimer Oct. 1988 29 p
(Contract DAAE07-87-C-R074)
(AD-A204694; TACOM-TR-13375) Avail: NTIS HC A03/MF A01 CSCL 17E

The vision block is essentially a window 8 in. wide, 2 in. high and 4 in. thick. Because of refraction, this gives a very wide (almost 90 deg) horizontal field of view, with a wide aperture which permits binocular vision over much of the field. It is impossible to achieve all these features with an intermediate focal plane within the space limitations. The design problem then is to make an optimum tradeoff among field of view, aperture and image quality, consistent with conforming to the 4 inch vision block dimensions and intended use. A unity-magnification telescope with an intermediate focal plane has been designed to fit into the outer housing of a standard No. 6300790 tank vision block. This has a 29 deg field of view with an exit pupil of 16 mm, at an eye relief of 70 mm. A slide permits insertion of test cells in the intermediate focal plane for evaluating laser protection devices. The intensity of an incident laser beam is increased by a factor of 50,000 at the intermediate focal plane. Two units have been built and tested. They show no degradation of normal vision over the entire focal plane. GRA

N89-23284# Oak Ridge Y-12 Plant, TN.
MACHINE REFERENCE MIRROR INSPECTION BY OPTICAL FABRY-PEROT CAVITY TESTING
R. C. Yoder, W. L. Goodwin, and G. K. Werner Jan. 1989 24 p
(Contract DE-AC05-84OS-21400)
(DE89-009635; Y-2402) Avail: NTIS HC A03/MF A01

The purpose of this endeavor was to design and validate an optical technique for measuring in situ the included dihedral angle of a pair of reference mirrors of a dual-YZ machine to a requested accuracy of 0.1 arc second. A whole-field optical test was investigated for application to this task; and optics were procured, characterized, and set up in a mockup machine test configuration. Data presented here were analyzed to validate the technique, and recommendations for its implementation are given. GRA

N89-23285# Lawrence Livermore National Lab., CA.
THERMAL BLOOMING THRESHOLD COMPUTATIONS WITH A MARKOV MODEL OF VELOCITY TURBULENCE
James A. Viecelli 30 Nov. 1988 49 p
(Contracts W-7405-eng-48; MIPR-W31RPD-7-D4041)
(DE89-009709; UCID-21589) Avail: NTIS HC A03/MF A01

A model of velocity turbulence based on first order Markov statistics is discussed. The coherence time of the scintillations in the optical intensity of a low power beam passing through the turbulence depends inversely on the root mean square amplitude of the velocity fluctuations. The relationship between coherence time and level of velocity turbulence is independent of both the velocity correlation length and the index structure constant. Application of the Markov model to atmospheric scintillation data yields estimates for the rms amplitude of velocity turbulence consistent with convective boundary layer theory. Computations of the optical field show that velocity turbulence introduces a threshold for stimulated thermal Rayleigh scattering. The threshold can be expressed in terms of a formula relating the limit on absorbed power to the rms amplitude of the velocity fluctuations. Above threshold the instability grows approximately exponentially reaching saturation after only a few waves of phase distortion have accumulated. Below threshold the instability is suppressed but there is a slow increase in the level of index turbulence caused by incoherent heating of the propagation medium. DOE

N89-23286# Lawrence Livermore National Lab., CA.
MEASUREMENTS OF OPTICAL LOSS IN TRANSPARENT SOLIDS USING A NOVEL SPECTROMETER BASED ON OPTICAL CAVITY DECAY
F. P. Milanovich, J. T. Hunt, and J. N. Roe 14 Dec. 1988 9 p Presented at the SPIE Symposium on Lasers and Optics, Los Angeles, CA, 15-20 Jan. 1989
(Contract W-7405-eng-48)
(DE89-009900; UCRL-100127; CONF-890142-4) Avail: NTIS HC A02/MF A01

Recent advances in High Average Power (HAP) solid state lasers and the development of new concept lasers with the potential of ultra-high average power output have put increasing demands on the transparency of optical window materials. To gain a better understanding of the current status of window materials and to direct research toward more nearly transparent materials, we have constructed an optical characterization facility with the purpose of making quantitative optical loss measurements in the sensitivity range of 10(-3) to 10(-6)/cm. . The cornerstone of this facility is a scanning optical lossmeter in which loss is determined by comparing the decay time of an optical cavity with and without a transparent solid present. The lossmeter has been successfully applied to measurements of the optical loss of witness samples of highly transparent fused silica. A description of the lossmeter and a compilation of preliminary loss measurements are presented here. DOE

N89-23287# Swedish Defence Research Establishment, Linkoeping. Dept. of Information Technology.
[ACTIVITIES REPORT OF THE DIVISION OF OPTICAL TECHNOLOGY (FOA 33)] Annual Report, fiscal year 1987/88
Dietmar Letalick, ed. Nov. 1988 21 p
(FOA-C-30507-3.1; ISSN-0347-3708; ETN-89-94307) Avail: NTIS HC A03/MF A01; Swedish Defence Research Establishment, P.O. Box 1165, S-581 11, Linkoeping, Sweden, 50 Swedish crowns

Research on hydro-optics; laser remote sensing; coherent CO2 laser radar; optical signatures; atmospheric transmission; ionizing radiation effects on electronics; fiber optics; optical processing; and terrain models is summarized. ESA

N89-23288# Limoges Univ. (France). Inst. de Recherches en Communications Optiques et Microondes.
STUDY OF LONG OPTICAL FIBERS Final Report
A. Barthelemy and C. Froehly Paris, France ESA 1989 45 p Partly in ENGLISH and FRENCH
(Contract ESTEC-6970/NL/IW(SC))
(ESA-CR(P)-2723; ETN-89-94455) Avail: NTIS HC A03/MF A01

Investigations of the distortions supported by wide bandwidth radiation after transmission across optical fibers a few meters long are presented. The potential of these optical fibers for the transport of coherent images is studied. The interference between two wide bandwidth waves of natural polarization transmitted by two fibers of the same optical length is analyzed. Applications to astronomical instrumentation are considered. The experimental analysis demonstrates the feasibility of a large base optical interferometer for the observation of astronomical sources of light. ESA

N89-23148# Martin Marietta Corp., Denver, CO.
GEOMETRIC CAMERA CALIBRATION USING SYSTEMS OF LINEAR EQUATIONS
Keith D. Gremban, Charles E. Thorpe, and Takeo Kanade (Carnegie-Mellon Univ., Pittsburgh, PA.) *In* Science Applications International Corp., Proceedings: Image Understanding Workshop, Volume 2 Apr. 1988 p 820-825 Previously announced in IAA as A89-11980 (For primary document see N89-23115 16-61)
(Contracts DACA76-85-C-0003; DACA76-84-C-0005; NSF DCR-84-19990; NSF DCR-86-04199)
Avail: NTIS HC A99/MF E03 CSCL 20F

75 PLASMA PHYSICS

Includes magnetohydrodynamics and plasma fusion.
For ionospheric plasmas see *46 Geophysics*. For space plasmas see *90 Astrophysics*.

N89-23289# Royal Inst. of Tech., Stockholm (Sweden). Dept. of Plasma Physics.
ANOMALOUS CROSS-FIELD VELOCITIES IN A CIV LABORATORY EXPERIMENT
Ingvar Axnaes Oct. 1988 21 p
(TRITA-EPP-88-06; ISSN-0348-7539) Avail: NTIS HC A03/MF A01

The axial and radial ion velocities and the electron radial velocity were determined in coaxial plasma gun operated under critical velocity conditions. The particle velocities were determined from probe measurements together with He I 3889 A absolute intensity measurements and the consideration of the total momentum balance of the current sheet. The ions were found to move axially and the electrons radially much faster than predicted by the Electrified/Magnetic Field (E/B) drift in the macroscopic fields. These results agree with what can be expected from the instability processes, which has earlier been proposed to operate in these experiments. It is therefore a direct experimental demonstration that instability processes have to be invoked not only for the electron heating, but also to explain the macroscopic velocities and currents. Author

N89-23290# General Atomics Technologies Corp., San Diego, CA.
H-MODE TRANSITION STUDIES IN DIII-D
T. N. Carlstrom, M. Shimada, K. H. Burrell, J. C. DeBoo, P. Gohil, R. J. Groebner, C. Hsieh, M. Matsumoto (Japan Atomic Energy Research Inst., Tokyo.), and P. Trost 1989 7 p Presented at the 16th European Conference on Controlled Fusion and Plasma Physics, Venice, Italy, 13-17 Mar. 1989
(Contract DE-AC03-84ER-51044; GA Proj. 3410)
(DE89-006913; GA-A-19564; CONF-890302-12) Avail: NTIS HC A02/MF A01

Determining the conditions necessary for the H-transition is important not only for scaling this important confinement regime to future machines but also to aid the understanding of H-mode physics with the hope of further exploiting H-mode confinement. We have done systematic scans of 1 sub P, bar n sub e, B sub T, and the X-point to divertor plate distance delta, in single-null diverted discharges, to ascertain their influence on the threshold power required for the L-H transition. During each of these scans, the neutral beam power was increased in a staircase fashion and the power required for the transition was noted. Over the ranges of: 1 less than 1 sub P (MA) less than 2, 1 less than B sub T (T) less than 2, 3 less than bar n sub e (10(19) m sup -3) less than 8, and 1 less than delta (cm) less than 23, the threshold power scales as bar n sub e B sub T, independent of 1 sub P, and is reduced when delta is small. This method also provided an L-mode power scan over the various plasma conditions, in which we looked for changes in the L-mode plasma, particularly in the edge region, that might trigger the H-transition. Over the range of conditions studied, we found that T sub e (r/a = 0.97)/B sub T approached a critical value before each L-H transition. Various theories have been put forth to explain the bifurcation observed at the L-H transition. We show that the prediction of several of these theories are inconsistent with the observations on DIII-D. DOE

N89-23291# Argonne National Lab., IL. Fusion Power Program.
MAXIMAL BOOTSTRAP CURRENT TOKAMAK EQUILIBRIA IN THE FIRST STABILITY REGIME
David A. Ehst and Kenneth Evans, Jr. Jan. 1989 31 p
(Contract W-31-109-eng-38)
(DE89-008201; ANL/FPP/TM-235) Avail: NTIS HC A03/MF A01

A series of tokamak equilibria are studied in order to identify characteristics which may maximize the proportion of toroidal current naturally provided by the bootstrap effect. These plasmas are typical of high field reactors considered by the ARIES (Advanced Reactor Innovation and Evaluation Study) collaboration and are assumed to have rather flat density profiles and broad pressure profiles. With the use of noninductive current drive to provide the seed current it is possible to operate with q sub axis approx. = 2.0; this results in a (bootstrap assissted) current drive power of P sup B sub CD - 117 MW and a figure of merit sub gamma sup B = 1.12 for reference reactor with bar T sub e approx. = 21 keV. For the reference reactor P sub f = 2880 MW so Q = 24. Without the bootstrap effect the absorbed current drive power would be P sub CD = 285 MW, so T equivalent to 1 - (sub gamma/sub gamma sup B) = 0.59. DOE

N89-23292# Lawrence Livermore National Lab., CA.
COMPUTATION OF LOWER HYBRID, NEUTRAL BEAM AND BOOTSTRAP CURRENTS IN CONSISTENT MHD EQUILIBRIA
R. S. Devoto, D. T. Blackfield, M. E. Fenstermacher, P. T. Bonoli, and M. Porkolab (Massachusetts Inst. of Tech., Cambridge.) 1 Feb. 1989 6 p Presented at the 16th European Conference on Controlled Fusion and Plasma Physics, Venice, Italy, 13 Mar. 1989
(Contract W-7405-eng-48)
(DE89-008892; UCRL-99981; CONF-890302-19) Avail: NTIS HC A02/MF A01

A possible scenario for steady state current drive in large, high- temperature tokamaks includes current driven by lower hybrid (LH) waves in the outer region with high-energy neutral beams (NB) used for current drive in the core. In addition, provided the poloidal beta is sufficiently high, there can be substantial bootstrap (BS) current, as observed in the TFTR and JET experiments. In work reported previously, a computer code, ACCOME, was written to obtain a solution to the MHD equations which is consistent with current driven by neutral beams, electric fields, and neoclassical (bootstrap) effects. For the computation of the solution to the Grad-Shafranov equation, the SELENE code is used. Iteration is necessary between SELENE and the current-drive computations to obtain a consistent solution. In this paper we describe modifications to ACCOME to enable the computation of LH current in addition to the NB, BS, and OH currents. The next section describes the models used and then the final section presents an application to ITER. DOE

N89-23293# Oxford Univ. (England). Dept. of Engineering Science.
BOUNDARIES AND PROBES IN ELECTRONEGATIVE PLASMAS
N. St. J. Braithwaite and J. E. Allen 1986 13 p
(OUEL-1636/86; ETN-89-94207) Avail: NTIS HC A03/MF A01

A simple model of a low pressure plasma containing two (or more) negative species (e.g., electron and negative ion) and one positive species is treated. Both negative species are described by assuming a thermal equilibrium between each and any electric potential, giving a two temperature description (T(e) and T(-)). The results have much in common with two electron temperature plasma models (Wickens and Allen, 1978). The positive ion is presumed to be significantly colder than the hotter negative particle and although T(+) may be referred to, positive ion dynamics do not include thermal effects. The main concern is to recover information about the relative particle concentration from currents

collected at a probe electrode; the plasma boundary is therefore generally of interest. A criterion for sheath formation (Bohm criterion, (Bohm, 1949)), space potential in the pre-sheath and negative/positive saturation currents is considered. ESA

N89-23294# Lawrence Livermore National Lab., CA.
FUSION POWER: EXPECTED ENVIRONMENTAL CHARACTERISTICS AND STATUS OF R AND D
T. Kenneth Fowler 24 Mar. 1989 16 p Presented at the International Energy Agency/Organization for Economic Cooperation and Development Expert Seminar on Energy Technologies for Reducing Emissions of Greenhouse Gases, Paris, France, 12 Apr. 1989
(Contract W-7405-eng-48)
(DE89-009232; UCRL-100623; CONF-8904158-1) Avail: NTIS HC A03/MF A01

From the outset in the 1950's, fusion research has been motivated by environmental concerns as well as long-term fuel supply issues. Compared to fossil fuels both fusion and fission would produce essentially zero emissions to the atmosphere. Compared to fission, fusion reactors should offer high demonstrability of public protection from accidents and a substantial amelioration of the radioactive waste problem. Fusion still requires lengthy development, the earliest commercial deployment being likely to occur around 2025 to 2050. However, steady scientific progress is being made and there is a wide consensus that it is time to plan large-scale engineering development. A major international effort, called the International Thermonuclear Experimental Reactor (ITER), is being carried out under IAEA auspices to design the world's first fusion engineering test reactor, which could be constructed in the 1990's. DOE

N89-23295# California Univ., Los Angeles. Dept. of Mechanical, Aerospace and Nuclear Engineering.
A FAST SPATIAL SCANNING COMBINATION EMISSIVE AND MACH PROBE FOR EDGE PLASMA DIAGNOSIS
R. D. Lehmer, B. LaBombard, and R. W. Conn Apr. 1989 76 p
(Contract DE-FG03-86ER-52134)
(DE89-009674; UCLA/PPG-1228) Avail: NTIS HC A05/MF A01

A fast spatially scanning emissive and Mach probe has been developed for the measurement of plasma profiles in the PISCES facility at UCLA. A pneumatic cylinder is used to drive a multiple tip probe along a 15 cm stroke in less than 400 msec, giving single shot profiles while limiting power deposition to the probe. A differentially pumped sliding O-ring seal allows the probe to be moved between shots to infer two and three dimensional profiles. The probe system has been used to investigate the plasma potential, density, and parallel Mach number profiles of the presheath induced by a wall surface and scrape-off-layer profile modifications in biased limiter simulation experiments. Details of the hardware, data acquisition electronics, and tests of probe reliability are discussed. DOE

N89-23296# Lodestar Research Corp., Boulder, CO.
A QUIVER KINETIC FORMULATION OF RADIO FREQUENCY HEATING AND CONFINEMENT IN COLLISIONAL EDGE PLASMAS
Peter J. Catto and J. R. Myra Jan. 1989 47 p
(Contract DE-FG02-88ER-53263)
(DE89-009675; DOE/ER-53263/2; LRC-89-3) Avail: NTIS HC A03/MF A01

The near fields in the collisional edge plasma of a radio frequency heated tokamak can cause one or more charged species to oscillate in the applied field with a quiver (or jitter) speed comparable to its thermal speed. By assuming the quiver motion dominates over drifts and gyromotion a completely new kinetic description of the flows in an edge plasma is formulated which retains Coulomb collisions and the relevant atomic processes. Moment equations are employed to obtain a description in which only a lowest order quiver kinetic equation need be solved to evaluate the slow time particle fluxes and current induced by the applied fields. The electron heating by collisional randomization of their quiver motion (inverse bremsstrahlung) is balanced by impact excitation losses since equilibration with the ions is too weak. A model plasma of electrons, neutrals, and a single cold ion species is considered to illustrate the utility of the quiver kinetic formulation. The model predicts local electrostatic potential changes and a local rvec E x rvec B convective flux that is of the same magnitude and scaling as would be predicted by Bohm diffusion. DOE

N89-23297# Mission Research Corp., Los Alamos, NM.
THEORETICAL AND COMPUTATIONAL STUDIES OF PLASMA OPENING SWITCHES
Erick L. Lindman, Jr. and Joseph M. Kindel Feb. 1989 187 p
(Contract DE-AC04-76DP-00789)
(DE89-009712; SAND-88-7154) Avail: NTIS HC A09/MF A01

Substantial progress has been made in understanding the operation of plasma opening switches (POS) in support of the Light-Ion Fusion Program at Sandia National Laboratories. Our efforts began with scoping studies using the particle-in-cell (PIC) code, MAGIC, which was written by Bruce Goplen and co-workers at MRC for pulsed-power applications. The version of MAGIC currently at Sandia National Laboratories is supported by Dave Seidel and Tim Pointon. MAGIC continues to play an important role as our studies moved into many different areas. Working closely with Cliff Mendel, we performed initial studies of switches using his fast B sub z concept. Working with Mary Ann Sweeney, Jeff Quintez and Cliff Mendel we performed studies of the effects of plasma density, cylindrical curvature, load impedance, rise time, and emission threshold on switch performance. In addition, we studied B-field penetration, turbulence, anomalous resistivity, and electron heating in plasma opening switches. This work has allowed us to identify the physical mechanisms that are important in the operation of plasma opening switches. Based on our knowledge of the physics we have established scaling relations for comparable switch performance under different experimental conditions. We studied the code requirements for POS simulation and numerical problems in MAGIC and in other PIC codes. And, more recently, we have begun to participate more strongly in the experimental program being carried out on PBFA II. Our conclusions based on these studies are summarized here. DOE

N89-23298# Oak Ridge National Lab., TN.
BINARY AND TERNARY GAS MIXTURES FOR USE IN GLOW DISCHARGE CLOSING SWITCHES Patent Application
Scott R. Hunter, inventor (to DOE) and Loucas G. Christophorou, inventor (to DOE) 27 Apr. 1988 20 p
(Contract DE-AC05-84OR-21400)
(DE89-009718; PATENTS-US-A7186856;
US-Patent-Appl-SN-186856) Avail: NTIS HC A03/MF A01

Highly efficient binary and ternary gas mixtures for use in diffuse glow discharge closing switches are disclosed. The binary mixtures are combinations of helium or neon and selected perfluorides. The ternary mixtures are combinations of helium, neon, or argon, a selected perfluoride, and a small amount of gas that exhibits enhanced ionization characteristics. These mixtures are shown to be the optimum choices for use in diffuse glow discharge closing switches by virtue of the combined physio-electric properties of the mixture components. DOE

N89-23299# Swedish Inst. of Space Physics, Uppsala.
A FLUID FLR MODEL OF THE MAGNETOPAUSE LAYER
K. Stasiewicz Nov. 1988 21 p
(IRF-Preprint-109; ISSN-0284-1711; ETN-89-94320) Avail: NTIS HC A03/MF A01

A model of the magnetopause current layer is constructed on the basis of fluid equations for collision-free plasmas with finite ion Larmor radius (FLR). The model provides self-consistent solutions for the plasma flow vector, magnetic field, and electric currents inside the magnetopause layer. It is shown that the erosion of the dayside magnetosphere can be explained by the normal component of the gyroviscous stress tensor that is related to the intensity of field-aligned currents inside the magnetopause layer. It is found that the sense of rotation of the magnetic field across the magnetopause is determined by the ratio of the normal

component of the Alfven velocity to the normal flow velocity. For a ratio larger than 1, the sense of rotation corresponds to electron polarization; ratio smaller than 1 yields proton polarization. It is argued that the case where the ratio = 1 corresponds to the formation of transient flux transfer events. The observed departures from MHD jump conditions across the magnetopause are explained by additional, finite Larmor radius terms in the moment equations. An expression for the characteristic thickness of the magnetopause layer is derived. ESA

N89-23300*# Information and Control Systems, Inc., Hampton, VA.
DEVELOPMENT AND SIMULATION STUDY OF A NEW INVERSE-PINCH HIGH COULOMB TRANSFER SWITCH Final Report
Sang H. Choi May 1989 42 p
(Contract NAS1-17685)
(NASA-CR-181768; FR-688102; NAS 1.26:181768) Avail: NTIS HC A03/MF A01 CSCL 20I

The inverse-pinch plasma switch was studied using a computer simulation code. The code was based on a 2-D, 2-temperature magnetohydrodynamic (MHD) model. The application of this code was limited to the disk-type inverse-pinch plasma switch. The results of the computer analysis appear to be in agreement with the experimental results when the same parameters are used. An inverse-pinch plasma switch for closing has been designed and tested for high-power switching requirements. An azimuthally uniform initiation of breakdown is a key factor in achieving an inverse-pinch current path in the switch. Thus, various types of triggers, such as trigger pins, wire-brush, ring trigger, and hypocycloidal-pinch (HCP) devices have been tested for uniform breakdown. Recently, triggering was achieved by injection of a plasma-ring (plasma puff) that is produced separately with hypocycloidal-pinch electrodes placed under the cathode of the main gap. The current paths at switch closing, initiated by the injection of a plasma-ring from the HCP trigger are azimuthally uniform, and the local current density is significantly reduced, so that damage to the electrodes and the insulator surfaces is minimized. The test results indicate that electron bombardment on the electrodes and the insulator surfaces is minimized. The test results indicate that electron bombardment on the electrodes is four orders of magnitude less than that of a spark-gap switch for the same switching power. Indeed, a few thousand shots with peak current exceeding a mega-ampere and with hold-off voltage up to 20 kV have been conducted without showing measurable damage to the electrodes and insulators. Author

N89-23301# Naval Research Lab., Washington, DC.
SIMULATIONS OF AXISYMMETRIC EROSION IN IFR-TRANSPORTED BEAMS Interim Report
Jonathan Krall, Khanh Nguyen, and Glenn Joyce 21 Feb. 1989 37 p Prepared in cooperation with Science Applications International Corp., McLean, VA
(AD-A205882) Avail: NTIS HC A03/MF A01 CSCL 20I

Erosion rates for relativistic electron beam propagating through low density plasma channel in the ion-focused regime are computed via axisymmetric particle simulation. We find steady-state inductive (ohmic) erosion rates that are in quantitative agreement with new theoretical results which correctly account for the relativistic dynamics of electrons at the beam head. In cases where the finite emittance of the beam is expected to be the dominant loss mechanism, the beam does not develop steady-state erosion, as suggested by previous analyses. Asymptotically, such a beam is characterized by a low emittance population at the beam head, a long rise length, and an erosion rate that tends toward zero. GRA

76 SOLID-STATE PHYSICS

Includes superconductivity.

For related information, see also *33 Electronics and Electrical Engineering* and *36 Lasers and Masers.*

N89-23302*# Howard Univ., Washington, DC.
EVALUATION, DEVELOPMENT, AND CHARACTERIZATION OF SUPERCONDUCTING MATERIALS FOR SPACE APPLICATION Semiannual Progress Report No. 2
A. N. Thorpe Jan. 1989 54 p
(Grant NAG5-1017)
(NASA-CR-184842; NAS 1.26:184842) Avail: NTIS HC A04/MF A01 CSCL 20L

Results are reported of low magnetic field studies of dc magnetic susceptibility and ac magnetic susceptibility of bulk samples and powders. These data are analyzed and compared with the microstructures and compositions of the samples as determined by scanning electron microscopic micrographs, X-ray and chemical analysis. Particular emphasis is given to the interpretation of the ac magnetic susceptibility data which were obtained as function of the magnitude and frequency of the ac measuring field, and low values of an applied dc magnetic field. Two general conclusions are given and briefly discussed. E.R.

N89-23303# Air Force Inst. of Tech., Wright-Patterson AFB, OH. School of Engineering.
TIME RESOLVED PHOTOLUMINESCENCE OF YTTERBIUM IN INDIUM PHOSPHIDE M.S. Thesis
Thad F. Bumgarner Dec. 1988 117 p
(AD-A202596; AD-E900870; AFIT/GEP/ENP/88D-1) Avail: NTIS HC A06/MF A01 CSCL 07B

Time resolved photoluminescence of ytterbium (Yb) implanted in indium phosphide (Inp) was the primary emphasis of this research. The decay lifetimes of the 1002 nm Yb emission were investigated as a function of temperature. Initial attempts were made to investigate as a function of temperature. Initial attempts were made to investigate aluminum gallium arsenide (AlGaAs) implanted with ytterbium. GRA

N89-23304# Air Force Inst. of Tech., Wright-Patterson AFB, OH. School of Engineering.
EFFECTS OF DIFFERENT FABRICATION TECHNIQUES ON THE YTTRIUM-BARIUM-COPPER OXIDE HIGH TEMPERATURE SUPERCONDUCTOR M.S. Thesis
Paul A. Rhea Dec. 1988 110 p
(AD-A202598; AD-E900870; AFIT/GE/ENG/88D-42) Avail: NTIS HC A06/MF A01 CSCL 20C

This study examines how several different parameters were changed in the yttrium-barium-copper oxide superconductor when the fabrication techniques were altered by using different barium precursors, including barium peroxide and barium carbonate; sintering at different temperatures, including 850, 900, 950 C; and annealing in an above ambient oxygen environment. Twelve different pellets were fabricated, and measurements were taken on them which included density, X-ray diffraction, critical temperature, critical current density, and magnetic susceptibility. The results showed that the barium peroxide derived samples had higher densities, better critical current densities and lower resistivities in the normal state. GRA

N89-23305# Harvard Univ., Cambridge, MA. Div. of Applied Sciences.
QUANTUM PHENOMENA IN MESOSCOPIC SUPERCONDUCTING TUNNEL JUNCTIONS Technical Report No. 27
Marco Iansiti Dec. 1988 186 p
(Contracts N00014-83-K-0383; N00014-84-K-0465; NSF DMR-84-04489)
(AD-A203354) Avail: NTIS HC A09/MF A01 CSCL 09A

We report a low temperature study of very small superconducting tunnel junctions. The samples were fabricated by using electron-beam lithography and thermal evaporation in single-junction, double-junction and eleven-junction-array

configurations. The junctions had normal resistances between 0.5 and 140 kilo-ohms and areas between 0.1 and 0.02 sq micron. We measured the current-voltage characteristics of the devices at low temperatures (20 mk -4 K), using a dilution refrigerator. In general, the devices had a large single electron charging energy E(c) is identical to sq e /2c of order 1 K. By varying the ratio of E(c) to the Josephson coupling energy E(j), we studied the crossover between the conventional Josephson regime, in which E(j) much greater than E(c), and the Coulomb blockade regime, in which charging effects are dominant. For comparable charging and Josephson energies the 1 to 5 curve is resistive at all currents, and exhibits a novel low-voltage resistance R(o) at currents less than the critical current 1c. GRA

N89-23306*# Alabama Univ., Huntsville. Center for Microgravity and Materials Research.
NOVEL PROTEIN CRYSTAL GROWTH TECHNOLOGY: PROOF OF CONCEPT Final Report, 1 Dec. 1987 - 31 Mar. 1989
Thomas A. Nyce and Franz Rosenberger 31 Mar. 1989 33 p
(Grant NAG8-98)
(NASA-CR-184959; NAS 1.26:184959) Avail: NTIS HC A03/MF A01 CSCL 20L

A technology for crystal growth, which overcomes certain shortcomings of other techniques, is developed and its applicability to proteins is examined. There were several unknowns to be determined: the design of the apparatus for suspension of crystals of varying (growing) diameter, control of the temperature and supersaturation, the methods for seeding and/or controlling nucleation, the effect on protein solutions of the temperature oscillations arising from the circulation, and the effect of the fluid shear on the suspended crystals. Extensive effort was put forth to grow lysozyme crystals. Under conditions favorable to the growth of tetragonal lysozyme, spontaneous nucleation could be produced but the number of nuclei could not be controlled. Seed transfer techniques were developed and implemented. When conditions for the orthorhombic form were tried, a single crystal 1.5 x 0.5 x 0.2 mm was grown (after in situ nucleation) and successfully extracted. A mathematical model was developed to predict the flow velocity as a function of the geometry and the operating temperatures. The model can also be used to scaleup the apparatus for growing larger crystals of other materials such as water soluble non-linear optical materials. This crystal suspension technology also shows promise for high quality solution growth of optical materials such as TGS and KDP. Author

N89-23307# California Univ., Berkeley. Lawrence Berkeley Lab. Materials and Chemical Sciences Div.
ELECTRON ENERGY-LOSS SPECTROSCOPY: FUNDAMENTALS AND APPLICATIONS IN THE CHARACTERIZATION OF MINERALS
Kannan M. Krishnan Nov. 1988 32 p Presented at the ACS Meeting on Structures and Active Sites of Minerals, Los Angeles, CA, 28 Sep. 1988
(Contract DE-AC03-76SF-00098)
(DE89-006613; LBL-26222; CONF-8809291-1) Avail: NTIS HC A03/MF A01

The combined use of an energy-loss spectrometer and an analytical electron microscope with fine probe forming capabilities provides a wealth of information about the sample at high spatial resolution. Fundamental principles governing the physics of the interaction between the fast electron and a thin foil sample, to account for the fine structure in the inelastically scattered fast electron distribution (EELS), will be reviewed. General application of EELS is in the area of low atomic number elements (Z is less than 11) microanalysis, where it significantly complements the more widely used EDX spectroscopy. However, a careful analysis of the low loss plasmon oscillations and the fine structure in the core-loss edges, can provide additional information related to the bonding and electronic structure of the sample. An illustration of this is presented from our study of C delta diamond residue from the Allende carbonaceous chondrite. Combination of EELS with channeling effects can provide specific site occupation/valence information in crystalline materials. Details of this novel crystallographic method will be outlined and illustrated with an example of the study of chromite spinels. DOE

N89-23308# Argonne National Lab., IL.
PHYSICAL PROPERTIES OF GRAIN-BOUNDARY MATERIALS: COMPARISON OF EAM (EMBEDDED-ATOM-METHOD) AND CENTRAL-FORCE POTENTIALS
D. Wolf, J. F. Lutsko, and M. Kluge Oct. 1988 19 p Presented at the Atomistic Modelling in Materials - Beyond Pair Potentials, Chicago, IL, 27 Sep. 1988
(Contract W-31-109-eng-38)
(DE89-007414; CONF-8809215-5) Avail: NTIS HC A03/MF A01

Three types of grain-boundary phenomena expected to be particularly sensitive functions of a local-volume dependence in the interatomic interaction potentials employed are investigated by means of many-body (embedded-atom and Finnis-Sinclair) and pair potentials. These phenomena are the zero-temperature volume expansion localized at the grain boundaries, the local elastic constants of grain-boundary materials, and their high-temperature stability. The same qualitative behavior is found in all these phenomena for both types of potentials, from which it is concluded that the local-volume dependence, incorporated in the many-body potentials only, does not have a strong effect on the predicted properties of grain-boundary materials. The reasons for these similarities are thought to arise from the fact that most grain-boundary properties are governed, as are those of liquids, by atoms in very close contact; i.e., by the short-range part of the interatomic potential which is of a central-force type in both sets of potentials. However, many-body potentials are expected to represent a given material better than pair-potentials since (1) they usually permit a larger number of adjustable parameters to be fitted to real-material properties, and (2) in contrast to equilibrium pair-potentials they do not satisfy the Cauchy relation. DOE

N89-23309# Argonne National Lab., IL. Materials Science Div.
GRAIN-BOUNDARY AND FREE-SURFACE INDUCED THERMODYNAMIC MELTING: A MOLECULAR DYNAMICS STUDY IN SILICON
S. R. Phillpot, J. F. Lutsko, D. Wolf, and S. Yip Oct. 1988 8 p Presented at the Atomistic Modelling in Materials - Beyond Pair Potentials, Chicago, IL, 27 Sep. 1988
(Contract W-31-109-eng-38)
(DE89-007415; CONF-8809215-4) Avail: NTIS HC A02/MF A01

Molecular dynamics simulations in silicon show that thermodynamic melting is rapidly nucleated at a grain boundary and at a free surface. Such an observation is entirely consistent with experiment. DOE

N89-23310# Stanford Univ., CA. Dept. of Applied Physics.
LOW FREQUENCY RESISTANCE FLUCTUATIONS IN FILMS OF HIGH TEMPERATURE SUPERCONDUCTORS
P. Rosenthal, R. H. Hammond, M. R. Beasley, R. Leoni, P. Lerch, and J. Clarke (California Univ., Berkeley.) Aug. 1988 5 p Presented at the Applied Superconductivity Conference, San Francisco, CA, 21 Aug. 1988 Prepared in cooperation with California Univ., Berkeley, Lawrence Berkeley Lab.
(Contract DE-AC03-76SF-00098)
(DE89-007489; LBL-26235; CONF-880812-41) Avail: NTIS HC A02/MF A01

Low frequency voltage fluctuations in thin films of YBa2Cu7O7-x at and above the superconducting transition have a spectral density S sub v (f) proportional to bar V squared/f, where bar V is the average voltage across the film and f is the frequency. The value of S sub v (f)/bar V squared decreases markedly as the microstructure of the films is improved. In contrast to classic superconductors, the noise at the resistive transition does not arise from equilibrium temperature fluctuations. DOE

N89-23311# California Univ., Berkeley. Lawrence Berkeley Lab. Dept. of Physics.
NUCLEAR MAGNETIC RESONANCE WITH dc SQUID (SUPER-CONDUCTING QUANTUM INTERFERENCE DEVICE) PREAMPLIFIERS
N. Q. Fan, Michael B. Heaney, John Clark, D. Newitt, Lawrence L. Wald, Erwin L. Hahn, A. Bierlecki, and A. Pines Aug. 1988 9 p Presented at the Applied Superconductivity Conference, San Francisco, CA, 21 Aug. 1988 Prepared in cooperation with California Univ., Berkeley, Lawrence Berkeley Lab.
(Contract DE-AC03-76SF-00098)
(DE89-007657; LBL-26234; CONF-880812-42) Avail: NTIS HC A02/MF A01

Sensitive radio-frequency (RF) amplifiers based on dc Superconducting QUantum Interface Devices (SQUIDS) are available for frequencies up to 200 MHz. At 4.2 K, the gain and noise temperature of a typical tuned amplifier are 18.6 + or - 0.5 dB and 1.7 + or - 0.5 K at 93 MHz. These amplifiers are being applied to a series of novel experiments on nuclear magnetic resonance (NMR) and nuclear quadrupole resonance (NQR). The high sensitivity of these amplifiers was demonstrated in the observation of nuclear spin noise, the emission of photons by Cl-35 nuclei in a state of zero polarization. In the more conventional experiments in which one applies a large RF pulse to the spins, a Q-spoiler, consisting of a series array of Josephson junctions, is used to reduce the Q of the input circuit to a very low value during the pulse. The Q-spoiler enables the circuit to recover quickly after the pulse, and has been used in an NQR experiment to achieve a sensitivity of about 2 x 10(16) nuclear Bohr magnetons in a single free precession signal with a bandwidth of 10 kHz. In a third experiment, a sample containing Cl-35 nuclei was placed in a capacitor and the signal detected electrically using a tuned SQUID amplifier and Q-spoiler. In this way, the electrical polarization induced by the precessing Cl nuclear quadrupole moments was detected: this is the inverse of the Stark effect in NQR. Two experiments involving NMR have been carried out. In the first, the 30 MHz resonance in Sn-119 nuclei is detected with a tuned amplifier and Q-spoiler, and a single pulse resolution of 10(18) nuclear Bohr magnetons in a bandwidth of 25 kHz has been achieved. For the second, a low frequency NMR system has been developed that uses an untuned input circuit coupled to the SQUID. The resonance in Pt-195 nuclei has been observed at 55 kHz in a field of 60 gauss. DOE

N89-23312# Columbia Univ., New York, NY. Dept. of Electrical Engineering.
MOLECULAR BEAM EPITAXIAL GROWTH AND CHARACTERIZATION OF METASTABLE COMPOUND SEMICONDUCTORS FOR INFRARED DETECTOR APPLICATIONS Annual Technical Report, 1 Feb. - 31 Oct. 1988
Wen I. Wang 25 Nov. 1988 7 p
(Grant AF-AFOSR-0126-88; AF Proj. 2306)
(AD-A205175; AFOSR-89-0092TR) Avail: NTIS HC A02/MF A01 CSCL 20L

Device quality narrow gap materials is discussed. During this sinitial phase, all the fundamental work necessary for future achievement of high quality metastable materials were completed. The growth of all the various buffer layer materials such as InAs, InSb, GaSb, and A1Sb, the calibration of the Auger system for quick feedback of alloy composition, and the in-situ Reflected High-Energy Diffraction (RHEED) oscillation calibration of growth rate are included. During this buffer layer studies, it was found that the growth of InAs and A1Sb are compatible in the temperature range of 450 to 500 C. AlSb/InAs/AlSb double range of 450 to 500 C. AlSb/InAs/AlSb double -barrier resonant tunneling structures therefore were grown and measured. Peak-to-valley ratios of 1.8:1 at room temperature and 9:1 at 77K were measured. Most importantly, the small effective mass of InAs makes it possible to demonstrate quantum effects in a 24 nm well, the longest coherent distance ever reported for double-barrier tunneling structures. It was estimated that an AlSb/InAs resonant tunneling transistor can significantly outperform similar devices based on A1GaAs/GaAs. GRA

N89-23313# Massachusetts Inst. of Tech., Cambridge.
DEVELOPMENT OF MAGNETIC FIELD ASSISTED MELT STABILIZATION WITH HEAT AND MASS TRANSFER CONTROL IN LOW PRESSURE LEC GROWTH OF GaAs Final Report, Mar. 1984 - Jul. 1987
S. Motakef, A. T. Patera, G. Stephanopoulos, J. Szekely, and A. F. Witt Oct. 1988 101 p
(Contract F33615-83-C-5089)
(AD-A205185; AFWAL-TR-88-4176) Avail: NTIS HC A06/MF A01 CSCL 20B

This research effort permits operation on a scale compatible with industry and establishes the basis for advanced science and technology transfer in the area of bulk crystal growth of elemental and compound semiconductors. It led to the development of a computer controlled, model-based magnetic LP-LEC facility for growth of GaAs at diameters in excess of 3 inches. In conjunction, a thermal imaging system was created which permits monitoring and control of the growth process as well as, from video-tape, the post-growth analysis of thermal field distribution and its changes. This capability makes it possible to analyze for correlations between the thermal history of a semiconductor and its properties. The imaging system is also an essential element for monitoring the effectiveness of heat transfer control and the viability of model-based feedforward growth control. The crystal growth research provided the background for major advances in our ability to characterize qualitatively on a micro- and macroscale the free charge carrier distribution (dopant distribution) in semiconductors. The opto-analytical approach taken provides for quantitative analyses of unprecedented spatial resolution and sensitivity within seconds and thus appears ideally suited for transfer to technology. GRA

N89-23314# Argonne National Lab., IL. Chemistry Div.
ESE (ELECTRON SPIN ECHO) AND CW-ESR STUDIES OF SYNTHETIC DIAMOND CRYSTALS: DISTRIBUTION OF NITROGEN AND NICKEL
J. Isoya, C. P. Lin, M. K. Bowman, J. R. Norris, S. Yazu, and S. Sato (Sumitomo Electric Industries Ltd., Itami, Japan) 1988 12 p Presented at the 1st International Conference on the New Diamond Science and Technology, Tokyo, Japan, 24 Oct. 1988
(Contract W-31-109-eng-38)
(DE89-007373; CONF-8810318-1) Avail: NTIS HC A03/MF A01

Both dispersed impurities and dispersed nickel impurities in synthetic type 1b diamond crystals give distinctive ESR spectra. We demonstrate that inhomogeneities in the distribution of the nitrogen and the nickel impurities can be characterized by instantaneous spectral diffusion measurements in two-pulse electron spin echo measurements. In a series of thirteen synthetic crystals, most (less than 90 percent) of the nitrogen centers are in regions with high local concentration. The remainder is present in regions of lower concentration. DOE

N89-23315# International Centre for Theoretical Physics, Trieste (Italy).
PERTURBATIVE TREATMENT OF LOCAL CORRELATIONS IN Cu-0 PLANES FOR HIGH TEMPERATURE SUPERCONDUCTORS
V. Zlatic, P. Entel, B. Horvatic, and D. Schulz Jul. 1988 16 p
(Grant JFP-NSF-707)
(DE88-705648; IC-88/122) Avail: NTIS (US Sales Only) HC A03/MF A01

Useful information about the high temperature superconductors might be obtained by studying the low-dimensional models in which the interplay between the short-range correlations and the geometry of the electron motion is taken into account. Here the short-range correlations are treated as a perturbation to 2-dimensional Cu-0 electrons. After defining the model Hamiltonian, the properties of the unperturbed part are briefly discussed and the perturbation expansions for various physical quantities are formulated. The

low-order expressions for the self-energy, the magnetic susceptibility and the pair correlation function are presented which should, in principle, allow a systematic study of the effects of the Coulomb interactions on the properties of the model. DOE

N89-23316# International Centre for Theoretical Physics, Trieste (Italy).
THEORETICAL STUDY OF THE Pd-B COMPLEX IN SILICON
Jian Wu, Zhou Jie, and Daren Zhang (Academia Sinica, Beijing, China) Jul. 1988 10 p
(DE88-705650; IC-88/159) Avail: NTIS (US Sales Only) HC A02/MF A01

We report the results for the electronic structure of the interstitial Pd-substitutional B complex in silicon. The self-consistent field calculations were performed within the framework of scattered-wave X alpha cluster method. Compared with the electronic structures of the isolated substitutional B in silicon and of the isolated interstitial Pd in silicon, we found that the shallow acceptor B impurity state is deepened by the perturbation from the Pd atom. The ionic model, which is currently accepted to describe interstitial 3d transition metal-3A group shallow acceptor impurity pair, is not quite suitable to deal with the system of Pd-B complex in silicon. DOE

N89-23317# International Centre for Theoretical Physics, Trieste (Italy).
ELECTRONIC PROPERTIES OF Ge SUB 1-x Si SUB x: A SIMPLIFIED TIGHT BINDING APPROACH
H. Gumus and Caglar Tuncay (Middle East Technical Univ., Ankara, Turkey) Sep. 1988 13 p Submitted for publication
(DE88-705671; IC-88/278) Avail: NTIS (US Sales Only) HC A03/MF A01

A simple method to predict the electronic properties of covalent materials will be outlined and applied to the alloy of Ge-Si. The method does not involve band structure calculations but gives equivalent results, and it can easily be generalized for compound alloys as well as to probe pressure effects on elements and on binary and compound alloys. DOE

N89-23318# International Centre for Theoretical Physics, Trieste (Italy).
ELECTRONIC STRUCTURE OF RARE-EARTH LUMINESCENT CENTRE IN ALKALINE-EARTH SULPHIDES
Qingqi Zheng, Wei Pan, Maichun Huang, and Xiaoguang He (Xiamen Univ., China) Sep. 1988 14 p
(DE88-705674; IC-88/281) Avail: NTIS (US Sales Only) HC A03/MF A01

The cluster method is used to investigate the electronic structure of rare-earth Eu(2+) and Ce(3+) doped SrS and CaS alkaline-earth sulphides in the local density theory regime. The ground state is obtained self-consistently by the DV-X sub alpha method, while the transition state theory is used to calculate the excited states. The energy difference between ground state and excited state is 2.95 eV (420 nm) for CaS:Eu is in good agreement with the experimental data of 430 nm for the absorption peak in SrS:Cu. The composition of ground state and excited state is also calculated which can give information about the EL excitation mechanism. DOE

N89-23319# International Centre for Theoretical Physics, Trieste (Italy).
INVESTIGATION OF THE VACUUM STRUCTURE OF THE GEORGI-GLASHOW MODEL ON THE LATTICE
V. G. Bornyakov, E. M. Ilgenfritz, V. K. Mitrjushkin, A. M. Zadorozhny, and M. Mueller-Preussker (Humboldt Univ., Berlin, German D.R.) Aug. 1988 26 p
(DE88-705676; IC-88/283) Avail: NTIS (US Sales Only) HC A03/MF A01

Distributions and correlations of magnetic fluxes as well as correlations between magnetic fluxes and other local observables are calculated numerically in order to explain the phase structure of the 4D Georgi-Glashow model on the lattice. We use and compare different definitions of magnetic fluxes. The data suggest a simple picture characterizing typical magnetic fluctuations in different regions of the phase space. A relaxation procedure exposes Abelian monopole-loop configurations in one of the phases. DOE

N89-23320# International Centre for Theoretical Physics, Trieste (Italy).
ELECTRONIC PROPERTIES OF Ge(1-X)Si(X): ALLOYING VERSUS PRESSURE
Caglar Tuncay (Middle East Technical Univ., Ankara, Turkey) Sep. 1988 19 p
(DE88-705678; IC-88/287) Avail: NTIS (US Sales Only) HC A03/MF A01

The electronic properties of Ge(sub 1-x(Si) sub x) solid solutions was studied using the second-neighbour tight binding theory in the virtual crystal approximation. The d(sup -2) scaling rule is followed for a uniform (hydrostatic) pressure. Outcoming trends are found as fairly consistent with the existing experimental and theoretical data. DOE

N89-23321# International Centre for Theoretical Physics, Trieste (Italy).
BAND STRUCTURE OF CdTe-ZnTe SUPERLATTICE
A. Camacho, F. Rodriquez, and L. Quiroga (Universidad de Los Andes, Bogota, Columbia) Sep. 1988 14 p
(DE88-705682; IC-88/297) Avail: NTIS (US Sales Only) HC A03/MF A01

We perform an empirical tight-binding band structure calculation for the superlattice CdTe-ZnTe. We examine the effect of strain and valence band offset on it. We find that the 6 percent lattice mismatch causes strain to play an important role. The trend of the superlattice band gap for all widths considered is to decrease as the valence band offset increases. We have found two interface states not reported before. This is our main result. They lie in energy about 100 MeV above the valence band edge. Since this energy is about equal to the difference between our calculated superlattice band gap and the value reported experimentally, we claim that optical absorption is measuring the transitions from these interface states to the conduction band. New more detailed experiments could settle this interesting problem. DOE

N89-23322# International Centre for Theoretical Physics, Trieste (Italy).
COEXISTENCE OF SPIN-GLASS AND TYPE-2 CERAMIC SUPERCONDUCTIVITY
R. Allub and J. Chela-Flores (Universidad Simon Bolivar, Caracas, Venezuela) Sep. 1988 15 p
(DE88-705684; IC-88/300) Avail: NTIS (US Sales Only) HC A03/MF A01

The new magnetic phase which has been observed recently in La(2-x)Ba(x)CuO4 at low temperatures for small concentrations of Ba, is studied in a phenomenological approach in which the superconducting (SC) and spin-glass (SG) phases are assumed to coexist. We are induced from recent experiments to the conclusion that the SG ordering enhances the SC ordering and viceversa. DOE

N89-23323# International Centre for Theoretical Physics, Trieste (Italy).
HYSTERESIS DEVELOPMENT IN SUPERCONDUCTING JOSEPHSON JUNCTIONS
T. F. Refai and L. N. Shehata (Atomic Energy Establishment, Cairo, Egypt) Sep. 1988 10 p Submitted for publication
(DE88-705693; IC-88/313) Avail: NTIS (US Sales Only) HC A02/MF A01

The resistively and capacitive shunted junction model is used to investigate hysteresis development in superconducting Josephson junctions. Two empirical formulas that relate the hysteresis width and the quasi-particle diffusion length in terms of the junctions electrical parameters, temperature and frequency are obtained. The obtained formulas provide a simple tool to investigate the full potentials of the hysteresis phenomena. DOE

N89-23324# International Centre for Theoretical Physics, Trieste (Italy).
ORDERING TRANSITIONS INDUCED BY COULOMB INTERACTIONS
M. Rovere, G. Senatore, and M. P. Tosi (Trieste Univ., Italy) Nov. 1988 28 p Submitted for publication
(DE88-705717; IC-88/368) Avail: NTIS (US Sales Only) HC A03/MF A01

We briefly review recent progress in treating phase transitions to ordered states driven by Coulomb interactions. Wigner crystallization of the one-component plasma, in the degenerate Fermi limit and in the classical limit, is the foremost example and developments in its theory are discussed in some detail. Attention is also given to quasi-two dimensional realizations of the plasma model in the laboratory. The usefulness of these ideas in relation to freezing and ordering transitions is illustrated with reference to alkali metals, elemental and polar semiconductors, and various types of ionic systems (molten salts, colloidal suspensions and astrophysical plasmas). DOE

N89-23325# Joint Inst. for Nuclear Research, Dubna (USSR). Lab. of High Energy.
POSSIBILITY OF OPERATION OF HIGH TEMPERATURE SUPERCONDUCTING YBa2Cu307 CERAMICS IN CYCLOTRONS AT IRRADIATION
A. A. Astapov, L. N. Zajtsev, V. I. Smirnov, and G. P. Reshetnikov 1988 12 p In RUSSIAN
(DE88-705783; JINR-14-88-57) Avail: NTIS (US Sales Only) HC A03/MF A01

Prospects for using the high temperature superconducting material in cryotron current transformers placed in radiation scattered field are considered. Adequacy of dose values of cryotron irradiation near accelerators and in cosmic space are shown. HTS-ceramics irradiation conditions at the JINR synchrophasotron are described: fluences of the projectile protons with 8.09 GeV energies are 4.5x10(sup 14) and 2x10(sup 14)/sq cm. Samples were placed behind the targets of 2x2 or 5x5 cu cm and PHI 10x13 sq cm in size, and received 10(sup 5) Gy (0.281 Gy/s) and 4.8x10(sup 4) Gy dose (14.5 Gy/s dose powers), respectively. Secondary particle differential spectra were computed by the Monte Carlo method. Changes of electrical resistance R(T) and critical currents j(sub c)(U) of superconducting samples are measured in order to predict maximum permissible doses of cryotron irradiation and other superconducting devices. DOE

N89-23326# Cornell Univ., Ithaca, NY. Dept. of Materials Science.
GRAIN BOUNDARY SLIDING PHENOMENA IN POLYCRYSTALLINE SOLIDS Ph.D. Thesis
Charles Haile Wilson Aug. 1988 180 p
(Contract DE-FG02-84ER-45055)
(DE89-007792; DOE/ER-45055/23) Avail: NTIS HC A09/MF A01

At elevated temperatures (T is greater than 0.4T sub m), grain boundary sliding (GBS) becomes a significant deformation mechanism which directly alters both the flow and failure properties of polycrystalline solids. In this work the nature of GBS, primarily in Incoloy 800H, is investigated in terms of the effects of stress, temperature and grain size on the flow behaviors obtained by using the load relaxation test. Flow behaviors are obtained for average grain diameters (d) of from 224 to 6 micrometers. The flow behavior of large grain size materials (d is greater than 10 micrometers), plotted as logarithmic stress versus logarithmic strain rate exhibits a sigmoidal shape which is traditionally associated with the effects of grain boundary sliding (GBS) on creep deformation. For small grain size materials (d is greater than 10 micrometers) the mechanical properties tend toward those characteristic of superplasticity as the grain size is decreased; the material becomes increasingly ductile and the strain rate sensitivity and material flow rate at a given stress increases. Reloading experiments and the observations of a scaling behavior with increasing level of work hardening show that the microstructure of the specimen during each test is stable. The change in flow behavior with decreasing grain size is shown to result from a change in the dominant mode of GBS accommodation. DOE

N89-23327# Sandia National Labs., Albuquerque, NM.
ELECTRICAL PROPERTIES AND DETECTION METHODS FOR CMOS IC DEFECTS
Jerry M. Soden and Charles F. Hawkins (New Mexico Univ., Albuquerque.) 1989 10 p Presented at the European Test Conference, Paris, France, 11 Apr. 1989
(Contract DE-AC04-76DP-00789)
(DE89-005775; SAND-88-3440C; CONF-890493-1) Avail: NTIS HC A02/MF A01

Defects in CMOS ICs cause unique electrical characteristics. Digital CMOS ICs may appear to perform their terminal logic functions in spite of significant imperfections such as open or short circuits. The effects of these commonly occurring defects must be understood to develop test strategies that minimize the escape of ICs with defects that either degrade reliability or compromise circuit performance. This paper summarizes and adds new information regarding electrical properties of CMOS IC defects. The parametric or logic measurements required to detect each type of defect in a production test environment are emphasized. DOE

N89-23328# California Univ., Berkeley. Lawrence Berkeley Lab. Engineering Div.
A VARIABLE TEMPERATURE CRYOSTAT THAT PRODUCES IN SITU CLEAN-UP GERMANIUM DETECTOR SURFACES
R. H. Pehl, N. W. Madden, D. F. Malone, C. P. Cork, D. A. Landis, J. S. Xing, and D. L. Friesel (Indiana Univ., Bloomington.) Nov. 1988 10 p Presented at the IEEE Nuclear Science Symposium, Orlando, FL, 9-11 Nov. 1988
(Contract DE-AC03-76SF-00098)
(DE89-008174; LBL-25223; CONF-881103-57) Avail: NTIS HC A03/MF A01

Variable temperature cryostats that can maintain germanium detectors at temperatures from 82 K to about 400 K while the thermal shield surrounding the detectors remains much colder when the detectors are warmed have been developed. Cryostats such as these offer the possibility of cryopumping material from the surface of detectors to the colder thermal shield. The diode characteristics of several detectors have shown very significant improvement following thermal cycles up to about 150 K in these cryostats. Important applications for cryostats having this attribute are many. DOE

N89-23329# Lawrence Livermore National Lab., CA.
ACCUMULATED SURFACE DAMAGE ON ZnS CRYSTALS PRODUCED BY CLOSELY SPACED PAIRS OF PICOSECOND LASER PULSES
Lloyd L. Chase and H. W. H. Lee Dec. 1988 17 p Presented at the Laser Induced Damage in Optical Materials, Boulder, CO, 26 Oct. 1988
(Contract W-7405-eng-48)
(DE89-008813; UCRL-99741; CONF-8810284-2) Avail: NTIS HC A03/MF A01

Excitation of a transparent ZnS crystal by repetitive picosecond dye laser pulses causes an accumulated surface modification leading to optical damage. The onset of the damage is detected by an abrupt increase in the emission of neutral Zn (and possibly S2) from the surface. Comparison of the neutral emission thresholds with pulse-pair and single-pulse excitation shows that linear absorption is the dominant laser-surface interaction. In general, this measurement technique shows considerable promise for investigating the possible influence of nonlinear absorption or excitation processes on damage mechanisms. The data suggest that heating of small absorbing regions produces the surface modification that leads to the observed surface ablation. The nature of the damage observed at fluences above the threshold suggests that it is caused by heating of a relatively large (approximately 10 to 100 micrometers) surface region that has been modified by the accumulation pulses. DOE

N89-23330# Lawrence Livermore National Lab., CA.
STORAGE IN SUPERCOMPUTER ENVIRONMENTS
Sam Coleman 1 Jun. 1988 8 p Presented at the Cray Users Group Meeting, Minneapolis, MN, 26 Apr. 1988
(Contract W-7405-eng-48)
(DE89-008895; UCRL-98924; CONF-8804136-3) Avail: NTIS HC A02/MF A01

The demand for storage in supercomputer environments is increasing and forcing an evolution toward distributed storage systems. In this paper, some existing storage systems and some requirements for future systems are described. The Storage Reference Model being developed by the IEEE Computer Society and a new storage system being developed at Livermore according to the IEEE model are also described. DOE

N89-23331# Technische Univ., Delft (Netherlands).
POSITRON LIFETIME TECHNIQUE WITH APPLICATIONS IN MATERIALS SCIENCE Ph.D. Thesis
Johannes DeVries 1987 158 p
(ETN-89-94141) Avail: NTIS HC A08/MF A01

The utilization of the positron lifetime technique to measure concentrations of cavities in materials is introduced, and efforts to increase the time resolution are described. The time resolution can be increased by optimizing the choice of the scintillator shape and surface treatment. The light yield of the scintillator has to be as high as possible. Applying a new type of photomultiplier (a microchannel plate) instead of a conventional one did not improve the time resolution. The reason is that a relatively low number of electrons reaches the amplification part of the photomultiplier. An improvement is obtained by combining a very fast pulse pick-off system with a especially designed time discrimination system. The conventional constant fraction method is replaced, to involve a pulse shaping step with division and addition of signals. Methods for data analysis are mentioned, and application examples are shown. ESA

N89-23332# Midwest Research Inst., Golden, CO.
SUPERCONDUCTIVITY FOR ELECTRIC POWER SYSTEMS: BUILDING TOWARD OUR FUTURE
Mar. 1989 20 p Prepared in cooperation with Energetics, Inc., Columbia, MD
(Contract DE-AC02-83CH-10093)
(DE89-000874; DOE/CH-10093/56) Avail: NTIS HC A03

Superconductivity for Electric Power Systems is a layman's overview of historical, current, and possible future aspects of superconductivity. DOE

N89-23333# Brookhaven National Lab., Upton, NY.
NEUTRON SCATTERING STUDIES OF MAGNETIC EXCITATIONS IN La/SUB 2-x/Sr/SUB x/CuO
M. A. Kastner, A. Aharony, R. J. Birgeneau, Y. Endoh, K. Fukuda, D. R. Gabbe, Y. Hidaka, H. P. Jenssen, T. Murakami, and M. Oda (Nippon Telegraph and Telephone Public Corp., Tokai, Japan) et al 1988 14 p Presented at the International Conference on the Electronic Structure of High Tc Symposium, Rome, Italy, 1 Aug. 1988 Prepared in cooperation with Defence Science and Technology Organization, Adelaide, Australia
(Contract DE-AC02-76CH-00016)
(DE89-008155; BNL-42265; CONF-8808138-1) Avail: NTIS HC A03/MF A01

The results of recent neutron scattering studies on La sub 2-x Sr sub x CuO4 are reviewed. For x = 0 the material is an antiferromagnetic insulator, and the spins in the CuO2 sheets are well-described by the 2D S = 1/2 square lattice Heisenberg model. With increasing x the Neel state is destroyed and is replaced at low temperatures, at least for samples which are nonmetallic or have low superconducting T sub c's, by a spin glass. The instantaneous correlations as well as those of the glass are incommensurate with the crystal lattice. The spin-spin correlation length in the doped CuO2 sheets equals the average separation between the holes which ultimately carry the supercurrent. DOE

N89-23334# Tennessee Univ., Knoxville.
EMISSION PROPERTIES OF EUROPIUM-DOPED LANTHANUM AND LUTETIUM ORTHOPHOSPHATE CRYSTALS FOR USE IN HIGH TEMPERATURE SENSOR APPLICATIONS
A. R. Bugos, S. W. Allison, and M. R. Cates (Oak Ridge National Lab., TN.) 1989 5 p Presented at the Southeastcon '89 Conference and Exhibition, Columbia, SC, 9 Apr. 1989
(Contracts DE-AC05-84OR-21400; W-7405-eng-36)
(DE89-008736; CONF-8904111-6) Avail: NTIS HC A02/MF A01

The emission properties of two crystalline europium activated thermographic phosphors, lanthanum phosphate (LaPO4:Eu³3+) and lutetium phosphate (LuPO4:Eu³3+) have been investigated for potential use in high temperature remote thermometry applications. Emissions and excitation spectra were taken for both crystals at room temperature and at elevated temperatures. In the excitation spectra taken from room temperature to approximately 400 C, lanthanum phosphate and lutetium phosphate exhibit a significant temperature dependent shift in their charge-transfer (C-T) absorption bands. DOE

N89-23335# Lehigh Univ., Bethlehem, PA. Materials Research Center.
THE EFFECT OF BORON ON MICROHARDNESS IN Ni3Al POLYCRYSTALS
X. R. Qian and Y. T. Chou 1988 6 p Presented at the MRS Symposium on High-Temperature Ordered Intermetallic Alloys, Boston, MA, 28 Nov. 1988
(Contract DE-FG02-86ER-45256)
(DE89-009124; CONF-8811161-4) Avail: NTIS HC A02/MF A01

In a recent MRS symposium, the effect of boron on grain boundary hardness (GBH) in Ni3Al was reported. Addition of 0.2 at. percent of boron decreased the GBH in all three sets of alloys tested (24, 25, and 26 at. percent Al). The present paper summarizes the study of the effect of boron on hardness within grains. Boron-induced softening was again observed in grain interiors. However, it occurred only in alloys with 24 and 25 at. percent Al, but not in the alloy with 26 at. percent Al. An explanation for this behavior is presented. DOE

N89-23336# Lawrence Livermore National Lab., CA.
DUCTILITY ENHANCEMENT IN UNREACTED INTERNAL-Sn Nb3Sn THROUGH LOW-TEMPERATURE ANNEALS
M. J. Strum, L. T. Summers, and J. R. Miller 19 Aug. 1988 18 p Presented at the Applied Superconductivity Conference, San Francisco, CA, 21 Aug. 1988
(Contract W-7405-eng-48)
(DE89-009125; UCRL-98739; CONF-880812-44) Avail: NTIS HC A03/MF A01

A lack of tensile ductility in as-drawn superconducting wires at room temperature can lead to damage during magnet fabrication steps such as cabling and coil winding. The tensile ductility of 0.42 mm internal-Sn Nb3Sn conductor in the as-drawn unreacted condition is limited to less than 3 percent at room temperature. Through low-temperature annealing treatments at 200 C the ductility can be substantially enhanced increasing to as high as 10 percent after 24 hr at 200 C. This effect is attributed to softening which reduces yield strengths up to 50 percent while maintaining 90 percent of the tensile strength. Fracture surfaces of annealed wires reveal increased adhesion between the Sn cores and the surrounding Cu as well as an increase in ductile void coalescence as the failure mechanism within the Cu. Preliminary results on the pre-reaction strain sensitivity of reacted wire critical currents confirm the increased strain tolerance in annealed wires. DOE

N89-23337# Brookhaven National Lab., Upton, NY. Dept. of Physics.
QUASICRYSTALS FROM CUTS IN SIX DIMENSIONS
Per Bak 1988 8 p Presented at MOSPOQ '88: International Conference on Modulated Structure, Polytypes and Quasicrystals, Varanasi, India, 19 Dec. 1988

(Contract DE-AC02-76CH-00016)
(DE89-009361; BNL-42478; CONF-881279-1) Avail: NTIS HC A02/MF A01

The principles for the six-dimensional crystallographic description of icosahedral crystals are briefly reviewed. The atomic arrangements are defined by three-dimensional atomic surfaces. In general, the crystals are not tilings formed by stacking a small number of basic building blocks. Recently, Gratias, Cahn, and Moser have determined the atomic surfaces in AlMnSi quasicrystals by analyzing X-ray and neutron scattering experiments. DOE

N89-23338# Los Alamos National Lab., NM.
INFLUENCE OF ION IRRADIATED SrTiO SUB 3 ON THE PROPERTIES OF THIN FILM OXIDE SUPERCONDUCTORS
Nicole Bordes, Michael Cohen, Michael Nastasi, Anthony D. Rollett, and Carl J. Maggiore 1989 20 p Presented at the 16th International Conference on Metallurgical Coatings and Equipment Exhibit, San Diego, CA, 12-17 Apr. 1989
(Contract W-7405-eng-36)
(DE89-009409; LA-UR-89-739; CONF-890468-3) Avail: NTIS HC A03/MF A01

The quality of high temperature superconducting thin films is dependent on the structure of the substrate used. The present work examines the effects of radiation damaged SrTiO3 substrates on the properties of Y1Ba2Cu3O7 thin film superconductors. Prior to film deposition, single crystal SrTiO3 substrates were cooled to 77 K and irradiated with 400 keV Ne ions to doses of 1 x 10(15) and 1 x 10(16) ions/sq cm. Following deposition the film/substrate couples were annealed in wet oxygen at either 850 or 900 C. Films on substrates irradiated at high doses showed an increase in transition width from 2 to 8 degrees and lowered transition temperature from 92 to 65 K relative to films on low dose and unirradiated substrates. These differences are discussed in terms of results obtained from high energy and Rutherford backscattering (RBS) and channeling experiments, scanning electron microscopy (SEM) observations and X-ray diffraction data (XRD). DOE

N89-23339# Department of Energy, Washington, DC.
BASIC RESEARCH IN SUPERCONDUCTOR, CERAMIC AND SEMICONDUCTOR SCIENCES AT SELECTED JAPANESE LABORATORIES BASED ON A 1988 VISIT: HIGHLIGHTS, SUMMARY AND OVERVIEW, DETAILED NOTES FROM SELECTED JAPANESE LABORATORIES
Feb. 1989 213 p Prepared in cooperation with Department of Commerce, Washington, DC; and Office of Naval Research, Arlington, VA
(DE89-009637; DOE/ER-0410) Avail: NTIS HC A10/MF A01

A summary and overview of basic research in superconductors at Japanese Laboratories was reported. The information was provided by individual Japanese researchers. GRA

N89-23340# Argonne National Lab., IL. Materials Science Div.
STRUCTURAL PROPERTIES OF SUPERCONDUCTING AND NONSUPERCONDUCTING Ba SUB 1-x K SUB x BIO3
B. Dabrowsi, D. G. Hinks, J. D. Jorgensen, D. R. Richards, Shiyou Pei, Y. Zheng, and A. W. Mitchell 1989 18 p Presented at the 4th International Conference on Ultrastructure Processing of Ceramics, Glasses and Composites, Tucson, AZ, 19-24 Feb. 1989
(Contract W-31-109-eng-38)
(DE89-009813; CONF-890275-1) Avail: NTIS HC A03/MF A01

Structural properties of Ba sub 1-x K sub x BiO3 prepared by powder- and melt-process methods are studied. The potassium solubility limit, x = 0.5, is about the same for both methods and probably is determined by the ionic sizes of the constituent ions. Melt- and powder-processed samples of very good quality for superconducting compositions (x greater than 0.3) can be produced by melting or by repeated grinding, respectively and quenching after N2 firing at 725 C. Single phase samples for x less than 0.3 can be made without reduction to the trivalent Bi-compound. Preparation of very homogeneous single phase samples for x less than 0.3 is difficult due to the low N2 synthesis temperatures and the phase separation which occurs above 725 C. DOE

N89-23341# Argonne National Lab., IL. Materials Science Div.
POINT DEFECTS AND OXYGEN DIFFUSION IN HIGH T SUB c SUPERCONDUCTORS
J. L. Routbort and S. J. Rothman Nov. 1988 12 p Presented at the 7th International Symposium on Ceramics, Bologna, Italy, 14-16 Dec. 1988 Submitted for publication
(Contract W-31-109-eng-38)
(DE89-009842; CONF-881207-4) Avail: NTIS HC A03/MF A01

This paper presents a review of the oxygen tracer diffusion data on the high-temperature oxide superconductors, La(sub 2-x) Sr(sub x) CuO4 and YBa2Cu3O sub 7-delta which have been obtained in our laboratory. The SIMS (Secondary Ion Mass Spectrometry) technique has been used to determine the depth profile of O to 18 from which the diffusion coefficient was calculated. Measurements in the La-Sr-Cu-O system have been performed for x = 0.1, 0.15 and 0.2 and the self-diffusion coefficient was found to decrease with increasing Sr substitution, a fact explained by a defect model in which oxygen vacancies are bound to Sr clusters. Recent measurements in polycrystals of Y-Ba-Cu-O were made in the temperature range of 300 to 600 C at an oxygen partial pressure of 1 atmosphere; they are given by D = 9 x 10 sup -6 exp -(0.89 eV/kT) sq cm/s. DOE

N89-23342# Argonne National Lab., IL. Engineering Div.
PROCESSING AND ELECTRICAL PROPERTIES OF HIGH-T SUB c SUPERCONDUCTORS
R. B. Poeppel, M. T. Lanagan, J. P. Singh, K. C. Goretta, J. T. Dusek, S. E. Dorris, U. Balachandran, C. L. Bohn, and J. R. Delayen Sep. 1988 3 p Presented at the 13th International Conference on Infrared and Millimeter Waves, Honolulu, HI, 5-9 Dec. 1988
(Contract W-31-109-eng-38)
(DE89-009852; CONF-881226-2) Avail: NTIS HC A02

This paper presents an overview of ceramic fabrication techniques and electrical properties of high-T sub c superconductors. Fabrication of bulk ceramic and composite, a high-T sub c superconducting wires and tapes is discussed. Direct-current critical current density data and surface resistance data at rf and microwave frequencies are presented for the YBa2Cu3O(7-x) and Ba2Sr2CaCu2O(8+y) phases. DOE

N89-23343# Argonne National Lab., IL. Materials Science Div.
GROWTH KINETICS OF GRAIN-BOUNDARY INDUCED MELTING: A MOLECULAR-DYNAMICS STUDY
S. R. Phillpot, J. F. Lutsko, D. Wolf, and S. Yip (Massachusetts Inst. of Tech., Cambridge.) Dec. 1988 7 p Presented at the Symposium on Atomic Scale Calculations in Materials Science, Boston, MA, 28 Nov. - 3 Dec. 1988
(Contract W-31-109-eng-38)
(DE89-009855; CONF-8811147-2) Avail: NTIS HC A02/MF A01

The growth kinetics of melting nucleation at a high-angle twist boundary in silicon are investigated using molecular dynamics. Melting is found to be a two-stage process. In the first stage order is lost within a single plane at the interface and the density of the solid increases to that of the liquid. In the second stage the atomic coordination changes and an isotropic liquid is formed. DOE

N89-23344# Etablissement Technique Central de l'Armement, Arcueil (France). Service Structure des Materiaux.
STUDY OF GRAIN BOUNDARIES IN POLYCRYSTALLINE ALUMINA [ETUDE DES JOINTS DE GRAINS DANS L'ALUMINE POLYCRISTALLINE]
S. Lartigue and L. Priester (Paris-Sud Univ., Orsay, France) 2 Dec. 1987 24 p In FRENCH Sponsored by Direction des Recherches, Etudes et Techniques, Paris, France
(ETCA-87-R-130; ETN-89-94345) Avail: NTIS HC A03/MF A01

Models describing the structure of grain boundaries and the theory of equilibrium intergranular segregation are studied emphasizing the differences between metals and ionic crystals. The experimental techniques and samples are described. The

results presented include the distribution of grain boundaries, the observation of intrinsic and extrinsic dislocations and the observation of faceted boundaries. ESA

N89-23345# Etablissement Technique Central de l'Armement, Arcueil (France). Service Structure des Materiaux.
STUDY OF GRAIN BOUNDARIES IN POLYCRYSTALLINE ALUMINA. EFFECT OF THE MANUFACTURING MODE AND OF THE MATERIAL COMPOSITION [ETUDE DES JOINTS DE GRAINS DANS L'ALUMINE POLYCRISTALLINE. EFFET DU MODE D'ELABORATION ET DE LA COMPOSITION DU MATERIAU]
S. Lartigue and L. Priester (Paris-Sud Univ., Orsay, France) 7 Oct. 1987 25 p In FRENCH Sponsored by Direction des Recherches, Etudes et Techniques, Paris, France
(ETCA-87-R-100; ETN-89-94346) Avail: NTIS HC A03/MF A01

High ductility ceramics such as MgO doped alumina are studied. The role of doping elements on microstructure and on the texture of grain boundaries is analyzed and detailed examples of reactions between intragranular and intergranular dislocations are presented. The study shows the existance of different mechanical behavior as a function of the type of grain joint. The ability to deform is related to the presence of extrinsic dislocations. ESA

N89-23346# Etablissement Technique Central de l'Armement, Arcueil (France). Service Structure des Materiaux.
PRELIMINARY STUDY OF CERAMIC-METAL INTERFACE IN THERMAL BOUNDARIES [ETUDE PRELIMINAIRE DE L'INTERFACE CERAMIQUE-METAL DANS LE CAS DES BARRIERES THERMIQUES]
G. Tremouilles and J. Luc Derep 7 Oct. 1987 49 p In FRENCH Sponsored by Direction des Recherches, Etudes et Techniques, Paris, France
(ETCA-87-R-101; ETN-89-94347) Avail: NTIS HC A03/MF A01

The interface of yttrium doped zircon ceramic on NiCrAlY alloy is studied. The different phases in the zircon are examined with electron microscopy. The presence of alumina in the interface is demonstrated. The possibility of damaging the NiCrAlY substrate when using a plasma gun is discussed. ESA

N89-23347# Battelle Inst., Frankfurt am Main (Germany, F.R.).
RADIATION HARDENED DETECTOR ARRAYS FOR THE FAR AND EXTREME INFRARED, PHASE 1 Final Report
D. Engemann, R. Faymonville, O. Frenzl, D. Haschberger, and K. Meyer Paris, France ESA Sep. 1988 63 p
(Contract ESTEC-6939/86/NL/PB(SC))
(BF-R-65.695-10; ESA-CR(P)-2722; ETN-89-94454) Avail: NTIS HC A04/MF A01

Results of the optimization of epitaxial double layer detector arrays are presented. Different types of blocked impurity band (BIB) detector arrays with different doping levels of the IR sensitive layer were fabricated and measured. The best performance data are: NEP = 5 times 10 to the minus 17th power W/sqrt Hz, and current responsivity S = 2 A/W using a doping concentration of 4 times 10 to the 17th power P/cc. A two dimensional 4x10 elements BIB array was connected to a multiplexing cryogenic read out circuit giving NEP = 10 to the minus 16th power W/sqrt Hz; S = 2 A/W. The results are obtained without enhancing the low sensitivity of these devices to ionizing radiation which remains an order of magnitude lower than that of conventional extrinsic photoconducting detectors. ESA

N89-23348# Utah Univ., Salt Lake City. Dept. of Physics.
CONDUCTIVITY FLUCTUATIONS IN MIXED Na/Ca BETA ALUMINA Technical Report, 1 Jan. 1988 - 17 Feb. 1989
Chu K. Kuo and James J. Brophy 17 Feb. 1989 14 p Submitted for publication
(Contract N00014-82-K-0603)
(AD-A205416; TR-20-ONR) Avail: NTIS HC A03/MF A01 CSCL 20C

Conductivity fluctuations in mixed Na/Ca beta alumina ceramics for different values of the Na/Ca ratio are observed to be similar to diffusion noise of the mobile ions seen in Na, Ag, and Pb beta alumina. Measured noise levels increase two orders of magnitude in changing from 100 percent Na to 100 percent Ca ions in the structure. In mixed Na/Ca ceramics the noise is greater for NaI solution current electrodes than for CaBr2 solution current electrodes. These differences are attributed to different correlation effects between the mobile ions. GRA

N89-23349# Illinois Univ., Urbana. Coll. of Engineering.
EXPERIMENTAL INVESTIGATION OF HOT ELECTRON AND RELATED EFFECTS IN GALLIUM (ALUMINUM) ARSENIDE DEVICES Technical Report, 1985 - 1988
Ted K. Higman Jan. 1989 85 p
(Contract N00014-84-C-0149)
(AD-A205442; UILU-ENG-89-2209) Avail: NTIS HC A05/MF A01 CSCL 20B

The advance of crystal growth technology, specifically metalorganic chemical vapor deposition (MOCVD) as it relates to this work, has made it practical to manufacture an entirely new class of heterojunction devices. Physical properties of semiconductor heterojunction devices such as resonant tunneling and ballistic transport and various hot electron effects discussed within, have been moved from the status of academic curiosity to physically realizable, useful effects. The theoretical and experimental results from the heterostructure hot electron diode (HHED) a two-terminal device which exhibits S-shaped negative differential resistance, are presented, which shed new light on the transport processes involved in the tunneling, resonant tunneling and thermionic emission processes in semiconductor heterostructures. GRA

N89-23350# California Univ., Davis. Dept. of Electrical and Computer Engineering.
ORGANIC AND POLYMER CRYSTALLINE FILMS FOR SPATIAL LIGHT MODULATION Final Report, 1 Oct. 1985 - 8 Dec. 1986
Stephen T. Kowell Jan. 1989 14 p
(Contract F29601-84-C-0080)
(AD-A205906; AFWL-TR-87-98) Avail: NTIS HC A03/MF A01 CSCL 07C

In this report, the work done during the last phase of this program is described. The efforts involved two components of the program in polymeric ultrathin films, second; harmonic generation measurements to characterize the second order nonlinearities, and capacitance measurements of deposition quality and water entrapment during deposition. With regard to second harmonic generation, the components of x (2) and the molecular orientation in Langmuir/Blodgett films of hemicyanine dye on glass substrates are reported. Decay of the signal because of molecular rearrangement and diffusion of impurities is discussed. For the capacitance sensor, subphase (water) entrainment is described as a function of deposition speed and of material composition. GRA

77 THERMODYNAMICS AND STATISTICAL PHYSICS

Includes quantum mechanics; theoretical physics; and Bose and Fermi statistics.

For related information see also *25 Inorganic and Physical Chemistry* and *34 Fluid Mechanics and Heat Transfer.*

N89-23351# International Centre for Theoretical Physics, Trieste (Italy).
TWO DIMENSIONAL (4,0) SUPERGRAVITY IN HARMONIC SUPERSPACE. THE ACTION AND THE MATTER COUPLINGS
T. Lhallabi and E.H. Saidi (Mohammed V Univ., Rabat, Morocco) Aug. 1988 20 p Submitted for publication
(DE88-705661; IC-88/238) Avail: NTIS (US Sales Only) HC A03/MF A01

The superfield formulation of the two dimensional (4,0)

supergravity is developed using the harmonic superspace techniques. The different sets of constraints are given and their solutions are expressed in terms of a SU(2) self dual torsion superfield and harmonic prepotentials. The pure auxiliary (4,0) Einstein action generalizing the (2,0) one is written down and the most general (4,0) matter couplings are given. DOE

N89-23352# International Centre for Theoretical Physics, Trieste (Italy).
NATURE OF CONDENSATION IN THE MOMENTUM SPACE FOR AN INTERACTING BOSE SYSTEM
R. I. M. A. Rashid (Dacca Univ., Bangladesh) Sep. 1988 10 p
(DE88-705679; IC-88/288) Avail: NTIS (US Sales Only) HC A02/MF A01

Earlier it has been shown that the properties of superfluid helium four have an intimate connection with a non-vanishing coherent pairing as well as the generalized Bose-Einstein condensation. Here, the nature of condensation for an interacting Bose system is re-examined. It is shown that, under conditions of constant temperature and pressure, minimization of the Gibbs free energy leads to a generalized condensation of the type first proposed by Girardeau. Extrapolation of these ideas to quasiparticle models of interacting Bose systems such as helium-2 lead to conclude that the condensation in momentum space should also be regarded as generalized in the same sense. A bonus of this approach is the disappearance of macroscopic fluctuations in the density encountered in the usual theory of the condensed ideal Bose system. DOE

N89-23353# International Centre for Theoretical Physics, Trieste (Italy).
CONSTRUCTION OF HARMONIC MAPS BETWEEN PSEUDO-RIEMANNIAN SPHERES AND HYPERBOLIC SPACES
J. Konderak (Jagellonian Univ., Cracow, Poland) Sep. 1988 11 p Submitted for publication
(DE88-705695; IC-88/319) Avail: NTIS (US Sales Only) HC A03/MF A01

Defined here is an orthogonal multiplication for vector spaces with indefinite nondegenerate scalar product. This is then used, via the Hopf construction, to obtain harmonic maps between pseudo-Riemannian spheres and hyperbolic spaces. Examples of harmonic maps are constructed using Clifford algebras. DOE

N89-23354# International Centre for Theoretical Physics, Trieste (Italy).
ON SPACE-TIME ESCAPE MECHANISMS
M. D. Maia (Brasilia Univ., Brazil) Sep. 1988 12 p Submitted for publication
(DE88-705699; IC-88/325) Avail: NTIS (US Sales Only) HC A03/MF A01

The Rubakov-Shaposhnikov space-time escape mechanism is further investigated as a strong gravity phenomena. It is suggested that this process is complementary to Hawking's particle creation mechanism in a high dimensional theory, with non-compact internal space. DOE

N89-23355# International Centre for Theoretical Physics, Trieste (Italy).
IMPROVED EFFECTIVE POTENTIAL IN THE EINSTEIN METRIC
G. Denardo and E. Spallucci (Istituto Nazionale di Fisica Nucleare, Trieste, Italy) Oct. 1988 16 p Prepared in cooperation with Trieste Univ., Italy
(DE88-705716; IC-88/360) Avail: NTIS (US Sales Only) HC A03/MF A01

We present a self-consistent evaluation of the effective potential for a lambda phi sup 4 non-minimally coupled to an Einstein background geometry. This method takes into account the contribution from the multiloop Feynman diagrams with non-overlapping bubbles. It results that, even if the classical potential is double-well shaped, the vacuum expectation value of the scalar field is always vanishing because of a finite size effect, and no phase transitions can occur. A similar result can be obtained also in the de Sitter S sup 4 space, where the present approach holds as well. The implications of the results on the dynamics of the early universe are briefly discussed. DOE

N89-23356# International Centre for Theoretical Physics, Trieste (Italy).
INDUCED QUANTUM CONFORMAL GRAVITY
Yuri V. Novozhilov and D. V. Vassilevich (Leningrad State Univ., USSR) Nov. 1988 11 p Submitted for publication
(DE88-705718; IC-88/382) Avail: NTIS (US Sales Only) HC A03/MF A01

Quantum gravity is considered as induced by matter degrees of freedom and related to the symmetry breakdown in the low energy region of a non-Abelian gauge theory of fundamental fields. An effective action for quantum conformal gravity is derived where both the gravitational constant and conformal kinetic term are positive. Relation with induced classical gravity is established. DOE

N89-23357# Nationaal Inst. voor Kernfysica en Hoge Energiefysica, Amsterdam (Netherlands).
QUANTUM THEORY OF A MASSLESS SPINNING PARTICLE
J. W. vanHolten May 1988 18 p Sponsored in part by Stichting voor Fundamenteel Onderzoek der Materie, Amsterdam, Netherlands
(NIKHEF-H/88-7; ETN-89-94252) Avail: NTIS HC A03/MF A01

The classical and quantum mechanics of a free massless pointlike fermion is presented. The action is invariant under local one-dimensional reparameterizations and supersymmetry, as well as a large set of rigid symmetries, including conformal and chiral symmetries. An infinite set of rigid symmetries is derived, starting from the chiral invariance, but only a finite subset does not vanish on shell. The BRST transformations corresponding to the d=1 local symmetries are constructed and the quantization is performed. The BRST cohomology is investigated and the conditions producing the physical states are derived. ESA

N89-23358# Nationaal Inst. voor Kernfysica en Hoge Energiefysica, Amsterdam (Netherlands).
LOCAL BRST INVARIANCE AND THE DYNAMICAL ORIGIN OF THE BRST CONDITION
J. W. vanHolten Sep. 1988 30 p Sponsored in part by Stichting voor Fundamenteel Onderzoek der Materie, Amsterdam, Netherlands
(NIKHEF-H/88-15; ETN-89-94254) Avail: NTIS HC A03/MF A01

It is shown that the BRST invariance of theories with local space-time symmetries, such as the reparametrization-invariant point-particle or d-dimensional general relativity, and of theories with local internal symmetries, like abelian and nonabelian gauge theories, can be gauged without changing the physical content of the theory, at least at the level of perturbation theory. In such a formulation the BRST condition Q=0 can be derived from the dynamics, instead of having to be imposed as an additional constraint needed to distinguish between the physical and unphysical solutions of the theory. This construction then leads to an infinite hierarchy of BRST symmetries, all with the same cohomology. ESA

80 SOCIAL SCIENCES (GENERAL)

Includes educational matters.

No abstracts in this category.

81 ADMINISTRATION AND MANAGEMENT

Includes management planning and research.

N89-23359# Kienbaum Unternehmensberatung, Gummersbach (Germany, F.R.).
ANALYSIS OF THE PRESENT KNOWLEDGE OF COSTS AND BENEFITS OF THE GOVERNMENTAL ADVANCEMENT OF ASTRONAUTICS [ANALYSE BISHERIGER ERKENNTNISSE ZU KOSTEN UND NUTZEN DER STAATLICHEN FOERDERUNG DER RAUMFAHRT]
Hans-Juergen Mortsiefer, Ulrich Bender, and Guenter Boehm Oct. 1987 192 p In GERMAN Sponsored by the BMFT, Bonn, Fed. Republic of Germany
(ETN-89-93770) Avail: NTIS HC A09/MF A01

A literature study of the costs and benefits of governmental advancement of astronautics was performed. An up-to-date overview of the status and contribution of the economic sciences to the research field cost-benefit analysis and related methods is given. The cost-benefit analyses performed in the field of astronautics and analogous technology domains are reviewed and analyzed with respect to their fields of research, methods, and results. ESA

N89-23360# Bundesministerium fuer Forschung und Technologie, Bonn (Germany, F.R.).
AGREEMENT ON THE INTERNATIONAL SPACE STATION AND COLUMBUS PROGRAM [UEBEREINKOMMEN UEBER DIE INTERNATIONALE RAUMSTATION UND DAS PROGRAMM COLUMBUS]
29 Sep. 1988 95 p In GERMAN
(Rept-34/88; ETN-89-93985) Avail: NTIS HC A05/MF A01

Articles of the agreement between USA and European member countries, Japan, and Canada for the cooperation on the international space station programs are described. Main phases are: detailed design and development, use and operation of the civil manned space station, personnel, transport, communication, and financial management. Other topics of the agreement concern exchange of goods and scientific data, handling of data in transit, intellectual property regulations, consulting, modification procedure, and withdrawal. ESA

N89-23361# Advisory Group for Aerospace Research and Development, Neuilly-Sur-Seine (France).
CALENDAR OF SELECTED AERONAUTICAL AND SPACE MEETINGS
Jun. 1988 144 p In ENGLISH and FRENCH
(AGARD-CAL-88/2; ISBN-92-835-0470-4) Avail: NTIS HC A07/MF A01

A schedule is presented of some aeronautical and space meetings and workshops which are of interest to the aforementioned community. This calendar is published every six months, in June and December of each year. Details concerning the meetings listed in this particular issue of the calendar were obtained form National and International Organizations which sponsor aeronautical and space meetings and from other sources such as journals and periodicals. E.R.

82 DOCUMENTATION AND INFORMATION SCIENCE

Includes information management; information storage and retrieval technology; technical writing; graphic arts; and micrography.

For computer documentation see *61 Computer Programming and Software.*

N89-23362# Advisory Group for Aerospace Research and Development, Neuilly-Sur-Seine (France). Technical Information Panel.
THE ORGANISATION AND FUNCTIONS OF DOCUMENTATION AND INFORMATION CENTRES IN DEFENCE AND AEROSPACE ENVIRONMENTS
Mar. 1989 114 p Meeting held in Athens, Greece, 19-20 Oct. 1988
(AGARD-CP-445; ISBN-92-835-0496-8) Avail: NTIS HC A06/MF A01

Topics addressed include the information scene in the civil and defence sectors in Greece, ways to identify users and their needs, sources of information for a documentation center, ways of handling and managing information including the problems caused by security requirements, and ways of using multiple data bases in information retrieval. For individual titles, see N89-23363 through N89-23374.

N89-23363# National Hellenic Research Foundation, Athens (Greece).
THE OBJECTIVES AND ROLE OF THE GREEK NATIONAL DOCUMENTATION CENTRE
V. Bouboukas, C. Skourlas, and E. Poulakaki *In* AGARD, The Organisation and Functions of Documentation and Information Centres in Defence and Aerospace Environments Mar. 1989 4 p (For primary document see N89-23362 16-82)
Avail: NTIS HC A06/MF A01

A brief overview of the Greek information scene is presented. The objectives and the role of the National Documentation Centre are outlined together with some of its activities which proved to function within such an information environment as well as plans for continuity. Author

N89-23364# Hellenic National Defence General Staff, Athens (Greece). Communication and Informatics Directorate.
THE STATUS OF DEFENCE INFORMATION PROGRAMS IN GREECE
George N. Tzovlas *In* AGARD, The Organisation and Functions of Documentation and Information Centres in Defence and Aerospace Environments Mar. 1989 7 p (For primary document see N89-23362 16-82)
Avail: NTIS HC A06/MF A01

The present situation, problems, needs, and benefits of a Documentation and Information Centre for the Hellenic National Defence are described. It also describes the efforts which started in 1985 by the Hellenic Airforce for the creation of a pilot information program which was developed to satisfy its own needs. The problems encountered in the realization of this effort which seem to be common with those of other countries and are caused by the variety of objectives, the multitude of user groups, the wide spectrum of information topics and the relatively limited number of users are presented. The problem of the language barrier is also mentioned in relation to the implementation of modern information systems. The results of a study for the Hellenic National Defence Documentation and Information Centre are described. The importance of a coordinated and efficiently managed effort for the development, organization, and operation of such a center is stressed. The impacts of state of the art high technology means and a gradual implementation strategy for a feasible solution is addressed. Author

N89-23365# Royal Aircraft Establishment, Farnborough (England).
USER NEEDS AND HOW TO DETERMINE THEM

Richard H. Searle *In* AGARD, The Organisation and Functions of Documentation and Information Centres in Defence and Aerospace Environments Mar. 1989 7 p (For primary document see N89-23362 16-82)
Avail: NTIS HC A06/MF A01

Without users libraries and information centers have no purpose. It is essential therefore that the customers and their needs are fully known and understood. Knowing and understanding the users must be essentially a process of two-way commmunication involving regular dialog. Libraries and information centers need to operate within clearly defined terms of reference which give authority to activities and form the basis for the user dialog. Once the customers know and understand this, why we exist and what is offered them, they are better equipped to express their needs. Some of the customers will have little or no requirement for the offered services and this fact must be known and appreciated. Author

N89-23366# Technisch Documentatie en Informatie Centrum voor de Krijgsmacht, The Hague (Netherlands).
SOURCES OF INFORMATION
B. H. A. Zijlstra *In* AGARD, The Organisation and Functions of Documentation and Information Centres in Defence and Aerospace Environments Mar. 1989 14 p (For primary document see N89-23362 16-82)
Avail: NTIS HC A06/MF A01

The Scientific and Technical Documentation and Information Centre of the Armed Forces (TDCK) publishes monthly abstract bulletins concerning 15 subject areas, each bulletin containing 50 to 100 abstracts of maximum 200 words concerning scientific or technical reports and articles. Details are given about the information sources from which the reports and articles are selected and deals with external on-line or on-disc data bases that are used. The TDCK also publishes the monthly acquisitions list of the Central Military Catalogue (CMC) and coordinates the production of the automated cumulative catalog of books. Details are given about the information sources (books, reference works, and encyclopedia) that are present in major Defense libraries. Attention is given to other information sources such as standards, manuals, loose leaf publications, videotapes, and to information guides and registries. Author

N89-23367# Defence Research Establishment Atlantic, Dartmouth (Nova Scotia). Information Services.
STANDARDIZED BIBLIOGRAPHIC PROCESSING
D. I. Richardson *In* AGARD, The Organisation and Functions of Documentation and Information Centres in Defence and Aerospace Environments Mar. 1989 8 p (For primary document see N89-23362 16-82)
Avail: NTIS HC A06/MF A01

Because of an ever growing number of publications, and ever dwindling economic resources, those who work in the information community have always seen the need to share resources through standardization. Since the 1960s computer technologies have made the sharing and exchange of bibliographic records feasible. Throughout this period, standards for descriptive cataloging were refined so that the records being exchanged will be compatible. Based on these standard machine readable records, both libraries and the abstracting/indexing communities have developed various formal exchange formats. An overview is presented of the development of standardized bibliographic processing from the first cataloging rules through to computer exchange formats. The use of these standards by the defence and aerospace community is examined with particular emphasis on the treatment of technical reports. Author

N89-23368# Federal Armed Forces Documentation and Information Centre, Bonn (Germany, F.R.).
INDEXING AND ABSTRACTING
Jan Mueller *In* AGARD, The Organisation and Functions of Documentation and Information Centres in Defence and Aerospace Environments Mar. 1989 8 p (For primary document see N89-23362 16-82)
Avail: NTIS HC A06/MF A01

The aim of content analysis of documents is to describe the intention of documents in condensed form as a document unit, to order and store it, and to retrieve the document by user request. To do this, formal systems of ordering (classifications), indexing terms of natural language-based or artificial documentation languages as well as abstracts formulated in a natural language are employed. Whereas classing establishes paradigmatic relations, indexing (keywords, subject headings, descriptors) provides the possibility to identify the content in a natural language and to establish syntagmatic relations; the processing of indexing, indexing principles, methods, and results will be described; the existence and basic principles of thesauri will also be discussed in this connection. In contrast, an abstract is a statement of contents formulated in a natural language with the purpose of setting forth not only the relevance but also the contents of a document concerning a specific subject; the different types of abstracts and abstracting procedures will be covered. It is emphasized that retrieval is the reversal of the intellectual processes classing, indexing and abstracting, which is indicative of the special importance of these processes for the efficacy of technical information systems. Author

N89-23369# Federal Armed Forces Documentation and Information Centre, Bonn (Germany, F.R.).
DATA SECURITY
Helmut Braun *In* AGARD, The Organisation and Functions of Documentation and Information Centres in Defence and Aerospace Environments Mar. 1989 9 p (For primary document see N89-23362 16-82)
Avail: NTIS HC A06/MF A01

Maintaining adequate security standards for classified documents in military information systems is of eminent importance. Handling commercially sensitive information requires similar precautions. Basically, there are two approaches to solve these problems: to produce and operate a classified database, in which case national and NATO security regulations must be observed in handling documents and references to these documents; or to work with an unclassified databases which contains only unclassified information, in which case the reference to classified documents have to be kept unclassified. Questions are discussed which are related to preparing unclassified references to classified documents, deals with release procedures, and with problems relating to housekeeping problems. Author

N89-23370# National Technical Information Service, Springfield, VA.
IDENTIFYING USERS AND HOW TO REACH THEM
Joseph F. Caponio, Frederick L. Haynes, and A. Rahman Khan *In* AGARD, The Organisation and Functions of Documentation and Information Centres in Defence and Aerospace Environments Mar. 1989 5 p (For primary document see N89-23362 16-82)
Avail: NTIS HC A06/MF A01

The importance of timely use of scientific and technical information is increasingly being recognized by the developing nations as well as the developed nations. It is recognized that it is not only important to develop a better mouse-trap but also it is equally important to ascertain that there is proper diffusion of such an innovation. Knowledge could lay dormant if it does not reach the end-users when they most need it. An attempt is made to address why this is important and focuses on some of the factors involved in identifying and reaching the end-users.
Author

N89-23371# Horton (Forest W., Jr.), Washington, DC.
INFORMATION RESOURCES MANAGEMENT
Forest W. Horton, Jr. *In* AGARD, The Organisation and Functions of Documentation and Information Centres in Defence and Aerospace Environments Mar. 1989 5 p (For primary document see N89-23362 16-82)
Avail: NTIS HC A06/MF A01

The transfer of scientific and technical information between and among nations poses increasing challenges because of: larger and larger volumes of data exchanged; the increasing variety of

information interchange media; larger and larger numbers of intermediaries and end-users all along the information transfer chain; and increasing incompatibility of bibliographic and telecommunications formatting conventions. The emerging field of Information Resources Management (IRM) offers promise in helping to cope with these serious information exchanges. In particular, experiments in the U.S. Federal Government with a technique called information mapping, helps information managers identify, describe, inventory/survey, and control their total data, document, and literature flows and holdings, whether automated or manual, more completely. This approach of IRM, and the technique of information mapping, in several organizational contexts - one private (an Australian mineral and mining company), the other public (the U.S. Department of State) are introduced. Author

N89-23372# Telsystemes Questel, Paris (France).
TRANSDOC-ELECTRONIC DELIVERY PROGRAMME
J. Soule *In* AGARD, The Organisation and Functions of Documentation and Information Centres in Defence and Aerospace Environments Mar. 1989 7 p (For primary document see N89-23362 16-82)
Avail: NTIS HC A06/MF A01

The TRANSDOC test has yielded positive results and has made it possible to confirm the following: It is technically possible to perform archiving electronically and the organizations needed to implement these technologies do work. There is a good match between the services tested and the needs of the users; services can be created and current ones improved. Beyond purely technical tests, the significance of such testing which is oriented towards routine use and the evaluation of the needs of future customers is, by now, completely obvious. TRANSDOC has made it possible to confirm that the arrival of these technologies will considerably modify the information market in all its forms very quickly.
Author

N89-23373# Bergen Univ. (Norway). Library.
DECENTRALIZATION OF DATABASES AND THE COMMUNICATION BETWEEN THEM
Leif Magne Iversland *In* AGARD, The Organisation and Functions of Documentation and Information Centres in Defence and Aerospace Environments Mar. 1989 5 p (For primary document see N89-23362 16-82)
Avail: NTIS HC A06/MF A01

Database management systems (DBMS) were for many years used to develop centralized information systems, where the database and the application programs are stored at a central computer. The DBMS have also resulted in decentralized information systems in which data and programs are stored at several sites with none or very little communication between the sites. With the advent of distributed database management systems (DDBMS) possibilities for developing information systems have emerged. An ideal DDBMS supports an information system database stored at several sites in a computer network in such a way that users can access data at any site in the network as if they were stored at the local site. Some of the necessary properties of an ideal DDBMS including location, replication, and fragmentation transparencies are examined. Author

N89-23374# Defense Applied Information Technology Center, Alexandria, VA.
FOSTERING INTERACTION OF GOVERNMENT, DEFENSE, AND AEROSPACE DATABASES
Viktor E. Hampel *In* AGARD, The Organisation and Functions of Documentation and Information Centres in Defence and Aerospace Environments Mar. 1989 20 p (For primary document see N89-23362 16-82)
Avail: NTIS HC A06/MF A01

The Department of Defense (DOD) knowledge worker needs rapid access to select information contained in government, defense, and aerospace databases. In the United States, information of use to defense and aerospace specialists are contained in multiple government databases as well as in commercial databases. Policy and technology strategies are addressed, which are being developed by the Defense Technical Information Center (DTIC) to foster better interaction among government, defense, and aerospace databases. To improve interactions, considerable progress was made by evolving standards in communication protocols, operating systems of computers, database management systems, and command structures, but it is the Defense Gateway technology that permits interconnectivity and interoperability in the interim period. This makes it possible to make the growing number of heterogeneous databases available to the defense community in a progressively more unified and automated manner. The results of several projects that introduce a high degree of information robotics to Information Resource Management (IRM) with substantial increases in human productivity are described. Author

N89-23375 Rutgers - The State Univ., New Brunswick, NJ.
R AND D PRODUCTIVITY: RELATIONSHIP TO SELECTIVE DISSEMINATION OF INFORMATION (SDI) IN THE CORPORATE ENVIRONMENT Ph.D. Thesis
Lawrence Geoffrey Mondschein 1988 320 p
Avail: Univ. Microfilms Order No. DA8901101

Selective Dissemination of Information (SDI) is an information alerting service designed to keep individuals informed of new developments in their particular field of interest. The use of SDI was evaluated by basic research scientists working at six major research companies located in the United States. The following conceptual areas were reviewed in developing the best model of SDI use and productivity: (1) background of the individual; (2) work environment; (3) need to keep abreast of new research developments; (4) use of information sources; and (5) productivity or number of papers published. Two hundred and eight responses were received from the mailing of 244 questionnaires to basic research scientists at the six companies. One hundred and fifty six individuals met the entrance criteria and were analyzed using both descriptive and inferential statistics. Frequency of SDI use was found to be related to the environment, need to keep abreast of research developments, and use of primary and secondary information sources, including patents. Productivity was found to be related to background characteristics of the scientist, environment, need to keep abreast, and use of various information sources. Based on these research findings, scientists who use SDI on a regular basis are more productive than their colleagues who are infrequent users, or who do not subscribe to the service. Finally, two models on SDI use and productivity were presented for the purposes of testing new hypotheses that will, it is hoped, contribute to a better understanding of scientific communication.
Dissert. Abstr.

N89-23376# GMD-German National Research Center for Computer Science, Washington, DC.
GERMANY: FOCUS ON SCIENTIFIC AND TECHNICAL INFORMATION, VOLUME 4, NUMBER 1, APRIL 1988
Apr. 1988 16 p
(AD-A204054) Avail: NTIS HC A03/MF A01 CSCL 05A

The report is a quarterly newsletter edited in Washington, D.C. by the office of the GMD (German National Research Center for Computer Science). Some of the news topics covered include: R&D Programs and Funding; Information Technology - Industrial Outlook for Germany; Telecommunication Issues; Information Technology for Education and Research; News from German Online Vendors; Rewards for Outstanding Achievements in Information and Technology; A Glance at Selected GMD Research Results; International Cooperation. GRA

N89-23377# RANA Associates, Santa Clara, CA.
MICROFILM AND COMPUTER FULL TEXT OF ARCHIVAL DOCUMENTS
13 Oct. 1988 9 p
(Contract N00014-85-C-0653)
(AD-A204055) Avail: NTIS HC A02/MF A01 CSCL 14D

The development of the computer, and more recently the personal computer, has provided a possible solution to the major logistics problem of the storage and retrieval of archival data. An

efficient or economical manual solution was precluded by the number of people necessary to support a very large data-base and the main bottleneck has occurred in the retrieval and later refiling of the data of interest. In addition, original documents have a finite lifetime, which is adversely affected each time a document is handled. Microfilm retention of data has provided a partial solution, but does suffer from several serious drawbacks. In general, it has very poor spatial resolution especially when archival information contains diagrams, figures, and photographs in addition to alpha-numeric data. Storage parameters such as heat and humidity, as well as the amount of usage by individuals also affect the lifetime of the microfilm itself. A very large microfilm data-base requires the services of information retrieval specialists to provide an efficient library function for users, thereby increasing the overhead. The intent of this contract is to develop and demonstrate the archival storage of documents using computer-based imaging techniques and the retrieval of these documents by standard database management software. GRA

N89-23378# Pacific Northwest Labs., Richland, WA.
A PROGRAMMATIC APPROACH TO ACHIEVING DATA QUALITY OBJECTIVES
Randy R. LaBarge Jan. 1989 12 p Presented at the 2nd Ecological Quality Assurance Workshop, Las Vegas, NV, 8 Feb. 1989
(Contract DE-AC06-76RL-01830)
(DE89-008248; PNL-SA-16579; CONF-890284-1) Avail: NTIS HC A03/MF A01

The U.S. Environmental Protection Agency (EPA) requires that all EPA-sponsored programs follow the Quality Assurance (QA) Plan preparation guidelines of the QAMS-005/80, Guidelines and Specifications for Preparing Quality Assurance Project Plans. The QAMS-005/80 format requires the preparer of the QA Project Plan to develop a set of objectives for measurement data in terms of precision, accuracy, completeness, representativeness and comparability, better known as Data Quality Objectives (DQOs). Data Quality Objectives (DQOs) are quantitative and qualitative statements describing the quality of data needed to support a specific environmental decision or action (RQAMO 1988). Usually expressed in terms of precision, accuracy, completeness, representativeness, and comparability, DQOs are the attributes of the data produced that make it suitable for reiterating into the decision making and planning process and provide for defensibility if challenged either in litigation or as to professional credibility. DOE

N89-23379 Texas Univ., Austin.
IMPACT OF INFORMATION TECHNOLOGY ON ORGANIZATIONAL STRUCTURE: A CONTROL PERSPECTIVE Ph.D. Thesis
Tae Kyung Sung 1988 166 p
Avail: UNiv. Microfilms Order No. DA8901402

Past research linking information technology and organizational structure were inconclusive and contradictory. This confusion is resolved by taking into consideration two theoretical issues and three methodological problems. The two theoretical issues are: an assessment of the importance of organizational control as an important intervening internal variable between information technology and organizational structure, and an assessment of the importance of environment as a key external variable constraining organizational structure and the use of information technology. The three methodological issues concern measurement problems associated with controlling for different levels of analysis, establishing a clear operationalization of information technology, and institutional and questionnaire approaches to data collection. The investigation resulted in four conclusions. First, data confirms the importance of organizational control as an intervening internal variable and environment as a key external variable in the linkage between information technology and organizational structure. Second, three central dimensions of information technology are identified: symbolic information technology, extensiveness of information technology use, and information technology sophistication. Third, in order to maximize the explanatory power of information technology on other organizational constructs it is necessary to differentiate between the actual use of information technology as opposed to the mere presence of information technology. Fourth, carefully designed questionnaire measures reveal no significant differences from institutional measures in the assessment of key organizational constructs. Dissert. Abstr.

N89-23132# SRI International Corp., Menlo Park, CA. Artificial Intelligence Center.
CORE KNOWLEDGE SYSTEM: STORAGE AND RETRIEVAL OF INCONSISTENT INFORMATION
Thomas M. Strat and Grahame B. Smith *In* Science Applications International Corp., Proceedings: Image Understanding Workshop, Volume 2 Apr. 1988 p 660-665 (For primary document see N89-23115 16-61)
Avail: NTIS HC A99/MF E03 CSCL 05B

83 ECONOMICS AND COST ANALYSIS

Includes cost effectiveness studies.

No abstracts in this category.

84 LAW, POLITICAL SCIENCE AND SPACE POLICY

Includes NASA appropriation hearings; aviation law; space law and policy; international law; international cooperation; and patent policy.

N89-23380# Los Alamos National Lab., NM.
RELEVANCE OF INTERNATIONAL RESEARCH FACILITIES TO INTERNATIONAL STABILITY
Louis Rosen 20 Mar. 1989 14 p Presented at the 4th European Physical Society Seminar on International Research Facilities, Zagreb, Yugoslavia, 17 Mar. 1989
(Contract W-7405-eng-36)
(DE89-009400; LA-UR-89-813; CONF-890388-1) Avail: NTIS HC A03/MF A01

International Facilities have played an important play in expanding and keeping open a dialog between east and west. The advent of glasnost has dramatically reduced inhibitions on communications and opened new opportunities for international facilities to facilitate the understanding and appreciation of common goals and common threats. This is accomplished through frank discussions in which real problems are identified and assessed while fictitious ones are laid to rest. DOE

85 URBAN TECHNOLOGY AND TRANSPORTATION

Includes applications of space technology to urban problems; technology transfer; technology assessment; and surface and mass transportation.

For related information see also *03 Air Transportation and Safety, 16 Space Transportation,* and *44 Energy Production and Conversion.*

N89-23381# New Mexico Technet, Inc., Albuquerque.
TECHNOLOGY TRANSFER REPORT Final Report
15 Jun. 1988 19 p
(Contract DE-FG04-84AL-26034)
(DE89-009044; DOE/AL-26034/T6) Avail: NTIS HC A03/MF A01

For the past year New Mexico Technet, Inc. (Technet), has been working with the national laboratories, the universities and private industry to develop ways in which Technet can be used to

provide and enhance technology transfer. This final report will track our progress toward creating a technology transfer data base, establishing industry-laboratory pilot projects and identifying other types of assistance Technet can provide industry and state government. This report will follow the outline of the Scope of Work set forth in our contract with the Department of Energy. A chronology of progress is included, as well as written documentation of requests Technet has made to the laboratories and meetings Technet staff has held with industries, laboratories and universities. Following our discussion of the work undertaken this year, Technet will provide its conclusions on the strengths and weaknesses of the project, how we feel its mission can be continued, and suggestions the Department of Energy might make to its laboratories in the area of technology transfer through the new tools available in various states, including communications networks and technology foundations, such as Riotech. DOE

N89-23382*# Ricardo-ITI, Westmont, IL.
METHODS FOR HEAT TRANSFER AND TEMPERATURE FIELD ANALYSIS OF THE INSULATED DIESEL, PHASE 3 Final Report
Thomas Morel, Syed Wahiduzzaman, Edward F. Fort, Rifat Keribar, and Paul N. Blumberg Dec. 1988 171 p
(Contracts DEN3-342; DE-AI01-86CE-50162)
(NASA-CR-182237; DOE/NASA/0342-3; NAS 1.26:182237)
Avail: NTIS HC A08/MF A01 CSCL 20D

Work during Phase 3 of a program aimed at developing a comprehensive heat transfer and thermal analysis methodology for design analysis of insulated diesel engines is described. The overall program addresses all the key heat transfer issues: (1) spatially and time-resolved convective and radiative in-cylinder heat transfer, (2) steady-state conduction in the overall structure, and (3) cyclical and load/speed temperature transients in the engine structure. These are all accounted for in a coupled way together with cycle thermodynamics. This methodology was developed during Phases 1 and 2. During Phase 3, an experimental program was carried out to obtain data on heat transfer under cooled and insulated engine conditions and also to generate a database to validate the developed methodology. A single cylinder Cummins diesel engine was instrumented for instantaneous total heat flux and heat radiation measurements. Data were acquired over a wide range of operating conditions in two engine configurations. One was a cooled baseline. The other included ceramic coated components (0.050 inches plasma sprayed zirconia)-piston, head and valves. The experiments showed that the insulated engine has a smaller heat flux than the cooled one. The model predictions were found to be in very good agreement with the data. Author

88 SPACE SCIENCES (GENERAL)

No abstracts in this category.

89 ASTRONOMY

Includes radio, gamma-ray, and infrared astronomy, and astrometry.

N89-23383 California Univ., Berkeley.
STUDIES OF HOT WHITE DWARFS AND INSTRUMENTATION FOR STELLAR EXTREME ULTRAVIOLET ASTRONOMY PH.D. Thesis
David Starr Finley 1988 227 p
Avail: Univ. Microfilms Order No. DA8902085

The extreme ultraviolet explorer (EUVE) all-sky survey will enlarge the sample of known hot white dwarfs (T(eff) greater than 20,000K) from approx. 80 to perhaps 2000. The EUV measurements, used in conjunction with observations in other wavelength ranges, will give accurate effective temperatures, helium abundances and interstellar hydrogen columns for significant numbers of hot white dwarfs. Study of multiple stars will result in many more direct mass determinations of white dwarfs. Optimum utilization of the EUV survey data will be achieved by complementing the EUV observations with observations in other wavelength ranges. The efficacy of far ultraviolet (FUV) continuum measurements was evaluated by taking FUV spectra of several hot DA white dwarfs with the international ultraviolet explorer (IUE) satellite. These spectra were analyzed by means of our white dwarf model atmosphere code. In the course of this effort, accurate effective temperatures were obtained for the target stars, the IUE sensitivity was calibrated more accurately, and the visible photometry temperature scale for white dwarfs was revised. A satellite-borne telescope was built which will perform a photometric partial sky survey in a portion of the EUV band, between 80 and 300A. Calibration of this instrument demonstrated that it achieved the sensitivity and resolution necessary for detecting and locating stellar sources of EUV radiation. Further instrumental advances were made in the fabrication of the flight mirrors for the EUVE experiment. The imaging quality of the best of these mirrors exceeds that of the mirror used in the Einstein satellite X-ray telescope. As a result, EUVE will be able to perform a very sensitive all-sky survey which spans the entire EUV band of 70 to 900A.
Dissert. Abstr.

N89-23384 Manchester Univ. (England).
ECHELLE OBSERVATIONS OF H2 COMPLEXES Ph.D. Thesis
Christopher A. Clayton 1987 339 p
Avail: Univ. Microfilms Order No. BRD-83912

The dynamics of H2 complexes varying in visual luminosity by factors of up to one thousand were studied in detail using the Manchester echelle spectrometers in conjunction with the Anglo-Australian and Isaac Newton telescopes. In M17, several velocity components are found to be continuous over large areas of its extent. Two of these are closely associated with molecular clouds. Over the bright nebular core, the third component changes systematically to more negative velocities over a distance of a few parsecs. The approaching side of a radially expanding shell is suggested. At the position exhibiting the highest negative radial velocity of this shell, a collimated stream of ionized material is emerging. In NGC 3603, several continuous components are visible across its core with peak-to-peak velocity differences of up to 150km/s. In the ring nebula Hubble 3 in NGC 6822 a remarkable symmetric radially expanding bubble is observed with smaller expanding bubbles over its surface. Several possible dynamical origins are examined and models involving stellar wind-driven bubbles are found to be the most convincing. In NGC 604 in M33, expanding shells round Wolf-Rayet stars have been clearly detected. Area spectroscopy of 30 Doradus has revealed a mean velocity gradient across its core which is believed to indicate the presence of two ionized sheets of material whose emission line intensities vary spatially. The focal ratio degrading and image scrambling properties of curved step index fibers are examined and the fiber optics image reformatters which have been built for the echelles are described. Dissert. Abstr.

N89-23385 Manchester Univ. (England).
OBSERVATIONAL ASPECTS OF INTERACTING GALAXIES Ph.D. Thesis
A. P. Marston 1987 294 p
Avail: Univ. Microfilms Order No. BRD-83930

Various aspects of galaxy-galaxy and galaxy-environment interactions were investigated using observations in various waveband. Ultra Violet (UV) radiation from young stars heat dust associated with the star forming regions which in turn reradiates the UV in the far infrared. The IRAS satellite results were therefore used as part of the investigations. These observations provide far infrared maps of an elliptical galaxy and indicate that far infrared emission comes from a disc component in the galaxy provided by a merger. Other galaxies mapped by IRAS are NGC 7582, NGC 5033, NGC 7552 and NGC 4569, the first two of which are Seyfert galaxies, which show extended emitting regions at their centers.

The dynamics of the Large Magellanic Cloud (LMC) were investigated using H I profile measurements taken at the Parkes radio telescope. These have shown the LMC to have a system of sheets which were probably caused by the interaction between our galaxy and the LMC. Dynamics of the peculiar galaxy ESO 217-G09 were investigated using longslit spectra taken with the Manchester Echelle Spectrograph at the Anglo Australian Telescope. These show the galaxy to have a solid body rotation curve which indicate a galaxy mass of 2 x 10(10) solar masses. Lastly, the technique of digital plate coaddition is presented. The coadded plates were fully calibrated and provide calibrated data down to the lowest surface brightness ever produced. Together with spectroscopy observations an estimate of the galaxy mass were made. Dissert. Abstr.

N89-22623# Joint Publications Research Service, Arlington, VA.
PROJECT RADIOASTRON
B. Konovalov *In its* JPRS Report: Science and Technology. USSR: Space 17 Aug. 1988 p 15-16 Transl. into ENGLISH from Izvestiya (Moscow, USSR), 10 Apr. 1988 p 2 (For primary document see N89-22622 16-12)
Copyright Avail: NTIS HC A05/MF A01

90 ASTROPHYSICS

Includes cosmology; celestial mechanics; space plasmas; and interstellar and interplanetary gases and dust.
For related information see also *75 Plasma Physics*.

N89-23386 Florida Univ., Gainesville.
CO IN THE GALACTIC CENTER: A COMPLETE SURVEY OF CARBON MONOXIDE EMISSION IN THE INNER 4 kpc OF THE GALAXY Ph.D. Thesis
Mauricio Ernesto BitranCarreno 1987 249 p
Avail: Univ. Microfilms Order No. DA8817767

The first well-sampled, large scale survey of CO-12 (J = 1 yields 0) emission from the inner 4 kpc of the Galaxy is presented and used to study the distribution of molecular clouds and the kinematics of the molecular gas in the inner Galaxy. The survey samples a 4 deg wide strip along the Galactic equator from 1 = -12 deg to 1 = 13 deg. The over 8000 spectra obtained with the Columbia University Southern millimeter telescope (La Serena, Chile) have a velocity resolution of 1.3 km/s, a rms sensitivity better than 0.12 K, and are spaced by approximately one beamwidth (8.8 minutes). This is the first survey to encompass the complete latitude and velocity spans of the CO emission from the inner Galaxy. The survey is presented as a collection of 1-V, b-V, and 1-b maps. Features with the largest CO luminosities and velocity widths in the inner Galaxy, outside the nuclear regions, were fully mapped and analyzed. Molecular clouds in the surveyed area were identified and cataloged. The inclination and thickness of the molecular layer in the inner Galaxy were measured and their relevance to current models of the regions discussed. A lower limit for the surface density at the center was found and a CO rotation curve was calculated and compared to available H I rotation curves. Dissert. Abstr.

N89-23387# Fermi National Accelerator Lab., Batavia, IL.
DARK MATTER CANDIDATES
Michael S. Turner Jan. 1989 9 p Presented at the 3rd ESO-CERN Symposium on Astronomy, Cosmology, and Fundamental Physics, Bologna, Italy, 16 May 1988
(Contracts DE-AC02-76CH-03000; DE-AC02-80ER-10587)
(DE89-006579; FNAL/C-89/16-A; CONF-8805229-2) Avail: NTIS HC A02/MF A01

One of the simplest, yet most profound, questions we can ask about the Universe is, how much stuff is in it, and further what is that stuff composed of. Needless to say, the answer to this question has very important implications for the evolution of the Universe, determining both the ultimate fate and the course of structure formation. Remarkably, at this late date in the history of the Universe we still do not have a definitive answer to this simplest of questions---although we have some very intriguing clues. It is known with certainty that most of the material in the Universe is dark, and we have the strong suspicion that the dominant component of material in the Cosmos is not baryons, but rather is exotic relic elementary particles left over from the earliest, very hot epoch of the Universe. If true, the Dark Matter question is a most fundamental one facing both particle physics and cosmology. The leading particle dark matter candidates are: the axion, the neutralino, and a light neutrino species. All three candidates are accessible to experimental tests, and experiments are now in progress. In addition, there are several dark horse, long shot, candidates, including the superheavy magnetic monopole and soliton stars. DOE

N89-23388# Florida Univ., Gainesville. Dept. of Physics.
GENERATING A HOT BIG BANG VIA A CHANGE IN TOPOLOGY
H. E. Kandrup and P. O. Mazur Jan. 1989 7 p Presented at the 14th Texas Symposium on Relativistic Astrophysics, Dallas, TX, 11 Dec. 1988
(Contract DE-FG05-86ER-40272)
(DE89-007561; DOE/ER-40272/73; CONF-881268-2) Avail: NTIS HC A02/MF A01

The objective here is to use ideas developed recently in semiclassical quantum gravity to provide a possible explanation of the Hot Big Bang generally assumed in cosmology. DOE

N89-23389# International Centre for Theoretical Physics, Trieste (Italy).
REVERSED SENSE OF THE OUTWARD DIRECTION FOR DYNAMICAL EFFECTS OF ROTATION CLOSE TO A SCHWARZSCHILD BLACK HOLE
Marek A. Abramowicz and A. R. Prasanna (Physical Research Lab., Ahmedabad, India) Oct. 1988 23 p Submitted for publication
(DE88-705670; IC-88/275) Avail: NTIS (US Sales Only) HC A03/MF A01

Anderson and Lemos (1988) noticed that the direction in which viscous torque transports angular momentum changes, close to a black hole, from outwards to inwards. We find here that close to a black hole the centrifugal force attracts particles towards the hole. We argue that these are particular examples of a general reversal in sense of the inward and outward directions for all dynamical effects of rotation close to the hole. Using results from the recent paper by Abramowicz, Carter and Lasota (1988) we explain that the reversal is not connected with dragging of inertial frames or with the difference between the angular velocities of the hole and of the surrounding matter but rather, it is an effect of curvature. For a Schwarzschild black hole the reversal takes place at the circular photon orbit (r=3M-tilde) because the geodesic curvature, R-tilde=r(1-3M-tilde/r), of the circles r = const. changes its sign there. DOE

N89-23390# International Centre for Theoretical Physics, Trieste (Italy).
SUPERCONDUCTING COSMIC STRING EVOLUTION OF QUASARS
Yulin Liu (Academia Sinica, Beijing, China) Sep. 1988 6 p
(DE88-705672; IC-88/279) Avail: NTIS (US Sales Only) HC A02/MF A01

The quasars may have been undergoing two evolutionary processes after they formed. As a result of the string loops shrinking at the first stage, the luminosities of the quasars increased gradually up to their maximum value at the redshift z is approximately 2, after then the second evolutionary stage began and the luminosity reduced. This result can be fitted by luminosity counting of quasars. Observable limit of quasars can be obtained naturally. Many phenomena, such as radiomorphology, density distribution between fuzz structure and broad line region and rotational curve may also originate from the first evolutionary stage of quasars as cosmic string. DOE

N89-23391# International Centre for Theoretical Physics, Trieste (Italy).
FAR INFRARED PECULIAR BEHAVIOR OF QUASARS
Yulin Liu and Jiying Liu (Academia Sinica, Beijing, China) Sep. 1988 9 p
(DE88-705673; IC-88/280) Avail: NTIS (US Sales Only) HC A02/MF A01

Many quasars possibly have nebulous envelopes with far infrared radiation. These nebulosities may be similar to fuzz in the optical region in morphology. These quasars have many properties in common. DOE

N89-23392# Los Alamos National Lab., NM. Space Astronomy and Astrophysics Group.
THE ALEXIS PROJECT AND THE LOCAL INTERSTELLAR MEDIUM
J. J. Bloch and B. W. Smith 1989 10 p Presented at the Berkeley Colloquium on Extreme Ultraviolet Astronomy, Berkeley, CA, 19 Jan. 1989
(Contract W-7405-eng-36)
(DE89-009246; LA-UR-89-1077; CONF-890189-6) Avail: NTIS HC A02/MF A01

The ALEXIS satellite will be a valuable tool for studying the diffuse soft X-ray background (SXRB). The SXRB emission (0.07 to 0.25 KeV) is thought to originate in a plasma at about 10 K that exists in the local interstellar medium. Emission models of such a plasma (Raymond and Smith 1977, 1987) with normal cosmic elemental abundances predict that about 34 percent of the atomic cooling power comes from a set of closely-spaced lines around 70 eV from Fe VII through XII. Two passbands of the ALEXIS telescopes will be centered at 66 and 72 eV to include the Fe line emission. The flux from these lines in the SXRB could produce a signal of as much as 150 counts per second for ALEXIS telescopes with these passbands. With the narrow spectral response of the ALEXIS telescopes, an unambiguous measurement of the flux from the lines will be possible. When combined with other data sets, the intensities of the SXRB in the 66 and 72 eV bands allow distinction between models of emission from hot gas having normal and depleted abundances. ALEXIS' spatial resolution and estimated year-long operating lifetime will allow the generation of all-sky maps of the SXRB in these Fe lines with about one degree resolution and considerable sensitivity. These maps will be more sensitive to absorption features due to nearby low-column-density clouds than maps done in higher energy bands. DOE

N89-23393 Texas Univ., Dallas.
PROBLEMS IN MODERN COSMOLOGY Ph.D. Thesis
Daniel Jeffrey Suson 1988 92 p
Avail: Univ. Microfilms Order No. DA8903268

Two problems in modern cosmology were studied. The first problem involved the study of a spherically symmetric universe, while the second considered the calculation of the annihilation cross section for two photino annihilation into two photons. The spherically symmetric universe problem studied the question of whether the metric for the model could be determined by considering the relationship between perfect observations and their theoretical counterparts. It was found that the combinations of the solid angle subtended by a galaxy vs. the cross sectional area of the galaxy and the number of galaxies per unit area vs. density could determine the metric uniquely, when used in conjunction with the field equations of general relativity. The annihilation cross section problem develops the exact calcuation up to a point where it can be replaced with an approximate Lagrangian. The cross section is then determined based on this Lagrangian and the result is compared with calculations performed by previous authors. This comparison shows that previous calcuations have underestimated the strength of the cross section. Dissert. Abstr.

N89-23394 California Univ., Berkeley.
GRAVITATIONAL EFFECTS OF COSMIC STRINGS IN FRIEDMANN UNIVERSES Ph.D. Thesis
Shoba Veeraraghavan 1988 147 p
Avail: Univ. Microfilms Order No. DA8902306

Cosmic strings were invoked recently as a possible source of the primordial density fluctuations in matter which gave rise to large-scale structure by the process of gravitational collapse. If cosmic strings did seed structure formation then they would also leave an observable imprint upon the microwave and gravitational wave backgrounds, and upon structure on the very largest scales. The energy-momentum tensor appropriate to a cosmic string configuration in the flat Friedmann universe is obtained and used in the linearized Einstein equations to obtain the perturbations of the background space-time and the ambient matter. The calculation is fully self-consistent to linear order and is valid for an arbitrarily curved and moving configuration everywhere except very close to a string segment. The single constraint is that the dimensionless string tension G(micro)/c squared must be small compared to unity. The gravitational wave spectrum and the microwave background temperature fluctuations from a single infinite straight and static string are calculated. The statistically expected fluctuations from an ensemble of such strings with a mean density equal to that found in computer simulations of the evolution of string networks is also calculated. These fluctuations are compared with the observational data on the microwave background to constrain G micro. The role of infinite strings in the formation of the large-scale structure on scales of tens of Megaparsecs observed in deep redshift surveys is examined. Based on the current values for the fraction of the total energy density in long strings and in subhorizonsized loops, it appears that gravitational collapse of matter in the wakes behind infinite strings could be responsible for the Megaparsec scale structure. Dissert. Abstr.

N89-23395 Edinburgh Univ. (Scotland).
OPTICAL AND INFRARED OBSERVATIONS OF THE NATURE AND EVOLUTION OF ACTIVE GALAXIES Ph.D. Thesis
Mark Guy Yates 1988 187 p
Avail: Univ. Microfilms Order No. BRD-84187

The evolution of the environments of powerful, high-redshift radio galaxies, and the astrophysics of low-redshift active galaxies as inferred from optical, near- and far-infrared observations are studied. The relationship between the radio and infrared luminosities of a sample of 60 high-redshift 3C radio galaxies reveals that the two quantities are correlated for the most powerful (and thus most distant) examples. It is suggested that the most powerful radio galaxies are subject to galaxy cannibalism, and will tend to lie in rich environments. Imaging of a sample of 26 powerful radio galaxies (0.15 is less than z is less than 0.82) is presented in order to test this hypothesis. It is found that radio galaxies at z is greater than 0.3 lie in environments as rich as Abell class 0-1 clusters. The environments of these galaxies are four to five times richer than those at low redshift (z is less than 0.3). However, it is not possible to establish unequivocally whether radio luminosity or epoch is the fundamental parameter determining the richness of the environment. Deep Infrared Astronomy Satellite (IRAS) observations of 18 3C radio galaxies (0.01 is less than z is less than 0.2) are discussed, and the spectral energy distributions of the six detected objects constructed. The two broad-line radio galaxies show a peak at 25 micrometer, possible associated with a warm (T approximately equals 180 K) dust component. The narrow-line radio galaxies have large far-infrared luminosities, and this component has a much greater luminosity than either the X-ray or radio components. However, there is no evidence for a 25 micro peak. Near-simultaneous optical and infrared spectrophotometry of a sample of eight optically bright quasars and one broad-line radio galaxy are presented. Study of their Pa(alpha)/H(alpha) and H(alpha)/H(beta) ratios reveals that they can not be well modelled by either reddened or unreddened photoionization models. Dissert. Abstr.

N89-22624# Joint Publications Research Service, Arlington, VA.
METHODS AND ALGORITHMS FOR PROCESSING TELEVISION IMAGES OF NUCLEUS OF HALLEY'S COMET. SOME RESULTS Abstract Only

R. Z. Sagdeyev, G. A. Avanesov, Ya. L. Ziman, V. A. Shamis, and V. A. Krasikov *In its* JPRS Report: Science and Technology. USSR: Space 17 Aug. 1988 p 26 Transl. into ENGLISH from Kosmicheskiye Issledovaniya (Moscow, USSR), v. 25, no. 6, Nov.-Dec. 1987 p 820-830 (For primary document see N89-22622 16-12)
Copyright Avail: NTIS HC A05/MF A01

91 LUNAR AND PLANETARY EXPLORATION

Includes planetology; and manned and unmanned flights.
For spacecraft design or space stations see *18 Spacecraft Design, Testing and Performance.*

N89-23396# International Centre for Theoretical Physics, Trieste (Italy).
DYNAMICS OF PARTICLES IN THE BENDING WAVES OF THE PLANETARY RINGS
S. K. Chakrabarti (Tata Inst. of Fundamental Research, Bombay, India) Oct. 1988 26 p Prepared in cooperation with California Inst. of Tech., Pasadena
(Grants AST-86-15325; AST-85-19411)
(DE88-705714; IC-88/354) Avail: NTIS (US Sales Only) HC A03/MF A01

We study the motion of a single particle in the bending wave of finite thickness in the planetary ring. We include the forcing due to the planet, the moon, the coriolis force and the self gravity of the ring. In particular, we study the variation of the velocity arising due to the variation of the amplitude and the phase of the epicyclic motion across the height of the ring. We suggest that the dissipation of energy of this shear layer through collisions of ring particles from different heights may contribute significantly to the damping of the bending waves observed in the Voyger data. DOE

N89-23397*# National Aeronautics and Space Administration. Lewis Research Center, Cleveland, OH.
COMPARISON OF SOLAR PHOTOVOLTAIC AND NUCLEAR REACTOR POWER SYSTEMS FOR A HUMAN-TENDED LUNAR OBSERVATORY
J. M. Hickman and H. S. Bloomfield 1989 7 p Proposed for presentation at the 24th Intersociety Energy Conversion Engineering Conference, Washington, DC, 6-11 Aug. 1989; sponsored by IEEE, AIAA, ANS, ASME, SAE, ACS and AIChE
(NASA-TM-102015; E-4729; NAS 1.15:102015) Avail: NTIS HC A02/MF A01 CSCL 03B

Photovoltaic and nuclear surface power systems were examined at the 20 to 100 kW power level range for use at a human-tended lunar astronomical observatory, and estimates of the power system masses were made. One system, consisting of an SP-100 thermoelectric nuclear power supply integrated with a lunar lander, is recommended for further study due to its low system mass, potential for modular growth, and applicability to other surface power missions, particularly in the Martian system. Author

N89-23398 New Mexico State Univ., University Park.
A HISTORICAL INTERPRETATION OF THE STUDY OF THE VISIBLE CLOUD MORPHOLOGY ON THE PLANET JUPITER: 1610-1878 Ph.D. Thesis
Thomas Arnold Hockey 1988 396 p
Avail: Univ. Microfilms Order No. DA8900316

The majority of the literature discussing the perceived physical appearance of Jupiter published prior to 1878 was examined in order to determine to what extent observations were biased by technical limitations and preconceptions of their day and, in lieu of these, how useful this body of work is in characterizing the behavior of the Jovian upper atmosphere over the last three hundred years. The biographies of the historical observers; their instrumentation, available viewing conditions, and observational techniques; their means of communication with their fellows; and the primary interpretive references available to their libraries were investigated in order to attempt to explain discrepancies and agreement between what was reported in pre-photographic times and what is presently seen. It was found that nearly all of the prominent feature-types found on Jupiter today existed during the nineteenth century and, in some cases, earlier. The longevity and frequency of the appearance of features can not be accurately determined from the time before objective surveys of the planet were organized. This is because, during each apparition of Jupiter, nonprofessional part-time observers, working independently chose to use their finite time and resources to follow the progress of specific discoveries on its disk to the exclusion of the rest of the planet. Interpretation of Jovian features were subject to three major impediments: the belief in and search for a solid surface of Jupiter at moderate depth below the clouds; a lack of appreciation for the two or more orders of magnitude differences of scale between the dimensions of Jupiter's area, mass, and properties of its atmosphere compared to those of the Earth; and an inability to differentiate between real and phantom features watched through seeing-limited telescopes. Dissert. Abstr.

92 SOLAR PHYSICS

Includes solar activity, solar flares, solar radiation and sunspots.
For related information see *93 Space Radiation.*

N89-23399*# California Univ., Berkeley. Space Sciences Lab.
OBSERVATIONAL TECHNIQUES FOR SOLAR FLARE GAMMA-RAYS, HARD X-RAYS, AND NEUTRONS Final Report, 1 Nov. 1983 - 30 Nov. 1988
Robert P. Lin 18 Apr. 1989 62 p
(Grant NAGw-516)
(NASA-CR-184910; NAS 1.26:184910) Avail: NTIS HC A04/MF A01 CSCL 03B

The development of new instrumentation and techniques for solar hard X-ray, gamma ray and neutron observations from spacecraft and/or balloon-borne platforms is examined. The principal accomplishments are: (1) the development of a two segment germanium detector which is near ideal for solar hard X-ray and gamma ray spectroscopy; (2) the development of long duration balloon flight techniques and associated instrumentation; and (3) the development of innovative new position sensitive detectors for hard X-ray and gamma rays. Author

93 SPACE RADIATION

Includes cosmic radiation; and inner and outer earth's radiation belts.
For biological effects of radiation see *52 Aerospace Medicine.* For theory see *73 Nuclear and High-Energy Physics.*

N89-23400*# Hampton Inst., VA. Dept. of Physics.
EFFECTS OF COSMIC RAYS ON SINGLE EVENT UPSETS Status Report
D. D. Venable, V. Zajic, C. W. Lowe, A. Olidapupo, and T. N. Fogarty Feb. 1989 84 p
(Grant NAG5-929)
(NASA-CR-184835; NAS 1.26:184835) Avail: NTIS HC A05/MF A01 CSCL 03B

Assistance was provided to the Brookhaven Single Event Upset (SEU) Test Facility. Computer codes were developed for fragmentation and secondary radiation affecting Very Large Scale Integration (VLSI) in space. A computer controlled CV (HP4192) test was developed for Terman analysis. Also developed were high speed parametric tests which are independent of operator judgment and a charge pumping technique for measurement of D(sub it) (E). The X-ray secondary effects, and parametric degradation as a function of dose rate were simulated. The SPICE simulation of static RAMs with various resistor filters was tested. B.G.

N89-23401# Severn Communications Corp., Millersville, MD.
EQUATIONS OF COSMIC-RAY TRANSPORT WITH DISTRIBUTED ACCELERATION
John R. Letaw and Jacob Roginsky 13 Jan. 1989 24 p
(Contract N00014-87-C-2251)
(AD-A204599; SCC-89-01) Avail: NTIS HC A03/MF A01 CSCL 03B

The equations of cosmic-ray transport used in our galactic cosmic-ray propagation model are described. The equations include distributed acceleration terms associated with weak reacceleration of cosmic-ray ions in supernova remnants. Reacceleration may occur at any time during the diffusion of cosmic rays through the interstellar medium. GRA

N89-23402# Lawrence Livermore National Lab., CA. Physics Dept.
THERMAL COMPTONIZATION MODELS FOR GAMMA-RAY EMISSION FROM BLACK-HOLE SOURCES
Charles D. Dermer 16 Mar. 1989 16 p Presented at the 14th Texas Symposium on Relativistic Astrophysics, Dallas, TX, 11 Dec. 1988
(Contract W-7405-eng-48)
(DE89-009918; UCRL-100749; CONF-881268-4) Avail: NTIS HC A03/MF A01

Black holes power the variable luminous emission observed from quasars and the nuclei of active galaxies; at least it is assumed so here. The list of black-hole candidates detected at gamma-ray energies includes the galactic binary X-ray source Cygnus X-1, the Galactic Center, and the extragalactic sources Cen A (NGC 5128), NGC 4151, MCG 8-11-11 and 3C 273. The luminosity of these objects peaks in the photon energy range 0.1 equal to or less than epsilon equal to or less than 10 MeV and dominates the total energy output in the observable wavebands. SAS-2 and COS-B upper limits and observations indicate a cutoff or softening in their spectra between approx. 1 and approx. 30 MeV, which is probably due to absorption of gamma rays by photon-photon pair production or a break in the underlying particle spectrum. Indeed, spectral softening at MeV energies seems to be required of active galactic nuclei (AGN) in general; otherwise the superposition of the emission from these sources would conflict with observations of the diffuse gamma-ray background radiation. The salient features associated with gamma-ray emission from the above-mentioned sources are summarized in this paper, beginning with Cygnus X-1, the best-studied black-hole candidate. Because of similarity in properties, models developed to explain the X-ray and gamma-ray observations of Cygnus X-1 can be equally applied to AGN. In this review, successes and limitations of thermal Comptonization models for the high-energy emission of black-hole sources are considered. GRA

99 GENERAL

N89-23403# Advisory Group for Aerospace Research and Development, Neuilly-Sur-Seine (France).
AGARD HIGHLIGHTS 88/2
Sep. 1988 39 p
Copyright Avail: NTIS HC A03/MF A01

Topics addressed include: a review of fluid dynamics; military pilot ergonomics; and future air operations. The award of the von Karman Medal for 1988 is presented. B.G.

N89-23404*# Tennessee Univ., Tullahoma. Center for Aerospace Research.
CENTER FOR ADVANCED SPACE PROPULSION (CASP) Annual Report, 1 Oct. 1987 - 30 Oct. 1988
1988 99 p Prepared in cooperation with Boeing Aerospace Co., Seattle, WA, Calspan Corp., Arnold AFS, TN, Rockwell International Corp., Canoga Park, CA, Saturn Corp., Cheverly, MD, Symbolics, Inc., Cambridge, MA and Technion, Inc., Irvine, CA
(Grant NAGw-1195)
(NASA-CR-184936; NAS 1.26:184936) Avail: NTIS HC A05/MF A01 CSCL 05A

With a mission to initiate and conduct advanced propulsion research in partnership with industry, and a goal to strengthen U.S. national capability in propulsion technology, the Center for Advanced Space Propulsion (CASP) is the only NASA Center for Commercial Development of Space (CCDS) which focuses on propulsion and associated technologies. Meetings with industrial partners and NASA Headquarters personnel provided an assessment of the constraints placed on, and opportunities afforded commercialization projects. Proprietary information, data rights, and patent rights were some of the areas where well defined information is crucial to project success and follow-on efforts. There were five initial CASP projects. At the end of the first year there are six active, two of which are approaching the ground test phase in their development. Progress in the current six projects has met all milestones and is detailed. Working closely with the industrial counterparts it was found that the endeavors in expert systems development, computational fluid dynamics, fluid management in microgravity, and electric propulsion were well received. One project with the Saturn Corporation which dealt with expert systems application in the assembly process, was placed on hold pending further direction from Saturn. The Contamination Measurment and Analysis project was not implemented since CASP was unable to identify an industrial participant. Additional propulsion and related projects were investigated during the year. A subcontract was let to a small business, MicroCraft, Inc., to study rocket engine certification standards. The study produced valuable results; however, based on a number of factors it was decided not to pursue this project further. Author

N89-23405# Centre National d'Etudes Spatiales, Toulouse (France).
HISTORY OF MANNED FLIGHT [HISTORIQUE DES VOLS HABITES]
Philippe Lebocq Jan. 1989 87 p In FRENCH; ENGLISH summary
(CNES-NT-121; ETN-89-94369) Avail: NTIS HC A05/MF A01

A compilation of Soviet and U.S. space missions is presented. The flight parameters are indicated for each case, including identity of crew members, flight dates, type of mission, type of vehicle and launcher, duration of flight, and extravehicular activity. Explanations are given about intricate missions, with crew transfer and inversion of flight spacecraft. ESA

Typical Subject Index Listing

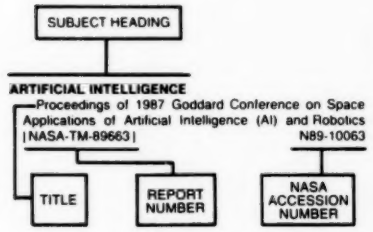

The subject heading is the key to the subject content of the document. Titles, report numbers, and accession numbers of pertinent documents are provided under each subject heading. When the title is insufficiently descriptive of the document content, a title extension has been added, separated from the title by three hyphens. The report number helps to indicate the type of document cited (e.g., NASA report, NASA translation, NASA contractor report). The NASA accession number is the number by which the document abstracts are arranged in this journal and by which the document is sold or requested. The titles, with title extensions if present, are arranged under each subject heading in ascending accession number order. The subject headings have been selected from the latest revision of the *NASA Thesaurus* (NASA SP-7064).

A

ABSORPTION SPECTRA
Gamma ray laser pump diagnostic
[AD-A205221] N89-22683

ABSTRACTS
Beam research technical abstracts, 1987
[DE89-009013] N89-23282
Sources of information N89-23366
Indexing and abstracting N89-23368

ABUNDANCE
The ALEXIS project and the local interstellar medium
[DE89-009246] N89-23392

ACCELERATED LIFE TESTS
Electrochemical technique for rapidly evaluating protective coatings on metals
[PB89-134209] N89-22748

ACCELERATION (PHYSICS)
Acceleration test for aircraft low-pass filter
[PB89-116263] N89-22807
Equations of cosmic-ray transport with distributed acceleration
[AD-A204599] N89-23401

ACCESS CONTROL
Fostering interaction of government, defense, and aerospace databases N89-23374

ACCIDENT PREVENTION
Safe skies for tomorrow: Aviation safety in a competitive environment
[PB89-114318] N89-22591

ACCIDENTS
Space Propulsion Hazards Analysis Manual (SPHAM). Volume 2: Appendices
[AD-A204601] N89-22650

ACCRETION DISKS
Direct numerical simulations of turbulent convection with a variable gravity and Keplerian rotation N89-22831

ACOUSTIC EXCITATION
Experimental observation of the nonlinear response of single bubbles to an applied acoustic field
[AD-A205191] N89-23271

ACOUSTIC MEASUREMENT
Measurements of a barotropic planetary vorticity mode in an eddy-resolving quasi-geostrophic model using acoustic tomography
[AD-A205409] N89-23058

ACOUSTIC VELOCITY
Measurements of a barotropic planetary vorticity mode in an eddy-resolving quasi-geostrophic model using acoustic tomography
[AD-A205409] N89-23058

ACOUSTICS
Detection of known signals in arbitrary backgrounds
[AD-A204076] N89-22784
Environmental noise characteristics of the MOD5-B (3.2 MW) wind turbine generator
[NASA-TM-101567] N89-23272
Acoustic wave device using plate modes with surface-parallel displacement
[DE89-009719] N89-23273

ACOUSTO-OPTICS
Parallel Optical Random Access Memory (PORAM)
[NASA-CR-4241] N89-22890

ACRYLIC RESINS
Environmentally induced discontinuities in transparent polymers
[AD-A205483] N89-22768

ACTIVE CONTROL
Active vibration control for flexible rotor by optimal direct-output feedback control
[NASA-TM-101972] N89-22605

ACTIVE GALACTIC NUCLEI
Thermal Comptonization models for gamma-ray emission from black-hole sources
[DE89-009918] N89-23402

ACTIVE GALAXIES
Optical and infrared observations of the nature and evolution of active galaxies N89-23395

ADA (PROGRAMMING LANGUAGE)
Implementation of the NETOS (Network Operating System) operated system in Ada with modifications to allow variable length messages
[AD-A202602] N89-23185
Use of language features in the implementation and validation of a standardized generic package of elementary functions for Ada
[DE89-007385] N89-23187
A statistical package in Ada
[FOA-C-20740-2.7] N89-23201
HOOD Toolset Development Project: ECLIPSE/HOOD/REP, issue 1.1
[ESA-CR(P)-2746] N89-23204

ADAPTIVE CONTROL
Control of free-flying space robot manipulator systems
[NASA-CR-184837] N89-22918
Adaptive LQ control: Conflict between identification and control
[MEMO-718] N89-23216

ADAPTIVE FILTERS
Adaptive smoothing for feature extraction N89-23173

ADHESION
Interfacial adhesion and mechanical properties of polyamide-6/glass bead composites
[ETN-89-94136] N89-22759
Internal debonding of solid rocket fuel: An experimental investigation
[AD-A205903] N89-22772

ADHESIVE BONDING
Signal treatment and data analysis methods applied to nondestructive control of adhesive bonded joints
[ISAL-IDI-8809] N89-22936
Analysis of the mechanical behavior of adhesively bonded composite joints
[AD-A202616] N89-22938

ADIABATIC CONDITIONS
A study of high strain rate generation of adiabatic shear bands in a titanium alloy N89-22967

ADIABATIC EQUATIONS
Compression and shear wave propagation in explosives
[AD-A205917] N89-22665

ADSORPTION
Measurement uncertainty of adsorption testing of desiccant materials
[DE89-000841] N89-22681
Adsorption studies in the critical region of a pure fluid. Development of an apparatus for adsorption measurements under microgravity conditions
[ETN-89-93767] N89-22774

AERIAL PHOTOGRAPHY
Image understanding research at the University of Maryland, December 1986 - January 1988 N89-23078
Image understanding research at SRI International N89-23080
Cooperative methods for road tracking in aerial imagery N89-23101
PACE: An environment for intelligence analysis N89-23102
Multiresolution aerial image interpretation N89-23116
Perceptual grouping for the detection and description of structures in aerial images N89-23117

AERODYNAMIC CHARACTERISTICS
Comparison of boundary layer trips of disk and grit types on airfoil performance at transonic speeds
[AD-A205206] N89-22575

AERODYNAMIC FORCES
Aerodynamics of nonrigid bodies undergoing large amplitude time-dependent motions N89-22586

AERODYNAMIC HEAT TRANSFER
Control of embedded vortices using wall jets
[AD-A202606] N89-22835

AERODYNAMIC HEATING
Transition to turbulence in laminar hypersonic flow N89-22830

AERODYNAMIC LOADS
Prediction of loads on wing/body/external store/fins pylon-configurations at transonic speeds
[FFA-TN-1988-44] N89-22602

AERODYNAMIC STABILITY
Aerodynamic detuning of a loaded airfoil cascade in an incompressible flow by a locally analytical method N89-22588

AERODYNAMICS
Visting China's aerodynamics research and development center
[AD-A203980] N89-22615
A vortex panel analysis of circular-arc bluff-bodies in unsteady flow
[DE89-007141] N89-22845
A real-time simulator for man-in-the-loop testing of aircraft control systems (SIMTACS-RT)
[AD-A202599] N89-23067

AEROELASTICITY
Aerodynamic detuning of a loaded airfoil cascade in an incompressible flow by a locally analytical method N89-22588
Structural dynamics branch research and accomplishments for FY 1988
[NASA-TM-101406] N89-22939

AERONAUTICAL ENGINEERING
Future advanced aero-engines: The materials challenge N89-22659

AERONAUTICS
Calendar of selected aeronautical and space meetings
[AGARD-CAL-88/2] N89-23361

AEROSPACE ENGINEERING
JPRS report: Science and technology. USSR: Space
[JPRS-USP-88-003] N89-22622
Construction in weightlessness N89-22626
Development of orbital welding technology N89-22628

AEROSPACE MEDICINE
Historical survey of biosatellites N89-22625

AEROSPACE SAFETY
Space Propulsion Hazards Analysis Manual (SPHAM). Volume 2: Appendices
[AD-A204601] N89-22650
Space Nuclear Safety Program
[DE89-008308] N89-23281

AEROSPACE SCIENCES
Calendar of selected aeronautical and space meetings
[AGARD-CAL-88/2] N89-23361
AEROSPACE SYSTEMS
Space Electrochemical Research and Technology Conference: Abstracts
[NASA-CP-10029] N89-22982
AEROTHERMODYNAMICS
Future advanced aero-engines: The materials challenge N89-22659
AGING (MATERIALS)
Spinodal decomposition of austenite in long-term-aged duplex stainless steel
[DE89-009827] N89-22737
AGREEMENTS
A multinational verification satellite: A preliminary investigation — arms control
[FOA-C-10312-9.3] N89-22974
AIR DEFENSE
AGARD highlights 88/2 N89-23403
AIR MASSES
Preliminary results of the MLAM (Multi-Layer Air Mass) Lagrangian transport model simulation of ANATEX (Across North America Tracer Experiment)
[DE89-008123] N89-23036
AIR POLLUTION
Quantitative analysis of atmospheric trace gases
[BPT-10/88] N89-23027
AIR TRAFFIC CONTROL
National airspace system plan: Facilities, equipment, associated development and other capital needs
[AD-A202615] N89-22596
AIR TRAFFIC CONTROLLERS (PERSONNEL)
Studies of poststrike air traffic control specialist trainees. Part 2: Selection and screening programs
[AD-A199177] N89-22595
AIR WATER INTERACTIONS
Measurements of a barotropic planetary vorticity mode in an eddy-resolving quasi-geostrophic model using acoustic tomography
[AD-A205409] N89-23058
AIRBORNE/SPACEBORNE COMPUTERS
An experimental environment and laboratory for studying human information processing in Naval Air ASW (Naval air antisubmarine warfare)
[AD-A204774] N89-23069
AIRCRAFT
Geodetic positioning system for flying aircraft (May 1987)
[REPT-013/88] N89-22598
AIRCRAFT ACCIDENT INVESTIGATION
Aircraft accident report: Trans-Colorado Airlines, Inc., Flight 2286, Fairchild Metro 3, SA227 AC, N68TC Bayfield, Colorado, January 19, 1988
[PB89-910401] N89-22593
AIRCRAFT COMPARTMENTS
Evaluation of the ride quality of a light twin engine airplane using a ride quality meter
[NASA-TP-2913] N89-22568
AIRCRAFT CONSTRUCTION MATERIALS
Tests of new materials with second generation carbon fibers, test report
[REPT-47-188/F] N89-22702
CSPC test 319.30: Study on impact tolerance of preimpregnated carbon-epoxy systems
[REPT-47-323/F] N89-22703
A survey of poly-ether-ether-ketone and its advanced composites
[FFA-TN-1988-37] N89-22707
AIRCRAFT CONTROL
A real-time simulator for man-in-the-loop testing of aircraft control systems (SIMTACS-RT)
[AD-A202599] N89-23057
AIRCRAFT DESIGN
An efficient inverse method for the design of blended wing-body configurations N89-22603
Computational fluid dynamics research in three-dimensional zonal techniques
[NASA-CR-181406] N89-22838
AIRCRAFT ENGINES
Application of Advanced Material for Turbomachinery and Rocket Propulsion
[AGARD-CP-449] N89-22654
AIRCRAFT HAZARDS
NASA's program on icing research and technology
[NASA-TM-101980] N89-22569
AIRCRAFT LANDING
Aircraft accident report: Trans-Colorado Airlines, Inc., Flight 2286, Fairchild Metro 3, SA227 AC, N68TC Bayfield, Colorado, January 19, 1988
[PB89-910401] N89-22593
AIRCRAFT NOISE
Evaluation of the ride quality of a light twin engine airplane using a ride quality meter
[NASA-TP-2913] N89-22568
AIRCRAFT SAFETY
Safe skies for tomorrow: Aviation safety in a competitive environment
[PB89-114318] N89-22591
AIRCRAFT SPECIFICATIONS
Testing of a new recovery parachute system for the F111 aircraft crew escape module: An update
[DE89-007139] N89-22592
AIRCRAFT STRUCTURES
Electro-impulse de-icing research: Fatigue and electromagnetic interference tests
[DOT/FAA/CT-88/27] N89-22594
An efficient inverse method for the design of blended wing-body configurations N89-22603
AIRFOIL PROFILES
Wind tunnel tests of 16 percent thick airfoil section with spoilers at different chordwise positions — wind turbines
[FFA-TN-1987-39] N89-22582
Computational investigation of incompressible airfoil flows at high angles of attack
[AD-A205885] N89-22590
AIRFOILS
A study of unsteady turbulent flow past airfoils N89-22587
Hardware and operating features of the adaptive wall test section for the 0.3-meter transonic cryogenic tunnel
[NASA-TM-4114] N89-22614
A vortex panel analysis of circular-arc bluff-bodies in unsteady flow
[DE89-007141] N89-22845
Surface temperature measurements using a thin film thermal array
[NASA-TM-101549] N89-22868
AIRFRAME MATERIALS
Development and testing of critical components for technological preparation of an Airbus-CFRP-fuselage, phase 2
[MBB-UT-129/87] N89-22600
AIRFRAMES
Tests of new materials with second generation carbon fibers, test report
[REPT-47-188/F] N89-22702
ALGEBRA
An algorithm for the three-index assignment problem
[AD-A205172] N89-23190
Optimization for object localization of the constrained algebraic reconstruction technique
[DE89-007755] N89-23193
On a functional equation over Hilbert spaces
[DE88-705645] N89-23267
ALGORITHMS
Dynamic image interpretation for autonomous vehicle navigation
[AD-A204167] N89-22597
Methods and algorithms for processing television images of nucleus of Halley's Comet. Some results N89-22624
HIFI: A design method for implementing signal processing algorithms on VLSI processor arrays
[ETN-89-94138] N89-22795
Evaluation of several state-of-charge algorithms
[DE89-009752] N89-22812
Computational fluid dynamics research in three-dimensional zonal techniques
[NASA-CR-181406] N89-22838
MIT progress in understanding images N89-23075
Image understanding research at the University of Maryland, December 1986 - January 1988 N89-23078
CMU image understanding program N89-23079
Progress in image understanding at the University of Rochester N89-23082
Image understanding research at GE N89-23085
Algorithms and architectures for smart sensing N89-23090
An integrated approach to stereo matching, surface reconstruction and depth segmentation using consistent smoothness assumptions N89-23092
Kalman filter-based algorithms for estimating depth from image sequences N89-23094
Parallel architectures for image processing and vision N89-23126
Pyramid algorithms implementation on the connection machine N89-23129
Robust parallel computation of 2-D model-based recognition N89-23130
Evaluation of quantization error in computer vision N89-23138
Algebraic reasoning in view consistency and parameterized model matching problems N89-23139
Test results from SRI's stereo system N89-23140
Stochastic stereo matching over scale N89-23143
The integration of information from stereo and multiple shape-form-texture cues N89-23145
Combining information in low-level vision N89-23152
Issues in extracting motion parameters and depth from approximate translational motion N89-23157
Structure recognition by connectionist relaxation: Formal analysis N89-23160
Ribbons, symmetries and skewed symmetries N89-23170
Image segmentation using geometric and physical constraints N89-23172
An optimal algorithm for the derivation of shape from shadows N89-23176
Texture edge localization N89-23178
Parallel processors and nonlinear structural dynamics algorithms and software
[NASA-CR-184938] N89-23184
An algorithm for the three-index assignment problem
[AD-A205172] N89-23190
A new modified cholesky factorization
[AD-A205174] N89-23191
Automating the identification of structural model parameters
[DE89-006327] N89-23194
Two time stepping algorithms for parallel computers
[DE89-008679] N89-23196
MIRAP, microcomputer reliability analysis program
[DE89-009749] N89-23200
New stable, vectorisable Kalman filter algorithms based on orthogonal transformations
[ESA-TT-1108] N89-23203
The stable evaluation of a simple rational function and its application to spline approximation
[NPL-DITC-135/88] N89-23253
Statistical smoothing methods and image analysis
[AD-A205643] N89-23256
The multigroup and cylindrical geometry formulation of the Sn Monte Carlo hybrid method
[DE89-000326] N89-23260
ALIGNMENT
Magnetic axis alignment and the Poisson alignment reference system
[DE89-007687] N89-22880
Recognizing solid objects by alignment N89-23174
ALKALINE BATTERIES
Oxygen electrodes for rechargeable alkaline fuel cells N89-22998
Corrosion testing of candidates for the alkaline fuel cell cathode N89-23000
ALKALINE EARTH METALS
Electronic structure of rare-earth luminescent centre in alkaline-earth sulphides
[DE88-705674] N89-23318
ALKYL COMPOUNDS
Formation of lubricating films at elevated temperatures from the gas phase
[PB89-129530] N89-22747
ALLOCATIONS
On the expected number of assignments in reduced matrices for the linear assignment problem
[MEMO-728] N89-23263
ALLOYS
Mechanisms of crevice corrosion in chlorinated environments
[AD-A204621] N89-22724
ALTITUDE
Development of a differential temperature probe for the measurement of atmospheric turbulence at all levels
[AD-A205893] N89-23047
ALTITUDE SIMULATION
Efficacy of conventional and high-frequency ventilation at altitude
[AD-A205922] N89-23071
ALUMINIDES
Behavior of iron aluminides in oxidizing and sulfidizing environments
[DE89-008919] N89-22693
Temperature effects on the break-in of nickel aluminide alloys
[DE89-005341] N89-22729
ALUMINUM ALLOYS
Atomic imaging of Au/Ni multilayers
[DE89-009903] N89-22698
Investigation and synthesis of high temperature and increased stiffness RSP aluminum alloys
[AD-A204162] N89-22723
Processing and properties of advanced aluminum alloys
[AD-A205187] N89-22725
Role of aluminium concentration on the structure behaviour of Cu-Al alloys
[DE88-705647] N89-22727
Ab initio calculations of ordered intermetallic phase equilibria
[DE89-009974] N89-22741
Fracture toughness and mechanical behavior of steel and aluminum alloys
[ETCA-87-R-090] N89-22743
Application of electrochemical noise spectral analysis to the study of the pitting corrosion of aluminum alloys
[ETCA-87-R-102] N89-22744

Tribological characterization of 15 surface treatments for aluminum alloys
[ETCA-87-R-132] N89-22928
The effect of boron on microhardness in Ni3Al polycrystals
[DE89-009124] N89-23335

ALUMINUM ARSENIDES
Experimental investigation of hot electron and related effects in gallium (aluminum) arsenide devices
[AD-A205442] N89-23349

ALUMINUM GALLIUM ARSENIDES
Time resolved photoluminescence of ytterbium in indium phosphide
[AD-A202596] N89-23303

ALUMINUM OXIDES
Alumina reinforced tetragonal zirconia (TZP) composites
[DE89-008880] N89-22690
Observations on the toughening of Al2O3-SiC composites
[DE89-009843] N89-22695
Criteria for selection of phase names for oxides
[NPL-DMA(A)169] N89-22714
Current and thermal noise in mixed Na/Ag beta alumina
[AD-A205869] N89-22816
Study of grain boundaries in polycrystalline alumina
[ETCA-87-R-130] N89-23344
Study of grain boundaries in polycrystalline alumina. Effect of the manufacturing mode and of the material composition
[ETCA-87-R-100] N89-23345
Conductivity fluctuations in mixed Na/Ca beta alumina
[AD-A205418] N89-23348

AMBIENT TEMPERATURE
Advances in ambient temperature secondary lithium cells N89-23011

AMORPHOUS SILICON
Diagnostics of glow discharges used to produce hydrogenated amorphous silicon films
[DE89-000887] N89-22760
Research on amorphous-silicon-based, thin-film photovoltaic devices, task B
[DE89-000885] N89-23021
Research on amorphous-silicon-based, thin-film photovoltaic devices, task B
[DE89-000886] N89-23022

AMPLIFICATION
On the small-signal gain of free-electron lasers in the low-current region
[ESA-TT-1120] N89-22889

AMPLIFIERS
Progress toward the delivery of high energy pulses with the Aurora KrF/ICF laser system
[DE89-007750] N89-22885

ANALOG DATA
Benzodiazepines and caffeine: Effect on daytime sleepiness, performance, and mood
[AD-A205862] N89-23066

ANALOG SIMULATION
Image understanding research at SRI International N89-23080

ANALYSIS (MATHEMATICS)
Projections of vector addition system reachability sets are semilinear
[AD-A205914] N89-23257

ANALYZERS
Distortions in the output signals of conventional spectrum analyzers
[DE88-705656] N89-22871

ANGLE OF ATTACK
Computational investigation of incompressible airfoil flows at high angles of attack
[AD-A205885] N89-22590

ANGULAR MOMENTUM
Turbulent transport in the solar nebula N89-22829
Reversed sense of the outward direction for dynamical effects of rotation close to a Schwarzschild black hole
[DE88-705670] N89-23389

ANGULAR VELOCITY
Rotor instability due to a gear coupling connected to a bearingless sun wheel of a planetary gear N89-22893

ANISOTROPY
The length scale for sub-grid-scale parameterization with anisotropic resolution N89-22818

ANNEALING
Effects of different fabrication techniques on the Yttrium-Barium-Copper oxide high temperature superconductor
[AD-A202598] N89-23304
Ductility enhancement in unreacted internal-Sn Nb3Sn through low-temperature anneals
[DE89-009125] N89-23336

ANNIHILATION REACTIONS
Problems in modern cosmology N89-23393

ANNUAL VARIATIONS
Seasonal and latitudinal variations of the temporal variance of ozone and of the potential temperature
[BPT-3/88] N89-23026
Determination of the dynamic CO2 source-sink function of different biomes with the object of verifying seasonality and trend of atmospheric CO2 measurements of different stations
[ETN-89-93763] N89-23038
Characteristics of winter lightning to high structures. Observation from December 1978 to March 1987
[DE88-756454] N89-23049
Reports from the German Meteorological Service. No. 177: Small-scale variability of solar radiation
[ISBN-3-88148-224-X] N89-23053
Seafloor temperature and conductivity data from coastal waters of the US Beaufort Sea
[AD-A205428] N89-23059

ANNULAR DUCTS
Annular honeycomb seals: Test results for leakage and rotordynamic coefficients; comparisons to labyrinth and smooth configurations N89-22899

ANNULAR FLOW
Two-phase flow characteristic of inverted bubbly, slug and annular flow in post-critical heat flux region
[DE89-007384] N89-22839

ANODIZING
Tribological characterization of 15 surface treatments for aluminum alloys
[ETCA-87-R-132] N89-22928

ANTENNA DESIGN
Study of a wideband telecommunications satellite for Europe
[ATES/DMA/TRM/162-86] N89-22641
Study of a DRS experimental payload for single and multiple access at S band: Executive summary
[PSD88/00017] N89-22648

ANTENNA RADIATION PATTERNS
Approximation technique for determining gain and radiation pattern of the horn antenna
[DE89-006136] N89-22786
The radiation performance of offset reflector antennas with horn feeds excited by high order modes
[FI-454-TB-43] N89-22792

ANTIEMETICS AND ANTINAUSEANTS
A new perspective in the etiology, treatment, prevention and prediction of space motion sickness
[AD-A205660] N89-23065

ANTIMISSILE DEFENSE
Compact, lightweight CO2 lasers for SDIO applications
[AD-A204300] N89-22882

ANTISUBMARINE WARFARE
An experimental environment and laboratory for studying human information processing in Naval Air ASW (Naval air antisubmarine warfare)
[AD-A204774] N89-23069

ANTISUBMARINE WARFARE AIRCRAFT
An experimental environment and laboratory for studying human information processing in Naval Air ASW (Naval air antisubmarine warfare)
[AD-A204774] N89-23069

APPLICATIONS PROGRAMS (COMPUTERS)
Orbiter Flying Qualities (OFQ) Workstation user's guide
[NASA-CR-179440] N89-22812
Integration effort in knowledge-based vision techniques for the autonomous land vehicle program N89-23108

APPROXIMATION
Approximation technique for determining gain and radiation pattern of the horn antenna
[DE89-006136] N89-22786
On multivariate polynomial interpolation
[AD-A204099] N89-23226
Approximate Bayesian methods for nonlinear measurement error models
[DE89-009224] N89-23233
Approximation of surfaces constrained by a differential equation using simplex splines
[MEMO-739] N89-23249
The stable evaluation of a simple rational function and its application to spline approximation
[NPL-DITC-135/88] N89-23253
Monte Carlo approximations in Bayesian decision theory. Part 3: Limiting behavior of Monte Carlo approximations
[AD-A204173] N89-23258

ARABSAT
Electrodynamic transient tests --- satellites
[CNES-CT/DRT/TVE/SM-024] N89-22644

ARC MELTING
A calorimetric-based comparison of gas tungsten and plasma arc welding processes
[DE89-008712] N89-22924

ARCHITECTURE (COMPUTERS)
Evaluation of several state-of-charge algorithms
[DE89-009752] N89-22812
Enhancements to the IBM version of COSMIC/NASTRAN N89-22948
Remote sensing information sciences research group: Browse in the EOS era
[NASA-CR-184637] N89-22979
CMU image understanding program N89-23079
Summary of image understanding research at the University of Massachusetts N89-23081
An integrated image understanding benchmark: Recognition of a 2 1/2 D mobile N89-23088
Some sample algorithms for the image understanding architecture N89-23089
Algorithms and architectures for smart sensing N89-23090
PACE: An environment for intelligence analysis N89-23102
Autonomous navigation in cross-country terrain N89-23107
Machine-independent image processing: Performance of Apply on diverse architectures N89-23125
Parallel architectures for image processing and vision N89-23126
Scan line array processors: Work in progress N89-23128
Pyramid algorithms implementation on the connection machine N89-23129
IU software environments N89-23133
Use of language features in the implementation and validation of a standardized generic package of elementary functions for Ada
[DE89-007385] N89-23187
Developing software to use parallel processing effectively
[AD-A205184] N89-23192
Automating the identification of structural model parameters
[DE89-006327] N89-23194
A new approach to system testing
[DE89-008660] N89-23195
Engineering Graphics System (EGS) user's manual
[DE89-009668] N89-23199
Expert systems on multiprocessor architectures, phase 1
[AD-A204907] N89-23206
Systolic implementation of neural networks
[DE89-008031] N89-23210

ARCTIC OCEAN
Optical studies of the magnetospheric cusp from Svalbard
[AD-A205432] N89-23044

ARGON
Precipitation of Ar, Kr and Xe in Ni at room temperature
[DE89-009879] N89-22713

ARGON LASERS
Kinetic studies of the electron-beam-pumped ArF laser
[DE89-004041] N89-22884

ARIANE LAUNCH VEHICLE
Ariane 5 Transfer Vehicle (ATV)
[REPT-OX-1-005] N89-22645
ATV: Ariane 5 transfer vehicle study
[STF/E-39-005/CB] N89-22648

AROMATIC COMPOUNDS
Formation of lubricating films at elevated temperatures from the gas phase
[PB89-129530] N89-22747

ARRAYS
Surface temperature measurements using a thin film thermal array
[NASA-TM-101549] N89-22868

ARTIFICIAL INTELLIGENCE
Proceedings: Image Understanding Workshop, volume 1
[AD-A197558] N89-23074
Image understanding research at GE N89-23085
The Maryland approach to image understanding N89-23091
Three-dimensional object recognition using surface descriptions N89-23105
Proceedings: Image Understanding Workshop, volume 2
[AD-A197559] N89-23115
Multiresolution aerial image interpretation N89-23116
TRIPLE: A multi-strategy machine learning approach to target recognition N89-23119
An operational perception system for cross-country navigation N89-23121
Stochastic stereo matching over scale N89-23143
Parallel problem solving system, PRISM (Parallel Inference System)
[AD-A204915] N89-23207
Some methods for uncertain reasoning
[FOA-C-30492-3.3] N89-23212
Fusion of multisensor data: A summary of the JASMIN project
[FOA-C-30498-3.3] N89-23213

Automatic generation of noncolliding trajectories and manipulation task planning in robotics
[LAAS-89-002] N89-23222
Contributions of expert systems to logistics
[REPT-882-320-101] N89-23223
Fostering interaction of government, defense, and aerospace databases N89-23374

ASSEMBLING
Construction in weightlessness N89-22626

ASTRONAUTICS
Analysis of the present knowledge of costs and benefits of the governmental advancement of astronautics
[ETN-89-93770] N89-23359

ASTRONAUTS
Astronaut radiation exposure in low-earth orbit. Part 1: Galactic cosmic radiation
[AD-A204598] N89-23063

ASTRONOMICAL MODELS
Generating a hot big bang via a change in topology
[DE89-007561] N89-23388

ASTRONOMICAL OBSERVATORIES
Comparison of solar photovoltaic and nuclear reactor power systems for a human-tended lunar observatory
[NASA-TM-102015] N89-23397

ASTRONOMICAL SPECTROSCOPY
Echelle observations of H2 complexes N89-23384

ASTROPHYSICS
Dark matter candidates
[DE89-006579] N89-23387

ASYMMETRY
Scaling relations for a beam-deflecting TM(110) mode in an asymmetric cavity
[DE89-009277] N89-22796

ASYMPTOTIC METHODS
Asymptotic expansions with error bounds for solutions of difference equations of level 1 sup +
[MEMO-724] N89-23241

ASYMPTOTIC PROPERTIES
On the asymptotic behavior of the coefficients of asymptotic power series and its relevance to Stokes phenomena
[MEMO-738] N89-23248
On the maximum period of a permutation of N elements
[MEMO-743] N89-23251
Asymptotically optimal nonparametric experimental design tests for the log linear model under censoring
[MEMO-727] N89-23262

ASYMPTOTIC SERIES
A Borel-Ritt theorem with prescribed error bounds
[MEMO-723] N89-23240
Asymptotic expansions with error bounds for solutions of difference equations of level 1 sup +
[MEMO-724] N89-23241
On the asymptotic behavior of the coefficients of asymptotic power series and its relevance to Stokes phenomena
[MEMO-738] N89-23248

ATMOSPHERIC BOUNDARY LAYER
The Large Eddy Simulation (LES) of MESOSCOP for atmospheric boundary layer flows including passive scalars
[DFVLR-MITT-88-28] N89-23041
Hazard index calculation for 31 May 1984 microburst at Erie, Colorado
[NASA-CR-184968] N89-23048
Radiative cooling in the nocturnal boundary layer
[KNMI-WR-88-05] N89-23054

ATMOSPHERIC CHEMISTRY
Seasonal and latitudinal variations of the temporal variance of ozone and of the potential temperature
[BPT-3/88] N89-23026
Coupling of a chemiluminescence detector with a gas chromatograph for the selective measurement of oxidized nitrogen bonds in the atmosphere
[JUEL-2217] N89-23029
Mass-spectroscopic measurements of stratospheric ions, trace gases and precondensation nuclei using balloon-borne measuring probes
[BPT-7/88] N89-23037

ATMOSPHERIC CIRCULATION
Investigation of the effects of increased sophistication of simulation of the atmospheric wind in wind tunnels N89-22620
Preliminary results of the MLAM (Multi-Layer Air Mass) Lagrangian transport model simulation of ANATEX (Across North America Tracer Experiment)
[DE89-008123] N89-23036
The Large Eddy Simulation (LES) of MESOSCOP for atmospheric boundary layer flows including passive scalars
[DFVLR-MITT-88-28] N89-23041
Diabatic circulations in the stratosphere N89-23043
Hazard index calculation for 31 May 1984 microburst at Erie, Colorado
[NASA-CR-184968] N89-23048

ATMOSPHERIC COMPOSITION
Coupling of a chemiluminescence detector with a gas chromatograph for the selective measurement of oxidized nitrogen bonds in the atmosphere
[JUEL-2217] N89-23029

ATMOSPHERIC EFFECTS
Ten year lifetime orbits about the planet Mars N89-22633
Ionospheric scintillation studies
[AD-A205210] N89-23034

ATMOSPHERIC ELECTRICITY
Characteristics of winter lightning to high structures. Observation from December 1978 to March 1987
[DE88-756454] N89-23049

ATMOSPHERIC GENERAL CIRCULATION MODELS
The response of thermospheric nitric oxide to an auroral storm N89-23031

ATMOSPHERIC LASERS
Development of an efficient high brightness Ti:Al2O3 laser amplifier
[AD-A204187] N89-22881

ATMOSPHERIC MODELS
Ionospheric scintillation studies
[AD-A205210] N89-23034
The Large Eddy Simulation (LES) of MESOSCOP for atmospheric boundary layer flows including passive scalars
[DFVLR-MITT-88-28] N89-23041
Radiative cooling in the nocturnal boundary layer
[KNMI-WR-88-05] N89-23054
Surface flux parameterization schemes: Developments and experiences at KNMI — Earth surface
[KNMI-WR-88-06] N89-23055

ATMOSPHERIC OPTICS
Activities report of the Division of Optical Technology (FOA 33)
[FOA-C-30507-3.1] N89-23287

ATMOSPHERIC PHYSICS
Technical support for optical turbulence research
[AD-A204776] N89-23033

ATMOSPHERIC PRESSURE
Efficacy of conventional and high-frequency ventilation at altitude
[AD-A205922] N89-23071

ATMOSPHERIC SOUNDING
Technical support for optical turbulence research
[AD-A204776] N89-23033

ATMOSPHERIC TURBULENCE
Development of a differential temperature probe for the measurement of atmospheric turbulence at all levels
[AD-A205893] N89-23047

ATOMIC ENERGY LEVELS
Gamma ray laser pump diagnostic
[AD-A205221] N89-22883

ATOMIC EXCITATIONS
Neutron scattering studies of magnetic excitations in La/sub 2-x/Sr/sub x/CuO
[DE89-008155] N89-23333

ATOMIC STRUCTURE
Atomic imaging of Au/Ni multilayers
[DE89-009903] N89-22898
The half-metallic ferromagnetic NiMnSb: A positron-annihilation study
[ECN-209] N89-23269
Electron energy-loss spectroscopy: Fundamentals and applications in the characterization of minerals
[DE89-006613] N89-23307
Theoretical study of the Pd-B complex in silicon
[DE88-705650] N89-23316
Electronic properties of Ge sub 1-x Si sub x: A simplified tight binding approach
[DE88-705671] N89-23317
Electronic structure of rare-earth luminescent centre in alkaline-earth sulphides
[DE88-705674] N89-23318
Electronic properties of Ge(1-X)Si(X): Alloying versus pressure
[DE88-705678] N89-23320

AUDIOMETRY
Detection of known signals in arbitrary backgrounds
[AD-A204076] N89-22784

AUDITORY PERCEPTION
Detection of known signals in arbitrary backgrounds
[AD-A204076] N89-22784
Coordinated Noninvasive Studies (CNS) Project
[AD-A205413] N89-22804
Motor theory of auditory perception
[AD-A204951] N89-23064

AUDITORY SIGNALS
Motor theory of auditory perception
[AD-A204951] N89-23064

AUDITORY STIMULI
Motor theory of auditory perception
[AD-A204951] N89-23064

AUGER SPECTROSCOPY
Chemical state depth profiling by Auger signal decomposition: Silicon oxynitride
[DE89-009830] N89-22784

AURORAL IRRADIATION
Kilometric radiation power flux dependence on area of discrete aurora
[NASA-CR-184993] N89-23040

AURORAS
The response of thermospheric nitric oxide to an auroral storm N89-23031
Optical studies of the magnetospheric cusp from Svalbard
[AD-A205432] N89-23044

AUSTENITE
Spinodal decomposition of austenite in long-term-aged duplex stainless steel
[DE89-009827] N89-22737

AUSTENITIC STAINLESS STEELS
Improved high temperature creep resistant austenitic alloy
[DE89-009864] N89-22736
Fracture toughness and mechanical behavior of steel and aluminum alloys
[ETCA-87-R-090] N89-22743

AUTOCORRELATION
Surface orientation from projective foreshortening of isotropic texture autocorrelation N89-23179

AUTOMOBILES
Survey of development trends of methanol automobiles and methanol fuel in China
[DE88-756492] N89-22771

AUTONOMOUS NAVIGATION
Dynamic image interpretation for autonomous vehicle navigation
[AD-A204167] N89-22597
MIT progress in understanding images N89-23075
USC image understanding research: 1987-1988 N89-23076
Image understanding research at the University of Maryland, December 1986 - January 1988 N89-23078
Summary of image understanding research at the University of Massachusetts N89-23081
Image understanding and robotics research at Columbia University N89-23083
Knowledge-based vision technology progress at Hughes AI Center N89-23084
Qualitative reasoning and modeling for robust target tracking and recognition from a mobile platform N89-23086
The Maryland approach to image understanding N89-23091
The MIT vision machine N89-23093
Qualitative motion detection and tracking of targets from a mobile platform N89-23099
Qualitative navigation 2 N89-23100
Self calibration of motion and stereo vision for mobile robot navigation N89-23106
Autonomous navigation in cross-country terrain N89-23107
Integration effort in knowledge-based vision techniques for the autonomous land vehicle program N89-23108
Generic models for robot navigation N89-23112
Using flow field divergence for obstacle avoidance in visual navigation N89-23120
An operational perception system for cross-country navigation N89-23121
On the computational complexity of linear navigation N89-23123
Three-dimensional vision for outdoor navigation by an autonomous vehicle N89-23124

AXIAL LOADS
A NASTRAN DMAP alter for linear buckling analysis under dynamic loading N89-22948

AXIAL STRAIN
The Hertzian cone crack: Theoretical, munerical and experimental studies
[OUEL-1743/88] N89-22961

AXISYMMETRIC FLOW
The inviscid axisymmetric stability of the supersonic flow along a circular cylinder
[NASA-CR-181816] N89-22574

B

BACKGROUND NOISE
Detection of known signals in arbitrary backgrounds
[AD-A204076] N89-22784

BACKGROUND RADIATION
The ALEXIS project and the local interstellar medium
[DE89-009246] N89-23392

BACKSCATTERING
Probabilities and statistics for backscatter estimates obtained by a scatterometer with applications to new scatterometer design data
[NASA-CR-4228] N89-22779
BACKWARD FACING STEPS
Experimental investigation of flow over a backward facing step-progress report N89-22832
BALLOON-BORNE INSTRUMENTS
Mass-spectroscopic measurements of stratospheric ions, trace gases and precondensation nuclei using balloon-borne measuring probes
[BPT-7/88] N89-23037
BAND STRUCTURE OF SOLIDS
Electronic properties of Ge sub 1-x Si sub x: A simplified tight binding approach
[DE88-705671] N89-23317
BANDPASS FILTERS
Magnetic bearing stiffness control using frequency band filtering N89-22910
BANDSTOP FILTERS
Magnetic bearing stiffness control using frequency band filtering N89-22910
BARIUM COMPOUNDS
Effects of different fabrication techniques on the Yttrium-Barium-Copper oxide high temperature superconductor
[AD-A202598] N89-23304
Structural properties of superconducting and nonsuperconducting Ba sub 1-x K sub x BiO3
[DE89-009813] N89-23340
BARIUM OXIDES
Material degradation in a barium hydroxide latent heat storage pilot unit
[ESA-TT-1107] N89-22715
BARRIER LAYERS
The long-term climate change assessment task of the Hanford Site, Washington, Protective Barrier Development Program
[DE89-008704] N89-23030
BATTERY CHARGERS
Evaluation of several state-of-charge algorithms
[DE89-009752] N89-22812
BAYES THEOREM
Some methods for uncertain reasoning
[FOA-C-30492-3.3] N89-23212
Approximate Bayesian methods for nonlinear measurement error models
[DE89-009224] N89-23233
Monte Carlo approximations in Bayesian decision theory. Part 3: Limiting behavior of Monte Carlo approximations
[AD-A204173] N89-23258
BEADS
Interfacial adhesion and mechanical properties of polyamide-6/glass bead composites
[ETN-89-94136] N89-22759
BEAM CURRENTS
Model calculations of the electron-optical properties of compact Faraday cups
[NPL-DMA(A)165] N89-23268
Computation of lower hybrid, neutral beam and bootstrap currents in consistent MHD equilibria
[DE89-006892] N89-23292
BEAM INJECTION
H-Mode transition studies in DIII-D
[DE89-006913] N89-23290
BEARING (DIRECTION)
Relative orientation N89-23149
BEARING ALLOYS
Cryogenic turbopump bearing materials N89-22678
BEARINGS
Temperature effects on the break-in of nickel aluminide alloys
[DE89-005341] N89-22729
Rotordynamic Instability Problems in High-Performance Turbomachinery, 1988
[NASA-CP-3026] N89-22891
Cavitation effects on the pressure distribution of a squeeze film damper bearing N89-22897
Incorporating general race and housing flexibility and deadband in rolling element bearing analysis N89-22912
Experimental verification of an eddy-current bearing N89-22913
BEAUFORT SEA (NORTH AMERICA)
Seafloor temperature and conductivity data from coastal waters of the US Beaufort Sea
[AD-A205428] N89-23059
BENDING
Dynamics of particles in the bending waves of the planetary rings
[DE88-705714] N89-23396
BIBLIOGRAPHIES
Beam research technical abstracts, 1987
[DE89-009013] N89-23282
The status of defence information programs in Greece N89-23364
Standardized bibliographic processing N89-23367
BIG BANG COSMOLOGY
Generating a hot big bang via a change in topology
[DE89-007561] N89-23388
BIHARMONIC EQUATIONS
Numerical solution of the biharmonic equation using different types of bivariate spline functions
[MEMO-734] N89-23247
BINARY SYSTEMS (MATERIALS)
Binary and ternary gas mixtures for use in glow discharge closing switches
[DE89-009718] N89-23298
BIOASTRONAUTICS
Historical survey of biosatellites N89-22625
BIOINSTRUMENTATION
Nondestructive evaluation of stress using ultrasound and pulsed heat
[AD-A205176] N89-22932
BIOMETEOROLOGY
Derivation of a large-scale map of heat load in the region Freiburg-Basel (Germany, F.R.) using satellite data. A contribution to the production of bioclimate data based on a geographic information system
[REPT-27] N89-22972
BIOSATELLITES
Historical survey of biosatellites N89-22625
BIOTECHNOLOGY
New developments in biotechnology: US investment in biotechnology, part 4
[PB88-246939] N89-23060
BIPOLARITY
Characterization testing of a 40 Ahr bipolar nickel hydrogen battery N89-22992
BISMUTH COMPOUNDS
Superconductivity for electric power systems: Building toward our future
[DE89-000874] N89-23332
BISMUTH OXIDES
Structural properties of superconducting and nonsuperconducting Ba sub 1-x K sub x BiO3
[DE89-009813] N89-23340
BISTATIC REFLECTIVITY
Verification and limitations of the monostatic-bistatic radar cross section derived by Kell
[AD-A202601] N89-22782
BIVARIATE ANALYSIS
Smooth interpolation to scattered data by bivariate piecewise polynomials of odd degree
[MEMO-732] N89-23245
Numerical solution of the biharmonic equation using different types of bivariate spline functions
[MEMO-734] N89-23247
BLACK HOLES (ASTRONOMY)
Reversed sense of the outward direction for dynamical effects of rotation close to a Schwarzschild black hole
[DE88-705670] N89-23389
Thermal Comptonization models for gamma-ray emission from black-hole sources
[DE89-009918] N89-23402
BLUFF BODIES
A vortex panel analysis of circular-arc bluff-bodies in unsteady flow
[DE89-007141] N89-22845
BLUNT LEADING EDGES
The influence of the leading edge geometry on the wave drag for a 65 degree delta wing at low supersonic speed and small angles of attack
[FFA-141] N89-22583
BODY WEIGHT
Inhalation developmental toxicology studies: Teratology study of methyl ethyl ketone in mice
[DE89-009563] N89-23062
BODY-WING AND TAIL CONFIGURATIONS
Unsteady aerodynamic computational method of non-coplanar wing-tail combinations in subsonic flow
[PB89-111470] N89-22571
Prediction of loads on wing/body/external store/fins pylon-configurations at transonic speeds
[FFA-TN-1988-44] N89-22602
BODY-WING CONFIGURATIONS
Transonic and supersonic wind tunnel tests on control effectiveness on schematic missile configurations with canard controls
[FFA-TN-1988-11] N89-22601
An efficient inverse method for the design of blended wing-body configurations N89-22603
BOILERS
Some in-field experiences of non-synchronous vibrations in large rotating machinery N89-22894
Multifrequency eddy current testing, optimization of the method for steam generator testing. Phase 2: Nonlinear description of signal location curves dynamics of the signal location curves
[REPT-860142-TW] N89-22933
BOREL SETS
A Borel-Ritt theorem with prescribed error bounds
[MEMO-723] N89-23240
BORON
Theoretical study of the Pd-B complex in silicon
[DE88-705650] N89-23316
The effect of boron on microhardness in Ni3Al polycrystals
[DE89-009124] N89-23335
BORON CARBIDES
Microwave sintering of boron carbide
[DE89-009652] N89-22763
BOUNDARY ELEMENT METHOD
Calculation of low frequency vibrational resonances of submerged structures N89-22951
BOUNDARY LAYER CONTROL
Comparison of boundary layer trips of disk and grit types on airfoil performance at transonic speeds
[AD-A205206] N89-22575
Wind tunnel tests of 16 percent thick airfoil section with spoilers at different chordwise positions — wind turbines
[FFA-TN-1987-39] N89-22582
Annual research briefs, 1988
[NASA-CR-184906] N89-22817
BOUNDARY LAYER EQUATIONS
On the Lagrangian description of unsteady boundary layer separation. Part 2: The spinning sphere
[NASA-TM-102027] N89-22861
BOUNDARY LAYER FLOW
The inviscid axisymmetric stability of the supersonic flow along a circular cylinder
[NASA-CR-181816] N89-22574
Flow over a leading edge with distributed roughness
[DFVLR-FB-88-45] N89-22581
Sidewall boundary layer study, with and without suction, for the 150 mm chord CAST 7 airfoil at the T2 wind tunnel N89-22584
Transition to turbulence in laminar hypersonic flow N89-22830
Experimental investigation of flow over a backward facing step-progress report N89-22832
The Large Eddy Simulation (LES) of MESOSCOP for atmospheric boundary layer flows including passive scalars
[DFVLR-MITT-88-28] N89-23041
BOUNDARY LAYER SEPARATION
Computational investigation of incompressible airfoil flows at high angles of attack
[AD-A205885] N89-22590
BOUNDARY LAYER STABILITY
The inviscid axisymmetric stability of the supersonic flow along a circular cylinder
[NASA-CR-181816] N89-22574
Study of unsteady boundary layers with adverse pressure gradient N89-22863
BOUNDARY LAYER TRANSITION
Comparison of boundary layer trips of disk and grit types on airfoil performance at transonic speeds
[AD-A205206] N89-22575
Transition to turbulence in laminar hypersonic flow N89-22830
Non-linear evolution of a second mode wave in supersonic boundary layers
[NASA-CR-181811] N89-22836
BOUNDARY LAYERS
On the Lagrangian description of unsteady boundary layer separation. Part 2: The spinning sphere
[NASA-TM-102027] N89-22861
BOUNDARY VALUE PROBLEMS
Non-linear evolution of a second mode wave in supersonic boundary layers
[NASA-CR-181811] N89-22836
Forced and free convection flow with viscous dissipation effects: The method of parametric differentiation
[DE88-705649] N89-22840
A higher-order scheme for the Burgers equation
[FFA-TN-1988-43] N89-22859
On the Lagrangian description of unsteady boundary layer separation. Part 2: The spinning sphere
[NASA-TM-102027] N89-22861
A pseudo singular value decomposition and inner functions in super optimal control
[OUEL-1738/88] N89-23214
Smoothing and likelihood ratio for Gaussian boundary value processes
[MEMO-726] N89-23242
Numerical solution of the biharmonic equation using different types of bivariate spline functions
[MEMO-734] N89-23247
The influence of open boundary conditions and difference operators on the time-integration of the Burger's equation
[FFA-TN-1988-57] N89-23254
BRANCHING (MATHEMATICS)
An algorithm for the three-index assignment problem
[AD-A205172] N89-23190

BRAYTON CYCLE
Megawatt Class Nuclear Space Power Systems (MCNSPS) conceptual design and evaluation report. Volume 3, technologies 2: Power conversion
[NASA-CR-179614-VOL-3] N89-22980
BRAZING
Metallurgical study of superalloy brazing alloys N89-22680
BREMSSTRAHLUNG
Gamma ray laser pump diagnostic
[AD-A205221] N89-22883
BRIGHTNESS TEMPERATURE
Remote sensing of oceanic rainrates by passive microwave sensors: A statistical-physical approach N89-23057
BRITTLENESS
Hydrogen embrittlement in nickel-hydrogen cells N89-23008
BROADBAND
Study of a wideband telecommunications satellite for Europe
[ATES/DMA/TRM/162-86] N89-22641
BROKEN SYMMETRY
Improved effective potential in the Einstein metric
[DE88-705716] N89-23355
BUBBLES
Experimental observation of the nonlinear response of single bubbles to an applied acoustic field
[AD-A205191] N89-23271
BUCKLING
A NASTRAN DMAP alter for linear buckling analysis under dynamic loading N89-22948
BUILDINGS
Investigation of the effects of increased sophistication of simulation of the atmospheric wind in wind tunnels N89-22620
BURGER EQUATION
A higher-order scheme for the Burgers equation
[FFA-TN-1988-43] N89-22859
The influence of open boundary conditions and difference operators on the time-integration of the Burger's equation
[FFA-TN-1988-57] N89-23254
BURNING RATE
Theoretical predictions of turbulent burning velocities of steady and accelerating unconfined turbulent flames with premixed reactants N89-22716

C

C-130 AIRCRAFT
Pre and post modification electromagnetic compatibility test report for the C-130H self contained navigation system with MLS A-kit, revision
[AD-A205167] N89-22604
CADMIUM TELLURIDES
Band structure of CdTe-ZnTe superlattice
[DE88-705682] N89-23321
CAFFEINE
Benzodiazepines and caffeine: Effect on daytime sleepiness, performance, and mood
[AD-A205862] N89-23066
CALCULUS OF VARIATIONS
Ab initio calculations of ordered intermetallic phase equilibria
[DE89-009974] N89-22741
CALENDARS
Calendar of selected aeronautical and space meetings
[AGARD-CAL-88/2] N89-23361
CALIBRATING
Measurement uncertainty of adsorption testing of desiccant materials
[DE89-000641] N89-22681
A computer controlled 100 kV pulse generator
[DE89-005922] N89-22808
Finite element analysis for calibration curve computation for measurement of crack propagation of ellipse shaped surface cracks
[GKSS-88/E/34] N89-22960
Geometric camera calibration using systems of linear equations N89-23148
Report on round robin measurements of 6 digital magnetic tapes
[NPL-DES-91] N89-23202
Machine reference mirror inspection by optical Fabry-Perot cavity testing
[DE89-009635] N89-23284
A programmatic approach to achieving data quality objectives
[DE89-006248] N89-23378
CALORIMETERS
Experimental study of uranium plastic scintillator calorimeters
[NIKHEF-H/88-4] N89-22678
CAMERAS
Geometric camera calibration using systems of linear equations N89-23148
CANARD CONFIGURATIONS
Compressible Euler solution around a wing canard sting configuration
[FFA-TN-1988-62] N89-22578
Transonic and supersonic wind tunnel tests on control effectiveness on schematic missile configurations with canard controls
[FFA-TN-1988-11] N89-22601
Transonic and supersonic wind tunnel tests on control effectiveness on schematic missile configuration with canard control
[FFA-TN-1988-11-SUPPL] N89-22613
CAPACITANCE
Advanced double layer capacitors N89-22993
Nickel-hydrogen capacity loss on storage N89-23007
Advanced high-temperature batteries N89-23010
CAPACITORS
Advanced double layer capacitors N89-22993
CAPILLARY FLOW
The effect of thermocapillary flow on weld-pool profile
[NPL-DMA(A)167] N89-22927
CARBON COMPOUNDS
Carbonaceous film coating
[DE89-009592] N89-22762
CARBON CYCLE
Determination of the dynamic CO2 source-sink function of different biomes with the object of verifying seasonality and trend of atmospheric CO2 measurements of different stations
[ETN-89-93763] N89-23038
CARBON DIOXIDE
Aqueous impurity effects on stainless steel IGSCC (intergranular stress corrosion cracking): A central composite matrix analysis
[DE88-017382] N89-22726
Determination of the dynamic CO2 source-sink function of different biomes with the object of verifying seasonality and trend of atmospheric CO2 measurements of different stations
[ETN-89-93763] N89-23038
CARBON DIOXIDE LASERS
Compact, lightweight CO2 lasers for SDIO applications
[AD-A204300] N89-22882
CARBON FIBER REINFORCED PLASTICS
Development and testing of critical components for technological preparation of an Airbus-CFRP-fuselage, phase 2
[MBB-UT-129/87] N89-22600
Influence of conditioning on the trapezoidal fatigue behavior of a carbon epoxy composite
[ETCA-87-R-052] N89-22700
Dynamic behavior of a carbon epoxy composite
[ETCA-87-R-001] N89-22701
Tests of new materials with second generation carbon fibers, test report
[REPT-47-188/F] N89-22702
CSPC test 319.30: Study on impact tolerance of preimpregnated carbon-epoxy systems
[REPT-47-323/F] N89-22703
Improving hole boring yield in carbon epoxy composites with tensile loading
[REPT-47-324/F] N89-22704
Ultrasonic detection of damage in carbon epoxy composite materials
[ONERA-RT-3/7256-RY-071-R] N89-22705
Mechanical properties and damage mechanisms of carbon fiber reinforced composites: Compression loading
[DFVLR-FB-88-41] N89-22706
CARBON FIBERS
High-performance refractory composite materials N89-22675
CARBON MONOXIDE
Models for surface intermediates in CO hydrogenation
[DE89-004348] N89-22712
CO in the galactic center: A complete survey of carbon monoxide emission in the inner 4 kpc of the Galaxy N89-23386
CARBON-CARBON COMPOSITES
Composite material systems for high temperature applications N89-22666
Silicon-carbide coated carbon-carbon: An advanced material for rocket systems N89-22672
High temperature composite materials for rocket propulsion N89-22676
Damage initiation in two-dimensional, woven, carbon-carbon composites
[AD-A202617] N89-22683
Three-dimensional response of composites
[AD-A204623] N89-22687
CARRIER MOBILITY
Basic research in superconductor, ceramic and semiconductor sciences at selected Japanese laboratories based on a 1988 visit: Highlights, summary and overview, detailed notes from selected Japanese laboratories
[DE89-009637] N89-23339
CARTRIDGES
Advanced cartridge technology: Executive summary — spacecraft furnaces
[SEP-TS/F-6972/88-RP] N89-22636
CASCADE FLOW
Transonic viscous flow calculations for a turbine cascade with a two equation turbulence model
[NASA-TM-101944] N89-22607
CATHODES
Preparation, characterization and performance of MoS3 as an active cathode material
[AD-A205886] N89-22717
A survey of advanced battery systems for space applications N89-22986
Advanced rechargeable sodium batteries with novel cathodes N89-22988
Oxygen electrodes for rechargeable alkaline fuel cells N89-22996
CATHODIC COATINGS
Coating of silicon carbide fibers
[CERT-423900/RF] N89-22787
CATIONS
Polymer electrolytes with exclusively cationic conductivity
[DE89-009521] N89-22761
CAUCHY PROBLEM
Localization of solutions of a nonlinear Fokker-Planck equation with Dirichlet boundary conditions — soil moisture infiltration
[MEMO-733] N89-23248
CAVITATION FLOW
Cavitation in a submerged jet at constant pressure
[OUEL-1658/86] N89-22848
Cavitation effects on the pressure distribution of a squeeze film damper bearing N89-22897
Experimental observation of the nonlinear response of single bubbles to an applied acoustic field
[AD-A205191] N89-23271
CAVITIES
Computer aided design of three-dimensional waveguide loaded cavities
[DE89-007733] N89-22783
Scaling relations for a beam-deflecting TM(110) mode in an asymmetric cavity
[DE89-009277] N89-22796
Comparison of a cavity solar receiver numerical model and experimental data
[DE89-003609] N89-23016
Machine reference mirror inspection by optical Fabry-Perot cavity testing
[DE89-009635] N89-23284
Positron lifetime technique with applications in materials science
[ETN-89-94141] N89-23331
CELL CATHODES
Corrosion testing of candidates for the alkaline fuel cell cathode N89-23000
CENSORED DATA (MATHEMATICS)
Asymptotically optimal nonparametric experimental design tests for the log linear model under censoring
[MEMO-727] N89-23262
CENTRIFUGAL COMPRESSORS
Some field experience with subsynchronous vibration of centrifugal compressors N89-22892
High stability design for new centrifugal compressor N89-22917
CENTRIFUGAL FORCE
Reversed sense of the outward direction for dynamical effects of rotation close to a Schwarzschild black hole
[DE88-705670] N89-23389
CENTRIFUGAL PUMPS
Influence of different types of seals on the stability behavior of turbopumps N89-22902
Influence of impeller and diffuser geometries on the lateral fluid forces of whirling centrifugal impeller N89-22907
Influence of impeller shroud forces on turbopump rotor dynamics N89-22909
CENTRIFUGING
Innovation in separation technology for fine gravity semi-products
[PB89-112478] N89-22719
CERAMIC COATINGS
CVD and diffusion coatings for high temperature applications in turbomachinery and rocket motors N89-22658
Initial results of tests on metal-ceramic guide vanes N89-22666

Application of indentation to the study of the toughness of yttrium-zircon plasma coatings
[ETCA-87-R-040] N89-22765
CERAMIC FIBERS
Monolithic and fiber ceramic components for turboengines and rockets N89-22657
High-performance refractory composite materials N89-22675
The isothermal fatigue behavior of a unidirectional SiC/Ti composite and the Ti alloy matrix
[NASA-TM-101984] N89-22684
CERAMIC MATRIX COMPOSITES
Material/manufacturing process interaction in advanced material technologies N89-22662
Composite material systems for high temperature applications N89-22666
Utilization of high temperature composites in turbojet engines N89-22667
Fiber matrix interface effects in failure of ceramic matrix fiber composites
[AD-A204618] N89-22686
Alumina reinforced tetragonal zirconia (TZP) composites
[DE89-008880] N89-22690
Internal stresses in ceramic composite constituents determined by neutron diffraction technique
[DE89-009883] N89-22697
Coating of silicon carbide fibers
[CERT-423900/RF] N89-22767
Basic research in superconductor, ceramic and semiconductor sciences at selected Japanese laboratories based on a 1988 visit: Highlights, summary and overview, detailed notes from selected Japanese laboratories
[DE89-009637] N89-23339
CERAMICS
Advanced cartridge technology: Executive summary — spacecraft furnaces
[SEP-TS/F-6972/88-RP] N89-22636
The demonstration of monolithic and composite ceramics in aircraft gas turbine combustors N89-22665
Silicon-carbide coated carbon-carbon: An advanced material for rocket systems N89-22672
Ceramic heat exchangers and turbine blades: Theory and experimental results N89-22677
Technical feasibility study on the development of ceramic thermoelectric conversion, part 2
[DE88-756481] N89-22755
Basic program for the development of a reliable high strength construction ceramic mode of SiC
[MTU-TB-87/927] N89-22757
Current and thermal noise in mixed Na/Ag beta alumina
[AD-A205869] N89-22816
Solid oxide fuel cell matrix and modules
[DE89-009607] N89-23024
Coexistence of spin-glass and type-2 ceramic superconductivity
[DE88-705684] N89-23322
Possibility of operation of high temperature superconducting YBa2Cu307 ceramics in cyclotrons at irradiation
[DE88-705783] N89-23325
Processing and electrical properties of high-T sub c superconductors
[DE89-009852] N89-23342
Conductivity fluctuations in mixed Na/Ca beta alumina
[AD-A205416] N89-23348
CERMETS
Far- and mid-infrared properties of metal-insulator composite materials
[AD-A204914] N89-22689
CHANNEL FLOW
Numerical study of a multipurpose transonic wind tunnel with an adaptable injection-suction system N89-22621
Non-linear evolution of a second mode wave in supersonic boundary layers
[NASA-CR-181811] N89-22836
Computerized simulation of turbulent flow in a channel
[ONERA-RSF-16/3419-AY-112-A] N89-22852
Theoretical study of the unsteady flow in a straight channel with variable and constant cross section
[VKI-TN-168] N89-22857
On the structure of pressure fluctuations in simulated turbulent channel flow
[NASA-TM-101084] N89-22860
Low Reynolds number calculation of turbulent channel flow: A general discussion
[AD-A205883] N89-22864
CHAOS
Low-dimensional chaos in turbulence N89-22822
CHARGE EFFICIENCY
Characterization testing of a 40 Ahr bipolar nickel hydrogen battery N89-22992
Advances in lightweight nickel electrode technology N89-23005
Advanced high-temperature batteries N89-23010
CHARGED PARTICLES
Calculation of longitudinal and transverse wake-field effects in dielectric structures
[DE89-009814] N89-22798
CHEMICAL ANALYSIS
Effects of X-rays on isotactic polypropylene. Volume 2: Polymers and ceramics
[DE88-705606] N89-22751
CHEMICAL ATTACK
Mechanisms of crevice corrosion in chlorinated environments
[AD-A204621] N89-22724
CHEMICAL BONDS
Models for surface intermediates in CO hydrogenation
[DE89-004348] N89-22712
Internal debonding of solid rocket fuel: An experimental investigation
[AD-A205903] N89-22772
CHEMICAL COMPOSITION
Development of an asbestos-free insulant for rocket motors N89-22679
Metallurgical study of superalloy brazing alloys N89-22680
Spinodal decomposition of austenite in long-term-aged duplex stainless steel
[DE89-009827] N89-22737
Chemical state depth profiling by Auger signal decomposition: Silicon oxynitride
[DE89-009830] N89-22764
Current and thermal noise in mixed Na/Ag beta alumina
[AD-A205869] N89-22816
Coupling of a chemiluminescence detector with a gas chromatograph for the selective measurement of oxidized nitrogen bonds in the atmosphere
[JUEL-2217] N89-23029
CHEMICAL EFFECTS
KOH concentration effect on the cycle life of nickel-hydrogen cells. 4: Results of failure analyse N89-23004
CHEMICAL PROPERTIES
Structural comparison of nickel electrodes and precursor phases N89-23001
CHEMICAL REACTIONS
Spinodal decomposition in polymer blends
[DE88-705687] N89-22754
CHEMICAL TESTS
Material degradation in a barium hydroxide latent heat storage pilot unit
[ESA-TT-1107] N89-22715
Spinodal decomposition in polymer blends
[DE88-705687] N89-22754
CHEMILUMINESCENCE
Coupling of a chemiluminescence detector with a gas chromatograph for the selective measurement of oxidized nitrogen bonds in the atmosphere
[JUEL-2217] N89-23029
CHINA
Visting China's aerodynamics research and development center
[AD-A203980] N89-22615
Survey of development trends of methanol automobiles and methanol fuel in China
[DE88-756492] N89-22771
CHLORINATION
Mechanisms of crevice corrosion in chlorinated environments
[AD-A204621] N89-22724
CHOLESKY FACTORIZATION
A new modified cholesky factorization
[AD-A205174] N89-23191
CHROMIUM
Microstructural studies of IAD and PVD Cr coatings by cross section transmission electron microscopy
[DE89-009877] N89-22739
Tunable chromium lasers
[DE89-008814] N89-22886
CHROMIUM OXIDES
Fracture toughness of MgCr2O4-based refractory composites
[DE89-009847] N89-22696
CIRCUIT BOARDS
Double sided circuit board and a method for its manufacture
[DE89-009601] N89-22809
Technical support for optical turbulence research
[AD-A204776] N89-23033
CIRCUIT RELIABILITY
Electrical properties and detection methods for CMOS IC defects
[DE89-005775] N89-23327
CIRCUITS
Experimental investigation of flow over a backward facing step-progress report N89-22832
CIRCULAR CYLINDERS
The inviscid axisymmetric stability of the supersonic flow along a circular cylinder
[NASA-CR-181816] N89-22574
CIVIL AVIATION
Safe skies for tomorrow: Aviation safety in a competitive environment
[PB89-114318] N89-22591
CLASSICAL MECHANICS
A general non-linear dynamical theory of elastic curved beams N89-22930
Quantum theory of a massless spinning particle
[NIKHEF-H/88-7] N89-23357
CLASSIFICATIONS
Image understanding: Intelligent systems N89-23077
Indexing and abstracting N89-23388
CLEANING
A variable temperature cryostat that produces in situ clean-up germanium detector surfaces
[DE89-008174] N89-23328
CLEARANCES
Incorporating general race and housing flexibility and deadband in rolling element bearing analysis N89-22912
CLIMATE
Solar radiation at the earth's surface: What are we doing to it and with it?
[DE89-008446] N89-23018
Climatological and statistical fundamentals for the explanation of climate data processing
[ETN-89-93775] N89-23051
CLIMATE CHANGE
The long-term climate change assessment task of the Hanford Site, Washington, Protective Barrier Development Program
[DE89-008704] N89-23030
CLIMATOLOGY
Climatological and statistical fundamentals for the explanation of climate data processing
[ETN-89-93775] N89-23051
CLOUD PHYSICS
Coherent polarimetric radar techniques for microwave propagation and cloud physics research
[DFVLR-FB-88-47] N89-22800
CLOUDS
A historical interpretation of the study of the visible cloud morphology on the planet Jupiter: 1610-1878 N89-23398
CLOUDS (METEOROLOGY)
Reports from the German Meteorological Service. No. 175: Global radiation during twilight
[ISBN-3-88148-241-5] N89-23052
Retrieving the distribution of liquid water content in clouds from observations of thermal microwave radiation N89-23056
CLUSTER ANALYSIS
Ab initio calculations of ordered intermetallic phase equilibria
[DE89-009974] N89-22741
TRIPLE: A multi-strategy machine learning approach to target recognition N89-23119
CLUTTER
Remote sensing of earth terrain
[NASA-CR-184937] N89-22971
CMOS
Electrical properties and detection methods for CMOS IC defects
[DE89-005775] N89-23327
Effects of cosmic rays on single event upsets
[NASA-CR-184835] N89-23400
COBALT ALLOYS
Corrosion of iron, nickel and cobalt based alloys in high temperature environments contaminated with chlorine
[DE89-009829] N89-22738
COLD ACCLIMATIZATION
Acclimatization to cold in humans
[NASA-TM-101012] N89-23061
COLD TOLERANCE
Acclimatization to cold in humans
[NASA-TM-101012] N89-23061
COLLAPSE
Mechanisms of cascade collapse
[DE89-009882] N89-22740
COLLATING
Perceptual grouping for the detection and description of structures in aerial images N89-23117
COLLISION AVOIDANCE
Automatic generation of noncolliding trajectories and manipulation task planning in robotics
[LAAS-89-002] N89-23222
COLLISIONAL PLASMAS
A quiver kinetic formulation of radio frequency heating and confinement in collisional edge plasmas
[DE89-009675] N89-23296
COLOR
CMU image understanding program N89-23079

Image segmentation and reflection analysis through color N89-23150
A color metric for computer vision N89-23151
COLUMBUS SPACE STATION
GPS terminal: Study of a GPS receiver for Columbus platform elements, executive summary [GPS-REP-SEL-002] N89-22643
Ariane 5 Transfer Vehicle (ATV) [REPT-OX-1-005] N89-22645
ATV: Ariane 5 transfer vehicle study [STF/E-39-005/CB] N89-22646
Columbus MTFF utilisation, phase B2X: Executive summary for main study [CUT-MBER-800-RP-220] N89-22647
Study on communications costs for Columbus utilization [REPT-871126/1/FR] N89-22801
Agreement on the International Space Station and Columbus Program [REPT-34/88] N89-23360
COMBUSTIBLE FLOW
Inviscid spatial stability of a compressible mixing layer. Part 2: The flame sheet model [NASA-CR-181815] N89-22837
COMBUSTION
Direct simulation of compressible reacting flows N89-22828
COMBUSTION CHAMBERS
Investigation of low NOx staged combustor concept in high-speed civil transport engines [NASA-TM-101977] N89-22606
The demonstration of monolithic and composite ceramics in aircraft gas turbine combustors N89-22685
Combustor flow visualization using innovative infrared thermographics techniques [AD-A205905] N89-22718
COMBUSTION EFFICIENCY
Investigation of low NOx staged combustor concept in high-speed civil transport engines [NASA-TM-101977] N89-22606
COMBUSTION TEMPERATURE
Ignition characteristics of the iron-based alloy UNS S66286 in pressurized oxygen [NASA-CR-183612] N89-22722
COMMAND AND CONTROL
Overview of the software technology project RS34C71, documentation, management/technical advanced concepts for software engineering [AD-A204921] N89-23189
COMMUNICATION
R and D productivity: Relationship to Selective Dissemination of Information (SDI) in the corporate environment N89-23375
COMMUNICATION NETWORKS
Study of a wideband telecommunications satellite for Europe [ATES/DMA/TRM/162-86] N89-22641
COMMUNICATION SATELLITES
PSDE/SAT-2: Communication system architecture study, executive summary [ESA-CR(P)-2732] N89-22802
COMMUTATION
Generalized multicomponent KP-hierarchies [MEMO-708] N89-23234
COMPATIBILITY
Paint compatibility test [I-266/88] N89-22758
COMPENSATORY TRACKING
Nonlinear model matching with prescribed tracking error with an application to Hamiltonian systems [MEMO-731] N89-23244
COMPONENT RELIABILITY
Monolithic and fiber ceramic components for turboengines and rockets N89-22657
Transmission overhaul and replacement predictions using Weibull and renewal theory [NASA-TM-102022] N89-22925
COMPOSITE MATERIALS
Future advanced aero-engines: The materials challenge N89-22659
Three-dimensional response of composites [AD-A204623] N89-22687
Fracture toughness of MgCr2O4-based refractory composites [DE89-009647] N89-22696
A NASTRAN DMAP alter for linear buckling analysis under dynamic loading N89-22948
COMPOSITE STRUCTURES
Three-dimensional response of composites [AD-A204623] N89-22687
Analysis of the mechanical behavior of adhesively bonded composite joints [AD-A202616] N89-22938
COMPRESSIBLE FLOW
Compressible Euler solution around a wing canard sting configuration [FFA-TN-1988-62] N89-22578
Turbulence modeling N89-22819
Direct numerical simulation of compressible free shear flows [AIAA-89-0374] N89-22827
Direct simulation of compressible reacting flows N89-22828
Inviscid spatial stability of a compressible mixing layer. Part 2: The flame sheet model [NASA-CR-181815] N89-22837
Rotordynamic coefficients for stepped labyrinth gas seals N89-22901
COMPRESSION LOADS
Mechanical properties and damage mechanisms of carbon fiber reinforced composites: Compression loading [DFVLR-FB-88-41] N89-22706
Compression and shear wave propagation in explosives [AD-A205917] N89-22865
COMPRESSORS
Development of advanced heat pumps. Part 3: Fundamental approach on two-stage compression system [DE88-756842] N89-22842
Rotordynamic Instability Problems in High-Performance Turbomachinery, 1988 [NASA-CP-3026] N89-22891
COMPTON EFFECT
Thermal Comptonization models for gamma-ray emission from black-hole sources [DE89-009918] N89-23402
COMPUTATIONAL FLUID DYNAMICS
Unsteady aerodynamic computational method of non-coplanar wing-tail combinations in subsonic flow [PB89-111470] N89-22571
A numerical study of viscous vortex rings using a spectral method N89-22572
The influence of the leading edge geometry on the wave drag for a 65 degree delta wing at low supersonic speed and small angles of attack [FFA-141] N89-22583
Prediction of loads on wing/body/external store/fins pylon-configurations at transonic speeds [FFA-TN-1988-44] N89-22602
Transonic viscous flow calculations for a turbine cascade with a two equation turbulence model [NASA-TM-101944] N89-22607
Close interactions of 3-D vortex tubes N89-22823
The effects of particle loading on turbulence structure and modelling N89-22825
Analysis of turbulence structures in shear flows N89-22826
An experimental investigation of a low Reynolds number turbulent boundary layer subject to an adverse pressure gradient N89-22834
Non-linear evolution of a second mode wave in supersonic boundary layers [NASA-CR-181811] N89-22836
Computational fluid dynamics research in three-dimensional zonal techniques [NASA-CR-181406] N89-22838
Numerical simulation of vortex breakdown [ONERA-RSF-3/4368-AY-502-A] N89-22853
A flux splitting method for hyperbolic systems: Application to the solution of the Euler equations [CERT-RF-1/3290/DERI] N89-22854
Lectures in Fluid Physics held at the Physics Department of the Georg-August-University. Volume 1: Source Strength of Vorticity [DFVLR-MITT-88-26-VOL-1] N89-22855
Lectures in Fluid Physics held at the Physics Department of the Georg-August-University. Volume 2: Examples of the Application of Dimensional Analysis [DFVLR-MITT-88-27-VOL-2] N89-22856
Theoretical study of the unsteady flow in a straight channel with variable and constant cross section [VKI-TN-168] N89-22857
Center for Advanced Space Propulsion (CASP) [NASA-CR-184936] N89-23404
COMPUTATIONAL GRIDS
Convergence of discrete-vortex induced-flow calculations by optimum choice of mesh N89-22585
General grid finite difference methods for time dependent electromagnetic problems in two dimensions [DE89-007225] N89-22788
Computational fluid dynamics research in three-dimensional zonal techniques [NASA-CR-181406] N89-22838
Multigrid for the steady-state incompressible Navier-Stokes equation: A survey [GMD-322] N89-22846
Improved performance in NASTRAN (R) N89-22941
Parallel architectures for image processing and vision N89-23126
COMPUTER AIDED DESIGN
Ab initio calculations of ordered intermetallic phase equilibria [DE89-009974] N89-22741
Preliminary blade design using integrated computer codes [FFA-TN-1988-67] N89-22777
Computer aided design of three-dimensional waveguide loaded cavities [DE89-007733] N89-22783
The use of COSMIC NASTRAN in an integrated conceptual design environment N89-22944
Definition of NASTRAN sets by use of parametric geometry N89-22958
A knowledge-based tool for multilevel decomposition of a complex design problem [NASA-TP-2903] N89-23181
The design and implementation of a graphical VHDL (VHSIC Hardware Description Language) user interface [AD-A202619] N89-23186
COMPUTER AIDED MAPPING
Cooperative methods for road tracking in aerial imagery N89-23101
Overview of the SRI cartographic modeling environment N89-23122
On the computational complexity of linear navigation N89-23123
Three-dimensional vision for outdoor navigation by an autonomous vehicle N89-23124
COMPUTER ANIMATION
Physically based modeling for vision and graphics N89-23097
COMPUTER ASSISTED INSTRUCTION
Story problem solver: A schema-based system of instruction [AD-A205594] N89-23205
COMPUTER COMPATIBLE TAPES
Report on round robin measurements of 6 digital magnetic tapes [NPL-DES-91] N89-23202
COMPUTER DESIGN
Design of a new high precision computer numerical control [DE89-008032] N89-23211
COMPUTER GRAPHICS
Using Patran and Supertab as pre- and postprocessors to COSMIC/NASTRAN N89-22942
Physically based modeling for vision and graphics N89-23097
Overview of the SRI cartographic modeling environment N89-23122
Using probabilistic domain knowledge to reduce the expected computational cost of matching N89-23134
Recognizing animal motion N89-23156
Labeling polyhedral images N89-23180
The design and implementation of a graphical VHDL (VHSIC Hardware Description Language) user interface [AD-A202619] N89-23186
Engineering Graphics System (EGS) user's manual [DE89-009668] N89-23199
COMPUTER INFORMATION SECURITY
Implementing security measures for computer-based security systems [DE89-008995] N89-23072
The Organisation and Functions of Documentation and Information Centres in Defence and Aerospace Environments [AGARD-CP-445] N89-23362
Data security N89-23369
COMPUTER NETWORKS
PixMail: Pictures through mail [DE89-009682] N89-22797
Implementing security measures for computer-based security systems [DE89-008995] N89-23072
Pyramid algorithms implementation on the connection machine N89-23129
IU software environments N89-23133
Structure recognition by connectionist relaxation: Formal analysis N89-23160
Overview of the software technology project RS34C71, documentation, management/technical advanced concepts for software engineering [AD-A204921] N89-23189
Decentralization of databases and the communication between them N89-23373
Technology transfer report [DE89-009044] N89-23381
COMPUTER PROGRAMMING
Numerical simulation of blast waves [REPT-882-320-102] N89-22858
A generalized one-dimensional computer code for turbomachinery cooling passage flow calculations [NASA-TM-102079] N89-22862

Implementation of the NETOS (Network Operating System) operated system in Ada with modifications to allow variable length messages
[AD-A202602] N89-23185
Overview of the software technology project RS34C71, documentation, management/technical advanced concepts for software engineering
[AD-A204921] N89-23189
A new approach to system testing
[DE89-008660] N89-23195
Expert systems for real-time monitoring and fault diagnosis
[NASA-CR-179441] N89-23209
Some methods for uncertain reasoning
[FOA-C-30492-3.3] N89-23212

COMPUTER PROGRAMS
Ultrasonic detection of damage in carbon epoxy composite materials
[ONERA-RT-3/7256-RY-071-R] N89-22705
SUPERFISH accuracy dependence on mesh size
[DE89-007992] N89-22790
A generalized one-dimensional computer code for turbomachinery cooling passage flow calculations
[NASA-TM-102079] N89-22862
Numerical method to predict projectile penetration
[DE89-007140] N89-22923
Design of a lightweight, low-cost geophysical survey vehicle
[DE89-009383] N89-22926
Interactive ultrasonic nondestructive evaluation
[AD-A204166] N89-22931
The project ASKA-SPACE, phase 1 — finite element method
[ETN-89-93768] N89-22959
Generalized finite strains, generalized stresses, and a hybrid variational principle for finite-element computer programs using curvilinear coordinates
[DE89-009923] N89-22962
A new perspective in the etiology, treatment, prevention and prediction of space motion sickness
[AD-A205660] N89-23065
SEAPAK user's guide, version 1.0
[NASA-TM-100728] N89-23182
Parallel processors and nonlinear structural dynamics algorithms and software
[NASA-CR-184938] N89-23184
Developing software to use parallel processing effectively
[AD-A205184] N89-23192
Simulation and analysis of physical mapping
[DE89-009399] N89-23198
MIRAP, microcomputer reliability analysis program
[DE89-009749] N89-23200
Techniques for applying sets code procedures to large fault trees in PRA (Probabilistic Risk Assessment) analysis
[DE89-004823] N89-23261
Theoretical and computational studies of plasma opening switches
[DE89-009712] N89-23297
The objectives and role of the Greek National Documentation Centre N89-23363
Microfilm and computer full text of archival documents
[AD-A204055] N89-23377

COMPUTER STORAGE DEVICES
Story problem solver: A schema-based system of instruction
[AD-A205594] N89-23205
Storage in supercomputer environments
[DE89-008895] N89-23330

COMPUTER SYSTEMS DESIGN
Integration effort in knowledge-based vision techniques for the autonomous land vehicle program N89-23108
Parallel hardware for constraint satisfaction N89-23127
Design of a new high precision computer numerical control
[DE89-008032] N89-23211

COMPUTER SYSTEMS PERFORMANCE
An integrated image understanding benchmark: Recognition of a 2 1/2 D mobile N89-23088
Specifying real-time systems with interval logic
[NASA-CR-181804] N89-23183
Parallel processors and nonlinear structural dynamics algorithms and software
[NASA-CR-184938] N89-23184
A new approach to system testing
[DE89-008660] N89-23195
Two time stepping algorithms for parallel computers
[DE89-008679] N89-23196
Reduction of a general matrix to tridiagonal form using a hypercube multiprocessor
[DE89-008721] N89-23197
Engineering Graphics System (EGS) user's manual
[DE89-009668] N89-23199
Factoring very large numbers using a massively parallel computer
[DE89-008198] N89-23208

COMPUTER SYSTEMS PROGRAMS
A statistical package in Ada
[FOA-C-20740-2.7] N89-23201

COMPUTER TECHNIQUES
Statistical smoothing methods and image analysis
[AD-A205643] N89-23256

COMPUTER VISION
Dynamic image interpretation for autonomous vehicle navigation
[AD-A204167] N89-22597
Proceedings: Image Understanding Workshop, volume 1
[AD-A197558] N89-23074
MIT progress in understanding images N89-23075
USC image understanding research: 1987-1988 N89-23076
Image understanding: Intelligent systems N89-23077
Image understanding research at the University of Maryland, December 1986 - January 1988 N89-23078
CMU image understanding program N89-23079
Image understanding research at SRI International N89-23080
Summary of image understanding research at the University of Massachusetts N89-23081
Progress in image understanding at the University of Rochester N89-23082
Image understanding and robotics research at Columbia University N89-23083
Qualitative reasoning and modeling for robust target tracking and recognition from a mobile platform N89-23086
Knowledge based vision for terrestrial robots N89-23087
An integrated image understanding benchmark: Recognition of a 2 1/2 D mobile N89-23088
Some sample algorithms for the image understanding architecture N89-23089
Algorithms and architectures for smart sensing N89-23090
The Maryland approach to image understanding N89-23091
An integrated approach to stereo matching, surface reconstruction and depth segmentation using consistent smoothness assumptions N89-23092
The MIT vision machine N89-23093
Kalman filter-based algorithms for estimating depth from image sequences N89-23094
Multimodal reconstruction and segmentation with Markov random fields and HCF optimization N89-23095
IU at UI: An overview and an example on shape from texture N89-23096
Physically based modeling for vision and graphics N89-23097
Perception with feedback N89-23098
Qualitative motion detection and tracking of targets from a mobile platform N89-23099
Qualitative navigation 2 N89-23100
Cooperative methods for road tracking in aerial imagery N89-23101
Affine invariant matching N89-23103
Constructing simple stable descriptions for image partioning N89-23104
Three-dimensional object recognition using surface descriptions N89-23105
Self calibration of motion and stereo vision for mobile robot navigation N89-23106
Autonomous navigation in cross-country terrain N89-23107
Integration effort in knowledge-based vision techniques for the autonomous land vehicle program N89-23108
Contour correspondences in dynamic imagery N89-23109
Spatio-temporal analysis of an image sequence with occlusion N89-23110
Generic models for robot navigation N89-23112
Mathematical morphology and the morphological sampling theorem N89-23113
Proceedings: Image Understanding Workshop, volume 2
[AD-A197559] N89-23115
Perceptual grouping for the detection and description of structures in aerial images N89-23117
Dynamic model matching for target recognition from a mobile platform N89-23118
TRIPLE: A multi-strategy machine learning approach to target recognition N89-23119
Using flow field divergence for obstacle avoidance in visual navigation N89-23120
An operational perception system for cross-country navigation N89-23121
On the computational complexity of linear navigation N89-23123
Three-dimensional vision for outdoor navigation by an autonomous vehicle N89-23124
Machine-independent image processing: Performance of Apply on diverse architectures N89-23125
Parallel architectures for image processing and vision N89-23126
Scan line array processors: Work in progress N89-23128
IU software environments N89-23133
Object recognition from a large database using a decision tree N89-23135
Modeling sensors and applying sensor model to automatic generation of object recognition program N89-23136
Evaluation of quantization error in computer vision N89-23138
Algebraic reasoning in view consistency and parameterized model matching problems N89-23139
Test results from SRI's stereo system N89-23140
Preliminary design of a programmed picture logic N89-23141
An introduction to generalized stereo techniques N89-23142
Stochastic stereo matching over scale N89-23143
Qualitative versus quantitative depth and shape from stereo N89-23144
The integration of information from stereo and multiple shape-form-texture cues N89-23145
Structural correspondence in stereo vision N89-23146
Curved surface reconstruction using stereo correspondence N89-23147
Geometric camera calibration using systems of linear equations N89-23148
Image segmentation and reflection analysis through color N89-23150
A color metric for computer vision N89-23151
Combining information in low-level vision N89-23152
Computation of motion in depth parameters: A first step in stereoscopic motion interpretation N89-23153
Is correspondence necessary for the perception of structure from motion N89-23154
Motion from a sequence of images N89-23155
Recognizing animal motion N89-23156
Issues in extracting motion parameters and depth from approximate translational motion N89-23157
A real time hierarchical model for optic flow determination via spatiotemporal frequency channels N89-23158
Structure recognition by connectionist relaxation: Formal analysis N89-23160
Extracting generic shapes using model-driven optimization N89-23161
Texture models and image measures for segmentation N89-23162
Building surfaces of evolution: The weaving wall N89-23165
Generation of face-edge-vertex models directly from images N89-23166
Depth from looming structure N89-23167
On the recovery of superellipsoids N89-23168
Straight homogeneous generalized cylinders: Differential geometry and uniqueness results N89-23169
Symbolic pixel labeling for curvilinear feature detection N89-23171
Image segmentation using geometric and physical constraints N89-23172
Adaptive smoothing for feature extraction N89-23173
Recognizing solid objects by alignment N89-23174
Projective invariants of shapes N89-23175
An optimal algorithm for the derivation of shape from shadows N89-23176
Predicting material classes N89-23177
Texture edge localization N89-23178
Surface orientation from projective foreshortening of isotropic texture autocorrelation N89-23179
Labeling polyhedral images N89-23180

COMPUTERIZED SIMULATION
Orbiter Flying Qualities (OFQ) Workstation user's guide
[NASA-CR-179440] N89-22612
The isothermal fatigue behavior of a unidirectional SiC/Ti composite and the Ti alloy matrix
[NASA-TM-101984] N89-22684
Simulation of a refrigerant evaporator
[ETN-89-94133] N89-22776
Special techniques used for time domain, three dimensional finite element modeling of electromagnetics
[DE89-007227] N89-22789
Annual research briefs, 1988
[NASA-CR-184906] N89-22817
Turbulence modeling N89-22819
Direct simulation of compressible reacting flows N89-22828

Non-linear evolution of a second mode wave in supersonic boundary layers
[NASA-CR-181811] N89-22836
A vortex panel analysis of circular-arc bluff-bodies in unsteady flow
[DE89-007141] N89-22845
Computerized simulation of turbulent flow in a channel
[ONERA-RSF-16/3419-AY-112-A] N89-22852
Numerical simulation of blast waves
[REPT-882-320-102] N89-22858
Enhanced rotor modeling tailored for rub dynamic stability analysis and simulation N89-22916
Topology of modified helical gears and Tooth Contact Analysis (TCA) program
[NASA-CR-4224] N89-22920
Numerical method to predict projectile penetration
[DE89-007140] N89-22923
Preliminary results of the MLAM (Multi-Layer Air Mass) Lagrangian transport model simulation of ANATEX (Across North America Tracer Experiment)
[DE89-008123] N89-23036
Retrieving the distribution of liquid water content in clouds from observations of thermal microwave radiation N89-23056
A real-time simulator for man-in-the-loop testing of aircraft control systems (SIMTACS-RT)
[AD-A202599] N89-23067
Physically based modeling for vision and graphics N89-23097
Optimization for object localization of the constrained algebraic reconstruction technique
[DE89-007755] N89-23193
Simulation and analysis of physical mapping
[DE89-009399] N89-23198
Nonlinear finite element simulation of the large angle motion of flexible bodies
[DE89-006505] N89-23230
Molecular dynamics and irreversibility, from Boltzmann to Nose
[DE89-006740] N89-23274
Theoretical and computational studies of plasma opening switches
[DE89-009712] N89-23297
Development and simulation study of a new inverse-pinch high Coulomb transfer switch
[NASA-CR-181768] N89-23300
Physical properties of grain-boundary materials: Comparison of EAM (Embedded-Atom-Method) and central-force potentials
[DE89-007414] N89-23308

CONCENTRATION (COMPOSITION)
Role of aluminium concentration on the structure behaviour of Cu-Al alloys
[DE88-705647] N89-22727
ESE (Electron Spin Echo) and CW-ESR studies of synthetic diamond crystals: Distribution of nitrogen and nickel
[DE89-007373] N89-23314

CONCENTRATORS
Innovation in separation technology for fine gravity semi-products
[PB89-112478] N89-22719
Advances in concentrator cell technology
[DE89-007432] N89-23013

CONDENSATION NUCLEI
Mass-spectroscopic measurements of stratospheric ions, trace gases and precondensation nuclei using balloon-borne measuring probes
[BPT-7/88] N89-23037

CONDENSING
Nature of condensation in the momentum space for an interacting Bose system
[DE88-705679] N89-23352

CONDUCTIVITY
The induced current in parallel wires over an imperfect ground from an incident EMP
[DE89-007209] N89-22787

CONFERENCES
Rotordynamic Instability Problems in High-Performance Turbomachinery, 1988
[NASA-CP-3026] N89-22891
Seventeenth NASTRAN (R) Users' Colloquium
[NASA-CP-3029] N89-22940
Space Electrochemical Research and Technology Conference: Abstracts
[NASA-CP-10029] N89-22962
Proceedings: Image Understanding Workshop, volume 1
[AD-A197558] N89-23074
Proceedings: Image Understanding Workshop, volume 2
[AD-A197559] N89-23115
Calendar of selected aeronautical and space meetings
[AGARD-CAL-88/2] N89-23361

CONFIDENCE LIMITS
A statistical package in Ada
[FOA-C-20740-2.7] N89-23201

CONFORMAL MAPPING
Knowledge based vision for terrestrial robots N89-23087
Induced quantum conformal gravity
[DE88-705718] N89-23356

CONSERVATION LAWS
Second-order accurate nonoscillatory schemes for scalar conservation laws
[NASA-TM-102010] N89-22573

CONSTITUTIVE EQUATIONS
A general non-linear dynamical theory of elastic curved beams N89-22930

CONTACT LOADS
Adaptive contact elements for three-dimensional explicit transient analysis
[DE89-008436] N89-22958

CONTAMINATION
Corrosion of iron, nickel and cobalt based alloys in high temperature environments contaminated with chlorine
[DE89-009829] N89-22738
Investigation on long time dispersion and washout factor. Vegetation contamination computation with meteorological whole year or summer statistics
[JUEL-SPEZ-449] N89-23028

CONTINENTAL SHELVES
Seafloor temperature and conductivity data from coastal waters of the US Beaufort Sea
[AD-A205428] N89-23059

CONTINUOUS RADIATION
Radiation control at the Continuous Electron Beam Accelerator Facility (CEBAF), a new high power CW electron accelerator installation
[CEBAF-PR-89-001] N89-23280

CONTINUUM MECHANICS
A general non-linear dynamical theory of elastic curved beams N89-22930

CONTOURS
Contour correspondences in dynamic imagery N89-23109

CONTRACT MANAGEMENT
Agreement on the International Space Station and Columbus Program
[REPT-34/88] N89-23360

CONTRACTS
Center for Advanced Space Propulsion (CASP)
[NASA-CR-184936] N89-23404

CONTROL CONFIGURED VEHICLES
An experimental and analytical synthesis of controlled structure design
[DE89-006505] N89-22957

CONTROL STABILITY
On the stabilization of bilinear systems via constant feedback
[MEMO-706] N89-23215
The local disturbance decoupling problem with stability for nonlinear systems
[MEMO-721] N89-23217
On the use of stable distributions in design programs
[MEMO-736] N89-23219

CONTROL SYSTEMS DESIGN
Single channel test controllers
[AD-A204088] N89-22611
Microcomputer based controller for the Langley 0.3-meter Transonic Cryogenic Tunnel
[NASA-CR-181808] N89-22616
Magnetic bearing stiffness control using frequency band filtering N89-22910
A magnetic damper for first mode vibration reduction in multimass flexible rotors N89-22911
Control of free-flying space robot manipulator systems
[NASA-CR-184837] N89-22918
Ritz method for transient response in systems having unsymmetric stiffness N89-22954
Expert systems for real-time monitoring and fault diagnosis
[NASA-CR-179441] N89-23209
On the use of stable distributions in design programs
[MEMO-736] N89-23219
Robust stabilization of an inverted double pendulum system via a polynomial approach to H(infinity) optimal control
[MEMO-742] N89-23220
Model matching for linear Hamiltonian systems
[MEMO-730] N89-23243
Nonlinear model matching with prescribed tracking error with an application to Hamiltonian systems
[MEMO-731] N89-23244
Radiation control at the Continuous Electron Beam Accelerator Facility (CEBAF), a new high power CW electron accelerator installation
[CEBAF-PR-89-001] N89-23280

CONTROL THEORY
Optimal low thrust trajectories for planetary capture
[AD-A202604] N89-22632
Selected aspects of discrete-time filtering techniques as applied to sensor control and signal processing problems
[ETN-89-94134] N89-22794
The structure and control of three-dimensional shock wave turbulent boundary layer interactions
[AD-A205923] N89-22866
Magnetic bearing stiffness control using frequency band filtering N89-22910
Control of free-flying space robot manipulator systems
[NASA-CR-184837] N89-22918
An experimental and analytical synthesis of controlled structure design
[DE89-006505] N89-22957
A real-time simulator for man-in-the-loop testing of aircraft control systems (SIMTACS-RT)
[AD-A202599] N89-23067
Expert systems for real-time monitoring and fault diagnosis
[NASA-CR-179441] N89-23209
Adaptive LQ control: Conflict between identification and control
[MEMO-718] N89-23216
Optimal processes described by a parabolic differential equation with control in the coefficients, part 3
[MEMO-725-PT-3] N89-23218
Some local results for linear systems and implications for state variable feedback
[MATHS-RES-202] N89-23221

CONTROLLERS
Single channel test controllers
[AD-A204088] N89-22611
A NASTRAN/TREETOPS solution to a flexible, multi-body dynamics and controls problem on a UNIX workstation N89-22945
A powerful enhancement to the DMAP alter capability N89-22947
Design of a new high precision computer numerical control
[DE89-008032] N89-23211

CONVECTION
On curve and surface stretching in turbulent flow N89-22820

CONVECTIVE FLOW
Forced and free convection flow with viscous dissipation effects: The method of parametric differentiation
[DE88-705649] N89-22840

CONVERGENCE
Monte Carlo approximations in Bayesian decision theory. Part 3: Limiting behavior of Monte Carlo approximations
[AD-A204173] N89-23258

COOLING
Development of advanced heat pump. Part 2: Preliminary test of two-stage compression heat pump
[DE88-756838] N89-22841

COOLING SYSTEMS
Numerical model of solar dynamic radiator for parametric analysis
[NASA-TM-102054] N89-22653

COOPERATION
Relationships between the prenucleolus, ENSC-solution and related solution concepts for cooperative games
[MEMO-729] N89-23266

COPOLYMERS
Dynamic scattering from multicomponent polymer systems
[DE88-705677] N89-22752
Application of the Ornstein-Zernike formalism to polymer and copolymer blends
[DE88-705686] N89-22753
Physical-chemical studies of solutions processing of nematic polymers
[AD-A205921] N89-22770

COPPER
Effects of grain size and strain rate on the mechanical response of copper
[DE89-008811] N89-22731
Mechanisms of cascade collapse
[DE89-009682] N89-22740
Physical properties of grain-boundary materials: Comparison of EAM (Embedded-Atom-Method) and central-force potentials
[DE89-007414] N89-23308
Ductility enhancement in unreacted internal-Sn Nb3Sn through low-temperature anneals
[DE89-009125] N89-23336

COPPER ALLOYS
Role of aluminium concentration on the structure behaviour of Cu-Al alloys
[DE88-705647] N89-22727

COPPER OXIDES
Evaluation, development, and characterization of superconducting materials for space application
[NASA-CR-184842] N89-23302
Effects of different fabrication techniques on the Yttrium-Barium-Copper oxide high temperature superconductor
[AD-A202598] N89-23304
Perturbative treatment of local correlations in Cu-O planes for high temperature superconductors
[DE88-705648] N89-23315
CORRELATION
Position, scale, and rotation invariant optical pattern recognition for target extraction and identification
[AD-A202600] N89-22781
CORROSION
Behavior of iron aluminides in oxidizing and sulfidizing environments
[DE89-008919] N89-22693
Corrosion monitoring with acoustic wave devices
[DE89-005235] N89-22728
Thermal healing of defects in oxide films on metals and alloys
[DE89-009580] N89-22735
Hydrogen embrittlement in nickel-hydrogen cells N89-23006
CORROSION PREVENTION
Electrochemical technique for rapidly evaluating protective coatings on metals
[PB89-134209] N89-22748
CORROSION RESISTANCE
Application of electrochemical noise spectral analysis to the study of the pitting corrosion of aluminum alloys
[ETCA-87-R-102] N89-22744
CORROSION TESTS
Corrosion testing of candidates for the alkaline fuel cell cathode N89-23000
COSMIC RAYS
Effects of cosmic rays on single event upsets
[NASA-CR-184835] N89-23400
COSMOLOGY
Induced quantum conformal gravity
[DE88-705718] N89-23356
Dark matter candidates
[DE89-006579] N89-23387
Problems in modern cosmology N89-23393
COSMOS SATELLITES
Mini Protein Crystallization Facility (MPCF), phase A study: Executive summary
[ESA-CR(P)-2709] N89-22775
COST ANALYSIS
Study on communications costs for Columbus utilization
[REPT-871126/1/FR] N89-22801
Development of advanced heat pumps. Part 3: Fundamental approach on two-stage compression system
[DE88-756842] N89-22842
Analysis of the present knowledge of costs and benefits of the governmental advancement of astronautics
[ETN-89-93770] N89-23359
COST ESTIMATES
Launch options for the future: Special report
[PB89-114268] N89-22637
Study on communications costs for Columbus utilization
[REPT-871126/1/FR] N89-22801
COST REDUCTION
The use of COSMIC NASTRAN in an integrated conceptual design environment N89-22944
Using probabilistic domain knowledge to reduce the expected computational cost of matching N89-23134
COUETTE FLOW
Low-dimensional chaos in turbulence N89-22822
COULOMB COLLISIONS
Ordering transitions induced by Coulomb interactions
[DE88-705717] N89-23324
COULOMB POTENTIAL
Development and simulation study of a new inverse-pinch high Coulomb transfer switch
[NASA-CR-181768] N89-23300
COUPLING
ICRF waveguide launcher research
[DE89-009151] N89-22791
Two dimensional (4,0) supergravity in harmonic superspace. The action and the matter couplings
[DE88-705661] N89-23351
CRACK GEOMETRY
The Hertzian cone crack: Theoretical, munerical and experimental studies
[OUEL-1743/88] N89-22961
CRACK INITIATION
Damage development, property degradation and life prediction in composite laminates N89-22708
The Hertzian cone crack: Theoretical, munerical and experimental studies
[OUEL-1743/88] N89-22961
CRACK PROPAGATION
Damage development, property degradation and life prediction in composite laminates N89-22708
Assessing hydrogen assisted cracking modes in high strength steel welds
[AD-A205431] N89-22746
Environmentally induced discontinuities in transparent polymers
[AD-A205483] N89-22768
Finite element analysis for calibration curve computation for measurement of crack propagation of ellipse shaped surface cracks
[GKSS-88/E/34] N89-22960
Recent advances in modeling creep crack growth
[W-2/88] N89-22964
Corrosion fatigue crack growth: The role of crack-tip deformation and film formation kinetics N89-22966
CRACK TIPS
Corrosion fatigue crack growth: The role of crack-tip deformation and film formation kinetics N89-22966
CRACKING (CHEMICAL ENGINEERING)
Environmentally induced discontinuities in transparent polymers
[AD-A205483] N89-22768
CRACKING (FRACTURING)
Fiber matrix interface effects in failure of ceramic matrix fiber composites
[AD-A204618] N89-22686
Corrosion fatigue crack growth: The role of crack-tip deformation and film formation kinetics N89-22966
CRACKS
Alumina reinforced tetragonal zirconia (TZP) composites
[DE89-008880] N89-22690
Mechanisms of crevice corrosion in chlorinated environments
[AD-A204821] N89-22724
CRASH LANDING
Aircraft accident report: Trans-Colorado Airlines, Inc., Flight 2286, Fairchild Metro 3, SA227 AC, N68TC Bayfield, Colorado, January 19, 1988
[PB89-910401] N89-22593
CREEP PROPERTIES
Development of stress and lifing criteria for single crystal turbine blades N89-22663
Recent advances in modeling creep crack growth
[W-2/88] N89-22964
CREEP STRENGTH
Investigation and synthesis of high temperature and increased stiffness RSP aluminum alloys
[AD-A204162] N89-22723
Improved high temperature creep resistant austenitic alloy
[DE89-009664] N89-22736
CRITERIA
Indexing and abstracting N89-23368
CRITICAL VELOCITY
Some in-field experiences of non-synchronous vibrations in large rotating machinery N89-22894
Anomalous cross-field velocities in a CIV laboratory experiment
[TRITA-EPP-88-06] N89-23289
CRYOGENIC EQUIPMENT
Analysis of the nonvented fill of a 4.96-cubic-meter lightweight liquid hydrogen tank
[NASA-TM-102039] N89-22652
Cryogenic turbopump bearing materials N89-22678
Performance of all-metal demountable cryogenic seals at superfluid helium temperatures
[NASA-TM-102190] N89-22850
CRYOGENIC FLUIDS
Analysis of the nonvented fill of a 4.96-cubic-meter lightweight liquid hydrogen tank
[NASA-TM-102039] N89-22652
CRYOGENIC TEMPERATURE
Performance of all-metal demountable cryogenic seals at superfluid helium temperatures
[NASA-TM-102190] N89-22850
CRYOGENIC WIND TUNNELS
Hardware and operating features of the adaptive wall test section for the 0.3-meter transonic cryogenic tunnel
[NASA-TM-4114] N89-22614
Microcomputer based controller for the Langley 0.3-meter Transonic Cryogenic Tunnel
[NASA-CR-181808] N89-22616
CRYOGENICS
New thermocouple: Characteristic investigation of Au+Pd+Ni/Ni+Cr thermocouple below 273K
[PB89-112940] N89-22867
CRYOSTATS
A variable temperature cryostat that produces in situ clean-up germanium detector surfaces
[DE89-008174] N89-23328
CRYSTAL DISLOCATIONS
Mechanisms of cascade collapse
[DE89-009882] N89-22740
Study of grain boundaries in polycrystalline alumina
[ETCA-87-R-130] N89-23344
Study of grain boundaries in polycrystalline alumina. Effect of the manufacturing mode and of the material composition
[ETCA-87-R-100] N89-23345
CRYSTAL GROWTH
Experimental investigation of hot electron and related effects in gallium (aluminum) arsenide devices
[AD-A205442] N89-23349
CRYSTAL LATTICES
Electronic properties of Ge(1-X)Si(X): Alloying versus pressure
[DE88-705678] N89-23320
CRYSTAL STRUCTURE
Internal stresses in ceramic composite constituents determined by neutron diffraction technique
[DE89-009883] N89-22697
Transmission electron microscopy: Imaging of materials
[DE89-007418] N89-22870
Electron energy-loss spectroscopy: Fundamentals and applications in the characterization of minerals
[DE89-006613] N89-23307
Quasicrystals from cuts in six dimensions
[DE89-009361] N89-23337
Structural properties of superconducting and nonsuperconducting Ba sub 1-x K sub x BiO3
[DE89-009813] N89-23340
CRYSTAL SURFACES
Accumulated surface damage on ZnS crystals produced by closely spaced pairs of picosecond laser pulses
[DE89-008813] N89-23329
CRYSTALLIZATION
Mini Protein Crystallization Facility (MPCF), phase A study: Executive summary
[ESA-CR(P)-2709] N89-22775
Novel protein crystal growth technology: Proof of concept
[NASA-CR-184959] N89-23306
Ordering transitions induced by Coulomb interactions
[DE88-705717] N89-23324
Influence of ion irradiated SrTiO sub 3 on the properties of thin film oxide superconductors
[DE89-009409] N89-23338
CRYSTALLOGRAPHY
Quasicrystals from cuts in six dimensions
[DE89-009361] N89-23337
CRYSTALS
Quasicrystals from cuts in six dimensions
[DE89-009361] N89-23337
CUBIC EQUATIONS
Approximate large deflection analysis of simply supported orthotropic plates
[NPL-DMA(A)171] N89-22963
CURRENT DENSITY
Variational analysis of railgun plasma-arc-armature for acceleration of solid hydrogen pellets for fusion reactor refueling
[DE89-009556] N89-22634
ITER equilibrium with bootstrap currents, lower hybrid current drive and fast wave current drive
[DE89-009676] N89-22810
CURVATURE
The effects of stabilizing and destabilizing longitudinal curvature on the structure of turbulent, two-stream mixing layers N89-22833
CURVE FITTING
Curved surface reconstruction using stereo correspondence N89-23147
CURVED BEAMS
A general non-linear dynamical theory of elastic curved beams N89-22930
CURVES (GEOMETRY)
On curve and surface stretching in turbulent flow N89-22820
CYCLES
Short proofs of some Fan-type results
[MEMO-711] N89-23237
CYCLIC LOADS
Environmental program on durability of graphite/epoxy honeycomb specimens with representative damage and repairs
[AR-005-504] N89-22685
CYCLOTRON RESONANCE
Effects of ion collisions on quasilinear heating by the current-driven ion cyclotron instability in the high latitude ionosphere
[AD-A202512] N89-23032

CYCLOTRONS
Possibility of operation of high temperature superconducting YBa2Cu3O7 ceramics in cyclotrons at irradiation
[DE88-705783] N89-23325
CYLINDRICAL BODIES
Straight homogeneous generalized cylinders: Differential geometry and uniqueness results N89-23169
The multigroup and cylindrical geometry formulation of the Sn Monte Carlo hybrid method
[DE89-000326] N89-23260
CZOCHRALSKI METHOD
Development of magnetic field assisted melt stabilization with heat and mass transfer control in low pressure LEC growth of GaAs
[AD-A205185] N89-23313

D

DAMAGE
Damage development, property degradation and life prediction in composite laminates N89-22708
DAMAGE ASSESSMENT
Damage tolerance concepts for advanced materials and engines N89-22661
The effects of plastic media blasting paint removal on the microstructure of graphite/epoxy composite materials
[AD-A204801] N89-22688
Ultrasonic detection of damage in carbon epoxy composite materials
[ONERA-RT-3/7256-RY-071-R] N89-22705
Mechanical properties and damage mechanisms of carbon fiber reinforced composites: Compression loading
[DFVLR-FB-88-41] N89-22706
DAMPERS
Rotordynamic Instability Problems in High-Performance Turbomachinery, 1988
[NASA-CP-3026] N89-22891
DAMPING
Modal strain energies in COSMIC NASTRAN N89-22955
Hysteresis development in superconducting Josephson junctions
[DE88-705693] N89-23323
DARK MATTER
Dark matter candidates
[DE89-006579] N89-23367
DATA ACQUISITION
Measurement uncertainty of adsorption testing of desiccant materials
[DE89-000841] N89-22681
Coordinated Noninvasive Studies (CNS) Project
[AD-A205413] N89-22804
An experimental environment and laboratory for studying human information processing in Naval Air ASW (Naval air antisubmarine warfare)
[AD-A204774] N89-23069
Perception with feedback N89-23098
A programmatic approach to achieving data quality objectives
[DE89-008246] N89-23378
DATA BASE MANAGEMENT SYSTEMS
Core knowledge system: Storage and retrieval of inconsistent information N89-23132
Simulation and analysis of physical mapping
[DE89-009399] N89-23198
Decentralization of databases and the communication between them N89-23373
Microfilm and computer full text of archival documents
[AD-A204055] N89-23377
Technology transfer report
[DE89-009044] N89-23381
DATA BASES
Improved performance in NASTRAN (R) N89-22941
Multi-mission Ni-H2 battery cell for the 1990's N89-23006
Gravity wave and turbulence studies using a high-resolution ST radar
[AD-A205592] N89-23046
Sources of information N89-23366
DATA INTEGRATION
Image understanding research at the University of Maryland, December 1986 - January 1988 N89-23078
Summary of image understanding research at the University of Massachusetts N89-23081
An integrated approach to stereo matching, surface reconstruction and depth segmentation using consistent smoothness assumptions N89-23092
The MIT vision machine N89-23093
Kalman filter-based algorithms for estimating depth from image sequences N89-23094
Multimodal reconstruction and segmentation with Markov random fields and HCF optimization N89-23095
IU at UI: An overview and an example on shape from texture N89-23096
Qualitative navigation 2 N89-23100
PACE: An environment for intelligence analysis N89-23102
Affine invariant matching N89-23103
Overview of the SRI cartographic modeling environment N89-23122
On the computational complexity of linear navigation N89-23123
The integration of information from stereo and multiple shape-form-texture cues N89-23145
Combining information in low-level vision N89-23152
Building surfaces of evolution: The weaving wall N89-23165
DATA LINKS
PSDE/SAT-2: Communication system architecture study, executive summary
[ESA-CR(P)-2732] N89-22802
DATA MANAGEMENT
The Organisation and Functions of Documentation and Information Centres in Defence and Aerospace Environments
[AGARD-CP-445] N89-23362
The objectives and role of the Greek National Documentation Centre N89-23363
The status of defence information programs in Greece N89-23364
Sources of information N89-23366
Identifying users and how to reach them N89-23370
Information resources management N89-23371
Impact of information technology on organizational structure: A control perspective N89-23379
DATA PROCESSING
National airspace system plan: Facilities, equipment, associated development and other capital needs
[AD-A202615] N89-22596
Project Radioastron N89-22623
Space Propulsion Hazards Analysis Manual (SPHAM). Volume 2: Appendices
[AD-A204601] N89-22650
Climatological and statistical fundamentals for the explanation of climate data processing
[ETN-89-93775] N89-23051
SEAPAK user's guide, version 1.0
[NASA-TM-100728] N89-23182
Systolic implementation of neural networks
[DE89-008031] N89-23210
Standardized bibliographic processing N89-23367
Information resources management N89-23371
TRANSDOC-electronic delivery programme N89-23372
DATA REDUCTION
Measurement uncertainty of adsorption testing of desiccant materials
[DE89-000841] N89-22681
CMU image understanding program N89-23079
DATA RETRIEVAL
Microfilm and computer full text of archival documents
[AD-A204055] N89-23377
DATA SAMPLING
Mathematical morphology and the morphological sampling theorem N89-23113
DATA SMOOTHING
An integrated approach to stereo matching, surface reconstruction and depth segmentation using consistent smoothness assumptions N89-23092
Adaptive smoothing for feature extraction N89-23173
Smoothing and likelihood ratio for Gaussian boundary value processes
[MEMO-726] N89-23242
Smooth interpolation to scattered data by bivariate piecewise polynomials of odd degree
[MEMO-732] N89-23245
DATA STORAGE
Core knowledge system: Storage and retrieval of inconsistent information N89-23132
TRANSDOC-electronic delivery programme N89-23372
Microfilm and computer full text of archival documents
[AD-A204055] N89-23377
DATA SYSTEMS
Overview of the software technology project RS34C71, documentation, management/technical advanced concepts for software engineering
[AD-A204921] N89-23189
DECISION MAKING
Object recognition from a large database using a decision tree N89-23135
Fostering interaction of government, defense, and aerospace databases N89-23374
DECISION THEORY
Progress in image understanding at the University of Rochester N89-23082
Monte Carlo approximations in Bayesian decision theory. Part 3: Limiting behavior of Monte Carlo approximations
[AD-A204173] N89-23258
DECOMPOSITION
Spinodal decomposition of austenite in long-term-aged duplex stainless steel
[DE89-009627] N89-22737
DECOUPLING
The local disturbance decoupling problem with stability for nonlinear systems
[MEMO-721] N89-23217
DEFECTS
Electrical properties and detection methods for CMOS IC defects
[DE89-005775] N89-23327
DEFENSE PROGRAM
Space control: A national imperative
[AD-A202612] N89-22631
Transitional strategic defense architectures
[DE89-008312] N89-23265
DEFLECTION
Approximate large deflection analysis of simply supported orthotropic plates
[NPL-DMA(A)171] N89-22963
DEFORMATION
Aerodynamics of nonrigid bodies undergoing large amplitude time-dependent motions N89-22586
Damage development, property degradation and life prediction in composite laminates N89-22708
Effects of grain size and strain rate on the mechanical response of copper
[DE89-008811] N89-22731
On curve and surface stretching in turbulent flow N89-22820
Adaptive contact elements for three-dimensional explicit transient analysis
[DE89-008436] N89-22958
Cohomology theory and deformations of Z sub 2-graded Lie algebras
[DE88-705694] N89-23229
DEGRADATION
Formation of lubricating films at elevated temperatures from the gas phase
[PB89-129530] N89-22747
The application of electrochemical impedance spectroscopy for characterizing the degradation of Ni(OH)2/NiOOH electrodes N89-23003
DEICING
NASA's program on icing research and technology
[NASA-TM-101989] N89-22569
Electro-impulse de-icing research: Fatigue and electromagnetic interference tests
[DOT/FAA/CT-88/27] N89-22594
DELTA WINGS
Transonic and supersonic flow past a 65 deg delta wing with rounded leading edges: Analysis of experimental data
[DFVLR-FB-88-44] N89-22580
The influence of the leading edge geometry on the wave drag for a 65 degree delta wing at low supersonic speed and small angles of attack
[FFA-141] N89-22583
DENSITY MEASUREMENT
Determination of the He3 number density for the proportional counter used in the NPL Bonner sphere system
[NPL-RS(EXT)104] N89-23275
DEOXYRIBONUCLEIC ACID
Simulation and analysis of physical mapping
[DE89-009399] N89-23198
DEPLOYMENT
Construction in weightlessness N89-22626
DEPOSITION
Carbonaceous film coating
[DE89-009592] N89-22762
DEPTH
Chemical state depth profiling by Auger signal decomposition: Silicon oxynitride
[DE89-009830] N89-22764
An integrated approach to stereo matching, surface reconstruction and depth segmentation using consistent smoothness assumptions N89-23092
Kalman filter-based algorithms for estimating depth from image sequences N89-23094
Qualitative versus quantitative depth and shape from stereo N89-23144
Computation of motion in depth parameters: A first step in stereoscopic motion interpretation N89-23153
Issues in extracting motion parameters and depth from approximate translational motion N89-23157
Depth from looming structure N89-23167

DESCENT
Aircraft accident report: Trans-Colorado Airlines, Inc., Flight 2286, Fairchild Metro 3, SA227 AC, N68TC Bayfield, Colorado, January 19, 1988
[PB89-910401] N89-22593

DESCRIPTIVE GEOMETRY
Approximation of surfaces constrained by a differential equation using simplex splines
[MEMO-739] N89-23249

DESICCANTS
Measurement uncertainty of adsorption testing of desiccant materials
[DE89-000841] N89-22681

DESIGN ANALYSIS
An efficient inverse method for the design of blended wing-body configurations N89-22603
Development of behaviorist models to simulate commuted power switches
[ISAL-88-0065] N89-22815
Development of advanced heat pumps. Part 3: Fundamental approach on two-stage compression system
[DE88-756842] N89-22842
Experimental verification of an eddy-current bearing N89-22913
Characterization testing of a 40 Ahr bipolar nickel hydrogen battery N89-22992
Multi-mission Ni-H2 battery cell for the 1990's N89-23006
Advances in ambient temperature secondary lithium cells N89-23011
Automatic generation of noncolliding trajectories and manipulation task planning in robotics
[LAAS-89-002] N89-23222

DESTABILIZATION
A theoretical study of fluid forces on a centrifugal impeller rotating and whirling in a vaned diffuser N89-22908

DIAMONDS
ESE (Electron Spin Echo) and CW-ESR studies of synthetic diamond crystals: Distribution of nitrogen and nickel
[DE89-007373] N89-23314

DIELECTRICS
Calculation of longitudinal and transverse wake-field effects in dielectric structures
[DE89-009814] N89-22798
Predicting material classes N89-23177

DIESEL ENGINES
Methods for heat transfer and temperature field analysis of the insulated diesel, phase 3
[NASA-CR-182237] N89-23382

DIFFERENCE EQUATIONS
Asymptotic expansions with error bounds for solutions of difference equations of level 1 sup +
[MEMO-724] N89-23241
The influence of open boundary conditions and difference operators on the time-integration of the Burger's equation
[FFA-TN-1988-57] N89-23254

DIFFERENTIAL EQUATIONS
Approximation of surfaces constrained by a differential equation using simplex splines
[MEMO-739] N89-23249
Projections of vector addition system reachability sets are semilinear
[AD-A205914] N89-23257

DIFFERENTIAL GEOMETRY
Straight homogeneous generalized cylinders: Differential geometry and uniqueness results N89-23169
Image segmentation using geometric and physical constraints N89-23172

DIFFUSION
CVD and diffusion coatings for high temperature applications in turbomachinery and rocket motors N89-22658
Mie scattering calculations for heat radiation
[FOA-C-20738-2.1] N89-23279

DIFFUSION ELECTRODES
Current and thermal noise in mixed Na/Ag beta alumina
[AD-A205869] N89-22816
Conductivity fluctuations in mixed Na/Ca beta alumina
[AD-A205416] N89-23348

DIFFUSION FLAMES
Inviscid spatial stability of a compressible mixing layer. Part 2: The flame sheet model
[NASA-CR-181815] N89-22837

DIFFUSION THEORY
Localization of solutions of a nonlinear Fokker-Planck equation with Dirichlet boundary conditions — soil moisture infiltration
[MEMO-733] N89-23246

DIGITAL FILTERS
Selected aspects of discrete-time filtering techniques as applied to sensor control and signal processing problems
[ETN-89-94134] N89-22794

DIGITAL SIMULATION
Position, scale, and rotation invariant optical pattern recognition for target extraction and identification
[AD-A202600] N89-22781
Using generic geometric and physical models for representing solids N89-23114

DIGITAL SYSTEMS
Interactive ultrasonic nondestructive evaluation
[AD-A204166] N89-22931

DIGITAL TECHNIQUES
Evaluation of quantization error in computer vision N89-23138
Report on round robin measurements of 6 digital magnetic tapes
[NPL-DES-91] N89-23202

DIHEDRAL ANGLE
Machine reference mirror inspection by optical Fabry-Perot cavity testing
[DE89-009635] N89-23284

DIMENSIONAL ANALYSIS
Lectures in Fluid Physics held at the Physics Department of the Georg-August-University. Volume 2: Examples of the Application of Dimensional Analysis
[DFVLR-MITT-88-27-VOL-2] N89-22856

DIMENSIONLESS NUMBERS
Lectures in Fluid Physics held at the Physics Department of the Georg-August-University. Volume 2: Examples of the Application of Dimensional Analysis
[DFVLR-MITT-88-27-VOL-2] N89-22856

DIRICHLET PROBLEM
Incorporation of a boundary condition to numerical solution of POISSON's equation
[DE89-007132] N89-23231
Localization of solutions of a nonlinear Fokker-Planck equation with Dirichlet boundary conditions — soil moisture infiltration
[MEMO-733] N89-23246

DISCRIMINANT ANALYSIS (STATISTICS)
Statistical smoothing methods and image analysis
[AD-A205643] N89-23256

DISCRIMINATION
Motor theory of auditory perception
[AD-A204951] N89-23064

DISPERSIONS
Investigation and synthesis of high temperature and increased stiffness RSP aluminum alloys
[AD-A204162] N89-22723
Investigation on long time dispersion and washout factor. Vegetation contamination computation with meteorological whole year or summer statistics
[JUEL-SPEZ-449] N89-23028

DISPLACEMENT
On the physical causes of ENSO events and the ITCZ's extreme latitudinal displacements
[DE88-705654] N89-23050
Acoustic wave device using plate modes with surface-parallel displacement
[DE89-009719] N89-23273

DISPLAY DEVICES
Model-based analysis and cooperative synthesis of control and display augmentation for piloted flight vehicles N89-22610
An experimental environment and laboratory for studying human information processing in Naval Air ASW (Naval air antisubmarine warfare)
[AD-A204774] N89-23069

DISSIPATION
Ionospheric scintillation studies
[AD-A205210] N89-23034

DISTORTION
Distortions caused by the signal processing in analog AM modulators
[DE88-705657] N89-22785
Analysis of turbulence structures in shear flows N89-22826
Distortions in the output signals of conventional spectrum analyzers
[DE88-705656] N89-22871

DISTRIBUTED PROCESSING
Specifying real-time systems with interval logic
[NASA-CR-181804] N89-23183
Systolic implementation of neural networks
[DE89-008031] N89-23210
Decentralization of databases and the communication between them N89-23373

DISTRIBUTING
TRANSDOC-electronic delivery programme N89-23372

DOCUMENT STORAGE
Microfilm and computer full text of archival documents
[AD-A204055] N89-23377

DOCUMENTS
Sources of information N89-23366
TRANSDOC-electronic delivery programme N89-23372

DRAG REDUCTION
The influence of the leading edge geometry on the wave drag for a 65 degree delta wing at low supersonic speed and small angles of attack
[FFA-141] N89-22583

DRIFT RATE
Electron drift velocity close to a sense wire
[NIKHEF-H/88-5] N89-23277

DROP TESTS
A preliminary characterization of parachute wake recontact
[DE89-006442] N89-22576

DUCTILITY
Hydrogen embrittlement in nickel-hydrogen cells N89-23008
Ductility enhancement in unreacted internal-Sn Nb3Sn through low-temperature anneals
[DE89-009125] N89-23336
Study of grain boundaries in polycrystalline alumina. Effect of the manufacturing mode and of the material composition
[ETCA-87-R-100] N89-23345

DYE LASERS
Accumulated surface damage on ZnS crystals produced by closely spaced pairs of picosecond laser pulses
[DE89-008813] N89-23329

DYNAMIC CHARACTERISTICS
Dynamic behavior of a carbon epoxy composite
[ETCA-87-R-001] N89-22701
Dynamic scattering from multicomponent polymer systems
[DE88-705677] N89-22752
A 3-dimensional finite-difference method for calculating the dynamic coefficients of seals N89-22903
An experimental study on the static and dynamic characteristics of pump annular seals N89-22904
A seal test facility for the measurement of isotropic and anisotropic linear rotordynamic characteristics N89-22905
Finite difference analysis of rotordynamic seal coefficients for an eccentric shaft position N89-22906
Role of circumferential flow in the stability of fluid-handling machine rotors N89-22915
Configuration comparison analysis for the AFIT/AAMRL anthropomorphic robotic manipulator
[AD-A202618] N89-22921
Molecular dynamics and irreversibility, from Boltzmann to Nose
[DE89-006740] N89-23274
Dynamics of particles in the bending waves of the planetary rings
[DE88-705714] N89-23396

DYNAMIC CONTROL
Optimal low thrust trajectories for planetary capture
[AD-A202604] N89-22632

DYNAMIC MODELS
Theoretical predictions of turbulent burning velocities of steady and accelerating unconfined turbulent flames with premixed reactants N89-22716
A general non-linear dynamical theory of elastic curved beams N89-22930
A real-time simulator for man-in-the-loop testing of aircraft control systems (SIMTACS-RT)
[AD-A202599] N89-23067
Dynamic model matching for target recognition from a mobile platform N89-23118
Boundaries and probes in electronegative plasmas
[OUEL-1636/86] N89-23293

DYNAMIC RESPONSE
Annealing studies on a fully cured epoxy resin: Effect of thermal prehistory, and time and temperature of annealing
[AD-A205875] N89-22769
Influence of different types of seals on the stability behavior of turbopumps N89-22902
A 3-dimensional finite-difference method for calculating the dynamic coefficients of seals N89-22903
Incorporating general race and housing flexibility and deadband in rolling element bearing analysis N89-22912
Structural dynamics branch research and accomplishments for FY 1988
[NASA-TM-101406] N89-22939

DYNAMIC STABILITY
Rotordynamic Instability Problems in High-Performance Turbomachinery, 1988
[NASA-CP-3026] N89-22891
Influence of different types of seals on the stability behavior of turbopumps N89-22902

DYNAMIC STRUCTURAL ANALYSIS
Structural dynamics branch research and accomplishments for FY 1988
[NASA-TM-101406] N89-22939
Using Patran and Supertab as pre- and postprocessors to COSMIC/NASTRAN N89-22942
Power flows and Mechanical Intensities in structural finite element analysis N89-22952
An experimental and analytical synthesis of controlled structure design
[DE89-006506] N89-22957
A study of high strain rate generation of adiabatic shear bands in a titanium alloy N89-22967
Parallel processors and nonlinear structural dynamics algorithms and software
[NASA-CR-184938] N89-23154
DYNAMICAL SYSTEMS
Expert systems for real-time monitoring and fault diagnosis
[NASA-CR-179441] N89-23209
On Hausdorff dimension of invariant manifolds of infinite-dimensional dynamic systems
[DE88-705628] N89-23227
Input-output decoupling with stability for Hamiltonian systems
[MEMO-722] N89-23239
Model matching for linear Hamiltonian systems
[MEMO-730] N89-23243
Local BRST invariance and the dynamical origin of the BRST condition
[NIKHEF-H/88-15] N89-23358

E

EARTH ATMOSPHERE
Monte Carlo applied to resonance scattering of high altitude fluorescent radiation
[DE89-006519] N89-23035
EARTH ENVIRONMENT
Earth system science: A program for global change
[NASA-TM-101186] N89-22969
EARTH IONOSPHERE
Design of an ELF/VLF satellite for under the ice submarine communications
[AD-A202607] N89-22639
Ionospheric scintillation studies
[AD-A205210] N89-23034
EARTH MAGNETOSPHERE
Optical studies of the magnetospheric cusp from Svalbard
[AD-A205432] N89-23044
EARTH OBSERVING SYSTEM (EOS)
Remote sensing information sciences research group: Browse in the EOS era
[NASA-CR-184637] N89-22979
EARTH ORBITAL ENVIRONMENTS
Orbital debris environment for spacecraft designed to operate in low Earth orbit
[NASA-TM-100471] N89-22638
In-space technology development: Atomic oxygen and orbital debris effects
[NASA-TM-102154] N89-22682
EARTH SURFACE
Remote sensing of earth terrain
[NASA-CR-184937] N89-22971
Surface flux parameterization schemes: Developments and experiences at KNMI — Earth surface
[KNMI-WR-88-06] N89-23055
Image understanding research at SRI International N89-23080
EARTH-MOON TRAJECTORIES
Optimal low thrust trajectories for planetary capture
[AD-A202604] N89-22632
EAST GERMANY
Germany: Focus on Scientific and Technical Information, volume 4, number 1, April 1988
[AD-A204054] N89-23376
ECONOMICS
Progress in crystalline silicon research
[DE89-007423] N89-22749
EDDY CURRENTS
Experimental verification of an eddy-current bearing N89-22913
Multifrequency eddy current testing, optimization of the method for steam generator testing. Phase 2: Nonlinear description of signal location curves dynamics of the signal location curves
[REPT-880142-TW] N89-22933
EDDY VISCOSITY
The length scale for sub-grid-scale parameterization with anisotropic resolution N89-22818
Renormalization group analysis of turbulence N89-22821
EDGES
Modal driven edge detection N89-23163
Texture edge localization N89-23176
EIGENVALUES
Semilinear elliptic eigenvalue problems
[ETN-89-94142] N89-23232
A divide and conquer method for unitary and orthogonal eigenproblems
[AD-A205433] N89-23255
EIGENVECTORS
Semilinear elliptic eigenvalue problems
[ETN-89-94142] N89-23232
A divide and conquer method for unitary and orthogonal eigenproblems
[AD-A205433] N89-23255
EL NINO
On the physical causes of ENSO events and the ITCZ's extreme latitudinal displacements
[DE88-705654] N89-23050
ELASTIC BARS
A general non-linear dynamical theory of elastic curved beams N89-22930
ELASTIC DEFORMATION
Compression and shear wave propagation in explosives
[AD-A205917] N89-22865
ELASTIC PLATES
On the semi-elliptical surface crack problem: Detailed numerical solutions for complete elastic stress fields
[FFA-TN-1988-74] N89-22965
ELASTIC WAVES
Direct simulation of compressible reacting flows N89-22828
Compression and shear wave propagation in explosives
[AD-A205917] N89-22865
ELASTOMERS
Reactions of inorganic high polymers as a route to tailored solids
[AD-A204602] N89-22750
ELECTRIC BATTERIES
Assessment of EV batteries and application to R and D planning
[DE89-009720] N89-22811
Evaluation of several state-of-charge algorithms
[DE89-009752] N89-22812
A survey of advanced battery systems for space applications N89-22986
Novel nitrogen-based organosulfur electrodes for advanced intermediate temperature batteries N89-22987
Multi-mission Ni-H2 battery cell for the 1990's N89-23006
Advanced high-temperature batteries N89-23010
Advances in ambient temperature secondary lithium cells N89-23011
ELECTRIC CHARGE
Nickel-hydrogen capacity loss on storage N89-23007
ELECTRIC CONDUCTORS
Double sided circuit board and a method for its manufacture
[DE89-009601] N89-22809
Monolithic Solid Oxide Fuel Cell development N89-22989
ELECTRIC CURRENT
Current and thermal noise in mixed Na/Ag beta alumina
[AD-A205869] N89-22816
Evaluation, development, and characterization of superconducting materials for space application
[NASA-CR-184842] N89-23302
ELECTRIC DISCHARGES
Lightweight fibrous nickel electrodes for nickel-hydrogen batteries
[NASA-TM-101997] N89-22710
A new concept for high-cycle-life LEO: Rechargeable MnO2-hydrogen N89-22991
ELECTRIC ENERGY STORAGE
Nickel-hydrogen capacity loss on storage N89-23007
Technology base research project for electrochemical energy storage
[DE89-008860] N89-23019
ELECTRIC GENERATORS
Rotor instability due to a gear coupling connected to a bearingless sun wheel of a planetary gear N89-22893
Superconductivity for electric power systems: Building toward our future
[DE89-000874] N89-23332
Comparison of solar photovoltaic and nuclear reactor power systems for a human-tended lunar observatory
[NASA-TM-102015] N89-23397
ELECTRIC HYBRID VEHICLES
Assessment of EV batteries and application to R and D planning
[DE89-009720] N89-22811
Advanced batteries for electric vehicles
[DE89-009771] N89-22813
ELECTRIC MOTOR VEHICLES
Advanced batteries for electric vehicles
[DE89-009771] N89-22813
Laboratory evaluation of advanced battery technologies for electric vehicle applications
[DE89-009810] N89-22814
ELECTRIC POTENTIAL
An electroviscous damper N89-22898
ELECTRIC POWER SUPPLIES
Superconductivity for electric power systems: Building toward our future
[DE89-000874] N89-23332
ELECTRIC PROPULSION
Center for Advanced Space Propulsion (CASP)
[NASA-CR-184936] N89-23404
ELECTRIC SWITCHES
Development of behaviorist models to simulate commuted power switches
[ISAL-88-0065] N89-22815
Development and simulation study of a new inverse-pinch high Coulomb transfer switch
[NASA-CR-181768] N89-23300
ELECTRICAL GROUNDING
ELF communications system terminal grounds seasonal variation pilot study
[AD-A205900] N89-22806
ELECTRICAL MEASUREMENT
ELF communications system terminal grounds seasonal variation pilot study
[AD-A205900] N89-22806
ELECTRICAL PROPERTIES
Finite element analysis of a micromechanical deformable mirror device N89-22953
Acoustic wave device using plate modes with surface-parallel displacement
[DE89-009719] N89-23273
Processing and electrical properties of high-T sub c superconductors
[DE89-009852] N89-23342
ELECTRICAL RESISTIVITY
Current and thermal noise in mixed Na/Ag beta alumina
[AD-A205869] N89-22816
Oxygen electrodes for rechargeable alkaline fuel cells N89-22998
Seafloor temperature and conductivity data from coastal waters of the US Beaufort Sea
[AD-A205428] N89-23059
ELECTRO-OPTICS
Model calculations of the electron-optical properties of compact Faraday cups
[NPL-DMA(A)165] N89-23268
ELECTROCATALYSTS
Space Electrochemical Research and Technology Conference: Abstracts
[NASA-CP-10029] N89-22982
Electrocatalysts for oxygen electrodes in fuel cells and water electrolyzers for space applications N89-22997
Oxygen electrodes for rechargeable alkaline fuel cells N89-22998
Non-noble electrocatalysts for alkaline fuel cells N89-22999
ELECTROCHEMICAL CELLS
Overview of battery usage in NASA/GSFC LEO and GEO missions N89-22983
Novel nitrogen-based organosulfur electrodes for advanced intermediate temperature batteries N89-22987
Structural comparison of nickel electrodes and precursor phases N89-23001
ELECTROCHEMICAL CORROSION
Application of electrochemical noise spectral analysis to the study of the pitting corrosion of aluminum alloys
[ETCA-87-R-102] N89-22744
Corrosion fatigue crack growth: The role of crack-tip deformation and film formation kinetics N89-22966
ELECTROCHEMISTRY
Lightweight fibrous nickel electrodes for nickel-hydrogen batteries
[NASA-TM-101997] N89-22710
Electrochemical technique for rapidly evaluating protective coatings on metals
[PB89-134209] N89-22748
Space Electrochemical Research and Technology Conference: Abstracts
[NASA-CP-10029] N89-22982
The electrochemical generation of useful chemical species from lunar materials N89-22990
Structural comparison of nickel electrodes and precursor phases N89-23001
Advances in ambient temperature secondary lithium cells N89-23011
Fabrication of solid oxide fuel cell by electrochemical vapor deposition
[DE89-009605] N89-23023

ELECTRODE MATERIALS
Electrocatalysts for oxygen electrodes in fuel cells and water electrolyzers for space applications N89-22997
Oxygen electrodes for rechargeable alkaline fuel cells N89-22998
Non-noble electrocatalysts for alkaline fuel cells N89-22999

ELECTRODEPOSITION
Preparation, characterization and performance of MoS3 as an active cathode material
[AD-A205866] N89-22717

ELECTRODES
Lightweight fibrous nickel electrodes for nickel-hydrogen batteries
[NASA-TM-101997] N89-22710
Space Electrochemical Research and Technology Conference: Abstracts
[NASA-CP-10029] N89-22982
Advanced double layer capacitors N89-22993
Electrocatalysts for oxygen electrodes in fuel cells and water electrolyzers for space applications N89-22997
Non-noble electrocatalysts for alkaline fuel cells N89-22999
Corrosion testing of candidates for the alkaline fuel cell cathode N89-23000
Structural comparison of nickel electrodes and precursor phases N89-23001
Impedance studies of Ni/Cd and Ni/H cells using the cell case as reference electrode N89-23002
The application of electrochemical impedance spectroscopy for characterizing the degradation of Ni(OH)2/NiOOH electrodes N89-23003
Advances in lightweight nickel electrode technology N89-23005
Nickel-hydrogen capacity loss on storage N89-23007
Sodium sulfur battery flight experiment definition study N89-23009
Advanced high-temperature batteries N89-23010
Technology base research project for electrochemical energy storage
[DE89-008860] N89-23019

ELECTRODYNAMICS
Design of an ELF/VLF satellite for under the ice submarine communications
[AD-A202607] N89-22639

ELECTROENCEPHALOGRAPHY
A new perspective in the etiology, treatment, prevention and prediction of space motion sickness
[AD-A205660] N89-23065

ELECTROFORMING
Thrust chamber thermal barrier coating techniques N89-22671

ELECTROLYTES
Polymer electrolytes with exclusively cationic conductivity
[DE89-009521] N89-22761
Advanced batteries for electric vehicles
[DE89-009771] N89-22813
Measuring electrode assembly
[DE89-009591] N89-22875
Hydrogen-oxygen proton-exchange membrane fuel cells and electrolyzers N89-22996
The application of electrochemical impedance spectroscopy for characterizing the degradation of Ni(OH)2/NiOOH electrodes N89-23003
Sodium sulfur battery flight experiment definition study N89-23009
Advanced high-temperature batteries N89-23010

ELECTROLYTIC CELLS
Advanced high-temperature batteries N89-23010

ELECTROMAGNETIC COMPATIBILITY
Pre and post modification electromagnetic compatibility test report for the C-130H self contained navigation system with MLS A-kit, revision
[AD-A205167] N89-22604

ELECTROMAGNETIC FIELDS
Computer aided design of three-dimensional waveguide loaded cavities
[DE89-007733] N89-22783
General grid finite difference methods for time dependent electromagnetic problems in two dimensions
[DE89-007225] N89-22788
Calculation of longitudinal and transverse wake-field effects in dielectric structures
[DE89-009814] N89-22798
Finite element modeling of electromagnetic fields and waves using NASTRAN N89-22950

ELECTROMAGNETIC INTERACTIONS
Experimental verification of an eddy-current bearing N89-22913

ELECTROMAGNETIC INTERFERENCE
Electro-impulse de-icing research: Fatigue and electromagnetic interference tests
[DOT/FAA/CT-88/27] N89-22594

ELECTROMAGNETIC NOISE
Current and thermal noise in mixed Na/Ag beta alumina
[AD-A205869] N89-22816

ELECTROMAGNETIC PULSES
The induced current in parallel wires over an imperfect ground from an incident EMP
[DE89-007209] N89-22787
Gamma ray laser pump diagnostic
[AD-A205221] N89-22883

ELECTROMAGNETIC RADIATION
Theoretical investigation of EM wave generation and radiation in the ULF, ELF, and VLF bands by the electrodynamic orbiting tether
[NASA-CR-181560] N89-22780
Effect of pump-induced density depletions on the spectrum of stimulated electromagnetic emissions --- ionosphere
[IRF-PREPRINT-107] N89-22799

ELECTROMAGNETIC WAVE TRANSMISSION
Theoretical investigation of EM wave generation and radiation in the ULF, ELF, and VLF bands by the electrodynamic orbiting tether
[NASA-CR-181560] N89-22780

ELECTROMAGNETISM
Theoretical investigation of EM wave generation and radiation in the ULF, ELF, and VLF bands by the electrodynamic orbiting tether
[NASA-CR-181560] N89-22780
Special techniques used for time domain, three dimensional finite element modeling of electromagnetics
[DE89-007227] N89-22789

ELECTRON ACCELERATORS
Radiation control at the Continuous Electron Beam Accelerator Facility (CEBAF), a new high power CW electron accelerator installation
[CEBAF-PR-89-001] N89-23280

ELECTRON BEAMS
Kinetic studies of the electron-beam-pumped ArF laser
[DE89-004041] N89-22884
Model calculations of the electron-optical properties of compact Faraday cups
[NPL-DMA(A)165] N89-23268
Beam research technical abstracts, 1987
[DE89-009013] N89-23282

ELECTRON DENSITY (CONCENTRATION)
Compact, lightweight CO2 lasers for SDIO applications
[AD-A204300] N89-22882

ELECTRON DISTRIBUTION
Electron energy-loss spectroscopy: Fundamentals and applications in the characterization of minerals
[DE89-006613] N89-23307

ELECTRON EMISSION
Ion-induced kinetic electron emission on clean and gas coated metal surfaces
[JUEL-2201] N89-22732

ELECTRON ENERGY
Kilometric radiation power flux dependence on area of discrete aurora
[NASA-CR-184993] N89-23040
Anomalous cross-field velocities in a CIV laboratory experiment
[TRITA-EPP-88-06] N89-23289
H-Mode transition studies in DIII-D
[DE89-006913] N89-23290

ELECTRON FLUX DENSITY
Ion-induced kinetic electron emission on clean and gas coated metal surfaces
[JUEL-2201] N89-22732

ELECTRON MICROSCOPY
Microstructural studies of IAD and PVD Cr coatings by cross section transmission electron microscopy
[DE89-009877] N89-22739
Transmission electron microscopy: Imaging of materials
[DE89-007418] N89-22870
Electron energy-loss spectroscopy: Fundamentals and applications in the characterization of minerals
[DE89-006613] N89-23307

ELECTRON PARAMAGNETIC RESONANCE
ESE (Electron Spin Echo) and CW-ESR studies of synthetic diamond crystals: Distribution of nitrogen and nickel
[DE89-007373] N89-23314

ELECTRON PRECIPITATION
Parallel Optical Random Access Memory (PORAM)
[NASA-CR-4241] N89-22890

ELECTRON PUMPING
Gamma ray laser pump diagnostic
[AD-A205221] N89-22883

ELECTRON SOURCES
Compact, lightweight CO2 lasers for SDIO applications
[AD-A204300] N89-22882

ELECTRON SPECTROSCOPY
Chemical state depth profiling by Auger signal decomposition: Silicon oxynitride
[DE89-009830] N89-22764
Electron energy-loss spectroscopy: Fundamentals and applications in the characterization of minerals
[DE89-006613] N89-23307

ELECTRON SPIN
ESE (Electron Spin Echo) and CW-ESR studies of synthetic diamond crystals: Distribution of nitrogen and nickel
[DE89-007373] N89-23314

ELECTRON TRAJECTORIES
Electron drift velocity close to a sense wire
[NIKHEF-H/88-5] N89-23277

ELECTRON TUNNELING
Quantum phenomena in mesoscopic superconducting tunnel junctions
[AD-A203354] N89-23305

ELECTRONIC MAIL
PixMail: Pictures through mail
[DE89-009682] N89-22797
TRANSDOC-electronic delivery programme N89-23372

ELEMENTARY PARTICLES
On space-time escape mechanisms
[DE88-705699] N89-23354

ELLIPSOIDS
On the recovery of superellipsoids N89-23168

ELLIPTIC FUNCTIONS
Semilinear elliptic eigenvalue problems
[ETN-89-94142] N89-23232

EMBEDDING
Control of embedded vortices using wall jets
[AD-A202606] N89-22835

EMISSION SPECTRA
Echelle observations of H2 complexes N89-23384

EMITTERS
Parallel Optical Random Access Memory (PORAM)
[NASA-CR-4241] N89-22890

ENDOTHERMIC REACTIONS
Ignition characteristics of the iron-based alloy UNS S66286 in pressurized oxygen
[NASA-CR-183612] N89-22722

ENERGY CONVERSION
Megawatt Class Nuclear Space Power Systems (MCNSPS) conceptual design and evaluation report. Volume 3, technologies 2: Power conversion
[NASA-CR-179614-VOL-3] N89-22980
Technology base research project for electrochemical energy storage
[DE89-008860] N89-23019
Comparison of solar photovoltaic and nuclear reactor power systems for a human-tended lunar observatory
[NASA-TM-102015] N89-23387

ENERGY CONVERSION EFFICIENCY
The NASA Space Solar Cell Advanced Research Program
[NASA-TM-102020] N89-22651
Progress in crystalline silicon research
[DE89-007423] N89-22749
Development of an efficient high brightness Ti:Al2O3 laser amplifier
[AD-A204187] N89-22881
Photovoltaic systems for today's remote power applications
[DE89-007431] N89-23012
Advances in concentrator cell technology
[DE89-007432] N89-23013
Solar thermal program summary. Volume 1: Overview, fiscal year 1988
[DE89-000860] N89-23020
Research on amorphous-silicon-based, thin-film photovoltaic devices, task B
[DE89-000886] N89-23022

ENERGY DISSIPATION
An experimental study of turbulent mixing of viscoelastic fluids
[ETN-89-94140] N89-22847
Research on amorphous-silicon-based, thin-film photovoltaic devices, task B
[DE89-000885] N89-23021
Measurements of optical loss in transparent solids using a novel spectrometer based on optical cavity decay
[DE89-009900] N89-23286
Electron energy-loss spectroscopy: Fundamentals and applications in the characterization of minerals
[DE89-006613] N89-23307

ENERGY GAPS (SOLID STATE)
Band structure of CdTe-ZnTe superlattice
[DE88-705682] N89-23321

ENERGY STORAGE
Space Electrochemical Research and Technology Conference: Abstracts
[NASA-CP-10029] N89-22982

Solar radiation at the earth's surface: What are we doing to it and with it?
[DE89-008446] N89-23018
ENERGY TRANSFER
Analysis of turbulence structures in shear flows N89-22826
Power flows and Mechanical Intensities in structural finite element analysis N89-22952
Design considerations for heat-pipe solar receivers
[DE89-004037] N89-23017
Gravity wave and turbulence studies using a high-resolution ST radar
[AD-A205592] N89-23046
ENGINE DESIGN
Technical evaluation report N89-22655
ENGINE PARTS
Monolithic and fiber ceramic components for turboengines and rockets N89-22657
Basic program for the development of a reliable high strength construction ceramic mode of SiC
[MTU-TB-87/927] N89-22757
Implementation of active magnetic bearings on advanced rocket engine turbopumps
[ETN-89-94365] N89-22929
ENGINE TESTS
The demonstration of monolithic and composite ceramics in aircraft gas turbine combustors N89-22665
Initial results of tests on metal-ceramic guide vanes N89-22668
The spectral analysis of an aero-engine assembly incorporating a squeeze-film damper N89-22895
ENGINES
The spectral analysis of an aero-engine assembly incorporating a squeeze-film damper N89-22895
ENVIRONMENTAL MONITORING
The new experimental areas oxygen monitor
[DE89-009700] N89-22876
ENVIRONMENTAL SURVEYS
Investigation on long time dispersion and washout factor. Vegetation contamination computation with meteorological whole year or summer statistics
[JUEL-SPEZ-449] N89-23028
EPOXY COMPOUNDS
Low-density foams from macroporous epoxy gels
[DE89-004042] N89-22756
EPOXY MATRIX COMPOSITES
Influence of conditioning on the trapezoidal fatigue behavior of a carbon epoxy composite
[ETCA-87-R-052] N89-22700
Ultrasonic detection of damage in carbon epoxy composite materials
[ONERA-RT-3/7256-RY-071-R] N89-22705
Damage development, property degradation and life prediction in composite laminates N89-22708
Glass transition temperature of the M10 resin associated to carbon, Kevlar or glass fibers
[ETCA-87-R-022] N89-22766
EPOXY RESINS
Low-density foams from macroporous epoxy gels
[DE89-004042] N89-22756
Annealing studies on a fully cured epoxy resin: Effect of thermal prehistory, and time and temperature of annealing
[AD-A205875] N89-22769
EQUATIONS OF MOTION
On the numerical integration of viscoelastic flow equations
[DE89-007135] N89-22844
A theoretical study of fluid forces on a centrifugal impeller rotating and whirling in a vaned diffuser N89-22908
Dynamics of particles in the bending waves of the planetary rings
[DE88-705714] N89-23396
EQUATIONS OF STATE
Compression and shear wave propagation in explosives
[AD-A205917] N89-22865
EQUILIBRIUM EQUATIONS
Ab initio calculations of ordered intermetallic phase equilibria
[DE89-009974] N89-22741
EQUILIBRIUM FLOW
Multigrid for the steady-state incompressible Navier-Stokes equation: A survey
[GMD-322] N89-22845
EQUIPMENT SPECIFICATIONS
Project Radioastron N89-22623
ERROR ANALYSIS
Evaluation of quantization error in computer vision N89-23138
Qualitative versus quantitative depth and shape from stereo N89-23144
Curved surface reconstruction using stereo correspondence N89-23147
Approximate Bayesian methods for nonlinear measurement error models
[DE89-009224] N89-23233
ERROR FUNCTIONS
The concept of an effective viewpoint N89-23131
ERRORS
Improvements to the CONTINUE feature in transient analysis N89-22949
ERS-1 (ESA SATELLITE)
Development of a satellite SAR image spectra and altimeter wave height data assimilation system for ERS-1
[NASA-CR-182685] N89-22975
Theoretical studies for ERS-1 wave mode, volume 1
[GEC-MTR-87/110-VOL-1] N89-22977
ESA SATELLITES
Study of a DRS experimental payload for single and multiple access at S band: Executive summary
[PSD86/00017] N89-22648
PSDE/SAT-2: Communication system architecture study, executive summary
[ESA-CR(P)-2732] N89-22802
ESCAPE SYSTEMS
Testing of a new recovery parachute system for the F111 aircraft crew escape module: An update
[DE89-007139] N89-22592
ETHYL COMPOUNDS
Inhalation developmental toxicology studies: Teratology study of methyl ethyl ketone in mice
[DE89-009563] N89-23062
ETIOLOGY
A new perspective in the etiology, treatment, prevention and prediction of space motion sickness
[AD-A205660] N89-23065
EULER EQUATIONS OF MOTION
Compressible Euler solution around a wing canard sting configuration
[FFA-TN-1988-62] N89-22578
The influence of the leading edge geometry on the wave drag for a 65 degree delta wing at low supersonic speed and small angles of attack
[FFA-141] N89-22583
A flux splitting method for hyperbolic systems: Application to the solution of the Euler equations
[CERT-RF-1/3290/DERI] N89-22854
EUROPEAN AIRBUS
Development and testing of critical components for technological preparation of an Airbus-CFRP-fuselage, phase 2
[MBB-UT-129/87] N89-22600
EUROPEAN SPACE PROGRAMS
Ariane 5 Transfer Vehicle (ATV)
[REPT-OX-1-005] N89-22645
ATV: Ariane 5 transfer vehicle study
[STF/E-39-005/CB] N89-22646
EUROPIUM
Emission properties of europium-doped lanthanum and lutetium orthophosphate crystals for use in high temperature sensor applications
[DE89-008736] N89-23334
EVAPORATIVE COOLING
Simulation of a refrigerant evaporator
[ETN-89-94133] N89-22776
EVAPORATORS
Simulation of a refrigerant evaporator
[ETN-89-94133] N89-22776
EXCITATION
An electroviscous damper N89-22898
EXERCISE PHYSIOLOGY
Acclimatization to cold in humans
[NASA-TM-101012] N89-23061
EXHAUST EMISSION
Investigation of low NOx staged combustor concept in high-speed civil transport engines
[NASA-TM-101977] N89-22606
EXHAUST NOZZLES
Rectangular nozzle plume velocity modeling for use in jet noise prediction
[NASA-TM-102047] N89-22577
EXHAUST VELOCITY
Rectangular nozzle plume velocity modeling for use in jet noise prediction
[NASA-TM-102047] N89-22577
EXOBIOLOGY
Mini Protein Crystallization Facility (MPCF), phase A study: Executive summary
[ESA-CR(P)-2709] N89-22775
EXPANSION
Velocity measurements downstream of a sudden expansion using LDV. Part 2: Experimental results
[FOA-C-20736-2.1-PT-2] N89-22849
Dynamic fracture in solids
[PB89-112650] N89-22937
EXPECTANCY HYPOTHESIS
On the expected number of assignments in reduced matrices for the linear assignment problem
[MEMO-728] N89-23263
EXPERIMENT DESIGN
The low-speed wind tunnel at DVFLR in Brunswick (Fed. Republic of Germany)
[DFVLR-MITT-88-25] N89-22619
Mini Protein Crystallization Facility (MPCF), phase A study: Executive summary
[ESA-CR(P)-2709] N89-22775
Asymptotically optimal nonparametric experimental design tests for the log linear model under censoring
[MEMO-727] N89-23262
EXPERT SYSTEMS
MIT progress in understanding images N89-23075
Image understanding research at the University of Maryland, December 1986 - January 1988 N89-23078
Summary of image understanding research at the University of Massachusetts N89-23081
Progress in image understanding at the University of Rochester N89-23082
Qualitative reasoning and modeling for robust target tracking and recognition from a mobile platform N89-23086
Knowledge based vision for terrestrial robots N89-23087
Algorithms and architectures for smart sensing N89-23090
Using flow field divergence for obstacle avoidance in visual navigation N89-23120
Core knowledge system: Storage and retrieval of inconsistent information N89-23132
Consensus theory in expert systems: An adaptive inference framework and application to image understanding
[AD-A204253] N89-23188
Expert systems on multiprocessor architectures, phase 1
[AD-A204907] N89-23206
Expert systems for real-time monitoring and fault diagnosis
[NASA-CR-179441] N89-23209
Contributions of expert systems to logistics
[REPT-882-320-101] N89-23223
Center for Advanced Space Propulsion (CASP)
[NASA-CR-184936] N89-23404
EXPLOSIONS
Numerical simulation of blast waves
[REPT-882-320-102] N89-22858
EXPOSURE
Environmental program on durability of graphite/epoxy honeycomb specimens with representative damage and repairs
[AR-005-504] N89-22685
EXTERNAL STORES
Prediction of loads on wing/body/external store/fins pylon-configurations at transonic speeds
[FFA-TN-1988-44] N89-22602
EXTRATERRESTRIAL RADIATION
The NASA Space Solar Cell Advanced Research Program
[NASA-TM-102020] N89-22651
EXTREME ULTRAVIOLET RADIATION
Studies of hot white dwarfs and instrumentation for stellar extreme ultraviolet astronomy N89-23383
EXTREMELY LOW FREQUENCIES
Design of an ELF/VLF satellite for under the ice submarine communications
[AD-A202607] N89-22639
ELF communications system terminal grounds seasonal variation pilot study
[AD-A205900] N89-22806
EYE MOVEMENTS
Progress in image understanding at the University of Rochester N89-23082
EYE PROTECTION
Unity vision block with focal plane
[AD-A204894] N89-23283

F

FABRICATION
Alumina reinforced tetragonal zirconia (TZP) composites
[DE89-008880] N89-22690
Diagnostics of glow discharges used to produce hydrogenated amorphous silicon films
[DE89-000887] N89-22760
Development of advanced heat pump. Part 2: Preliminary test of two-stage compression heat pump
[DE88-756838] N89-22841
Processing and electrical properties of high-T sub c superconductors
[DE89-009852] N89-23342

FABRY-PEROT INTERFEROMETERS
Machine reference mirror inspection by optical Fabry-Perot cavity testing
[DE89-009635] N89-23264
FACTORIZATION
Factoring very large numbers using a massively parallel computer
[DE89-008198] N89-23208
FAILURE
Fiber matrix interface effects in failure of ceramic matrix fiber composites
[AD-A204618] N89-22686
FAILURE ANALYSIS
Damage initiation in two-dimensional, woven, carbon-carbon composites
[AD-A202617] N89-22683
KOH concentration effect on the cycle life of nickel-hydrogen cells. 4: Results of failure analyse N89-23004
FALLOUT
Investigation on long time dispersion and washout factor. Vegetation contamination computation with meteorological whole year or summer statistics
[JUEL-SPEZ-449] N89-23028
FAR INFRARED RADIATION
Radiation hardened detector arrays for the far and extreme infrared, phase 1
[BF-R-65.895-10] N89-23347
Far infrared peculiar behavior of quasars
[DE88-705673] N89-23391
FARADAY EFFECT
Model calculations of the electron-optical properties of compact Faraday cups
[NPL-DMA(A)165] N89-23268
FATIGUE (MATERIALS)
Corrosion fatigue crack growth: The role of crack-tip deformation and film formation kinetics N89-22966
FATIGUE LIFE
Fatigue evaluation of WTS-3 wind turbine blade and retention
[FFA-TN-1987-81] N89-22618
Damage tolerance concepts for advanced materials and engines N89-22661
Thrust chamber thermal barrier coating techniques N89-22671
Fiber reinforced superalloys for rocket engines N89-22673
Cryogenic turbopump bearing materials N89-22678
The isothermal fatigue behavior of a unidirectional SiC/Ti composite and the Ti alloy matrix
[NASA-TM-101984] N89-22684
Damage development, property degradation and life prediction in composite laminates N89-22708
Transmission overhaul and replacement predictions using Weibull and renewal theory
[NASA-TM-102022] N89-22925
FATIGUE TESTS
Electro-impulse de-icing research: Fatigue and electromagnetic interference tests
[DOT/FAA/CT-88/27] N89-22594
Influence of conditioning on the trapezoidal fatigue behavior of a carbon epoxy composite
[ETCA-87-R-052] N89-22700
FAULT TOLERANCE
Self calibration of motion and stereo vision for mobile robot navigation N89-23106
Expert systems for real-time monitoring and fault diagnosis
[NASA-CR-179441] N89-23209
FAULT TREES
Techniques for applying sets code procedures to large fault trees in PRA (Probabilistic Risk Assessment) analysis
[DE89-004823] N89-23261
FEASIBILITY ANALYSIS
Technical feasibility study on the development of ceramic thermoelectric conversion, part 2
[DE88-756481] N89-22755
Transitional strategic defense architectures
[DE89-008312] N89-23265
FEEDBACK
Perception with feedback N89-23098
FEEDBACK CONTROL
Active vibration control for flexible rotor by optimal direct-output feedback control
[NASA-TM-101972] N89-22605
Single channel test controllers
[AD-A204088] N89-22611
Microcomputer based controller for the Langley 0.3-meter Transonic Cryogenic Tunnel
[NASA-CR-181808] N89-22616
Piezoelectric pushers for active vibration control of rotating machinery N89-22896
A recursive formulation for flexible multibody dynamics N89-22968
On the stabilization of bilinear systems via constant feedback
[MEMO-706] N89-23215
The local disturbance decoupling problem with stability for nonlinear systems
[MEMO-721] N89-23217
Robust stabilization of an inverted double pendulum system via a polynomial approach to H(infinity) optimal control
[MEMO-742] N89-23220
Some local results for linear systems and implications for state variable feedback
[MATHS-RES-202] N89-23221
Model matching for linear Hamiltonian systems
[MEMO-730] N89-23243
FERMIONS
Quantum theory of a massless spinning particle
[NIKHEF-H/88-7] N89-23357
FERROMAGNETIC MATERIALS
The half-metallic ferromagnetic NiMnSb: A positron-annihilation study
[ECN-209] N89-23269
FIBER COMPOSITES
Composite material systems for high temperature applications N89-22666
Fiber reinforced superalloys for rocket engines N89-22673
High-performance refractory composite materials N89-22675
Fiber matrix interface effects in failure of ceramic matrix fiber composites
[AD-A204618] N89-22686
New theoretical model of stress transfer between fibre and matrix in a uniaxially fibre reinforced composite
[NPL-DMA(A)168] N89-22691
Filament winding manufacturing of long fiber composite materials in thermoplastic matrix
[ETCA-87-R-047] N89-22699
FIBER OPTICS
Fiber optic laser rod
[DE89-009598] N89-22887
Design of a lightweight, low-cost geophysical survey vehicle
[DE89-009383] N89-22926
Activities report of the Division of Optical Technology (FOA 33)
[FOA-C-30507-3.1] N89-23287
Study of long optical fibers
[ESA-CR(P)-2723] N89-23288
FIBER ORIENTATION
Dynamic behavior of a carbon epoxy composite
[ETCA-87-R-001] N89-22701
Improving hole boring yield in carbon epoxy composites with tensile loading
[REPT-47-324/F] N89-22704
FIBER STRENGTH
Fiber matrix interface effects in failure of ceramic matrix fiber composites
[AD-A204618] N89-22686
FIELD OF VIEW
The concept of an effective viewpoint N89-23131
Labeling polyhedral images N89-23180
FIELD THEORY (PHYSICS)
Improved effective potential in the Einstein metric
[DE88-705716] N89-23355
Generating a hot big bang via a change in topology
[DE89-007561] N89-23388
FILAMENT WINDING
Filament winding manufacturing of long fiber composite materials in thermoplastic matrix
[ETCA-87-R-047] N89-22699
FINANCE
Center for Advanced Space Propulsion (CASP)
[NASA-CR-184936] N89-23404
FINE STRUCTURE
EXAFS studies of multilayer interfaces
[DE89-009527] N89-22694
FINITE DIFFERENCE THEORY
General grid finite difference methods for time dependent electromagnetic problems in two dimensions
[DE89-007225] N89-22788
Direct numerical simulation of compressible free shear flows
[AIAA-89-0374] N89-22827
Numerical simulation of vortex breakdown
[ONERA-RSF-3/4368-AY-502-A] N89-22853
Rotordynamic coefficients for labyrinth seals calculated by means of a finite difference technique N89-22900
A 3-dimensional finite-difference method for calculating the dynamic coefficients of seals N89-22903
Finite difference analysis of rotordynamic seal coefficients for an eccentric shaft position N89-22906
FINITE ELEMENT METHOD
Three-dimensional response of composites
[AD-A204623] N89-22687
Special techniques used for time domain, three dimensional finite element modeling of electromagnetics
[DE89-007227] N89-22789
Incorporating general race and housing flexibility and deadband in rolling element bearing analysis N89-22912
Enhanced rotor modeling tailored for rub dynamic stability analysis and simulation N89-22916
Seventeenth NASTRAN (R) Users' Colloquium
[NASA-CP-3029] N89-22940
Improved performance in NASTRAN (R) N89-22941
Using Patran and Supertab as pre- and postprocessors to COSMIC/NASTRAN N89-22942
The use of COSMIC NASTRAN in an integrated conceptual design environment N89-22944
Finite element modeling of electromagnetic fields and waves using NASTRAN N89-22950
Calculation of low frequency vibrational resonances of submerged structures N89-22951
Power flows and Mechanical Intensities in structural finite element analysis N89-22952
Finite element analysis of a micromechanical deformable mirror device N89-22953
Definition of NASTRAN sets by use of parametric geometry N89-22956
Adaptive contact elements for three-dimensional explicit transient analysis
[DE89-008436] N89-22958
The project ASKA-SPACE, phase 1 — finite element method
[ETN-89-93768] N89-22959
Finite element analysis for calibration curve computation for measurement of crack propagation of ellipse shaped surface cracks
[GKSS-88/E/34] N89-22960
Generalized finite strains, generalized stresses, and a hybrid variational principle for finite-element computer programs using curvilinear coordinates
[DE89-009923] N89-22962
On the semi-elliptical surface crack problem: Detailed numerical solutions for complete elastic stress fields
[FFA-TN-1988-74] N89-22965
Nonlinear finite element simulation of the large angle motion of flexible bodies
[DE89-006505] N89-23230
Numerical solution of the biharmonic equation using different types of bivariate spline functions
[MEMO-734] N89-23247
FINS
Prediction of loads on wing/body/external store/fins pylon-configurations at transonic speeds
[FFA-TN-1988-44] N89-22602
FIXED WINGS
Convergence of discrete-vortex induced-flow calculations by optimum choice of mesh N89-22585
FLAME PROPAGATION
Theoretical predictions of turbulent burning velocities of steady and accelerating unconfined turbulent flames with premixed reactants N89-22716
FLAME STABILITY
Theoretical predictions of turbulent burning velocities of steady and accelerating unconfined turbulent flames with premixed reactants N89-22716
FLASH LAMPS
Development of an efficient high brightness Ti:Al2O3 laser amplifier
[AD-A204187] N89-22881
FLAT SURFACES
Study of grain boundaries in polycrystalline alumina
[ETCA-87-R-130] N89-23344
FLEXIBILITY
Fracture toughness of MgCr2O4-based refractory composites
[DE89-009847] N89-22696
Incorporating general race and housing flexibility and deadband in rolling element bearing analysis N89-22912
FLEXIBLE BODIES
Aerodynamics of nonrigid bodies undergoing large amplitude time-dependent motions N89-22586
A recursive formulation for flexible multibody dynamics N89-22968
Nonlinear finite element simulation of the large angle motion of flexible bodies
[DE89-006505] N89-23230
FLIGHT CHARACTERISTICS
Orbiter Flying Qualities (OFQ) Workstation user's guide
[NASA-CR-179440] N89-22612
FLIGHT CONTROL
Orbiter Flying Qualities (OFQ) Workstation user's guide
[NASA-CR-179440] N89-22612

FLIGHT CREWS
Testing of a new recovery parachute system for the F111 aircraft crew escape module: An update
[DE89-007139] N89-22592
FLIGHT ENVELOPES
Ten year lifetime orbits about the planet Mars
N89-22633
FLIGHT HAZARDS
Hazard index calculation for 31 May 1964 microburst at Erie, Colorado
[NASA-CR-184968] N89-23048
FLIGHT SAFETY
Safe skies for tomorrow: Aviation safety in a competitive environment
[PB89-114318] N89-22591
National airspace system plan: Facilities, equipment, associated development and other capital needs
[AD-A202615] N89-22596
FLIGHT SIMULATION
Orbiter Flying Qualities (OFQ) Workstation user's guide
[NASA-CR-179440] N89-22612
Electrodynamic transient tests — satellites
[CNES-CT/DRT/TVE/SM-024] N89-22644
A real-time simulator for man-in-the-loop testing of aircraft control systems (SIMTACS-RT)
[AD-A202599] N89-23067
FLIGHT TESTS
NASA's program on icing research and technology
[NASA-TM-101989] N89-22569
An in-flight investigation of workload assessment techniques for civil aircraft operations
[NLR-TR-87119-U] N89-23070
FLOTATION
Innovation in separation technology for fine gravity semi-products
[PB89-112478] N89-22719
FLOW CHARACTERISTICS
Two-phase flow characteristic of inverted bubbly, slug and annular flow in post-critical heat flux region
[DE89-007384] N89-22839
FLOW DISTORTION
Hardware and operating features of the adaptive wall test section for the 0.3-meter transonic cryogenic tunnel
[NASA-TM-4114] N89-22614
FLOW DISTRIBUTION
Unsteady aerodynamic computational method of non-coplanar wing-tail combinations in subsonic flow
[PB89-111470] N89-22571
Transonic and supersonic flow past a 65 deg delta wing with rounded leading edges: Analysis of experimental data
[DFVLR-FB-88-44] N89-22580
Flow over a leading edge with distributed roughness
[DFVLR-FB-88-45] N89-22581
Sidewall boundary layer study, with and without suction, for the 150 mm chord CAST 7 airfoil at the T2 wind tunnel N89-22584
Convergence of discrete-vortex induced-flow calculations by optimum choice of mesh N89-22585
Aerodynamic detuning of a loaded airfoil cascade in an incompressible flow by a locally analytical method
N89-22588
Computational investigation of incompressible airfoil flows at high angles of attack
[AD-A205885] N89-22590
LDV measurements and investigation of flow field through radial turbine guide vanes N89-22609
Hardware and operating features of the adaptive wall test section for the 0.3-meter transonic cryogenic tunnel
[NASA-TM-4114] N89-22614
Two-phase flow characteristic of inverted bubbly, slug and annular flow in post-critical heat flux region
[DE89-007384] N89-22839
A vortex panel analysis of circular-arc bluff-bodies in unsteady flow
[DE89-007141] N89-22845
A generalized one-dimensional computer code for turbomachinery cooling passage flow calculations
[NASA-TM-102079] N89-22862
FLOW EQUATIONS
Second-order accurate nonoscillatory schemes for scalar conservation laws
[NASA-TM-102010] N89-22573
Lectures in Fluid Physics held at the Physics Department of the Georg-August-University. Volume 1: Source Strength of Vorticity
[DFVLR-MITT-88-26-VOL-1] N89-22855
Compression and shear wave propagation in explosives
[AD-A205917] N89-22865
FLOW GEOMETRY
Cavitation in a submerged jet at constant pressure
[OUEL-1658/86] N89-22848
Theoretical study of the unsteady flow in a straight channel with variable and constant cross section
[VKI-TN-168] N89-22857
FLOW MEASUREMENT
LDV measurements and investigation of flow field through radial turbine guide vanes N89-22609
Implementation of a two-component laser anemometer at the T2 wind tunnel
[A-501-H] N89-22879
FLOW STABILITY
Annual research briefs, 1988
[NASA-CR-184906] N89-22817
Low-dimensional chaos in turbulence N89-22822
The effects of stabilizing and destabilizing longitudinal curvature on the structure of turbulent, two-stream mixing layers N89-22833
Non-linear evolution of a second mode wave in supersonic boundary layers
[NASA-CR-181811] N89-22836
Inviscid spatial stability of a compressible mixing layer. Part 2: The flame sheet model
[NASA-CR-181815] N89-22837
Application of the Single-Axis-rate-Table (SAT) of the DFVLR for the evaluation of stationary and dynamic gyro properties
[ESA-TT-1122] N89-22877
FLOW THEORY
The effect of thermocapillary flow on weld-pool profile
[NPL-DMA(A)167] N89-22927
FLOW VELOCITY
LDV measurements and investigation of flow field through radial turbine guide vanes N89-22609
Velocity measurements downstream of a sudden expansion using LDV. Part 2: Experimental results
[FOA-C-20736-2.1-PT-2] N89-22849
Implementation of a two-component laser anemometer at the T2 wind tunnel
[A-501-H] N89-22879
Role of circumferential flow in the stability of fluid-handling machine rotors N89-22915
FLOW VISUALIZATION
Combustor flow visualization using innovative infrared thermographics techniques
[AD-A205905] N89-22718
FLUERICS
Developing software to use parallel processing effectively
[AD-A205184] N89-23192
FLUID DYNAMICS
AGARD highlights 88/2 N89-23403
FLUID FLOW
Experimental and theoretical studies of vertical annular liquid jets
[DE89-009153] N89-22851
Influence of impeller and diffuser geometries on the lateral fluid forces of whirling centrifugal impeller
N89-22907
A theoretical study of fluid forces on a centrifugal impeller rotating and whirling in a vaned diffuser N89-22908
FLUID MANAGEMENT
Analysis of the nonvented fill of a 4.96-cubic-meter lightweight liquid hydrogen tank
[NASA-TM-102039] N89-22652
Center for Advanced Space Propulsion (CASP)
[NASA-CR-184936] N89-23404
FLUORESCENCE
Monte Carlo applied to resonance scattering of high altitude fluorescent radiation
[DE89-006519] N89-23035
Emission properties of europium-doped lanthanum and lutetium orthophosphate crystals for use in high temperature sensor applications
[DE89-006736] N89-23334
FLUTTER
A study of unsteady turbulent flow past airfoils
N89-22587
FLUX DENSITY
Lightweight fibrous nickel electrodes for nickel-hydrogen batteries
[NASA-TM-101997] N89-22710
Compact, lightweight CO2 lasers for SDIO applications
[AD-A204300] N89-22882
Advanced rechargeable sodium batteries with novel cathodes N89-22988
A new concept for high-cycle-life LEO: Rechargeable MnO2-hydrogen N89-22991
Advances in lightweight nickel electrode technology
N89-23005
FLUX QUANTIZATION
A flux splitting method for hyperbolic systems: Application to the solution of the Euler equations
[CERT-RF-1/3290/DERI] N89-22854
FOAMS
Low-density foams from macroporous epoxy gels
[DE89-004042] N89-22756
FOKKER-PLANCK EQUATION
Localization of solutions of a nonlinear Fokker-Planck equation with Dirichlet boundary conditions — soil moisture infiltration
[MEMO-733] N89-23246
FOOTPRINTS
Minimum number of satellites for periodic coverage
[FOA-C-30511-9.4] N89-22976
FORCED CONVECTION
Forced and free convection flow with viscous dissipation effects: The method of parametric differentiation
[DE88-705649] N89-22840
FORCED VIBRATION
Some field experience with subsynchronous vibration of centrifugal compressors N89-22892
FORECASTING
The long-term climate change assessment task of the Hanford Site, Washington, Protective Barrier Development Program
[DE89-008704] N89-23030
FORMALISM
Application of the Ornstein-Zernike formalism to polymer and copolymer blends
[DE88-705686] N89-22753
FORMAT
Ritz method for transient response in systems having unsymmetric stiffness N89-22954
FOURIER TRANSFORMATION
Far- and mid-infrared properties of metal-insulator composite materials
[AD-A204914] N89-22689
Solution of multi-center molecular integrals of Slater-type orbitals
[NASA-TM-101545] N89-22692
The induced current in parallel wires over an imperfect ground from an incident EMP
[DE89-007209] N89-22787
FRACTURE MECHANICS
Internal stresses in ceramic composite constituents determined by neutron diffraction technique
[DE89-009883] N89-22697
Dynamic behavior of a carbon epoxy composite
[ETCA-87-R-001] N89-22701
Mechanical properties and damage mechanisms of carbon fiber reinforced composites: Compression loading
[DFVLR-FB-88-41] N89-22706
Processing and properties of advanced aluminum alloys
[AD-A205187] N89-22725
Assessing hydrogen assisted cracking modes in high strength steel welds
[AD-A205431] N89-22746
Internal debonding of solid rocket fuel: An experimental investigation
[AD-A205903] N89-22772
The Hertzian cone crack: Theoretical, numerical and experimental studies
[OUEL-1743/88] N89-22961
Recent advances in modeling creep crack growth
[W-2/88] N89-22964
FRACTURE STRENGTH
Alumina reinforced tetragonal zirconia (TZP) composites
[DE89-008880] N89-22690
Observations on the toughening of Al2O3-SiC composites
[DE89-009843] N89-22695
Fracture toughness of MgCr2O4-based refractory composites
[DE89-009847] N89-22696
Hydrogen embrittlement study and positron annihilation response of hydrogen in aisi 4340 steel N89-22720
Processing and properties of advanced aluminum alloys
[AD-A205187] N89-22725
Fracture toughness and mechanical behavior of steel and aluminum alloys
[ETCA-87-R-090] N89-22743
Environmentally induced discontinuities in transparent polymers
[AD-A205483] N89-22768
FRACTURES (MATERIALS)
Processing and properties of advanced aluminum alloys
[AD-A205187] N89-22725
Dynamic fracture in solids
[PB89-112650] N89-22937
FRACTURING
Hydrogen embrittlement study and positron annihilation response of hydrogen in aisi 4340 steel N89-22720
Hydrogen embrittlement in nickel-hydrogen cells
N89-23008
FREE CONVECTION
Direct numerical simulations of turbulent convection with a variable gravity and Keplerian rotation N89-22831

Forced and free convection flow with viscous dissipation effects: The method of parametric differentiation
[DE88-705649] N89-22840

FREE ELECTRON LASERS
Magnetic axis alignment and the Poisson alignment reference system
[DE89-007687] N89-22880
On the small-signal gain of free-electron lasers in the low-current region
[ESA-TT-1120] N89-22889
Beam research technical abstracts, 1987
[DE89-009013] N89-23282

FREE FLOW
Direct numerical simulation of compressible free shear flows
[AIAA-89-0374] N89-22627

FREQUENCY DISTRIBUTION
Reports from the German Meteorological Service. No. 177: Small-scale variability of solar radiation
[ISBN-3-88148-224-X] N89-23053

FREQUENCY STABILITY
Magnetic bearing stiffness control using frequency band filtering N89-22910

FRICTION
Effects of lubrication on the performance of high speed spur gears
[NASA-TM-101969] N89-22919

FRICTION REDUCTION
Tribological characterization of 15 surface treatments for aluminum alloys
[ETCA-87-R-132] N89-22928

FROUDE NUMBER
Experimental and theoretical studies of vertical annular liquid jets
[DE89-009153] N89-22851

FUEL CELLS
Monolithic Solid Oxide Fuel Cell development N89-22989
The application of Dow Chemical's perfluorinated membranes in proton-exchange membrane fuel cells N89-22995
Electrocatalysts for oxygen electrodes in fuel cells and water electrolyzers for space applications N89-22997
Non-noble electrocatalysts for alkaline fuel cells N89-22999
Corrosion testing of candidates for the alkaline fuel cell cathode N89-23000
Technology base research project for electrochemical energy storage
[DE89-008860] N89-23019
Fabrication of solid oxide fuel cell by electrochemical vapor deposition
[DE89-009605] N89-23023
Solid oxide fuel cell matrix and modules
[DE89-009607] N89-23024

FUEL CONSUMPTION
Ceramic heat exchangers and turbine blades: Theory and experimental results N89-22677
Methods for heat transfer and temperature field analysis of the insulated diesel, phase 3
[NASA-CR-182237] N89-23382

FUNCTIONAL DESIGN SPECIFICATIONS
Surface temperature measurements using a thin film thermal array
[NASA-TM-101549] N89-22868
The new experimental areas oxygen monitor
[DE89-009700] N89-22876
Monolithic Solid Oxide Fuel Cell development N89-22989

FURNACES
Advanced cartridge technology: Executive summary — spacecraft furnaces
[SEP-TS/F-6972/88-RP] N89-22636

FUSELAGES
Development and testing of critical components for technological preparation of an Airbus-CFRP-fuselage, phase 2
[MBB-UT-129/87] N89-22600

FUSION REACTORS
Variational analysis of railgun plasma-arc-armature for acceleration of solid hydrogen pellets for fusion reactor refueling
[DE89-009556] N89-22634

FUZZY SYSTEMS
Some methods for uncertain reasoning
[FOA-C-30492-3.3] N89-23212

G

GALACTIC COSMIC RAYS
Astronaut radiation exposure in low-earth orbit. Part 1: Galactic cosmic radiation
[AD-A204598] N89-23063
Equations of cosmic-ray transport with distributed acceleration
[AD-A204599] N89-23401

GALACTIC EVOLUTION
Topics in gravitational theory N89-23042
Optical and infrared observations of the nature and evolution of active galaxies N89-23395

GALACTIC MASS
Observational aspects of interacting galaxies N89-23385

GALACTIC RADIATION
Observational aspects of interacting galaxies N89-23385

GALACTIC STRUCTURE
Dark matter candidates
[DE89-006579] N89-23387

GALAXIES
Topics in gravitational theory N89-23042

GALERKIN METHOD
On the numerical integration of viscoelastic flow equations
[DE89-007135] N89-22844
Application of the Single-Axis-rate-Table (SAT) of the DFVLR for the evaluation of stationary and dynamic gyro properties
[ESA-TT-1122] N89-22877

GALLIUM ARSENIDES
The NASA Space Solar Cell Advanced Research Program
[NASA-TM-102020] N89-22651
Development of magnetic field assisted melt stabilization with heat and mass transfer control in low pressure LEC growth of GaAs
[AD-A205185] N89-23313
Experimental investigation of hot electron and related effects in gallium (aluminum) arsenide devices
[AD-A205442] N89-23349

GAME THEORY
Relationships between the prenucleolus, ENSC-solution and related solution concepts for cooperative games
[MEMO-729] N89-23266

GAMMA RAY LASERS
Gamma ray laser pump diagnostic
[AD-A205221] N89-22883

GAMMA RAYS
Gamma ray laser pump diagnostic
[AD-A205221] N89-22883
Observational techniques for solar flare gamma-rays, hard X-rays, and neutrons
[NASA-CR-184910] N89-23399
Thermal Comptonization models for gamma-ray emission from black-hole sources
[DE89-009918] N89-23402

GAS ANALYSIS
Measurement of the total gas content of a liquid
[OUEL-1643/86] N89-22711

GAS CHROMATOGRAPHY
Coupling of a chemiluminescence detector with a gas chromatograph for the selective measurement of oxidized nitrogen bonds in the atmosphere
[JUEL-2217] N89-23029

GAS DENSITY
Determination of the He3 number density for the proportional counter used in the NPL Bonner sphere system
[NPL-RS(EXT)104] N89-23275

GAS DETECTORS
Supersonic particle probes: Measurement of internal wall losses
[AD-A205863] N89-22589

GAS EXCHANGE
Efficacy of conventional and high-frequency ventilation at altitude
[AD-A205922] N89-23071

GAS MIXTURES
Binary and ternary gas mixtures for use in glow discharge closing switches
[DE89-009718] N89-23298

GAS TRANSPORT
Efficacy of conventional and high-frequency ventilation at altitude
[AD-A205922] N89-23071

GAS TUNGSTEN ARC WELDING
A calorimetric-based comparison of gas tungsten and plasma arc welding processes
[DE89-008712] N89-22924

GAS TURBINE ENGINES
Application of advanced materials for turbomachinery and rocket propulsion N89-22656
Monolithic and fiber ceramic components for turboengines and rockets N89-22657
CVD and diffusion coatings for high temperature applications in turbomachinery and rocket motors N89-22658
New metallic materials for gas turbines N89-22660
Damage tolerance concepts for advanced materials and engines N89-22661
Material/manufacturing process interaction in advanced material technologies N89-22662
The demonstration of monolithic and composite ceramics in aircraft gas turbine combustors N89-22665

GAS TURBINES
Ceramic heat exchangers and turbine blades: Theory and experimental results N89-22677
Rotor instability due to a gear coupling connected to a bearingless sun wheel of a planetary gear N89-22893

GAS-SOLID INTERFACES
Ion-induced kinetic electron emission on clean and gas coated metal surfaces
[JUEL-2201] N89-22732

GASTROINTESTINAL SYSTEM
A new perspective in the etiology, treatment, prevention and prediction of space motion sickness
[AD-A205660] N89-23085

GAUGE INVARIANCE
Local BRST invariance and the dynamical origin of the BRST condition
[NIKHEF-H/88-15] N89-23358

GAUGE THEORY
Investigation of the vacuum structure of the Georgi-Glashow model on the lattice
[DE88-705676] N89-23319
Induced quantum conformal gravity
[DE88-705718] N89-23356
Local BRST invariance and the dynamical origin of the BRST condition
[NIKHEF-H/88-15] N89-23358

GEAR TEETH
Effects of lubrication on the performance of high speed spur gears
[NASA-TM-101969] N89-22919
Topology of modified helical gears and Tooth Contact Analysis (TCA) program
[NASA-CR-4224] N89-22920

GEARS
Rotor instability due to a gear coupling connected to a bearingless sun wheel of a planetary gear N89-22893
Topology of modified helical gears and Tooth Contact Analysis (TCA) program
[NASA-CR-4224] N89-22920

GELS
Low-density foams from macroporous epoxy gels
[DE89-004042] N89-22756

GENETIC CODE
Simulation and analysis of physical mapping
[DE89-009399] N89-23198

GENETIC ENGINEERING
New developments in biotechnology: US investment in biotechnology, part 4
[PB88-246939] N89-23060
Simulation and analysis of physical mapping
[DE89-009399] N89-23198

GEODETIC COORDINATES
Geodetic positioning system for flying aircraft (May 1987)
[REPT-013/88] N89-22598

GEODIMETERS
Geodetic positioning system for flying aircraft (May 1987)
[REPT-013/88] N89-22598

GEOGRAPHIC INFORMATION SYSTEMS
Derivation of a large-scale map of heat load in the region Freiburg-Basel (Germany, F.R.) using satellite data. A contribution to the production of bioclimate data based on a geographic information system
[REPT-27] N89-22972
Remote sensing information sciences research group: Browse in the EOS era
[NASA-CR-184637] N89-22979

GEOLOGICAL SURVEYS
Design of a lightweight, low-cost geophysical survey vehicle
[DE89-009383] N89-22926

GEOMAGNETISM
Design of an ELF/VLF satellite for under the ice submarine communications
[AD-A202607] N89-22639

GEOMETRY
Internal debonding of solid rocket fuel: An experimental investigation
[AD-A205903] N89-22772
Using Patran and Supertab as pre- and postprocessors to COSMIC/NASTRAN N89-22942
Definition of NASTRAN sets by use of parametric geometry N89-22956
Using generic geometric and physical models for representing solids N89-23114
The multigroup and cylindrical geometry formulation of the Sn Monte Carlo hybrid method
[DE89-000326] N89-23260

GERMANIUM
A variable temperature cryostat that produces in situ clean-up germanium detector surfaces
[DE89-008174] N89-23328
GERMANIUM ALLOYS
Electronic properties of Ge sub 1-x Si sub x: A simplified tight binding approach
[DE88-705671] N89-23317
Electronic properties of Ge(1-X)Si(X): Alloying versus pressure
[DE88-705678] N89-23320
GET AWAY SPECIALS (STS)
Consortium for materials development in space
[NASA-CR-181405] N89-22773
GLASS
Interfacial adhesion and mechanical properties of polyamide-6/glass bead composites
[ETN-89-94136] N89-22759
Annealing studies on a fully cured epoxy resin: Effect of thermal prehistory, and time and temperature of annealing
[AD-A205875] N89-22769
GLASS ELECTRODES
Measuring electrode assembly
[DE89-009591] N89-22875
GLASS FIBER REINFORCED PLASTICS
Glass transition temperature of the M10 resin associated to carbon, Kevlar or glass fibers
[ETCA-87-R-022] N89-22766
Blade root design: A state of art survey
[FFAP-201] N89-22778
GLASS FIBERS
Composite material systems for high temperature applications N89-22666
GLOBAL POSITIONING SYSTEM
Geodetic positioning system for flying aircraft (May 1987)
[REPT-013/88] N89-22598
GPS terminal: Study of a GPS receiver for Columbus platform elements, executive summary
[GPS-REP-SEL-002] N89-22643
GLOW DISCHARGES
Diagnostics of glow dischargee used to produce hydrogenated amorphous silicon films
[DE89-000887] N89-22760
Binary and ternary gas mixtures for use in glow discharge closing switches
[DE89-009718] N89-23298
GOVERNMENT PROCUREMENT
New developments in biotechnology: US investment in biotechnology, part 4
[PB88-246939] N89-23060
GOVERNMENT/INDUSTRY RELATIONS
New developments in biotechnology: US investment in biotechnology, part 4
[PB88-246939] N89-23060
Analysis of the present knowledge of costs and benefits of the governmental advancement of astronautics
[ETN-89-93770] N89-23359
GRAIN BOUNDARIES
Microstructural studies of IAD and PVD Cr coatings by cross section transmission electron microscopy
[DE89-009877] N89-22739
Physical properties of grain-boundary materials: Comparison of EAM (Embedded-Atom-Method) and central-force potentials
[DE89-007414] N89-23308
Grain-boundary and free-surface induced thermodynamic melting: A molecular dynamics study in silicon
[DE89-007415] N89-23309
Grain boundary sliding phenomena in polycrystalline solids
[DE89-007792] N89-23326
Growth kinetics of grain-boundary induced melting: A molecular-dynamics study
[DE89-009855] N89-23343
Study of grain boundaries in polycrystalline alumina
[ETCA-87-R-130] N89-23344
Study of grain boundaries in polycrystalline alumina. Effect of the manufacturing mode and of the material composition
[ETCA-87-R-100] N89-23345
GRAIN SIZE
Effects of grain size and strain rate on the mechanical response of copper
[DE89-008811] N89-22731
Thermal healing of defects in oxide films on metals and alloys
[DE89-009580] N89-22735
GRAND UNIFIED THEORY
Investigation of the vacuum structure of the Georgi-Glashow model on the lattice
[DE88-705676] N89-23319
GRAPH THEORY
Restrictions on induced subgraphs ensuring Hamiltonicity or pancyclicity of K sub 1,3-free graphs
[MEMO-709] N89-23235
The separation number
[MEMO-710] N89-23236
GRAPHITE-EPOXY COMPOSITES
Environmental program on durability of graphite/epoxy honeycomb specimens with representative damage and repairs
[AR-005-504] N89-22685
The effects of plastic media blasting paint removal on the microstructure of graphite/epoxy composite materials
[AD-A204801] N89-22688
Mechanical properties and damage mechanisms of carbon fiber reinforced composites: Compression loading
[DFVLR-FB-88-41] N89-22706
Damage development, property degradation and life prediction in composite laminates N89-22708
Analysis of the mechanical behavior of adhesively bonded composite joints
[AD-A202616] N89-22938
GRAPHS (CHARTS)
Finite element analysis for calibration curve computation for measurement of crack propagation of ellipse shaped surface cracks
[GKSS-88/E/34] N89-22960
GRAVIMETRY
Detailed gravity anomalies derived form Seasat altimeter data. A comparison of two alternative approaches: Least squares collocation and a method based on FFT
[ETN-89-94144] N89-23039
GRAVITATION
Induced quantum conformal gravity
[DE88-705718] N89-23356
GRAVITATION THEORY
Topics in gravitational theory N89-23042
GRAVITATIONAL COLLAPSE
Gravitational effects of cosmic strings in Friedmann universes N89-23394
GRAVITATIONAL EFFECTS
Gravitational effects of cosmic strings in Friedmann universes N89-23394
GRAVITATIONAL FIELDS
On space-time escape mechanisms
[DE88-705699] N89-23354
Generating a hot big bang via a change in topology
[DE89-007561] N89-23388
GRAVITATIONAL LENSES
Topics in gravitational theory N89-23042
GRAVITY ANOMALIES
Detailed gravity anomalies derived form Seasat altimeter data. A comparison of two alternative approaches: Least squares collocation and a method based on FFT
[ETN-89-94144] N89-23039
GRAVITY WAVES
Gravity wave and turbulence studies using a high-resolution ST radar
[AD-A205592] N89-23046
GRAY SCALE
Combustor flow visualization using innovative infrared thermographics techniques
[AD-A205905] N89-22718
Mathematical morphology and the morphological sampling theorem N89-23113
Symbolic pixel labeling for curvilinear feature detection N89-23171
GREEN'S FUNCTIONS
On the structure of pressure fluctuations in simulated turbulent channal flow
[NASA-TM-101084] N89-22860
Low Reynolds number calculation of turbulent channel flow: A general discussion
[AD-A205883] N89-22864
GRID GENERATION (MATHEMATICS)
SUPERFISH accuracy dependence on mesh size
[DE89-007992] N89-22790
Using Patran and Supertab as pre- and postprocessors to COSMIC/NASTRAN N89-22942
Definition of NASTRAN sets by use of parametric geometry N89-22956
GROOVES
Influence of different types of seals on the stability behavior of turbopumps N89-22902
GROUND TESTS
NASA's program on icing research and technology
[NASA-TM-101989] N89-22569
GROUND TRUTH
Integration of tie-points in digital mosaicing
[ETN-89-94147] N89-22973
GUIDE VANES
LDV measurements and investigation of flow field through radial turbine guide vanes N89-22609
Initial results of tests on metal-ceramic guide vanes N89-22668

H

H I REGIONS
CO in the galactic center: A complete survey of carbon monoxide emission in the inner 4 kpc of the Galaxy N89-23386
H II REGIONS
Echelle observations of H2 complexes N89-23384
HALLEY'S COMET
Methods and algorithms for processing television images of nucleus of Halley's Comet. Some results N89-22624
HAMILTONIAN FUNCTIONS
Restrictions on induced subgraphs ensuring Hamiltonicity or pancyclicity of K sub 1,3-free graphs
[MEMO-709] N89-23235
Input-output decoupling with stability for Hamiltonian systems
[MEMO-722] N89-23239
Model matching for linear Hamiltonian systems
[MEMO-730] N89-23243
Nonlinear model matching with prescribed tracking error with an application to Hamiltonian systems
[MEMO-731] N89-23244
HANDBOOKS
Spacecraft thermal control design data handbook
[LAMF-8712] N89-22642
HARDWARE
SEAPAK user's guide, version 1.0
[NASA-TM-100728] N89-23182
HARMONIC GENERATORS
Organic and polymer crystalline films for spatial light modulation
[AD-A205906] N89-23350
HARMONICS
Two dimensional (4,0) supergravity in harmonic superspace. The action and the matter couplings
[DE88-705661] N89-23351
Construction of harmonic maps between pseudo-Riemannian spheres and hyperbolic spaces
[DE88-705695] N89-23353
HAZARDS
Space Propulsion Hazards Analysis Manual (SPHAM). Volume 2: Appendices
[AD-A204601] N89-22650
HEALING
Thermal healing of defects in oxide films on metals and alloys
[DE89-009580] N89-22735
HEART RATE
A new perspective in the etiology, treatment, prevention and prediction of space motion sickness
[AD-A205660] N89-23065
HEAT EXCHANGERS
Ceramic heat exchangers and turbine blades: Theory and experimental results N89-22677
Development of advanced heat pumps. Part 3: Fundamental approach on two-stage compression system
[DE88-756842] N89-22842
Heat transfer and pressure drop measurements in an air/molten salt direct-contact heat exchanger
[DE89-000837] N89-22843
HEAT FLUX
Two-phase flow characteristic of inverted bubbly, slug and annular flow in post-critical heat flux region
[DE89-007384] N89-22839
Surface flux parameterization schemes: Developments and experiences at KNMI — Earth surface
[KNMI-WR-88-06] N89-23055
HEAT PIPES
Megawatt Class Nuclear Space Power Systems (MCNSPS) conceptual design and evaluation report. Volume 2, technologies 1: Reactors, heat transport, integration issues
[NASA-CR-179614-VOL-2] N89-22981
Design considerations for heat-pipe solar receivers
[DE89-004037] N89-23017
HEAT PUMPS
Development of advanced heat pump. Part 2: Preliminary test of two-stage compression heat pump
[DE88-756838] N89-22841
Development of advanced heat pumps. Part 3: Fundamental approach on two-stage compression system
[DE88-756842] N89-22842
HEAT RADIATORS
Megawatt Class Nuclear Space Power Systems (MCNSPS) conceptual design and evaluation report. Volume 2, technologies 1: Reactors, heat transport, integration issues
[NASA-CR-179614-VOL-2] N89-22981

HEAT RESISTANT ALLOYS
Advanced cartridge technology: Executive summary --- spacecraft furnaces
[SEP-TS/F-6972/88-RP] N89-22636
Application of Advanced Material for Turbomachinery and Rocket Propulsion
[AGARD-CP-449] N89-22654
Advanced materials to combat the high temperature degradation processes in turbomachinery N89-22664
Fiber reinforced superalloys for rocket engines N89-22673
High temperature composite materials for rocket propulsion N89-22676
Metallurgical study of superalloy brazing alloys N89-22680
Development of metastable processing paths for high temperature alloys
[AD-A202614] N89-22721
Investigation and synthesis of high temperature and increased stiffness RSP aluminum alloys
[AD-A204162] N89-22723
Improved high temperature creep resistant austenitic alloy
[DE89-009664] N89-22736
HEAT STORAGE
Material degradation in a barium hydroxide latent heat storage pilot unit
[ESA-TT-1107] N89-22715
HEAT TRANSFER
Two-phase flow characteristic of inverted bubbly, slug and annular flow in post-critical heat flux region
[DE89-007384] N89-22839
Forced and free convection flow with viscous dissipation effects: The method of parametric differentiation
[DE88-705649] N89-22840
Heat transfer and pressure drop measurements in an air/molten salt direct-contact heat exchanger
[DE89-000837] N89-22843
A generalized one-dimensional computer code for turbomachinery cooling passage flow calculations
[NASA-TM-102079] N89-22862
The effect of thermocapillary flow on weld-pool profile
[NPL-DMA(A)167] N89-22927
Comparison of a cavity solar receiver numerical model and experimental data
[DE89-003609] N89-23016
Design considerations for heat-pipe solar receivers
[DE89-004037] N89-23017
A fast spatial scanning combination emissive and Mach probe for edge plasma diagnosis
[DE89-009674] N89-23295
Development of magnetic field assisted melt stabilization with heat and mass transfer control in low pressure LEC growth of GaAs
[AD-A205185] N89-23313
Methods for heat transfer and temperature field analysis of the insulated diesel, phase 3
[NASA-CR-182237] N89-23382
HEATING
ITER equilibrium with bootstrap currents, lower hybrid current drive and fast wave current drive
[DE89-009676] N89-22810
HELIOSTATS
An assessment of the optical performance of stretched-membrane mirror modules
[DE88-017347] N89-23015
HELIUM ISOTOPES
High accuracy thermal conductivity measurements near the lambda transition of helium with very high temperature resolution
[NASA-CR-184836] N89-22709
Determination of the He3 number density for the proportional counter used in the NPL Bonner sphere system
[NPL-RS(EXT)104] N89-23275
HEURISTIC METHODS
Translating optical flow into token matches N89-23159
An algorithm for the three-index assignment problem
[AD-A205172] N89-23190
HIERARCHIES
Rapid object recognition from a large model base using prediction hierarchies N89-23137
A real time hierarchical model for optic flow determination via spatiotemporal frequency channels N89-23158
Generalized multicomponent KP-hierarchies
[MEMO-708] N89-23234
Geometrical interpretation of the bilinear equations for the KP-hierarchy
[MEMO-720] N89-23238
HIGH ALTITUDE
Monte Carlo applied to resonance scattering of high altitude fluorescent radiation
[DE89-006519] N89-23035
HIGH FREQUENCIES
Efficacy of conventional and high-frequency ventilation at altitude
[AD-A205922] N89-23071
HIGH POLYMERS
Reactions of inorganic high polymers as a route to tailored solids
[AD-A204602] N89-22750
HIGH POWER LASERS
Development of an efficient high brightness Ti:Al2O3 laser amplifier
[AD-A204187] N89-22881
Progress toward the delivery of high energy pulses with the Aurora KrF/ICF laser system
[DE89-007750] N89-22885
HIGH RESOLUTION
Interactive ultrasonic nondestructive evaluation
[AD-A204166] N89-22931
HIGH REYNOLDS NUMBER
Transonic and supersonic flow past a 65 deg delta wing with rounded leading edges: Analysis of experimental data
[DFVLR-FB-88-44] N89-22580
HIGH STRENGTH
Basic program for the development of a reliable high strength construction ceramic mode of SiC
[MTU-TB-87/927] N89-22757
HIGH STRENGTH STEELS
Hydrogen embrittlement study and positron annihilation response of hydrogen in aisi 4340 steel N89-22720
Assessing hydrogen assisted cracking modes in high strength steel welds
[AD-A205431] N89-22746
HIGH TEMPERATURE
Formation of lubricating films at elevated temperatures from the gas phase
[PB89-129530] N89-22747
Annealing studies on a fully cured epoxy resin: Effect of thermal prehistory, and time and temperature of annealing
[AD-A205875] N89-22769
Advanced high-temperature batteries N89-23010
HIGH TEMPERATURE ENVIRONMENTS
Corrosion of iron, nickel and cobalt based alloys in high temperature environments contaminated with chlorine
[DE89-009829] N89-22738
HIGH TEMPERATURE GASES
Initial results of tests on metal-ceramic guide vanes N89-22668
HIGH TEMPERATURE RESEARCH
Improved high temperature creep resistant austenitic alloy
[DE89-009664] N89-22736
HIGH TEMPERATURE SUPERCONDUCTORS
Evaluation, development, and characterization of superconducting materials for space application
[NASA-CR-184842] N89-23302
Effects of different fabrication techniques on the Yttrium-Barium-Copper oxide high temperature superconductor
[AD-A202598] N89-23304
Low frequency resistance fluctuations in films of high temperature superconductors
[DE89-007489] N89-23310
Perturbative treatment of local correlations in Cu-O planes for high temperature superconductors
[DE88-705648] N89-23315
Possibility of operation of high temperature superconducting YBa2Cu3O7 ceramics in cyclotrons at irradiation
[DE88-705783] N89-23325
Neutron scattering studies of magnetic excitations in La/sub 2-x/Sr/sub x/CuO
[DE89-008155] N89-23333
Point defects and oxygen diffusion in high T sub c superconductors
[DE89-009842] N89-23341
Processing and electrical properties of high-T sub c superconductors
[DE89-009852] N89-23342
HILBERT SPACE
An optimal algorithm for the derivation of shape from shadows N89-23176
On Hausdorff dimension of invariant manifolds of infinite-dimensional dynamic systems
[DE88-705628] N89-23227
On the averaging method for quasilinear hyperbolic equations
[DE88-705629] N89-23228
Implementation of comparative probability by Gleason measures: Infinite dimensional case
[DE88-705683] N89-23259
On a functional equation over Hilbert spaces
[DE88-705645] N89-23267
HISTORIES
A historical interpretation of the study of the visible cloud morphology on the planet Jupiter: 1610-1878 N89-23398
History of manned flight
[CNES-NT-121] N89-23405
HOLE GEOMETRY (MECHANICS)
Improving hole boring yield in carbon epoxy composites with tensile loading
[REPT-47-324/F] N89-22704
HOMOGENEITY
Straight homogeneous generalized cylinders: Differential geometry and uniqueness results N89-23169
HOMOGENIZING
An experimental study of turbulent mixing of viscoelastic fluids
[ETN-89-94140] N89-22847
HOMOLOGY
Cohomology theory and deformations of Z sub 2-graded Lie algebras
[DE88-705694] N89-23229
HONEYCOMB STRUCTURES
Annular honeycomb seals: Test results for leakage and rotordynamic coefficients; comparisons to labyrinth and smooth configurations N89-22899
HORIZONTAL ORIENTATION
Unity vision block with focal plane
[AD-A204694] N89-23283
HORN ANTENNAS
Approximation technique for determining gain and radiation pattern of the horn antenna
[DE89-006136] N89-22786
HOT CORROSION
Corrosion of iron, nickel and cobalt based alloys in high temperature environments contaminated with chlorine
[DE89-009829] N89-22738
HOT STARS
Studies of hot white dwarfs and instrumentation for stellar extreme ultraviolet astronomy N89-23383
HOT-WIRE ANEMOMETERS
Experimental investigation of flow over a backward facing step-progress report N89-22832
HOUSINGS
Incorporating general race and housing flexibility and deadband in rolling element bearing analysis N89-22912
HUMAN BEHAVIOR
Coordinated Noninvasive Studies (CNS) Project
[AD-A205413] N89-22804
HUMAN BEINGS
Benzodiazepines and caffeine: Effect on daytime sleepiness, performance, and mood
[AD-A205862] N89-23066
HUMAN FACTORS ENGINEERING
Model-based analysis and cooperative synthesis of control and display augmentation for piloted flight vehicles N89-22610
A real-time simulator for man-in-the-loop testing of aircraft control systems (SIMTACS-RT)
[AD-A202599] N89-23067
The Space Station Flight Telerobotic Servicer and the human
[NASA-TM-100615] N89-23068
AGARD highlights 88/2 N89-23403
HUMAN FACTORS LABORATORIES
An experimental environment and laboratory for studying human information processing in Naval Air ASW (Naval air antisubmarine warfare)
[AD-A204774] N89-23069
HUMAN PERFORMANCE
Benzodiazepines and caffeine: Effect on daytime sleepiness, performance, and mood
[AD-A205862] N89-23066
HYDRAULIC EQUIPMENT
Acta Aeronautica et Astronautica Sinica (selected articles)
[AD-A205128] N89-22570
HYDRODYNAMICS
Renormalization group analysis of turbulence N89-22821
Direct numerical simulations of turbulent convection with a variable gravity and Keplerian rotation N89-22831
An experimental study of turbulent mixing of viscoelastic fluids
[ETN-89-94140] N89-22847
HYDROGEN
Variational analysis of railgun plasma-arc-armature for acceleration of solid hydrogen pellets for fusion reactor refueling
[DE89-009556] N89-22634
HYDROGEN EMBRITTLEMENT
Hydrogen embrittlement study and positron annihilation response of hydrogen in aisi 4340 steel N89-22720
Assessing hydrogen assisted cracking modes in high strength steel welds
[AD-A205431] N89-22746

Corrosion fatigue crack growth: The role of crack-tip deformation and film formation kinetics N89-22966
Hydrogen embrittlement in nickel-hydrogen cells N89-23008

HYDROGEN OXYGEN FUEL CELLS
Space Electrochemical Research and Technology Conference: Abstracts [NASA-CP-10029] N89-22982
Recent advances in solid polymer electrolyte fuel cell technology with low platinum loading electrodes N89-22994
Hydrogen-oxygen proton-exchange membrane fuel cells and electrolyzers N89-22996

HYDROGEN PEROXIDE
Aqueous impurity effects on stainless steel IGSCC (intergranular stress corrosion cracking): A central composite matrix analysis [DE88-017382] N89-22726

HYDROGENATION
Models for surface intermediates in CO hydrogenation [DE89-004348] N89-22712
Diagnostics of glow discharges used to produce hydrogenated amorphous silicon films [DE89-000887] N89-22760

HYDROSTATICS
Polymer electrolytes with exclusively cationic conductivity [DE89-009521] N89-22761

HYDROXIDES
Material degradation in a barium hydroxide latent heat storage pilot unit [ESA-TT-1107] N89-22715

HYPERBOLIC COORDINATES
Construction of harmonic maps between pseudo-Riemannian spheres and hyperbolic spaces [DE88-705695] N89-23353

HYPERBOLIC DIFFERENTIAL EQUATIONS
A flux splitting method for hyperbolic systems: Application to the solution of the Euler equations [CERT-RF-1/3290/DERI] N89-22854
On the averaging method for quasilinear hyperbolic equations [DE88-705629] N89-23228

HYPERCUBE MULTIPROCESSORS
Pyramid algorithms implementation on the connection machine N89-23129
Reduction of a general matrix to tridiagonal form using a hypercube multiprocessor [DE89-008721] N89-23197

HYPERSONIC FLIGHT
New hypersonic facility capability at NASA Lewis Research Center [NASA-TM-102028] N89-22617

HYPERSONIC FLOW
Transition to turbulence in laminar hypersonic flow N89-22830

HYPERSONIC VEHICLES
New hypersonic facility capability at NASA Lewis Research Center [NASA-TM-102028] N89-22617

HYPERSONIC WIND TUNNELS
New hypersonic facility capability at NASA Lewis Research Center [NASA-TM-102028] N89-22617

HYSTERESIS
A study of unsteady turbulent flow past airfoils N89-22587
Hysteresis development in superconducting Josephson junctions [DE88-705693] N89-23323

I

IBM COMPUTERS
Enhancements to the IBM version of COSMIC/NASTRAN N89-22946

ICE FORMATION
NASA's program on icing research and technology [NASA-TM-101989] N89-22569

ICE PREVENTION
NASA's program on icing research and technology [NASA-TM-101989] N89-22569
Electro-impulse de-icing research: Fatigue and electromagnetic interference tests [DOT/FAA/CT-88/27] N89-22594

ICOSAHEDRONS
Quasicrystals from cuts in six dimensions [DE89-009361] N89-23337

IGNITION
Ignition characteristics of the iron-based alloy UNS S66286 in pressurized oxygen [NASA-CR-183612] N89-22722

IGNITION TEMPERATURE
Ignition characteristics of the iron-based alloy UNS S66286 in pressurized oxygen [NASA-CR-183612] N89-22722

IMAGE ANALYSIS
Proceedings: Image Understanding Workshop, volume 1 [AD-A197558] N89-23074
Image understanding: Intelligent systems N89-23077
CMU image understanding program N89-23079
Summary of image understanding research at the University of Massachusetts N89-23081
Progress in image understanding at the University of Rochester N89-23082
An integrated image understanding benchmark: Recognition of a 2 1/2 D mobile N89-23088
Some sample algorithms for the image understanding architecture N89-23089
Algorithms and architectures for smart sensing N89-23090
Multimodal reconstruction and segmentation with Markov random fields and HCF optimization N89-23095
IU at UI: An overview and an example on shape from texture N89-23096
Cooperative methods for road tracking in aerial imagery N89-23101
PACE: An environment for intelligence analysis N89-23102
Affine invariant matching N89-23103
Contour correspondences in dynamic imagery N89-23109
Mathematical morphology and the morphological sampling theorem N89-23113
Using generic geometric and physical models for representing solids N89-23114
Proceedings: Image Understanding Workshop, volume 2 [AD-A197559] N89-23115
Perceptual grouping for the detection and description of structures in aerial images N89-23117
The concept of an effective viewpoint N89-23131
Preliminary design of a programmed picture logic N89-23141
An introduction to generalized stereo techniques N89-23142
Qualitative versus quantitative depth and shape from stereo N89-23144
Structural correspondence in stereo vision N89-23146
Image segmentation and reflection analysis through color N89-23150
A color metric for computer vision N89-23151
A real time hierarchical model for optic flow determination via spatiotemporal frequency channels N89-23158
Translating optical flow into token matches N89-23159
Structure recognition by connectionist relaxation: Formal analysis N89-23160
Extracting generic shapes using model-driven optimization N89-23161
Generalizing epipolar-plane image analysis on the spatiotemporal surface N89-23164
Building surfaces of evolution: The weaving wall N89-23165
Ribbons, symmetries and skewed symmetries N89-23170
Symbolic pixel labeling for curvilinear feature detection N89-23171
Predicting material classes N89-23177
Consensus theory in expert systems: An adaptive inference framework and application to image understanding [AD-A204253] N89-23188

IMAGE CONTRAST
Ultra-sensitive X-ray sensors give improved contrast sensitivity [DE89-003581] N89-22872

IMAGE CORRELATORS
Contour correspondences in dynamic imagery N89-23109
Spatio-temporal analysis of an image sequence with occlusion N89-23110

IMAGE ENHANCEMENT
Consensus theory in expert systems: An adaptive inference framework and application to image understanding [AD-A204253] N89-23188

IMAGE MOTION COMPENSATION
Qualitative reasoning and modeling for robust target tracking and recognition from a mobile platform N89-23086
Kalman filter-based algorithms for estimating depth from image sequences N89-23094
Qualitative motion detection and tracking of targets from a mobile platform N89-23099
Self calibration of motion and stereo vision for mobile robot navigation N89-23106
Integration effort in knowledge-based vision techniques for the autonomous land vehicle program N89-23108
Spatio-temporal analysis of an image sequence with occlusion N89-23110
Natural representation of motion in space-time N89-23111

IMAGE PROCESSING
Dynamic image interpretation for autonomous vehicle navigation [AD-A204167] N89-22597
Methods and algorithms for processing television images of nucleus of Halley's Comet. Some results N89-22624
Combustor flow visualization using innovative infrared thermographics techniques [AD-A205905] N89-22718
Transmission electron microscopy: Imaging of materials [DE89-007418] N89-22870
Ultra-sensitive X-ray sensors give improved contrast sensitivity [DE89-003581] N89-22872
ALEXIS: A narrow-band survey/monitor of the ultrasoft X-ray sky [DE89-007980] N89-22873
Integration of tie-points in digital mosaicing [ETN-89-94147] N89-22973
Image understanding and robotics research at Columbia University N89-23083
Knowledge-based vision technology progress at Hughes AI Center N89-23084
Image understanding research at GE N89-23085
Qualitative reasoning and modeling for robust target tracking and recognition from a mobile platform N89-23086
An integrated image understanding benchmark: Recognition of a 2 1/2 D mobile N89-23088
The Maryland approach to image understanding N89-23091
An integrated approach to stereo matching, surface reconstruction and depth segmentation using consistent smoothness assumptions N89-23092
The MIT vision machine N89-23093
Kalman filter-based algorithms for estimating depth from image sequences N89-23094
Multimodal reconstruction and segmentation with Markov random fields and HCF optimization N89-23095
IU at UI: An overview and an example on shape from texture N89-23096
Physically based modeling for vision and graphics N89-23097
Perception with feedback N89-23098
Qualitative navigation 2 N89-23100
Constructing simple stable descriptions for image partioning N89-23104
Three-dimensional object recognition using surface descriptions N89-23105
Autonomous navigation in cross-country terrain N89-23107
Integration effort in knowledge-based vision techniques for the autonomous land vehicle program N89-23108
Contour correspondences in dynamic imagery N89-23109
Spatio-temporal analysis of an image sequence with occlusion N89-23110
Natural representation of motion in space-time N89-23111
Mathematical morphology and the morphological sampling theorem N89-23113
Using flow field divergence for obstacle avoidance in visual navigation N89-23120
Three-dimensional vision for outdoor navigation by an autonomous vehicle N89-23124
Machine-independent image processing: Performance of Apply on diverse architectures N89-23125
Parallel architectures for image processing and vision N89-23126
IU software environments N89-23133
Using probabilistic domain knowledge to reduce the expected computational cost of matching N89-23134
Modeling sensors and applying sensor model to automatic generation of object recognition program N89-23136
Evaluation of quantization error in computer vision N89-23138
Algebraic reasoning in view consistency and parameterized model matching problems N89-23139
Test results from SRI's stereo system N89-23140
Stochastic stereo matching over scale N89-23143
Modal driven edge detection N89-23163
Generation of face-edge-vertex models directly from images N89-23166

Depth from looming structure N89-23167
Image segmentation using geometric and physical constraints N89-23172
Recognizing solid objects by alignment N89-23174
Optimization for object localization of the constrained algebraic reconstruction technique [DE89-007755] N89-23193
Statistical smoothing methods and image analysis [AD-A205643] N89-23256

IMAGE RECONSTRUCTION
Knowledge based vision for terrestrial robots N89-23087
An integrated approach to stereo matching, surface reconstruction and depth segmentation using consistent smoothness assumptions N89-23092
Multimodal reconstruction and segmentation with Markov random fields and HCF optimization N89-23095
Physically based modeling for vision and graphics N89-23097
Qualitative motion detection and tracking of targets from a mobile platform N89-23099
Constructing simple stable descriptions for image partioning N89-23104
Three-dimensional object recognition using surface descriptions N89-23105
Mathematical morphology and the morphological sampling theorem N89-23113
Using generic geometric and physical models for representing solids N89-23114
Perceptual grouping for the detection and description of structures in aerial images N89-23117
Overview of the SRI cartographic modeling environment N89-23122
Curved surface reconstruction using stereo correspondence N89-23147
Combining information in low-level vision N89-23152
Is correspondence necessary for the perception of structure from motion N89-23154
Generalizing epipolar-plane image analysis on the spatiotemporal surface N89-23164
Building surfaces of evolution: The weaving wall N89-23165
Generation of face-edge-vertex models directly from images N89-23166
On the recovery of superellipsoids N89-23168
Symbolic pixel labeling for curvilinear feature detection N89-23171
Adaptive smoothing for feature extraction N89-23173
Projective invariants of shapes N89-23175
Predicting material classes N89-23177
Surface orientation from projective foreshortening of isotropic texture autocorrelation N89-23179
Optimization for object localization of the constrained algebraic reconstruction technique [DE89-007755] N89-23193

IMAGE RESOLUTION
Multiresolution aerial image interpretation N89-23116
Perceptual grouping for the detection and description of structures in aerial images N89-23117
Dynamic model matching for target recognition from a mobile platform N89-23118
Using probabilistic domain knowledge to reduce the expected computational cost of matching N89-23134
Structural correspondence in stereo vision N89-23146

IMAGING RADAR
Imaging radar applications in Europe. Illustrated experimental results (1978-1987) [ESA-TM-01] N89-22978

IMAGING TECHNIQUES
Atomic imaging of Au/Ni multilayers [DE89-009903] N89-22698
Imaging radar applications in Europe. Illustrated experimental results (1978-1987) [ESA-TM-01] N89-22978
Motion from a sequence of images N89-23155
Development of magnetic field assisted melt stabilization with heat and mass transfer control in low pressure LEC growth of GaAs [AD-A205185] N89-23313
Microfilm and computer full text of archival documents [AD-A204055] N89-23377

IMPACT DAMAGE
In-space technology development: Atomic oxygen and orbital debris effects [NASA-TM-102154] N89-22682

IMPACT LOADS
Compression and shear wave propagation in explosives [AD-A205917] N89-22865
Adaptive contact elements for three-dimensional explicit transient analysis [DE89-008436] N89-22958

IMPACT TESTS
CSPC test 319.30: Study on impact tolerance of preimpregnated carbon-epoxy systems [REPT-47-323/F] N89-22703
Space Nuclear Safety Program [DE89-008308] N89-23281

IMPEDANCE
Impedance studies of Ni/Cd and Ni/H cells using the cell case as reference electrode N89-23002
The application of electrochemical impedance spectroscopy for characterizing the degradation of Ni(OH)2/NiOOH electrodes N89-23003

IMPEDANCE MEASUREMENT
Impedance studies of Ni/Cd and Ni/H cells using the cell case as reference electrode N89-23002

IMPELLERS
Rotordynamic instability Problems in High-Performance Turbomachinery, 1988 [NASA-CP-3026] N89-22891
Some field experience with subsynchronous vibration of centrifugal compressors N89-22892
Influence of impeller and diffuser geometries on the lateral fluid forces of whirling centrifugal impeller N89-22907
A theoretical study of fluid forces on a centrifugal impeller rotating and whirling in a vaned diffuser N89-22908
Influence of impeller shroud forces on turbopump rotor dynamics N89-22909

IMPURITIES
Theoretical study of the Pd-B complex in silicon [DE88-705650] N89-23316

INCOMPRESSIBLE FLOW
Aerodynamics of nonrigid bodies undergoing large amplitude time-dependent motions N89-22586
Aerodynamic detuning of a loaded airfoil cascade in an incompressible flow by a locally analytical method N89-22588
Computational investigation of incompressible airfoil flows at high angles of attack [AD-A205885] N89-22590
Close interactions of 3-D vortex tubes N89-22823
Forced and free convection flow with viscous dissipation effects: The method of parametric differentiation [DE88-705649] N89-22840
Multigrid for the steady-state incompressible Navier-Stokes equation: A survey [GMD-322] N89-22846
Computerized simulation of turbulent flow in a channel [ONERA-RSF-16/3419-AY-112-A] N89-22852

INCONEL (TRADEMARK)
Preliminary study of ceramic-metal interface in thermal boundaries [ETCA-87-R-101] N89-23346

INDENTATION
Application of indentation to the study of the toughness of yttrium-zircon plasma coatings [ETCA-87-R-040] N89-22765

INDEXES (DOCUMENTATION)
Indexing and abstracting N89-23368

INDIUM PHOSPHIDES
The NASA Space Solar Cell Advanced Research Program [NASA-TM-102020] N89-22651
InP (Indium Phosphide): Into the future [NASA-TM-102058] N89-23025
Time resolved photoluminescence of ytterbium in indium phosphide [AD-A202596] N89-23303

INELASTIC SCATTERING
Neutron scattering studies of magnetic excitations in La/sub 2-x/Sr/sub x/CuO [DE89-008155] N89-23333

INERTIAL CONFINEMENT FUSION
Progress toward the delivery of high energy pulses with the Aurora KrF/ICF laser system [DE89-007750] N89-22885

INERTIAL NAVIGATION
Pre and post modification electromagnetic compatibility test report for the C-130H self contained navigation system with MLS A-kit, revision [AD-A205167] N89-22604

INFERENCE
Consensus theory in expert systems: An adaptive inference framework and application to image understanding [AD-A204253] N89-23188
Parallel problem solving system, PRISM (Parallel Inference System) [AD-A204915] N89-23207

INFILTRATION
CVD and diffusion coatings for high temperature applications in turbomachinery and rocket motors N89-22658

INFORMATION DISSEMINATION
The Organisation and Functions of Documentation and Information Centres in Defence and Aerospace Environments [AGARD-CP-445] N89-23362
The objectives and role of the Greek National Documentation Centre N89-23363
The status of defence information programs in Greece N89-23364
Identifying users and how to reach them N89-23370
TRANSDOC-electronic delivery programme N89-23372
Impact of information technology on organizational structure: A control perspective N89-23379

INFORMATION FLOW
R and D productivity: Relationship to Selective Dissemination of Information (SDI) in the corporate environment N89-23375

INFORMATION PROCESSING (BIOLOGY)
Motor theory of auditory perception [AD-A204951] N89-23064

INFORMATION RETRIEVAL
Core knowledge system: Storage and retrieval of inconsistent information N89-23132
The Organisation and Functions of Documentation and Information Centres in Defence and Aerospace Environments [AGARD-CP-445] N89-23362
User needs and how to determine them N89-23365
Indexing and abstracting N89-23368
Fostering interaction of government, defense, and aerospace databases N89-23374

INFORMATION SYSTEMS
Earth system science: A program for global change [NASA-TM-101188] N89-22969
Implementing security measures for computer-based security systems [DE89-008995] N89-23072
The Organisation and Functions of Documentation and Information Centres in Defence and Aerospace Environments [AGARD-CP-445] N89-23362
The objectives and role of the Greek National Documentation Centre N89-23363
The status of defence information programs in Greece N89-23364
User needs and how to determine them N89-23365
Sources of information N89-23366
Data security N89-23369
Decentralization of databases and the communication between them N89-23373
R and D productivity: Relationship to Selective Dissemination of Information (SDI) in the corporate environment N89-23375
Germany: Focus on Scientific and Technical Information, volume 4, number 1, April 1988 [AD-A204054] N89-23376

INFORMATION THEORY
Statistical smoothing methods and image analysis [AD-A205643] N89-23256

INFORMATION TRANSFER
Impact of information technology on organizational structure: A control perspective N89-23379
Technology transfer report [DE89-009044] N89-23381

INFRARED ASTRONOMY
Optical and infrared observations of the nature and evolution of active galaxies N89-23395

INFRARED DETECTORS
Molecular beam epitaxial growth and characterization of metastable compound semiconductors for infrared detector applications [AD-A205175] N89-23312
Radiation hardened detector arrays for the far and extreme infrared, phase 1 [BF-R-65.695-10] N89-23347

INFRARED IMAGERY
Combustor flow visualization using innovative infrared thermographics techniques [AD-A205905] N89-22718

INFRARED RADIATION
Far- and mid-infrared properties of metal-insulator composite materials [AD-A204914] N89-22689

INFRARED SPECTRA
Optical and infrared observations of the nature and evolution of active galaxies N89-23395

INJECTION
Numerical study of a multipurpose transonic wind tunnel with an adaptable injection-suction system N89-22621
Development and study of a 3.2-mm-diameter, 1.2-m-long two-stage plasma-arc-driven railgun for hypervelocity hydrogen pellet injection [DE89-009557] N89-22635

INLET FLOW
Two-phase flow characteristic of inverted bubbly, slug and annular flow in post-critical heat flux region
[DE89-007384] N89-22839
INOCULATION
Novel protein crystal growth technology: Proof of concept
[NASA-CR-184959] N89-23306
INSTRUMENTS
A historical interpretation of the study of the visible cloud morphology on the planet Jupiter: 1610-1878
N89-23398
INTEGRAL EQUATIONS
Application of the Ornstein-Zernike formalism to polymer and copolymer blends
[DE88-705686] N89-22753
Statistical smoothing methods and image analysis
[AD-A205843] N89-23256
INTEGRALS
Solution of multi-center molecular integrals of Slater-type orbitals
[NASA-TM-101545] N89-22692
INTEGRATED CIRCUITS
Electrical properties and detection methods for CMOS IC defects
[DE89-005775] N89-23327
INTEGRATED OPTICS
Technical support for optical turbulence research
[AD-A204776] N89-23033
INTERACTING GALAXIES
Observational aspects of interacting galaxies
N89-23385
INTERACTIONAL AERODYNAMICS
Interaction between an isolated vortex and a wing profile
[ETN-89-94384] N89-22579
Computational investigation of incompressible airfoil flows at high angles of attack
[AD-A205885] N89-22590
INTERACTIVE CONTROL
Expert systems for real-time monitoring and fault diagnosis
[NASA-CR-179441] N89-23209
INTERATOMIC FORCES
Physical properties of grain-boundary materials: Comparison of EAM (Embedded-Atom-Method) and central-force potentials
[DE89-007414] N89-23308
INTERFACES
Alumina reinforced tetragonal zirconia (TZP) composites
[DE89-008880] N89-22690
EXAFS studies of multilayer interfaces
[DE89-009527] N89-22694
Atomic imaging of Au/Ni multilayers
[DE89-009903] N89-22698
Microstructural studies of IAD and PVD Cr coatings by cross section transmission electron microscopy
[DE89-009877] N89-22739
Preliminary study of ceramic-metal interface in thermal boundaries
[ETCA-87-R-101] N89-23346
INTERFACIAL TENSION
Interfacial adhesion and mechanical properties of polyamide-6/glass bead composites
[ETN-89-94136] N89-22759
INTERGRANULAR CORROSION
Aqueous impurity effects on stainless steel IGSCC (intergranular stress corrosion cracking): A central composite matrix analysis
[DE88-017382] N89-22726
INTERMETALLICS
Development of metastable processing paths for high temperature alloys
[AD-A202614] N89-22721
Ab initio calculations of ordered intermetallic phase equilibria
[DE89-009974] N89-22741
INTERMOLECULAR FORCES
Physical properties of grain-boundary materials: Comparison of EAM (Embedded-Atom-Method) and central-force potentials
[DE89-007414] N89-23308
INTERNATIONAL COOPERATION
Relevance of international research facilities to international stability
[DE89-009400] N89-23380
INTERNATIONAL RELATIONS
Relevance of international research facilities to international stability
[DE89-009400] N89-23380
INTERPOLATION
Compressible Euler solution around a wing canard sting configuration
[FFA-TN-1988-62] N89-22578
On multivariate polynomial interpolation
[AD-A204099] N89-23226
Smooth interpolation to scattered data by bivariate piecewise polynomials of odd degree
[MEMO-732] N89-23245
Monotonicity-preserving quadratic C sup 1-spline interpolation to scattered data
[MEMO-744] N89-23252
INTERSTELLAR MATTER
The ALEXIS project and the local interstellar medium
[DE89-009246] N89-23392
INTERSTELLAR SPACE
The ALEXIS project and the local interstellar medium
[DE89-009246] N89-23392
INVARIANCE
Affine invariant matching N89-23103
INVENTIONS
Microwave sintering of boron carbide
[DE89-009652] N89-22763
Double sided circuit board and a method for its manufacture
[DE89-009601] N89-22809
INVENTORIES
Information resources management N89-23371
INVERSIONS
Nonlinear optimization involving polynomial matrices and their generalized inverses
[AD-A202620] N89-23224
INVISCID FLOW
Inviscid spatial stability of a compressible mixing layer. Part 2: The flame sheet model
[NASA-CR-181815] N89-22837
ION BEAMS
Model calculations of the electron-optical properties of compact Faraday cups
[NPL-DMA(A)165] N89-23268
ION CURRENTS
Monolithic Solid Oxide Fuel Cell development
N89-22989
ION CYCLOTRON RADIATION
ICRF waveguide launcher research
[DE89-009151] N89-22791
ION EXCHANGE MEMBRANE ELECTROLYTES
Advanced double layer capacitors N89-22993
Recent advances in solid polymer electrolyte fuel cell technology with low platinum loading electrodes
N89-22994
The application of Dow Chemical's perfluorinated membranes in proton-exchange membrane fuel cells
N89-22995
Hydrogen-oxygen proton-exchange membrane fuel cells and electrolyzers N89-22996
Electrocatalysts for oxygen electrodes in fuel cells and water electrolyzers for space applications N89-22997
ION IMPLANTATION
Precipitation of Ar, Kr and Xe in Ni at room temperature
[DE89-009879] N89-22713
ION INJECTION
Current and thermal noise in mixed Na/Ag beta alumina
[AD-A205869] N89-22816
ION MOTION
Anomalous cross-field velocities in a CIV laboratory experiment
[TRITA-EPP-88-06] N89-23289
ION TEMPERATURE
Effects of ion collisions on quasilinear heating by the current-driven ion cyclotron instability in the high latitude ionosphere
[AD-A202512] N89-23032
IONIC COLLISIONS
Effects of ion collisions on quasilinear heating by the current-driven ion cyclotron instability in the high latitude ionosphere
[AD-A202512] N89-23032
IONIC DIFFUSION
Equations of cosmic-ray transport with distributed acceleration
[AD-A204599] N89-23401
IONIZATION
Anomalous cross-field velocities in a CIV laboratory experiment
[TRITA-EPP-88-06] N89-23289
IONIZATION FREQUENCIES
Compact, lightweight CO2 lasers for SDIO applications
[AD-A204300] N89-22882
IONOSPHERES
Effect of pump-induced density depletions on the spectrum of stimulated electromagnetic emissions --- ionosphere
[IRF-PREPRINT-107] N89-22799
IONOSPHERIC HEATING
Effects of ion collisions on quasilinear heating by the current-driven ion cyclotron instability in the high latitude ionosphere
[AD-A202512] N89-23032
IONS
Mass-spectroscopic measurements of stratospheric ions, trace gases and precondensation nuclei using balloon-borne measuring probes
[BPT-7/88] N89-23037
IRON
Behavior of iron aluminides in oxidizing and sulfidizing environments
[DE89-008919] N89-22693
IRON ALLOYS
Ignition characteristics of the iron-based alloy UNS S66286 in pressurized oxygen
[NASA-CR-183612] N89-22722
Corrosion of iron, nickel and cobalt based alloys in high temperature environments contaminated with chlorine
[DE89-009829] N89-22738
IRON OXIDES
Criteria for selection of phase names for oxides
[NPL-DMA(A)169] N89-22714
Thermal healing of defects in oxide films on metals and alloys
[DE89-009580] N89-22735
IRRADIATION
Mechanisms of cascade collapse
[DE89-009882] N89-22740
Possibility of operation of high temperature superconducting YBa2Cu3O7 ceramics in cyclotrons at irradiation
[DE88-705783] N89-23325
Influence of ion irradiated SrTiO sub 3 on the properties of thin film oxide superconductors
[DE89-009409] N89-23338
ISOMORPHISM
Parallel hardware for constraint satisfaction
N89-23127
ISOTROPIC TURBULENCE
On curve and surface stretching in turbulent flow
N89-22820
A seal test facility for the measurement of isotropic and anisotropic linear rotordynamic characteristics
N89-22905
ISOTROPY
Surface orientation from projective foreshortening of isotropic texture autocorrelation N89-23179
ITERATION
Renormalization group analysis of turbulence
N89-22821
ITERATIVE SOLUTION
Relative orientation N89-23149

J

JET AIRCRAFT NOISE
Rectangular nozzle plume velocity modeling for use in jet noise prediction
[NASA-TM-102047] N89-22577
JET ENGINES
Supersonic particle probes: Measurement of internal wall losses
[AD-A205863] N89-22589
JET FLOW
Cavitation in a submerged jet at constant pressure
[OUEL-1658/86] N89-22848
Experimental and theoretical studies of vertical annular liquid jets
[DE89-009153] N89-22851
JOINTS (JUNCTIONS)
Traction-drive force transmission for telerobotic joints
[NASA-CR-183331] N89-22922
Signal treatment and data analysis methods applied to nondestructive control of adhesive bonded joints
[ISAL-IDI-8809] N89-22936
Analysis of the mechanical behavior of adhesively bonded composite joints
[AD-A202616] N89-22938
JOSEPHSON JUNCTIONS
Quantum phenomena in mesoscopic superconducting tunnel junctions
[AD-A203354] N89-23305
Nuclear magnetic resonance with dc SQUID (Super-conducting QUantum Interference Device) preamplifiers
[DE89-007657] N89-23311
Hysteresis development in superconducting Josephson junctions
[DE88-705693] N89-23323
JUPITER ATMOSPHERE
A historical interpretation of the study of the visible cloud morphology on the planet Jupiter: 1610-1878
N89-23398

K

K-EPSILON TURBULENCE MODEL
Transonic viscous flow calculations for a turbine cascade with a two equation turbulence model
[NASA-TM-101944] N89-22607
Renormalization group analysis of turbulence N89-22821
Rotordynamic coefficients for labyrinth seals calculated by means of a finite difference technique N89-22900
Finite difference analysis of rotordynamic seal coefficients for an eccentric shaft position N89-22906

KALMAN FILTERS
Kalman filter-based algorithms for estimating depth from image sequences N89-23094
New stable, vectorisable Kalman filter algorithms based on orthogonal transformations
[ESA-TT-1108] N89-23203

KETONES
Inhalation developmental toxicology studies: Teratology study of methyl ethyl ketone in mice
[DE89-009563] N89-23062

KILOMETRIC WAVES
Kilometric radiation power flux dependence on area of discrete aurora
[NASA-CR-184993] N89-23040

KINEMATICS
Aerodynamics of nonrigid bodies undergoing large amplitude time-dependent motions N89-22586
On the numerical integration of viscoelastic flow equations
[DE89-007135] N89-22844
Configuration comparison analysis for the AFIT/AAMRL anthropomorphic robotic manipulator
[AD-A202618] N89-22921
A recursive formulation for flexible multibody dynamics N89-22968
CO in the galactic center: A complete survey of carbon monoxide emission in the inner 4 kpc of the Galaxy N89-23386

KINETIC HEATING
A quiver kinetic formulation of radio frequency heating and confinement in collisional edge plasmas
[DE89-009675] N89-23296

KLYSTRONS
Beam research technical abstracts, 1987
[DE89-009013] N89-23282

KNOWLEDGE BASES (ARTIFICIAL INTELLIGENCE)
Remote sensing information sciences research group: Browse in the EOS era
[NASA-CR-184637] N89-22979
Image understanding research at SRI International N89-23080
Summary of image understanding research at the University of Massachusetts N89-23081
Knowledge-based vision technology progress at Hughes AI Center N89-23084
Knowledge based vision for terrestrial robots N89-23087
Some sample algorithms for the image understanding architecture N89-23089
Affine invariant matching N89-23103
Integration effort in knowledge-based vision techniques for the autonomous land vehicle program N89-23108
Dynamic model matching for target recognition from a mobile platform N89-23118
TRIPLE: A multi-strategy machine learning approach to target recognition N89-23119
Core knowledge system: Storage and retrieval of inconsistent information N89-23132
IU software environments N89-23133
Rapid object recognition from a large model base using prediction hierarchies N89-23137
A knowledge-based tool for multilevel decomposition of a complex design problem
[NASA-TP-2903] N89-23181
Expert systems on multiprocessor architectures, phase 1
[AD-A204907] N89-23206

KNOWLEDGE REPRESENTATION
Image understanding: Intelligent systems N89-23077
Summary of image understanding research at the University of Massachusetts N89-23081
Image understanding and robotics research at Columbia University N89-23083
Some sample algorithms for the image understanding architecture N89-23089
Qualitative navigation 2 N89-23100
Affine invariant matching N89-23103
Natural representation of motion in space-time N89-23111
Generic models for robot navigation N89-23112
Using generic geometric and physical models for representing solids N89-23114
IU software environments N89-23133
Expert systems for real-time monitoring and fault diagnosis
[NASA-CR-179441] N89-23209

KRYPTON
Precipitation of Ar, Kr and Xe in Ni at room temperature
[DE89-009879] N89-22713

KRYPTON FLUORIDE LASERS
Progress toward the delivery of high energy pulses with the Aurora KrF/ICF laser system
[DE89-007750] N89-22885

L

LABORATORY EQUIPMENT
Mini Protein Crystallization Facility (MPCF), phase A study: Executive summary
[ESA-CR(P)-2709] N89-22775

LABYRINTH SEALS
Annular honeycomb seals: Test results for leakage and rotordynamic coefficients; comparisons to labyrinth and smooth configurations N89-22899
Rotordynamic coefficients for labyrinth seals calculated by means of a finite difference technique N89-22900
Rotordynamic coefficients for stepped labyrinth gas seals N89-22901
Rotordynamic stability problems and solutions in high pressure turbocompressors N89-22914

LAGRANGE MULTIPLIERS
An algorithm for the three-index assignment problem
[AD-A205172] N89-23190

LAGRANGIAN EQUILIBRIUM POINTS
Optimal low thrust trajectories for planetary capture
[AD-A202604] N89-22632

LAMINAR BOUNDARY LAYER
An experimental investigation of a low Reynolds number turbulent boundary layer subject to an adverse pressure gradient N89-22834

LAMINAR FLOW
Comparison of boundary layer trips of disk and grit types on airfoil performance at transonic speeds
[AD-A205206] N89-22575
Transition to turbulence in laminar hypersonic flow N89-22830

LAMINAR MIXING
The effects of stabilizing and destabilizing longitudinal curvature on the structure of turbulent, two-stream mixing layers N89-22833

LANDAU FACTOR
Nature of condensation in the momentum space for an interacting Bose system
[DE88-705679] N89-23352

LANDING GEAR
Acta Aeronautica et Astronautica Sinica (selected articles)
[AD-A205128] N89-22570

LANDMARKS
Qualitative motion detection and tracking of targets from a mobile platform N89-23099
Qualitative navigation 2 N89-23100
Autonomous navigation in cross-country terrain N89-23107

LANGUAGE PROGRAMMING
Use of language features in the implementation and validation of a standardized generic package of elementary functions for Ada
[DE89-007385] N89-23187

LANGUAGES
The objectives and role of the Greek National Documentation Centre N89-23363
The status of defence information programs in Greece N89-23364

LANTHANUM
Emission properties of europium-doped lanthanum and lutetium orthophosphate crystals for use in high temperature sensor applications
[DE89-006736] N89-23334

LANTHANUM COMPOUNDS
Superconductivity for electric power systems: Building toward our future
[DE89-000874] N89-23332
Neutron scattering studies of magnetic excitations in La/sub 2-x/Sr/sub x/CuO
[DE89-008155] N89-23333

LARGE SPACE STRUCTURES
Construction in weightlessness N89-22626

LARMOR RADIUS
A fluid FLR model of the magnetopause layer
[IRF-PREPRINT-109] N89-23299

LASER ANEMOMETERS
Study of unsteady boundary layers with adverse pressure gradient N89-22863
Implementation of a two-component laser anemometer at the T2 wind tunnel
[A-501-H] N89-22879

LASER BEAMS
Development of a differential temperature probe for the measurement of atmospheric turbulence at all levels
[AD-A205893] N89-23047

LASER CAVITIES
Measurements of optical loss in transparent solids using a novel spectrometer based on optical cavity decay
[DE89-009900] N89-23286

LASER DAMAGE
Unity vision block with focal plane
[AD-A204694] N89-23283
Accumulated surface damage on ZnS crystals produced by closely spaced pairs of picosecond laser pulses
[DE89-008813] N89-23329

LASER DOPPLER VELOCIMETERS
LDV measurements and investigation of flow field through radial turbine guide vanes N89-22609
Velocity measurements downstream of a sudden expansion using LDV. Part 2: Experimental results
[FOA-C-20736-2.1-PT-2] N89-22849

LASER FUSION
Progress toward the delivery of high energy pulses with the Aurora KrF/ICF laser system
[DE89-007750] N89-22885

LASER HEATING
Ignition characteristics of the iron-based alloy UNS S66286 in pressurized oxygen
[NASA-CR-183612] N89-22722

LASER MATERIALS
Cr3(+)-doped colquiite solid state laser material
[DE89-010106] N89-22888
Measurements of optical loss in transparent solids using a novel spectrometer based on optical cavity decay
[DE89-009900] N89-23286

LASER MODES
Kinetic studies of the electron-beam-pumped ArF laser
[DE89-004041] N89-22884

LASER OUTPUTS
Magnetic axis alignment and the Poisson alignment reference system
[DE89-007687] N89-22880
Fiber optic laser rod
[DE89-009598] N89-22887
Unity vision block with focal plane
[AD-A204694] N89-23283

LASER RANGE FINDERS
Knowledge-based vision technology progress at Hughes AI Center N89-23084
An operational perception system for cross-country navigation N89-23121

LASER SPECTROMETERS
Quantitative analysis of atmospheric trace gases
[BPT-10/88] N89-23027
Measurements of optical loss in transparent solids using a novel spectrometer based on optical cavity decay
[DE89-009900] N89-23286

LASER SPECTROSCOPY
Development of an efficient high brightness Ti:Al2O3 laser amplifier
[AD-A204187] N89-22881
Tunable chromium lasers
[DE89-006814] N89-22886

LASER WEAPONS
Transitional strategic defense architectures
[DE89-008312] N89-23265

LATITUDE
Seasonal and latitudinal variations of the temporal variance of ozone and of the potential temperature
[BPT-3/88] N89-23026
On the physical causes of ENSO events and the ITCZ's extreme latitudinal displacements
[DE88-705654] N89-23050

LATTICE PARAMETERS
Precipitation of Ar, Kr and Xe in Ni at room temperature
[DE89-009879] N89-22713
Investigation and synthesis of high temperature and increased stiffness RSP aluminum alloys
[AD-A204162] N89-22723
Physical properties of grain-boundary materials: Comparison of EAM (Embedded-Atom-Method) and central-force potentials
[DE89-007414] N89-23308
Electronic properties of Ge(1-X)Si(X): Alloying versus pressure
[DE88-705678] N89-23320
Growth kinetics of grain-boundary induced melting: A molecular-dynamics study
[DE89-009855] N89-23343

LATTICES (MATHEMATICS)
Investigation of the vacuum structure of the Georgi-Glashow model on the lattice
[DE88-705676] N89-23319

LAUNCH VEHICLES
Launch options for the future: Special report
[PB89-114268] N89-22637

LAUNCHERS
ICRF waveguide launcher research
[DE89-009151] N89-22791
LEAD ACID BATTERIES
Laboratory evaluation of advanced battery technologies for electric vehicle applications
[DE89-009810] N89-22814
LEADING EDGES
Flow over a leading edge with distributed roughness
[DFVLR-FB-88-45] N89-22581
Electro-impulse de-icing research: Fatigue and electromagnetic interference tests
[DOT/FAA/CT-88/27] N89-22594
LEAKAGE
Performance of all-metal demountable cryogenic seals at superfluid helium temperatures
[NASA-TM-102190] N89-22850
Annular honeycomb seals: Test results for leakage and rotordynamic coefficients; comparisons to labyrinth and smooth configurations N89-22899
LENNARD-JONES POTENTIAL
Physical properties of grain-boundary materials: Comparison of EAM (Embedded-Atom-Method) and central-force potentials
[DE89-007414] N89-23308
LIBRARIES
User needs and how to determine them N89-23365
LIE GROUPS
Cohomology theory and deformations of Z sub 2-graded Lie algebras
[DE88-705694] N89-23229
Nonlocal higher order symmetries for the Federbush model
[MEMO-740] N89-23250
LIFE (DURABILITY)
Technical evaluation report N89-22655
Environmental program on durability of graphite/epoxy honeycomb specimens with representative damage and repairs
[AR-005-504] N89-22685
Lightweight fibrous nickel electrodes for nickel-hydrogen batteries
[NASA-TM-101997] N89-22710
Acceleration test for aircraft low-pass filter
[PB89-116263] N89-22807
Laboratory evaluation of advanced battery technologies for electric vehicle applications
[DE89-009810] N89-22814
KOH concentration effect on the cycle life of nickel-hydrogen cells. 4: Results of failure analyse N89-23004
Asymptotically optimal nonparametric experimental design tests for the log linear model under censoring
[MEMO-727] N89-23262
Positron lifetime technique with applications in materials science
[ETN-89-94141] N89-23331
LIFE SCIENCES
JPRS report: Science and technology. USSR: Space
[JPRS-USP-88-003] N89-22622
LIFTING ROTORS
Development of stress and lifing criteria for single crystal turbine blades N89-22663
LIGHT (VISIBLE RADIATION)
Gamma ray laser pump diagnostic
[AD-A205221] N89-22883
LIGHT AMPLIFIERS
Development of an efficient high brightness Ti:Al2O3 laser amplifier
[AD-A204187] N89-22881
LIGHT EMISSION
Kilometric radiation power flux dependence on area of discrete aurora
[NASA-CR-184993] N89-23040
Optical studies of the magnetospheric cusp from Svalbard
[AD-A205432] N89-23044
LIGHT MODULATION
Organic and polymer crystalline films for spatial light modulation
[AD-A205906] N89-23350
LIGHT SCATTERING
Dynamic scattering from multicomponent polymer systems
[DE88-705677] N89-22752
Experimental observation of the nonlinear response of single bubbles to an applied acoustic field
[AD-A205191] N89-23271
LIGHTNING
Characteristics of winter lightning to high structures. Observation from December 1978 to March 1987
[DE88-756454] N89-23049
LIKELIHOOD RATIO
Smoothing and likelihood ratio for Gaussian boundary value processes
[MEMO-726] N89-23242
LINEAR ACCELERATORS
SUPERFISH accuracy dependence on mesh size
[DE89-007992] N89-22790
Beam research technical abstracts, 1987
[DE89-009013] N89-23282
LINEAR ARRAYS
Scan line array processors: Work in progress N89-23128
LINEAR ENERGY TRANSFER (LET)
Astronaut radiation exposure in low-earth orbit. Part 1: Galactic cosmic radiation
[AD-A204598] N89-23063
Effects of cosmic rays on single event upsets
[NASA-CR-184835] N89-23400
LINEAR EQUATIONS
Geometric camera calibration using systems of linear equations N89-23148
Geometrical interpretation of the bilinear equations for the KP-hierarchy
[MEMO-720] N89-23238
LINEAR SYSTEMS
On the stabilization of bilinear systems via constant feedback
[MEMO-706] N89-23215
Some local results for linear systems and implications for state variable feedback
[MATHS-RES-202] N89-23221
LINEAR TRANSFORMATIONS
The concept of an effective viewpoint N89-23131
LINEARIZATION
Acta Aeronautica et Astronautica Sinica (selected articles)
[AD-A205128] N89-22570
LIQUID CRYSTALS
Physical-chemical studies of solutions processing of nematic polymers
[AD-A205921] N89-22770
LIQUID HELIUM
Nature of condensation in the momentum space for an interacting Bose system
[DE88-705679] N89-23352
LIQUID HYDROGEN
Analysis of the nonvented fill of a 4.96-cubic-meter lightweight liquid hydrogen tank
[NASA-TM-102039] N89-22652
LIQUID INJECTION
Analysis of the nonvented fill of a 4.96-cubic-meter lightweight liquid hydrogen tank
[NASA-TM-102039] N89-22652
LIQUID PROPELLANT ROCKET ENGINES
Application of advanced materials for turbomachinery and rocket propulsion N89-22656
LITHIUM ALLOYS
Ab initio calculations of ordered intermetallic phase equilibria
[DE89-009974] N89-22741
LITHIUM COMPOUNDS
Advances in ambient temperature secondary lithium cells N89-23011
LITHIUM OXIDES
The electrochemical generation of useful chemical species from lunar materials N89-22990
LITHIUM SULFUR BATTERIES
Advanced batteries for electric vehicles
[DE89-009771] N89-22813
Advanced high-temperature batteries N89-23010
LOAD TESTING MACHINES
Single channel test controllers
[AD-A204088] N89-22611
LOADS (FORCES)
A theoretical study of fluid forces on a centrifugal impeller rotating and whirling in a vaned diffuser N89-22908
Influence of impeller shroud forces on turbopump rotor dynamics N89-22909
Ritz method for transient response in systems having unsymmetric stiffness N89-22954
A recursive formulation for flexible multibody dynamics N89-22968
LOCAL AREA NETWORKS
Implementation of the NETOS (Network Operating System) operated system in Ada with modifications to allow variable length messages
[AD-A202602] N89-23185
LOGIC DESIGN
Preliminary design of a programmed picture logic N89-23141
Specifying real-time systems with interval logic
[NASA-CR-181804] N89-23183
LOGIC PROGRAMMING
Preliminary design of a programmed picture logic N89-23141
LOGISTICS
Contributions of expert systems to logistics
[REPT-882-320-101] N89-23223
Microfilm and computer full text of archival documents
[AD-A204055] N89-23377
LONG TERM EFFECTS
Environmental program on durability of graphite/epoxy honeycomb specimens with representative damage and repairs
[AR-005-504] N89-22685
Spinodal decomposition of austenite in long-term-aged duplex stainless steel
[DE89-009827] N89-22737
LOW DENSITY MATERIALS
Low-density foams from macroporous epoxy gels
[DE89-004042] N89-22756
LOW FREQUENCIES
Calculation of low frequency vibrational resonances of submerged structures N89-22951
Low frequency resistance fluctuations in films of high temperature superconductors
[DE89-007489] N89-23310
LOW FREQUENCY BANDS
Theoretical investigation of EM wave generation and radiation in the ULF, ELF, and VLF bands by the electrodynamic orbiting tether
[NASA-CR-181560] N89-22780
LOW PASS FILTERS
Acceleration test for aircraft low-pass filter
[PB89-116263] N89-22807
LOW REYNOLDS NUMBER
An experimental investigation of a low Reynolds number turbulent boundary layer subject to an adverse pressure gradient N89-22834
Low Reynolds number calculation of turbulent channel flow: A general discussion
[AD-A205883] N89-22864
LOW SPEED WIND TUNNELS
The low-speed wind tunnel at DVFLR in Brunswick (Fed. Republic of Germany)
[DFVLR-MITT-88-25] N89-22619
LOW THRUST
Optimal low thrust trajectories for planetary capture
[AD-A202604] N89-22632
LOWER ATMOSPHERE
Gravity wave and turbulence studies using a high-resolution ST radar
[AD-A205592] N89-23046
LUBRICANTS
Formation of lubricating films at elevated temperatures from the gas phase
[PB89-129530] N89-22747
LUBRICATING OILS
Effects of lubrication on the performance of high speed spur gears
[NASA-TM-101969] N89-22919
LUMINESCENCE
Electronic structure of rare-earth luminescent centre in alkaline-earth sulphides
[DE88-705674] N89-23318
LUMINOSITY
Far infrared peculiar behavior of quasars
[DE88-705673] N89-23391
Optical and infrared observations of the nature and evolution of active galaxies N89-23395
LUMINOUS INTENSITY
Experimental observation of the nonlinear response of single bubbles to an applied acoustic field
[AD-A205191] N89-23271
LUNAR BASES
Comparison of solar photovoltaic and nuclear reactor power systems for a human-tended lunar observatory
[NASA-TM-102015] N89-23397
LUNAR EXPLORATION
Human exploration mission studies N89-22985
LUNAR OBSERVATORIES
Comparison of solar photovoltaic and nuclear reactor power systems for a human-tended lunar observatory
[NASA-TM-102015] N89-23397
LUNAR ROCKS
The electrochemical generation of useful chemical species from lunar materials N89-22990
LUTETIUM
Emission properties of europium-doped lanthanum and lutetium orthophosphate crystals for use in high temperature sensor applications
[DE89-008736] N89-23334
LYSOZYME
Novel protein crystal growth technology: Proof of concept
[NASA-CR-184959] N89-23306

M

MACH NUMBER
A fast spatial scanning combination emissive and Mach probe for edge plasma diagnosis
[DE89-009674] N89-23295

MACHINE LEARNING
TRIPLE: A multi-strategy machine learning approach to target recognition N89-23119
MACHINE TRANSLATION
The objectives and role of the Greek National Documentation Centre N89-23363
MAGELLANIC CLOUDS
Observational aspects of interacting galaxies N89-23385
MAGNESIUM OXIDES
Fracture toughness of MgCr2O4-based refractory composites
[DE89-009847] N89-22696
MAGNETIC BEARINGS
Magnetic bearing stiffness control using frequency band filtering N89-22910
Implementation of active magnetic bearings on advanced rocket engine turbopumps
[ETN-89-94365] N89-22929
MAGNETIC CIRCUITS
Experimental verification of an eddy-current bearing N89-22913
MAGNETIC EFFECTS
A magnetic damper for first mode vibration reduction in multimass flexible rotors N89-22911
MAGNETIC FIELDS
Development of magnetic field assisted melt stabilization with heat and mass transfer control in low pressure LEC growth of GaAs
[AD-A205185] N89-23313
Neutron scattering studies of magnetic excitations in La/sub 2-x/Sr/sub x/CuO
[DE89-008155] N89-23333
MAGNETIC FLUX
Investigation of the vacuum structure of the Georgi-Glashow model on the lattice
[DE88-705676] N89-23319
MAGNETIC PERMEABILITY
Evaluation, development, and characterization of superconducting materials for space application
[NASA-CR-184842] N89-23302
MAGNETIC STORMS
The response of thermospheric nitric oxide to an auroral storm N89-23031
MAGNETO-OPTICS
Parallel Optical Random Access Memory (PORAM)
[NASA-CR-4241] N89-22890
MAGNETOHYDRODYNAMIC FLOW
Spacecraft charge as a source of electrical power for spacecraft
[AD-A202621] N89-22649
MAGNETOHYDRODYNAMIC STABILITY
Effects of ion collisions on quasilinear heating by the current-driven ion cyclotron instability in the high latitude ionosphere
[AD-A202512] N89-23032
Anomalous cross-field velocities in a CIV laboratory experiment
[TRITA-EPP-88-06] N89-23289
Maximal bootstrap current tokamak equilibria in the first stability regime
[DE89-008201] N89-23291
Simulations of axisymmetric erosion in IFR-Transported beams
[AD-A205882] N89-23301
MAGNETOHYDRODYNAMICS
ITER equilibrium with bootstrap currents, lower hybrid current drive and fast wave current drive
[DE89-009676] N89-22810
Computation of lower hybrid, neutral beam and bootstrap currents in consistent MHD equilibria
[DE89-008892] N89-23292
A fluid FLR model of the magnetopause layer
[IRF-PREPRINT-109] N89-23299
MAGNETOPAUSE
A fluid FLR model of the magnetopause layer
[IRF-PREPRINT-109] N89-23299
MAINTENANCE
Transmission overhaul and replacement predictions using Weibull and renewel theory
[NASA-TM-102022] N89-22925
MALES
Benzodiazepines and caffeine: Effect on daytime sleepiness, performance, and mood
[AD-A205862] N89-23066
MAN ENVIRONMENT INTERACTIONS
An experimental environment and laboratory for studying human information processing in Naval Air ASW (Naval air antisubmarine warfare)
[AD-A204774] N89-23069
MAN MACHINE SYSTEMS
Model-based analysis and cooperative synthesis of control and display augmentation for piloted flight vehicles N89-22610
The Space Station Flight Telerobotic Servicer and the human
[NASA-TM-100615] N89-23068
MAN-COMPUTER INTERFACE
An experimental environment and laboratory for studying human information processing in Naval Air ASW (Naval air antisubmarine warfare)
[AD-A204774] N89-23069
Integration effort in knowledge-based vision techniques for the autonomous land vehicle program N89-23108
MANAGEMENT
Implementing security measures for computer-based security systems
[DE89-008995] N89-23072
MANAGEMENT METHODS
A programmatic approach to achieving data quality objectives
[DE89-008248] N89-23378
MANIFOLDS (MATHEMATICS)
On Hausdorff dimension of invariant manifolds of infinite-dimensional dynamic systems
[DE88-705628] N89-23227
MANIPULATORS
Control of free-flying space robot manipulator systems
[NASA-CR-184837] N89-22918
Configuration comparison analysis for the AFIT/AAMRL anthropomorphic robotic manipulator
[AD-A202618] N89-22921
Automatic generation of noncolliding trajectories and manipulation task planning in robotics
[LAAS-89-002] N89-23222
MANNED MARS MISSIONS
Future space projects discussed at Moscow Space F orum N89-22630
Human exploration mission studies N89-22985
MANNED SPACE FLIGHT
JPRS report: Science and technology. USSR: Space
[JPRS-USP-88-003] N89-22622
History of manned flight
[CNES-NT-121] N89-23405
MANNED SPACECRAFT
Glavkosmos official Yu. P. Semenov interviewed on development of USSR space program N89-22629
History of manned flight
[CNES-NT-121] N89-23405
MANUAL CONTROL
Model-based analysis and cooperative synthesis of control and display augmentation for piloted flight vehicles N89-22610
MANUFACTURING
Filament winding manufacturing of long fiber composite materials in thermoplastic matrix
[ETCA-87-R-047] N89-22699
MANY BODY PROBLEM
Physical properties of grain-boundary materials: Comparison of EAM (Embedded-Atom-Method) and central-force potentials
[DE89-007414] N89-23308
MAPPING
ALEXIS: A narrow-band survey/monitor of the ultrasoft X-ray sky
[DE89-007980] N89-22873
Interactive ultrasonic nondestructive evaluation
[AD-A204166] N89-22931
Ionospheric scintillation studies
[AD-A205210] N89-23034
Image understanding and robotics research at Columbia University N89-23083
Qualitative motion detection and tracking of targets from a mobile platform N89-23099
Information resources management N89-23371
CO in the galactic center: A complete survey of carbon monoxide emission in the inner 4 kpc of the Galaxy N89-23386
MAPS
Relative orientation N89-23149
Construction of harmonic maps between pseudo-Riemannian spheres and hyperbolic spaces
[DE88-705695] N89-23353
MARKETING
Development of advanced heat pump. Part 2: Preliminary test of two-stage compression heat pump
[DE88-756838] N89-22841
Increasing marketability and profitability of product line thru PATRAN and NASTRAN N89-22943
Identifying users and how to reach them N89-23370
MARKOV PROCESSES
Multimodal reconstruction and segmentation with Markov random fields and HCF optimization N89-23095
Statistical smoothing methods and image analysis
[AD-A205643] N89-23256
Thermal blooming threshold computations with a Markov model of velocity turbulence
[DE89-009709] N89-23285
MASERS
Kilometric radiation power flux dependence on area of discrete aurora
[NASA-CR-184993] N89-23040
MASS SPECTROSCOPY
Mass-spectroscopic measurements of stratospheric ions, trace gases and precondensation nuclei using balloon-borne measuring probes
[BPT-7/88] N89-23037
MASS TRANSFER
Turbulent transport in the solar nebula N89-22829
Heat transfer and pressure drop measurements in an air/molten salt direct-contact heat exchanger
[DE89-000837] N89-22843
Development of magnetic field assisted melt stabilization with heat and mass transfer control in low pressure LEC growth of GaAs
[AD-A205185] N89-23313
MASSIVELY PARALLEL PROCESSORS
MIT progress in understanding images N89-23075
Image understanding research at GE N89-23085
Parallel hardware for constraint satisfaction N89-23127
Pyramid algorithms implementation on the connection machine N89-23129
Factoring very large numbers using a massively parallel computer
[DE89-008198] N89-23208
MATCHING
An integrated approach to stereo matching, surface reconstruction and depth segmentation using consistent smoothness assumptions N89-23092
Affine invariant matching N89-23103
Contour correspondences in dynamic imagery N89-23109
MATERIALS RECOVERY
Innovation in separation technology for fine gravity semi-products
[PB89-112478] N89-22719
Processing and properties of advanced aluminum alloys
[AD-A205187] N89-22725
The electrochemical generation of useful chemical species from lunar materials N89-22990
MATHEMATICAL MODELS
Acta Aeronautica et Astronautica Sinica (selected articles)
[AD-A205128] N89-22570
Rectangular nozzle plume velocity modeling for use in jet noise prediction
[NASA-TM-102047] N89-22577
Aerodynamic detuning of a loaded airfoil cascade in an incompressible flow by a locally analytical method N89-22588
Orbital debris environment for spacecraft designed to operate in low Earth orbit
[NASA-TM-100471] N89-22638
Spacecraft charge as a source of electrical power for spacecraft
[AD-A202621] N89-22649
Numerical model of solar dynamic radiator for parametric analysis
[NASA-TM-102054] N89-22653
Solution of multi-center molecular integrals of Slater-type orbitals
[NASA-TM-101545] N89-22692
Damage development, property degradation and life prediction in composite laminates N89-22708
Locating pitting sites from propagating surface potential transients
[DE89-006171] N89-22730
Simulation of a refrigerant evaporator
[ETN-89-94133] N89-22776
Verification and limitations of the monostatic-bistatic radar cross section derived by Keil
[AD-A202601] N89-22782
Approximation technique for determining gain and radiation pattern of the horn antenna
[DE89-006136] N89-22786
Special techniques used for time domain, three dimensional finite element modeling of electromagnetics
[DE89-007227] N89-22789
Development of behaviorist models to simulate commuted power switches
[ISAL-88-0065] N89-22815
Low-dimensional chaos in turbulence N89-22822
Direct simulation of compressible reacting flows N89-22828
Turbulent transport in the solar nebula N89-22829
Transition to turbulence in laminar hypersonic flow N89-22830
Direct numerical simulations of turbulent convection with a variable gravity and Keplerian rotation N89-22831
The propagation of noise through streak systems
[DE89-006600] N89-22869

Rotordynamic Instability Problems in High-Performance Turbomachinery, 1988
[NASA-CP-3026] N89-22891
A seal test facility for the measurement of isotropic and anisotropic linear rotordynamic characteristics
N89-22905
A magnetic damper for first mode vibration reduction in multimass flexible rotors N89-22911
Incorporating general race and housing flexibility and deadband in rolling element bearing analysis
N89-22912
Enhanced rotor modeling tailored for rub dynamic stability analysis and simulation N89-22916
Dynamic fracture in solids
[PB89-112650] N89-22937
Using Patran and Supertab as pre- and postprocessors to COSMIC/NASTRAN N89-22942
Recent advances in modeling creep crack growth
[W-2/88] N89-22964
On the semi-elliptical surface crack problem: Detailed numerical solutions for complete elastic stress fields
[FFA-TN-1988-74] N89-22965
Remote sensing of earth terrain
[NASA-CR-184937] N89-22971
Comparison of a cavity solar receiver numerical model and experimental data
[DE89-003609] N89-23016
The long-term climate change assessment task of the Hanford Site, Washington, Protective Barrier Development Program
[DE89-008704] N89-23030
Preliminary results of the MLAM (Multi-Layer Air Mass) Lagrangian transport model simulation of ANATEX (Across North America Tracer Experiment)
[DE89-008123] N89-23036
Retrieving the distribution of liquid water content in clouds from observations of thermal microwave radiation
N89-23056
A new perspective in the etiology, treatment, prevention and prediction of space motion sickness
[AD-A205660] N89-23065
Image understanding research at GE N89-23085
Perception with feedback N89-23098
Constructing simple stable descriptions for image partioning N89-23104
Three-dimensional object recognition using surface descriptions N89-23105
Generic models for robot navigation N89-23112
Mathematical morphology and the morphological sampling theorem N89-23113
Robust parallel computation of 2-D model-based recognition N89-23130
Modeling sensors and applying sensor model to automatic generation of object recognition program
N89-23136
Rapid object recognition from a large model base using prediction hierarchies N89-23137
Algebraic reasoning in view consistency and parameterized model matching problems N89-23139
An introduction to generalized stereo techniques
N89-23142
Extracting generic shapes using model-driven optimization N89-23161
Texture models and image measures for segmentation
N89-23162
Modal driven edge detection N89-23163
Generation of face-edge-vertex models directly from images N89-23166
On the recovery of superellipsoids N89-23168
Automating the identification of structural model parameters
[DE89-006327] N89-23194
Contributions of expert systems to logistics
[REPT-682-320-101] N89-23223
Molecular dynamics and irreversibility, from Boltzmann to Nose
[DE89-006740] N89-23274
Thermal blooming threshold computations with a Markov model of velocity turbulence
[DE89-009709] N89-23285
A quiver kinetic formulation of radio frequency heating and confinement in collisional edge plasmas
[DE89-009675] N89-23296

MATRICES (MATHEMATICS)
A new modified cholesky factorization
[AD-A205174] N89-23191
Reduction of a general matrix to tridiagonal form using a hypercube multiprocessor
[DE89-008721] N89-23197
A pseudo singular value decomposition and inner functions in super optimal control
[OUEL-1738/88] N89-23214
Nonlinear optimization involving polynomial matrices and their generalized inverses
[AD-A202620] N89-23224

MATRIX MATERIALS
High temperature composite materials for rocket propulsion N89-22676

MATTER (PHYSICS)
Two dimensional (4,0) supergravity in harmonic superspace. The action and the matter couplings
[DE88-705661] N89-23351

MAXWELL EQUATION
General grid finite difference methods for time dependent electromagnetic problems in two dimensions
[DE89-007225] N89-22788
Special techniques used for time domain, three dimensional finite element modeling of electromagnetics
[DE89-007227] N89-22789
Finite element modeling of electromagnetic fields and waves using NASTRAN N89-22950

MEASURE AND INTEGRATION
Implementation of comparative probability by Gleason measures: Infinite dimensional case
[DE88-705683] N89-23259

MEASURING INSTRUMENTS
Nondestructive evaluation of stress using ultrasound and pulsed heat
[AD-A205176] N89-22932
Acoustic wave device using plate modes with surface-parallel displacement
[DE89-009719] N89-23273
A programmatic approach to achieving data quality objectives
[DE89-008248] N89-23378

MECHANICAL PROPERTIES
Tests of new materials with second generation carbon fibers, test report
[REPT-47-188/F] N89-22702
CSPC test 319.30: Study on impact tolerance of preimpregnated carbon-epoxy systems
[REPT-47-323/F] N89-22703
Fracture toughness and mechanical behavior of steel and aluminum alloys
[ETCA-87-R-090] N89-22743
Configuration comparison analysis for the AFIT/AAMRL anthropomorphic robotic manipulator
[AD-A202618] N89-22921
Finite element analysis of a micromechanical deformable mirror device N89-22953
The project ASKA-SPACE, phase 1 — finite element method
[ETN-89-93768] N89-22959
Grain boundary sliding phenomena in polycrystalline solids
[DE89-007792] N89-23326

MELTING
Melting behavior of heavy metal batch components
[ETN-89-93986] N89-22734
Grain-boundary and free-surface induced thermodynamic melting: A molecular dynamics study in silicon
[DE89-007415] N89-23309
Growth kinetics of grain-boundary induced melting: A molecular-dynamics study
[DE89-009855] N89-23343

MELTS (CRYSTAL GROWTH)
Development of magnetic field assisted melt stabilization with heat and mass transfer control in low pressure LEC growth of GaAs
[AD-A205185] N89-23313

MEMBRANE STRUCTURES
The application of Dow Chemical's perfluorinated membranes in proton-exchange membrane fuel cells
N89-22995

MEMBRANES
An assessment of the optical performance of stretched-membrane mirror modules
[DE88-017347] N89-23015

MEMORY (COMPUTERS)
MIRAP, microcomputer reliability analysis program
[DE89-009749] N89-23200

MENTAL PERFORMANCE
Consensus theory in expert systems: An adaptive inference framework and application to image understanding
[AD-A204253] N89-23188

MESOSPHERE
Gravity wave and turbulence studies using a high-resolution ST radar
[AD-A205592] N89-23046

MESSAGE PROCESSING
Implementation of the NETOS (Network Operating System) operated system in Ada with modifications to allow variable length messages
[AD-A202602] N89-23185

METAL AIR BATTERIES
Laboratory evaluation of advanced battery technologies for electric vehicle applications
[DE89-009810] N89-22814
Technology base research project for electrochemical energy storage
[DE89-008860] N89-23019

METAL COATINGS
Interaction of coatings with base metals at high temperature N89-22669

METAL COMBUSTION
Ignition characteristics of the iron-based alloy UNS S66286 in pressurized oxygen
[NASA-CR-183612] N89-22722

METAL FIBERS
Fiber reinforced superalloys for rocket engines
N89-22673

METAL FILMS
Corrosion monitoring with acoustic wave devices
[DE89-005235] N89-22728

METAL MATRIX COMPOSITES
Material/manufacturing process interaction in advanced material technologies N89-22662
The isothermal fatigue behavior of a unidirectional SiC/Ti composite and the Ti alloy matrix
[NASA-TM-101984] N89-22684
Investigation and synthesis of high temperature and increased stiffness RSP aluminum alloys
[AD-A204162] N89-22723

METAL OXIDE SEMICONDUCTORS
Development of behaviorist models to simulate commuted power switches
[ISAL-88-0065] N89-22815
Effects of cosmic rays on single event upsets
[NASA-CR-184835] N89-23400

METAL OXIDES
Melting behavior of heavy metal batch components
[ETN-89-93986] N89-22734

METAL SURFACES
Mechanisms of crevice corrosion in chlorinated environments
[AD-A204621] N89-22724
Ion-induced kinetic electron emission on clean and gas coated metal surfaces
[JUEL-2201] N89-22732
Reconstruction and relaxation of metal surfaces
[JUEL-2213] N89-22733

METALLIC GLASSES
Melting behavior of heavy metal batch components
[ETN-89-93986] N89-22734

METALLOGRAPHY
Metallurgical study of superalloy brazing alloys
N89-22680
Tribological characterization of 15 surface treatments for aluminum alloys
[ETCA-87-R-132] N89-22928

METALS
Mechanisms of crevice corrosion in chlorinated environments
[AD-A204621] N89-22724
Locating pitting sites from propagating surface potential transients
[DE89-006171] N89-22730
Diagnostics of phase formation in metastable solidification of metals
[DFVLR-FB-88-43] N89-22745
Predicting material classes N89-23177

METASTABLE STATE
Development of metastable processing paths for high temperature alloys
[AD-A202614] N89-22721
Diagnostics of phase formation in metastable solidification of metals
[DFVLR-FB-88-43] N89-22745
Compact, lightweight CO2 lasers for SDIO applications
[AD-A204300] N89-22882
Molecular beam epitaxial growth and characterization of metastable compound semiconductors for infrared detector applications
[AD-A205175] N89-23312

METEOROLOGICAL PARAMETERS
Characteristics of winter lightning to high structures. Observation from December 1978 to March 1987
[DE88-756454] N89-23049

METEOROLOGICAL RADAR
Coherent polarimetric radar techniques for microwave propagation and cloud physics research
[DFVLR-FB-88-47] N89-22800

METEOROLOGICAL SERVICES
Climatological and statistical fundamentals for the explanation of climate data processing
[ETN-89-93775] N89-23051

METEOSAT SATELLITE
Second generation Meteosat pre-phase A system study
[BA-SGM-FR-01] N89-22640

METHOD OF MOMENTS
Turbulence modeling N89-22819

METHYL ALCOHOL
Survey of development trends of methanol automobiles and methanol fuel in China
[DE88-756492] N89-22771
METHYL COMPOUNDS
Inhalation developmental toxicology studies: Teratology study of methyl ethyl ketone in mice
[DE89-009563] N89-23062
MICROANALYSIS
Electron energy-loss spectroscopy: Fundamentals and applications in the characterization of minerals
[DE89-006613] N89-23307
MICROBURSTS (METEOROLOGY)
Hazard index calculation for 31 May 1984 microburst at Erie, Colorado
[NASA-CR-184968] N89-23048
MICROCOMPUTERS
Microcomputer based controller for the Langley 0.3-meter Transonic Cryogenic Tunnel
[NASA-CR-181808] N89-22616
MIRAP, microcomputer reliability analysis program
[DE89-009749] N89-23200
MICROHARDNESS
Role of aluminium concentration on the structure behaviour of Cu-Al alloys
[DE88-705647] N89-22727
The effect of boron on microhardness in Ni3Al polycrystals
[DE89-009124] N89-23335
MICROMECHANICS
Finite element analysis of a micromechanical deformable mirror device N89-22953
MICROPROCESSORS
A signal processing system using MC68000 and TMS320 microprocessors
[USIP-88-07] N89-22803
MICROSTRUCTURE
The effects of plastic media blasting paint removal on the microstructure of graphite/epoxy composite materials
[AD-A204801] N89-22688
Behavior of iron aluminides in oxidizing and sulfidizing environments
[DE89-008919] N89-22693
Observations on the toughening of Al2O3-SiC composites
[DE89-009643] N89-22695
Fracture toughness of MgCr2O4-based refractory composites
[DE89-009647] N89-22696
Internal stresses in ceramic composite constituents determined by neutron diffraction technique
[DE89-009883] N89-22697
Atomic imaging of Au/Ni multilayers
[DE89-009903] N89-22698
Development of metastable processing paths for high temperature alloys
[AD-A202614] N89-22721
Processing and properties of advanced aluminum alloys
[AD-A205187] N89-22725
Microstructural studies of IAD and PVD Cr coatings by cross section transmission electron microscopy
[DE89-009877] N89-22739
Effects of X-rays on isotactic polypropylene. Volume 2: Polymers and ceramics
[DE88-705606] N89-22751
Transmission electron microscopy: Imaging of materials
[DE89-007418] N89-22870
Evaluation, development, and characterization of superconducting materials for space application
[NASA-CR-184842] N89-23302
Low frequency resistance fluctuations in films of high temperature superconductors
[DE89-007489] N89-23310
Grain boundary sliding phenomena in polycrystalline solids
[DE89-007792] N89-23326
MICROWAVE FREQUENCIES
Coherent polarimetric radar techniques for microwave propagation and cloud physics research
[DFVLR-FB-88-47] N89-22800
Fiber optic laser rod
[DE89-009598] N89-22887
MICROWAVE LANDING SYSTEMS
Pre and post modification electromagnetic compatibility test report for the C-130H self contained navigation system with MLS A-kit, revision
[AD-A205167] N89-22604
MICROWAVE RADIOMETERS
Retrieving the distribution of liquid water content in clouds from observations of thermal microwave radiation N89-23056
Remote sensing of oceanic rainrates by passive microwave sensors: A statistical-physical approach N89-23057
MICROWAVE SENSORS
Remote sensing of earth terrain
[NASA-CR-184937] N89-22971
Remote sensing of oceanic rainrates by passive microwave sensors: A statistical-physical approach N89-23057
MICROWAVES
Microwave sintering of boron carbide
[DE89-009652] N89-22763
MIE SCATTERING
Retrieving the distribution of liquid water content in clouds from observations of thermal microwave radiation N89-23056
Mie scattering calculations for heat radiation
[FOA-C-20738-2.1] N89-23279
MILITARY OPERATIONS
A multinational verification satellite: A preliminary investigation — arms control
[FOA-C-10312-9.3] N89-22974
Transitional strategic defense architectures
[DE89-008312] N89-23265
MILITARY SPACECRAFT
Space control: A national imperative
[AD-A202612] N89-22631
MILITARY TECHNOLOGY
The status of defence information programs in Greece N89-23364
Sources of information N89-23366
MILKY WAY GALAXY
CO in the galactic center: A complete survey of carbon monoxide emission in the inner 4 kpc of the Galaxy N89-23386
MINERAL OILS
Formation of lubricating films at elevated temperatures from the gas phase
[PB89-129530] N89-22747
MIRRORS
Finite element analysis of a micromechanical deformable mirror device N89-22953
An assessment of the optical performance of stretched-membrane mirror modules
[DE88-017347] N89-23015
Machine reference mirror inspection by optical Fabry-Perot cavity testing
[DE89-009635] N89-23284
MISALIGNMENT
Topology of modified helical gears and Tooth Contact Analysis (TCA) program
[NASA-CR-4224] N89-22920
MISSILE CONFIGURATIONS
Transonic and supersonic wind tunnel tests on control effectiveness on schematic missile configurations with canard controls
[FFA-TN-1988-11] N89-22601
Transonic and supersonic wind tunnel tests on control effectiveness on schematic missile configuration with canard control
[FFA-TN-1988-11-SUPPL] N89-22613
MISSILE CONTROL
Transonic and supersonic wind tunnel tests on control effectiveness on schematic missile configurations with canard controls
[FFA-TN-1988-11] N89-22601
Transonic and supersonic wind tunnel tests on control effectiveness on schematic missile configuration with canard control
[FFA-TN-1988-11-SUPPL] N89-22613
MISSION PLANNING
Future space projects discussed at Moscow Space F orum N89-22630
Human exploration mission studies N89-22985
MIXING
Conductivity fluctuations in mixed Na/Ca beta alumina
[AD-A205416] N89-23348
MIXING LAYERS (FLUIDS)
Direct numerical simulation of compressible free shear flows
[AIAA-89-0374] N89-22827
The effects of stabilizing and destabilizing longitudinal curvature on the structure of turbulent, two-stream mixing layers N89-22833
Inviscid spatial stability of a compressible mixing layer. Part 2: The flame sheet model
[NASA-CR-181815] N89-22837
MODAL RESPONSE
Modal strain energies in COSMIC NASTRAN N89-22955
MODELS
Models for surface intermediates in CO hydrogenation
[DE89-004348] N89-22712
MODES (STANDING WAVES)
The radiation performance of offset reflector antennas with horn feeds excited by high order modes
[FI-454-TB-43] N89-22792
MODULATORS
Distortions caused by the signal processing in analog AM modulators
[DE88-705657] N89-22785
MOISTURE CONTENT
Influence of conditioning on the trapezoidal fatigue behavior of a carbon epoxy composite
[ETCA-87-R-052] N89-22700
Retrieving the distribution of liquid water content in clouds from observations of thermal microwave radiation N89-23056
MOLECULAR BEAM EPITAXY
Molecular beam epitaxial growth and characterization of metastable compound semiconductors for infrared detector applications
[AD-A205175] N89-23312
MOLECULAR CLOUDS
CO in the galactic center: A complete survey of carbon monoxide emission in the inner 4 kpc of the Galaxy N89-23386
MOLECULAR DIFFUSION
Efficacy of conventional and high-frequency ventilation at altitude
[AD-A205922] N89-23071
Organic and polymer crystalline films for spatial light modulation
[AD-A205906] N89-23350
MOLECULAR ORBITALS
Solution of multi-center molecular integrals of Slater-type orbitals
[NASA-TM-101545] N89-22692
MOLECULES
Reactions of inorganic high polymers as a route to tailored solids
[AD-A204602] N89-22750
MOLTEN SALT ELECTROLYTES
A survey of advanced battery systems for space applications N89-22986
The electrochemical generation of useful chemical species from lunar materials N89-22990
MOLYBDENUM ALLOYS
Behavior of tungsten, molybdenum and alloys under unusual heating conditions N89-22674
MOMENTUM
Nature of condensation in the momentum space for an interacting Bose system
[DE88-705679] N89-23352
MOMENTUM TRANSFER
Application of the Ornstein-Zernike formalism to polymer and copolymer blends
[DE88-705686] N89-22753
MONITORS
Evaluation of several state-of-charge algorithms
[DE89-009752] N89-22812
ALEXIS: A narrow-band survey/monitor of the ultrasoft X-ray sky
[DE89-007980] N89-22873
The new experimental areas oxygen monitor
[DE89-009700] N89-22876
MONOMERS
Dynamic scattering from multicomponent polymer systems
[DE88-705677] N89-22752
MONOTONE FUNCTIONS
Second-order accurate nonoscillatory schemes for scalar conservation laws
[NASA-TM-102010] N89-22573
Monotonicity-preserving quadratic C sup 1-spline interpolation to scattered data
[MEMO-744] N89-23252
MONTE CARLO METHOD
Monte Carlo applied to resonance scattering of high altitude fluorescent radiation
[DE89-006519] N89-23035
Monte Carlo approximations in Bayesian decision theory. Part 3: Limiting behavior of Monte Carlo approximations
[AD-A204173] N89-23258
The multigroup and cylindrical geometry formulation of the Sn Monte Carlo hybrid method
[DE89-000326] N89-23260
Possibility of operation of high temperature superconducting YBa2Cu307 ceramics in cyclotrons at irradiation
[DE88-705783] N89-23325
MORPHOLOGY
Atomic imaging of Au/Ni multilayers
[DE89-009903] N89-22698
Corrosion of iron, nickel and cobalt based alloys in high temperature environments contaminated with chlorine
[DE89-009829] N89-22738
Mathematical morphology and the morphological sampling theorem N89-23113

Far infrared peculiar behavior of quasars
[DE88-705673] N89-23391
A historical interpretation of the study of the visible cloud morphology on the planet Jupiter: 1610-1878 N89-23398

MOSAICS
Integration of tie-points in digital mosaicing
[ETN-89-94147] N89-22973

MOTION PERCEPTION
Dynamic image interpretation for autonomous vehicle navigation
[AD-A204167] N89-22597
USC image understanding research: 1987-1988 N89-23076
Image understanding and robotics research at Columbia University N89-23083
Using flow field divergence for obstacle avoidance in visual navigation N89-23120
Computation of motion in depth parameters: A first step in stereoscopic motion interpretation N89-23153
Is correspondence necessary for the perception of structure from motion N89-23154
Recognizing animal motion N89-23156
A real time hierarchical model for optic flow determination via spatiotemporal frequency channels N89-23158

MOTION PICTURES
Cavitation effects on the pressure distribution of a squeeze film damper bearing N89-22697

MOTORS
Experimental verification of an eddy-current bearing N89-22913

MULTIPROCESSING (COMPUTERS)
Control of free-flying space robot manipulator systems
[NASA-CR-184837] N89-22918
Developing software to use parallel processing effectively
[AD-A205184] N89-23192
Reduction of a general matrix to tridiagonal form using a hypercube multiprocessor
[DE89-008721] N89-23197
Expert systems on multiprocessor architectures, phase II
[AD-A204907] N89-23206

MULTISENSOR APPLICATIONS
Fusion of multisensor data: A summary of the JASMIN project
[FOA-C-30498-3.3] N89-23213

MULTISTATIC RADAR
Verification and limitations of the monostatic-bistatic radar cross section derived by Kell
[AD-A202601] N89-22782

N

NAMING
Criteria for selection of phase names for oxides
[NPL-DMA(A)169] N89-22714

NASA PROGRAMS
Earth system science: A program for global change
[NASA-TM-101186] N89-22969

NASA SPACE PROGRAMS
Human exploration mission studies N89-22985
Agreement on the International Space Station and Columbus Program
[REPT-34/88] N89-23360
History of manned flight
[CNES-NT-121] N89-23405

NASTRAN
Damage initiation in two-dimensional, woven, carbon-carbon composites
[AD-A202617] N89-22683
Seventeenth NASTRAN (R) Users' Colloquium
[NASA-CP-3029] N89-22940
Improved performance in NASTRAN (R) N89-22941
Using Patran and Supertab as pre- and postprocessors to COSMIC/NASTRAN N89-22942
Increasing marketability and profitability of product line thru PATRAN and NASTRAN N89-22943
The use of COSMIC NASTRAN in an integrated conceptual design environment N89-22944
A NASTRAN/TREETOPS solution to a flexible, multi-body dynamics and controls problem on a UNIX workstation N89-22945
Enhancements to the IBM version of COSMIC/NASTRAN N89-22946
A powerful enhancement to the DMAP alter capability N89-22947
A NASTRAN DMAP alter for linear buckling analysis under dynamic loading N89-22948
Improvements to the CONTINUE feature in transient analysis N89-22949
Finite element modeling of electromagnetic fields and waves using NASTRAN N89-22950
Calculation of low frequency vibrational resonances of submerged structures N89-22951
Power flows and Mechanical Intensities in structural finite element analysis N89-22952
Ritz method for transient response in systems having unsymmetric stiffness N89-22954
Modal strain energies in COSMIC NASTRAN N89-22955
Definition of NASTRAN sets by use of parametric geometry N89-22956

NATIONAL AIRSPACE SYSTEM
National airspace system plan: Facilities, equipment, associated development and other capital needs
[AD-A202615] N89-22596

NATIONAL AIRSPACE UTILIZATION SYSTEM
National airspace system plan: Facilities, equipment, associated development and other capital needs
[AD-A202615] N89-22596

NAVIER-STOKES EQUATION
Numerical simulation of viscous vortex rings N89-22824
Non-linear evolution of a second mode wave in supersonic boundary layers
[NASA-CR-181811] N89-22836
Computational fluid dynamics research in three-dimensional zonal techniques
[NASA-CR-181406] N89-22838
Multigrid for the steady-state incompressible Navier-Stokes equation: A survey
[GMD-322] N89-22846
The Large Eddy Simulation (LES) of MESOSCOP for atmospheric boundary layer flows including passive scalars
[DFVLR-MITT-88-28] N89-23041

NEAR INFRARED RADIATION
Far- and mid-infrared properties of metal-insulator composite materials
[AD-A204914] N89-22689

NETWORK ANALYSIS
Study of a wideband telecommunications satellite for Europe
[ATES/DMA/TRM/162-86] N89-22641

NEUMANN PROBLEM
Incorporation of a boundary condition to numerical solution of POISSON's equation
[DE89-007132] N89-23231

NEURAL NETS
Algorithms and architectures for smart sensing N89-23090
Systolic implementation of neural networks
[DE89-008031] N89-23210

NEUTRAL BEAMS
Computation of lower hybrid, neutral beam and bootstrap currents in consistent MHD equilibria
[DE89-008892] N89-23292

NEUTRINOS
Neutrino helicity flips via electroweak interactions and SN1987a
[NIKHEF-H/88-18] N89-23278

NEUTRON SCATTERING
Neutron scattering studies of magnetic excitations in La/sub 2-x/Sr/sub x/CuO
[DE89-008155] N89-23333

NEUTRONS
Observational techniques for solar flare gamma-rays, hard X-rays, and neutrons
[NASA-CR-184910] N89-23399

NICKEL
Precipitation of Ar, Kr and Xe in Ni at room temperature
[DE89-009879] N89-22713
Mechanisms of cascade collapse
[DE89-009862] N89-22740
A calorimetric-based comparison of gas tungsten and plasma arc welding processes
[DE89-008712] N89-22924
ESE (Electron Spin Echo) and CW-ESR studies of synthetic diamond crystals: Distribution of nitrogen and nickel
[DE89-007373] N89-23314

NICKEL ALLOYS
New metallic materials for gas turbines N89-22680
Material/manufacturing process interaction in advanced material technologies N89-22662
Interaction of coatings with base metals at high temperature N89-22669
Vacuum plasma spray coating N89-22670
Atomic imaging of Au/Ni multilayers
[DE89-009903] N89-22698
Temperature effects on the break-in of nickel aluminide alloys
[DE89-005341] N89-22729
Corrosion of iron, nickel and cobalt based alloys in high temperature environments contaminated with chlorine
[DE89-009829] N89-22738
The effect of boron on microhardness in Ni3Al polycrystals
[DE89-009124] N89-23335

NICKEL CADMIUM BATTERIES
Overview of battery usage in NASA/GSFC LEO and GEO missions N89-22983
The importance of batteries in unmanned missions N89-22984
Impedance studies of Ni/Cd and Ni/H cells using the cell case as reference electrode N89-23002

NICKEL HYDROGEN BATTERIES
Lightweight fibrous nickel electrodes for nickel-hydrogen batteries
[NASA-TM-101997] N89-22710
The importance of batteries in unmanned missions N89-22984
A new concept for high-cycle-life LEO: Rechargeable MnO2-hydrogen N89-22991
Characterization testing of a 40 Ahr bipolar nickel hydrogen battery N89-22992
Impedance studies of Ni/Cd and Ni/H cells using the cell case as reference electrode N89-23002
KOH concentration effect on the cycle life of nickel-hydrogen cells. 4: Results of failure analyse N89-23004
Nickel-hydrogen capacity loss on storage N89-23007
Hydrogen embrittlement in nickel-hydrogen cells N89-23008

NICKEL IRON BATTERIES
Laboratory evaluation of advanced battery technologies for electric vehicle applications
[DE89-009610] N89-22814

NIOBIUM ALLOYS
Ductility enhancement in unreacted internal-Sn Nb3Sn through low-temperature anneals
[DE89-009125] N89-23336

NIOBIUM COMPOUNDS
The half-metallic ferromagnetic NiMnSb: A positron-annihilation study
[ECN-209] N89-23269

NIOBIUM OXIDES
Coating of silicon carbide fibers
[CERT-423900/RF] N89-22767

NITRIC OXIDE
The response of thermospheric nitric oxide to an auroral storm N89-23031

NITRIDING
Wear protection coatings and treatments for the TA6V alloy
[ETCA-88-R-003] N89-22742

NITROGEN
Formation of lubricating films at elevated temperatures from the gas phase
[PB89-129530] N89-22747
ESE (Electron Spin Echo) and CW-ESR studies of synthetic diamond crystals: Distribution of nitrogen and nickel
[DE89-007373] N89-23314

NITROGEN COMPOUNDS
Carbonaceous film coating
[DE89-009592] N89-22762

NITROGEN OXIDES
Investigation of low NOx staged combustor concept in high-speed civil transport engines
[NASA-TM-101977] N89-22606
Coupling of a chemiluminescence detector with a gas chromatograph for the selective measurement of oxidized nitrogen bonds in the atmosphere
[JUEL-2217] N89-23029

NOCTURNAL VARIATIONS
Radiative cooling in the nocturnal boundary layer
[KNMI-WR-88-05] N89-23054

NOISE GENERATORS
Environmental noise characteristics of the MOD5-B (3.2 MW) wind turbine generator
[NASA-TM-101567] N89-23272

NOISE INTENSITY
Current and thermal noise in mixed Na/Ag beta alumina
[AD-A205869] N89-22816
Effects of lubrication on the performance of high speed spur gears
[NASA-TM-101989] N89-22919
Comparison of measured and calculated sound pressure levels around a large horizontal axis wind turbine generator
[NASA-TM-100654] N89-23270

NOISE MEASUREMENT
Current and thermal noise in mixed Na/Ag beta alumina
[AD-A205869] N89-22816
Comparison of measured and calculated sound pressure levels around a large horizontal axis wind turbine generator
[NASA-TM-100654] N89-23270

Environmental noise characteristics of the MOD5-B (3.2 MW) wind turbine generator
[NASA-TM-101567] N89-23272

NOISE POLLUTION
Comparison of measured and calculated sound pressure levels around a large horizontal axis wind turbine generator
[NASA-TM-100654] N89-23270

NOISE PREDICTION (AIRCRAFT)
Rectangular nozzle plume velocity modeling for use in jet noise prediction
[NASA-TM-102047] N89-22577

NOISE PROPAGATION
The propagation of noise through streak systems
[DE89-006600] N89-22869

NOISE SPECTRA
Application of electrochemical noise spectral analysis to the study of the pitting corrosion of aluminum alloys
[ETCA-87-R-102] N89-22744
Cavitation in a submerged jet at constant pressure
[OUEL-1658/88] N89-22848

NOISE TOLERANCE
Evaluation of the ride quality of a light twin engine airplane using a ride quality meter
[NASA-TP-2913] N89-22568

NONAQUEOUS ELECTROLYTES
Preparation, characterization and performance of MoS3 as an active cathode material
[AD-A205866] N89-22717

NONDESTRUCTIVE TESTS
Ultrasonic detection of damage in carbon epoxy composite materials
[ONERA-RT-3/7256-RY-071-R] N89-22705
Interactive ultrasonic nondestructive evaluation
[AD-A204166] N89-22931
Nondestructive evaluation of stress using ultrasound and pulsed heat
[AD-A205176] N89-22932
Multifrequency eddy current testing, optimization of the method for steam generator testing. Phase 2: Nonlinear description of signal location curves dynamics of the signal location curves
[REPT-880142-TW] N89-22933
Reconstruction of defects from amplitude location curves
[REPT-780852-TW] N89-22934
NDT results for comparability program SPF/DB
[I-264/88] N89-22935
Signal treatment and data analysis methods applied to nondestructive control of adhesive bonded joints
[ISAL-IDI-8809] N89-22936

NONLINEAR EQUATIONS
Asymptotic expansions with error bounds for solutions of difference equations of level 1 sup +
[MEMO-724] N89-23241

NONLINEAR FEEDBACK
The local disturbance decoupling problem with stability for nonlinear systems
[MEMO-721] N89-23217

NONLINEAR SYSTEMS
Interactive ultrasonic nondestructive evaluation
[AD-A204166] N89-22931
Parallel processors and nonlinear structural dynamics algorithms and software
[NASA-CR-184938] N89-23184
The local disturbance decoupling problem with stability for nonlinear systems
[MEMO-721] N89-23217
On the use of stable distributions in design programs
[MEMO-736] N89-23219
Organic and polymer crystalline films for spatial light modulation
[AD-A205906] N89-23350

NONLINEARITY
Acta Aeronautica et Astronautica Sinica (selected articles)
[AD-A205128] N89-22570
A general non-linear dynamical theory of elastic curved beams N89-22930
Nonlinear optimization involving polynomial matrices and their generalized inverses
[AD-A202620] N89-23224
Nonlinear finite element simulation of the large angle motion of flexible bodies
[DE89-006505] N89-23230
Experimental observation of the nonlinear response of single bubbles to an applied acoustic field
[AD-A205191] N89-23271

NONOSCILLATORY ACTION
Second-order accurate nonoscillatory schemes for scalar conservation laws
[NASA-TM-102010] N89-22573

NONPARAMETRIC STATISTICS
Statistical smoothing methods and image analysis
[AD-A205643] N89-23256

NORMAL DENSITY FUNCTIONS
Smoothing and likelihood ratio for Gaussian boundary value processes
[MEMO-726] N89-23242

NOZZLE DESIGN
Supersonic particle probes: Measurement of internal wall losses
[AD-A205863] N89-22589
Numerical study of a multipurpose transonic wind tunnel with an adaptable injection-suction system N89-22621
High temperature composite materials for rocket propulsion N89-22676

NOZZLE FLOW
Rectangular nozzle plume velocity modeling for use in jet noise prediction
[NASA-TM-102047] N89-22577

NUCLEAR AUXILIARY POWER UNITS
Power supply in space N89-22627

NUCLEAR FUSION
Fusion power: Expected environmental characteristics and status of R and D
[DE89-009232] N89-23294

NUCLEAR MAGNETIC RESONANCE
Nuclear magnetic resonance with dc SQUID (Superconducting QUantum Interference Device) preamplifiers
[DE89-007657] N89-23311

NUCLEAR RADIATION SPECTROSCOPY
Observational techniques for solar flare gamma-rays, hard X-rays, and neutrons
[NASA-CR-184910] N89-23399

NUCLEAR REACTORS
Development and study of a 3.2-mm-diameter, 1.2-m-long two-stage plasma-arc-driven railgun for hypervelocity hydrogen pellet injection
[DE89-009557] N89-22635
Fusion power: Expected environmental characteristics and status of R and D
[DE89-009232] N89-23294

NUCLEATION
Novel protein crystal growth technology: Proof of concept
[NASA-CR-184959] N89-23306
Growth kinetics of grain-boundary induced melting: A molecular-dynamics study
[DE89-009855] N89-23343

NUMERICAL ANALYSIS
Numerical study of a multipurpose transonic wind tunnel with an adaptable injection-suction system N89-22621
Application of the Single-Axis-rate-Table (SAT) of the DFVLR for the evaluation of stationary and dynamic gyro properties
[ESA-TT-1122] N89-22877
Configuration comparison analysis for the AFIT/AAMRL anthropomorphic robotic manipulator
[AD-A202618] N89-22921

NUMERICAL CONTROL
A computer controlled 100 kV pulse generator
[DE89-005922] N89-22808
Design of a new high precision computer numerical control
[DE89-008032] N89-23211

NUMERICAL DIFFERENTIATION
Projections of vector addition system reachability sets are semilinear
[AD-A205914] N89-23257

NUMERICAL FLOW VISUALIZATION
Direct numerical simulation of compressible free shear flows
[AIAA-89-0374] N89-22827

NUMERICAL INTEGRATION
Configuration comparison analysis for the AFIT/AAMRL anthropomorphic robotic manipulator
[AD-A202618] N89-22921

O

OBSERVABILITY (SYSTEMS)
Input-output decoupling with stability for Hamiltonian systems
[MEMO-722] N89-23239

OBSTACLE AVOIDANCE
Knowledge-based vision technology progress at Hughes AI Center N89-23084
Self calibration of motion and stereo vision for mobile robot navigation N89-23106
Autonomous navigation in cross-country terrain N89-23107
Using flow field divergence for obstacle avoidance in visual navigation N89-23120
An operational perception system for cross-country navigation N89-23121

OCCLUSION
Spatio-temporal analysis of an image sequence with occlusion N89-23110

OCEAN BOTTOM
Measurements of a barotropic planetary vorticity mode in an eddy-resolving quasi-geostrophic model using acoustic tomography
[AD-A205409] N89-23058

OCEAN CURRENTS
Development of a satellite SAR image spectra and altimeter wave height data assimilation system for ERS-1
[NASA-CR-182685] N89-22975
Measurements of a barotropic planetary vorticity mode in an eddy-resolving quasi-geostrophic model using acoustic tomography
[AD-A205409] N89-23058

OCEAN MODELS
Development of a satellite SAR image spectra and altimeter wave height data assimilation system for ERS-1
[NASA-CR-182685] N89-22975

OCEAN SURFACE
Theoretical studies for ERS-1 wave mode, volume 1
[GEC-MTR-87/110-VOL-1] N89-22977
Measurements of a barotropic planetary vorticity mode in an eddy-resolving quasi-geostrophic model using acoustic tomography
[AD-A205409] N89-23058

ON-LINE SYSTEMS
Standardized bibliographic processing N89-23367
Germany: Focus on Scientific and Technical Information, volume 4, number 1, April 1988
[AD-A204054] N89-23376

OPERATING SYSTEMS (COMPUTERS)
Enhancements to the IBM version of COSMIC/NASTRAN N89-22946
A powerful enhancement to the DMAP alter capability N89-22947
Improvements to the CONTINUE feature in transient analysis N89-22949
Implementation of the NETOS (Network Operating System) operated system in Ada with modifications to allow variable length messages
[AD-A202602] N89-23185
Storage in supercomputer environments
[DE89-008895] N89-23330

OPERATING TEMPERATURE
Material/manufacturing process interaction in advanced material technologies N89-22662
The demonstration of monolithic and composite ceramics in aircraft gas turbine combustors N89-22665
Composite material systems for high temperature applications N89-22666
Utilization of high temperature composites in turbojet engines N89-22667
High-performance refractory composite materials N89-22675

OPERATORS (MATHEMATICS)
The influence of open boundary conditions and difference operators on the time-integration of the Burger's equation
[FFA-TN-1988-57] N89-23254
On a functional equation over Hilbert spaces
[DE88-705645] N89-23267

OPTICAL DATA PROCESSING
Perception with feedback N89-23098

OPTICAL MEASUREMENT
Study of long optical fibers
[ESA-CR(P)-2723] N89-23288

OPTICAL MEMORY (DATA STORAGE)
Parallel Optical Random Access Memory (PORAM)
[NASA-CR-4241] N89-22890

OPTICAL PATHS
Study of long optical fibers
[ESA-CR(P)-2723] N89-23288

OPTICAL PROPERTIES
Technical support for optical turbulence research
[AD-A204776] N89-23033
Using generic geometric and physical models for representing solids N89-23114
Predicting material classes N89-23177
Measurements of optical loss in transparent solids using a novel spectrometer based on optical cavity decay
[DE89-009900] N89-23286

OPTICAL RADAR
Development of an efficient high brightness Ti:Al2O3 laser amplifier
[AD-A204187] N89-22881

OPTICAL TRANSITION
Optical studies of the magnetospheric cusp from Svalbard
[AD-A205432] N89-23044

OPTIMAL CONTROL
Active vibration control for flexible rotor by optimal direct-output feedback control
[NASA-TM-101972] N89-22605

Model-based analysis and cooperative synthesis of control and display augmentation for piloted flight vehicles N89-22610
A pseudo singular value decomposition and inner functions in super optimal control
[OUEL-1738/88] N89-23214
Optimal processes described by a parabolic differential equation with control in the coefficients, part 3
[MEMO-725-PT-3] N89-23218
Robust stabilization of an inverted double pendulum system via a polynomial approach to H(infinity) optimal control
[MEMO-742] N89-23220

OPTIMIZATION
Multifrequency eddy current testing, optimization of the method for steam generator testing. Phase 2: Nonlinear description of signal location curves dynamics of the signal location curves
[REPT-860142-TW] N89-22933
Multi-mission Ni-H2 battery cell for the 1990's N89-23006
A new modified cholesky factorization
[AD-A205174] N89-23191
Optimization for object localization of the constrained algebraic reconstruction technique
[DE89-007755] N89-23193
Nonlinear optimization involving polynomial matrices and their generalized inverses
[AD-A202620] N89-23224

ORBIT CALCULATION
Ten year lifetime orbits about the planet Mars N89-22633

ORBIT TRANSFER VEHICLES
Ariane 5 Transfer Vehicle (ATV)
[REPT-OX-1-005] N89-22645
ATV: Ariane 5 transfer vehicle study
[STF/E-39-005/CB] N89-22646

ORBITAL LIFETIME
Ten year lifetime orbits about the planet Mars N89-22633

ORBITAL MECHANICS
Minimum number of satellites for periodic coverage
[FOA-C-30511-9.4] N89-22976

ORBITAL SERVICING
Ariane 5 Transfer Vehicle (ATV)
[REPT-OX-1-005] N89-22645
ATV: Ariane 5 transfer vehicle study
[STF/E-39-005/CB] N89-22646
Columbus MTFF utilisation, phase B2X: Executive summary for main study
[CUT-MBER-800-RP-220] N89-22647

ORDER-DISORDER TRANSFORMATIONS
Coexistence of spin-glass and type-2 ceramic superconductivity
[DE88-705684] N89-23322
Ordering transitions induced by Coulomb interactions
[DE88-705717] N89-23324

ORGANIC COMPOUNDS
Carbonaceous film coating
[DE89-009592] N89-22762

ORGANIC SULFUR COMPOUNDS
Novel nitrogen-based organosulfur electrodes for advanced intermediate temperature batteries N89-22987

ORGANIZING
Impact of information technology on organizational structure: A control perspective N89-23379

ORGANOMETALLIC COMPOUNDS
Experimental investigation of hot electron and related effects in gallium (aluminum) arsenide devices
[AD-A205442] N89-23349

ORTHOGONAL FUNCTIONS
New stable, vectorisable Kalman filter algorithms based on orthogonal transformations
[ESA-TT-1108] N89-23203

ORTHOGONALITY
A divide and conquer method for unitary and orthogonal eigenproblems
[AD-A205433] N89-23255

ORTHOTROPIC PLATES
Approximate large deflection analysis of simply supported orthotropic plates
[NPL-DMA(A)171] N89-22963

OSCILLATING FLOW
Experimental observation of the nonlinear response of single bubbles to an applied acoustic field
[AD-A205191] N89-23271

OVERVOLTAGE
Recent advances in solid polymer electrolyte fuel cell technology with low platinum loading electrodes N89-22964

OXIDATION
Behavior of iron aluminides in oxidizing and sulfidizing environments
[DE89-008919] N89-22693

OXIDATION RESISTANCE
Utilization of high temperature composites in turbojet engines N89-22667
Silicon-carbide coated carbon-carbon: An advanced material for rocket systems N89-22672

OXIDATION-REDUCTION REACTIONS
Electrocatalysts for oxygen electrodes in fuel cells and water electrolyzers for space applications N89-22997

OXIDE FILMS
Thermal healing of defects in oxide films on metals and alloys
[DE89-009580] N89-22735

OXYGEN
Aqueous impurity effects on stainless steel IGSCC (intergranular stress corrosion cracking): A central composite matrix analysis
[DE88-017382] N89-22726
The new experimental areas oxygen monitor
[DE89-009700] N89-22876

OXYGEN ATOMS
In-space technology development: Atomic oxygen and orbital debris effects
[NASA-TM-102154] N89-22682

OXYGEN PRODUCTION
The electrochemical generation of useful chemical species from lunar materials N89-22990

OXYGEN SPECTRA
Optical studies of the magnetospheric cusp from Svalbard
[AD-A205432] N89-23044

OXYGEN 18
Point defects and oxygen diffusion in high T sub c superconductors
[DE89-009842] N89-23341

OXYNITRIDES
Chemical state depth profiling by Auger signal decomposition: Silicon oxynitride
[DE89-009830] N89-22764

OZONE
Seasonal and latitudinal variations of the temporal variance of ozone and of the potential temperature
[BPT-3/88] N89-23026
Diabatic circulations in the stratosphere N89-23043

OZONOMETRY
Quantitative analysis of atmospheric trace gases
[BPT-10/88] N89-23027

P

PAINTS
The effects of plastic media blasting paint removal on the microstructure of graphite/epoxy composite materials
[AD-A204801] N89-22688
Paint compatibility test
[I-266/88] N89-22758

PALLADIUM
Theoretical study of the Pd-B complex in silicon
[DE88-705650] N89-23316

PANEL METHOD (FLUID DYNAMICS)
A vortex panel analysis of circular-arc bluff-bodies in unsteady flow
[DE89-007141] N89-22845

PARABOLIC ANTENNAS
The radiation performance of offset reflector antennas with horn feeds excited by high order modes
[FI-454-TB-43] N89-22792

PARACHUTES
A preliminary characterization of parachute wake recontact
[DE89-006442] N89-22576

PARALLEL PROCESSING (COMPUTERS)
Parallel Optical Random Access Memory (PORAM)
[NASA-CR-4241] N89-22890
USC image understanding research: 1987-1988 N89-23076
Progress in image understanding at the University of Rochester N89-23082
Some sample algorithms for the image understanding architecture N89-23089
Machine-independent image processing: Performance of Apply on diverse architectures N89-23125
Parallel architectures for image processing and vision N89-23126
Parallel hardware for constraint satisfaction N89-23127
Scan line array processors: Work in progress N89-23128
Robust parallel computation of 2-D model-based recognition N89-23130
Parallel processors and nonlinear structural dynamics algorithms and software
[NASA-CR-184938] N89-23184
Developing software to use parallel processing effectively
[AD-A205184] N89-23192
Two time stepping algorithms for parallel computers
[DE89-008679] N89-23196
Reduction of a general matrix to tridiagonal form using a hypercube multiprocessor
[DE89-008721] N89-23197
Expert systems on multiprocessor architectures, phase 1
[AD-A204907] N89-23206
Parallel problem solving system, PRISM (Parallel Inference System)
[AD-A204915] N89-23207
Factoring very large numbers using a massively parallel computer
[DE89-008198] N89-23208

PARALLEL PROGRAMMING
Implementing nested conditional statements in SIMD machines
[NASA-CR-181832] N89-23073

PARAMETER IDENTIFICATION
Observation parameters for a ground-based radar station to survey near-earth satellites
[REPT-4-88] N89-22793
Computation of motion in depth parameters: A first step in stereoscopic motion interpretation N89-23153

PARAMETERIZATION
ELF communications system terminal grounds seasonal variation pilot study
[AD-A205900] N89-22806
The length scale for sub-grid-scale parameterization with anisotropic resolution N89-22818
Surface flux parameterization schemes: Developments and experiences at KNMI --- Earth surface
[KNMI-WR-88-06] N89-23055
Automating the identification of structural model parameters
[DE89-006327] N89-23194

PARTIAL DIFFERENTIAL EQUATIONS
On Hausdorff dimension of invariant manifolds of infinite-dimensional dynamic systems
[DE88-705628] N89-23227
On the averaging method for quasilinear hyperbolic equations
[DE88-705629] N89-23228

PARTIAL PRESSURE
Point defects and oxygen diffusion in high T sub c superconductors
[DE89-009842] N89-23341

PARTICLE ACCELERATION
Calculation of longitudinal and transverse wake-field effects in dielectric structures
[DE89-009814] N89-22798

PARTICLE ENERGY
Internal debonding of solid rocket fuel: An experimental investigation
[AD-A205903] N89-22772

PARTICLE IN CELL TECHNIQUE
Theoretical and computational studies of plasma opening switches
[DE89-009712] N89-23297

PARTICLE SPIN
Quantum theory of a massless spinning particle
[NIKHEF-H/88-7] N89-23357

PARTICLES
The effects of particle loading on turbulence structure and modelling N89-22825
Dynamics of particles in the bending waves of the planetary rings
[DE88-705714] N89-23396

PARTITIONS (MATHEMATICS)
On the maximum period of a permutation of N elements
[MEMO-743] N89-23251

PASSENGER AIRCRAFT
Propulsion systems with improved efficiency for future passenger aircraft. Main task A: Conceptual investigations of future propulsion systems with enhanced propulsive efficiency
[MTU-TB-87/010] N89-22608

PATTERN RECOGNITION
Position, scale, and rotation invariant optical pattern recognition for target extraction and identification
[AD-A202600] N89-22781
Interactive ultrasonic nondestructive evaluation
[AD-A204166] N89-22931
Proceedings: Image Understanding Workshop, volume 1
[AD-A197558] N89-23074
MIT progress in understanding images N89-23075
CMU image understanding program N89-23079
Image understanding research at SRI International N89-23080
Summary of image understanding research at the University of Massachusetts N89-23081

Qualitative reasoning and modeling for robust target tracking and recognition from a mobile platform N89-23086
Knowledge based vision for terrestrial robots N89-23087
The Maryland approach to image understanding N89-23091
The MIT vision machine N89-23093
Multimodal reconstruction and segmentation with Markov random fields and HCF optimization N89-23095
Cooperative methods for road tracking in aerial imagery N89-23101
PACE: An environment for intelligence analysis N89-23102
Affine invariant matching N89-23103
Constructing simple stable descriptions for image partioning N89-23104
Three-dimensional object recognition using surface descriptions N89-23105
Contour correspondences in dynamic imagery N89-23109
Proceedings: Image Understanding Workshop, volume 2
[AD-A197559] N89-23115
Perceptual grouping for the detection and description of structures in aerial images N89-23117
Dynamic model matching for target recognition from a mobile platform N89-23118
TRIPLE: A multi-strategy machine learning approach to target recognition N89-23119
Three-dimensional vision for outdoor navigation by an autonomous vehicle N89-23124
Robust parallel computation of 2-D model-based reconition N89-23130
The concept of an effective viewpoint N89-23131
IU software environments N89-23133
Using probabilistic domain knowledge to reduce the expected computational cost of matching N89-23134
Object recognition from a large database using a decision tree N89-23135
Modeling sensors and applying sensor model to automatic generation of object recognition program N89-23136
Rapid object recognition from a large model base using prediction hierarchies N89-23137
Algebraic reasoning in view consistency and parameterized model matching problems N89-23139
Test results from SRI's stereo system N89-23140
Preliminary design of a programmed picture logic N89-23141
The integration of information from stereo and multiple shape-form-texture cues N89-23145
Structural correspondence in stereo vision N89-23146
Curved surface reconstruction using stereo correspondence N89-23147
Combining information in low-level vision N89-23152
Recognizing animal motion N89-23156
Issues in extracting motion parameters and depth from approximate translational motion N89-23157
Translating optical flow into token matches N89-23159
Structure recognition by connectionist relaxation: Formal analysis N89-23160
Extracting generic shapes using model-driven optimization N89-23161
Texture models and image measures for segmentation N89-23162
Modal driven edge detection N89-23163
Generalizing epipolar-plane image analysis on the spatiotemporal surface N89-23164
Building surfaces of evolution: The weaving wall N89-23165
Depth from looming structure N89-23167
Adaptive smoothing for feature extraction N89-23173
Recognizing solid objects by alignment N89-23174
Projective invariants of shapes N89-23175
Texture edge localization N89-23178
Surface orientation from projective foreshortening of isotropic texture autocorrelation N89-23179
Labeling polyhedral images N89-23180

PEEK
A survey of poly-ether-ether-ketone and its advanced composites
[FFA-TN-1988-37] N89-22707

PELLETS
Variational analysis of railgun plasma-arc-armature for acceleration of solid hydrogen pellets for fusion reactor refueling
[DE89-009556] N89-22634
Development and study of a 3.2-mm-diameter, 1.2-m-long two-stage plasma-arc-driven railgun for hypervelocity hydrogen pellet injection
[DE89-009557] N89-22635

PENDULUMS
Robust stabilization of an inverted double pendulum system via a polynomial approach to H(infinity) optimal control
[MEMO-742] N89-23220

PENETRATION
Numerical method to predict projectile penetration
[DE89-007140] N89-22923

PERFLUORO COMPOUNDS
The application of Dow Chemical's perfluorinated membranes in proton-exchange membrane fuel cells N89-22995

PERFORMANCE PREDICTION
A study of unsteady turbulent flow past airfoils N89-22587
Aerodynamic detuning of a loaded airfoil cascade in an incompressible flow by a locally analytical method N89-22588
Transonic viscous flow calculations for a turbine cascade with a two equation turbulence model
[NASA-TM-101944] N89-22607
High accuracy thermal conductivity measurements near the lambda transition of helium with very high temperature resolution
[NASA-CR-184836] N89-22709
Theoretical predictions of turbulent burning velocities of steady and accelerating unconfined turbulent flames with premixed reactants N89-22716
Computational fluid dynamics research in three-dimensional zonal techniques
[NASA-CR-181406] N89-22838
Overview of battery usage in NASA/GSFC LEO and GEO missions N89-22983
Automating the identification of structural model parameters
[DE89-006327] N89-23194

PERFORMANCE TESTS
Testing of a new recovery parachute system for the F111 aircraft crew escape module: An update
[DE89-007139] N89-22592
Development and testing of critical components for technological preparation of an Airbus-CFRP-fuselage, phase 2
[MBB-UT-129/87] N89-22600
Development and study of a 3.2-mm-diameter, 1.2-m-long two-stage plasma-arc-driven railgun for hypervelocity hydrogen pellet injection
[DE89-009557] N89-22635
Internal debonding of solid rocket fuel: An experimental investigation
[AD-A205903] N89-22772
Assessment of EV batteries and application to R and D planning
[DE89-009720] N89-22811
Advanced batteries for electric vehicles
[DE89-009771] N89-22813
Laboratory evaluation of advanced battery technologies for electric vehicle applications
[DE89-009810] N89-22814
Heat transfer and pressure drop measurements in an air/molten salt direct-contact heat exchanger
[DE89-000837] N89-22843
Evaluation of the Portable Instantaneous Display Analysis Spectrometer (PIDAS)
[NASA-CR-184878] N89-22970
Characterization testing of a 40 Ahr bipolar nickel hydrogen battery N89-22992
Research on amorphous-silicon-based, thin-film photovoltaic devices, task B
[DE89-000886] N89-23022
Developing software to use parallel processing effectively
[AD-A205184] N89-23192
Environmental noise characteristics of the MOD5-B (3.2 MW) wind turbine generator
[NASA-TM-101567] N89-23272
Theoretical and computational studies of plasma opening switches
[DE89-009712] N89-23297

PERMUTATIONS
On the maximum period of a permutation of N elements
[MEMO-743] N89-23251

PEROXIDES
Effects of different fabrication techniques on the Yttrium-Barium-Copper oxide high temperature superconductor
[AD-A202598] N89-23304

PERSONNEL SELECTION
Studies of poststrike air traffic control specialist trainees. Part 2: Selection and screening programs
[AD-A199177] N89-22595

PERTURBATION
Gravitational effects of cosmic strings in Friedmann universes N89-23394

PERTURBATION THEORY
Hard scattering of (almost) real photons at HERA
[NIKHEF-H/88-3] N89-23276
Perturbative treatment of local correlations in Cu-O planes for high temperature superconductors
[DE88-705648] N89-23315

PH
Measuring electrode assembly
[DE89-009591] N89-22875

PHASE DIAGRAMS
Development of metastable processing paths for high temperature alloys
[AD-A202614] N89-22721
Ab initio calculations of ordered intermetallic phase equilibria
[DE89-009974] N89-22741

PHASE SEPARATION (MATERIALS)
Role of aluminium concentration on the structure behaviour of Cu-Al alloys
[DE88-705647] N89-22727

PHASE TRANSFORMATIONS
Fracture toughness of MgCr2O4-based refractory composites
[DE89-009847] N89-22696
Criteria for selection of phase names for oxides
[NPL-DMA(A)169] N89-22714
Physical-chemical studies of solutions processing of nematic polymers
[AD-A205921] N89-22770
Ordering transitions induced by Coulomb interactions
[DE88-705717] N89-23324

PHOTOCHEMICAL REACTIONS
The response of thermospheric nitric oxide to an auroral storm N89-23031

PHOTOGRAMMETRY
MIT progress in understanding images N89-23075
Relative orientation N89-23149

PHOTOGRAPHS
PixMail: Pictures through mail
[DE89-009682] N89-22797

PHOTOINTERPRETATION
Image understanding research at the University of Maryland, December 1986 - January 1988 N89-23078
CMU image understanding program N89-23079
Image understanding research at SRI International N89-23080
Summary of image understanding research at the University of Massachusetts N89-23081
IU at UI: An overview and an example on shape from texture N89-23096
Qualitative motion detection and tracking of targets from a mobile platform N89-23099
Cooperative methods for road tracking in aerial imagery N89-23101
PACE: An environment for intelligence analysis N89-23102
Spatio-temporal analysis of an image sequence with occlusion N89-23110
Multiresolution aerial image interpretation N89-23116
Preliminary design of a programmed picture logic N89-23141

PHOTOLUMINESCENCE
Time resolved photoluminescence of ytterbium in indium phosphide
[AD-A202596] N89-23303

PHOTOMAPPING
USC image understanding research: 1987-1988 N89-23076

PHOTOMETRY
A color metric for computer vision N89-23151
Extracting generic shapes using model-driven optimization N89-23161
Modal driven edge detection N89-23163

PHOTOPRODUCTION
Hard scattering of (almost) real photons at HERA
[NIKHEF-H/88-3] N89-23276

PHOTOVOLTAIC CELLS
Research on amorphous-silicon-based, thin-film photovoltaic devices, task B
[DE89-000885] N89-23021
Research on amorphous-silicon-based, thin-film photovoltaic devices, task B
[DE89-000886] N89-23022

PHOTOVOLTAIC CONVERSION
The NASA Space Solar Cell Advanced Research Program
[NASA-TM-102020] N89-22651
Progress in crystalline silicon research
[DE89-007423] N89-22749
Photovoltaic systems for today's remote power applications
[DE89-007431] N89-23012
Advances in concentrator cell technology
[DE89-007432] N89-23013
InP (Indium Phosphide): Into the future
[NASA-TM-102058] N89-23025

PHOTOVOLTAIC EFFECT
Effects of cosmic rays on single event upsets
[NASA-CR-184935] N89-23400
PHYSIOLOGICAL EFFECTS
Acclimatization to cold in humans
[NASA-TM-101012] N89-23061
Benzodiazepines and caffeine: Effect on daytime sleepiness, performance, and mood
[AD-A205862] N89-23066
Efficacy of conventional and high-frequency ventilation at altitude
[AD-A205922] N89-23071
PIEZOELECTRIC CERAMICS
Piezoelectric pushers for active vibration control of rotating machinery N89-22896
PILOT ERROR
Aircraft accident report: Trans-Colorado Airlines, Inc., Flight 2286, Fairchild Metro 3, SA227 AC, N68TC Bayfield, Colorado, January 19, 1988
[PB89-910401] N89-22593
PILOT PERFORMANCE
Model-based analysis and cooperative synthesis of control and display augmentation for piloted flight vehicles N89-22610
An in-flight investigation of workload assessment techniques for civil aircraft operations
[NLR-TR-87119-U] N89-23070
AGARD highlights 88/2 N89-23403
PITTING
Locating pitting sites from propagating surface potential transients
[DE89-006171] N89-22730
Application of electrochemical noise spectral analysis to the study of the pitting corrosion of aluminum alloys
[ETCA-87-R-102] N89-22744
PIXELS
Symbolic pixel labeling for curvilinear feature detection N89-23171
PLANAR STRUCTURES
Ribbons, symmetries and skewed symmetries N89-23170
PLANETARY EVOLUTION
Earth system science: A program for global change
[NASA-TM-101186] N89-22969
PLANETARY STRUCTURE
Earth system science: A program for global change
[NASA-TM-101186] N89-22969
PLASMA ARC WELDING
A calorimetric-based comparison of gas tungsten and plasma arc welding processes
[DE89-008712] N89-22924
PLASMA CONDUCTIVITY
Spacecraft charge as a source of electrical power for spacecraft
[AD-A202621] N89-22649
PLASMA CONTROL
H-Mode transition studies in DIII-D
[DE89-006913] N89-23290
Maximal bootstrap current tokamak equilibria in the first stability regime
[DE89-008201] N89-23291
Computation of lower hybrid, neutral beam and bootstrap currents in consistent MHD equilibria
[DE89-008892] N89-23292
A quiver kinetic formulation of radio frequency heating and confinement in collisional edge plasmas
[DE89-009675] N89-23296
PLASMA CURRENTS
Anomalous cross-field velocities in a CIV laboratory experiment
[TRITA-EPP-88-06] N89-23289
A fluid FLR model of the magnetopause layer
[IRF-PREPRINT-109] N89-23299
PLASMA DENSITY
Ionospheric scintillation studies
[AD-A205210] N89-23034
PLASMA DIAGNOSTICS
A fast spatial scanning combination emissive and Mach probe for edge plasma diagnosis
[DE89-009674] N89-23295
The ALEXIS project and the local interstellar medium
[DE89-009248] N89-23392
PLASMA DYNAMICS
Simulations of axisymmetric erosion in IFR-Transported beams
[AD-A205882] N89-23301
PLASMA EQUILIBRIUM
Maximal bootstrap current tokamak equilibria in the first stability regime
[DE89-008201] N89-23291
PLASMA HEATING
Effects of ion collisions on quasilinear heating by the current-driven ion cyclotron instability in the high latitude ionosphere
[AD-A202512] N89-23032
H-Mode transition studies in DIII-D
[DE89-006913] N89-23290
PLASMA JETS
Development and study of a 3.2-mm-diameter, 1.2-m-long two-stage plasma-arc-driven railgun for hypervelocity hydrogen pellet injection
[DE89-009557] N89-22635
PLASMA PHYSICS
Boundaries and probes in electronegative plasmas
[OUEL-1636/86] N89-23293
PLASMA PINCH
Development and simulation study of a new inverse-pinch high Coulomb transfer switch
[NASA-CR-181768] N89-23300
PLASMA PROBES
Boundaries and probes in electronegative plasmas
[OUEL-1636/86] N89-23293
PLASMA SPRAYING
Vacuum plasma spray coating N89-22670
PLASMA WAVES
Effect of pump-induced density depletions on the spectrum of stimulated electromagnetic emissions — ionosphere
[IRF-PREPRINT-107] N89-22799
PLASMAS (PHYSICS)
Theoretical and computational studies of plasma opening switches
[DE89-009712] N89-23297
Ordering transitions induced by Coulomb interactions
[DE88-705717] N89-23324
PLASTIC DEFORMATION
A study of high strain rate generation of adiabatic shear bands in a titanium alloy N89-22967
PLATE THEORY
Approximate large deflection analysis of simply supported orthotropic plates
[NPL-DMA(A)171] N89-22963
PLUMES
Rectangular nozzle plume velocity modeling for use in jet noise prediction
[NASA-TM-102047] N89-22577
Preliminary results of the MLAM (Multi-Layer Air Mass) Lagrangian transport model simulation of ANATEX (Across North America Tracer Experiment)
[DE89-008123] N89-23036
POINT DEFECTS
Point defects and oxygen diffusion in high T sub c superconductors
[DE89-009842] N89-23341
POINTING CONTROL SYSTEMS
An experimental and analytical synthesis of controlled structure design
[DE89-008506] N89-22957
POISSON EQUATION
Incorporation of a boundary condition to numerical solution of POISSON's equation
[DE89-007132] N89-23231
POLAR REGIONS
Gravity wave and turbulence studies using a high-resolution ST radar
[AD-A205592] N89-23046
POLARIMETRY
Coherent polarimetric radar techniques for microwave propagation and cloud physics research
[DFVLR-FB-88-47] N89-22800
POLARIZATION (CHARGE SEPARATION)
Oxygen electrodes for rechargeable alkaline fuel cells N89-22995
Characteristics of winter lightning to high structures. Observation from December 1978 to March 1987
[DE88-756454] N89-23049
POLICIES
Safe skies for tomorrow: Aviation safety in a competitive environment
[PB89-114316] N89-22591
JPRS report: Science and technology. USSR: Space
[JPRS-USP-88-003] N89-22622
Survey of development trends of methanol automobiles and methanol fuel in China
[DE88-756492] N89-22771
Fostering interaction of government, defense, and aerospace databases N89-23374
POLLUTION MONITORING
Investigation on long time dispersion and washout factor. Vegetation contamination computation with meteorological whole year or summer statistics
[JUEL-SPEZ-449] N89-23028
POLYAMIDE RESINS
Interfacial adhesion and mechanical properties of polyamide-6/glass bead composites
[ETN-89-94136] N89-22759
Polymer electrolytes with exclusively cationic conductivity
[DE89-009521] N89-22761
Physical-chemical studies of solutions processing of nematic polymers
[AD-A205921] N89-22770
POLYCRYSTALS
Grain boundary sliding phenomena in polycrystalline solids
[DE89-007792] N89-23326
The effect of boron on microhardness in Ni3Al polycrystals
[DE89-009124] N89-23335
POLYHEDRONS
Labeling polyhedral images N89-23180
POLYMER CHEMISTRY
Reactions of inorganic high polymers as a route to tailored solids
[AD-A204602] N89-22750
Spinodal decomposition in polymer blends
[DE88-705687] N89-22754
POLYMER MATRIX COMPOSITES
Development of an asbestos-free insulant for rocket motors N89-22679
A survey of poly-ether-ether-ketone and its advanced composites
[FFA-TN-1988-37] N89-22707
POLYMERIC FILMS
Electrochemical technique for rapidly evaluating protective coatings on metals
[PB89-134209] N89-22748
Organic and polymer crystalline films for spatial light modulation
[AD-A205906] N89-23350
POLYMERIZATION
Low-density foams from macroporous epoxy gels
[DE89-004042] N89-22756
POLYNOMIALS
Nonlinear optimization involving polynomial matrices and their generalized inverses
[AD-A202620] N89-23224
On polynomial ideals of finite codimension with applications to box spline theory
[AD-A204095] N89-23225
Smooth interpolation to scattered data by bivariate piecewise polynomials of odd degree
[MEMO 732] N89-23245
POLYPHENYL ETHER
Formation of lubricating films at elevated temperatures from the gas phase
[PB89-129530] N89-22747
POLYPROPYLENE
Effects of X-rays on isotactic polypropylene. Volume 2: Polymers and ceramics
[DE88-705606] N89-22751
POROUS MATERIALS
Low-density foams from macroporous epoxy gels
[DE89-004042] N89-22756
PORTABLE EQUIPMENT
Evaluation of the Portable Instantaneous Display Analysis Spectrometer (PIDAS)
[NASA-CR-184878] N89-22970
POSITION (LOCATION)
Locating pitting sites from propagating surface potential transients
[DE89-006171] N89-22730
Optimization for object localization of the constrained algebraic reconstruction technique
[DE89-007755] N89-23193
POSITION SENSING
Position, scale, and rotation invariant optical pattern recognition for target extraction and identification
[AD-A202600] N89-22781
POSITRON ANNIHILATION
Hydrogen embrittlement study and positron annihilation response of hydrogen in aisi 4340 steel N89-22720
POSITRONS
Positron lifetime technique with applications in materials science
[ETN-89-94141] N89-23331
POTASSIUM COMPOUNDS
Structural properties of superconducting and nonsuperconducting Ba sub 1-x K sub x BiO3
[DE89-009813] N89-23340
POTASSIUM HYDROXIDES
KOH concentration effect on the cycle life of nickel-hydrogen cells. 4: Results of failure analyse N89-23004
POWDER METALLURGY
Behavior of tungsten, molybdenum and alloys under unusual heating conditions N89-22674
Microwave sintering of boron carbide
[DE89-009652] N89-22763
POWER CONVERTERS
Numerical model of solar dynamic radiator for parametric analysis
[NASA-TM-102054] N89-22653

POWER EFFICIENCY
Effects of lubrication on the performance of high speed spur gears
[NASA-TM-101969] N89-22919
POWER SERIES
A Borel-Ritt theorem with prescribed error bounds
[MEMO-723] N89-23240
Asymptotic expansions with error bounds for solutions of difference equations of level 1 sup +
[MEMO-724] N89-23241
On the asymptotic behavior of the coefficients of asymptotic power series and its relevance to Stokes phenomena
[MEMO-738] N89-23248
POWER SPECTRA
On the structure of pressure fluctuations in simulated turbulent channel flow
[NASA-TM-101084] N89-22860
PREAMPLIFIERS
Nuclear magnetic resonance with dc SQUID (Super-conducting QUantum Interference Device) preamplifiers
[DE89-007657] N89-23311
PRECIPITATION (CHEMISTRY)
Precipitation of Ar, Kr and Xe in Ni at room temperature
[DE89-009879] N89-22713
PREDICTION ANALYSIS TECHNIQUES
Damage development, property degradation and life prediction in composite laminates N89-22708
The spectral analysis of an aero-engine assembly incorporating a squeeze-film damper N89-22895
A new perspective in the etiology, treatment, prevention and prediction of space motion sickness
[AD-A205660] N89-23065
Rapid object recognition from a large model base using prediction hierarchies N89-23137
Environmental noise characteristics of the MOD5-B (3.2 MW) wind turbine generator
[NASA-TM-101567] N89-23272
PREMIXED FLAMES
Theoretical predictions of turbulent burning velocities of steady and accelerating unconfined turbulent flames with premixed reactants N89-22716
PREPROCESSING
Using Patran and Supertab as pre- and postprocessors to COSMIC/NASTRAN N89-22942
PRESSURE DISTRIBUTION
Cavitation effects on the pressure distribution of a squeeze film damper bearing N89-22897
PRESSURE EFFECTS
Influence of impeller and diffuser geometries on the lateral fluid forces of whirling centrifugal impeller N89-22907
Electronic properties of Ge sub 1-x Si sub x: A simplified tight binding approach
[DE88-705671] N89-23317
Electronic properties of Ge(1-X)Si(X): Alloying versus pressure
[DE88-705678] N89-23320
PRESSURE GRADIENTS
An experimental investigation of a low Reynolds number turbulent boundary layer subject to an adverse pressure gradient N89-22834
On the structure of pressure fluctuations in simulated turbulent channel flow
[NASA-TM-101084] N89-22860
Study of unsteady boundary layers with adverse pressure gradient N89-22863
PRESSURE REDUCTION
Heat transfer and pressure drop measurements in an air/molten salt direct-contact heat exchanger
[DE89-000837] N89-22843
PRESSURE SENSORS
Supersonic particle probes: Measurement of internal wall losses
[AD-A205863] N89-22589
PRIMERS (COATINGS)
Paint compatibility test
[I-266/88] N89-22758
PRINTED CIRCUITS
Double sided circuit board and a method for its manufacture
[DE89-009601] N89-22809
PROBABILITY DENSITY FUNCTIONS
Probabilities and statistics for backscatter estimates obtained by a scatterometer with applications to new scatterometer design data
[NASA-CR-4228] N89-22779
On the structure of pressure fluctuations in simulated turbulent channel flow
[NASA-TM-101084] N89-22860
Evaluation of quantization error in computer vision N89-23138
PROBABILITY DISTRIBUTION FUNCTIONS
On the use of stable distributions in design programs
[MEMO-736] N89-23219
Asymptotically optimal nonparametric experimental design tests for the log linear model under censoring
[MEMO-727] N89-23262
On the expected number of assignments in reduced matrices for the linear assignment problem
[MEMO-728] N89-23263
PROBABILITY THEORY
Space Propulsion Hazards Analysis Manual (SPHAM). Volume 2: Appendices
[AD-A204601] N89-22650
Consensus theory in expert systems: An adaptive inference framework and application to image understanding
[AD-A204253] N89-23188
Implementation of comparative probability by Gleason measures: Infinite dimensional case
[DE88-705683] N89-23259
Techniques for applying sets code procedures to large fault trees in PRA (Probabilistic Risk Assessment) analysis
[DE89-004823] N89-23261
Limiting exact efficiency of quadratic statistics
[MEMO-737] N89-23264
PROBLEM SOLVING
Methods and algorithms for processing television images of nucleus of Halley's Comet. Some results N89-22624
Finite element modeling of electromagnetic fields and waves using NASTRAN N89-22950
Story problem solver: A schema-based system of instruction
[AD-A205594] N89-23205
Parallel problem solving system, PRISM (Parallel Inference System)
[AD-A204915] N89-23207
A divide and conquer method for unitary and orthogonal eigenproblems
[AD-A205433] N89-23255
The multigroup and cylindrical geometry formulation of the Sn Monte Carlo hybrid method
[DE89-000326] N89-23260
Relationships between the prenucleolus, ENSC-solution and related solution concepts for cooperative games
[MEMO-729] N89-23266
PROCESS CONTROL (INDUSTRY)
New metallic materials for gas turbines N89-22660
PRODUCT DEVELOPMENT
Development and testing of critical components for technological preparation of an Airbus-CFRP-fuselage, phase 2
[MBB-UT-129/87] N89-22600
Basic program for the development of a reliable high strength construction ceramic mode of SiC
[MTU-TB-87/927] N89-22757
Adsorption studies in the critical region of a pure fluid. Development of an apparatus for adsorption measurements under microgravity conditions
[ETN-89-93767] N89-22774
Increasing marketability and profitability of product line thru PATRAN and NASTRAN N89-22943
PRODUCTIVITY
Increasing marketability and profitability of product line thru PATRAN and NASTRAN N89-22943
PROGRAM VERIFICATION (COMPUTERS)
An integrated image understanding benchmark: Recognition of a 2 1/2 D mobile N89-23088
Use of language features in the implementation and validation of a standardized generic package of elementary functions for Ada
[DE89-007385] N89-23187
Developing software to use parallel processing effectively
[AD-A205184] N89-23192
HOOD Toolset Development Project: ECLIPSE/HOOD/REP, issue 1.1
[ESA-CR(P)-2746] N89-23204
Parallel problem solving system, PRISM (Parallel Inference System)
[AD-A204915] N89-23207
PROGRAMMING LANGUAGES
Machine-independent image processing: Performance of Apply on diverse architectures N89-23125
PROJECT MANAGEMENT
Assessment of EV batteries and application to R and D planning
[DE89-009720] N89-22611
PROJECT PLANNING
Human exploration mission studies N89-22985
PROJECTILES
Numerical method to predict projectile penetration
[DE89-007140] N89-22923
PROMOTION
Analysis of the present knowledge of costs and benefits of the governmental advancement of astronautics
[ETN-89-93770] N89-23359
PROPAGATION VELOCITY
Corrosion monitoring with acoustic wave devices
[DE89-005235] N89-22728
PROPELLANT TANKS
Analysis of the nonvented fill of a 4.96-cubic-meter lightweight liquid hydrogen tank
[NASA-TM-102039] N89-22652
PROPELLANT TRANSFER
Analysis of the nonvented fill of a 4.96-cubic-meter lightweight liquid hydrogen tank
[NASA-TM-102039] N89-22652
PROPORTIONAL COUNTERS
Determination of the He3 number density for the proportional counter used in the NPL Bonner sphere system
[NPL-RS(EXT)104] N89-23275
PROPULSION SYSTEM CONFIGURATIONS
Propulsion systems with improved efficiency for future passenger aircraft. Main task A: Conceptual investigations of future propulsion systems with enhanced propulsive efficiency
[MTU-TB-87/010] N89-22608
Center for Advanced Space Propulsion (CASP)
[NASA-CR-184936] N89-23404
PROPULSION SYSTEM PERFORMANCE
Propulsion systems with improved efficiency for future passenger aircraft. Main task A: Conceptual investigations of future propulsion systems with enhanced propulsive efficiency
[MTU-TB-87/010] N89-22608
New hypersonic facility capability at NASA Lewis Research Center
[NASA-TM-102028] N89-22617
Technical evaluation report N89-22655
Application of advanced materials for turbomachinery and rocket propulsion N89-22656
Monolithic and fiber ceramic components for turboengines and rockets N89-22657
Future advanced aero-engines: The materials challenge N89-22659
Damage tolerance concepts for advanced materials and engines N89-22661
Material/manufacturing process interaction in advanced material technologies N89-22662
PROPULSIVE EFFICIENCY
Propulsion systems with improved efficiency for future passenger aircraft. Main task A: Conceptual investigations of future propulsion systems with enhanced propulsive efficiency
[MTU-TB-87/010] N89-22608
PROTECTIVE COATINGS
Advanced materials to combat the high temperature degradation processes in turbomachinery N89-22664
In-space technology development: Atomic oxygen and orbital debris effects
[NASA-TM-102154] N89-22682
Wear protection coatings and treatments for the TA6V alloy
[ETCA-88-R-003] N89-22742
Electrochemical technique for rapidly evaluating protective coatings on metals
[PB89-134209] N89-22748
Coating of silicon carbide fibers
[CERT-423900/RF] N89-22767
PROTEIN CRYSTAL GROWTH
Novel protein crystal growth technology: Proof of concept
[NASA-CR-184959] N89-23306
PROTEINS
Mini Protein Crystallization Facility (MPCF), phase A study: Executive summary
[ESA-CR(P)-2709] N89-22775
PROTOCOL (COMPUTERS)
PixMail: Pictures through mail
[DE89-009682] N89-22797
Specifying real-time systems with interval logic
[NASA-CR-181804] N89-23183
Decentralization of databases and the communication between them N89-23373
PROVING
Specifying real-time systems with interval logic
[NASA-CR-181804] N89-23183
PSYCHOMOTOR PERFORMANCE
Motor theory of auditory perception
[AD-A204951] N89-23064
PSYCHOTROPIC DRUGS
Aircraft accident report: Trans-Colorado Airlines, Inc., Flight 2286, Fairchild Metro 3, SA227 AC, N68TC Bayfield, Colorado, January 19, 1988
[PB89-910401] N89-22593

PULSE DURATION
Development of an efficient high brightness Ti:Al2O3 laser amplifier
[AD-A204187] N89-22881
PULSE GENERATORS
A computer controlled 100 kV pulse generator
[DE89-005922] N89-22808
PULSED LASERS
Accumulated surface damage on ZnS crystals produced by closely spaced pairs of picosecond laser pulses
[DE89-006813] N89-23329
PUMP SEALS
Influence of different types of seals on the stability behavior of turbopumps N89-22902
A 3-dimensional finite-difference method for calculating the dynamic coefficients of seals N89-22903
An experimental study on the static and dynamic characteristics of pump annular seals N89-22904
PYLONS
Prediction of loads on wing/body/external store/fins pylon-configurations at transonic speeds
[FFA-TN-1988-44] N89-22602
PYROLYSIS
Non-noble electrocatalysts for alkaline fuel cells N89-22999

Q

QUADRATIC EQUATIONS
Monotonicity-preserving quadratic C sup 1-spline interpolation to scattered data
[MEMO-744] N89-23252
Limiting exact efficiency of quadratic statistics
[MEMO-737] N89-23264
QUALITY CONTROL
Signal treatment and data analysis methods applied to nondestructive control of adhesive bonded joints
[ISAL-IDI-8809] N89-22936
The importance of batteries in unmanned missions N89-22984
A programmatic approach to achieving data quality objectives
[DE89-008248] N89-23378
QUANTITATIVE ANALYSIS
Quantitative analysis of atmospheric trace gases
[BPT-10/88] N89-23027
QUANTUM CHROMODYNAMICS
Hard scattering of (almost) real photons at HERA
[NIKHEF-H/88-3] N89-23276
QUANTUM EFFICIENCY
The propagation of noise through streak systems
[DE89-006600] N89-22869
QUANTUM MECHANICS
Implementation of comparative probability by Gleason measures: Infinite dimensional case
[DE88-705683] N89-23259
Molecular dynamics and irreversibility, from Boltzmann to Nose
[DE89-006740] N89-23274
QUANTUM STATISTICS
Nature of condensation in the momentum space for an interacting Bose system
[DE88-705679] N89-23352
QUANTUM THEORY
Quantum phenomena in mesoscopic superconducting tunnel junctions
[AD-A203354] N89-23305
Improved effective potential in the Einstein metric
[DE88-705718] N89-23355
Quantum theory of a massless spinning particle
[NIKHEF-H/88-7] N89-23357
QUANTUM WELLS
Molecular beam epitaxial growth and characterization of metastable compound semiconductors for infrared detector applications
[AD-A205175] N89-23312
QUASARS
Superconducting cosmic string evolution of quasars
[DE88-705672] N89-23390
Far infrared peculiar behavior of quasars
[DE88-705673] N89-23391
QUENCHING (COOLING)
Processing and properties of advanced aluminum alloys
[AD-A205187] N89-22725

R

RADAR CROSS SECTIONS
Probabilities and statistics for backscatter estimates obtained by a scatterometer with applications to new scatterometer design data
[NASA-CR-4228] N89-22779
Verification and limitations of the monostatic-bistatic radar cross section derived by Kell
[AD-A202601] N89-22782
RADAR DATA
Development of a satellite SAR image spectra and altimeter wave height data assimilation system for ERS-1
[NASA-CR-182685] N89-22975
RADAR IMAGERY
Development of a satellite SAR image spectra and altimeter wave height data assimilation system for ERS-1
[NASA-CR-182685] N89-22975
Theoretical studies for ERS-1 wave mode, volume 1
[GEC-MTR-87/110-VOL-1] N89-22977
Imaging radar applications in Europe. Illustrated experimental results (1978-1987)
[ESA-TM-01] N89-22978
RADAR MEASUREMENT
Observation parameters for a ground-based radar station to survey near-earth satellites
[REPT-4-88] N89-22793
RADAR PHOTOGRAPHY
Imaging radar applications in Europe. Illustrated experimental results (1978-1987)
[ESA-TM-01] N89-22978
RADAR SCATTERING
Probabilities and statistics for backscatter estimates obtained by a scatterometer with applications to new scatterometer design data
[NASA-CR-4228] N89-22779
RADAR TRACKING
Observation parameters for a ground-based radar station to survey near-earth satellites
[REPT-4-88] N89-22793
RADIAL FLOW
LDV measurements and investigation of flow field through radial turbine guide vanes N89-22609
Influence of impeller and diffuser geometries on the lateral fluid forces of whirling centrifugal impeller N89-22907
RADIAL VELOCITY
Anomalous cross-field velocities in a CIV laboratory experiment
[TRITA-EPP-88-06] N89-23289
RADIANT FLUX DENSITY
Monolithic Solid Oxide Fuel Cell development N89-22989
Recent advances in solid polymer electrolyte fuel cell technology with low platinum loading electrodes N89-22994
Advances in ambient temperature secondary lithium cells N89-23011
RADIATION DAMAGE
InP (Indium Phosphide): Into the future
[NASA-TM-102058] N89-23025
RADIATION DETECTORS
Observational techniques for solar flare gamma-rays, hard X-rays, and neutrons
[NASA-CR-184910] N89-23399
RADIATION DOSAGE
Astronaut radiation exposure in low-earth orbit. Part 1: Galactic cosmic radiation
[AD-A204598] N89-23063
RADIATION EFFECTS
Effects of X-rays on isotactic polypropylene. Volume 2: Polymers and ceramics
[DE88-705606] N89-22751
InP (Indium Phosphide): Into the future
[NASA-TM-102058] N89-23025
Influence of ion irradiated SrTiO sub 3 on the properties of thin film oxide superconductors
[DE89-009409] N89-23338
RADIATION HARDENING
Radiation hardened detector arrays for the far and extreme infrared, phase 1
[BF-R-65.695-10] N89-23347
RADIATION HAZARDS
Astronaut radiation exposure in low-earth orbit. Part 1: Galactic cosmic radiation
[AD-A204598] N89-23063
RADIATION MEASUREMENT
Reports from the German Meteorological Service. No. 175: Global radiation during twilight
[ISBN-3-88148-241-5] N89-23052
RADIATION PROTECTION
Radiation control at the Continuous Electron Beam Accelerator Facility (CEBAF), a new high power CW electron accelerator installation
[CEBAF-PR-89-001] N89-23280
Space Nuclear Safety Program
[DE89-008308] N89-23281
RADIATION TRANSPORT
Equations of cosmic-ray transport with distributed acceleration
[AD-A204599] N89-23401
RADIATIVE HEAT TRANSFER
Radiative cooling in the nocturnal boundary layer
[KNMI-WR-88-05] N89-23054
Mie scattering calculations for heat radiation
[FOA-C-20738-2.1] N89-23279
RADIO CONTROL
Design of a lightweight, low-cost geophysical survey vehicle
[DE89-009383] N89-22926
RADIO DIRECTION FINDERS
Geodetic positioning system for flying aircraft (May 1987)
[REPT-013/88] N89-22598
RADIO FREQUENCIES
Scaling relations for a beam-deflecting TM(110) mode in an asymmetric cavity
[DE89-009277] N89-22796
RADIO FREQUENCY HEATING
ICRF waveguide launcher research
[DE89-009151] N89-22791
A quiver kinetic formulation of radio frequency heating and confinement in collisional edge plasmas
[DE89-009675] N89-23296
RADIO GALAXIES
Optical and infrared observations of the nature and evolution of active galaxies N89-23385
RADIO RECEIVERS
GPS terminal: Study of a GPS receiver for Columbus platform elements, executive summary
[GPS-REP-SEL-002] N89-22643
RADIOACTIVE DECAY
Time resolved photoluminescence of ytterbium in indium phosphide
[AD-A202596] N89-23303
RADIOACTIVE WASTES
The long-term climate change assessment task of the Hanford Site, Washington, Protective Barrier Development Program
[DE89-008704] N89-23030
RADIOSONDES
Technical support for optical turbulence research
[AD-A204776] N89-23033
RAILGUN ACCELERATORS
Variational analysis of railgun plasma-arc-armature for acceleration of solid hydrogen pellets for fusion reactor refueling
[DE89-009556] N89-22634
Development and study of a 3.2-mm-diameter, 1.2-m-long two-stage plasma-arc-driven railgun for hypervelocity hydrogen pellet injection
[DE89-009557] N89-22635
RAIN GAGES
Remote sensing of oceanic rainrates by passive microwave sensors: A statistical-physical approach N89-23057
RAMAN SPECTRA
Preparation, characterization and performance of MoS3 as an active cathode material
[AD-A205866] N89-22717
Structural comparison of nickel electrodes and precursor phases N89-23001
RANDOM ACCESS MEMORY
Parallel Optical Random Access Memory (PORAM)
[NASA-CR-4241] N89-22890
Effects of cosmic rays on single event upsets
[NASA-CR-184835] N89-23400
RANDOM NOISE
Signal detection in fractional Gaussian noise and an RKHS (Reproducing Kernel Hilbert Space) approach to robust detection and estimation
[AD-A205441] N89-22805
RANGE FINDERS
Image understanding research at the University of Maryland, December 1986 - January 1988 N89-23078
RANKINE CYCLE
Megawatt Class Nuclear Space Power Systems (MCNSPS) conceptual design and evaluation report. Volume 3, technologies 2: Power conversion
[NASA-CR-179614-VOL-3] N89-22980
RAPID QUENCHING (METALLURGY)
Development of metastable processing paths for high temperature alloys
[AD-A202614] N89-22721
RARE EARTH ELEMENTS
Electronic structure of rare-earth luminescent centre in alkaline-earth sulphides
[DE88-705674] N89-23318
RATIONAL FUNCTIONS
The stable evaluation of a simple rational function and its application to spline approximation
[NPL-DITC-135/88] N89-23253
REACTION KINETICS
Models for surface intermediates in CO hydrogenation
[DE89-004348] N89-22712

Growth kinetics of grain-boundary induced melting: A molecular-dynamics study
[DE89-009655] N89-23343
REACTOR DESIGN
Megawatt Class Nuclear Space Power Systems (MCNSPS) conceptual design and evaluation report. Volume 3, technologies 2: Power conversion
[NASA-CR-179614-VOL-3] N89-22980
Megawatt Class Nuclear Space Power Systems (MCNSPS) conceptual design and evaluation report. Volume 2, technologies 1: Reactors, heat transport, integration issues
[NASA-CR-179614-VOL-2] N89-22981
REACTOR SAFETY
Adaptive contact elements for three-dimensional explicit transient analysis
[DE89-008436] N89-22958
Techniques for applying sets code procedures to large fault trees in PRA (Probabilistic Risk Assessment) analysis
[DE89-004823] N89-23261
Space Nuclear Safety Program
[DE89-008308] N89-23281
REAL TIME OPERATION
A signal processing system using MC68000 and TMS320 microprocessors
[USIP-88-07] N89-22803
Control of free-flying space robot manipulator systems
[NASA-CR-184837] N89-22918
A real-time simulator for man-in-the-loop testing of aircraft control systems (S!MTACS-RT)
[AD-A202599] N89-23067
Algorithms and architectures for smart sensing N89-23090
A real time hierarchical model for optic flow determination via spatiotemporal frequency channels N89-23158
Specifying real-time systems with interval logic
[NASA-CR-181804] N89-23183
Expert systems for real-time monitoring and fault diagnosis
[NASA-CR-179441] N89-23209
RECEIVERS
Geodetic positioning system for flying aircraft (May 1987)
[REPT-013/88] N89-22598
RECHARGING
Evaluation of several state-of-charge algorithms
[DE89-009752] N89-22812
Advanced rechargeable sodium batteries with novel cathodes N89-22988
A new concept for high-cycle-life LEO: Rechargeable MnO2-hydrogen N89-22991
Oxygen electrodes for rechargeable alkaline fuel cells N89-22998
RECONNAISSANCE
Fusion of multisensor data: A summary of the JASMIN project
[FOA-C-30498-3.3] N89-23213
RECONSTRUCTION
Reconstruction and relaxation of metal surfaces
[JUEL-2213] N89-22733
Reconstruction of defects from amplitude location curves
[REPT-780852-TW] N89-22934
RECOVERY PARACHUTES
Testing of a new recovery parachute system for the F111 aircraft crew escape module: An update
[DE89-007139] N89-22592
RECOVERY VEHICLES
Dynamic image interpretation for autonomous vehicle navigation
[AD-A204167] N89-22597
RECRYSTALLIZATION
Processing and properties of advanced aluminum alloys
[AD-A205187] N89-22725
RECURSIVE FUNCTIONS
A recursive formulation for flexible multibody dynamics N89-22968
REDOX CELLS
Novel nitrogen-based organosulfur electrodes for advanced intermediate temperature batteries N89-22987
REDUCED GRAVITY
Adsorption studies in the critical region of a pure fluid. Development of an apparatus for adsorption measurements under microgravity conditions
[ETN-89-93767] N89-22774
REDUNDANT COMPONENTS
A recursive formulation for flexible multibody dynamics N89-22968
REFLECTANCE
Image segmentation and reflection analysis through color N89-23150
REFLECTORS
The radiation performance of offset reflector antennas with horn feeds excited by high order modes
[FI-454-TB-43] N89-22792
REFRACTORIES
Advanced cartridge technology: Executive summary — spacecraft furnaces
[SEP-TS/F-6972/88-RP] N89-22636
REFRACTORY MATERIALS
Behavior of tungsten, molybdenum and alloys under unusual heating conditions N89-22674
High-performance refractory composite materials N89-22675
REFRACTORY METALS
Fracture toughness of MgCr2O4-based refractory composites
[DE89-009847] N89-22696
REFRIGERANTS
Simulation of a refrigerant evaporator
[ETN-89-94133] N89-22776
REGENERATIVE FUEL CELLS
A survey of advanced battery systems for space applications N89-22986
Hydrogen-oxygen proton-exchange membrane fuel cells and electrolyzers N89-22996
REGRESSION ANALYSIS
Aqueous impurity effects on stainless steel IGSCC (intergranular stress corrosion cracking): A central composite matrix analysis
[DE88-017382] N89-22726
REGULATIONS
Safe skies for tomorrow: Aviation safety in a competitive environment
[PB89-114318] N89-22591
Agreement on the International Space Station and Columbus Program
[REPT-34/88] N89-23360
Standardized bibliographic processing N89-23367
Data security N89-23369
RELATIVISTIC ELECTRON BEAMS
Simulations of axisymmetric erosion in IFR-Transported beams
[AD-A205882] N89-23301
RELATIVITY
Improved effective potential in the Einstein metric
[DE88-705716] N89-23355
RELAXATION METHOD (MATHEMATICS)
Structure recognition by connectionist relaxation: Formal analysis N89-23160
An algorithm for the three-index assignment problem
[AD-A205172] N89-23190
Incorporation of a boundary condition to numerical solution of POISSON's equation
[DE89-007132] N89-23231
RELAXATION TIME
Effects of ion collisions on quasilinear heating by the current-driven ion cyclotron instability in the high latitude ionosphere
[AD-A202512] N89-23032
RELIABILITY ANALYSIS
Transmission overhaul and replacement predictions using Weibull and renewal theory
[NASA-TM-102022] N89-22925
MIRAP, microcomputer reliability analysis program
[DE89-009749] N89-23200
REMOTE MANIPULATOR SYSTEM
A NASTRAN/TREETOPS solution to a flexible, multi-body dynamics and controls problem on a UNIX workstation N89-22945
REMOTE SENSING
Earth system science: A program for global change
[NASA-TM-101186] N89-22969
Evaluation of the Portable Instantaneous Display Analysis Spectrometer (PIDAS)
[NASA-CR-184878] N89-22970
Remote sensing of earth terrain
[NASA-CR-184937] N89-22971
Imaging radar applications in Europe. Illustrated experimental results (1978-1987)
[ESA-TM-01] N89-22978
Remote sensing information sciences research group: Browse in the EOS era
[NASA-CR-184637] N89-22979
Retrieving the distribution of liquid water content in clouds from observations of thermal microwave radiation N89-23056
Remote sensing of oceanic rainrates by passive microwave sensors: A statistical-physical approach N89-23057
REMOTE SENSORS
Selected aspects of discrete-time filtering techniques as applied to sensor control and signal processing problems
[ETN-89-94134] N89-22794
REMOTELY PILOTED VEHICLES
Design of a lightweight, low-cost geophysical survey vehicle
[DE89-009383] N89-22926
REQUIREMENTS
Project Radioastron N89-22623
Construction in weightlessness N89-22626
Power supply in space N89-22627
Surface temperature measurements using a thin film thermal array
[NASA-TM-101549] N89-22868
Overview of battery usage in NASA/GSFC LEO and GEO missions N89-22983
The design and implementation of a graphical VHDL (VHSIC Hardware Description Language) user interface
[AD-A202619] N89-23186
RESEARCH
Historical survey of biosatellites N89-22625
Earth system science: A program for global change
[NASA-TM-101186] N89-22969
RESEARCH AND DEVELOPMENT
Japan's sunshine project 1987 annual summary of solar energy R and D program
[DE88-756452] N89-23014
New developments in biotechnology: US investment in biotechnology, part 4
[PB88-246939] N89-23060
RESEARCH FACILITIES
Visting China's aerodynamics research and development center
[AD-A203980] N89-22615
Interactive ultrasonic nondestructive evaluation
[AD-A204166] N89-22931
New developments in biotechnology: US investment in biotechnology, part 4
[PB88-246939] N89-23060
Relevance of international research facilities to international stability
[DE89-009400] N89-23380
RESEARCH MANAGEMENT
Germany: Focus on Scientific and Technical Information, volume 4, number 1, April 1988
[AD-A204054] N89-23376
RESIDUAL STRESS
Fiber matrix interface effects in failure of ceramic matrix fiber composites
[AD-A204618] N89-22686
Three-dimensional response of composites
[AD-A204623] N89-22687
RESIN MATRIX COMPOSITES
Material/manufacturing process interaction in advanced material technologies N89-22662
Development of an asbestos-free insulant for rocket motors N89-22679
A survey of poly-ether-ether-ketone and its advanced composites
[FFA-TN-1988-37] N89-22707
RESONANCE
Calculation of low frequency vibrational resonances of submerged structures N89-22951
RESONANCE SCATTERING
Monte Carlo applied to resonance scattering of high altitude fluorescent radiation
[DE89-006519] N89-23035
RESONANT FREQUENCIES
Electrodynamic transient tests — satellites
[CNES-CT/DRT/TVE/SM-024] N89-22644
Rotor instability due to a gear coupling connected to a bearingless sun wheel of a planetary gear N89-22893
RESONANT TUNNELING
Molecular beam epitaxial growth and characterization of metastable compound semiconductors for infrared detector applications
[AD-A205175] N89-23312
RESOURCES MANAGEMENT
User needs and how to determine them N89-23365
Information resources management N89-23371
Fostering interaction of government, defense, and aerospace databases N89-23374
RESPIRATION
Inhalation developmental toxicology studies: Teratology study of methyl ethyl ketone in mice
[DE89-009563] N89-23062
RESPIRATORY RATE
Efficacy of conventional and high-frequency ventilation at altitude
[AD-A205922] N89-23071
REYNOLDS NUMBER
Experimental and theoretical studies of vertical annular liquid jets
[DE89-009153] N89-22851
REYNOLDS STRESS
Turbulence modeling N89-22819
Direct numerical simulations of turbulent convection with a variable gravity and Keplerian rotation N89-22831

RIEMANN MANIFOLD
Construction of harmonic maps between pseudo-Riemannian spheres and hyperbolic spaces
[DE88-705695] N89-23353
RIGID STRUCTURES
A recursive formulation for flexible multibody dynamics N89-22968
RINGS (MATHEMATICS)
On polynomial ideals of finite codimension with applications to box spline theory
[AD-A204095] N89-23225
RISK
Techniques for applying sets code procedures to large fault trees in PRA (Probabilistic Risk Assessment) analysis
[DE89-004823] N89-23261
ROADS
Cooperative methods for road tracking in aerial imagery N89-23101
ROBOTICS
Control of free-flying space robot manipulator systems
[NASA-CR-184837] N89-22918
Configuration comparison analysis for the AFIT/AAMRL anthropomorphic robotic manipulator
[AD-A202618] N89-22921
Traction-drive force transmission for telerobotic joints
[NASA-CR-183331] N89-22922
Structural dynamics branch research and accomplishments for FY 1988
[NASA-TM-101406] N89-22939
The Space Station Flight Telerobotic Servicer and the human
[NASA-TM-100615] N89-23068
Proceedings: Image Understanding Workshop, volume 1
[AD-A197558] N89-23074
USC image understanding research: 1987-1988 N89-23076
Progress in image understanding at the University of Rochester N89-23082
Image understanding and robotics research at Columbia University N89-23083
Qualitative reasoning and modeling for robust target tracking and recognition from a mobile platform N89-23086
Knowledge based vision for terrestrial robots N89-23087
Kalman filter-based algorithms for estimating depth from image sequences N89-23094
Perception with feedback N89-23098
Qualitative navigation 2 N89-23100
Self calibration of motion and stereo vision for mobile robot navigation N89-23106
Autonomous navigation in cross-country terrain N89-23107
Contour correspondences in dynamic imagery N89-23109
Spatio-temporal analysis of an image sequence with occlusion N89-23110
Proceedings: Image Understanding Workshop, volume 2
[AD-A197559] N89-23115
Automatic generation of noncolliding trajectories and manipulation task planning in robotics
[LAAS-89-002] N89-23222
ROBOTS
Generic models for robot navigation N89-23112
Motion from a sequence of images N89-23155
Depth from looming structure N89-23167
ROBUSTNESS (MATHEMATICS)
Robust parallel computation of 2-D model-based recognition N89-23130
Robust stabilization of an inverted double pendulum system via a polynomial approach to H(infinity) optimal control
[MEMO-742] N89-23220
ROCKET ENGINE DESIGN
Application of Advanced Material for Turbomachinery and Rocket Propulsion
[AGARD-CP-449] N89-22654
Future advanced aero-engines: The materials challenge N89-22659
New metallic materials for gas turbines N89-22660
Damage tolerance concepts for advanced materials and engines N89-22661
ROCKET ENGINES
CVD and diffusion coatings for high temperature applications in turbomachinery and rocket motors N89-22658
Thrust chamber thermal barrier coating techniques N89-22671
Fiber reinforced superalloys for rocket engines N89-22673
Development of an asbestos-free insulant for rocket motors N89-22679
Implementation of active magnetic bearings on advanced rocket engine turbopumps
[ETN-89-94365] N89-22929
ROCKET LININGS
The demonstration of monolithic and composite ceramics in aircraft gas turbine combustors N89-22665
ROCKET NOZZLES
Silicon-carbide coated carbon-carbon: An advanced material for rocket systems N89-22672
High-performance refractory composite materials N89-22675
High temperature composite materials for rocket propulsion N89-22676
RODS
Fiber optic laser rod
[DE89-009598] N89-22887
ROLLING CONTACT LOADS
Incorporating general race and housing flexibility and deadband in rolling element bearing analysis N89-22912
ROOTS OF EQUATIONS
Semilinear elliptic eigenvalue problems
[ETN-89-94142] N89-23232
ROTARY STABILITY
Rotor instability due to a gear coupling connected to a bearingless sun wheel of a planetary gear N89-22893
Rotordynamic stability problems and solutions in high pressure turbocompressors N89-22914
ROTARY WING AIRCRAFT
NASA's program on icing research and technology
[NASA-TM-101989] N89-22569
Convergence of discrete-vortex induced-flow calculations by optimum choice of mesh N89-22585
ROTATING BODIES
Some in-field experiences of non-synchronous vibrations in large rotating machinery N89-22894
ROTATING SHAFTS
Piezoelectric pushers for active vibration control of rotating machinery N89-22896
ROTATING STALLS
Some field experience with subsynchronous vibration of centrifugal compressors N89-22892
ROTATION
Influence of impeller and diffuser geometries on the lateral fluid forces of whirling centrifugal impeller N89-22907
A theoretical study of fluid forces on a centrifugal impeller rotating and whirling in a vaned diffuser N89-22908
Influence of impeller shroud forces on turbopump rotor dynamics N89-22909
Finite element analysis of a micromechanical deformable mirror device N89-22953
Nonlinear finite element simulation of the large angle motion of flexible bodies
[DE89-006505] N89-23230
Reversed sense of the outward direction for dynamical effects of rotation close to a Schwarzschild black hole
[DE88-705670] N89-23389
ROTOR AERODYNAMICS
A study of unsteady turbulent flow past airfoils N89-22587
Rotordynamic Instability Problems in High-Performance Turbomachinery, 1988
[NASA-CP-3026] N89-22891
Annular honeycomb seals: Test results for leakage and rotordynamic coefficients; comparisons to labyrinth and smooth configurations N89-22899
Rotordynamic coefficients for labyrinth seals calculated by means of a finite difference technique N89-22900
Rotordynamic coefficients for stepped labyrinth gas seals N89-22901
A seal test facility for the measurement of isotropic and anisotropic linear rotordynamic characteristics N89-22905
Finite difference analysis of rotordynamic seal coefficients for an eccentric shaft position N89-22906
Influence of impeller shroud forces on turbopump rotor dynamics N89-22909
Magnetic bearing stiffness control using frequency band filtering N89-22910
Incorporating general race and housing flexibility and deadband in rolling element bearing analysis N89-22912
Role of circumferential flow in the stability of fluid-handling machine rotors N89-22915
Enhanced rotor modeling tailored for rub dynamic stability analysis and simulation N89-22916
High stability design for new centrifugal compressor N89-22917
ROTOR BLADES (TURBOMACHINERY)
A study of unsteady turbulent flow past airfoils N89-22587
Rotordynamic coefficients for labyrinth seals calculated by means of a finite difference technique N89-22900
Rotordynamic coefficients for stepped labyrinth gas seals N89-22901
Role of circumferential flow in the stability of fluid-handling machine rotors N89-22915
Enhanced rotor modeling tailored for rub dynamic stability analysis and simulation N89-22916
ROTORS
Aerodynamic detuning of a loaded airfoil cascade in an incompressible flow by a locally analytical method N89-22588
Active vibration control for flexible rotor by optimal direct-output feedback control
[NASA-TM-101972] N89-22605
Some in-field experiences of non-synchronous vibrations in large rotating machinery N89-22894
The spectral analysis of an aero-engine assembly incorporating a squeeze-film damper N89-22895
An electroviscous damper N89-22898
A seal test facility for the measurement of isotropic and anisotropic linear rotordynamic characteristics N89-22905
A magnetic damper for first mode vibration reduction in multimass flexible rotors N89-22911
Experimental verification of an eddy-current bearing N89-22913
ROVING VEHICLES
Knowledge-based vision technology progress at Hughes AI Center N89-23084
RUBY LASERS
Gamma ray laser pump diagnostic
[AD-A205221] N89-22883
RUN TIME (COMPUTERS)
Enhancements to the IBM version of COSMIC/NASTRAN N89-22946
Object recognition from a large database using a decision tree N89-23135

S

SADDLE POINTS
A Borel-Ritt theorem with prescribed error bounds
[MEMO-723] N89-23240
SAFETY MANAGEMENT
Safe skies for tomorrow: Aviation safety in a competitive environment
[PB89-114318] N89-22591
SAMPLING
Far- and mid-infrared properties of metal-insulator composite materials
[AD-A204914] N89-22689
Evaluation of the Portable Instantaneous Display Analysis Spectrometer (PIDAS)
[NASA-CR-184878] N89-22970
SATELLITE ALTIMETRY
Development of a satellite SAR image spectra and altimeter wave height data assimilation system for ERS-1
[NASA-CR-182685] N89-22975
Detailed gravity anomalies derived form Seasat altimeter data. A comparison of two alternative approaches: Least squares collocation and a method based on FFT
[ETN-89-94144] N89-23039
SATELLITE ANTENNAS
Design of an ELF/VLF satellite for under the ice submarine communications
[AD-A202607] N89-22639
Study of a DRS experimental payload for single and multiple access at S band: Executive summary
[PSD88/00017] N89-22648
SATELLITE COMMUNICATION
Design of an ELF/VLF satellite for under the ice submarine communications
[AD-A202607] N89-22639
PSDE/SAT-2: Communication system architecture study, executive summary
[ESA-CR(P)-2732] N89-22802
SATELLITE CONFIGURATIONS
Second generation Meteosat pre-phase A system study
[BA-SGM-FR-01] N89-22640
SATELLITE DESIGN
Design of an ELF/VLF satellite for under the ice submarine communications
[AD-A202607] N89-22639
Second generation Meteosat pre-phase A system study
[BA-SGM-FR-01] N89-22640
Study of a wideband telecommunications satellite for Europe
[ATES/DMA/TRM/162-86] N89-22641
SATELLITE IMAGERY
A multinational verification satellite: A preliminary investigation — arms control
[FOA-C-10312-9.3] N89-22974
Theoretical studies for ERS-1 wave mode, volume 1
[GEC-MTR-87/110-VOL-1] N89-22977

Imaging radar applications in Europe. Illustrated experimental results (1978-1987)
[ESA-TM-01] N89-22978
The response of thermospheric nitric oxide to an auroral storm N89-23031
SEAPAK user's guide, version 1.0
[NASA-TM-100728] N89-23162

SATELLITE NETWORKS
Study of a wideband telecommunications satellite for Europe
[ATES/DMA/TRM/162-86] N89-22641
Minimum number of satellites for periodic coverage
[FOA-C-30511-9.4] N89-22976

SATELLITE OBSERVATION
Derivation of a large-scale map of heat load in the region Freiburg-Basel (Germany, F.R.) using satellite data. A contribution to the production of bioclimate data based on a geographic information system
[REPT-27] N89-22972
A multinational verification satellite: A preliminary investigation — arms control
[FOA-C-10312-9.3] N89-22974
Diabatic circulations in the stratosphere N89-23043
Observational aspects of interacting galaxies N89-23385

SATELLITE ORBITS
Overview of battery usage in NASA/GSFC LEO and GEO missions N89-22983

SATELLITE TRACKING
Observation parameters for a ground-based radar station to survey near-earth satellites
[REPT-4-88] N89-22793

SATURN RINGS
Dynamics of particles in the bending waves of the planetary rings
[DE88-705714] N89-23396

SCALARS
The Large Eddy Simulation (LES) of MESOSCOP for atmospheric boundary layer flows including passive scalars
[DFVLR-MITT-88-28] N89-23041

SCALE MODELS
Investigation of the effects of increased sophistication of simulation of the atmospheric wind in wind tunnels N89-22620

SCALING LAWS
Scaling relations for a beam-deflecting TM(110) mode in an asymmetric cavity
[DE89-009277] N89-22796

SCANNERS
A fast spatial scanning combination emissive and Mach probe for edge plasma diagnosis
[DE89-009674] N89-23295

SCATTER PROPAGATION
Analysis of regional phases using three component data
[AD-A205480] N89-23045

SCATTERING CROSS SECTIONS
Hard scattering of (almost) real photons at HERA
[NIKHEF-H/88-3] N89-23276

SCATTERING FUNCTIONS
Dynamic scattering from multicomponent polymer systems
[DE88-705677] N89-22752
Monotonicity-preserving quadratic C sup 1-spline interpolation to scattered data
[MEMO-744] N89-23252

SCENE ANALYSIS
Image understanding research at SRI International N89-23080
Image understanding and robotics research at Columbia University N89-23083
Knowledge-based vision technology progress at Hughes AI Center N89-23084
Image understanding research at GE N89-23085
Qualitative reasoning and modeling for robust target tracking and recognition from a mobile platform N89-23086
Some sample algorithms for the image understanding architecture N89-23089
Algorithms and architectures for smart sensing N89-23090
The Maryland approach to image understanding N89-23091
The MIT vision machine N89-23093
Perception with feedback N89-23098
Qualitative motion detection and tracking of targets from a mobile platform N89-23099
Constructing simple stable descriptions for image partioning N89-23104
Three-dimensional object recognition using surface descriptions N89-23105
Generic models for robot navigation N89-23112
Multiresolution aerial image interpretation N89-23116
Perceptual grouping for the detection and description of structures in aerial images N89-23117
Object recognition from a large database using a decision tree N89-23135
Computation of motion in depth parameters: A first step in stereoscopic motion interpretation N89-23153
Generalizing epipolar-plane image analysis on the spatiotemporal surface N89-23164
Building surfaces of evolution: The weaving wall N89-23165
Image segmentation using geometric and physical constraints N89-23172
Adaptive smoothing for feature extraction N89-23173
An optimal algorithm for the derivation of shape from shadows N89-23176

SCHEDULING
A knowledge-based tool for multilevel decomposition of a complex design problem
[NASA-TP-2903] N89-23181

SCHROEDINGER EQUATION
Optical studies of the magnetospheric cusp from Svalbard
[AD-A205432] N89-23044

SCHWARZSCHILD METRIC
Reversed sense of the outward direction for dynamical effects of rotation close to a Schwarzschild black hole
[DE88-705670] N89-23389

SCINTILLATION
Ionospheric scintillation studies
[AD-A205210] N89-23034

SCINTILLATION COUNTERS
Experimental study of uranium plastic scintillator calorimeters
[NIKHEF-H/88-4] N89-22878
Positron lifetime technique with applications in materials science
[ETN-89-94141] N89-23331

SEALS (STOPPERS)
Performance of all-metal demountable cryogenic seals at superfluid helium temperatures
[NASA-TM-102190] N89-22650
Rotordynamic Instability Problems in High-Performance Turbomachinery, 1988
[NASA-CP-3026] N89-22891
Annular honeycomb seals: Test results for leakage and rotordynamic coefficients; comparisons to labyrinth and smooth configurations N89-22899
Rotordynamic coefficients for labyrinth seals calculated by means of a finite difference technique N89-22900
Rotordynamic coefficients for stepped labyrinth gas seals N89-22901
A seal test facility for the measurement of isotropic and anisotropic linear rotordynamic characteristics N89-22905
Finite difference analysis of rotordynamic seal coefficients for an eccentric shaft position N89-22906
Rotordynamic stability problems and solutions in high pressure turbocompressors N89-22914

SECURITY
Relevance of international research facilities to international stability
[DE89-009400] N89-23380

SEDATIVES
Benzodiazepines and caffeine: Effect on daytime sleepiness, performance, and mood
[AD-A205862] N89-23066

SEEBECK EFFECT
New thermocouple: Characteristic investigation of Au+Pd+Ni/Ni+Cr thermocouple below 273K
[PB89-112940] N89-22867

SEGMENTS
An integrated approach to stereo matching, surface reconstruction and depth segmentation using consistent smoothness assumptions N89-23092
Image segmentation and reflection analysis through color N89-23150
Texture models and image measures for segmentation N89-23162
Image segmentation using geometric and physical constraints N89-23172

SEISMIC WAVES
Analysis of regional phases using three component data
[AD-A205480] N89-23045

SELECTIVE DISSEMINATION OF INFORMATION
Data security N89-23369
R and D productivity: Relationship to Selective Dissemination of Information (SDI) in the corporate environment N89-23375

SELF CONSISTENT FIELDS
Improved effective potential in the Einstein metric
[DE88-705716] N89-23355

SELF DIFFUSION (SOLID STATE)
Interaction of coatings with base metals at high temperature N89-22669
Point defects and oxygen diffusion in high T sub c superconductors
[DE89-009642] N89-23341

SELF EXCITATION
Some field experience with subsynchronous vibration of centrifugal compressors N89-22892
Some in-field experiences of non-synchronous vibrations in large rotating machinery N89-22894
Rotordynamic stability problems and solutions in high pressure turbocompressors N89-22914

SELF INDUCED VIBRATION
Some field experience with subsynchronous vibration of centrifugal compressors N89-22892

SEMICONDUCTOR DEVICES
Experimental investigation of hot electron and related effects in gallium (aluminum) arsenide devices
[AD-A205442] N89-23349

SEMICONDUCTORS (MATERIALS)
Reactions of inorganic high polymers as a route to tailored solids
[AD-A204602] N89-22750
Molecular beam epitaxial growth and characterization of metastable compound semiconductors for infrared detector applications
[AD-A205175] N89-23312
Development of magnetic field assisted melt stabilization with heat and mass transfer control in low pressure LEC growth of GaAs
[AD-A205185] N89-23313
Electronic properties of Ge sub 1-x Si sub x: A simplified tight binding approach
[DE88-705671] N89-23317
Basic research in superconductor, ceramic and semiconductor sciences at selected Japanese laboratories based on a 1988 visit: Highlights, summary and overview, detailed notes from selected Japanese laboratories
[DE89-009637] N89-23339

SENSITIVITY
Ultra-sensitive X-ray sensors give improved contrast senaitivity
[DE89-003581] N89-22872

SEPARATED FLOW
On the Lagrangian description of unsteady boundary layer separation. Part 2: The spinning sphere
[NASA-TM-102027] N89-22861

SEPARATORS
The importance of batteries in unmanned missions N89-22984
The application of Dow Chemical's perfluorinated membranes in proton-exchange membrane fuel cells N89-22995
The separation number
[MEMO-710] N89-23236

SERIES EXPANSION
A Borel-Ritt theorem with prescribed error bounds
[MEMO-723] N89-23240
Asymptotic expansions with error bounds for solutions of difference equations of level 1 sup +
[MEMO-724] N89-23241

SERVICE LIFE
Transmission overhaul and replacement predictions using Weibull and renewel theory
[NASA-TM-102022] N89-22925

SERVICES
User needs and how to determine them N89-23365

SERVOMECHANISMS
Traction-drive force transmission for telerobotic joints
[NASA-CR-183331] N89-22922

SET THEORY
Short proofs of some Fan-type results
[MEMO-711] N89-23237

SHADOWS
An optimal algorithm for the derivation of shape from shadows N89-23176

SHAFTS (MACHINE ELEMENTS)
Finite difference analysis of rotordynamic seal coefficients for an eccentric shaft position N89-22906

SHAPES
Affine invariant matching N89-23103
The integration of information from stereo and multiple shape-form-texture cues N89-23145
Combining information in low-level vision N89-23152
Projective invariants of shapes N89-23175
An optimal algorithm for the derivation of shape from shadows N89-23176

SHEAR FLOW
Analysis of turbulence structures in shear flows N89-22826
Direct numerical simulation of compressible free shear flows
[AIAA-89-0374] N89-22827

SHEAR LAYERS
The effects of stabilizing and destabilizing longitudinal curvature on the structure of turbulent, two-stream mixing layers N89-22833

SHEAR PROPERTIES
Damage initiation in two-dimensional, woven, carbon-carbon composites
[AD-A202617] N89-22683

A study of high strain rate generation of adiabatic shear bands in a titanium alloy N89-22967
SHELLS (STRUCTURAL FORMS)
Dynamic fracture in solids
[PB89-112650] N89-22937
SHOCK WAVE INTERACTION
Numerical simulation of blast waves
[REPT-882-320-102] N89-22858
The structure and control of three-dimensional shock wave turbulent boundary layer interactions
[AD-A205923] N89-22866
SHOCK WAVE PROPAGATION
Numerical simulation of blast waves
[REPT-882-320-102] N89-22858
SHORT CIRCUITS
Electrical properties and detection methods for CMOS IC defects
[DE89-005775] N89-23327
SHROUDED TURBINES
Influence of impeller shroud forces on turbopump rotor dynamics N89-22909
SIGNAL ANALYSIS
Chemical state depth profiling by Auger signal decomposition: Silicon oxynitride
[DE89-009530] N89-22764
SIGNAL DETECTION
Verification and limitations of the monostatic-bistatic radar cross section derived by Keil
[AD-A202601] N89-22782
Detection of known signals in arbitrary backgrounds
[AD-A204076] N89-22784
Signal detection in fractional Gaussian noise and an RKHS (Reproducing Kernel Hilbert Space) approach to robust detection and estimation
[AD-A205441] N89-22805
SIGNAL DETECTORS
Signal detection in fractional Gaussian noise and an RKHS (Reproducing Kernel Hilbert Space) approach to robust detection and estimation
[AD-A205441] N89-22805
Organic and polymer crystalline films for spatial light modulation
[AD-A205906] N89-23350
SIGNAL DISTORTION
Wavelength streak camera
[DE89-009612] N89-22874
SIGNAL MEASUREMENT
Organic and polymer crystalline films for spatial light modulation
[AD-A205906] N89-23350
SIGNAL PROCESSING
Distortions caused by the signal processing in analog AM modulators
[DE88-705657] N89-22785
Selected aspects of discrete-time filtering techniques as applied to sensor control and signal processing problems
[ETN-89-94134] N89-22794
HIFI: A design method for implementing signal processing algorithms on VLSI processor arrays
[ETN-89-94138] N89-22795
A signal processing system using MC68000 and TMS320 microprocessors
[USIP-88-07] N89-22803
The propagation of noise through streak systems
[DE89-006600] N89-22869
Distortions in the output signals of conventional spectrum analyzers
[DE88-705656] N89-22871
Interactive ultrasonic nondestructive evaluation
[AD-A204166] N89-22931
A divide and conquer method for unitary and orthogonal eigenproblems
[AD-A205433] N89-23255
SIGNAL RECEPTION
Wavelength streak camera
[DE89-009612] N89-22874
SILICON
Grain-boundary and free-surface induced thermodynamic melting: A molecular dynamics study in silicon
[DE89-007415] N89-23309
Theoretical study of the Pd-B complex in silicon
[DE88-705650] N89-23316
SILICON ALLOYS
Electronic properties of Ge sub 1-x Si sub x: A simplified tight binding approach
[DE88-705671] N89-23317
Electronic properties of Ge(1-X)Si(X): Alloying versus pressure
[DE88-705678] N89-23320
SILICON CARBIDES
Utilization of high temperature composites in turbojet engines N89-22667
Silicon-carbide coated carbon-carbon: An advanced material for rocket systems N89-22672
High temperature composite materials for rocket propulsion N89-22676
The isothermal fatigue behavior of a unidirectional SiC/Ti composite and the Ti alloy matrix
[NASA-TM-101984] N89-22684
Observations on the toughening of Al2O3-SiC composites
[DE89-009843] N89-22695
Basic program for the development of a reliable high strength construction ceramic mode of SiC
[MTU-TB-87/927] N89-22757
Coating of silicon carbide fibers
[CERT-423900/RF] N89-22767
SILICON FILMS
Diagnostics of glow discharges used to produce hydrogenated amorphous silicon films
[DE89-000887] N89-22760
SILICON NITRIDES
Chemical state depth profiling by Auger signal decomposition: Silicon oxynitride
[DE89-009530] N89-22764
SILICON OXIDES
Criteria for selection of phase names for oxides
[NPL-DMA(A)169] N89-22714
SILICON TRANSISTORS
Radiation hardened detector arrays for the far and extreme infrared, phase 1
[BF-R-65.695-10] N89-23347
SIMD (COMPUTERS)
Implementing nested conditional statements in SIMD machines
[NASA-CR-181832] N89-23073
Pyramid algorithms implementation on the connection machine N89-23129
SIMPLEX METHOD
Approximation of surfaces constrained by a differential equation using simplex splines
[MEMO-739] N89-23249
SINGLE CRYSTALS
Development of stress and lifing criteria for single crystal turbine blades N89-22663
Conductivity fluctuations in mixed Na/Ca beta alumina
[AD-A205416] N89-23348
SINGLE EVENT UPSETS
Effects of cosmic rays on single event upsets
[NASA-CR-184835] N89-23400
SINGULARITY (MATHEMATICS)
A pseudo singular value decomposition and inner functions in super optimal control
[OUEL-1738/88] N89-23214
SINKS
Determination of the dynamic CO2 source-sink function of different biomes with the object of verifying seasonality and trend of atmospheric CO2 measurements of different stations
[ETN-89-93763] N89-23038
SINTERING
Microwave sintering of boron carbide
[DE89-009652] N89-22763
Effects of different fabrication techniques on the Yttrium-Barium-Copper oxide high temperature superconductor
[AD-A202598] N89-23304
SISO (CONTROL SYSTEMS)
Nonlinear model matching with prescribed tracking error with an application to Hamiltonian systems
[MEMO-731] N89-23244
SKEWNESS
Ribbons, symmetries and skewed symmetries N89-23170
SLATER ORBITALS
Solution of multi-center molecular integrals of Slater-type orbitals
[NASA-TM-101545] N89-22692
SLEEP
Benzodiazepines and caffeine: Effect on daytime sleepiness, performance, and mood
[AD-A205862] N89-23066
SLIDING
Grain boundary sliding phenomena in polycrystalline solids
[DE89-007792] N89-23326
SLIDING FRICTION
Alumina reinforced tetragonal zirconia (TZP) composites
[DE89-008880] N89-22690
Temperature effects on the break-in of nickel aluminide alloys
[DE89-005341] N89-22729
SODIUM COMPOUNDS
Polymer electrolytes with exclusively cationic conductivity
[DE89-009521] N89-22761
SODIUM SULFUR BATTERIES
Laboratory evaluation of advanced battery technologies for electric vehicle applications
[DE89-009810] N89-22814
Novel nitrogen-based organosulfur electrodes for advanced intermediate temperature batteries N89-22987
Advanced rechargeable sodium batteries with novel cathodes N89-22988
Sodium sulfur battery flight experiment definition study N89-23009
Advanced high-temperature batteries N89-23010
SOFTWARE ENGINEERING
SEAPAK user's guide, version 1.0
[NASA-TM-100728] N89-23182
HOOD Toolset Development Project: ECLIPSE/HOOD/REP, issue 1.1
[ESA-CR(P)-2746] N89-23204
Expert systems on multiprocessor architectures, phase 1
[AD-A204907] N89-23206
SOFTWARE TOOLS
A knowledge-based tool for multilevel decomposition of a complex design problem
[NASA-TP-2903] N89-23181
Developing software to use parallel processing effectively
[AD-A205184] N89-23192
HOOD Toolset Development Project: ECLIPSE/HOOD/REP, issue 1.1
[ESA-CR(P)-2746] N89-23204
SOIL MOISTURE
Localization of solutions of a nonlinear Fokker-Planck equation with Dirichlet boundary conditions --- soil moisture infiltration
[MEMO-733] N89-23248
SOLAR ARRAYS
Japan's sunshine project 1987 annual summary of solar energy R and D program
[DE88-756452] N89-23014
SOLAR CELLS
The NASA Space Solar Cell Advanced Research Program
[NASA-TM-102020] N89-22651
Progress in crystalline silicon research
[DE89-007423] N89-22749
Advances in concentrator cell technology
[DE89-007432] N89-23013
Japan's sunshine project 1987 annual summary of solar energy R and D program
[DE88-756452] N89-23014
Research on amorphous-silicon-based, thin-film photovoltaic devices, task B
[DE89-000885] N89-23021
Comparison of solar photovoltaic and nuclear reactor power systems for a human-tended lunar observatory
[NASA-TM-102015] N89-23397
SOLAR COLLECTORS
Comparison of a cavity solar receiver numerical model and experimental data
[DE89-003609] N89-23016
Design considerations for heat-pipe solar receivers
[DE89-004037] N89-23017
Solar radiation at the earth's surface: What are we doing to it and with it?
[DE89-008446] N89-23018
SOLAR CORONA
Turbulent transport in the solar nebula N89-22829
Direct numerical simulations of turbulent convection with a variable gravity and Keplerian rotation N89-22831
SOLAR DYNAMIC POWER SYSTEMS
Numerical model of solar dynamic radiator for parametric analysis
[NASA-TM-102054] N89-22653
SOLAR ENERGY
Power supply in space N89-22627
Progress in crystalline silicon research
[DE89-007423] N89-22749
Photovoltaic systems for today's remote power applications
[DE89-007431] N89-23012
Advances in concentrator cell technology
[DE89-007432] N89-23013
Japan's sunshine project 1987 annual summary of solar energy R and D program
[DE88-756452] N89-23014
An assessment of the optical performance of stretched-membrane mirror modules
[DE88-017347] N89-23015
Design considerations for heat-pipe solar receivers
[DE89-004037] N89-23017
Solar radiation at the earth's surface: What are we doing to it and with it?
[DE89-008446] N89-23018

SOLAR ENERGY CONVERSION
Material degradation in a barium hydroxide latent heat storage pilot unit
[ESA-TT-1107] N89-22715
Japan's sunshine project 1987 annual summary of solar energy R and D program
[DE88-756452] N89-23014
Solar thermal program summary. Volume 1: Overview, fiscal year 1988
[DE89-000860] N89-23020
SOLAR FLARES
Observational techniques for solar flare gamma-rays, hard X-rays, and neutrons
[NASA-CR-184910] N89-23399
SOLAR HEATING
Japan's sunshine project 1987 annual summary of solar energy R and D program
[DE88-756452] N89-23014
Development of a differential temperature probe for the measurement of atmospheric turbulence at all levels
[AD-A205893] N89-23047
SOLAR ORBITS
Measurements of a barotropic planetary vorticity mode in an eddy-resolving quasi-geostrophic model using acoustic tomography
[AD-A205409] N89-23058
SOLAR RADIATION
Solar radiation at the earth's surface: What are we doing to it and with it?
[DE89-008446] N89-23018
Reports from the German Meteorological Service. No. 177: Small-scale variability of solar radiation
[ISBN-3-88148-224-X] N89-23053
SOLAR REFLECTORS
An assessment of the optical performance of stretched-membrane mirror modules
[DE88-017347] N89-23015
SOLAR SPECTRA
Optical studies of the magnetospheric cusp from Svalbard
[AD-A205432] N89-23044
SOLAR X-RAYS
Observational techniques for solar flare gamma-rays, hard X-rays, and neutrons
[NASA-CR-184910] N89-23399
SOLID CRYOGENS
Variational analysis of railgun plasma-arc-armature for acceleration of solid hydrogen pellets for fusion reactor refueling
[DE89-009556] N89-22634
SOLID ELECTRODES
Recent advances in solid polymer electrolyte fuel cell technology with low platinum loading electrodes N89-22994
Hydrogen-oxygen proton-exchange membrane fuel cells and electrolyzers N89-22996
SOLID ELECTROLYTES
Reactions of inorganic high polymers as a route to tailored solids
[AD-A204602] N89-22750
Fabrication of solid oxide fuel cell by electrochemical vapor deposition
[DE89-009605] N89-23023
Solid oxide fuel cell matrix and modules
[DE89-009607] N89-23024
SOLID ROCKET PROPELLANTS
Internal debonding of solid rocket fuel: An experimental investigation
[AD-A205903] N89-22772
SOLID STATE LASERS
Cr3(+)-doped colquiriite solid state laser material
[DE89-010106] N89-22888
SOLIDIFICATION
Development of metastable processing paths for high temperature alloys
[AD-A202614] N89-22721
Mechanisms of cascade collapse
[DE89-009882] N89-22740
Diagnostics of phase formation in metastable solidification of metals
[DFVLR-FB-88-43] N89-22745
SOLIDS
Using generic geometric and physical models for representing solids N89-23114
Recognizing solid objects by alignment N89-23174
Grain boundary sliding phenomena in polycrystalline solids
[DE89-007792] N89-23326
SOLVENTS
The effects of plastic media blasting paint removal on the microstructure of graphite/epoxy composite materials
[AD-A204801] N89-22688
Dynamic scattering from multicomponent polymer systems
[DE88-705677] N89-22752
SOUND PRESSURE
Comparison of measured and calculated sound pressure levels around a large horizontal axis wind turbine generator
[NASA-TM-100654] N89-23270
SOUND TRANSMISSION
Evaluation of the ride quality of a light twin engine airplane using a ride quality meter
[NASA-TP-2913] N89-22568
Power flows and Mechanical Intensities in structural finite element analysis N89-22952
SOUND WAVES
Corrosion monitoring with acoustic wave devices
[DE89-005235] N89-22728
Acoustic wave device using plate modes with surface-parallel displacement
[DE89-009719] N89-23273
SOUTHERN OSCILLATION
On the physical causes of ENSO events and the ITCZ's extreme latitudinal displacements
[DE88-705654] N89-23050
SOVIET SPACECRAFT
JPRS report: Science and technology. USSR: Space
[JPRS-USP-88-003] N89-22622
SPACE ADAPTATION SYNDROME
Historical survey of biosatellites N89-22625
SPACE DEBRIS
Orbital debris environment for spacecraft designed to operate in low Earth orbit
[NASA-TM-100471] N89-22638
In-space technology development: Atomic oxygen and orbital debris effects
[NASA-TM-102154] N89-22682
SPACE EXPLORATION
Glavkosmos official Yu. P. Semenov interviewed on development of USSR space program N89-22629
Future space projects discussed at Moscow Space Forum N89-22630
Launch options for the future: Special report
[PB89-114268] N89-22637
Human exploration mission studies N89-22985
SPACE FLIGHT
Launch options for the future: Special report
[PB89-114268] N89-22637
SPACE HEATING (BUILDINGS)
Development of advanced heat pump. Part 2: Preliminary test of two-stage compression heat pump
[DE88-756838] N89-22841
SPACE INDUSTRIALIZATION
Human exploration mission studies N89-22985
SPACE MANUFACTURING
Consortium for materials development in space
[NASA-CR-181405] N89-22773
SPACE MISSIONS
Space control: A national imperative
[AD-A202612] N89-22631
A survey of advanced battery systems for space applications N89-22986
SPACE NAVIGATION
Navigation experiment NAVEX: The reading differences between all ground station measuring clocks during Spacelab pass of the D1 mission
[ESA-TT-1113] N89-22599
SPACE PERCEPTION
Unity vision block with focal plane
[AD-A204694] N89-23283
SPACE POWER REACTORS
Megawatt Class Nuclear Space Power Systems (MCNSPS) conceptual design and evaluation report. Volume 3, technologies 2: Power conversion
[NASA-CR-179614-VOL-3] N89-22980
Megawatt Class Nuclear Space Power Systems (MCNSPS) conceptual design and evaluation report. Volume 2, technologies 1: Reactors, heat transport, integration issues
[NASA-CR-179614-VOL-2] N89-22981
Space Nuclear Safety Program
[DE89-008308] N89-23281
Comparison of solar photovoltaic and nuclear reactor power systems for a human-tended lunar observatory
[NASA-TM-102015] N89-23397
SPACE PROCESSING
Consortium for materials development in space
[NASA-CR-181405] N89-22773
SPACE PROGRAMS
Navigation experiment NAVEX: The reading differences between all ground station measuring clocks during Spacelab pass of the D1 mission
[ESA-TT-1113] N89-22599
SPACE SHUTTLE ORBITERS
Orbiter Flying Qualities (OFQ) Workstation user's guide
[NASA-CR-179440] N89-22612
SPACE STATION POLAR PLATFORMS
GPS terminal: Study of a GPS receiver for Columbus platform elements, executive summary
[GPS-REP-SEL-002] N89-22643
SPACE STATION POWER SUPPLIES
Numerical model of solar dynamic radiator for parametric analysis
[NASA-TM-102054] N89-22653
SPACE STATIONS
The Space Station Flight Telerobotic Servicer and the human
[NASA-TM-100615] N89-23068
SPACE TRANSPORTATION
Launch options for the future: Special report
[PB89-114268] N89-22637
SPACE WEAPONS
Space control: A national imperative
[AD-A202612] N89-22631
Transitional strategic defense architectures
[DE89-008312] N89-23265
SPACE-TIME FUNCTIONS
Natural representation of motion in space-time N89-23111
On space-time escape mechanisms
[DE88-705699] N89-23354
SPACEBORNE EXPERIMENTS
Future space projects discussed at Moscow Space Forum N89-22630
Consortium for materials development in space
[NASA-CR-181405] N89-22773
SPACEBORNE TELESCOPES
Project Radioastron N89-22623
SPACECRAFT CHARGING
Spacecraft charge as a source of electrical power for spacecraft
[AD-A202621] N89-22649
SPACECRAFT DESIGN
Ten year lifetime orbits about the planet Mars N89-22633
Orbital debris environment for spacecraft designed to operate in low Earth orbit
[NASA-TM-100471] N89-22638
Spacecraft thermal control design data handbook
[LAMF-8712] N89-22642
Ariane 5 Transfer Vehicle (ATV)
[REPT-OX-1-005] N89-22645
ATV: Ariane 5 transfer vehicle study
[STF/E-39-005/CB] N89-22646
Numerical model of solar dynamic radiator for parametric analysis
[NASA-TM-102054] N89-22653
Transition to turbulence in laminar hypersonic flow N89-22830
SPACECRAFT EQUIPMENT
Advanced cartridge technology: Executive summary — spacecraft furnaces
[SEP-TS/F-8972/88-RP] N89-22636
Columbus MTFF utilisation, phase B2X: Executive summary for main study
[CUT-MBER-800-RP-220] N89-22647
SPACECRAFT GLOW
In-space technology development: Atomic oxygen and orbital debris effects
[NASA-TM-102154] N89-22682
SPACECRAFT MAINTENANCE
Technical evaluation report N89-22655
SPACECRAFT MODELS
Electrodynamic transient tests — satellites
[CNES-CT/DRT/TVE/SM-024] N89-22644
SPACECRAFT ORBITS
Ten year lifetime orbits about the planet Mars N89-22633
SPACECRAFT POWER SUPPLIES
Power supply in space N89-22627
Spacecraft charge as a source of electrical power for spacecraft
[AD-A202621] N89-22649
Megawatt Class Nuclear Space Power Systems (MCNSPS) conceptual design and evaluation report. Volume 3, technologies 2: Power conversion
[NASA-CR-179614-VOL-3] N89-22980
Megawatt Class Nuclear Space Power Systems (MCNSPS) conceptual design and evaluation report. Volume 2, technologies 1: Reactors, heat transport, integration issues
[NASA-CR-179614-VOL-2] N89-22981
The importance of batteries in unmanned missions N89-22984
SPACECRAFT PROPULSION
Space Propulsion Hazards Analysis Manual (SPHAM). Volume 2: Appendices
[AD-A204601] N89-22650
Application of Advanced Material for Turbomachinery and Rocket Propulsion
[AGARD-CP-449] N89-22654
Technical evaluation report N89-22655

Application of advanced materials for turbomachinery and rocket propulsion N89-22656
Center for Advanced Space Propulsion (CASP) [NASA-CR-184936] N89-23404
SPACECRAFT RADIATORS
Numerical model of solar dynamic radiator for parametric analysis [NASA-TM-102054] N89-22653
SPACECRAFT STRUCTURES
The project ASKA-SPACE, phase 1 --- finite element method [ETN-89-93768] N89-22959
SPACECRAFT SURVIVABILITY
Ten year lifetime orbits about the planet Mars N89-22633
SPACECRAFT TEMPERATURE
Spacecraft thermal control design data handbook [LAMF-8712] N89-22642
SPACECRAFT TRAJECTORIES
Optimal low thrust trajectories for planetary capture [AD-A202604] N89-22632
SPACELAB
Navigation experiment NAVEX: The reading differences between all ground station measuring clocks during Spacelab pass of the D1 mission [ESA-TT-1113] N89-22599
SPATIAL DISTRIBUTION
Generalizing epipolar-plane image analysis on the spatiotemporal surface N89-23164
SPATIAL RESOLUTION
Ultra-sensitive X-ray sensors give improved contrast sensitivity [DE89-003581] N89-22872
SPECIFICATIONS
Specifying real-time systems with interval logic [NASA-CR-181804] N89-23183
SPECIMEN GEOMETRY
Improving hole boring yield in carbon epoxy composites with tensile loading [REPT-47-324/F] N89-22704
SPECTRAL BANDS
Gamma ray laser pump diagnostic [AD-A205221] N89-22883
SPECTRAL EMISSION
Kilometric radiation power flux dependence on area of discrete aurora [NASA-CR-184993] N89-23040
SPECTRAL METHODS
A numerical study of viscous vortex rings using a spectral method N89-22572
SPECTRAL REFLECTANCE
A color metric for computer vision N89-23151
SPECTROMETERS
Evaluation of the Portable Instantaneous Display Analysis Spectrometer (PIDAS) [NASA-CR-184878] N89-22970
SPECTROSCOPY
Far- and mid-infrared properties of metal-insulator composite materials [AD-A204914] N89-22689
The application of electrochemical impedance spectroscopy for characterizing the degradation of Ni(OH)2/NiOOH electrodes N89-23003
SPECTRUM ANALYSIS
Chemical state depth profiling by Auger signal decomposition: Silicon oxynitride [DE89-009830] N89-22764
Distortions in the output signals of conventional spectrum analyzers [DE88-705656] N89-22871
The spectral analysis of an aero-engine assembly incorporating a squeeze-film damper N89-22895
Interactive ultrasonic nondestructive evaluation [AD-A204166] N89-22931
SPHERICAL COORDINATES
Generalized finite strains, generalized stresses, and a hybrid variational principle for finite-element computer programs using curvilinear coordinates [DE89-009923] N89-22962
Symbolic pixel labeling for curvilinear feature detection N89-23171
SPIN GLASS
Coexistence of spin-glass and type-2 ceramic superconductivity [DE88-705684] N89-23322
SPIN-ORBIT INTERACTIONS
Neutrino helicity flips via electroweak interactions and SN1987a [NIKHEF-H/88-18] N89-23278
SPLICING
Parallel problem solving system, PRISM (Parallel Inference System) [AD-A204915] N89-23207
SPLINE FUNCTIONS
On polynomial ideals of finite codimension with applications to box spline theory [AD-A204095] N89-23225
Numerical solution of the biharmonic equation using different types of bivariate spline functions [MEMO-734] N89-23247
Approximation of surfaces constrained by a differential equation using simplex splines [MEMO-739] N89-23249
Monotonicity-preserving quadratic C sup 1-spline interpolation to scattered data [MEMO-744] N89-23252
The stable evaluation of a simple rational function and its application to spline approximation [NPL-DITC-135/88] N89-23253
SPOILERS
Wind tunnel tests of 16 percent thick airfoil section with spoilers at different chordwise positions --- wind turbines [FFA-TN-1987-39] N89-22582
SQUEEZE FILMS
The spectral analysis of an aero-engine assembly incorporating a squeeze-film damper N89-22895
Cavitation effects on the pressure distribution of a squeeze film damper bearing N89-22897
SQUID (DETECTORS)
Nuclear magnetic resonance with dc SQUID (Super-conducting QUantum Interference Device) preamplifiers [DE89-007657] N89-23311
STABILITY
Piezoelectric pushers for active vibration control of rotating machinery N89-22896
High stability design for new centrifugal compressor N89-22917
Relevance of international research facilities to international stability [DE89-009400] N89-23380
STAGNATION FLOW
Flow over a leading edge with distributed roughness [DFVLR-FB-88-45] N89-22581
STAGNATION POINT
Supersonic particle probes: Measurement of internal wall losses [AD-A205863] N89-22589
STAINLESS STEELS
Aqueous impurity effects on stainless steel IGSCC (intergranular stress corrosion cracking): A central composite matrix analysis [DE88-017382] N89-22726
Spinodal decomposition of austenite in long-term-aged duplex stainless steel [DE89-009827] N89-22737
A calorimetric-based comparison of gas tungsten and plasma arc welding processes [DE89-008712] N89-22924
STANDARD DEVIATION
Limiting exact efficiency of quadratic statistics [MEMO-737] N89-23264
STANDARDIZATION
A programmatic approach to achieving data quality objectives [DE89-006248] N89-23378
STANDARDS
Measurement uncertainty of adsorption testing of desiccant materials [DE89-000841] N89-22681
Standardized bibliographic processing N89-23367
STANDING WAVES
Effect of pump-induced density depletions on the spectrum of stimulated electromagnetic emissions --- ionosphere [IRF-PREPRINT-107] N89-22799
STATE ESTIMATION
Some local results for linear systems and implications for state variable feedback [MATHS-RES-202] N89-23221
STATIC CHARACTERISTICS
An experimental study on the static and dynamic characteristics of pump annular seals N89-22904
STATIC LOADS
A study of unsteady turbulent flow past airfoils N89-22587
STATIONS
ELF communications system terminal grounds seasonal variation pilot study [AD-A205900] N89-22806
STATISTICAL ANALYSIS
Low Reynolds number calculation of turbulent channel flow: A general discussion [AD-A205883] N89-22864
Remote sensing of oceanic rainrates by passive microwave sensors: A statistical-physical approach N89-23057
A statistical package in Ada [FOA-C-20740-2.7] N89-23201
Approximate Bayesian methods for nonlinear measurement error models [DE89-009224] N89-23233
STATISTICAL DISTRIBUTIONS
Climatological and statistical fundamentals for the explanation of climate data processing [ETN-89-93775] N89-23051
STATISTICAL MECHANICS
High accuracy thermal conductivity measurements near the lambda transition of helium with very high temperature resolution [NASA-CR-184836] N89-22709
Annual research briefs, 1988 [NASA-CR-184906] N89-22817
Renormalization group analysis of turbulence N89-22821
Lectures in Fluid Physics held at the Physics Department of the Georg-August-University. Volume 2: Examples of the Application of Dimensional Analysis [DFVLR-MITT-88-27-VOL-2] N89-22856
Molecular dynamics and irreversibility, from Boltzmann to Nose [DE89-006740] N89-23274
STEADY FLOW
Theoretical predictions of turbulent burning velocities of steady and accelerating unconfined turbulent flames with premixed reactants N89-22716
STEADY STATE
The influence of open boundary conditions and difference operators on the time-integration of the Burger's equation [FFA-TN-1988-57] N89-23254
Simulations of axisymmetric erosion in IFR-Transported beams [AD-A205882] N89-23301
STELLAR COMPOSITION
Studies of hot white dwarfs and instrumentation for stellar extreme ultraviolet astronomy N89-23383
STELLAR EVOLUTION
Turbulent transport in the solar nebula N89-22829
Superconducting cosmic string evolution of quasars [DE88-705672] N89-23390
Far infrared peculiar behavior of quasars [DE88-705673] N89-23391
STEREOPHOTOGRAPHY
IU at UI: An overview and an example on shape from texture N89-23096
Perceptual grouping for the detection and description of structures in aerial images N89-23117
STEREOSCOPIC VISION
An integrated approach to stereo matching, surface reconstruction and depth segmentation using consistent smoothness assumptions N89-23092
The MIT vision machine N89-23093
Kalman filter-based algorithms for estimating depth from image sequences N89-23094
Self calibration of motion and stereo vision for mobile robot navigation N89-23106
Generic models for robot navigation N89-23112
On the computational complexity of linear navigation N89-23123
Three-dimensional vision for outdoor navigation by an autonomous vehicle N89-23124
Modeling sensors and applying sensor model to automatic generation of object recognition program N89-23136
Test results from SRI's stereo system N89-23140
An introduction to generalized stereo techniques N89-23142
Stochastic stereo matching over scale N89-23143
Qualitative versus quantitative depth and shape from stereo N89-23144
The integration of information from stereo and multiple shape-form-texture cues N89-23145
Structural correspondence in stereo vision N89-23146
Curved surface reconstruction using stereo correspondence N89-23147
Relative orientation N89-23149
Computation of motion in depth parameters: A first step in stereoscopic motion interpretation N89-23153
STEREOSCOPY
Dynamic image interpretation for autonomous vehicle navigation [AD-A204167] N89-22597
STIFFNESS
Magnetic bearing stiffness control using frequency band filtering N89-22910
Role of circumferential flow in the stability of fluid-handling machine rotors N89-22915
STIFFNESS MATRIX
Ritz method for transient response in systems having unsymmetric stiffness N89-22954

STIMULATED EMISSION
Effect of pump-induced density depletions on the spectrum of stimulated electromagnetic emissions --- ionosphere
[IRF-PREPRINT-107] N89-22799
STIRLING ENGINES
Megawatt Class Nuclear Space Power Systems (MCNSPS) conceptual design and evaluation report. Volume 3, technologies 2: Power conversion
[NASA-CR-179614-VOL-3] N89-22980
Design considerations for heat-pipe solar receivers
[DE89-004037] N89-23017
STOCHASTIC PROCESSES
Stochastic stereo matching over scale N89-23143
STOKES THEOREM (VECTOR CALCULUS)
On the asymptotic behavior of the coefficients of asymptotic power series and its relevance to Stokes phenomena
[MEMO-738] N89-23248
STORAGE BATTERIES
Power supply in space N89-22627
Space Electrochemical Research and Technology Conference: Abstracts
[NASA-CP-10029] N89-22982
A survey of advanced battery systems for space applications N89-22986
STORAGE STABILITY
Nickel-hydrogen capacity loss on storage N89-23007
STRAIN ENERGY METHODS
Seventeenth NASTRAN (R) Users' Colloquium
[NASA-CP-3029] N89-22940
Modal strain energies in COSMIC NASTRAN N89-22955
A study of high strain rate generation of adiabatic shear bands in a titanium alloy N89-22967
STRAIN HARDENING
Grain boundary sliding phenomena in polycrystalline solids
[DE89-007792] N89-23326
STRAIN RATE
Effects of grain size and strain rate on the mechanical response of copper
[DE89-008811] N89-22731
Fracture toughness and mechanical behavior of steel and aluminum alloys
[ETCA-87-R-090] N89-22743
A study of high strain rate generation of adiabatic shear bands in a titanium alloy N89-22967
STRATEGY
Transitional strategic defense architectures
[DE89-008312] N89-23265
Fostering interaction of government, defense, and aerospace databases N89-23374
STRATOSPHERE
Mass-spectroscopic measurements of stratospheric ions, trace gases and precondensation nuclei using balloon-borne measuring probes
[BPT-7/88] N89-23037
Diabatic circulations in the stratosphere N89-23043
STREAK CAMERAS
Wavelength streak camera
[DE89-008612] N89-22874
STRESS ANALYSIS
Fatigue evaluation of WTS-3 wind turbine blade and retention
[FFA-TN-1987-81] N89-22618
The isothermal fatigue behavior of a unidirectional SiC/Ti composite and the Ti alloy matrix
[NASA-TM-101984] N89-22684
Three-dimensional response of composites
[AD-A204623] N89-22687
New theoretical model of stress transfer between fibre and matrix in a uniaxially fibre reinforced composite
[NPL-DMA(A)168] N89-22691
Nondestructive evaluation of stress using ultrasound and pulsed heat
[AD-A205176] N89-22932
Generalized finite strains, generalized stresses, and a hybrid variational principle for finite-element computer programs using curvilinear coordinates
[DE89-009923] N89-22962
On the semi-elliptical surface crack problem: Detailed numerical solutions for complete elastic stress fields
[FFA-TN-1988-74] N89-22965
STRESS CONCENTRATION
Assessing hydrogen assisted cracking modes in high strength steel welds
[AD-A205431] N89-22746
On the semi-elliptical surface crack problem: Detailed numerical solutions for complete elastic stress fields
[FFA-TN-1988-74] N89-22965
STRESS CORROSION
Aqueous impurity effects on stainless steel IGSCC (intergranular stress corrosion cracking): A central composite matrix analysis
[DE88-017382] N89-22726
STRESS CORROSION CRACKING
Aqueous impurity effects on stainless steel IGSCC (intergranular stress corrosion cracking): A central composite matrix analysis
[DE88-017382] N89-22726
STRESS DISTRIBUTION
Damage initiation in two-dimensional, woven, carbon-carbon composites
[AD-A202617] N89-22683
STRESS FUNCTIONS
Limiting exact efficiency of quadratic statistics
[MEMO-737] N89-23264
STRESS MEASUREMENT
Fiber matrix interface effects in failure of ceramic matrix fiber composites
[AD-A204618] N89-22686
STRESS PROPAGATION
New theoretical model of stress transfer between fibre and matrix in a uniaxially fibre reinforced composite
[NPL-DMA(A)168] N89-22691
STRESS RELAXATION
Reconstruction and relaxation of metal surfaces
[JUEL-2213] N89-22733
Grain boundary sliding phenomena in polycrystalline solids
[DE89-007792] N89-23326
STRESS TENSORS
A general non-linear dynamical theory of elastic curved beams N89-22930
STRESS-STRAIN RELATIONSHIPS
The isothermal fatigue behavior of a unidirectional SiC/Ti composite and the Ti alloy matrix
[NASA-TM-101984] N89-22684
New theoretical model of stress transfer between fibre and matrix in a uniaxially fibre reinforced composite
[NPL-DMA(A)168] N89-22691
Internal stresses in ceramic composite constituents determined by neutron diffraction technique
[DE89-009883] N89-22697
STRETCHING
On curve and surface stretching in turbulent flow N89-22820
Hydrogen embrittlement in nickel-hydrogen cells N89-23008
STRING THEORY
Gravitational effects of cosmic strings in Friedmann universes N89-23394
STRINGS
Superconducting cosmic string evolution of quasars
[DE88-705672] N89-23390
STRONTIUM COMPOUNDS
Influence of ion irradiated SrTiO sub 3 on the properties of thin film oxide superconductors
[DE89-009409] N89-23338
STRUCTURAL ANALYSIS
Seventeenth NASTRAN (R) Users' Colloquium
[NASA-CP-3029] N89-22940
A NASTRAN DMAP alter for linear buckling analysis under dynamic loading N89-22948
Modal strain energies in COSMIC NASTRAN N89-22955
Definition of NASTRAN sets by use of parametric geometry N89-22956
Approximate large deflection analysis of simply supported orthotropic plates
[NPL-DMA(A)171] N89-22963
Structural comparison of nickel electrodes and precursor phases N89-23001
Nonlinear finite element simulation of the large angle motion of flexible bodies
[DE89-006505] N89-23230
STRUCTURAL BASINS
Measurements of a barotropic planetary vorticity mode in an eddy-resolving quasi-geostrophic model using acoustic tomography
[AD-A205409] N89-23058
STRUCTURAL DESIGN
Power supply in space N89-22627
Blade root design: A state of art survey
[FFAP-201] N89-22778
High stability design for new centrifugal compressor N89-22917
Increasing marketability and profitability of product line thru PATRAN and NASTRAN N89-22943
The use of COSMIC NASTRAN in an integrated conceptual design environment N89-22944
A NASTRAN/TREETOPS solution to a flexible, multi-body dynamics and controls problem on a UNIX workstation N89-22945
An experimental and analytical synthesis of controlled structure design
[DE89-006506] N89-22957
Radiation control at the Continuous Electron Beam Accelerator Facility (CEBAF), a new high power CW electron accelerator installation
[CEBAF-PR-89-001] N89-23280
STRUCTURAL FAILURE
Mechanisms of crevice corrosion in chlorinated environments
[AD-A204821] N89-22724
STRUCTURAL STABILITY
A NASTRAN DMAP alter for linear buckling analysis under dynamic loading N89-22948
STRUCTURAL STRAIN
Fatigue evaluation of WTS-3 wind turbine blade and retention
[FFA-TN-1987-81] N89-22618
STRUCTURAL VIBRATION
Structural dynamics branch research and accomplishments for FY 1988
[NASA-TM-101406] N89-22939
Power flows and Mechanical Intensities in structural finite element analysis N89-22952
An experimental and analytical synthesis of controlled structure design
[DE89-006506] N89-22957
SUBMERGED BODIES
Calculation of low frequency vibrational resonances of submerged structures N89-22951
SUBSONIC FLOW
Unsteady aerodynamic computational method of non-coplanar wing-tail combinations in subsonic flow
[PB89-111470] N89-22571
Supersonic particle probes: Measurement of internal wall losses
[AD-A205863] N89-22589
SUCTION
Sidewall boundary layer study, with and without suction, for the 150 mm chord CAST 7 airfoil at the T2 wind tunnel N89-22584
Numerical study of a multipurpose transonic wind tunnel with an adaptable injection-suction system N89-22621
SULFIDATION
Behavior of iron aluminides in oxidizing and sulfidizing environments
[DE89-008919] N89-22693
Corrosion monitoring with acoustic wave devices
[DE89-005235] N89-22728
SUPERCOMPUTERS
Storage in supercomputer environments
[DE89-008895] N89-23330
SUPERCONDUCTIVITY
Effects of different fabrication techniques on the Yttrium-Barium-Copper oxide high temperature superconductor
[AD-A202598] N89-23304
Quantum phenomena in mesoscopic superconducting tunnel junctions
[AD-A203354] N89-23305
Perturbative treatment of local correlations in Cu-O planes for high temperature superconductors
[DE88-705648] N89-23315
Coexistence of spin-glass and type-2 ceramic superconductivity
[DE88-705684] N89-23322
Hysteresis development in superconducting Josephson junctions
[DE88-705693] N89-23323
Possibility of operation of high temperature superconducting YBa2Cu307 ceramics in cyclotrons at irradiation
[DE88-705783] N89-23325
Ductility enhancement in unreacted internal-Sn Nb3Sn through low-temperature anneals
[DE89-009125] N89-23336
Basic research in superconductor, ceramic and semiconductor sciences at selected Japanese laboratories based on a 1988 visit: Highlights, summary and overview, detailed notes from selected Japanese laboratories
[DE89-009637] N89-23339
Structural properties of superconducting and nonsuperconducting Ba sub 1-x K sub x BiO3
[DE89-009813] N89-23340
Point defects and oxygen diffusion in high T sub c superconductors
[DE89-009842] N89-23341
Superconducting cosmic string evolution of quasars
[DE88-705672] N89-23390
SUPERCONDUCTORS
Quantum phenomena in mesoscopic superconducting tunnel junctions
[AD-A203354] N89-23305
Superconductivity for electric power systems: Building toward our future
[DE89-000874] N89-23332
Influence of ion irradiated SrTiO sub 3 on the properties of thin film oxide superconductors
[DE89-009409] N89-23338

Basic research in superconductor, ceramic and semiconductor sciences at selected Japanese laboratories based on a 1988 visit: Highlights, summary and overview, detailed notes from selected Japanese laboratories
[DE89-009637] N89-23339
SUPERCRITICAL AIRFOILS
Comparison of boundary layer trips of disk and grit types on airfoil performance at transonic speeds
[AD-A205206] N89-22575
SUPERCRITICAL FLUIDS
Adsorption studies in the critical region of a pure fluid. Development of an apparatus for adsorption measurements under microgravity conditions
[ETN-89-93767] N89-22774
SUPERGRAVITY
Two dimensional (4,0) supergravity in harmonic superspace. The action and the matter couplings
[DE88-705661] N89-23351
SUPERHIGH FREQUENCIES
Study of a DRS experimental payload for single and multiple access at S band: Executive summary
[PSD88/00017] N89-22648
SUPERLATTICES
Band structure of CdTe-ZnTe superlattice
[DE88-705682] N89-23321
Basic research in superconductor, ceramic and semiconductor sciences at selected Japanese laboratories based on a 1988 visit: Highlights, summary and overview, detailed notes from selected Japanese laboratories
[DE89-009637] N89-23339
SUPERNOVA 1987A
Neutrino helicity flips via electroweak interactions and SN1987a
[NIKHEF-H/88-18] N89-23278
SUPERSONIC BOUNDARY LAYERS
Non-linear evolution of a second mode wave in supersonic boundary layers
[NASA-CR-181811] N89-22836
SUPERSONIC DRAG
The influence of the leading edge geometry on the wave drag for a 65 degree delta wing at low supersonic speed and small angles of attack
[FFA-141] N89-22583
SUPERSONIC FLOW
The inviscid axisymmetric stability of the supersonic flow along a circular cylinder
[NASA-CR-181816] N89-22574
Transonic and supersonic flow past a 65 deg delta wing with rounded leading edges: Analysis of experimental data
[DFVLR-FB-88-44] N89-22580
Supersonic particle probes: Measurement of internal wall losses
[AD-A205863] N89-22589
The structure and control of three-dimensional shock wave turbulent boundary layer interactions
[AD-A205923] N89-22866
SUPERSONIC SPEED
Investigation of low NOx staged combustor concept in high-speed civil transport engines
[NASA-TM-101977] N89-22606
SUPERSONIC WIND TUNNELS
Transonic and supersonic wind tunnel tests on control effectiveness on schematic missile configuration with canard control
[FFA-TN-1988-11-SUPPL] N89-22613
New hypersonic facility capability at NASA Lewis Research Center
[NASA-TM-102028] N89-22617
SUPERSYMMETRY
Two dimensional (4,0) supergravity in harmonic superspace. The action and the matter couplings
[DE88-705661] N89-23351
SURFACE ACOUSTIC WAVE DEVICES
Corrosion monitoring with acoustic wave devices
[DE89-005235] N89-22728
SURFACE CRACKS
Environmentally induced discontinuities in transparent polymers
[AD-A205483] N89-22768
Finite element analysis for calibration curve computation for measurement of crack propagation of ellipse shaped surface cracks
[GKSS-88/E/34] N89-22960
On the semi-elliptical surface crack problem: Detailed numerical solutions for complete elastic stress fields
[FFA-TN-1988-74] N89-22965
SURFACE DEFECTS
Multifrequency eddy current testing, optimization of the method for steam generator testing. Phase 2: Nonlinear description of signal location curves dynamics of the signal location curves
[REPT-860142-TW] N89-22933
Reconstruction of defects from amplitude location curves
[REPT-780852-TW] N89-22934
SURFACE FINISHING
Wear protection coatings and treatments for the TA6V alloy
[ETCA-88-R-003] N89-22742
SURFACE GEOMETRY
Three-dimensional object recognition using surface descriptions N89-23105
SURFACE LAYERS
Reconstruction and relaxation of metal surfaces
[JUEL-2213] N89-22733
SURFACE NAVIGATION
Image understanding research at SRI International N89-23080
SURFACE PROPERTIES
Image understanding: Intelligent systems N89-23077
Using generic geometric and physical models for representing solids N89-23114
Image segmentation and reflection analysis through color N89-23150
SURFACE REACTIONS
In-space technology development: Atomic oxygen and orbital debris effects
[NASA-TM-102154] N89-22682
Models for surface intermediates in CO hydrogenation
[DE89-004348] N89-22712
Locating pitting sites from propagating surface potential transients
[DE89-006171] N89-22730
SURFACE ROUGHNESS EFFECTS
Flow over a leading edge with distributed roughness
[DFVLR-FB-88-45] N89-22581
SURFACE TEMPERATURE
Surface temperature measurements using a thin film thermal array
[NASA-TM-101549] N89-22668
SURGES
Locating pitting sites from propagating surface potential transients
[DE89-006171] N89-22730
SURVEILLANCE RADAR
Observation parameters for a ground-based radar station to survey near-earth satellites
[REPT-4-88] N89-22793
SWAGING
Increasing marketability and profitability of product line thru PATRAN and NASTRAN N89-22943
SWATH WIDTH
Minimum number of satellites for periodic coverage
[FOA-C-30511-9.4] N89-22976
SWITCHES
Theoretical and computational studies of plasma opening switches
[DE89-009712] N89-23297
Binary and ternary gas mixtures for use in glow discharge closing switches
[DE89-009718] N89-23298
SYMMETRY
Ribbons, symmetries and skewed symmetries N89-23170
Nonlocal higher order symmetries for the Federbush model
[MEMO-740] N89-23250
Problems in modern cosmology N89-23393
SYNCHRONOUS PLATFORMS
Columbus MTFF utilisation, phase B2X: Executive summary for main study
[CUT-MBER-800-RP-220] N89-22647
SYNTHESIS (CHEMISTRY)
Investigation and synthesis of high temperature and increased stiffness RSP aluminum alloys
[AD-A204162] N89-22723
Reactions of inorganic high polymers as a route to tailored solids
[AD-A204602] N89-22750
SYNTHETIC APERTURE RADAR
Theoretical studies for ERS-1 wave mode, volume 1
[GEC-MTR-87/110-VOL-1] N89-22977
Imaging radar applications in Europe. Illustrated experimental results (1978-1987)
[ESA-TM-01] N89-22978
SYSTEM IDENTIFICATION
Adaptive LQ control: Conflict between identification and control
[MEMO-718] N89-23216
SYSTEMS ANALYSIS
Control of free-flying space robot manipulator systems
[NASA-CR-184837] N89-22918
Automating the identification of structural model parameters
[DE89-006327] N89-23104
SYSTEMS ENGINEERING
Advanced cartridge technology: Executive summary --- spacecraft furnaces
[SEP-TS/F-6972/88-RP] N89-22636
Measurement of the total gas content of a liquid
[OUEL-1643/86] N89-22711
HIFI: A design method for implementing signal processing algorithms on VLSI processor arrays
[ETN-89-94138] N89-22795
PSDE/SAT-2: Communication system architecture study, executive summary
[ESA-CR(P)-2732] N89-22802
A signal processing system using MC68000 and TMS320 microprocessors
[USIP-88-07] N89-22803
Benzodiazepines and caffeine: Effect on daytime sleepiness, performance, and mood
[AD-A205862] N89-23066
A knowledge-based tool for multilevel decomposition of a complex design problem
[NASA-TP-2903] N89-23181
SYSTEMS STABILITY
Influence of impeller shroud forces on turbopump rotor dynamics N89-22909
On the stabilization of bilinear systems via constant feedback
[MEMO-706] N89-23215
Robust stabilization of an inverted double pendulum system via a polynomial approach to H(infinity) optimal control
[MEMO-742] N89-23220

T

TACTILE DISCRIMINATION
Image understanding and robotics research at Columbia University N89-23083
TARGET ACQUISITION
Position, scale, and rotation invariant optical pattern recognition for target extraction and identification
[AD-A202600] N89-22781
TARGET MASKING
Detection of known signals in arbitrary backgrounds
[AD-A204076] N89-22784
TARGET RECOGNITION
Position, scale, and rotation invariant optical pattern recognition for target extraction and identification
[AD-A202600] N89-22781
Proceedings: Image Understanding Workshop, volume 1
[AD-A197558] N89-23074
Image understanding: Intelligent systems N89-23077
Image understanding research at GE N89-23085
Qualitative reasoning and modeling for robust target tracking and recognition from a mobile platform N89-23086
Multiresolution aerial image interpretation N89-23116
Dynamic model matching for target recognition from a mobile platform N89-23118
TRIPLE: A multi-strategy machine learning approach to target recognition N89-23119
TAYLOR INSTABILITY
Low-dimensional chaos in turbulence N89-22822
The effects of stabilizing and destabilizing longitudinal curvature on the structure of turbulent, two-stream mixing layers N89-22833
TDR SATELLITES
Study of a DRS experimental payload for single and multiple access at S band: Executive summary
[PSD88/00017] N89-22648
TECHNOLOGY ASSESSMENT
Launch options for the future: Special report
[PB89-114268] N89-22637
A survey of poly-ether-ether-ketone and its advanced composites
[FFA-TN-1988-37] N89-22707
Technical feasibility study on the development of ceramic thermoelectric conversion, part 2
[DE88-756481] N89-22755
Assessment of EV batteries and application to R and D planning
[DE89-009720] N89-22811
Solar thermal program summary. Volume 1: Overview, fiscal year 1988
[DE89-000860] N89-23020
New developments in biotechnology: US investment in biotechnology, part 4
[PB88-246939] N89-23060
TECHNOLOGY TRANSFER
The Organisation and Functions of Documentation and Information Centres in Defence and Aerospace Environments
[AGARD-CP-445] N89-23362
Sources of information N89-23366
Information resources management N89-23371
R and D productivity: Relationship to Selective Dissemination of Information (SDI) in the corporate environment N89-23375
Impact of information technology on organizational structure: A control perspective N89-23379

Technology transfer report
[DE89-009044] N89-23381
TECHNOLOGY UTILIZATION
Solar thermal program summary. Volume 1: Overview, fiscal year 1988
[DE89-000860] N89-23020
Impact of information technology on organizational structure: A control perspective N89-23379
TELECOMMUNICATION
Study on communications costs for Columbus utilization
[REPT-871126/1/FR] N89-22801
Signal detection in fractional Gaussian noise and an RKHS (Reproducing Kernel Hilbert Space) approach to robust detection and estimation
[AD-A205441] N89-22805
ELF communications system terminal grounds seasonal variation pilot study
[AD-A205900] N89-22806
TELEOPERATORS
Traction-drive force transmission for telerobotic joints
[NASA-CR-183331] N89-22922
The Space Station Flight Telerobotic Servicer and the human
[NASA-TM-100615] N89-23068
TELESCOPES
ALEXIS: A narrow-band survey/monitor of the ultrasoft X-ray sky
[DE89-007980] N89-22873
TEMPERATURE CONTROL
Filament winding manufacturing of long fiber composite materials in thermoplastic matrix
[ETCA-87-R-047] N89-22699
TEMPERATURE DEPENDENCE
Role of aluminium concentration on the structure behaviour of Cu-Al alloys
[DE88-705647] N89-22727
TEMPERATURE DISTRIBUTION
Diabatic circulations in the stratosphere N89-23043
On the physical causes of ENSO events and the ITCZ's extreme latitudinal displacements
[DE88-705654] N89-23050
Methods for heat transfer and temperature field analysis of the insulated diesel, phase 3
[NASA-CR-182237] N89-23382
TEMPERATURE EFFECTS
Interaction of coatings with base metals at high temperature N89-22669
Influence of conditioning on the trapezoidal fatigue behavior of a carbon epoxy composite
[ETCA-87-R-052] N89-22700
Temperature effects on the break-in of nickel aluminide alloys
[DE89-005341] N89-22729
Acceleration test for aircraft low-pass filter
[PB89-116263] N89-22807
TEMPERATURE GRADIENTS
A variable temperature cryostat that produces in situ clean-up germanium detector surfaces
[DE89-008174] N89-23328
TEMPERATURE MEASUREMENT
Surface temperature measurements using a thin film thermal array
[NASA-TM-101549] N89-22868
Seafloor temperature and conductivity data from coastal waters of the US Beaufort Sea
[AD-A205428] N89-23059
TEMPERATURE MEASURING INSTRUMENTS
New thermocouple: Characteristic investigation of Au+Pd+Ni/Ni+Cr thermocouple below 273K
[PB89-112940] N89-22867
TEMPERATURE PROBES
Development of a differential temperature probe for the measurement of atmospheric turbulence at all levels
[AD-A205893] N89-23047
TEMPERATURE PROFILES
Development of a differential temperature probe for the measurement of atmospheric turbulence at all levels
[AD-A205893] N89-23047
TEMPERATURE SENSORS
Emission properties of europium-doped lanthanum and lutetium orthophosphate crystals for use in high temperature sensor applications
[DE89-008736] N89-23334
TEMPORAL DISTRIBUTION
Is correspondence necessary for the perception of structure from motion N89-23154
Generalizing epipolar-plane image analysis on the spatiotemporal surface N89-23164
TEMPORAL RESOLUTION
Time resolved photoluminescence of ytterbium in indium phosphide
[AD-A202596] N89-23303
TENSILE CREEP
Internal stresses in ceramic composite constituents determined by neutron diffraction technique
[DE89-009883] N89-22697
TENSILE PROPERTIES
The isothermal fatigue behavior of a unidirectional SiC/Ti composite and the Ti alloy matrix
[NASA-TM-101984] N89-22684
Ductility enhancement in unreacted internal-Sn Nb3Sn through low-temperature anneals
[DE89-009125] N89-23336
TENSILE STRENGTH
Fracture toughness and mechanical behavior of steel and aluminum alloys
[ETCA-87-R-090] N89-22743
Application of indentation to the study of the toughness of yttrium-zircon plasma coatings
[ETCA-87-R-040] N89-22765
TERMINAL BALLISTICS
Numerical method to predict projectile penetration
[DE89-007140] N89-22923
TERNARY SYSTEMS
Binary and ternary gas mixtures for use in glow discharge closing switches
[DE89-009718] N89-23298
TERRAIN ANALYSIS
Remote sensing of earth terrain
[NASA-CR-184937] N89-22971
Image understanding research at SRI International N89-23080
PACE: An environment for intelligence analysis N89-23102
Autonomous navigation in cross-country terrain N89-23107
An operational perception system for cross-country navigation N89-23121
Overview of the SRI cartographic modeling environment N89-23122
TEST CHAMBERS
Hardware and operating features of the adaptive wall test section for the 0.3-meter transonic cryogenic tunnel
[NASA-TM-4114] N89-22614
TEST FACILITIES
ELF communications system terminal grounds seasonal variation pilot study
[AD-A205900] N89-22806
A seal test facility for the measurement of isotropic and anisotropic linear rotordynamic characteristics N89-22905
TETHERED SATELLITES
Design of an ELF/VLF satellite for under the ice submarine communications
[AD-A202607] N89-22639
Theoretical investigation of EM wave generation and radiation in the ULF, ELF, and VLF bands by the electrodynamic orbiting tether
[NASA-CR-181560] N89-22780
TEXTURES
IU at UI: An overview and an example on shape from texture N89-23096
The integration of information from stereo and multiple shape-form-texture cues N89-23145
Texture models and image measures for segmentation N89-23162
Texture edge localization N89-23178
Surface orientation from projective foreshortening of isotropic texture autocorrelation N89-23179
THALLIUM COMPOUNDS
Superconductivity for electric power systems: Building toward our future
[DE89-000874] N89-23332
THERMAL ANALYSIS
The project ASKA-SPACE, phase 1 — finite element method
[ETN-89-93768] N89-22959
Methods for heat transfer and temperature field analysis of the insulated diesel, phase 3
[NASA-CR-182237] N89-23382
THERMAL BARRIERS (PLASMA CONTROL)
Vacuum plasma spray coating N89-22670
Thrust chamber thermal barrier coating techniques N89-22671
Application of indentation to the study of the toughness of yttrium-zircon plasma coatings
[ETCA-87-R-040] N89-22765
THERMAL BLOOMING
Thermal blooming threshold computations with a Markov model of velocity turbulence
[DE89-009709] N89-23285
THERMAL CONDUCTIVITY
High accuracy thermal conductivity measurements near the lambda transition of helium with very high temperature resolution
[NASA-CR-184836] N89-22709
THERMAL CONTROL COATINGS
Application of indentation to the study of the toughness of yttrium-zircon plasma coatings
[ETCA-87-R-040] N89-22765
Preliminary study of ceramic-metal interface in thermal boundaries
[ETCA-87-R-101] N89-23346
THERMAL CYCLING TESTS
Thrust chamber thermal barrier coating techniques N89-22671
Environmental program on durability of graphite/epoxy honeycomb specimens with representative damage and repairs
[AR-005-504] N89-22685
THERMAL DEGRADATION
Advanced materials to combat the high temperature degradation processes in turbomachinery N89-22684
Interaction of coatings with base metals at high temperature N89-22669
Behavior of tungsten, molybdenum and alloys under unusual heating conditions N89-22674
THERMAL ENERGY
Annealing studies on a fully cured epoxy resin: Effect of thermal prehistory, and time and temperature of annealing
[AD-A205875] N89-22769
THERMAL EXPANSION
Monolithic Solid Oxide Fuel Cell development N89-22989
THERMAL FATIGUE
Development of stress and lifing criteria for single crystal turbine blades N89-22663
Utilization of high temperature composites in turbojet engines N89-22667
Metallurgical study of superalloy brazing alloys N89-22680
The isothermal fatigue behavior of a unidirectional SiC/Ti composite and the Ti alloy matrix
[NASA-TM-101984] N89-22684
THERMAL INSULATION
Development of an asbestos-free insulant for rocket motors N89-22679
Methods for heat transfer and temperature field analysis of the insulated diesel, phase 3
[NASA-CR-182237] N89-23382
THERMAL MAPPING
Derivation of a large-scale map of heat load in the region Freiburg-Basel (Germany, F.R.) using satellite data. A contribution to the production of bioclimate data based on a geographic information system
[REPT-27] N89-22972
THERMAL NOISE
Ionospheric scintillation studies
[AD-A205210] N89-23034
THERMAL PROTECTION
Thrust chamber thermal barrier coating techniques N89-22671
THERMAL SHOCK
Silicon-carbide coated carbon-carbon: An advanced material for rocket systems N89-22672
Metallurgical study of superalloy brazing alloys N89-22680
THERMAL STRESSES
Behavior of tungsten, molybdenum and alloys under unusual heating conditions N89-22674
THERMALIZATION (ENERGY ABSORPTION)
Thermal Comptonization models for gamma-ray emission from black-hole sources
[DE89-009918] N89-23402
THERMIONIC CONVERTERS
Megawatt Class Nuclear Space Power Systems (MCNSPS) conceptual design and evaluation report. Volume 3, technologies 2: Power conversion
[NASA-CR-179614-VOL-3] N89-22980
THERMIONIC EMISSION
Experimental investigation of hot electron and related effects in gallium (aluminum) arsenide devices
[AD-A205442] N89-23349
THERMOCOUPLES
New thermocouple: Characteristic investigation of Au+Pd+Ni/Ni+Cr thermocouple below 273K
[PB89-112940] N89-22867
Surface temperature measurements using a thin film thermal array
[NASA-TM-101549] N89-22868
THERMODYNAMIC EFFICIENCY
Comparison of a cavity solar receiver numerical model and experimental data
[DE89-003609] N89-23016
THERMODYNAMICS
Precipitation of Ar, Kr and Xe in Ni at room temperature
[DE89-009879] N89-22713
Molecular dynamics and irreversibility, from Boltzmann to Nose
[DE89-006740] N89-23274

Grain-boundary and free-surface induced thermodynamic melting: A molecular dynamics study in silicon
[DE89-007415] N89-23309

THERMOELASTICITY
Development of magnetic field assisted melt stabilization with heat and mass transfer control in low pressure LEC growth of GaAs
[AD-A205185] N89-23313

THERMOELECTRIC POWER GENERATION
Technical feasibility study on the development of ceramic thermoelectric conversion, part 2
[DE88-756481] N89-22755
Comparison of solar photovoltaic and nuclear reactor power systems for a human-tended lunar observatory
[NASA-TM-102015] N89-23397

THERMOELECTRICITY
New thermocouple: Characteristic investigation of Au+Pd+Ni/Ni+Cr thermocouple below 273K
[PB89-112940] N89-22867

THERMOGRAPHY
Combustor flow visualization using innovative infrared thermographics techniques
[AD-A205905] N89-22718

THERMONUCLEAR POWER GENERATION
Comparison of solar photovoltaic and nuclear reactor power systems for a human-tended lunar observatory
[NASA-TM-102015] N89-23397

THERMOPLASTICITY
Composite material systems for high temperature applications N89-22666
Filament winding manufacturing of long fiber composite materials in thermoplastic matrix
[ETCA-87-R-047] N89-22699

THERMOREGULATION
Acclimatization to cold in humans
[NASA-TM-101012] N89-23061

THERMOSIPHONS
Novel protein crystal growth technology: Proof of concept
[NASA-CR-184959] N89-23306

THERMOSPHERE
The response of thermospheric nitric oxide to an auroral storm N89-23031

THIN AIRFOILS
Convergence of discrete-vortex induced-flow calculations by optimum choice of mesh N89-22585

THIN FILMS
Microstructural studies of IAD and PVD Cr coatings by cross section transmission electron microscopy
[DE89-009877] N89-22739
Diagnostics of glow discharges used to produce hydrogenated amorphous silicon films
[DE89-000887] N89-22760
Carbonaceous film coating
[DE89-009592] N89-22762
Surface temperature measurements using a thin film thermal array
[NASA-TM-101549] N89-22868
Research on amorphous-silicon-based, thin-film photovoltaic devices, task B
[DE89-000885] N89-23021
Research on amorphous-silicon-based, thin-film photovoltaic devices, task B
[DE89-000886] N89-23022
Low frequency resistance fluctuations in films of high temperature superconductors
[DE89-007489] N89-23310
Influence of ion irradiated SrTiO sub 3 on the properties of thin film oxide superconductors
[DE89-009409] N89-23338

THIN WALLED SHELLS
The inviscid axisymmetric stability of the supersonic flow along a circular cylinder
[NASA-CR-181816] N89-22574

THREE DIMENSIONAL BODIES
Image understanding research at GE N89-23085
Qualitative reasoning and modeling for robust target tracking and recognition from a mobile platform N89-23086
Multimodal reconstruction and segmentation with Markov random fields and HCF optimization N89-23095
Physically based modeling for vision and graphics N89-23097
Three-dimensional object recognition using surface descriptions N89-23105
Using generic geometric and physical models for representing solids N89-23114
The concept of an effective viewpoint N89-23131
Curved surface reconstruction using stereo correspondence N89-23147
Recognizing animal motion N89-23156
On the recovery of superellipsoids N89-23168
Labeling polyhedral images N89-23180

THREE DIMENSIONAL BOUNDARY LAYER
The structure and control of three-dimensional shock wave turbulent boundary layer interactions
[AD-A205923] N89-22866

THREE DIMENSIONAL FLOW
Close interactions of 3-D vortex tubes N89-22823
Numerical simulation of viscous vortex rings N89-22824

THREE DIMENSIONAL MODELS
Computer aided design of three-dimensional waveguide loaded cavities
[DE89-007733] N89-22783
Special techniques used for time domain, three dimensional finite element modeling of electromagnetics
[DE89-007227] N89-22789
A 3-dimensional finite-difference method for calculating the dynamic coefficients of seals N89-22903

THREE DIMENSIONAL MOTION
Image understanding research at the University of Maryland, December 1986 - January 1988 N89-23078
CMU image understanding program N89-23079
Summary of image understanding research at the University of Massachusetts N89-23081
Natural representation of motion in space-time N89-23111
Computation of motion in depth parameters: A first step in stereoscopic motion interpretation N89-23153
Is correspondence necessary for the perception of structure from motion N89-23154
Motion from a sequence of images N89-23155
Recognizing animal motion N89-23156
A real time hierarchical model for optic flow determination via spatiotemporal frequency channels N89-23158
Translating optical flow into token matches N89-23159

THRUST CHAMBERS
Thrust chamber thermal barrier coating techniques N89-22671

TIME DEPENDENCE
Aerodynamics of nonrigid bodies undergoing large amplitude time-dependent motions N89-22586
General grid finite difference methods for time dependent electromagnetic problems in two dimensions
[DE89-007225] N89-22788

TIME MARCHING
Two time stepping algorithms for parallel computers
[DE89-006679] N89-23196

TIME MEASUREMENT
Navigation experiment NAVEX: The reading differences between all ground station measuring clocks during Spacelab pass of the D1 mission
[ESA-TT-1113] N89-22599

TIME SERIES ANALYSIS
A preliminary characterization of parachute wake recontact
[DE89-006442] N89-22576

TIME SIGNALS
Nondestructive evaluation of stress using ultrasound and pulsed heat
[AD-A205176] N89-22932

TIME TEMPERATURE PARAMETER
Annealing studies on a fully cured epoxy resin: Effect of thermal prehistory, and time and temperature of annealing
[AD-A205875] N89-22769

TIN ALLOYS
Ductility enhancement in unreacted internal-Sn Nb3Sn through low-temperature anneals
[DE89-009125] N89-23336

TIN OXIDES
Innovation in separation technology for fine gravity semi-products
[PB89-112478] N89-22719

TITAN LAUNCH VEHICLES
Launch options for the future: Special report
[PB89-114268] N89-22637

TITANIUM ALLOYS
New metallic materials for gas turbines N89-22660
The isothermal fatigue behavior of a unidirectional SiC/Ti composite and the Ti alloy matrix
[NASA-TM-101984] N89-22684
Wear protection coatings and treatments for the TA6V alloy
[ETCA-88-R-003] N89-22742
A study of high strain rate generation of adiabatic shear bands in a titanium alloy N89-22967

TITANIUM OXIDES
Influence of ion irradiated SrTiO sub 3 on the properties of thin film oxide superconductors
[DE89-009409] N89-23338

TOKAMAK DEVICES
Maximal bootstrap current tokamak equilibria in the first stability regime
[DE89-008201] N89-23291
Computation of lower hybrid, neutral beam and bootstrap currents in consistent MHD equilibria
[DE89-008892] N89-23292
Fusion power: Expected environmental characteristics and status of R and D
[DE89-009232] N89-23294

TOLERANCES (MECHANICS)
Technical evaluation report N89-22655
Monolithic and fiber ceramic components for turboengines and rockets N89-22657
Damage tolerance concepts for advanced materials and engines N89-22661
Environmental program on durability of graphite/epoxy honeycomb specimens with representative damage and repairs
[AR-005-504] N89-22685

TOLERANCES (PHYSIOLOGY)
Astronaut radiation exposure in low-earth orbit. Part 1: Galactic cosmic radiation
[AD-A204598] N89-23063

TOOLS
Dynamic image interpretation for autonomous vehicle navigation
[AD-A204167] N89-22597
Increasing marketability and profitability of product line thru PATRAN and NASTRAN N89-22943

TOPOLOGY
Generating a hot big bang via a change in topology
[DE89-007561] N89-23388

TOXICITY
Inhalation developmental toxicology studies: Teratology study of methyl ethyl ketone in mice
[DE89-009563] N89-23062

TRACE ELEMENTS
Quantitative analysis of atmospheric trace gases
[BPT-10/88] N89-23027
Mass-spectroscopic measurements of stratospheric ions, trace gases and precondensation nuclei using balloon-borne measuring probes
[BPT-7/88] N89-23037

TRACKING (POSITION)
Qualitative reasoning and modeling for robust target tracking and recognition from a mobile platform N89-23086
Cooperative methods for road tracking in aerial imagery N89-23101
Motion from a sequence of images N89-23155

TRACKING PROBLEM
Nonlinear model matching with prescribed tracking error with an application to Hamiltonian systems
[MEMO-731] N89-23244

TRAJECTORY ANALYSIS
Motion from a sequence of images N89-23155

TRAJECTORY OPTIMIZATION
Optimal low thrust trajectories for planetary capture
[AD-A202604] N89-22632
Knowledge-based vision technology progress at Hughes AI Center N89-23084

TRANSFORMATIONS (MATHEMATICS)
An introduction to generalized stereo techniques N89-23142
Recognizing solid objects by alignment N89-23174
New stable, vectorisable Kalman filter algorithms based on orthogonal transformations
[ESA-TT-1108] N89-23203
Nonlocal higher order symmetries for the Federbush model
[MEMO-740] N89-23250

TRANSIENT RESPONSE
Ritz method for transient response in systems having unsymmetric stiffness N89-22954

TRANSISTORS
Molecular beam epitaxial growth and characterization of metastable compound semiconductors for infrared detector applications
[AD-A205175] N89-23312

TRANSITION FLOW
Comparison of boundary layer trips of disk and grit types on airfoil performance at transonic speeds
[AD-A205206] N89-22575

TRANSITION PROBABILITIES
Optical studies of the magnetospheric cusp from Svalbard
[AD-A205432] N89-23044

TRANSITION TEMPERATURE
Glass transition temperature of the M10 resin associated to carbon, Kevlar or glass fibers
[ETCA-87-R-022] N89-22766
Annealing studies on a fully cured epoxy resin: Effect of thermal prehistory, and time and temperature of annealing
[AD-A205875] N89-22769
Evaluation, development, and characterization of superconducting materials for space application
[NASA-CR-184842] N89-23302

Neutron scattering studies of magnetic excitations in La/sub 2-x/Sr/sub x/CuO
[DE89-008155] N89-23333
Point defects and oxygen diffusion in high T sub c superconductors
[DE89-009842] N89-23341

TRANSLATIONAL MOTION
Issues in extracting motion parameters and depth from approximate translational motion N89-23157

TRANSMISSIONS (MACHINE ELEMENTS)
Traction-drive force transmission for telerobotic joints
[NASA-CR-183331] N89-22922
Transmission overhaul and replacement predictions using Weibull and renewal theory
[NASA-TM-102022] N89-22925

TRANSONIC FLOW
Transonic and supersonic flow past a 65 deg delta wing with rounded leading edges: Analysis of experimental data
[DFVLR-FB-88-44] N89-22580
An efficient inverse method for the design of blended wing-body configurations N89-22603

TRANSONIC NOZZLES
Numerical study of a multipurpose transonic wind tunnel with an adaptable injection-suction system N89-22621

TRANSONIC SPEED
Comparison of boundary layer trips of disk and grit types on airfoil performance at transonic speeds
[AD-A205206] N89-22575
Prediction of loads on wing/body/external store/fins pylon-configurations at transonic speeds
[FFA-TN-1988-44] N89-22602

TRANSONIC WIND TUNNELS
Sidewall boundary layer study, with and without suction, for the 150 mm chord CAST 7 airfoil at the T2 wind tunnel N89-22584
Transonic and supersonic wind tunnel tests on control effectiveness on schematic missile configuration with canard control
[FFA-TN-1988-11-SUPPL] N89-22613
Hardware and operating features of the adaptive wall test section for the 0.3-meter transonic cryogenic tunnel
[NASA-TM-4114] N89-22614
Microcomputer based controller for the Langley 0.3-meter Transonic Cryogenic Tunnel
[NASA-CR-181808] N89-22616
Numerical study of a multipurpose transonic wind tunnel with an adaptable injection-suction system N89-22621
Implementation of a two-component laser anemometer at the T2 wind tunnel
[A-501-H] N89-22879

TRANSPARENCE
Measurements of optical loss in transparent solids using a novel spectrometer based on optical cavity decay
[DE89-009900] N89-23286

TRANSPORT AIRCRAFT
Investigation of low NOx staged combustor concept in high-speed civil transport engines
[NASA-TM-101977] N89-22606

TRANSPORT PROPERTIES
High accuracy thermal conductivity measurements near the lambda transition of helium with very high temperature resolution
[NASA-CR-184836] N89-22709
Preliminary results of the MLAM (Multi-Layer Air Mass) Lagrangian transport model simulation of ANATEX (Across North America Tracer Experiment)
[DE89-008123] N89-23036

TREES (MATHEMATICS)
Object recognition from a large database using a decision tree N89-23135

TRENDS
Survey of development trends of methanol automobiles and methanol fuel in China
[DE88-756492] N89-22771

TRIBOLOGY
Tribological characterization of 15 surface treatments for aluminum alloys
[ETCA-87-R-132] N89-22928

TRIGGER CIRCUITS
Development and simulation study of a new inverse-pinch high Coulomb transfer switch
[NASA-CR-181768] N89-23300

TROPICAL REGIONS
On the physical causes of ENSO events and the ITCZ's extreme latitudinal displacements
[DE88-705654] N89-23050

TRUSSES
An experimental and analytical synthesis of controlled structure design
[DE89-006506] N89-22957

TUNABLE LASERS
Tunable chromium lasers
[DE89-008814] N89-22886
Cr3(+)-doped colquiriite solid state laser material
[DE89-010106] N89-22868

TUNGSTEN ALLOYS
Behavior of tungsten, molybdenum and alloys under unusual heating conditions N89-22674

TURBINE BLADES
Fatigue evaluation of WTS-3 wind turbine blade and retention
[FFA-TN-1987-81] N89-22618
Development of stress and lifing criteria for single crystal turbine blades N89-22663
Advanced materials to combat the high temperature degradation processes in turbomachinery N89-22664
Initial results of tests on metal-ceramic guide vanes N89-22668
Vacuum plasma spray coating N89-22670
Fiber reinforced superalloys for rocket engines N89-22673
Ceramic heat exchangers and turbine blades: Theory and experimental results N89-22677
Preliminary blade design using integrated computer codes
[FFA-TN-1988-67] N89-22777
Blade root design: A state of art survey
[FFAP-201] N89-22778

TURBINE ENGINES
Transonic viscous flow calculations for a turbine cascade with a two equation turbulence model
[NASA-TM-101944] N89-22607

TURBINE PUMPS
Cryogenic turbopump bearing materials N89-22678
Influence of different types of seals on the stability behavior of turbopumps N89-22902
A 3-dimensional finite-difference method for calculating the dynamic coefficients of seals N89-22903
An experimental study on the static and dynamic characteristics of pump annular seals N89-22904
Influence of impeller shroud forces on turbopump rotor dynamics N89-22909
Implementation of active magnetic bearings on advanced rocket engine turbopumps
[ETN-89-94365] N89-22929

TURBINES
LDV measurements and investigation of flow field through radial turbine guide vanes N89-22609
Some field experience with subsynchronous vibration of centrifugal compressors N89-22892
Some in-field experiences of non-synchronous vibrations in large rotating machinery N89-22894

TURBOCOMPRESSORS
Rotordynamic stability problems and solutions in high pressure turbocompressors N89-22914

TURBOGENERATORS
Megawatt Class Nuclear Space Power Systems (MCNSPS) conceptual design and evaluation report. Volume 3, technologies 2: Power conversion
[NASA-CR-179614-VOL-3] N89-22980

TURBOMACHINERY
Application of Advanced Material for Turbomachinery and Rocket Propulsion
[AGARD-CP-449] N89-22654
Advanced materials to combat the high temperature degradation processes in turbomachinery N89-22664
Utilization of high temperature composites in turbojet engines N89-22667
A generalized one-dimensional computer code for turbomachinery cooling passage flow calculations
[NASA-TM-102079] N89-22862
Rotordynamic Instability Problems in High-Performance Turbomachinery, 1988
[NASA-CP-3026] N89-22891
High stability design for new centrifugal compressor N89-22917
Structural dynamics branch research and accomplishments for FY 1988
[NASA-TM-101406] N89-22939

TURBULENCE
A preliminary characterization of parachute wake recontact
[DE89-006442] N89-22576
Renormalization group analysis of turbulence N89-22821
Low-dimensional chaos in turbulence N89-22822
Turbulent transport in the solar nebula N89-22829
Transition to turbulence in laminar hypersonic flow N89-22830
Direct numerical simulations of turbulent convection with a variable gravity and Keplerian rotation N89-22831
The effects of stabilizing and destabilizing longitudinal curvature on the structure of turbulent, two-stream mixing layers N89-22833
Thermal blooming threshold computations with a Markov model of velocity turbulence
[DE89-009709] N89-23285

TURBULENCE EFFECTS
Theoretical predictions of turbulent burning velocities of steady and accelerating unconfined turbulent flames with premixed reactants N89-22716

TURBULENCE MODELS
A study of unsteady turbulent flow past airfoils N89-22587
Annual research briefs, 1988
[NASA-CR-184906] N89-22817
Turbulence modeling N89-22819
The effects of particle loading on turbulence structure and modelling N89-22825
Analysis of turbulence structures in shear flows N89-22826
Computational fluid dynamics research in three-dimensional zonal techniques
[NASA-CR-181406] N89-22838

TURBULENT BOUNDARY LAYER
Annual research briefs, 1988
[NASA-CR-184906] N89-22817
The effects of stabilizing and destabilizing longitudinal curvature on the structure of turbulent, two-stream mixing layers N89-22833
An experimental investigation of a low Reynolds number turbulent boundary layer subject to an adverse pressure gradient N89-22834
Control of embedded vortices using wall jets
[AD-A202606] N89-22835
Study of unsteady boundary layers with adverse pressure gradient N89-22863
The structure and control of three-dimensional shock wave turbulent boundary layer interactions
[AD-A205923] N89-22866

TURBULENT FLOW
A study of unsteady turbulent flow past airfoils N89-22587
Theoretical predictions of turbulent burning velocities of steady and accelerating unconfined turbulent flames with premixed reactants N89-22716
Annual research briefs, 1988
[NASA-CR-184906] N89-22817
Turbulence modeling N89-22819
On curve and surface stretching in turbulent flow N89-22820
Close interactions of 3-D vortex tubes N89-22823
Numerical simulation of viscous vortex rings N89-22824
The effects of particle loading on turbulence structure and modelling N89-22825
Analysis of turbulence structures in shear flows N89-22826
Direct simulation of compressible reacting flows N89-22828
Computerized simulation of turbulent flow in a channel
[ONERA-RSF-16/3419-AY-112-A] N89-22852
Numerical simulation of vortex breakdown
[ONERA-RSF-3/4368-AY-502-A] N89-22853
On the structure of pressure fluctuations in simulated turbulent channel flow
[NASA-TM-101084] N89-22860
Low Reynolds number calculation of turbulent channel flow: A general discussion
[AD-A205883] N89-22864
Finite difference analysis of rotordynamic seal coefficients for an eccentric shaft position N89-22906

TURBULENT HEAT TRANSFER
Turbulent transport in the solar nebula N89-22829

TURBULENT MIXING
An experimental study of turbulent mixing of viscoelastic fluids
[ETN-89-94140] N89-22847

TURBULENT WAKES
Application of the Single-Axis-rate-Table (SAT) of the DFVLR for the evaluation of stationary and dynamic gyro properties
[ESA-TT-1122] N89-22877

TWILIGHT GLOW
Reports from the German Meteorological Service. No. 175: Global radiation during twilight
[ISBN-3-88148-241-5] N89-23052

TWO DIMENSIONAL FLOW
Interaction between an isolated vortex and a wing profile
[ETN-89-94364] N89-22579
Low-dimensional chaos in turbulence N89-22822
A theoretical study of fluid forces on a centrifugal impeller rotating and whirling in a vaned diffuser N89-22908

TWO PHASE FLOW
The effects of particle loading on turbulence structure and modelling N89-22825
Two-phase flow characteristic of inverted bubbly, slug and annular flow in post-critical heat flux region
[DE89-007384] N89-22839

U

U.S.S.R. SPACE PROGRAM
JPRS report: Science and technology. USSR: Space
[JPRS-USP-88-003] N89-22622

Project Radioastron N89-22623
Glavkosmos official Yu. P. Semenov interviewed on development of USSR space program N89-22629
Future space projects discussed at Moscow Space Forum N89-22630
History of manned flight [CNES-NT-121] N89-23405

ULTRAHIGH FREQUENCIES
Study of a DRS experimental payload for single and multiple access at S band: Executive summary [PSD88/00017] N89-22648

ULTRASONIC FLAW DETECTION
Ultrasonic detection of damage in carbon epoxy composite materials [ONERA-RT-3/7256-RY-071-R] N89-22705
Reconstruction of defects from amplitude location curves [REPT-780852-TW] N89-22934
NDT results for comparability program SPF/DB [I-264/88] N89-22935
Signal treatment and data analysis methods applied to nondestructive control of adhesive bonded joints [ISAL-IDI-8809] N89-22936

ULTRASONIC TESTS
Nondestructive evaluation of stress using ultrasound and pulsed heat [AD-A205176] N89-22932

ULTRAVIOLET ASTRONOMY
Studies of hot white dwarfs and instrumentation for stellar extreme ultraviolet astronomy N89-23383

ULTRAVIOLET RADIATION
Observational aspects of interacting galaxies N89-23385

UNDERWATER ENGINEERING
Seafloor temperature and conductivity data from coastal waters of the US Beaufort Sea [AD-A205428] N89-23059

UNDERWATER OPTICS
Activities report of the Division of Optical Technology (FOA 33) [FOA-C-30507-3.1] N89-23287

UNIQUENESS
Straight homogeneous generalized cylinders: Differential geometry and uniqueness results N89-23169

UNIVERSE
Dark matter candidates [DE89-006579] N89-23387
Problems in modern cosmology N89-23393

UNIX (OPERATING SYSTEM)
Improved performance in NASTRAN (R) N89-22941
A NASTRAN/TREETOPS solution to a flexible, multi-body dynamics and controls problem on a UNIX workstation N89-22945
The design and implementation of a graphical VHDL (VHSIC Hardware Description Language) user interface [AD-A202619] N89-23186

UNMANNED SPACECRAFT
Glavkosmos official Yu. P. Semenov interviewed on development of USSR space program N89-22629

UNSTEADY AERODYNAMICS
Unsteady aerodynamic computational method of non-coplanar wing-tail combinations in subsonic flow [PB89-111470] N89-22571
Aerodynamics of nonrigid bodies undergoing large amplitude time-dependent motions N89-22586
Aerodynamic detuning of a loaded airfoil cascade in an incompressible flow by a locally analytical method N89-22588
On the Lagrangian description of unsteady boundary layer separation. Part 2: The spinning sphere [NASA-TM-102027] N89-22861

UNSTEADY FLOW
A study of unsteady turbulent flow past airfoils N89-22587
A vortex panel analysis of circular-arc bluff-bodies in unsteady flow [DE89-007141] N89-22845
Theoretical study of the unsteady flow in a straight channel with variable and constant cross section [VKI-TN-168] N89-22857

URANIUM
Experimental study of uranium plastic scintillator calorimeters [IIKHEF-H/88-4] N89-22876

USER MANUALS (COMPUTER PROGRAMS)
Orbiter Flying Qualities (OFQ) Workstation user's guide [NASA-CR-179440] N89-22612
SEAPAK user's guide, version 1.0 [NASA-TM-100728] N89-23182
Engineering Graphics System (EGS) user's manual [DE89-009668] N89-23199

USER REQUIREMENTS
Minimum number of satellites for periodic coverage [FOA-C-30511-9.4] N89-22976
The Organisation and Functions of Documentation and Information Centres in Defence and Aerospace Environments [AGARD-CP-445] N89-23362
The status of defence information programs in Greece N89-23364
User needs and how to determine them N89-23365
Identifying users and how to reach them N89-23370

V

VACANCIES (CRYSTAL DEFECTS)
Mechanisms of cascade collapse [DE89-009882] N89-22740

VACUUM
Investigation of the vacuum structure of the Georgi-Glashow model on the lattice [DE88-705676] N89-23319

VACUUM DEPOSITION
Vacuum plasma spray coating N89-22670

VALENCE
Band structure of CdTe-ZnTe superlattice [DE88-705682] N89-23321

VAN SLYKE METHOD
Measurement of the total gas content of a liquid [OUEL-1643/86] N89-22711

VANELESS DIFFUSERS
Influence of impeller and diffuser geometries on the lateral fluid forces of whirling centrifugal impeller N89-22907

VANES
A theoretical study of fluid forces on a centrifugal impeller rotating and whirling in a vaned diffuser N89-22908

VAPOR DEPOSITION
CVD and diffusion coatings for high temperature applications in turbomachinery and rocket motors N89-22658
Fabrication of solid oxide fuel cell by electrochemical vapor deposition [DE89-009605] N89-23023

VAPOR PHASES
Formation of lubricating films at elevated temperatures from the gas phase [PB89-129530] N89-22747

VAPORIZING
Melting behavior of heavy metal batch components [ETN-89-93986] N89-22734

VARIATIONAL PRINCIPLES
Generalized finite strains, generalized stresses, and a hybrid variational principle for finite-element computer programs using curvilinear coordinates [DE89-009923] N89-22962

VECTOR ANALYSIS
Enhancements to the IBM version of COSMIC/NASTRAN N89-22946
Projections of vector addition system reachability sets are semilinear [AD-A205914] N89-23257

VEGETATION
Investigation on long time dispersion and washout factor. Vegetation contamination computation with meteorological whole year or summer statistics [JUEL-SPEZ-449] N89-23028
Determination of the dynamic CO2 source-sink function of different biomes with the object of verifying seasonality and trend of atmospheric CO2 measurements of different stations [ETN-89-93763] N89-23038

VELOCITY
Thermal blooming threshold computations with a Markov model of velocity turbulence [DE89-009709] N89-23285

VELOCITY MEASUREMENT
Velocity measurements downstream of a sudden expansion using LDV. Part 2: Experimental results [FOA-C-20736-2.1-PT-2] N89-22849
Implementation of a two-component laser anemometer at the T2 wind tunnel [A-501-H] N89-22879

VELOCITY MODULATION
Organic and polymer crystalline films for spatial light modulation [AD-A205906] N89-23350

VERY LARGE SCALE INTEGRATION
HIFI: A design method for implementing signal processing algorithms on VLSI processor arrays [ETN-89-94138] N89-22795
Parallel hardware for constraint satisfaction N89-23127
Scan line array processors: Work in progress N89-23128

VERY LONG BASE INTERFEROMETRY
Study of long optical fibers [ESA-CR(P)-2723] N89-23288

VERY LOW FREQUENCIES
Design of an ELF/VLF satellite for under the ice submarine communications [AD-A202607] N89-22639

VHSIC (CIRCUITS)
The design and implementation of a graphical VHDL (VHSIC Hardware Description Language) user interface [AD-A202619] N89-23186

VIBRATION
Evaluation of the ride quality of a light twin engine airplane using a ride quality meter [NASA-TP-2913] N89-22568
Rotor instability due to a gear coupling connected to a bearingless sun wheel of a planetary gear N89-22893
Some in-field experiences of non-synchronous vibrations in large rotating machinery N89-22894
The spectral analysis of an aero-engine assembly incorporating a squeeze-film damper N89-22895
Magnetic bearing stiffness control using frequency band filtering N89-22910
Calculation of low frequency vibrational resonances of submerged structures N89-22951

VIBRATION DAMPING
Acta Aeronautica et Astronautica Sinica (selected articles) [AD-A205128] N89-22570
Active vibration control for flexible rotor by optimal direct-output feedback control [NASA-TM-101972] N89-22605
The spectral analysis of an aero-engine assembly incorporating a squeeze-film damper N89-22895
Piezoelectric pushers for active vibration control of rotating machinery N89-22896
An electroviscous damper N89-22898
A magnetic damper for first mode vibration reduction in multimass flexible rotors N89-22911
High stability design for new centrifugal compressor N89-22917
Structural dynamics branch research and accomplishments for FY 1988 [NASA-TM-101406] N89-22939

VIBRATION ISOLATORS
A magnetic damper for first mode vibration reduction in multimass flexible rotors N89-22911

VIBRATION TESTS
Electrodynamic transient tests — satellites [CNES-CT/DRT/TVE/SM-024] N89-22644

VIDEO LANDMARK ACQUISITION AND TRACKING
Knowledge based vision for terrestrial robots N89-23087

VIDEO SIGNALS
Combustor flow visualization using innovative infrared thermographics techniques [AD-A205905] N89-22718

VISCOELASTICITY
Influence of conditioning on the trapezoidal fatigue behavior of a carbon epoxy composite [ETCA-87-R-052] N89-22700
Dynamic behavior of a carbon epoxy composite [ETCA-87-R-001] N89-22701
On the numerical integration of viscoelastic flow equations [DE89-007135] N89-22844
An experimental study of turbulent mixing of viscoelastic fluids [ETN-89-94140] N89-22847
Analysis of the mechanical behavior of adhesively bonded composite joints [AD-A202616] N89-22938

VISCOUS FLOW
A numerical study of viscous vortex rings using a spectral method N89-22572
Aerodynamics of nonrigid bodies undergoing large amplitude time-dependent motions N89-22586
Transonic viscous flow calculations for a turbine cascade with a two equation turbulence model [NASA-TM-101944] N89-22607
Forced and free convection flow with viscous dissipation effects: The method of parametric differentiation [DE88-705649] N89-22840
On the numerical integration of viscoelastic flow equations [DE89-007135] N89-22844

VISCOUS FLUIDS
An electroviscous damper N89-22898

VISUAL OBSERVATION
A historical interpretation of the study of the visible cloud morphology on the planet Jupiter: 1610-1878 N89-23398

VISUAL PERCEPTION
Using flow field divergence for obstacle avoidance in visual navigation N89-23120
Unity vision block with focal plane [AD-A204894] N89-23283

VOCAL CORDS
Motor theory of auditory perception
[AD-A204951] N89-23064
VOICE COMMUNICATION
National airspace system plan: Facilities, equipment, associated development and other capital needs
[AD-A202615] N89-22596
VOICE DATA PROCESSING
Coordinated Noninvasive Studies (CNS) Project
[AD-A205413] N89-22804
VOLUMETRIC ANALYSIS
Adsorption studies in the critical region of a pure fluid. Development of an apparatus for adsorption measurements under microgravity conditions
[ETN-89-93767] N89-22774
VORTEX BREAKDOWN
Numerical simulation of vortex breakdown
[ONERA-RSF-3/4368-AY-502-A] N89-22853
VORTEX FILAMENTS
Aerodynamics of nonrigid bodies undergoing large amplitude time-dependent motions N89-22586
VORTEX RINGS
A numerical study of viscous vortex rings using a spectral method N89-22572
Numerical simulation of viscous vortex rings N89-22824
VORTEX SHEETS
Aerodynamics of nonrigid bodies undergoing large amplitude time-dependent motions N89-22586
VORTICES
Interaction between an isolated vortex and a wing profile
[ETN-89-94364] N89-22579
Close interactions of 3-D vortex tubes N89-22823
Numerical simulation of viscous vortex rings N89-22824
Control of embedded vortices using wall jets
[AD-A202606] N89-22835
VORTICITY
The length scale for sub-grid-scale parameterization with anisotropic resolution N89-22818
The effects of particle loading on turbulence structure and modelling N89-22825
Lectures in Fluid Physics held at the Physics Department of the Georg-August-University. Volume 1: Source Strength of Vorticity
[DFVLR-MITT-88-26-VOL-1] N89-22855
VORTICITY EQUATIONS
Convergence of discrete-vortex induced-flow calculations by optimum choice of mesh N89-22585
VULNERABILITY
Orbital debris environment for spacecraft designed to operate in low Earth orbit
[NASA-TM-100471] N89-22638

W

WAKES
A preliminary characterization of parachute wake recontact
[DE89-006442] N89-22576
WALL FLOW
Sidewall boundary layer study, with and without suction, for the 150 mm chord CAST 7 airfoil at the T2 wind tunnel N89-22584
Non-linear evolution of a second mode wave in supersonic boundary layers
[NASA-CR-181811] N89-22836
Lectures in Fluid Physics held at the Physics Department of the Georg-August-University. Volume 1: Source Strength of Vorticity
[DFVLR-MITT-88-26-VOL-1] N89-22855
On the structure of pressure fluctuations in simulated turbulent channel flow
[NASA-TM-101084] N89-22860
WARFARE
Space control: A national imperative
[AD-A202612] N89-22631
WASTE DISPOSAL
The long-term climate change assessment task of the Hanford Site, Washington, Protective Barrier Development Program
[DE89-008704] N89-23030
WATER HEATING
Development of advanced heat pump. Part 2: Preliminary test of two-stage compression heat pump
[DE88-756838] N89-22841
WATER TUNNEL TESTS
Study of unsteady boundary layers with adverse pressure gradient N89-22863
WATER VAPOR
Diabatic circulations in the stratosphere N89-23043
WATER WAVES
Probabilities and statistics for backscatter estimates obtained by a scatterometer with applications to new scatterometer design data
[NASA-CR-4228] N89-22779
Theoretical studies for ERS-1 wave mode, volume 1
[GEC-MTR-87/110-VOL-1] N89-22977
WAVE GENERATION
ITER equilibrium with bootstrap currents, lower hybrid current drive and fast wave current drive
[DE89-009676] N89-22810
Non-linear evolution of a second mode wave in supersonic boundary layers
[NASA-CR-181811] N89-22836
WAVE INTERACTION
Gravity wave and turbulence studies using a high-resolution ST radar
[AD-A205592] N89-23046
WAVE PROPAGATION
Coherent polarimetric radar techniques for microwave propagation and cloud physics research
[DFVLR-FB-88-47] N89-22800
Theoretical study of the unsteady flow in a straight channel with variable and constant cross section
[VKI-TN-168] N89-22857
Magnetic axis alignment and the Poisson alignment reference system
[DE89-007687] N89-22880
On the small-signal gain of free-electron lasers in the low-current region
[ESA-TT-1120] N89-22889
Simulations of axisymmetric erosion in IFR-Transported beams
[AD-A205882] N89-23301
WAVE REFLECTION
Effect of pump-induced density depletions on the spectrum of stimulated electromagnetic emissions — ionosphere
[IRF-PREPRINT-107] N89-22799
WAVE SCATTERING
Analysis of regional phases using three component data
[AD-A205480] N89-23045
WAVEGUIDES
Computer aided design of three-dimensional waveguide loaded cavities
[DE89-007733] N89-22783
ICRF waveguide launcher research
[DE89-009151] N89-22791
Scaling relations for a beam-deflecting TM(110) mode in an asymmetric cavity
[DE89-009277] N89-22796
WAVELENGTHS
Wavelength streak camera
[DE89-008612] N89-22874
Fiber optic laser rod
[DE89-009598] N89-22887
WEAK ENERGY INTERACTIONS
Neutrino helicity flips via electroweak interactions and SN1987a
[NIKHEF-H/88-18] N89-23278
WEAR
Temperature effects on the break-in of nickel aluminide alloys
[DE89-005341] N89-22729
WEAR RESISTANCE
Cryogenic turbopump bearing materials N89-22678
WEAR TESTS
Wear protection coatings and treatments for the TA6V alloy
[ETCA-88-R-003] N89-22742
Effects of lubrication on the performance of high speed spur gears
[NASA-TM-101969] N89-22919
Tribological characterization of 15 surface treatments for aluminum alloys
[ETCA-87-R-132] N89-22926
WEATHER STATIONS
Determination of the dynamic CO2 source-sink function of different biomes with the object of verifying seasonality and trend of atmospheric CO2 measurements of different stations
[ETN-89-93763] N89-23038
WEIBULL DENSITY FUNCTIONS
Transmission overhaul and replacement predictions using Weibull and renewal theory
[NASA-TM-102022] N89-22925
WEIGHT REDUCTION
Lightweight fibrous nickel electrodes for nickel-hydrogen batteries
[NASA-TM-101997] N89-22710
Advances in lightweight nickel electrode technology N89-23005
WEIGHTLESSNESS
Construction in weightlessness N89-22626
WELDABILITY
The effect of thermocapillary flow on weld-pool profile
[NPL-DMA(A)167] N89-22927
WELDED STRUCTURES
Development of orbital welding technology N89-22628
WELDING
Development of orbital welding technology N89-22628
Assessing hydrogen assisted cracking modes in high strength steel welds
[AD-A205431] N89-22748
WEST GERMANY
Navigation experiment NAVEX: The reading differences between all ground station measuring clocks during Spacelab pass of the D1 mission
[ESA-TT-1113] N89-22599
Germany: Focus on Scientific and Technical Information, volume 4, number 1, April 1988
[AD-A204054] N89-23378
WHISKER COMPOSITES
Observations on the toughening of Al2O3-SiC composites
[DE89-009843] N89-22695
WHITE DWARF STARS
Studies of hot white dwarfs and instrumentation for stellar extreme ultraviolet astronomy N89-23383
WIGGLER MAGNETS
On the small-signal gain of free-electron lasers in the low-current region
[ESA-TT-1120] N89-22889
WIND (METEOROLOGY)
Investigation of the effects of increased sophistication of simulation of the atmospheric wind in wind tunnels N89-22620
Thermal blooming threshold computations with a Markov model of velocity turbulence
[DE89-009709] N89-23285
WIND PROFILES
Hazard index calculation for 31 May 1984 microburst at Erie, Colorado
[NASA-CR-184968] N89-23048
WIND TUNNEL APPARATUS
Implementation of a two-component laser anemometer at the T2 wind tunnel
[A-501-H] N89-22879
WIND TUNNEL MODELS
Investigation of the effects of increased sophistication of simulation of the atmospheric wind in wind tunnels N89-22620
WIND TUNNEL TESTS
NASA's program on icing research and technology
[NASA-TM-101988] N89-22569
Interaction between an isolated vortex and a wing profile
[ETN-89-94364] N89-22579
The influence of the leading edge geometry on the wave drag for a 65 degree delta wing at low supersonic speed and small angles of attack
[FFA-141] N89-22583
Transonic and supersonic wind tunnel tests on control effectiveness on schematic missile configurations with canard controls
[FFA-TN-1988-11] N89-22601
Transonic and supersonic wind tunnel tests on control effectiveness on schematic missile configuration with canard control
[FFA-TN-1988-11-SUPPL] N89-22613
Microcomputer based controller for the Langley 0.3-meter Transonic Cryogenic Tunnel
[NASA-CR-181808] N89-22616
The low-speed wind tunnel at DVFLR in Brunswick (Fed. Republic of Germany)
[DFVLR-MITT-88-25] N89-22619
Investigation of the effects of increased sophistication of simulation of the atmospheric wind in wind tunnels N89-22620
Experimental investigation of flow over a backward facing step-progress report N89-22832
An experimental investigation of a low Reynolds number turbulent boundary layer subject to an adverse pressure gradient N89-22834
Control of embedded vortices using wall jets
[AD-A202606] N89-22835
WIND TUNNEL WALLS
Sidewall boundary layer study, with and without suction, for the 150 mm chord CAST 7 airfoil at the T2 wind tunnel N89-22584
Hardware and operating features of the adaptive wall test section for the 0.3-meter transonic cryogenic tunnel
[NASA-TM-4114] N89-22614
WIND TUNNELS
Visting China's aerodynamics research and development center
[AD-A203980] N89-22615

Investigation of the effects of increased sophistication of simulation of the atmospheric wind in wind tunnels N89-22620

WIND TURBINES
Wind tunnel tests of 16 percent thick airfoil section with spoilers at different chordwise positions --- wind turbines [FFA-TN-1987-39] N89-22582
Fatigue evaluation of WTS-3 wind turbine blade and retention [FFA-TN-1987-81] N89-22618
Preliminary blade design using integrated computer codes [FFA-TN-1988-67] N89-22777
Blade root design: A state of art survey [FFAP-201] N89-22778
Comparison of measured and calculated sound pressure levels around a large horizontal axis wind turbine generator [NASA-TM-100654] N89-23270
Environmental noise characteristics of the MOD5-B (3.2 MW) wind turbine generator [NASA-TM-101567] N89-23272

WIND VELOCITY MEASUREMENT
Probabilities and statistics for backscatter estimates obtained by a scatterometer with applications to new scatterometer design data [NASA-CR-4226] N89-22779

WING PROFILES
Interaction between an isolated vortex and a wing profile [ETN-89-94364] N89-22579

WING TIP VORTICES
Convergence of discrete-vortex induced-flow calculations by optimum choice of mesh N89-22585

WIRE
The induced current in parallel wires over an imperfect ground from an incident EMP [DE89-007209] N89-22787

WORKLOADS (PSYCHOPHYSIOLOGY)
An in-flight investigation of workload assessment techniques for civil aircraft operations [NLR-TR-87119-U] N89-23070

WORKSTATIONS
The Space Station Flight Telerobotic Servicer and the human [NASA-TM-100615] N89-23068

X

X RAY ABSORPTION
EXAFS studies of multilayer interfaces [DE89-009527] N89-22694

X RAY DIFFRACTION
Effects of X-rays on isotactic polypropylene. Volume 2: Polymers and ceramics [DE88-705606] N89-22751

X RAY IMAGERY
Ultra-sensitive X-ray sensors give improved contrast sensitivity [DE89-003581] N89-22872
ALEXIS: A narrow-band survey/monitor of the ultrasoft X-ray sky [DE89-007980] N89-22873

X RAY SOURCES
Thermal Comptonization models for gamma-ray emission from black-hole sources [DE89-009918] N89-23402

X RAYS
The ALEXIS project and the local interstellar medium [DE89-009246] N89-23392

X-Y PLOTTERS
Engineering Graphics System (EGS) user's manual [DE89-009668] N89-23199

XENON
Precipitation of Ar, Kr and Xe in Ni at room temperature [DE89-009879] N89-22713

Y

YAW
A study of unsteady turbulent flow past airfoils N89-22587

YIELD STRENGTH
Ductility enhancement in unreacted internal-Sn Nb3Sn through low-temperature anneals [DE89-009125] N89-23336

YTTERBIUM
Time resolved photoluminescence of ytterbium in indium phosphide [AD-A202596] N89-23303

YTTRIUM
Effects of different fabrication techniques on the Yttrium-Barium-Copper oxide high temperature superconductor [AD-A202598] N89-23304

YTTRIUM COMPOUNDS
Superconductivity for electric power systems: Building toward our future [DE89-000874] N89-23332

Z

ZINC SULFIDES
Accumulated surface damage on ZnS crystals produced by closely spaced pairs of picosecond laser pulses [DE89-008813] N89-23329

ZINC TELLURIDES
Band structure of CdTe-ZnTe superlattice [DE88-705682] N89-23321

ZIRCONIUM OXIDES
Alumina reinforced tetragonal zirconia (TZP) composites [DE89-008880] N89-22690
Preliminary study of ceramic-metal interface in thermal boundaries [ETCA-87-R-101] N89-23346

Typical Personal Author Index Listing

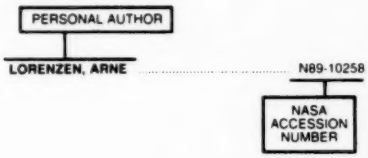

Listings in this index are arranged alphabetically by personal author. The NASA accession number denotes the number by which the citation is identified.

A

ABDELHAY, ABDELHAY MOHAMED N89-22967
ABRAMOWICZ, MAREK A. N89-23389
ACKERMAN, NEEL B., JR. N89-23071
ACOSTA, ALLAN J. N89-22908
ADAMIC, K. J. N89-22761
ADAMS, M. L. N89-22905
ADKINS, DOUGLAS R. N89-23017
AHARONY, A. N89-23333
AHUJA, NARENDRA N89-23096
AIELLO, ROBERT A. N89-22848
ALCOUFFE, R. E. N89-23260
ALDRED, P. N89-22726
ALESTEDT, EDDIE N89-22803
ALEXANDER, R. M. N89-22896
ALLAIRE, P. E. N89-22911
ALLCOCK, HARRY R. N89-22750
ALLEN, J. E. N89-23293
ALLEN, JAMES J. N89-22957
N89-23194
ALLEN, PETER K. N89-23083
N89-23158
ALLISON, S. W. N89-23334
ALLUB, R. N89-23322
ALOIMONOS, JOHN N89-23078
N89-23091
N89-23120
N89-23152
N89-23154
ALPERT, D. J. N89-23015
ALPHONSE, G. A. N89-22890
AMES, K. R. N89-22926
AN, JIGUANG N89-22571
ANDERSON, B. D. O. N89-23214
ANDERSON, KEVIN K. N89-23233
ANDERSON, R. G. N89-22885
ANDERSON, R. R. N89-23040
ANDERSON, WALLACE L. N89-22932
ANDERSSON, BORJE N89-22965
ANDREES N89-22757
ANNEVELINK, JURGEN N89-22795
ANZ-MEADOR, PHILLIP D. N89-22638
APPLEBY, A. JOHN N89-22991
N89-22994
AQUILINA, ALAN T. N89-23071
ARBAD, O. N89-22840
ARCHAMBAUD, J. P. N89-22584
N89-22879
ARNOLD, F. N89-23037
ARVIZU, DAN E. N89-22749
ARZPAYMA, F. N89-22641
ASH, R. L. N89-22868
ASTAPOV, A. A. N89-23325
ASTHEIMER, ROBERT W. N89-23283
ATTIA, ALAN I. N89-22986
AVANESOV, G. A. N89-22624
AVERBACK, R. S. N89-22740
AVRAN, P. N89-22677
AXNAES, INGVAR N89-23289

B

BAGCHI, ARUNABHA N89-23242
BAIN, RODNEY DONALD N89-22633
BAJCSY, RUZENA N89-23098
BAK, PER N89-23337
BAKER, H. HARLYN N89-23164
N89-23165
BAKER, R. S. N89-23260
BALACHANDRAN, U. N89-23342
BALAKRISHNA, S. N89-22616
BALAS, EGON N89-23190
BALASUBRAMANYAM, POORNIMA N89-23153
BALDWIN, R. N89-22996
BAMBERGER, A. N89-22878
BANKSTON, C. P. N89-22988
BANNING, DOUGLAS W. N89-22650
BARKER, RAYMOND H., JR. N89-22631
BARNARD, STEPHEN T. N89-23143
BARREIRO, F. N89-22878
BARRETT, L. E. N89-22911
BARRY, T. I. N89-22714
BARTELS, PAUL VINCENT N89-22847
BARTHELEMY, A. N89-23288
BARTHULI, KATHRYN E. N89-23205
BARTON, RICHARD J. N89-22805
BASU, ANUP N89-23152
BATAILLON, C. N89-22744
BAUER, EVA N89-22975
BAUGHN, TERRY V. N89-22956
BAUMANN, GERHARD N89-22959
BAUMANN, LEE S. N89-23074
N89-23115
BEASLEY, M. R. N89-23310
BECKER, R. N89-22933
BELJAARS, A. C. M. N89-23055
BELYTSCHKO, TED N89-23184
BENAVENTE, JAVIER E. N89-22945
BENDER, ULRICH N89-23359
BENEDEK, R. N89-22740
BENGTSSON, ANDERS N89-23254
BENMOUNA, MUSTAPHA N89-22752
N89-22753
N89-22754
BENTLY, D. E. N89-22915
BERGHOLTER, UWE N89-23052
BERGLIND, TORSTEN N89-22578
N89-22583
BERGMANN, HEINRICH W. N89-22706
BERNARD, J. N89-22767
BERNARDI, E. N89-22878
BERRY, GUY C. N89-22770
BETZOLD, K. N89-22933
BEX, W. N89-22680
BHANU, BIR N89-23086
N89-23099
N89-23118
N89-23119
BHAT, BILIYAR N. N89-22678
BIDA, THOMAS A. N89-22884
BIERLECKI, A. N89-23311
BILDSTEIN, H. N89-22674
BILLARD, PHILLIP A. N89-22722
BINFORD, THOMAS O. N89-23077
N89-23112
N89-23146
N89-23147
N89-23151
N89-23172
N89-23177
BINGHAM, CARL E. N89-22681
BIRGENEAU, R. J. N89-23333
BIRTCHER, R. C. N89-22713
BITRANCARRENO, MAURICIO ERNESTO N89-23386
BITTKER, DAVID A. N89-22606
BJORCK, ANDERS N89-22582
BJORSET, LARS N89-22794
BLACK, PAUL K. N89-23188
BLACKFIELD, D. T. N89-23292
BLAKE, RODGER D. N89-22763
BLATTNER, MEERA N89-22797
BLAU, PETER J. N89-22729
BLOCH, J. J. N89-22873
N89-23392
BLOM, ANDERS F. N89-22618
N89-22965
BLOOMFIELD, H. S. N89-23397
BLUMBERG, PAUL N. N89-23382
BOEHM, GUENTER N89-23359
BOETTINGER, WILLIAM J. N89-22721
BOGDONOFF, SEYMOUR M. N89-22866
BOHN, C. L. N89-23342
BOHN, MARK S. N89-22843
BOICOURT, G. P. N89-22790
BOLLES, ROBERT C. N89-23080
N89-23164
BONNAL, C. N89-22646
BONNET, J. L. N89-22879
BONOLI, P. T. N89-23292
BOOKER, STANLEY R. N89-22808
BORDENICK, JOHN E. N89-22875
BORDES, NICOLE N89-23336
BORETTI, A. A. N89-22607
BORNYAKOV, V. G. N89-23319
BOSCH, J. P. N89-22928
BOSCH, R. N89-22775
BOTTENBERG, W. N89-23021
BOUBOUKAS, V. N89-23363
BOUDIGUES, S. N89-22677
BOULT, TERRANCE E. N89-23083
N89-23092
N89-23145
N89-23168
BOURDEL, FRANCOISE N89-22854
BOUVART, DANIEL N89-22766
BOWMAN, M. K. N89-23314
BOYER, K. N89-22881
BRAAKSMA, B. L. J. N89-23240
BRAITHWAITE, N. ST. J. N89-23293
BRANDHORST, HENRY W., JR. N89-23025
BRANSFORD, JAMES W. N89-22722
BRAUN, HELMUT N89-23389
BREIL, J. F. N89-22584
BREUS, TAMARA N89-22630
BREWER, JEFFREY C. N89-22992
BREWER, MARGARET A. N89-23205
BRILL, JACK N89-23006
BRITTON, DORIS L. N89-22710
BROCA, JACQUES N89-22676
BROERSMA, H. J. N89-23235
N89-23251
BROOKS, RODNEY A. N89-23106
BROPHY, JAMES J. N89-22816
N89-23348
BROWN, C. M. N89-23095
BROWN, CHRISTOPHER M. N89-23082
BROWN, JENNIE H. N89-22768
BROWN, LISA GOTTESFELD N89-23179
BROWN, W. KEITH N89-22948
BROWNE, L. W. B. N89-22832
BRUENING, CLAUS N89-22975
BUEHLMANN, E. T. N89-22893
BUELTHOFF, H. N89-23093
BUENDIA, A. N89-22758
BUENING, HANS KLEINE N89-23257
BUGOS, A. R. N89-23334
BUMGARNER, THAD F. N89-23303
BURCH, J. L. N89-23040
BURGER, WILHELM N89-23099
BURKE, A. F. N89-22812
BURNS, J. BRIAN N89-23137
BURRELL, K. H. N89-23290
BURT, PETER J. N89-23090
BUTLER, THOMAS G. N89-22954

C

CABOT, WILLIAM H. N89-22831
CAGLAYAN, A. K. N89-23209
CALLAGHAN, BRIAN P. N89-22784
CAMACHO, A. N89-23321
CAMPO, E. N89-22663
CANAVAN, GREGORY H. N89-23265
CANNING, JOHN N89-23171
CANNON, ROBERT H., JR. N89-22918
CAPONIO, JOSEPH F. N89-23370
CAPPEL, A. N89-23051

CARLSTROM, T. N. N89-23290
CASKEY, G. R. N89-22726
CASPI, S. N89-23231
CASS, TODD ANTHONY N89-23093
N89-23130
CATALDO, ROBERT L. N89-22985
CATES, M. R. N89-23334
CATTO, PETER J. N89-23296
CAZENEUVE, C. N89-22700
N89-22701
CEDERSTAM, PER N89-23279
CENTER, JULIAN N89-23192
CHAKRABARTI, S. K. N89-23396
CHALK, C. D. N89-22658
CHALKLEY, P. D. N89-22685
CHAMBERLIN, ROGER N89-22617
CHAN, GORDON C. N89-22941
CHAN, Y. Y. N89-22575
CHANDRA, MADHUKAR N89-22800
CHANDRASHEKARA, S. N89-22687
CHANG, REBECCA R. N89-23009
CHANG, S. C. N89-22735
CHASE, LLOYD L. N89-22686
N89-22688
N89-23329
CHATO, DAVID J. N89-22652
CHATURVEDI, P. K. N89-23032
CHAVEZ, J. N89-22973
CHEKALIN, SERGEY VASILYEVICH N89-22626
N89-22627
CHELA-FLORES, J. N89-23322
CHELBERG, DAVID M. N89-23100
CHEN, C. H. N89-22931
CHEN, DANIAN N89-22937
CHEN, H. MING N89-22910
CHEN, JUDY N89-23182
CHEN, KANGYAN N89-22571
CHEN, LIANG-HUA N89-23092
CHENG, C. C. N89-22739
CHESTER, R. J. N89-22685
CHIANG, HSIAO-WEI DAVID N89-22588
CHIQIER, N. N89-22851
CHILDRESS, TIMOTHY G. N89-22781
CHILDS, DARA W. N89-22899
N89-22909
CHIU, YIHWAN DANNY N89-22585
CHO, W. D. N89-22735
CHOE, W. H. N89-22634
CHOI, SANG H. N89-23300
CHOU, P. B. N89-23095
CHOU, Y. T. N89-23335
CHRISPIN, W. J. N89-22659
CHRIST, DIETMAR N89-22619
CHRISTOPHOROU, LOUCAS G. N89-23298
CHUNG, H. M. N89-22737
CHURCHILL, P. N. N89-22978
CLARK, JOHN N89-23311
CLARK, KENNETH N89-22688
CLARKE, J. N89-23310
CLARKE, W. L. N89-22726
CLAYTON, CHRISTOPHER A. N89-23364
CLISSON, J. N89-22743
COATES, DWAINE N89-23005
COHEN, MARVIN S. N89-23188
COHEN, MICHAEL N89-23338
COLEMAN, SAM N89-23330
COLLINS, C. B. N89-22883
COLLINS, DAVE N89-23035
COLLINS, WILLIAM E. N89-22595
COLNAGO, GIUSEPPE N89-22894
COMBES, C. N89-22641
CONN, R. W. N89-23295
CONNOLLY, C. I. N89-23166
COOK, DAVID R. N89-23018
COOK, W. A. N89-22962
COOPER, PAUL R. N89-23127
N89-23160
COQUERELLE, G. N89-22742
CORBY, N. R. N89-23102
CORDEY, R. A. N89-22977
CORDOVA, F. N89-22873
CORK, C. P. N89-23326
CORNILSEN, BAHNE C. N89-23001
CORTES, V. N89-22935
COUGNET, C. N89-22645
COUTURE, G. N89-22679
COWPERTHWAITE, M. N89-22865
COX, M. G. N89-23253
COZIAN, GILDAS N89-22598
CRUM, LAWRENCE A. N89-23271
CULLEN, D. N89-22881
CUSICK, ALLAN HODGSON N89-22620
CYRLUK, DAVID A. N89-23139
CZUCHLEWSKI, S. J. N89-22865

D

DABROWSKI, B. N89-23340
DAGOSTINI, G. N89-22878
DAILY, MICHAEL J. N89-23121
DALLMANN, UWE N89-22581
DALLY, M. J. N89-23084
DAMERON, GARY G. N89-23067
DANG, K. N89-22852
DANIEL, SHARON L. N89-23261
DARDEL, R. N89-22644
DARIVA, I. N89-22642
DARYABEIGI, K. N89-22868
DARZI, MICHAEL N89-23182
DAUGHERTY, PAUL N89-23005
DAVENPORT, ALISON J. N89-22730
DAVIS, FRANK G. N89-22665
DAVIS, JAMES A. N89-23206
DAVIS, LARRY S. N89-23078
N89-23091
N89-23141
DAVIS, R. R. N89-22912
N89-22916
DAVIS, WILLIAM E. N89-23036
DEBOO, J. C. N89-23290
DEBOOR, CARL N89-23225
N89-23226
DEDE, M. M. N89-22695
DEFONTAINE, D. N89-22741
DEGROOT, A. J. N89-23210
DEHNE, KLAUS N89-23052
DEJONG, SIJBRAND J. N89-23276
DEJONGHE, L. C. N89-22987
DELAHOY, A. E. N89-23022
DELAMARE N89-22699
DELAYEN, J. R. N89-23342
DELIGIANNIS, F. N89-23011
DELUCA, W. H. N89-22814
DENARDO, G. N89-23355
DENDIS, JAMES C. N89-22683
DENLINGER, JERRY L. N89-23101
DENTEN, JAMES P. N89-22839
DEREP, J. LUC N89-23346
DERMER, CHARLES D. N89-23402
DEUTSCHER, N. N89-22645
DEVAN, J. H. N89-22693
DEVATY, ROBERT P. N89-22689
DEVORE, C. E. N89-22729
DEVOTO, R. S. N89-23292
DEVRIES, JOHANNES N89-23331
DHAR, Y. J. N89-22991
DIAZDELARUBIA, T. N89-22740
DICUS, JOHN H. N89-22617
DIERKS, K. N89-22878
DIETRICH, R. A. N89-22960
DIETZEN, F. J. N89-22903
N89-22906
DIEWALD, W. N89-22902
DILL, J. A. N89-23062
DILLON-TOWNES, L. A. N89-22668
DIRUSSO, ELISEO N89-22605
DISTEFANO, J. R. N89-22693
DISTEFANO, S. N89-22988
DIVER, R. B. N89-23016
DODSON, GARY N89-23006
DONGUY, PAUL N89-22676
DOR, J. B. N89-22584
DORHOUT, B. N89-23263
DORRIS, S. E. N89-23342
DOUGHTY, D. A. N89-22760
DOYLE, J. N89-22760
DRAKE, A. E. N89-23202
DRAKE, JAMES FREDERICK N89-23056
DREWS, G. N89-22878
DREXLER, R. G. N89-22606
DRIESSEN, THEO N89-23266
DROUGGE, GEORG N89-22583
DU, YUN-TIAN N89-22892
DUCK, PETER W. N89-22574
DUDA, J. L. N89-22747
DUPUY, SERGE N89-23223
DUSEK, J. T. N89-23342
DUTTA, R. N89-23157
DYE, JOHN W. N89-23100

E

EAGAR, THOMAS W. N89-22746
EATON, J. K. N89-22825
ECK, R. N89-22674
EDWARDS, S. J. N89-23209
EHST, DAVID A. N89-22810
N89-23291
EISMAN, G. A. N89-22995
EKBLAD, ULF N89-22974
N89-22976
EL-MOSSALAMY, S. N89-22727
ELIASSON, PETER N89-22583
ELLISTON, A. E. N89-23204
ELROD, DAVID N89-22899
ENAYATULLAH, MOHAMMAD N89-22994
ENDOH, Y. N89-23333
ENDRES, DANIEL N89-23182
ENGELEN, JOS J. N89-22878
N89-23276
ENGELMORE, ROBERT S. N89-23206
ENGEMANN, D. N89-23347
ENTEL, P. N89-23315
ERB, TRUDY A. N89-23036
ERCK, R. A. N89-22739
ERDAHL, DAVID C. N89-22650
ERICKSON, GEORGE F. N89-22887
ERIKSSON, JAN N89-22849
ERLEBACHER, GORDON N89-22836
EROGLU, HASAN N89-22609
ESER, E. N89-23022
ESKOW, ELIZABETH N89-23191
ESPINOSA, J. M. N89-22812
ESTES, JOHN E. N89-22979
ESTES, ROBERT D. N89-22780
ETEMADI, NASSROLLAH N89-22820
EVANOFF, J. J. N89-23062
EVANS, E. N89-22873
EVANS, KENNETH, JR. N89-23291
EVERSTINE, GORDON C. N89-22951
EWING, PAUL D. N89-22786

F

FACULJAK, DEBRA A. N89-23072
FAIRBANK, WILLIAM M. N89-22709
FAN, N. Q. N89-23311
FAN, T. J. N89-23105
FARMER, T. E. N89-22661
FAYMONVILLE, R. N89-23347
FEA, M. N89-22978
FEIGENBAUM, EDWARD A. N89-23206
FENSKE, G. R. N89-22739
FENSTERMACHER, M. E. N89-23292
FERGUSON, MONA M. N89-22732
FERRISS, D. H. N89-22963
FEUERBACHER, BERNDT N89-22745
FIELD, S. P. N89-22658
FIELDER, WILLIAM L. N89-23000
FIGUEIRA, J. F. N89-22885
FILIPPONE, W. L. N89-23260
FINDENEGG, GERHARD HELMUT N89-22774
FINE, MORRIS E. N89-22723
FINLEY, DAVID STARR N89-23383
FIRESTONE, JAMES N89-23182
FISCHLER, MARTIN A. N89-23080
FISHER, ALLAN L. N89-23128
FLEISCHER, KURT N89-23097
FLEMING, DAVID P. N89-22605
FLOCKE, FRANK N89-23029
FLOOD, DENNIS J. N89-22651
FLOOD, P. N89-23204
FLORYAN, JERZY M. N89-22581
FLOWER, R. N89-22640
FLYNN, ANITA M. N89-23106
FOGARTY, T. N. N89-23400
FORCHIONE, J. N89-22993
FORNEY, L. J. N89-22589
FORT, EDWARD F. N89-23382
FOUCHER, B. N89-22766
FOUJANET, M. C. N89-22785
FOWLER, T. KENNETH N89-23294
FRANKLIN, R. E. N89-22711
N89-22848
FRANZEN, WOLFGANG O. N89-23111
FREED, ALAN D. N89-22684
FREEMAN, A. J. N89-22741
FRENZL, O. N89-23347
FRIEDBERG, R. A. N89-22594
FRIESEL, D. L. N89-23328
FRIGERI, CLAUDIO N89-22694
FRISCHAT, G. H. N89-22734
FRITTS, DAVID C. N89-23048
FROEHLY, C. N89-23288
FROLOW, P. N89-22734
FUA, PASCAL N89-23161
N89-23163
FUERSCHBACH, PHILLIP W. N89-22924
FUKUDA, K. N89-23333
FUNAKI, YUKIHIKO N89-23266

G

GABB, TIMOTHY P. N89-22684
GABBE, D. R. N89-23333
GAEMERS, K. J. F. N89-23278
GAHN, RANDALL F. N89-22992
GAI, W. N89-22798
GAJDECZKO, BOGUSLAW FELIX N89-22863
GALE, WAYNE N89-22649
GALLAGHER, A. N89-22760
GAMBLE, E. N89-23093
GANDHI, R. N89-23278
GARCIA, M. N89-22878
GARG, SANJAY N89-22610
GARNERO, PASCAL N89-22858
GAUGER, J. R. N89-22806
GAYDA, JOHN, JR. N89-22684
GAYLOR, DAVID E. N89-22632
GAZIT, S. L. N89-23109
GEDEON, STEVEN A. N89-22748
GEHRMANN, E. N89-22734
GEIDEL N89-22606
GEIGER, D. N89-23093
GEIST, G. A. N89-23197
GELBAND, PATRICE N89-23087
GENONI, THOMAS C. N89-22884
GEORGE, T. G. N89-23281
GILDING, B. H. N89-23246
GILLETT, W. N89-23093
GILLHAM, JOHN K. N89-22769
GINER, J. N89-22999
GIRAULT, J. P. N89-22929
GLASSER, F. P. N89-22714
GMELIG-MEYLING, R. H. J. N89-23245
N89-23247
N89-23252
GODDARD, NIGEL H. N89-23156
GOEBEL, F. N89-23236
N89-23251
GOHIL, P. N89-23290
GOMEZ, S. A. N89-23066
GOODWIN, GENE M. N89-22736
GOODWIN, W. L. N89-23284
GOREN, YEHUDA N89-22783
GORETTA, K. C. N89-23342
GRABER, HANS N89-22975
GRADY, JOSEPH E. N89-22948
GRAGG, WILLIAM N89-23255
GRAHN, SVEN N89-22974
GRANT, BRYDON J. N89-23071
GRANT, J. BRIAN N89-22789
GRAY, HOWARD LESTER N89-22716
GREENBAUM, S. G. N89-22761
GREENLEAF, JOHN E. N89-23061
GREMBAN, KEITH D. N89-23148
GRIFFITH, LEE V. N89-22880
GRISHIN, SERGEY DMITRIYEVICH N89-22626
N89-22627
GROEBNER, R. J. N89-23290
GROSCH, C. E. N89-22837
GROSS, ARI D. N89-23168
GROSS, SIDNEY N89-23008
GROSSI, MARIO D. N89-22780
GRUBER, U. N89-22672
GRUENLING, HERMANN W. N89-22669
GU, D.-W. N89-23214
GU, JIN-CHU N89-22892
GUDMUNDSON, SVEN ERIK N89-22601
N89-22613
GUIBE, C. N89-22766
GUMUCIO N89-22608
GUMUS, H. N89-23317
GUO, X. Q. N89-22741
GUPTA, Y. M. N89-22865
GURNETT, D. A. N89-23040
GUSTAVSSON, ANDERS I. N89-22618
GUYENNE, T.-D. N89-22978

H

HAAGMANS, ROGERS H. N. N89-23039
HAAS, JEFFREY E. N89-22617
HADDAD, W. N89-22881
HAHN, ERWIN L. N89-23311
HALE, KEITH N89-22899
HALPERT, G. N89-23011
HAMAMATSU, TERUHIDE N89-22841
N89-22842
HAMBRIC, STEPHEN A. N89-22952
HAMEL, OLIVIER N89-22815
HAMMOND, R. H. N89-23310
HAMPEL, VIKTOR E. N89-23374
HANCOCK, P. N89-22664
HANDLER, R. A. N89-22864
HANLEY, JAMES N. N89-22772
HANLON, J. A. N89-22885
HANNAH, MARSHA JO N89-23140
HANSON, A. J. N89-23102
HANSON, ALLEN R. N89-22597
N89-23081
N89-23088
N89-23159
N89-23167
HANSON, ANDREW J. N89-23122
N89-23161
HANSON, KENNETH M. N89-23193
HANSSEN, KARL N89-23289
HARALICK, ROBERT M. N89-23113
HARDTKE, P. G. N89-22640
HARRIS, JOHN G. N89-23084
N89-23121
HARRIS, P. M. N89-23253
HARTJES, FRED N89-23277
HARTMANN, KLAUS N89-22580
HARWOOD, DAVID N89-23141
HASCHBERGER, D. N89-23347
HASHIMOTO, TSUYOSHI N89-22771
HASSELMANN, KLAUS N89-22975
HASSELMANN, SUSANNE N89-22975
HATZITHEODOROU, MICHAEL N89-23176
HAWKINS, CHARLES F. N89-23327
HAYMAN, C. N89-22658
HAYNES, FREDERICK L. N89-23370
HAYTON, G. E. N89-23221
HAZARIKA, NEEP N89-22603
HE, JUAN-ZHI N89-22719
HE, M. N89-22760
HE, XIAOGUANG N89-23318
HEALD, S. M. N89-22694
HEALEY, GLENN N89-23114
N89-23151
N89-23172
N89-23177
HEANEY, MICHAEL B. N89-23311
HEBERT, MARTIAL N89-23124
HEDMAN, SVEN G. N89-22602
HEINEMANN, K. N89-23028
HELLER, A. J. N89-23131
HELM, M. N89-23231
HELMINCK, G. F. N89-23234
N89-23238
HENDRICKS, E. W. N89-22864
HENRIKSEN, GARY L. N89-22811
HENRIKSEN, KJELL N89-23044
HENRION, X. N89-22641
HENRY, ARTHUR L. N89-23282
HERROU, P. N89-22700
HICKMAN, J. M. N89-23397
HICKS, M. A. N89-22660
HIDAKA, Y. N89-23333
HIGHNAM, PETER T. N89-23128
HIGHTON, D. R. N89-22659
HIGMAN, TED K. N89-23349
HILL, RAYMOND R., JR. N89-23224
HILLS, D. A. N89-22961
HINKS, D. G. N89-23340
HINSHAW, GARY FREEMAN N89-23042
HOCKEY, THOMAS ARNOLD N89-23398
HOGAN, R. E. N89-23016
HOGREFE, R. L. N89-22814
HOGUE, JEFFREY R. N89-22612
HOLD, R. GLYNN N89-23271
HOLDRIDGE, DIANE B. N89-23208
HOLLAND, REDUS N89-23035
HOLMES, R. N89-22895
HOLMES, RICHARD R. N89-22670
HOLTSLAG, A. A. M. N89-23055
HOOVER, WILLIAM G. N89-23274
HOQUE, M. S. N89-22898
HORAK, HENRY N89-23035
HORDONNEAU, A. N89-22675
HORN, BERTHOLD K. P. N89-23149
HORNBECK, L. J. N89-22953
HORNUNG, HANS G. N89-22855
N89-22856
HORTON, FOREST W., JR. N89-23371
HORVATIC, B. N89-23315
HOSSAIN, M. A. N89-22840
HOTOP, HANS-JURGEN N89-23203
HOUSER, R. M. N89-23015
HSEIH, H. N89-22740
HSIAO, TEN-LU N89-22687
HSIEH, ALEX J. N89-22768
HSIEH, C. N89-23290
HSU, S. N89-22747
HU, YONGDAI N89-22615
HUA, YONG-LI N89-22692
HUANG, C-K. N89-23011
HUANG, MAICHUN N89-23318
HUANG, THOMAS N89-23096
HUBBARD, HARVEY H. N89-23270
N89-23272
HUDAK, STEPHEN JOHN, JR. N89-22966
HUDSON, DALE A. N89-22665
HUETHER, W. N89-22668
N89-22757
HUIJBERTS, H. J. C. N89-23239
N89-23243
N89-23244
HUMMEL, ROBERT N89-23103
HUMPHRIS, R. R. N89-22911
HUNT, J. T. N89-23286
HUNTER, SCOTT R. N89-23298
HURLEY, JAMES A. N89-22722
HUSSAINI, M. Y. N89-22836
HUTTENLOCHER, DANIEL P. N89-23174
HUYNH, HUNG T. N89-22573
HYATT, ART N89-22943

I

IANSITI, MARCO N89-23305
IBRAHIM, HUSSEIN A. H. N89-23083
N89-23129
IKEUCHI, KATSUSHI N89-23136
ILGENFRITZ, E. M. N89-23319
IMMINK, G. K. N89-23240
N89-23241
N89-23248
INGRAM, G. D. N89-23268
INOUE, ATSUYUKI N89-23049
ISAACS, HUGH S. N89-22730
ISHII, M. N89-22839
ISIKAWA, YUUICHI N89-22919
ISOYA, J. N89-23314
ITO, EIKI N89-23154
IVERSLAND, LEIF MAGNE N89-23373
IVIE, J. J. N89-22589
IWATSUBO, T. N89-22904
IWATSUBO, TETSUSHIRO N89-22841
N89-22842

J

JACKSON, T. L. N89-22837
JACOB, JONAH N89-22882
JANKOWSKI, A. F. N89-22698
JARROUSSE, B. N89-22641
JEHEE, J. N. T. N89-23200
JENNISON, C. N89-23256
JENSSEN, H. P. N89-23333
JESTEADT, WALT N89-22784
JEURNINK, G. A. M. N89-23264
JIE, ZHOU N89-23316
JOHNSON, DONALD W. N89-22592
JOHNSON, L. C. N89-23066
JOHNSON, P. B. N89-22868
JOHNSTON, J. P. N89-22833
JONES, R. G. N89-22885
JORGENSEN, J. D. N89-23340
JOYCE, GLENN N89-23301

K

KACIUBA-USCILKO, HANNA N89-23061
KACKLEY, N. N89-22998
KACZMAREK, H. N89-22705
KAFAI, A. N89-23221
KALB, M. N89-23051
KALLENBERG, W. C. M. N89-23264
KAMAEV, D. A. N89-23227
N89-23228
KAMGAR-PARSI, BEHROOZ N89-23138
KAMGAR-PARSI, BEHZAD N89-23138
KAMPAS, F. N89-23022
KANADE, TAKEO N89-23079
N89-23094
N89-23124
N89-23136
N89-23148
N89-23150
KANDRUP, H. E. N89-23388
KANG, M. N89-22885
KANKI, H. N89-22917
KAPUR, DEEPAK N89-23139
KASARDA, M. E. F. N89-22911
KASCAK, A. F. N89-22896
KASS, MICHAEL N89-23097
KASTEN, FRITZ N89-23052
N89-23053
KASTNER, M. A. N89-23333
KATAYAMA, K. N89-22917
KATZ, JOEL D. N89-22763
KAUSCHE, GERHARD N89-22619

KAWANO, YOSHIO N89-22705
KEENE, B. J. N89-22927
KEGG, PAMELA S. N89-22595
KEIRSEY, DAVID M. N89-23107
KEMPEMA, EDWARD W. N89-23059
KENDER, JOHN R. N89-23083
N89-23123
N89-23176
KERIBAR, RIFAT N89-23382
KERSTEN, P. H. M. N89-23250
KESKINEN, M. J. N89-23032
KESSLER, DONALD J. N89-22636
KEUNINGS, R. N89-22844
KHAN, A. RAHMAN N89-23370
KIHM, K. N89-22851
KIKUCHI, TOMOYA N89-22771
KILGORE, W. ALLEN N89-22616
KIM, J. JOHN N89-23171
KIM, JOHN N89-22660
KIM, KEVIN N89-22634
N89-22635
KIM, SUNG-SOO N89-22966
KINDEL, JOSEPH M. N89-23297
KING, DAVID L. N89-22749
N89-23013
KINOSHITA, KIM N89-23019
KITCHEN, LESLIE J. N89-23137
KITTEL, PETER N89-22850
KLANNER, R. N89-22678
KLAUS, E. E. N89-22747
KLEIN, JOHN W. N89-22984
KLEY, DIETER N89-23029
KLINKER, GUDRUN J. N89-23150
KLOCKE, ROBERT A. N89-23071
KLOCKE, ULRICH N89-23027
KLUGE, M. N89-23308
KNOROVSKY, GERALD A. N89-22924
KNOTHE, MANFRED N89-23027
KOBLAX, M. N89-22600
KOCHENDOERFER, R. N89-22657
KOETZ, U. N89-22678
KOHLMAIER, GUNDOLF HANS N89-23038
KOHN, WOLFGANG N89-23027
KOITZSCH, KERRY V. N89-23100
KONDERAK, J. N89-23353
KONG, J. A. N89-22971
KONIJN, JAN N89-23277
KONOVALOV, B. N89-22623
KOO, J. N89-22674
KOWELL, STEPHEN T. N89-23350
KOZOL, JOSEPH N89-22688
KRALL, JONATHAN N89-23301
KRASIKOV, V. A. N89-22624
KRAUSE, SIEGFRIED N89-22715
KRIEGMAN, DAVID J. N89-23112
KRISHNAN, KANNAN M. N89-23307
KROPFLI, R. A. N89-23048
KRUEGER, W. N89-22668
KRUPKE, WILLIAM F. N89-22888
KUBAN, D. P. N89-22922
KUCHYNKA, DANIEL J. N89-22990
KULAGA, J. E. N89-22814
KULAK, R. F. N89-22958
KUMAR, GANESH N. N89-22862
KUO, CHU K. N89-23348
KUPFERMAN, STUART L. N89-22808
KUPPERMAN, D. S. N89-22697

L

LABARGE, RANDY R. N89-23378
LABOMBARD, B. N89-23295
LACONTI, A. B. N89-22993
LAMBLE, G. M. N89-22694
LANAGAN, M. T. N89-23342
LAND, PATRICIA A. N89-23071
LANDIS, D. A. N89-23328
LARSON, N. N89-23093
LARTIGUE, S. N89-23344
N89-23345
LASKEY, KATHRYN B. N89-23188
LASLETT, L. J. N89-23231
LASSILA, DAVID H. N89-22731
LATTIMER, J. M. N89-23278
LAUFFER, JAMES P. N89-22957
LAUTER, JUDITH N89-22604
LAWRENCE, WENDY B. N89-23058
LAWTON, DARYL T. N89-23087
N89-23100
N89-23133
LE, T. H. N89-22853
LEBOCQ, PHILIPPE N89-23405
LECLERC, YVAN G. N89-23104
N89-23163
LECOMTE-MERTENS, CH. N89-22680
LEE, BYUNG-UK N89-23172
LEE, H. W. H. N89-23329
LEE, JAE-WON N89-22708
LEE, KUN-IK N89-22930
LEE, MOON J. N89-22826
LEFF, AVRAHAM N89-23123
LEHMER, R. D. N89-23295
LEHNER, SUSANNE N89-22975
LEIGHTON, R. I. N89-22864
LEIS, H. N89-22672
LELE, SANJIVA K. N89-22827
LEMAY, JAMES D. N89-22756
LENORMAND, R. N89-22641
LEONI, R. N89-23310
LEONIDA, A. N89-22998
LERCH, P. N89-23310
LESSNER, P. N89-22993
N89-22999
LETALICK, DIETMAR N89-23287
LETAW, JOHN R. N89-23063
N89-23401
LETHIECQ, MARC N89-22936
LETTMANN, THEODOR N89-23257
LEVITT, TOD S. N89-23087
N89-23100
LEWANDOWSIJ, HANS N89-22774
LEWICKI, D. G. N89-22925
LEYSER, T. B. N89-22799
LHALLABI, T. N89-23351
LI, YANNIAN N89-22937
LI, YAPING N89-22615
LICHTENEGGER, J. N89-22978
LILLY, DOUGLAS K. N89-22818
LIM, H. S. N89-23004
LIM, HONG SEH N89-23146
N89-23147
LIN, C. P. N89-23314
LIN, CHANGJIAN N89-22748
LIN, G. H. N89-22760
LIN, R. R. N89-22896
LIN, ROBERT P. N89-23399
LINDEN, JOHANNES N89-22846
LINDENMEYER, CARL W. N89-22809
LINDMAN, ERICK L., JR. N89-23297
LIONELLO, PIERO N89-22975
LIPA, JOHN A. N89-22709
LIPMAN, ROBERT R. N89-22942
LITTLE, J. N89-23093
LITVIN, FAYDOR L. N89-22920
LIU, A. S. N89-22713
LIU, H. N89-22761
LIU, JIYING N89-23391
LIU, MENG-XING N89-22719
LIU, YULIN N89-23390
N89-23391
LIVINGSTON, ROBERT C. N89-23034
LOEHR, JOHN JOSEPH N89-23198
LONGDON, N. N89-22978
LONSDALE, GUY N89-22848
LOWE, C. W. N89-23400
LOYSELLE, PATRICIA N89-23001
LUCAS, DIDIER N89-22699
LUCE, NORRIS R. N89-22945
LUEBECK, EGMAR N89-22877
LUESINK, R. N89-23215
LUTSKO, J. F. N89-23308
N89-23309
N89-23343
LUZI, A. N89-22893
LYON, R. J. P. N89-22970

M

MA, SHONGHE N89-22937
MACDONALD, DIGBY D. N89-23003
MACHA, J. MICHAEL N89-22576
MACKLIN, J. T. N89-22977
MACLENNAN, JEFFREY M. N89-22762
MADDEN, N. W. N89-23328
MAESTAS, FRANK A. N89-22923
MAGGIORE, CARL J. N89-23338
MAIA, M. D. N89-23354
MAJUMDAR, S. N89-22697
MALONE, D. F. N89-23328
MANKO, DAVID J. N89-22994
MANMATHA, R. N89-23157
MANNING, CAROL A. N89-22595
MANOUKIAN, M. N89-22999
MANSFIELD, C. R. N89-22885
MANZO, MICHELLE A. N89-22992
N89-23007
MAO, YUZHU N89-22867
MARGALIT, AVRAHAM N89-23134
MARILL, THOMAS N89-23106
MARRE, J. P. N89-22641
MARSHALL, D. N89-22686
MARSHALL, H. N89-22873
MARSHALL, SANDRA P. N89-23205
MARSTON, A. P. N89-23385
MARTIN, J. M. N89-22935
MARTIN, M. E. N89-22812
MARTIN, S. J. N89-22728
MARTIN, STEPHEN J. N89-23273
MARTINEZ, DAVID R. N89-23194
MASSOUD, J. P. N89-22742
MAST, TERRYL J. N89-23062
MATECHIK, STEPHEN M. N89-23186
MATHRE, JOHN M. N89-22590
MATSUMOTO, M. N89-23290
MATSUMOTO, T. N89-22904
MATTHIES, LARRY N89-23094
MAYA, LEON N89-22762
MAYR, ERNST W. N89-23257
MAZET, PIERRE-ALAIN N89-22854
MAZIASZ, PHILIP J. N89-22736
MAZUR, P. O. N89-23388
MCCARTNEY, L. N. N89-22691
MCCLAIN, CHARLES R. N89-23182
MCCONAGHY, C. N89-22874
MCCONNELL, CHRISTOPHER C. N89-23133
MCDERMOTT, KATHLEEN M. N89-22722
MCELROY, J. N89-22996
MCINTYRE, JAMES R. N89-23188
MCKECHNIE, TIMOTHY N. N89-22670
MCKEOWN, DAVID M., JR. N89-23101
MCNALLAN, MICHAEL N89-22738
MCPHEETERS, C. C. N89-22989
MEDIONI, GERARD N89-23105
N89-23109
N89-23110
N89-23173
MEETHAM, G. W. N89-22662
MEHRHOLZ, DIETER N89-22793
MEISCHNER, PETER N89-22800
MEISSNER, HEIDI J. N89-22808
MEITNER, PETER L. N89-22862
MELANDER, MOGENS V. N89-22823
MENZ, GUNTER N89-22972
MERCIER, F. N89-22644
MERSON, J. L. N89-22790
MESEGUER, J. N89-22642
MESSERLE, LOUIS N89-22712
MESTRE, R. N89-22667
MEYER, K. N89-23347
MIDDLETON, DAVID N89-23073
MIGNERY, L. A. N89-22938
MIGNOSI, A. N89-22879
MILANOVICH, F. P. N89-23286
MILLEN, PHYLLIS K. N89-23068
MILLER, A. KEITH N89-22957
MILLER, J. R. N89-23336
MILLER, LEE N89-23006
MINCK, ROBERT N89-23009
MINECK, RAYMOND E. N89-22614
MING, JOHN C. N89-23119
MINKER, JACK N89-23207
MITANI, HIROSHI N89-23049
MITCHELL, A. W. N89-23340
MITCHELL, K. N89-23021
MITRJUSHKIN, V. K. N89-23319
MIYAKE, KUNIHIKO N89-23049
MIZUTANI, HACHIRO N89-22919
MOERDLER, MARK L. N89-23145
MOHAMMAD, NOOR N89-23267
MOHAN, RAKESH N89-23117
MONDSCHEIN, LAWRENCE GEOFFREY N89-23375
MONTAGUE, J. N89-22896
MOODY, E. S. N89-22611
MOORE, JOSEPH B. N89-22656
MORALES, ROGELIO, JR. N89-23065
MORAN, PATRICK J. N89-22724
MOREL, THOMAS N89-23382
MORII, S. N89-22917
MORTSIEFER, HANS-JUERGEN N89-23359
MOTAKEF, S. N89-23313
MOUGINOT, R. N89-22765
MOURI, Y. N89-22917
MOYER, E. THOMAS, JR. N89-22950
MUELLER-PREUSSKER, M. N89-23319
MUELLER, JAN N89-23368
MUELLER, W. N89-22934
MUNDY, JOSEPH L. N89-23085
N89-23102
N89-23131
N89-23139
MUNRO, R. G. N89-22747
MURAKAMI, T. N89-23333
MURPHY, O. J. N89-22991
MUSZYNSKA, A. N89-22915
MUTANGADURA, SIMBA A. N89-23259
MYERS, THOMAS T. N89-22612

MYLES, K. M. N89-22989
MYRA, J. R. N89-23296

N

NAIDU, S. K. N89-22747
NALETTE, T. N89-22996
NARAYAN, KRISHNASWAMI YEGNA N89-22580
NASR, HATEM N89-23118
NASSAR, A. M. N89-22727
NASTASI, MICHAEL N89-23338
NAWIJN, W. M. N89-23263
NEFF, DONNA L. N89-22784
NEFF, HERBERT P., JR. N89-22787
NELSON, G. C. N89-22764
NELSON, PAUL A. N89-22813
N89-23010
NELSON, RANDAL C. N89-23120
NELSON, W. E. N89-22953
NERON, J. N89-22648
NETANYAHU, NATHAN N89-23171
NEVATIA, RAMAKANT N89-23076
N89-23105
N89-23117
NEWITT, D. N89-23311
NEWKIRK, HERBERT W. N89-22888
NGUYEN, HUNG LEE N89-22606
NGUYEN, KHANH N89-23301
NGUYEN, TINH N89-22748
NGUYEN, VAN-DUC N89-23180
NIEDZWIECKI, RICHARD W. N89-22606
NIELSEN, SVEND MOLLER N89-22801
NIJMEIJER, H. N89-23215
N89-23217
NIKOLAJSEN, JORGEN L. N89-22896
N89-22913
NILSSON, SOREN N89-22707
NISHIHAMA, JIRO N89-22907
NJAU, ERNEST C. N89-22785
N89-22871
N89-23050
NONAMI, KENZOU N89-22605
NORDMANN, R. N89-22900
N89-22902
N89-22903
N89-22906
NORDSTROM, JAN N89-23254
NORRIS, J. R. N89-23314
NOTTROT, R. N89-23218
NOVOZHILOV, YURI V. N89-23356
NYCE, THOMAS A. N89-23306

O

ODA, M. N89-23333
ODA, T. N89-22917
ODORICO, J. N89-22702
N89-22703
N89-22704
OHASHI, HIDEO N89-22907
OHASHI, MAKOTO N89-22970
OKAMOTO, Y. N89-22761
OLANDER, NILS N89-23212
N89-23213
OLIDAPUPO, A. N89-23400
OLIN, K. E. N89-23084
OLMSTEAD, MICHAEL R. N89-23047
OLSEN, ANTHONY R. N89-23036
ONDREJCIN, R. S. N89-22726
ONN, SHING-CHUNG N89-22621
ORHAUG, TROLIEV N89-22974
OSSAKOW, S. L. N89-23032
OTTO, HORST N89-22619
OZAWA, U. N89-22917

P

PACE, S. E. N89-22905
PAK, Y. S. N89-22761
PALAZZOLO, A. B. N89-22896
PAMIDI, P. R. N89-22947
N89-22949
PAN, WEI N89-23318
PANDA, DURGA N89-23086
PANG, K. P. N89-22789
PARKER, S. R. N89-23210
PARKER, STEVEN L. N89-22921
PARSEGHIAN, ZAREH N89-22612
PATERA, A. T. N89-23313
PATIL, PANDIT G. N89-22811
PATRA, M. K. N89-23229
PAUL, GARY N89-23005
PAVLIN, IGOR N89-23108
N89-23155
PAWSON, STEVEN N89-23043
PAYNE, ARTHUR C., JR. N89-23261
PAYNE, STEPHEN A. N89-22886
N89-22888
PAYTON, DAVID W. N89-23107
PEHL, R. H. N89-23328
PEI, SHIYOU N89-23340
PELLAN, G. N89-22702
N89-22704
PENG, SHOU-LING N89-23110
PERRIER, R. N89-22702
PESARAN, AHMAD A. N89-22681
PETERSEN, K. L. N89-23030
PETERSON, LEE D. N89-22957
N89-23230
PETIT, R. N89-22636
PETRASEK, DONALD W. N89-22673
PETROVIC, JOHN J. N89-22763
PFLUGER, P. R. N89-23245
PHAM, M. N89-22996
PHILLPOT, S. R. N89-23309
N89-23343
PIELOU, J. M. N89-22977
PIERSON, WILLARD J., JR. N89-22779
PINES, A. N89-23311
PISHCHIK, V. B. N89-22625
PLESNIAK, MICHAEL W. N89-22833
PODLOUCKY, R. N89-22741
POEPPEL, R. B. N89-22696
N89-23342
POGGIO, T. N89-23075
N89-23093
POINSOT, THIERRY J. N89-22628
POLDERMAN, J. W. N89-23216
POLLAK, FRED H. N89-22717
POMPLUN, E. N89-23028
PONCE, JEAN N89-23114
N89-23169
N89-23170
N89-23172
PORKOLAB, M. N89-23292
POST, G. F. N89-23234
N89-23238
POST, H. N. N89-23012
POSTLETHWAITE, I. N89-23214
POTTER, ANDREW E., JR. N89-22682
POULAKAKI, E. N89-23363
POWLESLAND, I. N89-22611
PRAKASH, JAI N89-22997
PRANGE, MICHAEL N89-23045
PRASANNA-KUMAR, V. K. N89-23126
PRASANNA, A. R. N89-23389
PRASANNAPPA, RAJU N89-23141
PRASSINOS, PETER N89-22797
PRICE, KEITH N89-23108
PRIEDHORSKY, W. C. N89-22873
PRIESTER, L. N89-23344
N89-23345
PUGH, A. C. N89-23221

Q

QIAN, X. R. N89-23335
QIU, CHUANREN N89-22571
QUAM, LYNN H. N89-23102
N89-23122
QUENTMEYER, RICHARD J. N89-22671
QUIROGA, L. N89-23321

R

RAGAB, K. A. N89-22727
RAMOS, J. I. N89-22851
RANAUDO, RICHARD J. N89-22569
RASHID, R. I. M. A. N89-23352
RATNAKUMAR, B. V. N89-22988
RATNER, ELLIOT Z. N89-22811
RAY, SCOTT L. N89-22788
REED, DENNIS A. N89-22787
REFAI, T. F. N89-23323
REGAN, FRANK C., JR. N89-23033
REICHEL, L. N89-23255
REID, MARGARET A. N89-23002
REIMNITZ, ERK N89-23059
REINMANN, JOHN J. N89-22569
REISER, KURT N89-23084
N89-23121
REISIS, DIONISIOS N89-23126
RENARD, J. N89-22705
RENE, D. N89-22641
RESHETNIKOV, G. P. N89-23325
RESTALL, J. E. N89-22658
RESTALL, J. F. N89-22664
REYNOLDS, ROBERT C. N89-22638
RHATIGAN, JENNIFER L. N89-22653
RHEA, PAUL A. N89-23304
RHODES, C. K. N89-22881
RICCO, A. J. N89-22728
RICCO, ANTONIO J. N89-23273
RICHARDS, D. R. N89-23340
RICHARDSON, D. I. N89-23367
RIEDEL, H. N89-22964
RIEDEL, WOLFGANG JULIUS N89-23027
RILEY, BRIAN N89-23023
N89-23024
RISEMAN, EDWARD M. N89-22597
N89-23081
N89-23088
N89-23157
RISSER, V. VERNON N89-23012
RIVAS, D. N89-22642
ROACH, R. L. N89-22589
ROBERTSON, I. M. N89-22740
ROCKOFF, TODD E. N89-23128
RODRIGUEZ, ROBERT N89-23185
RODRIQUEZ, F. N89-23321
ROE, J. N. N89-23286
ROELKE, RICHARD J. N89-22862
ROETH, ERNEST-PETER N89-23026
ROGERS, JAMES L. N89-23181
ROGINSKY, JACOB N89-23401
ROLLETT, ANTHONY D. N89-23338
ROMAN, NILS N89-23201
ROMAN, WILLIAM G. N89-23188
ROMMEREIM, R. L. N89-23062
RON, AMOS N89-23225
N89-23226
ROSE, FREDERIC E. N89-23205
ROSEN, BENGT N89-23213
ROSEN, LOUIS N89-23380
ROSENBERG, J. N89-22844
ROSENBERGER, FRANZ N89-23306
ROSENBLATT, J. KENNETH N89-23107
ROSENFELD, AZRIEL N89-23078
N89-23088
N89-23091
N89-23134
N89-23171
ROSENTHAL, P. N89-23310
ROSOCHA, L. A. N89-22885
ROSSMANN N89-22757
ROTHMAN, S. J. N89-23341
ROUTBORT, J. L. N89-23341
ROVERE, M. N89-23324
ROZEWICZ, J. N89-22711
N89-22848
RUBIN, TOD N89-22970
RULON, PHILIP J. N89-22730
RUSHBY, JOHN N89-23183
RYAN, ARVE N89-22777
RYKS, HERMAN N89-22973

S

SAFLEKOS, N. A. N89-23040
SAGDEYEV, R. Z. N89-22624
SAIDI, E. H. N89-23351
SAIKAWA, MICHINORI N89-22841
N89-22842
SAINT-MARC, PHILIPPE N89-23173
SAKURAI, AKIRA N89-22907
SALERNO, LOUIS J. N89-22850
SALGUERO, DAVID E. N89-23199
SALTZMAN, ALAN R. N89-23071
SALTZMAN, MATTHEW J. N89-23190
SALVANO, S. N89-22663
SAMMELLS, ANTHONY F. N89-22990
SANDBERG, OLOF N89-22778
SANSCHAGRIN, D. N89-22679
SANTOSH, U. N89-22687
SARANGAPANI, S. N89-22993
N89-22999
SATO, S. N89-23314
SATO, TAKEHIKO N89-22771
SATYANARAYANA, P. N89-23032
SAVAGE, M. N89-22925
SCATTERGOOD, R. O. N89-22695
SCHAPERY, R. A. N89-22938
SCHARER, J. E. N89-22791
SCHARRER, JOSEPH K. N89-22901
SCHENZ, RICHARD F. N89-22880
SCHILD, HERBERT N89-22599
SCHILL N89-22608
SCHLAGER, H. N89-23037
SCHMIDT, H. N89-23051
SCHMIDT, HELMUT N89-23041
SCHMIDTKE, GERHARD N89-23027
SCHMIED, J. N89-22914
SCHNABEL, ROBERT B. N89-23191

SCHNEIDER, K. N89-22669
SCHOENFELD, W. N89-22960
SCHOO, D. N89-22676
SCHOOF, LARRY A. N89-22923
SCHROEDER, ERWIN N89-22950
SCHROTH, ARNO N89-22800
SCHULZ, D. N89-23315
SCHWARTZ, GEOFFREY E. N89-22835
SCHWARTZ, J. A. N89-22594
SEAH, M. P. N89-23268
SEARLE, RICHARD H. N89-23365
SEIGMUND, O. H. W. N89-22873
SELLMANN, PAUL V. N89-23059
SENATORE, G. N89-23324
SERAUDIE, A. N89-22879
SHAFER, STEVEN A. N89-23150
SHAMIS, V. A. N89-22624
SHAN, XIAOYIN N89-23001
SHAO, JUN N89-23258
SHAW, BARBARA A. N89-22724
SHAW, ROBERT J. N89-22569
SHEEHAN, R. E. N89-23040
SHEERER, T. J. N89-22953
SHEHATA, L. N. N89-23323
SHEINBERG, HASKELL N89-22763
SHEN, D. H. N89-23011
SHEN, QIN-GEN N89-22892
SHENG, B. C. N89-22904
SHEPHERD, KEVIN P. N89-23270
N89-23272
SHETTY, D. K. N89-22690
SHI, GONGXUN N89-22937
SHIH, TSAN-HSING N89-22819
SHIM, IN-OK N89-22720
SHIMADA, M. N89-23290
SHORT, DAVID ALLEN N89-23057
SHVAYTSER, HAIM N89-23179
SIDERIS, M. T. N89-22857
SIEBER, A. J. N89-22978
SIEBERT, RUEDIGER N89-22619
SIERRA, FRANCISCO N89-22797
SIFFRE, J. N89-22767
SILBERBERG, TERESA M. N89-23116
SILVERMAN, B. W. N89-23256
SIMADER, F. N89-22674
SIMEON, THIERRY N89-23222
SIMON, ELVIS D. N89-22650
SIN, S. K. N89-22931
SINGER, JOSEPH N89-23000
SINGH, AJIT N89-23158
SINGH, J. P. N89-22695
N89-22696
N89-22697
N89-23342
SINGH, JATINDER N89-22586
SINGHEISER, L. N89-22669
SIROTKIN, KARL N89-23198
SISKIND, DAVID ERIC N89-23031
SITARAMAN, RAMESHKUMAR N89-23134
SKOTHEIM, T. N89-22761
SKOURLAS, C. N89-23363
SLUIS, W. M. N89-23250
SLUITER, M. N89-22741
SMALINSKAS, K. N89-22740
SMIRNOV, V. I. N89-23325
SMITH, B. W. N89-22873
N89-23392
SMITH, G. B. N89-23102
SMITH, GRAHAME B. N89-23132
SMITH, LESLIE M. N89-22821
SMITH, S. N89-22695
SNIDER, C. N89-22604
SNYDER, B. D. N89-22955
SNYDER, M. A. N89-23153
N89-23157
SOARES, SANDRA N89-22751
SODEN, JERRY M. N89-23327
SOMMARGREN, GARY E. N89-22880
SONG, DEHUA N89-22867
SONI, S. R. N89-22687
SOOCHAK, N. N89-23275
SORENSEN, NICOLAJ N89-22801
SORENSON, N. R. N89-22728
SOULE, J. N89-23372
SOULEZELLE, B. N89-22703
SPALLUCCI, E. N89-23355
SPINDLER, GERHARD N89-22869
SPINWEBER, C. L. N89-23066
SPIVAK, ALAN L. N89-22850
SQUIRES, KYLE D. N89-22825
SRINIVASAN, SUPRAMANIAM N89-22991
N89-22994
STANAWAY, SHARON KAY N89-22572
N89-22824
STANISCI, M. N89-22663
STAPELMANN N89-22775
STAPLETON, GEOFFREY B. N89-23280
STAR, JEFFREY L. N89-22979
STARKE, EDGAR A., JR. N89-22725
STASIEWICZ, K. N89-23299
STECKEL, BARBARA N89-22846
STENSTROM, J. R. N89-23166
STEPHANOPOULOS, G. N89-23313
STEPHENS, JOSEPH R. N89-22673
STEWART, ERIC C. N89-22566
STICKLER, R. N89-22674
STINE, W. B. N89-23016
STORCH, NANCY N89-23195
STRAT, THOMAS M. N89-23102
N89-23132
STREBY, GARY D. N89-22718
STRICKLAND, JAMES H. N89-22576
N89-22845
STRUM, M. J. N89-23336
STUEBEN, KLAUS N89-22846
STUPIN, DAVID M. N89-22872
SUBBARAO, S. N89-23011
SUNANAWEERA, THILAKA S. N89-23112
N89-23172
SUMMERS, L. T. N89-23336
SUN, XIANCHAI N89-22571
SUNG, TAE KYUNG N89-23379
SUSON, DANIEL JEFFREY N89-23393
SUTHERLAND, DEXTER N89-23035
SUZUKI, RYO N89-22771
SVEDING, ULF N89-22974
SWAIN, MICHAEL J. N89-23127
N89-23135
SWEENEY, DOUGLAS J. N89-23211
SWEERS, GUIDO N89-23232
SWETTE, L. N89-22998
SWINDEMAN, ROBERT W. N89-22736
SWISHER, J. H. N89-22735
SZEKELY, J. N89-23313
SZELISKI, RICHARD N89-23094
SZREDERS, BERNARD E. N89-23023

T

TAHA, A. S. N89-22727
TAI, H. N89-22692
TAKEDA, H. N89-22796
TALLAN, NORMAN M. N89-22655
TANDON, G. P. N89-22687
TANG, PING TAK PETER N89-23187
TARASOV, A. N89-22628
TERPSTRA, T. J. N89-23262
TERZOPOULOS, DEMETRI N89-23097
THAHEEM, A. B. N89-23267
THIDE, B. N89-22799
THIELEN, HERBERT N89-22792
THOMAN, STEVEN N89-22688
THOMAS, D. J. N89-23275
THOMAS, GARETH N89-22870
THOMAS, M. G. N89-23012
THOMAS, RALPH H. N89-23280
THOMAS, S. J. N89-22885
THOMPSON, D. W. N89-23131
THOMPSON, EARL R. N89-22666
THOMPSON, GARY C. N89-22639
THOMPSON, KEVIN W. N89-22829
THORPE, A. N. N89-23302
THORPE, CHARLES E. N89-23148
TINZL, J. N89-22674
TIV, MEHRAN N89-22956
TJEMKES, S. A. N89-23054
TOICHI, TSUTOMU N89-22771
TOKSOZ, M. N. N89-23045
TORNGREN, LARS N89-22601
N89-22613
TORTORELLI, P. F. N89-22693
TOSI, M. P. N89-23324
TOWNSEND, DENNIS P. N89-22919
TRAAS, C. R. N89-23249
TRACKSDORF N89-22608
TRAPP, REINHARD N89-23053
TREMOUILLES, G. N89-23346
TRIPATHY, K. C. N89-23229
TROST, P. N89-23290
TRYK, DONALD N89-22997
TSAI, KAN J. N89-22990
TSAI, M. C. N89-23214
TSUJIMOTO, YOSHINOBU N89-22908
TUMMILO, A. F. N89-22814
TUNCAY, CAGLAR N89-23317
N89-23320
TURNER, MICHAEL S. N89-23387
TZOVLAS, GEORGE N. N89-23364

U

ULIBARRI, M. N89-22873
ULLMAN, SHIMON N89-23174
UMEMURA, S. N89-22917

V

V.GELLHORN, E. N89-22672
VALLANCE, C. S. N89-22912
VALLERGA, J. N89-22873
VALLINI, ANDREA N89-22894
VANCE, JOHN M. N89-22897
VANDEGRAAF, R. C. N89-23070
VANDENBRAEMBUSSCHE, R. A. N89-22857
VANDERMEER, JAKOB STEFANUS N89-22776
VANDERSCHAFT, A. J. N89-23239
VANDERVEGT, JAAP N89-22830
VANDERWAGEN, L. L. M. N89-23217
VANDERWEGEN, L. L. M. N89-23219
VANDOMMELEN, LEON L. N89-22861
VANHARTINGSVELDT, EDWIN ADRIAAN ANDRE
N89-22759
VANHOLTEN, J. W. N89-23357
N89-23358
VANMARLE, E. A. N89-23218
VANSELOW, JANICE J. N89-22768
VANWANDERHAM, M. C. N89-22661
VASSILEVICH, D. V. N89-23356
VASTANO, JOHN A. N89-22822
VAZQUEZ, ISAURA N89-22722
VEERARAGHAVAN, SHOBA N89-23394
VELDMAN, H. J. N89-23235
N89-23237
VENABLE, D. D. N89-23400
VENKAYYA, V. B. N89-22955
VERZWYVELT, S. A. N89-23004
VIECELLI, JAMES A. N89-23285
VILLALBA, M. N89-23093
VISCO, S. J. N89-22987
VISENTINE, JAMES T. N89-22682
VISTNES, RICHARD N89-23162
N89-23178
VOLZ, ANDREAS N89-23029
VONBRADKE, MICHAEL N89-22715
VONGLAHN, U. H. N89-22577
VROBEL, P. A. N89-23102

W

WAHIDUZZAMAN, SYED N89-23382
WALD, LAWRENCE L. N89-23311
WALL, M. A. N89-22698
WALLACE, RICHARD S. N89-23125
WALLIN, LARS B. N89-22974
WALROND, J. T. N89-22781
WALTE, F. N89-22934
WALTERS, ROBERT W. N89-22838
WANG, DESHENG N89-22937
WANG, DIEQIAN N89-22602
WANG, WEN I. N89-23312
WANG, XI-XUAN N89-22892
WARDE, CHARLES J. N89-22811
WATMUFF, JONATHAN H. N89-22834
WATT, R. G. N89-22885
WATZIN, JAMES G. N89-23068
WEBB, JON A. N89-23125
WEBSTER, C. E. N89-22814
WEEMS, CHARLES C. N89-23088
N89-23089
WEERTMAN, JULIA R. N89-22723
WEIGEL, RICHARD J. N89-23062
WEINERT, GEORGE F. N89-23211
WEINSHALL, DAPHNA N89-23093
N89-23144
WEISER, P. N89-22900
WEISS, ISAAC N89-23175
WERNER, G. K. N89-23284
WERNEYER, R. N89-22934
WERT, JOHN A. N89-22725
WESTDIJK, HANS N89-23242
WESTERBERG, R. BRUCE N89-23062
WETCH, J. R. N89-22980
N89-22981
WHEELER, JAMES R. N89-23005
WHIPPLE, J. C. N89-22868
WHITE, GIL N89-22944
WHITESON, ADAM N89-22869
WILDE, PETER N89-22859
WILDNER N89-22608
WILLIAMS, D. M. N89-22922
WILLIAMS, HEATHER N89-23064
WILLIAMS, JIM P. N89-22909

WILLIAMS, LANCE R. N89-23159
N89-23167
WILLSHIRE, KELLI F. N89-23068
WILLSHIRE, WILLIAM L., JR. N89-23270
WILSON, CHARLES HAILE N89-23326
WILSON, S. A. N89-22726
WITKIN, ANDREW N89-23097
WITT, A. F. N89-23313
WOLF, D. N89-23308
N89-23309
N89-23343
WOLF, HELMUT N89-23027
WOLFF, LAWRENCE BRILL N89-23142
WOLFSON, HAIM N89-23103
WOMBLE, DAVID E. N89-23196
WOODGATE, K. G. N89-23220
WOODING, M. G. N89-22978
WRIGHT, LAWRENCE A. N89-22884
WU, I-CHEN N89-23125
WU, JIAN N89-23316
WU, JIUNN-CHI N89-22567
WUTTIG, MATTHIAS N89-22733

X

XIAO, JICHUN N89-22867
XING, J. S. N89-23328

Y

YAN, MING N89-22571
YAN, ZHEN N89-22571
YANG, T. N89-22905
YATES, MARK GUY N89-23395
YAZU, S. N89-23314
YEAGER, ERNEST N89-22997
YI, THOMAS N89-22983
YINGZHI, LI N89-22961
YIP, S. N89-23309
N89-23343
YODER, R. C. N89-23284
YOKOYAMA, SHIGERU N89-23049
YOSHIDA, YOSHIKI N89-22908
YOUNG, C. WAYNE N89-22923
YU, DAVID U. L. N89-22783

Z

ZACHARY, WAYNE N89-23069
ZADOROZHNY, A. M. N89-23319
ZAJIC, V. N89-23400
ZAJTSEV, L. N. N89-23325
ZANETTA, GIAN ANTONIO N89-22894
ZEIDAN, FOUAD Y. N89-22897
ZELCK, G. N89-22647
ZHANG, DAREN N89-23316
ZHANG, DAVID N89-22635
ZHANG, JIAO N89-22920
ZHANG, ZHUFENG N89-22807
ZHENG, QINGQI N89-23318
ZHENG, Y. N89-23340
ZHOU, WENBO N89-22571
ZHU, LAN-SHENG N89-22892
ZIAKOULI, EVDOKIA N89-23254
ZIJLSTRA, B. H. A. N89-23366
ZIMAN, YA. L. N89-22624
ZLATIC, V. N89-23315
ZUBRITZKY, MONICA C. N89-23069
ZUMWALT, G. W. N89-22594

Typical Corporate Source Index Listing

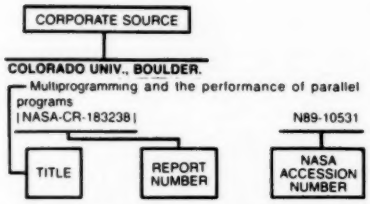

Listings in this index are arranged alphabetically by corporate source. The title of the document provides the user with a brief description of the subject matter. The report number helps to indicate the type of document cited (e.g., NASA report, translation, NASA contractor report). The NASA accession number denotes the number by which the citation is identified. The titles are arranged under each corporate source in ascending accession number order.

A

ADTECH SYSTEMS RESEARCH, INC., DAYTON, OH.
Three-dimensional response of composites
[AD-A204623] N89-22687

ADVANCED DECISION SYSTEMS, MOUNTAIN VIEW, CA.
Knowledge based vision for terrestrial robots N89-23087
Qualitative navigation 2 N89-23100
IU software environments N89-23133

ADVISORY GROUP FOR AEROSPACE RESEARCH AND DEVELOPMENT, NEUILLY-SUR-SEINE (FRANCE).
Application of Advanced Material for Turbomachinery and Rocket Propulsion
[AGARD-CP-449] N89-22654
Calendar of selected aeronautical and space meetings
[AGARD-CAL-88/2] N89-23361
The Organisation and Functions of Documentation and Information Centres in Defence and Aerospace Environments
[AGARD-CP-445] N89-23362
AGARD highlights 88/2 N89-23403

AEROJET TECHSYSTEMS CO., SACRAMENTO, CA.
Incorporating general race and housing flexibility and deadband in rolling element bearing analysis N89-22912
Enhanced rotor modeling tailored for rub dynamic stability analysis and simulation N89-22916

AERONAUTICAL RESEARCH INST. OF SWEDEN, STOCKHOLM.
Compressible Euler solution around a wing canard sting configuration
[FFA-TN-1988-62] N89-22578
Wind tunnel tests of 16 percent thick airfoil section with spoilers at different chordwise positions
[FFA-TN-1987-39] N89-22582
The influence of the leading edge geometry on the wave drag for a 65 degree delta wing at low supersonic speed and small angles of attack
[FFA-141] N89-22583
Transonic and supersonic wind tunnel tests on control effectiveness on schematic missile configurations with canard controls
[FFA-TN-1988-11] N89-22601
Prediction of loads on wing/body/external store/fins pylon-configurations at transonic speeds
[FFA-TN-1988-44] N89-22602
Transonic and supersonic wind tunnel tests on control effectiveness on schematic missile configuration with canard control
[FFA-TN-1988-11-SUPPL] N89-22613
Fatigue evaluation of WTS-3 wind turbine blade and retention
[FFA-TN-1987-81] N89-22618
A survey of poly-ether-ether-ketone and its advanced composites
[FFA-TN-1988-37] N89-22707
Preliminary blade design using integrated computer codes
[FFA-TN-1988-67] N89-22777
Blade root design: A state of art survey
[FFAP-201] N89-22778
A higher-order scheme for the Burgers equation
[FFA-TN-1988-43] N89-22859
On the semi-elliptical surface crack problem: Detailed numerical solutions for complete elastic stress fields
[FFA-TN-1988-74] N89-22965
The influence of open boundary conditions and difference operators on the time-integration of the Burger's equation
[FFA-TN-1988-57] N89-23254

AERONAUTICAL RESEARCH LABS., MELBOURNE (AUSTRALIA).
Single channel test controllers
[AD-A204088] N89-22611
Environmental program on durability of graphite/epoxy honeycomb specimens with representative damage and repairs
[AR-005-504] N89-22685

AEROSPATIALE, LES MUREAUX (FRANCE).
ATV: Ariane 5 transfer vehicle study
[STF/E-39-005/CB] N89-22646

AEROSPATIALE, PARIS (FRANCE).
Contributions of expert systems to logistics
[REPT-882-320-101] N89-23223

AEROSPATIALE, SAINT MEDARD-EN-JALLES (FRANCE).
High-performance refractory composite materials N89-22675

AEROSPATIALE, SURESNES (FRANCE).
Tests of new materials with second generation carbon fibers, test report
[REPT-47-188/F] N89-22702
CSPC test 319.30: Study on impact tolerance of preimpregnated carbon-epoxy systems
[REPT-47-323/F] N89-22703
Improving hole boring yield in carbon epoxy composites with tensile loading
[REPT-47-324/F] N89-22704

AIR FORCE FLIGHT DYNAMICS LAB., WRIGHT-PATTERSON AFB, OH.
Modal strain energies in COSMIC NASTRAN N89-22955

AIR FORCE INST. OF TECH., WRIGHT-PATTERSON AFB, OH.
Optimal low thrust trajectories for planetary capture
[AD-A202604] N89-22632
Spacecraft charge as a source of electrical power for spacecraft
[AD-A202621] N89-22649
Damage initiation in two-dimensional, woven, carbon-carbon composites
[AD-A202617] N89-22683
Internal debonding of solid rocket fuel: An experimental investigation
[AD-A205903] N89-22772
Position, scale, and rotation invariant optical pattern recognition for target extraction and identification
[AD-A202600] N89-22781
Verification and limitations of the monostatic-bistatic radar cross section derived by Kell
[AD-A202601] N89-22782
Configuration comparison analysis for the AFIT/AAMRL anthropomorphic robotic manipulator
[AD-A202618] N89-22921
A new perspective in the etiology, treatment, prevention and prediction of space motion sickness
[AD-A205660] N89-23065
A real-time simulator for man-in-the-loop testing of aircraft control systems (SIMTACS-RT)
[AD-A202599] N89-23067
Implementation of the NETOS (Network Operating System) operated system in Ada with modifications to allow variable length messages
[AD-A202602] N89-23185
The design and implementation of a graphical VHDL (VHSIC Hardware Description Language) user interface
[AD-A202619] N89-23186
Nonlinear optimization involving polynomial matrices and their generalized inverses
[AD-A202620] N89-23224
Time resolved photoluminescence of ytterbium in indium phosphide
[AD-A202596] N89-23303
Effects of different fabrication techniques on the Yttrium-Barium-Copper oxide high temperature superconductor
[AD-A202598] N89-23304

AIR FORCE MATERIALS LAB., WRIGHT-PATTERSON AFB, OH.
Technical evaluation report N89-22655

AIR FORCE SYSTEMS COMMAND, WRIGHT-PATTERSON AFB, OH.
Acta Aeronautica et Astronautica Sinica (selected articles)
[AD-A205128] N89-22570
Visting China's aerodynamics research and development center
[AD-A203980] N89-22615

AIR WAR COLL., MAXWELL AFB, AL.
Space control: A national imperative
[AD-A202612] N89-22631

ALABAMA UNIV., HUNTSVILLE.
Consortium for materials development in space
[NASA-CR-181405] N89-22773
Novel protein crystal growth technology: Proof of concept
[NASA-CR-184959] N89-23306

ALABAMA UNIV., UNIVERSITY.
A study of high strain rate generation of adiabatic shear bands in a titanium alloy N89-22967

ALASKA UNIV., FAIRBANKS.
Gravity wave and turbulence studies using a high-resolution ST radar
[AD-A205592] N89-23046

ALCATEL ESPACE, TOULOUSE (FRANCE).
Study of a wideband telecommunications satellite for Europe
[ATES/DMA/TRM/162-86] N89-22641
Study of a DRS experimental payload for single and multiple access at S band: Executive summary
[PSD88/00017] N89-22648

APPLIED RESEARCH ASSOCIATES, INC., ALBUQUERQUE, NM.
Numerical method to predict projectile penetration
[DE89-007140] N89-22923

ARGONNE NATIONAL LAB., IL.
Observations on the toughening of Al2O3-SiC composites
[DE89-009843] N89-22695
Fracture toughness of MgCr2O4-based refractory composites
[DE89-009847] N89-22696
Internal stresses in ceramic composite constituents determined by neutron diffraction technique
[DE89-009883] N89-22697
Precipitation of Ar, Kr and Xe in Ni at room temperature
[DE89-009879] N89-22713
Spinodal decomposition of austenite in long-term-aged duplex stainless steel
[DE89-009827] N89-22737
Microstructural studies of IAD and PVD Cr coatings by cross section transmission electron microscopy
[DE89-009877] N89-22739
Calculation of longitudinal and transverse wake-field effects in dielectric structures
[DE89-009814] N89-22798
ITER equilibrium with bootstrap currents, lower hybrid current drive and fast wave current drive
[DE89-009676] N89-22810
Advanced batteries for electric vehicles
[DE89-009771] N89-22813
Laboratory evaluation of advanced battery technologies for electric vehicle applications
[DE89-009810] N89-22814

Two-phase flow characteristic of inverted bubbly, slug and annular flow in post-critical heat flux region
[DE89-007384] N89-22839
Adaptive contact elements for three-dimensional explicit transient analysis
[DE89-008436] N89-22958
Monolithic Solid Oxide Fuel Cell development N89-22989
Advanced high-temperature batteries N89-23010
Solar radiation at the earth's surface: What are we doing to it and with it?
[DE89-008446] N89-23018
Fabrication of solid oxide fuel cell by electrochemical vapor deposition
[DE89-009605] N89-23023
Solid oxide fuel cell matrix and modules
[DE89-009607] N89-23024
Use of language features in the implementation and validation of a standardized generic package of elementary functions for Ada
[DE89-007385] N89-23187
Maximal bootstrap current tokamak equilibria in the first stability regime
[DE89-008201] N89-23291
Physical properties of grain-boundary materials: Comparison of EAM (Embedded-Atom-Method) and central-force potentials
[DE89-007414] N89-23308
Grain-boundary and free-surface induced thermodynamic melting: A molecular dynamics study in silicon
[DE89-007415] N89-23309
ESE (Electron Spin Echo) and CW-ESR studies of synthetic diamond crystals: Distribution of nitrogen and nickel
[DE89-007373] N89-23314
Structural properties of superconducting and nonsuperconducting Ba sub 1-x K sub x BiO3
[DE89-009813] N89-23340
Point defects and oxygen diffusion in high T sub c superconductors
[DE89-009842] N89-23341
Processing and electrical properties of high-T sub c superconductors
[DE89-009852] N89-23342
Growth kinetics of grain-boundary induced melting: A molecular-dynamics study
[DE89-009855] N89-23343

ARIZONA UNIV., TUCSON.
Coordinated Noninvasive Studies (CNS) Project
[AD-A205413] N89-22804

ARMY COLD REGIONS RESEARCH AND ENGINEERING LAB., HANOVER, NH.
Seafloor temperature and conductivity data from coastal waters of the US Beaufort Sea
[AD-A205428] N89-23059

ARMY LAB. COMMAND, WATERTOWN, MA.
Assessing hydrogen assisted cracking modes in high strength steel welds
[AD-A205431] N89-22746

ARMY MATERIALS TECHNOLOGY LAB., WATERTOWN, MA.
Environmentally induced discontinuities in transparent polymers
[AD-A205483] N89-22768

AT AND T TECHNOLOGIES, INC., GREENSBORO, NC.
Acoustic wave device using plate modes with surface-parallel displacement
[DE89-009719] N89-23273

AULE-TEK, INC., SCHENECTADY, NY.
Generation of face-edge-vertex models directly from images N89-23166

AURORAL OBSERVATORY, TROMSO (NORWAY).
Optical studies of the magnetospheric cusp from Svalbard
[AD-A205432] N89-23044

B

BATH UNIV. (ENGLAND).
Statistical smoothing methods and image analysis
[AD-A205643] N89-23256

BATTELLE INST., FRANKFURT AM MAIN (GERMANY, F.R.).
Radiation hardened detector arrays for the far and extreme infrared, phase 1
[BF-R-65.695-10] N89-23347

BELL TELEPHONE LABS., INC., HOLMDEL, NJ.
An introduction to generalized stereo techniques N89-23142

BELL TELEPHONE MFG. CO., ANTWERP (BELGIUM).
GPS terminal: Study of a GPS receiver for Columbus platform elements, executive summary
[GPS-REP-SEL-002] N89-22643

BENTLY ROTOR DYNAMICS RESEARCH CORP., MINDEN, NV.
Role of circumferential flow in the stability of fluid-handling machine rotors N89-22915

BERGEN UNIV. (NORWAY).
Decentralization of databases and the communication between them N89-23373

BOEING AEROSPACE CO., SEATTLE, WA.
Hydrogen embrittlement in nickel-hydrogen cells N89-23006
Center for Advanced Space Propulsion (CASP)
[NASA-CR-184936] N89-23404

BOYS TOWN NATIONAL INST., OMAHA, NE.
Detection of known signals in arbitrary backgrounds
[AD-A204076] N89-22784

BRITISH AEROSPACE PUBLIC LTD. CO., BRISTOL (ENGLAND).
Second generation Meteosat pre-phase A system study
[BA-SGM-FR-01] N89-22640

BROOKHAVEN NATIONAL LAB., UPTON, NY.
EXAFS studies of multilayer interfaces
[DE89-009527] N89-22694
Locating pitting sites from propagating surface potential transients
[DE89-008171] N89-22730
Neutron scattering studies of magnetic excitations in La/sub 2-x/Sr/sub x/CuO
[DE89-008155] N89-23333
Quasicrystals from cuts in six dimensions
[DE89-009361] N89-23337

BROWN, BOVERI UND CIE A.G., MANNHEIM (GERMANY, F.R.).
Interaction of coatings with base metals at high temperature N89-22669

BUNDESMINISTERIUM FUER FORSCHUNG UND TECHNOLOGIE, BONN (GERMANY, F.R.).
Agreement on the International Space Station and Columbus Program
[REPT-34/88] N89-23360

BUTLER ANALYSES, TOWSON, MD.
Ritz method for transient response in systems having unsymmetric stiffness N89-22954

C

CALIFORNIA INST. OF TECH., PASADENA.
Dynamics of particles in the bending waves of the planetary rings
[DE88-705714] N89-23396

CALIFORNIA UNIV., BERKELEY.
Studies of hot white dwarfs and instrumentation for stellar extreme ultraviolet astronomy N89-23383
Gravitational effects of cosmic strings in Friedmann universes N89-23394
Observational techniques for solar flare gamma-rays, hard X-rays, and neutrons
[NASA-CR-184910] N89-23399

CALIFORNIA UNIV., BERKELEY. LAWRENCE BERKELEY LAB.
Ab initio calculations of ordered intermetallic phase equilibria
[DE89-009974] N89-22741
On the numerical integration of viscoelastic flow equations
[DE89-007135] N89-22844
Transmission electron microscopy: Imaging of materials
[DE89-007418] N89-22870
Novel nitrogen-based organosulfur electrodes for advanced intermediate temperature batteries N89-22987
Technology base research project for electrochemical energy storage
[DE89-006860] N89-23019
Incorporation of a boundary condition to numerical solution of POISSON's equation
[DE89-007132] N89-23231
Electron energy-loss spectroscopy: Fundamentals and applications in the characterization of minerals
[DE89-006613] N89-23307
Low frequency resistance fluctuations in films of high temperature superconductors
[DE89-007489] N89-23310
Nuclear magnetic resonance with dc SQUID (Super-conducting QUantum Interference Device) preamplifiers
[DE89-007657] N89-23311
Nuclear magnetic resonance with dc SQUID (Super-conducting QUantum Interference Device) preamplifiers
[DE89-007657] N89-23311
A variable temperature cryostat that produces in situ clean-up germanium detector surfaces
[DE89-008174] N89-23328

CALIFORNIA UNIV., DAVIS.
PixMail: Pictures through mail
[DE89-009682] N89-22797
Molecular dynamics and irreversibility, from Boltzmann to Nose
[DE89-006740] N89-23274
Organic and polymer crystalline films for spatial light modulation
[AD-A205906] N89-23350

CALIFORNIA UNIV., LOS ANGELES.
Retrieving the distribution of liquid water content in clouds from observations of thermal microwave radiation N89-23056
A fast spatial scanning combination emissive and Mach probe for edge plasma diagnosis
[DE89-009674] N89-23295

CALIFORNIA UNIV., SANTA BARBARA.
Remote sensing information sciences research group: Browse in the EOS era
[NASA-CR-184637] N89-22979

CALSPAN CORP., ARNOLD AFS, TN.
Center for Advanced Space Propulsion (CASP)
[NASA-CR-184936] N89-23404

CARNEGIE-MELLON UNIV., PITTSBURGH, PA.
Physical-chemical studies of solutions processing of nematic polymers
[AD-A205921] N89-22770
Experimental and theoretical studies of vertical annular liquid jets
[DE89-009153] N89-22851
CMU image understanding program N89-23079
Kalman filter-based algorithms for estimating depth from image sequences N89-23094
Cooperative methods for road tracking in aerial imagery N89-23101
Three-dimensional vision for outdoor navigation by an autonomous vehicle N89-23124
Machine-independent image processing: Performance of Apply on diverse architectures N89-23125
Scan line array processors: Work in progress N89-23126
Image segmentation and reflection analysis through color N89-23150
An algorithm for the three-index assignment problem
[AD-A205172] N89-23190

CARRAR (FRANCE).
Mini Protein Crystallization Facility (MPCF), phase A study: Executive summary
[ESA-CR(P)-2709] N89-22775

CASE WESTERN RESERVE UNIV., CLEVELAND, OH.
A seal test facility for the measurement of isotropic and anisotropic linear rotordynamic characteristics N89-22905
Electrocatalysts for oxygen electrodes in fuel cells and water electrolyzers for space applications N89-22997

CENTRAL RESEARCH INST. OF ELECTRIC POWER INDUSTRY, TOKYO (JAPAN).
Development of advanced heat pump. Part 2: Preliminary test of two-stage compression heat pump
[DE88-756838] N89-22841
Development of advanced heat pumps. Part 3: Fundamental approach on two-stage compression system
[DE88-756842] N89-22842
Characteristics of winter lightning to high structures. Observation from December 1978 to March 1987
[DE88-756454] N89-23049

CENTRE D'ETUDES AERODYNAMIQUES ET THERMIQUES, POITIERS (FRANCE).
Interaction between an isolated vortex and a wing profile
[ETN-89-94364] N89-22579

CENTRE D'ETUDES ET DE RECHERCHES, TOULOUSE (FRANCE).
Sidewall boundary layer study, with and without suction, for the 150 mm chord CAST 7 airfoil at the T2 wind tunnel N89-22584
Coating of silicon carbide fibers
[CERT-423900/RF] N89-22767
A flux splitting method for hyperbolic systems: Application to the solution of the Euler equations
[CERT-RF-1/3290/DERI] N89-22854
Implementation of a two-component laser anemometer at the T2 wind tunnel
[A-501-H] N89-22879

CENTRE DE RECHERCHES METALLURGIQUES, LIEGE (BELGIUM).
Metallurgical study of superalloy brazing alloys N89-22680

CENTRE DE VILLAROCHE, MOISSY (FRANCE).
Utilization of high temperature composites in turbojet engines N89-22667

CENTRE NATIONAL D'ETUDES SPATIALES, TOULOUSE (FRANCE).
Electrodynamic transient tests
[CNES-CT/DRT/TVE/SM-024] N89-22644

History of manned flight
[CNES-NT-121] N89-23405

CENTRE NATIONAL DE LA RECHERCHE SCIENTIFIQUE, TOULOUSE (FRANCE).
Automatic generation of noncolliding trajectories and manipulation task planning in robotics
[LAAS-89-002] N89-23222

CESI, MILAN (ITALY).
Some in-field experiences of non-synchronous vibrations in large rotating machinery N89-22894

CHARLES RIVER ANALYTICS, INC., CAMBRIDGE, MA.
Expert systems for real-time monitoring and fault diagnosis
[NASA-CR-179441] N89-23209

CHI SYSTEMS, INC., BLUE BELL, PA.
An experimental environment and laboratory for studying human information processing in Naval Air ASW (Naval air antisubmarine warfare)
[AD-A204774] N89-23069

CHINA AERONAUTICAL ESTABLISHMENT, BEIJING.
Acceleration test for aircraft low-pass filter
[PB89-116263] N89-22807

CINCINNATI UNIV., OH.
LDV measurements and investigation of flow field through radial turbine guide vanes N89-22609

CISI INGENIERIE, TOULOUSE (FRANCE).
HOOD Toolset Development Project: ECLIPSE/HOOD/REP, issue 1.1
[ESA-CR(P)-2746] N89-23204

CITY COLL. OF THE CITY UNIV. OF NEW YORK, NY.
Probabilities and statistics for backscatter estimates obtained by a scatterometer with applications to new scatterometer design data
[NASA-CR-4226] N89-22779

CITY UNIV. OF NEW YORK, BROOKLYN.
Preparation, characterization and performance of MoS3 as an active cathode material
[AD-A205866] N89-22717

CIVIL AEROMEDICAL INST., OKLAHOMA CITY, OK.
Studies of poststrike air traffic control specialist trainees. Part 2: Selection and screening programs
[AD-A199177] N89-22595

COLORADO UNIV., BOULDER.
Numerical study of a multipurpose transonic wind tunnel with an adaptable injection-suction system N89-22621
Ten year lifetime orbits about the planet Mars N89-22633
The response of thermospheric nitric oxide to an auroral storm N89-23031
A new modified cholesky factorization
[AD-A205174] N89-23191

COLUMBIA UNIV., NEW YORK, NY.
Image understanding and robotics research at Columbia University N89-23083
An integrated approach to stereo matching, surface reconstruction and depth segmentation using consistent smoothness assumptions N89-23092
On the computational complexity of linear navigation N89-23123
Pyramid algorithms implementation on the connection machine N89-23129
Modeling sensors and applying sensor model to automatic generation of object recognition program N89-23136
An introduction to generalized stereo techniques N89-23142
The integration of information from stereo and multiple shape-form-texture cues N89-23145
A real time hierarchical model for optic flow determination via spatiotemporal frequency channels N89-23158
On the recovery of superellipsoids N89-23168
An optimal algorithm for the derivation of shape from shadows N89-23176
Surface orientation from projective foreshortening of isotropic texture autocorrelation N89-23179
Molecular beam epitaxial growth and characterization of metastable compound semiconductors for infrared detector applications
[AD-A205175] N89-23312

COMBUSTION ENGINEERING, INC., STAMFORD, CT.
Fabrication of solid oxide fuel cell by electrochemical vapor deposition
[DE89-009605] N89-23023
Solid oxide fuel cell matrix and modules
[DE89-009607] N89-23024

COMMERCE DEPT., WASHINGTON, DC.
Basic research in superconductor, ceramic and semiconductor sciences at selected Japanese laboratories based on a 1988 visit: Highlights, summary and overview, detailed notes from selected Japanese laboratories
[DE89-009637] N89-23339

COMPUTER RESOURCES INTERNATIONAL A/S (DENMARK).
HOOD Toolset Development Project: ECLIPSE/HOOD/REP, issue 1.1
[ESA-CR(P)-2746] N89-23204

COMPUTER SOFTWARE MANAGEMENT AND INFORMATION CENTER, ATHENS, GA.
Seventeenth NASTRAN (R) Users' Colloquium
[NASA-CP-3029] N89-22940

CONSTRUCCIONES AERONAUTICAS S.A., MADRID (SPAIN).
Paint compatibility test
[I-266/88] N89-22758
NDT results for comparability program SPF/DB
[I-264/88] N89-22935

CONTINUOUS ELECTRON BEAM ACCELERATOR FACILITY, NEWPORT NEW, VA.
Radiation control at the Continuous Electron Beam Accelerator Facility (CEBAF), a new high power CW electron accelerator installation
[CEBAF-PR-89-001] N89-23280

CORNELL UNIV., ITHACA, NY.
Grain boundary sliding phenomena in polycrystalline solids
[DE89-007792] N89-23326

COSURVEY (BELGIUM).
Mini Protein Crystallization Facility (MPCF), phase A study: Executive summary
[ESA-CR(P)-2709] N89-22775

COUNCIL FOR NATIONAL ACADEMIC AWARDS (ENGLAND).
Investigation of the effects of increased sophistication of simulation of the atmospheric wind in wind tunnels N89-22620

CRANFIELD INST. OF TECH., BEDFORD (ENGLAND).
Advanced materials to combat the high temperature degradation processes in turbomachinery N89-22664

D

DAVID SARNOFF RESEARCH CENTER, PRINCETON, NJ.
Parallel Optical Random Access Memory (PORAM)
[NASA-CR-4241] N89-22890
Algorithms and architectures for smart sensing N89-23090

DECISION SCIENCE CONSORTIUM, INC., RESTON, VA.
Consensus theory in expert systems: An adaptive inference framework and application to image understanding
[AD-A204253] N89-23188

DEFENCE RESEARCH ESTABLISHMENT ATLANTIC, DARTMOUTH (NOVA SCOTIA).
Standardized bibliographic processing N89-23367

DEFENCE RESEARCH ESTABLISHMENT VALCARTIER (QUEBEC).
Development of an asbestos-free insulant for rocket motors N89-22679

DEFENCE SCIENCE AND TECHNOLOGY ORGANIZATION, ADELAIDE (AUSTRALIA).
Neutron scattering studies of magnetic excitations in La/sub 2-x/Sr/sub x/CuO
[DE89-008155] N89-23333

DEFENSE APPLIED INFORMATION TECHNOLOGY CENTER, ALEXANDRIA, VA.
Fostering interaction of government, defense, and aerospace databases N89-23374

DEPARTMENT OF ENERGY, WASHINGTON, DC.
Basic research in superconductor, ceramic and semiconductor sciences at selected Japanese laboratories based on a 1988 visit: Highlights, summary and overview, detailed notes from selected Japanese laboratories
[DE89-009637] N89-23339

DEUTSCHE FORSCHUNGS- UND VERSUCHSANSTALT FUER LUFT- UND RAUMFAHRT, BRUNSWICK (GERMANY, F.R.).
The low-speed wind tunnel at DVFLR in Brunswick (Fed. Republic of Germany)
[DFVLR-MITT-88-25] N89-22619
Mechanical properties and damage mechanisms of carbon fiber reinforced composites: Compression loading
[DFVLR-FB-88-41] N89-22706

DEUTSCHE FORSCHUNGS- UND VERSUCHSANSTALT FUER LUFT- UND RAUMFAHRT, COLOGNE (GERMANY, F.R.).
Diagnostics of phase formation in metastable solidification of metals
[DFVLR-FB-88-43] N89-22745

DEUTSCHE FORSCHUNGS- UND VERSUCHSANSTALT FUER LUFT- UND RAUMFAHRT, GOETTINGEN (GERMANY, F.R.).
Transonic and supersonic flow past a 65 deg delta wing with rounded leading edges: Analysis of experimental data
[DFVLR-FB-88-44] N89-22580
Flow over a leading edge with distributed roughness
[DFVLR-FB-88-45] N89-22581
Lectures in Fluid Physics held at the Physics Department of the Georg-August-University. Volume 1: Source Strength of Vorticity
[DFVLR-MITT-88-26-VOL-1] N89-22855
Lectures in Fluid Physics held at the Physics Department of the Georg-August-University. Volume 2: Examples of the Application of Dimensional Analysis
[DFVLR-MITT-88-27-VOL-2] N89-22856

DEUTSCHE FORSCHUNGS- UND VERSUCHSANSTALT FUER LUFT- UND RAUMFAHRT, OBERPFAFFENHOFEN (WEST GERMANY).
Coherent polarimetric radar techniques for microwave propagation and cloud physics research
[DFVLR-FB-88-47] N89-22800
The Large Eddy Simulation (LES) of MESOSCOP for atmospheric boundary layer flows including passive scalars
[DFVLR-MITT-88-28] N89-23041

DEUTSCHE FORSCHUNGS- UND VERSUCHSANSTALT FUER LUFT- UND RAUMFAHRT, STUTTGART (GERMANY, F.R.).
Monolithic and fiber ceramic components for turboengines and rockets N89-22657

DEUTSCH METAL COMPONENTS, GARDENA, CA.
Increasing marketability and profitability of product line thru PATRAN and NASTRAN N89-22943

DEUTSCHER WETTERDIENST, OFFENBACH AM MAIN (GERMANY, F.R.).
Climatological and statistical fundamentals for the explanation of climate data processing
[ETN-89-93775] N89-23051
Reports from the German Meteorological Service. No. 175: Global radiation during twilight
[ISBN-3-88148-241-5] N89-23052
Reports from the German Meteorological Service. No. 177: Small-scale variability of solar radiation
[ISBN-3-88148-224-X] N89-23053

DORNIER-WERKE G.M.B.H., FRIEDRICHSHAFEN (GERMANY, F.R.).
Columbus MTFF utilisation, phase B2X: Executive summary for main study
[CUT-MBER-800-RP-220] N89-22647
Mini Protein Crystallization Facility (MPCF), phase A study: Executive summary
[ESA-CR(P)-2709] N89-22775

DOW CHEMICAL CO., FREEPORT, TX.
The application of Dow Chemical's perfluorinated membranes in proton-exchange membrane fuel cells N89-22995

DU PONT DE NEMOURS (E. I.) AND CO., AIKEN, SC.
Aqueous impurity effects on stainless steel IGSCC (intergranular stress corrosion cracking): A central composite matrix analysis
[DE88-017382] N89-22726

DYNACS ENGINEERING CO., INC., CLEARWATER, FL.
A NASTRAN/TREETOPS solution to a flexible, multi-body dynamics and controls problem on a UNIX workstation N89-22945

DYNAMICS RESEARCH CORP., ANDOVER, MA.
Developing software to use parallel processing effectively
[AD-A205184] N89-23192

E

EAGLE-PICHER INDUSTRIES, INC., JOPLIN, MO.
Advances in lightweight nickel electrode technology N89-23005
Multi-mission Ni-H2 battery cell for the 1990's N89-23006

EDGERTON, GERMESHAUSEN AND GRIER, INC., IDAHO FALLS, ID.
Assessment of EV batteries and application to R and D planning
[DE89-009720] N89-22811
Evaluation of several state-of-charge algorithms
[DE89-009752] N89-22812
MIRAP, microcomputer reliability analysis program
[DE89-009749] N89-23200

EDINBURGH UNIV. (SCOTLAND).
Diabatic circulations in the stratosphere N89-23043
Optical and infrared observations of the nature and evolution of active galaxies N89-23395

EDO CORP., SHELTON, CT.
Unity vision block with focal plane
[AD-A204694] N89-23283

EG AND G ENERGY MEASUREMENTS, INC., LOS ALAMOS, NM.
The propagation of noise through streak systems
[DE89-006600] N89-22869
ELTRON RESEARCH, INC., AURORA, IL.
The electrochemical generation of useful chemical species from lunar materials N89-22990
ENERGETICS, INC., COLUMBIA, MD.
Superconductivity for electric power systems: Building toward our future
[DE89-000874] N89-23332
ERNO RAUMFAHRTTECHNIK G.M.B.H., BREMEN (GERMANY, F.R.).
Ariane 5 Transfer Vehicle (ATV)
[REPT-OX-1-005] N89-22645
Columbus MTFF utilisation, phase B2X: Executive summary for main study
[CUT-MBER-800-RP-220] N89-22647
ETABLISSEMENT TECHNIQUE CENTRAL DE L'ARMEMENT, ARCUEIL (FRANCE).
Filament winding manufacturing of long fiber composite materials in thermoplastic matrix
[ETCA-87-R-047] N89-22699
Influence of conditioning on the trapezoidal fatigue behavior of a carbon epoxy composite
[ETCA-87-R-052] N89-22700
Dynamic behavior of a carbon epoxy composite
[ETCA-87-R-001] N89-22701
Wear protection coatings and treatments for the TA6V alloy
[ETCA-88-R-003] N89-22742
Fracture toughness and mechanical behavior of steel and aluminum alloys
[ETCA-87-R-090] N89-22743
Application of electrochemical noise spectral analysis to the study of the pitting corrosion of aluminum alloys
[ETCA-87-R-102] N89-22744
Application of indentation to the study of the toughness of yttrium-zircon plasma coatings
[ETCA-87-R-040] N89-22765
Glass transition temperature of the M10 resin associated to carbon, Kevlar or glass fibers
[ETCA-87-R-022] N89-22766
Tribological characterization of 15 surface treatments for aluminum alloys
[ETCA-87-R-132] N89-22928
Study of grain boundaries in polycrystalline alumina
[ETCA-87-R-130] N89-23344
Study of grain boundaries in polycrystalline alumina. Effect of the manufacturing mode and of the material composition
[ETCA-87-R-100] N89-23345
Preliminary study of ceramic-metal interface in thermal boundaries
[ETCA-87-R-101] N89-23346
EUROPEAN SPACE AGENCY, PARIS (FRANCE).
Navigation experiment NAVEX: The reading differences between all ground station measuring clocks during Spacelab pass of the D1 mission
[ESA-TT-1113] N89-22599
Material degradation in a barium hydroxide latent heat storage pilot unit
[ESA-TT-1107] N89-22715
Application of the Single-Axis-rate-Table (SAT) of the DFVLR for the evaluation of stationary and dynamic gyro properties
[ESA-TT-1122] N89-22877
On the small-signal gain of free-electron lasers in the low-current region
[ESA-TT-1120] N89-22889
Imaging radar applications in Europe. Illustrated experimental results (1978-1987)
[ESA-TM-01] N89-22978
New stable, vectorisable Kalman filter algorithms based on orthogonal transformations
[ESA-TT-1108] N89-23203

F

FEDERAL ARMED FORCES DOCUMENTATION AND INFORMATION CENTRE, BONN (GERMANY, F.R.).
Indexing and abstracting N89-23368
Data security N89-23369
FEDERAL AVIATION ADMINISTRATION, WASHINGTON, DC.
National airspace system plan: Facilities, equipment, associated development and other capital needs
[AD-A202615] N89-22596
FERMI NATIONAL ACCELERATOR LAB., BATAVIA, IL.
The new experimental areas oxygen monitor
[DE89-009700] N89-22876
Dark matter candidates
[DE89-006579] N89-23367
FIAT AVIAZIONE S.P.A., TURIN (ITALY).
Development of stress and lifing criteria for single crystal turbine blades N89-22563
FLORIDA UNIV., GAINESVILLE.
CO in the galactic center: A complete survey of carbon monoxide emission in the inner 4 kpc of the Galaxy N89-23386
Generating a hot big bang via a change in topology
[DE89-007561] N89-23388
FOKKER B.V., AMSTERDAM (NETHERLANDS).
Columbus MTFF utilisation, phase B2X: Executive summary for main study
[CUT-MBER-800-RP-220] N89-22647
FORD AEROSPACE AND COMMUNICATIONS CORP., PALO ALTO, CA.
Sodium sulfur battery flight experiment definition study N89-23009
FORSCHUNGSINSTITUT DER DEUTSCHEN BUNDESPOST, DARMSTADT (GERMANY, F.R.).
The radiation performance of offset reflector antennas with horn feeds excited by high order modes
[FI-454-TB-43] N89-22792
FORSCHUNGSINSTITUT FUER HOCHFREQUENZPHYSIK, WERTHHOVEN (GERMANY, F.R.).
Observation parameters for a ground-based radar station to survey near-earth satellites
[REPT-4-88] N89-22793
FRAUNHOFER-INST. FUER ZERSTOERUNGSFREIE PRUEFVERFAHREN, SAARBRUECKEN (GERMANY, F.R.).
Multifrequency eddy current testing, optimization of the method for steam generator testing. Phase 2: Nonlinear description of signal location curves dynamics of the signal location curves
[REPT-860142-TW] N89-22933
Reconstruction of defects from amplitude location curves
[REPT-780852-TW] N89-22934
FRAUNHOFER INST. FUER WERKSTOFFMECHANIK, FREIBURG (GERMANY, F.R.).
Recent advances in modeling creep crack growth
[W-2/88] N89-22964
FREIBURG UNIV. (GERMANY, F.R.).
Derivation of a large-scale map of heat load in the region Freiburg-Basel (Germany, F.R.) using satellite data. A contribution to the production of bioclimate data based on a geographic information system
[REPT-27] N89-22972

G

GARRETT TURBINE ENGINE CO., PHOENIX, AZ.
The demonstration of monolithic and composite ceramics in aircraft gas turbine combustors N89-22665
GEC-MARCONI ELECTRONICS LTD., CHELMSFORD (ENGLAND).
Theoretical studies for ERS-1 wave mode, volume 1
[GEC-MTR-87/110-VOL-1] N89-22977
GENERAL ATOMICS TECHNOLOGIES CORP., SAN DIEGO, CA.
H-Mode transition studies in DIII-D
[DE89-006913] N89-23290
GENERAL COHERENT TECHNOLOGY, INC., RICHARDSON, TX.
Gamma ray laser pump diagnostic
[AD-A205221] N89-22883
GENERAL ELECTRIC CO., SCHENECTADY, NY.
Image understanding research at GE N89-23085
PACE: An environment for intelligence analysis N89-23102
The concept of an effective viewpoint N89-23131
Algebraic reasoning in view consistency and parameterized model matching problems N89-23139
Labeling polyhedral images N89-23180
GEORGE WASHINGTON UNIV., WASHINGTON, DC.
Finite element modeling of electromagnetic fields and waves using NASTRAN N89-22950
GEORGIA INST. OF TECH., ATLANTA.
Convergence of discrete-vortex induced-flow calculations by optimum choice of mesh N89-22585
Aerodynamics of nonrigid bodies undergoing large amplitude time-dependent motions N89-22586
A study of unsteady turbulent flow past airfoils N89-22587
An efficient inverse method for the design of blended wing-body configurations N89-22603
GEORGIA TECH RESEARCH INST., ATLANTA.
Supersonic particle probes: Measurement of internal wall losses
[AD-A205863] N89-22589
GESELLSCHAFT FUER MATHEMATIK UND DATENVERARBEITUNG, SAINT AUGUSTIN (GERMANY, F.R.).
Multigrid for the steady-state incompressible Navier-Stokes equation: A survey
[GMD-322] N89-22846
GESELLSCHAFT FUER STRAHLEN- UND UMWELTFORSCHUNG M.B.H., MUNICH (GERMANY, F.R.).
Seasonal and latitudinal variations of the temporal variance of ozone and of the potential temperature
[BPT-3/88] N89-23026
Quantitative analysis of atmospheric trace gases
[BPT-10/88] N89-23027
Mass-spectroscopic measurements of stratospheric ions, trace gases and precondensation nuclei using balloon-borne measuring probes
[BPT-7/88] N89-23037
GINER, INC., WALTHAM, MA.
Advanced double layer capacitors N89-22993
Oxygen electrodes for rechargeable alkaline fuel cells N89-22998
Non-noble electrocatalysts for alkaline fuel cells N89-22999
GKSS-FORSCHUNGSZENTRUM GEESTHACHT (GERMANY, F.R.).
Finite element analysis for calibration curve computation for measurement of crack propagation of ellipse shaped surface cracks
[GKSS-88/E/34] N89-22960
GMD-GERMAN NATIONAL RESEARCH CENTER FOR COMPUTER SCIENCE, WASHINGTON, DC.
Germany: Focus on Scientific and Technical Information, volume 4, number 1, April 1988
[AD-A204054] N89-23376
GOSUDARSTVENNYI KOMITET PO ISPOLZOVANIYU ATOMNOI ENERGII, OBNINSK (USSR).
On Hausdorff dimension of invariant manifolds of infinite-dimensional dynamic systems
[DE88-705626] N89-23227
On the averaging method for quasilinear hyperbolic equations
[DE88-705629] N89-23228

H

HAMPTON INST., VA.
Effects of cosmic rays on single event upsets
[NASA-CR-184835] N89-23400
HARVARD UNIV., CAMBRIDGE, MA.
Development of metastable processing paths for high temperature alloys
[AD-A202614] N89-22721
Topics in gravitational theory N89-23042
Quantum phenomena in mesoscopic superconducting tunnel junctions
[AD-A203354] N89-23305
HELLENIC NATIONAL DEFENCE GENERAL STAFF, ATHENS (GREECE).
The status of defence information programs in Greece N89-23364
HONEYWELL SYSTEMS AND RESEARCH CENTER, MINNEAPOLIS, MN.
Qualitative reasoning and modeling for robust target tracking and recognition from a mobile platform N89-23086
Qualitative motion detection and tracking of targets from a mobile platform N89-23099
Dynamic model matching for target recognition from a mobile platform N89-23118
TRIPLE: A multi-strategy machine learning approach to target recognition N89-23119
HORTON (FOREST W., JR.), WASHINGTON, DC.
Information resources management N89-23371
HOUSTON UNIV., TX.
Nondestructive evaluation of stress using ultrasound and pulsed heat
[AD-A205176] N89-22932
HOWARD UNIV., WASHINGTON, DC.
Evaluation, development, and characterization of superconducting materials for space application
[NASA-CR-184842] N89-23302
HUGHES AIRCRAFT CO., LOS ANGELES, CA.
KOH concentration effect on the cycle life of nickel-hydrogen cells. 4: Results of failure analyse N89-23004
HUGHES RESEARCH LABS., CALABASAS, CA.
Knowledge-based vision technology progress at Hughes AI Center N89-23084
Autonomous navigation in cross-country terrain N89-23107
Multiresolution aerial image interpretation N89-23116
An operational perception system for cross-country navigation N89-23121

Machine-independent image processing: Performance of Apply on diverse architectures N89-23125
Recognizing animal motion N89-23156

I

IIT RESEARCH INST., CHICAGO, IL.
ELF communications system terminal grounds seasonal variation pilot study
[AD-A205900] N89-22806
IKO SOFTWARE SERVICE G.M.B.H., STUTTGART (GERMANY, F.R.).
The project ASKA-SPACE, phase 1
[ETN-89-93768] N89-22959
ILLINOIS UNIV., CHICAGO.
Corrosion of iron, nickel and cobalt based alloys in high temperature environments contaminated with chlorine
[DE89-009829] N89-22738
Topology of modified helical gears and Tooth Contact Analysis (TCA) program
[NASA-CR-4224] N89-22920
ILLINOIS UNIV., URBANA.
Variational analysis of railgun plasma-arc-armature for acceleration of solid hydrogen pellets for fusion reactor refueling
[DE89-009556] N89-22634
Development and study of a 3.2-mm-diameter, 1.2-m-long two-stage plasma-arc-driven railgun for hypervelocity hydrogen pellet injection
[DE89-009557] N89-22635
Mechanisms of cascade collapse
[DE89-009882] N89-22740
Signal detection in fractional Gaussian noise and an RKHS (Reproducing Kernel Hilbert Space) approach to robust detection and estimation
[AD-A205441] N89-22805
IU at UI: An overview and an example on shape from texture N89-23096
Experimental investigation of hot electron and related effects in gallium (aluminum) arsenide devices
[AD-A205442] N89-23349
INDUSTRIAL SCIENCE AND TECHNOLOGY AGENCY, TOKYO (JAPAN).
Japan's sunshine project 1987 annual summary of solar energy R and D program
[DE88-756452] N89-23014
INFORMATION AND CONTROL SYSTEMS, INC., HAMPTON, VA.
Development and simulation study of a new inverse-pinch high Coulomb transfer switch
[NASA-CR-181768] N89-23300
INFORMATION RESEARCH LAB., INC., DARTMOUTH, MA.
Interactive ultrasonic nondestructive evaluation
[AD-A204166] N89-22931
INSTITUT NATIONAL DES SCIENCES APPLIQUEES, LYON (FRANCE).
Development of behaviorist models to simulate commuted power switches
[ISAL-88-0065] N89-22815
Signal treatment and data analysis methods applied to nondestructive control of adhesive bonded joints
[ISAL-IDI-8809] N89-22936
INSTITUTE FOR COMPUTER APPLICATIONS IN SCIENCE AND ENGINEERING, HAMPTON, VA.
The inviscid axisymmetric stability of the supersonic flow along a circular cylinder
[NASA-CR-181816] N89-22574
Non-linear evolution of a second mode wave in supersonic boundary layers
[NASA-CR-181811] N89-22836
Inviscid spatial stability of a compressible mixing layer. Part 2: The flame sheet model
[NASA-CR-181815] N89-22837
Implementing nested conditional statements in SIMD machines
[NASA-CR-181832] N89-23073
INTERGRAPH CORP., HUNTSVILLE, AL.
The use of COSMIC NASTRAN in an integrated conceptual design environment N89-22944
INTERNATIONAL CENTRE FOR THEORETICAL PHYSICS, TRIESTE (ITALY).
Role of aluminium concentration on the structure behaviour of Cu-Al alloys
[DE88-705647] N89-22727
Dynamic scattering from multicomponent polymer systems
[DE88-705677] N89-22752
Application of the Ornstein-Zernike formalism to polymer and copolymer blends
[DE88-705686] N89-22753
Spinodal decomposition in polymer blends
[DE88-705687] N89-22754
Distortions caused by the signal processing in analog AM modulators
[DE88-705657] N89-22785
Forced and free convection flow with viscous dissipation effects: The method of parametric differentiation
[DE88-705649] N89-22840
Distortions in the output signals of conventional spectrum analyzers
[DE88-705656] N89-22871
On the physical causes of ENSO events and the ITCZ's extreme latitudinal displacements
[DE88-705654] N89-23050
Cohomology theory and deformations of Z sub 2-graded Lie algebras
[DE88-705694] N89-23229
Implementation of comparative probability by Gleason measures: Infinite dimensional case
[DE88-705683] N89-23259
On a functional equation over Hilbert spaces
[DE88-705645] N89-23267
Perturbative treatment of local correlations in Cu-O planes for high temperature superconductors
[DE88-705648] N89-23315
Theoretical study of the Pd-B complex in silicon
[DE88-705650] N89-23316
Electronic properties of Ge sub 1-x Si sub x: A simplified tight binding approach
[DE88-705671] N89-23317
Electronic structure of rare-earth luminescent centre in alkaline-earth sulphides
[DE88-705674] N89-23318
Investigation of the vacuum structure of the Georgi-Glashow model on the lattice
[DE88-705676] N89-23319
Electronic properties of Ge(1-X)Si(X): Alloying versus pressure
[DE88-705678] N89-23320
Band structure of CdTe-ZnTe superlattice
[DE88-705682] N89-23321
Coexistence of spin-glass and type-2 ceramic superconductivity
[DE88-705684] N89-23322
Hysteresis development in superconducting Josephson junctions
[DE88-705693] N89-23323
Ordering transitions induced by Coulomb interactions
[DE88-705717] N89-23324
Two dimensional (4,0) supergravity in harmonic superspace. The action and the matter couplings
[DE88-705661] N89-23351
Nature of condensation in the momentum space for an interacting Bose system
[DE88-705679] N89-23352
Construction of harmonic maps between pseudo-Riemannian spheres and hyperbolic spaces
[DE88-705695] N89-23353
On space-time escape mechanisms
[DE88-705699] N89-23354
Improved effective potential in the Einstein metric
[DE88-705716] N89-23355
Induced quantum conformal gravity
[DE88-705718] N89-23356
Reversed sense of the outward direction for dynamical effects of rotation close to a Schwarzschild black hole
[DE88-705670] N89-23389
Superconducting cosmic string evolution of quasars
[DE88-705672] N89-23390
Far infrared peculiar behavior of quasars
[DE88-705673] N89-23391
Dynamics of particles in the bending waves of the planetary rings
[DE88-705714] N89-23396
IOWA UNIV., IOWA CITY.
Models for surface intermediates in CO hydrogenation
[DE89-004348] N89-22712
A recursive formulation for flexible multibody dynamics N89-22968
ITALSPAZIO, ROME (ITALY).
PSDE/SAT-2: Communication system architecture study, executive summary
[ESA-CR(P)-2732] N89-22802

J

JET PROPULSION LAB., CALIFORNIA INST. OF TECH., PASADENA.
The importance of batteries in unmanned missions N89-22984
A survey of advanced battery systems for space applications N89-22986
Advanced rechargeable sodium batteries with novel cathodes N89-22988
Advances in ambient temperature secondary lithium cells N89-23011

JIAOTONG UNIV., SHANGHAI (CHINA).
Unsteady aerodynamic computational method of non-coplanar wing-tail combinations in subsonic flow
[PB89-111470] N89-22571
JOHANN-WOLFGANG-GOETHE-UNIV., FRANKFURT AM MAIN (GERMANY, F.R.).
Determination of the dynamic CO2 source-sink function of different biomes with the object of verifying seasonality and trend of atmospheric CO2 measurements of different stations
[ETN-89-93763] N89-23038
JOHNS HOPKINS UNIV., BALTIMORE, MD.
Mechanisms of crevice corrosion in chlorinated environments
[AD-A204821] N89-22724
JOINT INST. FOR NUCLEAR RESEARCH, DUBNA (USSR).
Possibility of operation of high temperature superconducting YBa2Cu3O7 ceramics in cyclotrons at irradiation
[DE88-705783] N89-23325
JOINT PUBLICATIONS RESEARCH SERVICE, ARLINGTON, VA.
JPRS report: Science and technology. USSR: Space
[JPRS-USP-88-003] N89-22622
Project Radioastron N89-22623
Methods and algorithms for processing television images of nucleus of Halley's Comet. Some results N89-22624
Historical survey of biosatellites N89-22625
Construction in weightlessness N89-22626
Power supply in space N89-22627
Development of orbital welding technology N89-22628
Glavkosmos official Yu. P. Semenov interviewed on development of USSR space program N89-22629
Future space projects discussed at Moscow Space Forum N89-22630

K

KAISERSLAUTERN UNIV. (GERMANY, F.R.).
Rotordynamic coefficients for labyrinth seals calculated by means of a finite difference technique N89-22900
Influence of different types of seals on the stability behavior of turbopumps N89-22902
A 3-dimensional finite-difference method for calculating the dynamic coefficients of seals N89-22903
Finite difference analysis of rotordynamic seal coefficients for an eccentric shaft position N89-22906
KERNFORSCHUNGSANLAGE, JUELICH (GERMANY, F.R.).
Ion-induced kinetic electron emission on clean and gas coated metal surfaces
[JUEL-2201] N89-22732
Reconstruction and relaxation of metal surfaces
[JUEL-2213] N89-22733
Investigation on long time dispersion and washout factor. Vegetation contamination computation with meteorological whole year or summer statistics
[JUEL-SPEZ-449] N89-23028
Coupling of a chemiluminescence detector with a gas chromatograph for the selective measurement of oxidized nitrogen bonds in the atmosphere
[JUEL-2217] N89-23029
KIENBAUM UNTERNEHMENSBERATUNG, GUMMERSBACH (GERMANY, F.R.).
Analysis of the present knowledge of costs and benefits of the governmental advancement of astronautics
[ETN-89-93770] N89-23359
KOBE UNIV. (JAPAN).
An experimental study on the static and dynamic characteristics of pump annular seals N89-22904

L

LAWRENCE LIVERMORE NATIONAL LAB., CA.
Atomic imaging of Au/Ni multilayers
[DE89-009903] N89-22698
Effects of grain size and strain rate on the mechanical response of copper
[DE89-008811] N89-22731
Low-density foams from macroporous epoxy gels
[DE89-004042] N89-22756
General grid finite difference methods for time dependent electromagnetic problems in two dimensions
[DE89-007225] N89-22788
Special techniques used for time domain, three dimensional finite element modeling of electromagnetics
[DE89-007227] N89-22789
PixMail: Pictures through mail
[DE89-009882] N89-22797
Wavelength streak camera
[DE89-008612] N89-22874

Magnetic axis alignment and the Poisson alignment reference system
[DE89-007687] N89-22880
Tunable chromium lasers
[DE89-008814] N89-22886
Cr3(+)-doped colquiriite solid state laser material
[DE89-010106] N89-22888
A new approach to system testing
[DE89-008660] N89-23195
Systolic implementation of neural networks
[DE89-008031] N89-23210
Design of a new high precision computer numerical control
[DE89-008032] N89-23211
Approximate Bayesian methods for nonlinear measurement error models
[DE89-009224] N89-23233
Molecular dynamics and irreversibility, from Boltzmann to Nose
[DE89-006740] N89-23274
Beam research technical abstracts, 1987
[DE89-009013] N89-23282
Thermal blooming threshold computations with a Markov model of velocity turbulence
[DE89-009709] N89-23285
Measurements of optical loss in transparent solids using a novel spectrometer based on optical cavity decay
[DE89-009900] N89-23286
Computation of lower hybrid, neutral beam and bootstrap currents in consistent MHD equilibria
[DE89-008892] N89-23292
Fusion power: Expected environmental characteristics and status of R and D
[DE89-009232] N89-23294
Accumulated surface damage on ZnS crystals produced by closely spaced pairs of picosecond laser pulses
[DE89-006813] N89-23329
Storage in supercomputer environments
[DE89-008895] N89-23330
Ductility enhancement in unreacted internal-Sn Nb3Sn through low-temperature anneals
[DE89-009125] N89-23336
Thermal Comptonization models for gamma-ray emission from black-hole sources
[DE89-009918] N89-23402

LEHIGH UNIV., BETHLEHEM, PA.
Corrosion fatigue crack growth: The role of crack-tip deformation and film formation kinetics N89-22966
The effect of boron on microhardness in Ni3Al polycrystals
[DE89-009124] N89-23335

LIAONING INST. OF METROLOGY, SHENYANG (CHINA).
New thermocouple: Characteristic investigation of Au+Pd+Ni/Ni+Cr thermocouple below 273K
[PB89-112940] N89-22867

LIMOGES UNIV. (FRANCE).
Study of long optical fibers
[ESA-CR(P)-2723] N89-23288

LOCKHEED ENGINEERING AND SCIENCES CO., HOUSTON, TX.
Orbital debris environment for spacecraft designed to operate in low Earth orbit
[NASA-TM-100471] N89-22638

LODESTAR RESEARCH CORP., BOULDER, CO.
A quiver kinetic formulation of radio frequency heating and confinement in collisional edge plasmas
[DE89-009575] N89-23296

LOS ALAMOS NATIONAL LAB., NM.
Microwave sintering of boron carbide
[DE89-009652] N89-22763
SUPERFISH accuracy dependence on mesh size
[DE89-007992] N89-22790
Scaling relations for a beam-deflecting TM(110) mode in an asymmetric cavity
[DE89-009277] N89-22796
Ultra-sensitive X-ray sensors give improved contrast sensitivity
[DE89-003561] N89-22872
ALEXIS: A narrow-band survey/monitor of the ultrasoft X-ray sky
[DE89-007960] N89-22873
Progress toward the delivery of high energy pulses with the Aurora KrF/ICF laser system
[DE89-007750] N89-22885
Fiber optic laser rod
[DE89-009568] N89-22887
Generalized finite strains, generalized stresses, and a hybrid variational principle for finite-element computer programs using curvilinear coordinates
[DE89-009923] N89-22962
Monte Carlo applied to resonance scattering of high altitude fluorescent radiation
[DE89-006519] N89-23035
Optimization for object localization of the constrained algebraic reconstruction technique
[DE89-007755] N89-23193
Simulation and analysis of physical mapping
[DE89-009399] N89-23198
The multigroup and cylindrical geometry formulation of the Sn Monte Carlo hybrid method
[DE89-000326] N89-23260
Transitional strategic defense architectures
[DE89-008312] N89-23265
Space Nuclear Safety Program
[DE89-008308] N89-23281
Influence of ion irradiated SrTiO sub 3 on the properties of thin film oxide superconductors
[DE89-009409] N89-23338
Relevance of international research facilities to international stability
[DE89-009400] N89-23380
The ALEXIS project and the local interstellar medium
[DE89-009246] N89-23392

LOUGHBOROUGH UNIV. OF TECHNOLOGY (ENGLAND).
Some local results for linear systems and implications for state variable feedback
[MATHS-RES-202] N89-23221

M

MANCHESTER UNIV. (ENGLAND).
Echelle observations of H2 complexes N89-23384
Observational aspects of interacting galaxies N89-23385

MARTIN MARIETTA CORP., DENVER, CO.
Space Propulsion Hazards Analysis Manual (SPHAM). Volume 2: Appendices
[AD-A204601] N89-22650
Geometric camera calibration using systems of linear equations N89-23148

MARYLAND UNIV., COLLEGE PARK.
Image understanding research at the University of Maryland, December 1986 - January 1988 N89-23078
The Maryland approach to image understanding N89-23091
Using flow field divergence for obstacle avoidance in visual navigation N89-23120
Using probabilistic domain knowledge to reduce the expected computational cost of matching N89-23134
Evaluation of quantization error in computer vision N89-23138
Preliminary design of a programmed picture logic N89-23141
Combining information in low-level vision N89-23152
Is correspondence necessary for the perception of structure from motion N89-23154
Symbolic pixel labeling for curvilinear feature detection N89-23171
Projective invariants of shapes N89-23175
Parallel problem solving system, PRISM (Parallel Inference System)
[AD-A204915] N89-23207

MASSACHUSETTS INST. OF TECH., CAMBRIDGE.
Remote sensing of earth terrain
[NASA-CR-184937] N89-22971
Analysis of regional phases using three component data
[AD-A205480] N89-23045
MIT progress in understanding images N89-23075
The MIT vision machine N89-23093
Self calibration of motion and stereo vision for mobile robot navigation N89-23106
Robust parallel computation of 2-D model-based recognition N89-23130
Qualitative versus quantitative depth and shape from stereo N89-23144
Relative orientation N89-23149
Recognizing solid objects by alignment N89-23174
Development of magnetic field assisted melt stabilization with heat and mass transfer control in low pressure LEC growth of GaAs
[AD-A205185] N89-23313

MASSACHUSETTS UNIV., AMHERST.
Dynamic image interpretation for autonomous vehicle navigation
[AD-A204167] N89-22597
Summary of image understanding research at the University of Massachusetts N89-23081
An integrated image understanding benchmark: Recognition of a 2 1/2 D mobile N89-23088
Some sample algorithms for the image understanding architecture N89-23089
Rapid object recognition from a large model base using prediction hierarchies N89-23137
Computation of motion in depth parameters: A first step in stereoscopic motion interpretation N89-23153
Motion from a sequence of images N89-23155
Issues in extracting motion parameters and depth from approximate translational motion N89-23157
Translating optical flow into token matches N89-23159
Depth from looming structure N89-23167

MATRA ESPACE, TOULOUSE (FRANCE).
HOOD Toolset Development Project: ECLIPSE/HOOD/REP, Issue 1.1
[ESA-CR(P)-2746] N89-23204

MAX-PLANCK-INST. FUER METEOROLOGIE, HAMBURG (GERMANY, F.R.).
Development of a satellite SAR image spectra and altimeter wave height data assimilation system for ERS-1
[NASA-CR-182685] N89-22975

MCR TECHNOLOGY CORP., CHICAGO, IL.
Development of an efficient high brightness Ti:Al2O3 laser amplifier
[AD-A204187] N89-22881

MECHANICAL TECHNOLOGY, INC., LATHAM, NY.
Magnetic bearing stiffness control using frequency band filtering N89-22910

MESSERSCHMITT-BOELKOW-BLOHM G.M.B.H., BREMEN (GERMANY, F.R.).
Development and testing of critical components for technological preparation of an Airbus-CFRP-fuselage, phase 2
[MBB-UT-129/87] N89-22600

METALLWERK PLANSEE, A.G., REUTTE (AUSTRIA).
Behavior of tungsten, molybdenum and alloys under unusual heating conditions N89-22674

MICHIGAN TECHNOLOGICAL UNIV., HOUGHTON.
Structural comparison of nickel electrodes and precursor phases N89-23001

MIDWEST RESEARCH INST., GOLDEN, CO.
Measurement uncertainty of adsorption testing of desiccant materials
[DE89-000841] N89-22681
Heat transfer and pressure drop measurements in an air/molten salt direct-contact heat exchanger
[DE89-000837] N89-22843
Solar thermal program summary. Volume 1: Overview, fiscal year 1988
[DE89-000860] N89-23020
Research on amorphous-silicon-based, thin-film photovoltaic devices, task B
[DE89-000885] N89-23021
Research on amorphous-silicon-based, thin-film photovoltaic devices, task B
[DE89-000886] N89-23022
Superconductivity for electric power systems: Building toward our future
[DE89-000874] N89-23332

MINISTRY OF DEFENCE, LONDON (ENGLAND).
Future advanced aero-engines: The materials challenge N89-22659

MISSION RESEARCH CORP., ALBUQUERQUE, NM.
Kinetic studies of the electron-beam-pumped ArF laser
[DE89-004041] N89-22884

MISSION RESEARCH CORP., LOS ALAMOS, NM.
Theoretical and computational studies of plasma opening switches
[DE89-009712] N89-23297

MITSUBISHI HEAVY-INDUSTRIES LTD., TAKASAGO (JAPAN).
High stability design for new centrifugal compressor N89-22917

MOTOREN- UND TURBINEN-UNION MUENCHEN G.M.B.H. (GERMANY, F.R.).
Propulsion systems with improved efficiency for future passenger aircraft. Main task A: Conceptual investigations of future propulsion systems with enhanced propulsive efficiency
[MTU-TB-87/010] N89-22608
Initial results of tests on metal-ceramic guide vanes N89-22668
Basic program for the development of a reliable high strength construction ceramic mode of SiC
[MTU-TB-87/927] N89-22757

N

NATIONAAL INST. VOOR KERNFYSICA EN HOGE ENERGIEFYSICA, AMSTERDAM (NETHERLANDS).
Experimental study of uranium plastic scintillator calorimeters
[NIKHEF-H/88-4] N89-22878
Hard scattering of (almost) real photons at HERA
[NIKHEF-H/88-3] N89-23276
Electron drift velocity close to a sense wire
[NIKHEF-H/88-5] N89-23277
Neutrino helicity flips via electroweak interactions and SN1987a
[NIKHEF-H/88-18] N89-23278

Quantum theory of a massless spinning particle
[NIKHEF-H/88-7] N89-23357
Local BRST invariance and the dynamical origin of the BRST condition
[NIKHEF-H/88-15] N89-23358

NATIONAL AERONAUTICAL ESTABLISHMENT, OTTAWA (ONTARIO).
Comparison of boundary layer trips of disk and grit types on airfoil performance at transonic speeds
[AD-A205206] N89-22575

NATIONAL AERONAUTICS AND SPACE ADMINISTRATION, WASHINGTON, DC.
Earth system science: A program for global change
[NASA-TM-101186] N89-22969

NATIONAL AERONAUTICS AND SPACE ADMINISTRATION. AMES RESEARCH CENTER, MOFFETT FIELD, CA.
Performance of all-metal demountable cryogenic seals at superfluid helium temperatures
[NASA-TM-102190] N89-22850
On the structure of pressure fluctuations in simulated turbulent channel flow
[NASA-TM-101084] N89-22860
Acclimatization to cold in humans
[NASA-TM-101012] N89-23061

NATIONAL AERONAUTICS AND SPACE ADMINISTRATION. GODDARD SPACE FLIGHT CENTER, GREENBELT, MD.
Overview of battery usage in NASA/GSFC LEO and GEO missions N89-22983
SEAPAK user's guide, version 1.0
[NASA-TM-100728] N89-23182

NATIONAL AERONAUTICS AND SPACE ADMINISTRATION. LYNDON B. JOHNSON SPACE CENTER, HOUSTON, TX.
Orbital debris environment for spacecraft designed to operate in low Earth orbit
[NASA-TM-100471] N89-22638
In-space technology development: Atomic oxygen and orbital debris effects
[NASA-TM-102154] N89-22682

NATIONAL AERONAUTICS AND SPACE ADMINISTRATION. LANGLEY RESEARCH CENTER, HAMPTON, VA.
Evaluation of the ride quality of a light twin engine airplane using a ride quality meter
[NASA-TP-2913] N89-22568
Hardware and operating features of the adaptive wall test section for the 0.3-meter transonic cryogenic tunnel
[NASA-TM-4114] N89-22614
Solution of multi-center molecular integrals of Slater-type orbitals
[NASA-TM-101545] N89-22692
Surface temperature measurements using a thin film thermal array
[NASA-TM-101549] N89-22868
The Space Station Flight Telerobotic Servicer and the human
[NASA-TM-100615] N89-23068
Implementing nested conditional statements in SIMD machines
[NASA-CR-181832] N89-23073
A knowledge-based tool for multilevel decomposition of a complex design problem
[NASA-TP-2903] N89-23181
Comparison of measured and calculated sound pressure levels around a large horizontal axis wind turbine generator
[NASA-TM-100654] N89-23270
Environmental noise characteristics of the MOD5-B (3.2 MW) wind turbine generator
[NASA-TM-101567] N89-23272

NATIONAL AERONAUTICS AND SPACE ADMINISTRATION. LEWIS RESEARCH CENTER, CLEVELAND, OH.
NASA's program on icing research and technology
[NASA-TM-101989] N89-22569
Second-order accurate nonoscillatory schemes for scalar conservation laws
[NASA-TM-102010] N89-22573
Rectangular nozzle plume velocity modeling for use in jet noise prediction
[NASA-TM-102047] N89-22577
Active vibration control for flexible rotor by optimal direct-output feedback control
[NASA-TM-101972] N89-22605
Investigation of low NOx staged combustor concept in high-speed civil transport engines
[NASA-TM-101977] N89-22606
Transonic viscous flow calculations for a turbine cascade with a two equation turbulence model
[NASA-TM-101944] N89-22607
New hypersonic facility capability at NASA Lewis Research Center
[NASA-TM-102028] N89-22617
The NASA Space Solar Cell Advanced Research Program
[NASA-TM-102020] N89-22651
Analysis of the nonvented fill of a 4.96-cubic-meter lightweight liquid hydrogen tank
[NASA-TM-102039] N89-22652
Numerical model of solar dynamic radiator for parametric analysis
[NASA-TM-102054] N89-22653
Thrust chamber thermal barrier coating techniques N89-22671
Fiber reinforced superalloys for rocket engines N89-22673
The isothermal fatigue behavior of a unidirectional SiC/Ti composite and the Ti alloy matrix
[NASA-TM-101984] N89-22684
Lightweight fibrous nickel electrodes for nickel-hydrogen batteries
[NASA-TM-101997] N89-22710
On the Lagrangian description of unsteady boundary layer separation. Part 2: The spinning sphere
[NASA-TM-102027] N89-22861
A generalized one-dimensional computer code for turbomachinery cooling passage flow calculations
[NASA-TM-102079] N89-22862
Rotordynamic Instability Problems in High-Performance Turbomachinery, 1988
[NASA-CP-3026] N89-22891
Effects of lubrication on the performance of high speed spur gears
[NASA-TM-101969] N89-22919
Transmission overhaul and replacement predictions using Weibull and renewal theory
[NASA-TM-102022] N89-22925
Structural dynamics branch research and accomplishments for FY 1988
[NASA-TM-101406] N89-22939
A NASTRAN DMAP alter for linear buckling analysis under dynamic loading N89-22948
Space Electrochemical Research and Technology Conference: Abstracts
[NASA-CP-10029] N89-22982
Human exploration mission studies N89-22985
Hydrogen-oxygen proton-exchange membrane fuel cells and electrolyzers N89-22996
Corrosion testing of candidates for the alkaline fuel cell cathode N89-23000
Impedance studies of Ni/Cd and Ni/H cells using the cell case as reference electrode N89-23002
Nickel-hydrogen capacity loss on storage N89-23007
InP (Indium Phosphide): Into the future
[NASA-TM-102058] N89-23025
Comparison of solar photovoltaic and nuclear reactor power systems for a human-tended lunar observatory
[NASA-TM-102015] N89-23397

NATIONAL AERONAUTICS AND SPACE ADMINISTRATION. MARSHALL SPACE FLIGHT CENTER, HUNTSVILLE, AL.
Vacuum plasma spray coating N89-22670
Cryogenic turbopump bearing materials N89-22678
Characterization testing of a 40 Ahr bipolar nickel hydrogen battery N89-22992

NATIONAL AEROSPACE LAB., AMSTERDAM (NETHERLANDS).
An in-flight investigation of workload assessment techniques for civil aircraft operations
[NLR-TR-87119-U] N89-23070

NATIONAL CENTER FOR PHYSICAL ACOUSTICS, UNIVERSITY, MS.
Experimental observation of the nonlinear response of single bubbles to an applied acoustic field
[AD-A205191] N89-23271

NATIONAL HELLENIC RESEARCH FOUNDATION, ATHENS (GREECE).
The objectives and role of the Greek National Documentation Centre N89-23363

NATIONAL INST. OF STANDARDS AND TECHNOLOGY, BOULDER, CO.
Ignition characteristics of the iron-based alloy UNS S66286 in pressurized oxygen
[NASA-CR-183612] N89-22722
Diagnostics of glow discharges used to produce hydrogenated amorphous silicon films
[DE89-000887] N89-22760

NATIONAL INST. OF STANDARDS AND TECHNOLOGY, GAITHERSBURG, MD.
Formation of lubricating films at elevated temperatures from the gas phase
[PB89-129530] N89-22747
Electrochemical technique for rapidly evaluating protective coatings on metals
[PB89-134209] N89-22748

NATIONAL OCEANIC AND ATMOSPHERIC ADMINISTRATION, BOULDER, CO.
Hazard index calculation for 31 May 1984 microburst at Erie, Colorado
[NASA-CR-184968] N89-23048

NATIONAL PHYSICAL LAB., TEDDINGTON (ENGLAND).
New theoretical model of stress transfer between fibre and matrix in a uniaxially fibre reinforced composite
[NPL-DMA(A)168] N89-22691
Criteria for selection of phase names for oxides
[NPL-DMA(A)169] N89-22714
The effect of thermocapillary flow on weld-pool profile
[NPL-DMA(A)167] N89-22927
Approximate large deflection analysis of simply supported orthotropic plates
[NPL-DMA(A)171] N89-22963
Report on round robin measurements of 6 digital magnetic tapes
[NPL-DES-91] N89-23202
The stable evaluation of a simple rational function and its application to spline approximation
[NPL-DITC-135/88] N89-23253
Model calculations of the electron-optical properties of compact Faraday cups
[NPL-DMA(A)165] N89-23268
Determination of the He3 number density for the proportional counter used in the NPL Bonner sphere system
[NPL-RS(EXT)104] N89-23275

NATIONAL TECHNICAL INFORMATION SERVICE, SPRINGFIELD, VA.
Identifying users and how to reach them N89-23370

NATIONAL TRANSPORTATION SAFETY BOARD, WASHINGTON, DC.
Aircraft accident report: Trans-Colorado Airlines, Inc., Flight 2286, Fairchild Metro 3, SA227 AC, N68TC Bayfield, Colorado, January 19, 1988
[PB89-910401] N89-22593

NAVAL AIR DEVELOPMENT CENTER, WARMINSTER, PA.
The effects of plastic media blasting paint removal on the microstructure of graphite/epoxy composite materials
[AD-A204801] N89-22688

NAVAL HEALTH RESEARCH CENTER, SAN DIEGO, CA.
Benzodiazepines and caffeine: Effect on daytime sleepiness, performance, and mood
[AD-A205862] N89-23066

NAVAL POSTGRADUATE SCHOOL, MONTEREY, CA.
Computational investigation of incompressible airfoil flows at high angles of attack
[AD-A205885] N89-22590
Design of an ELF/VLF satellite for under the ice submarine communications
[AD-A202607] N89-22639
Control of embedded vortices using wall jets
[AD-A202606] N89-22835
Development of a differential temperature probe for the measurement of atmospheric turbulence at all levels
[AD-A205893] N89-23047
A divide and conquer method for unitary and orthogonal eigenproblems
[AD-A205433] N89-23255

NAVAL RESEARCH LAB., WASHINGTON, DC.
Low Reynolds number calculation of turbulent channel flow: A general discussion
[AD-A205883] N89-22864
Effects of ion collisions on quasilinear heating by the current-driven ion cyclotron instability in the high latitude ionosphere
[AD-A202512] N89-23032
Simulations of axisymmetric erosion in IFR-Transported beams
[AD-A205882] N89-23301

NAVAL SHIP RESEARCH AND DEVELOPMENT CENTER, BETHESDA, MD.
Using Patran and Supertab as pre- and postprocessors to COSMIC/NASTRAN N89-22942
Calculation of low frequency vibrational resonances of submerged structures N89-22951
Power flows and Mechanical Intensities in structural finite element analysis N89-22952

NETHERLANDS ENERGY RESEARCH FOUNDATION, PETTEN.
The half-metallic ferromagnetic NiMnSb: A positron-annihilation study
[ECN-209] N89-23269

NEW ENERGY DEVELOPMENT ORGANIZATION, TOKYO (JAPAN).
Technical feasibility study on the development of ceramic thermoelectric conversion, part 2
[DE88-756481] N89-22755
Survey of development trends of methanol automobiles and methanol fuel in China
[DE88-756492] N89-22771

NEW MEXICO STATE UNIV., UNIVERSITY PARK.
A historical interpretation of the study of the visible cloud morphology on the planet Jupiter: 1610-1878 N89-23398
NEW MEXICO TECHNET, INC., ALBUQUERQUE.
Technology transfer report [DE89-009044] N89-23381
NEW YORK UNIV., NEW YORK.
Affine invariant matching N89-23103
NORTHWESTERN UNIV., EVANSTON, IL.
Damage development, property degradation and life prediction in composite laminates N89-22708
Investigation and synthesis of high temperature and increased stiffness RSP aluminum alloys [AD-A204162] N89-22723
Parallel processors and nonlinear structural dynamics algorithms and software [NASA-CR-184938] N89-23184

O

OAK RIDGE NATIONAL LAB., TN.
Behavior of iron aluminides in oxidizing and sulfidizing environments [DE89-008919] N89-22693
Temperature effects on the break-in of nickel aluminide alloys [DE89-005341] N89-22729
Improved high temperature creep resistant austenitic alloy [DE89-009664] N89-22736
Carbonaceous film coating [DE89-009592] N89-22762
Approximation technique for determining gain and radiation pattern of the horn antenna [DE89-006136] N89-22786
The induced current in parallel wires over an imperfect ground from an incident EMP [DE89-007209] N89-22787
Traction-drive force transmission for telerobotic joints [NASA-CR-183331] N89-22922
Reduction of a general matrix to tridiagonal form using a hypercube multiprocessor [DE89-006721] N89-23197
Binary and ternary gas mixtures for use in glow discharge closing switches [DE89-009718] N89-23298
OAK RIDGE Y-12 PLANT, TN.
Machine reference mirror inspection by optical Fabry-Perot cavity testing [DE89-009635] N89-23284
OFFICE NATIONAL D'ETUDES ET DE RECHERCHES AEROSPATIALES, PALAISEAU (FRANCE).
Ceramic heat exchangers and turbine blades: Theory and experimental results N89-22677
OFFICE NATIONAL D'ETUDES ET DE RECHERCHES AEROSPATIALES, PARIS (FRANCE).
Ultrasonic detection of damage in carbon epoxy composite materials [ONERA-RT-3/7256-RY-071-R] N89-22705
Computerized simulation of turbulent flow in a channel [ONERA-RSF-16/3419-AY-112-A] N89-22852
Numerical simulation of vortex breakdown [ONERA-RSF-3/4368-AY-502-A] N89-22853
OFFICE OF NAVAL RESEARCH, ARLINGTON, VA.
Basic research in superconductor, ceramic and semiconductor sciences at selected Japanese laboratories based on a 1988 visit: Highlights, summary and overview, detailed notes from selected Japanese laboratories [DE89-009637] N89-23339
OFFICE OF TECHNOLOGY ASSESSMENT, WASHINGTON, DC.
Safe skies for tomorrow: Aviation safety in a competitive environment [PB89-114318] N89-22591
Launch options for the future: Special report [PB89-114268] N89-22637
New developments in biotechnology: US investment in biotechnology, part 4 [PB88-246939] N89-23060
OSAKA UNIV., TOYONAKA (JAPAN).
A theoretical study of fluid forces on a centrifugal impeller rotating and whirling in a vaned diffuser N89-22908
OXFORD UNIV. (ENGLAND).
Measurement of the total gas content of a liquid [OUEL-1643/86] N89-22711
Cavitation in a submerged jet at constant pressure [OUEL-1658/86] N89-22848
The Hertzian cone crack: Theoretical, munerical and experimental studies [OUEL-1743/88] N89-22961
A pseudo singular value decomposition and inner functions in super optimal control [OUEL-1738/88] N89-23214
Boundaries and probes in electronegative plasmas [OUEL-1636/86] N89-23293

P

PACIFIC NORTHWEST LABS., RICHLAND, WA.
Design of a lightweight, low-cost geophysical survey vehicle [DE89-009383] N89-22926
Preliminary results of the MLAM (Multi-Layer Air Mass) Lagrangian transport model simulation of ANATEX (Across North America Tracer Experiment) [DE89-008123] N89-23036
Inhalation developmental toxicology studies: Teratology study of methyl ethyl ketone in mice [DE89-009563] N89-23062
A programmatic approach to achieving data quality objectives [DE89-006248] N89-23378
PASCO CORP. (JAPAN).
Evaluation of the Portable Instantaneous Display Analysis Spectrometer (PIDAS) [NASA-CR-184878] N89-22970
PENNSYLVANIA STATE UNIV., UNIVERSITY PARK.
Reactions of inorganic high polymers as a route to tailored solids [AD-A204602] N89-22750
PENNSYLVANIA UNIV., PHILADELPHIA.
Perception with feedback N89-23095
PITTSBURGH UNIV., PA.
Far- and mid-infrared properties of metal-insulator composite materials [AD-A204914] N89-22689
POLYTECHNIC UNIV., BROOKLYN, NY.
Polymer electrolytes with exclusively cationic conductivity [DE89-009521] N89-22761
PRATT AND WHITNEY AIRCRAFT, WEST PALM BEACH, FL.
Application of advanced materials for turbomachinery and rocket propulsion N89-22656
Damage tolerance concepts for advanced materials and engines N89-22661
PRINCETON UNIV., NJ.
Annealing studies on a fully cured epoxy resin: Effect of thermal prehistory, and time and temperature of annealing [AD-A205875] N89-22769
The structure and control of three-dimensional shock wave turbulent boundary layer interactions [AD-A205923] N89-22866
PURDUE UNIV., WEST LAFAYETTE, IN.
Aerodynamic detuning of a loaded airfoil cascade in an incompressible flow by a locally analytical method N89-22588
Model-based analysis and cooperative synthesis of control and display augmentation for piloted flight vehicles N89-22610
Two-phase flow characteristic of inverted bubbly, slug and annular flow in post-critical heat flux region [DE89-007384] N89-22839
Monte Carlo approximations in Bayesian decision theory. Part 3: Limiting behavior of Monte Carlo approximations [AD-A204173] N89-23258

R

RAHA ASSOCIATES, SANTA CLARA, CA.
Microfilm and computer full text of archival documents [AD-A204055] N89-23377
RICARDO-ITI, WESTMONT, IL.
Methods for heat transfer and temperature field analysis of the insulated diesel, phase 3 [NASA-CR-182237] N89-23382
ROCHESTER UNIV., NY.
Progress in image understanding at the University of Rochester N89-23082
Multimodal reconstruction and segmentation with Markov random fields and HCF optimization N89-23095
Parallel hardware for constraint satisfaction N89-23127
Object recognition from a large database using a decision tree N89-23135
Recognizing animal motion N89-23156
Structure recognition by connectionist relaxation: Formal analysis N89-23160
ROCKWELL INTERNATIONAL CORP., CANOGA PARK, CA.
Rotordynamic coefficients for stepped labyrinth gas seals N89-22901
Center for Advanced Space Propulsion (CASP) [NASA-CR-184936] N89-23404
ROCKWELL INTERNATIONAL SCIENCE CENTER, THOUSAND OAKS, CA.
Fiber matrix interface effects in failure of ceramic matrix fiber composites [AD-A204618] N89-22686
ROLLS-ROYCE LTD., DERBY (ENGLAND).
New metallic materials for gas turbines N89-22660
Material/manufacturing process interaction in advanced material technologies N89-22662
ROTOR BEARING DYNAMICS, INC., WELLSVILLE, NY.
A magnetic damper for first mode vibration reduction in multimass flexible rotors N89-22911
ROYAL AIRCRAFT ESTABLISHMENT, FARNBOROUGH (ENGLAND).
CVD and diffusion coatings for high temperature applications in turbomachinery and rocket motors N89-22658
User needs and how to determine them N89-23365
ROYAL INST. OF TECH., STOCKHOLM (SWEDEN).
Anomalous cross-field velocities in a CIV laboratory experiment [TRITA-EPP-88-06] N89-23289
ROYAL NETHERLANDS METEOROLOGICAL INST., DE BILT.
Radiative cooling in the nocturnal boundary layer [KNMI-WR-88-05] N89-23054
Surface flux parameterization schemes: Developments and experiences at KNMI [KNMI-WR-88-06] N89-23055
RPK CORP., COLUMBIA, MD.
A powerful enhancement to the DMAP alter capability N89-22947
Improvements to the CONTINUE feature in transient analysis N89-22949
RPK CORP., HAYES, VA.
Enhancements to the IBM version of COSMIC/NASTRAN N89-22946
RUHR UNIV., BOCHUM (GERMANY, F.R.).
Adsorption studies in the critical region of a pure fluid. Development of an apparatus for adsorption measurements under microgravity conditions [ETN-89-93767] N89-22774
RUTGERS - THE STATE UNIV., NEW BRUNSWICK, NJ.
R and D productivity: Relationship to Selective Dissemination of Information (SDI) in the corporate environment N89-23375

S

SAAB SPACE A.B., GOETEBORG (SWEDEN).
Ariane 5 Transfer Vehicle (ATV) [REPT-OX-1-005] N89-22645
SAN DIEGO STATE UNIV., CA.
Story problem solver: A schema-based system of instruction [AD-A205594] N89-23205
SANDIA NATIONAL LABS., ALBUQUERQUE, NM.
A preliminary characterization of parachute wake recontact [DE89-006442] N89-22578
Testing of a new recovery parachute system for the F111 aircraft crew escape module: An update [DE89-007139] N89-22592
Corrosion monitoring with acoustic wave devices [DE89-005235] N89-22728
Progress in crystalline silicon research [DE89-007423] N89-22749
Chemical state depth profiling by Auger signal decomposition: Silicon oxynitride [DE89-009830] N89-22764
A computer controlled 100 kV pulse generator [DE89-005922] N89-22808
A vortex panel analysis of circular-arc bluff-bodies in unsteady flow [DE89-007141] N89-22845
A calorimetric-based comparison of gas tungsten and plasma arc welding processes [DE89-008712] N89-22924
An experimental and analytical synthesis of controlled structure design [DE89-006506] N89-22957
Photovoltaic systems for today's remote power applications [DE89-007431] N89-23012
Advances in concentrator cell technology [DE89-007432] N89-23013
An assessment of the optical performance of stretched-membrane mirror modules [DE88-017347] N89-23015
Comparison of a cavity solar receiver numerical model and experimental data [DE89-003609] N89-23016
Design considerations for heat-pipe solar receivers [DE89-004037] N89-23017

Implementing security measures for computer-based security systems
[DE89-008995] N89-23072
Automating the identification of structural model parameters
[DE89-006327] N89-23194
Two time stepping algorithms for parallel computers
[DE89-008679] N89-23196
Engineering Graphics System (EGS) user's manual
[DE89-009668] N89-23199
Factoring very large numbers using a massively parallel computer
[DE89-008198] N89-23208
Nonlinear finite element simulation of the large angle motion of flexible bodies
[DE89-006505] N89-23230
Techniques for applying sets code procedures to large fault trees in PRA (Probabilistic Risk Assessment) analysis
[DE89-004823] N89-23261
Electrical properties and detection methods for CMOS IC defects
[DE89-005775] N89-23327

SAO PAULO UNIV. (BRAZIL).
Effects of X-rays on isotactic polypropylene. Volume 2: Polymers and ceramics
[DE88-705606] N89-22751

SATURN CORP., CHEVERLY, MD.
Center for Advanced Space Propulsion (CASP)
[NASA-CR-184936] N89-23404

SCHLUMBERGER PALO ALTO RESEARCH, CA.
Physically based modeling for vision and graphics
N89-23097

SCIENCE APPLICATIONS INTERNATIONAL CORP., MCLEAN, VA.
Proceedings: Image Understanding Workshop, volume 1
[AD-A197558] N89-23074
Proceedings: Image Understanding Workshop, volume 2
[AD-A197559] N89-23115
Simulations of axisymmetric erosion in IFR-Transported beams
[AD-A205882] N89-23301

SCIENCE RESEARCH LAB., INC., SOMERVILLE, MA.
Compact, lightweight CO2 lasers for SDIO applications
[AD-A204300] N39-22882

SENER S.A., MADRID (SPAIN).
GPS terminal: Study of a GPS receiver for Columbus platform elements, executive summary
[GPS-REP-SEL-002] N89-22643

SERVICE HYDROGRAPHIQUE ET OCEANOGRAPHIQUE DE LA MARINE, PARIS (FRANCE).
Geodetic positioning system for flying aircraft (May 1987)
[REPT-013/88] N89-22598

SEVERN COMMUNICATIONS CORP., MILLERSVILLE, MD.
Astronaut radiation exposure in low-earth orbit. Part 1: Galactic cosmic radiation
[AD-A204598] N89-23063
Equations of cosmic-ray transport with distributed acceleration
[AD-A204599] N89-23401

SIGRI ELECTROGRADHIT G.M.B.H., MEITINGEN (GERMANY, F.R.).
Silicon-carbide coated carbon-carbon: An advanced material for rocket systems N89-22672

SLI AVIONIC SYSTEMS CORP., GRAND RAPIDS, MI.
Pre and post modification electromagnetic compatibility test report for the C-130H self contained navigation system with MLS A-kit, revision
[AD-A205167] N89-22604

SMITHSONIAN ASTROPHYSICAL OBSERVATORY, CAMBRIDGE, MA.
Theoretical investigation of EM wave generation and radiation in the ULF, ELF, and VLF bands by the electrodynamic orbiting tether
[NASA-CR-181560] N89-22780

SOCIETE EUROPEENE DE PROPULSION, SAINT-MEDARD-EN-JALLES (FRANCE).
High temperature composite materials for rocket propulsion N89-22676

SOCIETE EUROPEENNE DE PROPULSION, VERNON (FRANCE).
Advanced cartridge technology: Executive summary
[SEP-TS/F-6972/88-RP] N89-22636
Implementation of active magnetic bearings on advanced rocket engine turbopumps
[ETN-89-94365] N89-22929

SOCIETE NATIONALE INDUSTRIELLE AEROSPATIALE, PARIS (FRANCE).
Numerical simulation of blast waves
[REPT-882-320-102] N89-22858

SOFTWARE SCIENCES LTD., FARNBOROUGH (ENGLAND).
HOOD Toolset Development Project: ECLIPSE/HOOD/REP, issue 1.1
[ESA-CR(P)-2746] N89-23204

SOUTHAMPTON UNIV. (ENGLAND).
Theoretical predictions of turbulent burning velocities of steady and accelerating unconfined turbulent flames with premixed reactants N89-22716
The spectral analysis of an aero-engine assembly incorporating a squeeze-film damper N89-22895

SOUTHERN METHODIST UNIV., DALLAS, TX.
Definition of NASTRAN sets by use of parametric geometry N89-22956

SOUTHWEST INST. OF FLUID PHYSICS, CHENGDU (CHINA).
Dynamic fracture in solids
[PB89-112650] N89-22937

SPACE POWER, INC., SAN JOSE, CA.
Megawatt Class Nuclear Space Power Systems (MCNSPS) conceptual design and evaluation report. Volume 3, technologies 2: Power conversion
[NASA-CR-179614-VOL-3] N89-22980
Megawatt Class Nuclear Space Power Systems (MCNSPS) conceptual design and evaluation report. Volume 2, technologies 1: Reactors, heat transport, integration issues
[NASA-CR-179614-VOL-2] N89-22981

SRI INTERNATIONAL CORP., MENLO PARK, CA.
Compression and shear wave propagation in explosives
[AD-A205917] N89-22865
The application of electrochemical impedance spectroscopy for characterizing the degradation of Ni(OH)2/NiOOH electrodes N89-23003
Ionospheric scintillation studies
[AD-A205210] N89-23034
Image understanding research at SRI International N89-23080
Constructing simple stable descriptions for image partioning N89-23104
Overview of the SRI cartographic modeling environment N89-23122
Core knowledge system: Storage and retrieval of inconsistent information N89-23132
Test results from SRI's stereo system N89-23140
Stochastic stereo matching over scale N89-23143
Extracting generic shapes using model-driven optimization N89-23161
Modal driven edge detection N89-23163
Generalizing epipolar-plane image analysis on the spatiotemporal surface N89-23164
Building surfaces of evolution: The weaving wall N89-23165
Specifying real-time systems with interval logic
[NASA-CR-181804] N89-23183

STANDARD ELEKTRIK LORENZ A.G., STUTTGART (GERMANY, F.R.).
GPS terminal: Study of a GPS receiver for Columbus platform elements, executive summary
[GPS-REP-SEL-002] N89-22643

STANFORD LINEAR ACCELERATOR CENTER, CA.
Computer aided design of three-dimensional waveguide loaded cavities
[DE89-007733] N89-22783

STANFORD UNIV., CA.
A numerical study of viscous vortex rings using a spectral method N89-22572
High accuracy thermal conductivity measurements near the lambda transition of helium with very high temperature resolution
[NASA-CR-184836] N89-22709
Annual research briefs, 1988
[NASA-CR-184906] N89-22817
The length scale for sub-grid-scale parameterization with anisotropic resolution N89-22818
Turbulence modeling N89-22819
On curve and surface stretching in turbulent flow N89-22820
Renormalization group analysis of turbulence N89-22821
Low-dimensional chaos in turbulence N89-22822
Close interactions of 3-D vortex tubes N89-22823
Numerical simulation of viscous vortex rings N89-22824
The effects of particle loading on turbulence structure and modelling N89-22825
Analysis of turbulence structures in shear flows N89-22826
Direct numerical simulation of compressible free shear flows
[AIAA-89-0374] N89-22827
Direct simulation of compressible reacting flows N89-22828
Turbulent transport in the solar nebula N89-22829
Transition to turbulence in laminar hypersonic flow N89-22830
Direct numerical simulations of turbulent convection with a variable gravity and Kepierian rotation N89-22831
Experimental investigation of flow over a backward facing step-progress report N89-22832
The effects of stabilizing and destabilizing longitudinal curvature on the structure of turbulent, two-stream mixing layers N89-22833
An experimental investigation of a low Reynolds number turbulent boundary layer subject to an adverse pressure gradient N89-22834
Control of free-flying space robot manipulator systems
[NASA-CR-184837] N89-22918
Evaluation of the Portable Instantaneous Display Analysis Spectrometer (PIDAS)
[NASA-CR-184878] N89-22970
Image understanding: Intelligent systems N89-23077
Generic models for robot navigation N89-23112
Using generic geometric and physical models for representing solids N89-23114
Structural correspondence in stereo vision N89-23146
Curved surface reconstruction using stereo correspondence N89-23147
A color metric for computer vision N89-23151
Texture models and image measures for segmentation N89-23162
Straight homogeneous generalized cylinders: Differential geometry and uniqueness results N89-23169
Ribbons, symmetries and skewed symmetries N89-23170
Image segmentation using geometric and physical constraints N89-23172
Predicting material classes N89-23177
Texture edge localization N89-23178
Expert systems on multiprocessor architectures, phase 1
[AD-A204907] N89-23206
Projections of vector addition system reachability sets are semilinear
[AD-A205914] N89-23257
Low frequency resistance fluctuations in films of high temperature superconductors
[DE89-007489] N89-23310

STATE UNIV. OF NEW YORK, BUFFALO.
Efficacy of conventional and high-frequency ventilation at altitude
[AD-A205922] N89-23071

STOCKHOLM UNIV. (SWEDEN).
A signal processing system using MC68000 and TMS320 microprocessors
[USIP-88-07] N89-22803

SULZER BROS. LTD., WINTERTHUR (SWITZERLAND).
Rotor instability due to a gear coupling connected to a bearingless sun wheel of a planetary gear N89-22893

SULZER-ESCHER WYSS LTD., ZURICH (SWITZERLAND).
Rotordynamic stability problems and solutions in high pressure turbocompressors N89-22914

SWEDISH DEFENCE RESEARCH ESTABLISHMENT, LINKOEPING.
Minimum number of satellites for periodic coverage
[FOA-C-30511-9.4] N89-22976
Some methods for uncertain reasoning
[FOA-C-30492-3.3] N89-23212
Fusion of multisensor data: A summary of the JASMIN project
[FOA-C-30498-3.3] N89-23213
Activities report of the Division of Optical Technology (FOA 33)
[FOA-C-30507-3.1] N89-23287

SWEDISH DEFENCE RESEARCH ESTABLISHMENT, STOCKHOLM.
Velocity measurements downstream of a sudden expansion using LDV. Part 2: Experimental results
[FOA-C-20736-2.1-PT-2] N89-22849
A multinational verification satellite: A preliminary investigation
[FOA-C-10312-9.3] N89-22974
A statistical package in Ada
[FOA-C-20740-2.7] N89-23201
Mie scattering calculations for heat radiation
[FOA-C-20738-2.1] N89-23279

SWEDISH INST. OF SPACE PHYSICS, UPPSALA.
Effect of pump-induced density depletions on the spectrum of stimulated electromagnetic emissions
[IRF-PREPRINT-107] N89-22799
A fluid FLR model of the magnetopause layer
[IRF-PREPRINT-109] N89-23299

SYMBOLICS, INC., CAMBRIDGE, MA.
Center for Advanced Space Propulsion (CASP)
[NASA-CR-184936] N89-23404

SYSTEMS INTEGRATION ENGINEERING, INC., LEXINGTON, MA.
Technical support for optical turbulence research
[AD-A204776] N89-23033
SYSTEMS TECHNOLOGY, INC., HAWTHORNE, CA.
Orbiter Flying Qualities (OFQ) Workstation user's guide
[NASA-CR-179440] N89-22612

T

TECHNION, INC., IRVINE, CA.
Center for Advanced Space Propulsion (CASP)
[NASA-CR-184936] N89-23404
TECHNISCH DOCUMENTATIE EN INFORMATIE CENTRUM VOOR DE KRIJGSMACHT, THE HAGUE (NETHERLANDS).
Sources of information N89-23366
TECHNISCHE HOGESCHOOL TWENTE, ENSCHEDE (NETHERLANDS).
On the stabilization of bilinear systems via constant feedback
[MEMO-706] N89-23215
Adaptive LQ control: Conflict between identification and control
[MEMO-718] N89-23216
The local disturbance decoupling problem with stability for nonlinear systems
[MEMO-721] N89-23217
Optimal processes described by a parabolic differential equation with control in the coefficients, part 3
[MEMO-725-PT-3] N89-23218
On the use of stable distributions in design programs
[MEMO-736] N89-23219
Robust stabilization of an inverted double pendulum system via a polynomial approach to H(infinity) optimal control
[MEMO-742] N89-23220
Generalized multicomponent KP-hierarchies
[MEMO-708] N89-23234
Restrictions on induced subgraphs ensuring Hamiltonicity or pancyclicity of K sub 1,3-free graphs
[MEMO-709] N89-23235
The separation number
[MEMO-710] N89-23236
Short proofs of some Fan-type results
[MEMO-711] N89-23237
Geometrical interpretation of the bilinear equations for the KP-hierarchy
[MEMO-720] N89-23238
Input-output decoupling with stability for Hamiltonian systems
[MEMO-722] N89-23239
A Borel-Ritt theorem with prescribed error bounds
[MEMO-723] N89-23240
Asymptotic expansions with error bounds for solutions of difference equations of level 1 sup +
[MEMO-724] N89-23241
Smoothing and likelihood ratio for Gaussian boundary value processes
[MEMO-726] N89-23242
Model matching for linear Hamiltonian systems
[MEMO-730] N89-23243
Nonlinear model matching with prescribed tracking error with an application to Hamiltonian systems
[MEMO-731] N89-23244
Smooth interpolation to scattered data by bivariate piecewise polynomials of odd degree
[MEMO-732] N89-23245
Localization of solutions of a nonlinear Fokker-Planck equation with Dirichlet boundary conditions
[MEMO-733] N89-23246
Numerical solution of the biharmonic equation using different types of bivariate spline functions
[MEMO-734] N89-23247
On the asymptotic behavior of the coefficients of asymptotic power series and its relevance to Stokes phenomena
[MEMO-738] N89-23248
Approximation of surfaces constrained by a differential equation using simplex splines
[MEMO-739] N89-23249
Nonlocal higher order symmetries for the Federbush model
[MEMO-740] N89-23250
On the maximum period of a permutation of N elements
[MEMO-743] N89-23251
Monotonicity-preserving quadratic C sup 1-spline interpolation to scattered data
[MEMO-744] N89-23252
Asymptotically optimal nonparametric experimental design tests for the log linear model under censoring
[MEMO-727] N89-23262
On the expected number of assignments in reduced matrices for the linear assignment problem
[MEMO-728] N89-23263
Limiting exact efficiency of quadratic statistics
[MEMO-737] N89-23264
Relationships between the prenucleolus, ENSC-solution and related solution concepts for cooperative games
[MEMO-729] N89-23266
TECHNISCHE UNIV., CLAUSTHAL-ZELLERFELD (GERMANY, F.R.).
Melting behavior of heavy metal batch components
[ETN-89-93986] N89-22734
TECHNISCHE UNIV., DELFT (NETHERLANDS).
Interfacial adhesion and mechanical properties of polyamide-6/glass bead composites
[ETN-89-94136] N89-22759
Simulation of a refrigerant evaporator
[ETN-89-94133] N89-22776
Selected aspects of discrete-time filtering techniques as applied to sensor control and signal processing problems
[ETN-89-94134] N89-22794
HIFI: A design method for implementing signal processing algorithms on VLSI processor arrays
[ETN-89-94138] N89-22795
An experimental study of turbulent mixing of viscoelastic fluids
[ETN-89-94140] N89-22847
Integration of tie-points in digital mosaicing
[ETN-89-94147] N89-22973
Detailed gravity anomalies derived form Seasat altimeter data. A comparison of two alternative approaches: Least squares collocation and a method based on FFT
[ETN-89-94144] N89-23039
Semilinear elliptic eigenvalue problems
[ETN-89-94142] N89-23232
Positron lifetime technique with applications in materials science
[ETN-89-94141] N89-23331
TECHPLAN CORP., SAN DIEGO, CA.
Overview of the software technology project RS34C71, documentation, management/technical advanced concepts for software engineering
[AD-A204921] N89-23189
TELEBIT, COPENHAGEN (DENMARK).
Study on communications costs for Columbus utilization
[REPT-871126/1/FR] N89-22801
TELESPAZIO, S.P.A., ROME (ITALY).
PSDE/SAT-2: Communication system architecture study, executive summary
[ESA-CR(P)-2732] N89-22802
TELSYSTEMES QUESTEL, PARIS (FRANCE).
TRANSDOC-electronic delivery programme N89-23372
TENNESSEE UNIV., KNOXVILLE.
Emission properties of europium-doped lanthanum and lutetium orthophosphate crystals for use in high temperature sensor applications
[DE89-008736] N89-23334
TENNESSEE UNIV., TULLAHOMA.
Center for Advanced Space Propulsion (CASP)
[NASA-CR-184936] N89-23404
TEXAS A&M UNIV., COLLEGE STATION.
Piezoelectric pushers for active vibration control of rotating machinery N89-22896
Cavitation effects on the pressure distribution of a squeeze film damper bearing N89-22897
An electroviscous damper N89-22898
Annular honeycomb seals: Test results for leakage and rotordynamic coefficients; comparisons to labyrinth and smooth configurations N89-22899
Experimental verification of an eddy-current bearing N89-22913
Analysis of the mechanical behavior of adhesively bonded composite joints
[AD-A202616] N89-22938
A new concept for high-cycle-life LEO: Rechargeable MnO2-hydrogen N89-22991
Recent advances in solid polymer electrolyte fuel cell technology with low platinum loading electrodes N89-22994
Remote sensing of oceanic rainrates by passive microwave sensors: A statistical-physical approach N89-23057
TEXAS INSTRUMENTS, INC., DALLAS.
Finite element analysis of a micromechanical deformable mirror device N89-22953
TEXAS UNIV., AUSTIN.
Impact of information technology on organizational structure: A control perspective N89-23379
TEXAS UNIV., DALLAS.
Problems in modern cosmology N89-23393
TEXAS UNIV., SAN ANTONIO.
Kilometric radiation power flux dependence on area of discrete aurora
[NASA-CR-184993] N89-23040
TEXTRON BELL HELICOPTER, FORT WORTH, TX.
Influence of impeller shroud forces on turbopump rotor dynamics N89-22909
TOKYO UNIV. (JAPAN).
Influence of impeller and diffuser geometries on the lateral fluid forces of whirling centrifugal impeller N89-22907
TORONTO UNIV. (ONTARIO).
Experimental study of uranium plastic scintillator calorimeters
[NIKHEF-H/88-4] N89-22878
TRIESTE UNIV. (ITALY).
Improved effective potential in the Einstein metric
[DE88-705716] N89-23355

U

UNISYS CORP., HUNTSVILLE, AL.
Improved performance in NASTRAN (R) N89-22941
UNITED TECHNOLOGIES RESEARCH CENTER, EAST HARTFORD, CT.
Composite material systems for high temperature applications N89-22666
UNIVERSAL ENERGY SYSTEMS, INC., DAYTON, OH.
Combustor flow visualization using innovative infrared thermographics techniques
[AD-A205905] N89-22718
UNIVERSIDAD POLITECNICA DE MADRID (SPAIN).
Spacecraft thermal control design data handbook
[LAMF-8712] N89-22642
UNIVERSITIES RESEARCH ASSOCIATION, INC., BATAVIA, IL.
Double sided circuit board and a method for its manufacture
[DE89-009601] N89-22809
UNIVERSITY OF SOUTHERN CALIFORNIA, LOS ANGELES.
USC image understanding research: 1987-1988 N89-23076
Three-dimensional object recognition using surface descriptions N89-23105
Integration effort in knowledge-based vision techniques for the autonomous land vehicle program N89-23108
Contour correspondences in dynamic imagery N89-23109
Spatio-temporal analysis of an image sequence with occlusion N89-23110
Natural representation of motion in space-time N89-23111
Perceptual grouping for the detection and description of structures in aerial images N89-23117
Parallel architectures for image processing and vision N89-23126
Adaptive smoothing for feature extraction N89-23173
UNIVERSITY OF SOUTHERN ILLINOIS, CARBONDALE.
Thermal healing of defects in oxide films on metals and alloys
[DE89-009580] N89-22735
UTAH DIV. OF WATER RESOURCES, SALT LAKE CITY.
Current and thermal noise in mixed Na/Ag beta alumina
[AD-A205869] N89-22816
UTAH UNIV., SALT LAKE CITY.
Alumina reinforced tetragonal zirconia (TZP) composites
[DE89-008880] N89-22690
Hydrogen embrittlement study and positron annihilation response of hydrogen in aisi 4340 steel N89-22720
Conductivity fluctuations in mixed Na/Ca beta alumina
[AD-A205416] N89-23348

V

VIGYAN RESEARCH ASSOCIATES, INC., HAMPTON, VA.
Microcomputer based controller for the Langley 0.3-meter Transonic Cryogenic Tunnel
[NASA-CR-181808] N89-22616
VIRGINIA POLYTECHNIC INST. AND STATE UNIV., BLACKSBURG.
Computational fluid dynamics research in three-dimensional zonal techniques
[NASA-CR-181406] N89-22838
VIRGINIA UNIV., CHARLOTTESVILLE.
Processing and properties of advanced aluminum alloys
[AD-A205187] N89-22725

VON KARMAN INST. FOR FLUID DYNAMICS, RHODE-SAINT-GENESE (BELGIUM).
Theoretical study of the unsteady flow in a straight channel with variable and constant cross section
[VKI-TN-168] N89-22857

W

WASHINGTON STATE UNIV., PULLMAN.
Study of unsteady boundary layers with adverse pressure gradient N89-22863
WASHINGTON UNIV., SEATTLE.
Mathematical morphology and the morphological sampling theorem N89-23113
WAYNE STATE UNIV., DETROIT, MI.
A general non-linear dynamical theory of elastic curved beams N89-22830
WESTINGHOUSE ELECTRIC CORP., COCKEYSVILLE, MD.
Motor theory of auditory perception
[AD-A204951] N89-23084
WESTINGHOUSE ELECTRIC CORP., WEST MIFFLIN, PA.
Measuring electrode assembly
[DE89-009591] N89-22875
WESTINGHOUSE HANFORD CO., RICHLAND, WA.
The long-term climate change assessment task of the Hanford Site, Washington, Protective Barrier Development Program
[DE89-008704] N89-23030
WICHITA STATE UNIV., KS.
Electro-impulse de-icing research: Fatigue and electromagnetic interference tests
[DOT/FAA/CT-88/27] N89-22594
WISCONSIN UNIV., MADISON.
ICRF waveguide launcher research
[DE89-009151] N89-22791
On polynomial ideals of finite codimension with applications to box spline theory
[AD-A204095] N89-23225
On multivariate polynomial interpolation
[AD-A204099] N89-23226
WOODS HOLE OCEANOGRAPHIC INSTITUTION, MA.
Measurements of a barotropic planetary vorticity mode in an eddy-resolving quasi-geostrophic model using acoustic tomography
[AD-A205409] N89-23058

Y

YUNNAN TIN CORP., GEJIU (CHINA).
Innovation in separation technology for fine gravity semi-products
[PB89-112478] N89-22719

Z

ZHEJIANG UNIV. (CHINA).
Some field experience with subsynchronous vibration of centrifugal compressors N89-22892

Typical Contract Number Index Listing

Listings in this index are arranged alphanumerically by contract number. Under each contract number the NASA accession numbers denoting documents that have been produced as a result of research done under that contract are arranged in ascending order. The NASA accession number denotes the number by which the citation is identified.

AF PROJ. SM-MMK-87-10-324 ..... N89-22592
AF PROJ. 2304 ..... N89-23207
AF PROJ. 2306 ..... N89-22723
N89-23312
AF PROJ. 2313 ..... N89-22784
N89-22804
N89-23064
AF-AFOSR-0021-86 ..... N89-23081
AF-AFOSR-0082-87 ..... N89-22725
AF-AFOSR-0125-88 ..... N89-23312
AF-AFOSR-0303-82 ..... N89-23207
AF-AFOSR-0336-86 ..... N89-23054
AF-AFOSR-0337-85 ..... N89-22723
AF-AFOSR-0374-87 ..... N89-22784
AF-AFOSR-0379-85 ..... N89-22804
ARPA ORDER 4976 ..... N89-23128
N89-23136
N89-23150
ARPA ORDER 5605 ..... N89-23074
N89-23115
AST-85-19411 ..... N89-23396
AST-86-15325 ..... N89-23396
BMFT-FKZ-0704562 ..... N89-23037
BMFT-FKZ-0704569-8 ..... N89-23027
BMFT-GRS-150610 ..... N89-22933
BMFT-KF-2007/4 ..... N89-23038
BMFT-KF-3012/4 ..... N89-23041
BMFT-LFT-8510/4 ..... N89-22608
BMFT-LKF-8652/7 ..... N89-22600
BMFT-RS-102-17 ..... N89-22934
BMFT-01-QV-070 ..... N89-22774
BMFT-01-TB-8503 ..... N89-22959
BMFT-01-YQ-113-6 ..... N89-22734
BMFT-01-ZH-85062 ..... N89-22734
BMFT-07-KR-2121 ..... N89-22975
BMFT-0704590-4 ..... N89-23026
BMVG-T/RF31/D0038/D1332 ..... N89-22793
DA PROJ. 1L1-61102-AH-45 ..... N89-22862
DA PROJ. 1L1-61103-BH-57 ..... N89-23256
DA PROJ. 1L1-62209-A-47-A N89-22920
N89-22925
DAAB07-86-K-F073 ..... N89-23091
N89-23134
N89-23152
N89-23154
DAAE07-87-C-R074 ..... N89-23283
DAAG29-84-K-0018 ..... N89-22865
DAAG29-84-K-0061 ..... N89-23098
DAAG29-84-9-0027 ..... N89-23098
DAAG29-85-K-0118 ..... N89-22717
DAAL03-87-K-0009 ..... N89-22932
DAAL03-87-K-0030 ..... N89-23225
N89-23226
DAAL03-88-K-0086 ..... N89-23191
DAAL04-88-C-0003 ..... N89-22931
DACA72-84-C-0002 ..... N89-23101
DACA72-86-C-0003 ..... N89-23188
DACA76-84-C-0005 ..... N89-23148
DACA76-85-C-0001 ..... N89-23095
DACA76-85-C-0002 ..... N89-23125
DACA76-85-C-0003 ..... N89-23124
N89-23148
DACA76-85-C-0004 ..... N89-23080
N89-23143
N89-23163
N89-23164
N89-23165
DACA76-85-C-0005 ..... N89-23087
N89-23133
DACA76-85-C-0007 ..... N89-23084
DACA76-85-C-0008 ..... N89-22597
N89-23081
N89-23155
N89-23157
N89-23167
DACA76-85-C-0009 ..... N89-23076
N89-23108
N89-23109
N89-23110
N89-23173
DACA76-85-C-0010 ..... N89-23130
N89-23174
DACA76-85-C-0017 ..... N89-23084
N89-23107
DACA76-85-C-0100 ..... N89-23149
DACA76-86-C-0007 ..... N89-23085
N89-23102
N89-23131
N89-23139
N89-23186
DACA76-86-C-0015 ..... N89-23081
N89-23088
N89-23089
DACA76-86-C-0017 ..... N89-23118
DACA76-86-C-0024 ..... N89-23083
N89-23123
N89-23129
DACA87-85-C-0007 ..... N89-23121
DAJA45-86-C-0054 ..... N89-23256
DARPA ORDER 3119 ..... N89-23117
N89-23126
DARPA ORDER 4976 ..... N89-23101
DCA/STPA-86-96-901 ..... N89-22742
DE-AC02-76CH-00016 ..... N89-22694
N89-22730
N89-22761
N89-23333
N89-23337
DE-AC02-76CH-03000 ..... N89-22809
N89-22876
N89-23387
DE-AC02-80ER-10567 ..... N89-23387
DE-AC02-83CH-10093 ..... N89-22681
N89-22760
N89-22843
N89-23020
N89-23021
N89-23022
N89-23332
DE-AC02-87ER-40317 ..... N89-23278
DE-AC02-87ER-80500 ..... N89-22999
DE-AC03-76SF-00098 ..... N89-22741
N89-22844
N89-22870
N89-23019
N89-23231
N89-23307
N89-23310
N89-23311
N89-23328
DE-AC03-76SF-00515 ..... N89-22783
DE-AC03-84ER-51044 ..... N89-23290
DE-AC03-87ER-80529 ..... N89-22783
DE-AC04-76DP-00789 ..... N89-22576
N89-22592
N89-22726
N89-22749
N89-22764
N89-22808
N89-22845
N89-22884
N89-22923
N89-22924
N89-22957
N89-23012
N89-23013
N89-23015
N89-23016
N89-23017
N89-23072
N89-23194
N89-23198
N89-23199
N89-23208
N89-23230
N89-23261
N89-23273
N89-23297
N89-23327
DE-AC05-84ER-40150 ..... N89-23280
DE-AC05-84OR-21400 ..... N89-22693
N89-22729
N89-22736
N89-22762
N89-22786
N89-22787
N89-22922
N89-23197
N89-23298
N89-23334
DE-AC05-84OS-21400 ..... N89-23284
DE-AC06-76RL-01830 ..... N89-22926
N89-23036
N89-23062
N89-23378
DE-AC06-87RL-10930 ..... N89-23030
DE-AC07-76ID-01570 ..... N89-22811
N89-22812
N89-23200
DE-AC08-88NV-10617 ..... N89-22689
DE-AC09-76SR-00001 ..... N89-22726
DE-AC11-76PN-00014 ..... N89-22875
DE-AI01-86CE-50162 ..... N89-23382
DE-FC22-88PC-88861 ..... N89-22735
DE-FG02-84ER-45055 ..... N89-23326
DE-FG02-84ER-52111 ..... N89-22634
N89-22635
DE-FG02-85ER-45178 ..... N89-22738
DE-FG02-86ER-13597 ..... N89-22851
DE-FG02-86ER-45256 ..... N89-23335
DE-FG02-86ER-52133 ..... N89-22791
DE-FG02-87ER-45312 ..... N89-22690
DE-FG02-88ER-53263 ..... N89-23296
DE-FG03-86ER-52134 ..... N89-23295
DE-FG04-84AL-26034 ..... N89-23381
DE-FG05-86ER-40272 ..... N89-23386
DE-FG22-85PC-80513 ..... N89-22712
DEN3-342 ..... N89-23382
DMA800-85-C-0008 ..... N89-23117
DMA800-85-C-0012 ..... N89-23081
N89-23159
DRET-85-092 ..... N89-22579
DRET-86-002-15 ..... N89-22767
DRET-87-34-001 ..... N89-22852
DRET-87-002-21 ..... N89-22854
DRET/RP-87-34-001 ..... N89-22853
DRET/SDCE-85-1487 ..... N89-22609
DRET/SDCE/MA-841471 ..... N89-22785
DRET/SDR-84-1022 ..... N89-22701
N89-22743
DRET/SDR/G8-83-1028 ..... N89-22700
N89-22926
DRET/SDR/G8-84-1022 ..... N89-22786
ER1/9/4/093-ARE(T) N89-22848
ER1/9/4/2057/093 ..... N89-22711
ESA-6875/87/HGE/I(SC) N89-22975
ESA-6878/87/HGE/I(SC) N89-22977
ESA-7197/87/NL/JS N89-22640
ESA-7266/87/D/IM N89-22801
ESA-7403/87/F/FL(SC) N89-22775
ESA-7451/87/F/SC N89-22647
ESTEC-5847/84/NL/GM(SC) N89-22641
ESTEC-6115/84/NL/MA(SC) N89-22642
ESTEC-6328/85/NL/BP N89-22644
ESTEC-6818/86/NL/PB(SC) N89-22643
ESTEC-6939/86/NL/PB(SC) N89-23347
ESTEC-6970/NL/IW(SC) N89-23288

ESTEC-7140/87/NL/DG N89-22648
ESTEC-7358/87/NL/MA N89-22646
ESTEC-7357/87/NL/MA(SC) N89-22645
ESTEC-7435/87/NL/MAC N89-23204
ESTEC-7502/87 ..... N89-22636
ESTEC-7570/88/NL/DG N89-22602
FMV-FFL-82250-86-169-25-001 ..... N89-22707
FMV-FLYGFL-82223-78-170-21-001 ..... N89-22601
N89-22613
FMV-FLYGFL-82260-88-061-73-001 ..... N89-22578
N89-22602
F04611-84-C-0003 ..... N89-22650
F09603-85-C-1224 ..... N89-22604
F19628-84-K-0019 ..... N89-23034
F19628-85-C-0052 ..... N89-23033
F19628-86-D-0006 ..... N89-23192
F19628-87-K-0054 ..... N89-23045
F29601-84-C-0080 ..... N89-23350
F30602-85-C-0008 ..... N89-23095
N89-23127
N89-23160
F30602-85-C-0012 ..... N89-23206
F30602-87-C-0140 ..... N89-23081
N89-23137
N89-23157
N89-23159
N89-23167
F33615-81-K-1539 ..... N89-23125
F33615-83-C-5089 ..... N89-23313
F33615-83-D-0601 ..... N89-23071
F33615-84-K-1520 ..... N89-23101
N89-23136
N89-23150
F33615-85-C-5034 ..... N89-22687
F33615-85-C-5106 ..... N89-23077
N89-23112
N89-23114
N89-23151
N89-23169
N89-23170
N89-23172
N89-23177
F33615-86-C-2670 ..... N89-22718
F33615-87-C-1436 ..... N89-23076
N89-23105
N89-23117
N89-23126
F33615-87-C-1499 ..... N89-23094
N89-23124
F33615-87-K-1499 ..... N89-23128
F33615-98-C-1436 ..... N89-23173
F40600-86-K-0004 ..... N89-22599
F49620-82-K-0033 ..... N89-22699
F49620-85-C-0140 ..... N89-22770
F49620-85-C-1040 ..... N89-22770
F49620-85-K-0018 ..... N89-23098
F49620-86-C-0041 ..... N89-23089
F49620-86-C-0094 ..... N89-22866
F49620-87-C-0024 ..... N89-23046
F49620-87-C-0066 ..... N89-22881
GA PROJ. 3410 ..... N89-23290
JFP-NSF-707 ..... N89-23315
JPL-957652 ..... N89-22975
MDA903-83-C-0027 ..... N89-23140
MDA903-86-C-0084 ..... N89-23080
N89-23104
N89-23122
N89-23140
N89-23143
N89-23161
N89-23163
MIPR-W31RPD-7-D4041 ..... N89-23285
NAGW-516 ..... N89-23399
NAGW-690 ..... N89-22779
NAGW-812 ..... N89-22773
NAGW-967 ..... N89-22979
NAGW-1195 ..... N89-23404
NAGW-1252 ..... N89-22970
NAGW-1254 ..... N89-23040
NAG1-650 ..... N89-23184
NAG1-868 ..... N89-22838
NAG2-276 ..... N89-22709
NAG3-181 ..... N89-22899
NAG3-655 ..... N89-22920
NAG5-227 ..... N89-23040
NAG5-270 ..... N89-22971
NAG5-929 ..... N89-23400
NAG5-1017 ..... N89-23302
NAG8-98 ..... N89-23306
NAG8-638 ..... N89-22780
NASA ORDER H-43201-B N89-22722
NAS1-17067 ..... N89-23183
NAS1-17685 ..... N89-23300
NAS1-17919 ..... N89-22616
NAS1-17993 ..... N89-22868
NAS1-18107 ..... N89-22574
N89-22837
NAS1-18226 ..... N89-22890
NAS1-18605 ..... N89-22574
N89-22836
N89-22837
N89-23073
N89-22612
NAS2-12454 ..... N89-23209
NAS2-12725 ..... N89-22980
NAS3-23667 ..... N89-22961
N89-22998
NAS3-24635 ..... N89-23000
NAS3-25119 ..... N89-23182
NAS5-29371 ..... N89-22975
NAS7-918 ..... N89-22990
NAS9-17991 ..... N89-22918
NCC2-333 ..... N89-22817
NCC2-460 ..... N89-23070
NIVR-01406N N89-23125
NR-SDRJ-007 ..... N89-23125
NR-048-659 ..... N89-23040
NSF ATM-85-21590 ..... N89-23040
NSF ATM-86-46122 ..... N89-23040
NSF ATM-88-05819 ..... N89-23191
NSF CCR-87-02403 ..... N89-23098
NSF DCR-82-19196 ..... N89-23103
NSF DCR-83-20085 ..... N89-23095
NSF DCR-83-20136 ..... N89-23098
NSF DCR-84-10771 ..... N89-23148
NSF DCR-84-19990 ..... N89-23150
N89-23191
NSF DCR-84-20944 ..... N89-23081
NSF DCR-85-00332 ..... N89-23137
N89-23157
N89-23124
NSF DCR-86-04199 ..... N89-23148
N89-23305
NSF DMR-84-04489 ..... N89-23225
NSF DMS-87-01275 ..... N89-23226
N89-23258
NSF DMS-87-17799 ..... N89-23190
NSF ECS-86-01660 ..... N89-23103
NSF IRI-87-03335 ..... N89-23126
NSF IRI-87-10863 ..... N89-23122
NSF IST-85-11751 ..... N89-23098
NSF MCS-82-19196 ..... N89-23125
N00014-80-C-0236 ..... N89-22805
N00014-81-K-0014 ..... N89-23095
N00014-82-K-0193 ..... N89-23103
N00014-82-K-0381 ..... N89-23081
N00014-82-K-0464 ..... N89-23155
N89-22816
N00014-82-K-0603 ..... N89-23348
N89-22975
N00014-83-G-0126 ..... N89-23305
N00014-83-K-0383 ..... N89-23349
N00014-84-C-0149 ..... N89-22769
N00014-84-K-0021 ..... N89-23305
N00014-84-K-0465 ..... N89-22750
N00014-84-K-0477 ..... N89-22686
N00014-85-C-0416 ..... N89-23377
N00014-85-C-0653 ..... N89-23257
N00014-85-C-0731 ..... N89-23103
N00014-85-K-0077 ..... N89-23130
N00014-85-K-0124 ..... N89-23149
N89-23174
N89-23125
N00014-85-K-0152 ..... N89-23190
N00014-85-K-0198 ..... N89-23205
N00014-85-K-0661 ..... N89-23098
N00014-85-K-0807 ..... N89-22689
N00014-85-K-0808 ..... N89-23074
N00014-86-C-0700 ..... N89-23115
N89-23271
N00014-86-K-0134 ..... N89-22938
N00014-86-K-0590 ..... N89-23130
N00014-86-K-0685 ..... N89-23174
N89-22721
N00014-86-K-0753 ..... N89-23069
N00014-87-C-0814 ..... N89-23063
N00014-87-C-2251 ..... N89-23401
N89-22724
N00014-87-K-0294 ..... N89-22882
N00014-88-C-0727 ..... N89-22883
N00014-88-C-2257 ..... N89-23258
N00014-88-K-1070 ..... N89-22993
N00014-88-0391 ..... N89-22805
N00014-89-J-1321 ..... N89-23092
N00039-84-C-0165 ..... N89-23123
N89-23142
N89-23145
N89-23168
N89-23179
N00039-84-C-0211 ..... N89-23148
N89-23147
N00039-88-C-0065 ..... N89-22806
N00039-95-C-0134 ..... N89-23125
N00228-85-G-3262 ..... N89-23058
N66001-86-D-0020 ..... N89-23189
PHASE-3075-AN-225-D N89-22584
RR04206 ..... N89-23205
STPA-83-96-003 ..... N89-22702
STPA-84-96-023 ..... N89-22704
STPA-85-95-004 ..... N89-22705
ST2J-0044-8-D N89-22975
ST2J-0101-2-NL(ED8) N89-23220
W-31-109-ENG-38 ..... N89-22695
N89-22696
N89-22697
N89-22713
N89-22737
N89-22739
N89-22740
N89-22798
N89-22810
N89-22813
N89-22814
N89-22839
N89-22958
N89-23018
N89-23023
N89-23024
N89-23187
N89-23291
N89-23308
N89-23309
N89-23314
N89-23340
N89-23341
N89-23342
N89-23343
W-7405-ENG-36 ..... N89-22763
N89-22790
N89-22796
N89-22872
N89-22873
N89-22885
N89-22887
N89-22962
N89-23035
N89-23193
N89-23198
N89-23260
N89-23265
N89-23281
N89-23334
N89-23338
N89-23360
N89-23392
W-7405-ENG-48 ..... N89-22696
N89-22731
N89-22756
N89-22788
N89-22789
N89-22797
N89-22874
N89-22880
N89-22886
N89-22888
N89-23195
N89-23210
N89-23211
N89-23233
N89-23274
N89-23282
N89-23285
N89-23286
N89-23292
N89-23294
N89-23329
N89-23330
N89-23336
N89-23402
199-21-12-07 ..... N89-23061
326-31-31 ..... N89-23397
474-52-10 ..... N89-22653
505-60 ..... N89-22860
505-61-01-05 ..... N89-22868
505-61-01-09 ..... N89-22616
505-61-21-03 ..... N89-22614
505-61-41-02 ..... N89-22568
505-62-3B N89-22617
505-62-21 ..... N89-22573
N89-22607
505-62-51 ..... N89-22606
505-62-91 ..... N89-22577
505-63-1A N89-22684
505-63-1B N89-22605
N89-22939
505-63-01-01 ..... N89-22692
505-63-51 ..... N89-22919
N89-22920

N89-22925
505-66-21-01 ..... N89-23183
505-66-71 ..... N89-23209
505-68-11 ..... N89-22569
505-90-21-01 ..... N89-22574
N89-22836
N89-22837
N89-23073
506-41-11 ..... N89-22651
N89-23025
506-41-21 ..... N89-22710
N89-22982
506-41-41-02 ..... N89-23300
506-43-41-01 ..... N89-23181
506-44-21-01 ..... N89-22890
506-48 ..... N89-22612
506-49-31-03 ..... N89-23068
535-03-11-03 ..... N89-23270
N89-23272
535-05-10 ..... N89-22862
553-13 ..... N89-22891
586-01-11 ..... N89-22980
N89-22981
591-23-21 ..... N89-22652
778-34-22 ..... N89-23382
928-30-05 ..... N89-22850

Typical Report Number Index Listing

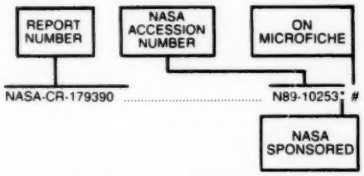

Listings in this index are arranged alphanumerically by report number. The NASA accession number denotes the number by which the citation is identified. An asterisk (*) indicates that the item is a NASA report. A pound sign (#) indicates that the item is available on microfiche.

A-501-H ..... N89-22879 #
A-68223 ..... N89-23061* #
A-89073 ..... N89-22860* #
A-89101 ..... N89-22850* #

ACIESP-60-VOL-2 ..... N89-22751 #

AD-A197558 ..... N89-23074 #
AD-A197559 ..... N89-23115 #
AD-A199177 ..... N89-22595 #
AD-A202512 ..... N89-23032 #
AD-A202596 ..... N89-23303 #
AD-A202598 ..... N89-23304 #
AD-A202599 ..... N89-23067 #
AD-A202600 ..... N89-22781 #
AD-A202601 ..... N89-22782 #
AD-A202602 ..... N89-23185 #
AD-A202604 ..... N89-22632 #
AD-A202606 ..... N89-22835 #
AD-A202607 ..... N89-22639 #
AD-A202612 ..... N89-22631 #
AD-A202614 ..... N89-22721 #
AD-A202615 ..... N89-22596 #
AD-A202616 ..... N89-22938 #
AD-A202617 ..... N89-22683 #
AD-A202618 ..... N89-22921 #
AD-A202619 ..... N89-23186 #
AD-A202620 ..... N89-23224 #
AD-A202621 ..... N89-22649 #
AD-A203354 ..... N89-23305 #
AD-A203980 ..... N89-22615 #
AD-A204054 ..... N89-23376 #
AD-A204055 ..... N89-23377 #
AD-A204076 ..... N89-22784 #
AD-A204088 ..... N89-22611 #
AD-A204095 ..... N89-23225 #
AD-A204099 ..... N89-23226 #
AD-A204162 ..... N89-22723 #
AD-A204166 ..... N89-22931 #
AD-A204167 ..... N89-22597 #
AD-A204173 ..... N89-23258 #
AD-A204187 ..... N89-22881 #
AD-A204253 ..... N89-23188 #
AD-A204300 ..... N89-22882 #
AD-A204598 ..... N89-23063 #
AD-A204599 ..... N89-23401 #
AD-A204601 ..... N89-22650 #
AD-A204602 ..... N89-22750 #
AD-A204618 ..... N89-22686 #
AD-A204621 ..... N89-22724 #
AD-A204623 ..... N89-22687 #
AD-A204694 ..... N89-23283 #
AD-A204774 ..... N89-23069 #
AD-A204776 ..... N89-23033 #
AD-A204801 ..... N89-22688 #
AD-A204907 ..... N89-23206 #
AD-A204914 ..... N89-22689 #
AD-A204915 ..... N89-23207 #
AD-A204921 ..... N89-23189 #
AD-A204951 ..... N89-23064 #
AD-A205128 ..... N89-22570 #
AD-A205167 ..... N89-22604 #
AD-A205172 ..... N89-23190 #
AD-A205174 ..... N89-23191 #
AD-A205175 ..... N89-23312 #
AD-A205176 ..... N89-22932 #
AD-A205184 ..... N89-23192 #
AD-A205185 ..... N89-23313 #
AD-A205187 ..... N89-22725 #
AD-A205191 ..... N89-23271 #
AD-A205206 ..... N89-22575 #
AD-A205210 ..... N89-23034 #
AD-A205221 ..... N89-22683 #
AD-A205409 ..... N89-23058 #
AD-A205413 ..... N89-22804 #
AD-A205416 ..... N89-23348 #
AD-A205428 ..... N89-23059 #
AD-A205431 ..... N89-22746 #
AD-A205432 ..... N89-23044 #
AD-A205433 ..... N89-23255 #
AD-A205441 ..... N89-22805 #
AD-A205442 ..... N89-23349 #
AD-A205480 ..... N89-23045 #
AD-A205483 ..... N89-22768 #
AD-A205592 ..... N89-23046 #
AD-A205594 ..... N89-23205 #
AD-A205643 ..... N89-23256 #
AD-A205660 ..... N89-23065 #
AD-A205662 ..... N89-23066 #
AD-A205863 ..... N89-22589 #
AD-A205866 ..... N89-22717 #
AD-A205869 ..... N89-22816 #
AD-A205875 ..... N89-22769 #
AD-A205882 ..... N89-23301 #
AD-A205883 ..... N89-22864 #
AD-A205885 ..... N89-22590 #
AD-A205893 ..... N89-23047 #
AD-A205900 ..... N89-22806 #
AD-A205903 ..... N89-22772 #
AD-A205905 ..... N89-22718 #
AD-A205906 ..... N89-23350 #
AD-A205914 ..... N89-23257 #
AD-A205917 ..... N89-22865 #
AD-A205921 ..... N89-22770 #
AD-A205922 ..... N89-23071 #
AD-A205923 ..... N89-22866 #

AD-E801786 ..... N89-22882 #
AD-E900870 ..... N89-22596 #
AD-E900870 ..... N89-22631 #
AD-E900870 ..... N89-22632 #
AD-E900870 ..... N89-22639 #
AD-E900870 ..... N89-22649 #
AD-E900870 ..... N89-22683 #
AD-E900870 ..... N89-22721 #
AD-E900870 ..... N89-22781 #
AD-E900870 ..... N89-22782 #
AD-E900870 ..... N89-22835 #
AD-E900870 ..... N89-22921 #
AD-E900870 ..... N89-22938 #
AD-E900870 ..... N89-23067 #
AD-E900870 ..... N89-23185 #
AD-E900870 ..... N89-23186 #
AD-E900870 ..... N89-23224 #
AD-E900870 ..... N89-23303 #
AD-E900870 ..... N89-23304 #

AEDC-TR-88-37 ..... N89-22589 #

AFAL-TR-88-096-VOL-2 ..... N89-22650 #

AFGL-TR-88-0148 ..... N89-23034 #
AFGL-TR-88-0269 ..... N89-23033 #
AFGL-TR-88-0322 ..... N89-23045 #

AFIT/EN/AA/88D-04 ..... N89-22632 #

AFIT/GA/AA/88D-08 ..... N89-22921 #

AFIT/GAE/AA/88D-7 ..... N89-22683 #
AFIT/GAE/AA/88D-19 ..... N89-22772 #

AFIT/GE/ENG/88D-4 ..... N89-22781 #
AFIT/GE/ENG/88D-8 ..... N89-23067 #
AFIT/GE/ENG/88D-24 ..... N89-22782 #
AFIT/GE/ENG/88D-25 ..... N89-23186 #
AFIT/GE/ENG/88D-42 ..... N89-23304 #
AFIT/GE/ENG/88D-43 ..... N89-23185 #

AFIT/GEP/ENP/88D-1 ..... N89-23303 #

AFIT/GOR/MA/88D-4 ..... N89-23224 #

AFIT/GSO/ENG/88D-2 ..... N89-23065 #

AFIT/GSO/ENP/88D-2 ..... N89-22649 #

AFOSR-88-1227TR ..... N89-22784 #
AFOSR-88-1311TR ..... N89-22881 #
AFOSR-89-0081TR ..... N89-22723 #
AFOSR-89-0092TR ..... N89-23312 #
AFOSR-89-0113TR ..... N89-23207 #
AFOSR-89-0213TR ..... N89-23064 #
AFOSR-89-0230TR ..... N89-22725 #
AFOSR-89-0264TR ..... N89-22804 #
AFOSR-89-0284TR ..... N89-23046 #
AFOSR-89-0285TR ..... N89-22866 #
AFOSR-89-0288TR ..... N89-22770 #

AFWAL-TR-88-4176 ..... N89-23313 #
AFWAL-TR-88-4242 ..... N89-22687 #

AFWL-TR-87-98 ..... N89-23350 #

AGARD-CAL-88/2 ..... N89-23361 #

AGARD-CP-445 ..... N89-23362 #
AGARD-CP-449 ..... N89-22654 #

AIAA-89-0374 ..... N89-22827* #
AIAA-89-0930 ..... N89-22845 #
AIAA-89-1201 ..... N89-23230 #
AIAA-89-2357 ..... N89-22577* #
AIAA-89-2534 ..... N89-22617* #
AIAA-89-2919 ..... N89-22925* #
AIAA-89-2942 ..... N89-22606* #

AIST-8805 ..... N89-23014 #

ANL-HEP-CP-89-24 ..... N89-22798 #

ANL/FPP/TM-235 ..... N89-23291 #
ANL/FPP/TM-238 ..... N89-22810 #

ANL/PPRNT-89-98 ..... N89-23018 #
ANL/PPRNT-89-111 ..... N89-22958 #

AR-005-504 ..... N89-22685 #

ARL-MAT-TM-397 ..... N89-22685 #

ARL-STRUC-TM-488 ..... N89-22611 #

ARO-21117.2-EG ..... N89-22865 #
ARO-22450.1-CH ..... N89-22717 #
ARO-24513.8-EG ..... N89-22932 #
ARO-24923.3-MA ..... N89-23191 #

ATES/DMA/TRM/162-86 ..... N89-22641 #

AVSCOM-TR-89-C-002 ..... N89-22920* #
AVSCOM-TR-89-C-007 ..... N89-22925* #
AVSCOM-TR-89-C-013 ..... N89-22862* #

BA-SGM-FR-01 ..... N89-22640 #

BF-R-65.895-10 ..... N89-23347 #

BNL-41404 ..... N89-22694 #
BNL-42094 ..... N89-22730 #
BNL-42265 ..... N89-23333 #
BNL-42371 ..... N89-22761 #
BNL-42478 ..... N89-23337 #

BPT-3/88 ..... N89-23026 #
BPT-7/88 ..... N89-23037 #
BPT-10/88 ..... N89-23027 #

CEBAF-PR-89-001 ..... N89-23260 #

CERT-RF-1/3290/DERI ..... N89-22854 #

CERT-423900/RF ..... N89-22767 #

CMS-TSR-89-17 ..... N89-23226 #
CMS-TSR-89-21 ..... N89-23225 #

CNES-CT/DRT/TVE/SM-024 ..... N89-22644 #

CNES-NT-121 ..... N89-23405 #

CONF-880812-41 ..... N89-23310 #
CONF-880812-42 ..... N89-23311 #
CONF-880812-44 ..... N89-23336 #
CONF-880887-31 ..... N89-22669 #
CONF-880887-33 ..... N89-23211 #
CONF-880894-4 ..... N89-23195 #
CONF-880901-18 ..... N89-22870 #
CONF-881103-57 ..... N89-23328 #
CONF-881125-5 ..... N89-22697 #
CONF-881155-54 ..... N89-22761 #
CONF-881155-55 ..... N89-22694 #
CONF-881155-57 ..... N89-22739 #
CONF-881155-58 ..... N89-22713 #
CONF-881155-59 ..... N89-22740 #
CONF-881155-69 ..... N89-22741 #
CONF-881207-2 ..... N89-22695 #
CONF-881207-3 ..... N89-22696 #
CONF-881207-4 ..... N89-23341 #
CONF-881226-2 ..... N89-23342 #
CONF-881244-9 ..... N89-22665 #
CONF-881268-2 ..... N89-23366 #
CONF-881268-4 ..... N89-23402 #
CONF-881278-1 ..... N89-23198 #
CONF-881279-1 ..... N89-23337 #
CONF-890115-1 ..... N89-23193 #
CONF-890135-8 ..... N89-23036 #
CONF-890142-4 ..... N89-23286 #
CONF-890145-19 ..... N89-23210 #
CONF-890145-23 ..... N89-22686 #
CONF-890153-3 ..... N89-22922* #
CONF-890180-1 ..... N89-23274 #
CONF-890189-3 ..... N89-22873 #
CONF-890189-6 ..... N89-23392 #
CONF-890197-6 ..... N89-22798 #
CONF-890211-1 ..... N89-23013 #
CONF-890211-2 ..... N89-23012 #
CONF-890211-3 ..... N89-22749 #
CONF-890215-5 ..... N89-22737 #
CONF-890240-2 ..... N89-22811 #
CONF-890240-5 ..... N89-22814 #
CONF-890275-1 ..... N89-23340 #
CONF-890284-1 ..... N89-23378 #
CONF-890302-12 ..... N89-23290 #
CONF-890302-19 ..... N89-23292 #
CONF-890304-35 ..... N89-22926 #
CONF-890315-1 ..... N89-22813 #
CONF-890324-5 ..... N89-22731 #
CONF-890335-4 ..... N89-22790 #
CONF-890335-33 ..... N89-22796 #
CONF-890372-1 ..... N89-23208 #
CONF-890372-2 ..... N89-23196 #
CONF-890372-3 ..... N89-23197 #
CONF-890385-1 ..... N89-23030 #
CONF-890388-1 ..... N89-23380 #
CONF-890394-1 ..... N89-22693 #
CONF-890405-10 ..... N89-23261 #
CONF-890408-8 ..... N89-23035 #
CONF-890423-4 ..... N89-22864 #
CONF-890436-2 ..... N89-23015 #
CONF-890436-3 ..... N89-23016 #
CONF-890436-5 ..... N89-23017 #
CONF-890436-7 ..... N89-22843 #
CONF-890436-8 ..... N89-22681 #
CONF-890437-1 ..... N89-22726 #
CONF-890437-7 ..... N89-22730 #
CONF-890437-9 ..... N89-22728 #
CONF-890438-1 ..... N89-23260 #
CONF-890466-3 ..... N89-23338 #
CONF-890468-4 ..... N89-22698 #
CONF-890468-5 ..... N89-22764 #
CONF-890478-1 ..... N89-22872 #
CONF-890479-4 ..... N89-22844 #
CONF-890479-5 ..... N89-22789 #
CONF-890479-6 ..... N89-23231 #
CONF-890479-7 ..... N89-22788 #
CONF-890483-1 ..... N89-22756 #
CONF-890493-1 ..... N89-23327 #
CONF-8904136-3 ..... N89-23330 #
CONF-8905106-3 ..... N89-22851 #
CONF-8905229-2 ..... N89-23387 #
CONF-8907159-1 ..... N89-22851 #
CONF-8908138-1 ..... N89-23333 #
CONF-8908156 ..... N89-22751 #

CONF-8909105-13 ..... N89-22874 #
CONF-8909215-4 ..... N89-23309 #
CONF-8909215-5 ..... N89-23308 #
CONF-8909291-1 ..... N89-23307 #
CONF-8910155-43 ..... N89-22839 #
CONF-8910176-4 ..... N89-22924 #
CONF-8910284-2 ..... N89-23329 #
CONF-8910318-1 ..... N89-23314 #
CONF-8910320-1 ..... N89-23187 #
CONF-8911147-2 ..... N89-23343 #
CONF-8911161-4 ..... N89-23335 #
CONF-8904103-1 ..... N89-22729 #
CONF-8904111-3 ..... N89-22786 #
CONF-8904111-4 ..... N89-22787 #
CONF-8904111-6 ..... N89-23334 #
CONF-8904112-1 ..... N89-22957 #
CONF-8904112-2 ..... N89-23230 #
CONF-8904112-3 ..... N89-23194 #
CONF-8904116-1 ..... N89-22808 #
CONF-8904118-2 ..... N89-22845 #
CONF-8904118-3 ..... N89-22576 #
CONF-8904118-4 ..... N89-22592 #
CONF-8904119-1 ..... N89-22923 #
CONF-8904155-1 ..... N89-23233 #
CONF-8904159-1 ..... N89-23294 #

CRIE-T-37040 ..... N89-23049 #

CRIE-W-87020-PT-2 ..... N89-22841 #
CRIE-W-87029-PT-3 ..... N89-22842 #

CRMSE-RN-89-01 ..... N89-23205 #

CRREL-89-1 ..... N89-23059 #

CUT-MBER-800-RP-220 ..... N89-22647 #

DE88-017347 ..... N89-23015 #
DE88-017382 ..... N89-22726 #
DE88-705606 ..... N89-22751 #
DE88-705628 ..... N89-23227 #
DE88-705629 ..... N89-23228 #
DE88-705645 ..... N89-23267 #
DE88-705647 ..... N89-22727 #
DE88-705648 ..... N89-23315 #
DE88-705649 ..... N89-22840 #
DE88-705650 ..... N89-23316 #
DE88-705654 ..... N89-23050 #
DE88-705656 ..... N89-22871 #
DE88-705657 ..... N89-22785 #
DE88-705661 ..... N89-23351 #
DE88-705670 ..... N89-23389 #
DE88-705671 ..... N89-23317 #
DE88-705672 ..... N89-23390 #
DE88-705673 ..... N89-23391 #
DE88-705674 ..... N89-23318 #
DE88-705676 ..... N89-23319 #
DE88-705677 ..... N89-22752 #
DE88-705678 ..... N89-23320 #
DE88-705679 ..... N89-23352 #
DE88-705682 ..... N89-23321 #
DE88-705683 ..... N89-23259 #
DE88-705684 ..... N89-23322 #
DE88-705686 ..... N89-22753 #
DE88-705687 ..... N89-22754 #
DE88-705693 ..... N89-23323 #
DE88-705694 ..... N89-23229 #
DE88-705695 ..... N89-23353 #
DE88-705699 ..... N89-23354 #
DE88-705714 ..... N89-23396 #
DE88-705716 ..... N89-23355 #
DE88-705717 ..... N89-23324 #
DE88-705718 ..... N89-23356 #
DE88-705783 ..... N89-23325 #
DE88-756452 ..... N89-23014 #
DE88-756454 ..... N89-23049 #
DE88-756481 ..... N89-22755 #
DE88-756492 ..... N89-22771 #
DE88-756636 ..... N89-22841 #
DE88-756842 ..... N89-22842 #
DE89-000326 ..... N89-23260 #
DE89-000837 ..... N89-22843 #
DE89-000841 ..... N89-22681 #
DE89-000860 ..... N89-23020 #
DE89-000874 ..... N89-23332 #
DE89-000885 ..... N89-23021 #
DE89-000886 ..... N89-23022 #
DE89-000887 ..... N89-22760 #
DE89-003581 ..... N89-22872 #
DE89-003609 ..... N89-23016 #
DE89-004037 ..... N89-23017 #
DE89-004041 ..... N89-22684 #
DE89-004042 ..... N89-22756 #
DE89-004348 ..... N89-22712 #
DE89-004823 ..... N89-23261 #
DE89-005235 ..... N89-22728 #

DE89-005341 ..... N89-22729 #
DE89-005775 ..... N89-23327 #
DE89-005922 ..... N89-22808 #
DE89-006136 ..... N89-22786 #
DE89-006171 ..... N89-22730 #
DE89-006327 ..... N89-23194 #
DE89-006442 ..... N89-22576 #
DE89-006505 ..... N89-23230 #
DE89-006506 ..... N89-22957 #
DE89-006519 ..... N89-23035 #
DE89-006579 ..... N89-23387 #
DE89-006600 ..... N89-22869 #
DE89-006613 ..... N89-23307 #
DE89-006687 ..... N89-22922* #
DE89-006740 ..... N89-23274 #
DE89-006913 ..... N89-23290 #
DE89-007132 ..... N89-23231 #
DE89-007135 ..... N89-22844 #
DE89-007139 ..... N89-22592 #
DE89-007140 ..... N89-22923 #
DE89-007141 ..... N89-22845 #
DE89-007209 ..... N89-22787 #
DE89-007225 ..... N89-22788 #
DE89-007227 ..... N89-22789 #
DE89-007373 ..... N89-23314 #
DE89-007384 ..... N89-22839 #
DE89-007385 ..... N89-23187 #
DE89-007414 ..... N89-23308 #
DE89-007415 ..... N89-23309 #
DE89-007416 ..... N89-22870 #
DE89-007423 ..... N89-22749 #
DE89-007431 ..... N89-23012 #
DE89-007432 ..... N89-23013 #
DE89-007489 ..... N89-23310 #
DE89-007561 ..... N89-23388 #
DE89-007657 ..... N89-23311 #
DE89-007667 ..... N89-22880 #
DE89-007733 ..... N89-22783 #
DE89-007750 ..... N89-22885 #
DE89-007755 ..... N89-23193 #
DE89-007792 ..... N89-23326 #
DE89-007980 ..... N89-22873 #
DE89-007992 ..... N89-22790 #
DE89-008031 ..... N89-23210 #
DE89-008032 ..... N89-23211 #
DE89-008123 ..... N89-23036 #
DE89-008155 ..... N89-23333 #
DE89-008174 ..... N89-23328 #
DE89-008198 ..... N89-23208 #
DE89-008201 ..... N89-23291 #
DE89-008248 ..... N89-23378 #
DE89-008308 ..... N89-23281 #
DE89-008312 ..... N89-23265 #
DE89-008436 ..... N89-22958 #
DE89-008446 ..... N89-23018 #
DE89-008612 ..... N89-22874 #
DE89-008660 ..... N89-23195 #
DE89-008679 ..... N89-23196 #
DE89-008704 ..... N89-23030 #
DE89-008712 ..... N89-22924 #
DE89-008721 ..... N89-23197 #
DE89-008736 ..... N89-23334 #
DE89-008811 ..... N89-22731 #
DE89-008813 ..... N89-23329 #
DE89-008814 ..... N89-22886 #
DE89-008860 ..... N89-23019 #
DE89-008880 ..... N89-22690 #
DE89-008892 ..... N89-23292 #
DE89-008895 ..... N89-23330 #
DE89-008919 ..... N89-22693 #
DE89-008995 ..... N89-23072 #
DE89-009013 ..... N89-23282 #
DE89-009044 ..... N89-23381 #
DE89-009124 ..... N89-23335 #
DE89-009125 ..... N89-23336 #
DE89-009151 ..... N89-22791 #
DE89-009153 ..... N89-22851 #
DE89-009224 ..... N89-23233 #
DE89-009232 ..... N89-23294 #
DE89-009246 ..... N89-23392 #
DE89-009277 ..... N89-22796 #
DE89-009361 ..... N89-23337 #
DE89-009383 ..... N89-22926 #
DE89-009399 ..... N89-23198 #
DE89-009400 ..... N89-23380 #
DE89-009409 ..... N89-23338 #
DE89-009521 ..... N89-22761 #
DE89-009527 ..... N89-22694 #
DE89-009556 ..... N89-22634 #
DE89-009557 ..... N89-22635 #
DE89-009563 ..... N89-23062 #
DE89-009580 ..... N89-22735 #
DE89-009591 ..... N89-22875 #
DE89-009592 ..... N89-22762 #
DE89-009598 ..... N89-22887 #
DE89-009601 ..... N89-22809 #

DE89-009605 ..... N89-23023 #
DE89-009607 ..... N89-23024 #
DE89-009635 ..... N89-23284 #
DE89-009637 ..... N89-23339 #
DE89-009652 ..... N89-22763 #
DE89-009664 ..... N89-22736 #
DE89-009668 ..... N89-23199 #
DE89-009674 ..... N89-23295 #
DE89-009675 ..... N89-23296 #
DE89-009676 ..... N89-22810 #
DE89-009682 ..... N89-22797 #
DE89-009700 ..... N89-22876 #
DE89-009709 ..... N89-23285 #
DE89-009712 ..... N89-23297 #
DE89-009718 ..... N89-23298 #
DE89-009719 ..... N89-23273 #
DE89-009720 ..... N89-22811 #
DE89-009749 ..... N89-23200 #
DE89-009752 ..... N89-22812 #
DE89-009771 ..... N89-22813 #
DE89-009810 ..... N89-22814 #
DE89-009813 ..... N89-23340 #
DE89-009814 ..... N89-22796 #
DE89-009827 ..... N89-22737 #
DE89-009829 ..... N89-22738 #
DE89-009830 ..... N89-22764 #
DE89-009842 ..... N89-23341 #
DE89-009843 ..... N89-22695 #
DE89-009847 ..... N89-22696 #
DE89-009852 ..... N89-23342 #
DE89-009855 ..... N89-23343 #
DE89-009877 ..... N89-22739 #
DE89-009879 ..... N89-22713 #
DE89-009882 ..... N89-22740 #
DE89-009883 ..... N89-22697 #
DE89-009900 ..... N89-23286 #
DE89-009903 ..... N89-22698 #
DE89-009918 ..... N89-23402 #
DE89-009923 ..... N89-22962 #
DE89-009974 ..... N89-22741 #
DE89-010106 ..... N89-22888 #

DFVLR-FB-87-10 ..... N89-22889 #
DFVLR-FB-87-49 ..... N89-22715 #
DFVLR-FB-87-52 ..... N89-23203 #
DFVLR-FB-88-41 ..... N89-22706 #
DFVLR-FB-88-43 ..... N89-22745 #
DFVLR-FB-88-44 ..... N89-22580 #
DFVLR-FB-88-45 ..... N89-22581 #
DFVLR-FB-88-47 ..... N89-22800 #

DFVLR-MITT-87-23 ..... N89-22599 #
DFVLR-MITT-88-09 ..... N89-22877 #
DFVLR-MITT-88-25 ..... N89-22619 #
DFVLR-MITT-88-26-VOL-1 ..... N89-22855 #
DFVLR-MITT-88-27-VOL-2 ..... N89-22856 #
DFVLR-MITT-88-28 ..... N89-23041 #

DODA-AR-005-525 ..... N89-22611 #

DOE/AL-26034/T6 ..... N89-23381 #

DOE/CH-10093/45-VOL-1 ..... N89-23020 #
DOE/CH-10093/56 ..... N89-23332 #

DOE/ER-0410 ..... N89-23339 #
DOE/ER-40272/73 ..... N89-23388 #
DOE/ER-45055/23 ..... N89-23326 #
DOE/ER-45178/3 ..... N89-22738 #
DOE/ER-45312/1 ..... N89-22690 #
DOE/ER-52111/T4 ..... N89-22634 #
DOE/ER-52111/T5 ..... N89-22635 #
DOE/ER-52133/3 ..... N89-22791 #
DOE/ER-53263/2 ..... N89-23296 #

DOE/ID-10214 ..... N89-22812 #

DOE/NASA/0342-3 ..... N89-23382* #

DOE/PC-80513/T5 ..... N89-22712 #
DOE/PC-88861/T13 ..... N89-22735 #

DOT/FAA/AM-88/3 ..... N89-22595 #

DOT/FAA/CT-88/27 ..... N89-22594 #

DP-MS-88-177 ..... N89-22726 #

DSCI-TR-88-16 ..... N89-23188 #

E-4071 ..... N89-22606* #
E-4227 ..... N89-22891* #
E-4498 ..... N89-22939* #
E-4626 ..... N89-22920* #
E-4634 ..... N89-22607* #
E-4666 ..... N89-22919* #
E-4672 ..... N89-22605* #
E-4683 ..... N89-22684* #
E-4692 ..... N89-22569* #
E-4701 ..... N89-22710* #
E-4708 ..... N89-22962* #
E-4721 ..... N89-22573* #
E-4729 ..... N89-23397* #
E-4739 ..... N89-22577* #
E-4747 ..... N89-22651* #
E-4750 ..... N89-22652* #
E-4756 ..... N89-22925* #
E-4760 ..... N89-22617* #
E-4771 ..... N89-22861* #
E-4807 ..... N89-22653* #
E-4818 ..... N89-23025* #
E-4839 ..... N89-22862* #

ECN-209 ..... N89-23269 #

EGG-M-88460 ..... N89-22811 #

EGG-SSRE-8137 ..... N89-23200 #

ESA-CR(P)-2706 ..... N89-22640 #
ESA-CR(P)-2707 ..... N89-22641 #
ESA-CR(P)-2709 ..... N89-22775 #
ESA-CR(P)-2710 ..... N89-22975* #
ESA-CR(P)-2712 ..... N89-22642 #
ESA-CR(P)-2716 ..... N89-22636 #
ESA-CR(P)-2719 ..... N89-22643 #
ESA-CR(P)-2722 ..... N89-23347 #
ESA-CR(P)-2723 ..... N89-23288 #
ESA-CR(P)-2727 ..... N89-22644 #
ESA-CR(P)-2731 ..... N89-22801 #
ESA-CR(P)-2732 ..... N89-22802 #
ESA-CR(P)-2735 ..... N89-22645 #
ESA-CR(P)-2738 ..... N89-22646 #
ESA-CR(P)-2744 ..... N89-22647 #
ESA-CR(P)-2746 ..... N89-23204 #
ESA-CR(P)-2750 ..... N89-22977 #
ESA-CR(P)-2751 ..... N89-22648 #

ESA-TM-01 ..... N89-22978 #

ESA-TT-1107 ..... N89-22715 #
ESA-TT-1108 ..... N89-23203 #
ESA-TT-1113 ..... N89-22599 #
ESA-TT-1120 ..... N89-22889 #
ESA-TT-1122 ..... N89-22877 #

ETCA-87-R-001 ..... N89-22701 #
ETCA-87-R-022 ..... N89-22766 #
ETCA-87-R-040 ..... N89-22765 #
ETCA-87-R-047 ..... N89-22699 #
ETCA-87-R-052 ..... N89-22700 #
ETCA-87-R-090 ..... N89-22743 #
ETCA-87-R-100 ..... N89-23345 #
ETCA-87-R-101 ..... N89-23346 #
ETCA-87-R-102 ..... N89-22744 #
ETCA-87-R-130 ..... N89-23344 #
ETCA-87-R-132 ..... N89-22928 #
ETCA-88-R-003 ..... N89-22742 #

ETL-0516 ..... N89-22597 #
ETL-0524 ..... N89-23188 #

ETN-89-93759 ..... N89-22846
ETN-89-93760 ..... N89-23026 #
ETN-89-93761 ..... N89-23037 #
ETN-89-93762 ..... N89-23027 #
ETN-89-93763 ..... N89-23038 #
ETN-89-93764 ..... N89-22757
ETN-89-93765 ..... N89-22608
ETN-89-93767 ..... N89-22774 #
ETN-89-93768 ..... N89-22959 #
ETN-89-93769 ..... N89-22600 #
ETN-89-93770 ..... N89-23359 #
ETN-89-93771 ..... N89-22792 #
ETN-89-93772 ..... N89-22933 #
ETN-89-93773 ..... N89-22934 #
ETN-89-93774 ..... N89-22793
ETN-89-93775 ..... N89-23051
ETN-89-93776 ..... N89-23052
ETN-89-93777 ..... N89-23053
ETN-89-93781 ..... N89-22972 #
ETN-89-93953 ..... N89-22960 #
ETN-89-93957 ..... N89-23028 #
ETN-89-93958 ..... N89-22732 #
ETN-89-93961 ..... N89-22733 #
ETN-89-93962 ..... N89-23029 #
ETN-89-93985 ..... N89-23360 #
ETN-89-93986 ..... N89-22734 #
ETN-89-94125 ..... N89-23212 #
ETN-89-94126 ..... N89-23213 #
ETN-89-94127 ..... N89-22935 #
ETN-89-94128 ..... N89-22758 #
ETN-89-94133 ..... N89-22776 #
ETN-89-94134 ..... N89-22794 #
ETN-89-94136 ..... N89-22759 #
ETN-89-94138 ..... N89-22795 #
ETN-89-94140 ..... N89-22847 #
ETN-89-94141 ..... N89-23331 #
ETN-89-94142 ..... N89-23232 #
ETN-89-94144 ..... N89-23039 #
ETN-89-94147 ..... N89-22973 #
ETN-89-94153 ..... N89-23054
ETN-89-94154 ..... N89-23055
ETN-89-94197 ..... N89-23070 #
ETN-89-94204 ..... N89-23268
ETN-89-94205 ..... N89-22891
ETN-89-94206 ..... N89-23275
ETN-89-94207 ..... N89-23293 #
ETN-89-94208 ..... N89-22711 #
ETN-89-94209 ..... N89-22848 #
ETN-89-94215 ..... N89-23214 #
ETN-89-94216 ..... N89-22961 #
ETN-89-94221 ..... N89-22974 #
ETN-89-94222 ..... N89-22849 #
ETN-89-94234 ..... N89-22889 #
ETN-89-94235 ..... N89-22877 #
ETN-89-94238 ..... N89-22640 #
ETN-89-94239 ..... N89-22641 #
ETN-89-94240 ..... N89-22775 #
ETN-89-94241 ..... N89-22975* #
ETN-89-94242 ..... N89-22642 #
ETN-89-94248 ..... N89-23269 #
ETN-89-94249 ..... N89-23276 #
ETN-89-94250 ..... N89-22878 #
ETN-89-94251 ..... N89-23277 #
ETN-89-94252 ..... N89-23357 #
ETN-89-94254 ..... N89-23358 #
ETN-89-94257 ..... N89-23278 #
ETN-89-94258 ..... N89-23215 #
ETN-89-94260 ..... N89-23234 #
ETN-89-94261 ..... N89-23235 #
ETN-89-94262 ..... N89-23236 #
ETN-89-94263 ..... N89-23237 #
ETN-89-94264 ..... N89-23216 #
ETN-89-94265 ..... N89-23238 #
ETN-89-94266 ..... N89-23217 #
ETN-89-94267 ..... N89-23239 #
ETN-89-94268 ..... N89-23240 #
ETN-89-94269 ..... N89-23241 #
ETN-89-94270 ..... N89-23218 #
ETN-89-94271 ..... N89-23242 #
ETN-89-94272 ..... N89-23262 #
ETN-89-94273 ..... N89-23263 #
ETN-89-94274 ..... N89-23266 #
ETN-89-94275 ..... N89-23243 #
ETN-89-94276 ..... N89-23244 #
ETN-89-94277 ..... N89-23245 #
ETN-89-94278 ..... N89-23246 #
ETN-89-94279 ..... N89-23247 #
ETN-89-94280 ..... N89-23219 #
ETN-89-94281 ..... N89-23264 #
ETN-89-94282 ..... N89-23248 #
ETN-89-94283 ..... N89-23249 #
ETN-89-94284 ..... N89-23250 #
ETN-89-94285 ..... N89-23220 #
ETN-89-94286 ..... N89-23251 #
ETN-89-94287 ..... N89-23252 #
ETN-89-94302 ..... N89-23279 #
ETN-89-94303 ..... N89-23201 #
ETN-89-94307 ..... N89-23287 #
ETN-89-94308 ..... N89-22976 #
ETN-89-94313 ..... N89-22616 #
ETN-89-94314 ..... N89-22601 #
ETN-89-94315 ..... N89-22613 #
ETN-89-94316 ..... N89-22578 #
ETN-89-94317 ..... N89-22777 #
ETN-89-94318 ..... N89-22778 #
ETN-89-94319 ..... N89-22799 #
ETN-89-94320 ..... N89-23299 #
ETN-89-94321 ..... N89-23221 #
ETN-89-94338 ..... N89-22927
ETN-89-94339 ..... N89-22714
ETN-89-94340 ..... N89-22963
ETN-89-94341 ..... N89-23202
ETN-89-94342 ..... N89-23253
ETN-89-94343 ..... N89-22765 #
ETN-89-94344 ..... N89-22766 #
ETN-89-94345 ..... N89-23344 #
ETN-89-94346 ..... N89-23345 #
ETN-89-94347 ..... N89-23346 #
ETN-89-94348 ..... N89-22742 #
ETN-89-94349 ..... N89-22699 #
ETN-89-94350 ..... N89-22928 #
ETN-89-94351 ..... N89-22700 #
ETN-89-94352 ..... N89-22701 #
ETN-89-94353 ..... N89-22743 #
ETN-89-94354 ..... N89-22744 #
ETN-89-94355 ..... N89-22702 #

ETN-89-94356 N89-22703 #
ETN-89-94357 N89-22704 #
ETN-89-94358 N89-22598 #
ETN-89-94359 N89-22852 #
ETN-89-94360 N89-22853 #
ETN-89-94361 N89-22705 #
ETN-89-94362 N89-22767 #
ETN-89-94363 N89-22854 #
ETN-89-94364 N89-22579 #
ETN-89-94365 N89-22929 #
ETN-89-94367 N89-22815 #
ETN-89-94368 N89-22936 #
ETN-89-94369 N89-23405 #
ETN-89-94370 N89-23222 #
ETN-89-94371 N89-22619 #
ETN-89-94372 N89-22855 #
ETN-89-94373 N89-22856 #
ETN-89-94374 N89-23041 #
ETN-89-94376 N89-22706 #
ETN-89-94377 N89-22745 #
ETN-89-94378 N89-22580 #
ETN-89-94379 N89-22581 #
ETN-89-94380 N89-22800 #
ETN-89-94402 N89-22964 #
ETN-89-94443 N89-22715 #
ETN-89-94444 N89-23203 #
ETN-89-94445 N89-22599 #
ETN-89-94450 N89-22857 #
ETN-89-94452 N89-22636 #
ETN-89-94453 N89-22643 #
ETN-89-94454 N89-23347 #
ETN-89-94455 N89-23288 #
ETN-89-94456 N89-22644 #
ETN-89-94457 N89-22801 #
ETN-89-94458 N89-22802 #
ETN-89-94461 N89-22645 #
ETN-89-94463 N89-22646 #
ETN-89-94466 N89-22647 #
ETN-89-94467 N89-23204 #
ETN-89-94471 N89-22977 #
ETN-89-94472 N89-22648 #
ETN-89-94474 N89-22978 #
ETN-89-94479 N89-23223 #
ETN-89-94480 N89-22858 #
ETN-89-94544 N89-22582 #
ETN-89-94545 N89-22707 #
ETN-89-94546 N89-22859 #
ETN-89-94547 N89-22602 #
ETN-89-94548 N89-23254 #
ETN-89-94549 N89-22965 #
ETN-89-94550 N89-22583 #
ETN-89-94551 N89-22803 #

FEI-1906 N89-23227 #
FEI-1908 N89-23228 #

FFA-TN-1987-39 N89-22582 #
FFA-TN-1987-81 N89-22618 #
FFA-TN-1988-11 N89-22601 #
FFA-TN-1988-11-SUPPL N89-22613 #
FFA-TN-1988-37 N89-22707 #
FFA-TN-1988-43 N89-22859 #
FFA-TN-1988-44 N89-22602 #
FFA-TN-1988-57 N89-23254 #
FFA-TN-1988-62 N89-22578 #
FFA-TN-1988-67 N89-22777 #
FFA-TN-1988-74 N89-22965 #

FFA-141 N89-22583 #

FFAP-801 N89-22778 #

FI-454/TB-43 N89-22792 #

FNAL-TM-1567 N89-22876 #

FNAL/C-89/16-A N89-23387 #

FOA-C-10312-9.3 N89-22974 #
FOA-C-20736-2.1-PT-2 N89-22849 #
FOA-C-20736-2.1 N89-23279 #
FOA-C-20740-2.7 N89-23201 #
FOA-C-30492-3.3 N89-23212 #
FOA-C-30498-3.3 N89-23213 #
FOA-C-30507-3.1 N89-23287 #
FOA-C-30511-9.4 N89-22976 #

FR-688102 N89-23300* #

FTD-ID(RS)T-0630-88 N89-22615 #
FTD-ID(RS)T-0912-88 N89-22570 #

GA-A-19564 N89-23290 #

GEC-MTR-87/110-VOL-1 N89-22977 #

GKSS-88/E/34 N89-22960 #

GMD-322 N89-22846

GPS-REP-SEL-002 N89-22643 #

H-1537 N89-22612* #
H-1540 N89-23209* #

HJB-860367 N89-22807 #

I-264/88 N89-22935 #
I-266/88 N89-22758 #

IC-88/38-REV N89-23267 #
IC-88/115 N89-22727 #
IC-88/122 N89-23315 #
IC-88/141 N89-22840 #
IC-88/159 N89-23316 #
IC-88/205 N89-23050 #
IC-88/224 N89-22871 #
IC-88/225 N89-22785 #
IC-88/238 N89-23351 #
IC-88/275 N89-23389 #
IC-88/278 N89-23317 #
IC-88/279 N89-23390 #
IC-88/280 N89-23391 #
IC-88/281 N89-23318 #
IC-88/283 N89-23319 #
IC-88/285 N89-22752 #
IC-88/287 N89-23320 #
IC-88/288 N89-23352 #
IC-88/297 N89-23321 #
IC-88/299 N89-23259 #
IC-88/300 N89-23322 #
IC-88/302 N89-22753 #
IC-88/303 N89-22754 #
IC-88/313 N89-23323 #
IC-88/314 N89-23229 #
IC-88/319 N89-23353 #
IC-88/325 N89-23354 #
IC-88/354 N89-23396 #
IC-88/360 N89-23355 #
IC-88/368 N89-23324 #
IC-88/382 N89-23356 #

ICASE-89-15 N89-22836* #
ICASE-89-18-PT-2 N89-22837* #
ICASE-89-19 N89-22574* #
ICASE-89-27 N89-23073* #

IITRI-E06595-4 N89-22806 #

IRF-PREPRINT-107 N89-22799 #
IRF-PREPRINT-109 N89-23299 #

ISAL-IDI-8809 N89-22936 #

ISAL-88-0065 N89-22815 #

ISBN-3-88148-224-X N89-23053
ISBN-3-88148-241-5 N89-23052
ISBN-92-835-0470-4 N89-23361 #
ISBN-92-835-0496-8 N89-23362 #
ISBN-92-835-0498-4 N89-22654 #

ISSN-0072-4130 N89-23052
ISSN-0072-4130 N89-23053
ISSN-0081-5640 N89-22583 #
ISSN-0143-7305 N89-23202
ISSN-0143-7313 N89-22691
ISSN-0143-7313 N89-22714
ISSN-0143-7313 N89-22927
ISSN-0143-7313 N89-22963
ISSN-0143-7313 N89-23266
ISSN-0143-7315 N89-23275
ISSN-0169-1651 N89-23054
ISSN-0169-1651 N89-23055
ISSN-0169-2690 N89-23219 #
ISSN-0169-2690 N89-23220 #
ISSN-0169-2690 N89-23246 #
ISSN-0169-2690 N89-23247 #
ISSN-0169-2690 N89-23248 #
ISSN-0169-2690 N89-23249 #
ISSN-0169-2690 N89-23250 #
ISSN-0169-2690 N89-23251 #
ISSN-0169-2690 N89-23252 #
ISSN-0169-2690 N89-23264 #
ISSN-0171-1342 N89-22580 #
ISSN-0171-1342 N89-22581 #
ISSN-0171-1342 N89-22706 #
ISSN-0171-1342 N89-22745 #
ISSN-0171-1342 N89-22800 #
ISSN-0176-0777 N89-23026 #
ISSN-0176-0777 N89-23027 #
ISSN-0176-0777 N89-23037 #
ISSN-0176-7739 N89-22619 #
ISSN-0176-7739 N89-22855 #
ISSN-0176-7739 N89-22856 #
ISSN-0176-7739 N89-23041 #
ISSN-0262-5369 N89-23253
ISSN-0281-0247 N89-22974 #
ISSN-0284-1711 N89-22799 #
ISSN-0284-1711 N89-23299 #
ISSN-0343-7639 N89-23026 #
ISSN-0344-9629 N89-22960 #
ISSN-0347-3694 N89-22849 #
ISSN-0347-3694 N89-23201 #
ISSN-0347-3694 N89-23279 #
ISSN-0347-3706 N89-22976 #
ISSN-0347-3706 N89-23212 #
ISSN-0347-3706 N89-23213 #
ISSN-0347-3706 N89-23287 #
ISSN-0348-7539 N89-23289 #
ISSN-0366-0885 N89-22732 #
ISSN-0366-0885 N89-22733 #
ISSN-0366-0885 N89-23029 #
ISSN-0723-0506 N89-22846
ISSN-0921-1969 N89-23215 #
ISSN-0921-1969 N89-23216 #
ISSN-0921-1969 N89-23217 #
ISSN-0921-1969 N89-23218 #
ISSN-0921-1969 N89-23234 #
ISSN-0921-1969 N89-23235 #
ISSN-0921-1969 N89-23236 #
ISSN-0921-1969 N89-23237 #
ISSN-0921-1969 N89-23238 #
ISSN-0921-1969 N89-23239 #
ISSN-0921-1969 N89-23240 #
ISSN-0921-1969 N89-23241 #
ISSN-0921-1969 N89-23242 #
ISSN-0921-1969 N89-23243 #
ISSN-0921-1969 N89-23244 #
ISSN-0921-1969 N89-23245 #
ISSN-0921-1969 N89-23262 #
ISSN-0921-1969 N89-23263 #
ISSN-0921-1969 N89-23266 #

ISTIC-TR-C-000139 N89-22937 #
ISTIC-TR-C-000157 N89-22719 #
ISTIC-TR-C-000181 N89-22867 #
ISTIC-TR-C-000196 N89-22571 #

JINR-14-88-57 N89-23325 #

JPRS-USP-88-003 N89-22622 #

JUEL-SPEZ-449 N89-23028 #

JUEL-2201 N89-22732 #
JUEL-2213 N89-22733 #
JUEL-2217 N89-23029 #

KNMI-WR-88-05 N89-23054
KNMI-WR-88-06 N89-23055

L-16524 N89-22568* #
L-16548 N89-22614* #
L-16557 N89-23181* #

LA-UR-88-3281 N89-23260 #
LA-UR-88-3665 N89-22872 #
LA-UR-89-265 N89-23035 #
LA-UR-89-266 N89-23193 #
LA-UR-89-366 N89-22685 #
LA-UR-89-479 N89-22873 #
LA-UR-89-599 N89-22790 #
LA-UR-89-739 N89-23336 #
LA-UR-89-813 N89-23380 #
LA-UR-89-817 N89-23198 #
LA-UR-89-949 N89-22796 #
LA-UR-89-1077 N89-23392 #

LA-11440-PR N89-23281 #
LA-11524-MS N89-23265 #
LA-11546-MS N89-22962 #

LAAS-89-002 N89-23222 #

LAMF-8712 N89-22642 #

LBL-24106 N89-23231 #
LBL-25223 N89-23328 #
LBL-25507 N89-23019 #
LBL-26144 N89-22870 #
LBL-26222 N89-23307 #
LBL-26234 N89-23311 #
LBL-26235 N89-23310 #
LBL-26467 N89-22844 #
LBL-26727 N89-22741 #

LC-88-600538 N89-23060 #

LC-88-600540 ..... N89-22637 #
LC-88-600550 ..... N89-22591 #
LC-88-600554 ..... N89-22747 #

LFD-273 ..... N89-22793

LRC-89-3 ..... N89-23296 #

MAE-1851 ..... N89-22666 #

MATHS-RES-202 ..... N89-23221 #

MBB-UT-129/87 ..... N89-22600 #

MCR-88-590-VOL-2 ..... N89-22650 #

MEMO-648 ..... N89-23239 #
MEMO-706 ..... N89-23215 #
MEMO-708 ..... N89-23234 #
MEMO-709 ..... N89-23235 #
MEMO-710 ..... N89-23236 #
MEMO-711 ..... N89-23237 #
MEMO-718 ..... N89-23216 #
MEMO-719 ..... N89-23250 #
MEMO-720 ..... N89-23238 #
MEMO-721 ..... N89-23217 #
MEMO-722 ..... N89-23239 #
MEMO-723 ..... N89-23240 #
MEMO-724 ..... N89-23241 #
MEMO-725-PT-3 ..... N89-23218 #
MEMO-726 ..... N89-23242 #
MEMO-727 ..... N89-23262 #
MEMO-728 ..... N89-23263 #
MEMO-729 ..... N89-23266 #
MEMO-730 ..... N89-23243 #
MEMO-731 ..... N89-23244 #
MEMO-732 ..... N89-23245 #
MEMO-733 ..... N89-23246 #
MEMO-734 ..... N89-23247 #
MEMO-736 ..... N89-23219 #
MEMO-737 ..... N89-23264 #
MEMO-738 ..... N89-23248 #
MEMO-739 ..... N89-23249 #
MEMO-740 ..... N89-23250 #
MEMO-742 ..... N89-23220 #
MEMO-743 ..... N89-23251 #
MEMO-744 ..... N89-23252 #

MM-5558-88-20 ..... N89-22938 #

MSRR-550 ..... N89-23190 #

MTL-TR-88-34 ..... N89-22931 #
MTL-TR-88-44 ..... N89-22746 #
MTL-TR-89-11 ..... N89-22768 #

MTU-TB-87/010 ..... N89-22608
MTU-TB-87/927 ..... N89-22757

NADC-88109-60 ..... N89-22688 #

NAE-AN-56 ..... N89-22575 #

NAS 1.15:4114 ..... N89-22614* #
NAS 1.15:100471 ..... N89-22638* #
NAS 1.15:100615 ..... N89-23068* #
NAS 1.15:100654 ..... N89-23270* #
NAS 1.15:100728 ..... N89-23182* #
NAS 1.15:101012 ..... N89-23061* #
NAS 1.15:101084 ..... N89-22860* #
NAS 1.15:101186 ..... N89-22969* #
NAS 1.15:101406 ..... N89-22939* #
NAS 1.15:101545 ..... N89-22692* #
NAS 1.15:101549 ..... N89-22868* #
NAS 1.15:101567 ..... N89-23272* #
NAS 1.15:101944 ..... N89-22607* #
NAS 1.15:101969 ..... N89-22919* #
NAS 1.15:101972 ..... N89-22605* #
NAS 1.15:101977 ..... N89-22606* #
NAS 1.15:101984 ..... N89-22684* #
NAS 1.15:101989 ..... N89-22569* #
NAS 1.15:101997 ..... N89-22710* #
NAS 1.15:102010 ..... N89-22573* #
NAS 1.15:102015 ..... N89-23397* #
NAS 1.15:102020 ..... N89-22651* #
NAS 1.15:102022 ..... N89-22925* #
NAS 1.15:102027 ..... N89-22661* #
NAS 1.15:102028 ..... N89-22617* #
NAS 1.15:102039 ..... N89-22652* #
NAS 1.15:102047 ..... N89-22577* #
NAS 1.15:102054 ..... N89-22653* #
NAS 1.15:102058 ..... N89-23025* #
NAS 1.15:102079 ..... N89-22662* #
NAS 1.15:102154 ..... N89-22682* #
NAS 1.15:102190 ..... N89-22850* #
NAS 1.26:4224 ..... N89-22920* #
NAS 1.26:4228 ..... N89-22779* #
NAS 1.26:4241 ..... N89-22890* #
NAS 1.26:179440 ..... N89-22612* #
NAS 1.26:179441 ..... N89-23209* #
NAS 1.26:179614-VOL-2 ..... N89-22981* #
NAS 1.26:179614-VOL-3 ..... N89-22980* #
NAS 1.26:181405 ..... N89-22773* #
NAS 1.26:181406 ..... N89-22838* #
NAS 1.26:181560 ..... N89-22780* #
NAS 1.26:181768 ..... N89-23300* #
NAS 1.26:181804 ..... N89-23183* #
NAS 1.26:181808 ..... N89-22616* #
NAS 1.26:181811 ..... N89-22636* #
NAS 1.26:181815 ..... N89-22637* #
NAS 1.26:181816 ..... N89-22574* #
NAS 1.26:181832 ..... N89-23073* #
NAS 1.26:182237 ..... N89-23382* #
NAS 1.26:182685 ..... N89-22975* #
NAS 1.26:183331 ..... N89-22922* #
NAS 1.26:183612 ..... N89-22722* #
NAS 1.26:184637 ..... N89-22979* #
NAS 1.26:184835 ..... N89-23400* #
NAS 1.26:184836 ..... N89-22709* #
NAS 1.26:184837 ..... N89-22918* #
NAS 1.26:184842 ..... N89-23302* #
NAS 1.26:184878 ..... N89-22970* #
NAS 1.26:184906 ..... N89-22817* #
NAS 1.26:184910 ..... N89-23399* #
NAS 1.26:184936 ..... N89-23404* #
NAS 1.26:184937 ..... N89-22971* #
NAS 1.26:184938 ..... N89-23184* #
NAS 1.26:184959 ..... N89-23306* #
NAS 1.26:184968 ..... N89-23048* #
NAS 1.26:184993 ..... N89-23040* #
NAS 1.55:3026 ..... N89-22891* #
NAS 1.55:3029 ..... N89-22940* #
NAS 1.55:10029 ..... N89-22982* #
NAS 1.60:2903 ..... N89-23181* #
NAS 1.60:2913 ..... N89-22568* #

NASA-CP-3026 ..... N89-22891* #
NASA-CP-3029 ..... N89-22940* #
NASA-CP-10029 ..... N89-22982* #

NASA-CR-4224 ..... N89-22920* #
NASA-CR-4228 ..... N89-22779* #
NASA-CR-4241 ..... N89-22890* #
NASA-CR-179440 ..... N89-22612* #
NASA-CR-179441 ..... N89-23209* #
NASA-CR-179614-VOL-2 ..... N89-22981* #
NASA-CR-179614-VOL-3 ..... N89-22980* #
NASA-CR-181405 ..... N89-22773* #
NASA-CR-181406 ..... N89-22838* #
NASA-CR-181560 ..... N89-22780* #
NASA-CR-181788 ..... N89-23300* #
NASA-CR-181804 ..... N89-23183* #
NASA-CR-181808 ..... N89-22616* #
NASA-CR-181811 ..... N89-22636* #
NASA-CR-181815 ..... N89-22637* #
NASA-CR-181816 ..... N89-22574* #
NASA-CR-181832 ..... N89-23073* #
NASA-CR-182237 ..... N89-23382* #
NASA-CR-182685 ..... N89-22975* #
NASA-CR-183331 ..... N89-22922* #
NASA-CR-183612 ..... N89-22722* #
NASA-CR-184637 ..... N89-22979* #
NASA-CR-184835 ..... N89-23400* #
NASA-CR-184836 ..... N89-22709* #
NASA-CR-184837 ..... N89-22918* #
NASA-CR-184842 ..... N89-23302* #
NASA-CR-184878 ..... N89-22970* #
NASA-CR-184906 ..... N89-22817* #
NASA-CR-184910 ..... N89-23399* #
NASA-CR-184936 ..... N89-23404* #
NASA-CR-184937 ..... N89-22971* #
NASA-CR-184938 ..... N89-23184* #
NASA-CR-184959 ..... N89-23306* #
NASA-CR-184968 ..... N89-23048* #
NASA-CR-184993 ..... N89-23040* #

NASA-TM-4114 ..... N89-22614* #
NASA-TM-100471 ..... N89-22638* #
NASA-TM-100615 ..... N89-23068* #
NASA-TM-100654 ..... N89-23270* #
NASA-TM-100728 ..... N89-23182* #
NASA-TM-101012 ..... N89-23061* #
NASA-TM-101084 ..... N89-22860* #
NASA-TM-101186 ..... N89-22969* #
NASA-TM-101406 ..... N89-22939* #
NASA-TM-101545 ..... N89-22692* #
NASA-TM-101549 ..... N89-22868* #
NASA-TM-101567 ..... N89-23272* #
NASA-TM-101944 ..... N89-22607* #
NASA-TM-101969 ..... N89-22919* #
NASA-TM-101972 ..... N89-22605* #
NASA-TM-101977 ..... N89-22606* #
NASA-TM-101984 ..... N89-22684* #
NASA-TM-101989 ..... N89-22569* #
NASA-TM-101997 ..... N89-22710* #
NASA-TM-102010 ..... N89-22573* #
NASA-TM-102015 ..... N89-23397* #
NASA-TM-102020 ..... N89-22651* #
NASA-TM-102022 ..... N89-22925* #
NASA-TM-102027 ..... N89-22661* #
NASA-TM-102028 ..... N89-22617* #
NASA-TM-102039 ..... N89-22652* #
NASA-TM-102047 ..... N89-22577* #
NASA-TM-102054 ..... N89-22653* #
NASA-TM-102058 ..... N89-23025* #
NASA-TM-102079 ..... N89-22662* #
NASA-TM-102154 ..... N89-22682* #
NASA-TM-102190 ..... N89-22850* #

NASA-TP-2903 ..... N89-23181* #
NASA-TP-2913 ..... N89-22568* #

NCPA-LC-02-1988 ..... N89-23271 #

NEDOJ-P-8708-PT-2 ..... N89-22755 #
NEDOJ-P-8743 ..... N89-22771 #

NHRC-88-51 ..... N89-23086 #

NIKHEF-H/88-3 ..... N89-23276 #
NIKHEF-H/88-4 ..... N89-22878 #
NIKHEF-H/88-5 ..... N89-23277 #
NIKHEF-H/88-7 ..... N89-23357 #
NIKHEF-H/88-15 ..... N89-23358 #
NIKHEF-H/88-18 ..... N89-23278 #

NIST/SP-744 ..... N89-22747 #

NIST/TN-1253 ..... N89-22748 #

NISTIR-88/3904 ..... N89-22722* #

NLR-TR-87119-U ..... N89-23070 #

NOAA-TM-ERL-WPL-155 ..... N89-23048* #

NOSC/TD-1301 ..... N89-23189 #

NOTE-E/ES4-21-387 ..... N89-23223 #

NPL-DES-91 ..... N89-23202

NPL-DITC-135/88 ..... N89-23253

NPL-DMA(A)165 ..... N89-23268
NPL-DMA(A)167 ..... N89-22927
NPL-DMA(A)168 ..... N89-22691
NPL-DMA(A)169 ..... N89-22714
NPL-DMA(A)171 ..... N89-22963

NPL-RS(EXT)104 ..... N89-23275

NPS53-89-007 ..... N89-23255 #
NPS61-89-003 ..... N89-23047 #

NRC-29908 ..... N89-22575 #

NRL-MEMO-6335 ..... N89-23032 #

NRL-MR-6410 ..... N89-22864 #

NTH-Y01-ES-70153 ..... N89-23062 #

NTSB/AAR-89/01 ..... N89-22593 #

ONERA-RSF-3/4368-AY-502-A ..... N89-22853 #
ONERA-RSF-16/3419-AY-112-A ..... N89-22852 #

ONERA-RT-3/7256-RY-071-R ..... N89-22705 #

OSP-92790 ..... N89-22971* #

OTA-BA-360-PT-4 ..... N89-23060 #

OTA-ISC-383 ..... N89-22637 #

OTA-SET-381 ..... N89-22591 #

OUEL-1636/88 ..... N89-23293 #
OUEL-1643/88 ..... N89-22711 #
OUEL-1658/88 ..... N89-22848 #
OUEL-1738/88 ..... N89-23214 #
OUEL-1743/88 ..... N89-22961 #

PATENTS-US-A7176014 ..... N89-22888 #
PATENTS-US-A7180839 ..... N89-22887 #
PATENTS-US-A7182671 ..... N89-22809 #
PATENTS-US-A7184476 ..... N89-23023 #

PATENTS-US-A7184918 ..... N89-23024 #
PATENTS-US-A7186419 ..... N89-22675 #
PATENTS-US-A7186427 ..... N89-22762 #
PATENTS-US-A7186856 ..... N89-23298 #
PATENTS-US-A7187776 ..... N89-23273 #
PATENTS-US-A7193705 ..... N89-22736 #
PATENTS-US-A7206153 ..... N89-22763 #

PB88-248939 ..... N89-23060 #
PB89-111470 ..... N89-22571 #
PB89-112478 ..... N89-22719 #
PB89-112650 ..... N89-22937 #
PB89-112940 ..... N89-22667 #
PB89-114268 ..... N89-22637 #
PB89-114318 ..... N89-22591 #
PB89-116263 ..... N89-22607 #
PB89-127831 ..... N89-23048* #
PB89-129530 ..... N89-22747 #
PB89-134209 ..... N89-22748 #
PB89-910401 ..... N89-22593 #

PNL-SA-16432 ..... N89-23036 #
PNL-SA-16548 ..... N89-22926 #
PNL-SA-16579 ..... N89-23378 #

PNL-6833 ..... N89-23062 #

PSD88/00017 ..... N89-22648 #

R/D-5421-MA-01 ..... N89-23256 #

RADC-TR-88-187 ..... N89-23206 #
RADC-TR-88-203 ..... N89-23192 #

REPT-OX-1-005 ..... N89-22645 #

REPT-4-88 ..... N89-22793
REPT-19 ..... N89-22975* #
REPT-27 ..... N89-22972 #
REPT-34/88 ..... N89-23360 #
REPT-47-186/F ..... N89-22702 #
REPT-47-323/F ..... N89-22703 #
REPT-47-324/F ..... N89-22704 #
REPT-013/88 ..... N89-22598 #
REPT-882-320-101 ..... N89-23223 #
REPT-882-320-102 ..... N89-22858 #
REPT-6216-055-REV ..... N89-22604 #
REPT-780852-TW ..... N89-22934 #
REPT-860142-TW ..... N89-22933 #
REPT-871126/1/FR ..... N89-22601 #

S-593 ..... N89-22682* #

SAND-88-1483C ..... N89-23261 #
SAND-88-1651C ..... N89-23015 #
SAND-88-1847C ..... N89-23016 #
SAND-88-2347C ..... N89-23194 #
SAND-88-2366C ..... N89-23230 #
SAND-88-2377C ..... N89-22957 #
SAND-88-2891C ..... N89-22728 #
SAND-88-2960C ..... N89-22808 #
SAND-88-3058C ..... N89-22576 #
SAND-88-3072C ..... N89-23017 #
SAND-88-3114 ..... N89-23072 #
SAND-88-3440C ..... N89-23327 #
SAND-88-7154 ..... N89-23297 #
SAND-88-7162C ..... N89-22884 #
SAND-89-0156 ..... N89-23199 #
SAND-89-0266C ..... N89-22923 #
SAND-89-0332C ..... N89-23012 #
SAND-89-0366C ..... N89-22845 #
SAND-89-0381C ..... N89-22749 #
SAND-89-0382C ..... N89-23013 #
SAND-89-0410C ..... N89-22592 #
SAND-89-0580C ..... N89-23196 #
SAND-89-0581C ..... N89-23208 #
SAND-89-0706C ..... N89-22764 #
SAND-89-0809C ..... N89-22924 #

SCC-88-01 ..... N89-23063 #
SCC-89-01 ..... N89-23401 #

SC5432.AR ..... N89-22686 #

SEP-TS/F-6972/88-RP ..... N89-22836 #

SERI/STR-211-3446 ..... N89-23021 #
SERI/STR-211-3473 ..... N89-22760 #
SERI/STR-211-3487 ..... N89-23022 #

SERI/TP-253-3426 ..... N89-22843 #
SERI/TP-254-3454 ..... N89-22681 #

SPI-25-1-VOL-2 ..... N89-22981* #
SPI-25-1-VOL-3 ..... N89-22980* #

SR-1 ..... N89-23045 #

SRL-P-01-1989 ..... N89-22882 #

SSC-MAG-166 ..... N89-23231 #

STF/E-39-005/CB ..... N89-22648 #

SU-SLAC/AP-73 ..... N89-22783 #

SU-STAN-CS-88-1199 ..... N89-23257 #

T-114-A ..... N89-22679 #

TACOM-TR-13375 ..... N89-23283 #

TR-20-ONR ..... N89-23348 #
TR-48 ..... N89-22750 #
TR-88-65C ..... N89-23256 #
TR-881020-8704 ..... N89-23069 #

TRITA-EPP-88-06 ..... N89-23289 #

UCID-21589 ..... N89-23285 #
UCID-21591 ..... N89-22880 #
UCID-21652 ..... N89-22797 #

UCLA/PPG-1228 ..... N89-23295 #

UCRL-53889 ..... N89-23282 #
UCRL-97689 ..... N89-22789 #
UCRL-98426 ..... N89-22874 #
UCRL-98739 ..... N89-23336 #
UCRL-98873 ..... N89-23195 #
UCRL-98924 ..... N89-23330 #
UCRL-98957 ..... N89-23211 #
UCRL-99077 ..... N89-22886 #
UCRL-99741 ..... N89-23329 #
UCRL-99853 ..... N89-22696 #
UCRL-99865 ..... N89-22788 #
UCRL-99981 ..... N89-23292 #
UCRL-99995 ..... N89-22756 #
UCRL-100127 ..... N89-23266 #
UCRL-100134 ..... N89-22731 #
UCRL-100259 ..... N89-23274 #
UCRL-100353 ..... N89-23210 #
UCRL-100623 ..... N89-23294 #
UCRL-100680 ..... N89-23233 #
UCRL-100749 ..... N89-23402 #

UILU-ENG-89-2203 ..... N89-22805 #
UILU-ENG-89-2209 ..... N89-23349 #

US-PATENT-APPL-SN-176014 ..... N89-22888 #
US-PATENT-APPL-SN-180939 ..... N89-22887 #
US-PATENT-APPL-SN-182671 ..... N89-22809 #
US-PATENT-APPL-SN-184476 ..... N89-23023 #
US-PATENT-APPL-SN-184918 ..... N89-23024 #
US-PATENT-APPL-SN-185419 ..... N89-22675 #
US-PATENT-APPL-SN-185427 ..... N89-22762 #
US-PATENT-APPL-SN-186856 ..... N89-23298 #
US-PATENT-APPL-SN-187776 ..... N89-23273 #
US-PATENT-APPL-SN-193705 ..... N89-22736 #
US-PATENT-APPL-SN-206153 ..... N89-22763 #

USAFSAM-TR-88-10 ..... N89-23071 #

USIP-88-07 ..... N89-22803 #

UVA/525671/MS89/101 ..... N89-22725 #

VKI-TN-168 ..... N89-22857 #

W-2/88 ..... N89-22964 #

WHC-SA-0537 ..... N89-23030 #

WHOI-88-36 ..... N89-23058 #

WP-88-89-23 ..... N89-23190 #

WRDC-TR-89-2015 ..... N89-22718 #

Y-2402 ..... N89-23284 #

☆ U.S. GOVERNMENT PRINTING OFFICE: 1989— 242-445/00107

FEDERAL REGIONAL DEPOSITORY LIBRARIES

ALABAMA

AUBURN UNIV. AT MONTGOMERY LIBRARY
Documents Department
Montgomery, AL 36193
(205) 271-9650

UNIV. OF ALABAMA LIBRARY
Documents Dept.-Box S
University, AL 35486
(205) 348-6046

ARIZONA

DEPT. OF LIBRARY, ARCHIVES AND PUBLIC RECORDS
Third Floor – State Cap.
1700 West Washington
Phoenix, AZ 85007
(602) 255-4121

UNIVERSITY OF ARIZONA LIB.
Government Documents Dept.
Tucson, AZ 85721
(602) 621-6433

ARKANSAS

ARKANSAS STATE LIBRARY
One Capitol Mall
Little Rock, AR 72201
(501) 371-2326

CALIFORNIA

CALIFORNIA STATE LIBRARY
Govt. Publications Section
P.O. Box 2037
Sacramento, CA 95809
(916) 324-4863

COLORADO

UNIV OF COLORADO LIB.
Government Pub. Division
Campus Box 184
Boulder, CO 80309
(303) 492-8834

DENVER PUBLIC LIBRARY
Govt. Pub. Department
1357 Broadway
Denver, CO 80203
(303) 571-2131

CONNECTICUT

CONNECTICUT STATE LIBRARY
Government Documents Unit
231 Capitol Avenue
Hartford, CT 06106
(203) 566-7029

FLORIDA

UNIV. OF FLORIDA LIBRARIES
Library West
Documents Department
Gainesville, FL 32611
(904) 392-0367

GEORGIA

UNIV. OF GEORGIA LIBRARIES
Government Reference Dept.
Athens, GA 30602
(404) 542-8949

HAWAII

UNIV. OF HAWAII LIBRARY
Govt. Documents Collection
2550 The Mall
Honolulu, HI 96822
(808) 948-8230

IDAHO

UNIV. OF IDAHO LIBRARY
Documents Section
Moscow, ID 83843
(208) 885-6344

ILLINOIS

ILLINOIS STATE LIBRARY
Information Services Branch
Centennial Building
Springfield, IL 62756
(217) 782-5185

INDIANA

INDIANA STATE LIBRARY
Serials Documents Section
140 North Senate Avenue
Indianapolis, IN 46204
(317) 232-3686

IOWA

UNIV. OF IOWA LIBRARIES
Govt. Documents Department
Iowa City, IA 52242
(319) 353-3318

KANSAS

UNIVERSITY OF KANSAS
Doc. Collect – Spencer Lib.
Lawrence, KS 66045-2800
(913) 864-4662

KENTUCKY

UNIV. OF KENTUCKY LIBRARIES
Govt. Pub. Department
Lexington, KY 40506-0039
(606) 257-3139

LOUISIANA

LOUISIANA STATE UNIVERSITY
Middleton Library
Govt. Docs. Dept.
Baton Rouge, LA 70803
(504) 388-2570

LOUISIANA TECHNICAL UNIV. LIBRARY
Documents Department
Ruston, LA 71272-0046
(318) 257-4962

MAINE

UNIVERSITY OF MAINE
Raymond H. Fogler Library
Tri-State Regional Documents Depository
Orono, ME 04469
(207) 581-1680

MARYLAND

UNIVERSITY OF MARYLAND
McKeldin Lib. – Doc. Div.
College Park, MD 20742
(301) 454-3034

MASSACHUSETTS

BOSTON PUBLIC LIBRARY
Government Docs. Dept.
Boston, MA 02117
(617) 536-5400 ext.226

MICHIGAN

DETROIT PUBLIC LIBRARY
Sociology Department
5201 Woodward Avenue
Detroit, MI 48202-4093
(313) 833-1409

MICHIGAN STATE LIBRARY
P.O. Box 30007
Lansing, MI 48909
(517) 373-1593

MINNESOTA

UNIVERSITY OF MINNESOTA
Government Pubs. Division
409 Wilson Library
309 19th Avenue South
Minneapolis, MN 55455
(612) 373-7870

MISSISSIPPI

UNIV. OF MISSISSIPPI LIB.
Documents Department
University, MS 38677
(601) 232-5857

MONTANA

UNIV. OF MONTANA
Mansfield Library
Documents Division
Missoula, MT 59812
(406) 243-6700

NEBRASKA

UNIVERSITY OF NEBRASKA - LINCOLN
Love Library
Documents Department
Lincoln, NE 68588-0410
(402) 472-2562

NEVADA

UNIVERSITY OF NEVADA LIB.
Govt. Pub. Department
Reno, NV 89557-0044
(702) 784-6579

NEW JERSEY

NEWARK PUBLIC LIBRARY
5 Washington Street
Newark, NJ 07101-0630
(201) 733-7812

NEW MEXICO

UNIVERSITY OF NEW MEXICO
Zimmerman Library
Government Pub. Dept.
Albuquerque, NM 87131
(505) 277-5441

NEW MEXICO STATE LIBRARY
Reference Department
325 Don Gaspar Avenue
Santa Fe, NM 87503
(505) 827-3826

NEW YORK

NEW YORK STATE LIBRARY
Empire State Plaza
Albany, NY 12230
(518) 474-5563

NORTH CAROLINA

UNIVERSITY OF NORTH CAROLINA AT CHAPEL HILL
Davis Library
BA/SS Documents Division
Chapel Hill, NC 27515
(919) 962-1151

NORTH DAKOTA

UNIVERSITY OF NORTH DAKOTA
Chester Fritz Library
Documents Department
Grand Forks, ND 58202
(701) 777-4629
In cooperation with North Dakota State Univ. Library

OHIO

STATE LIBRARY OF OHIO
Documents Department
65 South Front Street
Columbus, OH 43266-0334
(614) 462-7051

OKLAHOMA

OKLAHOMA DEPT. OF LIB.
Government Documents
200 NE 18th Street
Oklahoma City, OK 73105
(405) 521-2502, ext. 252

OKLAHOMA STATE UNIV. LIB.
Documents Department
Stillwater, OK 74078
(405) 624-6546

OREGON

PORTLAND STATE UNIV. LIB.
Documents Department
P.O. Box 1151
Portland, OR 97207
(503) 229-3673

PENNSYLVANIA

STATE LIBRARY OF PENN.
Government Pub. Section
P.O. Box 1601
Harrisburg, PA 17105
(717) 787-3752

TEXAS

TEXAS STATE LIBRARY
Public Services Department
P.O. Box 12927 – Cap. Sta.
Austin, TX 78711
(512) 475-2996

TEXAS TECH. UNIV. LIBRARY
Govt. Documents Department
Lubbock, TX 79409
(806) 742-2268

UTAH

UTAH STATE UNIVERSITY
Merrill Library, U.M.C. 30
Logan, UT 84322
(801) 750-2682

VIRGINIA

UNIVERSITY OF VIRGINIA
Alderman Lib. – Public Doc.
Charlottesville, VA 22903-2498
(804) 924-3133

WASHINGTON

WASHINGTON STATE LIBRARY
Documents Section
Olympia, WA 98504
(206) 753-4027

WEST VIRGINIA

WEST VIRGINIA UNIV. LIB.
Documents Department
Morgantown, WV 26506-6069
(304) 293-3640

WISCONSIN

MILWAUKEE PUBLIC LIBRARY
814 West Wisconsin Avenue
Milwaukee, WI 53233
(414) 278-3065

ST. HIST LIB. OF WISCONSIN
Government Pub. Section
816 State Street
Madison, WI 53706
(608) 262-4347

WYOMING

WYOMING STATE LIBRARY
Supreme Ct. & Library Bld.
Cheyenne, WY 82002
(307) 777-5919

National Aeronautics and
Space Administration
Code NTT-4
Washington, D.C.
20546

Official Business

Penalty for Private Use, $300

SPECIAL FOURTH-CLASS RATE
POSTAGE & FEES PAID
NASA
PERMIT No. G 27

NASA

POSTMASTER: If Undeliverable (Section 158
Postal Manual) Do Not Return